



www.segweb.org

REVIEWS IN ECONOMIC GEOLOGY

Volume 6, Part A

THE ENVIRONMENTAL GEOCHEMISTRY OF MINERAL DEPOSITS

PART A: PROCESSES, TECHNIQUES, AND HEALTH ISSUES

CONTENTS

INTRODUCTION

AN EARTH-SYSTEM SCIENCE TOOLKIT FOR ENVIRONMENTALLY FRIENDLY MINERAL RESOURCE DEVELOPMENT

G.S. Plumlee and M.J. Logsdon

AN OVERVIEW OF THE ABUNDANCE, RELATIVE MOBILITY, BIOAVAILABILITY, AND HUMAN TOXICITY OF METALS

K.S. Smith and H.L.O. Huyck

PROCESSES

THE ENVIRONMENTAL GEOLOGY OF MINERAL DEPOSITS

G.S. Plumlee

SOME FUNDAMENTALS OF AQUEOUS GEOCHEMISTRY

D.K. Nordstrom

THE ROLE OF BACTERIA IN ENVIRONMENTAL GEOCHEMISTRY

A.L. Mills

GEOCHEMISTRY OF ACID MINE WATERS

D.K. Nordstrom and C.N. Alpers

METAL SORPTION ON MINERAL SURFACES: AN OVERVIEW WITH EXAMPLES RELATING TO MINERAL DEPOSITS

K.S. Smith

GENERAL ASPECTS OF AQUATIC COLLOIDS IN ENVIRONMENTAL GEOCHEMISTRY *J.F. Ranville and R.L. Schmiermund*

GEOCHEMICAL PROCESSES CONTROLLING URANIUM

R.B. Wanty, W.R. Miller, P.H. Briggs, and J.B. McHugh

MOBILITY IN MINE DRAINAGES

GEOCHEMISTRY OF THE PROCESSES THAT ATTENUATE ACID MINE DRAINAGE IN WETLANDS *K. Walton-Day*

THE ENVIRONMENTAL GEOCHEMISTRY OF CYANIDE

A.C.S. Smith and T.I. Mudder

TECHNIQUES

FIELD METHODS FOR SAMPLING AND ANALYSIS OF ENVIRONMENTAL SAMPLES FOR UNSTABLE AND SELECTED STABLE CONSTITUENTS *W.H. Ficklin and E.L. Mosier*

LABORATORY METHODS FOR THE ANALYSIS OF ENVIRONMENTAL SAMPLES *J.G. Crock, B.F. Arbogast, and P.J. Lamothe*

GEOCHEMICAL MODELING OF WATER-ROCK INTERACTIONS IN MINING ENVIRONMENTS *C.N. Alpers and D.K. Nordstrom*

STATIC-TEST METHODS MOST COMMONLY USED TO PREDICT ACID-MINE DRAINAGE: PRACTICAL GUIDELINES FOR USE AND INTERPRETATION *W.W. White III, K.A. Lapakko, and R.L. Cox*

HEALTH ISSUES

THE HEALTH EFFECTS OF MINERAL DUSTS

M. Ross

BIOAVAILABILITY OF METALS IN THE ENVIRONMENT: IMPLICATIONS FOR HEALTH RISK ASSESSMENT

G.R. Krieger, H.A. Hattamer-Frey, and J.E. Kester

EFFECTS OF HEAVY METALS ON THE AQUATIC BIOTA

M.G. Kelly

Editors

G.S. Plumlee and M.J. Logsdon

SOCIETY OF ECONOMIC GEOLOGISTS, INC.



www.segweb.org

REVIEWS IN ECONOMIC GEOLOGY

Volume 6, Part B

THE ENVIRONMENTAL GEOCHEMISTRY OF MINERAL DEPOSITS

PART B: CASE STUDIES AND RESEARCH TOPICS

CONTENTS

- GEOLOGIC CONTROLS ON THE COMPOSITION OF NATURAL WATERS AND MINE WATERS DRAINING DIVERSE MINERAL-DEPOSIT TYPES *G.S. Plumlee, K.S. Smith, M.R. Montour, W.H. Ficklin, and E.L. Mosier*
- A MULTI-PHASED APPROACH TO PREDICT ACID PRODUCTION FROM PORPHYRY COPPER-GOLD WASTE ROCK IN AN ARID MONTANE ENVIRONMENT *L.H. Filipek, T.J. VanWyngharden, C.S.E. Papp, and J. Curry*
- THE HYDROGEOCHEMISTRY OF A NICKEL-MINE TAILINGS IMPOUNDMENT—COPPER CLIFF, ONTARIO *C.J. Coggans, D.W. Blowes, W.D. Robertson, and J.L. Jambor*
- SEASONAL VARIATION IN METAL CONCENTRATIONS IN A STREAM AFFECTED BY ACID MINE DRAINAGE, ST. KEVIN GULCH, COLORADO *B.A. Kimball*
- NATURAL ATTENUATIONS OF ACIDIC DRAINAGE FROM SULFIDIC TAILINGS AT A SITE IN WASHINGTON STATE *R.H. Lambeth*
- THE BEHAVIOR OF TRACE METALS IN WATER DURING NATURAL ACID SULFATE WEATHERING IN AN ALPINE WATERSHED *W.R. Miller, R.L. Bassett, J.B. McHugh, and W.H. Ficklin*
- CALCULATIONS OF GEOCHEMICAL BASELINES OF STREAM WATERS IN THE VICINITY OF SUMMITVILLE, COLORADO, BEFORE HISTORIC UNDERGROUND MINING AND PRIOR TO RECENT OPEN-PIT MINING *W.R. Miller and J.B. McHugh*
- A CASE STUDY ON THE AEROBIC AND ANAEROBIC REMOVAL OF MANGANESE BY WETLAND PROCESSES *L.A. Clayton, J.L. Bolis, T.R. Wildeman, and D.M. Updegraff*
- GEOCHEMICAL AND BIOGEOCHEMICAL CONTROLS ON ELEMENT MOBILITY IN AND AROUND URANIUM MILL TAILINGS *E.R. Landa*
- BIOOXIDATION PRETREATMENT OF REFRACTORY SULFIDIC AND SULFIDIC-CARBONACEOUS GOLD ORES AND CONCENTRATES *J.A. Brierley*
- DETERMINATION OF THE SOURCE AND PATHWAY OF CYANIDE-BEARING MINE WATER SEEPAGE *L.H. Filipek*
- USE OF LEAD ISOTOPES AS NATURAL TRACERS OF METAL CONTAMINATION—A CASE STUDY OF THE PENN MINE AND CAMANCHE RESERVOIR, CALIFORNIA *S.E. Church, C.N. Alpers, R.B. Vaughn, P.H. Briggs, and D.G. Slotton*

Editors

L.H. Filipek and G.S. Plumlee

SOCIETY OF ECONOMIC GEOLOGISTS, INC.

Society of Economic Geologists, Inc.

Reviews in Economic Geology, Vol. 6

The Environmental Geochemistry of Mineral Deposits
Part A: Processes, Techniques, and Health Issues
Part B: Case Studies and Research Topics

G.S. Plumlee and M.J. Logdson, Editors
J.M. Robertson, Series Editor

Additional copies of this publication can be obtained from

Society of Economic Geologists, Inc.
7811 Shaffer Parkway
Littleton, CO 80127
www.segweb.org

ISBN: 978-1-629495-64-4

Chapter 1

AN EARTH-SYSTEM SCIENCE TOOLKIT FOR ENVIRONMENTALLY FRIENDLY MINERAL RESOURCE DEVELOPMENT

G.S. Plumlee¹ and M.J. Logsdon²

¹*U.S. Geological Survey, Box 25046, MS 973, Federal Center, Denver, CO 80225-0046*

²*Geochimica, Inc., 206 North Signal, Suite M, Ojai, CA 93023*

INTRODUCTION

Environmental issues have become important, if not critical, factors in the success of proposed mining projects worldwide. In an ongoing and intense public debate about mining and its perceived environmental impacts, the mining industry points out that there are many examples of environmentally responsible mining currently being carried out (e.g., Todd and Struhsacker, 1997). The industry also emphasizes that the majority of mining-environmental problems facing society today are legacies from the past when environmental consequences of mining were poorly understood, not regulated, or viewed as secondary in importance to societal needs for the resources being extracted. On the other hand, environmental organizations (e.g., Mineral Policy Center, 1999) point to recent environmental problems, such as those stemming from open-pit gold mining at Summitville, Colorado, in the late 1980s (see Summitville summaries in Posey et al., 1995; Danielson and Alms, 1995; Williams, 1995; Plumlee, 1999), or those associated with a 1998 tailings dam collapse in Spain (van Geen and Chase, 1998), as an indication that environmental problems (whether accidental or resulting from inappropriate practices) can still occur in modern mining. Recent legislation imposing a moratorium on new mining in Wisconsin, and banning new mining in Montana using cyanide heap-leach extraction methods further underscore the seriousness of the debate and its implications for mineral resource extraction.

In this debate, one certainty exists: there will always be a need for mineral resources in developed and developing societies. Although recycling and substitution will help meet some of the world's resource needs, mining will always be relied upon to meet the remaining needs. The challenge will be to continue to improve the ways in which mining is done so as to minimize its environmental effects.

The earth, engineering, and life sciences (which we group here under the term "earth-system sciences," or ESS for short) provide an ample toolkit that can be drawn upon in the quest for environmentally friendly mineral resource development. The papers in this two-part volume provide many details on tools in the scientific toolkit, and how these tools can be used to better understand, anticipate, prevent, mitigate, and remediate the environmental effects of mining and mineral processing.

As with any toolkit, it is the professional's responsibility to choose the tool(s) best suited to a specific job. By describing the tools now available, we do not mean to imply that all of these tools need even be considered at any given site, nor that there are no other tools that may be useful. Rather, our intent is to provide a

brief overview of many of the tools in a growing toolkit and to illustrate ways in which they can be applied in all phases of environmentally-friendly mineral resource development, including exploration, mine planning and development, mitigation, and remediation.

OTHER SOURCES OF INFORMATION

There are a number of other excellent sources of general information on the environmental effects of mining, or that address specific aspects of environmental processes as they relate to mining.

Recent textbooks or overview books on mineral resources, mining, and their associated environmental issues include Kesler (1994), Holland and Petersen (1995), Ripley et al. (1996) and Hudson et al. (1999, in press). There are also many sources of information about the topic that reflect the perspective of the groups that publish the information. Da Rosa and Lyon (1997) present an overview of mining's environmental impacts from the perspective of an environmental advocacy organization, the Mineral Policy Center. The U.S. Environmental Protection Agency (U.S. EPA, 1997) recently published a CD-ROM about hardrock mining and related environmental issues from the perspective of an environmental regulatory agency. A multi-volume book set was also published by the Australia Environment Protection Agency (1997).

A large number of general information sources on mining-environmental issues have appeared on the internet in the last several years. These include, for example, web sites sponsored by government agencies (such as USGS MDIG, 1999; MEND, 1999), mining-environmental consultants (such as Enviromine, 1999), the mining industry (National Mining Association, 1999), and environmental groups (such as the Mineral Policy Center, 1999). Email discussion groups such as the Enviromine list server (accessible through the Enviromine web site) have also been established. These web sites, as well as several registries for environmental and earth science web sites (such as USGS Earth and Environment, 1999) provide many links to other sites that have earth science or environmental content. We have included in the reference list these and a number of other web sites that are current as of early 1999.

There are a number of journals and volumes available with papers that discuss the environmental aspects of mining from a geologic, geochemical, or ecological standpoint, including: the journals *Applied Geochemistry*, *Contaminant Hydrology*,

Environmental Geochemistry and Health, Environmental Geology, Environmental Science and Technology, Mine Water and the Environment, Journal of Geochemical Exploration, Journal of Hydrology, Science of the Environment, and Water Resources Research; and multi-paper conference proceedings or summary volumes such as Jambor and Blowes (1994), Alpers and Blowes (1994), Posey et al. (1995), and du Bray (1995).

TOOLS IN THE SCIENTIFIC TOOLKIT

A large number of techniques developed for earth-system science investigations are also directly applicable to mineral-environmental issues (Table 1.1), and include: geologic characterization studies (geologic mapping, mineralogic characterization, structural analysis); mineral deposit models and geoenvironmental models of mineral deposits; mineral resource, mineral-environmental, ecosystem, and abandoned mine lands assessments; geochemical characterization of waters, soils, sediments, plants, mine wastes, mineral processing wastes, and other media; other geochemical studies (laboratory simulation experiments, geochemical modeling, stable and radiogenic isotopes, age dating); geophysical characterization (including a variety of field methods such as resistivity, ground-penetrating radar, and seismic tomography surveys, and remote methods such as aeromagnetic and airborne electromagnetic surveys); remote sensing surveys; biological, toxicological, and ecological characterization and testing; and geospatial databases and geographic information systems (GIS) analysis of the data in the databases. Interdisciplinary studies that integrate these tools provide truly powerful insights into the environmental impacts of mineral deposits, mining, and mineral processing.

ESS information and tools can be used to help plan and implement all phases of environmentally friendly mineral resource development, from exploration through mine design, permitting, production, and closure, to environmental remediation of past mining and processing operations. In our following discussion of the ESS toolkit, we will progress through each of the phases of mineral-resource development and discuss the types of tools that are useful in each phase.

There are many spatial scales at which the ESS tools can be applied, and vary from: global-scale (such as global minerals information databases, and mineral-deposit or geoenvironmental-deposit models based on global deposit occurrences); to national-, regional-, or sub-regional-scale (such as regional geochemical or geophysical surveys and databases); to district- or deposit-scale (such as studies of the geology and mineral zoning within a mineral deposit or mining district, or studies of water quality within a district); to mine- or site-scale (e.g., studies of mineral zoning in a mine); to mine-working-scale (such as seasonal studies of water compositions draining a particular adit); down to hand sample- and microscopic-scale (e.g., mineralogical characterization of ore and gangue minerals, or characterization of colloids or suspended particulates that sorb metals in mine-drainage streams). In Table 1.1, we have listed the ESS tools in a very general order of increasing spatial detail at which they can suitably be applied; however, many of the tools can each be applied at a variety of spatial scales.

Many of the ESS tools can be applied at a variety of temporal scales as well. For example, regional geophysical or geochemical surveys may be sufficiently complex and costly that they cannot be repeated on a regular basis; however, some regional geochemical surveys may be worth repeating after an extended period of

time to measure long-term shifts in the geochemical landscape. On the other hand, more local studies such as water quality studies may need to be carried out on a regular basis (such as hourly, weekly, or monthly) to address short-term variations that result from diurnal, event-driven (such as a storm-related), or seasonal processes.

A watershed basis for environmentally friendly mineral resource development

In recent years, there has been a general recognition on the part of both scientists and regulators that the watershed (the area drained by a river or stream) is a fundamental basis for characterizing and understanding many of the environmental effects of mineral deposits, mining, and mineral processing. Watershed boundaries are natural hydrologic barriers that limit the flows of surface waters and most ground waters to within the watershed. The environmental effects of mineral deposits on a watershed are strongly influenced by the compositions of the watershed ground waters, surface waters, and sediments derived from the rocks within the watershed, which are in turn a function of the climate, geology, and ecology of the watershed. The major exceptions to this are particulates or gases transported by wind between watersheds (such as smelter emissions or windblown dust from mine waste or tailings piles), or ground water that, due to regional topographic gradients or the presence of conductive geologic structures, flows between watersheds (e.g., Winter et al., 1998). In our discussion, we will highlight how mineral-environmental characterization, prediction, mitigation, and remediation are generally best carried out within a watershed context.

DATABASES AND GIS ANALYSIS

Increasingly, mineral-resource and mineral-environmental decisions are being made on the basis of earth-system science data. Many of these data are being compiled in vast digital databases and interpreted using GIS analysis. The coverages of databases range in scale from global (for example, data on the global occurrences of mineral deposits) to microscopic (for example, data on microscopic variations in composition of a single mineral from a mineral deposit).

The sheer number and size of databases available for interpretation present formidable challenges in how to organize and interpret multiple data sets that are relevant to a particular problem. Increasingly, geospatial data (those that vary according to geographic location) are being interpreted digitally using GIS analysis. GIS analysis provides a means for integrating and interpreting diverse geospatial datasets (or layers) such as land-use, population, topography, climate, ecosystem, geology, geochemistry, mining, remote sensing, and many others. It allows the user to understand and quantify complex relationships between the data layers that are not readily apparent when examined separately. The theory of GIS analysis, as well as its applications to earth science issues, are summarized by Bonham-Carter (1994). Both databases and the GIS engines used to interpret the databases are becoming more and more available on the Internet; we have provided in the references the Internet addresses for examples of such databases and GIS engines.

TABLE 1.1—Scientific tools that are useful for successful mining-environmental prediction, mitigation, and remediation. For most of the tools, we have included one or more general references, as well as one or more references that illustrate application of the tool in a topical study. References from this two-volume set are indicated in italicized text. Other useful references are shown in plain text.

Tool	References	Use
Geographic Information Systems (GIS) Analysis	Bonham-Carter (1994); Lee (1999 in press); Lee et al. (1999b in press)	Very useful for integrating large amounts of geospatial data and interpreting spatial relationships between diverse data types.
Earth science databases, maps, and GIS coverages		
• Minerals information	USGS Minerals Information (1998); Natural Resources Canada (1999)	• Data on consumption, production, uses, and recycling of a number of mineral commodities are regularly compiled globally, nationally, and regionally.
• Mine site and production data (e.g., USGS MAS/MILS)	Babitzke et al. (1982); Berg and Carillo (1980); Ferderer (1996); McCartan et al. (1998); USGS Mineral Data Bases (1999 in press)	• Indicate the locations, commodities, amounts of production, and other information for present and past mining or processing sites.
• Mineral exploration databases	Wilburn (1998)	• Provide information on exploration activities on a yearly basis, including the location and commodities sought.
• Significant deposit databases	Bookstrom et al. (1996)	• Provide geologic, production, and commodity information on the major producing mineral deposits or mineral districts in a region.
• Deposit geology, mineralogy databases	USGS Mineral Data Bases (1999 in press)	• Document geologic and mineralogic information at mine sites, prospects.
• Regional geochemistry surveys, databases (“landscape geochemistry”)	Smith (1997); <i>Smith and Huyck (1999)</i>	• Determine regional variations in the geochemical composition of rocks, sediments, plants.
• Regional geophysics databases	Saltus and Simmons (1997); McCafferty et al. (1998)	• Mapping regional variations in rock magnetic, density, and radiometric properties provides important insights into regional variations in rock compositions and crustal structures.
• Regional geology maps, databases	Schruben et al. (1998)	• Geologic maps show the spatial distribution of rock units as differentiated by age, rock type, as well as major structures such as faults.
• Regional lithology maps, databases	Raines et al. (1996)	• Lithologic maps show the spatial distribution of rock units as differentiated by their geologic properties (e.g., rock type, hydrologic characteristics, acid-neutralizing capacity, etc.).
• National or regional seismic hazards maps, databases	USGS Earthquake Hazards (1999)	• Provide information on the risk for potential future earthquakes in a region, based on the frequency and magnitude of past earthquakes in that region.
• National or regional landslide hazards maps, databases	USGS Landslide Hazards (1999)	• Provide information on the potential hazards for landslides, based on the distribution of rock units that are geologically prone to generate landslides.
Climate/hydrologic databases, maps, GIS coverages		
• Climate	NOAA (1999)	• Climate plays an important role in influencing the environmental effects of mining and mineral deposits.
• Precipitation, evapotranspiration temperature	NOAA (1999); Shevenell (1996)	• Influence the amounts and types of vegetation, and the amounts of surface-water runoff versus ground-water recharge, etc.
• Watershed boundaries	USGS (1982)	• Watersheds are a fundamental basis for understanding the geologic, climatic, and environmental controls on surface- and ground-water flow and quality. • The scale of a watershed boundary can vary from local (e.g., of a short stream) to continental (e.g., of a major river).
• Water discharge, quality	USGS Water Data (1999); U.S. EPA STORET (1999)	• Flow volumes of surface waters and chemical compositions of surface and ground waters as a function of time and space are key to understanding the potential downstream effects of mineral deposits, mining, and mineral processing.
• Water use	USGS Water Data (1999); Solley et al. (1998)	• Provide insights into existing water use patterns and availability in areas where mineral resource development has occurred or may occur. Water availability may be an important consideration in resource development in some arid areas.
Ecoregion databases, maps, GIS coverages	Bailey (1995)	Ecoregions provide a means for interpreting the environmental effects of mineral deposits, mining, and mineral processing in a biological context. The spatial distribution and biological characteristics of ecosystems are strongly influenced by climate, topography, and geology.

TABLE 1.1—Continued

Tool	References	Use
Geologic and geoenvironmental models of mineral deposits and rock units		Mineral deposits can be typed according to similarities in their geology, size, and grade, as well as their environmental signatures. Rock units with similar lithologic characteristics commonly have similar environmental geology and geochemistry characteristics.
• Geologic mineral deposit models	<i>Plumlee (1999)</i> ; du Bray (1995); Guilbert and Park (1986); Cox and Singer (1986); Kirkham et al. (1993)	<ul style="list-style-type: none"> • Mineral deposit models summarize the key geologic, grade, and size characteristics of geologically similar mineral deposits of a given type. They also summarize key geologic and geochemical processes by which the deposits form. • Are widely used in mineral exploration; can also provide important insights into possible environmental issues such as the size of disturbance, and geologically associated deposit types.
• Geoenvironmental models of mineral deposits	<i>Plumlee (1999)</i> ; Wanty et al. (1999 in press); du Bray (1995)	<ul style="list-style-type: none"> • Geoenvironmental mineral deposit models summarize the key geologic, size, and grade characteristics of geologically similar deposits that influence environmental signatures and impacts of the deposits. • Also present empirical data on environmental signatures and impacts of mineral deposits mined by various methods in different climates.
• Geoenvironmental models of rock units	<i>Plumlee (1999)</i> ; <i>Smith and Huyck (1999)</i> ; <i>Miller and McHugh (1999)</i>	<ul style="list-style-type: none"> • For similar rock types, summarize important environmental geology characteristics (mineralogy, physical strength, manner in which the rocks fracture) geochemical characteristics (the content and geoavailability of trace elements, acid-buffering or acid-generating minerals, reactivity during weathering), and environmental signatures in different climates (such as pH, alkalinity, and major and trace-element contents of drainage waters).
Mineral-resource, mineral environmental, and geologic ecosystem assessments		
• Mineral resource assessments	Van Loenen and Gibbons (1997); USGS and Servicio Geológico de Bolivia (1992); Light et al. (1997)	<ul style="list-style-type: none"> • Compile and interpret information on the geology and mineral deposits in a nation or region, with the purpose of estimating the number of undiscovered mineral deposits of different types present.
• Mineral environmental assessments	<i>Plumlee (1999)</i> ; Plumlee et al. (1995c); Lee et al. (1999b in press); Price et al. (1995)	<ul style="list-style-type: none"> • Compile and interpret information on the past, current, and potential future environmental effects of mineral deposits, mining, and mineral processing within a region or area.
• Geologic ecosystem assessments	Frost et al. (1996); Raines et al. (1996); Bookstrom et al. (1996)	<ul style="list-style-type: none"> • Geology-based assessments interpret the links between geologic features and ecosystem characteristics in a region.
Abandoned mine lands assessments	Nimick and von Guerard (1998); Price et al. (1995); Pioneer Technical Services (1994)	Government agencies have recently begun assessing the extent of environmental problems caused by abandoned mine sites. These assessments, where available, provide valuable information on environmental issues in historic mining districts.
Geologic characterization		
• Geologic mapping (regional-, watershed-, district-, mine-, and ore body-scale)	<i>Plumlee (1999)</i> ; Guilbert and Park (1986); Peters (1987)	<ul style="list-style-type: none"> • Essential for understanding the distribution of rock types, geologic and mineralogic zones, wallrock alteration zones, faults, and other structures that are present at a site or in the surrounding watersheds.
• Mineralogic characterization	<i>Smith and Huyck (1999)</i> ; <i>Plumlee (1999)</i> ; <i>Nordstrom and Alpers (1999)</i>	<ul style="list-style-type: none"> • A knowledge of the minerals and mineral textures, reactivities, and trace element contents of mineral deposits, rocks, soils, and sediments is key to understanding the metals, their geologic form, and hence their geoavailability and bioavailability at a site.
• Structural analysis	NRC (1996); Ramsay and Huber (1987); <i>Plumlee (1999)</i>	<ul style="list-style-type: none"> • The distribution, origin, and degree of openness of fractures, faults, and joints is an important control on ground-water flow through a site.
Remote sensing studies	Swayze et al. (1996); King (1995); Lee et al. (1999a in press); Lillesand and Kiefer (1987); Clark and Roush (1984)	Images gathered by satellite- or airborne systems can be used to map regional to local variations in a variety of parameters such as mineral types and compositions or plant types and health, and therefore to interpret the distribution of environmental features such as potentially acid-generating rocks or mine dumps.
Environmental geophysics studies	Campbell et al. (1999 in press); NRC (1996); Custis (1994); Ackman and Cohen (1994)	Can provide extremely useful information on the geologic and hydrologic character of the subsurface, as well as on the migration of contaminants and ground water through the subsurface. Also aid in the remote (e.g., non-invasive) environmental characterization of mine waste piles (such as determining the amounts of sulfides present in mine wastes, or whether a waste pile is saturated with water.

TABLE 1.1—Continued

Tool	References	Use
• High resolution airborne magnetic surveys	Grauch and Millegan (1998)	• New technology permits close flight line spacings that provide detailed information on spatial variations in the magnetic properties of rocks, such as differences in rock types or locations of fractures. These have been successfully used, for example, to map fractures in magnetic alluvial sediments, volcanics, and crystalline rocks.
• High resolution airborne electromagnetic surveys	Fitterman (1990); Garney (1996)	• Useful for identifying the 3-dimensional subsurface distribution of electrically conductive rock units (such as clay units or water-saturated aquifers) or mineralized ground waters.
• Ground penetrating radar cross-hole seismic tomography	NRC (1996); Tura et al. (1992)	• Used to characterize the distribution of fractures in the subsurface.
• Induced polarization, electromagnetic sounding studies	Campbell et al. (1999); NRC (1996)	• Characterize the conductivity of rocks in the subsurface. Can be used to help identify the sulfide content of mine dumps, as well as the location of water-saturated zones within the mine dumps.
Hydrologic characterization	Domenico and Schwartz (1990); Freeze and Cherry (1979)	Essential to understanding surface- and ground-water flow through a mining or processing site and its surrounding watershed
• Water balance (precipitation vs. evapotranspiration)	Shevenell (1996)	• The amount of precipitation relative to evapotranspiration is an important control on the vegetation and amount of surface-water runoff and ground-water recharge in a watershed or at a site.
• Surface-water discharge	Rantz et al. (1982); <i>Ficklin and Mosier (1999)</i>	• Measuring temporal variations in flow from springs and streams at a site and in the watershed surrounding a site is crucial to understand the relative effects of water discharges (such as acid-drainage, etc.) from a mine site.
• Borehole geophysics	Paillet (1993); Paillet et al. (1987); NRC (1996)	• Acoustic televiewers provide information on the orientation of fractures in a drill hole that may transmit ground water. • Heat pulse flow meters test which of the fractures in a drill hole are hydrologically conductive.
• Hydraulic testing (single hole and multiple hole)	Domenico and Schwartz (1990)	• Provides information on rates of ground-water recharge and flow around a well or set of wells.
• Tracer studies	Domenico and Schwartz (1990); Kimball (1996); NRC (1996); Kimball et al. (1994); <i>Kimball (1999)</i>	• Injection of dyes or chemical tracers into wells, mines, streams, provides insights into ground-water residence times, interactions between ground and surface waters, and amounts of mixing with tributary waters downstream.
Water quality measurements		Water-quality measurements form the basis of any environmental study where water quality is an issue. Proper sampling and analytical procedures are crucial, as is collection of the different sample types necessary to adequately characterize the dissolved, colloidal, and suspended particulate compositions of waters.
• Waters with low trace metals	Horowitz et al. (1994); <i>Ficklin and Mosier (1999)</i> ; <i>Crock et al. (1999)</i>	• Rigorous field analysis and sampling procedures are needed for waters with low trace metal contents, in order to minimize contamination during sampling that could generate significant errors in results and interpretations.
• Waters with high trace metals	<i>Ficklin and Mosier (1999)</i> ; <i>Crock et al. (1999)</i>	• Simpler sampling procedures can be used for rapid evaluation of sites where acid mine waters or other metalliferous waters are present.
• Surface-water sampling	Edwards and Glysson (1988); Horowitz et al. (1990); von Guerard and Ortiz (1995); Kimball (1996); Kimball et al. (1994)	• Care must be taken to collect a representative sample from a surface stream that may be quite variable compositionally across its width-depth cross section. Point sampling from the stream bank may likely not be as accurate as integrated cross-section sampling.
• Ground-water sampling	<i>Ranville and Schmiernund (1999)</i> , Domenico and Schwartz (1990); Alley (1993a)	• Sampling of waters from wells requires specialized well development and sampling procedures to assure collection of representative samples (for example, to minimize mobilization of solids from around the wells) and to minimize chemical changes in the sample (such as oxygenation of reduced waters) during collection.
Geochemical analyses of rocks, soils, plants, organisms		The geochemical compositions of rocks, soils, sediments, plants and tissues can provide significant insights into the earth materials that are sources or sinks for potentially toxic elements, how readily the elements are mobilized into the environment, and how readily the elements are taken up by plants and organisms.

TABLE 1.1—Continued

Tool	References	Use
<ul style="list-style-type: none"> • Rocks, soils, earth materials, mining and mineral processing wastes 	<i>Crock et al (1999); Plumlee (1999); Smith and Huyck (1999)</i>	<ul style="list-style-type: none"> • Total geochemical analyses measure the concentrations of major and trace elements in solid samples, but provide no indication of how mobile the elements are. • Geochemical analyses of solids can be coupled with mineralogical characterization to fully understand the mineralogic residences of potentially toxic elements.
<ul style="list-style-type: none"> • Sequential chemical extractions of solid samples 	<i>Crock et al. (1999); Leinz et al. (1999)</i>	<ul style="list-style-type: none"> • Measure the concentrations of metals tied up in each of progressively less reactive solid phases. • Provide significant insights into the mineralogic residences and potential geoavailability (<i>Smith and Huyck, 1999</i>) and bioavailability of metals from the solids.
<ul style="list-style-type: none"> • Plants and organisms 	<i>Crock et al. (1999); Dwyer et al. (1988); Moore et al. (1991); Gray et al. (1996)</i>	<ul style="list-style-type: none"> • Chemical analyses of metals in tissues provide important information on how metals are taken up from the environment by plants and organisms; are often useful to evaluate metals in plants and organisms at progressively higher levels in food chains.
Paleontological analyses of sediments	<i>Brouwers et al. (1996); Dallinger and Rainbow (1993); Mezquita et al. (1997)</i>	Remains of organisms (including frog and fish bones, tests of microorganisms) in sediments preserve a stratigraphic record of past water quality in a lake, stream, or river.
Geostatistical and other numerical analyses of geochemical data		Important tools in the interpretation of geochemical data sets
<ul style="list-style-type: none"> • Factor analysis 	<i>Plumlee (1999); Davis (1973); Johnston (1980); Alley (1993a)</i>	<ul style="list-style-type: none"> • Very useful for discriminating different trace-element populations in geochemical data sets (such as natural versus smelter-related element signatures in soils developed on mineralized rocks).
<ul style="list-style-type: none"> • Kriging 	<i>Davis (1973); Johnston (1980); Peters (1987); Alley (1993a, b)</i>	<ul style="list-style-type: none"> • Technique commonly used to estimate ore grades in large blocks of rocks based on the grades of small samples in drill holes. Can also be used to estimate amounts of acid-generating sulfides or acid-consuming carbonates in large volumes of potential waste rocks based on smaller-volume core samples.
Stable isotope studies		Stable isotopes are useful for tracking sources of waters and contaminants, and for understanding geochemical processes that modify the waters or contaminants.
<ul style="list-style-type: none"> • Hydrogen and oxygen isotopic compositions of waters, minerals 	<i>Ingraham and Taylor (1991); Coplen (1993); Clark and Fritz (1997); Hamlin and Alpers (1996); Rye and Alpers (1997)</i>	<ul style="list-style-type: none"> • Track sources of ground and surface waters (snowmelt vs. rainfall), and processes (such as evaporation and water-rock interactions) that have affected the waters. Isotopic compositions of minerals indicate processes by which the minerals may have formed, or the sources of waters from which some minerals formed.
<ul style="list-style-type: none"> • Sulfur isotopic compositions of aqueous sulfate/sulfide, sulfide/sulfate minerals 	<i>Taylor and Wheeler (1994); Ohmoto and Rye (1979)</i>	<ul style="list-style-type: none"> • Track sources of aqueous sulfur species (e.g., sulfide oxidation vs. dissolution of sulfate minerals) and processes (such as bacterial sulfate reduction) that have affected the sulfur species.
<ul style="list-style-type: none"> • Oxygen isotopic compositions of aqueous sulfate and sulfate minerals 	<i>Taylor and Wheeler (1994)</i>	<ul style="list-style-type: none"> • Identify sources of sulfate, biological processes that have affected the sulfate, and relative roles of atmospheric oxygen versus ferric iron in sulfide oxidation and acid-mine drainage formation.
<ul style="list-style-type: none"> • Carbon and/or nitrogen isotopic composition of carbonates, nitrates, and cyanide 	<i>Ohmoto and Rye (1979); Johnson et al. (1998)</i>	<ul style="list-style-type: none"> • Identify sources of aqueous carbonate (atmospheric CO₂, soil CO₂, organic contaminants, dissolution of carbonate minerals) or aqueous nitrate (fertilizers, explosives, cyanide degradation), and processes that have affected aqueous cyanide (bacterial degradation, volatilization, etc.; <i>Smith and Mudder, 1999</i>)
Radiogenic isotope studies		Isotopes of elements that result from the radioactive decay of other elements (for example ²³⁸ U decays to ²⁰⁶ Pb) are useful for tracking sources of metals, rocks, and soils.
<ul style="list-style-type: none"> • Lead isotopes 	<i>Church et al. (1999); Östlund et al. (1995); Gulson et al. (1996); Faure (1986)</i>	<ul style="list-style-type: none"> • Track sources of lead in ores, rocks, soils, waters, organisms. For example, can help determine the proportions of lead in an environmental sample derived from the weathering of sulfides, local rocks, smelter emissions, leaded gasoline, paint or other sources.
<ul style="list-style-type: none"> • Strontium isotopes. 	<i>Faure (1986)</i>	<ul style="list-style-type: none"> • Useful for tracing source rocks of soil or sediment materials, or for identifying rocks with which waters have interacted.
Age dating of earth materials and waters		Very useful for establishing historical record of natural and anthropogenic contamination, and therefore for helping to establish pre-mining background and baseline conditions.

TABLE 1.1—Continued

Tool	References	Use
• ^{210}Pb , ^{137}Cs dating of sediments	Robbins (1978); Ritchie and McHenry (1984); Van Metre et al. (1997)	• Provide a means for dating recent sediments, such as overbank or lake sediments. Have been successfully used to track temporal changes in sediment metal concentrations that result from metal influx due to historic mining activities.
• $^{39}\text{Ar}/^{40}\text{Ar}$ dating; K/Ar dating	Dalrymple et al. (1995); Vasconcelos et al. (1994)	• Used to date the ages of potassium-bearing rocks, wallrock alteration, mineral deposits, and secondary minerals.
• Dating of ground waters (e.g., tritium, ^{14}C , ^{36}Cl , ^{85}Kr , chlorofluorocarbons)	Plummer et al., (1993); Coplen (1993); Fontes (1980); Mook (1980); Kimball (1984); Bentley et al. (1986)	• A variety of methods are used to date ground waters, each with its own range of applicability and limitations.
• ^{14}C dating of organic material	Faure (1986)	• Useful to date organic matter in soils and sediments.
Laboratory-based geochemical prediction experiments	Morin and Hutt (1997)	Useful for modeling and anticipating geochemical conditions that may result from a variety of environmental processes. It is challenging to design experimental procedures that adequately replicate the natural geochemical and physical conditions and rates that control the processes being modeled, and to use samples that adequately represent the range of rocks, minerals, and waters that will actually be present at a mine site.
• Static mine-waste tests (acid-base accounting, net acid production, consumption)	<i>White et al. (1999)</i> White et al. (1997); Morin and Hutt (1997)	• Predict the net acid-generating or acid-consuming potential of mine waste samples, based on chemical analyses of the sulfide and carbonate contents of the samples. • It is difficult to ensure that the samples used are representative of the actual range in mineralogic and geologic characteristics of the mine wastes. • Results are optimized when coupled with detailed mineralogic characterization of the sample to determine which minerals are generating or consuming acid.
• Kinetic mine-waste tests —Humidity cell tests	<i>White et al. (1999)</i> ; White and Jeffers (1994); ASTM (1996); Morin and Hutt (1997)	—Humidity cells react samples of mine wastes with humid air to simulate and predict the compositions of mine-drainage waters that may form from weathering of the wastes. —The same rate, scale, sampling, and characterization challenges exist as with static tests. Many tests are run for multiple weeks to months
—Column, tank tests	<i>Filipek et al. (1999)</i> ; Logsdon and Basse (1991)	—Test the attenuation capacity of metals or other contaminants by soils or rocks, the leaching efficiency of metals from ores by heap leach solutions, or the generation of acid and metals from mine wastes. —Tests should be done in conjunction with mineralogical characterization of the solids.
• Leach tests	Montour et al. (1998a, b); U.S. EPA (1986–1995); U.S. EPA (1995)	• Used to simulate and predict the mobility of metals from mine wastes, smelter slag, soils, or tailings solids as a result of reactions with rain or ground waters. • Several different techniques use different leach solution compositions, amounts of grinding of samples prior to leaching, and amounts of agitation during leaching. • Different techniques can produce significantly different results. • Tests should be done in conjunction with mineralogical characterization of the solids.
—EPA 1311 (TCLP)	U.S. EPA (1986–1995); U.S. EPA (1995); Montour et al. (1998a, b)	—Extracts metals from <1 cm solids using acetic acid extraction fluid and extensive agitation. —Acetic acid extraction fluids (designed to simulate municipal-industrial landfill waste fluids) over-solubilize Pb from mine wastes, due to efficient extraction by Pb-acetate complexes.
—U.S. EPA 1312 (SPLP)	U.S. EPA (1986–1995)	—Designed to extract metals from <1 cm solids using a slightly acidic synthetic rainfall extraction fluid and extensive agitation.
—USGS modified 1312	Montour et al. (1998a, b)	—Similar to 1312, but uses much less agitation.
—USGS field rainfall experiment	Montour et al. (1998a)	—Sample of mine wastes leached by rainfall passing directly through sample during rainstorm.

TABLE 1.1—Continued

Tool	References	Use
• Water mixing tests	<i>Plumlee (1999); Plumlee et al. (1995a)</i>	<ul style="list-style-type: none"> • Can be used to help simulate potential geochemical impacts of mine waters or mineral processing waters on water quality in the surrounding watershed. • Due to the difficulty in reproducing the actual watershed conditions, these tests should be used as only a guide to the potential impacts of a water on a watershed.
Geochemical and hydrologic modeling (computer driven)	<i>Alpers and Nordstrom (1999); Smith (1999); Appel and Reilly (1994); Domenico and Schwartz (1990)</i>	Very useful ways to simulate and interpret geochemical and hydrologic processes at a site or in a watershed or basin, when used with the proper recognition of appropriate constraints and limitations. Most useful when constrained by: detailed chemical and physical analyses of water samples (temperature, pH, redox, dissolved and suspended concentrations of major and trace elements), and hydrologic data (aquifer tests, tracer studies, recharge/discharge rates, etc.)
• Inverse (mass balance) geochemical modeling	<i>Alpers and Nordstrom (1999)</i>	<ul style="list-style-type: none"> • Useful for interpreting the possible amounts of minerals precipitated, gases given off, etc., that produced the change in chemical composition between water samples along a flow path. Also used to test hypotheses regarding mixing of water types.
• Forward (reaction-path) geochemical modeling	<i>Alpers and Nordstrom (1999); Smith (1999); Cogans et al. (1999)</i>	<ul style="list-style-type: none"> • Useful to anticipate changes in water composition that will result from environmental processes such as sulfide oxidation, fluid mixing, water-rock reactions, etc.
• Hydrologic modeling	<i>Mercer and Faust (1981); Huyakorn and Pinder (1983); Appel and Reilly (1994); Folger et al. (1997); NRC (1996)</i>	<ul style="list-style-type: none"> • Used to simulate flow of ground waters in subsurface. Most useful when constrained by field hydrologic data on recharge/discharge rates, aquifer testing results, etc. Methods to model flow through porous media (e.g., sandstone aquifers) are well established; fracture-flow modeling capabilities are still evolving.
• Coupled geochemical and hydrologic modeling	<i>Alpers and Nordstrom (1999)</i>	<ul style="list-style-type: none"> • Couple forward chemical modeling with hydrologic flow modeling to simulate fluid chemistry evolution along flow paths.
Limnology	<i>Cole (1994); Wetzel (1983)</i>	A good understanding of the hydrologic and geochemical characteristics of lakes is key to anticipating and understanding the development and evolution of open-pit lakes.
Biological Characterization		Provides needed information on the impacts of mineral deposits, mining, and mineral processing on humans, other organisms, and plants.
• Microbial characterization	<i>Mills (1999); Brierley (1999); Nordstrom and Alpers (1999); Smith and Mudder (1999); Schrenk et al. (1998); Chapelle et al. (1993)</i>	<ul style="list-style-type: none"> • Evaluate the types and contributions of microorganisms that contribute to environmental processes such as the formation of acid-mine drainage, or the degradation of cyanide. Also evaluate the impacts of metals on microbial communities.
• Aquatic ecology characterization	<i>Moore et al. (1991); Dwyer et al. (1988); Kelly (1999)</i>	<ul style="list-style-type: none"> • Integrate data on aquatic organism populations (including fish and benthic invertebrates) and metal contents of organisms with data on water quality and stream sediment compositions.
• Aquatic toxicology tests	<i>Kelly (1999); Gray and O'Neill (1997); Moore et al. (1991)</i>	<ul style="list-style-type: none"> • Laboratory experiments that test the effects of acid waters and other contaminated waters on the health of aquatic organisms and insects living near water.
• Human health studies	<i>Smith and Huyck (1999); Krieger et al. (1999); Ross (1999)</i>	<ul style="list-style-type: none"> • Examine the effects of metals and minerals on human health.
Examples of process-oriented earth-system science studies		
• Watershed characterization studies	<i>Miller and McHugh (1999); Miller et al. (1999); Church et al. (1999); Kimball (1999); Lambeth (1999); Posey et al. (1995); Church et al. (1993, 1997); Nimick and Von Guerard (1998)</i>	<ul style="list-style-type: none"> • Utilize many of the tools listed above to characterize the geologic, geochemical, hydrologic, and ecological properties of watersheds.
• Wetlands studies	<i>Walton-Day (1999); Clayton et al. (1999); Wildeman and Updegraf (1997)</i>	<ul style="list-style-type: none"> • Characterize the geochemical and biogeochemical processes in wetlands, which are a common treatment for acid-mine drainage.
• Cyanide geochemistry, degradation	<i>Smith and Mudder (1999); Filipek (1999); Johnson et al. (1998); Mudder (1999 in press)</i>	<ul style="list-style-type: none"> • Characterize the processes that degrade cyanide in the environment.
• Element mobility overviews	<i>Smith and Huyck (1999); Nordstrom (1999); Wanty et al. (1999)</i>	<ul style="list-style-type: none"> • Chapters in this volume covering the geochemical and biogeochemical processes that control element mobility in the environment.

MINERAL EXPLORATION

Mineral exploration decisions are driven by a complex combination of economic, political, and geologic factors. As environmental mitigation expenses continue to increase in importance to the economic bottom line of proposed mining ventures, environmental considerations will be increasingly factored into all stages of mineral exploration projects, including the planning on where to explore, collection of environmentally pertinent data during regional exploration, and characterization of specific exploration prospects. Although the focus of this section is geared toward mineral exploration, the same information and techniques may also be applied to a variety of issues such as identification and remediation of abandoned mine sites, and understanding the potential environmental effects of past, present, and future mineral resource development in a regional or national context.

Exploration planning

Exploration companies have traditionally used minerals information (e.g., USGS Mineral Resources Program, 1999; USGS Minerals Information, 1999; Natural Resources Canada, 1999) on the current and anticipated future global uses, production, recycling, and substitution of various mineral commodities to determine the commodities upon which they focus their exploration efforts. Mineral production databases and maps (e.g., USGS Mineral Resources Program, 1999; USGS Mineral Data Bases, 1999 in press; McCartan et al., 1998) compile data on the size, mining/processing type, and commodities produced by past and current producing mines and mineral processing facilities, and provide insights into the global or national distribution of commodity production.

Exploration geologists have traditionally guided their exploration efforts with mineral deposit models, which summarize the key geologic features, processes of formation, and grade-tonnage relationships of mineral deposit types (a deposit type is a group of geologically similar mineral deposits). Deposit types form within characteristic geologic and tectonic settings; as a result, exploration for deposits of a particular type focuses on geologically and tectonically favorable portions of the world, as elucidated by global geologic and tectonic maps and map databases, and mineral deposit databases (USGS Mineral Data Bases, 1999 in press). Political considerations (such as long-term political stability), economic considerations (such as favorable economic incentives, availability of transportation and other infrastructure, distance from markets, etc.), and, increasingly, environmental considerations (e.g., the length and complexity of the environmental permitting process) also factor in the decision of where in the world to explore.

Tools in the ESS toolkit can facilitate incorporation of environmental considerations into the earliest phases of mineral exploration planning. For example, geoenvironmental models of mineral deposit types (du Bray, 1995; Plumlee, 1999; Wanty et al., 1999 in press) provide an indication of the potential environmental effects that may need to be mitigated or prevented should a deposit be developed. These models could therefore help exploration companies decide not to explore for particular types of deposits that are geologically disposed for environmental problems requiring high environmental mitigation expenses (such as pyrite-rich, carbonate-poor deposits that are likely prone to

extreme acid-rock drainage problems). Or, the models could help focus exploration on deposit types with low environmental mitigation expenses, such as deposits with low pyrite contents and high carbonate contents that are not prone to acid drainage. Alternatively, the models may help focus exploration geographically in particular climates. For example, deposit types likely to be acid-generating may be more easily developed with lower environmental mitigation expenses in dry climates rather than wet climates. Or, exploration for acid-generating deposit types in wetter climates could be focused on higher-grade, lower-tonnage deposit types; the higher grades could help offset the increased acid-drainage treatment expenses and the lower volumes of wastes produced could help reduce acid-drainage generation.

The geoenvironmental mineral deposit models at present do not compile empirical data on actual environmental mitigation expenses paid by producing mines. Such a compilation for different deposit types in different climates could be very useful in both an exploration and mine planning context, as it would allow a more complete economic analysis of potential expenses (including environmental mitigation expenses) and returns for particular deposit types.

Environmental considerations in regional exploration

Environmental data collection and interpretation should be an integral part of any mineral exploration program. Many of the same earth science data used for the purpose of discovering mineral deposits can also be interpreted in an environmental context; the data and interpretations can thus provide advantageous and timely environmental information for the mine planning and permitting process, should the exploration program result in the discovery of an economic mineral deposit and development of a mine. Even if the exploration program is unsuccessful in a particular region, the compilation of environmental information for that region during exploration can contribute greatly to the general knowledge of environmental conditions developed on mineral deposits or mineralized rocks in particular climates.

For example, regional geologic maps are used by exploration geologists to focus on areas within regions that are geologically favorable for the occurrence of particular mineral deposit types. These maps (when interpreted in a lithologic or rock characteristic context; Raines et al., 1996) can also provide geologists with important insights into the regional distribution of rock units that may have particular beneficial or detrimental environmental geology characteristics, such as the potential to consume acid in acid-rock drainage or the potential to themselves produce acid-rock drainage. Similarly, regional geologic maps identify regional-scale faults or fractures that may control ground-water flow through a mine or mineral deposit, or that may be structurally indicative of other related smaller-scale fractures that control ground-water movement.

Regional geochemistry surveys measure spatial variations in the major- and trace-element compositions of rock, soil, sediment, and plant samples collected over a region (Rose et al., 1979; Smith, 1997; Plumlee, 1999); they are used in mineral exploration to help locate and delineate geologic sources (such as economic mineral deposits) for anomalous trace metals in the samples. Existing national or regional geochemistry databases, such as the USGS National Geochemical Database (Smith, 1997; USGS Mineral Resources Program, 1999) are useful in regions where

data coverage is adequate; however, many exploration programs carry out new geochemical surveys in regions of interest. These same geochemical data also can be used to establish regional variations in environmental/geochemical background conditions (those that exist prior to mining or other human activities in pristine areas) and baseline conditions (those that exist at the time of sampling prior to some anticipated change such as mining). Such baseline and background information will be crucial to document the pre-mining environmental geochemistry "landscape" (Smith and Huyck, 1999) in a region if an economic mineral deposit is discovered and developed into a mine. Whenever possible, splits of samples collected as part of a regional exploration geochemistry survey should be saved if there is a high likelihood of mine development in a region, both to provide material for reanalysis and verification of the survey results, as well as for other environmentally oriented analyses that would be helpful for the mine planning and permitting process (such as sequential chemical extractions to determine potential metal mobility from the samples; Crock et al., 1999).

Regional hydrogeochemistry surveys and water quality databases measure spatial variations in the composition (pH, conductivity, dissolved oxygen, concentrations of major and trace elements) of surface waters and ground waters throughout a region (Miller et al., 1982; Smith, 1997; Ficklin and Mosier, 1999; USGS Water Data, 1999). Exploration geologists have successfully used these surveys in a variety of climates to help locate and delineate the extent of mineral deposits that are releasing metals and other constituents into ground and surface waters. Although hydrogeochemical surveys carried out as part of mineral exploration programs are typically not implemented with sufficiently rigorous sampling, chain-of-custody, and analytical protocols (Ficklin and Mosier, 1999; Crock et al., 1999) to satisfy environmental permitting and regulatory requirements, they do provide excellent information on regional background and (or) baseline water quality that is present in a region prior to any mining that may result from the exploration.

Geostatistical analyses (such as factor analysis) of regional geochemistry data sets (see example in Plumlee, 1999) can help discriminate different geologic and (or) anthropogenic sources that contributed to the overall chemical composition of sediment, soil, plant, or water samples. Factor analysis can also indicate the relative contributions of different sources to the overall chemical makeup of each of the samples in a regional survey.

National and regional geophysical databases such as the USGS National Geophysical Database (Phillips et al., 1993; USGS Mineral Resources Program, 1999), interpretive geophysical maps made from the surveys (Saltus and Simmons, 1997; McCafferty et al., 1998), and regional geophysical surveys conducted by mineral exploration companies are an important component of many exploration programs. They provide information on the 3-dimensional spatial variations in magnetic, electromagnetic, gravity, and radiometric signatures of rocks, and so are particularly useful for locating concealed mineral deposits that do not crop out at the ground surface or locating rocks that may be favorable hosts for mineral deposits. These regional surveys, which generally are acquired using airborne geophysical techniques, can also be extremely useful for interpreting the 3-dimensional distribution of environmentally important features such as fractures or rock units that may conduct ground water, or for mapping the distribution of large volumes of altered, sulfide-bearing rocks that may be potential sources for acid-rock drainage.

National and regional mineral production databases and mineral deposit databases (USGS Mineral Data Bases, 1999 in press; Ferderer, 1996), significant deposit databases (Bookstrom et al., 1996), and maps developed from these databases (McCartan et al., 1998; Ferderer, 1996) provide explorationists with guides to the locations, amounts of production, mining methods used, commodities produced, processing types, and geologic characteristics of present and past producing major mining districts, mine sites and mineral prospects in a region. This information is useful because much current mineral exploration is focused on areas of past or present production. When coupled with geologic mineral deposit models, the databases can be used to help refine the geologic understanding of the mineral deposits already discovered in a region. From an environmental standpoint, these databases are also very useful for the exploration geologist to gauge the extent and nature of mining activity that may be contributing to environmental baseline conditions in a region or watershed.

Mineral exploration databases (Wilburn, 1998) document the locations of active mineral exploration projects on a regular basis. These databases not only keep the exploration geologists updated on the activities of their industry, they also provide an indication of where mineral resource development may occur in the foreseeable future. When coupled with geologic maps, mineral production and deposit databases, mineral deposit models and geo-environmental models of mineral deposits, these exploration databases also can be used to help anticipate potential environmental considerations that may accompany foreseeable future development.

Regional remote sensing methods (Lillesand and Kiefer, 1987; Lee et al., 1999a in press) are commonly used in mineral exploration programs. Multispectral satellite imaging (such as Landsat Multispectral Scanner, MSS, and Thematic Mapper, TM) measures the electromagnetic spectrum reflected from the Earth's surface in relatively broad bands, whereas hyperspectral imaging (such as the Airborne Visible and Infrared Imaging Spectrometer, AVIRIS; Clark and Roush, 1984) measure the reflectance spectrum in much narrower bands. Airborne thermal infrared imaging (such as the Thermal Infrared Mapping system, TIMS) collects digital thermal infrared spectra. The satellite techniques offer broad regional coverage, with generally lower resolution, whereas the airborne techniques offer somewhat more limited regional coverage at higher resolution; however, new satellite systems will be in place in the near future that will provide both broad regional coverage and high resolution (on the order of 1–2 meters). These different techniques, each with their own capabilities (Lee et al., 1999a in press) are commonly used to identify the spatial distribution of mineral types (such as clay alteration and secondary iron oxide minerals) and vegetation types that are commonly associated with exposed, weathering mineral deposits (King, 1995; Swayze et al., 1996). These methods are also used to identify major structural features (lineaments) in the Earth's crust thought to be zones of weakness that help localize mineral deposits. In an environmental context, remote sensing data provide the exploration geologist with important insights into the distribution and extent of mineralized rocks that may be contributing to natural environmental variations in a region or watershed. If sufficiently high resolution, the remote sensing techniques may also map the in-stream distribution of secondary minerals formed from weathering of mineral deposits (King, 1995).

Other national and regional geospatial databases provide insights useful for both exploration and environmental purposes. For example, data in regional climate databases and maps

(NOAA, 1999) can be used to estimate the spatial and seasonal variations in temperature, precipitation and evapotranspiration, which influence both the way that mineral deposits weather and the resulting environmental signatures of unmined mineral deposits and mining operations. Hydrologic databases and maps showing the locations of streams, rivers, and watershed boundaries (USGS, 1982), water flow data (USGS Water Data, 1999), and the ground-water component of stream flow (Winter et al., 1998) all provide information that can be used to understand better the spatial and temporal variations in hydrology of a region. The spatial distribution of ecosystems is closely linked to variations in climate. Ecoregion databases and maps (Bailey, 1995) provide insights into the distribution of vegetation and animal communities likely to be present in a region, and therefore that may be affected by mining. A variety of other geospatial databases containing pertinent information on roads, land use, land classification, cultural features, topography and other information are also readily available through the Internet for a number of countries and regions within countries.

Mineral resource, mineral-environmental, and ecosystems assessments

National, regional, and land-unit mineral resource assessments (USGS and Servicio Geológico de Bolivia, 1992; Van Loenen and Gibbons, 1997; Light et al., 1997) integrate many of the techniques in the ESS toolkit to provide an overview of the regional geology and known mineral deposits in a nation, region, or government land unit (such as a National Forest) within a region. The assessments also develop a qualitative or quantitative estimate of the numbers and sizes of undiscovered mineral deposits of given types that may be present. Such assessments compile existing information and collect new data on a reconnaissance scale. They are excellent sources of geologic information that are commonly used by exploration geologists to help guide mineral exploration; they are also used by government agencies and land managers to understand the potential mineral endowment of government lands.

Mineral-environmental assessments link the regional geology and mineral deposit information compiled in mineral resource assessments with geoenvironmental models of mineral deposits and geologic terrains to help understand the potential environmental effects of unmined mineral deposits, past mining, and future mining. Plumlee et al. (1995c) developed a prototype mineral-environmental map of Colorado to identify mining districts with the greatest geologic potential to generate acidic or metal-bearing drainage waters; Plumlee (1999) discusses ways in which the Colorado map approach could be improved by evaluating the impacts of the districts in a watershed context rather than as "point sources." Lee et al. (1999b, in press) present a GIS-based geoenvironmental assessment of Montana that uses GIS statistical analysis to integrate multiple data layers (such as the environmental geology of the rock units and mineral deposits, regional geochemistry and geophysics data, and others).

A prototype ecosystem assessment of the interior Columbia River basin, northwestern United States (Frost et al., 1996; Bookstrom et al., 1996; Raines et al., 1996), demonstrates how regional geologic, minerals information, mineral deposit, geochemical, and mineral-environmental data can be integrated and interpreted to help address ecosystem issues. For example, a lithologic map recast from the regional geologic map was used to map the distribution of cliff-forming limestones that comprise good

peregrine falcon habitat (Frost et al., 1996).

The mineral resource, mineral-environmental, and ecosystem assessments provide excellent earth science, environmental, and ecosystem data that can be used to guide environmentally friendly mineral exploration in the regions they cover. They also provide useful methodologies that can be drawn upon to help gather, integrate, and interpret mineral resource and mineral-environmental data in regions they do not cover.

Environmental considerations in sub-regional exploration or prospect evaluation

Once a regional exploration program has identified target areas with high geological potential for mineral deposit occurrences, detailed studies are then conducted to identify, characterize the geology, map the distribution, and estimate the size and grade of mineral deposit prospects in the target areas. These studies nearly always require extensive new data collection, usually involving more detailed application of many of the ESS techniques used to generate the regional databases and maps discussed previously, including: detailed geologic mapping; detailed rock, sediment, soil, water, and (or) plant geochemistry surveys; high-resolution ground or airborne geophysical surveys; and sampling of rocks in the subsurface using rotary or core drilling, accompanied by geological, mineralogical, and geochemical characterization of the drill samples and geophysical characterization of the rocks around the drill holes.

At this point in the exploration program, the main objective is to identify and delineate ore deposits that can be economically extracted. However, with relatively little additional effort and expense, a large amount of environmental characterization can be done simultaneously with the prospect evaluation activities that can greatly help constrain how big a role environmental mitigation costs may play in the economic viability of any prospects found.

Environmental characterization of exploration target areas or specific target prospects can be done both by interpretation of the data routinely collected as part of the exploration activity, and by some collection of environmental-specific data.

Prospect evaluation and characterization

Once a target prospect is identified, detailed site characterization is carried out using a variety of ESS tools to determine the size, subsurface distribution, grade, process mineralogy (suitability of the ore minerals for processing and extraction), and other geologic characteristics of the target. Environmental information should be compiled routinely as part of these prospect evaluation activities.

A variety of important environmental geology information (Plumlee, 1999) can be interpreted directly from the exploration-driven geological (geologic mapping, drill hole logging), mineralogical, geochemical, and geophysical characterization studies, such as:

- The 3-dimensional distribution and proportion of alteration types, ore minerals, and gangue minerals within a deposit that may help consume or generate acid during weathering (Plumlee, 1999).
- The extent of pre-mining sulfide oxidation.
- The textures and relative weatherabilities (or reactivities) of acid-generating sulfide minerals in the deposit (Plumlee,

1999). In drill hole samples, a general idea of sulfide reactivities can be gleaned by observing if secondary efflorescent salts gradually build up on the surfaces of exposed sulfides as moist core or drill chip samples are allowed to dry out. Spritzing dried core or drill chip samples with water and then measuring the pH with pH paper may also provide an indication whether or not soluble salts have formed on the sample as a result of oxidation of readily-weathered sulfides. Etching rates of sulfides in polished drill core slabs or rock chip aggregates may also help (Plumlee, 1999).

- The textures and relative reactivities of acid-consuming carbonate minerals in the mineral deposit. These may be estimated by observing the amount of fizzing triggered when hydrochloric acid is dropped on the carbonates; the greater the fizz, the greater the reactivity, and therefore the greater the ability of the minerals to react with and consume acid generated by sulfide oxidation (Plumlee, 1999). Etching of carbonate and silicate minerals in polished slabs may also help in the estimation of acid-buffering capacity.
- The concentrations of environmentally important trace elements (Smith and Huyck, 1999) in the deposit, wallrock alteration zones, and unaltered host rocks (Plumlee, 1999).
- The sulfide sulfur content (Crock et al., 1999) of the deposit, wallrock alteration zones, and unaltered host rocks. This can be used to estimate total amounts of acid that may be generated through weathering of waste rocks from a deposit.
- The distribution of hydrologically conductive joints or fractures. For example, major fracture zones, when encountered during drilling, result in a substantial loss in sample recovery and drilling fluid circulation.
- Porosity and permeability characteristics of the deposit host rocks.
- The locations of pre- and post-mining ground-water discharge points. In many sulfide-rich mineral deposits, the locations of pre-mining springs and post-mining discharge from workings or waste piles are marked by extensive deposits of iron- or manganese oxides (termed ferricrete or ferrosinter deposits; Plumlee, 1999).
- The potential for natural hazards (such as earthquakes and landslides: USGS Earthquake Hazards, 1999; USGS Landslide Hazards, 1999) at the mine site and in the surrounding watersheds, which may lead to physical disruption of mining and processing infrastructure such as tailings impoundments.

Exploration drilling characterization is used to understand the 3-dimensional geologic character and distribution of ore grades within mineral prospects in the subsurface. For exploration prospects that have a high potential for developing into economically viable mines, drill core and drill cutting samples can also be evaluated for their net acid-generating or acid-consuming potential through various static and kinetic testing methods such as acid-base accounting, humidity cell, and column or tank tests (Logsdon and Basse, 1991; White and Jeffers, 1994; White et al., 1997; White et al., 1999; Filipek et al., 1999). These tests are discussed in more detail in a subsequent section of this paper.

Data on the ore grades of exploration drill hole samples are routinely subjected to a variety of geostatistical analysis methods, such as kriging, to quantify the sizes, average grades, and distributions of ore zones within a mineral deposit. These same techniques can also be used to estimate better the environmental character of a mineral deposit. For example, the concentrations of environmentally important trace elements, sulfide sulfur, pyrite,

or carbonates, as well as acid-base accounting data, can be kriged to help better quantify the potential of waste zones within a deposit to generate acidic, metal-bearing mine drainage.

Remnants of past mining activity (such as mine adits, mine waste piles, or tailings impoundments) in or near an exploration prospect can provide valuable indications of the types of environmental issues that may develop should a new mine be developed. Waters draining mine adits, mine waste piles, or tailings impoundments should be sampled and analyzed for key environmental parameters such as pH, conductivity, redox conditions, and major and trace element concentrations (Ficklin and Mosier, 1999; Crock et al., 1999). Mine waste piles or tailings impoundments should be characterized mineralogically (including amounts of primary sulfides, secondary minerals and efflorescent salts; Plumlee, 1999). The immediate surroundings of the waste piles should also be investigated for the presence of vegetation kill zones that are usually manifested by iron-oxide hardpan, and that are typically indicative of acid waters emanating from the waste piles. Leach tests (U.S. EPA, 1986-1995; Montour et al., 1998a and b) of the solid waste materials can also be performed relatively easily to determine whether dissolution of soluble secondary salts from the mine wastes by snowmelt or rainfall will generate acidic, metalliferous waters. AVIRIS remote sensing techniques (USGS Speclab, 1998; Swayze et al., 1996) have also been used to identify mine dumps that have a high potential to generate acid, based on the remotely mapped presence of jarosite, a potassium-iron hydroxysulfate mineral that forms from the oxidation of pyrite and the evaporation of acid waters (Nordstrom and Alpers, 1999).

Hydrologic characterization of a prospect is important to establish the location of the ground-water table relative to the ore zones (and potential future mine workings), and to understand potential ground-water recharge through the ore zones and future mine workings. Depth to ground water can be easily established from exploration drill holes. Mapping of springs in a geologic context (e.g., in relation to mapped fractures, contacts between rock units, etc.) should be done during the wettest periods of the year so that all potential water discharge points from the deposit are fully understood; if possible, flows or discharge volumes of the springs relative to those of local streams should be measured. In competent rocks, exploration drill holes can be used to conduct hydraulic aquifer tests that enable an estimation of drawdown times and recharge rates in the drill holes, and hence the hydrologic transmissivity of the rocks surrounding the holes. Exploration drill holes, when properly developed (e.g., careful purging of multiple well volumes using slow pumping rates), may be used to sample ground waters for chemical analysis; however, the lack of casing and screening precludes sampling of potential multiple-producing intervals. As with wells that have been cased and screened, the sampling, analysis, and interpretation of ground-water data should be done with appropriate attention to methods, limitations, and cautions (Ranville and Schmiermund, 1999; Domenico and Schwartz, 1990; Alley, 1993a).

Sub-regional watershed characterization

Environmental characterization of sub-regional exploration target areas is most logically done on a watershed basis, including the major watersheds normally depicted on 1:1,000,000 or 1:2,000,000 scale maps, as well as lesser watersheds within these major watersheds. The major goal of this level of environmental

characterization should be to evaluate the overall environmental baseline conditions of the area, including contributions from both natural and anthropogenic sources. This characterization can be accomplished using data from existing regional databases (with some field verification), followed by remote sensing characterization, field characterization, and collection and interpretation of new data. New data collection during exploration would most likely be done primarily in areas around prospects that have high geologic and economic potential to be developed into mines. Important information to be compiled should include, for example:

- Boundaries of major and lesser watersheds within the area (these can be determined using topographic maps or digital elevation data).
- Climate and ecosystem variations within the major and lesser watersheds, including data on seasonal temperatures, precipitation, evaporation, and vegetation types.
- Where available, data (preferably seasonal) on the flow and water quality of major rivers and streams within the watersheds.
- Distribution and environmental geology characteristics (such as carbonate content, sulfide content, chemical reactivity, likely hydrologic conductivities, etc.) of rock units within the major and lesser watersheds.
- Distribution of major faults and fractures that may transmit ground waters.
- Locations, production, sizes, and, where available, environmental geology characteristics of mines, prospects, mineral processing sites, and other industrial facilities in the watersheds.
- The locations and distribution of unmined mineralized areas that may contribute acid-rock drainage to the watersheds.
- The locations of actively draining mines, or mine waste piles with extensive down-gradient vegetation kill zones.
- Where available, the geochemical compositions of stream sediments, soils, and waters that indicate the extent of metal mobility away from mineralized areas. These data are often compiled as part of routine exploration geochemistry and hydrogeochemistry surveys (e.g., Miller et al., 1982).
- If available from regional databases, or from prior ecological studies of the watersheds in question, data on the species, population sizes, and health of plant, animal, insect, and aquatic organism communities within the watersheds.

ENVIRONMENTAL CONSIDERATIONS IN MINE PLANNING AND DEVELOPMENT

If prospect exploration is successful and results in the discovery of an ore deposit of sufficiently large volume, high enough grade, and suitable process mineralogy to be mined and the metals extracted from the ore at a profit, then mine planning and development is initiated. Ideally, as mine planning commences, environmental information and data gathered as part of the prospect exploration have already provided a sufficient comfort level about the potential environmental economics of the deposit. However, detailed environmental impact statements (EIS's), involving substantial new environmental data collection and interpretation, are typically required by multiple government regulatory agencies before a mining permit is granted. These studies are needed to help anticipate and deal with potential environmental

problems before they occur—prevention and mitigation are always less costly and more easily accomplished than remediation after the problems develop. Many examples of EIS's are available from the regulatory agencies that require them, or from the mining companies themselves. Typically, these EIS's are prepared by environmental consulting companies under contract to the mining company. However, in particularly contentious cases, both regulators and industry may contract their own EIS's.

It is not the intent of this section to provide a cookbook on how to prepare an EIS. Rather, it is designed to show how tools in the ESS toolkit are already widely used in mine planning and development, and to show how a number of tools in the toolkit that have not been widely used can provide additional valuable information. The following sections will show how the ESS tools can be applied to help (a) characterize pre-mining background and baseline conditions at the proposed mine site and in its surrounding watershed(s); (b) predict potential future environmental impacts that may result from mine development, and; (c) monitor environmental conditions during mining. The application of ESS tools to help minimize and remediate any potential environmental problems will be discussed in the following section.

Characterizing pre-mining environmental baseline and background conditions

It is crucial that the pre-mining environmental baseline conditions (those that exist prior to the proposed mining) and background conditions (those that existed naturally prior to any mining or human activities) at a proposed mine site and within the watershed(s) surrounding the site be constrained in as much detail as possible prior to any mine development and production. This information will allow the potential environmental impacts that may result in the watershed from proposed mining at the site, given various levels of mitigation, to be understood more fully. In addition, this will allow the mining company, government land managers and regulators, and the general public to measure the relative contributions of the site to any environmental degradation that is observed after commencement of mining.

Quantification and verification

In general, environmental characterization and prediction activities carried out as part of the mine planning and development process require a substantially greater level of quantification and verification than is likely achievable or affordable during exploration programs. For example, a variety of detailed new data should be collected for both the site and its surrounding watershed, including: existing environmental and ecological conditions; surface- and ground-water quality and hydrology; and locations and environmental effects of mines, prospects, processing facilities, and unmined mineralized areas. Although existing data collected as part of regional studies or the exploration process will be useful for helping to guide the new sampling, the existing data may not have been collected in adequate spatial or temporal detail, or with appropriate methodologies and documentation to be suitable for preparation of site EIS's. For new data collection, detailed field laboratory and analytical records, results, and notes (summarizing methods and assumptions) should be archived in order to allow regulators, land managers, and the general public to reconstruct or trace the data gathering process, if necessary. Rigorous

QA/QC (Quality Assurance/Quality Control) protocols for all types of studies (including field mapping and other earth science investigations) also should be followed, or established if no others are available. The main goal should be to meet or exceed the quantification standards set by government land management or regulatory agencies.

Any ground- and surface-water quality measurements made should be as complete and detailed as possible (e.g., pH, conductivity, total dissolved solids, alkalinity, acidity, dissolved oxygen and other redox parameters, total and dissolved major- and trace-element concentrations, organic species). Although such detailed analyses are not typically required from a regulatory or mine-permitting standpoint, and hence may be viewed as an excess expense, they are in fact essential to adequately characterize the geochemical and biogeochemical processes controlling water quality (Ficklin and Mosier, 1999; Alpers and Nordstrom, 1999).

Finally, the prospect of legal actions is increasingly facing proposed mining projects. Hence, all data collected (as well as field notes, laboratory notebooks, etc.) should be considered as potential legal evidence, and so should be subjected to rigorous chain of custody and other evidentiary procedures that demonstrate that samples have not been tampered with between collection and analysis.

Mine site characterization

Much of the geologic information needed to help interpret a site's environmental geology characteristics will probably have been collected in sufficient detail as part of the detailed prospect evaluation (see previous discussions). However, further geological characterization may be warranted.

For example, fractures and joints are the dominant hydrologic conduits (NRC, 1996) in many mineral deposits. As a result, further detailed geologic mapping and analysis of structures and joints may provide needed information on fracture flow hydrology at a site. Ground based environmental geophysics studies such as ground penetrating radar, seismic tomography, or resistivity surveys may help supplement the geologic mapping by providing useful information on the location of hydrologically conductive (or non-conductive) structures or rock units in the subsurface (NRC, 1996; Tura et al., 1992).

Mineralogical and geochemical characterization (Plumlee, 1999) of any existing mine waste or tailings dumps from prior mining activities, as well as soils in any adjacent vegetation kill zones to the waste dumps should be coupled with leach studies (Montour, 1998a and b) of the wastes to assess the potential for environmentally detrimental surface runoff. For very large waste dumps or those that are of particularly high potential for environmental problems, characterization via drill sampling of the dump materials may be warranted. Geophysical characterization of the waste piles may help provide information on the subsurface distribution of moist or saturated zones within the dumps, as well as on geochemical processes going on within the dumps (Campbell et al., 1999 in press).

Mineralogical and geochemical characterization and age dating of any ferricrete deposits may provide information on the pre-mining quality of waters draining the site (e.g., Furniss and Hinman, 1998).

Pre-existing environmental conditions should be characterized through a careful analysis over the course of at least a full year,

and preferably longer, to allow the fullest range possible of seasonal and climatic variations to be measured. Detailed hydrologic and water-quality data should be collected regularly (monthly or even weekly) for any streams flowing through the site, and of any existing springs on the site that drain unmined rocks or existing adits, tailings piles, or mine waste piles (e.g., Lambeth, 1999)

Meteorological data (rain and snowfall amounts, maximum and minimum temperatures) measured on a regular (preferably daily) basis are needed to understand the site surface- and ground-water hydrology. In addition, calculation of seasonal evapotranspiration rates and a net water balance at the site (see Shevenell, 1996, and references therein) is absolutely crucial both from an environmental standpoint and a mineral processing standpoint; these affect ground-water recharge rates and water accumulation rates in mine-water storage ponds, heap leach impoundments, or mineral processing ponds.

The ground-water hydrology at the site should be analyzed via a network of wells sited to provide a maximum understanding of ground water relations to topography, geology (faults, rock units, etc.), and mine workings. Depth to water table, as well as ground-water quality, should be measured regularly (weekly or monthly). Aquifer tests should be completed in order to understand potential ground-water recharge and flow rates, as well as the conductivities of known fractures in between wells. Tracer tests (Kimball, 1996; Domenico and Schwartz, 1990; NRC, 1996) may also provide key information on the subsurface flow and relations between ground and surface waters at the site. Age dating of the ground waters, when linked with regular water-table measurements, may provide further insights to the sources, recharge rates, and flow rates of ground waters through the site.

Stable isotope studies of the site's mineral deposits, its ground and surface waters, and dissolved constituents of the waters can provide important information on sources for the waters and their constituents, as well as the geochemical or biogeochemical processes that have affected the waters. Stable hydrogen isotope analyses of surface and ground waters at the site provide insights into the sources of the waters and processes such as evaporation that may have affected the waters. For example, waters that are derived directly from snowmelt recharge will be quite light isotopically compared to those that are derived from rain-water recharge. Waters that have been subjected to evaporation (such as open-pit waters, or waters in hot underground workings where sulfide oxidation is rampant) will be quite heavy isotopically (Hamlin and Alpers, 1996). Stable hydrogen and oxygen isotope measurements of H- and O-bearing primary and secondary minerals can indicate the processes by which the minerals formed, and the isotopic compositions of the waters from which minerals were deposited (Rye and Alpers, 1997). Stable sulfur isotope compositions of aqueous sulfate, when compared to the sulfur isotopic compositions of sulfides present at an existing mine site, can provide an indication of the mineralogical source(s) of the sulfate (Taylor and Wheeler, 1994). Stable oxygen isotope measurements of aqueous sulfate can provide information on whether sulfide oxidation occurred as a result of oxidation by atmospheric oxygen or by ferric iron (Taylor and Wheeler, 1994; Alpers and Nordstrom, 1999). Bacterial reduction of aqueous sulfate in some environments (such as wetlands or flooded mine workings) may also be manifested in the sulfur and oxygen isotopic composition of the aqueous sulfate (Taylor and Wheeler, 1994; Hamlin and Alpers, 1996). Stable carbon isotope measurements of aqueous carbonate species can provide an indication of whether they were

derived from incorporation of soil gas by ground waters or dissolution of carbonate minerals.

As a result of the detailed geologic, hydrologic, and geochemical characterization studies, the mining company, its consultants, and the regulators overseeing the site should have developed as comprehensive an understanding as possible of the site's hydrology and geochemistry prior to the proposed mining. Hydrologic modeling and geochemical modeling studies also may help in this understanding. For example, inverse chemical modeling (Alpers and Nordstrom, 1999) may be useful in understanding the different ore and wallrock minerals that reacted with rain or snowmelt water to produce a given spring water composition measured at the site; this modeling is most successful when used in conjunction with detailed mineralogical characterization of the deposit and host rocks, coupled with detailed and complete water analyses (Alpers and Nordstrom, 1999; Ficklin and Mosier, 1999). Hydrologic modeling of the site (Domenico and Schwartz, 1990) will provide an indication of existing ground-water flow conditions, and can be used to anticipate the effects of mining on the local hydrology (discussed in a subsequent section).

Ecological characterization of the site, including an inventory of terrestrial and aquatic plant and organism populations, should also be completed to document the ecological *status quo* prior to the proposed mining.

Watershed characterization

Establishment of detailed environmental baseline conditions existing in the watershed(s) surrounding a proposed mine site is crucial, because any environmental impacts of the proposed mine will be measured and judged on a watershed basis. Among other examples, interdisciplinary studies examining the downstream effects of the Summitville Mine (Posey et al., 1995) provide excellent examples of the types of studies that must also be done on a watershed basis to evaluate pre-mining baseline conditions.

The locations of mineralized areas, other mine sites, and other potential sources of environmental degradation (such as industrial sources) must be identified; this may have been largely accomplished during exploration and prospect evaluation activities.

As discussed previously, remote sensing studies have been used successfully to identify mine dumps and tailings impoundments having the greatest potential to generate acid drainage in a district, based on identification of jarosite-bearing mineral assemblages within mine waste dumps, and goethite in soils immediately surrounding the dumps (Swayze et al., 1996).

Detailed measurements of surface-water discharge and quality should be made on a regular weekly or monthly basis (Walton-Day et al., 1995; Kimball, 1999). This level of detailed temporal and spatial sampling is necessary to quantify any impacts from the proposed mine site on surface-water quality relative to impacts from other sources. Measurement and sampling sites should be located on the major stream or river in a watershed below each of its confluences with major tributaries or tributaries along which environmental degradation is occurring. Sampling and measurement sites should also be spaced along any tributaries that may potentially be affected by the proposed mine, and should include sites both upstream and downstream from the mine. If possible, water discharge and quality measurements should also be made during one or more storm events to assess potential short-term variations in water flow and quality that may be superimposed on

longer-term seasonal variations (Ortiz et al., 1995); such short-term storm events may result in brief but potentially toxic pulses of metal-laden waters from the dissolution of soluble metal salts in mine wastes or natural weathering of mineralized rocks. Ideally, both filtered and unfiltered water samples (Ficklin and Mosier, 1999) should be collected to understand the contributions of both dissolved and suspended particulates to the total metal loads. In addition, specially filtered samples (Ficklin and Mosier, 1999) designed to understand the amounts of suspended colloidal materials should also be collected (Church et al., 1997). Turbidity measurements should also be made to help understand the amounts of suspended sediment present (Edwards and Glysson, 1988).

Collection of stream-water samples for water-quality analysis typically should involve an integrated cross-sectional sampling approach, rather than a point sampling approach from the stream bank (von Guerard and Ortiz, 1995); many streams and rivers can vary substantially in composition across any given width-depth cross section, and so point samples collected from the bank or in the center of a stream may not be representative of the cross-sectional average composition.

In-stream hydrologic tracer studies (Kimball, 1996) may be necessary to accurately determine flow and to determine how major streams in the watershed(s) gain water from or lose water to the ground-water reservoir (Winter et al., 1998). In addition, synoptic sampling methods, where all samples and flow measurements in a watershed or along a river stretch are collected within a short period of time, provide a snapshot of the entire river system that is very useful for interpreting the surface-water hydrology of the river or stream system (Kimball, 1996).

Ground-water characterization should also be carried out on a regular basis through sampling of wells located both up-gradient and down-gradient from the mine site in order to determine regional variations in ground-water quality, depth to water table, and other hydrologic parameters. If possible, aquifer tests should also be carried out on these wells to understand potential transit times of ground water from the mine site to the surrounding wells.

As discussed previously for mine site characterization, stable and radiogenic isotope studies of surface waters and ground waters in the watershed may provide useful information on the sources of and geochemical processes affecting the waters and their dissolved constituents.

At the same time surface water samples are collected and flow measurement are made, it is also beneficial to characterize the aquatic ecology (e.g., Moore et al., 1991) of the streams in the watershed(s) surrounding the proposed mine site. These assessments should be made at least once during each of low-flow and high-flow conditions.

Detailed stream sediment surveys of the watershed(s) surrounding a mine site, if not done as part of the sub-regional exploration and prospect evaluation, should also be done not only to establish a geochemical baseline in the sediments prior to proposed mining, but also to understand metal contributions to the sediment load from unmined mineralized areas and past mining activities. Sequential chemical extractions (Crock et al., 1999) of the sediment samples provide an indication of the availability of metals from the sediments. Radiogenic isotope studies of elements such as lead in the sediment samples can be used to help understand the proportions of each sediment sample's metal content that are derived from particular sources such as mining districts or unmined mineralized areas (Church et al., 1993, 1997, 1999). Geochemical studies of lake or stream sediment strata, coupled

with age dating studies such as Pb^{210} dating, measure temporal variations in metal loading to the sediments over time (Nimick and Moore, 1994; Horowitz et al., 1994; Church et al., 1993). Paleontological analyses of animal remains in the sedimentary strata also may provide an indication of temporal variations in past water quality. For example, different taxa of freshwater ostracods are viable in different pH ranges of water; when they die, the tests of the ostracods fall to the lake bottom, are incorporated into the sediments, and provide a stratigraphic record of past variations in pH (Brouwers et al., 1996; Mezquita et al., 1997).

Chemical analyses of plants in the watershed(s) surrounding the proposed mine may also provide important baseline information. Tree ring analyses of trees affected by surface and ground waters originating in part from the proposed mine site may provide insights into metal uptake over time (Gough et al., 1995). If surface waters or ground waters potentially affected by the mine site are used for irrigation, analysis of plants irrigated by the waters, coupled with analyses of the metal contents of the irrigation waters and the irrigated soils should also be done to establish pre-mining irrigation baselines (Erdman et al., 1997).

Anticipating the potential environmental effects of a mine

There are a number of different ESS tools that can be used to help anticipate the potential environmental effects that might develop from a proposed mine. Many of these predictive tests and models are required or routinely carried out as part of the preparation of the proposed mine's EIS. In addition, much of the information that will hopefully have been collected during pre-mining baseline studies, such as environmental characterization of existing mine dumps or draining adits, will also provide important insights. It is important to note that none of these predictive methods can provide an absolutely accurate and quantifiable prediction of a mine's potential environmental effects; however, especially when multiple methods are used in concert, a very useful, educated estimate of the potential effects can be obtained.

Predicting the composition of mine waters

A variety of methods are commonly used to predict the potential for mine workings, mine waste piles, or tailings solids to develop acidic or metalliferous drainage waters. Static tests such as acid-base accounting (White et al., 1999; Morin and Hutt, 1997; ICARD, 1997) typically involve measurement of the total acid generating potential (in the form of sulfide sulfur content) and acid consuming or neutralizing potential (in the form of carbonate content) of samples of prospective ore and waste rocks from the mineral deposit to be mined. Potential complications in interpreting these tests arise from verifying whether the samples analyzed are truly representative of the range of rock types in the deposit that will be exposed by mining. In addition, there is often the possibility that the measured carbonate content either underestimates or overestimates the acid-consuming capacity of the samples: other minerals such as some aluminosilicates may also react with and consume acid, some carbonate minerals (such as ankerite and magnesite) are slow to react with acid, and carbonates such as siderite (an iron carbonate) may actually generate acid upon weathering under some chemical conditions (Plumlee,

1999). Kinetic tests include humidity cell tests, which subject samples of ore and waste rocks to cycles of moist or dry air (White et al., 1997; White and Jeffers, 1994; ICARD, 1997; Filipek et al., 1999; Morin and Hutt, 1997), and flow-through column or tank tests (Logsdon and Basse, 1991), in which waters are run through containers of ore and waste rock samples. The effluent waters are then measured for pH and metal content. As with the static tests, these kinetic tests are complicated by the challenge of whether or not the samples are representative of the total range of rock types in the deposit. However, subjecting sufficient numbers of samples to the tests, and increasing the sample size (Logsdon and Basse, 1991) will help in this regard. It is also a challenge to develop experimental procedures that reproduce the environmental conditions and reaction rates that will occur at the mine site.

Empirical data on mine water compositions measured at geologically similar mines in similar climates (components of geo-environmental mineral deposit models; Plumlee et al., 1999; du Bray, 1995; Price et al., 1995) may also be used to help understand the range of mine water compositions that may develop at the prospective mine site. The advantage of such an empirical approach is that the data measured reflect actual rates of sulfide oxidation that occur in the field, and integrate large volumes of ore and (or) waste materials. The disadvantage is that the deposits for which empirical data are available may not be truly similar in geologic, hydrologic, or climatic setting to the deposit under development (Plumlee et al., 1999).

With appropriate recognition of its limitations, geochemical modeling (Alpers and Nordstrom, 1999) may also be used to help anticipate potential mine-drainage compositions. These calculations can be used, for example, to model the progressive change in water and rock compositions that could result from the reaction of oxygenated rain water with different ore and waste rock types based on observed proportions and reactivities of sulfide, carbonate, and aluminosilicate minerals. Various options such as sorption of metals onto secondary hydrous iron oxides can also be added to the calculations (Smith, 1999; Alpers and Nordstrom, 1999). The calculations are best accomplished when constrained by field measurements of actual water compositions, coupled with mineralogical characterization of the primary ore and wastes, and secondary minerals formed by the oxidation of these rocks. Inverse chemical modeling calculations (Alpers and Nordstrom, 1999) based on existing water compositions may also be used to help determine the minerals that are reactive and modifying water compositions at a site.

Another indication of the potential mine water compositions that may develop at a proposed mine site are any waters that are draining existing mine workings and wastes at the site. However, if the proposed mining involves extensive new ground disturbance and exposure of unoxidized sulfides to weathering, the use of existing water compositions as a model may underestimate the potential acidity and metal content of the waters generated by the proposed mining. For example, Reynolds adit waters draining the underground workings at Summitville prior to open-pit mining were quite acidic, with 8–10 ppm dissolved Cu (Plumlee et al., 1995b, 1999). As a result of the increased exposure of unoxidized sulfides and other hydrologic alterations by the open-pit mining (Plumlee et al., 1995a), the Reynolds adit waters increased rapidly in metal content during the 7 years of mining, with dissolved Cu concentrations eventually reaching as high as several hundreds of ppm.

Leach studies (e.g., Montour, 1998a and b) of existing mine

wastes, when coupled with mineralogical characterization of the wastes and characterization of vegetation and soils down-gradient from existing mine dumps, may also provide pertinent insights into water compositions that may develop from new mining at a site. However, the compositions of the resulting leachate waters may vary substantially depending upon the leach methods used, the ratio of water to rock used in the leach tests, and the degree of agitation used in the tests (Montour et al., 1998a and b).

Effluents from kinetic tests and mixing tests can also be used in toxicological studies (Kelly, 1999) to help estimate the potential effects of drainage from the site on aquatic organisms.

Predicting the composition of open-pit waters

Due to the great increase in the last several decades of open-pit mining operations, considerable effort and expense on the part of mining companies, regulators, and their consultants has been put into the prediction of water quality in pit lakes that develop after open-pit mining activity has ceased. The compositions of existing open-pit lake waters have been shown to vary with depth in the lake and seasonally, much the same as observed in many regular lakes. The compositions also vary as a function of the local topography and ground-water hydrology, the amounts of evaporation and precipitation, the type and extent of biological activity, the morphology of the pit (which influences the pit lake limnology), and the geology of the rocks surrounding the pit. Measuring the compositions of pit waters developed in ore deposits of similar geology and climate characteristics (Plumlee, 1999; Plumlee et al., 1999; Price et al., 1995) provides some insights into potential pit water compositions that may develop at a particular deposit. However, the number of pit lakes for which water quality data are available is somewhat limited, and hence integrated geochemical, hydrologic, and lake hydrodynamic modeling studies are increasingly called upon as predictive tools (e.g., Atkins et al., 1997; Kempton et al., 1997; Miller et al., 1996). Due to the many complex factors controlling pit lake compositions, and possible changes in these factors over the tens to hundreds of years that may be required for a pit lake to reach its maximum extent, the results of these predictive models should be viewed as approximations. As more pit lakes form for which detailed predictive hydrogeochemical models have been developed, and empirical data are collected on spatial and temporal variations in pit water quality (e.g., Atkins et al., 1997; Davis and Eary, 1997), the accuracy of the predictive models will undoubtedly be refined.

Estimating the potential impacts of mine waters and mineral processing waters

In addition to anticipating the potential compositions of mine waters that may develop at a mine site, it is also important to estimate the potential impacts of these waters, and any mineral processing waters and other solutions generated at the site, on ground- and surface-water quality. Measuring the effects of waters draining existing mine workings and mine wastes on water quality and ecology in the watershed, presumably done during pre-mining watershed baseline characterization, will provide some insights.

Mixing experiments (e.g., Plumlee et al., 1995b) may provide further information to help anticipate potential environmental impacts of the mine or mineral processing waters. In these experiments, effluents from kinetic mine waste tests, leach tests, or pre-

mining ore processing evaluations can be mixed with samples of the local ground or surface waters, and the resulting compositional changes measured. However, the actual physical and geochemical conditions present in the surface or ground waters down-gradient from a site will be difficult to replicate. Further, the potential variations in mine-water compositions and proportions in which the mine waters mix with local ground or surface waters will require a significant number of experimental runs. Hence, these mixing experiments should be viewed only as indicators of potential environmental effects.

Chemical modeling of the progressive downstream dilution of mine waters that may develop at a site can also be effective. See a similar approach used by Miller and McHugh (1999) as an example.

MINING-ENVIRONMENTAL PREVENTION AND REMEDIATION STRATEGIES

Ideally, with effective prediction, many mining-environmental problems should be anticipated and prevented before they occur at proposed and active mine sites. Prevention is generally much easier and cheaper to accomplish than remediation once the problems develop. Further, although preventative measures are generally accomplished at the mine site, remedial actions may not only be required at the site to stop the source of the problems, but also may be required in the surrounding watershed to repair damage well away from the site. Earth-system science data and tools are key to the development of effective engineered solutions to mining-environmental problems.

Prevention and treatment of acid-rock drainage

There are a variety of engineering approaches to the prevention and treatment of acid-rock drainage. Excellent summaries are included in Kwong (1993), Evangelou (1995), ICARD (1997), Filipek et al. (1999), and other general sources listed in the first part of this paper.

Prevention

Most preventative measures (which also may be used to help remediate existing drainage problems) involve prohibiting the oxidation of pyrite and other iron-bearing sulfides, which is the key contributor to severe acid-mine drainage problems (Nordstrom and Alpers, 1999; Plumlee, 1999; Evangelou, 1995).

Isolation of sulfide-bearing wastes from atmospheric oxygen and oxygenated waters is commonly used to decrease the generation of acid mine drainage. For example, capping of sulfide-rich waste dumps with impermeable barriers (e.g., Blowes et al., 1994; reports available through MEND, 1999) will help decrease the flow of oxygenated rain and snowmelt waters through the dump; however, the barriers must be designed to prevent the development of leaks. In addition, care must be taken in areas of steep topography to prevent flow of ground waters from springs into the dump beneath the cover.

Blending of acid-generating mine wastes with carbonate-rich rocks has been used at some mines in the anticipation that the carbonates will react with and consume the acid generated by sulfide oxidation, and that secondary minerals formed by neutralization of

the acid waters will decrease porosity and permeability. However, armoring of the carbonates by secondary iron oxides may reduce acid-consuming efficiency. Further, increasing the pH of waters flowing through the wastes does not guarantee that the waters will have low metal concentrations (Plumlee et al., 1999). Techniques in which liquid slurries of alkaline reagents are injected into the waste dumps have the same anticipated outcome and potential shortcomings.

Disposal of acid-generating tailings and wastes under water is commonly used, with the presumption that the limited quantities of oxygen carried by water that is out of contact with the atmosphere will greatly reduce sulfide oxidation and acid generation. For example, sulfidic tailings are often backfilled into underground mine workings below the water table, which then flood after mining. However, such a treatment strategy should also include an evaluation of the amounts and types of soluble secondary salts present in the underground workings. Such salts form by evaporation of acid waters or oxidation of sulfides by humid air (Alpers and Nordstrom, 1999; Plumlee, 1999) in the underground workings and can provide a ready source of ferric iron, which can then trigger sulfide oxidation in the absence of direct atmospheric oxygen. In mining operations close to the ocean, sulfidic tailings are increasingly being disposed of in the ocean; while sulfide oxidation and release of the acid and metals are greatly inhibited, assessments must also be made of the extent of metal uptake from the solids by benthic organisms (see, for example, studies of lead uptake by benthic organisms in streams affected by lead tailings in Dwyer et al., 1988).

Application of bactericides to sulfide-generating mine wastes has been used in recent years to kill the bacteria that catalyze sulfide oxidation (Evangelou, 1995; Mills, 1999; Nordstrom and Alpers, 1999). However, repeated application of the water-transported bactericides is necessary, and transport of the bactericides to all sulfide mineral surfaces is very difficult (Evangelou, 1995). Techniques that have recently been developed to process gold ores, which use bacteria to oxidize sulfides prior to heap leaching (Brierley, 1999), may also be used increasingly in the future to treat sulfidic mine wastes prior to final disposal.

Techniques that microencapsulate sulfides with non-reactive phases are currently under development (Evangelou, 1995). For example, treatment of pyritic wastes with solutions containing potassium phosphate and hydrogen peroxide causes the oxidation of the iron in the pyrite to ferric iron and the precipitation of ferric phosphate solid on the pyrite surface. The solid coating forms an armor that greatly decreases the rates of oxygen and water access to the pyrite surfaces.

Hydrologic isolation techniques have been proposed and put into limited use to prevent flow of ground waters through sulfide-bearing mineral deposits. Grout curtains (where impermeable grout is injected into fractures) have been used, for example up-gradient from mine workings to seal the fractures and divert ground-water flow around workings. Such techniques require detailed understanding of the fracture-flow hydrology of the site, as well as a long-lasting, effective grout.

Treatment

A variety of methods have been developed to treat acid-rock drainage once it forms (see, for example, Evangelou, 1995; Skousen and Ziemkeiwicz, 1995; and case studies in ICARD,

1997). Active treatment methods require continued addition of reagents to treat the waters, along with active maintenance and mechanical devices to mix the reagents with the waters. Passive systems require little or no input of reagents, active maintenance, or mechanical devices.

Passive treatment systems such as anoxic limestone drains have been used for quite some time to treat coal mine drainage (Hedin et al., 1994). Acid waters flow through cells with periodically replenished crushed limestone, which then reacts with the acid to raise the pH. However, the waters must first have low dissolved oxygen to prevent precipitation of hydrous ferric oxide armor on the carbonate surfaces. Aluminum-rich waters are not suitable for treatment because they can also armor the carbonates with Al precipitates (Wildeman et al., 1997). Further, once the waters leave the drain, oxidation of ferrous iron to ferric iron and formation of hydrous ferric oxide particulates can lead to a pH decrease (Nordstrom and Alpers, 1999).

Near-neutral waters commonly drain carbonate-rich rocks or rocks altered to contain carbonates that are present in or around some types of mineral deposits (Plumlee, 1999; Plumlee et al., 1999). These types of rocks may have potential for use as large anoxic limestone drain systems, if they can be suitably fractured to increase water-rock interactions, and if appropriate flow systems can be engineered that do not allow contamination of the surrounding ground and surface waters.

Wetlands (both natural and engineered) and bioreactors are two other passive treatment systems that are increasingly being used to treat acid rock drainage (Walton-Day, 1999; Clayton et al., 1999; Wildeman and Updegraff, 1997; Herbert et al., 1998). Aerobic and anaerobic wetlands can serve to filter particulates from waters. Anaerobic wetlands and bioreactors develop reduced geochemical conditions due to decay of organic matter; bacterial sulfate reduction then increases the pH and precipitates the metals as sulfides. Anaerobic wetlands and bioreactors can be quite effective; however, both produce sulfide precipitates that must remain isolated from the atmosphere, lest oxidation and acid generation start all over again.

A number of active treatment systems involve mechanical addition of lime or other reagents to the acid drainage. The treatment raises the pH of the waters and removes the metals into a sludge, which is then separated physically by settling (either by mechanical separators or passive settling ponds) and disposed of. A disadvantage of these systems is that they require periodic upkeep and addition of reagents over the life of the treatment system. They also require long-term disposal of large quantities of sludge produced by the treatment. A number of these systems also require mechanical devices to mix the reagents with the drainage waters.

Some of the alkaline-addition treatment systems only add alkaline reagents with or without flocculants. In these systems, the metals are largely removed through precipitation of iron, aluminum and manganese particulates and sorption of metals onto the particulates. These systems have the advantage of generating oxidized sludge that is a relatively non-reactive residence for the metals; however, some metals may be released from the disposed sludge if it comes into contact with ground waters having an appropriate pH to trigger metal desorption (Smith, 1999). Other treatment methods involve the addition of lime to raise the pH, as well as the addition of sodium sulfide or bisulfide to precipitate the metals as sulfides. The disadvantage of these methods is that the sulfide sludge must be disposed of in an anoxic environment

to prohibit re-oxidation and renewed acid generation.

Increasingly, innovative active treatment schemes also are being developed that use as reagents alkaline waste products from a variety of industrial processes (such as paper mill waste or cement kiln dust; Chtaini et al., 1997). However, the chemical makeup of these innovative reagents and samples of treated waters from pilot studies should be carefully analyzed to make sure that the waste reagents are not adding additional trace elements or other contaminants to the waters they are being used to treat.

In studies of a number of different mine drainage waters, Smith (1999) and Smith et al. (1992) demonstrated that dilution of acid-mine waters with surface waters may provide substantial mitigation of the acid without special addition of reagents. Thus, semi-passive treatment schemes that utilize dilution and particulate settling prior to discharge may be appropriate for some drainage and local water compositions. These studies also showed that dissolved metal concentrations in mine-drainage streams are strongly influenced by sorption onto suspended particulates, but not by sorption on bed sediments. These results indicate that drainage treatment plans which utilize sorption of metals onto particulates should be designed to maximize interactions between the waters and their suspended particulates (Smith, 1999). Therefore, settling ponds should be designed with partially submerged curtains that inhibit laminar flow of waters across the tops of the ponds, and that encourage circulation throughout the pond (Smith et al., 1992).

Geochemical modeling can be used to understand how amenable different acid water compositions are to some active treatment methods (Smith, 1999; Alpers and Nordstrom, 1999). For example, calculations modeling the progressive neutralization of acid waters by either lime addition or water dilution can be set up to estimate the amounts of particulates formed and the amounts of various metals sorbed onto the particulates (a function of the original pH and proportions of particulate forming metals to sorbing metals in the waters) over various target end pH values (Smith, 1999). The calculations can also be used to determine the optimal pH to which the waters should be treated; some metals such as those that form oxyanions (e.g., arsenic or molybdenum; Smith and Huyck, 1999) or strong carbonate complexes (such as uranium; Wanty et al., 1999) desorb at high pH values, and so treatment to excessively alkaline pH values may end up releasing potentially harmful concentrations of these elements.

Electrochemical methods are also being developed and tested to treat acid-mine waters. These methods employ the electrolytic properties of acid-mine drainage and the differences in electrical potential between a cathode (such as sulfidic rocks) and an anode (such as Fe, Al, or Zn) to set up a galvanic cell in the mine waters (see, for example, Shelp et al., 1996, 1995). In their experiments with Zn anodes, for example, Shelp et al. (1996) were able to raise the pH of low-dissolved oxygen waters from 3 to 6.7 over a two-month period, and achieve a corresponding significant decrease in the concentrations of wide variety of metals such as Fe, Al, Co, Cu, and Ni that were exchanged for Zn from the anode. However, these methods add metal dissolved from the electrode (such as Zn, Fe, or Al) into the waters, which may require further treatment to remove.

Finally, methods to economically extract one or more metals from the acid mine waters to help offset the treatment costs are being developed and applied. For many years, copper has been recovered from Cu-rich acid mine waters using a simple electrochemical method in which copper from the waters replaces and

plates out on scrap iron. A more sophisticated variation on this technique, solvent-extraction electrowinning, is increasingly used as the primary extraction technique in many copper deposits, and has been proposed to recover copper from acid-mine drainage as well (Miedecke et al., 1997).

Adit plugging

Adits and tunnels that were installed to drain underground mine workings are common sources of acid mine drainage. Plugging of draining adits and drainage tunnels has been proposed at many sites and carried out at several of these sites to reduce the amounts of drainage waters needing treatment. The reasoning behind plugging is that it not only removes a point source for acid drainage, but it also backs ground water up into the underground mine workings, thereby precluding atmospheric oxygen from reaching and oxidizing sulfides.

However, there are several potential disadvantages to adit plugging. First, if fractures, joints, or other hydrologic conduits are present that can transmit ground waters from behind the plug to the ground surface, then leakage around the plug may occur and the original single drainage point source is, in effect, converted to a number of smaller point sources. In some cases, the adit plugging may simply reactivate pre-mining ground-water discharge points, as indicated by the presence of pre-mining ferricrete deposits. Second, the flooding of underground mine workings will likely lead to the dissolution of any soluble secondary salts that have accumulated in the workings as a result of evaporation of acid waters or in-situ oxidation of sulfides by humid air. Release of ferric iron from the salts (Nordstrom and Alpers, 1999) will in turn trigger more sulfide oxidation without the need for direct contact with atmospheric oxygen. Adit plugging may therefore lead to at least a short-term increase in concentration of metals and acid in the ground waters behind the plug. If the water table behind the plug fluctuates seasonally, then there is a high likelihood that the cycle of soluble salt formation, salt dissolution, and sulfide oxidation will continue indefinitely, and there may be little to no overall gain in water quality.

Hence, before adit plugging is considered as a viable remedial action, several key bodies of geologic, geochemical, and hydrologic information should be gathered and interpreted. The locations and extrapolated surface outcrops of any fractures, rock contacts, or other hydrologic conduits behind the proposed plug locations should be carefully documented using geologic mapping or geophysical techniques. Locations of pre-mining springs should also be carefully mapped and linked to the fracture maps. The amounts and types of secondary salts present in the underground workings should be characterized. The site should be characterized in detail hydrologically, with special attention paid to identifying the distribution of hydrologically conductive mine workings and fractures, and the areas through which ground water is recharged into the underground workings. A detailed hydrologic model of the site should then be developed (which preferably incorporates fracture flow) to determine the extent to which the water table will rise as a result of the plugging, and the extent to which the water table will fluctuate seasonally. Geochemical models should be linked to the hydrologic models to understand how the composition of ground waters in the mine workings will change as a result of plugging and seasonal variations in water table level behind the plug once it is in place.

Treatment of mineral processing wastes and solutions

Many mineral processing solutions are recycled as much as possible during mining, in order to minimize water and reagent usage. However, disposal of these solutions is inevitable once their extractive capacities have been exhausted. The wastes left from mineral processing are also disposed of.

Mill tailings and tailings waters

In general, mill tailings left after the milling and physical or chemical extraction of the mineral commodity of interest are disposed of through discharge of a slurry to a tailings impoundment, where the solids settle from the slurry and much of the liquid decanted for reuse or disposal. The tailings solids have minerals similar to those in mine waste rocks from the deposit, only in potentially different proportions (for example, flotation tailings commonly are depleted in sulfides compared to the ores and waste rocks) and in much smaller particle size. The liquids that remain in the impoundment depend upon the type of milling process, but often contain some levels of organic chemicals (such as detergent-like surfactants), cyanide, and other reagents used to enhance the mineral recovery. With time, these chemicals tend to be diluted through addition of rain water, or are degraded as a result of bacterial action, photolytic degradation, or other processes. Due to reactions with the tailings solids, the tailings waters generally evolve over time to chemical compositions similar to those of mine waters draining the same deposit type, except that the tailings waters can contain higher concentrations of acid and (or) metals than corresponding mine waters due to the fine grain size of the tailings and evaporative concentration in dry climates (Plumlee et al., 1999). Reactions of acid waters with carbonates or other minerals in the tailings impoundments may produce higher-pH waters with lower metal contents. Also, reducing conditions may develop in the deeper portions of tailings impoundments. Both waters and solids from uranium mill tailings may have elevated concentrations of radioactive daughter products such as radon and radium that result from the radioactive decay of uranium (Landa, 1999); they may also have elevated concentrations of metals such as Co, Ni, Mo, and Se that are commonly associated with uranium ores, and elevated levels of total dissolved solids.

There are several potential environmental effects of mill tailings impoundments that are the focus of prevention and remediation efforts. In historic mining districts, mill tailings were commonly released directly into nearby streams and rivers. Erosion or failure of tailings impoundments may also release large volumes of finely ground tailings solids into the environment; substantial tailings deposits then can accumulate in low-flow portions of the streams into which they are released, where they can become a long-term, non-point source for acid drainage. Waters may leak from impoundments into the local ground or surface waters (e.g., Coggans et al., 1999), or may be released catastrophically into surface waters if the impoundment dam fails.

Prevention of environmental problems associated with mill tailings requires design of effective tailings impoundments that will not fail. Effective geotechnical characterization of the impoundment site, coupled with a detailed understanding of the risk for natural hazards such as earthquakes, landslides, and flash floods are therefore crucial in the design of the impoundments. Blending of sulfidic tailings with carbonate-rich material as the

tailings are placed in the impoundment may help to minimize the development of acid-rock drainage from the impoundment; however, tailings waters with near-neutral pH values may still carry elevated levels of metals such as Zn (Plumlee et al., 1999). A common method of tailings disposal that is quite effective from an environmental standpoint is the backfill of tailings-cement paste mixtures in underground workings; although this technique is primarily used to provide ground support, it may also help mitigate acid-rock drainage, as the cement helps neutralize acid generated by oxidation of sulfides in the tailings solids. In addition, backfilling of sulfide mill tailings in underground workings below the post-mining water table is carried out at a number of mining operations; once mining and pumping of ground water from the workings ceases, flooding of the backfilled workings submerges the tailings and precludes ready access of atmospheric oxygen.

As with acid-generating mine wastes, mill tailings can be remediated by isolation of acid-generating sulfides from the atmosphere; however, the large volumes of tailings that are typically generated by many large-scale mining operations may make such an approach quite expensive. For tailings that have been released into fluvial environments, removal of the tailings from the fluvial environment and isolation is an option. Alternatively, some remedial approaches have used lime addition to the upper portions of fluvial tailings deposits, which help mitigate (but do not entirely preclude) acid drainage generation in the deposits.

Organic chemicals and other reagents in tailings waters may be treated with a variety of chemical or bacterial destruction processes. Acid and metals in the tailings waters may be treated with the same types of approaches used to treat acid-mine drainage discussed previously.

Heap leach solids and processing solutions

At present, there are two main types of heap leach mineral processing utilized by the mining industry, including sulfuric acid heap leach processing of copper ores and cyanide heap leach processing of gold ores. Heap leach processing of copper ores involves application of sulfuric acid solutions to sulfide and (or) oxide copper ores. The copper is then leached from the ores and recovered using solvent extraction-electrowinning. The process solutions develop compositions similar to those of acid-mine drainage waters, but with generally lower pH and much higher acidities and concentrations of metals (due to the repeated recycling of the solutions in the heap), and so can be treated similarly to acid drainage. After efficient copper extraction has finished, the heaps may be treated by rinsing with dilute water; however, extremely large volumes of water may be required to accomplish sufficient rinsing. Alternatively, the heaps may be treated with alkaline solutions to raise the pH and precipitate secondary hydroxide and sulfate minerals in the heap pore spaces. If the heaps processed sulfide-rich ores, then the same potential for long-term acid generation exists as with sulfide-rich mine wastes, and the treatment options are the same as for the mine wastes.

Cyanide heap leach facilities use alkaline cyanide solutions to leach gold from oxide ores (Smith and Mudder, 1999; Mudder, 1999 in press). There are a number of geochemical and biogeochemical processes that degrade cyanide in the environment, including, for example, volatilization of HCN gas (triggered by mixing of the solutions with lower-pH surface waters), aerobic bacterial degradation to nitrate and carbon dioxide, precipitation

of insoluble cyanide compounds, and photolytic degradation (Smith and Mudder, 1999; Mudder, 1999 in press). These processes require time to completely degrade the cyanide, and the environmental effects of accidental cyanide spills may reflect the rate at which the cyanide is released to the environment compared to the rates of possible degradation mechanisms. In some cases, the environmental effects of accidental cyanide loss to the environment may more likely result from the adverse effects of metals such as Zn and Cu that had been complexed with the cyanide.

After cyanide heap leach processing is completed, or after the extraction capacity of the solutions is exhausted (due to buildup of thiocyanates, or other metal-cyanide complexes that reduce gold extraction efficiency) the leftover solutions are treated by a variety of processes such as peroxide or sulfur dioxide treatment to degrade the cyanide, land application (which spreads the cyanide over large enough areas to allow efficient photolytic degradation), or bacterial degradation (Smith and Mudder, 1999; Mudder, 1999 in press). As mentioned previously in the section on treatment of acid-mine drainage, mixing of spent cyanide solutions with acid-mine drainage may be a low-cost means to treat both at mine sites where both are an issue (Plumlee et al., 1995b).

Cyanide heap leach pads have in the past been treated after cessation of processing by repeated rinsing with dilute waters. In theory, the rinsing diluted the cyanide remaining in the pore spaces and dropped the pH of the cyanide solutions below the 9.36 value needed to maintain cyanide ions in solution, thereby leading to additional degradation by volatilization. However, large volumes of rinse water were needed for this process. Increasingly, mining companies are treating the process solutions draining from spent heaps by partially evaporating and then recycling them in the heaps; this is repeated until the volume of drainage is small enough to be treated through bioreactors or wetlands.

Studies evaluating cyanide and its degradation products provide important insights into the geochemical stability of cyanide in ground and surface waters (Smith and Mudder, 1999; Filipek, 1999). Recent stable isotope studies (Johnson et al., 1998) have shown that the stable carbon and nitrogen isotopic compositions of cyanide and possible degradation products (such as nitrates and aqueous carbonate) are also very useful for understanding the relative importance of the different cyanide degradation mechanisms present in active and abandoned heap leach pads.

Smelter wastes and soils affected by smelter emissions

Smelting and roasting extract metals from sulfide ores by combining the sulfides with fluxes (such as silica and carbonate minerals) in a high-temperature reducing environment. Native metals accumulate in the bottom of the furnace beneath slag, which forms by the combination of iron, calcium and other non-metallic elements in the ores and fluxes. The molten slag is then discarded; when it cools, solid slag is produced that contains abundant iron-silicate glass, and minerals. Calcium- and magnesium-bearing glasses and minerals also may be present depending upon the composition of the ores and fluxes used. The slags can have quite high metal contents, with the metals present as small inclusions of sulfides or metal oxides, or tied up within the silicate glasses and minerals (Parsons et al., 1998; references in Plumlee, 1999).

Gases rich in sulfur dioxide and carrying metal-rich particulates also are generated during smelting and roasting. Modern

smelters have extensive treatment procedures that scrub the gaseous emissions of much of their deleterious gases and their particulate load. However, historic smelting activities without such modern scrubbing equipment commonly left behind metal-rich deposits in the local soils, as well as vegetation killed by the effects of acid rain (generated by reactions of the sulfur dioxide with atmospheric water vapor).

The most common method for remediating smelter slag and soils affected by smelter emissions is isolation of the slag, and removal and isolation of affected topsoil.

ESS studies can be used to greatly increase the understanding of metal mobility from slag and soils (see references in Plumlee, 1999), information that can then be used to help guide and focus the remediation process. Mineralogical characterization, coupled with sequential chemical extraction studies of the slags and soils, can be used to understand how readily available the metals are in different slag types and soil horizons, thereby helping to focus the remedial efforts on the most problematic areas (Parsons et al., 1998). Analyses of plants and vegetables growing on the soils can show whether the metals are being taken up by the plants in sufficient quantities to be toxic to animals and humans that eat the plants. Lead isotope studies of soils and human lead (Gulson et al., 1996) can indicate the extent to which lead is being taken up from the soils relative from other sources such as lead-bearing paint. Smelters in many historic mining districts added metal-rich particulates to metal-rich soils derived from mineralized rocks; detailed geochemical sampling of the area affected by these smelters' emissions can be coupled with factor analysis of the geochemical data to help understand background metal levels and the distribution of sites most affected by the smelting (Chaffee, 1980, 1987).

SUMMARY

This chapter has given a very brief overview of a large number of earth-system science methods, studies, and reference links to other studies that can be used to better measure, understand, predict, mitigate, and remediate the environmental effects of mineral resource development. We have also shown examples of how these tools from the earth-system science toolkit can be applied in all phases of mineral resource development. The greatest benefits arise when methods from diverse disciplines (such as geology, geochemistry, hydrology, geophysics, ecology, and toxicology) are integrated and applied together to address mining-environmental issues.

We do not mean to imply that all tools that we have discussed here are suitable for application at all sites or in all instances; rather, the toolkit contains a wide variety of tools that are available for use at the discretion of those who best know the issues to be examined. However, many of the methods discussed here are already in widespread use by the mining industry, environmental consultants, and federal land managers and regulators as part of mine planning, permitting, and remediation. In the future, we expect that more of the methods and types of studies discussed here, as well as many new methods yet to be developed, will be widely used as a routine component of environmentally friendly mineral resource development.

REFERENCES

- Ackman, T.E., and Cohen, K.K., 1994, Geophysical methods: remote techniques applied to mining-related environmental and engineering problems: Proceedings, International Land Reclamation and Mine Drainage Conference and 3rd Internatl Conference on the Abatement of Acidic Drainage, U.S. Bureau of Mines Spec. Pub. No. SP 06D-94, v. 4, pp. 208–217.
- Alley, W.M. (ed.), 1993a, Regional ground-water quality: Van Nostrand Reinhold, New York, 634 pp.
- Alley, W.M., 1993b, Geostatistical models; *in* Alley, W.M. (ed.), Regional Ground-Water Quality: Van Nostrand Reinhold, New York, pp. 87–108.
- Alpers, C.N., and Blowes, D.W. (eds.), 1994, Environmental geochemistry of sulfide oxidation: American Chemical Society Symposium Series 550, 681 pp.
- Alpers, C.N., and Nordstrom, D.K., 1999, Geochemical modeling of water-rock interactions in mining environments; *in* Plumlee, G.S., and Logsdon, M.J. (eds.), The Environmental Geochemistry of Mineral Deposits, Part A. Processes, Techniques, and Health Issues: Society of Economic Geologists, Reviews in Economic Geology, v. 6A, pp. 289–323.
- Appel, C.A., and Reilly, T.E., 1994, Summary of selected computer programs produced by the U.S. Geological Survey for simulation of ground-water flow and quality, 1994: U.S. Geological Survey Circular 1104, 98 pp.
- ASTM, 1996, Standard test method for accelerated weathering of solid materials using a modified humidity cell: ASTM D5744-96, 13 pp.
- Atkins, D., Kempton, J.H., and Martin, T., 1997, Limnologic conditions in three existing Nevada pit lakes—Observations and modeling using CEQUAL-W2: Proceedings, 4th Internatl Conference on Acid Rock Drainage, Vancouver, B.C., Canada, May 31-June 6, v. 2, pp. 697–716.
- Australia Environment Protection Agency, 1997, Best Practice Environmental Management in Mining: Environment Australia, 13-volume set.
- Babitzke, H.R., Barsotti, A.F., Coffman, J.S., Thompson, J.G., and Bennett, H.J., 1982, The Bureau of Mines Mineral Availability System—An update of Information Circular 8654: U.S. Bureau of Mines Information Circular 8887, 54 pp.
- Bailey, R.G., 1995, Description of Ecoregions of the United States: U.S. Department of Agriculture, Forest Service, Miscellaneous Publication 1391, 108 pp., 1 plate.
- Bentley, H.W., Phillips, F.M., Davis, S.N., Habermehl, M.A., Airey, P.L., Calf, G.E., Elmore, D., Grove, H.E., and Torgersen, T., 1986, Chlorine-36 dating of very old groundwater 1. The great artesian basin, Australia: Water Resources Research, v. 22, pp. 1991–2001.
- Berg, A.W., and Carillo, F.V., 1980, MILS—The Mineral Industry Location System of the Federal Bureau of Mines: U.S. Bureau of Mines Information Circular 8815, 24 pp.
- Blowes, D.W., Ptacek, C.J., and Jambor, J.L., 1994, Remediation and prevention of low-quality drainage from tailings impoundments; *in* Jambor, J.L. and Blowes, D.W. (eds.), Environmental Geochemistry of Sulfide Mine-Wastes, Mineralogical Association of Canada, Short Course Notes, v. 22, pp. 365–379.
- Bonham-Carter, G.F., 1994, Geographic information systems for geoscientists—Modelling with GIS: Pergamon/Elsevier Science, Tarrytown, N.Y. and Kidlington, U.K., 398 pp.
- Bookstrom, A.A., Zientek, M.L., Box, S.E., Derkey, P.D., Elliott, J.E., Frishman, D., Ashley, R.P., Evarts, R.C., Stoesser, D.B., Moyer, L.A., Cox, D.P., and Ludington, S., 1996, Status and metal content of significant metallic mineral deposits in the Pacific Northwest—a contribution to the Interior Columbia Basin Ecosystem Management Project: U.S. Geological Survey Open-File Report 95-688 (also available online at <http://wrgis.wr.usgs.gov/open-file/of95-688/index.html>)
- Brierley, J.A., 1999, Biooxidation pretreatment of refractory sulfidic and sulfidic-carbonaceous gold ores and concentrates; *in* Filipek, L.H., and Plumlee, G.S. (eds.), The Environmental Geochemistry of Mineral Deposits, Part B. Case Studies and Research Topics: Society of Economic Geologists, Reviews in Economic Geology, v. 6B, pp. 539–547.
- Brouwers, E.M., Bradbury, J.P., and Nichols, D.J., 1996, Bioindicators of aquatic toxicity in Terrace Reservoir as related to Summitville Mine operations, Colorado: Geological Society of America, Abstracts with programs, v. 28, no. 7, p. 97.
- Campbell, D.L., Horton, R.J., Bisdorf, R.J., Fey, D.L., Powers, M.H., and Fitterman, D.V., 1999, Some geophysical methods for tailings/mine waste work: Proceedings, 6th Internatl Conference on Tailings and Mine Waste '99, Fort Collins, Colo., Jan. 24-27, A.A. Balkema, Rotterdam, ISBN 90 5809 025 6, pp. 35–43.
- Chaffee, M.A., 1980, Interpretation of geochemical anomalies in soil samples from a smelter-contaminated area, Eureka mining district, Nevada [abs.]: Technical Program, American Institute of Mining, Metallurgical, and Petroleum Engineers Annual Meeting, Feb. 1980, Las Vegas, Nev., pp. 56–57.
- Chaffee, M.A., 1987, Application of R-mode factor analysis to geochemical studies in the Eureka mining district and vicinity, Eureka and White Pine counties, Nevada; *in* Elliott, I.L., and Smee, B.M. (eds.), GEOEXPO/86, Exploration in the North American Cordillera: The Association of Exploration Geochemists, Vancouver, Canada, pp. 94–108.
- Chapelle, F.H., Bradley, P.M., and McMahon, P.B., 1993, Subsurface microbiology; *in* Alley, W.M. (ed.), Regional Ground-Water Quality: Van Nostrand Reinhold, New York, pp. 181–198.
- Chtaini, A., Bellaloui, A., Bailivy, G., Nariasiah, S., Lalancette, J., and Bilodeau, 1997, A study of acid mine drainage control by addition of alkaline mill paper waste: Proceedings, 4th Internatl Conference of Acid Rock Drainage, Vancouver, v. 3, pp. 1145–1162.
- Church, S.E., Holmes, C.W., Briggs, P.H., Vaughn, R.B., Cathcart, J., and Marot, M., 1993, Geochemical and Pb-isotope data from stream and lake sediments, and cores from the upper Arkansas River drainage—effects of mining at Leadville, Colorado, on heavy-metal concentrations in the Arkansas River: U.S. Geological Survey Open-File Report 93-534, 61 pp.
- Church, S.E., Kimball, B.A., Fey, D.L., Ferderer, D.A., Yager, T.J., and Vaughn, R.B., 1997, Source, transport, and partitioning of metals between water, colloids, and bed sediments of the Animas River, Colorado: U.S. Geological Survey Open-file Report 97-151, 135 pp.
- Church, S.E., Alpers, C.N., Vaughn, R.B., Briggs, P.H., and Slotton, D.G., 1999, Use of lead isotopes as natural tracers of metal contamination—A case study of the Penn Mine and Camanche Reservoir, California; *in* Filipek, L.H., and Plumlee, G.S. (eds.), The Environmental Geochemistry of Mineral Deposits, Part B. Case Studies and Research Topics: Society of Economic Geologists, Reviews in Economic Geology, v. 6B, pp. 567–582.
- Clark, I., and Fritz, P., 1997, Environmental Isotopes in Hydrogeology: Lewis Publishers with CRC Press, New York, 328 pp.
- Clark, R.N., and Roush, T.L., 1984, Reflectance spectroscopy—quantitative analysis techniques for remote sensing applications: Journal of Geophysical Research, v. 89, no. B7, pp. 6329–6340.
- Clayton, L.D., Bolis, J.L., Wildeman, L.R., and Updegraff, D.M., 1999, A case study on the aerobic and anaerobic removal of manganese by wetland processes; *in* Filipek, L.H., and Plumlee, G.S. (eds.), The Environmental Geochemistry of Mineral Deposits, Part B. Case Studies and Research Topics: Society of Economic Geologists, Reviews in Economic Geology, v. 6B, pp. 515–526.
- Coggans, C.J., Blowes, D.W., Robertson, W.D., and Jambor, J.L., 1999, The hydrogeochemistry of a nickel-mine tailings impoundment—Copper Cliff, Ontario; *in* Filipek, L.H., and Plumlee, G.S. (eds.), The Environmental Geochemistry of Mineral Deposits, Part B. Case Studies and Research Topics: Society of Economic Geologists, Reviews in Economic Geology, v. 6B, pp. 447–465.
- Cole, G.A., 1994, Textbook of Limnology: Waveland Press, Prospect Heights.
- Coplen, T.B., 1993, Uses of environmental isotopes; *in* Alley, W.M. (ed.), Regional Ground-Water Quality: Van Nostrand Reinhold, New York, pp. 227–254.
- Cox, D.P., and Singer, D.A. (eds.), 1986, Mineral deposit models: U.S.

- Geological Survey Bulletin 1693, 379 pp.
- Crock, J.G., Arbogast, B.F., and Lamothe, P.J., 1999, Laboratory methods for the analysis of environmental samples; *in* Plumlee, G.S., and Logsdon, M.J. (eds.), *The Environmental Geochemistry of Mineral Deposits, Part A. Processes, Techniques, and Health Issues*: Society of Economic Geologists, *Reviews in Economic Geology*, v. 6A, pp. 265–287.
- Custis, K., 1994, Application of geophysics to acid-mine drainage investigations, vol. 1—literature review and theoretical background: MS 09–06, California Department of Conservation, Office of Mine Reclamation, 100 pp.
- Da Rosa, C.D., and Lyon, J.S., 1997, *Golden dreams, poisoned streams*: Mineral Policy Center, Washington, 269 pp.
- Dallinger, R., and Rainbow, P.S. (eds.), 1993, *Ecotoxicology of metals in invertebrates*: Special Publication, Society of Environmental Toxicology and Chemistry, Lewis Publishers, 460 pp.
- Dalrymple, G.B., Czamanske, G.K., Fedorenko, V.A., Simonov, O.N., Lanphere, M.A., and Likhachev, A.P., 1995, A reconnaissance ⁴⁰Ar/³⁹Ar geochronologic study of ore-bearing and related rocks, Siberian Russia: *Geochimica et Cosmochimica Acta*, v. 59, pp. 2071–2083.
- Danielson, L.J., and Alms, L., 1995, The Summitville legacy—where do we go from here?; *in* Posey, H.H., Pendleton, J.A., and Van Zyl, D. (eds.), *Summitville Forum Proceedings*: Colorado Geological Survey Spec. Pub. No. 38, pp. 346–361.
- Davis, A., and Eary, L.E., 1997, Pit lake water quality in the western United States—An analysis of chemogenetic trends: *Mining Engineering*, v. 49, pp. 98–102.
- Davis, J.C., 1973, *Statistics and data analysis in geology*: John Wiley and Sons, New York, 550 pp.
- Domenico, P.A., and Schwartz, F.W., 1990, *Physical and chemical hydrogeology*: John Wiley and Sons, New York, 824 pp.
- du Bray, E.A. (ed.), 1995, Preliminary descriptive geoenvironmental models of mineral deposits: U.S. Geological Survey Open-File Report 95–231, 272 pp. (also available online at <http://minerals.cr.usgs.gov>)
- Dwyer, F.J., Schmitt, C.J., Finger, S.E., and Mehrle, P.M., 1988, Biochemical changes in longear sunfish, *Lepomis megalotis*, associated with lead, cadmium, and zinc from mine tailings: *Journal of Fisheries Biology*, v. 33, pp. 307–317.
- Edwards, T.K., and Glysson, G.D., 1988, Field methods for measurement of fluvial sediment: U.S. Geological Survey Open-File Report 86–531, 118 pp.
- Enviromine, 1999, Enviromine mining-environmental information website (http://www.enviromine.com/env_main.html).
- Erdman, J.A., Smith, K.S., and ter Kuile, M., 1997, Impact of the lower Alamosa river water on alfalfa, southwestern San Luis valley—1995 follow-up study of effects from the Summitville mine: U.S. Geological Survey Open-File Report 96–034, 32 pp.
- Evangelou, V.P., 1995, *Pyrite oxidation and its control*: CRC Press, Boca Raton, Fla., 293 pp.
- Faure, G., 1986, *Principles of isotope geology*: John Wiley and Sons, New York, 589 pp.
- Ferderer, D.A., 1996, National overview of abandoned mine land sites utilizing the Minerals Availability System (MAS) and Geographic Information Systems (GIS) technology: U.S. Geological Survey Open-File Report 96–549, 42 pp.
- Ficklin, W.H., and Mosier, E.L., 1999, Field methods for sampling and analysis of environmental samples for unstable and selected stable constituents; *in* Plumlee, G.S., and Logsdon, M.J. (eds.), *The Environmental Geochemistry of Mineral Deposits, Part A. Processes, Techniques, and Health Issues*: Society of Economic Geologists, *Reviews in Economic Geology*, v. 6A, pp. 249–264.
- Filipek, L.H., 1999, Determination of the source and pathway of cyanide-bearing mine water seepage; *in* Filipek, L.H., and Plumlee, G.S. (eds.), *The Environmental Geochemistry of Mineral Deposits, Part B. Case Studies and Research Topics*: Society of Economic Geologists, *Reviews in Economic Geology*, v. 6B, pp. 549–565.
- Filipek, L.H., VanWyngarden, T.J., Papp, C.S.E., and Curry, J., 1999, A multi-phased approach to predict acid production from porphyry copper-gold waste rock in an arid montane environment; *in* Filipek, L.H., and Plumlee, G.S. (eds.), *The Environmental Geochemistry of Mineral Deposits, Part B. Case Studies and Research Topics*: Society of Economic Geologists, *Reviews in Economic Geology*, v. 6B, pp. 433–445.
- Fitterman, D.V. (ed.), 1990, *Developments and applications of modern airborne electromagnetic surveys*: U.S. Geological Survey Bulletin 1925, 216 pp.
- Folger, P.F., Poeter, E., Wanty, R.B., Day, W., and Frishman, D., 1997, ²²²Rn transport in a fractured crystalline rock aquifer—results from numerical simulations: *Journal of Hydrology*, v. 195, pp. 45–77.
- Fontes, J.C., 1980, Environmental isotopes in groundwater hydrology; *in* Fritz, P., and Fontes, J.C. (eds.), *Handbook of Environmental Isotope Geochemistry*, vol. 1: Elsevier, N.Y., pp. 75–140.
- Freeze, R.A., and Cherry, J.A., 1979, *Groundwater*: Prentice Hall, Englewood Cliffs, N.J., 604 pp.
- Frost, T.P., Raines, G.L., Almqvist, C.A., and Johnson, B.R., 1996, Digital map of possible bat habitats in the Pacific Northwest—a contribution to the Interior Columbia Basin Ecosystem Management Project: U.S. Geological Survey Open-File Report 95–683, 24 pp., (also available on-line at <http://wrgis.wr.usgs.gov/open-file/>).
- Furniss, G., and Hinman, N.W., 1998, Ferricrete provides record of natural acid drainage, New World District, Montana; *in* Arehart, G.B., and Hulston, J.R. (eds.), *Water-Rock Interaction, Proceedings of the 9th Internat Symposium on Water-Rock Interaction*, Taupo, New Zealand: A.A. Balkema, Rotterdam, Brookfield, pp. 973–976.
- Garney, T.J., 1996, Acid mine drainage in northern Ontario; *in* Gibson, R.I., and Millegan, P.S. (eds.), *Geologic Applications of Gravity and Magnetism—Case Histories*: Society of Exploration Geophysicists *Geophysical References*, No. 8, pp. 112–113.
- Gough, L.P., Yanoski, T.M., Lichte, F.E., and Balistrieri, L.S., 1995, Preliminary interpretation of spatial and temporal trends in the chemistry of tree rings downstream from the Summitville Mine; *in* Posey, H.H., Pendleton, J.A., and Van Zyl, D. (eds.), *Summitville Forum Proceedings*: Colorado Geological Survey Spec. Pub. No. 38, pp. 236–243.
- Grauch, V.J.S., and Millegan, P.S., 1998, Mapping intrabasinal faults from high-resolution aeromagnetic data: *The Leading Edge*, pp. 53–55.
- Gray, J. E., Meier, A.L., O’Leary, R.M., Outwater, C., and Theodorakos, P.M., 1996, Environmental geochemistry of mercury deposits in southwestern Alaska—mercury contents in fish, stream-sediment, and stream-water samples; *in* Moore, T.E., and Dumolin, J.A. (eds.), *Geological Studies in Alaska by the U.S. Geological Survey, 1994*: U.S. Geological Survey Bulletin 2152, pp. 17–29.
- Gray, N.F., and O’Neill, C., 1997, Acid mine-drainage toxicity testing: *Environmental geochemistry and health*, v. 19, pp. 165–171.
- Guilbert, J., and Park, C., 1986, *The geology of ore deposits*: W.H. Freeman and Co., New York, 985 pp.
- Gulson, B.L., Pisaniello, D., McMichael, A.J., Mizon, K.J., Korsch, M.J., Luke, C., Ashbolt, R., Pederson, D.G., Vimpani, G., and Mahaffey, K.R., 1996, Stable lead isotope profiles in smelter and general urban communities—A comparison of environmental and blood measures: *Environmental Geochemistry and Health*, v. 18, pp. 147–163.
- Hamlin, S.N., and Alpers, C.N., 1996, Hydrogeology and geochemistry of acid mine drainage in ground water in the vicinity of Penn Mine and Camanche Reservoir, Calaveras County, California—second-year summary, 1992–93: U.S. Geological Survey Water-Resources Investigations Report 96-4257, 44 pp.
- Hedin, R.S., Nairn, R.W., and Kleinmann, R.L.P., 1994, Passive treatment of coal mine drainage: U.S. Bureau of Mines Information Circular IC 9389, 35 pp.
- Herbert, R.B., Benner, S.G., and Blowes, D.W., 1998, Reactive barrier treatment of groundwater contaminated by acid mine drainage—Sulfur accumulation and sulfide formation; *in* Herbert, M., and Kovar, K. (eds.), *Groundwater Quality—Remediation and Protection*: IAHS Pub. No. 250, International Assoc. of Hydrological Sciences, IAHS Press, Wallingford, pp. 451–457.

- Holland, H.D., and Petersen, U., 1995, Living dangerously—The earth, its resources, and the environment: Princeton University Press, Princeton, 490 pp.
- Horowitz, A.J., Demas, C.R., Fitzgerald, K.K., Miller, T.L., and Rickert, D.A., 1994, U.S. Geological Survey protocol for the collection and processing of surface-water samples for the subsequent determination of inorganic constituents in filtered water: U.S. Geological Survey Open-File Report 94-539, 57 pp.
- Horowitz, A.J., Rinella, F.A., Lamothe, P., Miller, T.L., Roche, R.L., and Rickert, D.A., 1990, Variations in suspended sediment and associated trace-element concentrations in selected riverine cross sections: *Environmental Science and Technology*, v. 24, pp. 1313–1320.
- Horowitz, A.J., Robbins, J.A., Elrick, K.A., and Cook, R.B., 1996, Bed sediment-trace element geochemistry of Terrace Reservoir, near Summitville, southwestern, Colorado: U.S. Geological Survey Open-File Report 96-344, 41 pp.
- Hudson, T.L., Fox, F.D., and Plumlee, G.S., 1999 in press, Metal mining and the environment: AGI Environmental Awareness Series, American Geological Institute, Alexandria, Va.
- Huyakorn, P., and Pinder, G.F., 1983, Computational methods in subsurface flow: Academic Press, New York, 473 pp.
- ICARD, 1997, Proceedings, 4th Internatl Conference on Acid Rock Drainage, Vancouver, B.C., Canada: 4 volume set.
- Ingraham, N.L., and Taylor, B.E., 1991, Light stable isotope systematics of large-scale hydrologic regimes in California and Nevada: *Water Resources Research*, v. 27, pp. 77–90.
- Jambor, J.L., and Blowes, D.W. (eds.), 1994, Short course on environmental geochemistry of sulfide-mine wastes: Mineralogical Association of Canada, Short Course Handbook, v. 22, 438 pp.
- Johnson, C.A., Grimes, D.J., and Rye, R.O., 1998, Accounting for cyanide and its degradation products at three Nevada gold mines—Constraints from stable C- and N-isotopes: U.S. Geological Survey Open-File Report 98-753, 16 pp. (also available online at: <http://greenwood.cr.usgs.gov/pub/open-file-reports/ofr-98-0753/>).
- Johnston, R.J., 1980, Multivariate Statistical Analysis in Geography: Longman, London, 280 pp.
- Kelly, M.G., 1999, Effects of heavy metals on the aquatic biota; *in* Plumlee, G.S., and Logsdon, M.J. (eds.), *The Environmental Geochemistry of Mineral Deposits, Part A. Processes, Techniques, and Health Issues*: Society of Economic Geologists, *Reviews in Economic Geology*, v. 6A, pp. 363–371.
- Kempton, J.H., Locke, W., Atkins, D., Nicholson, A.D., Bennett, M., and Bliss, L., 1997, Probabilistic prediction of water quality in the Twin Creeks Mine pit lake, Golconda, Nevada, USA: *Proceedings, 4th Internatl Conference on Acid Rock Drainage, Vancouver, B.C., Canada, May 31-June 6, v. 2, pp. 889–904.*
- Kesler, S.E., 1994, Mineral resources, economics and the environment: Macmillan, 391 pp.
- Kimball, B.A., 1984, Ground water age determinations, Piceance Creek Basin, Colorado; *in* Hichon, B., and Wallick, E.I. (eds.), *First Canadian/American Conference on Hydrogeology*: National Water Well Association, Dublin, Ohio, pp. 149–177.
- Kimball, B.A., 1996, Use of tracer injections and synoptic sampling to measure metal loading from acid mine drainage: U.S. Geological Survey Fact Sheet 245-96.
- Kimball, B.A., 1999, Seasonal variation in metal concentrations in a stream affected by acid mine drainage, St. Kevin Gulch, Colorado; *in* Filipek, L.H., and Plumlee, G.S. (eds.), *The Environmental Geochemistry of Mineral Deposits, Part B. Case Studies and Research Topics*: Society of Economic Geologists, *Reviews in Economic Geology*, v. 6B, pp. 467–478.
- Kimball, B.A., Broshears, R.E., Bencala, K.E., and McKnight, D.M., 1994, Coupling of hydrologic transport and chemical reactions in a stream affected by acid mine drainage: *Environmental Science and Technology*, v. 28, pp. 2065–2073.
- King, T.V.V. (ed.), 1995, Environmental considerations of active and abandoned mine lands—Lessons from Summitville, Colorado: U.S. Geological Survey Bulletin 2220, 38 pp. (available online at <http://minerals.cr.usgs.gov/pubs.html>)
- Kirkham, R.D., Sinclair, W.D., Thorpe, R.I., and Duke, J.M. (eds.), 1993, Mineral deposit modeling: Geological Association of Canada Spec. Paper 40, 770 pp.
- Krieger, G.R., Hattemer-Frey, H.A., and Kester, J.E., 1999, Bioavailability of metals in the environment—Implications for health risk assessment; *in* Plumlee, G.S., and Logsdon, M.J. (eds.), *The Environmental Geochemistry of Mineral Deposits, Part A. Processes, Techniques, and Health Issues*: Society of Economic Geologists, *Reviews in Economic Geology*, v. 6A, pp. 357–361.
- Kwong, Y.T.J., 1993, Prediction and prevention of acid rock drainage from a geological and mineralogical perspective: MEND Project 1.32.1, 47 pp. (available through <http://mend2000.nrcan.gc.ca/>)
- Lambeth, R.H., 1999, Natural attenuation of acidic drainage from sulfidic tailings at a site in Washington State; *in* Filipek, L.H., and Plumlee, G.S. (eds.), *The Environmental Geochemistry of Mineral Deposits, Part B. Case Studies and Research Topics*: Society of Economic Geologists, *Reviews in Economic Geology*, v. 6B, pp. 479–491.
- Landa, E.R., 1999, Geochemical and biogeochemical controls on element mobility in and around uranium mill tailings; *in* Filipek, L.H., and Plumlee, G.S. (eds.), *The Environmental Geochemistry of Mineral Deposits, Part B. Case Studies and Research Topics*: Society of Economic Geologists, *Reviews in Economic Geology*, v. 6B, pp. 527–538.
- Lee, G.K., 1999 in press, Multiple data layer modeling and analysis in assessments; *in* Fabbri, (ed.), *Proceedings, 1998 NATO Advanced Study Institute Workshop, Deposit and Geoenvironmental Models for Resource Exploitation and Environmental Security*: Kluwer Academic Publishers.
- Lee, G.K., Knepper, D., Jr., McCafferty, A., Miller, S., Sole, T., Swayze, G., and Watson, K., 1999a in press, Applications of remotely sensed data in geoenvironmental assessments; *in* Fabbri, (ed.), *Proceedings, 1998 NATO Advanced Study Institute Workshop, Deposit and Geoenvironmental Models for Resource Exploitation and Environmental Security*: Kluwer Academic Publishers.
- Lee, G.K., McCafferty, A.E., Alminas, H.V., Bankey, V., Elliott, J.E., Frishman, D., Knepper, D.H., Jr., Kulik, D.M., Marsh, S.P., Phillips, J.D., Pitkin, J.A., Smith, S.M., Stoesser, D.B., Tysdal, R.G., and Van Gosen, B.S., 1999b in press, *Geoenvironmental Assessment of Montana*: U.S. Geological Survey Digital Data Series.
- Leinz, R.W., Sutley, S.J., and Briggs, P.H., 1999, The use of sequential extractions for the chemical speciation of mine wastes: *Proceedings, 6th Internatl Conference on Tailings and Mine Waste '99, Fort Collins, Colo., Jan 24-27, A.A. Balkema, Rotterdam, ISBN 90 5809 025 6, pp. 555–561.*
- Light, T.D., Barnwell, C.E., and Andrade, J., 1997, Livengood geoexplorer—An interactive geologic database on CD-ROM, Livengood Quadrangle, Alaska: U.S. Geological Survey Open-File Report 97-484-E.
- Lillesand, T.M., and Kiefer, R.W., 1987, *Remote Sensing and Image Interpretation*: John Wiley and Sons, New York.
- Logsdon, M.J., and Basse, B., 1991, Quantitative evaluation of Pb-Zn mine wastes for subgrade disposal—Characterization versus classification in a Superfund environment: *Proceedings of the 1991 AIME Annual meeting, Denver, Colorado, Environmental Management for the 1990's*, pp. 207–212.
- McCafferty, A., Bankey, V., and Brenner, K.C., 1998, Montana aeromagnetic and gravity maps and data: U.S. Geological Survey Open-File-Report 98-333 (<http://greenwood.cr.usgs.gov/pub/open-file-reports/ofr-98-0333/mt.html>).
- McCartan, L., LaTurno, N.M., and Ambroziak, R.A., 1998, Mines and mineral processing sites in the United States: U.S. Geological Survey Geologic Investigations Series Map I-2654.
- MEND, 1999, Mine environment, neutral drainage: Natural Resources Canada website (<http://mend2000.nrcan.gc.ca/>).
- Mercer, J.W., and Faust, C.R., 1981, Groundwater modeling: National Water Well Association, Dublin, Ohio.
- Mezquita, F., Hernandez, R., and Rueda, J., 1997, Ecology and distribu-

- tion of ostracods in a polluted Mediterranean River: Abstracts Volume, 13th International Symposium on Ostracoda, University of Greenwich. (no pagination).
- Miedecke, J., Miller, S., Gowen, M., Ritchie, I., Johnston, J., and McBride, P., 1997, Remediation options (including copper recovery by SX/EW) to reduce acid drainage from historical mining operations at Mount Lyell, Western Tasmania, Australia: Proceedings, 4th International Conference on Acid Rock Drainage, Vancouver, v. 4, pp. 1451–1468.
- Miller, G.C., Lyons, W.B., and Davis, A., 1996, Understanding the water quality of pit lakes: *Environmental Science and Technology*, v. 30, pp. 117A–123A.
- Miller, W.R., and McHugh, J.B., 1999, Calculations of geochemical baselines of stream waters in the vicinity of Summitville, Colorado, before historic underground mining and prior to recent open-pit mining; *in* Filipek, L.H., and Plumlee, G.S. (eds.), *The Environmental Geochemistry of Mineral Deposits, Part B. Case Studies and Research Topics*: Society of Economic Geologists, *Reviews in Economic Geology*, v. 6B, pp. 505–514.
- Miller, W.R., Ficklin, W.H., and Learned, R.E., 1982, Hydrogeochemical prospecting for porphyry copper deposits in the tropical-marine climate of Puerto Rico: *Journal of Geochemical Exploration*, v. 16, pp. 217–233.
- Miller, W.R., Bassett, R.L., McHugh, J.B., and Ficklin, W.H., 1999, The behavior of trace metals in water during natural acid sulfate weathering in an Alpine Watershed; *in* Filipek, L.H., and Plumlee, G.S. (eds.), *The Environmental Geochemistry of Mineral Deposits, Part B. Case Studies and Research Topics*: Society of Economic Geologists, *Reviews in Economic Geology*, v. 6B, pp. 493–503.
- Mills, A.L., 1999, The role of bacteria in environmental geochemistry; *in* Plumlee, G.S., and Logsdon, M.J. (eds.), *The Environmental Geochemistry of Mineral Deposits, Part A. Processes, Techniques, and Health Issues*: Society of Economic Geologists, *Reviews in Economic Geology*, v. 6A, pp. 125–132.
- Mineral Policy Center, 1999, Mineral Policy Center website (<http://www.mineralpolicy.org/>)
- Montour, M.R., Hageman, P.L., Meier, A.L., Theodorakos, P., Briggs, P.H., 1998a, Leachate chemistry data for solid mine waste composite samples from Silverton and Leadville, Colorado: U.S. Geological Survey Open-File Report 98–621, 46 pp.
- Montour, M.R., Hageman, P.L., Meier, A.L., Theodorakos, P., and Briggs, P.H., 1998b, EPA method 1312 (synthetic precipitation leaching procedure) leachate chemistry for solid mine waste composite samples from Silverton and Leadville, Colorado: U.S. Geological Survey Open-File Report 98–624, 24 pp.
- Mook, W.G., 1980, Carbon-14 in hydrogeological studies; *in* Fritz, P., and Fontes, J.C. (eds.), *Handbook of Environmental Isotope Geochemistry*, Volume 1: Elsevier, New York, pp. 49–74.
- Moore, J.N., Luoma, S.N., and Peters, D., 1991, Downstream effects of mine effluent on an intermontane riparian system: *Canadian Journal of Fisheries and Aquatic Sciences*, v. 48, pp. 222–232.
- Morin, K.A., and Hutt, N.M., 1997, Environmental geochemistry of mine-site drainage—Practical theory and case studies: MDAG Publishing, Vancouver, B.C., Canada, 333 pp.
- Mudder, T.I. (ed.), 1999 in press, *The Cyanide Monograph*: Mining Journal Books.
- National Mining Association, 1999, National Mining Association website (<http://www.nma.org/>).
- Natural Resources Canada, 1999, Canadian Minerals Yearbook website (http://www.nrcan.gc.ca/mms/cmy/index_e.html).
- Nimick, D.A., and Moore, J.N., 1994, Stratigraphy and chemistry of sulfidic flood-plain sediments in the Upper Clark Fork valley, Montana; *in* Alpers, C.N., and Blowes, D.W. (eds.), *Environmental Geochemistry of Sulfide Oxidation*: American Chemical Society Symposium Series 550, pp. 276–288.
- Nimick, D.A., and von Guerard, P., 1998, Science for watershed decisions on abandoned mine lands—review of preliminary results, Denver, Colorado, February 4–5, 1998: U.S. Geological Survey Open-File Report 98–297, 71 pp.
- NOAA, 1999, National Oceanic and Atmospheric Administration, National Climatic Data Center web site: <http://www.noaa.ncdc.gov/>
- Nordstrom, D.K., 1999, Some fundamentals of aqueous geochemistry; *in* Plumlee, G.S., and Logsdon, M.J. (eds.), *The Environmental Geochemistry of Mineral Deposits, Part A. Processes, Techniques, and Health Issues*: Society of Economic Geologists, *Reviews in Economic Geology*, v. 6A, pp. 117–123.
- Nordstrom, D.K., and Alpers, C.N., 1999, Geochemistry of acid mine waters; *in* Plumlee, G.S., and Logsdon, M.J. (eds.), *The Environmental Geochemistry of Mineral Deposits, Part A. Processes, Techniques, and Health Issues*: Society of Economic Geologists, *Reviews in Economic Geology*, v. 6A, pp. 133–160.
- NRC, 1996, Rock fractures and fluid flow, contemporary understanding and applications: National Research Council, National Academy Press, 551 pp.
- Ohmoto, H., and Rye, R.O., 1979, Isotopes of sulfur and carbon; *in* Barnes, H. (ed.), *The geochemistry of hydrothermal ore deposits*: John Wiley and Sons, New York, pp. 509–567.
- Ortiz, R.F., von Guerard, P.B., and Walton-Day, K., 1995, Effect of a localized rainstorm on the water quality of the Alamosa River upstream from Terrace Reservoir, south-central Colorado, August 9–10, 1993; *in* Posey, H.H., Pendleton, J.A., and Van Zyl, D. (eds.), *Proceedings, Summitville Forum '95*: Colorado Geological Survey Spec. Pub. No. 38, pp. 171–177.
- Östlund, P., Torssander, P., Morth, C.M., and Claesson, S., 1995, Lead and sulfur isotope dilution during dispersion from the Falun mining area: *Journal of Geochemical Exploration*, v. 52, pp. 91–95.
- Paillet, F.L., 1993, Using borehole geophysics and cross-borehole flow testing to define hydraulic connections between fracture zones in bedrock aquifers: *Journal of Applied Geophysics*, v. 30, pp. 261–279.
- Paillet, F.L., Hess, A.H., Cheng, C.H., and Hardin, E., 1987, Characterization of fracture permeability with high-resolution vertical flow measurements during borehole pumping: *Ground Water*, v. 25, pp. 28–40.
- Parsons, M.B., Einaudi, M.T., Bird, I.K., and Alpers, C.N., 1998, Geochemical and mineralogical controls on trace-element release from base-metal slag deposits at Penn Mine, Calaveras County, California: *EOS, Transactions, American Geophysical Union*, v. 79, no. 45, supplement, pp. F354.
- Peters, W.C., 1987, *Exploration and mining geology*: John Wiley, New York.
- Phillips, J.D., Duval, J.S., and Ambroziak, R.A., 1993, National geophysical data grids—gamma-ray, gravity, magnetic, and topographic data for the conterminous United States: U.S. Geological Survey Digital Data Series DDS-9.
- Pioneer Technical Services, 1994, Abandoned hardrock mine priority sites, summary report: Montana Department of State Lands, Abandoned Mines and Reclamation Bureau, Engineering Services Agreement DSL-AMRB No. 004, Summary Report, 314 pp.
- Plumlee, G.S., 1999, The environmental geology of mineral deposits; *in* Plumlee, G.S., and Logsdon, M.J. (eds.), *The Environmental Geochemistry of Mineral Deposits, Part A. Processes, Techniques, and Health Issues*: Society of Economic Geologists, *Reviews in Economic Geology*, v. 6A, pp. 71–116.
- Plumlee, G.S., Gray, J.E., Roeber, M.M., Jr., Coolbaugh, M., Flohr, M., and Whitney, G., 1995a, The importance of geology in understanding and remediating environmental problems at Summitville; *in* Posey, H.H., Pendleton, J.A., and Van Zyl, D. (eds.), *Summitville Forum Proceedings*: Colorado Geological Survey Spec. Pub. No. 38, pp. 13–22.
- Plumlee, G.S., Smith, K.S., Mosier, E.L., Ficklin, W.H., Montour, M., Briggs, P.H., and Meier, A.L., 1995b, Geochemical processes controlling acid-drainage generation and cyanide degradation at Summitville; *in* Posey, H.H., Pendleton, J.A., and Van Zyl, D. (eds.), *Summitville Forum Proceedings*: Colorado Geological Survey Spec. Pub. No. 38, pp. 23–34.
- Plumlee, G.S., Streufert, R.K., Smith, K.S., Smith, S.M., Wallace, A.,

- Toth, M., Nash, J.T., Robinson, R., Ficklin, W.H., 1995c, Geology-based map of potential metal-mine drainage hazards in Colorado: U.S. Geological Survey Open-File Report 95-26 (also available online at <http://minerals.cr.usgs.gov>).
- Plumlee, G.S., Smith, K.S., Montour, M.R., Ficklin, W.H., and Mosier, E.L., 1999, Geologic controls on the composition of natural waters and mine waters draining diverse mineral-deposit types; in Filipek, L.H., and Plumlee, G.S. (eds.), *The Environmental Geochemistry of Mineral Deposits, Part B. Case Studies and Research Topics*: Society of Economic Geologists, *Reviews in Economic Geology*, v. 6B, pp. 373-432.
- Plummer, L.N., Michel, R.L., Thurman, E.M., and Glynn, P.D., 1993, Environmental tracers for age dating young ground water; in Alley, W.M. (ed.), *Regional Ground-Water Quality*: Van Nostrand Reinhold, New York, pp. 255-294.
- Posey, H.H., Pendleton, J.A., and Van Zyl, D. (eds.), 1995, *Summitville Forum Proceedings*: Colorado Geological Survey Spec. Pub. No. 38, 375 pp.
- Price, J.G., Shevenell, L., Henry, C.D., Rigby, J.G., Christensen, L.G., Lechler, P.J., Desilets, M.O., Fields, R., Driesner, D., Durbin, B., and Lombardo, W., 1995, Water quality at inactive and abandoned mines in Nevada: Nevada Bureau of Mines and Geology Open-File Report 95-4, 73 pp. (<http://www.nbmgn.unr.edu>).
- Raines, G.L., Johnson, B.R., Frost, T.P., and Zientek, M.L., 1996, Digital maps of compositionally classified lithologies derived from 1:500,000 scale geologic maps for the Pacific Northwest—A contribution to the Interior Columbia Basin Ecosystem Management Project: U.S. Geological Survey Open-File Report 95-685 (also available online at <http://wrgis.wr.usgs.gov/open-file/of95-685/index.html>).
- Ramsay, J.G., and Huber, M.I., 1987, *The techniques of modern structural geology, Volume 2—Folds and fractures*: Academic Press, Harcourt Brace Jovanovich Publishers, London, 700 pp.
- Rantz, S.E., and others, 1982, Measurement and computation of stream flow—v.1, measurement of stage and discharge—v.2, computation of discharge: U.S. Geological Survey Water Supply Paper 2175, 631 pp.
- Ranville, J.F., and Schmiermund, R.L., 1999, General aspects of aquatic colloids in environmental geochemistry; in Plumlee, G.S., and Logsdon, M.J. (eds.), *The Environmental Geochemistry of Mineral Deposits, Part A. Processes, Techniques, and Health Issues*: Society of Economic Geologists, *Reviews in Economic Geology*, v. 6A, pp. 183-199.
- Ripley, E.A., Redmann, R.E., Crowder, A.A., 1996, *Environmental Effects of Mining*: St. Lucie Press, Delray Beach, Fla., 356 pp.
- Ritchie, J.C., and McHenry, J.R., 1984, Application of radioactive ^{137}Cs for measuring soil erosion and sediment accumulation rates and patterns—a review: *Journal of Environmental Quality*, v. 19, pp. 215-233.
- Robbins, J.A., 1978, Geochemical and geophysical applications of radioactive lead isotopes; in *The Biogeochemistry of Lead in the Environment*: Elsevier/North Holland Biomedical Press, Amsterdam, pp. 285-383.
- Rose, A.W., Hawkes, H.E., and Webb, J.S., 1979, *Geochemistry in mineral exploration*, 2nd ed.: Academic Press, New York, 657 pp.
- Ross, M., 1999, The health effects of mineral dusts; in Plumlee, G.S., and Logsdon, M.J. (eds.), *The Environmental Geochemistry of Mineral Deposits, Part A. Processes, Techniques, and Health Issues*: Society of Economic Geologists, *Reviews in Economic Geology*, v. 6A, pp. 339-356.
- Rye, R.O., and Alpers, C.N., 1997, The stable isotope geochemistry of jarosite: U.S. Geological Survey Open-File Report 97-88, 28 pp.
- Saltus, R.W., and Simmons, G.C., 1997, Composite and merged aeromagnetic data for Alaska—a website for distribution of gridded data and plot files: U.S. Geological Survey Open-File-Report 97-520 (<http://greenwood.cr.usgs.gov/pub/open-file-reports/ofr-97-0520/alaskamag.html>).
- Schrenk, M.O., Edwards, K.J., Goodman, R.M., Hamers, R.J., and Banfield, J.F., 1998, Distribution of *Thiobacillus ferrooxidans* and *Leptospirillum ferrooxidans*—Implications for generation of acid mine drainage: *Science*, v. 279, pp. 1519-1522.
- Schruben, P.G., Arndt, R.E., and Bawiec, W.J., 1998, Geology of the conterminous United States at 1:2,500,000 scale—A digital representation of the 1974 P.B. King and H.M. Beikman map: U.S. Geological Survey Digital Data Series 11, Release 2 (<http://minerals.er.usgs.gov:80/kb/dd-11.html>).
- Shelp, G.S., Chesworth, W., and Spiers, G., 1995, The amelioration of acid mine drainage by an in situ electrochemical method, Part 1. Employing scrap iron as the sacrificial anode: *Applied Geochemistry*, v. 10, pp. 705-713.
- Shelp, G.S., Chesworth, W., and Spiers, G., 1996, The amelioration of acid mine drainage by an in situ electrochemical method, Part 2. Employing aluminum and zinc as sacrificial anodes: *Applied Geochemistry*, v. 11, pp. 425-432.
- Shevenell, L., 1996, Statewide potential evapotranspiration maps for Nevada: Nevada Bureau of Mines and Geology Report 48, 32 pp. (<http://www.nbmgn.unr.edu>).
- Skousen, J.G., and Ziemkeiwicz, P.F. (compilers), 1995, *Acid mine drainage—Control and Treatment*: National Mine Land Reclamation Center, West Virginia University, Morgantown, 255 pp.
- Smith, A.C.S., and Mudder, T.I., 1999, The environmental geochemistry of cyanide; in Plumlee, G.S., and Logsdon, M.J. (eds.), *The Environmental Geochemistry of Mineral Deposits, Part A. Processes, Techniques, and Health Issues*: Society of Economic Geologists, *Reviews in Economic Geology*, v. 6A, pp. 229-248.
- Smith, K.S., 1999, Metal sorption on mineral surfaces—An overview with examples relating to mineral deposits; in Plumlee, G.S., and Logsdon, M.J. (eds.), *The Environmental Geochemistry of Mineral Deposits, Part A. Processes, Techniques, and Health Issues*: Society of Economic Geologists, *Reviews in Economic Geology*, v. 6A, pp. 161-182.
- Smith, K.S., and Huyck, H.L.O., 1999, An overview of the abundance, relative mobility, bioavailability, and human toxicity of metals; in Plumlee, G.S., and Logsdon, M.J. (eds.), *The Environmental Geochemistry of Mineral Deposits, Part A. Processes, Techniques, and Health Issues*: Society of Economic Geologists, *Reviews in Economic Geology*, v. 6A, pp. 29-70.
- Smith, K.S., Ficklin, W. H., Plumlee, G. S., and Meier, A. L., 1992, Metal and arsenic partitioning between water and suspended sediment at mine-drainage sites in diverse geologic settings: *Proceedings, 7th Internat Water-Rock Interaction Conference*, Park City, Utah, July pp. 443-447.
- Smith, S.M., 1997, National geochemical database—reformatted data from the National Uranium Resource Evaluation (NURE) Hydrogeochemical and Stream Sediment Reconnaissance (HSSR) Program: U.S. Geological Survey Open-File Report 97-0492 (<http://greenwood.cr.usgs.gov/pub/open-file-reports/ofr-97-0492/>).
- Solley, W.B., Pierce, R.R., and Perlman, H.A., 1998, Estimated use of water in the United States in 1995: U.S. Geological Survey Circular 1200, 71 pp.
- Swayze, G.A., R.N. Clark, Pearson, R.M., Livo, K.E., 1996, Mapping acid-generating minerals at the California Gulch Superfund Site in Leadville, Colorado using imaging spectroscopy: *Summaries of the 6th Annual JPL Airborne Earth Science Workshop*, JPL Pub. No. 96-4, March 4-8, pp. 231-234.
- Taylor, B.E., and Wheeler, M.C., 1994, Sulfur- and oxygen-isotope geochemistry of acid-mine drainage in the western United States—Field and experimental studies revisited; in Alpers, C.N., and Blowes, D.W. (eds.), *Environmental Geochemistry of Sulfide Oxidation*: American Chemical Society Symposium Series 550, pp. 481-514.
- Todd, J.W., and Struhsacker, D.W., 1997, Environmentally responsible mining—results and thoughts regarding a survey of North American metallic mineral mines: Society for Mining, Metallurgy, and Exploration, Inc., Preprint 97-304, 15 pp.
- Tura, M.A.C., Johnson, L.R., Majer, E.L., and Peterson, J.E., 1992, Application of diffraction tomography to fracture detection: *Geophysics*, v. 57, pp. 245-257.
- U.S. EPA, 1986-1995, Test methods for evaluating solid waste, volumes I and II: U.S. Environmental Protection Agency (SW-846), 3rd ed., Nov. 1986, with revisions through revision 2b, April 4, 1995.

- U.S. EPA, 1995, Applicability of the toxicity characteristic leaching procedure to mineral processing wastes: U.S. Environmental Protection Agency, 25 pp. plus appendices.
- U.S. EPA, 1997, Introduction to Hard Rock Mining, A CD-ROM application: U.S. Environmental Protection Agency 530-C-97-005.
- U.S. EPA STORET, 1999, U.S. Environmental Protection Agency STORET water quality database overview website (<http://www.epa.gov/owow/wtr1/STORET/zip/overview.html>).
- USGS, 1982, A U.S. Geological Survey data standard—codes for the identification of hydrologic units in the United States and Caribbean outlying areas: U.S. Geological Survey Circular 878-A, 115 pp.
- USGS Earth and Environment, 1999, Earth and environmental internet resources registry: USGS website (<http://info.er.usgs.gov/network/science/earth/earth.html>).
- USGS Earthquake Hazards, 1999, U.S. Geological Survey Earthquake Hazards web site (<http://quake.wr.usgs.gov/hazprep/index.html#Hazards>).
- USGS Landslide Hazards, 1999, U.S. Geological Survey Landslide Hazards website (http://geohazards.cr.usgs.gov/html_files/landslides/nationalmap/national.html).
- USGS MDIG, 1999, Mine Drainage Interest Group, U.S. Geological Survey website (<http://mine-drainage.usgs.gov/mine/>).
- USGS Mineral Data Bases, 1999 in press, U.S. Geological Survey Mineral Data Bases, Release 1: U.S. Geological Survey Digital Data Series.
- USGS Minerals Information, 1999, U.S. Geological Survey minerals information website (<http://minerals.er.usgs.gov>).
- USGS Mineral Resources Program, 1999, U.S. Geological Survey Mineral Resources Program website (<http://minerals.er.usgs.gov>).
- USGS SpecLab, 1999, U.S. Geological Survey AVIRIS remote sensing website (<http://speclab.cr.usgs.gov>).
- USGS Water Data, 1999, Water Resources Division water data: U.S. Geological Survey website (<http://water.usgs.gov/data.html>).
- USGS and Servicio Geológico de Bolivia, 1992, Geology and mineral resources of the Altiplano and Cordillera Occidental, Bolivia: U.S. Geological Survey Bulletin 1975, 365 pp., 8 map plates.
- van Geen, A., and Chase, Z., 1998, Recent mine spill adds to contamination of southern Spain: EOS, Transactions, American Geophysical Union, v. 79, no. 38, pp. 449, 455.
- Van Loenen, R.E., and Gibbons, A.B., 1997, Mineral resource potential and geology of the San Juan National Forest, Colorado: U.S. Geological Survey Bulletin 2127, 140 pp., 4 map plates.
- Van Metre, P.C., Callender, E., and Fuller, C.C., 1997, Historical trends in organochlorine compounds in river basins identified using sediment cores from reservoirs: Environmental Science and Technology, v. 31, pp. 2339–2344.
- Vasconcelos, P.M., Becker, T.A., Renne, P.R., and Brimhall, G.H., 1994, Direct dating of weathering phenomena by ^{40}K - ^{40}Ar and ^{40}Ar - ^{39}Ar analysis of supergene K-Mn oxides: Geochimica et Cosmochimica Acta, v. 58, pp. 1635–1665.
- von Guerard, P., and Ortiz, R.F., 1995, Effects of sampling methods on copper and iron concentrations, Alamosa river, south-central Colorado, 1993; *in* Posey, H.H., Pendleton, J.A., and Van Zyl, D. (eds.), Summitville Forum Proceedings: Colorado Geological Survey Spec. Pub. No. 38, pp. 171–177.
- Walton-Day, K., 1999, Geochemistry of the processes that attenuate acid mine drainage in wetlands; *in* Plumlee, G.S., and Logsdon, M.J. (eds.), The Environmental Geochemistry of Mineral Deposits, Part A. Processes, Techniques, and Health Issues: Society of Economic Geologists, Reviews in Economic Geology, v. 6A, pp. 215–228.
- Walton-Day, K., Ortiz, R.F., and von Guerard, P.B., 1995, Sources of water having elevated metal concentrations in the upper Alamosa River from the headwaters to the outlet of Terrace Reservoir, south-central Colorado, April-September, 1993; *in* Posey, H.H., Pendleton, J.A., and Van Zyl, D. (eds.), Summitville Forum Proceedings: Colorado Geological Survey Spec. Pub. No. 38, pp. 160–170.
- Wanty, R.B., Miller, W.R., Briggs, P.H., and McHugh, J.B., 1999, Geochemical processes controlling uranium mobility in mine drainages; *in* Plumlee, G.S., and Logsdon, M.J. (eds.), The Environmental Geochemistry of Mineral Deposits, Part A. Processes, Techniques, and Health Issues: Society of Economic Geologists, Reviews in Economic Geology, v. 6A, pp. 201–213.
- Wanty, R.B., Berger, B.R., Plumlee, G.S., and King, T.V.V., 1999 in press, Geoenvironmental models; *in* Fabbri, (ed.), Proceedings, 1998 NATO Advanced Study Institute Workshop, Deposit and Geoenvironmental Models for Resource Exploitation and Environmental Security: Kluwer Academic Publishers.
- Wetzel, R.G., 1983, Limnology (2nd ed.): Saunders, Philadelphia, Pa.
- White III, W.W., and Jeffers, T.H., 1994, Chemical predictive modeling of acid mine drainage from metallic sulfide-bearing waste rock; *in* Alpers, C.N., and Blowes, D.W. (eds.), Environmental Geochemistry of Sulfide Oxidation: American Chemical Society Symposium Series 550, pp. 608–630.
- White III, W.W., Lapakko, K.A., and Cox, R.L., 1997, Effects of protocol variables and sample mineralogy on static-test NP: Proceedings, 11th Annual Conference of the Society of Mineral Analysts, Elko, Nev., April 7–10.
- White III, W.W., Lapakko, K.A., Cox, R.L., 1999, Static-test methods most commonly used to predict acid-mine drainage—Practical guidelines for use and interpretation; *in* Plumlee, G.S., and Logsdon, M.J. (eds.), The Environmental Geochemistry of Mineral Deposits, Part A. Processes, Techniques, and Health Issues: Society of Economic Geologists, Reviews in Economic Geology, v. 6A, pp. 325–338.
- Wilburn, D.R., 1998, Exploration overview: Mining engineering, Annual Review, v. 50, pp. 51–59.
- Wildeman, T.R., and Updegraff, D., 1997, Passive bioremediation of metals and inorganic contaminants; *in* Macalady, D.L., (ed.), Perspectives in Environmental Chemistry: Oxford University Press, New York, pp. 473–495.
- Wildeman, T.R., Dinkel, J.W., Smith, R.M., and McCallister, M.L., 1997, Field assessment of Fe (III), Al, and dissolved O_2 for passive treatment options: Proceedings, 4th Internat'l Conference on Acid Rock Drainage, Vancouver, B.C., Canada, May 31-June 6, v. 4, pp. 1659-1672.
- Williams, L.O., 1995, Is Summitville really unique?; *in* Posey, H.H., Pendleton, J.A., and Van Zyl, D. (eds.), Summitville Forum Proceedings: Colorado Geological Survey Spec. Pub. No. 38, pp. 362–368.
- Winter, T.C., Harvey, J.W., Franke, O.L., and Alley, W.M., 1998, Ground water and surface water—A single resource: U.S. Geological Survey Circular 1139, 79 pp.

Chapter 2

AN OVERVIEW OF THE ABUNDANCE, RELATIVE MOBILITY, BIOAVAILABILITY, AND HUMAN TOXICITY OF METALS

Kathleen S. Smith¹ and Holly L.O. Huyck²

¹*U.S. Geological Survey, Box 25046, MS 973, Federal Center, Denver, CO 80225-0046*

²*P.O. Box 28161-16, Lakewood, CO 80228*

“All things are poisonous and yet there is nothing that is poisonous; it is only the dose that makes a thing poisonous.”—P.A. Paracelsus (1493?–1541)

INTRODUCTION

A major reason for considering the environmental geochemistry of mineral deposits is the environmental impact from such deposits on human, animal, and plant life. Some human activities may perturb or alter natural cycles of metals in the environment leading to accumulation of many potentially toxic metals in the food chain. To adequately assess the impact of human activities on metals in the environment, one must approach the issue from both a geological/geochemical/physical viewpoint and a biological/biochemical/toxicological perspective.

This chapter provides a geochemical and a biological context for chapters in this volume that discuss specifics of environmental geochemistry of mineral deposits. We alternate between the geological/geochemical/physical and biological/biochemical/toxicological aspects of selected metals. Because the emphasis of this volume is the environmental geochemistry of mineral deposits, we present examples that relate to metals or mineral deposits rather than provide a review of the literature. We also place emphasis on geological, geochemical, and chemical factors that affect metal bioavailability and toxicity to highlight connections between the earth and biological sciences. Radioactive materials are beyond the scope of this chapter.

Definitions

In this chapter, we use the term “metal” in a general sense to mean an element that, in aqueous solution, displays cationic behavior or that has an oxide that is soluble in acids (Parish, 1977). By this definition, elements that are non-metals include hydrogen, the rare gases, boron, carbon, silicon, nitrogen, phosphorus, arsenic, oxygen, sulfur, selenium, tellurium, polonium, fluorine, chlorine, bromine, iodine, and astatine. In our compilations, we may include some of the non-metals under a heading of “metals” in order to provide as much of the available information as possible. McKinney and Rogers (1992) state that the elements of major interest to the U.S. Environmental Protection Agency (U.S. EPA) include aluminum, antimony, arsenic, barium, beryllium, cadmium, chromium, cobalt, copper, lead, manganese, mer-

cury, molybdenum, nickel, selenium, silver, sodium, thallium, vanadium, and zinc.

To understand toxicity of metals in humans, one must define various terms. “Toxicology” is the study of adverse effects of chemicals on living organisms. “Ecotoxicology” is the study of potentially harmful substances in the environment and involves the disciplines of environmental chemistry, toxicology, and ecology. “Toxicity” of an element or a chemical compound is the capacity of the material to adversely affect any biological function. A “toxicant” is a toxic material of non-biological origin whereas a “toxin” is a toxic material of biological origin.

Our definition for “bioavailability” is based upon Newman and Jagoe (1994): “Bioavailability is the degree to which a contaminant in a potential source is free for uptake (movement into or onto an organism).” Thus, we use the term bioavailability in a broad sense. Some definitions of bioavailability further imply that the toxicant must affect the organism. In environmental toxicity studies, the definition of bioavailability varies with the toxicant under study, the method of determining amount of toxicant absorbed, and the target organism (e.g., see Davis et al., 1992). In the field of toxicology, the term bioavailability is often used to compare resulting blood concentrations from a one-time oral dose with the same dose administered intravenously. Dickson et al. (1994) discuss various definitions of bioavailability and state that the term eludes a consensus definition. The term “bioaccessibility” refers to the amount of contaminant liberated under a specified set of test conditions (Ruby et al., 1993).

The term “geoavailability” (coined by W. Day, verbal commun., U.S. Geological Survey, 1993) was initially defined in Plumlee (1994). Geoavailability is that portion of a chemical element’s or a compound’s total content in an earth material that can be liberated to the surficial or near-surface environment (or biosphere) through mechanical, chemical, or biological processes. The geoavailability of a chemical element or a compound is related to the susceptibility and availability of its resident mineral phase(s) to alteration and weathering reactions.

PATHWAYS FROM TOTAL METAL CONTENT THROUGH TOXICITY

Figure 2.1 illustrates pathways and relationships between total metal content in an earth material and potential toxicity to an organism. Total metal is the abundance of a given metal in an earth material and geoavailability is a function of the total metal content, access to weathering, and susceptibility to weathering.

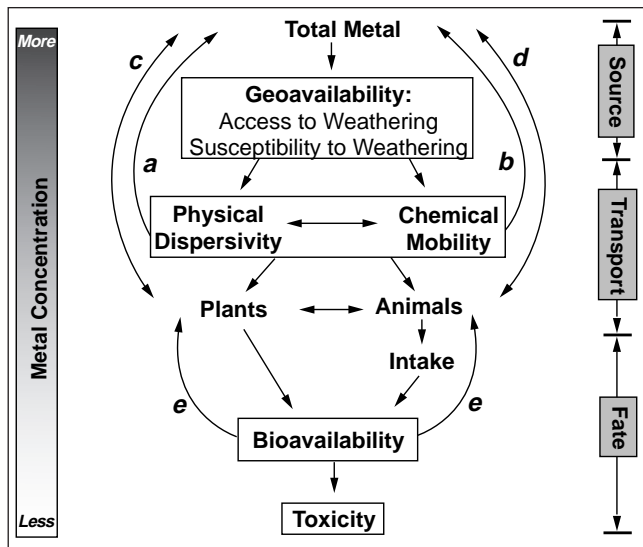


FIGURE 2.1—Diagram showing the pathways and relationships between total metal in an earth material and toxicity. As a metal or toxicant moves from one stage to another, generally less than 100% is transferred; not all of the total metal content in an earth material is usually geoavailable, bioavailable, or toxic. The gray scale on Figure 2.1 portrays this concept. Loops “a” and “b” signify transport and deposition of metals into another earth material (e.g., from weathering rocks to soil or sediment). Loops “c” and “d” denote direct uptake of the earth material by plants or animals (e.g., pica by children) and possible redeposition of metals by decay or excretion. Loops “e” illustrate biomagnification (see text).

“Dispersivity” refers to physical processes, or the ability to scatter via non-chemical means. Dispersion may occur via processes such as movement of bedload or suspended-sediment load in streams or as transport through air (e.g., smelter emissions, wind erosion). Mobility refers to chemical processes, which include chemical interactions with the surficial or near-surface environment, and the capacity for movement within fluids after dissolution. Mobility embodies the physicochemical characteristics and speciation of elements in aqueous systems.

Controls on geoavailability, dispersivity, and mobility incorporate both source characteristics and processes that interact with those characteristics, as summarized in Table 2.1. Plumlee (1999) discusses many of these characteristics and processes in detail; we note them here only in relation to controls on geoavailability, dispersivity, and mobility.

On Figure 2.1, we make a distinction between plants and animals because bioavailability is generally a prerequisite for uptake in plants, whereas animals may intake (ingest, inhale, etc.) toxicants that subsequently pass through their bodies without any systemic uptake. For animals, two levels of bioavailability distinguish (1) systemic uptake (e.g., into the bloodstream) from (2) uptake into target organs, where toxicants can accumulate and create specific toxicity symptoms (after Valberg et al., 1994; not shown on Fig. 2.1). For plants, metals can be either directly absorbed from the environment and stored by plant organs at the point of absorption (e.g., roots and leaves) or translocated and accumulated within plant tissues.

Bioavailability is a function of geoavailability, dispersivity, mobility, mode and pathway of exposure, biological specificity, and individual susceptibility of an organism. In this chapter, we

use a broad definition for bioavailability based upon Newman and Jagoe (1994) (see definition above). Bioavailability is generally less than 100% of the amount of a chemical element or compound to which an organism is exposed (by ingestion, breathing, etc.), and may be far less than the total content of that element or compound in an earth material. Bioavailability is a prerequisite for toxicity but does not necessarily result in toxicity; toxicity requires an adverse effect on an organism. Toxicity is discussed in detail in later sections of this chapter.

TABLE 2.1—Outline of the controls on geoavailability, dispersivity, and mobility of chemical elements.

- | |
|---|
| I. Controls on Geoavailability |
| A. Abundance (total metal content) |
| B. Access of weathering agents and degree of weathering |
| 1. Climate |
| 2. Porosity and permeability |
| a. Structural and lithologic factors |
| b. Surface exposure |
| 3. Topographic relief |
| C. Susceptibility of source mineral phases in earth materials to weathering |
| 1. Mineral properties |
| a. Mineral type |
| b. Solubility |
| c. Grain size, texture, and structure |
| d. Impurities |
| 2. Geochemical conditions |
| a. Aqueous concentration and speciation |
| b. pH and redox conditions |
| c. Kinetic constraints |
| II. Controls on Dispersivity (Physical Processes) |
| A. Abundance and geoavailability |
| B. Grain characteristics |
| 1. Size |
| 2. Shape |
| 3. Density |
| C. Access of erosional agents |
| 1. Climate |
| 2. Topographic relief |
| D. Access to transporting or retaining agents |
| 1. Movement through air |
| 2. Movement with or settling in water |
| a. Particle properties |
| b. Stream or river or aquifer hydrologic characteristics |
| c. Pond or lake characteristics |
| d. Aquifer characteristics |
| III. Controls on Mobility (Chemical Processes) |
| A. Abundance and geoavailability |
| B. Speciation |
| C. Solubility product of primary and secondary minerals |
| 1. Aqueous concentration and speciation |
| 2. pH and redox conditions |
| 3. Kinetic constraints |
| 4. Temperature |
| 5. Climate |
| D. Sorption, coprecipitation, or ion exchange reactions |
| 1. Aqueous concentration and speciation |
| 2. pH and redox conditions |
| 3. Soil properties and mineralogic characteristics |
| 4. Abundance of sorbent material |
| 5. Accessibility of sorbent material |
| E. Redox conditions |
| F. Photolysis |
| G. Tendency for volatilization |
| H. Tendency for biotransformation |

Each stage from total metal content in an earth material through toxicity in the surficial environment on Figure 2.1 is a reservoir with a distinct “half-life.” As a metal or toxicant moves from one stage to another, generally less than 100% is transferred. Therefore, not all of the total metal content in an earth material is usually geoavailable, bioavailable, or toxic. The gray scale on Figure 2.1 portrays this concept. Total metal content and geoavailability constitute the “source” factors; dispersivity and mobility comprise the “transport” factors; and intake, bioavailability, and toxicity constitute the “fate” of metals or toxicants. Biomagnification links the fate and transport segments of the diagram (as depicted by loops labeled “e” on Fig. 2.1). An example of biomagnification is the accumulation of mercury in marine biota.

HEALTH, TOXICITY, AND REGULATIONS

Metals can be essential to health and they also can be toxic. This section covers dietary requirements, essential effects, and toxic effects of metals. Huheey et al. (1993, Chapter 19) provide a detailed discussion of the inorganic chemistry of biological systems. Regulations and guidelines for metal concentrations in water also are discussed in this section.

Minimum human dietary requirements of “minerals” and electrolytes

Human health requires ingestion of many metals on a daily basis. Many people are aware of the need to consume sufficient iron, for example, to maintain hemoglobin in the blood. Relatively recently, dietary requirements have begun to emphasize other metals, e.g., zinc, as being necessary for maintaining health. Table 2.2A summarizes U.S. Recommended Daily Allowances (USRDA) and estimated safe and adequate daily dietary intakes for adults (National Research Council, 1989). Among the elements listed in Table 2.2A, fluorine is the only element that is not considered to be essential for human health. However, its usefulness in preventing tooth decay garners the designation of “beneficial element” for human health (National Research Council, 1989). Table 2.2B lists other metals that some researchers consider to be essential for good health, but whose roles have not been sufficiently defined by scientific research to list under USRDAs.

Some other elements are also considered by some researchers to be potentially important to human health, although clinical studies are equivocal. These elements are: bromine, lead, and tin (Ensminger et al., 1994; Nielsen, 1994). Some of these elements are important to plant health; deficiencies of others cause problems for laboratory animals in one or two studies. Further research

TABLE 2.2A—U.S. Recommended Daily Allowances (USRDA) and biological roles of elements that the National Research Council (1989) lists as essential to health.

Element	USRDA ⁽²⁾	Biological role ⁽⁴⁾
Calcium (Ca)	800 –1200 mg	Needed to build strong bones and teeth; for blood clotting, neural transmission, and muscle function
Chlorine/Chloride (Cl)	[750 –3600 mg]	Needed to maintain water balance, osmotic pressure, and acid-base balance, for digestive acid
Chromium (Cr)	50 –200 µg	Needed for glucose metabolism
Copper (Cu)	1.5 –3 mg	Respiratory and red blood cell function; present in oxidative enzymes
Fluorine/Fluoride (F) ⁽¹⁾	1.5 –4 mg	As fluoride, prevents tooth decay or disease
Iodine (I)	150 µg ⁽³⁾	Needed for thyroid hormones, to control body temperature, metabolism, reproduction, and growth
Iron (Fe)	10 –15 mg ⁽³⁾	Needed for hemoglobin in blood, energy production, and a healthy immune system
Magnesium (Mg)	280 –350 mg ⁽³⁾	Needed for healthy bones and blood vessels, muscle function, nerve transmission, and energy formation
Manganese (Mn)	2 –5 mg	Promotes growth, development, and cell function; cofactor in a number of enzymatic reactions
Molybdenum (Mo)	75 –250 µg	Promotes growth, development, and cell function; essential cofactor in certain enzymes
Phosphorous (P)	800 –1200 mg ⁽³⁾	Essential for healthy bones and energy production; present in almost every chemical reaction within the body
Potassium (K)	[2000 –3500 mg]	Regulates body fluid balance; aids muscle contraction and neural transmission
Selenium (Se)	55 –70 µg ⁽³⁾	Prevents cardiovascular disease and cancer; detoxifies several major pollutants, especially oxidants and free radicals
Sodium (Na)	[500 –2400 mg]	Aids muscle contraction and neural transmission; maintains blood pressure
Zinc (Zn)	12 –15 mg	Maintains senses of taste and smell, and healthy immune system and growth; protects liver from chemical damage

⁽¹⁾Although fluorine is not essential to health, the National Research Council (1989) considers it to have sufficient value to be included in this listing.

⁽²⁾[]: lower number is estimated minimum requirement for adults; upper limit is based upon text (National Research Council, 1989).

⁽³⁾Indicates USRDAs; all others are “estimated safe and adequate daily dietary intakes,” which are less well defined. All values are listed for adults >18 years old (excluding pregnant or lactating women).

⁽⁴⁾After Griffith (1988), National Research Council (1989), Christian and Greger (1991), and Nielsen (1994).

TABLE 2.2B—Biological roles of metals that may be vital to human health.^{(1) (2)}

Element	Biological Role
Boron (B)	Affects metabolism of some essential elements
Cobalt (Co) ⁽³⁾	Constituent in vitamin B ₁₂ and a factor in formation of red blood cells
Lithium (Li)	May be essential for slow respiration on intracellular level
Nickel (Ni)	Important in critical enzymes
Silicon (Si)	Important in metabolism, maintaining bone tissue
Sulfur (S) ⁽³⁾	Enables storage and release of energy; promotes enzyme reactions, aids in detoxification of body; constituent in thiamine, biotin, and required proteins
Vanadium (V)	May play a role in metabolism of bones and teeth

⁽¹⁾Elements listed in this table were noted as being potentially vital to humans in at least two sources.

Sources: Venugopal and Luckey (1978); Griffith (1988); National Research Council (1989); Goyer (1991); Ensminger et al. (1994); Nielsen (1994).

⁽²⁾Tin has no known biological role, but deficiency has been produced in experimental animals and thus tin may be essential in humans (Ensminger et al., 1994) and is noted as a possible nutrient or nutrient under special conditions in Luckey and Venugopal (1977). Similarly, arsenic's role is not well defined, but deficiency in experimental animals resulted in depressed growth and abnormal reproduction (Ensminger et al., 1994; Nielsen, 1994).

⁽³⁾Although National Research Council (1989) does not specifically list cobalt and sulfur as essential, Christian and Greger (1991) and Ensminger et al. (1994) note that each is a constituent of vitamins or proteins for which U.S. Recommended Daily Allowances (USRDA) have been established.

is necessary to define their benefits (or lack thereof) to humans. According to Robert Benson (U.S. EPA, personal commun., 1996), there are no credible data suggesting that lead is an essential element for humans; in fact, lead appears to have adverse effects on developing nervous systems at the lowest exposures that can be quantified. Figure 2.2 summarizes the current status of nutrients considered to be essential to mammalian health.

Toxicity of metals

Gossel and Bricker (1984), Hayes (1989), and Goyer (1991, 1995) provide useful reviews of metal toxicity in humans, and Gough et al. (1979) review element concentrations toxic to plants, animals, and humans. Many metals are essential to life in small amounts and such metals become toxic only when absorbed in excessive amounts. However, the level of toxicity for metals is

commonly only a few to several times the level necessary to sustain life in humans. For example, while the recommended daily ingestion of zinc for humans is 12–15 mg, researchers have found that daily intakes of as low as 18.5 or 25 mg zinc cause decreased retention of copper (an essential metal) in adult males (Festa et al., 1985; Fischer et al., 1984). Types of toxicity commonly encountered in ecotoxicology are summarized in Table 2.3. Definitions of “acute” and “chronic” exposure vary with source and target. For aquatic species, the time limits of acute and chronic exposure are one hour and four days, respectively; time limits are longer for humans.

Toxic effects

Tables 2.4A and 2.4B summarize the human pathways of metal absorption and the organs in which the metals concentrate or

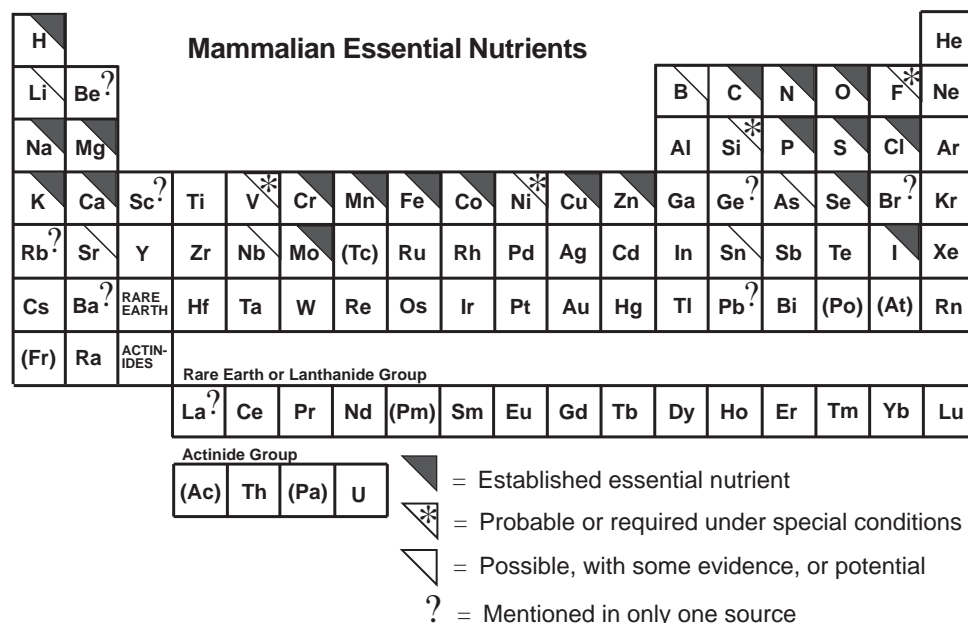


FIGURE 2.2—Periodic table of essential mammalian nutrients. Such nutrients are considered to be essential nutrients to humans, although many studies are based upon experiments on laboratory animals. Based on Luckey and Venugopal (1977), with modifications from National Research Council (1989), Griffith (1988), Nielsen (1994), and Ensminger et al. (1994). Lack of notation for rare earth and actinide group elements is due to lack of information about those elements.

TABLE 2.3—Types of toxicity (modified from Luckey and Venugopal, 1977; U.S. EPA, 1986; Hoffman, 1991; Klaassen and Eaton, 1991; Agency for Toxic Substances and Disease Registry (ATSDR), 1992).

Acute Exposure: (1) exposure to a toxic agent for 24 hours or less (Klaassen and Eaton, 1991); (2) exposure to a toxic agent for 14 days or less (ATSDR, 1992, Glossary); (3) exposure of aquatic life to a toxic agent for one hour (U.S. EPA, 1986, for setting water pollution standards)⁽¹⁾.

Acute Toxicity: adverse biological effects caused by a single dose or repeated doses over a short period of time (acute exposure).

Carcinogen: a biologic, chemical, or physical agent capable of producing uncontrolled cell proliferation in organs and tissues, or to induce cancer. Carcinogenicity depends on routes and times of exposure, dose, physical state of the agent, and host-specific factors.

Chronic Exposure: (1) exposure to a toxic agent for more than three months (Klaassen and Eaton, 1991); (2) exposure to a toxic agent for 365 days or more (ATSDR, 1992, Glossary); (3) exposure of aquatic life to a toxic agent for four days (U.S. EPA, 1986, for setting water pollution standards)⁽¹⁾.

Chronic Toxicity: (1) also called “cumulative poisoning” or “distal toxicity,” adverse biological effects caused by long and continuous exposure (chronic exposure).

Mutagen: (1) A substance that causes mutations. A mutation is a change in the genetic material of a body cell. Mutations can lead to birth defects, miscarriages, or cancer (ATSDR, 1992, Glossary). (2) Any agent that causes mutation [by mutagenesis]. Mutagenesis includes the induction of DNA damage and all kinds of genetic alterations, ranging from changes in one DNA base pair to gross changes in chromosome structure or in chromosome number (Hoffman, 1991).

Teratogen: a biological, chemical, or physical agent that interferes with growth and development of an embryo or a fetus, creating growth retardation, and functional or structural defects in the fetus.

⁽¹⁾See Table 2.7 for further clarification of definition (3). For purposes of setting water standards to protect aquatic life, the “acute” and “chronic” levels of toxicant concentrations may be reached on average only once every three years (U.S. EPA, 1986).

which the metals most strongly affect. This table is broken into two sets—metals that are “characteristically hazardous,” as defined by U.S. EPA (see below), and other metals that may be hazardous. The main pathways of exposure to metals are inhalation and ingestion. Ingestion by humans occurs dominantly via eating contaminated plants or animals or by drinking contaminated water. The pathway of exposure can influence which organs are targets for toxic interactions.

Figure 2.3 and Table 2.5 summarize toxic effects of elements on mammals (and presumably on humans). Rare earth elements and actinides are excluded from this summary. Figure 2.3 focuses on carcinogens, teratogens, or embryocides (see Table 2.3 for definitions). Toxicity may result in pathologies that are not related to any of these. Table 2.5 lists “toxic” metals, defined as those that have strong toxic effects aside from (or in addition to) carcinogenicity or reproductive effects. Selection of elements is based on Goyer (1991). Venugopal and Luckey (1978) consider antimony, arsenic, lead, mercury, selenium, tellurium, thallium, and tin to be particularly toxic. When metals that may create toxic side effects (e.g., aluminum, bismuth, gold, lithium, and platinum) are used in the treatment of illnesses, these metals are considered to be special cases. For example, the association of long-term ingestion of lithium with central nervous system disorders is a special case.

The Agency for Toxic Substances and Disease Registry (ATSDR) publishes reports on toxicological profiles for various

metals. A variety of information also is available through the ATSDR web site:

(<http://atsdr1.atsdr.cdc.gov:8080/atsdrhome.html>).

Regulatory response to metal toxicity

Within this chapter, we focus on regulations under the Resource Conservation and Recovery Act (RCRA), the Clean Water Act (CWA), and the Safe Drinking Water Act (SDWA). For an in-depth discussion of these regulations and their impact on mining, refer to Marcus (1997). Under the RCRA legislation (which regulates landfills and land-disposal sites), U.S. EPA distinguishes arsenic, barium, cadmium, chromium, lead, mercury, selenium, and silver as being sufficiently toxic to humans to warrant special regulation as “characteristically hazardous” metals. Based upon toxicity studies, the U.S. EPA set minimum extractable levels for metals in solid wastes for defining characteristically hazardous wastes under RCRA regulation (Table 2.6). The currently approved extraction method, “Toxicity Characteristic Leaching Procedure,” or TCLP (U.S. EPA Method 1311), involves leaching of solids by dilute acetic acid for 18 hours. The resulting leachate is used to define materials as hazardous, with the assumption that the test simulates leaching in a mixed organic/metal landfill. Whereas this test is an improvement over simply using total metal content in solid materials, it does not account for other factors affecting bioavailability or, ultimately, bioavailability. Additional leaching methods exist, such as the “Synthetic Precipitation Leaching Procedure” (SPLP; U.S. EPA Method 1312, which involves leaching of solids with a very dilute mixture of sulfuric and nitric acid), but none of these other methods is currently approved for use by U.S. EPA. Under RCRA, the Bevill Amendment temporarily exempts the regulation of mining wastes derived from extraction or beneficiation (referred to as “Bevill Wastes”) from regulation under Subtitle C (hazardous wastes). Instead, they are regulated under Subtitle D (solid wastes). This exemption defers the “cradle-to-grave” documentation and handling required under Subtitle C for mining wastes. In 1997, U.S. EPA proposed new restrictions on the Bevill Amendment for mining wastes. Information can be obtained from the internet at the following U.S. EPA sites:

<http://earth1.epa.gov/OSWRCRA/hazwaste/data/>
<http://www.epa.gov/epaoswer/other/mining.htm>

The Federal Water Pollution Control Act, along with its amendments, is commonly known as the Clean Water Act (CWA). The stated purpose of the CWA is to “restore and maintain the chemical, physical, and biological integrity of the nation’s waters.” This legislation includes regulations that set maximum allowable concentrations of toxicants in discharges and receiving waters, and establishes the National Pollutant Discharge Elimination System (NPDES) permit program. (As this paper goes to press, the CWA has not yet been reauthorized. New legislation may change regulations in the future.)

The Safe Drinking Water Act (SDWA; 1974, amended 1977, 1986, and 1996) establishes a federal regulatory system to ensure the safety of public drinking water, but applies only to drinking water facilities of a certain size. Under the SDWA, U.S. EPA must set “at-the-tap” maximum permissible levels for contaminants in water delivered by a public water system. A contaminant is defined in the Act as “any physical, chemical, biological, or radiological substance or matter in water.” For each contaminant, U.S. EPA must set a Maximum Contaminant Level Goal (MCLG) and

TABLE 2.4A—Toxicity of “characteristically hazardous” metals (after Goyer, 1991; National Research Council, 1989).

Element	Class ⁽¹⁾	Nutrient ⁽²⁾	Major forms of absorption ⁽³⁾	Organs toxicologically affected
Arsenic (As)	H	P	Ingestion Inhalation	Nervous System Liver Vascular Skin, Lungs (c) ⁽⁴⁾
Barium (Ba)	H	?	Inhalation Ingestion	Pulmonary Muscular
Cadmium (Cd)	S	No	Ingestion Inhalation	Renal Skeletal Cardiovascular Lungs (c)
Chromium (Cr)	H	Yes	Ingestion (Inhalation)	Renal (Nasal) Lungs (c) Skin
Lead (Pb)	B	?	Inhalation ($<0.5 \mu\text{m}$ size) Ingestion	Nervous System Blood Lungs, Renal (c) Reproductive
Mercury (Hg)	S	No	Inhalation (Ingestion)	Nervous System (Gastrointestinal) Renal
Selenium (Se)	--	Yes	Ingestion (Inhalation)	Muscular Nervous System Skin ⁽⁵⁾
Silver (Ag)	S	No	Ingestion	Gastrointestinal Skin

⁽¹⁾H = hard acid, S = soft acid, B = borderline acid (metal classification after Huheey et al., 1993), -- = insufficient information. See Figure 2.9.

⁽²⁾Yes = essential or probable nutrient, P = possible nutrient, ? = noted as a potential nutrient in only one source, No = not an essential nutrient.

⁽³⁾Parentheses indicate lower occurrence rate, lower toxicity, or less common route of absorption.

⁽⁴⁾Although U.S. EPA and the World Health Organization consider arsenic to be a well-established carcinogen (Goyer, 1991), association of arsenic with cancer is considered by some authors to be equivocal (Nielsen, 1994; Frost, 1978). Petito and Beck (1990) provide evidence that the threshold for ingested arsenic to cause skin cancer is significantly higher than originally thought.

⁽⁵⁾Selenium tests for carcinogenesis are conflicting. Human epidemiological studies indicate that, in some cases, selenium actually protects against cancer (Goyer, 1991).

(c)Well-established carcinogen in humans or lab animals. Based on varying mixes of laboratory animal studies and human epidemiological studies. Commonly, these are contradictory. Carcinogen designation is based on evidence from either laboratory animal studies or human epidemiological studies.

a Maximum Contaminant Level (MCL). The MCLG is a nonenforceable health goal set solely on the basis of human health effects. The MCL is the enforceable drinking water standard and is set as close to the MCLG as is technologically or economically feasible. Upon authorization, states may adopt the federal MCLs or establish independent ones that are the same or more stringent. Under the SDWA, contaminants are regulated as either primary or secondary drinking water standards. Primary standards regulate contaminants that may cause adverse human health effects whereas secondary standards, which are federally unenforceable, are limited to contaminants that may adversely affect public welfare (for example, contaminants that may affect the odor or appearance of drinking water; see below for associated contaminant limits). U.S. EPA procedures for setting drinking water standards are contained in 56 FR 3526–3597 (Jan. 30, 1991 Federal Register) and in 57 FR 31776–31849 (July 17, 1992 Federal Register). The SDWA drinking water standards are often used to set remedial standards for actions under RCRA and the Comprehensive Environmental Response, Compensation and Liability Act (CERCLA, also known as Superfund).

Risk assessment

The topic of risk assessment for metals is essential to the regulatory process. However, because it is a very broad topic, we do not discuss risk assessment in detail. Beck et al. (1995) provide a comprehensive introduction to health-based risk assessment for metals. They build their discussions around the “red book,” “Risk Assessment in the Federal Government: Managing the Process” (NRC, 1983), and on the report “Science and Judgment in Risk Assessment” (NRC, 1994). Davis and Elias (1996) also discuss risk assessment of metals and contrast key features of the U.S. EPA risk assessments for lead and manganese. Fan (1996) describes the process of risk assessment used for setting permissible levels in drinking water. The U.S. EPA report, “A Framework for Ecological Risk Assessment,” (U.S. EPA, 1992) develops guidelines and basic principles, and provides definitions of key terms for ecological risk assessment. Bartell et al. (1992), Suter (1993), and Landis and Yu (1995) discuss various aspects of ecological risk assessment.

Risk assessment includes hazard identification, dose-response

TABLE 2.4B—Toxicity of selected “other” metals (after Goyer, 1991; National Research Council, 1989; and Venugopal and Luckey, 1978).

Element	Class ⁽¹⁾	Nutrient ⁽²⁾	Major forms of absorption ⁽³⁾	Organs toxicologically affected
Aluminum (Al)	H	No	(Ingestion of large amounts; dialysis or P deficiency)	(Nervous system, bone, gastrointestinal)
Antimony (Sb)	B	No	Ingestion	Gastrointestinal (acute); Cardiac and liver (chronic)
Beryllium (Be)	H	?	Inhalation Dermal (Ingestion)	Lungs, air passages (c) Skin lesions (Bone, liver)
Cobalt (Co)	H/B	Yes	Ingestion Inhalation Dermal (Injection)	Muscle, liver, heart Lungs Allergic on skin (c)
Copper (Cu)	S/B	Yes	Ingestion (Dermal—burn treatment)	Liver, bone marrow (Blood—anemia)
Iodine (I)	--	Yes	Ingestion	Thyroid (either excess or deficiency)
Iron (Fe)	H/B	Yes	Ingestion Intravenously (Inhalation)	Liver, pancreas, endocrine system, heart (Lungs)
Lithium (Li)	H	P	Ingestion	Gastrointestinal, central nervous system, renal, cardiovascular, endocrine
Manganese (Mn)	H	Yes	Inhalation	Lungs/respiratory system (acute), central nervous system, liver (chronic)
Molybdenum (Mo)	--	Yes	Ingestion (Inhalation)	Renal, adrenal Bone, mucous membranes
Nickel (Ni)	B	Yes	Inhalation Dermal	Lungs (kidneys, liver, brain) (c) Allergic on skin
Thallium (Tl)	S	No	Ingestion Dermal Inhalation	Gastrointestinal, renal Nervous system, lungs Hair, bone, reproductive
Vanadium (V)	--	Yes	Inhalation (Dermal)	Respiratory Cardiovascular
Zinc (Zn)	B	Yes	(Ingestion) (Inhalation)	Central nervous system, gastrointestinal (Lungs—chills/fever, weakness (acute))

⁽¹⁾H = hard acid, S = soft acid, B = borderline acid (metal classification after Huheey et al., 1993), -- = insufficient information. See Figure 2.9.

⁽²⁾Yes = essential or probable nutrient, P = possible nutrient, ? = noted as a potential nutrient in only one source, No = not an essential nutrient.

⁽³⁾Parentheses indicate lower occurrence rate, lower toxicity, or less common route of absorption.

(c) Well-established carcinogen in humans or lab animals. Based on varying mixes of laboratory animal studies and human epidemiological studies. Commonly, these are contradictory. Carcinogen designation is based on evidence from either laboratory animal studies or human epidemiological studies.

assessment, exposure assessment, and risk characterization. NRC (1994) recommends an iterative approach with initial conservative assumptions to protect human health in the risk assessment process. Risk is usually inferred from epidemiological investigations or calculated from models. Ginevan and Splitstone (1997) discuss methods for modeling spatial distribution of risk.

Contaminant levels in water

Tables 2.7A and 2.7B summarize U.S. EPA guidelines for concentrations of a number of metals, sulfate, fluoride, and cyanide for protection of freshwater aquatic life and of human life, respectively. These guidelines are general, and state agencies or U.S. EPA should be contacted for information on specific water-quality criteria. In addition, many states publish standards for pH. (A typical secondary MCL for drinking water pH is 6.5–8.5.) State regulations may vary among states and within states with respect to specific bodies of water and their classifications. For example, the state of Colorado has adopted one-day (not one-hour) stan-

dards for “acute” aquatic life criteria and a 30-day average (not 4-hour average) for “chronic” aquatic life criteria (W. Wuerthele, U.S. EPA, personal commun., 1995; refer to Table 2.3 for definitions).

For situations in which humans may ingest water and fish, the “published” column in Table 2.7B shows water-quality criteria for human health published by U.S. EPA in 1980 (U.S. EPA, 1980). U.S. EPA has published a more recent water quality criteria document since this paper entered copy editing (U.S. EPA, 1998). The “updated” column is based upon more recent toxicity information in U.S. EPA’s “Integrated Risk Information System,” (IRIS) database (U.S. EPA, 1993a). This database is constantly changing, based upon new studies on carcinogenicity or other toxicity of chemicals, and revised thresholds for triggering toxicities. These are national guidelines, although states may define other local levels for specific waterway segments. States commonly incorporate these updated numbers in their triennial reviews of regulations based upon the CWA. The best way to decide what regulations currently apply to a particular mine site is to contact the appropriate state agency.

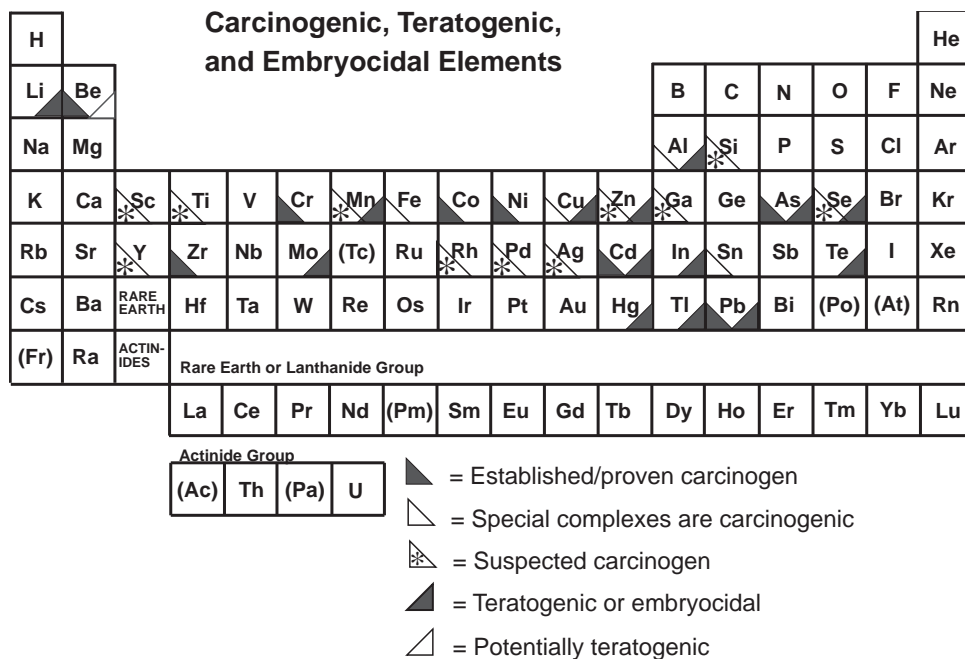


FIGURE 2.3—Periodic table of carcinogenic, teratogenic, and embryocidal elements, based upon epidemiological studies of humans and laboratory studies of humans and mammals. Based upon Luckey and Venugopal (1977), with modifications from Venugopal and Luckey (1978) and Goyer (1991). Lack of notation for rare earth and actinide group elements is due to lack of studies and should not be construed as meaning that these elements are not potentially toxic. This figure does not include toxic effects related to radioactivity.

TABLE 2.5—Summary of potential health-related effects of metals and other selected elements (after Luckey and Venugopal, 1977; Venugopal and Luckey, 1978; Griffith, 1988; National Research Council, 1989; Goyer, 1991; Enslinger et al., 1994; and Nielsen, 1994).

Element	Essential for human health	Toxicity	Carcinogenic	Teratogenic
Aluminum (Al)		S	S	P/E
Antimony (Sb)		t		
Arsenic (As)	P	T	Y	Y/E
Barium (Ba)	?	t		
Beryllium (Be)	?	T	Y ^{(1) (2)}	P
Bismuth (Bi)		S		
Boron (B)	P			
Bromine (Br)	?			
Cadmium (Cd)		T	Y ⁽¹⁾	Y/E
Calcium (Ca)	Y			
Chromium (Cr)	Y	T	Y ^{(1) (3)}	
Cobalt (Co)	Y	t	Y	
Copper (Cu)	Y	t	S	E
Fluorine (F)	H			
Gallium (Ga)		S	P	
Gold (Au)		S		
Iodine (I)	Y			
Iron (Fe)	Y	t	S	
Lanthanum (La)	?			
Lead (Pb)	?	T	Y	Y/E
Lithium (Li)	P	S		Y/E
Magnesium (Mg)	Y	t		
Manganese (Mn)	Y	t	P	E
Mercury (Hg)		T		Y/E
Molybdenum (Mo)	Y	t		Y
Nickel (Ni)	P	T	Y	
Niobium (Nb)	P			
Palladium (Pd)			P	
Phosphorus (P)	Y			
Platinum (Pt)		S		
Potassium (K)	Y			

TABLE 2.5—Continued

Element	Essential for human health	Toxicity	Carcinogenic	Teratogenic
Rhenium (Rh)			P	
Selenium (Se)	Y	t	P ⁽⁴⁾	Y/E
Silver (Ag)		t	P	
Strontium (Sr)	P			
Sulfur (S)	Y			
Tellurium (Te)		t		Y/E
Thallium (Tl)		t		Y/E
Tin (Sn)	P	t	S ⁽⁵⁾	
Titanium (Ti)		t	P	
Vanadium (V)	P	t		
Yttrium (Y)			P	
Zinc (Zn)	Y	t	P	Y/E
Zirconium (Zr)			Y	

Y = proven or established. For nutrients, “Y” is based solely on National Research Council (1989). Cobalt and sulfur are included as “Y” because they are constituents of vitamins or proteins considered to be essential by the National Research Council. P = possible or suspected, plus probable for nutrients. H = although fluorine is not essential to health, the National Research Council (1989) considers it to have sufficient value to be included in its USRDA listing. ? = nutrient cited in one source only. S = special complex or special conditions required. E = embryocidal. T = toxic metals with multiple effects (after Goyer, 1991). t = metals with potential for toxicity (after Goyer, 1991).
⁽¹⁾Carcinogenic to humans by inhalation only.
⁽²⁾Although beryllium has been implicated as a human carcinogen by inhalation, epidemiological studies are conflicting. U.S. EPA considers evidence for carcinogenicity to be sufficient in animals (which includes by injection), but limited in humans (Goyer, 1991).
⁽³⁾Cr(VI) is considered to be carcinogenic, whereas Cr(III) is not.
⁽⁴⁾Although laboratory studies of rats indicate carcinogenicity, some human epidemiological studies indicate that selenium can inhibit cancer.
⁽⁵⁾Carcinogenic as organic form only.

TABLE 2.6—Hazardous levels of constituent concentrations in waste extract (Toxicity Characteristic Leaching Procedure, TCLP), as listed in the Resource Conservation and Recovery Act (RCRA) regulations for characteristically hazardous metals. See Table 2.4A for toxicity characteristics. The EPA number refers to regulatory identification numbers; “D” is the designation for characteristically hazardous wastes (U.S. EPA, 1996).

EPA No.	Constituent	Regulatory level (mg/l)
D004	Arsenic	5.0
D005	Barium	100
D006	Cadmium	1.0
D007	Chromium	5.0
D008	Lead	5.0
D009	Mercury	0.20
D010	Selenium	1.0
D011	Silver	5.0

TABLE 2.7A—Water-quality guidelines for metals and cyanide for which water-quality standards or lowest observed effect levels (L.O.E.L.s) have been established for protection of aquatic life.⁽¹⁾

Constituent	Hardness-Dependent Criteria? ⁽²⁾	Published Section 304(a) Freshwater Criteria ⁽³⁾ (H=100 mg/l CaCO ₃)		Hardness-based equation for calculation of freshwater aquatic-life criteria ^(2, 5) (µg/l)
		Acute (µg/l)	Chronic	
Cyanide (total)		22	5.2	
Aluminum (pH 6.5—9.0 only)		750	87	
Antimony		9000 ⁽⁴⁾	1600 ⁽⁴⁾	
Arsenic		360	190	
Arsenic (V)		850 ⁽⁴⁾	48 ⁽⁴⁾	
Arsenic (III)		44 ⁽⁴⁾	40 ⁽⁴⁾	
Beryllium		130 ⁽⁴⁾	5.3 ⁽⁴⁾	
Cadmium	Yes	3.9	1.1	e (1.128 [ln (hardness)] - 3.828) (a) e (0.7852 [ln (hardness)] - 3.490) (b)
Chromium (III)	Yes	1700	210	e (0.8190 [ln (hardness)] + 3.688) (a) e (0.8190 [ln (hardness)] + 1.561) (b)
Chromium (VI)		16	11	
Copper	Yes	18	12	e (0.9422 [ln (hardness)] - 1.464) (a) e (0.8545 [ln (hardness)] - 1.465) (b)
Iron			1000	
Lead	Yes	82	3.2	e (1.273 [ln (hardness)] - 1.460) (a) e (1.273 [ln (hardness)] - 4.705) (b)
Mercury		2.4	0.012	
Nickel	Yes	1400	160	e (0.8460 [ln (hardness)] + 3.3612) (a) e (0.8460 [ln (hardness)] + 1.1645) (b)
Selenium		20	5	
Silver	Yes	4.1	0.12 ⁽⁴⁾	e (1.72 [ln (hardness)] - 6.52) (a)
Thallium		1400 ⁽⁴⁾	40 ⁽⁴⁾	
Zinc	Yes	120	110	e (0.8473 [ln (hardness)] + 0.8604) (a) e (0.8473 [ln (hardness)] + 0.7614) (b)

(1) Values are based on the Updated Version of EPA Region VIII Clean Water Act Section 304(a) Criteria Chart (U.S. EPA, 1993b). U.S. EPA has published guidelines for a different set of water-quality standards for specific river segments in the following locations: Arkansas, California, District of Columbia, Florida, Kansas, Michigan, New Jersey, Puerto Rico, Rhode Island, and Vermont (U.S. EPA, 1994). The values in this table should be used only as guidelines. Individual states and U.S. EPA should be contacted for updated and local water-quality criteria.

(2) Some freshwater criteria vary with water hardness. There is generally an inverse relationship between hardness and toxicity for a given metal concentration. Hardness is defined as the amount of polyvalent metal ions (primarily Ca²⁺ and Mg²⁺; U.S. EPA, 1986), and is expressed as mg/l calcium carbonate (CaCO₃).

(3) In the case of hardness-dependent criteria, a water hardness (H) of 100 mg/l CaCO₃ is used. Unless otherwise noted, “acute” means a 1-hour average and “chronic” means a 4-day average. These definitions of acute and chronic are specifically for aquatic life and differ from those that refer to human life (see Table 2.3; U.S. EPA, 1986; ATSDR, 1992; U.S. EPA, 1993b). Streams are considered to be protective of aquatic life if the criterion is not exceeded more than once in 3 years.

(4) Values represent established L.O.E.L.s, which do not meet sufficient standards to be considered as water-quality criteria for aquatic life. A L.O.E.L. (lowest observed effect level) is the lowest contaminant level at which target aquatic species exhibit negative effects. Although these are not U.S. EPA criteria, they are included as guidelines according to U.S. EPA (1986).

(5) These equations are in the form e^{(x [ln (hardness)] ± y)} and are used to calculate hardness-dependent freshwater aquatic-life criteria for a given water-hardness value. (a) = 1-hour average, or acute; (b) = 4-day average, or chronic.

TABLE 2.7B—Water-quality criteria for metals, cyanide, sulfate, and fluoride for which water-quality standards and maximum contaminant levels (MCLs) have been established for protection of human life.⁽¹⁾

Constituent	Water + Fish Ingestion ⁽²⁾		Drinking water MCLG and MCL (mg/l) ⁽³⁾
	Published	Updated	
Cyanide (total)	200 µg/l (m)	700 µg/l	0.2 (g); 0.2 (f)
Sulfate			500 (g); 500 (p); 250 (s)
Aluminum			0.05—0.2 (s, l)
Antimony	146 µg/l	14 µg/l (r)	0.006 (g); 0.006 (f)
Arsenic	2 ng/l	18 ng/l	0.05 (d)
Barium	1 mg/l (m)	1 mg/l (m)	2 (g); 2 (f)
Beryllium	3.7 ng/l	7.7 ng/l	0.004 (g); 0.004 (d)
Cadmium	10 µg/l (m); 29 µg/l (tx)	14 µg/l (r)	0.005 (g); 0.005 (f)
Chromium			0.1 (g); 0.1 (f)
Chromium (III)	50 µg/l (m); 170 mg/l (tx)	3.3 mg/l (r)	
Chromium (VI)	50 µg/l (m)	170 µg/l (r)	
Copper	1.0 mg/l (s)	1.3 mg/l	1.3 (g, tt); 1.0 (s)
Fluoride			4 (g); 4 (f); 2 (s)
Iron	0.3 mg/l (m)	0.3 mg/l (m)	0.3 (s)
Lead	50 µg/l (m)	— (r)	0 (g); 0.015 (tt)
Manganese	0.05 mg/l (m)	0.05 mg/l (m)	0.05 (s, l) ⁽⁴⁾
Mercury	144 ng/l	140 ng/l	0.002 (g); 0.002 (f)
Nickel	13.4 µg/l	610 µg/l (r)	0.1 (g, rr); 0.1 (f, rr)
Selenium	10 µg/l (m)	170 µg/l (r)	0.05 (g); 0.05 (f)
Silver	50 µg/l (m)	170 µg/l	0.1 (s)
Thallium	13 µg/l	1.7 µg/l	0.0005 (g); 0.002 (f)
Zinc	5 mg/l (s)	9.1 mg/l	5 (s, l)

⁽¹⁾After U.S. EPA (1993b; 1995). U.S. EPA (1993b) was used to define published and updated values. U.S. EPA (1995) was used to define drinking water MCLGs and MCLs. The values in this table should be used only as guidelines. Individual states and U.S. EPA should be contacted for updated and local water-quality criteria.

⁽²⁾These water-quality values apply to situations in which humans may ingest both water and fish. Values are based on the Updated Version of EPA Region VIII Clean Water Act Section 304(a) Criteria Chart (U.S. EPA, 1993b). Human-health criteria for ingestion of water + fish occur in two forms. The “published” criteria are those that have been officially published by U.S. EPA in Clean Water Act Section 304(a) criteria documents. The “updated” values (as of July 1993) are based upon the Integrated Risk Information System (IRIS), which is constantly changing, and which the states use for their triennial updates of water-quality regulations. Access to current versions of IRIS are available by commercial services. (m) = criteria based on drinking water MCL (after U.S. EPA, 1993b), (tx) = the calculated Section 304(a) toxicity-based value, if any, (r) = a more stringent final MCL has been issued by U.S. EPA under the Safe Drinking Water Act, and (s) = secondary criteria based on taste and odor.

⁽³⁾These MCLG and MCL values are published under the Safe Drinking Water Act (U.S. EPA, 1995). The MCLs are at various stages of regulatory development.

(f) = final, (rr) = being remanded, (l) = listed for regulation as a primary MCL, (d) = draft, under review as a primary MCL, (p) = proposed as a primary MCL, and (s) = secondary MCL. All secondary MCLs are set for look, taste, or odor, and are final. In addition to having secondary MCLs, aluminum, manganese, and zinc are listed for regulation as primary MCLs. (g) = MCLG; (tt) = “treatment technique.” Since in-house plumbing and soil characteristics can affect copper and lead contents of water, “action levels” (shown for copper and lead) are set under the treatment technique guideline. For example, if drinking water exceeds these action levels in a particular area, the water provider must initiate a variety of technical improvements to comply with each action level. These include corrosion controls and education of local residents. If the water provider implements all required technical improvements and still does not achieve action levels, it will not be sued to force compliance. For MCLs, however, the provider must be in compliance at the end user.

⁽⁴⁾A primary MCL for manganese is being considered at 0.8 mg/l (H. Fliniaux, U.S. EPA, personal commun., 1997).

Metals for which MCL criteria are listed exist mainly for protection of human health (U.S. EPA, 1995). A few metals—iron and manganese—have levels that are mainly aesthetic to minimize taste, odor, or color problems in drinking water. [U.S. EPA is considering regulating manganese in the future; at continuous and long-term exposure to high levels it may adversely affect the human brain (R. Benson, U.S. EPA, personal commun., 1996)]. Zinc and copper are considered to be pollutants in water because of their high toxicity to aquatic life, despite their relatively low toxicity to humans.

ABUNDANCES OF ELEMENTS

Introduction

This section provides tables and figures that present generalizations about the abundances of elements in earth materials, water, and vegetation. This section can stand alone and is not essential to understanding the remainder of this chapter. The pur-

pose of this section is to assemble element-abundance data in one place, with minimal explanation. These data are intended to serve only as a rough guide when evaluating the concentrations of chemical elements in the environment. Many of these types of data are still evolving as analytical-chemistry techniques are developed and refined. A standardized world geochemical atlas and global geochemical database are being prepared by the International Geological Correlation Program (IGCP, 1995; <http://www.unesco.org/general/eng/programmes/science/programme/environ/igcp/index.html>). The Geochemical Earth Reference Model (GERM) initiative is establishing a consensus on chemical characterization of the Earth (<http://www-ep.es.llnl.gov/germ/germ-home.html>).

Crustal abundance

There are numerous compilations of estimates of the average abundance of elements within the Earth’s crust (see Rickwood, 1983). These compilations tend to vary due to the different

approaches, methods, and assumptions used to derive estimates of crustal abundance. Our knowledge of the crustal abundance of most rock types (and hence their associated elements) is inadequate because the Earth's crust is so variable and so poorly exposed.

Table 2.8 lists approximate (order of magnitude) consensus values of various published estimates of crustal abundance and the range of these estimates (Rickwood, 1983). Clarke values, which refer to the average abundance of a particular element in the lithosphere, are also given in Table 2.8 (Fortescue, 1992); Clarke values are synonymous with crustal abundances. The "Clarke of Concentration" (KK), an expression for the relative abundance of an element in a given sample or set of samples, is the abundance of an element in the sample(s) divided by its Clarke value. The KK is used to delineate materials that are enriched or depleted in an element relative to average values.

Table 2.8 also includes the abundance of minor and trace elements in two different rock types, basalt and granite (Levinson, 1980). These data illustrate how the abundances of most minor and trace elements vary from mafic to granitic rocks, which in turn reflect magmatic differentiation. Figure 2.4 illustrates the range of minor and trace elements in rocks and the relationship between typical abundances (Rose et al., 1979). The trace-element content of specific rock types is the major control on background levels in soils, sediments, and waters.

Soil

Soils form from chemically and mechanically weathering rocks under the influence of climatic and topographic controls, microbiological processes, the abundance of an element in the parent rock, the nature and duration of the weathering processes operating on the parent rock, gains and losses by physical processes (e.g., wind transport), the solubility of the primary and secondary mineral phases present in the parent rock and in the soil (geoavailability), the type of vegetation, and the type and amount of organic matter in the soil. Solubility and kinetic reactions, and pore-water composition control the ability of solid phases to replenish an element as it is depleted from the soil's interstitial water. These factors are all related to geoavailability (see Table 2.1).

Soils normally contain different layers, which are referred to as soil horizons. These horizons commonly have very different properties and elemental distributions, and may range from a few millimeters to meters in thickness. When comparing the composition of different soils, it is important to be consistent in the soil horizon being considered.

Table 2.9 lists average concentrations and ranges of elements in soils compiled by different authors. Soil samples from the western and eastern United States (Shacklette and Boerngen, 1984) were collected from a depth of 20 cm. This depth was chosen because it is a depth below the plow zone that would include parts of the zone of illuviation (i.e., accumulation of dissolved or suspended soil materials as a result of transport) in most well-developed zonal soils (Shacklette and Boerngen, 1984). The selected average of Lindsay (1979) is an arbitrary reference level for elements in soils. Figure 2.5 compares minor and trace-element concentrations in topsoils to their abundance in the lithosphere (Kabata-Pendias and Pendias, 1992).

Vegetation

The ability of plants to absorb minor and trace elements is highly variable depending on the species, soil conditions, climate, and season. However, on average, this ability exhibits some general trends for particular elements, as illustrated on Figure 2.6 (Kabata-Pendias and Pendias, 1992). Table 2.10 lists concentration ranges of elements in plant leaf tissue as a function of typically measured range, deficiency, and toxicity. These ranges are only approximations. It is important to note that the typical range of concentrations of some elements in plant leaf tissue can be close to or even overlapping with excessive or toxic concentrations (e.g., boron, copper, and zinc). Markert (1994) has published the trace element content of a "reference plant" which represents the trace element content of plants in general (Table 2.10).

Dissolved and suspended riverine materials

Factors affecting the chemical composition of most surface waters are climate (especially intensity and frequency of rainfall), lithology, geoavailability of elements, vegetation, topography, biological activity, and time. It is difficult to predict which of these factors will be most important for a given situation. However, the composition of water is most often controlled by interactions with earth materials through which the water flows. For surface waters, these interactions generally take place in the soil zone. The composition of uncontaminated surface waters varies by several orders of magnitude depending on environmental conditions (Meybeck and Helmer, 1989), analytical techniques, and possible contamination.

Concentrations of trace elements in surface waters are still a matter of debate and uncertainty because water samples can be easily contaminated during collection or analysis, analytical detection limits are sometimes greater than the natural concentrations and few pristine surface waters have been analyzed cleanly for trace elements (Martin et al., 1980). Table 2.11 lists concentrations of dissolved constituents in surface waters compiled by various authors. The values listed in this table are meant only as a rough guide for element concentrations in surface water.

As a first approximation, the composition of suspended matter in rivers may be assumed to be that of proximal surficial rocks in the drainage basin (Whitfield and Turner, 1979; Martin and Whitfield, 1983). However, the degree of chemical weathering and individual element behavior will affect the ultimate element concentrations in suspended matter.

FACTORS AFFECTING METAL MOBILITY AND DISPERSIVITY

Chemical and physical properties of elements

Elements have certain inherent chemical and physical properties that influence their behavior in the environment (see Nordstrom, 1999). The chemistry of the elements is determined by how atoms exchange, interchange, and share the electrons that occupy their "outermost orbits" (the valence electrons). The term "electronegativity" refers to the relative tendency of an atom to acquire negative charge. Listings of electronegativities are common in most inorganic or physical chemistry textbooks (e.g.,

TABLE 2.8—Estimates of the crustal abundance of selected chemical elements by various authors, and the abundance of minor and trace elements in two different types of rocks. Data are as ppm; significant figures reflect those reported by the source.

Element	Estimates of crustal abundance (ppm)			Abundance in rocks (ppm)	
	Approximate consensus ⁽¹⁾	Consensus range ⁽²⁾	Clarke value ⁽³⁾	Basalt ⁽⁴⁾	Granite ⁽⁴⁾
Aluminum (Al)	80,000	74,500–88,649	83,600		
Antimony (Sb)		0.15–1	0.20	0.2	0.2
Arsenic (As)	2	1.7–5	1.80	2	1.5
Barium (Ba)	430	179–1070	390	250	600
Beryllium (Be)	3	1.3–10	2.00	0.5	5
Bismuth (Bi)	0.2	0.0029–0.2	0.0082 ⁽³⁾	0.15	0.1
Boron (B)	10	3–50	9.00	5	15
Bromine (Br)	3	0.26–10	2.50	3.6	2.9
Cadmium (Cd)	0.18	0.1–5	0.16	0.2	0.2
Calcium (Ca)	30,000	16,438–62,894	46,600		
Carbon (C)		200–4902	180		
Cerium (Ce)	45	29–96	66.4	35	46
Cesium (Cs)	3	1–10	2.60	1	5
Chlorine (Cl)	500(?)	100–2000	126	60	165
Chromium (Cr)	200	70–330	122	200	4
Cobalt (Co)	25	12–100	29.0	50	1
Copper (Cu)	60(?)	14–100	68.0	100	10
Dysprosium (Dy)	4.5	3–7.5	5.00	3	0.5
Europium (Eu)	1.2	0.2–1.4	2.14	1.27	
Fluorine (F)	500	270–800	544	400	735
Gadolinium (Gd)	7	5–10	6.14	4.7	2
Gallium (Ga)	17	1–19	19.0	12	18
Germanium (Ge)	15(?)	1.3–7	1.50	1.5	1.5
Gold (Au)	0.004	0.001–0.005	0.0040	0.004	0.004
Indium (In)	0.1	0.05–0.25	0.24	0.1	0.1
Iodine (I)	0.5	0.05–10	0.46	0.5	0.5
Iridium (Ir)	0.001	0.001–0.01	0.000002		
Iron (Fe)	50,000	30,888–64,668	62,200		
Lanthanum (La)		6.5–100	34.6	10.5	25
Lead (Pb)	16	12–20	13.0	5	20
Lithium (Li)	30	18–65	18.0	10	30
Lutetium (Lu)	0.9	0.27–1.7	0.54	0.2	0.01
Magnesium (Mg)	21,000	10,191–33,770	27,640		
Manganese (Mn)	900	155–1549	1,060	2200	500
Mercury (Hg)	0.08	0.03–0.5	0.086	0.08	0.08
Molybdenum (Mo)	2	1–15	1.20	1	2
Neodymium (Nd)	25	17–37	39.6	17.8	18
Nickel (Ni)	80	23–200	99.0	150	0.5
Niobium (Nb)	20	0.32–24	20.0	20	20
Nitrogen (N)	20(?)	15–400	19.0		
Oxygen (O)	470,000	452,341–495,200	456,000		
Palladium (Pd)	0.01	0.0084–0.05	0.015	0.02	0.002
Phosphorus (P)	1000	480–1309	1,120		
Platinum (Pt)	0.005	0.005–0.2	0.0005	0.02	0.008
Potassium (K)	26,000	15,773–32,625	18,400		
Rhenium (Re)	0.001	0.00042–0.001	0.0007	0.0005	0.0005
Rubidium (Rb)	120	78–310	78.0	30	150
Samarium (Sm)	7	6.5–8	7.02	4.2	3
Scandium (Sc)		5–22	25.0	38	5
Selenium (Se)	0.09	0.05–0.8	0.050	0.05	0.05
Silicon (Si)	270,000	257,500–315,896	273,000		
Silver (Ag)	0.07	0.02–0.1	0.080	0.1	0.04
Sodium (Na)	24,000	15,208–28,500	22,700		
Strontium (Sr)	350	150–480	384	465	285
Sulfur (S)	500	260–1200	340		
Tantalum (Ta)	2	0.24–3.4	1.70	0.5	3.5
Tellurium (Te)		0.00036–0.01	0.0040	0.001	0.001
Thallium (Tl)	1	0.1–3	0.72	0.1	0.75
Thorium (Th)	10	5.8–20	8.10	2.2	17
Tin (Sn)	2.5	2–80	2.10	1	3
Titanium (Ti)	5000	2458–9592	6320	9000	2300

TABLE 2.8—Continued

Element	Approximate consensus ⁽¹⁾	Estimates of crustal abundance (ppm)			Abundance in rocks (ppm)	
		Consensus range ⁽²⁾	Clarke value ⁽³⁾	Basalt ⁽⁴⁾	Granite ⁽⁴⁾	
Tungsten (W)	1	0.4–70	1.20	1	2	
Uranium (U)	3	1.7–80	2.30	0.6	4.8	
Vanadium (V)	150	53–200	136	250	20	
Ytterbium (Yb)	3	0.33–8	3.10	1.11	0.06	
Yttrium (Y)	30	19–50	31.0	25	40	
Zinc (Zn)	70	40–200	76.0	100	40	
Zirconium (Zr)	160	130–400	162	150	180	

⁽¹⁾Data are from Rickwood (1983, table A-II) and represent an approximate consensus (within an order of magnitude) of published estimates of crustal abundance.

⁽²⁾Data are from Rickwood (1983, table A-II) and give the range of the published estimates of crustal abundance used to compile the approximate consensus values in the previous column.

⁽³⁾Data are from Fortescue (1992, table 4). According to the author, the value for Bi appears to be too low.

⁽⁴⁾Data are from Levinson (1980, table 2-1) for two different types of rocks.

Huhey et al., 1993). Elements that have low electronegativity, such as metals, are relatively easily ionized and tend to combine with non-metallic elements of high electronegativity. Hence, electronegativity is indicative of the types of compounds and the types of chemical bonds that a given element will form.

The oxidation state (also referred to as oxidation number) represents the charge that an atom “appears” to have when electrons are counted. Oxidation states are used to track electrons in oxidation-reduction reactions. Ionic radii generally decrease with increasing oxidation state. Also, for a given element, the preferred geometry varies with different oxidation states. For example, the electronic structure of Co^{2+} is such that tetrahedral or octahedral coordination is energetically favored; in contrast, trigonal bipyramidal coordination is most stable for Co^+ (Cotton and Wilkinson, 1988). Finally, elements with variable oxidation states, such as iron and copper, can take part in oxidation-reductions reactions. Consequently, oxidation state can influence binding sites and chemical reactions for a given element.

The size of an ion primarily depends on its oxidation state. The ionic radius of an element is important in determining if it can take part in particular biochemical reactions. Also, elements with similar ionic radii and charge can sometimes substitute for one another. For example, Cd^{2+} can substitute for Ca^{2+} in many geochemical and biological systems.

Ionic potential (the ratio of oxidation number to ionic radius) of elements has been related to their mobility (see Rose et al., 1979). Figure 2.7 shows the mobility of various elements as a function of ionic potential. Elements with low ionic potential are generally mobile in the aquatic environment as simple cations (e.g., Na^+ , Ca^{2+}) and elements with high ionic potential are generally mobile as oxyanions (i.e., elements that combine with oxygen to form an anionic species in aqueous systems; e.g., SO_4^{2-} , MoO_4^{2-}). Elements with high ionic potential tend to form covalent bonds rather than ionic bonds. Elements with intermediate ionic potential have a tendency to strongly sorb or hydrolyze and exhibit low solubility; therefore, these elements are fairly immobile (Rose et al., 1979). The concept of ionic potential is useful in explaining how elements with apparently different chemical properties behave similarly during migration in the environment.

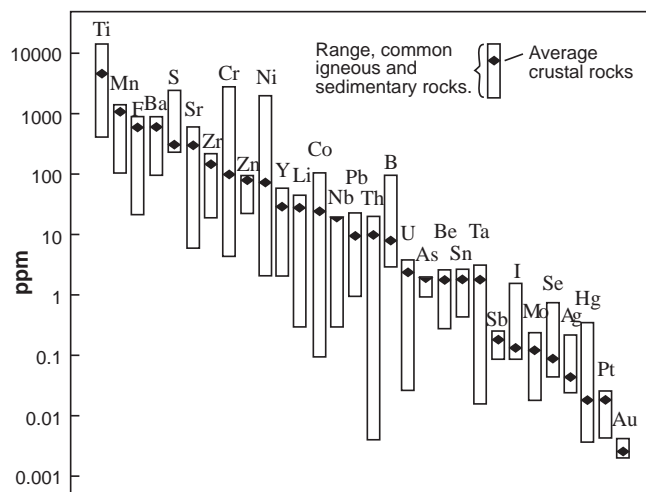


FIGURE 2.4—Average concentrations and ranges of trace elements in rocks. After Rose et al. (1979).

Classification systems

Goldschmidt's geochemical classification of the elements

Goldschmidt (1954) studied the distribution of elements in the Earth, meteorites, and smelter products. He grouped the elements into those that tend to occur with native iron and which are probably concentrated in the Earth's core (siderophile elements), those concentrated in sulfides and characteristic of sulfide ore deposits (chalcophile elements), those that generally occur with silica (lithophile elements), and those that exist in gaseous form (atmosphile elements). Figure 2.8 shows Goldschmidt's groupings of the elements in the context of the periodic table. Elements of each group generally exhibit similar geologic behavior. However, some elements have characteristics common to two groups. Although rough, the terminology of Goldschmidt's classification system is still used, and this system has provided the foundation for other more recent geochemical classification systems (e.g., Beus and Grigorian, 1977).

TABLE 2.9—Means and ranges of elemental concentrations in soils. Data are as ppm; significant figures reflect those reported by the source.

Element	Western United States ⁽¹⁾		Eastern United States ⁽²⁾		Lindsay (1979) Average ⁽⁵⁾
	Mean ⁽³⁾	Range ⁽⁴⁾	Mean ⁽³⁾	Range ⁽⁴⁾	
Aluminum (Al)	58,000	5,000->100,000	33,000	7,000->100,000	71,000
Antimony (Sb)	0.47	<1-2.6	0.52	<1-8.8	
Arsenic (As)	5.5	<0.10-97	4.8	<0.1-73	5
Barium (Ba)	580	70-5,000	290	10-1,500	430
Beryllium (Be)	0.68	<1-15	0.55	<1-7	6
Boron (B)	23	<20-300	31	<20-150	10
Bromine (Br)	0.52	<0.5-11	0.62	<0.5-5.3	5
Cadmium (Cd)					0.06
Calcium (Ca)	18,000	600-320,000	3,400	100-280,000	13,700
Carbon (C)	17,000	1,600-100,000	15,000	600-370,000	20,000
Cerium (Ce)	65	<150-300	63	<150-300	
Cesium (Cs)					6
Chlorine (Cl)					100
Chromium (Cr)	41	3-2,000	33	1-1,000	100
Cobalt (Co)	7.1	<3-50	5.9	<0.3-70	8
Copper (Cu)	21	2-300	13	<1-700	30
Fluorine (F)	280	<10-1,900	130	<10-3,700	200
Gallium (Ga)	16	<5-70	9.3	<5-70	14
Germanium (Ge)	1.2	0.58-2.5	1.1	<0.1-2.0	1
Iodine (I)	0.79	<0.5-9.6	0.68	<0.5-7.0	5
Iron (Fe)	21,000	1,000->100,000	14,000	100->100,000	38,000
Lanthanum (La)	30	<30-200	29	<30-200	30
Lead (Pb)	17	<10-700	14	<10-300	10
Lithium (Li)	22	5-130	17	<5-140	20
Magnesium (Mg)	7,400	300->100,000	2,100	50-50,000	5,000
Manganese (Mn)	380	30-5,000	260	<2-7,000	600
Mercury (Hg)	0.046	<0.01-4.6	0.081	0.01-3.4	0.03
Molybdenum (Mo)	0.85	<3-7	0.32	<3-15	2
Neodymium (Nd)	36	<70-300	46	<70-300	
Nickel (Ni)	15	<5-700	11	<5-700	40
Niobium (Nb)	8.7	<10-100	10	<10-50	
Nitrogen (N)					1,400
Oxygen (O)					490,000
Phosphorus (P)	320	40-4,500	200	<20-6,800	600
Potassium (K)	18,000	1,900-63,000	12,000	50-37,000	8,300
Rubidium (Rb)	69	<20-210	43	<20-160	10
Scandium (Sc)	8.2	<5-50	6.5	<5-30	7
Selenium (Se)	0.23	<0.1-4.3	0.30	<0.1-3.9	0.3
Silicon (Si)	300,000	150,000-440,000	340,000	17,000-450,000	320,000
Silver (Ag)					0.05
Sodium (Na)	9,700	500-100,000	2,500	<500-50,000	6,300
Strontium (Sr)	200	10-3,000	53	<5-700	200
Sulfur (S)	1,300	<800-48,000	1,000	<800-3,100	700
Thorium (Th)	9.1	2.4-31	7.7	2.2-23	
Tin (Sn)	0.90	<0.1-7.4	0.86	<0.1-10	10
Titanium (Ti)	2,200	500-20,000	2,800	70-15,000	4,000
Uranium (U)	2.5	0.68-7.9	2.1	0.29-11	
Vanadium (V)	70	7-500	43	<7-300	100
Ytterbium (Yb)	2.6	<1-20	2.6	<1-50	
Yttrium (Y)	22	<10-150	20	<10-200	50
Zinc (Zn)	55	10-2,100	40	<5-2,900	50
Zirconium (Zr)	160	<20-1,500	220	<20-2,000	300

⁽¹⁾Values observed in the western United States, west of the 96th meridian. Samples were collected at a depth of approximately 20 cm. Data are from Shacklette and Boerngen (1984, table 2).

⁽²⁾Values observed in the eastern United States, east of the 96th meridian. Samples were collected at a depth of approximately 20 cm. Data are from Shacklette and Boerngen (1984, table 2).

⁽³⁾Means are geometric means except for K and Si, which are arithmetic means.

⁽⁴⁾Ranges are those observed from the study. Data are from Shacklette and Boerngen (1984, table 2).

⁽⁵⁾Selected average for soils from Lindsay (1979, table 1.1; no information on depth or type of average).

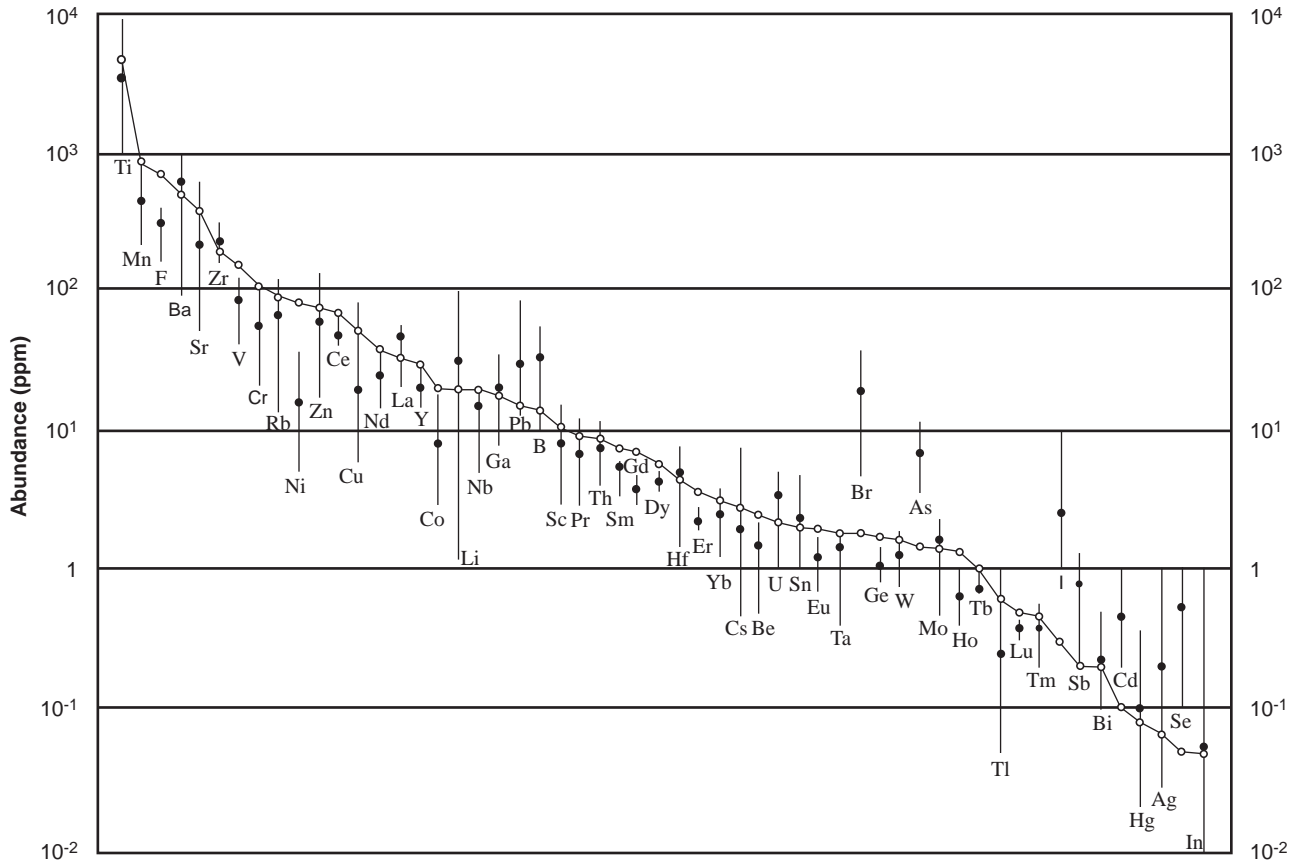


FIGURE 2.5—Abundance of trace elements in soils compared to their abundance in the lithosphere. Open circles are the mean content in the lithosphere. Filled circles are the mean content in topsoils and vertical lines indicate the range of values commonly found in topsoils. After Kabata-Pendias and Pendias (1992).

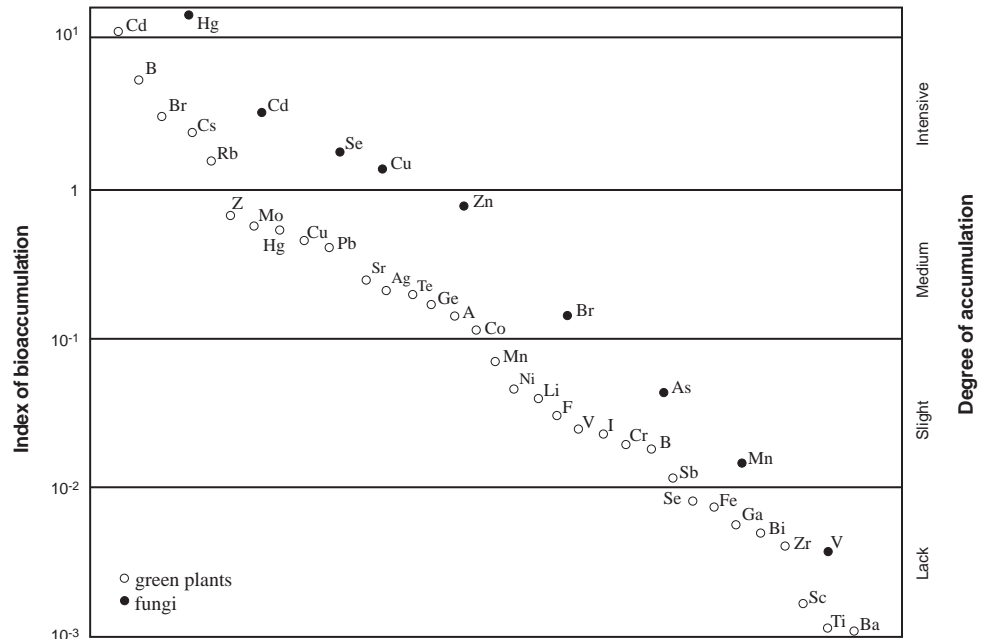


FIGURE 2.6—Generalized bioaccumulation of elements by plants from soils. Bioaccumulation by individual plants is highly variable and depends upon plant species, soil, climate, etc. The index of bioaccumulation is the ratio of the element concentration in plants to the concentration in soils. After Kabata-Pendias and Pendias (1992).

TABLE 2.10—Generalized concentration ranges of chemical elements in mature plant leaf tissue (as ppm on a dry-weight basis). Sensitive or highly tolerant species are not included. Significant figures reflect those reported by the source.

Element	Typical range ⁽¹⁾	Deficient ⁽¹⁾	Excessive or toxic ⁽¹⁾	Reference plant ⁽²⁾
Antimony (Sb)	7–50		150	0.1
Arsenic (As)	1–1.7		5–20	0.1
Barium (Ba)			500	40
Beryllium (Be)	<1–7		10–50	0.001
Boron (B)	10–200	5–30	50–200	40
Cadmium (Cd)	0.05–0.2		5–30	0.05
Chromium (Cr)	0.1–0.5		5–30	1.5
Cobalt (Co)	0.02–1		15–50	0.2
Copper (Cu)	5–30	2–5	20–100	10
Fluorine (F)	5–30		50–500	2.0
Lead (Pb)	5–10		30–300	1.0
Lithium (Li)	3		5–50	
Manganese (Mn)	20–300	15–25	300–500	200
Mercury (Hg)			1–3	0.1
Molybdenum (Mo)	0.2–1	0.1–0.3	10–50	0.5
Nickel (Ni)	0.1–5		10–100	1.5
Selenium (Se)	0.001–2		5–30	0.02
Silver (Ag)	0.5		5–10	0.2
Thallium (Tl)			20	0.05
Tin (Sn)			60	0.2
Titanium (Ti)	0.5–2.0	0.2–0.5	50–200	5.0
Vanadium (V)	0.2–1.5		5–10	0.5
Zinc (Zn)	27–150	10–20	100–400	50
Zirconium (Zr)	0.5–2.0	0.2–0.5	15	

⁽¹⁾Data are from Kabata-Pendias and Pendias (1992) with revisions by Pais and Jones (1997).

⁽²⁾Data are from Markert (1994). Represents the trace element content of plants in general.

Classifications of metals

Metals can be classified into groups based on their capacity for binding to different anions. Several classification systems have developed through the years (e.g., Whitfield and Turner, 1983), but the foundation is often built upon the empirical system of Ahrlund et al. (1958). They divided metal ions into Classes A and B, depending on whether the metal ions formed their most stable complexes with ligands of the first row of groups V, VI, or VII of the periodic table (i.e., nitrogen, oxygen, and fluorine, respectively), or with heavier lower-row ligands of those groups (i.e., phosphorus, sulfur, and iodine). Stable complexes are formed depending on the number of valence electrons of the metal ion.

Class A metal cations preferentially form aqueous complexes with fluoride and with ligands having oxygen as the electron donor (e.g., carboxyl groups (COOH) and PO₄³⁻). Water is strongly attracted to these metals, and no sulfides (complexes or precipitates) are formed by these ions in aqueous solution. Class A metals tend to form relatively insoluble precipitates with OH⁻, CO₃²⁻, and PO₄³⁻ (Stumm and Morgan, 1996). The stability of a Class A metal cation complex with a given ligand generally increases with an increase in charge on the metal ion, and ions with the smallest radii usually form the most stable complexes.

Class B metal cations form complexes preferentially with ligands containing iodine, sulfur, or nitrogen as donor atoms. These metal cations may bind ammonia more strongly than water, and

CN⁻ in preference to OH⁻. Class B metal cations form insoluble sulfides and soluble complexes with S²⁻ and HS⁻ (Stumm and Morgan, 1996). It is difficult to generalize about stability sequences for complexes in this class.

Pearson (1963, 1968a, 1968b) introduced the terms “hard” and “soft” acid and base to describe Class A and B metals and ligands. A “hard acid” is a Class A metal ion, a “soft acid” is a Class B metal ion, a “hard base” is a Class A ligand, and a “soft base” is a Class B ligand. Hard acids tend to bind to hard bases, and soft acids tend to bind to soft bases. The terms “hard” and “soft” are relative, and there are borderline cases between hard and soft for both acids and bases. Also, within each grouping, some acids are harder or softer than others and will behave accordingly. Figure 2.9 shows the periodic table with acids classified by the hard-soft-acid-base (HSAB) system according to Huheey et al. (1993); Table 2.12 lists the bases by this classification. Some of these classifications are mixed due to multiple common oxidation states of some elements. Generalizations about the speciation, behavior, and mobility of elements in aqueous systems can be made based on this type of classification system.

Transition-metal cations have a reasonably well-established rule for the sequence of complex stability based on empirical observation—the Irving-Williams order. According to this rule, the stability of complexes follows the order:

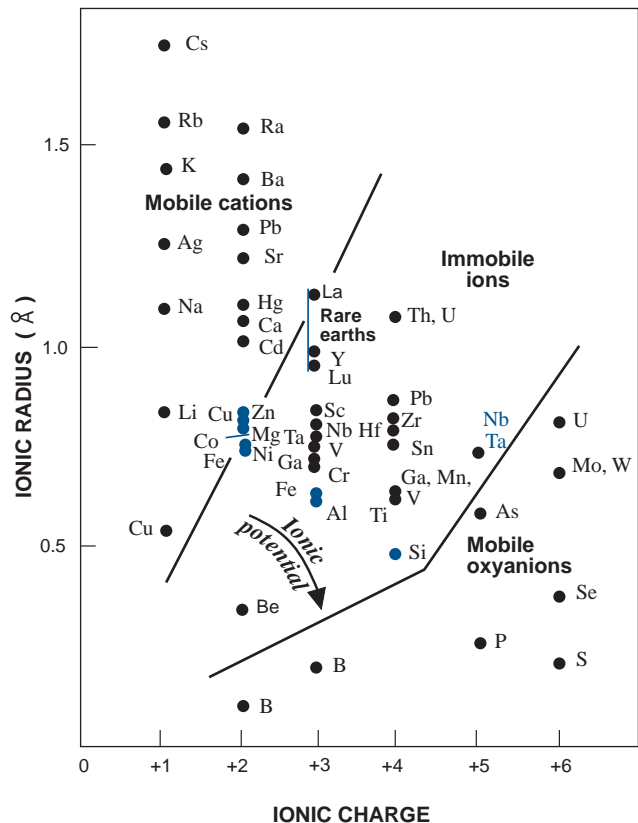


FIGURE 2.7—Mobility of chemical elements in the surficial environment as a function of ionic potential. After Rose et al. (1979).

TABLE 2.11—Summary of the average elemental composition of dissolved and suspended matter in surface water from a variety of sources and various authors.

Element	Martin and Whitfield (1983)		Meybeck (1988)	Hem (1985)
	Dissolved ⁽¹⁾ (µg/l)	Suspended ⁽¹⁾ (µg/g)	Dissolved ⁽²⁾ (µg/l)	Dissolved ⁽³⁾ (µg/l)
Aluminum (Al)	50	94,000	40 ± 20	
Antimony (Sb)	1	2.5		0.1–1s
Arsenic (As)	1.7	5	1 ± 0.5	0.1–1s
Barium (Ba)	60	600		10s
Beryllium (Be)				0.1s
Boron (B)	18	70	30 ± 20	
Bromine (Br)	20	5		
Cadmium (Cd)	0.02	(1)		0.1–1s
Calcium (Ca)	13,300	21,500		
Cerium (Ce)	0.08	95		
Cesium (Cs)	0.035	6	0.05 ± 0.03	
Chromium (Cr)	1	100	0.8 ± 0.3	0.1–1s
Cobalt (Co)	0.2	20	0.1 ± 0.05	0.1s
Copper (Cu)	1.5	100	2 ± 1	1–10s
Erbium (Er)	0.004	(3)		
Europium (Eu)	0.001	1.5		
Fluorine (F)			100 ± 20	
Gadolinium (Gd)	0.008	(5)		
Gallium (Ga)	0.09	25		
Gold (Au)	0.002	0.05		
Hafnium (Hf)	0.01	6		
Holmium (Ho)	0.001	(1)		
Iron (Fe)	40	48,000	50 ± 30	
Lanthanum (La)	0.05	45		
Lead (Pb)	0.1	100		0.1–1s
Lithium (Li)	12	25		
Lutetium (Lu)	0.001	0.5		
Magnesium (Mg)	3,100	11,800		
Manganese (Mn)	8.2	1,050	10 ± 5	
Mercury (Hg)				0.1s
Molybdenum (Mo)	0.5	3	0.8 ± 0.4	0.1–1s
Neodymium (Nd)	0.04	35		
Nickel (Ni)	0.5	90	0.4 ± 0.3	0.1–1s
Phosphorus (P)	115	1,150		
Potassium (K)	1,500	20,000		
Praseodymium (Pr)	0.007	(8)		
Rubidium (Rb)	1.5	100		
Samarium (Sm)	0.008	7		
Scandium (Sc)	0.004	18		
Selenium (Se)				0.1s
Silicon (Si)	5,000	285,000		
Silver (Ag)	0.3	0.07	0.4 ± 0.2	0.1s
Sodium (Na)	5,300	7,100		
Strontium (Sr)	60	150		
Tantalum (Ta)	<0.002	1.25		
Terbium (Tb)	0.001	1.0		
Thorium (Th)	0.1	14		0.01–0.1s
Thulium (Tm)	0.001	(0.4)		
Titanium (Ti)	10	5,600		
Uranium (U)	0.24	3	0.26	0.1–1s
Vanadium (V)	1	170		1s
Ytterbium (Yb)	0.004	3.5		
Yttrium (Y)		30		
Zinc (Zn)	30	250	10 ± 5	1–10s

⁽¹⁾Data are from Martin and Whitfield (1983, Table 4). Values are based on analytical results from world rivers.

⁽²⁾Data are from Meybeck (1988, p. 262). Ranges are based on more than ten rivers and represent an estimate of world averages.

⁽³⁾Data are from Hem (1985). Values are based on a variety of literature citations for element concentrations in a variety of water sources, including ground water.

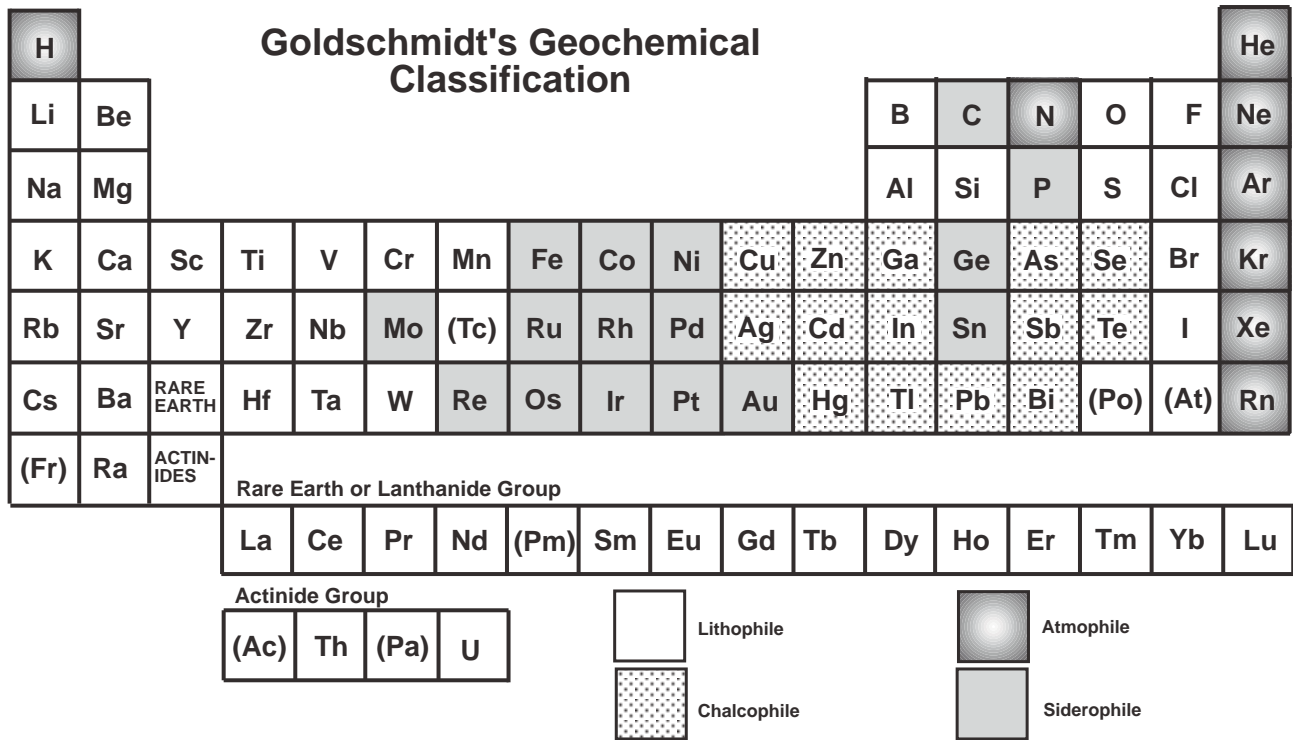


FIGURE 2.8—Periodic table showing Goldschmidt's geochemical classification of the elements. Siderophilic elements occur with native iron and are likely concentrated in the Earth's core, chalcophilic elements are concentrated in sulfides, lithophilic elements commonly occur with silica, and atmophilic elements exist as gases. After Levinson (1980).

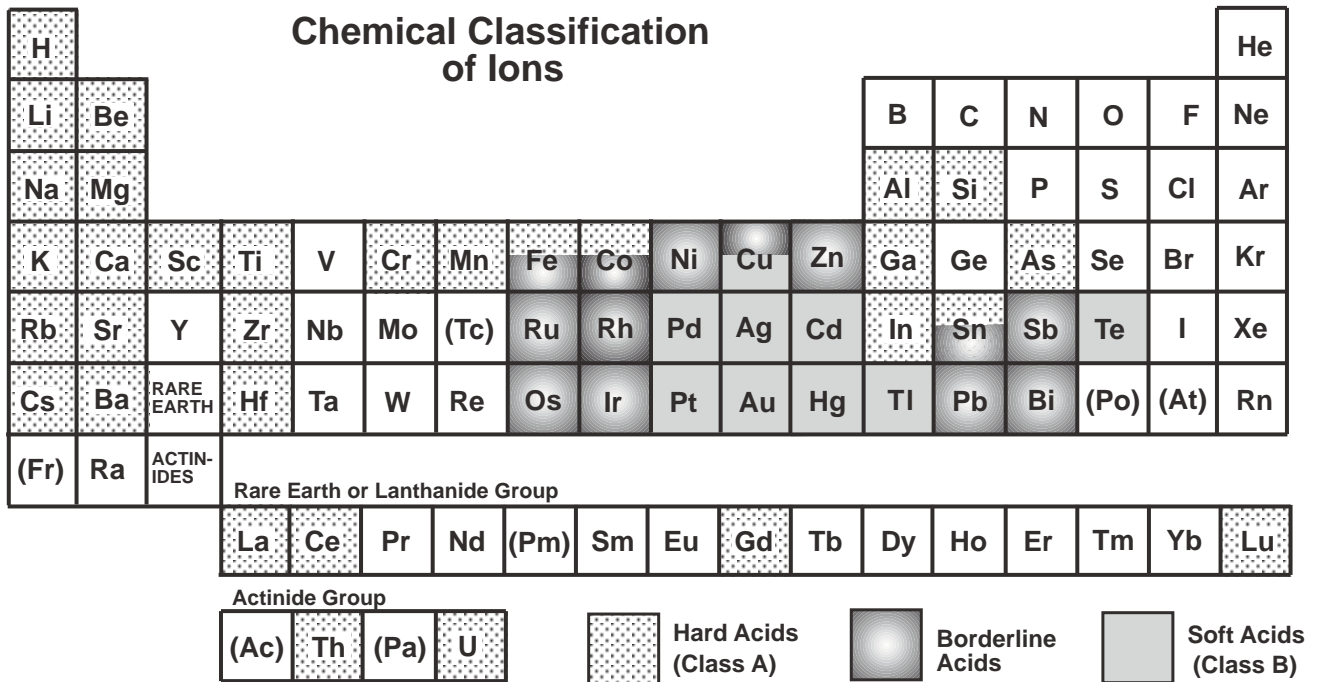
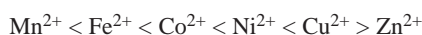


FIGURE 2.9—Periodic table showing the chemical classification of metal ions. Lack of shading or pattern is due to lack of information for that element or to its classification as a base. Information is from Huheey et al. (1993, table 9.7). Hybrid classifications are due to different valence states.



This sequence is the same sequence as the elements are located in the periodic table. Note that copper forms the most stable complexes with ligands in this series of metals.

TABLE 2.12—List of hard, borderline, and soft bases (after Huheey et al., 1993; “R” refers to an organic molecule).

Hard Bases

NH₃, RNH₂, N₂H₄
H₂O, OH⁻, O²⁻, ROH, RO⁻, R₂O
CH₃COO⁻, CO₃²⁻, NO₃⁻, PO₄³⁻, SO₄²⁻, ClO₄⁻
F⁻, (Cl⁻)

Borderline Bases

C₆H₅NH₂, C₅H₅N, N₃⁻, N₂
NO₂⁻, SO₃²⁻
Br⁻

Soft Bases

H⁻
R⁻, C₂H₄, C₆H₆, CN⁻, RNC, CO
SCN⁻, R₃P, (RO)₃P, R₃As
R₂S, RSH, RS⁻, S₂O₃²⁻
I⁻

General characteristics of elements in aqueous systems

A general overview of the characteristics of trace elements is given by Pais and Jones (1997). Mobility encompasses the general characteristics and speciation of elements in aqueous systems. Table 2.13 lists several elements that exist as cations or anions in aqueous systems. The behavior of cations and anions is quite different in aqueous systems. Dissolved metals do not normally occur only as free ions, but rather combine with other atoms into different aqueous complexes. Cations are generally more mobile under acidic conditions whereas anions are generally less mobile. This characteristic can have an effect on bioavailability. For example, aluminum, a cation which may be toxic to aquatic life, is fairly soluble at low pH but is relatively insoluble at circumneutral pH. Another example is elements that tend to form oxyanions in water (e.g., arsenic, boron, chromium, molybdenum, selenium, and vanadium) are often transported through living cell membranes by diffusion-controlled processes; the membranes generally do not provide a barrier to these oxyanionic species (Wood, 1988).

Elements sensitive to oxidation-reduction (redox) conditions are also tabulated in Table 2.13. A redox-sensitive element will generally undergo a change in mobility at oxidizing or reducing geochemical barriers. For example, chromium dissolves as it is oxidized to chromium (VI) and precipitates on reduction to chromium (III); this is important because chromium (VI) is much more toxic than is chromium (III). Similarly, uranium is immobile under reducing conditions but can be mobile under oxidizing conditions. On the other hand, iron and manganese may be soluble under reducing conditions; consequently, metals sorbed onto hydrous iron and manganese oxides can be released under reducing conditions.

TABLE 2.13—General characteristics of some chemical elements in simple surface or near-surface aqueous systems.⁽¹⁾⁽²⁾

Element	Anionic ⁽³⁾	Cationic	Redox-sensitive ⁽⁴⁾
Aluminum (Al)		X	
Antimony (Sb)	X		X
Arsenic (As)	X		X
Barium (Ba)		X	
Beryllium (Be)		X	
Boron (B)	X		
Cadmium (Cd)		X	
Chromium (Cr)	X	X	X
Cobalt (Co)		X	
Copper (Cu)		X	X
Iron (Fe)		X	X
Lead (Pb)		X	(X ⁽⁶⁾)
Lithium (Li)		X	
Manganese (Mn)		X	X
Mercury (Hg)		X	X
Molybdenum (Mo)	X	X ⁽⁵⁾	X
Nickel (Ni)		X	
Selenium (Se)	X		X
Silver (Ag)		X	
Thorium (Th)		X	(X ⁽⁶⁾)
Uranium (U)	X	X	X
Vanadium (V)	X	X	X
Zinc (Zn)		X	

⁽¹⁾This table is meant as a simple guide for element behavior under normal surface or near-surface aqueous conditions.

⁽²⁾This table does not include complexes with other elements.

⁽³⁾Anionic species exist as oxyanions.

⁽⁴⁾Elements that change oxidation state and oftentimes exhibit different behavior under different oxidation-reduction (redox) conditions.

⁽⁵⁾Cationic species exist for Mo but are rare and usually ignored in aqueous systems.

⁽⁶⁾Some of the elements, such as Pb and Th, are redox sensitive only under extreme conditions.

General geochemical concepts

Stability of minerals in the surficial environment

Minerals in the Earth’s crust are the ultimate source of metals. Metals are neither created nor destroyed in the environment, but are redistributed by several different kinds of mechanisms. Consequently, metals are not distributed uniformly in the Earth’s crust or among the various earth materials (e.g., rocks, soils, sediments).

There are two geochemical environments, (1) the deep-seated environment, which is not subject to surficial or near-surface processes, and (2) the surficial environment, which is subject to surficial or near-surface processes. Minerals formed in the deep-seated environment are unstable to varying degrees in the surficial environment, and elements contained in these minerals may be released, transported, and redistributed in the surficial environment. Table 2.14 lists some minor and trace elements found in common rock-forming minerals. When these minerals weather, the listed minor and trace elements may be expected to be released from the mineral matrix. From this type of information one may crudely predict which elements may be most readily remobilized in the surficial environment (geoavailability) based on the ease of weathering of the minerals in which they occur.

Bowen’s reaction series, illustrated on Figure 2.10, schematically depicts the magma differentiation process in the deep-seated

TABLE 2.14—Minor and trace elements found in common rock-forming minerals and relative stability of those minerals in the surficial environment. Characteristically hazardous metals, as defined by the Resource Conservation and Recovery Act (RCRA), are in bold (see Table 2.6 and text). Information is from Levinson (1980, Table 2-2.).

Mineral	X%	Range of concentration in crystal structure			Stability
		0.X%	0.0X%	0.00X% or less	
Olivine	--	Ni, Mn	Ca, Al, Cr , Ti, P, Co	Zn, V, Cu, Sc	
Pyroxene	--	Ti, Na, Mn, K	Cr , V, Ni, Cl, Sr	P, Cu, Co, Zn, Li, Rb, Ba	
Plagioclase	K	Sr	Ba , Rb, Ti, Mn	P, Ga, V, Zn, Ni, Pb , Cu, Li	
Amphibole (e.g., hornblende)	--	Ti, F, K, Mn, Cl, Rb	Zn, Cr , V, Sr, Ni	Ba , Cu, P, Co, Ga, Pb , Li, B	
Biotite	Ti, F	Ca, Na, Ba , Mn, Rb	Cl, Zn, V, Cr , Li, Ni	Cu, Sn, Sr, Co, P, Pb , Ga	
Potash Feldspar	Na	Ca, Ba , Sr	Rb, Ti	Pb , Ga, V, Zn, Ni, Cu, Li	
Muscovite	--	Ti, Na, Fe, Ba , Rb, Li	Cr , Mn, V, Cs, Ga	Zn, Sn, Cu, B, Nb	
Quartz	--	--	--	Fe, Mg, Al, Ti, Na, B, Ga, Ge, Mn, Zn	

environment. As a magma cools some elements in the magma are depleted as minerals form. Minerals crystallized at higher temperatures are less stable in the surficial environment and minerals formed at lower temperatures are more stable in the surficial environment. (An important exception to this generalization is calcite, which can be a late magmatic mineral phase and which is soluble in the surficial environment.)

Element cycles

A holistic approach is required to adequately understand and assess the environmental impacts of mineral development. Elements cycle through the Earth’s lithosphere, atmosphere, hydrosphere, and biosphere. Human activities, such as mining, can perturb these natural cycles and change the distribution, flux, and residence time of elements in various reservoirs (see Nriagu and Pacyna, 1988, and Nriagu, 1990, for world-wide inventories of industrial/municipal discharges of trace metals into air, soils, and aquatic ecosystems; Meybeck et al., 1989). To anticipate and assess the extent and degree of any perturbation one must understand and account for the various processes that control the distri-

bution, flux, and residence times of elements in natural systems. There is a complex web of interrelationships between factors involved in the flow of elements through a system, in the resulting environmental quality, and in the degree of reversible or irreversible effects on the environment or on human health. Many of these interrelationships are poorly understood and much work remains to be done to define and assess these factors. One also must try to determine metal budgets in contaminated systems (Merrington and Alloway, 1994). One can then place the situation into a broader perspective (e.g., watershed impact) and, if necessary, devise ways to eliminate, minimize, mitigate, or remediate the perturbation.

Landscape geochemistry

Landscape geochemistry can be applied to the understanding of metal distributions in the environment. Landscape geochemistry focuses on the interaction of the lithosphere with the hydrosphere, biosphere, and atmosphere, and links exploration geochemistry with environmental science (Fortescue, 1980). Landscape geochemistry is an holistic approach to the study of the geochemistry of the environment in that it involves element cycles and may involve local, regional, and global studies. Fortescue (1992) reviews the development of landscape geochemistry and provides the foundation of how it relates to environmental science.

Fortescue (1992) proposes the establishment of a discipline of “Global Landscape Geochemistry” (GLG), which may provide the foundation for future developments in applied and environmental geochemistry and which is necessary to adequately address current geoenvironmental problems. GLG regional geochemical mapping can be used to delineate geochemical provinces, identify local geochemical enrichments in mineral deposits, determine baseline environmental geochemistry, monitor environmental changes in soil and water geochemistry in response to human activities, evaluate the nutritional status of plants and animals, and

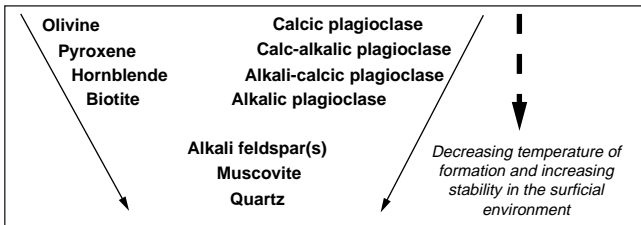


FIGURE 2.10—Bowen’s reaction series showing the sequence of mineralogical differentiation starting with a basaltic magma in the deep-seated environment. Minerals at the top of the series tend to be unstable in the surficial environment and subject to higher geoavailability.

study human health. Fortescue (1992) notes that there is a need to map geochemical landscapes as an essential preliminary step to the study of environmental geochemistry. Geochemical maps based on the analysis of rocks, soils, sediments, waters, and vegetation, originally compiled for mineral exploration purposes, may be extended to multi-purpose geochemical surveys that have applications in agriculture, pollution studies, and human health (Webb, 1964). However, geochemical analyses for mineral exploration purposes have generally been designed to be cost effective; consequently, the quality of the geochemical data often is inadequate for many environmental applications. Geochemical atlases have been prepared for Northern Ireland (Webb et al., 1973), England and Wales (Webb et al., 1978), the United Kingdom (Plant and Thornton, 1985), and several other countries. Darnley (1990) and IGCP (1995) discuss the International Geochemical Mapping Project, which proposes to produce geochemical maps of the world. A geology-based map of potential metal-mine drainage hazards in Colorado has been compiled by Plumlee et al. (1995).

Geochemical associations and pathfinder elements

Knowledge of geochemical associations and common pathfinder elements from the geochemical-exploration literature can be used for environmental purposes to determine which elements may be mobilized from a mined site for a given type of ore deposit. Ordinarily, a suite of elements is concentrated in a particular deposit. Geochemical exploration utilizes empirical knowledge of element associations that can serve as pathfinders for particular mineral deposit types. Boyle (1974), Beus and Grigorian (1977), Rose et al. (1979), Levinson (1980), Cox and Singer (1986), and du Bray (1995) compiled elemental associations for a variety of deposits. Table 2.15 lists geochemical signatures for selected types of mineral deposits. This information is useful for predicting element mobility and dispersivity in soils, sediments, water, and air from mined lands. For example, Li and Thornton (1993) report that the multi-element contamination of soils and plants in historical lead-zinc mining and smelting areas of the United Kingdom reflects the geochemical associations of the lead-zinc mineralization. Ficklin et al. (1992), Plumlee et al. (1992, 1993, 1999), and Ripley et al. (1996) relate the composition of mine-drainage waters to the geology of diverse mineral deposit types and discuss the environmental effects of mining various mineral deposit types. This topic is also discussed in Plumlee (1999).

Pathfinder elements are elements associated with a mineral deposit type that are used to explore for ore bodies. Elements enriched in an ore deposit will have different relative mobilities in surrounding wall rocks and in the weathering environment. The most useful pathfinder elements commonly are more easily analyzed or detected or are more mobile in the surficial environment than are the primary elements of the ore deposit. Additional elements may have been introduced at the ore deposit if ore processing occurred onsite. For example, if mercury has been used in gold amalgamation, this may be an element of concern during site characterization and remediation.

Geochemical gradients and barriers

As an outgrowth of landscape geochemistry, Perel'man (1977) discusses the importance of geochemical gradients, which

describe gradual changes of a landscape, and geochemical barriers, which describe abrupt changes. An example of a geochemical gradient might be the vertical and horizontal distribution of certain elements away from a mineral deposit within a constant lithology; for a given element an anomalous concentration eventually declines to a background concentration at some distance away from the deposit. Another example of a geochemical gradient is the concentration plume for some elements downwind from a smelter. Perel'man (1986) defines geochemical barriers as zones of the Earth's crust with sharp physical or chemical gradients that are commonly associated with accumulation of elements. Geochemical barriers represent abrupt changes in physical or chemical environments in the path of migration of elements causing the precipitation of certain elements from solution. Geochemical barriers include mechanical, physicochemical, biochemical, and anthropogenic (or technogenic) types. This chapter discusses physicochemical barriers including acidic, alkaline, reducing, oxidizing, evaporation, adsorption, and thermodynamic barriers. Complex barriers may be created when two or more barrier types are superimposed. Nordstrom and Alpers (1999) discuss the geochemistry of several physicochemical barriers.

Acidic barriers develop when pH drops. Under these conditions, elements that form anions (such as molybdenum) as well as certain complexes, generally become less mobile, whereas many metals that form cations (such as copper) generally become more mobile (see Table 2.13). Solubility relationships can play an important role. For example, aluminum is usually fairly mobile below a pH of about 4, but will precipitate between a pH of about 5 and 9. On the other hand, silicon (as SiO_2) is relatively insoluble at low pH and becomes more soluble at high pH. One of the most important effects of developing low-pH environments is the destruction of the carbonate-bicarbonate buffering system, a feedback mechanism that controls the extent of pH change in an aqueous system. Below a pH of about 4.5, carbonate and bicarbonate are converted to carbonic acid. Upon such acidification, the water loses its capacity to buffer changes in pH, and many photosynthetic organisms that use bicarbonate as their inorganic carbon source become stressed or die. Once damaged, the acid buffering capacity of a natural system may take significant time to recover, even if no further acid is added to the system. The carbonate-bicarbonate system may have both a direct and an indirect effect on the mobility of several elements.

Alkaline barriers develop where acidic waters encounter alkaline conditions over a short distance (e.g., oxidation zones of pyrite in limestone host rock). This type of barrier mostly retains those elements that migrate easily under acidic conditions and precipitate as hydroxides or carbonates under alkaline conditions (such as iron, aluminum, copper, nickel, and cobalt). During the shift to alkaline conditions, hydrous iron, aluminum, and manganese oxides may sorb trace metals and create an alkaline/adsorption complex barrier.

Reducing conditions develop in the absence of free oxygen (or other electron acceptors). They may result from inorganic or organic chemical reactions that are frequently mediated by microorganisms. Figure 2.11 illustrates the chemical-reaction sequence for oxidation-reduction reactions. This redox sequence is biologically mediated by a succession of microorganisms (see Stumm and Morgan, 1996). Reducing barriers can be divided into those that contain hydrogen sulfide and those that do not (referred to as "reducing gley" environments; Perel'man, 1986). Reducing hydrogen sulfide barriers develop where oxidizing or reducing

TABLE 2.15—Geochemical signatures for selected types of mineral deposits.⁽¹⁾⁽²⁾

Mineral deposit type	Model number(s) ⁽³⁾	Examples	Geochemical signature
Magmatic sulfide (Ni, Cu, PGE)	1; 2b; 5a, b; 6a, b; 7a	Noril'sk, Merensky Reef, Stillwater, Kambalda, Duluth	Ag, As, Au, Bi, Co, Cu, Cr, Fe, Hg, Mg, Ni, Pb, Sb, Se, Te, Ti, Zn, PGE (\pm Cd, Ga, In, Sn)
Carbonatite	10	Oka, Mountain Pass, Phalaborwa	Ba, Cu, F, Mn, Mo, Na, Nb, P, Pb, Th, Ti, U, V, Y, Zn, Zr, REE (B, Be, Hf, Li, Sn, Ta, W are rare)
Rare-metal pegmatite ⁽⁴⁾	13a, b	Petaca district, Black Hills district	B, Be, Cs, F, Li, Nb, Rb, Sn, Ta, Th, U, W, REE
Tin and (or) tungsten skarn replacement	14a-c	Pine Creek, Moina, Renison Bell	Ag, As, B, Be, Bi, Cs, Cu, F, Fe, Li, Mn, Mo, Pb, Rb, Re, Sn, W, Zn
Vein and greisen tin and tungsten	15a-c	Cornwall, Erzgebirge	Ag, As, B, Be, Bi, Cs, Cu, F, Li, Mo, Nb, P, Pb, Rb, Re, Rn, Sb, Sn, Ta, Th, U, W, Zn, REE
Climax molybdenum	16	Climax, Henderson, Questa	Al, Be, Cs, Cu, F, Fe, Li, Mo, Nb, Pb, Rb, Sn, Ta, Th, U, W, Zn
Porphyry copper	17	Bingham, El Salvador	Ag, As, Au, B, Ba, Bi, Cd, Co, Cr, Cs, Cu, F, Fe, Hg, K, La, Li, Mg, Mn, Mo, Na, Ni, Pb, Rb, Re, Sb, Se, Sr, Te, Tl, U, V, W, Zn
Copper, gold, and zinc-lead skarn	18b, c	Carr Fork, Fortitude, Bismark, New World	Ag, Al, As, Au, Be, Bi, Cd, Co, Cu, F, Fe, Mn, Mo, Pb, Sb, Se, Sn, Te, W, Zn (\pm Cr, Hg)
Polymetallic vein and replacement	19a; 22c	Leadville, New World, Park City, Eureka	Ag, Al, As, Au, Ba, Bi, Cu, F, Fe, Hg, Mn, Mo, P, Pb, Sb, Zn
Gold-silver-tellurium vein	22b	Sulpherets, Zortman-Landusky, Porgera	Ag, As, Au, Ba, Bi, Cu, F, Fe, Hg, Mn, Mo, Ni, Pb, Sb, Te, V, Zn, PGE (\pm Cd, Sc)
Volcanic-associated massive sulfide	24a, b; 28a	Cyprus, Kuroko, Besshi, Skouriotissa, Kidd Creek	Ag, As, Au, Ba, Bi, Cd, Co, Cr, Cu, Fe, Hg, Mn, Ni, Pb, Sb, Se, Sn, Zn (\pm Al, Mo)
Epithermal vein	25b-d	Creede, Comstock, Sado	Ag, Al, As, Au, Ba, Bi, Cu, Fe, Hg, Mn, Pb, Sb, Se, Te, U, W, Zn
Epithermal quartz-alunite	25e	Summitville, Julcani	Al, As, Au, Ba, Be, Bi, Co, Cu, Fe, Hg, Mn, Mo, Ni, Pb, Sb, Se, Sn, Te, Th, Tl, U, W, Zn, REE
Epithermal manganese	25g	Talamantes, Sardegna	Ag, As, Au, Ba, Cu, Fe, Mn, Mo, P, Pb, Sb, Sr, Tl, W, Zn
Rhyolite-hosted tin	25h	"Mexican-type" in the states of Durango and Zacatecas; Black Range, NM	As, Be, Bi, F, Fe, Li, Mo, Nb, Pb, Sb, Sn, Th, U, Zn, REE (\pm Ti, Y, Zr)
Low titanium iron oxide copper-uranium-REE	25i, 29b	Olympic Dam, Kiruna, Bayan Obo	Ag, As, Au, B, Ba, Bi, Cl, Co, Cu, F, Fe, K, Mn, Mo, Na, Nb, Ni, P, Te, U, V, REE
Sediment-hosted gold (Carlin type)	26a	Carlin, Jerritt Canyon, Mercur	Ag, As, Au, Ba, F, Hg, Mo, Sb, Se, Tl, W (\pm Cd, Cr, Cu, Ni, Pb, Zn)
Hot spring gold-silver or mercury ⁽⁴⁾	25a; 27a	McLaughlin, Round Mountain, McDermitt, Sulfur Bank	Ag, As, Au, Hg, Sb, Tl, W
Almaden mercury	27b	Almaden, Las Cuevas	As, Fe, Hg, Sb (\pm Cu, Ni, Pb, Zn, Zr)
Stibnite-quartz	27d, e; 36c	Lake George, Xiguanshan	As, Au, Ba, Cu, Fe, Hg, Pb, Sb, U, Zn (\pm Ag, W)
Algoma iron	28b	Sherman, Wadi Sawanin, Vermillion Iron Formation	Au, Fe
Sediment-hosted copper	30b	Kupferschiefer, African copper belt, Naciminto, Spar Lake, White Pine	Ag, As, Au, B, Ba, Bi, Cd, Co, Cr, Cu, Ge, Hg, Mo, Ni, Pb, Sc, Se, Sn, Sr, U, V, Zn, PGE
Sandstone uranium ⁽⁴⁾	30c	Grants district, Colorado Plateau	Ag, Cu, Mo, Pb, Rn, Se, U, V
Sedimentary exhalative zinc-lead-silver	31a	Sullivan, Red Dog, Rammelsberg, McArthur River, Tynagh, Broken Hill	Ag, Al, As, Au, B, Ba, Cd, Co, Cu, Fe, Hg, Mn, Ni, Pb, Sb, Zn
Mississippi Valley type lead-zinc	32a	Viburnum Trend, Mascot-Jefferson, Pine Point, Polaris, Silesian District, Lennard Shelf District	Ag, As, Au, Ba, Bi, Cd, Co, Cu, F, Fe, Ga, Ge, Hg, In, Mg, Mo, Ni, Pb, Sb, Sn, Zn
Solution-collapse breccia pipe uranium	32e	Arizona breccia pipe district, Tsumeb	Ag, As, Ba, Cd, Co, Cr, Cu, Hg, Mo, Ni, Pb, Rn, Sb, Se, Sr, U, V, Y, Zn
Superior iron	34a	Mesabi and Marquette iron ranges, Minas Gerais	Fe, P
Sedimentary manganese	34b	Molango, Nikopol, Groote Eylandt, Kalahari, Imini	Ba, Mn, P, Pb
Low sulfide gold quartz veins	36a	Yilgarn block, Abitibi belt, Mother Lode, Muruntau	Ag, As, Au, Bi, Cu, Fe, Hg, Mo, P, Pb, Sb, Te, W, Zn
Stratabound gold in iron formations	36b	Homestake, Lupine, Cuiaba, Champion	Ag, As, Au, B, Bi, Cu, Fe, Hg, Mo, Pb, Sb, Zn, PGE

⁽¹⁾Listings include enriched elements within or adjacent to mineral deposits. Groupings are based on du Bray (1995) unless otherwise noted. Examples and geochemical signatures are from du Bray (1995), Boyle (1974), Cox and Singer (1986), Beus and Grigorian (1977, adapted from Table 57), Rose et al., (1979, adapted from Table 4.2), and Levinson (1980, adapted from Table 2-3). Elements are listed alphabetically and not in order of abundance.

⁽²⁾Sulfur is present in many mineral deposits. However, due to variations within deposit types and within alteration types, sulfur may or may not be of environmental significance. Refer to du Bray (1995) for discussions relating to sulfur content of mineral deposits.

⁽³⁾Model numbers are based on Cox and Singer (1986). ⁽⁴⁾Grouping is based on Cox and Singer (1986).

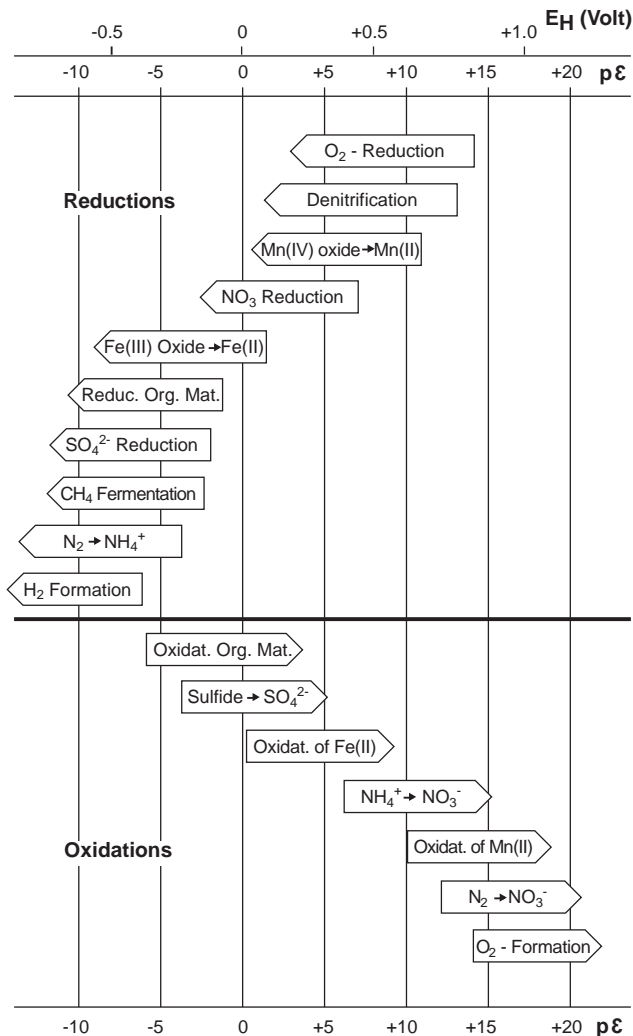


FIGURE 2.11—Sequence of microbially mediated oxidation-reduction reactions. This sequence is often observed in natural systems and represents the thermodynamic order of reactions. Modified from Stumm and Morgan (1996).

gley waters come into contact with a reducing hydrogen sulfide environment or with sulfide minerals, or where deoxygenated sulfate-rich water encounters an accumulation of organic matter. Insoluble sulfides of elements such as iron, copper, zinc, lead, cobalt, nickel, and silver may precipitate at reducing barriers that contain hydrogen sulfide. Reducing gley barriers can form where water infiltrates soil and the weathering crust, and free oxygen is lost or consumed. Depending on the pH, reducing gley waters are usually favorable for the transport of many ore-forming elements; additionally, elements such as selenium, copper, uranium, molybdenum, rhenium, vanadium, chromium, silver, and arsenic are known to accumulate at some reducing gley barriers (Perel'man, 1986). For example, roll-front-type uranium deposits may form under such conditions. See Table 2.13 for a list of redox-sensitive elements.

Oxidizing barriers occur where oxygen is introduced into anoxic waters or when anoxic ground water is discharged to the

surficial environment. Iron, and possibly manganese, may precipitate at these barriers (see Fig. 2.11). Since hydrous iron and manganese oxides are good sorbents for metals (such as copper and cobalt), a complex barrier may form by combining an oxidizing barrier with an adsorption barrier.

Figure 2.12 illustrates the ranges of pH and Eh (oxidizing-reducing conditions) of water commonly found in different natural environments. Nordstrom and Alpers (1999) discuss Eh-pH diagrams in more detail. This type of diagram helps distinguish the types of natural environments where geochemical barriers may be formed. The shaded area on Figure 2.12 represents the approximate conditions reported by Plumlee et al. (1999) for geologically and geochemically diverse mine-drainage waters; conditions are approximate because dissolved oxygen, rather than Eh, was determined in many of the waters. There is a wider range of pH in mine waters than shown on Figure 2.12. The pH of mine waters can range from -3.5 to >12 (D.K. Nordstrom, USGS, personal commun., 1997).

Evaporation barriers are often indicated by the presence of salt crusts or efflorescent salts. Sodium, magnesium, calcium, chlorine, sulfur, and carbonate salts may precipitate at these barriers. Evaporation barriers may be temporary and related to changing

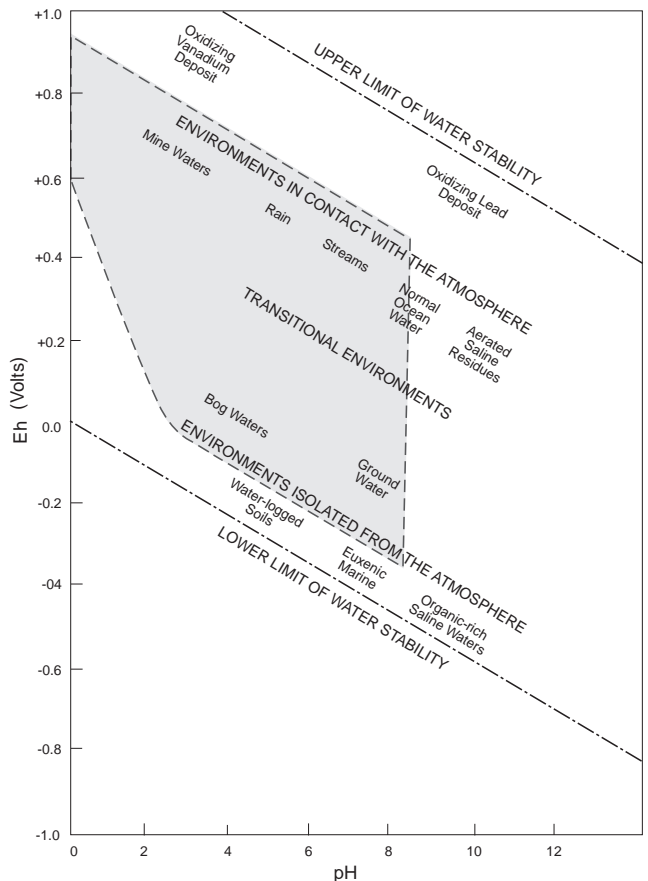


FIGURE 2.12—Eh-pH regimes of some natural near-surface environments. The shaded area represents the approximate conditions reported by Plumlee et al. (1999) for geologically and geochemically diverse mine-drainage waters (see text). Modified from Garrels and Christ (1965).

climatic conditions. For example, in some mine dumps efflorescent salts, enriched in elements such as iron, aluminum, copper, and sulfur, may form during the dry season. These salts will be flushed from the system during a subsequent wet period and may cause a brief spike in metal content and acidity of the stormwater runoff (see Nordstrom and Alpers, 1999).

Adsorption barriers are typically part of complex barriers. The most common sorbents (e.g., hydrous iron, aluminum, and manganese oxides; organic matter and clay minerals) have different affinities for elements under different geochemical conditions (see Smith, 1999). Adsorption reactions are known to control trace-metal concentrations in many natural systems.

Thermodynamic barriers are formed in areas with temperature and pressure variations. One example of such a barrier is the degassing of carbon-dioxide-rich ground water, as pressure drops, and subsequent deposition of carbonate minerals. Trace elements such as lead and cadmium can precipitate as carbonate minerals or coprecipitate with CaCO_3 .

Perel'man (1977, 1986) gives a more in-depth discussion of geochemical barriers. This concept can help anticipate element distributions in the surficial environment and understand metal transport and mobility.

Metal mobility in the surficial environment

In this chapter, mobility refers to the capacity of an element to move within fluids after dissolution. It is difficult to predict element mobility quantitatively in surficial environments. Rather, mobility should be considered in a relative sense by empirically comparing the behavior of elements under changing environmental conditions such as at geochemical barriers. Figure 2.13 illustrates the generalized relative mobility of elements expected under a variety of geochemical conditions. This figure takes into account the tendency of the elements to sorb onto hydrous oxides or to precipitate. Criteria for mobility distinctions are scaled by element abundance rather than being based on absolute solubility; no quantitative information can be inferred from Figure 2.13. By comparing the periodic tables (Fig. 2.13a-e), one may make qualitative statements about the behavior of a given element under changing conditions such as at geochemical barriers. Data for Figure 2.13 are derived from a wide range of information about mine-drainage systems as well as from Vlasov (1966), Fuller (1977), Parish (1977), Perel'man (1977, 1986), Callahan et al. (1979), Lindsay (1979), Rose et al. (1979), Levinson (1980), Greenwood and Earnshaw (1984), Lukashev (1984, 1986), Adriano (1986), Cotton and Wilkinson (1988), Hem (1985), and Kabata-Pendias and Pendias (1992).

Figure 2.13a shows the generalized relative mobility of elements under oxidizing acidic ($\text{pH} < 3$) conditions in aqueous systems and Figure 2.13b shows mobilities under circumneutral conditions. For redox-sensitive elements (see Table 2.13), the most oxidized form is assumed to be present. This is important because some redox-sensitive elements have different mobility and toxicity characteristics. For example, chromium (VI), the more toxic form, is more mobile in soils than chromium (III). By comparing data in these two periodic tables, it is possible to estimate the behavior of a given element at an acidic or alkaline geochemical barrier under oxidized conditions. For example, under acidic conditions iron remains dissolved, but it will precipitate when conditions become more alkaline. Figure 2.13c shows the generalized relative mobility of elements in the presence of such iron-rich pre-

cipitates and, when compared with Figures 2.13a and 2.13b, represents a complex alkaline and sorption geochemical barrier. Elements such as copper and arsenic become much less mobile under these conditions if sufficient iron-rich precipitates are present and if the pH for optimal sorption is attained (which is different for different elements and substrates; see Smith, 1999).

Figure 2.13d shows the generalized relative mobility of elements under reducing conditions without hydrogen sulfide (reducing gley environments) and Figure 2.13e shows mobilities in the presence of hydrogen sulfide. Comparing these two periodic tables illustrates the influence of sulfide-mineral formation. For example, copper and zinc become much less mobile when hydrogen sulfide is present because they form insoluble sulfide minerals.

It is also useful to compare the oxidizing-conditions periodic tables (Fig. 2.13a, b, and c) with the reducing-conditions periodic tables (Fig. 2.13d and e). For example, a reducing gley geochemical barrier could be simulated by comparing an initial condition with low-sulfate, oxidizing, circumneutral pH water (in the absence of abundant iron-rich particulates as on Fig. 2.13b) to the conditions represented on Figure 2.13d. In this situation, iron becomes more mobile and uranium will become less so. Another example is when sulfate-rich waters infiltrate a wetland system (e.g., passive mine-drainage treatment or natural systems; see Walton-Day, 1999), where it would be appropriate to compare Figures 2.13a or 2.13b with Figure 2.13e.

Figure 2.13 provides a general guide or first approximation to predict metal behavior in surficial environments. This approach does not substitute for in-depth field studies and topical research; there is no reliable "cookbook" approach. This approach may help to determine which elements could be mobile in a given environment and to anticipate the effects of various geochemical barriers. It should be kept in mind that there was a great degree of subjectivity in assigning the elements to the various categories on Figure 2.13. To use this approach in a natural setting, one must know something about the geochemical conditions. One must also have a good grasp of underlying chemical and geochemical principles (e.g., Garrels and Christ, 1965; Nordstrom and Munoz, 1994; Stumm and Morgan, 1996). Figure 2.13 should be used only in a relative sense and does not provide any information about absolute concentrations or quantitative data.

The rates of geochemical and biological reactions also can impact metal mobility; many reactions involving metals are kinetically controlled and biologically mediated. This rate dependence makes reactions extremely difficult to predict (e.g., Langmuir and Mahoney, 1984).

Success in estimating metal behavior in surficial environments also depends on scale. At a regional scale, generalizations often can be used to understand broad trends in metal mobility. As the scale becomes increasingly finer, however, estimating metal behavior usually becomes increasingly difficult. Many chemical interactions involve elements of interest as well as other elements and components such as acidity, rainfall, and factors that are involved in complicated synergisms or antagonisms. Once these other components are recognized and addressed, a more accurate assessment of metal mobility can be made.

It is often necessary to understand the mobility of major elements before data on the mobility of trace elements can be interpreted. For example, insoluble salts or solution complexes may form between trace metals and major elements, such as the formation of cadmium chloride complexes. Major or minor elements may modify the concentration or activity of a trace element. For example, cadmium and calcium compete to form chloro complex-

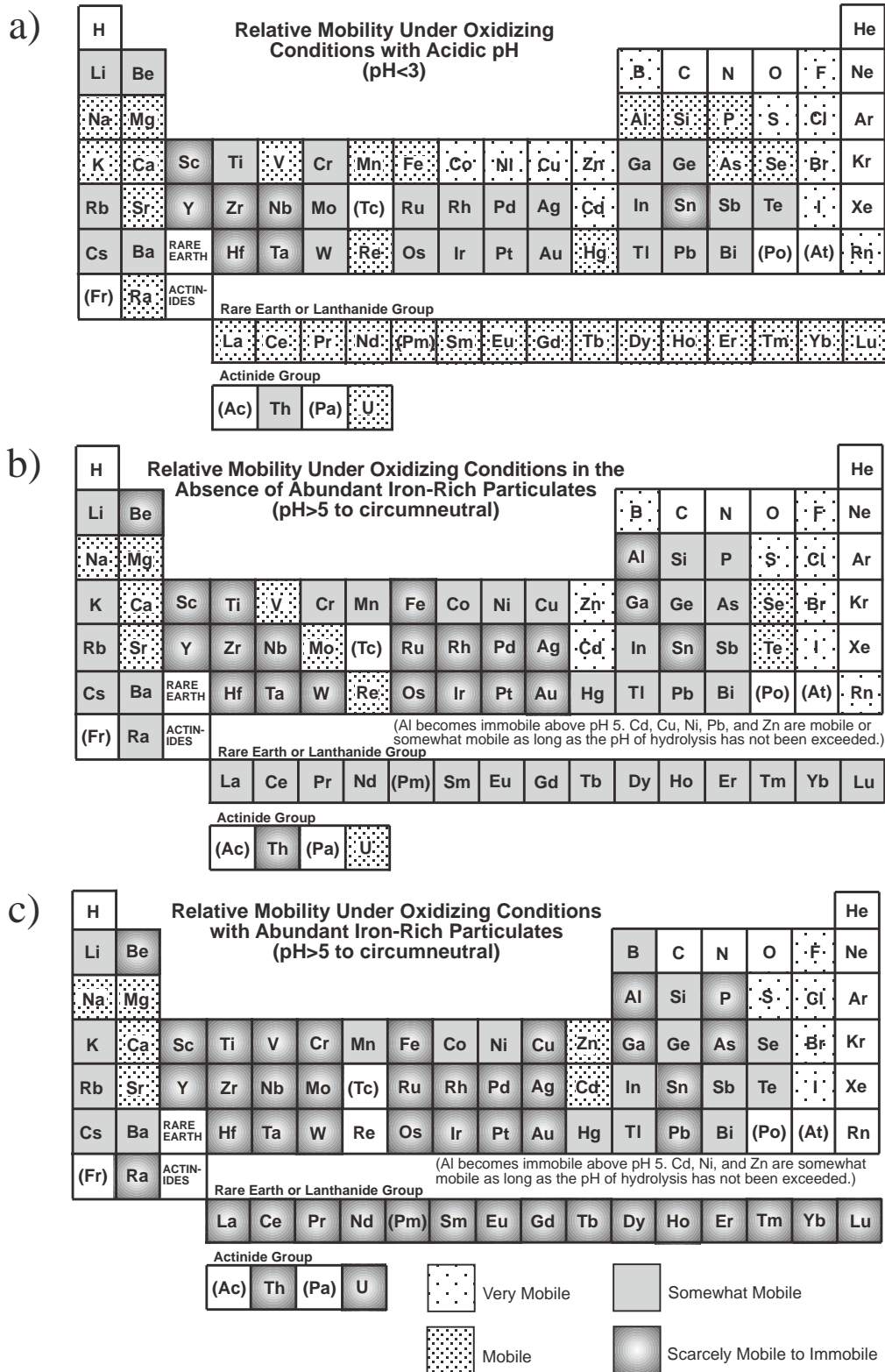


FIGURE 2.13a-c—Periodic tables of generalized relative mobility of chemical elements under different environmental conditions. For rare elements it is difficult to assign a mobility category due to their low abundance and lack of data. Lack of shading or pattern for some elements is due to either their existence in the gaseous state or a lack of information about that element.

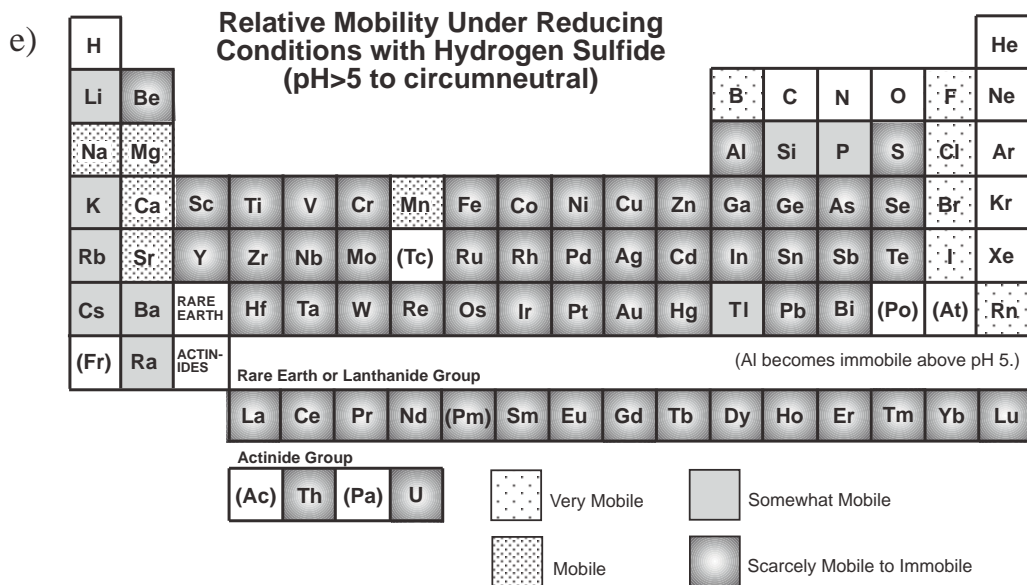
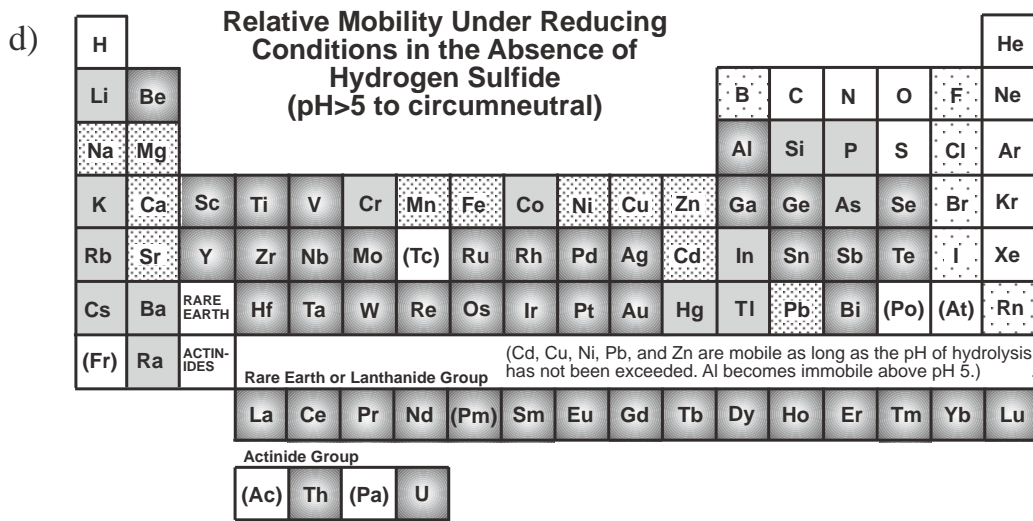


FIGURE 2.13d and e—Continued

es or insoluble carbonate and phosphate minerals. Another example is the iron system, where concentrations of many trace elements can be controlled by sorption onto iron-rich precipitates (see Smith, 1999; Smith et al., 1998).

Metal dispersivity in the surficial environment

Air

Atmospheric deposition of metals may impact the chemistry of soils, rivers, lakes, estuaries, and oceans. Metals enter the atmosphere as gases, vapors, aerosols, and particles originating from a

variety of natural and anthropogenic sources. Tables 2.16A and 2.16B list estimates of some of these sources and their relative importance. According to Nriagu (1989), wind-borne soil particles generally account for more than half of the chromium, cobalt, manganese, and vanadium, and for one-third to one-half of the molybdenum, nickel, and zinc emitted from natural sources (although metals in wind-blown dust are often of industrial origin). Volcanoes account for more than half of the cadmium, and significant amounts of arsenic, chromium, copper, lead, mercury, and nickel. Biogenic sources are the leading contributors of mercury and selenium, and significant sources of arsenic (Table 2.16A; Nriagu, 1989). In Table 2.16B, nonferrous metal produc-

TABLE 2.16A—Estimates of worldwide trace-metal emissions into the atmosphere from natural sources ($\times 10^3$ kg/yr). Data from Nriagu (1989, Table 1).

Source (median values)	As	Cd	Co	Cr	Cu	Hg	Mn
Wind-borne soil	2,600	210	4,100	27,000	8,000	50	221,000
Seasalt spray	1,700	60	70	70	3,600	20	860
Volcanoes	3,800	820	960	15,000	9,400	1,000	42,000
Forest fires	190	110	310	90	3,800	20	23,000
Biogenic							
Continental particulates	260	150	520	1,000	2,600	20	27,000
Continental volatiles	1,300	40	60	50	320	610	1,300
Marine	2,300	50	80	60	390	770	1,500
Total Natural Sources (Median value)	12,000	1,300	6,100	44,000	28,000	2,500	317,000

Source (median values)	Mo	Ni	Pb	Sb	Se	V	Zn
Wind-borne soil	1,300	11,000	3,900	780	180	16,000	19,000
Seasalt spray	220	1,300	1,400	560	550	3,100	440
Volcanoes	400	14,000	3,300	710	950	5,600	9,600
Forest fires	570	2,300	1,900	220	260	1,800	7,600
Biogenic							
Continental particulates	400	510	1,300	200	1,120	920	2,600
Continental volatiles	60	100	200	40	2,600	130	2,500
Marine	80	120	240	50	4,700	160	3,000
Total Natural Sources (Median value)	3,000	30,000	12,000	2,400	9,300	28,000	45,000

tion and use accounted for the largest fraction of lead (in addition to gasoline combustion), arsenic, cadmium, copper, and zinc emitted into the atmosphere in 1983 (Nriagu and Pacyna, 1988). Pacyna (1996) provides an in-depth discussion of trace metal emissions into the atmosphere. He states that trace metals emitted into the atmosphere can be transported a long distance and that atmospheric deposition is an important pathway for worldwide metal contamination of terrestrial and aquatic ecosystems.

Residence times of metals in the atmosphere are fairly short—generally on the order of days to weeks (Salomons and Forstner, 1984). However, volcanogenic particles can remain in the upper atmosphere for much longer periods of time. The distance of airborne transport depends on the source, size, shape, and density of the particles, on changes in particle characteristics during transport and on meteorological conditions. Particles in the atmosphere can undergo diffusion, coagulation, condensation, sedimentation, scavenging by precipitation, and reaction with atmospheric gases. Deposition varies with particle-size distribution, ground cover, and meteorological conditions.

Metals can be transported in different forms when associated with fly ash from urban waste incinerators. Fernandez et al. (1992) suggested that the behavior of elements in fly ash correlates with the following four classes originally suggested by Klein et al. (1975):

Class I: Elements that make up the matrix of the fly ash and are only minimally deposited on the fly-ash surface. These include Al, Ba, Be, Ca, Co, Fe, K, Mg, Mn, Si, Sr, and Ti.

Class II: Elements that volatilize during combustion and condense on the surface of fly-ash particles, forming soluble compounds. These elements also tend to be more enriched in smaller size fly ash particles (because of the particle's greater specific surface area) and include As, Cd, Cu, Ga, Pb, Sb, Se, and Zn.

Class III: Elements that volatilize but do not condense. These include Br, Cl, and Hg.

Class IV: Elements whose behavior is a combination of the above classes.

Several studies have examined metal contamination near smelters. The elements enriched in various smelter emissions are similar to the suite of elements enriched in fly ash, and are related to the ore deposit type. For example, Li and Thornton (1993) observed that lead, zinc, cadmium, antimony, and arsenic are enriched in a lead-zinc smelting area in England. Ragaini et al. (1977) found greater concentrations of cadmium, arsenic, lead, indium, scandium, antimony, zinc, silver, gold, nickel, and possibly copper in soils, grasses, and ambient aerosols near a lead smelting complex in Kellogg, Idaho. Small et al. (1981) studied emissions from five copper smelters in southeastern Arizona. They report that sulfur, copper, zinc, arsenic, selenium, silver, cadmium, indium, antimony, tungsten, gold, lead, and iodine are strongly enriched in the plumes relative to background, and that copper, arsenic, selenium, cadmium, and indium are enriched in the copper smelters far in excess of other sources. In a companion study, Germani et al. (1981) determined that variations in the elemental enrichments among plumes from the five copper smelters appear to be due to differences in the feed material, smelting conditions, and equipment used by the smelters. Researchers have also documented the distribution of smelter emissions (e.g., Gabriel and Patten, 1994) and the migration and mobility of metals in smelting areas (e.g., Scokart et al., 1983; Maskall et al., 1995).

Water

Physical transport of sediments is related to hydrologic and geomorphologic processes such as erosion, vertical and horizontal

TABLE 2.16B—Estimates of worldwide trace-metal emissions into the atmosphere in 1983 from anthropogenic sources (x 10³ kg/yr). Data from Nriagu and Pacyna (1988, Table 2).

Source	Arsenic	Cadmium	Chromium	Copper
Pyrometallurgical nonferrous metal production				
Mining	40.0–80	0.6–3		160–800
Pb production	780–1,560	39–195		234–312
Cu–Ni production	8,500–12,750	1,700–3,400		14,450–30,600
Zn–Cd production	230–690	920–4,600		230–690
Secondary nonferrous metal production		2.3–3.6		55–165
Steel and iron mfg.	355–2,480	28–284	2,840–28,400	142–2,840
Coal combustion				
electric utilities	232–1,550	77–387	1,240–7,750	930–3,100
industry and domestic	198–1,980	99–495	1,680–11,880	1,390–4,950
Oil combustion				
electric utilities	5.8–29	23–174	87–580	348–2,320
industry and domestic	7.2–72	18–72	358–1,790	179–1,070
Wood combustion	60–300	60–180		600–1,200
Refuse incineration				
municipal	154–392	56–1,400	98–980	980–1,960
sewage sludge	15–60	3–36	150–450	30–180
Phosphate fertilizers		68–274		137–685
Cement production	178–890	8.9–534	890–1,780	
Miscellaneous	1,250–2,800			
Total 1983 Emissions	12,000–25,630	3,100–12,040	7,340–53,610	19,860–50,870
Median value	18,820	7,570	30,480	35,370

Source	Mercury	Indium	Manganese	Molybdenum
Pyrometallurgical nonferrous metal production				
Mining			415–830	
Pb production	7.8–16			
Cu–Ni production	37–207	8.5–34.0	850–4,250	
Zn–Cd production		2.3–4.6		
Secondary nonferrous metal production			1,065–28,400	
Coal combustion				
electric utilities	155–542		1,080–6,980	232–2,320
industry and domestic	495–2,970		1,485–11,880	396–2,480
Oil combustion				
electric utilities			58–580	58–406
industry and domestic			358–1,790	107–537
Wood combustion	60–300			
Refuse incineration				
municipal	140–2,100		252–1,260	
sewage sludge	15–60		5,000–10,000	
Total 1983 Emissions	910–6,200	11–39	10,560–65,970	793–5,740
Median value	3,560	25	38,270	3,270

TABLE 2.16B—Continued

Source	Nickel	Lead	Antimony	Selenium
Pyrometallurgical nonferrous metal production				
Mining	800	1,700–3,400	18–176	18–176
Pb production	331	11,700–31,200	195–390	195–390
Cu–Ni production	7,650	11,050–22,100	425–1,700	427–1,280
Zn–Cd production		5,520–11,500	46–92	92–230
Secondary nonferrous metal production		90–1,440	3.8–19	3.8–19
Steel and iron mfg.	36–7,100	1,065–14,200	3.6–7.1	0.8–2.2
Coal combustion				
electric utilities	1,395–9,300	775–4650	155–775	108–775
industry and domestic	1,980–14,850	990–9,900	198–1,480	792–1,980
Oil combustion				
electric utilities	3,840–14,500	232–1,740		35–290
industry and domestic	7,160–28,640	716–2,150		107–537
Wood combustion	600–1,800	1,200–3,000		
Refuse incineration				
municipal	98–420	1,400–2,800	420–840	28–70
sewage sludge	30–180	240–300	15–60	3–30
Phosphate fertilizers	137–685	55–274		0.4–1.2
Cement production	89–890	18–14,240		
Mobile sources		248,030		
Miscellaneous		3,900–5,100		
Total 1983 Emissions	24,150–87,150	288,700–376,000	1,480–5,540	1,810–5,780
Median value	55,650	332,350	3,510	3,790
<hr/>				
Source	Tin	Thallium	Vanadium	Zinc
Pyrometallurgical nonferrous metal production				
Mining				310–620
Pb production				195–468
Cu–Ni production	425–1,700		43–85	4,250–8,500
Zn–Cd production				46,000–82,800
Secondary nonferrous metal production				270–1,440
Steel and iron mfg.			71–1,420	7,100–31,950
Coal combustion				
electric utilities	155–755	155–620	310–4,650	1,085–7,750
industry and domestic	99–990	495–990	990–9,900	1,485–11,880
Oil combustion				
electric utilities	348–2,320		6,960–52,200	174–1,280
industry and domestic	286–3,580		21,480–71,600	358–2,506
Wood combustion				1,200–6,000
Refuse incineration				
municipal	140–1,400			2,800–8,400
sewage sludge	15–60		300–2,000	150–450
Phosphate fertilizers				1,370–6,850
Cement production		2,670–5,340		1,780–17,800
Miscellaneous				1,724–4,783
Total 1983 Emissions	1,470–10,810	3,320–6,950	30,150–141,860	70,250–193,500
Median value	6,140	5,140	86,000	131,880

transport, sediment deposition, and compaction. In general, to transport sediment, flow rate of water must exceed a certain critical velocity, which depends on grain size and density; for deposition, the flow must decrease below another critical value. In rivers and estuaries, the sand- and gravel-size bedload fraction moves along the bottom by rolling or by a series of leaps. These particles usually are not transported long distances before deposition. Finer-grained sediments are carried in suspension and can be transported long distances before deposition (Horowitz, 1991). For example, Axtmann and Luoma (1991) document wide-scale fluvial distribution of fine-grained mining waste along the Clark Fork River in Montana.

In the water column, metals are commonly associated with suspended particulates. This suspended load can transport significant quantities of metals during spring runoff and storm events when the suspended load is highest. It is difficult to obtain a representative sample of suspended sediments and their associated metals (Horowitz et al., 1990).

Metals are not homogeneously distributed among the various grain-size fractions in sediments. Generally, the finer-grained clay-size fractions have the highest metal concentrations due to large specific surface areas and to the presence of metal-oxide and organic coatings on mineral surfaces that tend to sorb metals. In the silt and sand-size fractions, metal concentrations generally decrease due to the greater abundance of quartz and lower oxide and organic content. The coarse fractions either may increase in metal concentrations, if they include metal-containing minerals (e.g., sulfide minerals), or may decrease in metal concentrations. Filipek and Owen (1979) discuss the influence of grain size on metal distribution in lacustrine sediments.

Physical transport of particulates in ground water encompasses many of the factors involved in surface water plus such factors as complex flow paths and finite pore sizes. Ranville and Schmiermund (1999) provide a description of colloid transport in ground water.

FACTORS AFFECTING METAL BIOAVAILABILITY AND TOXICITY

Because the emphasis of this volume is the environmental geochemistry of mineral deposits, we place emphasis on geological, geochemical, and chemical factors that affect metal bioavailability and toxicity. We also present mining-related examples rather than provide a review of the literature. In doing so, we do not intend to overemphasize the importance of geological, geochemical, and chemical factors. Rather, we endeavor to familiarize earth scientists with some of the linkages that exist between the earth sciences and biological sciences.

Measurement of bioavailability

Because absorption pathways vary with metals, bioavailability for different hosts is measured differently for specific metals within specific biological systems. As noted in the discussion of Figure 2.1, bioavailability may be measured by systemic availability of a metal or by accumulation in organs. For example, the bioavailability of lead can be measured by dose response (or internal dose) of lead levels in blood. In contrast, cadmium levels in laboratory

animals are measured by content in livers or kidneys; urine content is not considered to be a reliable indicator of cadmium in test animals because, unlike other metals, cadmium is generally stored in tissue rather than excreted. There are also measurement differences for the same metal. For example, the bioavailability of ingested lead, as measured in Davis et al. (1992), is based on the amount of lead absorbed by digestion. This is not equivalent to blood-lead measurements since lead is transported by the blood to soft tissues and bone. Krieger et al. (1999) discuss bioavailability of arsenic, cadmium, and lead.

Host-related factors

Biologically related factors, such as mode of exposure, cumulative residence time in the host, ability of the host to absorb a particular size or compound, presence of other metals in the host, genetics, host species, and age and development of the host, affect the bioavailability of a particular metal. Host-related factors are very important to metal bioavailability and toxicity, and are also very complex; we include only a brief discussion of these factors in this chapter. For more detailed discussions relating to metals, refer to Fergusson (1990), Goyer (1991), Goyer et al. (1995), and Chang (1996).

Mode of exposure significantly affects bioavailability. Natural modes of exposure to humans include inhalation, ingestion, and transfer through the skin. Potential for airborne exposure to metals in the workplace and in ambient air is significant. Inhaled metals may increase susceptibility to respiratory infection, may be related to immune suppression (Selgrade and Gardner, 1996), or may be associated with pulmonary carcinomas (Gordon, 1995). Ingestion of toxicants commonly takes place through food or water. Ingestion of soil is a significant mode of exposure of metals to children. The significance of this mode of exposure is related to behavioral characteristics of small children (i.e., the hand-to-mouth action of most small children; Beck et al., 1995). Gulson et al. (1994a) found that ingestion of soil and dust is the main source for elevated blood-lead levels in children from a mining community in Australia. Skin does a good job of keeping out water, particles, ionic inorganic species, and materials of high molecular weight. However, skin does not keep out lipid-soluble substances and therefore is susceptible to the absorption of organometallic compounds (Fergusson, 1990).

Cumulative residence time in the host is different for different metals and different hosts. For example, lead is particularly toxic to children, who absorb it much more readily than adults. Hemphill et al. (1991) report that absorption of ingested lead is <20% in adults, and <53% in children. In contrast to lead, cadmium accumulates gradually in the human body, and so becomes increasingly concentrated in adults. Thus, adults generally exhibit higher cadmium levels than children.

Airborne particles exist in fine (<2.5 μm) and coarse (>2.5 μm) sizes; particles from anthropogenic sources (e.g., smelters) are usually fine. In the case of lead, inhalation is much more dangerous if the particle size is fine. Goyer (1991) reports that, for particle sizes smaller than 0.5 μm , human lungs retain 90% of the particles and absorb almost 100% of the retained lead. Larger particles are generally swallowed. This may help to explain why people living in mining communities that once had smelters generally have greater blood-lead levels than those living in mining areas without smelters.

As previously mentioned, the toxicity of chromium depends on its oxidation state, with chromium (VI) being more toxic than chromium (III). The National Research Council (1989) notes that most dietary chromium is trivalent, which is relatively nontoxic; humans cannot oxidize this to chromium (VI). Toxicity of chromium has been associated with bronchial cancer related to occupational exposure to dust in chromium metallurgical, refinery, or manufacturing operations. This dust is generally a mixture of chromium (III) and chromium (VI). A 1972 study of German workers exposed for 20–25 years to chromium (III) in manufacturing reveals no lung cancer among the workers (Luckey and Venugopal, 1977). However, chromium (III) is the metabolically active form within humans, and may be toxic in some cases (Goyer, 1991). Klein (1996) states that the carcinogenic risk associated with human exposure to chromium seems to be most directly correlated with particular chromium oxidation states, with the greatest observed risks associated with exposure to chromium(VI) compounds such as chromates. Whether chromium causes cancer outside the respiratory tract is unclear.

Some metal compounds are known to be more bioavailable than others. A variety of metal-carbon compounds are lipid soluble, and hence presumably can penetrate lipid membranes. For example, methyl mercury, tributyl tin, and tetraethyl lead can dissolve in cell membranes. Pelletier (1995) provides an overview of the environmental chemistry of these organometallic compounds.

Interactions among elements in the host affect the bioavailability and the dose response in the host. For example, people with low intake of calcium, iron, or phosphorous can increase absorption of lead from their diet. As noted above, even slightly greater than optimal concentrations of zinc can diminish absorption of copper by humans; but zinc can provide protection against cadmium and lead toxicities (Sandstead, 1980, 1988; Hill, 1988). In another example, phosphate depletion, negative phosphorous balance, or problems with phosphorous reactions can create aluminum toxicity, even though ingested aluminum generally is not a toxic substance to humans (Luckey and Venugopal, 1977). Cattle with excess dietary exposure to molybdenum can be treated by addition of copper sulfate to their diet (Goyer, 1991) because high concentrations of copper in the body decrease uptake of molybdenum. Selenium uptake by alfalfa may be diminished by moderate sulfur concentrations in the soil (Severson et al., 1991; Severson and Gough, 1992).

Genetic effects on the susceptibility and tolerance to contaminants are documented for several types of organisms. For example, Bryan (1976) provides a review of metal tolerance in estuarine invertebrates, and metal tolerance in plants is discussed in Shaw (1990). The importance of genetic factors in human metal toxicity is not well known; a National Academy of Sciences report states that the role of genetic factors in susceptibility to lead toxicity has received little attention (NRC, 1993).

Different types of plants absorb elements at different rates under otherwise similar circumstances. Plants may be classified as accumulators or excluders of metals (Fergusson, 1990). In smelter-contaminated soils in New Mexico containing 2,000–10,000 ppm lead, rabbitbrush contained approximately 3 times the lead level of adjacent cactus or creosote (Austin et al., 1992). Selenium is absorbed to an unusual degree by a limited number of plant species, some of which serve as livestock feed (Erdman et al., 1991). For example, in parts of the arid west some species of *Astragalus* contain several thousand ppm selenium compared with grasses in the same soil that contain only a few

ppm selenium (Thornton, 1982). Other plants, such as wheat, do not contain abnormal selenium even when grown in high-selenium soils. Selenium uptake in wheat requires “selenium converter plants” to change the soil selenium to a form that is absorbable by wheat (Ensminger et al., 1994).

Metal-tolerant plants avoid toxic effects in a variety of ways. Some species accumulate the metals in the roots and restrict access to shoots. Others may bind the metals in complexes that isolate them from sensitive sites (Thurman, 1982). Uptake from soil can be “passive” (due to diffusion based on concentration differences), “facilitated” (due to increased availability from chemical changes induced by roots), or “active” (due to metabolic selection and concentration by roots; Phipps, 1981). An example of facilitated uptake is organic-acid exudates from roots that are known to drop the pH of the rhizosphere, thus dissolving metal carbonates and freeing them for assimilation (Gough et al., 1980).

Age and development of the host play a role in bioavailability. For example, blood lead levels in humans appear to decrease during adolescence, evidently due to lead deposition in bone, and increase during menopause and osteoporosis, apparently due to demineralization of bone (Goyer, 1995). Many toxic metals exert their most serious adverse effects during fetal development. For example, lead and mercury can be transferred from the placenta to the fetus; however, the placenta selectively retains cadmium (Goyer, 1995).

Chemical, geochemical, and geological factors

Most metals cannot be considered solely detrimental because they commonly are also essential micronutrients for plants and animals. Uptake and accumulation of metals by organisms provides an essential link between the types, concentrations, forms, and species of metals in the environment and the effects that these have on living systems. Physical chemistry, geochemistry, and geology can significantly influence the bioavailability of metals to organisms. Kelly (1999) discusses toxic effects on aquatic biota of metals associated with mining activities.

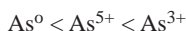
Chemical factors

Chemical factors, such as water composition (e.g., pH, hardness) and chemical and physical properties of elements (e.g., oxidation state), can influence element bioavailability in aquatic systems. The pH of a system is often a master variable that governs reactions and processes in the system; this, in turn, will influence bioavailability. For example, the bioavailability of cationic metals to aquatic organisms is generally greater in the acidic pH range than in the alkaline range. A study of metal bioavailability in lakes showed that fish in lakes with lower pH usually had higher body or tissue burdens of aluminum, cadmium, lead, and mercury than fish in nearby lakes with higher pH (Spry and Weiner, 1991). These relationships largely are due to pH-dependent metal speciation (see discussion below). Frequently, amendments are used to alter the pH of a soil in order to control metal availability because pH is a major factor in determining the free metal ion activity in the soil interstitial water (e.g., Pierzynski and Schwab, 1993). Kabata-Pendias and Pendias (1992) state that to provide an effective evaluation of the pool of bioavailable trace elements, techniques based on both soil tests and plant analyses should be used

together. For example, cadmium uptake by plants generally is inversely related to soil pH (Andersson and Nilsson, 1974). Alloway et al. (1988) report that cadmium concentrations in various crops are highest for crops grown on acidic soils, and Jackson and Alloway (1991) show that application of lime to soils amended with sewage sludge reduced cadmium bioavailability to cabbage and lettuce, but not to potatoes. Conversely, anionic metals, such as molybdenum, are usually more bioavailable in alkaline soils (e.g., Smith et al., 1997). This different behavior of cationic and anionic elements is due primarily to pH-dependent sorption reactions in the soils (see Smith, 1999).

Water hardness may affect the toxicity of some metals. Water hardness refers to the concentration of calcium and magnesium ions, as well as other polyvalent metals such as manganese, iron, and aluminum. In general, most metals are more toxic to aquatic life in soft (total hardness <75 mg/l) water rather than hard water (Zitko and Carson, 1976). According to Sprague (1985), heavy metals are an order of magnitude more toxic to aquatic life in very soft water than in very hard water; he attributed this increased toxicity to increased membrane permeability due low calcium concentrations. This toxicity-hardness relationship drives the hardness-based water quality criteria shown in Table 2.7A.

Oxidation state influences toxicity of metals. Molybdenum (VI) and chromium (VI), for example, are much more toxic than molybdenum (II) (commonly occurring as a sulfide mineral) or chromium (III). Similarly, toxicity of arsenic varies with oxidation state. Toxicity increases such that:



(Valberg et al., 1994).

Nieboer and Richardson (1980) modified existing systems of classification of metal ions, based upon those of Ahrlund et al. (1958) and Pearson (1963, 1968a, 1968b) (discussed briefly in a previous section) and presented them in a more biological context (Fig. 2.14). According to Nieboer and Richardson's classification, Class A metals, which tend to seek oxygen-containing ligands, comprise all the macronutrient metals (such as potassium and calcium). Class B metals, which tend to seek nitrogen- and sulfur-containing groups, include many of the more toxic metals. Borderline metals, which have intermediate properties, include most of the common metals. As shown on Figure 2.14, there is a distinct break between Class A metals and the borderline group, but there is little distinction between the borderline group and Class B metals. This type of approach can provide a general set of criteria by which the actions of different metals can be compared. For example, Class B metals may displace borderline metals, such as zinc or copper, from enzymes. The toxicity of a borderline metal depends on its Class B character; it will be able to displace many Class A metals and, depending upon their relative affinities, other borderline metals. With the exception of barium, characteristically hazardous metals (see Table 2.6) are either class B or borderline based on Nieboer and Richardson's (1980) classification.

Geochemical and geological factors

Simple relationships between metal concentrations in organisms and total metal concentrations in the food, water, or sediment to which the organisms are exposed, are seldom found in natural

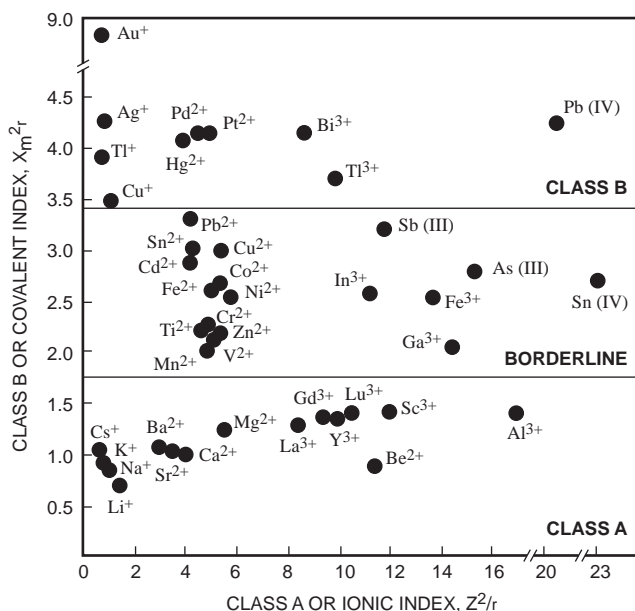


FIGURE 2.14—Chemical classification of metal ions according to Nieboer and Richardson (1980). X_m is the Pauling electronegativity, r is the effective ionic radius, and Z is the formal ion charge. Modified from Nieboer and Richardson (1980).

systems (Jenne and Luoma, 1977). Consequently, it is not sufficient to determine total metal concentrations in earth materials if the ultimate goal is to estimate bioavailability of the metals. (However, the total metal concentrations do place an upper limit on metal bioavailability.) Luoma (1989, p. 380) states, "extensive trace metal analyses of sediment, water and biotic tissues through the last decade demonstrate that bioaccumulation by plants and animals may vary considerably from one environment to the next, independent of concentration in sediment or water." For example, Erdman et al. (1976) found no strong correlation between element concentrations in crops and associated soils in Missouri. Pascoe et al. (1994) performed a food-chain transfer analysis for resident small mammals in a wetland habitat to evaluate the impacts of mining wastes on bioaccumulation of metals at the Milltown Reservoir Sediments Superfund site in Montana. Although several metals are present in high concentrations in the mining wastes, Pascoe et al. (1994) found limited bioavailability of these metals and arsenic to resident small mammals. On the other hand, in a study of invertebrates and vegetation associated with mine tailings from base-metal rich gold veins in British Columbia, Azcue et al. (1995) found arsenic, lead, and cadmium to be highly bioavailable; however, the metals appeared to be less bioavailable to invertebrates in a lake ecosystem that receives and accumulates the tailings.

Aquatic organisms may accumulate metals from the dissolved phase, suspended particulates, bottom sediments, and prey or food sources. However, it is not clear if water, particulate material, or food source is the primary route of exposure in natural systems. Questions remain as to what environmental variables should be monitored and regulated. Luoma and Carter (1993, p. 793) state that "understanding of the actual toxicity of sediments in nature is constrained by inadequate knowledge of processes in ecosystems

that contain contaminated sediments.” Figure 2.15 summarizes some of the processes and geochemical conditions that can redistribute dissolved metal cations among various reservoirs. Several publications address biological and geochemical processes that affect metal bioavailability in surface-water systems (e.g., Luoma, 1983; Morel and Hudson, 1985; Brezonik et al., 1991; Tessier and Turner, 1995).

Mineralogy and mode of occurrence can affect bioavailability of metals. For example, Mahaffey (1978) notes that, all other things being equal, bioavailability of ingested lead in lab rats increases in the following order:

lead chromate, lead sulfide, lead molybdate < lead acetate
< lead oxalate, lead carbonate.

Preliminary results from a study of lead bioavailability in soils and other test materials using juvenile swine indicate that ingested lead

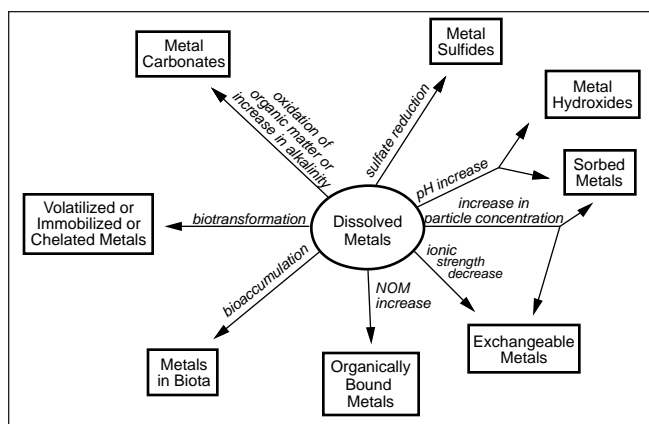


FIGURE 2.15—Some processes and geochemical conditions that can redistribute cationic dissolved metals in oxidizing, circumneutral-pH systems. Metals contained in each of the reservoirs (illustrated by boxes in the figure) also can be redistributed by geochemical or biological processes or by changing geochemical conditions. “NOM” refers to natural organic matter.

carbonate has high relative bioavailability, lead oxide and lead phosphate have intermediate relative bioavailability, and lead sulfide, lead sulfate, and native lead have low relative bioavailability (U.S. EPA, 1997). This sequence may differ from the order of increasing geoavailability, dispersivity, or mobility.

The bioavailability of soil-bound metals is related to the physicochemical form of the metal in the soil. Ingestion of soil by animals and humans can be an important route of exposure for metals. Generally, the more soluble a metal is, the more bioavailable it is (Sheppard et al., 1995). Ruby et al. (1992) demonstrate that dissolution kinetics must be considered when assessing metal availability from minerals or soils. The soluble metal salts often used in toxicological studies are not a good proxy for kinetically-controlled dissolution of minerals in the gut (Davis et al., 1992; Freeman et al., 1992; Ruby et al., 1992). Ruby et al. (1993) developed a screening method to evaluate the bioaccessibility of ingested lead. Wixson and Davies (1994) propose a protocol for decisions and guidelines concerning lead in soil.

Lead levels in blood provide an example of the variability in lead bioavailability from different sources. Recent studies of children living in and near inactive tailings or mill dumps in four Colorado areas—Leadville, Smuggler Mountain (Aspen), Telluride, and the Clear Creek-Black Hawk-Central City region—and in Park City, Utah, show relatively little enrichment of lead in blood compared to the national average, except for Leadville (Table 2.17). During the 1980s, the national average blood-lead level for children declined from 17 µg/dl to approximately 4–6 µg/dl (U.S. EPA, 1991). These statistics are for all children; Table 2.17 refers to children under 6 years of age. The first three studies shown in Table 2.17 are from blood samples taken in 1986–1987; the last three are from samples taken in 1990–1991. These are separated because the national blood-lead level of people continued to drop (to 2.9 µg/dl for people aged 1–74 years in 1989–1991) due to phasing out of leaded gasoline and lead solder in food containers (Univ. of Cincinnati, 1997). The current Centers for Disease Control “level of concern” for lead content in blood is 10 µg/dl. As Table 2.17 shows, only the 1987 blood samples for Leadville exhibit arithmetic mean blood-lead levels above 10 µg/dl; the more recent (and larger) study indicates that these levels have dropped even faster than the national trend and are within health safety ranges (Univ. of Cincinnati, 1997). It should be

TABLE 2.17—Blood-lead levels in children and soil-lead contents in mining towns. Sources: Colorado Dept. of Health (1990); Colorado Dept. of Health (1992); Colorado Dept. of Health (1993); Agency for Toxic Substances and Disease Registry (1988); Univ. of Cincinnati (1997). Means are arithmetic means unless otherwise noted.

Location	Blood sampling year	Mean blood lead in children ⁽¹⁾ (µg/dl)	Soil range (ppm)	Soil mean (ppm)
Telluride, Colorado	1986	6.7 ⁽³⁾ ; 7.4		641 ⁽³⁾ ; 1370
Park City, Utah	1987	7.8 ⁽³⁾	16–5,840	
Leadville, Colorado	1987	8.7 ⁽³⁾ ; 10.1		
front yard cores			49–15,100	1,108 ⁽³⁾ ; 1,762
rear yard cores			10–27,800	915 ⁽³⁾ ; 1,625
Leadville, Colorado ⁽⁴⁾	1991	4.8 ⁽³⁾ ; 5.53	118–15,403	812 ⁽³⁾
Aspen (Smuggler Mtn.), Colorado	1990	2.6 ⁽³⁾ ; 3.0	135–11,676 ⁽²⁾	641 ⁽³⁾ ; 1,370
Clear Creek/Central City, Colorado	1990	5.9 ⁽³⁾ ; 6.3	10–2,590 ⁽²⁾	201 ⁽³⁾ ; 375

⁽¹⁾Blood levels shown for children less than 6 years of age.

⁽²⁾Soil values for households with children less than 6 years of age. In Smuggler Mt., soil samples for adults and children’s yards range from 0–46,100 ppm Pb, with means of 505 ppm⁽³⁾ and 1,155 ppm Pb (Colorado Dept. of Health, 1992).

⁽³⁾Geometric mean.

⁽⁴⁾Two studies of Leadville show a drop in mean blood level in children over 4 years’ time (see text).

noted that some variation in the blood-lead levels of children may be due to differences in the studies; geometric mean soil contents for lead are slightly lower in the second study.

Blood-lead levels in children may depend partially on the geoavailability of the lead source. In a study at Butte, Montana, Davis et al. (1993) report that low blood-lead levels in young children are due to the low solubility of lead minerals in the soil and waste rock. Figure 2.16 shows that children living in the mining district of Butte, Montana, had lower blood-lead levels than children living in Cincinnati, urban Minnesota, or adjacent to smelters. Similar observations were noted in a study in a mining village in the United Kingdom where, although garden soils and household dust averaged 7,000 and 1,500 ppm lead, respectively, blood lead levels were within the normal range. The researchers found that the lead in lead-rich soils was primarily present as pyromorphite (Pb₅(PO₄)₃Cl), a relatively insoluble lead mineral. They attribute the lower-than-expected blood lead levels to the predominance of this mineral phase (Cotter-Howells and Thornton, 1991). Tingle et al. (1993) found that lead tends to be adsorbed onto mineral surfaces in tailings or soils with near-neutral pH. However, tailings with low-pH (pH~2) have little or no detectable surface-bound lead. Presence of surface-bound lead, and of smelter-impacted soils, may help to explain the higher blood-lead levels in children in the 1987 sampling at Leadville. Gulson et al. (1994b) applied mineral-exploration techniques to determine the sources and pathways of lead into children living in a zinc-lead mining district in Australia. They report some cases where elevated blood-lead levels in children appear to be derived from orebody lead, but they found other cases where lead appears to be derived from gasoline lead or paint.

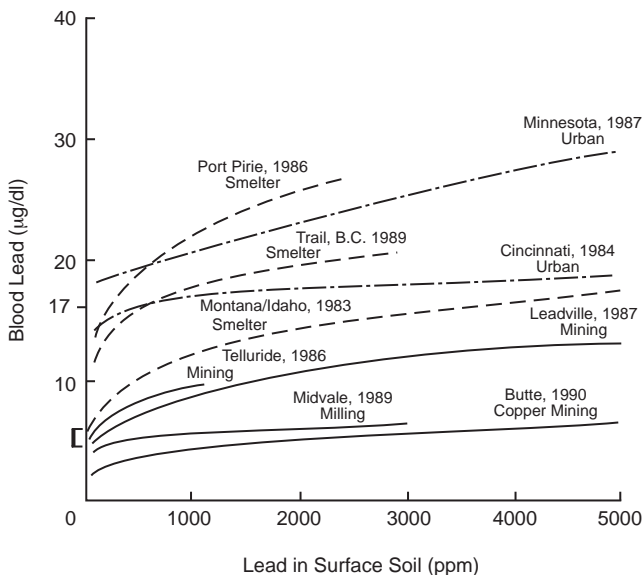


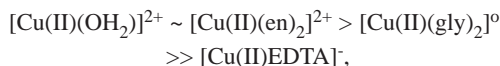
FIGURE 2.16—Blood-lead levels in children from mining (solid lines), smelter (dashed lines), and urban (dash-dot lines) sites in the United States. Modified from Gulson et al. (1994b, Fig. 12). During the 1980s, the national average blood-lead level for U.S. children declined from 17 µg/dl (noted) to approximately 4–6 µg/dl (bracket) (U.S. EPA, 1991). These ranges are shown because most of the studies were published in the 1980s. These averages are for all U.S. children under the age of 18 years.

Sediment texture can play a role in metal bioavailability. For example, Pesch and Morgan (1978) showed that a polychaete (a type of worm) exhibited greater bioaccumulation when exposed to metal-spiked water mixed with sandy sediment than when exposed to water mixed with fine-grained sediment. This is probably due to the higher metal-binding capacity of fine-grained sediment.

Metal speciation

Nieboer and Fletcher (1996) define speciation as “the occurrence of an element in separate, identifiable forms (i.e., chemical, physical, or morphological state).” The speciation of an element, rather than its total concentration, influences its effects on an organism. Factors that affect speciation include pH and redox conditions, the solubility of solid compounds, the oxidation state of the element, the availability and type of complexing agents, complex and ion-pair formation, sorption-desorption reactions, and biochemical processes.

The bioavailability and toxicity of metals may be strongly modified by the chemical partitioning of metals in food components (e.g., Luoma and Jenne, 1977), the speciation of metals in solution (e.g., Pagenkopf et al., 1974; Sunda and Guillard, 1976; Andrew et al., 1977; Driscoll et al., 1980), and the speciation of metals in sediments and soils (Luoma and Jenne, 1976, 1977). For example, Phipps (1981, p. 31) illustrates the importance of aqueous copper speciation on copper uptake by excised roots, with



where en, gly, and EDTA are organic ligands. This sequence of root uptake follows the overall charges of the copper complexes (Phipps, 1981).

Metal concentrations in soils and sediments are commonly several orders of magnitude greater than those found in associated waters. Metals can partition among various components of soils or sediments and may be (1) sorbed on hydrous metal oxides, organic matter, or clays, (2) present in the lattice of primary or secondary minerals, or (3) occluded in amorphous materials or remains of organisms. Salomons (1995) relates metal speciation to potential relative mobility with the following distinctions:

- Exchangeable cationsHigh mobility
- Metals associated with iron and manganese hydroxidesMedium mobility
- Metals bound or fixed inside organic substancesMedium mobility
- Metals bound or fixed inside mineral particlesLow mobility
- Metals associated with a sulfidic phaseStrongly dependent on environmental conditions

In a study of the Amazon and Yukon rivers, Gibbs (1973) found that copper and chromium are mainly associated with mineral particles, manganese is present in oxide coatings, and iron, nickel, and cobalt are equally distributed between solids and coatings. Differences in metal bioavailability occur when metals are bound

to different types of binding sites on particles (Luoma and Jenne, 1977; Campbell and Tessier, 1991). Luoma and Davis (1983, p. 161) state that "...with some exceptions, the metal particle reactions which are biologically most important in estuaries are those that affect metal distributions among the organic and inorganic components of fine-grained, oxidized sediments."

The composition of the suspended phase influences the physicochemical form in which a metal is transported, which in turn influences bioavailability (e.g., Luoma and Bryan, 1979). Bioavailability also can be affected by the preferential partitioning of metals to the suspended sediment and consequent removal from the dissolved phase since metals are generally more bioavailable when dissolved.

Geochemical methods to estimate metal speciation and bioavailability

In aqueous systems, the simplest speciation distinction is between what does and does not pass through a filter. The filter pore size determines what passes through a filtering unit (filtrate). The filtrate includes free ions and their complexes with various ligands and, perhaps, colloidal materials. Tanizaki et al. (1992) used filtration and ultrafiltration techniques to determine the physicochemical forms of several elements in river water (see Ranville and Schmiermund, 1999).

Generally, the free-ion concentrations of dissolved metals are the best indicator of bioavailability and toxic effects to aquatic organisms (O'Donnel et al., 1985) and crops (Kabata-Pendias and Pendias, 1992). Free metal ion concentrations in waters are determined either with specialized chemical and analytical techniques or with thermodynamically-based chemical-equilibrium calculations. These calculations are done with the aid of computer programs; when using these computer programs it is important to be aware of their limitations. Failure to (1) include all of the important species (e.g., major elements, organics), (2) consider all of the possible reactions (e.g., sorption), or (3) verify the validity of any inherent assumptions (e.g., thermodynamically versus kinetically-controlled reactions; reliability of stability constant data) may lead to erroneous conclusions. Hence, these models provide a qualitative estimate of the actual reactions and interrelationships between aqueous speciation and bioavailability. Turner (1995) provides a detailed discussion of problems in modeling trace metal speciation. An extension of the modeling approach is the free-ion activity model (FIAM; Morel, 1983), which was developed to link metal speciation with bioavailability in controlled laboratory studies, and has since been extrapolated to natural waters. Campbell (1995) describes and critiques the FIAM.

Quantification of metal speciation also requires specialized techniques. For example, it is necessary to distinguish the carcinogenic form of chromium (Cr(VI)) from the noncarcinogenic forms (Cr(III) and elemental chromium). Reliable analytical techniques, especially field techniques, have yet to be developed for many important speciation issues.

Predictions of metal bioavailability in soils and sediments have met with limited success. Metal speciation in soils and sediments can be determined by direct instrumental techniques (e.g., x-ray diffraction, electron microprobe, various spectroscopic methods), physical separation (e.g., size, density, magnetism), and chemical extractants. Partial chemical extractions or sequential extractions of soils and sediments are used to extract only the bioavailable

fraction of metal (e.g., Pickering, 1981) or only the fraction associated with particular components of the soil or sediment (e.g., Tessier et al., 1979; Filipek et al., 1981; Luoma and Bryan, 1981; Chao, 1984). However, incomplete knowledge of the complicated chemistry of soils and sediments, coupled with the lack of selectivity of some reagents, can make interpretation difficult (e.g., Luoma, 1989; Filipek and Theobald, 1981; Papp et al., 1991). Despite the limitations, partial extractions remain a useful technique for the examination of metals associated with various components in soils and sediments that serve as controls of metal mobility (Gatehouse et al., 1977; Lion et al., 1982; Chao, 1984). Positive assessment of partial dissolution techniques by Tessier et al. (1979) includes information about the origin and mode of occurrence of metals, physicochemical availability, and mobility of trace elements in the environment. In soil/plant studies with diverse soil types, the correlation between estimates of metal bioavailability and plant uptake is marginal (e.g., Gough et al., 1980). However, in agriculture partial dissolution techniques are used successfully to determine nutrient availability from soils to crops (Westerman, 1990). A few studies have been conducted with aquatic sediments and several different extraction procedures have shown correlations with metal bioavailability (e.g., Diks and Allen, 1983; Luoma, 1983), but no single approach is consistently successful (e.g., Weimin et al., 1992). Predictive capabilities may be improved by the use of normalizing parameters, such as iron (Luoma and Bryan, 1981), organic matter (Langston, 1982), or H⁺/iron oxyhydroxide (Tessier et al., 1984).

ENVIRONMENTAL GEOCHEMISTRY AND HEALTH

The field of environmental geochemistry and health involves the application of geochemistry, in particular geochemical mapping, to studies of plant, animal, and human health (Lag, 1983; Thornton, 1993; Cotter-Howells, 1996). This requires combining the disciplines of geochemistry, geology, chemistry, soil science, botany, zoology, microbiology, animal husbandry, veterinary science, epidemiology, and public health. Links between geochemistry and human health are usually difficult to establish. Warren (1989) provides an overview of potential health implications of exposure to Al, As, Au, Cd, Cu, Hg, I, Pt, Se, and Zn in the environment.

Geochemical maps have been used to correlate areas of trace-element deficiency or excess with problems in crops and animal nutrition (e.g., Thornton, 1983), and to identify areas where the population may be exposed to unusually great concentrations of metals (e.g., Morgan, 1988). A reconnaissance geochemical survey of Missouri by the U.S. Geological Survey provided information to epidemiologists in search of relationships between geochemistry of the environment and human health (see Miesch, 1976). Geochemical atlases have been generated for various European countries (e.g., Webb et al., 1978); they provide the geochemical basis for studies that seek links between geochemistry and health. Simpson (1995) describes the Geochemical Baseline Survey of the Environment (G-BASE) for the United Kingdom. Examples of other studies include Piispanen (1989), who compared disease maps with geochemical maps in Finland, and Irvine et al. (1988), who proposed a link between multiple sclerosis clusters in Saskatchewan and excess lead, nickel, and zinc in the soil. These types of studies do not demonstrate a direct association between trace elements and disease, but they do show that trace

elements may influence health. Accordingly, public-health measures can be taken to reduce exposure to trace elements in problem areas. Shaper (1979) and Thornton (1987) outline some of the potential problems associated with this approach.

There are several well-known correlations between health and trace elements. For example, iodine deficiency can result in enlargement of the thyroid gland, iron deficiency can cause anemia, fluoride deficiency has been associated with high rates of dental caries, and Keshan Disease in China has responded to treatment with selenium (McLaren, 1994).

The relationship between the environment and human health is illustrated by the mercury incident in Minamata Bay, Japan. In the 1930s a chemical plant began discharging mercury into Minamata Bay. The mercury was converted to methylmercury by microorganisms (Zakrzewski, 1991). In the 1960s, local residents began to show symptoms such as sensory impairment and approximately 6% of the infants born near Minamata had cerebral palsy (Eisler, 1987). By 1982, methylmercury poisoning was diagnosed in some local residents, more than 50 people died, and 700 were left permanently paralyzed (Kudo and Miyahara, 1984). The methylmercury accumulated in fish and birds, and because fish was a staple in the diet of the local residents, ingestion of the mercury-contaminated fish led to what has become known as Minamata disease.

Another example is a bone disease, known as itai-itai ("ouch-ouch") disease, found in people in Japan exposed to large amounts of cadmium in food during the later part of World War II. Itai-itai disease occurred in people living downstream from a lead-zinc mine who used contaminated river water for drinking and irrigation of rice paddies. The relationship between itai-itai disease and cadmium is based on increased disease prevalence in areas of highest cadmium exposure, concomitant kidney disease that corresponds to cadmium-related kidney disease in industrial workers, and high cadmium concentrations in blood, urine, and organs (Bhattacharyya et al., 1995).

Chronic thallium poisoning was reported in a rural area of Southwest Guizhou Province, China, in the 1960s and 1970s. Weathering of waste slag from coal and mercury mining released thallium to overlying soil, and the thallium accumulated in vegetables that were ingested by humans (Zhou and Liu, 1985).

CONCLUDING REMARKS

Metals can be both essential and toxic to humans (Maugh, 1973; Mertz, 1981). Unlike some organic contaminants, metals do not break down in the environment; they are neither created nor destroyed by human activities. However, human activities can perturb the natural cycles of metals and redistribute them throughout the various reservoirs of natural systems (Nriagu and Pacyna, 1988; Nriagu, 1990). Contamination associated with mineral extraction has prompted controversies about human-health issues (Moore and Luoma, 1990).

The metal content of biota is often influenced by the geochemical nature of their habitat. This reflects a general pattern of metal transfer from the terrestrial to the biotic environment (Chang and Page, 1996). There is considerable evidence that the bioavailability and toxicity of metals are influenced by the speciation and physicochemical forms in which metals are present in waters, sediments, and soils (Jenne and Luoma, 1977; Allen et al., 1980). The speciation of metals in the environment is controlled by an interrelated web of chemical, geochemical, and biological

processes that control the behavior and mobility of metals in the surficial environment. A first approximation of metal behavior and mobility often can be made based on a knowledge of the physicochemical properties of metals, and on empirical observations.

It is important to combine physicochemical, geochemical, geological, and biological information in the study of metal bioavailability and toxicity. Much remains to be learned about interactions and interferences among metals and their combined effects on physiology. However, it is clear that a holistic approach is required to adequately understand and assess the environmental impacts of metals on human health.

ACKNOWLEDGMENTS—Special thanks go to A. Rose and P. Valberg for their technical reviews of this manuscript. We acknowledge with much gratitude the comments and suggestions of the following persons: C. Alpers, D. Anderson, L. Balistrieri, R. Benson, B. Berger, T. Bowers, T. Chao, S. Church, J. Erdman, L. Filipek, S. Gebhard, R. Goldfarb, L. Gough, J. Leventhal, A. Lewis-Russ, S. Luoma, D. Macalady, W. Miller, A. Mills, M. Montour, A. Nicholson, K. Nordstrom, G. Plumlee, C. Russell, R. Schmiermund, R. Severson, K. Walton-Day, R. Wanty, and W. Wuerthele. We regret that we were unable to incorporate all of the proposed comments and suggestions; ultimately, we are responsible for any disparities or omissions in this chapter. We would also like to acknowledge B. Gebhard and K. O'Connell for their contributions. Finally, we want to thank our families for their understanding and support during the preparation of this article. K.S. was funded through the Mineral Resources and the Toxic Substances Hydrology Programs of the U.S. Geological Survey.

REFERENCES

- Adriano, D.C., 1986, Trace elements in the terrestrial environment: Springer-Verlag, New York, 533 pp.
- Agency for Toxic Substances and Disease Registry, 1988, The Silver Creek mine tailings exposure study: Final report, technical assistance to the Summit City/County, Utah, Health Dept., 48 pp.
- Agency for Toxic Substances and Disease Registry, 1992, Toxicological profile for aluminum: U.S. Dept. of Health and Human Services, TP-91/01, 136 pp.
- Agency for Toxic Substances and Disease Registry, 1993, Toxicological profile for arsenic: U.S. Dept. of Health and Human Services, TP-92/02, 175 pp.
- Ahrland, S., Chatt, J., and Davies, N.R., 1958, The relative affinities of ligand atoms for acceptor molecules and ions: Quarterly Reviews Chemical Society, v. 12, pp. 265–276.
- Allen, H.E., Hall, R.H., and Brisbin, T.D., 1980, Metal speciation effects on aquatic toxicity: Environmental Science and Technology, v. 14, pp. 441–443.
- Alloway, B.J., Thornton, I., Smart, G.A., Sherlock, J.C., and Quinn, M.J., 1988, Metal availability: Science of the Total Environment, v. 75, pp. 41–69.
- Andersson, A., and Nilsson, K.O., 1974, Influence of lime and soil pH on Cd availability to plants: Ambio, v. 3, pp. 198–200.
- Andrew, R.W., Biesinger, K.E., and Glass, G.E., 1977, Effects of inorganic complexing on the toxicity of copper to *Daphnia magna*: Water Research, v. 11, pp. 309–315.
- Austin, G.S., Branduold, L.A., Hawley, J.W., and Renault, J., 1992, Lead contamination at old smelter sites in the West—The Socorro, New Mexico case history: Society for Mining, Metallurgy, and Exploration, Inc., Preprint No. 92–99, 13 pp.
- Axtmann, E.V., and Luoma, S.N., 1991, Large scale distribution of metal contamination in fine-grained sediments of the Clark Fork River, Montana, USA: Applied Geochemistry, v. 6, pp. 75–88.

- Azcue, J.M., Mudroch, A., Rosa, F., Hall, G.E.M., Jackson, T.A., and Reynoldson, T., 1995, Trace elements in water, sediments, porewater, and biota polluted by tailings from an abandoned gold mine in British Columbia, Canada: *Journal of Geochemical Exploration*, v. 52, pp. 25–34.
- Bartell, S.M., Gardner, R.H., and O'Neill, R.V., 1992, Ecological risk estimation: Lewis Publishers, Chelsea, Mich., 252 pp.
- Beck, B.D., Rudel, R., Hook, G.C., and Bowers, T.S., 1995, Risk assessment; *in* Goyer, R.A., Klaassen, C.D., and Waalkes, M.P. (eds.), *Metal Toxicology*: Academic Press, San Diego, Calif., pp. 141–185.
- Beus, A.A., and Grigorian, S.V., 1977, Geochemical exploration methods for mineral deposits: Applied Publishing Ltd., Wilmette, Ill., 287 pp.
- Bhattacharyya, M.H., Wilson, A.K., Silbergeld, E.K., Watson, L., and Jeffery, E., 1995, Metal-induced osteotoxicities; *in* Goyer, R.A., Klaassen, C.D., and Waalkes, M.P. (eds.), *Metal Toxicology*: Academic Press, San Diego, Calif., pp. 465–510.
- Boyle, R.W., 1974, Elemental associations in mineral deposits and indicator elements of interest in geochemical prospecting: Geological Survey of Canada Paper 74–45, 40 pp.
- Brezonik, P.L., King, S.O., and Mach, C.E., 1991, The influence of water chemistry on trace metal bioavailability and toxicity to aquatic organisms; *in* Newman, M.C., and McIntosh, A.W. (eds.), *Metal Ecotoxicology, Concepts and Applications*: Lewis Publishers, Chelsea, Mich., pp. 1–31.
- Bryan, G., 1976, Some aspects of heavy metal tolerance in aquatic organisms; *in* Lockwood A. (ed.), *Effects of Pollutants on Aquatic Organisms*: Cambridge Univ. Press, Cambridge, Mass., pp. 7–34.
- Callahan, M.A., Slimak, M.W., Gabel, N.W., May, I.P., Fowler, C.F., Freed, J.R., Jennings, P., Durfee, R.L., Whitmore, F.C., Maestri, B., Mabey, W.R., Holt, B.R., and Gould, C., 1979, Water-related environmental fate of 129 priority pollutants, Vol. I, Introduction and technical background, metals and inorganics, pesticides and PCB's: U.S. Environmental Protection Agency, EPA-440/4-79-029a.
- Campbell, P.G.C., 1995, Interactions between trace metals and aquatic organisms—A critique of the free-ion activity model; *in* Tessier, A., and Turner, D.R. (eds.), *Metal Speciation and Bioavailability in Aquatic Systems*: John Wiley and Sons, New York, pp. 45–102.
- Campbell, P.G.C., and Tessier, Andre, 1991, Biological availability of metals in sediments—Analytical approaches; *in* Vernet, J.-P. (ed.), *Heavy Metals in the Environment*: Elsevier, N.Y., pp. 161–173.
- Chang, A.C., and Page, A.L., 1996, Assessment of ecological and health effects of soil-borne trace elements and metals; *in* Chang, L.W. (ed.), *Toxicology of Metals*: CRC Press, Boca Raton, Fla., pp. 29–38.
- Chang, L.W. (ed.), 1996, *Toxicology of metals*: CRC Press, Inc., Boca Raton, Fla., 1198 pp.
- Chao, T.T., 1984, Use of partial dissolution techniques in geochemical exploration: *Journal of Geochemical Exploration*, v. 20, pp. 101–135.
- Christian, J.L., and Greger, J.L., 1991, *Nutrition for living*, 3rd ed.: Benjamin/Cummings Pub. Co., Inc., Redwood City, Calif., 651 pp.
- Colorado Dept. of Health, 1990, Leadville metals exposure study: Colorado Dept. of Health, Denver, 89 pp.
- Colorado Dept. of Health, 1992, Final report, Clear Creek/Central City mine waste exposure study, Part I. Smuggler Mountain Site: Colorado Dept. of Health, Denver, 267 pp.
- Colorado Dept. of Health, 1993, Clear Creek/Central City mine waste exposure study, Part II. Clear Creek/Central City Mine Sites: Colorado Dept. of Health, Denver, 90 pp.
- Cotter-Howells, J., 1996, Environmental geochemistry and health: *Mineralogical Society Bulletin*, Sept. 1996, pp. 3–6.
- Cotter-Howells, J., and Thornton, I., 1991, Sources and pathways of environmental lead to children in a Derbyshire mining village: *Environmental Geochemistry and Health*, v. 13, pp. 127–135.
- Cotton, F.A., and Wilkinson, Geoffrey, 1988, *Advanced inorganic chemistry*, 5th ed.: John Wiley and Sons, New York, 1455 pp.
- Cox, D.P., and Singer, D.A., 1986, Mineral deposit models: U.S. Geological Survey Bulletin 1693, 379 pp.
- Darnley, A.G., 1990, International geochemical mapping—A new global project: *Journal of Geochemical Exploration*, v. 39, pp. 1–13.
- Davis, A., Ruby, M.V., and Bergstrom, P.D., 1992, Bioavailability of arsenic and lead in soils from the Butte, Montana, mining district: *Environmental Science and Technology*, v. 26, pp. 461–468.
- Davis, A., Drexler, J.W., Ruby, M.V., and Nicholson, A., 1993, Micromineralogy of mine wastes in relation to lead bioavailability, Butte, Montana: *Environmental Science and Technology*, v. 27, pp. 1415–1425.
- Davis, J.M., and Elias, R.W., 1996, Risk assessment of metals; *in* Chang, L.W. (ed.), *Toxicology of Metals*: CRC Press, Inc., Boca Raton, Fla., pp. 55–67.
- Dickson, K.L., Giesy, J.P., Parrish, R., and Wolfe, L., 1994, Closing remarks—summary and conclusions; *in* Hamelink, J.L., Landrum, P.F., Bergman, H.L., and Benson W.H. (eds.), *Bioavailability—Physical, Chemical, and Biological Interactions*, SETAC Spec. Pub. Series: CRC Press, Inc., Boca Raton, Fla., pp. 221–230.
- Diks, D.M., and Allen, H.E., 1983, Correlation of copper distribution in a freshwater-sediment system to bioavailability: *Bulletin of Environmental Contamination and Toxicology*, v. 30, pp. 37–43.
- Driscoll, C.T., Baker, J.P., Bisogni, J.J., and Schofield, C.L., 1980, Effect of aluminum speciation on fish in dilute acidified waters: *Nature*, v. 284, pp. 161–164.
- du Bray, E.A. (ed.), 1995, Preliminary compilation of descriptive geo-environmental mineral deposit models: U.S. Geological Survey Open-File Report 95–831, 272 pp.
- Eisler, R., 1987, Mercury hazards to fish, wildlife, and invertebrates—A synoptic review: *Biological Report 85(1.10)*, U.S. Dept. of the Interior, Fish and Wildlife Service, Laurel, Md.
- Ensminger, A.H., Ensminger, M.E., Konlande, J.E., and Robson, J.R., 1994, *Nutrition encyclopedia*, 2nd ed.: CRC Press, Ann Arbor, Mich., 2415 pp. (2 vols.).
- Erdman, J.A., Shacklette, H.T., and Keith, J.R., 1976, Elemental composition of corn grains, soybean seeds, pasture grasses, and associated soils from selected areas in Missouri: U.S. Geological Survey Professional Paper 954-D, 23 pp.
- Erdman, J.A., Severson, R.C., Crock, J.G., Harms, T.F., and Mayland, H.F., 1991, Selenium in soils and plants from native and irrigated lands at the Kendrick Reclamation Project Area, Wyoming; *in* Severson, R.C., Fisher, Jr., S.E., and Gough, L.P. (eds.), *Proceedings of the 1990 Billings Land Reclamation Symposium on Selenium in Arid and Semiarid Environments, Western United States*: U.S. Geological Survey Circular 1064, pp. 91–105.
- Fan, A.M., 1996, Assessment of metals in drinking water with specific references to lead, copper, arsenic, and selenium; *in* Chang, L.W. (ed.), *Toxicology of Metals*: CRC Press, Inc., Boca Raton, Fla., pp. 39–53.
- Fergusson, J.E., 1990, *The heavy elements—chemistry, environmental impact and health effects*: Pergamon Press, New York, 614 pp.
- Fernandez, M.A., Martinez, L., Segarra, M., Garcia, J.C., and Espiell, F., 1992, Behavior of heavy metals in the combustion gases of urban waste incinerators: *Environmental Science and Technology*, v. 26, pp. 1040–1047.
- Festa, M.D., Anderson, H.L., Dowdy, R.P., and Ellersieck, M.R., 1985, Effect of zinc intake on copper excretion and retention in men: *The American Journal of Clinical Nutrition*, v. 41, pp. 285–292.
- Ficklin, W.H., Plumlee, G.S., Smith, K.S., and McHugh, J.B., 1992, Geochemical classification of mine drainages and natural drainages in mineralized areas; *in* Kharaka, Y.K., and Maestri, A.S. (eds.), *Water-Rock Interaction*, v. 1, 7th Internatl Symposium on Water-Rock Interaction: A.A. Balkema, Rotterdam, pp. 381–384.
- Filipek, L.H., and Owen, R.M., 1979, Geochemical associations and grain-size partitioning of heavy metals in lacustrine sediments: *Chemical Geology*, v. 26, pp. 105–117.
- Filipek, L.H., and Theobald, P.K., Jr., 1981, Sequential extraction techniques applied to a porphyry copper deposit in the basin and range province: *Journal of Geochemical Exploration*, v. 14, pp. 155–174.
- Filipek, L.H., Chao, T.T., and Carpenter, R.H., 1981, Factors affecting the partitioning of Cu, Zn and Pb in boulder coatings and stream sediments in the vicinity of a polymetallic sulfide deposit: *Chemical Geology*, v. 33, pp. 45–64.

- Fischer, P.W.F., Giroux, A., and L'Abbé, M.R., 1984, Effect of zinc supplementation on copper status in adult men: *The American Journal of Clinical Nutrition*, v. 40, pp. 743–746.
- Fortescue, J.A.C., 1980, *Environmental geochemistry—a holistic approach*: Springer-Verlag, New York, 347 pp.
- Fortescue, J.A.C., 1992, Landscape geochemistry—Retrospect and prospect—1990: *Applied Geochemistry*, v. 7, pp. 1–53.
- Freeman, G.B., Johnson, J.D., Killinger, J.M., Liao, S.C., Feder, P.I., Davis, A.O., Ruby, M.V., Chaney, R.L., Lovre, S.C., and Bergstrom, P.D., 1992, Relative bioavailability of lead from mining waste soil in rats: *Fundamentals of Applied Toxicology*, v. 19, pp. 388–398.
- Frost, D.V., 1978, The arsenic problems; *in* Schrauzer, G.N. (ed.), *Inorganic and Nutritional Aspects of Cancer*: Plenum Press, New York, pp. 259–280.
- Fuller, W.H., 1977, Movement of selected metals, asbestos, and cyanide in soil—Applications to waste disposal problems: U.S. Environmental Protection Agency, EPA-600/2-77-020, 242 pp.
- Gabriel, I.E., and Patten, T., 1994, Distribution of copper smelter emissions in southeastern Arizona—using honey mesquite as a bioindicator: *Water, Air, and Soil Pollution*, v. 72, pp. 67–87.
- Garrels, R.M., and Christ, C.L., 1965, *Solutions, minerals, and equilibria*: Freeman, Cooper and Company, San Francisco, Calif., 450 pp.
- Gatehouse, S., Russell, D.W., and Van Moort, J.C., 1977, Sequential soil analysis in exploration geochemistry: *Journal of Geochemical Exploration*, v. 8, pp. 483–494.
- Germani, M.S., Small, M., Zoller, W.H., and Moyers, J.L., 1981, Fractionation of elements during copper smelting: *Environmental Science and Technology*, v. 15, pp. 299–305.
- Gibbs, R.J., 1973, Mechanisms of trace metal transport in rivers: *Science*, v. 180, pp. 71–73.
- Ginevan, M.E., and Splitstone, D.E., 1997, Improving remediation decisions at hazardous waste sites with risk-based geostatistical analysis: *Environ. Sci. Tech.*, v. 31, pp. 92A–96A.
- Goldschmidt, V.M., 1954, *Geochemistry*: Oxford Univ. Press, Fair Lawn, N.J.
- Gordon, T. 1995, Respiratory system; *in* Goyer, R.A., Klaassen, C.D., and Waalkes, M.P. (eds.), *Metal Toxicology*: Academic Press, San Diego, Calif., pp. 237–263.
- Gossel, T.A., and Bricker, J.D., 1984, Metals; *in* *Principles of Clinical Toxicology*: Raven Press, New York, pp. 153–187.
- Gough, L.P., Shacklette, H.T., and Case, A.A., 1979, Element concentrations toxic to plants, animals, and man: U.S. Geological Survey Bulletin 1466, 80 pp.
- Gough, L.P., McNeal, J.M., and Severson, R.C., 1980, Predicting native plant copper, iron, manganese and zinc levels using DTPA and EDTA soil extractants, Northern Great Plains: *Soil Science Society of America Journal*, v. 44, pp. 1030–1035.
- Goyer, R.A., 1991, Toxic effects of metals; *in* Amdur, M.O., Doull, J., and Klaassen, C.D. (eds.), *Casarett and Doull's Toxicology, The Basic Science of Poisons*, 4th ed.: Pergamon Press, New York, pp. 623–680.
- Goyer, R.A., 1995, Factors influencing metal toxicity; *in* Goyer, R.A., Klaassen, C.D., and Waalkes, M.P. (eds.), *Metal Toxicology*: Academic Press, San Diego, Calif., pp. 31–45.
- Goyer, R.A., Klaassen, C.D., and Waalkes, M.P. (eds.), 1995, *Metal toxicology*: Academic Press, San Diego, Calif., 525 pp.
- Greenwood, N.N., and Earnshaw, A., 1984, *Chemistry of the elements*: Pergamon Press, New York, 1542 pp.
- Griffith, W.H., 1988, Complete guide to vitamins, minerals and supplements: Fisher Books, Tucson, Ariz., 510 pp.
- Gulson, B.L., Davis, J.J., Mizon, K.J., Korsch, M.J., Law, A.J., and Howarth, D., 1994a, Lead bioavailability in the environment of children—Blood lead levels in children can be elevated in a mining community: *Archives of Environmental Health*, v. 49, pp. 326–331.
- Gulson, B.L., Mizon, K.J., Law, A.J., Korsch, M.J., Davis, J.J., and Howarth, D., 1994b, Source and pathways of lead in humans from the Broken Hill mining community—an alternative use of exploration methods: *Economic Geology*, v. 89, pp. 889–908.
- Hayes, J.A., 1989, Metal toxicity; *in* Marquis, J.A. (ed.), *A Guide to General Toxicology*, 2nd ed.: Karger, New York, pp. 179–189.
- Hem, J.D., 1985, Study and interpretation of the chemical characteristics of natural water, 3rd ed.: U.S. Geological Survey Water-Supply Paper 2254, 263 pp.
- Hemphill, C.P., Ruby, M.V., Beck, B.D., Davis, A., and Bergstrom, P.D., 1991, The bioavailability of lead in mining wastes—physical/chemical considerations: *Chemical Speciation and Bioavailability*, v. 3, pp. 135–148.
- Hill, C.H., 1988, Interactions among trace elements; *in* Prasad, A.S. (ed.), *Essential and Toxic Trace Elements in Human Health and Disease*: Alan R. Liss, Inc., New York, pp. 491–500.
- Hoffman, G.R., 1991, Genetic toxicology; *in* Amdur, M.O., Doull, J., and Klaassen, C.D. (eds.), *Casarett and Doull's Toxicology, the Basic Science of Poisons*: Pergamon Press, New York, pp. 201–225.
- Horowitz, A.J., 1991, A primer on sediment-trace element chemistry, 2nd ed.: Lewis Publishers, Chelsea, Mich., 136 pp.
- Horowitz, A.J., Rinella, F.A., Lamothe, P., Miller, T.L., Edwards, T.K., Roche, R.L., and Rickert, D.A., 1990, Variations in suspended sediment and associated trace element concentrations in selected riverine cross sections: *Environmental Science and Technology*, v. 24, pp. 1313–1320.
- Huheey, J.E., Keiter, E.A., and Keiter, R.L., 1993, *Inorganic chemistry—principles of structure and reactivity*, 4th ed.: Harper Collins College Publishers, New York, 964 pp.
- IGCP, 1995, A global geochemical database for environmental and resource management, recommendations for international geochemical mapping, final report of the International Geological Correlation Programme (IGCP) Project 259, by A.G. Darnley, A. Bjorklund, B. Bolviken, N. Gustavsson, P.V. Koval, J.A. Plant, A. Steinfeld, M. Tauchid, and X. Xuejing: UNESCO Publishing, France, 122 pp.
- Irvine, D.G., Schiefer, H.R., and Hader, W.J., 1988, Geotoxicology of multiple sclerosis—The Henribourg, Saskatchewan, cluster focus, II. The soil: *Science of the Total Environment*, v. 77, pp. 175–188.
- Jackson, A.P., and Alloway, B.J., 1991, The transfer of cadmium from sewage sludge amended soils into the edible components of food crops: *Water, Air, and Soil Pollution*, v. 57–58, pp. 873–881.
- Jenne, E.A., and Luoma, S.N., 1977, Forms of trace elements in soils, sediments and associated waters—An overview of their determination and biological availability; *in* Wildung, R.E., and Drucker, H. (eds.), *Biological Implications of Metals in the Environment*: Technical Information Center, Energy Research and Development Administration Symposium Series 42, NTIS, Springfield, Va., CONF-750929, pp. 110–143.
- Kabata-Pendias, A., and Pendias, H., 1992, *Trace elements in soils and plants*, 2nd ed.: CRC Press, Inc., Boca Raton, Fla., 342 pp.
- Kelly, M.G., 1999, Effects of heavy metals on the aquatic biota; *in* Plumlee, G.S., and Logsdon, M.J. (eds.), *The Environmental Geochemistry of Mineral Deposits, Part A. Processes, Techniques, and Health Issues*: Society of Economic Geologists, Reviews in Economic Geology, v. 6A, pp. 363–371.
- Klaassen, C.D., and Eaton, D.L., 1991, Principles of toxicology; *in* Amdur, M.O., Doull, J., and Klaassen, C.D. (eds.), *Casarett and Doull's Toxicology, The Basic Science of Poisons*: Pergamon Press, New York, pp. 12–49.
- Klein, C.B., 1996, Carcinogenicity and genotoxicity of chromium; *in* Chang, L.W. (ed.), *Toxicology of Metals*: CRC Press, Inc., Boca Raton, Fla., pp. 205–219.
- Klein, D.H., Andren, A.W., Carter, J.A., Emery, J.F., Feldman, C., Fulkerson, W., Lyon, W.S., Ogle, J.C., Talmi, Y., Van Hook, R.I., and Bolton, N., 1975, Pathways of thirty-seven elements through coal-fired power plant: *Environmental Science and Technology*, v. 9, pp. 973–979.
- Krieger, G.R., Hattemer-Frey, H.A., and Kester, J.E., 1999, Bioavailability of metals in the environment—Implications for health risk assessment; *in* Plumlee, G.S., and Logsdon, M.J. (eds.), *The Environmental Geochemistry of Mineral Deposits, Part A. Processes, Techniques, and Health Issues*: Society of Economic Geologists, Reviews in Economic Geology, v. 6A, pp. 357–361.

- Kudo, A., and Miyahara, S., 1984, Mercury dispersion from Minamata Bay to the Yatsushiro Sea during 1975–1980: *Ecotoxicol. Environ. Safety*, v. 8, pp. 507–510.
- Lag, J., 1983, Geomedicine in Scandinavia; *in* Thornton, I. (ed.), *Applied Environmental Geochemistry*: Academic Press, London, pp. 335–353.
- Landis, W.G., and Yu, M.-H., 1995, Introduction to environmental toxicology: CRC Press, Inc., Boca Raton, Fla., 328 pp.
- Langmuir, D., and Mahoney, J.J., 1984, Chemical equilibrium and kinetics of geochemical processes in ground water studies; *in* Hitchon, B., and Wallick, E. (eds.), *Practical Applications of Ground Water Geochemistry*: National Water Well Association, Dublin, Ohio, pp. 69–95.
- Langston, W.J., 1982, Distribution of mercury in British estuarine sediments and its availability to deposit-feeding bivalves: *J. Mar. Biol. Assoc. U.K.*, v. 62, pp. 667–684.
- Levinson, A.A., 1980, Introduction to exploration geochemistry, 2nd ed.: Applied Publishing Ltd., Wilmette, Ill., 924 pp.
- Li, X., and Thornton, I., 1993, Multi-element contamination of soils and plants in old mining areas, U.K.: *Applied Geochemistry, Suppl. Issue no. 2*, pp. 51–56.
- Lindsay, W.L., 1979, *Chemical equilibria in soils*: John Wiley and Sons, New York, 449 pp.
- Lion, L.W., Altmann, R.S., and Leckie, J.O., 1982, Trace-metal adsorption characteristics of estuarine particulate matter: evaluation of contributions of Fe/Mn oxide and organic surface coatings: *Environmental Science and Technology*, v. 16, pp. 660–666.
- Luckey, T.D., and Venugopal, B., 1977, *Metal toxicity in mammals, Vol. 1, Physiologic and chemical basis for metal toxicity*: Plenum Press, New York, 238 pp.
- Lukashev, V.K., 1984, Mode of occurrence of elements in secondary environments: *Journal of Geochemical Exploration*, v. 21, pp. 73–87.
- Lukashev, V.K., 1986, Some scientific and applied problems of supergene geochemistry in the U.S.S.R.: *Applied Geochemistry*, v. 1, pp. 441–449.
- Luoma, S.N., 1983, Bioavailability of trace metals to aquatic organisms—a review: *Science of the Total Environment*, v. 28, pp. 1–22.
- Luoma, S.N., 1989, Can we determine the biological availability of sediment bound trace elements?: *Hydrobiologia*, v. 176/177, pp. 379–396.
- Luoma, S.N., and Bryan, G.W., 1979, Trace metal bioavailability—modeling chemical and biological interactions of sediment-bound zinc; *in* Jenne, E.A. (ed.), *Chemical Modeling in Aqueous Systems—Speciation, Sorption, Solubility, and Kinetics, ACS Symposium Series 93*: American Chemical Society, Washington, D.C., pp. 577–609.
- Luoma, S.N., and Bryan, G.W., 1981, A statistical assessment of the form of trace metals in oxidized estuarine sediments employing chemical extractants: *Science of the Total Environment*, v. 17, pp. 165–196.
- Luoma, S.N., and Carter, J.L., 1993, Understanding the toxicity of contaminants in sediments—beyond the bioassay-based paradigm: *Environmental Toxicology and Chemistry*, v. 12, pp. 793–796.
- Luoma, S.N., and Davis, J.A., 1983, Requirements for modeling trace metal partitioning in oxidized estuarine sediments: *Marine Chemistry*, v. 12, pp. 159–181.
- Luoma, S.N., and Jenne, E.A., 1976, Estimating bioavailability of sediment-bound trace metals with chemical extractants; *in* Hemphill, D.D. (ed.), *Trace Substances in Environmental Health*: Univ. of Missouri Press, Columbia, pp. 343–353.
- Luoma, S.N., and Jenne, E.A., 1977, The availability of sediment-bound cobalt, silver and zinc to a deposit-feeding clam; *in* Wildung, R.E., and Drucker, H. (eds.), *The Biological Implications of Metals in the Environment*: Technical Information Center, Energy Research and Development Administration Symposium Series 42, NTIS, Springfield, Va., CONF-750929, pp. 213–230.
- Mahaffey, K.R., 1978, Environmental exposure to lead; *in* Nriagu, J.O. (ed.), *The Biogeochemistry of Lead in the Environment, Part B. Biological Effects*: Elsevier/North-Holland Biomedical Press, New York, pp. 1–36.
- Marcus, J.J. (ed.), 1997, *Mining environmental handbook*: Imperial College Press, London, 785 pp.
- Markert, B., 1994, Plants as biomonitors—potential advantages and problems; *in* Adriano, D.C., Chen, Z.S., and Yang, S.S. (eds.), *Biogeochemistry of Trace Elements*: Science and Technology Letters, Northwood, N.W., pp. 601–613.
- Martin, J.H., Knauer, G.A., and Flegal, A.R., 1980, Distribution of zinc in natural waters; *in* Nriagu, J.O. (ed.), *Zinc in the Environment, Part I. Ecological Cycling*: John Wiley and Sons, New York, pp. 193–197.
- Martin, J.-M., and Whitfield, M., 1983, The significance of the river input of chemical elements to the ocean; *in* Wong, C.S., Boyle, E., Bruland, K.W., Burton, J.D., and Goldberg, E.D. (eds.), *Trace Metals in Sea Water*: Plenum Press, New York, pp. 265–296.
- Maskall, J., Whitehead, K., and Thornton, I., 1995, Heavy metal migration in soils and rocks at historical smelting sites: *Environmental Geochemistry and Health*, v. 17, pp. 127–138.
- Maugh, T.H., II, 1973, Trace elements—a growing appreciation of their effects on man: *Science*, v. 181, pp. 253–254.
- McKinney, J.D., and Rogers, R., 1992, Metal bioavailability—EPA workshop identified research needs: *Environmental Science and Technology*, v. 26, pp. 1298–1299.
- McLaren, D.S., 1994, Clinical manifestations of human vitamin and mineral disorders—a resume; *in* Shils, M.E., Olsen, J.A., and Shike, M. (eds.), *Modern Nutritional Health and Disease, 8th ed.*, vol. 1: Lea and Febiger, Philadelphia, Pa., pp. 909–923.
- Merrington, G., and Alloway, B.J., 1994, The transfer and fate of Cd, Cu, Pb and Zn from two historic metalliferous mine sites in the U.K.: *Applied Geochemistry*, v. 9, pp. 677–687.
- Mertz, W., 1981, The essential trace elements: *Science*, v. 213, pp. 1332–1338.
- Meybeck, M., 1988, How to establish and use world budgets of riverine materials; *in* Lerman, A., and Meybeck, M. (eds.), *Physical and Chemical Weathering in Geochemical Cycles*: Kluwer Academic Publishers, Dordrecht, pp. 247–272.
- Meybeck, M., and Helmer, R., 1989, The quality of rivers—From pristine stage to global pollution: *Paleogeography, Paleoclimatology, Paleocology, Global and Planetary Change Section*, v. 75, pp. 283–309.
- Meybeck, M., Chapman, D.V., and Helmer, R. (eds.), 1989, *Global freshwater quality—a first assessment*: Published on behalf of the World Health Organization and the United Nations Environment Programme by Blackwell Reference, Oxford, 300 pp.
- Miesch, A.T., 1976, *Geochemical survey of Missouri—methods of sampling, laboratory analysis, and statistical reduction of data*: U.S. Geological Survey Professional Paper 954-A, 39 pp.
- Moore, J.N., and Luoma, S.N., 1990, Hazardous wastes from large-scale metal extraction: *Environmental Science and Technology*, v. 24, pp. 1278–1285.
- Morel, F.M.M., 1983, *Principles of aquatic chemistry*: Wiley Interscience, New York, 301 pp.
- Morel, F.M.M., and Hudson, R.J.M., 1985, The geobiological cycle of trace elements in aquatic systems—Redfield revisited; *in* Stumm, W. (ed.), *Chemical Processes in Lakes*: John Wiley and Sons, New York, pp. 251–281.
- Morgan, H. (ed.), 1988, *The Shipham report—an investigation into cadmium contamination and its implications for human health*: The Science of the Total Environment, v. 75, pp. 41–69.
- National Research Council, 1983, *Risk assessment in the federal government—Managing the process*: National Academy of Sciences, National Academy Press, Washington, D.C.
- National Research Council, 1989, *Recommended dietary allowances, 10th ed.*: National Academy of Sciences, National Academy Press, Washington, D.C., 284 pp.
- National Research Council, 1993, *Measuring lead exposure in infants, children, and other sensitive populations*: National Academy of Sciences, National Academy Press, Washington, D.C.
- National Research Council, 1994, *Science and judgment in risk assessment*: National Academy of Sciences, National Academy Press, Washington, D.C.
- Navarra, T., and Lipkowitz, M.A., 1996, *Encyclopedia of vitamins, miner-*

- als, and supplements: Facts on File, Inc., New York, 281 pp.
- Newman, M.C., and Jagoe, C.H., 1994, Inorganic toxicants—ligands and the bioavailability of metals in aquatic environments; *in* Hamelink, J.L., Landrum, P.F., Bergman, H.L., and Benson, W.H. (eds.), Bioavailability—Physical, Chemical, and Biological Interactions, SETAC Spec. Pub. Series: CRC Press, Inc., Boca Raton, Fla., pp. 39–61.
- Nieboer, E., and Fletcher, G.G., 1996, Determinants of reactivity in metal toxicology; *in* Chang, L.W. (ed.), Toxicology of Metals: CRC Press, Boca Raton, Fla., pp. 113–132.
- Nieboer, E., and Richardson, D.H.S., 1980, The replacement of the non-descript term “heavy metals” by a biologically and chemically significant classification of metal ions: *Environmental Pollution, Series B*, v. 1, pp. 3–26.
- Nielsen, F.H., 1994, Ultratrace minerals; *in* Shils, M.E., Olson, J.A., and Shike, M. (eds.), Modern Nutrition in Health and Disease, 8th ed., Vol. 1: Lea and Febiger, Philadelphia, Pa., pp. 269–296.
- Nordstrom, D.K., 1999, Some fundamentals of aqueous geochemistry; *in* Plumlee, G.S., and Logsdon, J.J. (eds.), The Environmental Geochemistry of Mineral Deposits, Part A. Processes, Techniques, and Health Issues: Society of Economic Geologists, Reviews in Economic Geology, v. 6A, pp. 117–123.
- Nordstrom, D.K., and Alpers, C.N., 1999, Geochemistry of acid mine waters; *in* Plumlee, G.S., and Logsdon, J.J. (eds.), The Environmental Geochemistry of Mineral Deposits, Part A. Processes, Techniques, and Health Issues: Society of Economic Geologists, Reviews in Economic Geology, v. 6A, pp. 133–160.
- Nordstrom, D.K., and Munoz, J.L., 1994, Geochemical thermodynamics, 2nd ed.: Blackwell Science, 493 pp.
- Nriagu, J.O., 1989, A global assessment of natural sources of atmospheric trace metals: *Nature*, v. 338, pp. 47–49.
- Nriagu, J.O., 1990, Global metal pollution: *Environment*, v. 32, no. 7, pp. 6–11, 28–33.
- Nriagu, J.O., and Pacyna, J.M., 1988, Quantitative assessment of worldwide contamination of air, water and soils by trace metals: *Nature*, v. 333, pp. 134–139.
- O’Donnel, J.R., Kaplan, B.M., and Allen, H.E., 1985, Bioavailability of trace metals in natural waters; *in* Cardwell, R.D., Purdy, R., and Bahner, R.C. (eds.), Aquatic Toxicology and Hazard Assessment, 7th Symposium, ASTM Spec. Tech. Pub. No. 854: American Society for Testing and Materials, Philadelphia, Pa., pp. 485–501.
- Pacyna, J.M., 1996, Monitoring and assessment of metal contaminants in the air; *in* Chang, L.W. (ed.), Toxicology of Metals: CRC Press, Inc., Boca Raton, Fla., pp. 9–28.
- Pagenkopf, G.K., Russo, R.C., and Thurston, R.V., 1974, Effect of complexation on toxicity of copper to fishes: *J. Fish Res. Bd. Can.*, v. 31, pp. 462–465.
- Pais, I., and Jones, J.B., Jr., 1997, The handbook of trace elements: St. Lucie Press, Boca Raton, Fla., 223 pp.
- Papp, C.S.E., Filipek, L.H., and Smith, K.S., 1991, Selectivity and effectiveness of extractants used to release metals associated with organic matter: *Applied Geochemistry*, v. 6, pp. 349–353.
- Parish, R.V., 1977, The metallic elements: Longman Inc., New York, 254 pp.
- Pascoe, G.A., Blanchet, R.J., and Linder, G., 1994, Bioavailability of metals and arsenic to small mammals at a mining waste-contaminated wetland: *Arch. Environ. Contam. Toxicol.*, v. 27, pp. 44–50.
- Pearson, R.G., 1963, Hard and soft acids and bases: *Journal of the American Chemical Society*, v. 85, pp. 3533–3539.
- Pearson, R.G., 1968a, Hard and soft acids and bases, HSAB, Part I. Fundamental principles: *Journal of Chemical Education*, v. 45, pp. 581–587.
- Pearson, R.G., 1968b, Hard and soft acids and bases, HSAB, Part II. Underlying theories: *Journal of Chemical Education*, v. 45, pp. 643–648.
- Pelletier, E., 1995, Environmental organometallic chemistry of mercury, tin, and lead—present status and perspectives; *in* Tessier, A., and Turner, D.R. (eds.), Metal Speciation and Bioavailability in Aquatic Systems: John Wiley and Sons, New York, pp. 103–148.
- Perel’man, A.I., 1977, Geochemistry of elements in the supergene zone (translated from Russian): Keter Publishing House Ltd., Jerusalem, 266 pp.
- Perel’man, A.I., 1986, Geochemical barriers—theory and practical applications: *Applied Geochemistry*, v. 1, pp. 669–680.
- Pesch, C.E., and Morgan, D., 1978, Influence of sediment in copper toxicity tests with the polychaete *Neathes arenaceodentata*: *Water Research*, v. 12, pp. 747–751.
- Petito, C.T., and Beck, B.D., 1990, Evaluation of evidence of nonlinearities in the dose-response curve for arsenic carcinogenesis: *Trace Substances in Environmental Health*, v. 24, pp. 143–176.
- Phipps, D.A., 1981, Chemistry and biochemistry of trace metals in biological systems; *in* Lepp, N.W. (ed.), Effect of Heavy Metal Pollution on Plants, Vol. 1, Effects of Trace Metals on Plant Function: Applied Science Publishers, London, pp. 1–54.
- Pickering, W.F., 1981, Selective chemical extraction of soil components and bound metal species: *CRC Critical Reviews in Analytical Chemistry*, v. 12, pp. 233–266.
- Pierzynski, G.M., and Schwab, A.P., 1993, Bioavailability of zinc, cadmium, and lead in a metal-contaminated alluvial soil: *Journal of Environmental Quality*, v. 22, pp. 247–254.
- Piispanen, R., 1989, Geochemical interpretation of cancer maps of Finland: *Environmental Geochemistry and Health*, v. 11, pp. 145–147.
- Plant, J.A., and Thornton, I., 1985, Geochemistry and health in the United Kingdom; *in* Thornton, I. (ed.), Proceedings of the 1st Internatl Symposium on Geochemistry and Health: Science Reviews, Northwood, pp. 1–15.
- Plumlee, G., 1994, Environmental geology models of mineral deposits: *SEG Newsletter*, January 1994, no. 16, pp. 5–6.
- Plumlee, G.S., 1999, The environmental geology of mineral deposits; *in* Plumlee, G.S., and Logsdon, M.J. (eds.), The Environmental Geochemistry of Mineral Deposits, Part A. Processes, Techniques, and Health Issues: Society of Economic Geologists, Reviews in Economic Geology, v. 6A, pp. 71–116.
- Plumlee, G.S., Smith, K.S., Ficklin, W.H., and Briggs, P.H., 1992, Geological and geochemical controls on the composition of mine drainages and natural drainages in mineralized areas; *in* Kharaka, Y.K., and Maest, A.S. (eds.), Water-Rock Interaction, Vol. 1, 7th Internatl Symposium on Water-Rock Interaction: A.A. Balkema, Rotterdam, pp. 419–422.
- Plumlee, G.S., Smith, K.S., Ficklin, W.H., Briggs, P.H., and McHugh, J.B., 1993, Empirical studies of diverse mine drainages in Colorado—Implications for the prediction of mine-drainage chemistry, Proceedings, Vol. 1: 1993 Mined Land Reclamation Symposium, Billings, Mont., pp. 176–186.
- Plumlee, G.S., Streufert, R.K., Smith, K.S., Smith, S.M., Wallace, A.R., Toth, M., Nash, J.T., Robinson, R., Ficklin, W.H., and Lee, G.K., 1995, Geology-based map of potential metal-mine drainage hazards in Colorado: U.S. Geological Survey Open-File Report 95–26.
- Plumlee, G.S., Smith, K.S., Montour, M.R., Mosier, E.L., and Ficklin, W.H., 1999, Geologic controls on the composition of natural waters and mine waters draining diverse mineral-deposit types; *in* Filipek, L.H., and Plumlee, G.S. (eds.), The Environmental Geochemistry of Mineral Deposits, Part B, Case Studies and Research Topics: Society of Economic Geologists, Reviews in Economic Geology, v. 6B, pp. 373–432.
- Purcell, K.F., and Kotz, J.C., 1980, An introduction to inorganic chemistry: Saunders College, Philadelphia, Pa., 637 pp.
- Ragaini, R.C., Ralston, H.R., and Roberts, N., 1977, Environmental trace metal contamination in Kellogg, Idaho, near a lead smelting complex: *Environmental Science and Technology*, v. 11, pp. 773–781.
- Ranville, J.F., and Schmiermund, R.L., 1999, General aspects of aquatic colloids in environmental geochemistry; *in* Plumlee, G.S., and Logsdon, M.J. (eds.), The Environmental Geochemistry of Mineral Deposits, Part A. Processes, Techniques, and Health Issues: Society of Economic Geologists, Reviews in Economic Geology, v. 6A, pp. 183–199.

- Rickwood, P.C., 1983, Crustal abundance, distribution, and crystal chemistry of the elements; *in* Govett, G.J.S., Handbook of Exploration Geochemistry, Vol. 3, Rock Geochemistry in Mineral Exploration: Elsevier Scientific Publishing Company, Amsterdam, pp. 347–387.
- Ripley, E.A., Redmann, R.E., and Crowder, A.A., 1996, Environmental effects of mining: St. Lucie Press, Delray Beach, Fla., 356 pp.
- Rose, A.W., Hawkes, H.E., and Webb, J.S., 1979, Geochemistry in mineral exploration, 2nd ed.: Academic Press, New York, 657 pp.
- Ruby, M.V., Davis, Andy, Kempton, J.H., Drexler, J.W., and Bergstrom, P.D., 1992, Lead bioavailability—Dissolution kinetics under simulated gastric conditions: *Environmental Science and Technology*, v. 26, pp. 1242–1248.
- Ruby, M.V., Davis, A., Link, T.E., School, R., Chaney, R.L., Freeman, G.B., and Bergstrom, P., 1993, Development of an *in vitro* screening test to evaluate the *in vivo* bioaccessibility of ingested mine-waste lead: *Environmental Science and Technology*, v. 27, pp. 2870–2877.
- Salomons, W., 1995, Environmental impact of metals derived from mining activities—processes, predictions, prevention: *Journal of Geochemical Exploration*, v. 52, pp. 5–23.
- Salomons, W., and Forstner, U., 1984, *Metals in the hydrocycle*: Springer-Verlag, Berlin, 349 pp.
- Sandstead, H.H., 1980, Interactions of toxic elements with essential elements—Introduction: *Ann. N.Y. Acad. Sci.*, v. 355, pp. 282–284.
- Sandstead, H.H., 1988, Interactions that influence bioavailability of essential metals to humans; *in* Kramer, J.R., and Allen, H.E. (eds.), *Metal Speciation—Theory, Analysis and Application*: Lewis Publishers, Chelsea, Mich., pp. 315–332.
- Scokart, P.O., Meeus-Verdinne, K., and de Borger, R., 1983, Mobility of heavy metals in polluted soils near zinc smelters: *Water, Air, and Soil Pollution*, v. 20, pp. 451–463.
- Selgrade, M.J.K., and Gardner, D.E., 1996, Altered host defenses and resistance to respiratory infections following exposure to airborne metals; *in* Chang, L.W. (ed.), *Toxicology of Metals*: CRC Press, Inc., Boca Raton, Fla., pp. 853–860.
- Severson, R.C., and Gough, L.P., 1992, Selenium and sulfur relationships in alfalfa and soil under field conditions, San Joaquin Valley, California: *Journal of Environmental Quality*, v. 21, pp. 353–358.
- Severson, R.C., Gough, L.P., Crock, J.G., Fey, D.L., Hageman, P.L., Love, A.H., and Peacock, T.R., 1991, Uptake and physiological antagonism of selenium and sulfur in alfalfa and wheat under field conditions, San Joaquin Valley, California: U.S. Geological Survey Open-File Report 91–16, 42 pp.
- Shacklette, H.T., and Boerngen, J.G., 1984, Element concentrations in soils and other surficial materials of the conterminous United States: U.S. Geological Survey Professional Paper 1270, 105 pp.
- Shaper, A.G., 1979, Epidemiology for geochemists: *Phil. Trans. R. Soc. London B*, v. 288, pp. 127–136.
- Shaw, A.J. (ed.), 1990, *Heavy metal tolerance in plants—evolutionary aspects*: CRC Press, Boca Raton, Fla.
- Sheppard, S.C., Evenden, W.G., and Schwartz, W.J., 1995, Ingested soil—bioavailability of sorbed lead, cadmium, cesium, iodine, and mercury: *Journal of Environmental Quality*, v. 24, pp. 498–505.
- Simpson, P.R., 1995, Geochemical baselines for sustainable development: *Mineralogical Society Bulletin*, no. 109, Dec. 1995, pp. 21–26.
- Small, M., Germani, M.S., Small, A.M., Zoller, W.H., and Moyers, J.L., 1981, Airborne plume study of emissions from the processing of copper ores in southeastern Arizona: *Environmental Science and Technology*, v. 15, pp. 293–299.
- Smith, K.S., 1999, Metal sorption on mineral surfaces—An overview of examples relating to mineral deposits; *in* Plumlee, G.S., and Logsdon, M.J. (eds.), *The Environmental Geochemistry of Mineral Deposits, Part A. Processes, Techniques, and Health Issues*: Society of Economic Geologists, Reviews in Economic Geology, v. 6A, pp. 161–182.
- Smith, K.S., Balistrieri, L.S., Smith, S.M., and Severson, R.C., 1997, Distribution and mobility of molybdenum in the terrestrial environment; *in* Gupta, U.C. (ed.), *Molybdenum in Agriculture*, Ch. 3: Cambridge Univ. Press, Cambridge, Mass., pp. 23–46.
- Smith, K.S., Ranville, J.F., Plumlee, G.S., and Macalady, D.L., 1998, Predictive double-layer modeling of metal sorption in mine-drainage systems; *in* Jenne, E.A. (ed.), *Adsorption of Metals by Geomedia*: Academic Press, San Diego, Calif., pp. 521–547.
- Sprague, J.B., 1985, Factors that modify toxicity; *in* Rand, G.M., and Petrocelli, S.R. (eds.), *Fundamentals of Aquatic Toxicology*: Hemisphere, Washington, D.C., pp. 123–163.
- Spry, D.J., and Weiner, J.G., 1991, Metal bioavailability and toxicity to fish in low-alkalinity lakes: a critical review: *Environmental Pollution*, v. 71, pp. 243–304.
- Stumm, W., and Morgan, J.J., 1996, *Aquatic chemistry—chemical equilibria and rates in natural waters*, 3rd ed.: John Wiley and Sons, New York, 1022 pp.
- Sunda, W.G., and Guillard, R.R., 1976, The relationship between cupric-ion activity and the toxicity of copper to phytoplankton: *Journal of Marine Research*, v. 34, pp. 511–529.
- Suter, G.W., II, 1993, *Ecological risk assessment*: Lewis Publishers, Chelsea, Mich., 538 pp.
- Tanizaki, Y., Shimokawa, T., and Nakamura, M., 1992, Physicochemical speciation of trace elements in river waters by size fractionation: *Environmental Science and Technology*, v. 26, pp. 1433–1444.
- Tessier, A., and Turner, D.R. (eds.), 1995, *Metal speciation and bioavailability in aquatic sediments*, IUPAC Series on Analytical and Physical Chemistry of Environmental Systems, Vol. 3: John Wiley and Sons, New York, 679 pp.
- Tessier, A., Campbell, P.G.C., and Bisson, M., 1979, Sequential extraction procedure for the speciation of particulate trace metals: *Analytical Chemistry*, v. 51, pp. 844–851.
- Tessier, A., Campbell, P.G.C., Anclair, J.C., and Bisson, M., 1984, Relationships between the partitioning of trace metals in sediments and their accumulation in the tissues of the freshwater mollusk *Elliptio complanata* in a mining area: *Can. J. Fish. Aquat. Sci.*, v. 41, pp. 1463–1472.
- Thornton, I., 1982, Geochemical aspects of the distribution and forms of heavy metals in soils; *in* Lepp, N.W. (ed.), *Effect of Heavy Metal Pollution on Plants*, Vol. 2, *Metals in the Environment*: Applied Science Publishers, London, pp. 1–33.
- Thornton, I., 1983, *Geochemistry applied to agriculture*; *in* Thornton, I. (ed.), *Applied Environmental Geochemistry*: Academic Press, London, pp. 231–266.
- Thornton, I., 1987, Mapping of trace elements in relation to human disease: *Clinical Nutrition*, v. 6, pp. 97–104.
- Thornton, I., 1993, Environmental geochemistry and health in the 1990's—A global perspective: *Applied Geochemistry*, Suppl. Issue No. 2, pp. 203–210.
- Thurman, D.A., 1982, Mechanism of metal tolerance in higher plants; *in* Lepp, N.W. (ed.), *Effect of Heavy Metal Pollution on Plants*, Vol. 2, *Metals in the Environment*: Applied Science Publishers, London, pp. 239–249.
- Tingle, T.N., Borch, R.S., Hochella, M.F., Jr., Becker, C.H., and Walker, W.J., 1993, Characterization of lead on mineral surfaces in soils contaminated by mining and smelting: *Applied Surface Science*, v. 72, pp. 301–306.
- Turner, D.R., 1995, Problems in trace metal speciation modeling; *in* Tessier, A., and Turner, D.R. (eds.), *Metal Speciation and Bioavailability in Aquatic Systems*: John Wiley and Sons, New York, pp. 149–203.
- University of Cincinnati, 1997, Leadville/Lake County environmental health lead study, final report: Dept. of Environmental Health, 82 pp. and 17 appendices.
- U.S. EPA, 1980, Notice of availability, ambient water quality criteria documents (64 documents), Office of Water Regulations and Standards, Criterion Standards Division: U.S. Environmental Protection Agency, Federal Register, v. 45, pp. 79,318–79,379.
- U.S. EPA, 1986, Quality criteria for water 1986, U.S. Environmental Protection Agency, EPA 440/5–86–001: U.S. Government Printing Office, Washington, D.C.
- U.S. EPA, 1989, Risk assessment guidance for Superfund, I. Human health evaluation manual, Part A, U.S. Environmental Protection Agency, EPA

- 540/1-89-002: U.S. Government Printing Office, Washington, D.C.
- U.S. EPA, 1991, Comprehensive review of lead in the environment under TSCA: U.S. Environmental Protection Agency, Federal Register, v. 56, pp. 22,096-22,098.
- U.S. EPA, 1992, A framework for ecological risk assessment, Risk Assessment Forum, February, 1992: U.S. Environmental Protection Agency, EPA 630/R-92/001, 56 pp.
- U.S. EPA, 1993a, Integrated Risk Information Service (IRIS) on-line database: U.S. Environmental Protection Agency, Washington, D.C.
- U.S. EPA, 1993b, EPA Region VIII Clean Water Act Section 304(a) criteria chart, July 1, 1993: U.S. Environmental Protection Agency, 12 pp.
- U.S. EPA, 1994, Code of Federal Regulations, Title 40, Part 131, July 1, 1994 edition, pp. 335-369.
- U.S. EPA, 1995, Drinking water regulations and health advisories, May 1995: U.S. Environmental Protection Agency, Office of Water, 11 pp.
- U.S. EPA, 1996, Code of Federal Regulations, Title 40, Sec. 261.24, July 1, 1996 edition, p. 52.
- U.S. EPA, 1997, Measurement of lead bioavailability in soils and other test materials using juvenile swine; June 1997 Working Draft by S.W. Casteel, L.D. Brown, M.E. Dunsmore, C.P. Weis, G.M. Henningsen, E. Hoffman, W.J. Brattin, and T.L. Hammon: U.S. Environmental Protection Agency, Region VIII, Denver, Colo.
- U.S. EPA, 1998, National recommended water quality criteria: U.S. Environmental Protection Agency, Federal Register, v. 63, pp. 68,354-68,364.
- Valberg, P., Boardman, P., Bowers, T., and Beck, B., 1994, Arsenic health risks in the mining environment—current controversies, National Western Mining Conference, March 23-25, 1994: Denver Region Exploration Geologists Society, reprint, 11 pp.
- Venugopal, B., and Luckey, T.D., 1978, Metal toxicity in mammals, Vol. 2, Chemical toxicity of metals and metalloids: Plenum Press, New York, 409 pp.
- Vlasov, K.A. (ed.), 1966, Geochemistry and mineralogy of rare elements and genetic types of their deposits, Vol. 1, Geochemistry of rare elements (translated from Russian): Israel Program for Scientific Translations Ltd., Jerusalem, 688 pp.
- Walton-Day, K., 1999, Geochemistry of the processes that attenuate acid mine drainage in wetlands; *in* Plumlee, G.S., and Logsdon, M.J. (eds.), The Environmental Geochemistry of Mineral Deposits, Part A. Processes, Techniques, and Health Issues: Society of Economic Geologists, Reviews in Economic Geology, v. 6A, pp. 215-228.
- Warren, H.V., 1989, Geology, trace elements and health: Soc. Sci. Med., v. 8, pp. 923-926.
- Webb, J.S., 1964, Geochemistry and life: New Scientist, v. 23, pp. 504-507.
- Webb, J.S., Nichol, I., Foster, R., Lowenstein, P.L., and Howarth, R.J., 1973, Provisional geochemical atlas of Northern Ireland: Applied Geochemistry Research Group, Imperial College of Science and Technology, London.
- Webb, J.S., Thornton, I., Thompson, M., Howarth, R.J., and Lowenstein, P.L., 1978, The Wolfson geochemical atlas of England and Wales: Oxford Univ. Press.
- Weimin, Y., Batley, G.E., and Ahsanullah, M., 1992, The ability of sediment extractants to measure the bioavailability of metals to three marine invertebrates: The Science of the Total Environment, v. 125, pp. 67-84.
- Westerman, R.L. (ed.), 1990, Soil testing and plant analysis, 3rd ed.: Soil Science Society of America, 784 pp.
- Whitfield, M., and Turner, D.R., 1979, Water-rock partition coefficients and the composition of sea water and river water: Nature, v. 278, pp. 132-137.
- Whitfield, M., and Turner, D.R., 1983, Chemical periodicity and the speciation and cycling of the elements; *in* Wong, C.S., Boyle, E., Bruland, K.W., Burton, J.D., and Goldberg, E.D. (eds.), Trace Metals in Sea Water: Plenum Press, New York, pp. 719-750.
- Wixson, B.G., and Davies, B.E., 1994, Guidelines for lead in soil: Environmental Science and Technology, v. 28, pp. 26A-31A.
- Wood, J.M., 1988, Transport, bioaccumulation, and toxicity of metals and metalloids in microorganisms under environmental stress; *in* Kramer, J.R., and Allen, H.E. (eds.), Metal Speciation—Theory, Analysis and Application: Lewis Publishers, Chelsea, Mich., pp. 295-314.
- Zakrzewski, S.F., 1991, Principles of environmental toxicology: American Chemical Society, Washington, D.C., pp. 270.
- Zhou, D., and Liu, D., 1985, Chronic thallium poisoning in a rural area of Guizhou Province, China: Journal of Environmental Health, v. 48, pp. 14-18.
- Zitko, V., and Carson, W.G., 1976, A mechanism of the effects of water hardness on the lethality of heavy metals to fish: Chemosphere, v. 5, pp. 299-303.

Chapter 3

THE ENVIRONMENTAL GEOLOGY OF MINERAL DEPOSITS

G.S. Plumlee

U.S. Geological Survey, Box 25046, MS 964, Federal Center, Denver, CO 80225-0046

INTRODUCTION

Mineral deposits are concentrations of metallic or other mineral commodities in the Earth's crust that result from a variety of complex geologic processes. The natural weathering and erosion of a mineral deposit at the Earth's surface disperses its constituents into the waters, soils, and sediments of its surrounding environment. There, the constituents may be taken up by plants and (or) organisms. The concentrations and chemical, mineralogical, or biological forms of metals and other constituents from a mineral deposit prior to mining in soils, waters, sediments, plants, and organisms are defined here to be the natural environmental signatures of the deposit.

Modern mining and mineral processing activities employ a wide variety of methods to prevent or minimize adverse environmental impacts (Ripley et al., 1996; Plumlee and Logsdon, 1999; references therein). However, if not carried out with appropriate mitigation and prevention practices (as was common in most historical operations), or as a result of accidental releases, mining and mineral processing can disperse potentially deleterious metals, other deposit constituents, and mineral processing chemicals or byproducts into the environment. Mining-related environmental signatures are defined here as the concentrations and chemical, mineralogical, or biological forms of these metals and chemicals *prior to mitigation or remediation* in mining and milling wastes, mine waters, mineral processing solutions and byproducts, and smelter emissions and byproducts.

The geologic characteristics of mineral deposits exert important and predictable controls on the natural environmental signatures of mineralized areas prior to mining, and on the environmental signatures that could result from mining and mineral processing if appropriate preventive and mitigative practices were not followed. A good understanding of the environmental geology of mineral deposits is therefore crucial to the development of effective mining-environmental prediction, mitigation, and remediation practices.

This chapter summarizes the important geologic characteristics of mineral deposits that influence their environmental signatures, how climate and mining and mineral processing methods modify the environmental signatures mandated by deposit geology, and how climate and geology influence the effects of the deposits on the surrounding environment. In addition, the chapter will show how mineral deposit types with similar geologic characteristics have generally similar and predictable environmental signatures, and will discuss the development of empirical geoenvironmental models of various mineral deposit types.

Mineral deposits and mineral deposit types

"Mineral deposits" as considered here include metallic, or hard-rock, deposits (those in which metals such as Au, Ag, Cu, Pb, Zn, Ni, or Co are the dominant commodity), energy mineral deposits (including coal and uranium deposits), and industrial mineral deposits (those which contain mineral commodities such as sand, gravel, zeolites, phosphates, etc.).

"Mineral deposit types" are groups of mineral deposits having similar geologic characteristics, geologic environments of occurrence, and geologic processes of formation (Guilbert and Park, 1986; Cox and Singer, 1986; Bliss, 1992). Different categories of metallic mineral deposit types can be identified based on their mode of formation. Magmatic deposits are those that form directly from magmas, such as Ni-sulfide deposits hosted by layered mafic intrusions. Magmatic hydrothermal deposit types form from fluids expelled from crystallizing magmas, and include types such as porphyry, skarn, and polymetallic replacement deposits. Hydrothermal deposit types form from heated waters circulating in the Earth's crust; common hydrothermal types include volcanogenic massive sulfide, epithermal, polymetallic vein, and Carlin-type sediment-hosted Au deposits. Supergene deposits form from surface and ground waters that weather and redeposit metals from an existing mineral deposit. Residual deposits are formed by the natural weathering of rocks, which removes most of the rock constituents and results in the residual enrichment of economic constituents in the highly weathered rock remnants; these include deposit types such as bauxite Al and laterite Ni. Placer deposits form by sedimentary accumulation of dense minerals eroded from rocks or mineral deposits, and include placer Au and beach-sand Ti deposits.

Industrial mineral deposit types have a broad spectrum of origins, including: chemical (those that form by chemical precipitation from water, such as phosphate and evaporite deposits); sedimentary (those that form by sedimentary processes, such as sand and gravel deposits); metamorphic (those that form by metamorphic processes, such as some garnet deposits); weathering (those that form by weathering of existing rocks, such as some clay deposits); igneous (those that form by igneous processes, such as deposits of perlite in volcanic domes); and hydrothermal (those that form by hydrothermal processes, such as hydrothermal clay deposits).

This discussion will focus primarily on the environmental geology of metallic deposits, but will also include some discussion of the environmental geology of uranium and industrial mineral deposits.

Other sources of geologic information

As part of this discussion, only some of the basic terms and concepts of economic geology will be discussed; for further details the interested reader is referred to general economic geology textbooks such as Guilbert and Park (1986). Holland and Petersen (1995) present an overview of the geologic, economic, and environmental issues related to mineral-resource development. For detailed geologic discussions of particular mineral deposits, mining districts, or mineral deposit types, see general journals such as *Economic Geology* or *Mineralium Deposita*, papers by national geological surveys (for example, U.S. Geological Survey Professional Papers or Bulletins are available for a number of historic U.S. mining districts), and special publications by professional associations such as the Society of Economic Geologists or the Geological Association of Canada (e.g., Kirkham et al., 1993).

There are also a number of journals and volumes available with papers that discuss the environmental aspects of mining from a geologic standpoint, including the journals *Environmental Geology*, *Applied Geochemistry*, *Journal of Geochemical Exploration*, and *Environmental Geochemistry and Health*, and volumes such as Jambor and Blowes (1994), Kwong (1993), Alpers and Blowes (1994), Pasava et al. (1995), and Ripley et al. (1996). Conceptual models that describe the important geo-environmental characteristics of a number of mineral-deposit types are presented in du Bray (1995). Many of the papers included in this two-part volume also discuss environmental processes in a geologic context.

ENVIRONMENTAL GEOLOGY CHARACTERISTICS OF MINERAL DEPOSITS

In general, the geologic characteristics of mineral deposits that control their environmental signatures (their environmental-geology characteristics) influence either the chemical or physical response of the deposits to weathering and environmental processes (Table 3.1). Geologic features such as the acid-generating or acid-consuming minerals in the deposit, host rocks, and wallrock alteration are examples of characteristics that influence the chemical response of the deposits to weathering. Other characteristics such as mineral textures, the presence of faults or joints, and the porosity and hydraulic conductivity of the deposit and associated host rocks, ultimately control the access of weathering agents into the deposit and the speed with which the deposit is weathered and dispersed into the environment. Some geologic characteristics such as the mineralogy and trace element content of minerals can affect both the chemical and physical response of the deposit to weathering and environmental dispersion.

Primary mineralogy

Primary minerals are defined as those that form during the original formation of the deposit. The primary ore (economically valuable) and gangue (non-economic) minerals present in a mineral deposit play a key role in determining how readily the deposit's constituents are dispersed into the environment (Tables 3.2–3.5, Figs. 3.1–3.3).

TABLE 3.1—Geologic characteristics of mineral deposits that affect their environmental signatures.

Characteristic	Controls	Remarks
Iron sulfide content	Chemical	Oxidation generates acid; also supplies ferric iron, which is an aggressive oxidant.
Content of other sulfides	Chemical	Many (but not all) may generate acid during oxidation.
Content of carbonates, aluminosilicates and other nonsulfide minerals	Chemical	Many of these minerals can consume acid; iron and manganese carbonates may generate acid under some conditions.
Mineral resistance to weathering	Physical	Function of the mineral (different minerals weather at different rates) and the texture and trace-element content of the mineral.
Secondary mineralogy	Chemical and physical	Soluble secondary minerals can store acid and metals, to be released when the minerals dissolve. Insoluble secondary minerals can armor reactive minerals, thereby restricting access of weathering agents.
Extent of pre-mining or pre-erosion weathering and oxidation	Chemical	Pre-mining oxidation greatly reduces potential for sulfide deposits to generate acid.
Host rock lithology	Chemical and physical	May consume or generate acid. Physical characteristics (porosity, permeability) control access of weathering agents.
Wallrock alteration	Chemical and physical	May increase or decrease the host rock's ability to consume acid. May increase or decrease host rock's ability to transmit ground waters. May also increase or decrease resistance to erosion.
Major-, trace-elements in deposit and host rocks	Chemical	Elemental composition of deposit and host rocks are typically reflected in environmental signatures.
Physical nature of ore body (vein, disseminated, massive)	Physical	Controls access of weathering agents.
Porosity, hydraulic conductivity of host rocks	Physical	Control access of weathering agents.
Presence and openness of faults, joints	Physical	Control access of weathering agents.
Deposit grade, size	Physical and chemical	Controls magnitude of natural, mining impacts on surroundings.

TABLE 3.2—Examples of sulfide oxidation reactions and other mineral dissolution reactions that may generate acid. The reactions depicted are idealized, and likely do not represent the appropriate reaction products for the entire range of ambient chemical conditions in nature. However, they illustrate the range of acid amounts that can be generated (moles acid >0) or consumed (moles acid <0) depending on the mineral, the oxidant (oxygen versus ferric iron) and the reaction products (oxidation state, chemical species, and minerals) produced.

Mineral	Formula	Acid generation/consumption reaction	Moles acid
Pyrite	FeS ₂	FeS ₂ + 3.5 O ₂ + H ₂ O = Fe ²⁺ + 2 SO ₄ ⁼ + 2 H ⁺	2
		FeS ₂ + 3.75 O ₂ + 0.5 H ₂ O = Fe ³⁺ + H ⁺ + 2 SO ₄ ⁼	1
		FeS ₂ + 3.75 O ₂ + 3.5 H ₂ O = 2 SO ₄ ⁼ + 4 H ⁺ + Fe(OH) ₃ (s)	4
		FeS ₂ + 14 Fe ³⁺ + 8 H ₂ O = 15 Fe ²⁺ + 2 SO ₄ ⁼ + 16 H ⁺	16
Pyrrhotite	Fe _{1-x} S	x = 0.1: Fe _{0.9} S + 1.95 O ₂ + 0.1 H ₂ O = 0.9 Fe ²⁺ + SO ₄ ⁼ + 0.2 H ⁺	0.2
		x = 0.1: Fe _{0.9} S + 2.175 O ₂ + 0.7 H ⁺ = 0.9 Fe ³⁺ + SO ₄ ⁼ + 0.35 H ₂ O	-0.7
		x = 0.1: Fe _{0.9} S + 2.175 O ₂ + 2.35 H ₂ O = SO ₄ ⁼ + 2 H ⁺ + 0.9 Fe(OH) ₃ (s)	2
		x = 0.1: Fe _{0.9} S + 7.8 Fe ³⁺ + 4 H ₂ O = 8.7 Fe ²⁺ + SO ₄ ⁼ + 8 H ⁺	8
Sphalerite, Covellite, Galena	ZnS, CuS, PbS	MS + 2 O ₂ = M ²⁺ + SO ₄ ⁼ (M = Zn, Cu, Pb)	0
		MS + 8 Fe ³⁺ + 4 H ₂ O = M ²⁺ + 8 Fe ²⁺ + SO ₄ ⁼ + 8 H ⁺	8
Galena	PbS	PbS + 2 O ₂ = PbSO ₄ (anglesite)	0
		PbS + 0.5 O ₂ + 2 H ⁺ = Pb ²⁺ + H ₂ O + S ^o (native sulfur)	-2
Chalcopyrite	CuFeS ₂	CuFeS ₂ + 4 O ₂ = Cu ²⁺ + Fe ²⁺ + 2 SO ₄ ⁼	0
		CuFeS ₂ + 16 Fe ³⁺ + 8 H ₂ O = Cu ²⁺ + 17 Fe ²⁺ + 2 SO ₄ ⁼ + 16 H ⁺	16
Enargite	Cu ₃ AsS ₄	Cu ₃ AsS ₄ + 8.75 O ₂ + 2.5 H ₂ O = 3 Cu ²⁺ + HAsO ₄ ⁼ + 4 SO ₄ ⁼ + 4 H ⁺	4
		Cu ₃ AsS ₄ + 35 Fe ³⁺ + 20 H ₂ O = 3 Cu ²⁺ + 35 Fe ²⁺ + HAsO ₄ ⁼ + 4 SO ₄ ⁼ + 39 H ⁺	39
Arsenopyrite	FeAsS	FeAsS + 3.25 O ₂ + 1.5 H ₂ O = Fe ²⁺ + HAsO ₄ ⁼ + SO ₄ ⁼ + 2 H ⁺	2
		FeAsS + 3.5 O ₂ + H ₂ O = Fe ³⁺ + HAsO ₄ ⁼ + SO ₄ ⁼ + H ⁺	1
		FeAsS + 13 Fe ³⁺ + 8 H ₂ O = 14 Fe ²⁺ + HAsO ₄ ⁼ + SO ₄ ⁼ + 15 H ⁺	15
		FeAsS + 3.5 O ₂ + 3 H ₂ O = SO ₄ ⁼ + 2 H ⁺ + FeAsO ₄ •2H ₂ O (scorodite)	2
Native sulfur	S ^o	S ^o + H ₂ O + 1.5 O ₂ = 2 H ⁺ + SO ₄ ⁼	2
Realgar	AsS	AsS + 2.75 O ₂ + 2.5 H ₂ O = HAsO ₄ ⁼ + SO ₄ ⁼ + 4 H ⁺	4
		AsS + 11 Fe ³⁺ + 8 H ₂ O = 11 Fe ²⁺ + HAsO ₄ ⁼ + SO ₄ ⁼ + 15 H ⁺	15
Siderite	FeCO ₃	FeCO ₃ + H ⁺ = Fe ²⁺ + HCO ₃ ⁻	-1
		FeCO ₃ + 2 H ⁺ + 0.25 O ₂ = Fe ³⁺ + 0.5 H ₂ O + HCO ₃ ⁻	-2
		FeCO ₃ + 0.25 O ₂ + 2.5 H ₂ O = Fe(OH) ₃ + H ⁺ + HCO ₃ ⁻	1
Alunite	KAl ₃ (SO ₄) ₂ (OH) ₆	KAl ₃ (SO ₄) ₂ (OH) ₆ + 6 H ⁺ = K ⁺ + 3Al ³⁺ + 2 SO ₄ ⁼ + 6 H ₂ O	-6
		KAl ₃ (SO ₄) ₂ (OH) ₆ + 3 H ₂ O = K ⁺ + 3Al(OH) ₃ + 2 SO ₄ ⁼ + 3 H ⁺	3

Acid-generating minerals

Many metallic mineral deposits that form beneath the Earth's surface contain sulfide minerals, a consequence of their formation under relatively reduced conditions out of contact with atmospheric oxygen. Sulfide minerals that are exposed by erosion or mining are unstable in the presence of atmospheric oxygen or oxygenated ground waters. Bacterially catalyzed oxidation of sulfides by oxygenated ground and surface waters is well known as the cause of acid-rock drainage (Nordstrom and Alpers, 1999). However, the amount of acid generated (Tables 3.2 and 3.3) is a complex function of the sulfide minerals present in an ore body, their resistance to weathering (see discussion below and Table 3.4), whether the sulfides contain iron, whether oxidized or reduced metal species are produced by the oxidation, whether other elements such as arsenic are major constituents of the sulfides, whether oxygen or aqueous ferric iron is the oxidant, and

whether hydrous metal oxides or other minerals precipitate as a result of the oxidation process. Iron sulfides (pyrite, FeS₂; marcasite, FeS₂; pyrrhotite, Fe_{1-x}S), sulfides with metal/sulfur ratios <1, and sulfosalts such as enargite (Cu₃AsS₄), generate acid when they react with oxygen and water. Other sulfides with metal/sulfur ratios = 1, such as sphalerite (ZnS), galena (PbS), and chalcopyrite (CuFeS₂) tend not to produce acid when oxygen is the oxidant. However, aqueous ferric iron is a very aggressive oxidant that, when it reacts with sulfides, generates significantly greater quantities of acid than are generated by oxygen-driven oxidation alone (Nordstrom and Alpers, 1999; Tables 3.2, 3.3). Sulfide oxidation by ferric iron also occurs more rapidly than by oxygen alone (Nordstrom and Alpers, 1999). Thus, because of their role in producing aqueous ferric iron, the amounts of iron sulfides present in a mineral assemblage play a crucial role in determining whether acid will be generated during weathering. In general, sulfide-rich mineral assemblages with high percentages of iron sulfides or sul-

TABLE 3.3—Common sulfides known or inferred to generate acid when oxidized. Sulfides listed as inferred to generate acid are postulated on the basis of idealized chemical reactions such as those listed in Table 3.2.

Mineral	Formula
Common sulfides known (<i>inferred</i>) to generate acid with oxygen as the oxidant:	
Pyrite, marcasite	FeS ₂
Pyrrhotite	Fe _{1-x} S
Bornite	Cu ₅ FeS ₄
Arsenopyrite	FeAsS
Enargite/famatinite	Cu ₃ AsS ₄ /Cu ₃ SbS ₄
Tennantite/tetrahedrite	(Cu,Fe,Zn) ₁₂ As ₄ S ₁₃ / (Cu,Fe,Zn) ₁₂ Sb ₄ S ₁₃
Realgar	AsS
Orpiment	As ₂ S ₃
Stibnite	Sb ₂ S ₃
Common sulfides that may generate acid with ferric iron as the oxidant: All of the above, plus:	
Sphalerite	ZnS
Galena	PbS
Chalcopyrite	CuFeS ₂
Covellite	CuS
Cinnabar	HgS
Millerite	NiS
Pentlandite	(Fe,Ni) ₉ S ₈
Greenockite	CdS
Common minerals that may generate acid if hydrous oxides are formed:	
Siderite	FeCO ₃
Rhodochrosite	MnCO ₃
Alunite	KAl ₃ (SO ₄) ₂ (OH) ₆

TABLE 3.4—Factors affecting resistance of sulfide minerals to oxidation, listed in order of increasing resistance from top to bottom of table. The mineral resistance ranking by Brock (1979), is modified to include arsenopyrite (Jambor, 1994) and other sulfides based on the authors' field observations. This ranking is only one of a number of published rankings that are in general agreement, but differ in a variety of specifics. Grain size, texture, and trace element content can substantially shift the relative resistance of the different sulfide minerals; for example, trace element-rich botryoidal pyrite and marcasite generally oxidize much more rapidly than coarse, euhedral sphalerite.

Mineralogy (Brock, 1979; Jambor, 1994)	Grain size	Texture	Trace element content	Resistance to oxidation
Pyrrhotite	Fine	Framboidal	High	Low
Chalcocite		Colloform		
Galena				
Sphalerite		Botryoidal		
Arsenopyrite ¹				
Pyrite,	Medium			Medium
Enargite		Massive		
Marcasite				
Bornite ²				
Chalcopyrite				
Argentite ²				
Cinnabar				
Molybdenite	Coarse	Euhedral	Low	High

¹Based on the observations of Jambor (1994).

²Based on the author's observations.

TABLE 3.5—Relative reactivities of common rock-forming and deposit-forming minerals, listed in order of decreasing reactivity. Originally produced by Sverdrup (1990) for soils, and modified by Kwong (1993) and the author (author modifications shown in italics) to include more minerals based on observations of weathering rates observed in mineral deposits. Dissolving minerals are those whose components are taken completely into solution. Weathering minerals are those whose components are partially removed into solution and partially converted to other minerals. For mineral formulas, the reader is referred to standard mineralogic texts such as Deer et al. (1978). Calc-silicates common in skarn deposits (garnet, diopside, wollastonite) are included in the intermediate-weathering group rather than the fast weathering group (as originally classified by Kwong and Sverdrup); the low pH of mine waters that drain some skarn deposits where these minerals are abundant indicate that these minerals do not react readily with acid waters (see Plumlee et al., 1999).

Mineral Group	Typical minerals
Readily dissolving	cerussite, calcite, aragonite, <i>strontianite</i>
<i>Less readily dissolving</i>	<i>rhodochrosite, siderite, dolomite, ankerite, magnesite, brucite, fluorite (?)</i>
Fast weathering	anorthite, nepheline, olivine, jadeite, leucite, spodumene, <i>volcanic glass</i>
Intermediate-weathering	epidote, zoisite, enstatite, hypersthene, augite, hedenbergite, hornblende, glaucophane, tremolite, actinolite, anthophyllite, serpentine, chrysotile, talc, chlorite, biotite, <i>diopside (?)</i> , <i>wollastonite (?)</i> , <i>garnet (?)</i> , <i>rhodonite (?)</i> , <i>hematite (?)</i>
Slow weathering	albite, oligoclase, labradorite, vermiculite, montmorillonite, gibbsite, kaolinite, magnetite
Very slow weathering	potassium feldspar, muscovite
Inert	quartz, rutile, zircon

fides having iron as a constituent (such as chalcopyrite or iron-rich sphalerite) will generate significantly more acidic waters than sphalerite- and galena-rich assemblages without iron sulfides.

Precipitation of hydrous oxides during the sulfide oxidation process can also lead to the formation of acid (Table 3.2). In fact, some non-sulfide minerals such as siderite (FeCO₃) and alunite (KAl₃(SO₄)₂(OH)₆) can also generate acid during weathering if hydrous iron or aluminum oxides precipitate.

Acid-consuming minerals

In most mineral deposits, acid-generating sulfide minerals are either intergrown with or occur in close proximity to a variety of carbonate and aluminosilicate minerals that can react with and consume acid generated during sulfide oxidation. However, like the sulfides, the ease and rapidity with which these minerals can react with acid varies substantially (Table 3.5).

Alkaline earth carbonates such as calcite (CaCO₃), dolomite [(Ca, Mg)(CO₃)₂], and magnesite (MgCO₃) typically react with acid according to reactions such as:



As discussed previously, if hydrous iron or manganese oxides form as a result of the dissolution of their respective carbonates (siderite and rhodochrosite), then a net generation of acid results;

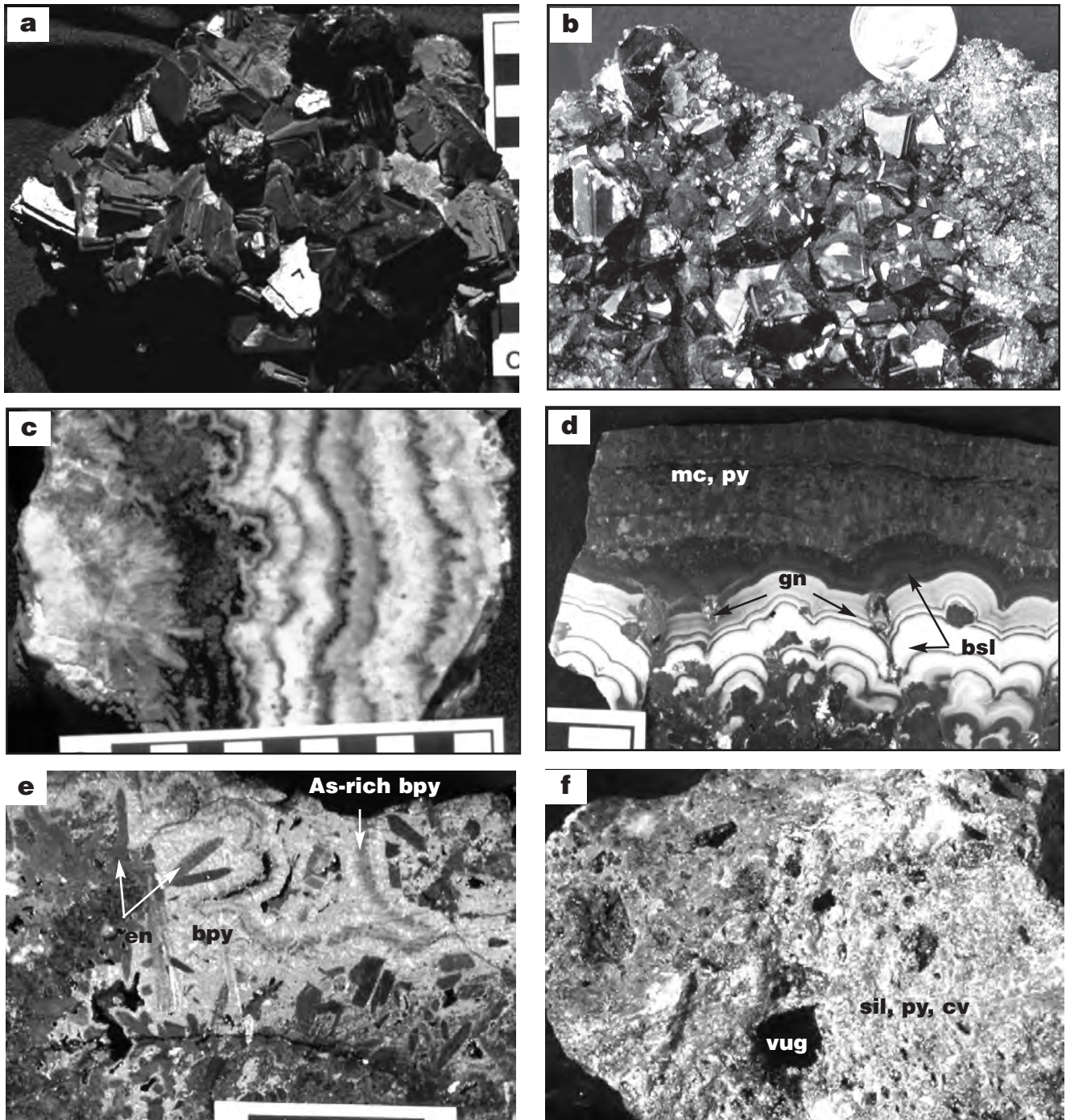


FIGURE 3.1—Examples of sulfide mineral assemblages found in a variety of mineral-deposit types, shown in general order of increasing reactivity and acid-generating potential. (a) Coarse-grained galena, Creede, Colorado. (b) Coarse-grained sphalerite, Creede, Colorado. Dime in upper right for scale. (c) Cut slab of fine-grained sphalerite and galena generations (dark) interbanded with fine- to coarse-grained barite (white). Such banding is termed crustification, and reflects the progressive growth (toward the right in the photo) of successive mineral bands on top of earlier-formed bands. (d) Cut slab of botryoidal marcasite and pyrite (mc, py) coating botryoidal sphalerite (alternating light and dark bands, labeled bsl) with intergrown galena (dark crystals cutting sphalerite bands, labeled gn). (e) Cut slab of arsenic-rich botryoidal pyrite (bpy) coating coarse-grained, euhedral laths of enargite (en), Cerro de Pasco, Peru. Scale bars are 1 cm long. (f) Vuggy silica alteration, Summitville, Colorado, with fine-grained silica (sil) replacing the original rock; pyrite (py) and covellite (cv) are disseminated in the silica. Vugs are left by the complete dissolution of a coarse-grained feldspar crystal from the original volcanic rock. Vug is approximately 1.5 cm wide.

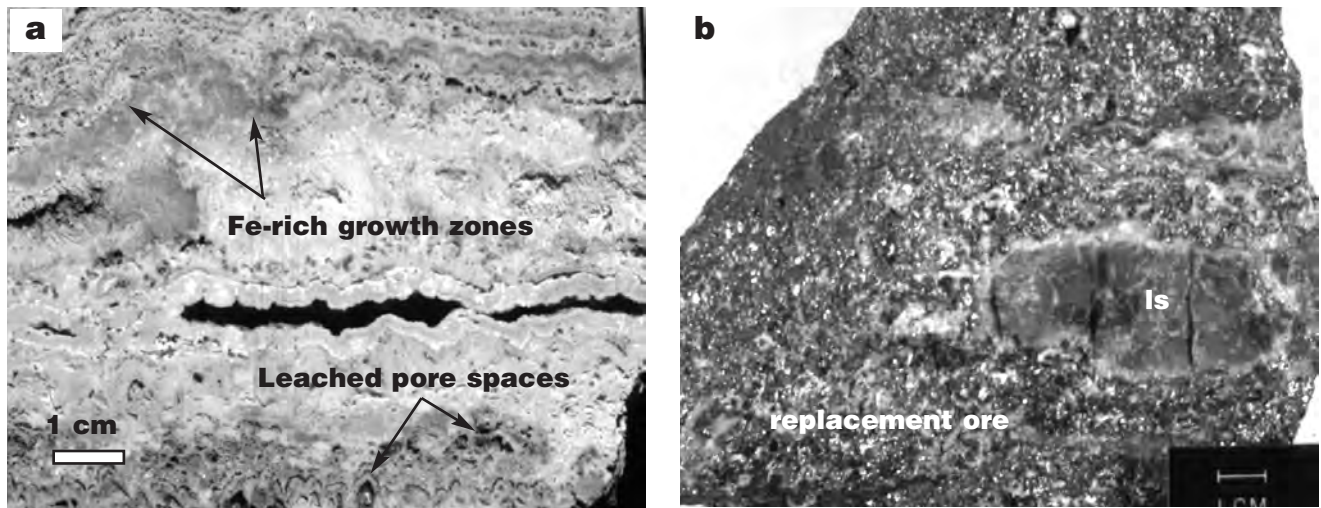


FIGURE 3.2—Examples of acid-consuming mineral assemblages. (a) Banded rhodochrosite, Creede, Colorado. Variations in color in part reflect variations in the Fe content of the rhodochrosite. The Fe preferentially oxidizes on the cut surface of the sample to form Fe-hydroxides. Some of the rhodochrosite growth zones were subsequently leached by hydrothermal fluids, which produced the many dark pores in the sample. The dark open space stretching horizontally across the middle of the sample is a fracture with sides coated by later rhodochrosite that did not completely fill the fracture. (b) Sphalerite-galena-pyrite-calcite-silica ore (labeled replacement ore) replacing limestone, from the polymetallic replacement deposits at Leadville, Colorado. Remnant limestone fragment labeled ls. Due to the high pyrite and sphalerite content, this assemblage would most likely generate near-neutral-pH drainage waters with elevated levels of zinc. Photograph by G. Landis.

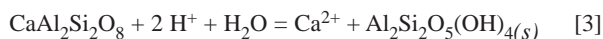
acid-base accounting schemes that simply total the amount of carbonate present in minerals can therefore underestimate the acid-generating potential of siderite- or rhodochrosite-bearing mine wastes or soils (see White et al., 1999).

A variety of metal carbonates, such as those of zinc (smithsonite), and copper (malachite and azurite) occur in the oxidized zones of sulfide mineral deposits in dry climates. These minerals are also effective acid consumers.

Aluminosilicate, calc-silicate, and some metal-silicate minerals are common components of many mineral deposits or their host rocks. Reactions of acid with aluminosilicate minerals are a well-known part of the rock weathering process (Stumm and Morgan, 1981). These acid-consuming reactions typically result in the release of some constituents into solution and the transformation of other constituents into more acid-stable and commonly less reactive (Table 3.5) minerals, such as is shown by the reaction below of potassium feldspar with acid to form aqueous potassium and silica and solid hydrous aluminum oxide,



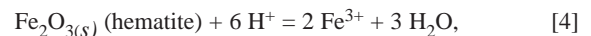
or the reaction of calcium-plagioclase to form kaolinite,



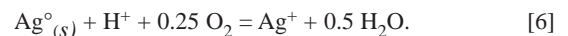
Calc-silicate minerals such as diopside, wollastonite, and garnets can similarly react to consume acid, as can rhodonite (MnSiO_3), a metal silicate common in some types of sulfide-bearing mineral deposits.

Iron-, manganese-, and aluminum- oxides and hydroxides, such as hematite, magnetite, pyrolusite, and gibbsite can theoretic-

cally react with acid, as indicated by the following reactions:



Native silver can also theoretically consume acid; however, it is a relatively stable and trace component of oxidized ore bodies, and so does not readily dissolve in oxygenated surface waters without the availability of complexing agents such as chloride:



Quartz, chalcedony, and other silica minerals, however, do not consume acid when they weather:



Fluorite (CaF_2), a common gangue mineral in a number of mineral deposits, is similarly not an effective acid-consumer:



Mineralogic controls on health effects

Environmental concerns about some industrial minerals stem from their direct effects on health. Mineralogy plays a well-

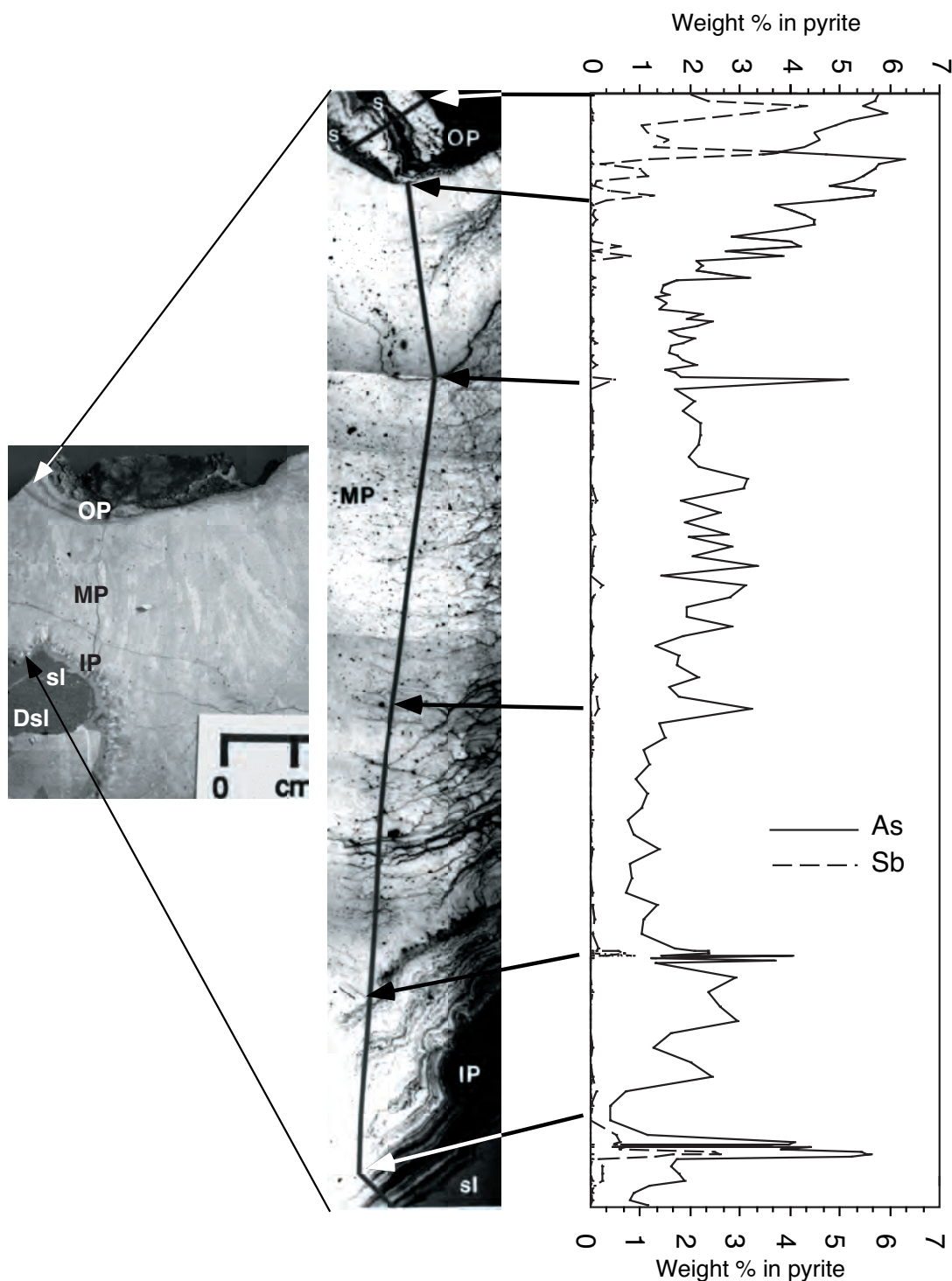


FIGURE 3.3—Relationship between etching rate and trace-element content in a botryoidal pyrite sample from Creede, Colorado. Left photo is photo of cut pyrite slab showing growth of botryoidal pyrite on top of coarse-grained sphalerite (sl, Dsl). Middle photo is composite reflected light photomicrograph across the pyrite stratigraphy. Darker growth zones are those that etched most rapidly when etched for 15 seconds with half-strength reagent-grade nitric acid. Right column shows variations of As, Sb, and Ag across the pyrite stratigraphy; note correlation between highly etched growth zones and elevated As and Sb contents. The etching of polished sulfide slabs with nitric acid and observing the rate of etching appears to be a reasonable proxy for understanding relative sulfide weathering and oxidation rates. Figure modified from Plumlee (1989).

known, important role in determining adverse health effects associated with ingestion or inhalation of asbestos minerals (see Ross, 1999). Chrysotile asbestos, the most common form of asbestos used in industrial applications in the United States, apparently has negligible effects on human cancer incidences. However, crocidolite and amosite asbestos varieties can clearly be linked to greatly increased human mortality rates from certain types of cancer. As another example, resistate minerals (those that are not readily soluble in ground and surface waters) occur in a variety of pegmatite, rare earth, or Ti-bearing beach sand deposits; some of these minerals can contain substantial amounts of radioactive uranium and thorium, which decay to release radon gas that can cause deleterious health effects.

Mineral resistance to weathering

The relative rates at which minerals weather have a major effect on the rates of acid production, acid consumption, and metal release from mineral deposits into the environment. The rates of weathering are a complex function of mineralogy, mineral textures, and trace element contents (Tables 3.4, 3.5).

Sulfide resistance to oxidation

Mineralogy: The relative weathering rates of various sulfide minerals have been evaluated through a variety of laboratory studies (summarized by Nordstrom and Alpers, 1999, and Jambor, 1994) and by field observations. Although the laboratory studies (i.e., Brock, 1979) are generally in overall agreement as to the sulfides which are most (cinnabar, molybdenite) and least (pyrrhotite, chalcocite) resistant to oxidation, they can vary substantially in detail as to whether a particular sulfide is more or less resistant than another sulfide (Jambor, 1994). It is possible that the disagreement between the laboratory studies is due to (at least in part) differences in grain size, texture, and trace element content of the sulfides examined, all of which can greatly influence resistance to oxidation (Table 3.4).

Grain size and textures: Due to greater surface area available for attack by weathering agents, fine-grained (< ~1 mm) sulfides tend to oxidize much more rapidly than their coarser equivalents. Sulfides with framboidal (agglomerations of many microscopic spherules) and colloform (intergrown, radiating crystal fibers) textures grew rapidly under highly supersaturated conditions; due to their very great surface area, they tend to be much less stable during weathering than sulfides having well-developed crystal faces (Figs. 3.1a, b). Using humidity cell tests of sulfide-bearing ores, White and Jeffers (1994) showed that framboidal pyrite weathers much more rapidly than fine-grained, euhedral pyrite, and so contributed to significant acid generation early in the tests; the euhedral pyrite, in contrast, weathered much more slowly, and so released low levels of acid throughout the tests. Botryoidal textures form when crystals grow outward simultaneously from a surface and coalesce; because their outer surfaces are euhedral crystal faces, their reactivity is less than colloform textures. Massive textures form when crystals grow together in a cavity and develop interlocking outer surfaces; due to the lack of pore spaces and crystal faces to weather, massive crystal growths that the author has observed tend to have moderate reactivities (Fig. 3.4).

Trace-element content: Trace elements present in a sulfide (either as impurities within the crystal structure or as minute

inclusions of other minerals) cause strain in the crystal structure, and therefore generally tend to diminish the sulfide's resistance to oxidation (Kwong, 1995; Jambor, 1994). Perhaps the best example of this is the occurrence of arsenic in pyrite, which greatly decreases oxidation resistance (Fig. 3.3). As shown on Figure 3.3, the rates at which botryoidal pyrite growth zones are etched by nitric acid (an effective proxy for natural oxidation) are clearly related to the arsenic and antimony content of the growth zones and the botryoidal crystal size (Plumlee, 1989); the higher the arsenic content, the more rapid the etching. A survey of arsenic-rich pyrite and marcasite from a variety of mineral deposits (Plumlee, 1989) indicates that pyrite and marcasite with greater than several weight percent arsenic (which imparts a distinctive bronze tint to the pyrite and marcasite) will weather rapidly even without liquid water, merely from the reactions of the mineral with water vapor in the air (Fig. 3.3); curated pyrite and marcasite samples with high arsenic contents were very easy to identify due to the acid-driven corrosion of their sample containers.

The role of other trace elements in sulfides other than pyrite is less well documented. Kwong (1993) has noted that Cu-bearing growth zones tended to increase pyrite oxidation rates in humidity cell tests of polished sections of sulfide ores, and that sphalerite containing microscopic inclusions of chalcopyrite weathered more rapidly than inclusion-free sphalerite. Jambor (1994) indicates that the presence of iron and other trace elements in sphalerite decreases its stability, and that the presence of Ag, Sb, and Bi in galena similarly decreases its resistance to oxidation.

Not all trace elements decrease a sulfide's resistance to oxidation, however. In his humidity cell study, Kwong (1993) noted that traces of Co and Ni in pyrite tended to increase its resistance to oxidation rather than decrease it. Kwong postulated that elements which substitute for an element to their left on the periodic table (such as Co for Fe), under semiconductor physics theory, should lead to positive effective charge and therefore suppress the electron transfer necessary for sulfide oxidation to occur.

Reactivity of sulfide assemblages: As noted by Kwong (1995), Sato (1992), and Nordstrom and Alpers (1999), sulfides in a mineral assemblage can weather preferentially due to galvanic reactions resulting from differences in their standard electrode reduction potentials. Minerals with low standard electrode reduction potentials (such as pyrrhotite, sphalerite, and galena) can preferentially oxidize when in electrochemical contact (i.e., via ion-bearing waters) with sulfides having higher standard electrode reduction potentials, such as argentite (Ag_2S), and pyrite; the pyrite and argentite are thus "protected" from oxidation by the pyrrhotite, sphalerite, and galena. As noted by other studies cited in Nordstrom and Alpers (1999), however, this galvanic effect is not always discernible.

The presence of readily-weathered sulfides in a mineral assemblage can also increase the reactivity of other, less readily weathered sulfides due to the formation of corrosive acids. For example, the author recently observed monomineralic bornite on one side of a mine drift that has remained unoxidized after 20 years of mining. On the other side of the mine drift, bornite intergrown with reactive marcasite has undergone extensive oxidation to secondary copper sulfate salts. The acid generated by marcasite oxidation has triggered the breakdown of the more resistive bornite. Similar effects were noted by Boyle (1994) in a weathering massive sulfide deposit, where the abundance of readily-weatherable pyrrhotite in the deposit could be directly correlated with the rate at which the intergrown sphalerite and pyrite oxidized.

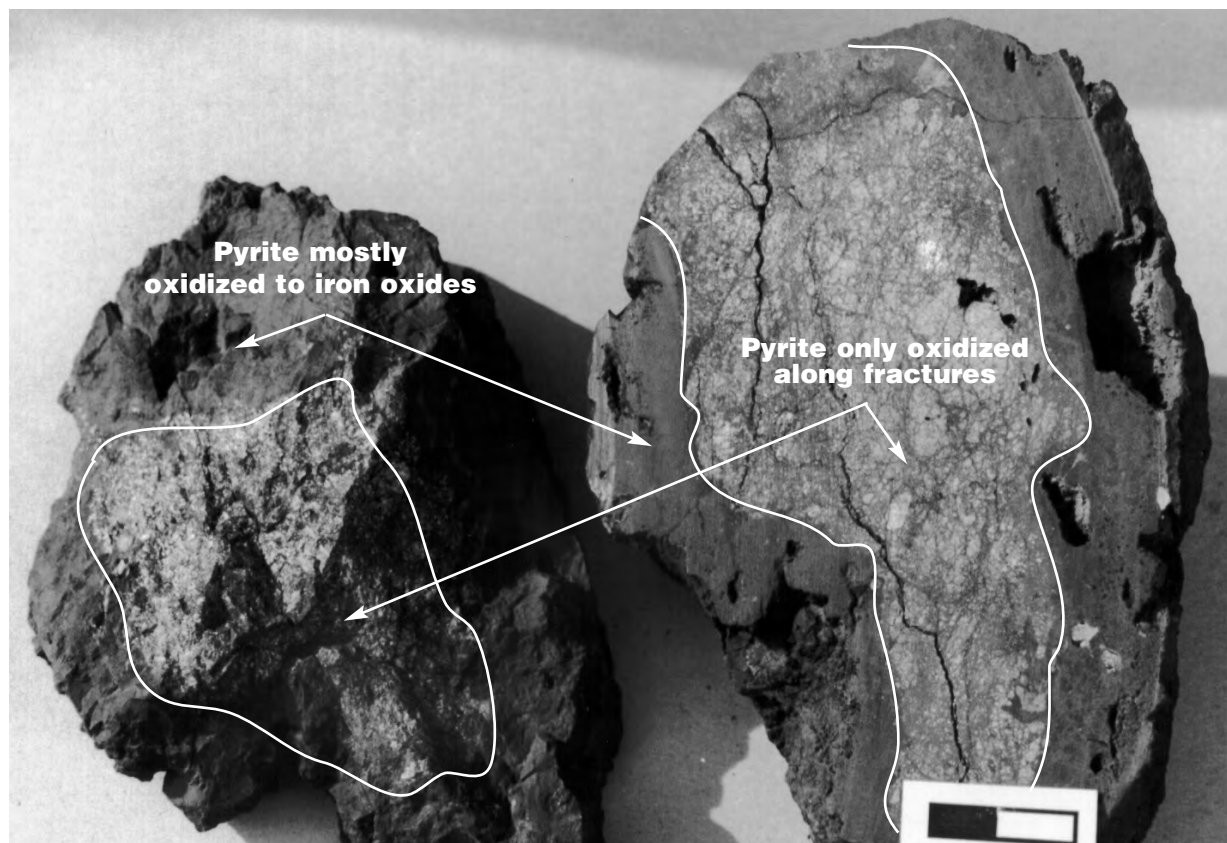


FIGURE 3.4—Massive pyrite sample from the polymetallic replacement deposits at Leadville, Colorado, showing the relative rates of pre-mining and post-mining oxidation. Pre-mining oxidation of the sample replaced the pyrite with iron-oxide minerals in a thick, dark rind around the edges of the samples and in veinlets crosscutting the unoxidized pyrite; this presumably occurred over the thousands of years since the last retreat of glaciers in the area some 10,000 years ago. The post-mining oxidation of the sample on the mine dump produced relatively little oxidation over the course of the ~100 years the sample was on the dump, as shown by the shiny pyrite faces on the uncut surface to the left.

Carbonate- and silicate-mineral resistance to weathering

As with the sulfides, the mineralogy, grain size, and textures of carbonates and silicates greatly influences their ability to react with acid generated during sulfide weathering. Sverdrup (1990) (as cited by Kwong, 1993) classified various rock-forming silicates, carbonates, and oxides according to their relative pH-dependent reactivities; a revised version of the classification provided by Kwong (1993) is shown in Table 3.5. Carbonate mineral reactivity generally decreases in the following sequence:

cerussite, aragonite, calcite > rhodochrosite >
siderite > magnesite, brucite

The presence of trace elements may increase or decrease carbonate resistance to weathering. For example, iron-rich growth zones in rhodochrosite can weather more rapidly than the surrounding Mn-rich growth zones, perhaps due to oxidation of the iron; this is illustrated by the development of iron oxide minerals on Fe-rich growth zones in sawed rhodochrosite slabs within a day or two of cutting (Fig. 3.2a).

Variable silicate resistance to weathering is well documented in the literature (for example, Goldich, 1938; Sverdrup, 1990; Kwong, 1993). Minerals that crystallize from magmas at high temperatures, such as olivine, pyroxene, and calcic plagioclase, tend to be more reactive than minerals that crystallize at lower temperatures such as alkali feldspars, biotite, muscovite, and quartz (see summary in Smith and Huyck, 1999). Clay minerals (such as montmorillonite and kaolinite) and zeolites have relatively low reactivity. Volcanic glass and devitrified volcanic glass (a mixture of very-fine-grained aluminosilicate and silica minerals) also can be quite reactive in the ground-water environment. As demonstrated by the high levels (as high as tens of thousands of mg/l or ppm) of aluminum found in acid rock drainage waters (Nordstrom and Alpers, 1999; Plumlee et al., 1999), aluminosilicate minerals do react with the acid generated by sulfide oxidation; however, the great abundances of the aluminosilicate minerals found in most mineral deposits or their host rocks means that the aluminum in the waters was derived from relatively limited acid consumption by the aluminosilicate weathering reactions.

The effects of grain size and texture on carbonate and silicate reactivities can be substantial. For example, mine waters draining pyrite-molybdenite ores and their host coarse-grained granites can

be quite acidic, due to the low reactivity of the coarse-grained feldspars; in contrast, very fine-grained potassium feldspars may consume acid to produce near-neutral mine waters draining Au-Te ores in alkalic volcanic rocks (Plumlee et al., 1999). Effects of climate on silicate weathering rates are discussed below in the section on climate.

Secondary mineralogy

Secondary minerals are those that form at or near the ground surface as mineral deposits are exposed by erosion or mining and weathered by ground waters, surface waters, and the atmosphere. Depending upon their compositions and solubilities, secondary minerals can be beneficial, by restricting access of weathering agents to sulfides, or detrimental, by storing acid and metals in a readily-released form. A detailed discussion is presented by Nordstrom and Alpers (1999) and Jambor (1994), so only a brief discussion is included here. Chemical formulas for minerals discussed here are given in the tables in Nordstrom and Alpers (1999).

Secondary minerals that form in the oxidized zone of weathering deposits

As a mineral deposit is exposed by erosion and weathered by surface waters descending through the unsaturated zone, a near-surface oxidized rind typically results. In this rind, the original constituents of the deposit and its host rocks are either removed in solution or converted to a wide variety of oxygen- and acid-stable minerals. As these minerals tend to be relatively insoluble in most ground and surface waters, they typically reduce the release of metals into the environment; as a result, completely oxidized sulfide orebodies tend to produce relatively non-acidic drainage waters with relatively low concentrations of heavy metals. The oxidized minerals can also form relatively impermeable coatings on remnant sulfides, thereby reducing the rates of sulfide oxidation and acid and metal generation where sulfides are still present in the rock (Nordstrom and Alpers, 1999).

Examples of minerals common in the secondary oxidized zone include: oxides and hydroxides of iron (goethite, lepidocrocite, hematite), aluminum (boehmite, gibbsite, diaspore), manganese (pyrolusite), copper (cuprite, tenorite); sulfates of calcium (gypsum) and lead (anglesite); hydroxysulfates of iron, aluminum, potassium, sodium, and lead (alunite, natroalunite, jarosite, natrojarosite, plumbojarosite); clays (kaolinite, halloysite, dickite); silicates of manganese (psilomelane), copper (chrysocolla), and zinc (hemimorphite); carbonates of copper (malachite and azurite), zinc (smithsonite), and lead (cerussite); phosphates (hinsdalite, turquoise); native metals (Ag, Cu, Au); molybdates (wulfenite); and halides of silver (chlorargyrite, bromyrite, embolite). Soluble sulfate salts of copper (such as chalcantite) and other metals also can form transiently during dry periods.

Lateritic or residual mineral deposits of Fe, Al, Mn, and Ni are formed as a result of weathering processes of rocks in humid, tropical to subtropical climates (Guilbert and Park, 1986). In general, these deposits result from the residual concentration of the Fe, Al, Mn, or Ni in intensely weathered rocks that were originally somewhat enriched in these constituents. Organic acids released from decaying vegetation play a substantial role in the

weathering process, but these deposits are not characterized by acid rock drainage caused by sulfide oxidation. Some transport of Ni in natural and mine-drainage waters does occur however, due to its relatively high mobility and lack of sorption onto particulates (W. Miller, oral commun., 1997; Smith, 1999).

Secondary minerals that form below the water table in weathering sulfide deposits

Some metals leached by waters in the unsaturated zone are re-deposited as sulfides under the reducing conditions present below the water table. This enrichment occurs via the replacement of existing sulfides, and is driven by the relative electrochemical properties of the sulfides (Guilbert and Park, 1986). Copper and silver are the metals most commonly enriched in the reduced supergene zone, and pyrite and the iron sulfides are the sulfides most commonly replaced. A suite of copper and copper-iron sulfides (including covellite, chalcocite, bornite, and djurleite) typically replace iron sulfides. Supergene acanthite (Ag_2S) typically replaces galena, pyrite, and sphalerite, and is itself commonly replaced by native silver.

The predominant environmental effects of the supergene sulfides result from the fact that the supergene process removes acid-generating iron sulfides from the deposit and replaces them with sulfides that commonly generate less acid. However, the supergene process typically does not lead to the complete removal of iron sulfides, and can lead to the precipitation of acid-generating supergene sulfides such as bornite; hence, the potential beneficial effects of supergene enrichment on acid-generating potential are rarely completely realized.

Soluble secondary salts

A complex array of soluble sulfates, hydrous sulfates, and some hydroxysulfates are a common result of sulfide oxidation in the surficial environment (Nordstrom and Alpers, 1999; Jambor, 1994). These soluble salts are of environmental concern because they store acid and metals in the solid phase. During periods of rainfall or snowmelt, their dissolution can result in potentially detrimental flushes of acid and metals into ground and surface waters. For example, seasonal flushing of soluble salts from tailings deposits along the Clark Fork River in Montana has been documented as the cause for seasonal fish kills along the river (see references in Nimick and Moore, 1994). These salts can also be a significant source of dissolved ferric iron which, when released, can trigger further sulfide oxidation.

Sulfates and hydrated sulfates of the major elements calcium (gypsum) and magnesium (epsomite, pickeringite), and the major metals iron and aluminum (melantherite, copiapite, coquimbite, rhomboclase, halotrichite, alunogen, and many others) are generally most abundant, due to the common occurrence of the iron sulfides in many mineral deposits and the abundance of Ca, Mg, and Al in deposit host rocks. Although considered to be relatively insoluble in the secondary oxidized zone of weathering mineral deposits (Nordstrom and Alpers, 1999), jarosite (an Fe-K-Na- H^+ hydroxysulfate) is a common salt in many mine waste materials that readily release acid and metals during rain storms or laboratory leach tests (for example, Plumlee et al., 1995a and b). The abundance of hydrated sulfates of heavy metals such as copper (chal-

canthite, brochantite), zinc (gummingite, zincosite), and nickel (morenosite) varies depending upon the abundance of these metals in the primary sulfides present. As shown by Alpers et al. (1994a and b), these heavy metals can also occur in significant concentrations as impurities within iron- and aluminum-sulfates and jarosite.

Soluble secondary salts are best known to form from the evaporation of acid-drainage waters (Nordstrom and Alpers, 1999). For example, efflorescent crusts are common on the surfaces of mine dumps and on the edges of natural- and mine-drainage streams and puddles. The mineralogy of the product salts can change with progressive evaporation, such as has been observed for hydrous iron sulfates (Nordstrom and Alpers, 1999). In general, the greatest salt growth occurs when the growing crusts are replenished by acid water, such as a flowing drainage stream or waters wicked to the surface of a mine waste dump by capillary action.

The soluble secondary salts can also form as weathering products of sulfides that are not in direct contact with liquid water, but that are in contact with atmospheric moisture; such occurrences are well documented in experimental weathering studies (Borek, 1994; White and Jeffers, 1994) and through field observations. For example, extensive growths of secondary iron and copper salts occur on the ribs of mine workings where there is no source of flowing water to evaporate. As another example, complex intergrowths of secondary salts formed on samples of arsenic-rich botryoidal pyrite from Creede, Colorado while the samples were stored in drawers; the only source of the moisture could have been humidity in the air.

Due to their high solubilities, secondary salts most commonly form where sulfides have been exposed directly to weathering by oxygenated waters. Mine waste piles, mine workings, and mill tailings piles are therefore common hosts for these minerals. However, they can also occur naturally where sulfide mineralization has been exposed at the ground surface by rapid mechanical erosion or glaciation. For example, largely unmined porphyry Cu-Mo systems occur in the Alamosa River basin south and east of Summitville, Colorado. Due to the extreme topographic relief and the highly altered rocks in these areas, physical erosion rates greatly exceed chemical weathering rates, thereby exposing unoxidized sulfides at the ground surface (Figs. 3.5d-f). A water quality study along the Alamosa River (Ortiz et al., 1995) showed that a single rainstorm which affected one of these mineralized areas lead to a transient pulse of acid and metals into the river; the most likely source of this pulse was the dissolution of soluble salts from the sulfide-rich rock material exposed in the mineralized area.

Secondary ferricrete deposits

As Fe-bearing ground waters flow onto the ground surface or mix with surface or near-surface waters, oxidation of the Fe results in the precipitation of Fe hydroxides and hydroxysulfates (Nordstrom and Alpers, 1999; Smith, 1999). In cases where supersaturation is extreme and precipitation is rapid (such as during dilution of acid waters by surface waters, or oxygenation of near-neutral pH waters), suspended particulates are produced (Nordstrom and Alpers, 1999; Smith, 1999). These suspended particulates settle out from surface waters in areas of low flow velocity, but can be easily resuspended and transported downstream in periods of high flow.

In contrast, in environments where supersaturation is less

extreme (such as where acid waters flow onto the ground surface and are oxidized), Fe hydroxides precipitate directly on pre-existing surfaces as ferricrete deposits. Ferricrete can occur as a cement around rock fragments in stream channel deposits or talus breccias (Figs. 3.5f, h), or as so-called ferrosinter terraces (Kirkham et al., 1995) on the ground surface (Fig. 3.5g). In most cases, ferricrete and ferrosinter deposits form at or near breaks in topographic slope, where the ground-water table intersects the ground surface or mixes with shallow ground water recharged from streams of different chemical composition. These deposits are typically quite resistant to erosion and form prominent ledges or ridges (Fig. 3.5h). These deposits also have generally low hydraulic conductivities (Fig. 3.5f), and can thus serve as confining beds that restrict the flow of ground water. Paleo-ferricrete deposits are very common around many sulfide-bearing mineral deposits, and are good indicators of naturally degraded ground-water quality for hundreds or thousands of years prior to mining (Furniss and Hinman, 1998).

Extent of sulfide oxidation prior to mining

As indicated in the previous section, pre-mining sulfide oxidation can substantially reduce the potential for a sulfide-bearing mineral deposit to generate acidic, metal-rich mine-drainage waters. The extent of pre-mining oxidation is typically a function of the deposit geology, topography, and climate (discussed subsequently). Oxidation is most extensive in deposits (a) with geologic characteristics that allow easy access to descending oxygenated ground waters (discussed below), (b) that occur in areas of high topographic relief (where the water table tends to be relatively deep), and (c) that occur in dry climates where the water table is deep. Prior to mining, the extent of oxidation should be carefully mapped in an originally sulfide-rich deposit; more than one mine that was planned on the assumption that the sulfides were completely oxidized has turned out to produce pockets of acid-generating, sulfide-bearing ores or wastes that substantially increased the need for and costs of acid-drainage mitigation, and may have affected metal recovery as well.

Host rock lithology

The same mineralogic, textural, and compositional characteristics that influence the environmental geochemistry of a mineral deposit also apply to the minerals making up the rocks that host the mineral deposit (Tables 3.1, 3.5).

Chemical characteristics of host rocks

Host rocks with moderate to high contents of carbonate minerals (for example, limestone, dolomite, marble, carbonate-cemented sandstone, and shale) or contents of reactive aluminosilicate minerals (for example, poorly welded volcanic tuff or ultramafic rocks such as dunite and gabbro) have moderate to very high acid-neutralizing capacity, and so can react directly with acid generated by oxidation of sulfides in the mineral deposit. In addition, ground waters draining these rock types typically have high alkalinities; mixing with and dilution of acid-rock drainage by waters draining these rock types can thus help neutralize the acid and

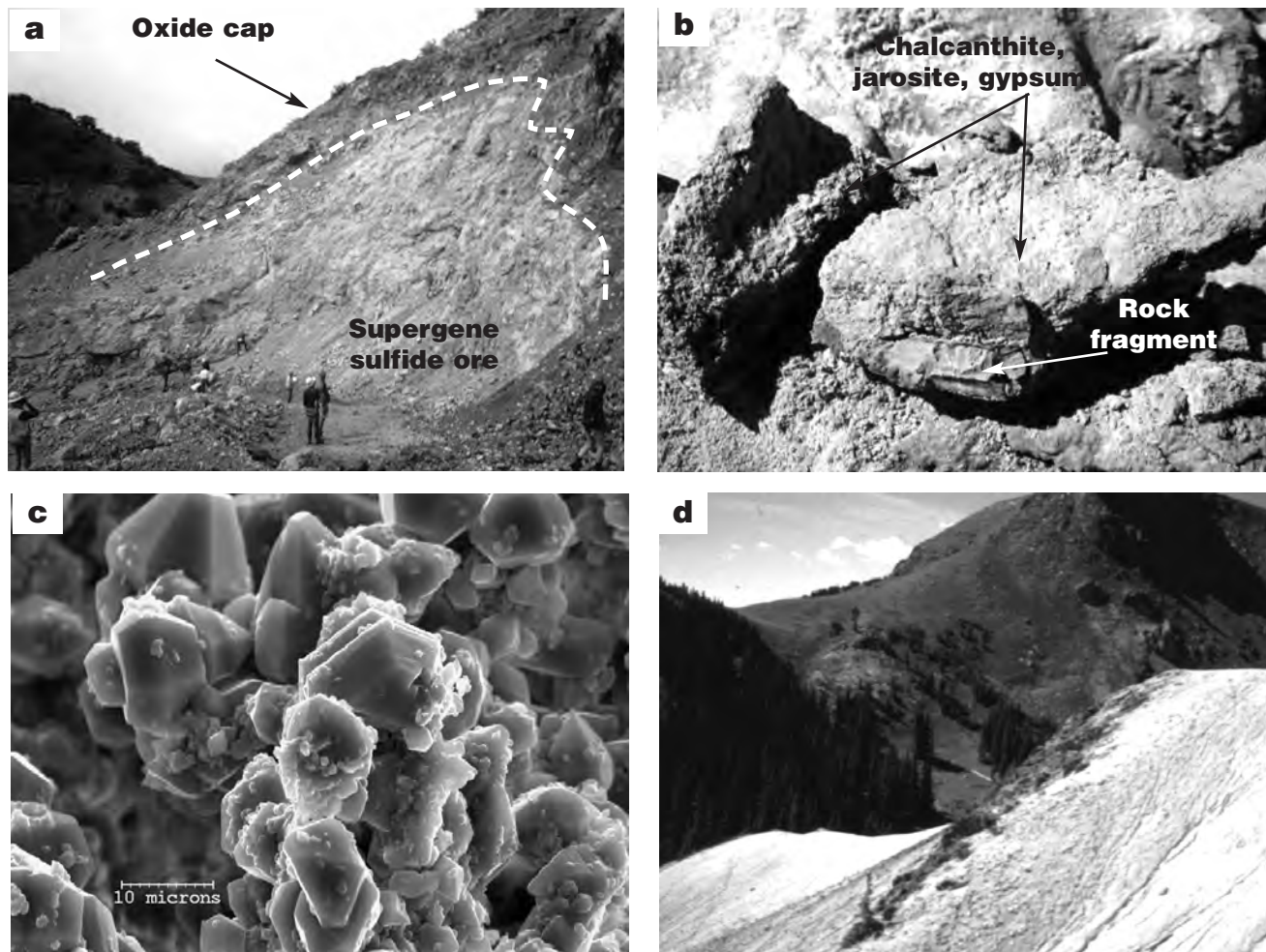


FIGURE 3.5—Examples of weathered mineral deposits. (a) Photographic cross section showing the oxide cap (dark rocks) and supergene sulfide zone (light rocks) of a porphyry-Cu deposit, Bisbee, Arizona. The oxide cap is composed primarily of relatively insoluble secondary oxides of Fe and some oxides and carbonates of Cu. The underlying supergene sulfide zone is characterized by supergene chalcocite replacement of primary pyrite and chalcocopyrite stockwork veins and disseminations in altered host rock. After exposure by mining, the sulfides are now weathering to soluble blue Cu sulfates and yellow-orange Fe-sulfates and jarosite. Photo by C. Taylor, USGS. (b) Concrete-like mixtures of chalcanthite, jarosite, and gypsum that form 3–5 cm-thick encrustations in a Cu-sulfide-rich tailings pile, 3-R Mine, Patagonia Mountains, Arizona. The crusts form by the progressive evaporation of acid waters during dry periods. When placed in deionized water, these coatings dissolve nearly completely within an hour, and form a solution with $\text{pH} < 3$ and a blue tint indicative of many hundreds of parts per million dissolved Cu. (c) Scanning electron microscope (SEM) image of copiapite growing on arsenic-rich botryoidal pyrite from Creede, Colorado. All of the growth occurred on a cut slab of the pyrite while the slab was stored in a sample drawer. The growth demonstrates the ease with which reactive sulfides can oxidize simply by reacting with moisture in the air. (d) Argillically-altered rocks (light color in foreground) that formed in the middle to upper levels of a low-grade porphyry Cu-Mo system, Alamosa River stock, south of Summitville, Colorado. The altered rocks erode much more rapidly than the unaltered volcanic rocks in the background; the light color reflects a several centimeter-thick oxidized rind of weathered clays and soluble secondary salts coating unoxidized sulfide-bearing rock.

cause some metals to sorb from solution onto particulates (Smith, 1999; Smith et al., 1994).

Rock types that generally afford little or no acid-neutralizing capacity include coarse-grained, silica-rich intrusive rocks (such as granites or granodiorites), silica-rich sedimentary rocks (such as quartz-rich, silica-cemented sandstones, and arkoses), and carbonate-poor metamorphic rocks (such as quartzites).

Rocks can themselves be enriched in a variety of trace metals (Thornton, 1995; Rose et al., 1979); however, the ease with which these elements are released into the environment from the rocks during weathering (termed their *geoavailability*; Smith and

Huyck, 1999) varies substantially among rock types. Some rock types, such as black shales, sulfidic schists, layered ultramafic intrusive rocks, sedimentary rocks mineralized by migrating basinal brines, and coal beds, contain abundant sulfide minerals as primary constituents. These rock types often have elevated concentrations of trace metals (such as As, Ni, Co, Cu, Zn, Se, etc.) that occur at least in part within sulfides. In many cases, these rocks were mineralized by the same processes that form mineral deposits, but that did not concentrate the metals sufficiently to form a deposit. Depending upon their acid-neutralizing capacity, these rocks, upon weathering, can generate acidic, metalliferous

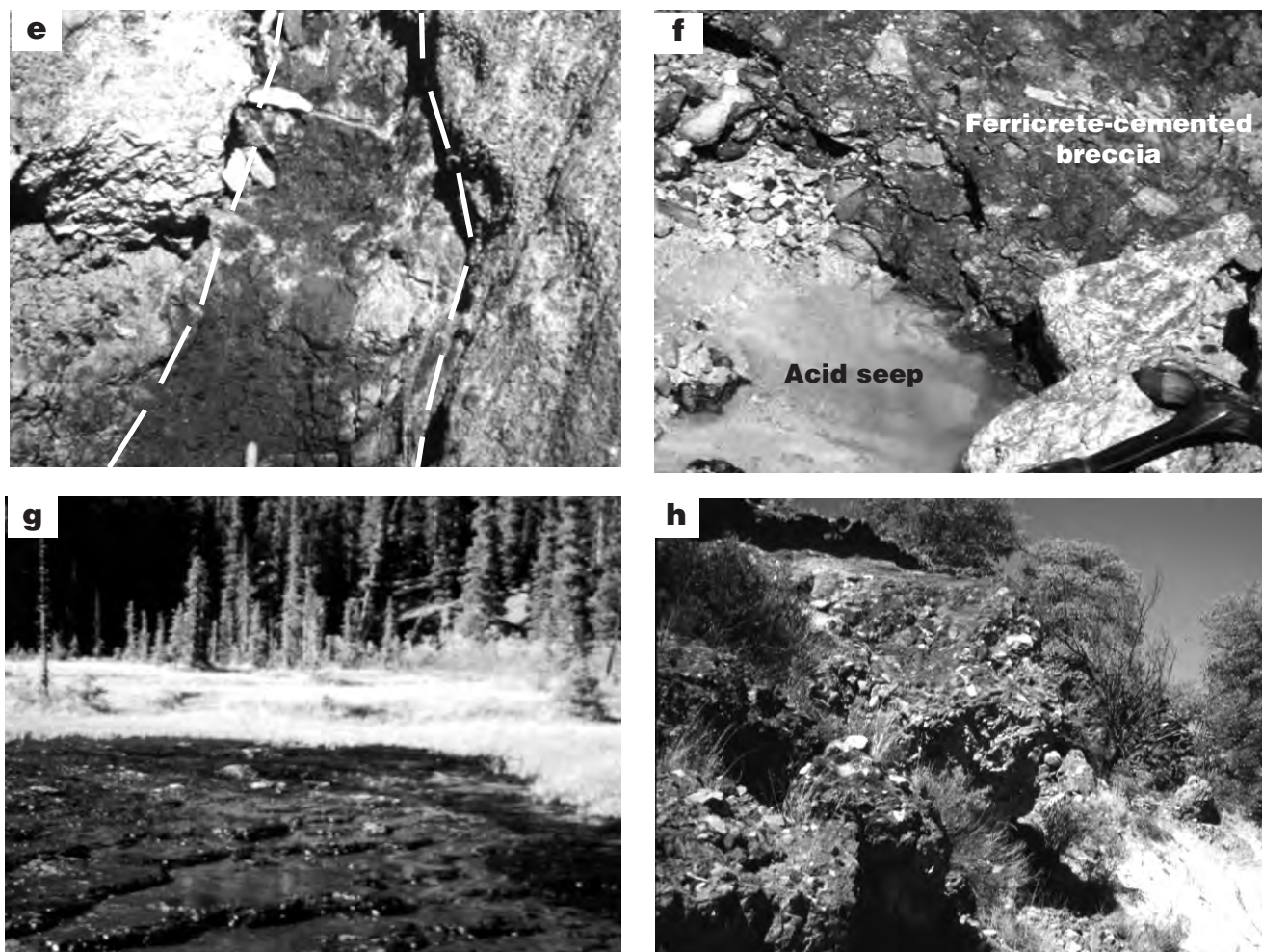


FIGURE 3.5 (Continued)—(e) Fresh sulfides exposed in a rivulet cutting through the weathered rock shown in (d). (f) Ferricrete-cemented breccia that occurs at the base of the altered rock slope shown in (d). The ferricrete has been deposited by acid spring waters since the last period of glaciation some 10–12 thousand years ago. Acid waters still seep from beneath the ferricrete, which serves as an impermeable confining bed. (g) Modern ferrosinter terraces (dark, foreground) being deposited by acid spring waters draining the Alamosa River stock. (h) Ferricrete-cemented breccias (left side of photo) formed in a stream channel on the flanks of a low-grade porphyry-Cu deposit, Patagonia Mountains, Arizona, during a past wet period. The highly cemented ferricrete erodes very slowly and now holds up ridges.

waters or less acidic waters with elevated concentrations of metals such as Zn, Se, U, or Ni that are mobile in near-neutral waters. In addition to their limited potential to help chemically mitigate drainage problems from nearby mineral deposits, these rocks can themselves generate a variety of environmental concerns. For example, locally pyrite-rich schists form the mountainous backbone of the Great Smoky Mountains. Exposure of these sulfide-rich rocks by past road building has enhanced natural acid-rock drainage from the schists. As another example, Se-rich black shales in the western foothills of the San Joaquin Valley of California were determined to be the source of Se that was concentrated by agricultural irrigation in the valley, and led to toxic effects on local waterfowl and aquatic life (Deverel and Fujii, 1988; Tidball et al., 1991). Phosphoria Formation phosphate deposits in the northern Rocky Mountains are phosphate-rich, sul-

fidic black shales that have similarly elevated levels of trace elements such as Se, U, and Ni.

In many rock types, metals occur as trace constituents within the rock-forming minerals, and so their geoavailability depends on the ease with which their host minerals weather. Some rocks such as pegmatites and silica-rich granites have high concentrations of elements such as U, Th, and rare-earth elements (REE). However, in these rock types, these elements typically occur in minerals that are highly resistant to weathering, such as tantalite, zircon, columbite, and monazite. As a result, their geoavailability and environmental mobility is generally quite low. The most significant environmental concern from these rock types is radioactive daughter products, such as radon, that are produced by the radioactive decay of the U and Th (see Landa, 1999, for a discussion of radioactive decay and its environmental effects). As another

er example, many granites also have elevated levels of Pb that occurs as a trace element within feldspars; in general, such feldspar-bound Pb is of relatively low geoavailability in most climates.

Physical characteristics of deposit host rocks

The environmentally important physical characteristics of deposit host rocks are those that control ground-water flow to the deposits (Fig. 3.6, Table 3.6) and those that affect the physical susceptibility of the rocks to mass wasting such as slumps and landslides.

Rock characteristics that control ground-water flow: The ability of a rock to transmit ground water is termed its hydraulic conductivity, and is a function of its porosity (the size and number of pore spaces) and permeability (the connectedness of the pore spaces). The porosity and permeability of rock can either be primary (provided by features such as pore spaces within the rocks), or secondary (provided by fractures, joints, etc., that cut the rocks). For a detailed discussion of the porosity and permeability of various rock types, the reader is referred to texts on hydrology such as Domenico and Schwartz (1990), and Freeze and Cherry (1979).

Published hydraulic conductivity values for given rock types can vary over many orders of magnitude (Fig. 3.6), but some generalizations can be made for different rock types. Carbonate rocks such as limestones tend to have low to moderate primary porosity and permeability. However, both limestones and dolomites can have high hydraulic conductivities if they are extensively fractured or have well-developed karst features. Dolomites may have greater fracture densities than limestones because they are more brittle. Karst features are secondary voids formed by the dissolution of carbonate rocks by ground waters flowing along fractures and joints. Karst features can be very large, spatially extensive, and highly irregular in shape and distribution; they can therefore be of potentially great environmental concern due to their ability to transmit ground waters to and from mineral deposits in great volumes and over great distances.

Clastic sedimentary rocks such as sandstone, conglomerate, and breccia have primary porosity and permeability that is a function of the size and interconnection of the pore spaces between their grains. The greatest porosities and permeabilities occur in rocks such as gravels that have the coarsest grain size, greatest sorting (i.e., smallest range in size of the grains), and lowest interstitial cement content.

Due to their clay contents, shales typically do not tend to transmit ground waters. Instead they serve as confining beds that restrict ground-water flow between aquifers. Faults and fractures also tend to be poorly developed in shales, and so do not transmit ground water across shale beds.

In most igneous and metamorphic rocks, ground-water flow occurs along fractures and joints within the rocks. In volcanic flows, brecciated flow tops and bottoms can serve as important sources of primary porosity and permeability, as can lava tubes. Vesicular basalts can also be quite conductive hydrologically (Fig. 3.6).

Rock characteristics that control physical erosion and mass wasting: Processes that lead to gravitational collapse of deposit host rocks can be of environmental concern because the collapses can expose large volumes of potentially mineralized rocks to weathering. In general, rocks with high clay contents are more susceptible to gravitationally driven collapse than those with low clay contents. For example, shales are well known for their susceptibility to landslides and debris flows. Further, recent studies of continental shales in the Colorado Plateau (host rocks to sandstone uranium and copper deposits) have shown that the types of clay minerals present also influence susceptibility to mass wasting; shales with high contents of kaolinite and illite are more prone to landslide generation than those with high smectite contents (Griffiths et al., 1996).

Rocks that have planar geologic structures (such as bedding, lava-flow surfaces, parallel joints, etc.) along which rock failure can occur may be prone to gravitational collapse. For example, the sulfidic schists noted previously in the Great Smoky Mountains National Park are prone to failure where the schistosity surfaces are steeply dipping. During periods of heavy rains, water seeping in along the schistosity surfaces lowers the coefficient of friction sufficiently to enable rock collapse and the formation of debris flows. The debris flows expose fresh sulfides in the schists to weathering and oxidation; the acid and metals released by the sulfide oxidation are toxic to fish and other aquatic organisms in the streams downgradient from the debris flows; the affected populations may require several years to recover.

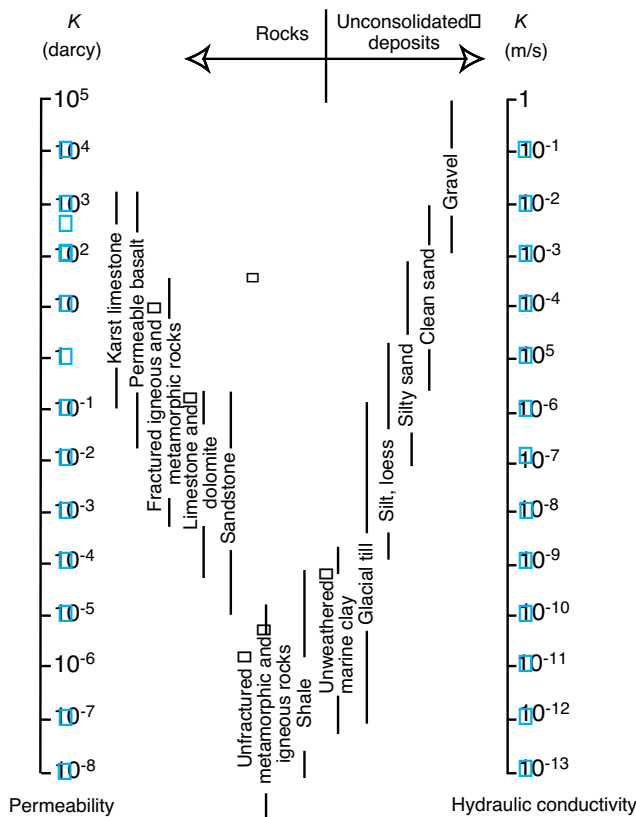


FIGURE 3.6—Hydraulic conductivities of various rock types. Modified from Freeze and Cherry (1979), and Cathles (1997).

TABLE 3.6—Environmental geology characteristics of rock types that commonly host mineral deposits. Acid buffering potential (N.P.) is a combination of the acid-neutralizing capacity of the rock-forming minerals, coupled with their reactivity (modified from Glass et al., 1982). Acid-generating potential (A.P.) is a combination of the sulfide content and reactivities. Rocks with high N.P. and A.P. may generate near-neutral, metal-rich waters. Trace elements from Thornton (1995), Guilbert and Park (1986), and other sources. Physical characteristics from Freeze and Cherry (1979), Domenico and Schwartz (1990).

Rock type	Acid-neutralizing generating potential	Trace elements (geoavailable)	Physical characteristics controlling ground-water flow
Sedimentary			
Limestone	High N.P.	(±F, Mn, Zn), Pb	Karst, fractures, joints
Dolomite	Mod-high N.P.	(± F, Mn, Zn), Pb	Karst, fractures, joints
Calcareous sandstone	Mod N.P.		Moderate intergranular, if little cement; otherwise fractures, joints
Black shales	Low-mod N.P.; low-mod A.P.	(U, Se, S, Ni, Te, Co, Mo, Zn, Cu) ¹ , P	Generally low permeability
Redbed shales	Mod N.P.	(U, V, Ni, Co, Cu, Se, Te, Mo) ²	Generally low permeability
Arkose	Low N.P.	(Cu) ¹	Moderate-high intergranular
Chert	Low N.P.		Fractures
Quartzose sandstone	Low N.P.		Low-moderate intergranular, if little cement; otherwise fractures, joints
Igneous intrusive			
Carbonatite	High N.P.; mod A.P. in sulfide-rich rocks	(Cu, Zn, Pb, S) ¹ , REE, Nb, Ta, Zr, Hf, U, Th, P, Ba	Fractures, joints
Ultramafic (dunite, norite, etc.)	Mod-high N.P.; mod A.P.	Cr, (Co, Ni, S) ¹	Fractures, joints
Granite	Low N.P.	Ba, Li, W, Mo, Sn, Zr, U, Hf, Th, Ti, F	Fractures, joints
Volcanic			
Komatiite	Mod-high N.P.; some A.P.	(Ni, Co, Cu, S) ¹	Fractures, joints
Basalt	Low-mod N.P.	Cu, Zn	Fractures, joints, interconnected vesicles, flow tops and bottoms
Andesites	Low-mod N.P.	Cu, Zn	Fractures, joints, brecciated flow tops
Poorly welded, volcanic tuffs	Mod-high N.P.	(As, Li, Zn, Cu, B) ³	Low fracture permeability
Highly welded volcanic tuffs	Low-mod N.P.	As, Li, Zn, Cu, Pb	Fractures, cooling joints
Rhyolite flows	Low-mod N.P.	As, Li, Zn, Cu, Pb	Fractures, cooling joints
Metamorphic			
Marble	High N.P.		Fractures, joints
Gneiss	Low N.P.	Ba, Li, W, Mo, Sn, Zr, U, Hf, Th, Ti	Fractures, joints, foliation, remnant bedding
Quartzite	Very low N.P.		Fractures, joints
Sulfidic schists	Low N.P., high A.P.	As, Zn, Co, Ni, Cu, U, Mo, Se	Fractures, joints, foliation, schistosity, remnant bedding

¹Geoavailable if in sulfides.

²Trace elements are typically concentrated at interface between oxidized and reduced ground waters, and are otherwise dispersed elsewhere in the rocks in relatively low concentrations.

³These and other trace elements, while not particularly high in concentration, can be relatively geoavailable in fresh volcanic glasses.

Wallrock alteration

Wallrock alteration, a common feature of many hydrothermal mineral deposits, results from the chemical and thermal interaction of hydrothermal fluids or magmas that form the deposits with surrounding wallrock. A number of wallrock alteration types with characteristic mineralogies are recognized in a number of different hydrothermal deposit types (Table 3.7). Wallrock alteration has important environmental consequences because it can affect both the chemical and physical properties of the surrounding rocks.

Chemical effects of wallrock alteration

Wallrock alteration can either increase or decrease the acid-generating capacity and (or acid-neutralizing capacity of a deposit's host rocks. Alteration types that increase the acid-generating capacity (by increasing the content of acid-generating sulfides in the rocks) and (or decrease the acid-neutralizing capacity (by removing minerals that react with acid) of a deposit's host rocks include acid-sulfate (also called advanced argillic), argillic, phyllic (quartz-sericite pyrite), coarse-grained potassic, skarn, and jasperoid. Alteration types that increase the acid neutralizing capacity of host rocks include propylitic, carbonate, and fine-grained potassic.

TABLE 3.7—The environmental characteristics of various wallrock alteration types common to hydrothermal mineral deposits. See discussion in Guilbert and Park (1986) for discussion of alteration origins.

Alteration type	Alteration products	Chemical effects	Physical effects
Acid-sulfate (advanced argillic)	Vuggy silica (+pyrite), quartz-alunite, kaolinite, \pm pyrophyllite, dickite	Greatly decreases acid-buffering capacity of host rocks, and increases acid-generating capacity	Vuggy silica zones highly permeable. Surrounding clay alteration zones impermeable
Argillic	Kaolinite, illite, montmorillonite, \pm pyrite, \pm chlorite	Decreases acid-buffering capacity	Substantially decreases rock and fracture permeability
Phyllic	Quartz, sericite, pyrite	Increases acid-generating capacity	Slightly decreases rock and fracture permeability
Potassic	Potassium feldspar, biotite, anhydrite	Coarse grain size of feldspars decreases rock reactivity	Shifts permeability to fracture permeability
Propylitic	Epidote, chlorite, calcite, albite, \pm pyrite	Increases acid-buffering capacity of rock	Chlorite-rich alteration somewhat decreases fracture permeability
Silica	Silica, quartz addition to rock and replacement of rock minerals	Decreases acid-buffering capacity of rock	Decreases rock permeability, porosity. Increases susceptibility of rocks to fracturing
Jasperoid	Silica, quartz replacement of carbonate sedimentary rocks	Greatly decreases acid-buffering capacity	Can increase porosity, permeability of rock; also increases susceptibility of rocks to fracturing
Greisen	Quartz, muscovite, topaz, fluorite, cassiterite, magnetite	Some decrease in acid-buffering capacity, reactivity	Moderate rock permeability, fracture permeability
Skarn	Carbonate rocks alter to calc-silicates, magnetite	Decrease acid-buffering capacity; increase acid-generating capacity	May decrease rock permeability
Dolomitization	Alteration of limestones to dolomites	May decrease acid-buffering capacity	May decrease or increase rock porosity, permeability
Carbonatization	Alteration of rock minerals to carbonates	Substantially increases acid-buffering capacity	Negligible effect
Sulfidation	Alteration of Fe minerals to Fe sulfides	Increases acid-generating capacity	Negligible effect
Decalcification (decarbonatization)	Removal of carbonate from rocks, some replacement by silica	Decreases acid-buffering capacity	Substantially increases porosity, permeability

Acid-sulfate alteration is common in the wallrocks around high sulfidation or quartz alunite-epithermal deposits, and is formed by reactions of acidic magmatic gas condensates with wallrocks. Vuggy silica, in which all of the major host rock constituents are removed except silica, and in which pyrite is introduced into the rock, is the most intense alteration adjacent to fractures; the vugs form from the complete dissolution of feldspar phenocrysts. Progressive neutralization of the acid leads to quartz-alunite-pyrite and quartz-kaolinite-pyrite (\pm pyrophyllite, dickite) away from the central silica zone. Intense acid leaching of the rocks prior to mineralization essentially removes any capacity the rocks may have had to react with and consume acid generated by sulfide oxidation; hence this alteration type is typically highly acid-generating.

Argillic alteration results in the conversion of rock-forming minerals such as feldspars to various mixtures of clay minerals such as illite, kaolinite, and montmorillonite. Pyrite and other sulfides are also commonly introduced into the rock. As the clay minerals are relatively acid-stable, they do not have any substantial acid-neutralizing capacity. The presence of sulfides typically transforms argillically altered rocks into acid-generating mineral assemblages.

Coarse-grained potassic alteration formed by saline magmatic-hydrothermal fluids in the high-temperature (600–700°C) cores of porphyry copper and other magmatic-hydrothermal deposit types is characterized by the replacement of rock minerals by coarse-grained (up to several centimeters) potassium feldspar, biotite, anhydrite, and sulfides such as pyrite and chalcopyrite. Due to the coarse grain size of the biotite and feldspars, the net result of this

alteration is to increase the acid-generating potential of the rock and decrease the acid-neutralizing capacity of the rock. In contrast, potassic alteration formed in epithermal and Au-Te deposits from dilute, near-neutral hydrothermal fluids at temperatures of 250–350°C is characterized by replacement of rock minerals by very fine-grained (<1–2 mm) potassium feldspar. The fine grain size of the feldspars may allow them to react more rapidly with acid generated by sulfide oxidation, and so may increase the acid-neutralizing capacity of the host rocks.

Phyllic alteration is characterized by the replacement of rock minerals by quartz, pyrite, and sericite (a fine-grained mica). Due to the substantial increase in pyrite content and the relatively non-reactive quartz and sericite, phyllic alteration typically has high acid-generating potential. A variation on phyllic alteration that occurs in magmatic-hydrothermal systems enriched in fluorine and tin is greisen alteration, in which tourmaline, fluorite, topaz, cassiterite, and wolframite are also added to the rock in addition to quartz, sericite, and pyrite; greisen alteration is potentially acid generating, depending upon the pyrite content.

Silica alteration, or silicification, is the replacement of rock materials by silica. Because silica minerals are typically nonreactive and do not consume acid, silica alteration generally decreases the acid-neutralizing capacity of the host rocks.

Several of the alteration assemblages mentioned thus far involve sulfidation, the introduction of H₂S into the rock and the reaction of the H₂S with Fe-bearing minerals (such as hematite, magnetite, and Fe-silicates) in the rock. Sulfidation can result in a substantial increase in the acid-generating capacity of the rock.

Propylitic alteration is marked by the conversion of rock min-

erals to a mixture of epidote, chlorite, sodium feldspar, carbonates, and pyrite. Due to the presence of carbonates, this alteration type can be an effective acid consumer. The acid-generating potential of the pyrite is generally insufficient to overcome the acid-neutralizing capacity of the carbonates.

Carbonate alteration, or carbonatization, occurs in relatively few mineral deposit types (such as low-sulfide Au-quartz vein deposits and carbonatite deposits), and involves the alteration of host rock silicate minerals to carbonates such as calcite, dolomite, ankerite, and magnesite. The acid-neutralizing capacity of this alteration type is substantial.

Hydrothermal mineral deposits hosted by carbonate-rich sedimentary rocks can have several types of alteration, including skarn alteration, dolomitization, jasperoid alteration, and decalcification/decarbonatization. Skarn alteration is marked by the conversion of calcite and dolomite in the sedimentary rocks to calc-silicate and Fe-rich silicate minerals such as diopside, wollastonite, tremolite, actinolite, and garnets (Guilbert and Park, 1986); sulfides such as chalcopyrite and pyrite, and oxides such as magnetite, also are common. Acidic waters draining skarn deposits indicate that the generally coarse grain size and relatively slow reaction kinetics of the calc-silicate minerals makes them ineffective acid consumers. Jasperoid forms by the extensive replacement of carbonate sedimentary rocks by silica. If few or none of the original carbonate minerals remain in the rock, jasperoid has a very low acid-neutralizing capacity. Dolomitization is the alteration of calcite and aragonite in limestones to dolomite. It generally results in a slight decrease in acid-neutralizing capacity due to the lower reactivity of dolomite. Carlin-type, sediment-hosted Au deposits commonly exhibit decalcification (or decarbonatization) alteration that involves large-scale dissolution of carbonate minerals by acidic hydrothermal fluids, coupled with the residual concentration of the remnant silica minerals originally present in the carbonate sedimentary rocks.

Physical effects of wallrock alteration

Alteration characteristics that control ground-water flow: Wallrock alteration can either increase or decrease the ability of rocks to transmit ground waters, either through rock pore spaces or through joints and fractures (Table 3.7). Alteration that results in extreme leaching of the host rocks, such as vuggy silica alteration in acid-sulfate-altered rocks and the formation of jasperoid in carbonate sedimentary rocks, can lead to increased hydraulic conductivities. Dolomitization may result in increased hydraulic conductivities, due to the volume decrease resulting from the replacement of calcite with denser dolomite; however, in many cases additional dolomite also precipitates in the rock pore spaces, and so results in a net permeability decrease. Decalcification/decarbonatization can result in a substantial increase in hydraulic conductivity of carbonate host rocks, due to the large scale dissolution of the host carbonates during the alteration process.

In contrast, alteration that forms large amounts of clay minerals (such as kaolinite and dickite in acid-sulfate and argillic alteration assemblages) can substantially decrease hydraulic conductivity, as well as decrease the rock's ability to develop hydrologically conductive fractures.

Alteration characteristics that control physical erosion and mass wasting: Various wallrock alteration types can impart varying degrees of resistance to erosion and mass wasting within min-

eral deposits. Alteration that adds silica to rocks typically increases a host rock's ability to withstand erosion. For example, vuggy silica alteration zones form prominent ledges and topographic highs within quartz-alunite epithermal deposits, and also serve as strong skeletal supports that minimize potential landslides and debris flows within the deposits. In contrast, wallrock alteration that substantially increases the clay-mineral component of wallrocks can greatly weaken the rock's resistance to rapid physical erosion and mass wasting. The argillically altered rocks in the Alamosa River stock shown on Figure 3.5 are an excellent example of this weakening; rapid physical erosion rates compared to chemical weathering rates continually expose fresh pyrite at the ground surface. Drainages in the stock that have oversteepened topography (usually where silicified ledges overlie argillically altered rock) are prone to debris flows during periods of rapid runoff, such as occur during summer thundershowers. As another example, rocks at the upper levels of the Mount Rainier volcano have been extensively altered by magmatic gas condensates to argillic and advanced argillic alteration assemblages very similar to those found at Summitville, Colorado, and other quartz-alunite-epithermal or high-sulfidation deposit types (Zimbelman, 1996; Crowley and Zimbelman, 1997). The structurally weakened, altered rocks at Mount Rainier have been the source areas for large debris flows and mudflows from the mountain, which, due to their high clay contents are very cohesive and can travel great distances downstream (Crandell, 1971; Scott et al., 1995). Detailed links between alteration type and the potential for landslide and debris flow generation remain to be examined.

Major- and trace-element content of deposits and their host rocks

The chemical composition of the geoavailable major and trace elements in mineral deposits is typically manifested in their environmental signatures, with some variability superimposed by geochemical processes such as oxidation, secondary mineral precipitation, and sorption (Nordstrom and Alpers, 1999; Smith, 1999). For example, deposits that are enriched in As (such as those that contain arsenopyrite or enargite) typically produce drainage waters, smelter emissions, etc., that are enriched in As relative to waters or smelter emissions from deposits that are not enriched in As.

Table 3.8 lists some common mineralogic hosts for major and trace elements found in environmental signatures of mineral deposits such as mine-drainage waters and smelter emissions.

The physical characteristics of mineral deposits

Mineral deposits can occur in a wide variety of physical forms, including veins, stockworks, breccias, disseminations, and massive lenses or pods (Fig. 3.7). These different forms influence the extent to which weathering agents can access deposits, either in place within the ground or on mine dumps.

Veins typically form when pre-existing fractures are filled by ore and gangue minerals (Figs. 3.7a, b); crustification sequences often develop in which the vein minerals are added in successive layers (Figs. 3.1c, d, e; Fig. 3.7a). Depending upon the extent to which the fractures are filled with minerals (Fig. 3.7a), veins can either focus or inhibit ground-water flow. Veins with considerable

open spaces can preferentially transmit ground water, and thus enhance the interactions of the waters with vein materials and minimize interaction with wallrock (Fig. 3.7a). In contrast, veins that are nearly completely filled typically transmit ground water only along later fractures within the vein. Unless well-crustified vein fill is permeable (Fig. 3.2a), fractured, or broken and exposed by mining, ground water typically interacts with the outermost coatings of the vein minerals; thus, acid-generating sulfides or acid-consuming carbonates that are coated by later, less reactive minerals may not have as strong an influence on ground-water chemistry.

Stockwork ore bodies (Fig. 3.7c) are composed of many intersecting small veins or veinlets. If the veinlets are at all permeable, they can distribute ground water to a large volume of mineralized rock.

TABLE 3.8—Common primary mineralogic sources for some environmentally important major and trace elements in mineral deposits. For each element, the minerals are listed in general decreasing order of reactivity in the surficial environment. For further details, see discussions in Smith and Huyck (1999) and appendix in Rose et al. (1979).

Element	Common mineralogic sources
Ca	Gypsum, anhydrite, calcite, fluorite, dolomite, calcic plagioclase, calc-silicates
Mg	Dolomite, pyroxenes, amphiboles, chlorite
Na	Sodic feldspars, micas
K	Sylvite, potassium feldspars, micas
Al	Aluminosilicate minerals
Si	Aluminosilicate, silica minerals
Fe	Pyrite, siderite and other carbonates, hematite, mafic silicates (pyroxene, amphibole, biotite), magnetite
Mn	Rhodochrosite, carbonates, aluminosilicate minerals, Mn-silicates
S	Sulfides, sulfosalts, sulfates
F	Fluorite, topaz, silicates
Ba	Feldspars, other aluminosilicates, barite
Zn	Sphalerite, other sulfides and sulfosalts, mafic silicates, Zn-silicates
Cd	Sphalerite, greenockite, other sulfides and sulfosalts
Cu	Cu-sulfides, mafic minerals
Pb	Galena, other sulfides and sulfosalts, feldspars
As	Realgar, orpiment, enargite, arsenopyrite, other sulfides and sulfosalts
Sb	Stibnite, other sulfides and sulfosalts
Ni	Ni-sulfides, other sulfides, olivine and other mafic silicates
Co	Co-sulfides, other sulfides, aluminosilicates
Cr	Mafic silicates, chromite (relatively nonreactive)
Hg	Native mercury, cinnabar, other sulfides and sulfosalts
Mo	Sulfides, molybdenite (relatively non-reactive)
Se	Sulfides, selenides, selenates
U	Uraninite, coffinite, carnotite, apatite, feldspars, zircon, allanite
Rare earth elements	Bastnaesite, silicates, monazite

Disseminated ore is characterized by ore minerals dispersed throughout the host rocks; the ore minerals are therefore available for interactions with ground water over relatively large host-rock volumes. In some deposits such as porphyry-Cu deposits, disseminated sulfides are controlled by microscopic stockwork fractures in the rock that may or may not transmit ground waters. In some sed-

iment-hosted mineral deposits, disseminated sulfides precipitate at the same time as their host sediments are deposited mechanically; if the rate of sulfide precipitation exceeds the rate of host sediment deposition, massive sulfide ore bodies result.

Breccia ore bodies typically form by the filling of open spaces in rocks brecciated by faulting, hydrothermal, or magmatic-hydrothermal processes. Like veins, breccias can either focus or inhibit ground-water flow, depending upon the extent to which their interstices are filled with material (Fig. 3.7e).

Massive ore bodies, as their name implies, are characterized by lenses or pods of massive, intergrown sulfides with few or no intergrown silicates or carbonates (Fig. 3.7f). Ground-water flow is typically along fractures or grain boundaries within the sulfides (Fig. 3.4). Water flowing within massive Fe-sulfide lenses can become quite acidic if flow paths do not intersect wallrocks surrounding the lenses; an example is the extremely acid water draining massive sulfide ore bodies at Iron Mountain, California (Alpers and Nordstrom, 1991; Nordstrom and Alpers, 1999).

Presence and openness of faults, joints

If they are open and interconnected, faults and joints that cross-cut ore bodies can serve as significant conduits for ground waters and their contained weathering agents. In general, flow along faults is generally much more effective than flow across them. The hydraulic conductivity of an open fracture is proportional to the cube of its dilation (or openness).

The openness of fractures is a function of the ability of their host rock to develop fractures, their ambient stress regime (geologic stresses lead to faulting and folding), and the presence or absence of minerals filling the fractures. For example, rocks that are composed of minerals that break rather than deform ductily (such as feldspars and quartz) tend to form more well-developed, open fractures than rocks composed of minerals that deform ductily (such as clays). Different structures in the same rock unit in the same mine can have different degrees of openness as a function of their orientation relative to ambient geologic stress directions; fractures that occur at an angle to compressive stresses tend to be closed, whereas those that are nearly co-planar with compressive stress directions tend to be more open structurally.

If faults and joints are not interconnected or are not open to the ground surface, their influence on ground-water flow is diminished. The interconnectedness of faults can in part be determined through careful structure mapping, but is determined with the greatest certainty through hydrologic testing techniques such as those discussed in Domenico and Schwartz (1990).

A detailed understanding of the structural characteristics of a mineral deposit is crucial to understand the potential role that fractures and joints will play in influencing ground-water flow through the deposit. Such an understanding can only be established through careful geologic mapping of structures, field or mine observations of the orientation and openness of structures, structural analysis, and hydrologic testing.

GEOLOGIC VARIABILITY IN MINERAL DEPOSITS

The previous section outlined the major geologic characteristics of mineral deposits that influence their environmental signatures. It is important to recognize that these characteristics can

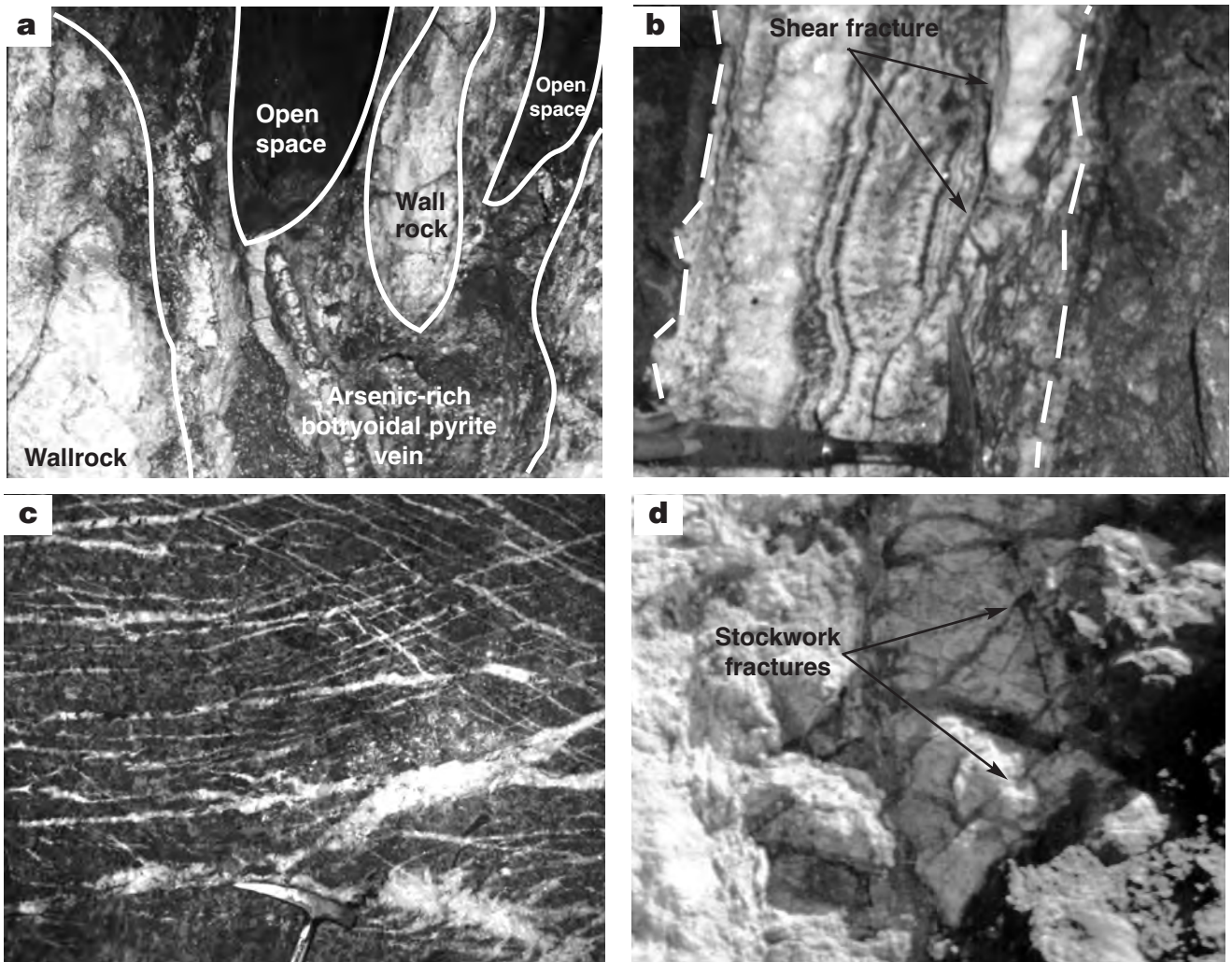


FIGURE 3.7—Examples of different ore types. (a) Vein of crustified, arsenic-rich botryoidal pyrite from Creede, Colorado. The pyrite was deposited in successive layers (a crustification sequence) growing out from the vein walls, completely filling the vein in the lower part of the photograph but only partially filling the vein in the upper part of the photograph. White lines mark approximate edges of vein and open space in the center of the vein. (b) Crustified barite-sulfide vein, Bulldog Mountain mine, Creede district, Colorado. Barite (light) and intergrown sphalerite and galena (dark) generations completely filled the vein, and were later partially truncated by shear fractures. (c) Gold-quartz veinlets in carbonatized wallrock from the low-sulfide gold-quartz vein deposits in the Kensington mine, Juneau, Alaska. The two intersecting sets of parallel veinlets reflect fracture formation along conjugate shear couples. Due to the carbonate alteration of the wallrocks, these deposits tend to have relatively low acid-generating potential, even though they contain several volume % pyrite and arsenopyrite in both the veins and wallrock (Goldfarb et al., 1997). Photo by C. Taylor, USGS. (d) Pyrite-chalcopyrite-quartz stockwork veinlets in altered submarine volcanic host rocks, Rio Tinto, Spain. The stockwork veins formed in the feeder zone for hydrothermal fluids that discharged onto the sea floor and produced massive sulfide deposits overlying the volcanic rocks. Photo by C. Taylor, USGS.

vary spatially and substantially within most mineral deposits. Thus, one portion of an ore body, mine, or mining district may have significantly different environmental geology considerations than those present in other portions of the same ore body, mine or district.

Primary mineral zoning

The primary minerals making up a mineral deposit commonly show systematic spatial variations, or zoning patterns, that ultimately result from the processes by which the deposit formed.

Substantial mineralogic variations can occur on a spectrum of scales ranging from several centimeters within an ore shoot, to tens to hundreds of meters within an ore body, to several kilometers across a mining district (Figs. 3.8, 3.9). From an environmental standpoint, such geologic variability can lead to substantial variations in environmental signatures within a deposit, mining district, or mine.

Creede and Central City, Colorado

Epithermal vein ores in the Bulldog Mountain vein system,

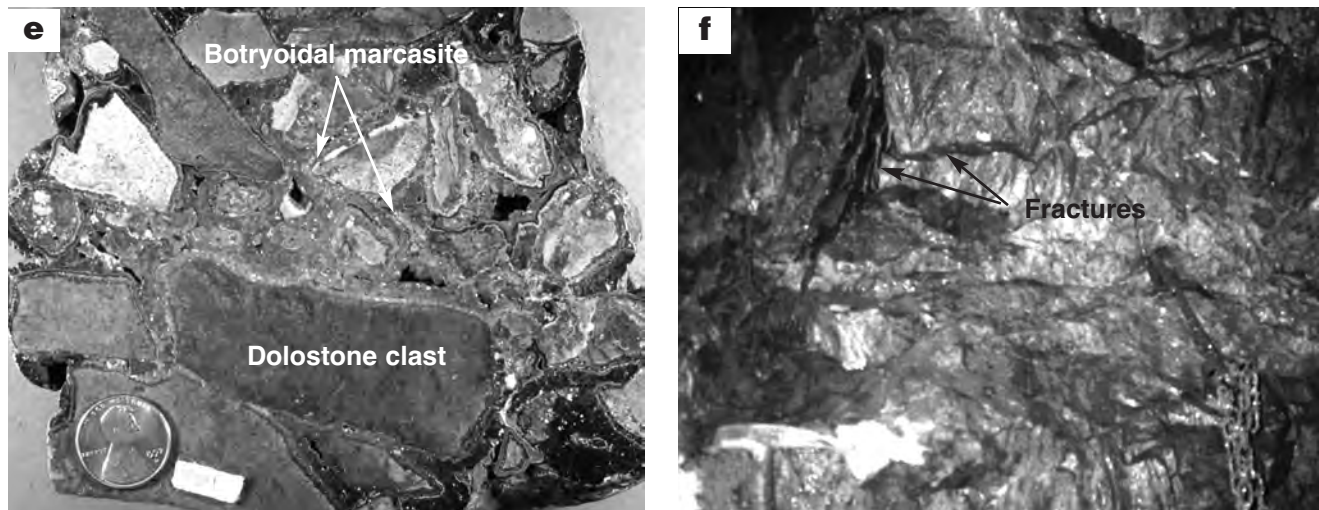


FIGURE 3.7 (Continued)—(e) Sample of a mineralized, partially replaced breccia from Mississippi-Valley-Type (MVT) deposits in the Pomerzany mine, Silesian-Cracow district, Poland. The breccia formed in part by collapse of pre-mineralization karst caverns, and in part by collapse resulting from hydrothermal dolomitization that replaced limestone with dolostone. The dolostone breccia clasts were then partially replaced by fine-grained sphalerite, which was then coated by trace-element-rich botryoidal marcasite. The breccia now has moderate porosity due to infilling of the pore spaces by mineralization. Photograph by D. Leach, reproduced from Leach et al. (1996). (f) Massive sulfide ore body, Windy Craggy deposit, British Columbia, Canada. The entire field of view is composed of massive pyrite-pyrrhotite-chalcocopyrite ore. Photo by C. Taylor, USGS.

Creede district, Colorado show complex mineralogic variations (Fig. 3.8) along the major veins in the system. These variations resulted from the geochemical evolution of the hydrothermal fluids that deposited the vein minerals, hydrothermal leaching of some minerals once they were deposited, and progressive closing (and in some cases opening) of the fractures by structural activity during mineral deposition (Plumlee and Whitehouse-Veaux, 1994; Plumlee, 1989).

Polymetallic veins are strongly zoned across Colorado's Central City mining district; pyrite-rich mineral assemblages in the core of the district grade laterally outward into progressively more sphalerite-, galena-, and carbonate-rich ores (Fig. 3.9); this zonation resulted from an overall decrease in formation temperature of the veins toward the lateral fringes of the mineralizing system. In both the Bulldog Mountain and Central City examples, the different mineral assemblages produce quite different environmental signatures, in waters draining both the mine workings and mine waste dumps.

Wallrock alteration zoning

Wallrock alteration assemblages can also vary substantially over the same spectrum of scales at which mineral zoning occurs.

Summitville, Colorado

The high-sulfidation, quartz-alunite epithermal Au-Cu-Ag deposit at Summitville, Colorado, is an excellent example of zoned alteration assemblages (Figs. 3.10–3.13). Summaries of Summitville's environmental geology are presented by Plumlee et al. (1995a, b) and Gray et al. (1994). The deposit formed in the core of a volcanic dome, as part of the waning stages of the dome-

forming cycle (Stoffregen, 1987; Rye et al., 1990; Gray and Coolbaugh, 1994). Prior to ore mineralization, magmatic gases released from a crystallizing magma at depth flowed upward along fractures in the dome rocks and condensed at shallow levels in the dome; the highly acidic condensates produced intense, pre-ore acid-sulfate alteration near the fractures (Figs. 3.10, 3.11). On a local scale (Fig. 3.12), progressive neutralization of acid in the condensates, coupled with mixing with ground waters, resulted in laterally zoned alteration assemblages that grade from vuggy silica nearest the fractures to quartz-alunite-pyrite, quartz-kaolinite, illite-montmorillonite, and propylitic farthest from the fractures (Gray et al., 1994, and references therein). On a district-scale (Fig. 3.11), the most intense alteration occurs in the core of the deposit; a central acid-sulfate alteration zone is surrounded by intermediate argillic and distal propylitic alteration zones. Subsequently, hydrothermal fluids deposited pyrite, marcasite, enargite, covellite, native sulfur, barite, and native gold in the central part of the deposit, grading laterally outward to sphalerite and galena. The permeable vuggy silica zones focused hydrothermal fluid flow, causing the bulk of the sulfide deposition to occur in the vuggy silica and adjacent alteration zones. However, some sulfides were also deposited in the argillic zones. Trace-metal zoning is directly related to the overall mineralogic zoning; Cu and As are dominant in the central part of the deposit, and Pb and Zn are more abundant on the lateral fringes of the deposit. Increasing Hg concentrations with increasing elevation resulted from the concentration of Hg in the near-surface levels of the hydrothermal system that formed the deposit; the Hg occurs primarily as a trace metal in sulfides such as pyrite.

Wallrock alteration at Summitville also strongly influenced the deposit's hydraulic conductivity and the way in which the deposit weathered prior to mining. The deepest pre-mining oxidation occurred along permeable vuggy silica zones, to depths as great as 100 m (Figs. 3.12, 3.13; Gray et al., 1994); oxidation concentrat-

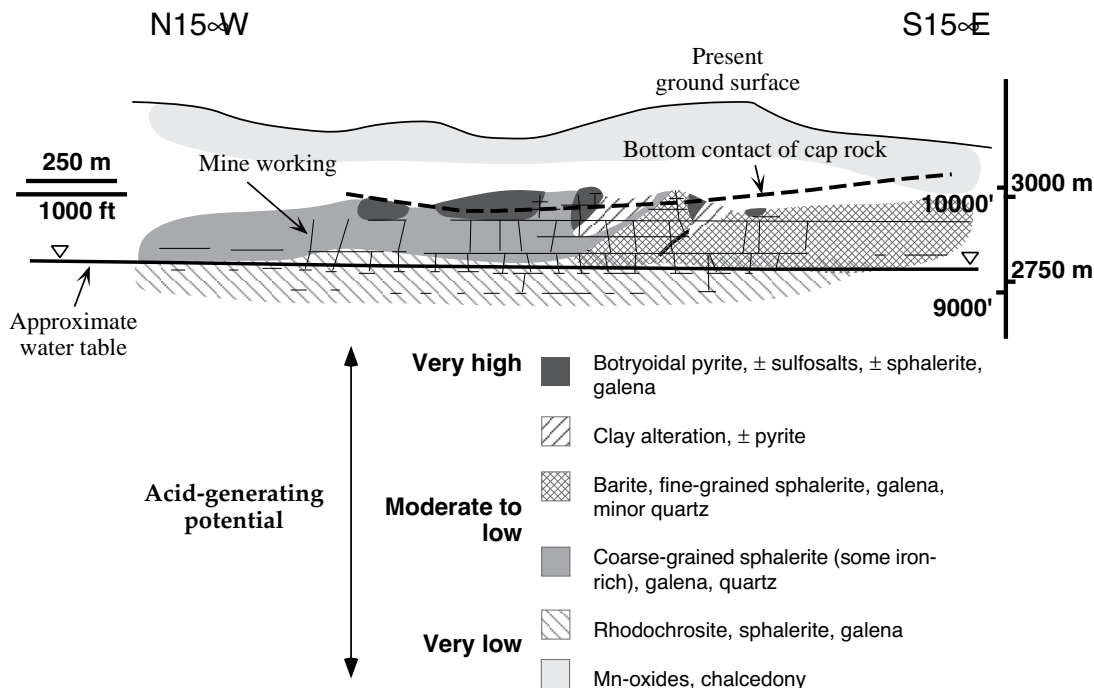


FIGURE 3.8—Longitudinal section of the A Vein, Bulldog Mountain Mine, Creede, Colorado, showing the distribution and environmental characteristics of dominant mineral assemblages along the vein. The pre-mining water table occurred primarily in acid-neutralizing rhodochrosite, and so the mine waters had near-neutral pH and relatively low levels of dissolved metals (R. Boppe, oral. commun., 1982). Acid-generating, arsenic-rich botryoidal pyrite (Figs. 3.3 and 3.7a) persists unoxidized above the water table due to the presence of an illite- and montmorillonite-rich hydrothermal alteration cap and a poorly welded ash-flow tuff above the main vein ore zone; these features combine to produce low hydraulic conductivity along the vein between the ground surface and the main ore zone. Figure modified from Plumlee and Whitehouse-Veaux (1994) and Plumlee and Nash (1995).

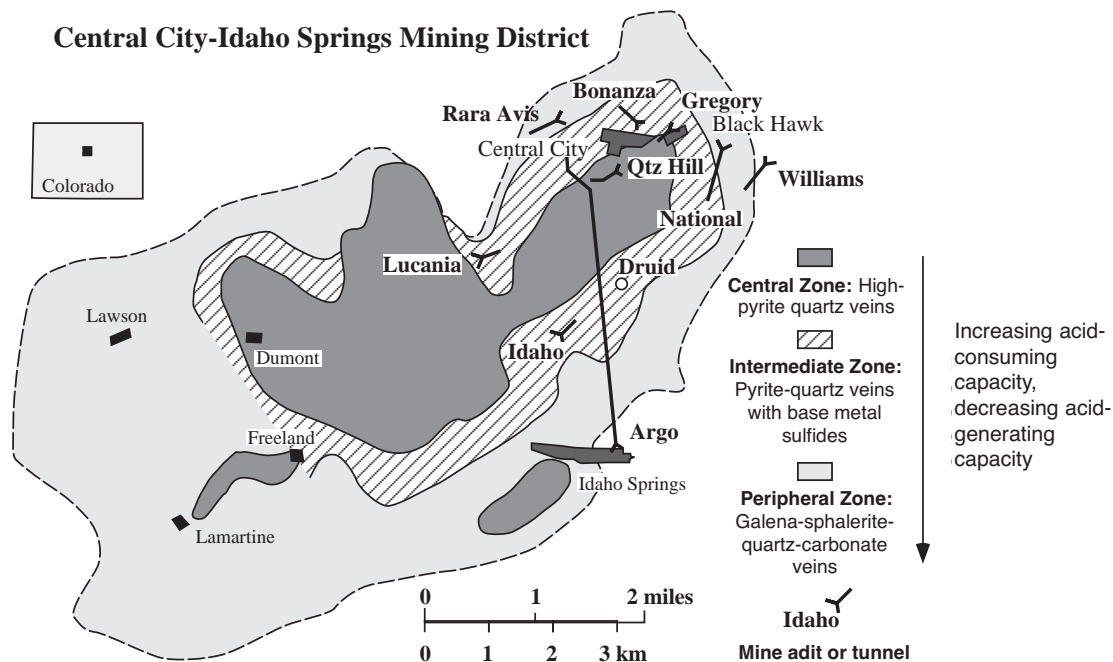


FIGURE 3.9—Map showing primary mineral zoning of polymetallic veins across the Central City-Idaho Springs mining districts, Colorado. Figure modified from Sims et al. (1963). A porphyry Mo deposit is inferred to be present at depth beneath the district.

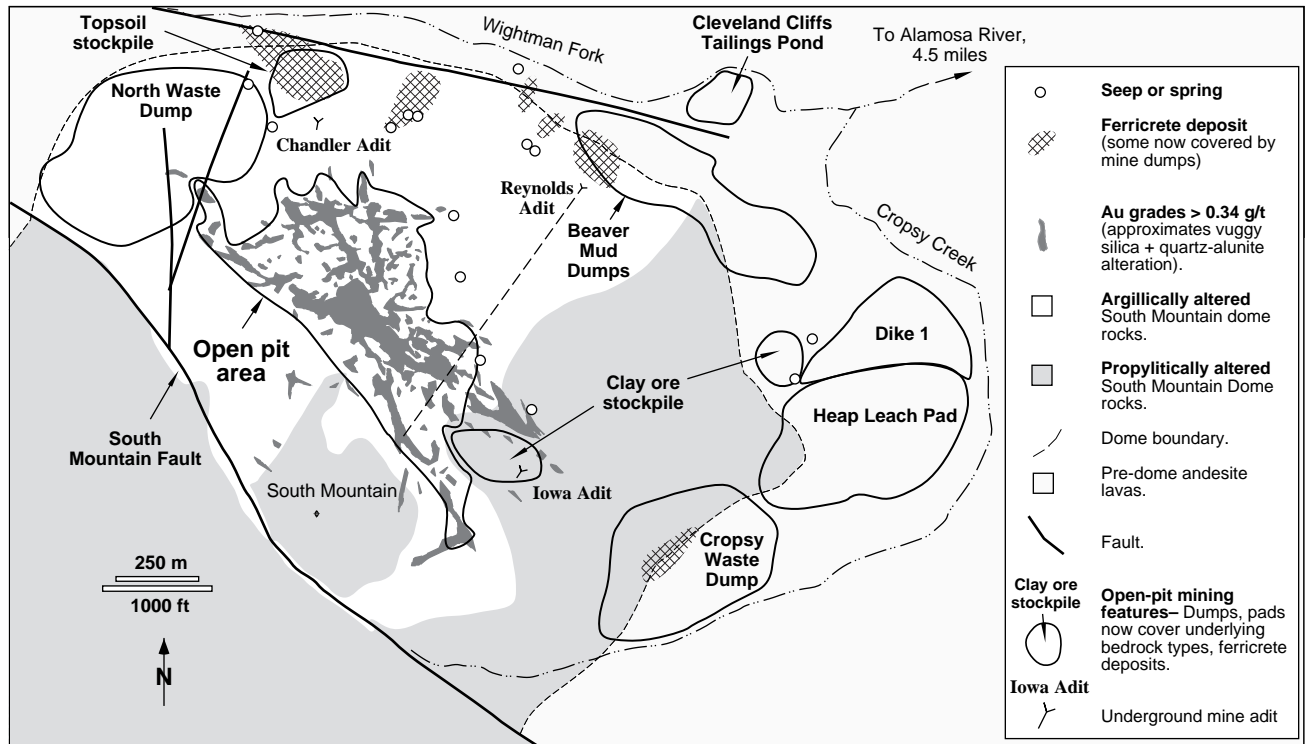


FIGURE 3.10—Geologic map of the Summitville quartz-alunite epithermal, Au-Cu-Ag deposit and mine, SW Colorado, showing the location of major mine features relative to important geologic features. The highest-grade Au ores occurred along vuggy silica alteration zones following original radial fractures in the host volcanic dome rocks. Underground mining in the late 1800s followed the vuggy silica zones. Recent open-pit mining from 1984-1992 used open-pit methods and heap leach processing to extract lower-grade gold ores from the rocks around the highest-grade vuggy silica. The mining company operating the open-pit mine declared bankruptcy in late 1992 as remediation of substantial environmental problems (such as extreme acid-mine drainage) was beginning, and the U.S. Environmental Protection Agency (EPA) took over the site under Superfund Emergency Response Authority. The site was added to the Superfund National Priorities list in 1994.

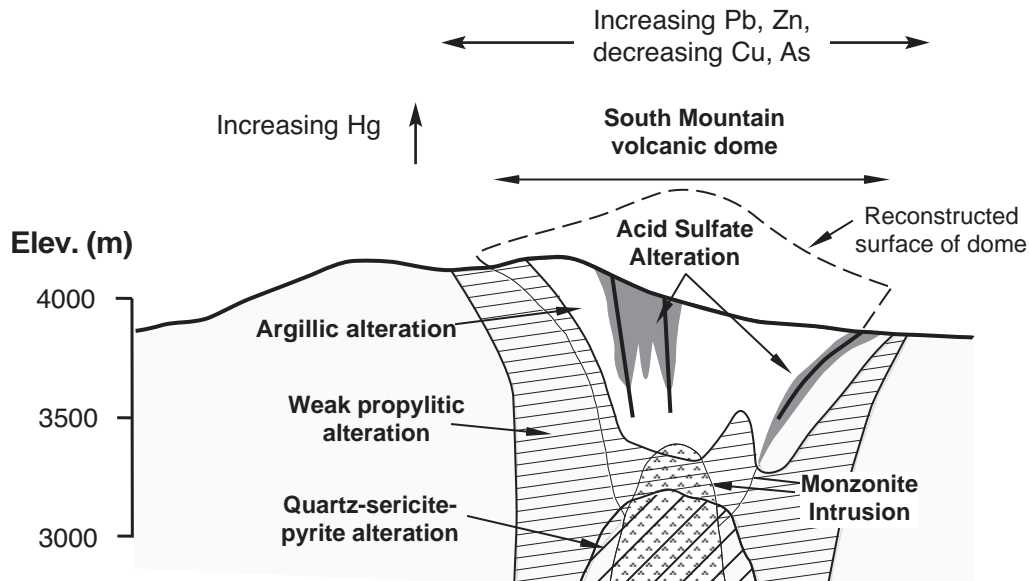


FIGURE 3.11—East-west geologic cross section of the Summitville deposit, SW Colorado, showing deposit-wide alteration and metal zoning. The quartz-sericite-pyrite alteration is associated with a low-grade porphyry-Cu deposit. Figure from Plumlee et al. (1995a), and originally modified from Rye et al. (1990).

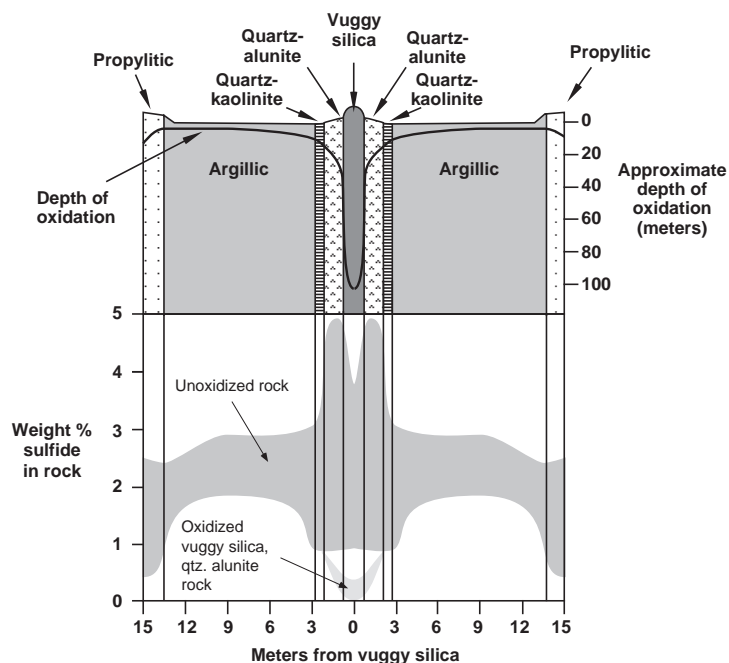


FIGURE 3.12—Schematic diagram showing distribution of alteration zones, sulfide content, and depth of oxidation away from fractures in the Summitville deposit, Colorado. Although the sulfide content of the alteration zones is not extremely high (<5 wt.%), the extreme lack of acid-buffering capacity in the acid-sulfate altered rocks gives the deposit very high acid-generating potential. Figure from Plumlee et al. (1995a), modified originally from a figure in Gray et al. (1994).

ed gold in the vuggy silica zones and therefore made the vuggy silica zones the main targets for exploration and mining (Fig. 3.10). In contrast, the clay-rich argillic alteration was much less permeable to descending ground waters, and so oxidation only occurred to depths as shallow as several meters (Figs. 3.12, 3.13). The vuggy silica zones also physically stabilized the deposit and prevented extensive erosion and exposure of sulfides in the argillic

alteration zones, such as occurred several kilometers to the south in the Alamosa River stock (Figs. 3.5d-g). The net product of the hydrothermal alteration-mineralization and pre-mining weathering at Summitville was a deposit with very high acid-generating capacity and very low acid-neutralizing capacity in the central (i.e., most mined) part of the deposit. Increased acid-neutralizing capacity of propylitically altered rocks toward the lateral fringes of the deposit is of relatively little environmental benefit due to the lack of mine workings in and ground-water flow through these rocks.

As at Summitville, district-scale alteration zoning is common in a variety of hydrothermal ore deposit types, including other acid-sulfate epithermal deposits (such as Round Mountain and Goldfield, Nevada), Cordilleran lode deposits (such as Julcani, Peru, and Butte, Montana), porphyry Cu and Cu-Mo, Climax-type porphyry-Mo (such as Climax and Henderson, Colorado), and zoned polymetallic vein systems (such as Central City, Colorado). In nearly all of these deposit types, acid-neutralizing propylitically-altered rocks occur in the distal parts of the deposits. Acid-sulfate epithermal and Cordilleran lode deposits (both are also termed high-sulfidation deposits) contain extensive acid-sulfate or advanced argillic alteration with extreme acid-generating potential in their central portions, and acid-neutralizing propylitic alteration on their distal fringes. Porphyry deposits typically have deep potassic alteration flanked by phyllic alteration and overlain by argillic alteration (Fig. 3.5d) in their central portions (all typically have high acid-generating potential), and distal propylitic alteration. Zoned polymetallic vein deposits also have phyllic and argillic alteration in their central portions, flanked by distal propylitic alteration; such zoning also coincides with the zoning in primary vein mineralogies shown on Figure 3.9.

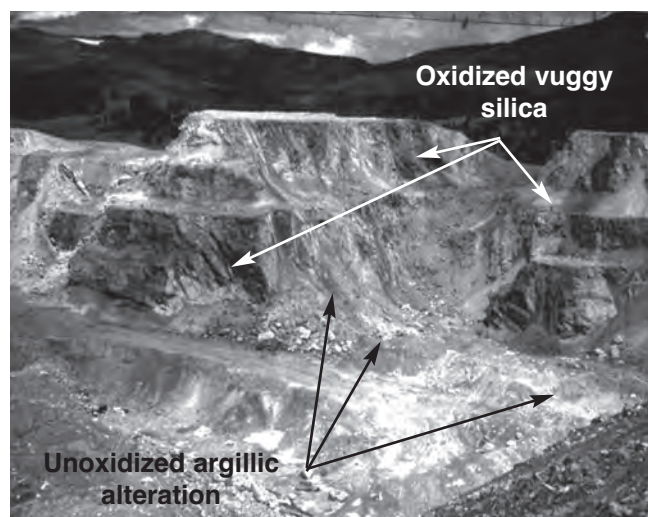


FIGURE 3.13—Photo of the Summitville open pit, taken in August 1993. Dark gray zones are oxidized vuggy silica zones, and lighter gray zones are sulfide-bearing argillic alteration zones.

Jerritt Canyon, Nevada

Carlin-type sediment-hosted Au deposits such as those at Jerritt Canyon, Nevada, also show both local and district-scale alteration and primary mineral zoning patterns. The deposits formed from moderately acidic, H_2S - and As-rich hydrothermal fluids that mixed with cooler, dilute, oxidized ground waters and reacted with Fe-bearing carbonate rocks (Hofstra et al., 1991). The cores of the deposits, where the hydrothermal fluids flowed into the carbonate rocks from feeder fractures (Fig. 3.14), are marked by extensive to complete decalcification of the host rocks and residual enrichment of silica. The decalcification occurred contemporaneously with deposition of hydrothermal quartz, formation of realgar-orpiment veins, and sulfidation of Fe minerals in the host rocks to produce disseminated arsenian pyrite, the main host for the gold (Fig. 3.14a). Grading outward from the feeder zones, the extent of decarbonatization, realgar-orpiment veining, disseminated pyrite, and gold grades progressively decrease; this is accompanied by a progressive increase in the amount of carbonate remaining in the wallrock, as well as an increase in the amounts of pre-ore and ore-stage calcite veins. In the intermediate zones of the deposits, local variations in the extent of decarbonatization can be abrupt, with the transition between extensively decarbonated, quartz-rich rock and carbonate-rich rock occurring over a space of several centimeters (Fig. 3.14b).

From an environmental standpoint, the highest grade ores in Jerritt Canyon and other Carlin-type deposits also have a relatively high potential to generate locally acidic drainage waters, due to the removal of acid-neutralizing carbonate minerals and deposition of reactive, acid-generating arsenian pyrite. However, the abundant carbonate minerals in host rocks surrounding the deposits increase the opportunities for any acid drainage waters that might form to be consumed through reaction with the carbonate minerals or mixing with alkaline waters draining the carbonate rocks. The abundance of As in the deposits, coupled with the mobility of As in higher-pH waters (Smith and Huyck, 1999; Smith, 1999), indicates that As should be the dominant element of environmental concern in this deposit type. However, the formation of Fe particulates in drainage waters should also lead to relatively effective sorption of As in all but the most acidic or alkaline drainage waters (Smith, 1999).

Variations in geology that affect hydraulic conductivity and ground-water flow

In addition to variations in hydraulic conductivity imparted by its alteration, Summitville is also an excellent example of the variations in hydraulic conductivity imparted by fractures and rock contacts. The location of ferricrete deposits and acid seeps in and around the deposit (Fig. 3.10) show that the primary geologic features which focus ground-water flow are the vuggy silica alteration zones, the South Mountain fault bounding the deposit on its western side, fractures within the dome (which follow dominant $N30^\circ W$, $N60^\circ W$, $N5^\circ W$, and $N30^\circ E$ trends; Gray et al., 1994; Gray and Coolbaugh, 1994), and the contact between the dome rocks and the surrounding andesite volcanic rocks. The andesites surrounding the Summitville dome have very low fracture and joint permeability (M. Roeber, oral commun., 1993), and so minimize ground-water flow from the dome into the surrounding rocks.

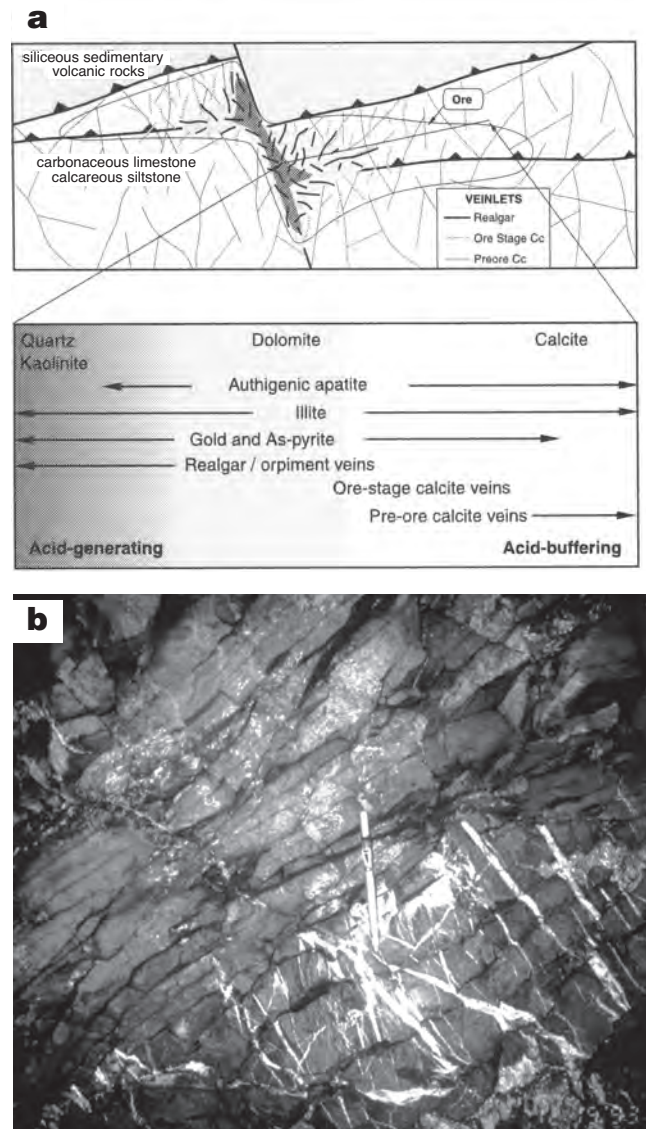


FIGURE 3.14—Spatial variations in alteration and mineralization in a Carlin-type, sediment-hosted Au deposit, Jerritt Canyon, Nevada. (a) Schematic cross section (upper) and primary and alteration mineral zoning patterns (lower) of Carlin-type, sediment-hosted Au deposits, Jerritt Canyon, Nevada. Figure modified from Hofstra et al. (1991). (b) Photo of mine face showing sharp break between highly decarbonated ore with abundant ore-stage realgar-orpiment veins (upper) and unaltered rock containing abundant host-rock carbonate and pre-ore calcite veinlets (white). The decalcification occurred preferentially along bedding planes (dark lines cutting diagonally from lower left to upper right). Photo by A. Hofstra, USGS.

Prior to the development of the Reynolds adit (which was installed in the early 1900s to drain the underground workings, ground-water recharge into the deposit was most likely from the South Mountain fault and the vuggy silica zones, and discharge was primarily along the dome-andesite contact and fractures that intersect

the ground surface. The Reynolds adit short-circuited the natural flow paths, and focused all discharge from most of the deposit. Plugging of the Reynolds adit in 1994 during environmental restoration at the site resulted in the predictable reactivation of the natural discharge seeps (Fig. 3.10), which will continue to serve as long-term, but relatively low-level, sources of acid drainage from the site.

In other deposit types, geologic variations in host rocks, alteration, faults, joints, and other geologic features can combine to create complex controls on porosity, permeability, and therefore hydrology. This again underscores the need for careful, integrated geologic and hydrologic site characterization prior to mining and remediation, in order to better understand the geologic controls on fracture-dominated ground-water flow.

Variations in deposit type within a mining district or mineralized area

In addition to local- to district-scale geologic variations within a given deposit type noted previously, many mineralized areas and mining districts can contain more than one deposit type, each with its own particular range of geologic characteristics. In many cases, these multiple deposit types are genetically-related parts of a larger mineralizing system. More rarely, they may be entirely unrelated in age or processes of formation.

One example of genetically-related, multiple deposit types in a given district is the occurrence of a low-grade porphyry-Cu deposit with stockwork pyrite-chalcopyrite veins and phyllic alteration at depth beneath the Summitville quartz-alunite epithermal deposit (Fig. 3.11). The porphyry deposit formed during the crystallization of the host monzonite intrusion. It is unclear whether the intrusion and the porphyry-Cu mineralization are truly contemporaneous with either the pre-mineralization acid-sulfate alteration or the hydrothermal mineralization in the Summitville quartz-alunite epithermal deposit; however, both clearly formed in the late stages of the Summitville volcanic dome formation (Gray and Coolbaugh, 1994; Rye et al., 1990). Quartz-alunite epithermal deposits and their deeper equivalents, Cordilleran lode deposits (such as Butte, Montana) commonly form in the upper levels and (or) late stages of porphyry-Cu or porphyry-Mo-Cu mineralizing systems; both require crystallization of magmas to produce magmatic-hydrothermal fluids that form the porphyry deposits, and the magmatic gases and magmatic heat source for the hydrothermal system that produce the acid-sulfate alteration and high sulfidation mineralization.

Another example of multiple deposit types occurring within a single district is shown on Figure 3.15, a schematic cross section of porphyry, skarn, breccia, igneous-hosted polymetallic vein, and sediment-hosted polymetallic vein and replacement deposits associated with the crystallization of a magmatic intrusion into a sedimentary rock sequence. Examples of such systems include Leadville and Gilman, Colorado; and New World, Montana. Districts developed on such deposit systems can have a wide range in environmental geology characteristics depending upon the deposit type(s) in which particular mines are developed. For example, the igneous-hosted porphyry deposits (with quartz-pyrite-chalcopyrite stockwork veins and disseminations) and polymetallic vein deposits (pyrite-sphalerite-galena, with occasional calcite) generally have high acid-generating capacity but low acid-neutralizing capacity. The breccia (sulfides cementing igneous or sedimentary rock breccias), skarn (sulfides and calc-silicate minerals

replacing carbonate rocks), and sediment-hosted polymetallic vein (pyrite-sphalerite-galena±calcite) and replacement deposits (massive pyrite-marcasite-sphalerite-galena±calcite) can display a variety of acid-generating and acid-neutralizing capacities, depending upon factors such as the carbonate content of the sedimentary host rocks, the reactivities of the calc-silicate skarn minerals, the thickness and permeability of the massive sulfide lenses, and the amount of calcite present in the ores. Metal contents can also vary substantially, with Cu typically enriched in the deeper porphyry and skarn deposits, and Pb and Zn enriched in the more shallow polymetallic vein and replacement deposits. Hence, environmental signatures such as natural- or mine-drainage compositions may vary greatly within these districts, depending upon which of the deposit types have been exposed at the surface by pre-mining erosion, and which have been mined.

THE ROLE OF CLIMATE AND MINING/ MINERAL PROCESSING METHOD

Climate and mining/mineral-processing method also influence the environmental signatures produced by weathering mineral deposits and by mining and mineral processing activities. However, the effects of climate and mining/processing methods generally serve to modify the environmental signatures that are ultimately governed by the deposit geology and geochemistry.

Effects of climate

Three main aspects of climate exert important controls on rock weathering and related environmental processes: temperature, humidity, and the amount of precipitation (rain + snow) relative to evapotranspiration (the combined evaporation from soils, rocks, and surface waters, and transpiration from plants).

Temperature and humidity influence potential evapotranspiration (the maximum possible evapotranspiration that could occur in an area), the rate of vegetation growth, and the rates at which weathering occurs.

In wet climates where precipitation exceeds evapotranspiration, abundant water is available to promote rock weathering, vegetation growth, and ground-water recharge. With increasing aridity, evapotranspiration increases and overtakes precipitation, and so less and less water becomes available for weathering, ground-water recharge, and vegetation growth. In most climates, precipitation and potential evapotranspiration vary as a function of season (Domenico and Schwartz, 1990), leading to significant variations in recharge, weathering rates, and vegetation growth over the course of a year. Relative precipitation and evapotranspiration can also vary seasonally on a regional and local basis. For example, the basins of northern Nevada are quite cool in late fall and winter and receive most of their precipitation in the form of snow in the early winter and spring; however, they are quite hot and dry during the summer months (Shevenell, 1996). The mountain ranges, due to their higher elevation and orographic precipitation effects, have higher precipitation and lower evapotranspiration than the adjacent valleys in the wet seasons. In contrast, southern Nevada receives its precipitation in the form of both winter rains and summer monsoonal rains; however, the basins of the area are hot enough throughout the year for potential evapotranspiration to predominate greatly over precipitation, and so the overall climate is quite arid (Shevenell, 1996). Local scale variations in precipi-

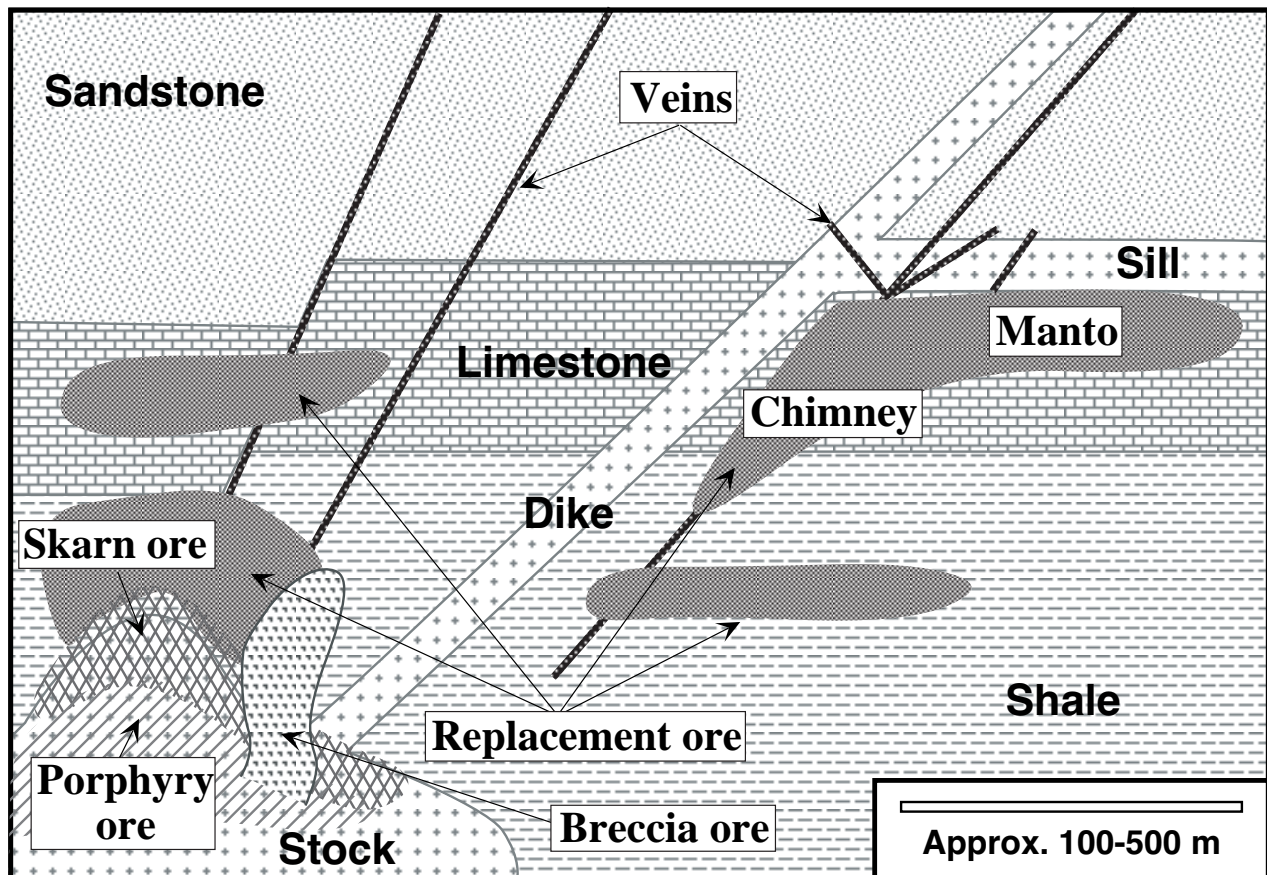


FIGURE 3.15—Schematic cross section of mineral-deposit types that may form from the intrusion of a magmatic stock into a sedimentary-rock sequence containing carbonates, shales, and sandstones.

tation relative to evapotranspiration can also result from variations in topography and the direction slopes face relative to the dominant sun direction. For example, in the eastern foothills of the Colorado Rocky Mountains, Douglas fir (indicative of relatively abundant water) grow on the shaded north-facing slope of a hill, whereas ponderosa pines and scrub junipers (indicative of less available water and higher evapotranspiration rates) grow on the sun-baked south-facing slopes, even though the overall precipitation rates are the same on both sides of the hill.

Links between climate, mineral-deposit geology, and environmental processes

The major links between climate, geology, and the environmental effects of mineral deposits are best known from studies of soil (FitzPatrick, 1980), hydrologic studies (Domenico and Schwartz, 1990, and references therein), and studies of supergene enrichment of ore deposits (Guilbert and Park, 1986). However, systematic studies of the environmental geology and geochemistry of mineral deposits as a function of climate are in their infancy. Nonetheless, some generalizations can be made.

In general, the water table is shallow in wet climates with high precipitation relative to evapotranspiration, and deep in semi-arid to arid climates with high evapotranspiration relative to precipita-

tion. Deep weathering and sulfide oxidation profiles therefore tend to develop in semi-arid climates due to the generally deep water tables. In wetter climates, shallow water tables tend to preclude very deep oxidation. However, even in semi-arid and wet climates, depths to water table and resulting depths of weathering can be quite variable depending upon the local topography and geologic conditions. For example, the depth to water table in individual mining districts in the mountain ranges of the semi-arid U.S. southwest can vary from 0 to several-hundred-meter depths, depending upon proximity to incised canyons.

Weathering of, and element leaching from, rocks and mineral deposits tend to be intense in humid tropical climates, due to the warm temperatures and organic acids generated by the abundant decaying vegetation. In contrast, element leaching and weathering rates are much less intense in arid deserts and cold arctic regions. In humid to semi-arid climates, leaching and transport tends to be downward, whereas in arid climates, evaporation-driven upward movement of water by capillary action becomes a significant process.

High rates of evaporation in arid and semi-arid climates also result in increased alkalinity in surface waters and ground waters in the unsaturated zone. Carbonate-rich waters can produce extensive carbonate cements and weathering rinds in soils and alluvial sediments in semi-arid to arid climates.

As shown by Plumlee et al. (1999), mine waters draining sul-

fide-mineral-bearing deposit types that generate acid mine waters tend to have lower pH and higher metal contents in dry climates than in wet climates due to lesser dilution by fresh waters and greater evaporative concentration of acid and metals. Evaporative processes can also have important effects in wet climates that have seasonal wet and dry periods; as discussed previously, evaporation of acid waters to dryness triggers the formation of soluble metal sulfate salts, which then dissolve readily during the next rain or snowmelt. However, data summarized by Plumlee et al. (1999) indicate that relative shifts in pH and metal content for a given deposit type in different climate settings are generally less than shifts due to differences in geologic characteristics.

Very cold climates can have several consequences for mineral environmental processes. First, weathering rates decrease substantially in very cold climates. For example, unweathered sulfide minerals may be abundant at the ground surface where climate favors permafrost formation. However, during short warmer summer seasons in areas dominated by otherwise very cold climate, weathering of sulfide minerals exposed at the ground surface can lead to formation of highly acidic water, depending upon the mineral-deposit geology (i.e., Kelley and Taylor, 1997). Partial freezing of acid waters can also lead to increased acidity and metal contents in the residual waters (W. Miller, oral commun., 1994).

Climate effects on environmental impacts downstream from mineral deposits can be significant. For example, downstream dilution (and therefore environmental mitigation) of acid mine water by dilute water draining unmineralized areas is much more efficient in wet climates than in dry climates. In contrast, downstream mitigation is enhanced in dry climates by the increased acid-neutralizing capacity of solid material in stream beds and soils, coupled with the generally higher alkalinities of surface waters draining unmineralized areas.

Effects of mining and mineral processing methods

The techniques used to extract and process ores can substantially affect the nature, volumes, and compositions of mine wastes, waters, byproducts, and airborne emissions needing treatment to prevent or minimize environmental impacts.

A wide variety of mining and mineral processing methods are currently in use; even more have been used over the course of historic mineral extraction activities. Ultimately, mining and mineral processing methods used to exploit a deposit are strongly dependent on the geologic and mineralogic characteristics of the ore. For example, vein ores continue to be most economically extracted by underground tunnels, adits, and stopes. In contrast, disseminated and stockwork deposits such as porphyry-Cu and -Mo deposits are at present most economically extracted using either surface open-pit methods or large-volume underground methods such as block caving. The large-scale underground and open pit mining methods have only become technologically feasible and widely used in the last 40–50 years.

The biggest environmental effect of mining method (open-pit vs. underground block caving vs. underground tunnels, stopes and adits) is in the amount of disturbance generated and the amount of mineralized rock exposed to weathering. Abundances of acid and metals in mine waters draining deposits with similar geologic characteristics tend to progressively increase from waters draining underground workings, to those draining mine dumps and mill tailings, to those which collect in open pits (Plumlee et al., 1999).

This trend is due to increasing access to weathering agents (water and atmospheric oxygen), increased surface area of sulfide minerals exposed to weathering, and increased opportunities for evaporative concentration.

Mineral processing methods have also evolved as new technological advances have been made, enabling the economic processing of lower-grade ores in higher volumes. As with mining method, however, the geologic nature of the ores controls the optimum mineral processing method used to extract metals from ore. In the past century, physical crushing and sorting methods, such as jig crushers, were followed by roasting or smelting to extract metals contained in sulfide ores, and amalgamation was used to extract Au from oxidized or pre-roasted ores. Cyanidation milling became popular for the treatment of Au ores in the early 1900s. In the 1950s and 60s, froth flotation of sulfides allowed economical processing of large volumes of sulfide-bearing porphyry ores. Cyanide heap leach methods (Smith and Mudder, 1999) have become economically in the last several decades to extract gold from oxidized low-grade ores. Heap leach solvent extraction (where the sulfide or oxide ores are treated with sulfuric acid to leach the metals, and the metals remove from the acid solution with organic solvents) have been used in the last decade to process lower-grade Cu ores.

The size of particles produced by milling and beneficiation processes can dramatically influence their environmental impacts. Particles in finely milled ore and tailings have very high surface areas and abundant broken crystal edges, which greatly enhance mineral reactivities relative to those of mined rock and waste rock. Thus, sulfide oxidation and acid-generation rates can increase substantially. In addition, tailings particles are more likely to be distributed by wind and water than their more coarse-grained equivalents in waste-rock piles.

One important way in which mineral processing techniques influence potential environmental impacts relates to the way in which potentially environmentally-problematic chemicals were utilized. For example, mercury amalgamation was widely used as a gold extraction technique in the United States in the last century. As a result, soil and sediments may be mercury-contaminated at many sites where amalgamation was practiced historically, but would not otherwise be characterized by elevated mercury abundances in the deposits themselves.

ENVIRONMENTAL SIGNATURES THAT ARE INFLUENCED BY DEPOSIT GEOLOGY

As discussed in previous sections, significant differences in the environmental-geology characteristics may exist between mineral deposits of different types, and within a given mineral deposit. These differences are clearly discernible in the environmental signatures produced during the natural weathering of mineral deposits and by the mining and processing of the mineral deposits. In this section, the links between the environmental-geology characteristics of mineral deposits and their environmental signatures will be discussed.

Drainage water compositions

Geologic controls on the compositions of mine waters and natural waters draining a number of mineral-deposit types are inter-

preted in detail by Plumlee et al. (1999), and so will only be discussed briefly here. Other studies examining the roles of deposit geology in controlling drainage-water compositions include Runnells et al. (1992), Price et al. (1995), Barry (1996), and Kelley and Taylor (1997). A subset of data presented by Plumlee et al. (1999) are summarized graphically on Figure 3.16 using element-pH plots, in which dissolved mine- and natural-water compositions are grouped according to the geologic characteristics of the specific ore types drained by the waters. This type of graphical portrayal is useful to examine compositional similarities of waters draining specific ore types that occur in more than one deposit type, such as waters draining propylitically altered rocks in porphyry, epithermal, and polymetallic vein systems.

The data show that, without considering geologic characteristics, both mine and natural drainage waters span a broad range of pH values (>9 pH units) and dissolved metal concentrations (for some metals, ranging ten orders of magnitude, from less than a part per billion [ppb] to tens of thousands of parts per million [ppm]). However, when grouped according to the dominant geologic characteristics of the ore types they drain, the drainage water compositions cluster in groups having much smaller ranges in pH (generally <several pH units) and metal concentrations (generally <several orders of magnitude). While clearly not sufficiently detailed to permit a precise and accurate prediction of the pH and metal concentrations of a specific water draining a specific ore type or deposit type, this type of graphical representation nicely illustrates the role of geology in influencing drainage compositions.

The groupings of data by geologic characteristic illustrate the integrated role of both deposit geology and geochemical processes in controlling drainage compositions. The overall trend of increasing metal content and decreasing pH results from the increasing acid-generating capacity (pyrite, sulfide content) and decreasing acid-neutralizing capacity (amounts and types of carbonates) of the deposits. For waters with a given pH, metal contents increase with increasing pyrite and sulfide content, and increasing exposure of Zn-, Cu-, and other metal-sulfides near the ground surface. The relative abundances of Zn, Cu, As, and U in the deposits are also manifested in their concentrations in the drainage waters.

Geochemical controls such as the solubility of Fe and sorption onto Fe particulates are also manifested in the plots. Waters with elevated Fe concentrations at near-neutral pH values have low dissolved oxygen levels, which preclude the formation of hydrous ferric oxide and hydroxysulfate particulates. Near-neutral pH waters with elevated Zn are due to high amounts of pyrite in sphalerite-galena ore bodies, coupled with the lack of Zn sorption onto particulates (Smith, 1999). The steep trends of decreasing U and As concentrations with increasing pH below pH 5 are due to sorption onto particulates, and the increasing abundance of particulates; however, both U and As show increasing concentrations with increasing pH above pH 5–6. For U, this results from desorption caused by the formation of aqueous uranyl carbonate complexes (Wanty et al., 1998, 1999). For As, this results from both desorption and the lack of Fe particulates to sorb the As in near-neutral waters with low dissolved oxygen.

As shown in detail by Plumlee et al. (1999), systematic variations in drainage composition can be linked to variations in geologic characteristics within mineral deposits. Figure 3.17 shows that the different mineralogic zones of the Central City-Idaho Springs, Colorado, mining district (Fig. 3.9) are marked by char-

acteristic and fairly distinct ranges in metal concentration and pH.

Natural and mine waters draining deposits of the same type and same geologic characteristics within a deposit type also have fairly characteristic and predictable ranges in pH and metal concentrations. Figure 3.18 depicts the compositions of mine waters (Summitville and Red Mountain Pass, Colorado; 3R mine, Patagonia Mountains, Arizona) and natural waters (Mt. Macintosh, B.C., Canada) draining quartz alunite epithermal deposits. Mine waters draining the core acid-sulfate alteration zones of these deposits all are highly acidic and metalliferous. Waters draining the intermediate argillic and distal propylitic alteration zones have progressively lower metal concentrations and higher pH values, resulting from progressively greater acid-neutralizing capacity.

In addition to the Al, Fe, Zn, and Cu found in most mine-drainage waters, the waters draining the advanced-argillic alteration zones of Summitville and other quartz-alunite epithermal deposits also have quite high dissolved concentrations of a number of more exotic elements such as Cr, Co, Ni, Be, and rare-earth elements (REE) (Fig. 3.19). It is likely that the elevated concentrations of these metals result from both release of trace metals via sulfide oxidation, and the partial dissolution of the altered host rocks. For example, Co, Ni, and Cr are unusually enriched in the volcanic host rocks in the area (T. Steven, oral commun., 1992), and so their elevated concentrations in mine waters most likely result from acid-attack of wallrock minerals containing these elements.

Waters draining the unmined quartz-alunite epithermal deposit at Mt. Macintosh, B.C., have similar ranges in pH and concentrations of Al and Fe as their mine-water counterparts, but have lower concentrations of Cu, Zn, As, and other trace metals (Fig. 3.18). Similar differences between natural water compositions and mine-water compositions are present in other mineral-deposit types where sulfides are not exposed at the ground surface. However, in unmined deposits where sulfides have been exposed at the ground surface by glaciation (i.e., SEDEX deposits in Alaska; Kelley and Taylor, 1997) or by rapid physical erosion (i.e., the Alamosa River stock, Colorado; Fig. 3.5e) the concentration ranges of Zn, Cu, and other trace metals are nearly identical to those measured in mine waters draining the same deposit types.

A plot of Cu concentrations in adit and seep outflows from Summitville in the 11 years following inception of open-pit mining (Fig. 3.20) illustrates both the rapidity with which acid-mine waters can develop if sulfides are reactive, and the major effect that dissolution of soluble salts can have on mine-drainage compositions. The soluble salts form in the historic underground mine workings and rock fractures beneath the open pit during dry periods in mid-summer and fall, and then are flushed out by snowmelt waters in late spring. In addition to Cu, the adit waters have very high concentrations of Fe^{2+} and many other metals, which mimic the concentration variations shown by Cu. Soluble Cu-sulfates and ferrous sulfates such as melanterite, and their contained trace elements are the likely sources for these metals (Nordstrom and Alpers, 1999). The dramatic increase in metal loadings from the Reynolds adit, especially during spring snowmelt (flows in excess of 1,000 gallons per minute were common in late May and early June of 1993), prompted the plugging of the adit as part of Superfund site remediation. The Chandler adit (located some 800 m north of and 80 m higher than the Reynolds; Fig. 3.10) was also plugged, but developed a substantial leak within 6 months of the Reynolds plugging, as the waters backed up in the underground

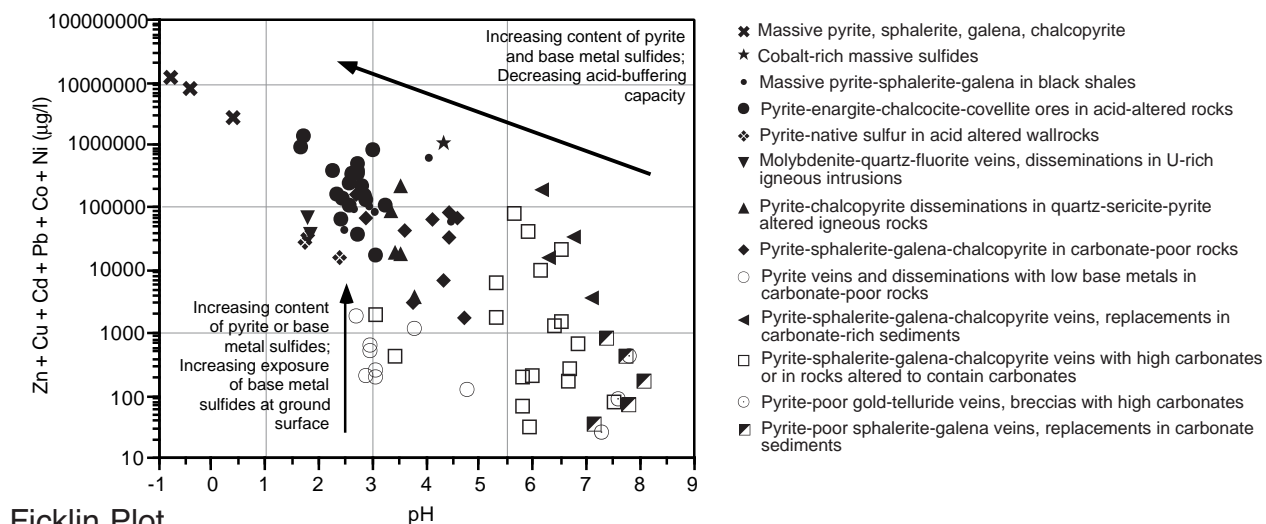
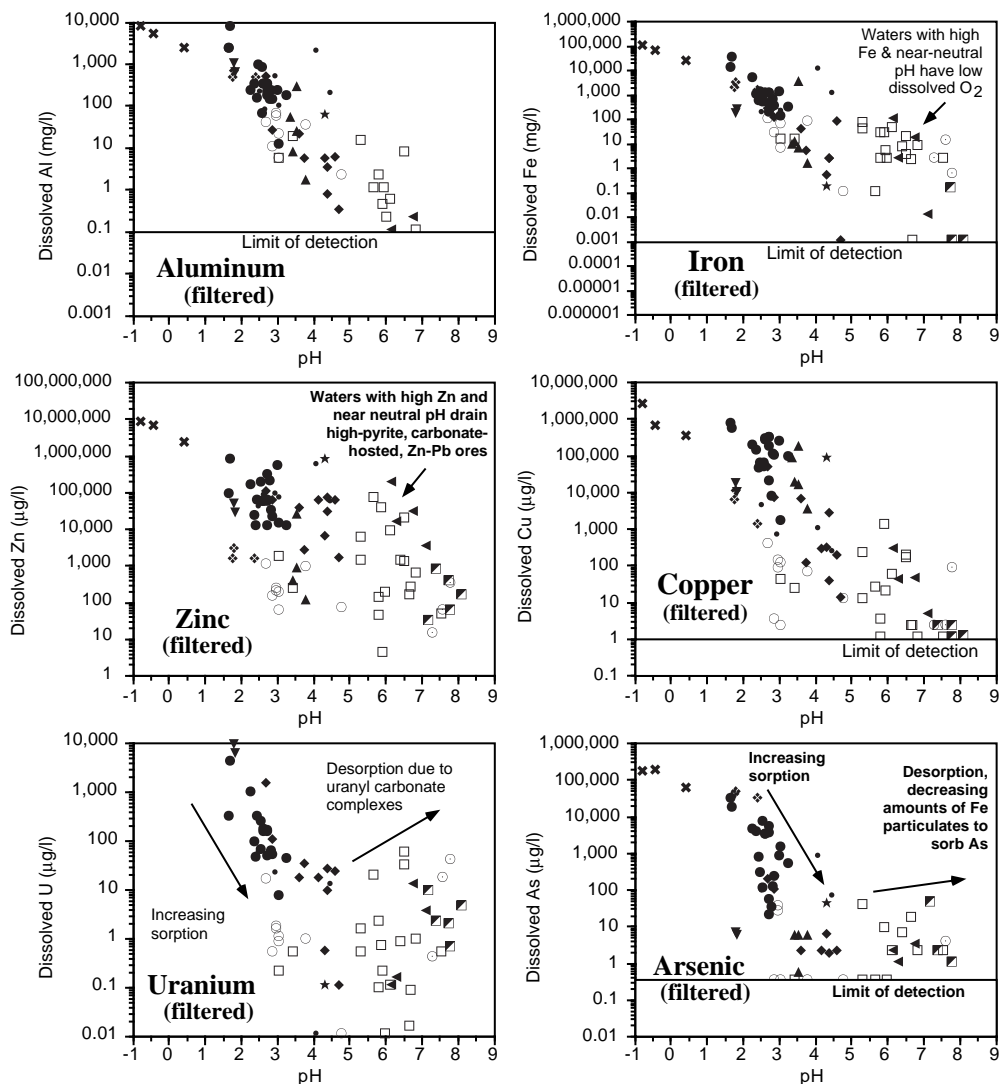


FIGURE 3.16—Plots showing the metal-pH compositions of mine waters and natural waters from mineralized areas, grouped according to the geologic characteristics of the ore types, alteration zones, etc., that they drain. The plots are from Smith et al. (1994), and show a subset of the data presented by Plumlee et al. (1999). The Ficklin plot at the top of the page shows the sum of base metals Zn, Cu, Cd, Pb, Co, and Ni, the generally predominant trace metals found in mine waters and natural waters draining unmined mineral deposits. See discussion in Plumlee et al. (1999) regarding metal concentration units used for the plots.



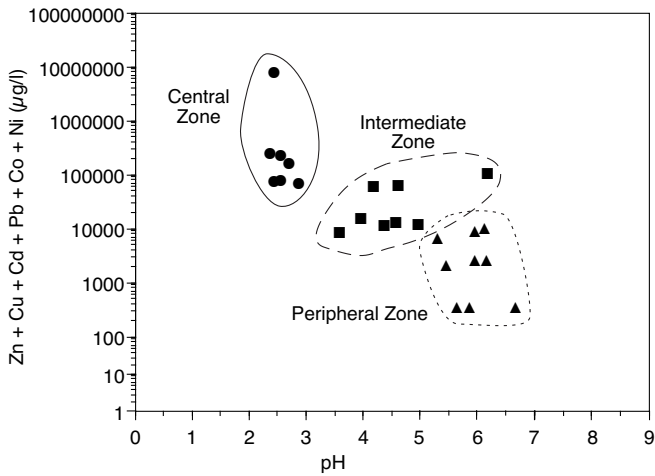


FIGURE 3.17—Ficklin plot showing the composition of mine waters draining different mineralogic zones of the Central City-Idaho Springs mining districts, Colorado (Fig. 3.9). Data from Plumlee et al. (1999) and Wildeman et al. (1974).

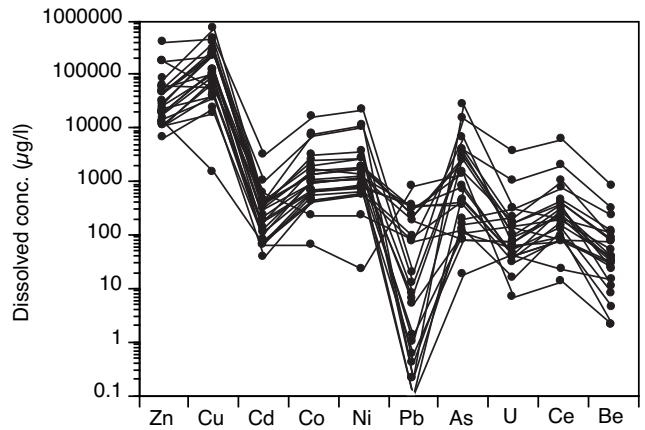


FIGURE 3.19—Concentrations of metals in waters draining acid sulfate alteration zones of quartz-alunite epithermal deposits. Data from Plumlee et al. (1999). Figure modified from Plumlee et al. (1995c).

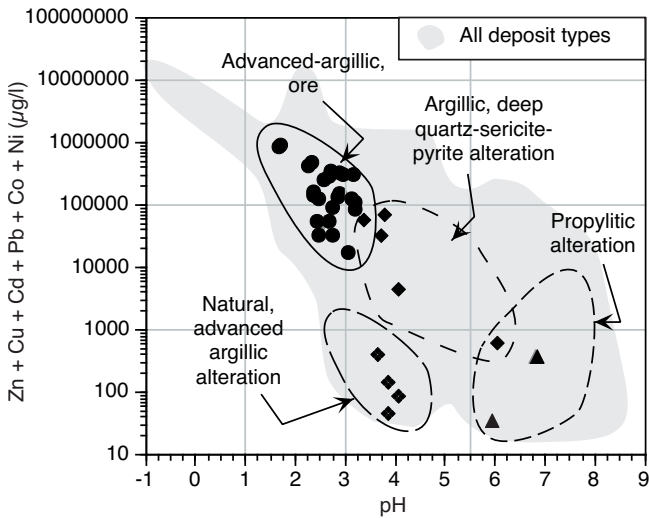


FIGURE 3.18—Ficklin plot showing the compositions of mine and natural waters draining quartz-alunite epithermal deposits. Data from Plumlee et al. (1999). Figure modified from Plumlee et al. (1995c) and Plumlee et al. (1999).

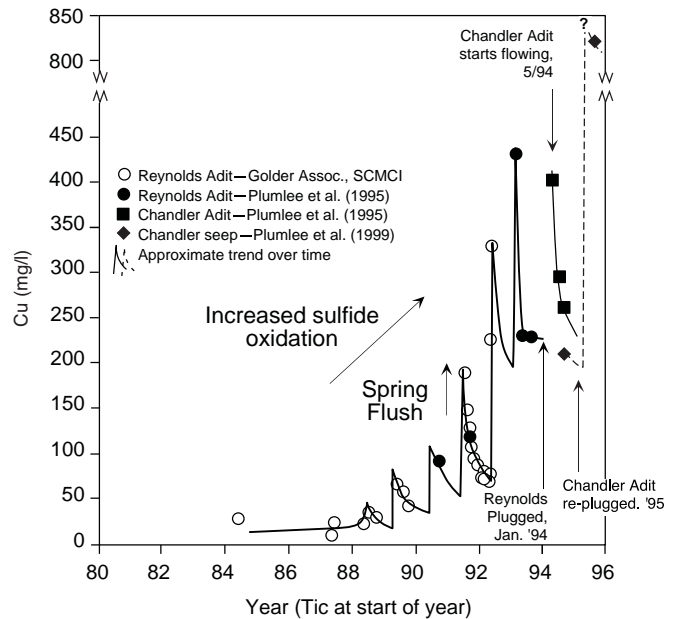


FIGURE 3.20—Plot of copper concentrations in adit and seep outflows from the area beneath the Summitville open pit since the start of open-pit mining in 1985. Figure modified from Plumlee et al. (1995b). The hollow symbols show data collected by Golder and Associates for the mining company, Summitville Consolidated Mining Co., Inc. (SCMCI) prior to the bankruptcy of the company in 1992.

workings. The Chandler adit was re-plugged in 1995, resulting in a substantial decrease in Cu loads leaving the site. However, the pre-mining seeps (Fig. 3.10) reactivated by the adit plugging had, as of 1995, higher Cu concentrations than the adit waters.

Simple loading and price calculations indicate that the gross (pre-extraction) value of major metals leaving Summitville in solution via Reynolds adit waters during 1993 peak spring flow

was in excess of \$20,000 U.S. per day (Fig. 3.21). At present, Cu is the only one of these metals that might have been economically extractable from the Summitville mine waters; Cu-rich mine waters have long been viewed as economic resources in many porphyry-Cu mines, which commonly extract the Cu with shredded auto parts and other scrap steel. In the future, mine-waters draining geologically favorable mineral deposit types such as

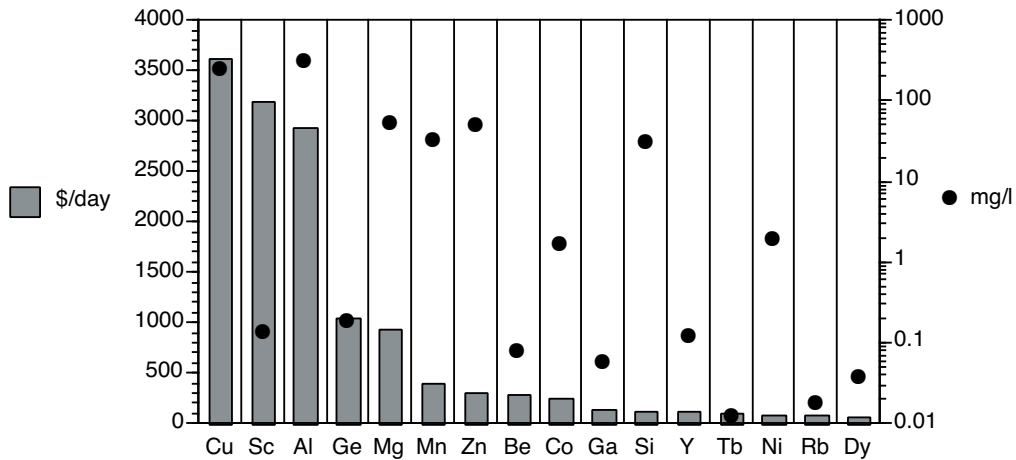


FIGURE 3.21—Concentrations and calculated gross (pre-extraction) values of various metals in Reynolds adit waters during peak spring flow, early June 1993. The values were calculated using estimated metal prices for that general time period. Mine-drainage data from Plumlee et al. (1995b). Flow value of 1000 gallons per minute was used to estimate total loadings of metals per day carried by the waters.

Summitville may at some point (with appropriate advances in metal extraction technology) be viewed as economic resources for a variety of metals, rather than as environmental liabilities.

Mine-drainage data from polymetallic vein and replacement deposits at Leadville, Gilman, and Silverton, Colorado, New World, Montana, and Nabesna, Alaska, illustrate the range in water compositions that can be produced by different deposit types in a given district (Fig. 3.22). Waters draining igneous-hosted polymetallic vein ores and skarn ores with low carbonate contents produce the most acidic waters, resulting from the lack of acid-neutralizing reactions with the igneous wallrocks and skarn calc-silicate minerals. Sediment-hosted skarn, vein, and replacement deposits can also produce mine waters with a wide range in metal

content and pH, depending upon the carbonate content of the sediments, the extent to which the waters react with the carbonates, and the pyrite content of the ores.

Climate and mining method controls on drainage compositions

The data presented on Figures 3.16–3.22 also illustrate the generally subordinate controls that climate and mining method exert on natural and mine-drainage compositions. For example, the data for pyrite-enargite-covellite ores in acid-sulfate altered rock (Fig. 3.16) include compositions from Summitville and Red Mountain Pass, Colorado (waters draining adits, mine waste piles, and open pit ponds in wet, cool mountainous climates). Data from the 3-R Mine, Arizona, located in a hot, semi-arid climate, are not shown on Figure 3.16 (Plumlee et al., 1999), but fall within the same range of pH and metal contents as those of Summitville and Red Mountain Pass. Although the compositions of the 3-R waters are similar to those of Summitville and Red Mountain Pass, their effects on the surrounding surface water environment are not; they flow for only a portion of the year, and when they do flow they do not persist far downstream due to loss by evaporation and loss into the vadose zone below the stream beds.

As discussed by Plumlee et al. (1999), waters draining mine waste piles and tailings impoundments can be quite acidic and metal-bearing in deposit types with large amounts of carbonate minerals. This likely results from the large surface area of sulfides exposed in the waste-rock piles and tailings impoundments, the lack of reaction with acid-neutralizing carbonates that are armored by secondary hydrous Fe- and Al-oxides, and the dissolution of soluble sulfate salts from sulfide surfaces by rain and snowmelt waters.

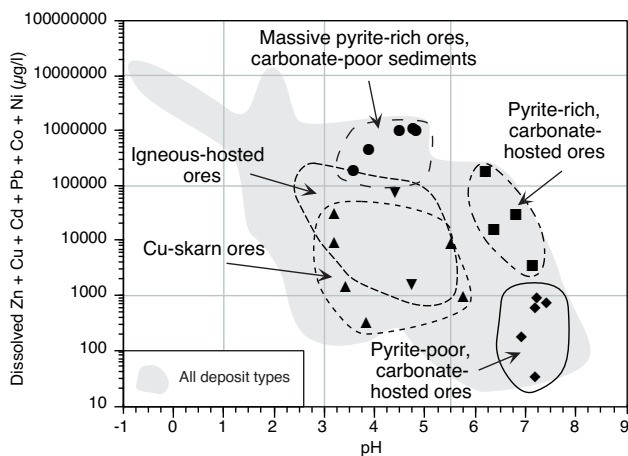


FIGURE 3.22—Ficklin plot comparing the concentrations of mine waters draining different ore types that are found in polymetallic vein and replacement deposits. Data are from Leadville, Gilman, and Bandora, Colorado (polymetallic replacements); New World, Montana (Cu-skarn; Pioneer Technical Services, 1994); Nabesna (Au skarn; Eppinger et al., 1997). Data are listed in Appendix of Plumlee et al. (1999).

Mineral processing waters

There are a variety of mineral processing (beneficiation) methods that use water-based reagents to either physically concentrate

ore minerals or chemically extract ore elements from the surrounding gangue material. For a detailed discussion of the chemical reagents used in mineral beneficiation, the reader is referred to general texts on the subject (e.g., Ripley et al., 1996). Although the chemical compositions of mineral processing solutions are largely controlled by the complex chemical reagent mixtures needed for the specific beneficiation processes, the solutions can be modified chemically through reactions with the ore and gangue materials, and thus can be influenced by the mineralogy and trace-element compositions of the ore being processed.

Froth flotation waters

Froth flotation processing of sulfide ores uses a variety of soap-like organic chemicals with high surface tension that, when frothed, create bubbles to which the milled sulfide particles adhere. Other reagents such as cyanide may also be added to the processing solutions to enhance the process. Although processing solutions are recycled repeatedly, they eventually end up in tailings impoundments, where the reagents may be isolated by impoundment reclamation, diluted by rainfall, concentrated by evaporation, or gradually degraded by bacterial, photolytic, or other geochemical processes. As the processing solutions react with the ore and gangue minerals, they can pick up dissolved heavy metals. In sulfide-rich tailings impoundments, the processing solutions, which typically are maintained to relatively alkaline pH during the beneficiation process, may be acidified by oxidation of sulfides and dissolve heavy metals from the sulfides. Due to the organic chemical degradation and sulfide oxidation, tailings impoundment waters can therefore eventually develop compositions that are quite similar to those draining mine dumps and mine workings of their deposit type (see above).

Cyanidation and cyanide heap-leach processing waters

Cyanidation milling and cyanide heap leach processing both use cyanide solutions to chemically extract gold and (or) silver (Smith and Mudder, 1999). Cyanidation solutions and heap leach processing solutions typically are maintained at pH values near 10 using lime in order to maximize CN^- concentrations and gold extraction efficiency. If the ores are very low sulfide or are completely oxidized (either naturally by pre-mining oxidation, or by pre-cyanidation roasting), then the process waters are composed primarily of free cyanide and gold- and silver-cyanide complexes, and gold extraction efficiency is greatest. Concentrations of Fe, Cu, and other metals are generally low because their oxides are relatively insoluble in the alkaline processing waters.

If appreciable amounts of sulfides are present in the ores being treated, then sulfide oxidation can reduce solution pH. It can also produce elevated concentrations of thiosulfate (derived by reactions of cyanide with intermediate oxidation-state sulfide species) and cyanide complexes with a variety of other metals (such as zinc, copper, cobalt, and nickel). In general, the concentrations of these metals in the processing solutions mimic their abundances in the ores. For example, heap leach processing of Cu-rich, sulfide-bearing ores at Summitville, Colorado (Plumlee et al., 1995b), produced processing waters with quite elevated thiocyanate and copper concentrations (as high as several hundred ppm), and relatively high concentrations of iron, cobalt, and nickel (several

ppm). Although iron sulfides are abundant in the Summitville ores, Fe concentrations were typically limited to several ppm by the precipitation of insoluble hydrous iron oxides or Fe (\pm Cu) cyanides. In contrast to the Summitville heap leach solutions, a solution produced during cyanide heap-leach testing of sphalerite-bearing polymetallic vein ores from Central City, Colorado, had several hundred ppm Zn, Ag, and thiocyanate (G. Plumlee, unpub. data). Experimental studies by Ficklin et al. (1995) showed that alkaline heap leach solutions are effective at extracting As from realgar, orpiment and other As-bearing minerals. Thus, heap leach solutions from As-rich deposits (such as Carlin-type sediment-hosted Au deposits) may contain up to several ppm As.

Heap-leach, solvent-extraction processing waters

In recent years, heap-leach processing and solvent-extraction/electrowinning have been used to extract copper from both oxide and sulfide ores. The ores are placed on a heap leach pad and treated with sulfuric acid, which dissolves metal sulfide, oxide, sulfate, and carbonate minerals from the ores. The Cu is then extracted from the processing waters using organic solvents, and the Cu extracted from the solvents using electrowinning. Due to the use of sulfuric acid, these processing waters develop compositions that are lower in pH but similar in their contained metals to acid-mine drainage. However, metal concentrations of the leach waters are substantially higher than those of mine waters, due to the repeated cycling of the processing waters through the heap leach. For example the leach waters may contain very high to extreme concentrations of Fe, Al, and sulfate (thousands of ppm), and Cu and Zn (many hundreds to low thousands of ppm).

Processing waters and byproducts from some industrial mineral deposits

Some industrial mineral deposits, such as phosphate deposits, rare earth deposits, and titanium deposits, have significant environmental considerations that result directly from mineral processing. The processing liberates and concentrates potentially deleterious trace elements contained in the ores as waste byproducts.

Rouse (1974) summarized the environmental issues related to the mining and processing of the phosphate deposits in Florida. The deposits are chemical sediments composed largely of nodules of apatite (a calcium phosphate mineral) that commonly contains high concentrations of U, F, Cl, REE, and Cr as trace impurities. The phosphate concentration process involves initial washing to remove fine phosphate particles as slimes, followed by amine flotation to remove silica sand particles. The phosphate concentrate is then ground and acidulated, where it is reacted with sulfuric acid to produce either a mixture of superphosphate and gypsum, or phosphoric acid and waste byproduct gypsum. The byproduct gypsum is a substantial waste product that is stored in large piles near the processing plants. Prior to the mid-1970s, environmental considerations such as the release of fluorine into the atmosphere from processing plants, disposal of highly acidic, F- and P-rich waste waters, dust, and SO_2 emissions from sulfuric acid plants were recognized and being largely remediated. However, the issue of potential radiochemical releases was largely not recognized until the 1970s (Rouse, 1974). Due to the high

levels of U in the original ore, the radioactive decay of U and its daughter products, primarily radium-226 and radon-222, in the waste processing waters, slimes, and gypsum byproducts were recognized to be of potentially significant environmental concern. As a result, new environmental mitigation measures were needed, such as better waste disposal procedures, and the prohibition of the use of byproduct gypsum in the manufacture of wallboards.

Titanium processing uses sulfuric acid to dissolve resistate minerals such as ilmenite and rutile. The processing also releases a variety of trace metals into the sulfuric acid. For example, Schuiling and van Gaans (1997) and van Gaans and Schuiling (1997) measured compositions of acid-discharge waters from a TiO₂ processing plant in the Ukraine, and found a pH of 0.85 and extreme concentrations of Fe, Na S, and Cl (tens of thousands of mg/l); Al, Ca, Ti, P, Si, Mn (hundreds of mg/l); Cu, Cr, Ce, V, Sr, and Ni (tens of mg/l). Although these studies did not determine concentrations of radionuclides such as U, Th, Ra, and Rn, it is possible that they may also be present in elevated concentrations. Placer sand deposits, the most common source of Ti ore, commonly contain other resistate minerals such as monazite, columbite, zircon, and tantalite that are enriched in these radionuclides (see, for example, Eisenbud, 1987; Filippidis et al., 1997; and references therein).

Effects of mine-drainage, natural-drainage, and mineral-processing waters on ground- and surface-water quality

The geochemical and biological effects of waters draining unmined mineral deposits and, if released into the environment, mine waters and mineral-processing waters, are a complex function of many interrelated factors. The composition and flow (volumes) of a poor-quality water relative to those of ground or surface-waters with which it mixes affects how rapidly and effectively the chemical effects of the degraded water are mitigated downstream. Other processes such as chemical precipitation (formation of particulates), sorption, photochemical processes (i.e., photoreduction of iron), physical processes (physical settling or resuspension of particulates), and biogeochemical processes (i.e., bacterially catalyzed reactions such as iron oxidation) also play important roles in the downstream mitigation of degraded waters (Nordstrom and Alpers, 1999; Smith, 1999).

As acid-rock drainage flows into a fresh stream, it is progressively diluted by the stream waters. This dilution triggers an increase in pH of the acid drainage, which leads to the precipitation of orange hydrous ferric oxide colloids and particulates; the precipitation of the iron particulates also results in part from the gradual oxidation of ferrous iron in the acid waters by oxygen in the oxygenated stream waters. Once the pH of the mixture rises above 4.5–5, white aluminum colloids and particulates form. As shown by Smith (1999), suspended Fe and Al particulates can effectively sorb most trace elements (As, Pb, and most Cu) in the manner and order discussed previously; Zn, Cd, Ni, and, to a lesser extent, Cu, are not as effectively sorbed. Suspended particulates settle as they reach low-velocity areas downstream, form coatings on the rocks and sediment in the stream bed, and remove (at least temporarily) their sorbed trace metals from the surface water system. Particulate-rich bed sediments are relatively ineffective at sorbing metals from the waters flowing over them, and are easily eroded from the stream bottom during periods of high flow.

Seasonal changes in water chemistry may lead to desorption of trace metals from the uppermost bed sediments and resuspended particulates. Process such as photoreduction of iron may also lead to dissolution of some of the particulates.

The controls of watershed geology

Geology (with the modifying effects of climate) can play an important role in controlling the downstream or down-gradient effects of mine- or natural-drainage waters. The influence that geologic characteristics of mineral deposits have on the compositions of mine, natural-drainage, and mineral-processing waters has been discussed previously. Similarly, the geologic characteristics of the rock units in a watershed around a mineral deposit can influence the compositions of the ambient ground and surface waters in the watershed, including their alkalinities, major-element concentrations, and trace-element concentrations. The compositions of these ambient waters influence the downstream chemical and biological effects of acid-mine drainage and mineral processing waters. For example, as discussed previously, the higher the alkalinity of a stream- or ground-water, the more effective a given volume of the water is at reacting with and consuming the acid in acid-mine waters. Hence, watersheds with carbonate-rich rocks (such as limestones or dolomites), or reactive silicate rocks (for example, ultramafic rocks such as dunites or serpentinites) generally produce surface waters with higher alkalinities and acid buffering capacities than watersheds with carbonate-poor, less-reactive rocks such as many granites.

The role of climate

Climate can substantially affect the acid-buffering capacities of waters in a watershed. In drier climates, high evaporation rates tend to increase the alkalinities and acid-buffering capacities of waters draining most rock types, including those with low carbonate contents or reactivities (W. Miller, oral commun., 1996). Thus, smaller volumes of alkaline surface waters draining many rock types in dry climates can mitigate the effects of acid drainage waters as effectively as larger volumes of less alkaline waters draining similar rock types in wetter climates.

A comparison of two watersheds affected by acid-rock drainage

The effects of watershed geology on the downstream impacts of acid-mine drainage can be seen by comparing two mineralized watersheds in southwestern Colorado, the Animas and Alamosa River basins (Fig. 3.23). Both watersheds originate in intermediate to felsic volcanic rocks of the San Juan volcanic field. Both are characterized by extensive mineralization in their headwaters, including quartz-alunite epithermal deposits (Summitville on the Alamosa, and Red Mountain Pass on the Animas) that produce highly acidic mine-drainage waters (Fig. 3.18) and polymetallic to adularia-sericite epithermal vein deposits that produce, depending upon the carbonate content of the veins and wallrock alteration, variably acidic and metalliferous drainage waters. Both also have their headwaters in high mountains with high precipitation (in excess of 1 meter annually); both have high snowfall in winter and

intermittent thundershowers and dry conditions in summer. Both flow from the mountains into adjacent lowlands that are very dry, with less than 10–20 cm total annual precipitation.

However, there are important geologic differences between the watersheds. The Animas drains extensive areas of propylitically altered volcanic rocks in its headwaters, and drains carbonate-rich sedimentary rocks downstream from its headwaters. In contrast, the Alamosa River drains several large, predominantly unmined areas of pyritic alteration that produce extensive natural acid drainage; although propylitically altered rocks are present on the fringes of the pyritically altered areas, they are relatively minor in volume. The Alamosa River also drains volcanic rocks throughout most of its length, and does not drain carbonate-rich sedimentary rocks.

As a result of the differences in their watershed geology, waters in the Alamosa and Animas Rivers have very different chemical compositions. Tributaries of the Animas River that drain the Red Mountain Pass mineralized systems are quite acidic and metalliferous; however, once these waters mix with waters from numerous other tributaries draining carbonate-bearing, propylitically altered rocks, and the carbonate-rich sedimentary rocks downstream, the pH of the Animas River rises to near-neutral levels, abundant Fe-, Al-, and Mn-rich colloids and particulates form, and most metals other than Zn and Cd sorb onto the particulates.

The Alamosa River water is quite acidic and metalliferous in its headwaters, due to largely natural acid rock drainage from the pyritically altered areas (Kirkham et al., 1995). Creek names such as Iron, Alum, Bitter attest to the naturally degraded water quality in the headwaters of the Alamosa. Few tributaries drain unmineralized rocks, and those that do are generally of relatively low volume. Thus, Alamosa River has a relatively limited capability to mitigate the effects of acid rock drainage. The tremendous increases in acid-rock drainage that resulted from recent open-pit mining at Summitville thus flowed into a river that was already quite acidic during most times of year. As a result, especially during dry periods when dilution from unaffected tributaries was minimal, quite acidic waters can persist well downstream. For example, in late summer, 1994 (when significant volumes of untreated acid waters were leaving the Summitville site), irrigation waters drawn from the Alamosa River some 60–70 km downstream from Summitville had pH values as low as 3.9 and dissolved Cu concentrations near 1 ppm (Fig. 3.24).

Possible downstream effects of cyanide heap leach solutions: Summitville as an example

Accidental releases of cyanide heap-leach processing solutions have occurred at several mine sites in recent years. The potential downstream environmental effects of cyanide-bearing processing solutions are influenced in part by the composition of the processing solutions (i.e., whether the cyanide is present as free cyanide, weak-acid dissociable cyanide complexes, or complexes that do not dissociate readily in weak acids) (Smith and Mudder, 1999). Geochemical and biogeochemical processes such as volatilization, bacterial degradation, precipitation of insoluble cyanide solids, and photolytic degradation influence how rapidly cyanide is degraded once in the environment (Smith and Mudder, 1999). In general, degradation is most rapid in systems open to the atmosphere, either in surface waters or in the vadose zone above the water table. As with acid-mine drainage, the climate and geology

of the watershed into which the heap solutions are released play an important role in the downstream persistence and environmental effects of the cyanide, most importantly by controlling the volumes and compositions of the waters with which the heap leach solutions interact. Summitville is an example of one extreme, in which heap leach solutions interacted with highly acidic waters affected by acid-mine drainage.

Summitville perhaps received more public attention for several accidental releases of cyanide heap leach processing solutions from the site during mining than it did for its acid-rock drainage problems. However, the exact number, magnitude, and sources (heap leach pad versus the french drain beneath the pad) of cyanide releases from Summitville are not well documented, nor are their actual downstream effects on surface water quality.

In an attempt to interpret the possible fate of cyanide accidentally released into the environment from Summitville, Plumlee et al. (1995b) carried out laboratory experiments in which they mixed samples of heap leach solutions from Summitville with water collected from the Wightman Fork of the Alamosa River (Fig. 3.25). The experiments were designed to simulate the chemical evolution of the Wightman Fork waters after receiving an influx of cyanide-bearing solutions from the heap leach impoundment. The mixing experiments were carried out in the sun (to take into account photolytic cyanide degradation), and compressed air was bubbled into the mixed solution to simulate the churning of the Wightman Fork waters as they flowed over the ~8-km course to the Alamosa River.

The experimental results suggest that, depending on the time of year and the magnitude of the release, acidic waters from Summitville may have helped degrade cyanide accidentally released from the heap-leach impoundment. Further, the alkaline heap leach solutions may have improved downstream water quality by neutralizing the acid Wightman Fork waters. The experimental results indicate that acid in the Wightman Fork waters broke down the Cu-cyanide complexes to form hydrogen cyanide, which then volatilized and caused water pH to increase further. In addition, ferric iron from the acid-mine drainage also likely combined with the Cu-cyanide complexes to precipitate insoluble Cu-Fe-cyanide solids. Copious orange (presumably hydrous ferric oxide) and white (presumably aluminum hydroxysulfate) precipitates also formed in the experiments, which helped to sorb Cu, Pb, and other metals from solution. The relatively positive effects indicated by these experiments may not have occurred, however, if: the flow volumes of heap leach solutions released were substantially greater than the flow volumes of Wightman Fork water at the times of release; if the releases occurred during winter when ice cover over the Wightman Fork inhibited cyanide volatilization; or if the cyanide releases were of acidic mixtures of heap leach waters and acid drainage from the french drain system underneath the heap leach pad.

In watersheds where acid drainage is not present, the likelihood increases that cyanide accidentally released into the environment will persist for appreciable distances downstream. The persistence and environmental effects of the cyanide will depend on the relative flow volumes of the released solutions versus those of the local surface waters, the degree of turbulence in the local surface waters, and the compositions of the local surface waters (a function of climate and watershed geology). Dilution of alkaline heap leach solutions by near-neutral surface waters (in most temperate climates) or acidic surface waters (in wet climates where decay of organic matter generates humic acids) will eventually lead to

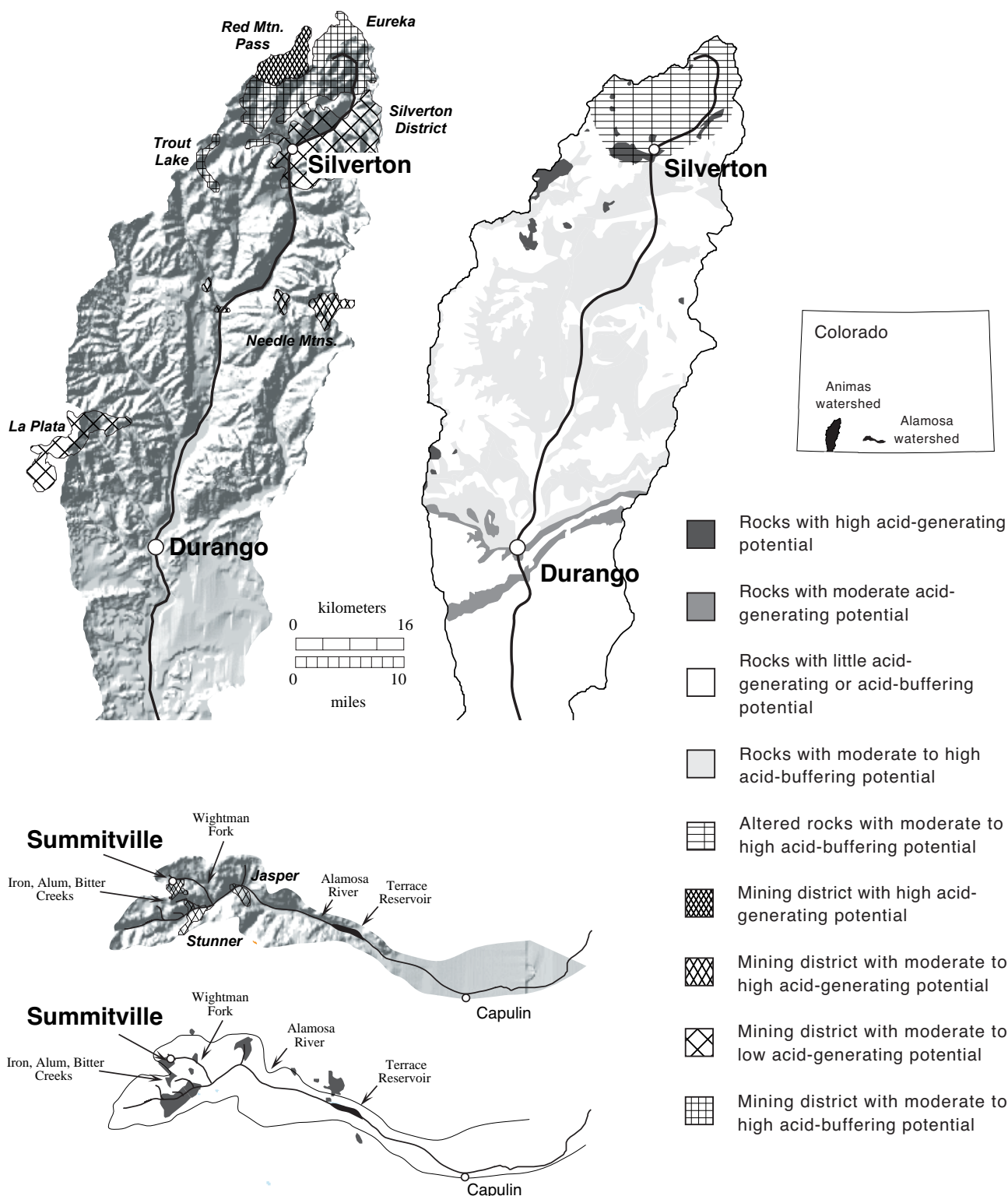


FIGURE 3.23—Maps comparing the environmental geology and mining districts of the Animas (upper) and Alamosa (lower) watersheds, southwest Colorado, that are affected by both natural acid rock drainage and mine drainage. The environmental geology of the watershed rock units is compiled from the Colorado state geologic map (Tweto, 1985; Green, 1992). Mining districts are from Plumlee et al. (1995d) and references therein.

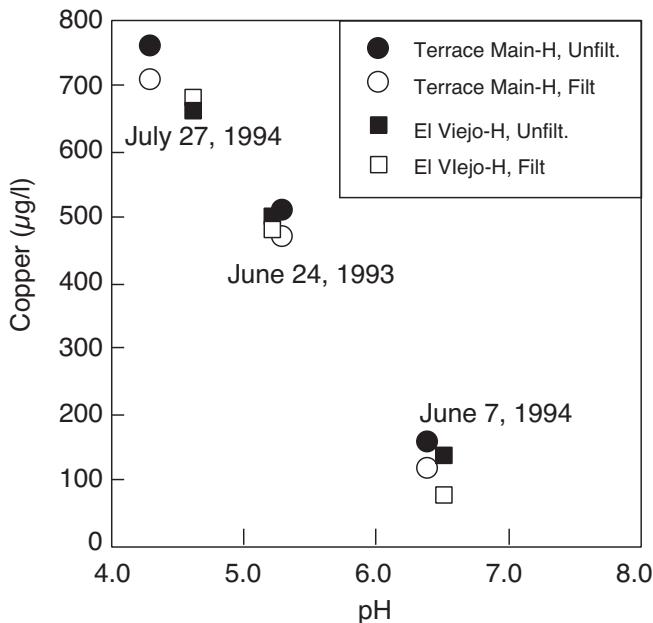


FIGURE 3.24—Plot of the pH and copper concentration in filtered (filt.) and unfiltered (unfilt.) irrigation waters taken from irrigation ditch headgates along the Alamosa River in 1993 and 1994, during the peak impacts of acid drainage resulting from open-pit mining at Summitville. The collection points for the water are some 60–70 km downstream from Summitville, and thus demonstrate the Alamosa River watershed’s lack of capacity to self-mitigate significant influxes of acid-rock drainage. Figure modified from Smith et al. (1995).

breakdown of weak cyanide complexes and cyanide volatilization (see Smith and Mudder, 1999). However, metals complexed by the cyanide may persist in solution if particulate matter is not present to sorb the metals. As with the experiments conducted by Plumlee et al. (1995b), the potential downstream effects of heap leach solutions from a site may be evaluated experimentally by mixing samples of the heap leach solutions and local surface waters.

Soil and sediment compositions

The mineralogic and geochemical compositions of soils that form on and stream sediments that are deposited downstream from a weathering mineral deposit are the complex result of many interacting geologic, geochemical, biological, and climatic processes. The byproducts of human resource extraction activities (such as mining and processing wastes, smelter emissions, etc.) add many more layers of geologic and geochemical complexity to interpret. However, there are a number of ways that geologic and geochemical information can be used to interpret the relative contributions to and environmental significance of multiple natural and anthropogenic sources in the overall makeup of soil or stream-sediment samples. Many examples are presented in the exploration geochemistry literature (see Rose et al., 1979, and the *Journal of Geochemical Exploration*, for example), and in the burgeoning literature on environmental geology (see, for example, the journals *Environmental Geology*, and *Environmental Geochemistry and Health*).

Soil compositions

Soils that form by the weathering of underlying rocks mimic in large part the original mineralogic and geochemical makeup of the rock, but also in part result from various aspects of the weathering process that are controlled by non-geologic factors (such as topography, rain and snowfall amounts, ambient temperature, vegetation types and amounts, etc.). Soils developed on unmineralized rocks that are not enriched in any trace metals tend to have low natural concentrations of metals of environmental concern (such as Hg, As, Cu, Zn, Pb, etc.). In contrast, metal concentrations in soils developed on trace-element-rich bedrocks or directly on weathering mineral deposits can have extremely high concentrations of many of the same elements enriched in the mineral deposits. For example, Chaffee (1987) measured very high total concentrations of Pb (as high as 10,000 ppm) and Zn (as high as 30,000 ppm), and moderate to high concentrations of Cu (up to

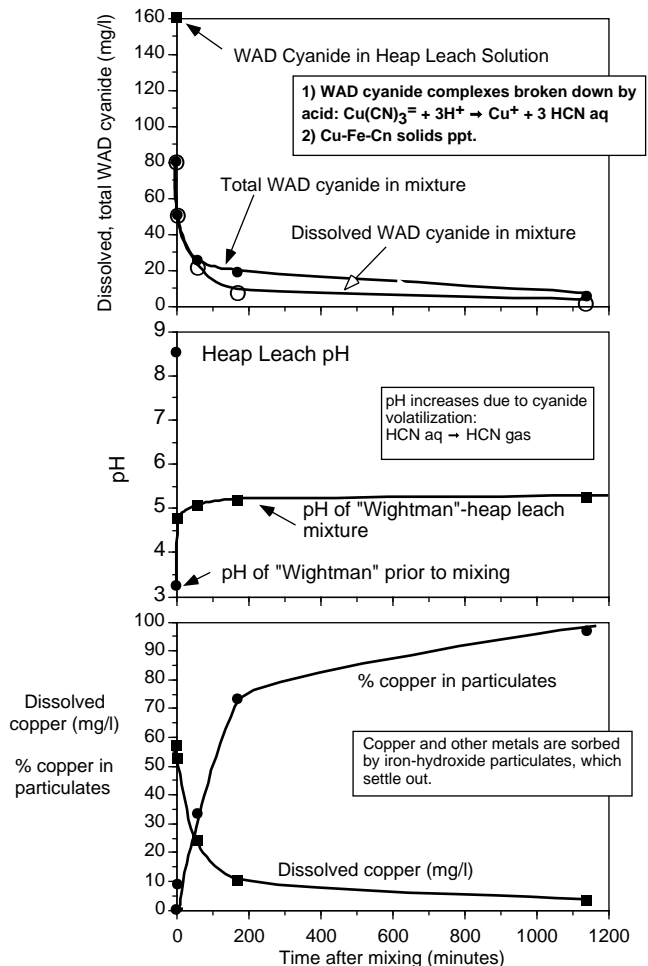


FIGURE 3.25—Plots of cyanide concentrations (upper), pH (middle), and dissolved copper (lower) over time in a mixing experiment simulating the mixing cyanide heap leach solutions from Summitville with Wightman Fork waters. “WAD”—weak acid-dissociable aqueous cyanide complexes (such as those with Zn and Cu). “Ppt.”—precipitates. Figure modified from Plumlee et al. (1995b).

500 ppm) and Sb (up to 400 ppm) in soils developed on mineralized carbonate host rocks of the polymetallic Pb-Zn-Cu replacement deposits, Eureka district, Nevada.

Stream sediment compositions

Stream sediments downstream from a weathering mineral deposit typically contain a mixture of minerals, including: the less easily weathered primary minerals of the deposit and host rocks (i.e., quartz, some feldspars, clays, and resistates such as Fe- and Fe-Ti-oxides, native Au, columbite, apatite, zircon, etc.); secondary minerals formed during the weathering process (clays, hydroxides, insoluble metal carbonates or sulfates); and secondary minerals precipitated from the surface waters (Fe-, Al-hydroxysulfates and hydrous oxides that contain sorbed metals). In drainages where sulfides are exposed at the surface by glaciation or high erosion rates, sulfides can comprise a significant portion of the stream sediment package as well. Organic detritus can also be present in trace to major amounts.

Natural concentrations of metals derived from a weathering mineral deposit can be quite high in stream sediments close to the deposit, but decrease with increasing distance downstream due to dilution by sediments from other sources. For example, pre-mining stream sediments downstream from polymetallic replacement deposits at Leadville, Colorado contained thousands of ppm lead in the form of secondary cerussite; in fact, the polymetallic nature of the deposits at Leadville was discovered because a heavy mineral that was greatly decreasing placer gold recovery was identified as cerussite. In the last several decades, stream sediment geochemistry surveys of unmined mineralized areas have been responsible for the discovery of a number of economic ore deposits.

Where mining and mineral processing activities have released material into the environment, still more complexities are added to the bulk geochemical compositions of stream sediments. Physical transport of solid materials from mine-waste dumps and mill-tailings adds a variety of minerals originally present in the deposit; these minerals add high concentrations of the metals that, depending upon the mineral, may be released into solution or taken up by plants and organisms. Secondary minerals (such as yellow- to orange hydrous ferric oxides and iron hydroxysulfates, and white aluminum hydroxysulfates) precipitate through chemical reactions such as dilution. These secondary particulates can settle out in slow-flow portions of the stream and contribute significantly to the composition of the stream sediments. Because they effectively scavenge other metals and As (Nordstrom and Alpers, 1999; Smith, 1999) these secondary precipitates can contribute significant concentrations of these elements in a readily-liberated form to the stream sediments.

A number of regional stream sediment geochemistry surveys were carried out as part of the United States National Uranium Reconnaissance Evaluation (NURE) program in the mid 1970s. Interpretations of the NURE data illustrate the combined effects of naturally elevated metal concentrations in stream sediments around mineralized areas and elevated metal concentrations in stream sediments resulting from human activities such as mining, mineral processing, smelting, and automobile use. In Colorado (Fig. 3.26), elevated lead concentrations in stream sediments highlight historic mining districts such as Leadville (which contributed metal loadings to the stream sediments both naturally prior to

mining and as a result of mining), locations of smelters, and other sources of lead such as particulate lead contributed by burning of leaded gasoline prior to the 1970s (prevalent in metropolitan areas). Areas with moderate lead concentrations in soils in some cases result from weathering of lead from lead-rich rocks such as granites.

The geoavailability of metals from soils and sediments

Surveys such as those depicted on Figure 3.26, which measure total metal concentrations in stream sediments, do not give an indication of how readily the metals may be taken up from the sediments by waters, plants and animals (i.e., how geoavailable they are; Smith and Huyck, 1999). However, geochemical surveys can be carried out that measure not only total metal concentrations but also concentrations released in each of a series of sequential chemical extractions (see Crock et al., 1999). Such extractions subject soil or sediment samples to sequential leaches of increasingly strong acids and other reagents, which dissolve increasingly resistant, less readily-weathered mineral phases. Such leaches commonly dissolve metals tied up in (listed in general order of decreasing geoavailability) (a) water-soluble minerals (such as soluble sulfate salts), (b) colloids, (c) poorly crystalline, fine-grained hydrous Fe- and or Al oxide and hydroxysulfate particulates, (d) carbonates, (e) sulfides and organics, (f) silicates, and (g) resistate minerals such as ilmenite, rutile, zircon, columbite, and others.

When coupled with detailed mineralogical studies of the sediments, these sequential extraction studies provide important insights into how readily the metals contained in stream sediments downstream from a mining district may be released into the environment. For example, Church et al. (1997) demonstrated that a significant component of the lead, zinc, copper, and arsenic in stream sediments in the Animas River watershed, Colorado are stored in readily available form, sorbed onto colloidal and more crystalline but fine-grained particulates. When ingested by invertebrates, the metals tied up in these particulates may be present in concentrations high enough to be toxic (Church et al., 1997).

The geoavailability of metals from soils and stream sediments also may be determined by directly measuring the amounts of metals taken up by waters, plants, or organisms that come in contact with or ingest the sediments. For example, Dwyer et al. (1988) studied metal uptake by longear sunfish living in a part of the Big River near Deslodge, Missouri, which had large amounts of Pb-, Zn- and Cd-rich mill tailings incorporated into its stream sediments as a result of accidental releases from a tailings impoundment. Dwyer et al. (1988) found elevated levels of Pb, Cd, and Zn in blood and muscle tissues of the fish, as well as biochemical indicators of the effects of these metals on the biologic activity of the fish.

Techniques to discriminate natural from anthropogenic contributions to metal concentrations in soils and sediments

It is generally very difficult to discern the relative geochemical contributions of multiple geologic and anthropogenic sources for soil or stream sediment samples, based solely on the concentrations of major and trace elements in the samples. However, a variety of statistical and isotopic techniques have been developed that,

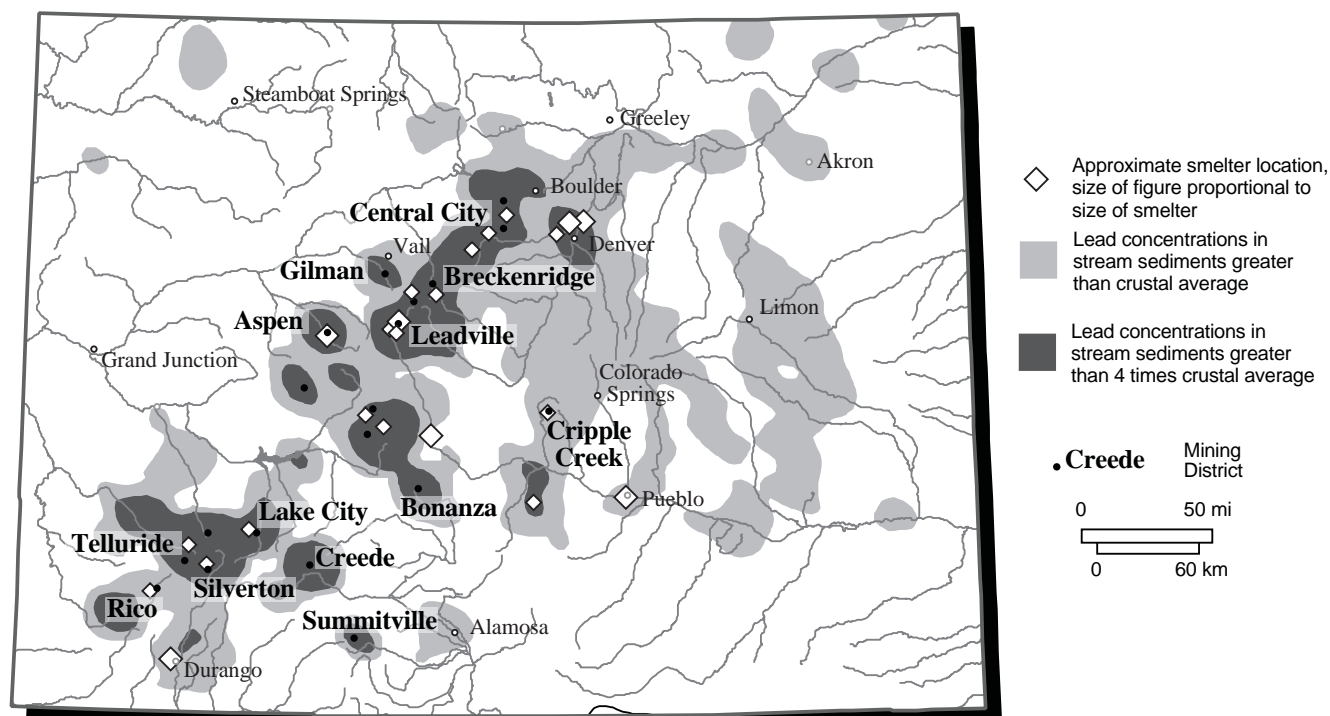


FIGURE 3.26—Map of Colorado showing contours of lead concentrations in stream sediments collected throughout the state as part of the NURE program. Names of mining districts are shown in bold dark text, and cities in plain text. Locations and relative sizes of some historic smelters (taken from Fell, 1979) are also shown.

when used in conjunction with surficial geology and geomorphology studies, significantly improve the chances of successfully differentiating relative contributions from multiple sources.

Multivariate statistical techniques such as factor analysis (i.e., Johnston, 1980) have been developed that can discriminate, for a sufficiently large population of samples, different suites of elements that are statistically associated. The analysis also estimates the relative proportions of different element suites, or factors, contained in a given sample of the population. The technique can be used for samples collected regionally, or locally within a smaller area such as a mining district.

Tidball et al. (1995) measured the geochemical compositions of soils, stream overbank sediments, and aeolian (windblown) sediments collected from throughout the San Luis Valley, Colorado, in order to examine the effects of acid-mine drainage and materials eroded from Summitville on soils and stream sediments in the southwestern part of the valley near the Alamosa River. They collected samples on a grid with spacing between samples varying from 2–5 km, and from 0–30 cm depth in the soil profile; they analyzed then analyzed these samples for 40 elements. Soil paste pH was also measured for each sample. The results were then interpreted with the aid of factor analysis. Seven factors, or geochemical associations of elements, were identified (Table 3.9), and then scores for each factor at each sample site were plotted and contoured on a map of the valley (see, for example, Fig. 3.27). Factors 1, 2, and 5 were interpreted to result from sediments derived primarily from volcanic or igneous rocks of various origins. Samples with high scores for these factors occur primarily on the margins of the valley, on or near alluvial fans

whose rivers drain areas underlain by these rock types in the adjacent mountains. Factors 3 and 5 result from geochemical enrichments caused by evaporation of shallow ground waters, and are greatest in samples collected in the central parts of the valley where evaporation rates are greatest. Factors 4 and 7 indicate high contributions from mineralized areas. Samples with high factor 4 scores occur on or near alluvial material deposited by streams draining Pb-Zn mining districts such as Creede and Bonanza to the west of the valley. Factor 7 scores are greatest in soils collected on the Alamosa River fan and in the floodplain of the Alamosa River, and therefore indicate a high contribution of elements from Summitville (Tidball et al., 1995) and other mineralized areas in the Alamosa River watershed.

In a soil geochemistry survey of the Eureka district, Nevada, Chaffee (1987) used factor analysis to help identify soils in and near the district that were not contaminated by heavy metals emitted from local smelting. Samples with anomalously high levels of a variety of heavy metals (Ag, As, Au, Mo, Hg, Pb, Cu, Zn, and others) occur both in soils derived from weathering of the mineralized rocks and in soils near smelters. In contrast, Ba, Co, Mn, and V are anomalous over mineralized areas but not near the smelters; elements with high factor scores for this association were therefore interpreted as having minimal smelter contamination. Factor analysis also identified two soil geochemical associations that Chaffee interpreted as being derived from two distinct mineral-deposit types in the district, including the polymetallic-replacement deposits from which the bulk of the district's historic production came, and sediment-hosted Au deposits previously unidentified in the district. These results show that factor analysis

TABLE 3.9—Compositions of element suites (or factors) determined by Tidball et al. (1995) using factor analysis for a large set of soil, aeolian sediment, and stream overbank sediment samples collected from the San Luis Valley, Colorado. For each factor, the elements that make up the factor are listed in decreasing order of dominance, based on the correlation between the factor scores and the concentrations of elements in the samples. Interpreted origins for each factor are also shown (from Tidball et al., 1995).

Correlation coefficients						
Factor 1	Factor 2	Factor 3	Factor 4	Factor 5	Factor 6	Factor 7
Nd, 0.953	Fe, 0.965	Mg, 0.917	Pb, 0.922	Cr, 0.895	Na, 0.882	As, 0.705
Ce, 0.942	V, 0.922	Ca, 0.849	Zn, 0.858	Ni, 0.882	K, 0.651	Cu, 0.616
La, 0.934	Ti, 0.892	Sr, 0.662		Co, 0.635		
Nb, 0.827	Co, 0.870	S, 0.456		Sc, 0.632		
Y, 0.822	Sc, 0.809					
Th, 0.683	Ga, 0.631					
Yb, 0.647						
Rhyolitic, granitic source	Andesitic source	Alkaline evaporative salts	Pb-Zn ores	Basalt source	Saline evaporative salts	High-sulfidation mineralization

is not only useful in a mineral exploration context, but also can be used to help establish pre-mining baseline geochemical conditions in districts having significant historic mining and smelting impacts.

A number of studies have successfully used radiogenic isotopes to help understand the sources and their relative contributions to the geochemical makeup of stream sediments or soils. Lead isotopes have proven extremely useful in identifying multiple sources of lead in mineralized watersheds, including different mining districts and different rock units that each have distinctive lead isotopic signatures (i.e., Church et al., 1993, 1997, 1999; Östlund et al., 1995). For example, the lead isotopic composition of stream sediments upstream and downstream from the Penn Mine, California (Church et al., 1999) clearly shows the significant contribution of lead (as much as 71%) and other related metals from the Penn Mine ores relative to contributions of lead from rocks upstream in the drainage basin.

Stratigraphic sampling of overbank or lake sediments, coupled with ^{210}Pb (Robbins, 1978), ^{137}Cs (Ritchie and McHenry, 1984) or other isotopic or geomorphic dating of the sediments, also provides an indication of variations in metal concentrations in stream sediments over time. If the sedimentary record is long enough, such techniques may permit determination of pre-mining baseline concentrations of metals in the sediments. For example, Horowitz et al. (1996) examined the bed-sediment geochemistry of Terrace Reservoir, located on the Alamosa River downstream from Summitville (see the location of the reservoir on Fig. 3.27). They found that the onset of enrichment of many metals (Cu, Pb, Zn, Cd, As, Hg, Fe, and Al) in the reservoir sediments substantially predates the open-pit mining at Summitville, and that the open-pit mining may have marginally increased the concentrations and fluxes of some of these metals in the reservoir sediments.

Mobility of metals from solid mine and mineral-processing wastes

Metals may be liberated from solid mine wastes and mineral processing wastes by weathering, sulfide oxidation, and dissolution of soluble secondary salts. In addition, animals or aquatic organisms that directly ingest the solids may take up metals into their systems. As discussed in the previous section on geologic

controls on mine-drainage compositions, the mineralogy of the waste material plays an important role in controlling how readily metals are liberated from the wastes into the environment. Waste rock piles with large amounts of soluble secondary salts (which therefore usually have high contents of reactive sulfides) will have a greater likelihood of producing acidic, metalliferous waters during storm or snowmelt events. Tailings solids, due to their fine grain size resulting from crushing and grinding, are likely to be more reactive than geologically similar waste rocks, and hence are likely to have greater potential metal mobility than the mine wastes.

There are a number of tests, including humidity cell tests (White and Jeffers, 1994), column tests (Filipek et al., 1999), tank tests (Logsdon and Basse, 1991), and leach tests (Montour, 1994), that may be used to help estimate potential metal mobility in aqueous form from solid mine and mineral processing wastes.

The extent of metal uptake directly by an organism that ingests solid mine or processing waste particles also is a function of the mineralogy of the wastes, coupled with the chemical conditions inside the organism's gastro-intestinal tract. Experiments have been developed to simulate metal mobility in gastro-intestinal tracts of some organisms such as rabbits (Davis et al., 1992). Metal uptake by organisms can also be evaluated by measuring the concentrations of metals in organism tissues and blood (for example, Dwyer et al., 1988).

Smelter slag and emissions

Sulfide ore smelting results in the formation of waste slag (through the reaction of iron in the ores with silica flux), and gaseous emissions containing both sulfur dioxide (an acid-generating gas) and particulates with high concentrations of the metals contained in the ores. Although modern smelters have scrubbers that remove much of the sulfur dioxide and metal-bearing particulates, emissions from past smelters lacking the scrubbers are a significant environmental concern in the areas immediately around and downwind from the smelters. Metal mobility from slag, although commonly low, may be potentially important at some sites.

A number of mineralogical and geochemical studies of smelter slag piles (e.g., Lasmanis et al., 1997) and of the soils and plants

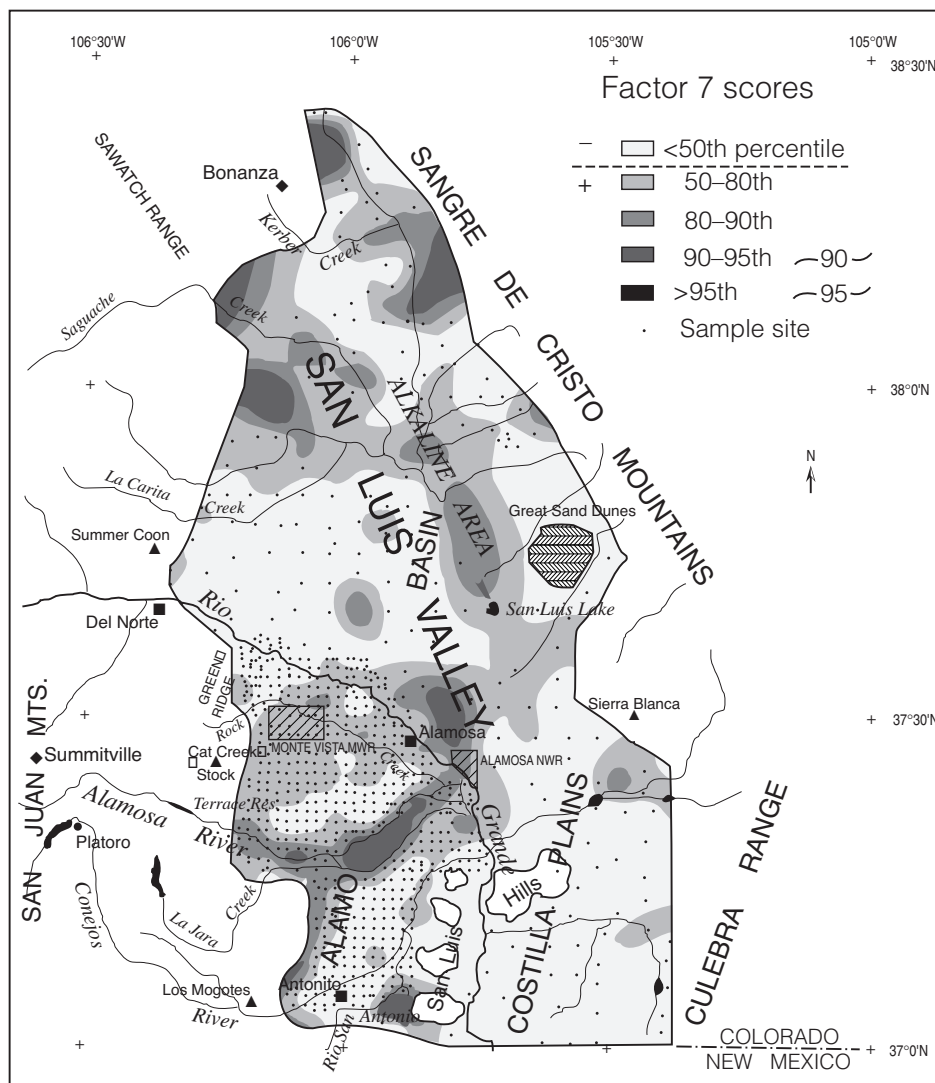


FIGURE 3.27—Map of the San Luis Valley, south-central Colorado, showing contours of factor 7 scores in soil samples for the As-Cu element association, as determined by R-mode factor analysis of the soil geochemistry data. Darker shades within contours indicate a greater component of the As-Cu element association in the geochemical makeup of soils. Note the very high levels in the floodplain sediments and soils of the Alamosa River alluvial fan in the SW corner of the valley. Figure modified from Tidball et al. (1995).

affected by particulate smelter emissions (e.g., Chaffee, 1980, 1987; Montour, 1994; Maskall et al., 1996; Karczewska, 1996) have been conducted. These studies show that the slags and soils are generally enriched in many of the same metals that were present in the ores being smelted, and that the metals can occur in very high concentrations from several hundreds to several thousands of ppm. The availability of the metals from slag is a function of the slag mineralogy, the degree to which more reactive minerals are encapsulated by less reactive phases, and the way in which the slag is cooled. The metal content of slag can be provided by remnant sulfides of the metals contained in the ores (Montour, 1994), or by less reactive oxide minerals, silicate minerals, or glass phases (Parsons et al., 1998). Slag poured on the ground surface to cool generally has lower metal availability than slag frothed into

the air to cool (J. Drexler, oral commun., 1993). Metal availability in soils affected by particulate smelter emissions is a function of the clay, organic, and moisture contents of the soil (e.g., Karczewska, 1996), coupled with the mineralogical form and geochemical properties (Smith and Huyck, 1999) of the metals in the emissions.

Plant compositions

A number of plant species can take up trace metals from waters and from the soils in which they grow. A number of studies of metal uptake by plants, as well as the application of plant chemistry as a mineral prospecting technique, are summarized by Rose

et al. (1979), other exploration geochemistry textbooks, journals such as the *Journal of Geochemical Exploration*, and textbooks such as Kabata-Pendias and Pendias (1984). Methods used to prepare plants for chemical analysis and to analyze the metal contents of plants are presented by Crock et al. (1999), and in the references cited in the following discussion.

Many trace elements (such as Cu, Zn, Mn, Fe, and Mo; Rose et al., 1979) are essential nutrients for plants. For example, Cu is involved in a variety of photosynthetic, respiration, oxidation-reduction, and other metabolic processes (Gupta, 1979). Zinc also has a variety of plant physiological functions, and is commonly associated with plant proteins and enzymes. However, excessive abundances of many otherwise beneficial trace metals may have an overall toxic effect upon a plant.

Trace metal uptake from a soil depends upon: the nutritive requirements of the different plant species growing in a soil (different plant species take up metals in greatly different amounts); the depth to which the plant roots penetrate (some plants may penetrate soil and underlying bedrock to depths of many tens of feet); the concentrations and geoavailabilities of the different trace elements in the soil or rocks in which the plant is growing; and the geochemical conditions within the soil (pH, soil moisture, oxidation state, organic matter content, etc.). Once taken up, trace elements may be stored in different concentrations in different parts of a plant such as the leaves, twigs, roots, and bark of a tree.

Many trace elements (such as Cu) are essential nutrients for plant-eating animals. However, the concentrations of particular trace elements in plants growing on mineralized rocks may reach sufficiently elevated levels that the plants become toxic to the animals that consume them. For example, selenosis and molybdenosis are two diseases in cattle that develop as a result of the cattle eating Se-rich (selenosis) or Mo-rich, Cu-poor (molybdenosis) forage.

The potential effects of acid-mine drainage from open-pit mining at Summitville on the metal contents of San Luis valley crops irrigated with Alamosa River water were a substantial concern in the years immediately following the mine closure. To address these concerns, studies were carried out in 1993 to measure the metal contents of SW San Luis valley alfalfa (Erdman et al., 1995, 1997), barley (Stout and Emerick, 1995), and wheat and potatoes (Cardon et al., 1995). Crops irrigated with Alamosa River water were found to have concentrations of various metals (such as Cu, Ni, and Mn) that were statistically higher than those of SW San Luis valley crops irrigated with near-neutral pH water from other sources (see Fig. 3.28 for the study results for alfalfa). However, the concentrations of these metals were also found to be well within the ranges of metal concentrations measured in these crops from throughout the United States. In the case of alfalfa (Fig. 3.28), the 1993 metal concentrations were well below levels considered toxic to cattle (Erdman et al., 1995). However, later sampling carried out in 1994 and 1995 (Erdman et al., 1997) indicated that concentrations of Cu in the alfalfa were increasing and beginning to approach potentially toxic levels for sheep, underscoring the need for environmental remediation at Summitville, and continued crop monitoring.

Gough et al. (1995) measured the metal content of tree rings in aspens and cottonwoods growing along the Alamosa River, to chart the spatial and temporal variations in metal contents of the river waters. Although the temporal trends (across ~30 years of tree rings) and spatial trends proved inconclusive for most elements measured, Gough et al. (1995) concluded that the analyti-

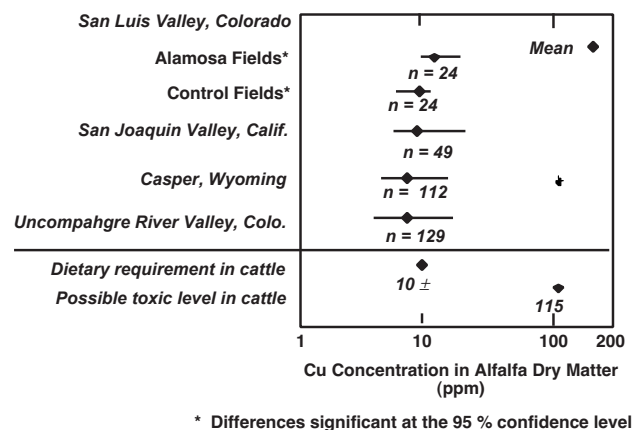


FIGURE 3.28—Plot comparing the Cu concentrations of alfalfa from fields irrigated with Alamosa River water (“Alamosa Fields”) to those of alfalfa from SW San Luis Valley fields irrigated with water from other sources (“Control Fields”), and alfalfa from elsewhere in the United States. Also shown is the dietary requirement for Cu in alfalfa fed to cattle, and the possible level of Cu in alfalfa that is toxic to cattle. Figure modified from Erdman et al. (1995). References for other data sources included on figure are also given in Erdman et al. (1995).

cal method used and the approach of dendrochemical trace element measurements hold promise for tracking metal variations over time, in spite of processes such as metal translocation across tree rings that tend to blur temporal metal variations. Gough et al. (1995) also list a number of useful references on trace metal uptake by trees and dendrochemical analytical methods.

GEOLOGY-BASED GEOENVIRONMENTAL MINERAL DEPOSIT MODELS

As shown by the discussion in the preceding sections, the same geologic characteristics that allow economic geologists to classify or type mineral deposits also play key roles in controlling the pre-mining and mining-related environmental signatures of mineral deposits. In the same way that economic geologists can develop deposit models for diverse mineral-deposit types (Cox and Singer, 1986; Kirkham et al., 1993), geology-based geoenvironmental models can also be developed for the same mineral deposit types (Plumlee and Nash, 1995; du Bray, 1995) that interpret the deposits’ environmental characteristics in a geologic context.

A preliminary compendium of descriptive geoenvironmental deposit models developed by the U.S. Geological Survey is presented in du Bray (1995). The geoenvironmental models are based on and extend the mineral deposit models originally included in Cox and Singer (1986) and Bliss (1992). The working definition of a geoenvironmental mineral deposit model given by Plumlee and Nash (1995) in the introduction of the du Bray volume is: “A compilation of geologic, geochemical, geophysical, hydrologic, and engineering information and data pertaining to the environmental behavior of geologically similar mineral deposits (a) prior to mining, and (b) resulting from mining, mineral processing, and smelting.”

For a given deposit type the geoenvironmental models included in du Bray (1995) summarize:

- Pertinent environmental geology characteristics, such as sulfide mineralogy, textures, and resistance to weathering; gangue mineralogy, textures, and resistance to weathering; wallrock alteration; host rock lithology; mineral zoning; trace element contents of the deposit and its host rocks; structural, lithologic controls on ground-water flow; and the nature and extent of pre-mining oxidation.
- Pertinent information on potential past and present mining methods (i.e., open-pit, underground, or block caving) and processing methods (froth flotation and roasting or smelting; jig concentration; mercury amalgamation; crushing, roasting, and cyanidation; crushing and cyanide heap leaching).
- As a function of climate, empirical data (where available) on environmental signatures from all mineralogic zones or ore types, including: pre-mining baseline geochemical conditions (compositions of seeps, soils, and stream sediments); compositions of mine-drainage, tailings, or cyanide heap leach waters; metal mobility from mine dumps, tailings, or smelter slag; smelter signatures in soils; and environmental effects on the surrounding ecosystem or watershed (which are a function of geology and climate).
- Useful geophysical techniques to identify, delineate, and monitor, environmental signatures associated with mined and unmined mineral deposits.
- Geoscientific guidelines for potential remediation/mitigation strategies.

Although the preliminary geoenvironmental mineral deposit models originally presented in du Bray (1995) are still evolving in concept and content (see Wanty et al., 1999 in press), they provide a very useful way in which to interpret and summarize the environmental signatures of mining and mineral deposits in a systematic geologic context. They cannot and should not be used to predict the absolute pH and metal concentrations that will develop from a particular mine dump in a particular ore zone of a particular mineral-deposit type. The models also should not be used in place of field characterization and study of mine sites. Rather, the models are best used as a series of geologic guidelines about the potential range of environmental signatures that may have been present in a district prior to mining, that may exist in a mining district as a result of historic mining activity, or that may develop as a result of mining a particular deposit (and therefore need to be accounted for in prevention and mitigation strategies).

The models underscore the utility of and need for the compilation and interpretation of empirical environmental data in a geologic context. An empirical study of mine waters draining diverse mineral deposit types presented by Plumlee et al. (1999) in the accompanying volume illustrates the utility of this empirical approach. However, the geoenvironmental models of specific mineral deposit types as presented in du Bray (1995) or Plumlee et al. (1999) do not provide on their own a complete estimation of potential environmental impacts of a mine site, mineral processing site, or unmined mineralized area on its surrounding ecosystem or watershed. These impacts are not only a function of the geology, climate, and mining/processing methods used for the particular deposit, but also of the bedrock geology, climate, and other characteristics of the surrounding watershed. An important next step in the development of geoenvironmental mineral-deposit models will therefore be the shift to a watershed- or ecosystem-based focus, where the deposits are considered not only in the context of their

geology, but also in the context of their surrounding watersheds (Wanty et al., 1999).

SUMMARY

This paper has summarized many key geologic characteristics of mineral deposits that control their environmental signatures and their effects on the surrounding environment, both prior to mining and that may result from mining and mineral processing. Careful attention to the environmental geology of mineral deposits is crucial to all aspects of mineral-resource development, from grass-roots exploration through mine development, closure, and remediation:

- *Establishment of pre-mining baseline conditions:* It is more cost-effective, technologically feasible, and realistic to remediate mine sites to the background conditions that existed in a mineralized area prior to mining, rather than to remediate to conditions found in unmineralized areas. Geologically constrained baseline data are crucial to establish reasonable pre-mining conditions for diverse deposit types in various climates. These baseline models can then be used to establish analogues for pre-mining conditions in districts where historic mining activities obscure pre-existing baseline conditions.
- *Mineral exploration:* Knowledge of the likely environmental effects associated with development of particular deposit types can be integrated into grass-roots exploration efforts. For example, development of deposit types with high geologic potential to generate very acidic mine drainage with extreme metal contents will have the lowest environmental mitigation expenses in arid climates, in deposits with extensive to complete pre-mining oxidation, or in geologic terranes with abundant carbonate rocks. Conversely, development of such acid-generating deposits in wet climates may require such expensive environmental mitigation measures as to either require high ore grades or make development non-profitable.
- *Mine planning and development:* Improved predictive capabilities provided by geologic knowledge enable mine planners to better anticipate, plan for, and mitigate potential environmental problems, rather than to try to treat (with much greater technical difficulties and costs) the environmental problems after they occur. Similarly, geologic characteristics of a particular deposit can be exploited to help mitigate potential environmental problems. For example, carbonate-bearing wallrock alteration that is often present on the fringes of deposits, or carbonate sediments that occur in the proximity of some deposits, may be useful in helping to mitigate acid drainage from sulfide-rich ore zones.
- *Remediation:* Accurate geological, geochemical, and hydrologic information (such as geologic controls on ground-water flow and ore mineralogy) is needed by engineers to develop the most effective remediation plans at mine sites. Many remedial plans implemented in the past ignored or dangerously oversimplified important geologic information. For example, adit plugging has been used or is proposed to reduce acid drainage from a number mine sites. Detailed geologic characterization is crucial to identify the location of faults or other hydrologic conduits that might reduce the effectiveness of adit plugging as a remedial solution.
- *Abandoned mine lands issues:* Although mineral resource extraction has been carried out for several millennia, relatively

little attention has been given until the last several decades to minimizing the effects of such extraction on the environment. As a result, a number of historic (meaning they were operated prior to the last several decades) mining and mineral processing sites that were abandoned once the profitable ores ran out are now potential or ongoing sources of environmental contamination. In the United States, land management agencies are currently faced with the daunting task of identifying and prioritizing for remediation all abandoned mine sites on public lands; although a large majority of these sites will not require remediation, the total number of sites to be investigated and prioritized for remediation is likely in excess of several hundred thousand. Geologic information provides land managers with a low-cost screening technique to help identify, prioritize for study, and remediate potentially hazardous mine sites on public lands.

- *Mineral deposits in a holistic context:* In the future, as metal extraction technologies improve (such as techniques to remove metals from waters) mineral deposits may be treated in a more holistic context. For example, acid-mine waters may be viewed as economic resources rather than as environmental liabilities. Techniques to extract metals in situ, or to extract environmentally problematic metals from solid mine wastes or mineral processing wastes may reduce the need for mining with physical extraction techniques, and may turn former wastes into ores. Geologic characterization and mineral-environmental deposit models will help identify mineral deposits or mineral deposit types amenable to such a holistic treatment.

Quite simply, geologic knowledge is a fundamental and critical component of environmentally friendly mineral-resource development.

REFERENCES

- Alpers, C.N., and Blowes, D.W. (eds.), 1994, Environmental geochemistry of sulfide oxidation: American Chemical Society Symposium Series 550, 681 pp.
- Alpers, C.N., and Nordstrom, D.K., 1991, Geochemical evolution of extremely acid mine waters at Iron Mountain, California—Are there any lower limits to pH?, Proceedings, 2nd Internatl Conference on the Abatement of Acidic Drainage: MEND (Mine Environment Neutral Drainage), Ottawa, Canada, v. 2., pp. 321–342.
- Alpers, C.N., Blowes, D.W., Nordstrom, D.K., and Jambor, J.L., 1994a, Secondary minerals and acid mine-water chemistry; *in* Jambor, J.L., and Blowes, D.W. (eds.), Short course on environmental geochemistry of sulfide mine-wastes: Mineralogical Association of Canada, Short Course Handbook, v. 22, pp. 247–270.
- Alpers, C.N., Nordstrom, D.K., and Thompson, J.M., 1994b, Seasonal variations of Zn/Cu ratios in acid mine water from Iron Mountain, California; *in* Alpers, C.N., and Blowes, D.W. (eds.), Environmental Geochemistry of Sulfide Oxidation: American Chemical Society Symposium Series 550, pp. 324–344.
- Barry, T.H., 1996, The geochemistry of natural waters draining hydrothermally altered and mineralized terrains in the upper Alamosa River basin, Colorado: Unpub. M.S. thesis, Auburn Univ., 220 pp.
- Bliss, J.D., 1992, Developments in mineral deposit modeling: U.S. Geological Survey Bulletin 2004, 168 pp.
- Borek, S.L., 1994, Effect of humidity on pyrite oxidation; *in* Alpers, C.N., and Blowes, D.W. (eds.), Environmental Geochemistry of Sulfide Oxidation: American Chemical Society Symposium Series 550, pp. 31–44.
- Boyle, D.R., 1994, Oxidation of massive sulfide deposits in the Bathurst mining camp, New Brunswick—natural analogues for acid drainage in temperate climates; *in* Alpers, C.N., and Blowes, D.W. (eds.), Environmental Geochemistry of Sulfide Oxidation: American Chemical Society Symposium Series 550, pp. 535–550.
- Brock, T.D., 1979, Biology of microorganisms, 3rd ed.: Prentice-Hall, Inc., Englewood Cliffs, N.J., 802 pp.
- Cardon, G.E., Ali, A.Y., McCann, J., and Lorenz, A., 1995, Metal content of wheat and potato tissue and associated soils irrigated with Alamosa river water; *in* Posey, H.H., Pendleton, J.A., and Van Zyl, D. (eds.), Summitville Forum Proceedings: Colorado Geological Survey Spec. Pub. No. 38, pp. 281–285.
- Cathles III, L.M., 1997, Thermal aspects of ore formation; *in* Barnes, H.L. (ed.), Geochemistry of Hydrothermal Ore Deposits, Third Edition: John Wiley and Sons, New York, pp. 191–228.
- Chaffee, M.A., 1980, Interpretation of geochemical anomalies in soil samples from a smelter-contaminated area, Eureka mining district, Nevada [abs.]: Technical Program, American Institute of Mining, Metallurgical, and Petroleum Engineers Annual Meeting, February, 1980, Las Vegas, Nev., pp. 56–57.
- Chaffee, M.A., 1987, Application of R-mode factor analysis to geochemical studies in the Eureka mining district and vicinity, Eureka and White Pine counties, Nevada; *in* Elliott, I.L., and Snee, B.M. (eds.), GEOEX-PO/86, Exploration in the North American Cordillera: The Association of Exploration Geochemists, Vancouver, Canada, pp. 94–108.
- Church, S.E., Holmes, C.W., Briggs, P.H., Vaughn, R.B., Cathcart, J., and Marot, M., 1993, Geochemical and Pb-isotope data from stream and lake sediments, and cores from the upper Arkansas River drainage—effects of mining at Leadville, Colorado, on heavy-metal concentrations in the Arkansas River: U.S. Geological Survey Open-File Report 93–534, 61 pp.
- Church, S.E., Kimball, B.A., Fey, D.L., Ferderer, D.A., Yager, T.J., and Vaughn, R.B., 1997, Source, transport, and partitioning of metals between water, colloids, and bed sediments of the Animas River, Colorado: U.S. Geological Survey Open-File Report 97–151, 135 pp.
- Church, S.E., Alpers, C.N., Vaughn, R.B., and Briggs, P.H., 1999, Use of lead isotopes as natural tracers of metal contamination—a case study of the Penn Mine and Camanche Reservoir, California; *in* Filipek, L.H., and Plumlee, G.S. (eds.), The Environmental Geochemistry of Mineral Deposits, Part B. Case Studies and Research Topics: Society of Economic Geologists, Reviews in Economic Geology, v. 6B, pp. 567–582.
- Cox, D.P., and Singer, D.A. (eds.), 1986, Mineral deposit models: U.S. Geological Survey Bulletin 1693, 379 pp.
- Crandell, D.R., 1971, Postglacial lahars from Mount Rainier volcano, Washington: U.S. Geological Survey Professional Paper 677, 75 pp.
- Crock, J.G., Arbogast, B.F., and Lamothe, P.J., 1999, Laboratory methods for the analysis of environmental samples; *in* Plumlee, G.S., and Logsdon, M.J. (eds.), The Environmental Geochemistry of Mineral Deposits, Part A. Processes, Techniques, and Health Issues: Society of Economic Geologists, Reviews in Economic Geology, v. 6A, pp. 265–287.
- Crowley, J.K., and Zimbelman, D.R., 1997, Mapping hydrothermally altered rocks on Mount Rainier, Washington, with Airborne Visible/Infrared Imaging Spectrometer (AVIRIS) data: Geology, v. 25, pp. 559–562.
- Davis, A., Ruby, M.V., and Bergstrom, P.D., 1992, Bioavailability of arsenic and lead in soils from the Butte, Montana, mining district: Environmental Science and Technology, v. 23, pp. 461–468.
- Deer, W.A., Howie, R.S.A., and Zussman, J., 1978, An introduction to the rock-forming minerals: Longman Group, Ltd., London, 528 pp.
- Deverell, S.J., and Fujii, R., 1988, Processes affecting the distribution of selenium in shallow ground water of agricultural areas, western San Joaquin Valley, California: Water Resources Research, v. 24, pp. 516–524.
- Domenico, P.A., and Schwartz, F.W., 1990, Physical and chemical hydrogeology: John Wiley and Sons, New York, 824 pp.
- du Bray, E.A. (ed.), 1995, Preliminary descriptive geoenvironmental models of mineral deposits: U.S. Geological Survey Open-File Report 95–231, 272 pp. (also available online at <http://minerals.cr.usgs.gov>)

- Dwyer, F.J., Schmitt, C.J., Finger, S.E., and Mehrle, P.M., 1988, Biochemical changes in longear sunfish, *Lepomis megalotis*, associated with lead, cadmium, and zinc from mine tailings: *Journal of Fisheries Biology*, v. 33, pp. 307–317.
- Eppinger, R.G., Sutley, S.J., and McHugh, J.B., 1997, Environmental geochemical study of the Nabesna gold skarn and Kennecott strata-bound copper deposits, Alaska; *in* Dumoulin, J.A., and Gray, J.G. (eds.), *Geologic Studies in Alaska by the U.S. Geological Survey*, 1995: U.S. Geological Survey Professional Paper 1574, pp. 19–40.
- Eisenbud, M., 1987, Environmental Radioactivity from Natural, Industrial, and Military Sources: Academic Press, San Diego, 475 pp.
- Erdman, J.A., Smith, K.S., Dillon, M.A., and ter Kuile, M., 1995, Impact of Alamosa river water on alfalfa, southwestern San Luis valley, Colorado; *in* Posey, H.H., Pendleton, J.A., and Van Zyl, D. (eds.), *Summitville Forum Proceedings: Colorado Geological Survey Spec. Pub. No. 38*, pp. 263–269.
- Erdman, J.A., Smith, K.S., and ter Kuile, M., 1997, Impact of the lower Alamosa river water on alfalfa, southwestern San Luis valley—1995 follow-up study of effects from the Summitville mine: U.S. Geological Survey Open-File Report 96–034, 32 pp.
- Fell, J.E., Jr., 1979, Ores to Metals, The Rocky Mountain Smelting Industry: University of Nebraska Press, Lincoln, 341 pp.
- Ficklin, W.H., Plumlee, G.S., and McHugh, J., 1995, Reactions of arsenic minerals and gold ores with alkaline cyanide solutions; *in* Morganwalp, D.W., and Aronson, D.A. (eds.), *U.S. Geological Survey Toxic Substances Hydrology Program, Proceedings of the Technical Meeting, Colorado Springs, Colorado, September 20–24, 1993: U.S. Geological Survey Water Resources Investigations Report 94–4015*.
- Filipek, L.H., VanWyngarden, T.J., Papp, C.S.E., and Curry, J., 1999, A multi-phased approach to predict acid production from porphyry copper-gold waste rock in an arid montane environment; *in* Filipek, L.H., and Plumlee, G.S. (eds.), *The Environmental Geochemistry of Mineral Deposits, Part B. Case Studies and Research Topics: Society of Economic Geologists, Reviews in Economic Geology*, v. 6B, pp. 433–445.
- Filippidis, A., Misaelides, P., Clouvas, A., Godelitsas, A., Barbayannis, N., and Anousis, I., 1997, Mineral, chemical, and radiological investigation of a black sand at Touzla Cape, near Thessaloniki, Greece: *Environmental Geochemistry and Health*, v. 19, pp. 83–88.
- FitzPatrick, E.A., 1980, Soils—Their formation, classification, and distribution: Longman, London, 353 pp.
- Freeze, R.A., and Cherry, J.A., 1979, *Groundwater*: Prentice Hall, Englewood Cliffs, N.J., 604 pp.
- Furniss, G., and Hinman, N.W., 1998, Ferricrete provides record of natural acid drainage, New World District, Montana; *in* Arehart, G.B., and Hulston, J.R. (eds.), *Water-Rock Interaction, Proceedings of the 9th Internat Symposium on Water-Rock Interaction, Taupo, New Zealand: A.A. Balkema, Rotterdam, Brookfield*, pp. 973–976.
- Glass, N.R., Arnold, D.E., Galloway, J.N., Henry, J.R., Lee, J.J., McFee, N.W., Norton, S.A., Powers, C.F., Rambo, D.L., and Schofield, C.L., 1982, Effects of acid precipitation: *Environmental Science and Technology*, v. 16, pp. 162A–169A.
- Goldich, S.S., 1938, A study in rock weathering: *Journal of Geology*, v. 46, pp. 17–58.
- Goldfarb, R.J., Taylor, C.D., Meier, A.L., d'Angelo, W.M., and O'Leary, R.M., 1997, Hydrogeochemistry of mine-drainage waters associated with low-sulfide, gold-quartz veins in Alaska; *in* Dumoulin, J.A., and Gray, J.E. (eds.), *Geologic Studies in Alaska by the U.S. Geological Survey*, 1995: U.S. Geological Survey Professional Paper 1574, pp. 3–18.
- Gough, L.P., Yanosky, T.M., Lichte, F.E., and Balistrieri, L.S., 1995, Preliminary interpretation of spatial and temporal trends in the chemistry of tree rings downstream from the Summitville mine; *in* Posey, H.H., Pendleton, J.A., and Van Zyl, D. (eds.), *Summitville Forum Proceedings: Colorado Geological Survey Spec. Pub. No. 38*, pp. 236–243.
- Gray, J.E., and Coolbaugh, M.F., 1994, Geology and geochemistry of Summitville, Colorado—An epithermal acid-sulfate deposit in a volcanic dome: *Economic Geology, Special Issue on Volcanic Centers as Exploration Targets*, v. 89, no. 4., pp. 1906–1923.
- Gray, J.E., Coolbaugh, M.F., Plumlee, G.S., and Atkinson, W.W., 1994, Environmental geology of the Summitville mine, Colorado: *Economic Geology, Special Issue on Volcanic Centers as Exploration Targets*, v. 89, no. 4., pp. 2006–2014.
- Green, G.N., 1992, The digital geologic map of Colorado in ARC/INFO Format: U.S. Geological Survey Open-File Report 92–507A–O, 9 pp. (<http://greenwood.cr.usgs.gov/pubs/maps/maps.html>)
- Griffiths, P.G., Webb, R.H., and Melis, T.S., 1996, Initiation and frequency of debris flows in Grand Canyon, Arizona: U.S. Geological Survey Open-File Report 96–491, 35 pp.
- Guilbert, J., and Park, C., 1986, *The Geology of Ore Deposits*: W.H. Freeman and Co., New York, 985 pp.
- Gupta, U.C., 1979, Copper in agricultural crops; *in* Nriagu, J. (ed.), *Copper in the Environment*: John Wiley and Sons, New York, pp. 255–288.
- Hofstra, A.H., Leventhal, J.S., Northrop, H.R.L., Andis, G.P., Rye, R.O., Birak, D.J., and Dahl, A.R., 1991, Genesis of sediment-hosted disseminated gold deposits by fluid mixing and sulfidation—chemical-reaction-path modeling of ore depositional processes documented in the Jerritt Canyon district, Nevada: *Geology*, v. 19, pp. 36–40.
- Holland, H.D., and Petersen, U., 1995, *Living Dangerously—The earth, its resources, and the environment*: Princeton University Press, Princeton, 490 pp.
- Horowitz, A.J., Robbins, J.A., Elrick, K.A., and Cook, R.B., 1996, Bed sediment-trace element geochemistry of Terrace Reservoir, near Summitville, southwestern, Colorado: U.S. Geological Survey Open-File Report 96–344, 41 pp.
- Jambor, J.L., 1994, Mineralogy of sulfide-rich tailings and their oxidation products; *in* Jambor, J.L., and Blowes, D.W. (eds.), *Short Course on Environmental Geochemistry of Sulfide-Mine Wastes: Mineralogical Association of Canada, Short Course Handbook*, v. 22, pp. 59–102.
- Jambor, J.L., and Blowes, D.W. (eds.), 1994, *Short course on environmental geochemistry of sulfide mine-wastes: Mineralogical Association of Canada, Short Course Handbook*, v. 22, 438 pp.
- Johnston, R.J., 1980, *Multivariate statistical analysis in geography*: Longman, London, 280 pp.
- Kabata-Pendias, A., and Pendias, H., 1984, *Trace Elements in Soils and Plants*: CRC Press, Inc., Boca Raton, Fla., 315 pp.
- Karczewska, A., 1996, Metal species distribution in top- and sub-soil in an area affected by copper smelter emissions: *Applied Geochemistry*, v. 11, pp. 35–42.
- Kelley, K.D., and Taylor, C.D., 1997, Environmental geochemistry of shale-hosted Ag-Pb-Zn massive sulfide deposits in northwest Alaska—Natural background concentrations of metals in water from mineralized areas: *Applied Geochemistry*, v. 12, pp. 397–409.
- Kirkham, R.D., Sinclair, W.D., Thorpe, R.I., and Duke, J.M. (eds.), 1993, *Mineral deposit modeling: Geological Association of Canada Special Paper 40*, 770 pp.
- Kirkham, R.M., Lovekin, J.R., and Sares, M.A., 1995, Sources of acidity and heavy metals in the Alamosa River basin outside of the Summitville mining area, Colorado; *in* Posey, H.H., Pendleton, J.A., and Van Zyl, D. (eds.), *Summitville Forum Proceedings: Colorado Geological Survey Spec. Pub. No. 38*, pp. 42–57.
- Kwong, Y.T.J., 1993, Prediction and prevention of acid rock drainage from a geological and mineralogical perspective: MEND Project 1.32.1, 47 pp.
- Kwong, Y.T.J., 1995, Influence of galvanic sulfide oxidation on mine water chemistry; *in* Hynes, T.P., and Blanchette, M.C. (eds.), *Proceedings of Sudbury '95—Mining and the Environment*, v. 2, May 28–June 1, 1995, Sudbury, Ontario: CANMET, Ottawa, pp. 477–484.
- Landa, E.R., 1999, Geochemical and biogeochemical controls on element mobility in and around uranium mill tailings; *in* Filipek, L.H., and Plumlee, G.S. (eds.), *The Environmental Geochemistry of Mineral Deposits, Part B. Case Studies and Research Topics: Society of Economic Geologists, Reviews in Economic Geology*, v. 6B, pp. 527–538.

- Lasmanis, R., Norman, D.K., and Cannon, B., 1997, Preliminary study of minerals in Tacoma smelter slags: *Washington Geology*, v. 25, no. 3, pp. 19–25.
- Leach, D.L., Viets, J.G., and Powell, J.W., 1996, Textures of ores from the Silesian-Cracow zinc-lead deposits, Poland—clues to the ore-forming environment; *in* Górczka, E., Leach, D.L., and Kozłowski, A. (eds.), Carbonate-hosted zinc-lead deposits in the Silesian-Cracow area, Poland: *Prace Panstowowego Instytutu Geologicznego*, Warsaw, Poland, pp. 37–50.
- Logsdon, M.J., and Basse, B., 1991, Quantitative evaluation of Pb-Zn mine wastes for subgrade disposal—Characterization versus classification in a Superfund environment: *Proceedings of the 1991 AIME Annual meeting*, Denver, Colorado, Environmental Management for the 1990's, pp. 207–212.
- Maskall, J., Whitehead, K., Gee, C., and Thornton, I., 1996, Long-term migration of metals at historical smelting sites: *Applied Geochemistry*, v. 11, pp. 43–51.
- Montour, M.R., 1994, Aqueous leachability of solid forms of lead in mining and smelting wastes, Leadville, Colorado: M.S. thesis, Univ. of Colorado, Boulder, 234 pp.
- Montour, M.R., Hageman, P.L., Meier, A.L., Theodorakos, P., Briggs, P.H., 1998, Leachate chemistry data for solid mine waste composite samples from Silverton and Leadville, Colorado: U.S. Geological Survey Open-File Report 98–621, 46 pp.
- Nimick, D.A., and Moore, J.N., 1994, Stratigraphy and chemistry of sulfidic flood-plain sediments in the Upper Clark Fork valley, Montana; *in* Alpers, C.N., and Blowes, D.W. (eds.), Environmental Geochemistry of Sulfide Oxidation: American Chemical Society Symposium Series 550, pp. 276–288.
- Nordstrom, D.K., and Alpers, C.N., 1999, Geochemistry of acid mine waters; *in* Plumlee, G.S., and Logsdon, M.J. (eds.), The Environmental Geochemistry of Mineral Deposits, Part A. Processes, Techniques, and Health Issues: Society of Economic Geologists, Reviews in Economic Geology, v. 6A, pp. 133–160.
- Ortiz, R.F., von Guerard, P.B., and Walton-Day, K., 1995, Effect of a localized rainstorm on the water quality of the Alamosa River upstream from Terrace Reservoir, south-central Colorado, August 9–10, 1993; *in* Posey, H.H., Pendleton, J.A., and Van Zyl, D. (eds.), *Proceedings, Summitville Forum '95*: Colorado Geological Survey Spec. Pub. No. 38, pp. 171–177.
- Östlund, P., Torssander, P., Morth, C.M., and Claesson, S., 1995, Lead and sulfur isotope dilution during dispersion from the Falun mining area: *Journal of Geochemical Exploration*, v. 52, pp. 91–95.
- Parsons, M.B., Einaudi, M.T., Bird, I.K., and Alpers, C.N., 1998, Geochemical and mineralogical controls on trace-element release from base-metal slag deposits at Penn Mine, Calaveras County, California: *EOS, Transactions, American Geophysical Union*, v. 79, no. 45, supplement, pp. F354.
- Pasava, J., Kribek, B., and Zak, K. (eds.), 1995, Mineral deposits—from their origin to their environmental impacts, *Proceedings, 3rd Biennial SGA Meeting, Prague, Czech Republic, August 1995*: A.A. Balkema, Rotterdam, 1018 pp.
- Pioneer Technical Services, 1994, Abandoned hardrock mine priority sites, summary report: Montana Department of State Lands, Abandoned Mines and Reclamation Bureau, Engineering Services Agreement DSL-AMRB No. 004, 314 pp.
- Plumlee, G.S., 1989, Processes controlling epithermal mineral distribution in the Creede mining district: Unpub. Ph.D. thesis, Harvard University, 379 pp.
- Plumlee, G.S., and Logsdon, M.J., 1999, An earth-system science toolkit for environmentally friendly mineral resource development; *in* Plumlee, G.S., and Logsdon, M.J. (eds.), The Environmental Geochemistry of Mineral Deposits, Part A. Processes, Techniques, and Health Issues: Society of Economic Geologists, Reviews in Economic Geology, v. 6A, pp. 1–27.
- Plumlee, G.S., and Nash, J.T., 1995, Geoenvironmental models of mineral deposits—fundamentals and applications; *in* du Bray, E.A. (ed.), Preliminary compilation of descriptive geoenvironmental mineral deposit models: U.S. Geological Survey Open-File Report 95–831, pp. 1–9.
- Plumlee, G.S., and Whitehouse-Veaux, P. H., 1994, Mineralogy, paragenesis, and mineral zoning along the Bulldog Mountain vein system, Creede District, Colorado: *Economic Geology, Special Issue on Volcanic Centers as Targets for Mineral Exploration*, v. 89, no. 8, pp. 1883–1905.
- Plumlee, G.S., Smith, K.S., Ficklin, W.H., Briggs, P.H., and McHugh, J.B., 1993, Empirical studies of diverse mine drainages in Colorado—implications for the prediction of mine-drainage chemistry: *Proceedings, 1993 Mined Land Reclamation Symposium*, Billings, Mont., v. 1, pp. 176–186.
- Plumlee, G.S., Gray, J.E., Roeber, M.M., Jr., Coolbaugh, M., Flohr, M., and Whitney, G., 1995a, The importance of geology in understanding and remediating environmental problems at Summitville; *in* Posey, H.H., Pendleton, J.A., and Van Zyl, D. (eds.), *Summitville Forum Proceedings*: Colorado Geological Survey Spec. Pub. No. 38, pp. 13–22.
- Plumlee, G.S., Smith, K.S., Mosier, E.L., Ficklin, W.H., Montour, M., Briggs, P.H., and Meier, A.L., 1995b, Geochemical processes controlling acid-drainage generation and cyanide degradation at Summitville; *in* Posey, H.H., Pendleton, J.A., and Van Zyl, D. (eds.), *Summitville Forum Proceedings*: Colorado Geological Survey Spec. Pub. No. 38, pp. 23–34.
- Plumlee, G.S., Smith, K.S., Gray, J.E., and Hoover, D.B., 1995c, Epithermal quartz-alunite deposits; *in* du Bray, E.A. (ed.), Preliminary compilation of descriptive geoenvironmental mineral deposit models: U.S. Geological Survey Open-File Report 95–831, p. 162–169.
- Plumlee, G.S., Streufert, R.K., Smith, K.S., Smith, S.M., Wallace, A., Toth, M., Nash, J.T., Robinson, R., Ficklin, W.H., 1995d, Geology-based map of potential metal-mine drainage hazards in Colorado: U.S. Geological Survey Open-File Report 95–26. (also available online at <http://minerals.cr.usgs.gov>)
- Plumlee, G.S., Smith, K.S., Montour, M., Ficklin, W.H., and Mosier, E.L., 1999, Geologic controls on the composition of natural waters and mine waters draining diverse mineral-deposit types; *in* Filipek, L.H., and Plumlee, G.S., (eds.), *The Environmental Geochemistry of Mineral Deposits, Part B. Case Studies and Research Topics*: Society of Economic Geologists, Reviews in Economic Geology, v. 6B, pp. 373–432.
- Price, J.G., Shevenell, L., Henry, C.D., Rigby, J.G., Christensen, L.G., Lechler, P.J., Desilets, M.O., Fields, R., Driesner, D., Durbin, B., and Lombardo, W., 1995, Water quality at inactive and abandoned mines in Nevada: Nevada Bureau of Mines and Geology Open-File Report 95–4, 73 pp.
- Ripley, E.A., Redmann, R.E., Crowder, A.A., 1996, Environmental Effects of Mining: St. Lucie Press, Delray Beach, Fla., 356 pp.
- Ritchie, J.C., and McHenry, J.R., 1984, Application of radioactive ¹³⁷Cs for measuring soil erosion and sediment accumulation rates and patterns—a review: *Journal of Environmental Quality*, v. 19, pp. 215–233.
- Robbins, J.A., 1978, Geochemical and geophysical applications of radioactive lead isotopes; *in* The Biogeochemistry of Lead in the Environment: Elsevier/North Holland Biomedical Press, Amsterdam, pp. 285–383.
- Rose, A.W., Hawkes, H.E., and Webb, J.S., 1979, Geochemistry in mineral exploration, 2nd ed.: Academic Press, New York, 657 pp.
- Ross, Malcolm, 1999, The health effects of mineral dusts; *in* Plumlee, G.S., and Logsdon, M.J. (eds.), The Environmental Geochemistry of Mineral Deposits, Part A. Processes, Techniques, and Health Issues: Society of Economic Geologists, Reviews in Economic Geology, v. 6A, pp. 339–356.
- Rouse, J.V., 1974, Radiochemical pollution from phosphate rock mining and milling; *in* Hadley, R.F., and Snow, D.T. (eds.), *Water Resources Problems Related to Mining*: American Water Resources Association Proc. No. 18, pp. 65–71.
- Runnells, D.D., Shepherd, T.A., and Angino, E.E., 1992, Metals in water—determining natural background concentrations in mineralized areas: *Environmental Science and Technology*, v. 26, pp. 2316–2323.

- Rye, R.O., Stoffregen, R., and Bethke, P.M., 1990, Stable isotope systematics and magmatic and hydrothermal processes in the Summitville, CO, gold deposit: U.S. Geological Survey Open-File Report 90-626, 31 pp.
- Sato, M., 1992, Persistency-field diagrams for sulfides and their application to supergene oxidation and enrichment of sulfide orebodies: *Geochimica et Cosmochimica Acta*, v. 56, pp. 3133-3156.
- Schuiling, R.D., and van Gaans, P.F.M., 1997, The waste sulfuric acid lake of the TiO₂-plant at Armyansk, Crimea, Ukraine. Part II. Modeling the chemical evolution with PHRQPITZ: *Applied Geochemistry*, v. 12, pp. 187-201.
- Scott, K.M., Pringle, P.T., and Vallance, J.W., 1995, Sedimentology, behavior, and hazards of debris flows at Mount Rainier Washington: U.S. Geological Survey Professional Paper 1547, 56 pp.
- Shevenell, L., 1996, Statewide potential evapotranspiration maps for Nevada: Nevada Bureau of Mines and Geology Report 48, 32 pp.
- Sims, P.K., Drake, A.A., Jr., and Tooker, E.W., 1963, Economic geology of the Central City district, Gilpin County, Colorado: U.S. Geological Survey Professional Paper 359, 231 pp.
- Smith, A.C.S., and Mudder, T.I., 1999, The environmental geochemistry of cyanide; in Plumlee, G.S., and Logsdon, M.J. (eds.), *The Environmental Geochemistry of Mineral Deposits, Part A. Processes, Techniques, and Health Issues: Society of Economic Geologists, Reviews in Economic Geology*, v. 6A, pp. 229-248.
- Smith, K.S., 1999, Metal sorption on mineral surfaces—An overview with examples relating to mineral deposits; in Plumlee, G.S., and Logsdon, M.J. (eds.), *The Environmental Geochemistry of Mineral Deposits, Part A. Processes, Techniques, and Health Issues: Society of Economic Geologists, Reviews in Economic Geology*, v. 6A, pp. 161-182.
- Smith, K.S., and Huyck, H.L.O., 1999, An overview of the abundance, relative mobility, bioavailability, and human toxicity of metals; in Plumlee, G.S., and Logsdon, M.J. (eds.), *The Environmental Geochemistry of Mineral Deposits, Part A. Processes, Techniques, and Health Issues: Society of Economic Geologists, Reviews in Economic Geology*, v. 6A, pp. 29-70.
- Smith, K.S., Plumlee, G.S., and Ficklin, W.H., 1994, Predicting water contamination from metal mines and mining waste; Notes, Workshop No. 2, Internatl Land Reclamation and Mine Drainage Conference and 3rd Internatl Conference on the Abatement of Acidic Drainage: U.S. Geological Survey Open-File Report 94-264, 112 pp.
- Smith, K.S., Mosier, E.L., Montour, M.R., Plumlee, G.S., Ficklin, W.H., Briggs, P.H., and Meier, A.L., 1995, Yearly and seasonal variations in acidity and metal content of irrigation waters from the Alamosa River, Colorado; in Posey, H.H., Pendleton, J.A., and Van Zyl, D. (eds.), *Summitville Forum Proceedings: Colorado Geological Survey Spec. Pub. No. 38*, pp. 293-297.
- Stoffregen, R.E., 1987, Genesis of acid-sulfate alteration and Au-Cu-Ag mineralization at Summitville, Colorado: *Economic Geology*, v. 82, pp. 1575-1591.
- Stout, P.R., and Emerick, J.C., 1995, Metal uptake by Moravian III barley irrigated with water affected by acid mine discharge in San Luis valley, Colorado; in Posey, H.H., Pendleton, J.A., and Van Zyl, D. (eds.), *Summitville Forum Proceedings: Colorado Geological Survey Spec. Pub. No. 38*, pp. 272-280.
- Stumm, W., and Morgan, J.J., 1981, *Aquatic chemistry—An introduction emphasizing chemical equilibria in natural waters*: John Wiley and Sons, New York, 780 pp.
- Sverdrup, H.U., 1990, The kinetics of base cation release due to chemical weathering: Lund University Press, Lund, 246 pp.
- Thornton, I., 1995, Metals in the global environment—facts and misconceptions: Internatl Council on Metals in the Environment, Ottawa, 103 pp.
- Tidball, R.R., Severson, R.C., Presser, T.S., and Swain, W.C., 1991, Selenium sources in the Diablo Range, western Fresno county, California; in Severson, R.C., Fisher, S.E., and Gough, L.P. (eds.), *Proceedings of the 1990 Billings Land Reclamation Symposium on Selenium in Arid and Semi-arid Environments, Western United States: U.S. Geological Survey Circular 1064*, pp. 107-114.
- Tidball, R.R., Stewart, K.C., Tripp, R.B., and Mosier, E.L., 1995, Geochemical mapping of surficial materials in the San Luis Valley, Colorado; in Posey, H.H., Pendleton, J.A., and Van Zyl, D. (eds.), *Summitville Forum Proceedings: Colorado Geological Survey Spec. Pub. No. 38*, pp. 244-262.
- Tweto, O., 1979, Geologic map of Colorado: U.S. Geological Survey Geologic Map, 1:500,000 scale, 1 plate.
- van Gaans, P.F.M., and Schuiling, R.D., 1997, The waste sulfuric acid lake of the TiO₂-plant at Armyansk, Crimea, Ukraine. Part I. Self-sealing as an environmental protection mechanism: *Applied Geochemistry*, v. 12, pp. 181-186.
- Viets, J.G., Leach, D.L., Lichte, F.E., Hopkins, R.T., Gent, C.A., and Powell, J.W., 1996, Paragenetic and minor- and trace-elements studies of Mississippi Valley-Type ore deposits of the Silesian-Cracow district, Poland; in Górcza, E., Leach, D.L., and Kozłowski, A. (eds.), *Carbonate-hosted zinc-lead deposits in the Silesian-Cracow area, Poland: Prace Panstowowego Instytutu Geologicznego, Warsaw, Poland*, pp. 37-50.
- Wanty, R.B., Miller, W.R., Zielinski, R.A., Plumlee, G.S., Bove, D.J., Lichte, F.E., Meier, A.L., and Smith, K.S., 1998, Uranium mobility in surface waters draining mineralized areas in the western U.S.; in Arehart, G.B., and Hulston, J.R. (eds.), *Water-Rock Interaction, Proceedings of the 9th Internatl Symposium on Water-Rock Interaction, Taupo, New Zealand: A.A. Balkema, Rotterdam, Brookfield*, pp. 1013-1016.
- Wanty, R.B., Miller, W.R., Briggs, P.H., and McHugh, J.B., 1999, Geochemical processes controlling uranium mobility in mine drainages; in Plumlee, G.S., and Logsdon, M.J. (eds.), *The Environmental Geochemistry of Mineral Deposits, Part A. Processes, Techniques, and Health Issues: Society of Economic Geologists, Reviews in Economic Geology*, v. 6A, pp. 201-213.
- Wanty, R.B., Berger, B.R., and Plumlee, G.S., 1999 in press, Geoenvironmental models; in Fabbri (ed.), *Proceedings, 1998 NATO Advanced Studies Institute Workshop on Geoenvironmental Models of Mineral Deposits: L. Kluwer Academic Publishers*.
- White, W.W., III, and Jeffers, T.H., 1994, Chemical predictive modeling of acid mine drainage from metallic sulfide-bearing waste rock; in Alpers, C.N., and Blowes, D.W. (eds.), *Environmental Geochemistry of Sulfide Oxidation: American Chemical Society Symposium Series 550*, pp. 608-630.
- White III, W.W., Lapakko, K.A., Cox, R.L., 1999, Static-test methods most commonly used to predict acid-mine drainage—Practical guidelines for use and interpretation; in Plumlee, G.S., and Logsdon, M.J. (eds.), *The Environmental Geochemistry of Mineral Deposits, Part A. Processes, Techniques, and Health Issues: Society of Economic Geologists, Reviews in Economic Geology*, v. 6A, pp. 325-338.
- Wildeman, T.R., Cain, D., and Ramiriz, R.A.J., 1974, The relation between water chemistry and mineral zonation in the Central City Mining district, Colorado; in Hadley, R.F., Snow, D.T. (eds.), *Water Resources Problems Related to Mining: American Water Resources Association Proc. No. 18*, pp. 219-229.
- Zimbelman, D.R., 1996, Hydrothermal alteration and its influence on volcanic hazards—Mount Rainier, Washington, a case history: Ph.D. thesis, University of Colorado, Boulder, 384 pp.

Chapter 4

SOME FUNDAMENTALS OF AQUEOUS GEOCHEMISTRY

D. Kirk Nordstrom

U.S. Geological Survey, 3215 Marine Street, Boulder, CO 80303-1066

INTRODUCTION

Aqueous geochemistry is the application of chemistry to reactions between rock and natural water. Analytical chemistry, inorganic and organic chemistry, and physical chemistry are used to understand and interpret the dominant processes that effect a redistribution of the elements in man's environment. Examples of these processes are the dissolution and precipitation of minerals, adsorption and desorption of ions, oxidation-reduction or redox reactions, gas uptake or production, transformations involving organic matter, complexation and chelation, evaporation, ion exchange, and anthropogenic changes. In the field of aqueous geochemistry these processes are known to occur in a variety of environments including rain, fog, snow, soils, bedrock weathering, streams, rivers, lakes, estuaries, ground waters, subsurface brines, diagenetic environments, the formation and weathering of mineral deposits, and the global movement of elements and compounds. Aqueous geochemistry is synonymous with low-temperature geochemistry, where the approximate temperature and pressure limits of 0–100°C and 1–500 bars commonly apply. The term environmental geochemistry is often used to emphasize the environmental aspects of geochemistry. Another common term, hydrogeochemistry, is usually applied to the aqueous geochemistry of ground waters. These four terms all refer to the same basic subject matter.

In physics and chemistry, great advances are made through theoretical research, experimental research, or optimally through a blend of both. In aqueous geochemistry, a third aspect plays an essential role: field observations. By applying the best that theoretical chemistry and physics can offer to the interpretation of field observations aided by reliable experimental and analytical determinations, the aqueous geochemist is at the crossroads of theory, experiment and the natural environment. Geological phenomena are of a much greater complexity than the carefully controlled systems investigated in physics and chemistry, so that the geochemist has had to expand his knowledge creatively beyond the traditional boundaries of the physical sciences. The challenge of this type of scientific research is not generally appreciated (Alvarez, 1990). There are far more unknown and uncontrolled variables in natural systems than in the typical physicochemical investigation carried out in the laboratory. The hydrological, microbiological, macrobiological, and meteorological sciences are all necessary in addition to geology and chemistry.

The same basic principles apply in aqueous geochemistry as in other fields of science. These are (1) the conservation of mass, (2) the conservation of energy, (3) the unidirectional nature of mass

and energy flow, (4) the continuity of mass and energy flow, (5) the constancy of radioactive decay, and (6) the evolutionary nature of the earth and its organisms over time.

Conservation of mass is the basis for mass balance and mass flow calculations on inputs and outputs at appropriate points in a natural system. Conservation of energy permits the calculation of energy balances and flows for specified processes. The unidirectional redistribution of mass and energy principle provides the basis for calculating that portion of the total energy available for useful work and chemical reaction, that is, for calculating what processes are energetically possible. The continuity principle allows the integrated formulation of mass flow, energy flow, and mass transfer. Radioactive decay constancy makes it possible to assign absolute ages to substances, flow rates, and mass transfer rates for natural processes. The evolutionary aspect of nature allows the extrapolation of current observable processes either backward or forward over long periods of time.

The experimental data used in aqueous geochemistry comes from a great many sources. They include basic material properties including thermodynamic, electrolyte, non-electrolyte, kinetic, and related physical properties. More recently, there has been the important addition of surface properties and the atomic and molecular bonding properties of both bulk and surface through new methods of spectroscopy and microscopy. Two major challenges facing geochemical research are to apply these experimental data to natural materials where impurities and heterogeneities are abundant and to relate experimental data on a molecular-scale or lab-scale to field-scale observations.

Field observations are often the starting point and the final goal of aqueous geochemical studies. Observations and interpretations of geological structure, hydrogeological properties, mineralogy, petrology, water chemistry, isotopic chemistry, gas chemistry, colloid chemistry, microbiological and macrobiological characteristics, and anthropogenic factors can provide valuable insights about natural processes functioning over time and space.

Physical chemistry, traditionally taught since Ostwald's time in the three fields of thermodynamics, kinetics, and quantum mechanics (Servos, 1990), embodies the fundamental theory used in aqueous geochemistry. *Thermodynamics* is the study of the energetics of chemical transformations that allows one to calculate whether a particular reaction is possible or not for a given set of conditions. Calculations of plausible or energetically feasible geochemical reactions is the first step toward quantifying chemical processes in the natural environment. The next step is knowledge of the reaction rate, i.e. the identification of which of all possible reactions is the slowest or the fastest. *Kinetics* is the study of reac-

tion rates and in aqueous geochemistry rates range from nanoseconds for aqueous hydrolysis reactions to many millions of years for the evolution of deep brines in sedimentary basins or crystalline basements. Finally, *quantum mechanics* is the study of bonding theory and how the electronic and nuclear structure of atoms and molecules (along with statistical mechanics) can describe the behavior of matter and radiant energy. Both thermodynamic and kinetic properties are based ultimately on the nature of chemical bonds and their rearrangement during reaction.

AQUEOUS GEOCHEMICAL THERMODYNAMICS

Thermodynamics is based on three fundamental laws: (1) the law of conservation of energy, (2) the law of the natural redistribution of energy, and (3) the law of absolute entropy. The first law recognizes that energy comes in many different forms but the total energy of a defined system is constant and equal to the sum of its parts in the energy balance equation:

$$\Delta U = Q + W \quad [1]$$

where ΔU is the net change in total energy, Q is the heat transferred into or out of the system, and W is work energy done by or on the system. Only changes in energy are considered because we don't know the absolute amount. Other forms of energy that might affect the energy budget are gravitational, electrochemical, and electromagnetic radiation where chemical sedimentation, pyrite oxidation, and photochemical reduction of iron, respectively, are geochemical examples. The historical development of thermodynamics focused on the relation between heat and work, especially with regard to the performance of engines. Aqueous geochemistry focuses on the heat exchanged during a geochemical process and whether the energy change for a geochemical reaction, such as pyrite oxidation, is favorable or not under a given set of conditions. The differential form of equation [1]:

$$dU = \delta Q + \delta W \quad [2]$$

points out that the internal energy is a function of the state of the system, i.e. it depends only on the initial condition and the final condition but not on how it got from one to the other. The differential, dU , is an exact differential whereas the differentials for heat and work, δQ , δW , are inexact differentials and not state functions, i.e. their value can change depending on what path was chosen for them to go from initial to final state. The sum of two inexact differentials, however, can produce an exact differential as shown in equation [2].

The second law of thermodynamics expresses the natural tendency for all processes to be unidirectional. The first law only states that energy is conserved during a process or reaction but the second law says that energy is redistributed only in a certain direction such that a more likely state or condition is achieved. For example, it is observed that heat flows from a higher to a lower temperature, that water flows from a higher to a lower head, that dissolved ions flow from a higher to a lower concentration and that electrons flow from a higher to a lower electrical potential. The state function that represents this natural redistribution of

energy is called the entropy. It is calculated from the heat transferred during a reversible process divided by the absolute temperature:

$$dS = \frac{\delta Q_{\text{rev}}}{T} \quad [3]$$

In an irreversible, or real, process, the heat flow is always less than that for a reversible process. Hence, for any process the most general expression for the second law is the famous Clausius inequality:

$$dS \geq \frac{\delta Q}{T} \quad [4]$$

The concept of entropy increase has often been equated with the concept of increasing disorder and randomness. The classic example is that of two gases mixing in an adiabatic container of fixed volume. After they mix, there is more "mixed-upness" of the gases than before. However, there are just as many examples of an increase in order for a spontaneous process. For example, a super-cooled liquid freezes to a more ordered state spontaneously, a mixture of hydrogen and argon separated from a vacuum by a palladium membrane permeable only to hydrogen will "unmix" with an increase in entropy, the evolution of the earth and its organisms could be described as progressing from disordered atoms, molecules and random molecular assemblages to more ordered and complex entities, disorder in molecular arrangements usually increase with temperature yet water is more dense and ordered at 4°C than at 0°C. Consequently, it is incorrect to give meaning to entropy by equating it only with disorder or randomness (McGlashan, 1979). Entropy, as a macroscopic property, is simply a state variable that is measurable, always increases for any real process, always reflects the loss of useful work for a real process, and has meaning in that it represents a natural tendency to redistribute energy. As a microscopic property it can refer to the distribution of energy states or "the number of accessible eigenstates" (McGlashan, 1979).

Substituting the work term PdV for the inexact differential in equation [2] and substituting the heat term TdS from equations [3] and [4] into equation [2] results in the fundamental Gibbs equation that combines the first and second laws of thermodynamics:

$$dU \leq TdS - PdV \quad [5]$$

for either reversible (equality) or irreversible (inequality) changes in a closed system. This equation contains all of the primary thermodynamic variables (U , S , P , V , and T) necessary to describe the state of a system. All other variables are derived from these.

The heat term in equation [1] is not a state function. J.W. Gibbs (1876–78) defined the enthalpy or heat content, H , to be a state function by making it equal to the internal energy plus PV work. The total derivative of H becomes

$$dH = TdS + VdP \quad [6]$$

when equation [5] is substituted.

The heat capacity is the differential change in the heat with respect to temperature

$$C = \frac{dQ}{dT} \quad [7]$$

The heat capacity at constant pressure is defined as the partial derivative of the enthalpy with respect to temperature

$$C_P = \left[\frac{\partial H}{\partial T} \right]_P \quad [8]$$

The heat capacity allows the calculation of the temperature dependence for all of the other thermodynamic functions. The enthalpy or heat content of a phase can be calculated at some temperature, T_2 , by integrating the heat capacity from a reference temperature, T_1

$$H_{T_2} = H_{T_1} + \int_{T_1}^{T_2} C_P dT \quad [9]$$

In a similar manner the temperature dependence of the entropy can be derived. Since

$$dS = \frac{dQ_{rev}}{T} \quad [10]$$

then

$$dS = \frac{C_P dT}{T} \text{ and } S_{T_2} = S_{T_1} + \int_{T_1}^{T_2} \frac{C_P}{T} dT \quad [11]$$

Gibbs defined one of the most useful state functions, G , by means of a Legendre transform which subtracted the TS term from the enthalpy

$$G \equiv U + PV - TS = H - TS \quad [12]$$

When the derivative of equation [12] is made and equation [5] is substituted, the result is the differential of the Gibbs free energy in terms of pressure and temperature

$$dG = -SdT + VdP \quad [13]$$

Equation [13] can be combined with the total derivative of equation [12] at constant pressure to obtain the derivative of the Gibbs free energy as a function of enthalpy and entropy

$$dG = dH - TdS \quad [14]$$

Enthalpies and entropies of substances can easily be found in tables of thermodynamic data to calculate free energies of geochemical reactions.

Gibbs also showed the change in free energy with the number of moles of a substance (the partial molar Gibbs free energy) is the driving force for chemical reaction, known as the chemical potential

$$\mu_i = \left[\frac{\partial G}{\partial n_i} \right]_{P,T,n_j} \quad [15]$$

where n_i is the number of moles of the i th component or species and n_j is the number of moles of all components or species for $i \neq j$. When dG is zero, there is no tendency for chemical reaction and we have a mathematical criterion for equilibrium.

By considering the effect of pressure on the chemical potential for a pure, ideal gas and with the aid of concepts introduced by G.N. Lewis, the chemical potential can be related to a much more practical quantity, the activity, a_i ,

$$\mu_i = \mu_i^0 + RT \ln a_i \quad [16]$$

where the standard state to which these quantities are referenced is given by the superscript zero.

The activity is an important concept that describes the "reactive" or "effective" concentration of a component or species in a phase. For example, acid mine waters usually have high concentrations of aluminum. A sample of acid mine water from Iron Mountain mine in California has an aluminum molality of 9.1 millimolal whereas the free aluminum ion is only 1.6 millimolal, or 17.4% of the total, because of complexing of the aluminum with sulfate ions. The activity of free aluminum, however, is only 0.1 on the millimolality scale (activity is dimensionless), or 1.1% of the total.

Another example is pH. The measurement of pH gives a value less than the total hydrogen ion concentration in an aqueous solution and the definition of pH is the negative logarithm of the hydrogen ion "activity." This activity is analogous to a concentration that has been corrected for non-ideal behavior

$$a_i = \gamma_i m_i \quad [17]$$

where γ_i is the activity coefficient (correction factor). The activity and activity coefficient terms will be discussed again later.

Equation [16] can be written for every species participating in a chemical reaction

$$\sum \nu_i \mu_i = \sum \nu_i \mu_i^0 + \sum \nu_i RT \ln a_i \quad [18]$$

By definition, equation [15], $\Delta G = \sum \nu_i \mu_i = 0$ at equilibrium and equation [18] becomes the equilibrium constant for a reaction

$$\Delta G_r^0 = \sum \nu_i \mu_i^0 = -RT \ln K \quad [19]$$

Another important concept commonly used in geochemical thermodynamics is electrochemical potential. The electrochemical energy is a type of free energy defined by $\Delta G = -nFE$, where F is the Faraday constant and E is the electrochemical potential. Combining this equation with equations [18] and [19] results in the Nernst equation

$$E = E^0 - \frac{RT}{nF} \ln \Pi a_i^{v_i} \quad [20]$$

For example, the electrochemical potential relative to the standard hydrogen electrode, E_h , for the redox reaction



is

$$E = 0.770 - 0.0592 \log \frac{a_{\text{Fe}^{2+}}}{a_{\text{Fe}^{3+}}} \quad [22]$$

SPECIATION, ACTIVITY COEFFICIENT MODELS, AND MINERAL SATURATION

Aqueous speciation refers to the equilibrium distribution of aqueous species between free ions such as Ca^{2+} , Mg^{2+} , and Al^{3+} , and ion pairs, complexes, and neutral species such as CaSO_4^0 , MgOH^+ , and AlSO_4^+ . The type and degree of speciation in natural waters is necessary for many purposes including the interpretation of toxicity, bioavailability, mineral solubilities, sorption reactions, redox reactions, gas reactions, and rate mechanisms. The calculation of speciation requires a chemical model and the details of the chemical modeling of mine wastes can be found in Alpers and Nordstrom (1999). In this section we will focus on how activity coefficients and saturation indices are calculated.

Equation [17] expresses the activity as simply the molality corrected for non-ideality by multiplying it by an activity coefficient. The activity coefficient is a single term that has to account for a multitude of solute-solute and solute-solvent interactions that are difficult to define and model. Two approaches to modeling activity coefficients are in general use: the ion-association theory (IA) and the specific-ion interaction (SI) theory of Pitzer (1991, 1995).

The IA theory explicitly defines electrostatic interactions between ions of opposite charge by equilibrium constants for ion pair or complex formation. For example, in acid mine waters a large percentage of divalent and trivalent metal cations (Al^{III} , Fe^{III} , Fe^{II} , Cu^{II} , Zn^{II} , etc.) will be attracted to SO_4^{2-} ions to form ion pairs such as AlSO_4^+ . If the thermodynamic stability constants for the formation of these ion pairs are known then they can be entered into a numerical algorithm to solve simultaneously the speciation among several competing ions. Water analyses can be used an input data along with the thermodynamic properties of ion-pair formation (equilibrium constants or free energies, enthalpies, entropies, and heat capacities) to solve mass balance equations for every component. More details on solving simulta-

neous mass-action and mass-balance expressions can be found in Alpers and Nordstrom (1999). The activity coefficients are usually some form of Debye-Hückel equation. The extended Debye-Hückel equation

$$\log \gamma_i = \frac{-Az_i^2 \sqrt{I}}{1 + B\hat{a}_i \sqrt{I}} \quad [23]$$

works well for dilute solutions. A significant improvement is made with the addition of a linear term

$$\log \gamma_i = \frac{-Az_i^2 \sqrt{I}}{1 + B\hat{a}_i \sqrt{I}} + b_1 I \quad [24]$$

where A and B are Debye-Hückel solvent parameters (functions of the temperature and the density and dielectric constant of water), z_i is the charge of the i th ion, and \hat{a}_i and b_1 are fitting parameters. The ionic strength, I , is the total ionic concentration of charged species in solution

$$I = \frac{1}{2} \sum_i m_i z_i^2 \quad [25]$$

Equation [24], when used in conjunction with simultaneous solution of mass-action and mass-balance equations, can often provide satisfactory results for speciation up to the ionic strength of seawater (0.7 molal). It is not reliable at ionic strengths of 1 molal and higher.

The SI, or Pitzer, approach incorporates the weak electrostatic interactions into the activity coefficient expression using a semi-empirical equation based on the virial expansion (Pitzer, 1995). The Pitzer method permits activity calculations to very high ionic strengths (in some cases up to 15–20 molal) but the range of components is more limited than with the IA method. Since most acid mine waters fall in the range of ionic strength less than seawater, often require redox calculations not available by the Pitzer method, and require trace element data, the IA method is preferable. The most successful approach arises with “hybrid” models that combine the best features of both methods. An excellent example of a hybrid model was reported by Millero and Schreiber (1982) in which the relevant stability constants for ions in seawater and estuarine waters were combined with modified Pitzer equations to calculate speciation.

Once speciation and activities of aqueous ions have been calculated then a saturation index calculation can be made. The saturation index is defined as the logarithm of the degree of saturation, Ω , which is the ratio of the ion activity product (IAP) to the solubility product constant. For example, the equilibrium solubility of gibbsite



is represented by the equilibrium-constant expression

$$K_{\text{sp}} = \frac{(a_{\text{Al}^{3+}})(a_{\text{OH}^-})^3}{a_{\text{gibbsite}}} \quad [27]$$

where the activity of gibbsite is unity when assumed to be in its standard state of pure phase at 25°C and 1 bar pressure. The IAP is the numerator in equation [27] and at solubility equilibrium is equal to the K_{sp} . The degree of saturation is unity at the equilibrium solubility and the saturation index

$$SI = \log \Omega = \log \left[\frac{IAP}{K_{sp}} \right] \quad [28]$$

will be zero.

Three possible results may arise when computing the SI for a natural water

$$\begin{array}{ll} SI > 0 & \text{indicates supersaturation} \\ SI = 0 & \text{indicates saturation} \\ SI < 0 & \text{indicates undersaturation} \end{array} \quad [29]$$

with respect to a given mineral. These results describe the tendency of a water sample to be saturated or not based on the model assumptions and the reliability of the reported water analysis. It is an interpreted signature of the water sample, not a conclusion regarding actual processes without further information. For example, equilibrium solubility may not be assumed even if the $SI = 0$ when mineralogical examination shows the mineral doesn't exist at a particular site.

A difficulty with SI values arises when attempting to define how close to zero is close enough to say the water appears to be in equilibrium with respect to a given mineral. A certain margin of error must be allowed to account for errors in the water analysis and errors in the thermodynamic data. An example of an uncertainty analysis demonstrating the propagation of errors from both the water analyses and the thermodynamic data on calculated SI values has been reported by Nordstrom and Ball (1989). The conclusion they reached was that for some common minerals such as calcite, fluorite, barite, gibbsite, and ferrihydrite, the SI values tend to be affected most by uncertainties in the water analyses.

Yet another difficulty arises when trying to compare saturation indices for minerals of different stoichiometries. A mineral such as jarosite, $KFe_3(SO_4)_2(OH)_6$, will have activities in the IAP raised to the 6th power for hydroxide ion and to the 3rd power for ferric ion, whereas the IAP for ferric hydroxide has an activity of ferric ion raised to the 1st power and hydroxide raised to the 3rd power. The stoichiometric coefficients will magnify any errors in computed IAP values when they are larger. The solution to this problem is to normalize to the total stoichiometry as pointed out by Zhang and Nancollas (1990). The total stoichiometric coefficient, v , is the total number of ions in the formula unit

$$v = v_+ + v_- \quad [30]$$

The saturation ratio, S , is the normalized degree of saturation

$$S = \left[\frac{IAP}{K_{sp}} \right]^{\frac{1}{v}} \quad [31]$$

and the normalized saturation index becomes

$$\log S = \frac{SI}{v} = \frac{1}{v} \log \left[\frac{IAP}{K_{sp}} \right] \quad [32]$$

Hence, a uniform approach for defining reasonable uncertainties around sets of saturation indices for different minerals should be possible with the normalized SI.

These fundamental concepts and relationships of geochemical thermodynamics are the foundation upon which quantitative interpretations of geochemical processes are built. Many more thermodynamic expressions can be derived from these and the interested reader is encouraged to seek out textbooks such as Atkins (1978), Crerar and Anderson (1993), Laidler and Meiser (1982), Nordstrom and Munoz (1994), and Pitzer (1995).

AQUEOUS GEOCHEMICAL KINETICS

The subject of thermodynamics can tell us a great deal about which reactions are possible and which ones aren't when applied to aqueous geochemical processes. It cannot tell us, however, which of many possible reactions are likely based on their rates. The rate of reactions is the subject of chemical kinetics, the study of the rates and mechanisms of molecular reactions. In aqueous geochemistry, molecular reactions are important but so are macroscale processes occurring in a ground-water system or a watershed where thousands of competing reactions have rates that should be known over a large range of conditions. Consequently, simplifications are necessary to interpret field data and the same approach used to interpret single reactions on the molecular scale might not be appropriate on the scale of a field site.

The scale problem might be termed the first principle of geochemical kinetics: the size, complexity, and time frame of a system will dictate the approach used. For example, if microbial growth kinetics is the dominant rate control on some aspect of the water chemistry then the rate equations not only will look different from those for inorganic reactions, but rates will then vary with climate, available nutrients, and biological competition. This principle is similar to the problem in applying thermodynamics to natural systems, i.e., the investigator is responsible for defining the boundaries and assumptions of the system to be studied.

The next important aspect of geochemical kinetics is the relationship between water flow rates and geochemical reaction rates. The hydrodynamics of the system can affect reaction rates. The relationship between flow rates and reaction rates also depends on whether the geochemical reaction is dominated by diffusion or surface reactions (Berner, 1978). Temporal variations in hydrology due to climatic changes have to be factored in for watershed or drainage basin scale studies. Mobility of aqueous contaminants can vary greatly with seasonal, diel, and storm events (Alpers et al., 1992; McKnight and Bencala, 1988; Nordstrom, 1985).

Microbiological processes may have a catalytic effect on some reactions, changing their rates by orders of magnitude. A classic example is the increase in the oxidation rate of aqueous ferrous iron by 5 to 6 orders of magnitude in the presence of iron-oxidizing bacteria (Nordstrom, 1985).

Photochemical reactions have been identified in acid mine waters and the discovery of the photoreduction of iron has changed our understanding of the rates and mechanisms of processes involving iron (McKnight et al., 1988).

The effect of organics on rates and mechanisms is also an

important topic. Organics can have a major influence on the mobility or immobility of metals by complexing metals and by promoting redox reactions.

Additional reviews of geochemical kinetics can be found in Lasaga (1984), Lasaga et al. (1994), Stumm (1990), and White and Brantley (1995).

Elementary reaction kinetics

The basic concepts and expressions used in chemical kinetics are presented here as a basis for discussing reaction rates in geochemical systems. The presentation is condensed and simplified to fit the scope of this volume but complete enough to give the reader a proper overview.

The rate of reaction is defined as

$$v = \frac{d\xi}{Vdt} = \frac{dn_i}{Vv_i dt} \quad [33]$$

where a differential change in the progress variable is defined as

$$d\xi = \frac{dn_i}{v_i} \quad [34]$$

if the volume is held constant then dn_i/V can be replaced by the concentration change dc_i and the reaction rate is

$$v = \frac{dc_i}{v_i dt} \quad [35]$$

which is to be distinguished from the rate of consumption or formation of the i th species, v_i ,

$$v_i = \frac{dc_i}{dt} \quad [36]$$

The order of a reaction is an empirically-derived power to which a reacting species is raised in the rate equation. If the rate is proportional to the first power of the concentration of A then,

$$v_A = k[A] \quad [37]$$

or, in general,

$$v = k[A]^n \quad [38]$$

where n is the order of the reaction. For example, for the rate oxidation of ferrous iron by dissolved oxygen, Stumm and Lee (1961) found

$$-\frac{d[\text{Fe}^{2+}]}{dt} = k[\text{Fe}^{2+}][\text{OH}^-]^2[\text{P}_{\text{O}_2}] \quad [39]$$

This oxidation rate is first order in ferrous iron, second order in hydroxide, first order in oxygen, and fourth order overall. Rates

can be zero order, first order, second order, or fractional order, but rarely more than second order.

Assuming constant volume conditions, a relation exists between the free energy of a reaction and its rate

$$v = \frac{d\xi}{dt} = ks(1 - e^{\frac{-n\Delta G}{RT}}) \quad [40]$$

where k is the rate constant and s is the reactive surface area (Lasaga, 1981; Aagaard and Helgeson, 1982). This form of the reaction rate can be derived either from transition state theory or from first principles of thermodynamics and kinetics (or from irreversible thermodynamic theory). These type of expressions are used to model and interpret water-rock interactions.

The temperature dependence of the rate constant is expressed by the Arrhenius equation

$$k = Ae^{-\frac{E}{RT}} \quad [41]$$

From a careful analysis of reaction rates and a determination of the order, an attempt can be made to determine the molecularity and the reaction mechanism. At the scale of a mine site, watershed, or ground water, however, these concepts become highly questionable. For example, the oxidation of ferrous iron in acid mine waters is governed by the growth rate and concentration of iron-oxidizing bacteria. Their growth rate is determined by nutrient availability and climatic variations. The quantitative expression of their growth rate is based on the Michaelis-Menten equation for enzyme catalysis which exhibits both zero order and first order properties. Michaelis-Menten kinetics does not imply that anything is known about the mechanism. Consequently, we must discuss the relative mass flow rate of different constituents through a given drainage system.

Consideration of mass attenuation rates (where the mass flow rate may be quite different from the water flow rate) gives us empirical field rates which we can then attempt to interpret in terms of known chemical, biological, and physical processes and their rates. For example, the calculation of arsenic, copper, and zinc attenuation rates were calculated at the Leviathan mine drainage system (Webster, et al., 1994).

Rate constants only apply to elementary reactions. When several elementary reactions are involved which may be coupled in unknown ways, then it should be referred to as a composite reaction and the proportionality constant is known as a rate coefficient. For hydrogeochemical processes where climatic factors, biological factors, and hydrogeologic factors are as important as chemical factors, rate should be described in terms of generalized fluxes or flows for specified regions of time and space.

REFERENCES

- Aagaard, P., and Helgeson, H.C., 1982, Thermodynamic and kinetic constraints on reaction rates among minerals and aqueous solutions, I. Theoretical considerations: *American Journal of Science* 282, pp. 237-285.
- Alpers, C.N., and Nordstrom, D.K., 1999, Geochemical modeling of water-rock interactions in mining environments; *in* Plumlee, G.S., and Logsdon, M.J. (eds.), *The Environmental Geochemistry of Mineral Deposits, Part A. Processes, Techniques, and Health Issues*: Society of

- Economic Geologists, *Reviews in Economic Geology*, v. 6A, pp. 289–323.
- Alpers, C.N., Nordstrom, D.K., and Burchard, J.M., 1992, Compilation and interpretation of water-quality and discharge data for acidic mine waters at Iron Mountain, Shasta County, California: U.S. Geological Survey Water-Resource Investigation Report 91–4160, 173 pp.
- Alvarez, W., 1990, Interdisciplinary aspects of research on impacts and mass extinctions—A personal view: Geological Society of America Spec. Paper No. 247, pp. 93–97.
- Atkins, P.W., 1978, *Physical chemistry*: W.H. Freeman, 1022 pp.
- Berner, R.A., 1978, Rate control of mineral dissolution under earth surface conditions: *American Journal of Science* 278, pp. 1235–1252.
- Crerar, D.A., and Anderson, G.M., 1993, *Thermodynamics in geochemistry—The equilibrium model*: Oxford University Press, 588 pp.
- Gibbs, J.W., 1876–78, On equilibrium of heterogeneous substances: *Trans. Conn. Acad.* vol III, 1876, pp. 108–248; 1878, pp. 343–524.
- Laidler, K.J., and Meiser, J.H., 1982, *Physical chemistry: Benjamin/Cummings*, 919 pp.
- Lasaga, A.C., 1981, Rate laws of chemical reactions; *in* Lasaga, A.C., and Kirkpatrick, R.J. (eds.), *Kinetics of Geochemical Processes: Rev. Mineral.*, vol. 8, Mineralogical Society of America, Washington, D.C., pp. 1–67.
- Lasaga, A.C., 1984, Chemical kinetics of water-rock interactions: *Journal of Geophysical Research* 89, 4009–4025.
- Lasaga, A.C., Soler, J.M., Ganor, J., Burch, T.E., and Nagy, K.L., 1994, Chemical weathering rate laws and global geochemical cycles: *Geochimica et Cosmochimica Acta* 58, 2361–2386.
- McGlashan, M.L., 1979, *Chemical thermodynamics*: Academic Press, 345 pp.
- McKnight, D., and Bencala, K., 1988, Diel variations in iron chemistry in an acidic stream in the Colorado Rocky Mountains, U.S.A.: *Arctic Alpine Res.* 20, pp. 492–500.
- McKnight, D.M., Kimball, B.A., and Bencala, K.E., 1988, Iron photoreduction and oxidation in an acidic mountain stream: *Science* 240, pp. 637–640.
- Millero, F.J., and Schreiber, D., 1982, Use of the ion pairing model to estimate activity coefficients of the ionic components of natural waters: *American Journal of Science* 282, pp. 1508–1540.
- Nordstrom, D.K., 1985, The rate of ferrous iron oxidation in a stream receiving acid mine effluent; *in* *Selected Papers in the Hydrologic Sciences 1985*: U.S. Geological Survey Water-Supply Paper 2270, pp. 113–119.
- Nordstrom, D.K., and Ball, J.W., 1989, Mineral saturation states in natural waters and their sensitivity to thermodynamic and analytic errors: *Scientific Geology Bulletin* 42, pp. 269–280.
- Nordstrom, D.K., and Munoz, J.L., 1994, *Geochemical thermodynamics*, 2nd ed.: Blackwell Science, 493 pp.
- Pitzer, K.S., 1991, Ion interaction approach—Theory and data correlation; *in* *Activity Coefficients in Electrolyte Solutions*, 2nd ed.: CRC Press, Boca Raton, Fla., pp. 75–153.
- Pitzer, K.S., 1995, *Thermodynamics*: McGraw-Hill, 626 pp.
- Servos, J.W., 1990, *Physical chemistry from Ostwald to Pauling—The making of a science in America*: Princeton University Press, 402 pp.
- Stumm, W. (ed.), 1990, *Aquatic chemical kinetics—Reaction rates of processes in natural waters*: John Wiley and Sons, New York, 540 pp.
- Stumm, W., and Lee, G.F., 1961, Oxidation of ferrous iron: *Industrial Engineering Chemistry* 53, pp. 143–146.
- Webster, J., Nordstrom, D.K., and Smith, K., 1994, Transport and natural attenuation of Cu, Zn, As, and Fe in the acid mine drainage of Leviathan and Bryant Creeks; *in* Alpers, C.N., and Blowes, D.W. (eds.), *Environmental Geochemistry of Sulfide Oxidation: American Chemical Society Symposium Series 550*, pp. 244–260.
- White, A.F., and Brantley, S.L. (eds.), 1995, *Chemical weathering rates of silicate minerals*, *Rev. Mineral.*, vol. 31: Mineralogical Society of America, Washington, D.C., 583 pp.
- Zhang and Nancollas, 1990, Mechanisms of growth and dissolution of sparingly soluble salts; *in* Hochella, Jr., M.F., and White, A.F. (eds.), *Mineral-Water Interface Geochemistry*, *Rev. Mineral.*, v. 23: Mineralogical Society of America, Washington, D.C., pp. 365–396.

Chapter 5

THE ROLE OF BACTERIA IN ENVIRONMENTAL GEOCHEMISTRY

A.L. Mills

*Department of Environmental Sciences, University of Virginia,
Clark Hall, Charlottesville, VA 22903*

INTRODUCTION

Many of the geochemical processes occurring at earth-surface temperature and pressure are influenced by microorganisms, particularly the bacteria. Like any other living entity, the bacteria as an aggregate have a single goal, to reproduce and perpetuate their life-form. To accomplish this goal the bacteria must utilize energy and materials that can only be obtained from their surrounding environment. As the process of growth and reproduction occurs, a variety of changes occur in the environment in which the microbe lives. The chemical makeup of waters inhabited by bacteria is altered, and any equilibrium reactions taking place in that water or between that water and associated solid phases may cause a shift in the chemical composition of aqueous- or solid-phase materials. Some materials, such as oxygen, may simply be consumed by the microbes. The resultant anoxic conditions may induce concomitant changes in some redox-sensitive species of elements such as sulfur. Bacterial utilization or production of oxidized or reduced chemical species may cause further large shifts in the redox status of the local environment. Production of acidogenic or proton-consuming species can cause radical shifts in pH in either direction, depending on the organism, the starting material, and the products formed. Indeed, the current state of the earth's surface conditions is due in large part to the action of microorganisms on the chemicals found in the environment. Photosynthetic organisms (including the cyanobacteria, which are often referred to as blue-green algae) created the oxidizing atmosphere. Many important geochemical reactions occur against thermodynamic predictions, while others occur at rates that would be considered impossible if only the abiotic reactions operated.

The importance of the microbes (in the context of all of the life on the planet) in shaping the condition of the surface environment was summarized by Krumbein and Dyer (1985):

- “1) Transfer of the rocks and minerals of the lithosphere through time and space is considerably speeded up and directed by biological processes on all scales....
- 2) Biological transfer of parts of objects of art and technology made of minerals, glasses and metals is considerable and by far exceeds the speed of inorganic transfer processes.
- 3) The transfer activity of the biosphere includes enrichments for practically all elements, purposeful arrangement according to the requirements of the biota, and rate limiting controls.
- 4) The abiotic transfer of rocks and minerals in a geomorphological sense is negligible under the thermodynamic conditions of earth.
- 5) Biotic and abiotic states of matter are in homeorhesis.”

To understand how the microorganisms play such a dominating role in geochemical processes, it is necessary to look both at what the organisms do geochemically and how and why they do it. This chapter will examine the most fundamental processes of microbial growth and reproduction, and it will link those fundamental processes with the geochemical changes that are often observed to occur in the presence of microbes. It is not the purpose of this presentation to provide an exhaustive discussion; indeed, that would (and has) filled several volumes. Rather it is more appropriate to leave the reader with the firm conclusion that many of the geochemical reactions associated with the formation of some and the weathering of all ore deposits are microbiologically mediated, and that any complete study of geochemistry therefore should pay attention to the biotic components of the system being examined.

Microbes interactions with the geochemical environment occur in a variety of ways, including utilization of geochemically reactive species, production of geochemically reactive species, and alteration of the geochemical environment. Individual compounds may be altered due to direct action by microbially produced enzymes, or by the consumption or production of molecules that react with the geochemical species of interest. Alternatively, microbial action may cause a change in the geochemical environment that leads to alteration of geochemically important species in the particular system of interest.

THE ABUNDANCE AND DISTRIBUTION OF MICROORGANISMS

Although the microbiologist often has great difficulty in keeping contaminating organisms out of laboratory cultures, it was commonly assumed for a long period of time that some areas of the Earth's surface are sterile. In the past 10–20 years, that common knowledge has been demonstrated to be inaccurate. Active bacteria have been found at very high hydrostatic pressures (600 to 1,000 atmospheres) in the deep ocean. Other active bacteria have been found to exist at high temperatures (up to 350°C) in combination with elevated pressures (about 600 atm), such as the conditions found in the geothermal rift vents in the ocean floor (Baross and Deming, 1983). Even more recently, abundant, diverse, and active communities of bacteria have been found in old sedimentary deposits at depths approaching a kilometer (Balkwill, 1989). The presence of these diverse communities seems to disprove the hypothesis that microbial life is generally (but not universally) limited to the top few meters of soil (e.g., Alexander, 1976).

Given the small size of bacteria (0.5 μm to about 5 μm), one

could legitimately ask the question of how they manage to be so important in the environment. The answer is quite simple: the bacteria are extraordinarily numerous, and they metabolize and reproduce very rapidly. Typical concentrations of bacteria in several habitat types are given in Table 5.1. As a means of illustration, let us assume that a person is taking a bath in “typical” lake water. If the concentration of bacterial cells is 1×10^6 and the bath contains 30 gallons (117 liters) of water, the bather shares the bath with 1.17×10^{11} other living beings! Further, given the typical numbers of bacteria, fungi, etc., recovered from surface agricultural soils, the mass of the microorganisms in an acre-furrow-slice (approximately the top 6 inches of soil covering an acre—estimated to weigh about 2 million pounds) is about 3,000 pounds.

TABLE 5.1—Typical abundance of microorganisms in various habitats.

Location	Concentration of microbes ⁽¹⁾	Reference
Agricultural soil	10^8 cm^{-3} (cultural counts)	Alexander, 1976
Coastal waters	10^6 ml^{-1}	Hobbie et al., 1977
Open ocean water	10^5 ml^{-1}	Atlas and Bartha, 1993
Terrestrial surface waters	10^6 ml^{-1}	Hobbie et al., 1977
Deep aquifers	$10^5\text{--}10^8 \text{ g}^{-1}$ wet sediment (cultural counts)	Balkwill, 1989
Sea floor		
Water	10^3 ml^{-1}	Deming, 1981
Sediment	$10^5\text{--}10^8 \text{ g}^{-1}$ dry sediment	Austin, 1988

⁽¹⁾Numbers are approximations based on multiple values given in the reference. The numbers are given as general guidelines only; specific sites may vary from these values by several orders of magnitude.

FUNDAMENTALS OF MICROBIAL METABOLISM

Microorganisms, as all other organisms, have several basic needs to maintain life and to grow and reproduce. Those needs can be classified by several schemes, but a fundamental one used by most microbial ecologists includes the need for energy, carbon, and a source of electrons. Along with the need for carbon goes a need for a number of other elements that are used to synthesize new biomass. For example, nitrogen, phosphorous, sulfur, potassium, calcium and several other metals and transition elements must be present in trace amounts for cell growth. Implicit in the need for a source of electrons is the need for a suitable terminal electron acceptor, a “place to put the electrons” after they have been used for energy production or reducing power.

With the exception of the phototrophs, which obtain their energy from light, all organisms are chemotrophs. That is, their energy for growth is obtained through the oxidation of either organic or inorganic chemicals (Fig. 5.1); the free energy change associated with oxidation reactions is usually negative, thus favorable for the progress of the reaction and thus resulting in a net release of energy that can be used by the organism. Life forms from microbes to man have evolved the capability of coupling the energy released from oxidation reactions to other reactions that result in the synthesis of new cellular biomass. Biosynthetic reactions are typically reductive in nature, and require an input of energy and, by definition, electrons. The exergonic oxidations are not coupled directly to the endergonic synthetic reactions. Instead, the free energy and the released electrons are held in carrier mole-

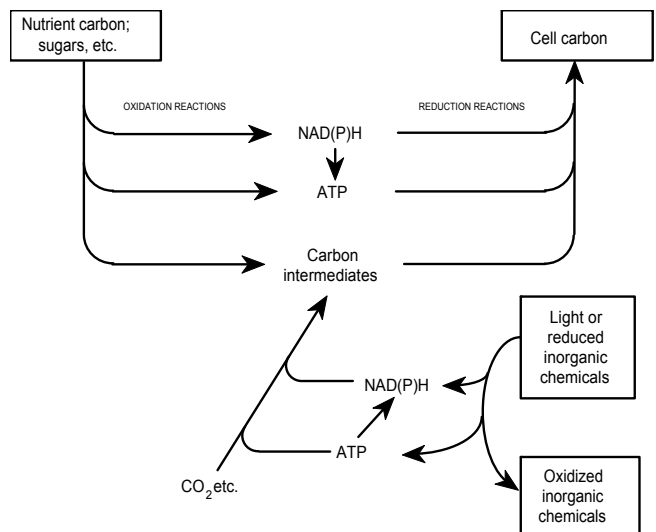


FIGURE 5.1—A summary of biological metabolism. Energy is gained from the oxidation of organic or inorganic chemicals (or light in the case of phototrophs), electrons are usually gained from those same compounds (phototrophs obtain electrons from the splitting of H_2O to yield O_2 or the splitting of H_2S to yield S^0). Carbon is obtained from the organic compound used by the heterotrophs or fixed from CO_2 in the autotrophs. Note that the energy yielding (exergonic) oxidation reactions are not coupled directly to the endergonic reduction reactions of biosynthesis. Rather they are indirectly coupled through the energy transfer compound ATP and the electron transfer compound NAD(P)H. Note that NAD(P)H is a phosphorylated form of the NADH molecule mentioned in the text (after Lynch and Poole, 1979).

cules. Energy is stored in the form of high-energy phosphate bonds in phosphorylated adenylate molecules (adenosine triphosphate, or ATP) and the electrons are transferred by electron carriers such as nicotinamide adenine dinucleotide (the reduced form is noted as NADH, the oxidized form as NAD^+). The ability to store energy and electrons in carrier molecules means that reactions with small changes in free energy can fuel reactions with larger changes in free energy without direct stoichiometric relationships.

Organisms that obtain carbon from an organic molecule are referred to as heterotrophs, whereas organisms that must reduce CO_2 to an organic form are called autotrophs (see Table 5.2). Heterotrophs most often utilize the same organic molecule as a source of energy, carbon, and electrons. While such organisms are technically chemoorganoheterotrophs, they are usually referred to simply as heterotrophs or conventional heterotrophs (Brock et al., 1979). In most (but certainly not all) chemolithotrophs, the source of energy and electrons is the same inorganic compound, while CO_2 serves as the carbon source. Thus, the two most frequently encountered nutritional types are the heterotrophs and the chemolithotrophs. In geochemically interesting systems such as ore deposits, these two broad groups are most often responsible for microbiological reactions of importance.

Chemolithotrophs are responsible for the oxidation of a variety of inorganic compounds including molecular hydrogen, reduced-sulfur and nitrogen compounds, iron(II), and even carbon monoxide (Table 5.3). The net reactions mediated by the chemolithotrophs are all favored thermodynamically, that is ΔG° is negative. Due to kinetic constraints, however, most of these

reactions proceed abiotically very slowly or not at all at earth surface temperature and pressure; a notable exception may be the oxidation of Fe^{2+} , as discussed later.

TABLE 5.2—Trophic grouping of microorganisms.

Substance	Source	Classification
Carbon	Organic	Heterotroph
	CO_2	Autotroph
Energy	Light	Phototroph
	Chemical	Chemotroph
Electrons	Organic	Organotroph
	Inorganic	Lithotroph

TABLE 5.3—Physiological groups of chemolithotrophs (taken from Gottschalk, 1986). Although the correct SI units for these values would be Joules, the author defers to the argument of Kleiber (1972) and Battley (1987), that the calorie is a preferable means of expressing changes in heat due to work done on or by a thermodynamic system.

Group	ATP yielding reaction	ΔG°	
		kcal/reaction	kcal/2e ⁻
Hydrogen bacteria	$\text{H}_2 + 1/2\text{O}_2 \rightarrow \text{H}_2\text{O}$	-56.7	-56.7
Carboxydo-bacteria	$\text{CO} + 1/2\text{O}_2 \rightarrow \text{CO}_2$	-61.5	-61.5
Sulfur bacteria	$\text{S}^{2-} + 2\text{O}_2 \rightarrow \text{SO}_4^{2-}$	-189.9	-47.5
	$\text{S}^0 + 1/2\text{O}_2 + \text{H}_2\text{O} \rightarrow \text{SO}_4^{2-} + 2\text{H}^+$	-139.8	-46.6
Iron bacteria	$\text{Fe}^{2+} + 1/4\text{O}_2 + \text{H}^+ \rightarrow \text{Fe}^{3+} + 1/2\text{H}_2\text{O}$	-10.6 ^a	-21.2 ^a
Ammonia oxidizers	$\text{NH}_4^+ + 1 1/2\text{O}_2 \rightarrow \text{NO}_2^- + 2\text{H}^+ + \text{H}_2\text{O}$	-64.7	-21.6
	Nitrite oxidizers	$\text{NO}_2^- + 1/2\text{O}_2 \rightarrow \text{NO}_3^-$	-18.5

^a ΔG° values for pH = 0 are given; iron bacteria can grow at acidic pH values only; the ΔG° value for pH = 7 would be -0.95 kcal/reaction.

Oxidation of a number of inorganic substances can support chemolithotrophs, and the potential (E_0') for some of these reactions is shown in Table 5.4 along with the NADH/NAD⁺ couple. These reactions usually occur under aerobic conditions, because of the high E_0' of the $\text{H}_2\text{O}/\text{O}_2$ couple.

TABLE 5.4—Redox potentials of reactions important in chemolithotrophic metabolism.

	E_0' (volts)
$\text{CO} + \text{H}_2\text{O} \rightarrow \text{CO}_2 + 2\text{H}^+ + 2e^-$	-0.54
$\text{H}_2 \rightarrow 2\text{H}^+ + 2e^-$	-0.41
$\text{NADH} + \text{H}^+ \rightarrow \text{NAD}^+ + 2e^- + 2\text{H}^+$	-0.32
$\text{H}_2\text{S} \rightarrow \text{S} + 2\text{H}^+ + 2e^-$	-0.25
$\text{S} + 3\text{H}_2\text{O} \rightarrow \text{SO}_3^{2-} + 6\text{H}^+ + 4e^-$	+0.05
$\text{SO}_3^{2-} + \text{H}_2\text{O} \rightarrow \text{SO}_4 + 2\text{H}^+ + 2e^-$	-0.28
$\text{NH}_4^+ + \text{H}_2\text{O} \rightarrow \text{NO}_2^- + 8\text{H}^+ + 6e^-$	+0.44
$\text{NO}_2^- + \text{H}_2\text{O} \rightarrow \text{NO}_3^- + \text{H}^+ + 2e^-$	+0.42
$\text{Fe}^{2+} \rightarrow \text{Fe}^{3+} + e^-$	+0.78
$\text{O}_2 + 4\text{H}^+ + 4e^- \rightarrow 2\text{H}_2\text{O}$	+0.86

Under anaerobic conditions, heterotrophs often oxidize organic carbon to CO_2 by using some oxidized inorganic (other than O_2) as the terminal electron acceptor. Such organisms include the denitrifiers (NO_3^- is reduced sequentially to NO_2^- then to N_2), iron reducers, sulfate reducers, and methanogens. The latter often follow a metabolic path wherein H_2 is oxidized to H_2O , and CO_2 serves as both the carbon source and as the terminal electron acceptor (i.e., $4\text{H}_2 + \text{CO}_2 \rightarrow \text{CH}_4 + 2\text{H}_2\text{O}$). Some relevant reduction reactions will be discussed below. However, it is important to note that the chemolithotrophic oxidation of reduced inorganic species, coupled with the anaerobic reduction of the oxidized species of the same element, constitutes a complete biogeochemical cycle, at least in terms of production and fate of the various redox species.

DIRECT TRANSFORMATIONS: ALTERATIONS OF MATERIALS FOUND IN ORE DEPOSITS

Sulfur

Many of the ore deposits in which microorganisms play an important role during weathering contain reduced sulfides. The sulfides were formed as part of igneous or hydrothermal processes. Sulfides of biogenic origin are present in some mineral deposits and coal deposits. In such circumstances, the sulfides arose from the bacterial reduction of sulfate during anaerobic oxidation of organic matter. Sulfides in mineral deposits, coal deposits, and rocks are preserved until exposed by erosion to oxygen and water. A number of metal sulfides are of interest (either because they can be formed biogenically or are decomposed biologically); the reader is referred to Alpers and Nordstrom (1999) for a list of important sulfide minerals.

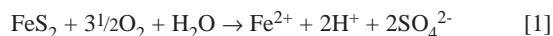
Sulfur oxidation

Microorganisms attack metal sulfides directly or indirectly, resulting in mineral dissolution or the combined dissolution of the mineral and the oxidation of one or more of the elements in the mineral. In the direct case, enzymes are produced by the microbes that react with the surface of the mineral grains. All studies conducted thus far suggest that close contact between the microbial cell and the mineral grain must occur for the direct dissolution/oxidation to proceed.

Metal sulfides are acted upon directly by a few microbes, generally of the genus *Thiobacillus*. Nearly all the sulfur oxidizers are chemolithoautotrophs that are capable of linking the free energy released during the oxidation with ATP and NADH formation to synthesize new cell material from autotrophically fixed CO_2 . While *Thiobacillus* sp. are the primary oxidizers of the metal sulfide ores, a few genera (including some *Thiobacillus* species) attack the sulfur in dissolved sulfides (H_2S); for example, much of the H_2S formed during sulfate reduction in salt marshes is reoxidized to S^0 by *Beggiatoa*. The S^0 is stored as granules in the cells; in the event that the H_2S supply becomes limited, the organism is capable of oxidizing the S^0 to SO_4^{2-} . In the case of *Beggiatoa*, the acidification normally seen in the oxidation of sulfide minerals such as pyrite does not occur.

In reactions involving iron-containing sulfides, it is difficult to separate the oxidation of sulfur from that of iron, and some men-

tion of both must be made when discussing either sulfur oxidation or iron oxidation. Typical chemical reaction for oxidation of pyrite sulfur is shown in equation [1], sulfur reduction in equations [2–4], and Fe oxidation in equations [5–8]. The oxidation of pyrite proceeds according to the reaction:



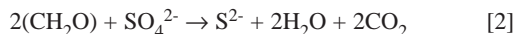
The ferrous iron generated by this process can be further oxidized to ferric iron (see equation [5]). Ferric iron is then free to participate in further “indirect” oxidation according to a reaction of the type given in equation [8]. The process depicted in equation [1] is carried out by *Thiobacillus thiooxidans*, *Thiobacillus ferrooxidans*, possibly other members of the genus *Thiobacillus*, and members of the genus *Sulfolobus* (Erlich, 1995). The reaction depicted in equation [1] is the rate limiting step in pyrite oxidation (Singer and Stumm, 1970), and while it will proceed in the absence of bacterial catalysis, the rates in the presence of active bacteria can be as much as a million times more rapid than those in the absence of bacterial activity.

T. ferrooxidans is the most intensively studied of the sulfur-oxidizing chemolitho-autotrophs. In addition to its oxidation of sulfur, *T. ferrooxidans* can also oxidize ferrous iron in pyrite and other sulfide minerals to drive its biosynthetic pathways. Indeed, to separate for laboratory studies *T. ferrooxidans* from *T. thiooxidans*, which can oxidize the sulfur but not the iron, a medium containing reduced iron added as FeSO_4 (the so-called 9K medium of Silverman and Lundgren, 1959) is used to grow the iron oxidizers. *T. ferrooxidans* cannot use ferrous iron at a pH above 4. There, the free energy change of the reaction becomes too small to allow efficient ATP synthesis for energy storage (see Table 5.3). *T. ferrooxidans* can oxidize sulfur at circumneutral pH levels, however.

Equation [1] shows the production of one mole of H^+ per mole of pyrite sulfur oxidized. This reaction, therefore, contributes to a number of acidification processes, including those that form acid mine drainage (AMD). As we shall see below, the oxidation of Fe^{2+} contributes even more acid to the water in which the reaction is taking place.

Sulfate reduction

In the absence of oxygen, a select but active and important group of microbes are capable of oxidizing organic matter while utilizing SO_4^{2-} as the terminal electron acceptor. This reaction is often written as



where CH_2O is used to represent organic matter (CH_2O is a good stoichiometric representation of carbohydrate, the most abundant material in plants). Work of the past 10 years has shown that equation [2] represents a community-level reaction in that organisms that actually reduce SO_4^{2-} (typified by members of the genus *Desulfovibrio*) cannot use carbohydrates. Rather they utilize the products of anaerobic bacterial fermentation such as acetate and H_2 , the most frequently used substrates for the direct reduction of SO_4^{2-} to H_2S .

Sulfate reduction is an important reaction in the geochemical processes associated with the formation of many sulfides in coal and some mineral deposit types. It represents the reverse of one of the important reactions that creates the acidic conditions associated with the oxidation of sulfide minerals. Indeed, sulfate reduction represents the source of sulfide in most coal deposits; seawater sulfate is reduced during the initial decomposition reactions associated with coal formation. Pyrite forms as a result of the simultaneous release of Fe^{2+} .

In addition to being the source of reduced sulfide in coal and some mineral deposits, sulfate reduction can have a definite mitigative effect on the acid conditions produced by oxidation of metal sulfides such as pyrite. The fate of the sulfide released by the reaction depicted in equation [2] is likely to be as follows (Bernier et al., 1970; Goldhaber and Kaplan, 1975):



Combining equations [2] and [3] yields

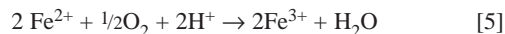


The alkalinity thus produced is permanent only if the H_2S is removed (by degassing) or if the sulfide reacts with a metal ion such as Fe^{2+} to form a solid phase that prevents diffusion of the sulfide to oxygenated waters. Formation of alkalinity in acidic wastes from ore deposits will be considered further in discussion of the reduction of iron below.

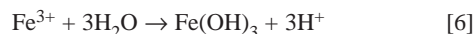
Iron

Iron oxidation

As pointed out above, microbial pyrite oxidation by *T. thiooxidans* and *T. ferrooxidans* results in the formation of sulfuric acid (equation [1]). Additionally, *T. ferrooxidans* oxidizes the Fe^{2+} to Fe^{3+} by the reaction:



This reaction would seem to consume the protons released during the oxidation of the sulfur, but hydrolysis of the Fe^{3+} generates a net increase in the proton concentration of the system by the formation of aqueous ferric hydroxide complexes or ferric hydroxide solids, by the reaction:



The formation of $\text{Fe}(\text{OH})_3$ solids is responsible for the reddish to yellowish staining of rocks commonly seen in acid mine streams. The formation of jarosite in sulfate-rich acid mine waters may decrease the ratio of protons generated per iron oxidized (Erlich, 1995):



where M^+ may be Na^+ , K^+ , NH_4^+ , or H_3O^+ . The ferric iron produced may also contribute to the abiotic oxidation of pyrite with a substantial net increase in the total acid production (Erllich, 1995):

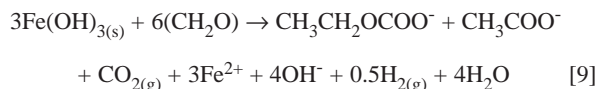


In this case, the dissolved ferric iron comes largely as a result of bacterial oxidation. The formation of the large amount of acidity contributes greatly to the oxidation of other metal sulfides that may be a part of the host rock in which the minerals exist.

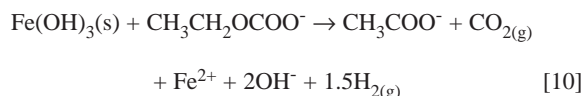
Iron reduction

Reduction of iron (and perhaps other metals) plays an important role in ion mobility due to the increased solubility of Fe(II) compounds compared to Fe(III) compounds. Increased iron concentrations in ground waters are often attributed to the action of microorganisms, either by direct reduction of the iron when it is used as a terminal electron acceptor for oxidation of organic matter, or by indirect iron reduction caused by production of suitable reducing agents by bacteria. For example, the reduction of sulfate results in production of sulfides that can reduce Fe(III) in many minerals in the absence of direct microbial activity on the iron itself. In the case of sulfides, however, the end product may be an iron mono- or di-sulfide solid phase, thereby creating another insoluble mineral phase. Some studies of direct iron reduction by bacteria suggest that the role of this process in nature may have been underestimated historically (Lovely, 1991).

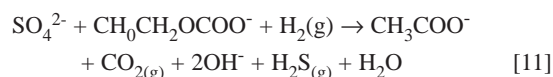
The formation of acidic effluents associated with reduced iron minerals exposed to oxygenated water relies to a great extent on the hydrolysis of the oxidized iron as shown in equations [6] and [8]. Conversely, if the iron is again reduced, consumption of that acidity occurs. This process is of particular interest in iron- and sulfur-rich acid mine waters. Given anaerobic conditions and appropriate bacteria, alkalinity can be produced from the oxidation of glucose by the community-level reaction (Mills et al., 1989):



Likewise, alkalinity is generated if lactate is used as a carbon and electron source for iron reduction, and the stoichiometry of the equations suggests that more alkalinity is generated per mole of iron reduced when lactate is used than when glucose is used:



Alkalinity is also generated by sulfate reduction using lactate as a carbon source:



In order for alkalinity generated during iron or sulfate reduction to be permanent, the reduced iron and sulfur must be either sequestered in, or removed from the sediments. Sequestration can occur by reactions of sulfide with metal cations to form insoluble metal sulfides and by reactions of sulfide to form organic sulfide compounds (Anderson and Schiff, 1987).

The reactions above indicate that iron reduction can be important in acid neutralization. In addition to direct acid neutralization, iron can also play a role in the delivery of SO_4^{2-} to anaerobic sites such as sediments, as well as influencing the final products of other microbial processes such as SO_4^{2-} reduction. Figure 5.2 shows a series of processes that have been shown to function in the Contrary Creek arm of Lake Anna in Virginia. Microcosm experiments utilizing sediment and water from this acid-mine-drainage-receiving impoundment have shown that removal of SO_4^{2-} from the water column is greatly enhanced by the addition of Fe^{3+} to sulfate-rich water overlying reducing sediment (Mills et al., 1989; Herlihy and Mills, 1989). The iron generates an iron oxyhydroxide floc that coprecipitates with adsorbed sulfate, enhancing delivery of SO_4^{2-} to the sediment; in contrast, direct diffusion of SO_4^{2-} into the sediments in Lake Anna accounted for only 5% of the observed sulfate retention in the acidified arm of the impoundment (Herlihy et al., 1987). The precipitation of the iron increases the acidity, but the acidity is neutralized by subsequent reactions in the sediment.

When the precipitate reaches the sediment/water interface, the iron oxyhydroxide dissolves as iron is reduced, both by direct bacterial activity and by redox reactions induced by microbial reactions not directly involving iron (Bell et al., 1987; Lovely, 1991; Lovely and Phillips, 1988). Reduction of iron neutralizes the acidity formed during the hydrolysis, and liberates adsorbed and precipitated SO_4^{2-} into the anaerobic sediments. At this point, reduc-

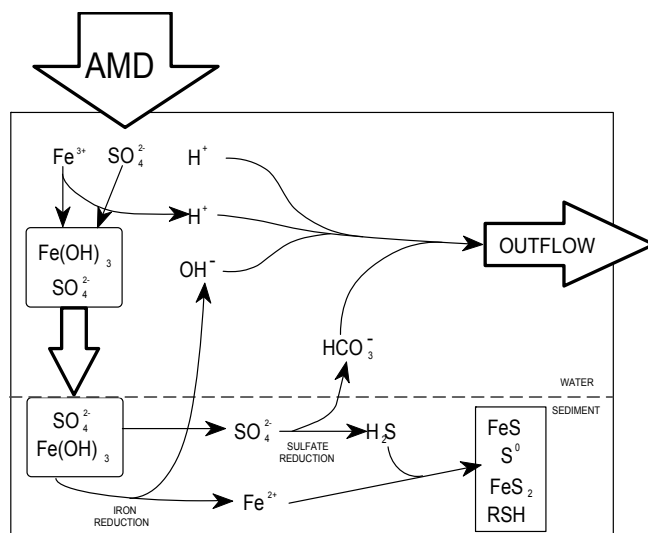


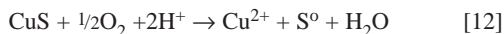
FIGURE 5.2—Role of iron and sulfate in the neutralization of acid mine drainage.

tion of both iron and SO_4^{2-} contributes to the neutralization of the acid mine drainage. While much of the neutralization contributed by iron reduction balances the acidity formed during the hydrolysis, any particulate ferric iron entering the lake can contribute to neutralization of the protons in the acid pollution.

In order to preserve the alkalinity generated by the reduction reactions the sulfides must be retained (as described above), or their reoxidation will generate protons and consume the alkalinity. Precipitation of reduced metal sulfides serves as an important mechanism for preservation of reduced sulfide. Thus, iron is a critical element in the biogeochemical neutralization of acid pollutants. In waters where iron is not abundant, other elements may also play an important role, i.e., aluminum oxides might help remove sulfate from water as would any solid-phase anion exchange complex; reduction of elements such as manganese can also contribute to the generation of alkalinity in some waters. While iron is not well studied with respect to reactions such as those described here, the role of the other elements is totally undocumented and also deserves attention to arrive at a complete picture of the overall neutralization process.

Other elements

Release of other metal ions to solution occurs during oxidation of sulfide ores either by acid production or dissolution of the solid phase. For example, the oxidation of CuS by *T. ferrooxidans* proceeds because of the oxidation of the S atom:

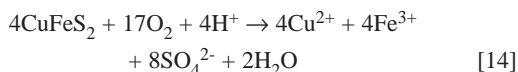


An additional, bacterially mediated step results in the formation of sulfate:

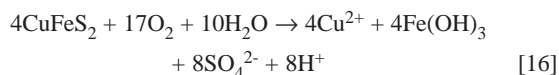


In some cases, such as that with *Thiobacillus thioparus*, the initial oxidation (equation [12]) is abiotic, and the only biotic oxidation is that depicted in equation [13] (Erlich, 1995).

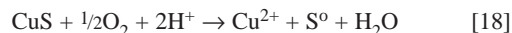
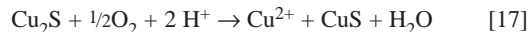
Erlich (1995) also provides evidence from the literature that suggests different oxidation mechanisms for different ores. For example, the oxidation of chalcopyrite probably proceeds by a pair of reactions, the first of which is bacterially mediated, and in which both the metal and sulfide moieties are attacked by different enzymes:



Summing reactions 14 and 15 yields:



Alternatively, bacteria may attack the metal before the sulfide. Chalcocite oxidation proceeds as described by Erlich (1995):



In this case it is not clear that energy or electrons needed for growth are actually obtained by the microorganism.

Similarly, in the case of reductions, it is not clear if the redox reaction is carried out actively by the microbes or whether it occurs secondarily as a result of microbial alteration of the environment. Note, however that there appears to be strong evidence for a mercury reductase system in several bacteria (Wood, 1974). The product of mercury reduction is elemental mercury, which readily volatilizes into the atmosphere.

Several elements (notably Hg, Sn, As, Se) are known to be methylated in anaerobic sediments to volatile methyl complexes such as mono- and dimethyl mercury. Because these compounds are vaporous, they diffuse rapidly through the water, and can even diffuse into the atmosphere. The volatilization/methylation reactions are thought to be part of a strategy on the part of the microbes to convert the toxic material to a form that rapidly dissipates from the vicinity of the cell. For these reactions, microorganisms and organic matter are essential. Methylation often occurs in environments conducive to methanogenesis (i.e., sediments and anaerobic waters), and all of the known organisms that carry out such reactions are heterotrophs (both bacteria and fungi are capable of participating in such reactions).

INDIRECT TRANSFORMATIONS: ALTERATIONS OF THE GEOCHEMICAL SETTING

Alteration of pH

The reactions surrounding the oxidation of metal sulfide ores generate large amounts of acidity (See equations [1], [5], [6], and [8], above). However, if a major component of the ore body consists of a nonsulfidic, reduced iron mineral, the lack of sulfide oxidation does not preclude acid formation.

Bacteria can also reduce the pH through the formation of organic acids. These acids usually are carboxylic acids (i.e., R-COOH). Although phenols (hydroxybenzene) can also display an acid character at high pH values. Such compounds are Lowry-Brønsted acids in that they donate protons to the solution. These acids and their conjugate bases can provide buffer capacity to an aqueous solution, and the conjugate bases (e.g., R-COO⁻) often complex with metal cations as described later.

Under some conditions, microbes can raise the pH through generation of bicarbonate alkalinity or generation of bases such as NH_3 or S^{2-} .

Alteration of Eh

Whenever microbial activity occurs, the effect is a lowering of the redox potential. In aerobic systems, the presence of oxygen poises the Eh so that visible effects are unlikely. When the oxygen is consumed, however, the measured or calculated redox potential can drop very quickly. Theoretical calculations of Eh using couples assumed to dominate under different sets of metabolic conditions indicate that the range of Eh conditions inhabited by bacteria ranges from about 800 mV (fully aerobic conditions) to about -350 to -400 mV, where methanogenesis occurs. Organic loading of any water can alter the Eh of the water if the oxygen demand exceeds the reaeration capability. The redox reactions that occur may cause the release of iron, manganese, (Evans et al., 1977; Graybeal and Heath, 1984; Brannon et al., 1985) and arsenic (Edenborn et al., 1986) to the water. Further, metals that are sorbed or precipitated with Fe and Mn oxides may also be released on dissolution of the oxide phases (Graybeal and Heath, 1984; Sawlen and Murray, 1983; Gunkel and Sztarka, 1986; Shaw et al., 1990). Recent laboratory experiments indicate the release of Cd, Cr, Ni, Pb, and Zn by this process (Francis and Dodge, 1990).

Production of chelators and complexing agents

An important microbial activity that can mobilize metals in waters associated with ore deposits is the formation of chelating agents. For example, there are a number of compounds that are used by bacteria for the transport of iron across the cell membrane. These compounds are called siderophores, and some examples of their structures are shown on Figure 5.3. Production of similar compounds for other metals is not well documented, although generation of some nonspecific complexing agents referred to as metallothioneins is frequently reported. Metallothioneins are small proteinaceous molecules with a high proportion of sulfur-containing amino acids that complex strongly with metal ions.

Microbial decomposition of organic matter often results in the release of metal-mobilizing humic substances into solution (Reuter and Perdue, 1977; Bovendeur et al., 1982). These substances contain a high concentration of acid functional groups that carry a negative charge at most environmental pH values. Thus, they tend to form strong ionic complexes, often multidentate, with dissolved metals. The affinity of the humic acids for metal ions is often strong enough to remove the ion from exchange surfaces in the solid phase of subaqueous environments. Lehman (1991) demonstrated that addition of humic acid to chambers placed on the sediment surface in Lake Anna, where the sediments are copper-enriched due to the inflow of acid mine drainage, resulted in the mobilization of copper at levels beyond that explained by mechanisms such as Eh change or reductive dissolution of copper-containing iron oxides (See Fig. 5.4)

REFERENCES

- Alexander, M., 1976, Introduction to soil microbiology: John Wiley and Sons, New York, 467 pp.
 Alpers, C.N., and Nordstrom, D.K., 1999, Geochemical modeling of water-rock interactions in mining environments; *in* Plumlee, G.S., and Logsdon, M.J. (eds.), The Environmental Geochemistry of Mineral Deposits, Part A. Processes, Techniques, and Health Issues: Society of Economic Geologists, Reviews in Economic Geology, v. 6A, pp. 289-323.

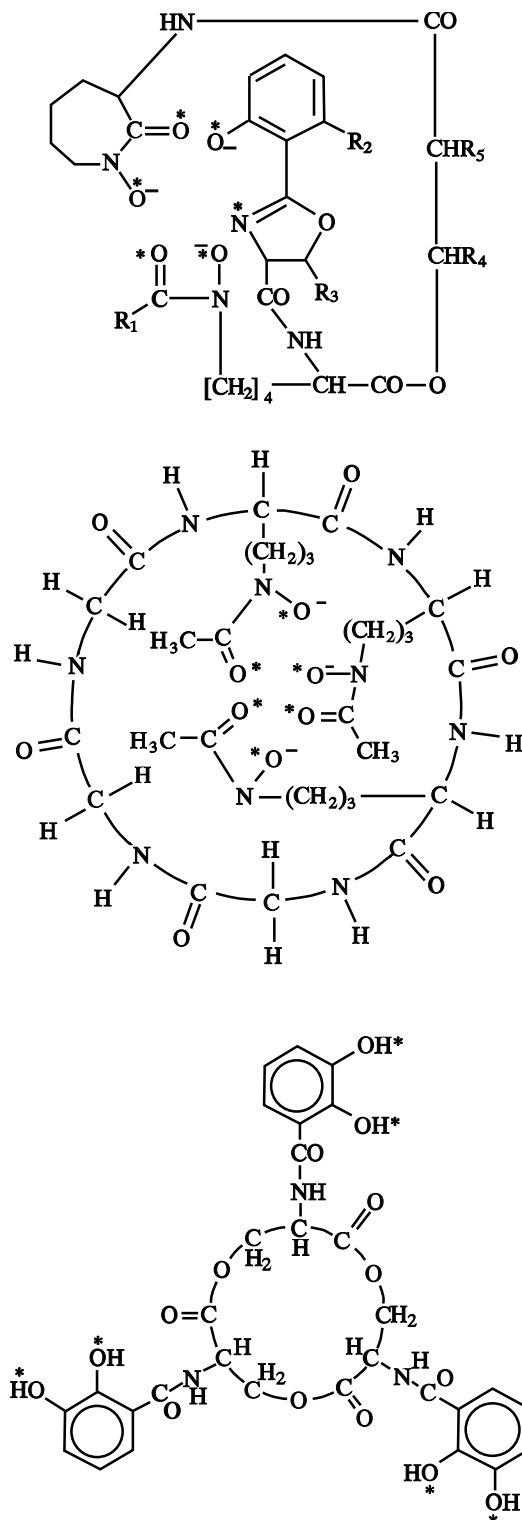


FIGURE 5.3—Structure of some siderophores. Note the variety of charge sites that can interact with a metal ion to form a multi-dentate complex.

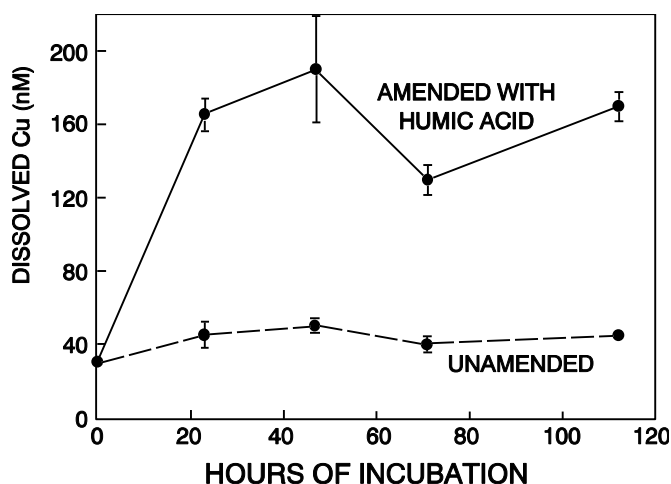


FIGURE 5.4—Release of copper from impoundment sediments due to the addition of humic acid to the overlying water. Addition of organic matter as dead (previously frozen) phytoplankton did not have the same effect on copper mobilization as did the addition of the humic acids (Lehman, 1991).

Anderson, R.A., and Schiff, S.L., 1987, Alkalinity generation and the fate of sulfur in lake sediments: *Can. J. Fish. Aquat. Sci.*, v. 44, pp. 188–193.

Atlas, R.M., and Bartha, R., 1993, *Microbial ecology—Fundamentals and applications*: Benjamin/Cummings, Inc., Redwood City, Calif., 563 pp.

Austin, B., 1988, *Marine microbiology*: Cambridge University Press, Cambridge, 222 pp.

Balkwill, D.L., 1989, Numbers, diversity, and morphological characteristics of aerobic, chemoheterotrophic bacteria in deep subsurface sediments from a site in South Carolina: *Geomicrobiology Journal*, v. 7, pp. 33–52.

Baross, J.A., and Deming, J.W., 1983, Growth of ‘black smoker’ bacteria at temperatures of at least 250°C: *Nature*, v. 303, pp. 423–426.

Battley, E.H., 1987, *Energetics of microbial growth*: John Wiley and Sons, New York, 450 pp.

Bell, P.E., Mills, A.L., and Herman, J.S., 1987, Biogeochemical conditions favoring formation of magnetite during anaerobic iron reduction: *Applied Environmental Microbiology*, v. 53, pp. 2610–2616.

Berner, R.A., Scott, M.R., and Thomlinson, C., 1970, Carbonate alkalinity in the porewaters of anoxic marine sediments: *Limnol. Oceanogr.*, v. 18, pp. 544–549.

Bovendeur, J., Van Burren, J.C.L., and Jacobs, J.A., 1982, Mobilization of copper from modified peat by dissolved organic matter in natural waters and biologically purified wastewaters: *Z. Wasser Abwasser Forsch.*, v. 15, pp. 181–186.

Brannon, J.M., Chen, R.L., and Gunnison, D., 1985, Sediment-water interactions and mineral cycling in reservoirs; *in* Gunnison, D. (ed.), *Microbial Processes in Reservoirs*: Dr. W. Junk Publishers, Dordrecht, pp. 121–135.

Brock, T.D., Smith, D.W., and Madigan, M.T., 1979, *Biology of microorganisms*: Prentice-Hall, Inc., Englewood Cliffs, N.J., 847 pp.

Deming, J.W., 1981, *Ecology of barophilic deep-sea bacteria*, Ph.D. Dissertation, Univ. of Maryland, College Park, Md., 160 pp.

Edenborn, H.M., Belzile, N., Mucci, A., Label, J., and Silverberg, M., 1986, Observations on the diagenetic behavior of arsenic in a deep coastal sediment: *Biogeochemistry*, v. 2, pp. 359–376.

Erlich, H.L., 1995, *Geomicrobiology*: 3rd ed., Marcel Dekker, Inc., New York, 719 pp.

Evans, D.W., Cutshall, N.H., Cross, F.A., and Wolfe, D.A., 1977, Manganese cycling in the Newport River Estuary, North Carolina: *Estuar. Coast. Mar. Sci.*, v. 5, pp. 71–80.

Francis, A.J., and Dodge, C.J., 1990, Anaerobic microbial remobilization of toxic metals coprecipitated with iron oxide: *Environmental Science and Technology*, v. 24, pp. 373–378.

Goldhaber, M.B., and Kaplan, I.R., 1975, Controls and consequences of sulfate reduction rates in recent marine sediments: *Soil Science*, v. 119, pp. 42–55.

Gottschalk, G., 1986, *Bacterial metabolism*: Springer-Verlag, New York, 359 pp.

Graybeal, A.L., and Heath, G.R., 1984, Remobilization of transition metals in surficial pelagic sediments from the Eastern Pacific: *Geochimica et Cosmochimica Acta*, v. 48, pp. 965–975.

Gunkel, V.G., and Sztraka, A., 1986, Investigations about the fate of heavy metals in lakes, 2. The role of iron and manganese mobilization to the hypolimnic enrichment of heavy metals: *Archives of Hydrobiology*, v. 106, pp. 91–117.

Herlihy, A.T., and Mills, A.L., 1989, Factors controlling the removal of sulfate and acidity from the waters of an acidified lake: *Water Air Soil Pollution*, v. 45, pp. 135–155.

Herlihy, A.T., Mills, A.L., Hornberger, G.M., and Bruckner, A.E., 1987, The importance of sediment sulfate reduction to the sulfate budget of an impoundment receiving acid mine drainage: *Water Resources Research*, v. 23, pp. 287–292.

Hobbie, J.E., Daley, R.J., and Jasper, S., 1977, Use of Nuclepore filters for counting bacteria by fluorescence microscopy: *Applied Environmental Microbiology*, v. 33, pp. 1225–1228.

Kleiber, M., 1972, Joules vs calories in nutrition: *Journal of Nutrition*, v. 102, pp. 309–312.

Krumbein, W.E., and Dyer, B.D., 1985, This planet is alive—Weathering and biology, a multi-faceted problem; *in* Drever, J.I. (ed.), *The Chemistry of Weathering*: Kluwer Academic Publishers, pp. 6–13.

Lehman, R.M., 1991, The effect of microbial formation of dissolved organic material on the mobilization of copper from reservoir sediments: M.S. thesis, Univ. of Virginia, Charlottesville, Va., 143 pp.

Lovely, D.R., 1991, Dissimilatory Fe(III) and Mn(IV) reduction: *Microbiology Review*, v. 55, pp. 259–287.

Lovley, D.R., and Phillips, E.J.P., 1988, Novel mode of microbial energy metabolism—Organic carbon oxidation coupled to dissimilatory reduction of iron or manganese: *Applied Environmental Microbiology*, v. 54, pp. 1472–1480.

Lynch, J.M., and Poole, N.J., 1979, *Microbial ecology—A conceptual approach*: Blackwell Scientific Publications, Oxford, 266 pp.

Mills, A.L., Bell, P.E., and Herlihy, A.T., 1989, Microbes, sediments, and acidified water—The importance of biological buffering; *in* Rao, S.S. (ed.), *Acid Stress and Aquatic Microbial Interactions*: CRC Press, Inc., Boca Raton, Fla., pp. 1–19.

Reuter, J.H., and Perdue, E.M., 1977, Importance of heavy metal-organic matter interactions in natural waters: *Geochimica et Cosmochimica Acta*, v. 41, pp. 325–334.

Sawlen, J.J., and Murray, J.W., 1983, Trace metal remobilization in the interstitial waters of red clay and hemipelagic marine sediments: *Earth Planet. Sci. Lett.*, v. 64, pp. 213–230.

Shaw, T.J., Gieskes, J.M., and Jahnke, R.A., 1990, Early diagenesis in differing depositional environments—The response of transition metals in porewater: *Geochimica et Cosmochimica Acta*, v. 54, pp. 1233–1246.

Silverman, M.P., and Lundgren, D.G., 1959, Studies on the chemoautotrophic iron bacterium *Ferrobacillus ferrooxidans*, I. An improved medium and a harvesting procedure for securing high cell yields: *Journal of Bacteriology*, v. 77, pp. 642–647.

Singer, P.C., and Stumm, W., 1970, Acidic mine drainage—The rate-determining step: *Science*, v. 167, pp. 1121–1123.

Strahler, A.N., 1977, *Principles of physical geology*: Harper and Row Publishing, New York, 374 pp.

Wood, J.M., 1974, Biological cycles for toxic elements in the environment: *Science*, v. 183, pp. 1049–1052.

Chapter 6

GEOCHEMISTRY OF ACID MINE WATERS

D. Kirk Nordstrom¹ and C.N. Alpers²

¹*U.S. Geological Survey, 3215 Marine Street, Boulder, CO 80303-1066*

²*U.S. Geological Survey, Placer Hall, 6000 J Street, Sacramento, CA 95879-6129*

INTRODUCTION

There are about a dozen major hydrogeochemical processes that can account for the chemical composition of most natural waters. One of these is the oxidation of pyrite, a process at least as important a source of sulfate in natural waters as seawater and sea spray, gypsum dissolution, and atmospheric emissions. The natural process of pyrite oxidation is fundamental to the supergene alteration of ore deposits, the formation of acid-sulfate soils, and the development of acidity and metal mobilization in natural waters. As mineral deposits continue to be mined, and inactive or abandoned mines with their associated waste-rock and tailings piles continue to be exposed to weathering, large concentrations of sulfate and heavy metals will continue to be found in both surface waters and ground waters. Nearly 5×10^{10} tons of mining and mineral processing wastes had been generated in the United States as of 1985 and about 10^9 tons continue to be generated each year (U.S. Environmental Protection Agency, 1985). A more recent estimate indicates that there may be more than 500,000 inactive or abandoned mine sites in the U.S. (Lyon et al., 1993). Hazardous mine sites in serious need of remediation are probably much fewer but may still range in the thousands. Inventories of mineral resources, mine sites, and their associated environmental hazards are being assembled at various scales by federal and state agencies to better assess the magnitude of the problem.

The water-quality hazard produced by pyrite oxidation is known as "acid rock drainage," or if from a mined area, "acid mine drainage." We use the terms "acid mine drainage" and "acid mine water" synonymously, reflecting popular usage. These waters drain from waste rock, tailings, open pits, and underground mines into surface streams, rivers, and lakes. Acid mine waters typically have pH values in the range of 2–4 and high concentrations of metals known to be toxic to living organisms (Ash et al., 1951; Martin and Mills, 1976; Nordstrom and Ball, 1985). Natural waters acidified by mine drainage have killed enormous numbers of fish and benthic organisms, harmed livestock, and destroyed crops and have made many rivers, streams, and lakes turbid, colored, and unfit for most beneficial purposes. In the United States, 10^7 fish were reported killed during 1961–1975 from the effects of mining activities (Biernacki, 1978), and this number can safely be considered a gross underestimate. For example, the eighth annual report of the Federal Water Pollution Control Administration (1968) states that of the 11.59×10^6 fish reported killed in 1967 from all types of pollution only 16,413 were reported killed from the state of California. The California Department of Fish and Game (Nordstrom et al., 1977), however, recorded

47,100 fish killed from mine drainage at one site during a 7-day period in January of 1967. Many other mining-related fish kills may not be adequately recorded in federal or state archives.

Kleinmann (1989) has estimated that about 19,300 km of rivers and streams and more than 180,000 acres of lakes and reservoirs in the continental U.S. have been seriously damaged by acid mine drainage. Although a quantitative assessment of environmental damage from mining activities may be difficult or impossible, the volume of water bodies affected by acid mine drainage could be comparable to that affected by acid rain or other industrial sources of acidification.

It is important to note that pyrite oxidation also occurs in the absence of mining and there are numerous localities world-wide where naturally acidic waters containing high concentrations of metals are known (Runnells et al., 1992). The geochemical processes of weathering may be very similar in terms of mineral oxidation and dissolution but the hydrologic regime, the rates of reaction, and the environmental consequences can be quite different. Geochemical reactions in mined areas are more rapid because of:

- 1) greater accessibility of air through mine workings, wastes, and tailings,
- 2) greater surface areas for sulfides in mine workings, wastes, and especially tailings, and
- 3) different compositions of tailings as a result of mineral processing.

The presence of flues and flue dust piles (typically high in arsenic, zinc, and cadmium), slag piles, and soils and rocks contaminated by smelter fumes can be particularly detrimental to flora and fauna. Erosion of these materials by both aeolian and fluvial transport can contaminate drainage systems for very long distances (Moore and Luoma, 1990). The slower weathering of unmined mineral deposits occurs over longer time frames and tends to lead to more stable and insoluble mineral phases than those at mined deposits.

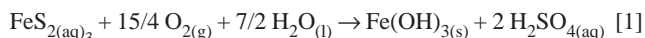
As an example of the extremes to which mine waters can develop acidity and high metal concentrations, the analyses of four of the most acidic mine waters ever reported are shown in Table 6.1. These waters were found in the Richmond mine workings at Iron Mountain, California (Nordstrom et al., 1991). Note that all samples have negative pH values and metal concentrations in grams per liter. These concentrations are some of the highest recorded metal and sulfate concentrations and the lowest pH values known. A survey of the literature indicates that only one known determination for copper, one for zinc, and one for arsenic have been found to be higher than those from the Richmond mine

waters (Table 6.1). Although these extreme values are rare, they do indicate the dramatic changes in water quality caused by natural processes and enhanced by mining activities.

TABLE 6.1—Comparison of four of the most acidic mine waters at Iron Mountain, California with the most acidic and metal-rich mine waters reported in the world (pH values in standard units, concentrations in grams per liter, Nordstrom et al., 1991; Nordstrom and Alpers, 1999).

	Iron Mountain					Other sites	References
pH	-0.7	-2.5	-2.6	-3.6	0.67		Goleva et al. (1970)
Cu	2.3	4.8	3.2	n.d.	48		Clarke (1916)
Zn	7.7	23.5	20	n.d.	50		Braeuning (1977)
Cd	0.048	0.21	0.17	n.d.	0.041		Lindgren (1928)
As	0.15	0.34	0.22	n.d.	0.40		Goleva (1977)
Fe (total)	86.2	111	101	16.3	48		Blowes et al. (1991)
Fe (II)	79.7	34.5	34.9	9.8	48		Blowes et al. (1991)
SO ₄	360	760	650	n.d.	209		Lindgren (1928)

The chemical reaction responsible for the formation of acid mine waters requires three basic ingredients: pyrite, oxygen, and water. The overall reaction is often written as:



where one mole of ferric hydroxide and 2 moles of sulfuric acid are produced for every mole of pyrite oxidized. For each mole of pyrite oxidized in equation [1], 1 electron is lost by oxidation of iron, 14 electrons are lost by oxidation of disulfide, and 15 electrons are gained by reduction of oxygen. Iron is also hydrolyzed and precipitated. All of these reactions cannot take place in a single step. Electron transfer reactions take place generally with only one or two electrons at a time (Basolo and Pearson, 1967). Hence, there could be 15 or more reactions with as many possible rate-determining steps to consider. To further complicate matters, several other oxidizing agents besides oxygen have been implicated in pyrite oxidation, e.g., ferric iron. Fortunately, all the intermediate reactions need not be determined to delineate the rate-controlling mechanisms involved with pyrite oxidation.

This chapter reviews the abiotic and microbial rates and mechanisms for sulfide mineral oxidation, the secondary minerals formed as a result of sulfide oxidation, and the major environmental factors that control the quality and quantity of acid water produced from mining activities.

HISTORICAL BACKGROUND

The history of mining and its environmental consequences, like technology in general, goes back several thousands of years, well before recorded history. Theophrastus (*ca.* 315 B.C.) mentions the degradation of pyrite to acid and salts (see Agricola, 1556). By the time of Pliny (23–79 A.D.), it was already well known that oil of vitriol (sulfuric acid), vitriol (ferrous sulfate), and alum (aluminum sulfates) were produced by the natural lixiviation (leaching) of pyritiferous rocks. Oil of vitriol was used to make other acids and compounds, vitriol was primarily used to blacken leather, and alum was used to tan hides. The acid waters and their

associated efflorescent (or flowering) salts produced from pyrite oxidation were also known to be highly toxic. Georgius Agricola (1546) wrote “When moisture corrodes cupriferous and friable pyrite it produces an acid juice from which *atramentum sutorium* forms and also liquid alum.... Experiments show that when porous, friable pyrite is attacked by moisture such an acid juice is produced.” *De Re Metallica* (Agricola, 1556), considered to be the first systematic book on mining and mineralogy, contains the following passage, “Since I have explained the nature of vitriol and its relatives which are attained from cupriferous pyrites I will next speak of an acrid solidified juice...; it is hard and white and so acrid that it kills mice, crickets and every kind of animal.” The “solidified juice” was later identified (by Herbert Hoover, translator) as goslarite, a hydrated zinc sulfate that likely contained some cadmium. With the dawn of the industrial revolution, acid mine drainage became a major source of water pollution on a large scale.

In the United States, occasional effort was directed towards the problem of acid mine drainage in the Appalachian coal mining region before 1900 (Vranesh, 1979). The State of Indiana has had a land reclamation act for coal-stripping since 1942 and a history of concern with the adverse effects of strip mining that can be traced back to 1917 (Wilber, 1969). Western mines were originally exempt from regulations on mine drainage or other environmental hazards because of the interest in attracting businesses and people to the West. Mining and metallurgical engineers occasionally investigated the problem (e.g., Burke and Downs, 1938), but primarily with an aim to alleviate coal mine drainage problems. From the 1920s through the 1940s, government agencies and the mining industry investigated acid mine drainage produced in the Appalachians from coal mines (Ash et al., 1951). Twenty years later the Appalachian Regional Commission reviewed the coal mine drainage problems (Appalachian Regional Commission, 1969). From the late 1960s through the late 1970s the National Coal Association and Bituminous Coal Research, Inc. sponsored a series of Coal Mine Drainage Research Symposia that resulted in several useful publications on the problem. About the same time, considerable research was supported by the Federal Water Pollution Control Federation and, later, the Environmental Protection Agency (EPA) on both the causes of acid mine drainage and its remediation. Even more attention has been given to the problem with the advent of the Comprehensive Environmental Response, Compensation and Liability Act (CERCLA or Superfund) in 1980. Several mining sites around the country were put on EPA's National Priority List for Superfund investigation and remediation.

FORMATION OF ACID MINE WATERS

The general description of the weathering of pyrite will now be examined in more detail. Equation [1], the overall reaction for the breakdown of pyrite to ferric hydroxide and sulfuric acid, is a gross oversimplification. It gives the correct picture in that oxygen is the ultimate driving force for the oxidation of pyrite and the final products are an insoluble form of oxidized iron and an aqueous sulfuric acid solution. Some problems with equation [1] are that it does not explain geochemical mechanisms or rates, it does not explain that ferric hydroxide is a fictitious, idealized phase, and it does not reflect the slow oxidation of aqueous ferrous iron in acid solutions that often results in high ferrous iron concentrations in

acid mine waters. Furthermore, factors such as microbial catalysis, neutralization reactions, sorption reactions, and climatic effects have an important influence on pyrite weathering, but are not considered explicitly in equation [1].

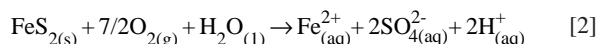
Mine operators as well as reclamation and remediation teams would like to know the potential or actual production of acid waters from a mine or from waste materials at a mine or a mineral processing facility. There is no simple, single test to assess metal and acid mobility in these settings because of the numerous variables that affect contaminant transport. The problem is multifaceted and we must emphasize that acid mine drainage forms within a complex environmental system where several factors need to be considered within the five general categories as shown in Table 6.2. These five categories are traditional scientific disciplines that must be integrated to characterize a field site.

TABLE 6.2—Environmental factors affecting acid mine water formation.

	Traditional Scientific Disciplines				
	Inorganic chemistry	Organic chemistry	Geology/mineralogy	Hydrology	Microbiology
Sulfide oxidation	✓	✓	✓	✓	✓
$\text{Fe}^{(II)}_{(aq)} \rightarrow \text{Fe}^{(III)}_{(aq)}$	✓	✓	✓	✓	✓
pH	✓	✓	✓	✓	✓
Temperature	✓	✓	✓	✓	✓
Gangue dissolution	✓		✓	✓	
Rock type/structure	✓		✓	✓	
Porosity			✓	✓	
Permeability			✓	✓	
Flow paths (recharge/discharge)	✓		✓	✓	
Climate	✓			✓	
Evapoconcentration/efflorescent salt formation	✓		✓	✓	
Efflorescent salt dissolution	✓		✓	✓	
Photochemistry	✓	✓		✓	✓

Stoichiometry and kinetics of abiotic pyrite oxidation

The voluminous literature on pyrite oxidation has been reviewed by Lawson (1982) with regard to abiotic chemical oxidation and by Nordstrom (1982a) with regard to biotic and abiotic geochemical oxidation. More recent contributions can be found in Goldhaber (1983), McKibben and Barnes (1986), Moses et al. (1987), Moses and Herman (1991), and Evangelou (1995). When pyrite oxidizes there are two species that can oxidize, the ferrous iron and the sulfidic sulfur. In studies on acid mine waters and pyrite oxidation, it has long been recognized that iron easily leaches out of pyrite but tends to stay in the ferrous state in acid solutions. Ancient history records the production of vitriol and oil of vitriol from washing pyritiferous ores and shales. During the last two centuries this vitriol was determined to be a mixture of ferrous sulfate and sulfuric acid. Hence, another common representation of the pyrite oxidation reaction is:



The sulfur moiety in pyrite oxidizes more quickly than the iron, but it must transfer a large number of electrons (14 times as many as iron per mole of pyrite). Consequently, there are several possible side reactions and sulfur intermediates that may occur during oxidation.

One side reaction is the formation of elemental sulfur during oxidation (Stokes, 1901; Bergholm, 1955; Clark, 1966). The yield is low and increases with higher temperatures, up to a maximum at about 100–150°C (Lowson, 1982). The lowest yield is at ambient temperatures but increases with increasing acidity. Field observations without laboratory identification are not reliable sources of information on elemental sulfur forming from pyrite oxidation because other minerals such as copiapite and jarosite may commonly be misidentified as elemental sulfur. Positive identification of elemental sulfur has been made at numerous inactive tailings impoundments (Blowes, 1995, written commun.). When acid waters react with minerals such as pyrrhotite and sphalerite they will produce H_2S , which readily oxidizes to elemental sulfur. Elemental sulfur is found commonly in nature where sulfur-rich, near-surface, hydrothermal solutions with temperatures around 100–150°C have oxidized or where H_2S -rich spring waters have oxidized on exposure to air.

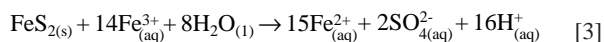
Another side reaction, or group of reactions, is the formation of intermediate sulfoxyanions of lower oxidation state than that found in sulfate: i.e., thiosulfate ($\text{S}_2\text{O}_3^{2-}$), polythionates ($\text{S}_n\text{O}_6^{2-}$), and sulfite (SO_3^{2-}). Steger and Desjardins (1978) reported a thiosulfate compound on the surface of oxidizing pyrite but their method did not distinguish between thiosulfate, polythionate, and sulfite. Goldhaber (1983) measured rates of reaction and reaction products for the pH range 6–9 and found that polythionates, thiosulfate, sulfite, and sulfate formed but only at high stirring rates. The proportions of intermediate sulfoxyanions were sensitive to pH in Goldhaber's (1983) experiments. Polythionates were found to be dominant at low pH and thiosulfate was dominant at high pH, with some sulfite formed at the highest pH values. Some ambiguity exists in his determination of polythionates and thiosulfate. He used the colorimetric method of Nor and Tabatai (1976), which assumes tetrathionate is the dominant polythionate and does not completely distinguish between thiosulfate and polythionate. The pyrite and sphalerite oxidation experiments of Moses et al. (1987) included more direct determination of sulfate, sulfite, polythionates, and thiosulfate by ion chromatography (Moses et al., 1984). Their results were similar to those of Goldhaber (1983) except that additional experiments carried out in the presence of $\text{Fe}^{3+}_{(aq)}$ did not produce any detectable intermediate sulfoxyanions. These results are also similar to those of aqueous H_2S oxidation with oxygen (Chen and Morris, 1971, 1972; Zhang and Millero, 1994; Vairavamurthy et al., 1994).

Experiments documenting the formation of intermediate sulfoxyanions during pyrite oxidation should not be taken as evidence that the same oxyanions are to be found in natural waters during sulfide weathering. In experimental systems, these compounds can only be detected in solution when the aqueous layer next to the mineral surface is strongly sheared by high stirring rates so that these metastable products can not back-react by further electron exchange with the solid. Such strong shearing is not found generally in ground-water systems and even rapidly-moving surface waters rarely exhibit such shearing at the mineral surface. Luther (1987, 1990) has pointed out that species such as thiosul-

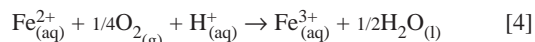
fate and sulfite would not be detected in solutions containing $\text{Fe}^{3+}_{(\text{aq})}$ because they oxidize so rapidly; experiments by Williamson and Rimstidt (1993) and references therein confirmed that this reaction is rapid. Furthermore, intermediate sulfoxyanions are an excellent source of energy for chemoautotrophic bacteria of the *Thiobacillus* genus and may be quickly biodegraded before detectable concentrations can accumulate (Gould et al., 1994).

The experiments of Granger and Warren (1969) are often cited as evidence for the formation of sulfoxyanions from pyrite oxidation and the role of sulfoxyanions in the genesis of ore deposits. However, these authors admitted that the thiosulfate they found in their column experiments may have been formed by the oxidation of residual aqueous Na_2S solution. They had first added H_2O_2 solution in an effort to sterilize the column and then added Na_2S solution to reduce the iron oxide stains that had formed from the peroxide treatment. After such a traumatic chemical treatment, significant quantities of thiosulfate would have formed from the aqueous sulfide solution and would have been difficult to remove completely from the column. The thiosulfate thus formed may have had nothing to do with pyrite oxidation.

It has long been known that ferric iron rapidly oxidizes pyrite (Stokes, 1901). Experiments carried out by Garrels and Thompson (1960) and McKibben and Barnes (1986) have confirmed the balanced reaction stoichiometry:



for the oxidation of pyrite by aqueous ferric ions. This reaction is considerably faster than the reaction with oxygen as the oxidant, but significant concentrations of oxidized iron only occur at low pH values because of the low solubility of hydrolyzed ferric iron at circumneutral pH values. Hence, it is thought that pyrite oxidation is initiated by oxygen at circumneutral pH (equation [2]) but as pH values reduce to about 4, the rate of oxidation becomes governed by equation [3]. Oxygen is still required to replenish the supply of ferric iron according to



but the oxygen does not have to diffuse all the way to the pyrite surfaces. It is quite possible for pyrite to oxidize in the absence of dissolved oxygen. Nevertheless, the overall rate of pyrite oxidation in a tailings pile, in a mine, or in a waste rock pile will largely be determined by the overall rate of oxygen transport (advection and diffusion).

Considerable speculation can be found in the literature on the question of the initiation and propagation of pyrite oxidation. Undoubtedly, during the initiation of pyrite oxidation, there are complex chemical and microbiological processes occurring in microenvironments (Williams et al., 1982), i.e., within a few tens of nanometers of the surface of a sulfide grain. These regions are inaccessible to normal sampling techniques and are not represented by the bulk aqueous phase. For example, when oxygen initially adsorbs to a pyrite surface and transfers electrons, an accumulation of protons will form at or near the surface. Acidophilic iron-oxidizing bacteria will begin to colonize and a film of acidic water will cover the mineral grain without affecting the bulk aqueous

phase. Even before some acidic water develops, neutrophilic *Thiobacilli* will catalyze the initial stage of pyrite oxidation (Blowes et al., 1995; Gould et al., 1994). The extent to which these microenvironmental gradients affect the bulk properties are dependent on many factors, not the least of which is the pyrite concentration in the rock, soil, or waste material. The existence and importance of these microenvironments is well illustrated by the formation of jarosite, a mineral that can only form under acid conditions and has been found in soil waters of circumneutral pH (Carson et al., 1982).

The oxidation of at least 18 different sulfide minerals has been investigated (Table 6.3). Most of these have been studied with and without microbial catalysis by *Thiobacillus ferrooxidans*. The microbial oxidation rate is usually greater than the abiotic rate, all other conditions being equal. Unfortunately, most of the microbial studies were done without measurement of surface area and without a consistent procedure for removing small particles or otherwise cleaning the samples before the experiment. The lack of these characteristics prevents any direct comparison of microbial oxidation rates except in a qualitative manner. The results for abiotic and biotic oxidation of pyrite, however, are of considerably better quality than for other sulfide minerals and some quantitative comparisons are possible.

It should be noted that arsenic-rich minerals such as arsenopyrite and orpiment are also subject to bacterially catalyzed oxidation (Ehrlich, 1963a, 1964). Indeed, the occurrence of arsenite-oxidizing bacteria in acid mine waters has been reported by Wakao et al. (1988) and one of the first reports of arsenite oxidation by heterotrophic bacteria was that of Turner (1949).

There are now numerous reports on the oxidation rates of pyrite and marcasite by oxygen (Bergholm, 1955; McKay and Halpern, 1958; Smith and Shumate, 1970; Mathews and Robins, 1974; Goldhaber, 1983; McKibben and Barnes, 1986; Moses et al., 1987; Nicholson et al., 1988; Moses and Herman, 1991), by ferric iron (Bergholm, 1955; Garrels and Thompson, 1960; Smith and Shumate, 1970; Mathews and Robins, 1972; Wiersma and Rimstidt, 1984; McKibben and Barnes, 1986; Moses et al., 1987; Brown and Jurinak, 1989; Moses and Herman, 1991), and by hydrogen peroxide (McKibben and Barnes, 1986). The oxidation rates of pyrrhotite in the presence of oxygen (Nicholson and Scharer, 1994) and marcasite, covellite, galena, sphalerite, chalcocopyrite, and arsenopyrite in the presence of ferric iron (Rimstidt et al., 1994) have been measured. Pyrite oxidation rates from different studies are generally comparable, but differences in experimental design, initial pH values, temperatures, grain size, mineral preparation, method for data reduction and rate law expression make a quantitative comparison difficult. For this paper, we use the results of McKibben and Barnes (1986) on pyrite to compare with the biotic rates in the next section. Table 6.4 summarizes the reaction rates from several studies cited above for a pH close to 2, $m_{\text{Fe(III)}} = 10^{-3}$, temperatures close to 25°C, and oxygen in equilibrium with the atmosphere.

The rates in Table 6.4 show that the oxidation of pyrite by ferric iron (according to the reaction stoichiometries given in equations [2] and [3]) can be about 2–3 orders of magnitude faster than by oxygen, that some minerals oxidize more rapidly than pyrite and some more slowly, and that oxidation rates can range over three orders of magnitude. These rates are demonstrably faster than the dissolution rates for aluminosilicate minerals (White and Brantley, 1995) by one to several orders of magnitude.

TABLE 6.3—Sulfide oxidation studies (more references can be found in Nordstrom and Southam, 1997).

Mineral	Formula	Oxidant	pH	Reference
Pyrite	FeS ₂	O ₂ , Fe ³⁺ , H ₂ O ₂	0-10	See references in next sections
Marcasite	FeS ₂	O ₂ , Fe ³⁺	2-3	Wiersma and Rimstidt (1984); Silverman et al. (1961)
Pyrrhotite	Fe _{1-x} S	O ₂	2-6	Nicholson and Scharer (1994)
Sphalerite	(Zn, Fe)S	O ₂ , Fe ³⁺	2-7	Rimstidt et al. (1994); Torma et al. (1972); Khalid and Ralph (1977)
Galena	PbS	O ₂ , Fe ³⁺	2	Rimstidt et al. (1994); Torma and Subramanian (1974)
Chalcopyrite	CuFeS ₂	O ₂ , Fe ³⁺	1.2-2.5	Rimstidt et al. (1994); Torma et al. (1976)
Arsenopyrite	FeAsS	O ₂ , Fe ³⁺	2	Rimstidt et al. (1994); Ehrlich (1964)
Covellite	CuS	O ₂ , Fe ³⁺	2	Walsh and Rimstidt (1986); Rickard and Vanselow (1978)
Chalcocite	Cu ₂ S	O ₂	2-4.8	Beck (1977); Sakaguchi et al. (1976)
Greenockite	CdS	O ₂	2.3	Torma et al. (1974)
Millerite	NiS	O ₂	2.3	Torma et al. (1974)
Cobalt sulfide	CoS	O ₂	2.3	Torma et al. (1974)
Klockmannite	CuSe	O ₂	2.3	Torma and Habashi (1972)
Cinnabar	HgS	Fe ³⁺	2	Burkstaller et al. (1975)
Enargite	Cu ₃ AsS ₄	O ₂	3	Ehrlich (1964)
Orpiment	As ₂ S ₃	O ₂		Ehrlich (1963a)
Bornite	Cu ₅ FeS ₄	O ₂		Landesman et al. (1966)
Molybdenite	MoS ₂	O ₂	2.5	Brierley and Murr (1973)
Tetrahedrite	(Cu,Fe) ₁₂ Sb ₄ S ₁₃	O ₂		Yakhontova et al. (1980)
Stibnite	Sb ₂ S ₃	O ₂		Torma et al. (1974)
Pentlandite	(Fe, Ni) ₉ S ₈	O ₂		Brierley and Le Roux (1977)

TABLE 6.4—Abiotic reaction rates (mol m⁻² s⁻¹) for sulfide mineral oxidation.

Mineral/Oxidant	MB86 ¹	BJ89 ²	R94 ^{3,7}	N94 ⁴	NS94 ⁵
Pyrite/O ₂	3.1 x 10 ⁻¹⁰			5.3 x 10 ⁻¹⁰	1.1 x 10 ⁻¹⁰
Pyrite/Fe ³⁺	9.6 x 10 ⁻⁹	1.8 x 10 ⁻⁸	1.9 x 10 ⁻⁸		
Pyrrhotite/O ₂				1.4 x 10 ⁻⁸	
Marcasite/Fe ³⁺			1.5 x 10 ⁻⁷		
Arsenopyrite/Fe ³⁺			1.7 x 10 ⁻⁶		
Galena/Fe ³⁺			1.6 x 10 ⁻⁶		
Sphalerite/Fe ³⁺			7.0 x 10 ⁻⁸		
Blau. covellite ⁶ /Fe ³⁺			7.1 x 10 ⁻⁸		
Chalcopyrite/Fe ³⁺			9.6 x 10 ⁻⁹		
Covellite/Fe ³⁺			9.1 x 10 ⁻⁹		

¹ McKibben and Barnes (1986); because there appears to be an error in the stated value for pyrite oxidation by oxygen we have used the corrected value from Nicholson (1994).

² Brown and Jurinak (1989); average from oxidation rates measured in different electrolytes.

³ Rimstidt et al. (1994).

⁴ Nicholson (1994); the value for pyrite is an average from four studies covering a pH range of 1-8.

⁵ Nicholson and Scharer (1994) and Tervari and Campbell (1976).

⁶ "blau. covellite" is blaubleibender or "blue-remaining" covellite having slightly different optical and X-ray properties than ordinary covellite.

⁷ The values listed for R94 are all given in terms of the amount of Fe(III) reduced except for pyrite. All values for pyrite are given in the same units, per mole of pyrite oxidized, for purposes of direct comparison.

Galvanic protection does occur during oxidative dissolution of coexisting sulfide minerals. This phenomenon is the same as that for galvanized iron. The more electroconductive metal sulfide (the one with the higher standard electrode reduction potential, see Sato, 1992) will oxidize at a slower rate and the less electroconductive sulfide will oxidize at a faster rate than either one would when not in contact. Sveshnikov and Dobyshin (1956) reported that rates of metal release from different sulfides are related to

their electrode potentials and that a mixture of sulfide minerals in contact releases more metals into solution and decreases the pH more than monomineralic samples. Sveshnikov and Ryss (1964) postulated that these electronic properties of co-existing conductive sulfides are important during the weathering of sulfide mineral deposits. Sato (1992) has used electrochemical data on metal sulfides, typical of heavy metal sulfide deposits, to explain the mineral assemblage that is found during supergene enrichment.

Nicholson and Scharer (1994) mixed pyrrhotite and pyrite in different proportions to see if there was any evidence for galvanic protection, but could not detect any such effect in their study. Kwong (1995) has done laboratory experiments to show the effect of galvanic protection during dissolution of multi-sulfide mineral assemblages. The relative rates of mineral dissolution follow the sequence indicated by standard electrode potentials as outlined by Sato (1992).

Because the oxidation rate for pyrite by $\text{Fe}_{(\text{aq})}^{3+}$ is faster than that by oxygen, it is important to know the oxidation rate for ferrous to ferric iron according to equation [4]. Numerous studies on the ferrous iron oxidation rate show that, under acid conditions, the rate becomes very slow and independent of pH. Singer and Stumm (1968) reported an abiotic rate of $2.7 \times 10^{-12} \text{ mol L}^{-1} \text{ s}^{-1}$ at pH values below 4. Similar rates have been reported elsewhere. Such rates are considerably slower than the rate of oxidation of pyrite by $\text{Fe}_{(\text{aq})}^{3+}$; hence, equation [4] would be the rate-limiting step were it not for the catalytic effect of bacteria.

Microbial oxidation: Historical perspective

Microorganisms are abundant in natural waters containing acid mine drainage; indeed, they are often the *only* form of life under such conditions. Powell and Parr (1919) and later Carpenter and Herndon (1933) suggested that pyrite oxidation and the consequent acid mine drainage from coal deposits may be catalyzed by bacteria. Lackey (1938) observed flagellates, rhizopods, ciliates, and green algae in 62 West Virginia streams. Joseph (1953) found gram-positive and gram-negative bacilli and cocci, fungi, green algae, diatoms, and actinomyces in acidified surface waters and soils in West Virginia and Pennsylvania. Acid mine waters from a copper mine in the southwestern U.S. were found to contain yeasts, flagellates, protozoa, and amoebae (Ehrlich, 1963b). "Acid slime streamers" have often been observed in acid mine waters (Dugan et al., 1970; Dugan, 1972).

As long ago as 1888 it was recognized by S.N. Winogradsky that certain microbes could oxidize reduced inorganic compounds, such as sulfur, to gain energy for the reduction of carbon dioxide for metabolism and growth (see Sokolova and Karavaiko, 1968). Microorganisms that utilize reduced inorganic substances are known as chemolithotrophic (see Mills, 1999). Nathansohn (1902) first isolated a *Thiobacillus* species and the acidophilic bacterium, *Thiobacillus thiooxidans*, was isolated and identified by Waksman and Jaffe (1921, 1922) from soils containing free sulfur and phosphate. Colmer and Hinkle (1947), Colmer et al. (1950), Temple and Colmer (1951), and Temple and Delchamps (1953) isolated a new chemoautotrophic and acidophilic bacterium, *Thiobacillus ferrooxidans*, and showed that microbial degradation of pyrite was an important factor in the production of acid mine waters.

The nutritional requirements for *T. ferrooxidans* are ubiquitous. Nitrogen and carbon dioxide are available in the atmosphere. Sulfur is readily available in mined environments, and only small amounts of phosphorous are needed. *Thiobacilli* have several adaptive techniques that permit them to tolerate low pH and high metal concentrations (Tuovinen et al., 1971; Kushner, 1978). Some studies have shown that *T. ferrooxidans* can tolerate g/l concentrations of Zn, Ni, Cu, Co, Mn, and Al (Tuovinen et al., 1971). Scala et al. (1982) found consistent and roughly equal concentrations of *T. thiooxidans* and *T. ferrooxidans* in mine effluents of different compositions from quite different mines, in different geo-

logical and climatological environments, in different parts of the country (from California to Virginia). The diversity of microorganisms and their populations in mineral deposit and mine waste environments is complex and not well understood. Further investigations on the microbial ecology of mines and mine wastes are certainly needed.

T. thiooxidans oxidizes elemental sulfur but not iron, *T. ferrooxidans* oxidizes both iron and sulfur compounds, and a third species, *Leptospirillum ferrooxidans*, behaves metabolically like *T. ferrooxidans* but has a helical-rod morphology first described by Markosyan (1972). *L. ferrooxidans* is now thought to be equally important as the other two bacilli (Sand et al., 1992). Mixed cultures oxidize reduced iron and sulfur compounds faster than single-species cultures (Kelly et al., 1979; Wakao et al., 1982). Apparently, bacteria are preconditioned by the medium in which they are cultured and may have a synergistic association with other species. For example, *T. ferrooxidans* grown in ferrous-containing solutions exhibited different surface chemistry than those grown on minerals such as pyrite, elemental sulfur, and chalcopyrite (Devasia et al., 1993) as exhibited by hydrophobicity and electrophoretic mobility measurements. The bacilli grown on mineral sulfides developed a proteinaceous cell surface appendage that adhered to the solid surface whereas the cells grown in ferrous iron solutions contained no such characteristic. The importance of these features bears on the mechanism of microbial oxidation. Free-floating bacteria can catalyze the oxidation of iron from ferrous to ferric in aqueous solution, and then the ferric iron directly oxidizes the pyrite. Silverman (1967) calls this the indirect mechanism. The direct contact mechanism works by direct adhesion of the bacteria to the pyrite surface. There has been a long-standing debate over whether the direct or indirect mechanism is dominant. We contend that the indirect mechanism is the dominant one, but there is some evidence for enhancement of the pyrite oxidation rate by direct microbial contact. Surface-etch patterns may result from bacterial attachment (Bennett and Tributsch, 1978), and direct microbial growth on pyrite surfaces has been observed (Konishi et al., 1990).

Microbial oxidation: Kinetics

The catalytic effect of *T. ferrooxidans* on the aqueous oxidation of ferrous to ferric iron is well-established. Singer and Stumm (1968, 1970a, b) found that bacteria increased the ferrous iron oxidation rate by 10^5 over the abiotic rate, from about $3 \times 10^{-12} \text{ mol L}^{-1} \text{ s}^{-1}$ to about $3 \times 10^{-7} \text{ mol L}^{-1} \text{ s}^{-1}$. Silverman and Lundgren (1959), Lundgren et al. (1964), and Lacey and Lawson (1977) grew *T. ferrooxidans* on culture media and typically measured oxidation rates of $2.8\text{--}8.3 \times 10^{-7} \text{ mol L}^{-1} \text{ s}^{-1}$. Wakao et al. (1977) measured field oxidation rates of ferrous iron oxidation in acid mine drainage and estimated $3 \times 10^{-6} \text{ mol L}^{-1} \text{ s}^{-1}$ but the stream velocity was not measured. Nordstrom (1985) measured stream velocities and iron oxidation rates of 2 to $8 \times 10^{-7} \text{ mol L}^{-1} \text{ s}^{-1}$ in a mountainous stream drainage containing acid mine waters, where the range of values depended on climatic conditions. From these studies we have chosen an average microbial oxidation rate for ferrous iron of $5 \times 10^{-7} \text{ mol L}^{-1} \text{ s}^{-1}$ for the purpose of comparison with the abiotic rates.

Table 6.5 summarizes abiotic and microbial rates of oxidation for ferrous iron and pyrite under roughly comparable conditions (except for the field rates cited here and discussed later). The

microbial oxidation rate of pyrite by oxygen is very similar to the abiotic oxidation rates of pyrite by either oxygen or ferric iron. Studies by Wakao et al. (1984) showed that adsorption of bacterial cells on pyrite surfaces actually inhibited pyrite oxidation and that it was the growth of free-floating ferrous-iron-oxidizing bacteria that contributed to pyrite oxidation. These results help to clarify the reaction mechanism. Pyrite oxidation is primarily accomplished by microbial catalysis by the indirect mechanism, as defined earlier.

Estimates of field oxidation rates of pyritiferous waste rock or tailings cover a wide range of values, from three orders of magnitude less than the microbial rate to two orders of magnitude greater (Table 6.5). The field rates are primarily based on flux rates of oxygen depletion upon reaction with pyrite in waste rock or tailings. There may be complications with the assumptions made in translating temperature and oxygen profiles into flux rates. The relation between flux rates and actual *in situ* rates of pyrite oxidation may be more difficult to quantify than previously realized. The main problem is estimating the reactive surface area of the sulfides. Other problems may include the consumption of oxygen by processes other than pyrite oxidation, the dependence of temperature profiles on the moisture content, the salinity of the moisture, the temperature dependence of the oxygen consumption rate, climatic variability in pressure and temperature, site heterogeneities, and variations in thermal conductivities of the various waste materials. Averaging hydrologic properties over spatial and temporal intervals may cause inaccurate estimations of flux rates and oxidation rates at some sites.

A direct comparison of the rates of microbial oxidation of aqueous ferrous iron with rates of microbial oxidation of pyrite would be helpful in discerning the rate-controlling step of these processes, but it is difficult to accomplish. Aqueous iron oxidation is expressed as a molar concentration change with respect to time ($\text{mol L}^{-1} \text{s}^{-1}$), whereas pyrite oxidation is a function of surface area and the ratio of pyrite mass to solution volume or porosity ($\text{mol m}^{-2} \text{s}^{-1}$). Two investigations make such a comparison possible: Southam and Beveridge (1992) described bacterial cell densities on pyrite surfaces and Olson (1991) conducted an interlaboratory comparison of pyrite bioleaching rates. Neither study reported pyrite surface area but both reported grain size, so that surface areas may be estimated from the relationship between surface area and grain size for sulfide minerals.

Figure 6.1 depicts the dependence of surface area (in $\text{cm}^2 \text{g}^{-1}$) on grain size for pyrite and other sulfide minerals. The solid line

represents the diameter-to-surface-area relationship for an ideal sphere or cube of pyrite with a density of 5.0 g cm^{-3} (see Parks, 1990; Nicholson, 1994). The dashed line is a best fit for cleaned quartz grains from Parks (1990). Two suggestions are evident from Figure 6.1. More recent determinations demonstrate the effect of more carefully sized and cleaned pyrite grains (compare museum pyrite of Braley, 1954, with any of the more recent non-diagenetic pyrite). Secondly, the diagenetic or framboidal pyrite has much more surface area for a given mass than coarse-grained pyrite. Several of the data points on Figure 6.1 lie close to the best fit of Parks (1990), which will be used as a lower limit and as an estimate of the relationship of surface area to grain diameter.

Southam and Beveridge (1992) determined values of 10^7 to 10^9 cells g^{-1} for *Thiobacilli* on surfaces of Lemoine tailings at Chibougamau, Quebec, Canada, by the most probable number method. Their tailings samples were in the size range of 200 mesh and higher, hence about 50 micrometers (μm) in diameter or about $500 \text{ cm}^2 \text{g}^{-1}$ in surface area. A cell count of 10^8 cells g^{-1} for a surface area of $500 \text{ cm}^2 \text{g}^{-1}$ works out to 2×10^5 cells cm^{-2} or 2×10^9 cells m^{-2} on pyrite surfaces. For a tailings aquifer with 30% porosity and assuming only pure pyrite in the solids, the cell concentration in the slurry becomes $(1 - \text{porosity})(\text{pyrite density})(\text{cell count}) = (0.7) \times (5 \text{ g ml}^{-1}) \times (10^8 \text{ cells g}^{-1}) = 3.5 \times 10^8$ cells ml^{-1} , which is the same concentration of cells in solution that would oxidize aqueous ferrous iron optimally at $5 \times 10^{-7} \text{ mol L}^{-1} \text{ s}^{-1}$ (Silverman and Lundgren, 1959). It is also in the same range of cell concentration found in acid mine waters in the environment (Scala et al., 1982). Therefore, it appears that the observed concentration of *Thiobacilli* on pyrite surfaces would produce aqueous Fe^{III} concentrations of the same order of magnitude as those formed by microbial oxidation of ferrous iron in aqueous solution by free-floating bacteria.

A preferable method of estimating the microbial rate of pyrite oxidation can be obtained from the interlaboratory comparison of pyrite bioleaching rates coordinated by the National Institute of Science and Technology (Olson, 1991). Eight laboratories participated in tests using a standardized method with 1 gram of pyrite from the same source. The pyrite was cleaned and sterilized after sizing to -165/+250 mesh (58 to 91 μm). Then sample was inoculated with a standard culture of *Thiobacillus ferrooxidans*. From Figure 6.1, the surface area would have been about $350 \text{ cm}^2 \text{g}^{-1}$. The reported oxidation rate ($12.4 \text{ mg Fe L}^{-1} \text{ h}^{-1}$ or about $6 \times 10^{-8} \text{ mol L}^{-1} \text{ s}^{-1}$) is about an order of magnitude lower than the microbial oxidation rate of aqueous ferrous iron (Table 6.5). Olson

TABLE 6.5—Comparison of abiotic, microbial, and field oxidation rates ($\text{pH} \approx 2$, $T \approx 25^\circ\text{C}$).

Reaction or Process (references)	Abiotic rate	Microbial rate	Field rate
Oxidation of aqueous ferrous iron (Singer and Stumm, 1968; Lacey and Lawson, 1977; Nordstrom, 1985)	3×10^{-12} $\text{mol L}^{-1} \text{ s}^{-1}$	5×10^{-7} $\text{mol L}^{-1} \text{ s}^{-1}$	5×10^{-7} $\text{mol L}^{-1} \text{ s}^{-1}$
Oxidation of pyrite by ferric iron (McKibben and Barnes, 1986; Rimstidt et al., 1994)	1 to 2×10^{-8} $\text{mol m}^{-2} \text{ s}^{-1}$		
Oxidation of pyrite by oxygen (McKibben and Barnes, 1986; Olson, 1991)	0.3 to 3×10^{-9} $\text{mol m}^{-2} \text{ s}^{-1}$	8.8×10^{-8} $\text{mol m}^{-2} \text{ s}^{-1}$	
Oxidation of waste dump (Ritchie, 1994a, b)			0.03×10^{-8} $\text{mol m}^{-2} \text{ s}^{-1}$
Oxidation of tailings (Elberling et al., 1993)			20 to 60×10^{-8} $\text{mol m}^{-2} \text{ s}^{-1}$

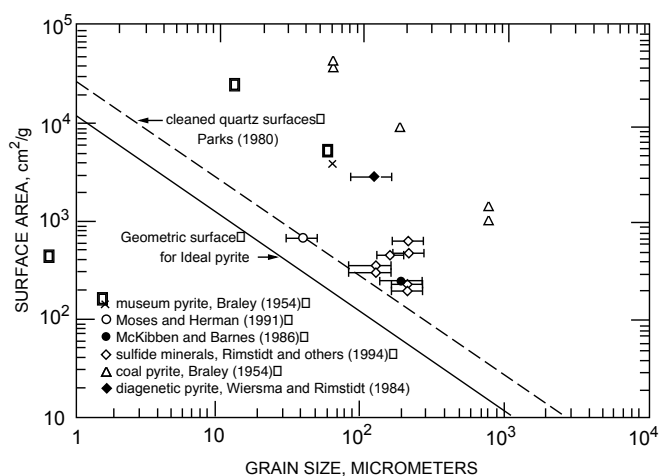


FIGURE 6.1—Surface area versus grain size for pyrite and other sulfide minerals.

(1991) used 1 g of pyrite in 50 ml of solution, so we can calculate the microbial oxidation rate of pyrite as

$$R = \frac{12.4 \text{ mg Fe L}^{-1}\text{h}^{-1}}{56 \text{ mg Fe mmol}^{-1}} \frac{50 \text{ ml}}{(1 \text{ g}) (350 \text{ cm}^2\text{g}^{-1})}$$

$$\frac{1 \text{ mol}}{10^3 \text{ mmol}} \frac{1 \text{ L}}{10^3 \text{ ml}} \frac{10^4 \text{ cm}^2}{\text{m}^2} \frac{1 \text{ h}}{3,600 \text{ s}}$$

$$= 8.8 \times 10^{-8} \text{ mol m}^{-2} \text{ s}^{-1} \quad [5]$$

This rate falls squarely between the abiotic oxidation of pyrite by ferric iron and the microbial oxidation of ferrous iron, i.e., within the uncertainty of the data, there is little difference between the oxidation rate of pyrite by ferric iron and the oxidation rate of ferrous iron by *T. ferrooxidans*. The lower rate of microbial pyrite oxidation compared to the oxidation rate of ferrous iron by *T. ferrooxidans* suggests that the heterogeneous reaction is the rate-determining step. We would suggest, however, that the uncertainties on the rates are large enough and the natural variation in the ferrous iron oxidation rate is large enough that there is not a significant difference. Hence, the rate of pyrite oxidation proceeds about as fast as the aqueous ferric iron can be produced from ferrous iron through microbial catalysis.

Field oxidation rates

What are the actual oxidation rates of pyritic mine waste in the field? What governs oxidation rates at field sites? Singer and Stumm (1970a) conceived of rates in the conventional sense of chemical kinetics. They described the abiotic oxidation of aqueous ferrous to ferric iron as the “rate-determining step” for the production of acid mine drainage because it is orders of magnitude slower than the oxidation of pyrite by ferric iron. This abiotic iron oxidation rate, however, has limited relevance because iron- and sulfur-oxidizing bacteria are ubiquitous in ground and surface waters, catalyzing aqueous iron and pyrite oxidation by orders of magnitude. Singer and Stumm (1970a, b) recognized

that microbial catalysis greatly speeds up the oxidation of aqueous ferrous iron and that either the complete elimination of oxygen or the use of bactericides would be necessary to eliminate microbial activity. The microbial oxidation of aqueous ferrous iron, under optimal conditions of temperature, oxygen supply, and nutrient availability, is the fastest rate known in the system. This rate provides an upper limit to the pyrite oxidation rate. The lower limit is zero (or negative if sulfate reduction is considered) in the absence of oxygen and water. These extremes of rate cover a wide range over which actual rates may occur in the field.

The effects of sulfide surface area, degree of crystallinity, and purity cannot be overstated. One has only to compare the spontaneous oxidation of “framboidal,” “microcrystalline,” or “cryptocrystalline” pyrite (see Pabst, 1940; Caruccio, 1970) with untarnished, large, euhedral pyrite cubes that have survived in museums for several centuries to notice the difference in oxidation rates. The signatures of kings, queens, and other dignitaries over the last century can still be seen clearly on an exposed surface of massive chalcopyrite in the Falun mine in Sweden. Caruccio (1970) and Caruccio et al. (1976) pointed out that the grain size and surface area of pyrite in coal deposits has a considerable influence on the production rate of acid mine drainage, with framboidal pyrite being the most reactive. Normalizing reaction rates to unit surface area is now routinely done when reporting dissolution rates of minerals but differences in degree of crystallinity and purity (solid solution substitutions) may also affect reaction rates. Furthermore, the “reactive surface area” may be significantly less than the total measured surface area as measured by standard techniques (Dzombak and Morel, 1990). Reactive surface area refers to those sites on the surface that are actively available to adsorb and chemically bond with aqueous species, and can be reduced by intergranular contact or inclusion within other minerals. Another complication in the field is that not all exposed surface sites are in the flow path of the water, thereby reducing further the reactive surface area.

Field oxidation rates for pyrite are complicated by air and water transport processes, microbial growth kinetics, microbial ecology, organic compounds, temperature gradients, secondary mineral formation, neutralization reactions, climatic patterns, and the site-specific design of mine workings, waste dumps, and tailings. The production rate of acid mine drainage is governed by rates of transport and attenuation processes, which tend to be slower than rates of pyrite oxidation. Some confusion exists in the literature because the distinction between oxidation rates and transport/attenuation rates has not been made clear. In this sense, an obvious parallel or analogy can be made with silicate mineral weathering rates and discrepancies between laboratory and field studies (see Alpers and Nordstrom, 1999, and White and Brantley, 1995).

Ritchie (1994a, b) has reviewed and analyzed the physical factors that pertain to the acid production rate from waste piles. He has shown that the limiting factor is the transport and reaction of oxygen in the waste. Three main processes are dominant in these systems: convection of oxygen, diffusion of oxygen, and the intrinsic oxidation rate which he has calculated for two sites and compared with results compiled from other sites. Ritchie (1994 a, b) described the “global oxidation rate” as the overall flux rate of acid mine drainage from a waste dump and the “intrinsic oxidation rate” as the oxygen consumption rate, measured from oxygen profiles in units of $\text{mol kg}^{-1} \text{ s}^{-1}$ or $\text{mol m}^{-3} \text{ s}^{-1}$. Several assumptions are involved in making these computations, including a stoichiometric

metric relationship between oxygen consumed and pyrite oxidized (i.e., that oxygen is consumed only by pyrite).

The oxidation of pyrite is a highly exothermic reaction, which can cause thermal air convection in waste dumps and underground mines (Zverev et al., 1983). Air temperatures of 50 to 65°C are commonly achieved in waste-rock piles and copper heap-leach dumps (Cathles and Apps, 1975; Harries and Ritchie, 1981; Cathles, 1994; Ritchie, 1994a) and a water temperature of 47°C was reported from the Richmond Mine at Iron Mountain, California (Alpers and Nordstrom, 1991). Temperature and density gradients resulting from heat generation cause convective air transport, which can be a significant oxygen-supply mechanism (Ritchie, 1994a). Cathles (1994) indicated that convective gas flux driven by thermal gradients was dominant in the well-instrumented Midas Test Dump and other larger dumps at Kennecott's Bingham Canyon Mine (Cathles and Apps, 1975). However, Ritchie (1994a) asserted that the convective flux in a large dump generally applies over a much smaller area than the diffusive oxygen flux.

The relative importance of diffusion vs. convection depends primarily upon the range of air permeability. Ritchie (1994a) suggested a cutoff permeability value of 10^{-9} m². Above this value, convection should dominate and below this value, diffusion should dominate. Ritchie (1994a) also pointed out that he has found the global oxidation rate to be insensitive to changes in the intrinsic oxidation rate. Hence, for unsaturated waste rock, the dominant rate-limiting process should be oxygen diffusion, especially in a newly built waste-rock dump (Ritchie, 1994a). Parts of waste rock piles, usually located near the center, are typically dominated by diffusion whereas the outer edges may be dominated by convection. With time, convective gas transport will penetrate further into the dump as it ages (Ritchie 1994a).

Other factors that affect the ultimate release of acid drainage include the climate, hydrologic variables, mineralogy of the waste materials, physical structure of the waste and geological structure and setting of the mine site, historical evolution of mineral-processing practices, materials used and discarded in mineral processing, geomorphology of the terrain, and vegetation. Discussion of these subjects is beyond the scope of this chapter and can be found in other chapters of this volume or in other review papers. For example, Moore and Luoma (1990) have outlined the sources, transport mechanisms, and sinks for mining and mineral-processing wastes. They use the categories "primary," "secondary," and "tertiary" according to how many times the mining waste has been retransported. A comprehensive overview of tailings problems and their management has been published by Ritcey (1989).

REDOX CHEMISTRY AND MINERAL SOLUBILITIES

Eh-pH diagrams and redox chemistry

The traditional graphical method of delineating the stabilities of reduction-oxidation (or redox) species in geochemical systems (and in corrosion systems) has been through the use of Eh-pH (or pE-pH) diagrams. These are a type of master variable diagram where the independent or master variable is pH. Originally developed by Pourbaix (1945, 1966; also see Pourbaix and Pourbaix, 1992; Sato, 1992) to portray equilibrium relationships in metal corrosion systems, they were introduced and championed in the geochemical literature by Krumbein and Garrels (1952), Garrels

(1954) and Garrels and Christ (1965). Hem (1961, 1985), Krauskopf (1967), Krauskopf and Bird (1995) and many others have used the concepts of Eh and pH as a convenient means of representing redox relationships for ions and minerals. The reader is referred to these sources as well as discussions by Stumm and Morgan (1981) and Nordstrom and Munoz (1994) for an introduction to the construction of these diagrams from thermodynamic data.

A pE-pH diagram for the Fe-S-K-O₂-H₂O system is shown on Figure 6.2 with the thermodynamic stability fields of several major ions and minerals of iron. The formation and occurrence of jarosite, goethite, and other secondary iron minerals are discussed in the next section. The stability boundary between goethite and jarosite can vary over several units of pH depending on the crystallinity and particle size of these minerals. Metastable phases such as ferrihydrite may form more readily than the thermodynamically stable phase in some conditions, and thus can play an important role in controlling aqueous metal concentrations.

Figure 6.2 indicates that goethite is stable under mildly acidic to basic oxidizing conditions, jarosite is stable under acidic oxidizing conditions, and pyrite is stable under a large range of strongly reducing conditions. Acidity tends to promote dissolution of minerals under a range of redox conditions. Additional iron minerals can be shown on diagrams similar to Figure 6.2, if additional components such as carbonate, silica, phosphate, and uranium are included, but such multi-component diagrams can become very cluttered and most of these additional minerals are not particularly relevant to acid mine waters.

These pE-pH diagrams can be very useful in showing the general stability relations among redox-sensitive ions and minerals but their limitations must be clearly understood:

- 1) The redox chemistry of a solution or a natural water cannot be measured by a simple "Eh" parameter. There is no such thing as a single representative redox potential or an Eh of a water. A measurement of electromotive force (EMF) with a platinum

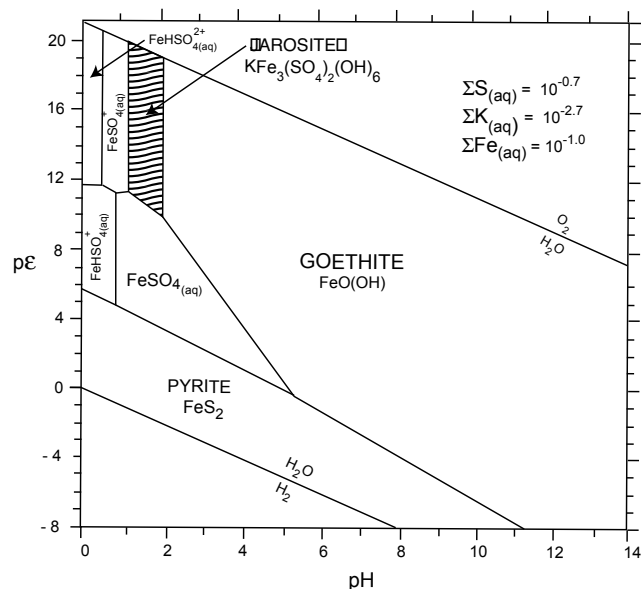


FIGURE 6.2—pE-pH diagram, showing stable solid phases in Fe-S-K-O-H system at 25°C (modified from Alpers et al., 1989).

electrode (converted to Eh by subtracting the reference electrode half-cell potential) for a water sample may or may not reflect an equilibrium potential for a single redox couple but there is no single Eh that represents the water (Thorstenson, 1984; Hostetler, 1984). Hence, Eh measurements may be quantitatively correlated to a specific redox couple such as Fe(II/III) but otherwise they are of little use.

- 2) Redox couples of different elements rarely, if ever, reach equilibrium at temperatures below 100°C. This fact is one of the reasons why a single Eh cannot be assigned to a water sample. Redox disequilibrium is the rule, not the exception. Lindberg and Runnells (1984) showed that when different redox couples are measured in the same water sample, none of them appear to be in equilibrium. The reasons for this are largely kinetic. Electrons transfer much more readily between redox-sensitive ions and surfaces such as electroconductive minerals (most sulfides) and bacteria than with other ions in solution.
- 3) Redox potential measurements respond to electroactive aqueous ions. To be electroactive an ion must have a sufficiently high exchange current density (Bricker, 1982) so that there is no kinetic hindrance to the transfer of electrons. This criterion requires both sufficiently high concentrations of the redox-sensitive ions as well as the lack of kinetic barriers to electron transfer. Only two common elements clearly meet this requirement: iron (II/III) and sulfur (sulfide). All other elements and ions found in natural waters (with the possible exception of uranium and cobalt under unusual circumstances) do not.
- 4) The redox conditions of a water sample are best characterized analytically by determining the concentrations of multiple redox species for each redox-active element in the sample. Acid mine waters are easily analyzed for Fe(II) and Fe(total) (with Fe(III) computed by difference or by direct determination, To et al., 1999) by visible spectrophotometry using a ferrous reagent such as bipyridine, orthophenanthroline, or ferrozine. The more precise and sensitive nature of methods using a colorimetric reagent such as ferrozine make them preferable to atomic absorption or inductively-coupled plasma atomic-emission spectroscopy (Ball and Nordstrom, 1994). Once the concentrations of redox species have been determined then the classification of Berner (1981) can be used to describe the redox chemistry. Berner suggests a practical lower limit of detection as 10^{-6} molar for oxygen, iron, sulfide, and methane. The presence of oxygen classifies a water as "oxic," the absence of oxygen and presence of ferrous iron classifies it as "post-oxic," the presence of sulfide classifies it as "sulfidic," and the presence of methane classifies it as "methanic." This general classification works well for the typical ground water evolving into more reducing conditions with time and depth, but not for acid mine waters. Acid mine waters and other types of surface waters are usually of a mixed redox chemistry and only by determining relevant redox species can you interpret the redox chemistry of the water.

Nordstrom et al. (1979) showed that acid mine waters typically have sufficient iron concentrations to give an equilibrium potential at the platinum electrode for the Fe (II/III) redox couple but that the O_2/H_2O redox couple was far from equilibrium with respect to the iron couple. Careful analyses of acid mine waters from the Leviathan/Bryant Creek system demonstrate the limits of redox measurements for mine waters even more clearly (Ball and Nordstrom, 1989, 1994). Figures 6.3a and 6.3b compare platinum electrode Eh measurements with Eh values calculated from Fe

(II/III) determinations and speciated with the WATEQ4F code (Ball and Nordstrom, 1991; see Alpers and Nordstrom, 1999). The comparison of measured and calculated Eh on Figures 6.3a and 6.3b shows an excellent correlation for samples with total iron concentrations greater than 10^{-5} m. Most of the deviations are found at the lowest Eh values where the iron concentrations are so low (less than 10^{-6} m) that iron is no longer electroactive. Furthermore, these waters are saturated with atmospheric oxygen so that a mixed potential results from the oxygen competing with the low concentrations of iron. Poor comparisons of calculated and measured Eh are occasionally found at very high iron concentrations and low pH values because of inherent problems with the chemical model under these conditions (see Alpers and Nordstrom, 1999).

Iron photoreduction

Iron (II) concentrations in oxygenated surface waters have not only been detected but have been found to vary from night to day. The concentrations of Fe (II) reach a peak during midday, at the peak of insolation. The solar radiation reduces both dissolved Fe (III) and colloidal ferric hydroxide in natural waters (Waite and

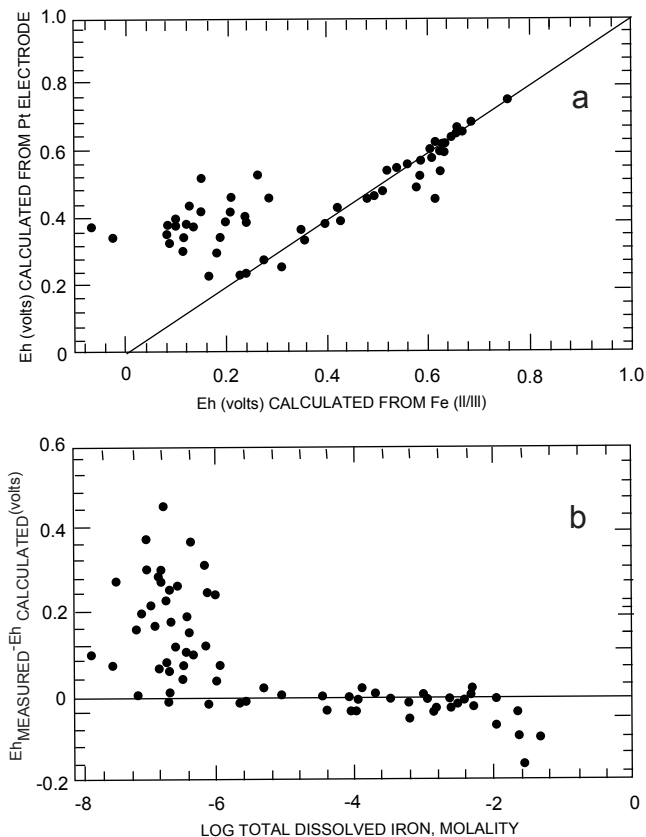


FIGURE 6.3—(a) Comparison of Eh calculated from the Fe (II/III) redox couple to Eh measured with a platinum electrode. (b) Difference between calculated and measured Eh plotted as function of total dissolved iron concentrations in molal units. Data from Leviathan/Bryant Creek watershed, California and Nevada (Ball and Nordstrom, 1989; 1994).

Morel, 1984). The same effect has been found for acid mine waters that have dissolved iron <5 mg/l (McKnight et al., 1988; McKnight and Bencala, 1988). McKnight et al. (1988) found the daytime production of Fe(II) to be nearly 4 times faster than the nighttime oxidation of Fe(II). These results might also be enhanced by light inhibition of iron- and sulfur-oxidizing bacteria (Le Roux and Marshall, 1977). The continual exposure of acid mine waters to the sun promotes recycling of the iron between dissolved and particulate phases and may have important consequences on the sorption of metals. Solar radiation could lead to Ostwald ripening of iron colloids which would increase the iron hydroxide particle size and decrease the reactive surface area. Alternatively, recycling of iron hydroxides and recreation of fresh colloidal surfaces would promote surface area and the opportunity for increased adsorption of metals (McKnight and Bencala, 1989). These effects, however, may only be detectable in streams with relatively small concentrations of iron. Acid mine waters with more typical iron concentrations of 20–1000 mg/l may not show this effect. In wetlands, an opposite effect has been observed, where Fe (II) concentrations reach a minimum during daylight hours; this effect has been attributed to daytime oxygenation by algae (Wieder, 1994).

Saturation indices (SI) and mineral solubilities

When complete water analyses for the major ions are available, a speciation computation can be done to determine the state of saturation with respect to any particular minerals for which thermodynamic data are available (see Alpers and Nordstrom, 1999). Numerous acid mine waters and tailings pore waters have been subject to these calculations to achieve more quantitative interpretations on the control of metal concentrations by mineral solubilities. Some brief examples of the usefulness of this approach are shown here.

Acid mine waters are characterized by low pH, high iron and aluminum concentrations, high metal concentrations, and high sulfate concentrations. Minerals that might be stable under these conditions should be hydrolyzed iron- and aluminum-sulfate minerals and insoluble metal-sulfate minerals. Prime candidates include jarosite, alunite, barite, anglesite, gypsum, and a suite of ferric- and aluminum-hydroxysulfate compounds. Figures 6.4a-d show two examples of SI values for barite, one for alunite, and one for anglesite. If equilibrium solubility is achieved and if it exerts the dominant control on the concentration of one or more elements, then the SI values should show a linear and horizontal trend close to zero. Such a pattern signifies that the water chemistry reflects the stoichiometry of the given mineral and may have reached equilibrium saturation. As expected, the values tend to plateau with the appropriate stoichiometry of the mineral but generally in the region of supersaturation. This effect might be explained by the particle size effect on solubility because the solubility product constant usually refers to a coarse-grained, well-crystallized material and it might also be due to solid solution substitution of trace components. Some of the apparent supersaturation could also be due to inadequacies in the chemical model, especially in the activity coefficient and stability constant expressions.

The behavior of aluminum and iron as reflected in saturation indices can be seen on Figures 6.5a-d. On Figure 6.5a, a plateau in the SI values for Al(OH)₃ is seen at pH values above about 4.5.

At pH values above 4.5, solubility equilibrium is apparently reached with respect to microcrystalline or amorphous Al(OH)₃ and seems to be maintained at all higher pH values. This phenomenon was pointed out by Nordstrom and Ball (1986) and can be more clearly seen on Figure 6.5b in which the activity of the free aluminum ion is plotted against pH. The rate of aluminum leaching from common minerals at low pH is not generally fast enough relative to the flow rate of surface and ground waters to reach equilibrium with gibbsite. Furthermore, gibbsite solubility is so high at very low pH that it becomes an unstable or metastable phase with respect to other aluminous minerals, especially in the presence of high sulfate concentrations (Nordstrom, 1982b).

When acid mine drainage is diluted by neutral surface waters, the pH and aluminum concentrations eventually reach the gibbsite solubility curve and aluminum concentrations become controlled by one of 3 possibilities: (1) solubility of a solid phase (such as gibbsite), (2) a surface coating control with a stoichiometry similar to gibbsite, or (3) a common aluminosilicate mineral with an exchange ratio of Al³⁺ to H⁺ of 1:3. A pH of 5 is also equal to the pK₁, the negative logarithm of the first hydrolysis constant for aluminum, and without hydrolysis the precipitation of hydrolyzed aluminum would not be possible. Hem and Roberson (1990) have shown that the rate of aluminum hydrolysis increases as pH values rise to about 5 so that the hydrolysis kinetics for dissolved aluminum favors the tendency toward equilibrium. Nordstrom et al. (1984) have shown that, when rapid mixing causes precipitation of aluminum in acid mine waters, the solid produced is an amorphous aluminum-hydroxysulfate material that might best be described as an amorphous basaluminite.

Comparable diagrams for iron are shown on Figures 6.5c-d. Apparent supersaturation with respect to ferric hydroxide or ferrihydrite occurs at pH values above about 4. The supersaturation might be explained by substitution of sulfate for hydroxide ions in the ferrihydrite and the formation of a schwertmannite-like phase. Schwertmannite [Fe₈O₈(OH)₆(SO₄)₂] was described by Bigham et al. (1990) and Bigham (1994) and is discussed in more detail in a later section of this chapter. The apparent supersaturation with respect to ferric hydroxide might also be explained by the formation of colloidal iron particles that cannot be filtered out by 0.1 micrometer pore size membranes. This apparent supersaturation behavior for ferric hydroxide is commonly seen for both surface waters and ground waters.

In general, the stoichiometry of a phase controlling the solubility of an aqueous constituent can be derived from an appropriately-selected ion-activity plot. For example, if pure ferric hydroxide were controlling the solubility of ferric iron, the reaction



and its log equilibrium constant expression

$$\log K = \log a_{\text{Fe}^{3+}} - 3 \log a_{\text{H}^+} + 3 \log a_{\text{H}_2\text{O}} \quad [6b]$$

would indicate that a plot of Fe³⁺ activity versus pH (= -log a_{H+}) should have a slope of -3.

The observed slope of -2.4 on Figure 6.5d is clearly inconsistent with solubility control by pure ferric hydroxide having a molar Fe:OH ratio of 1:3 (Nordstrom, 1991). Similar results (a

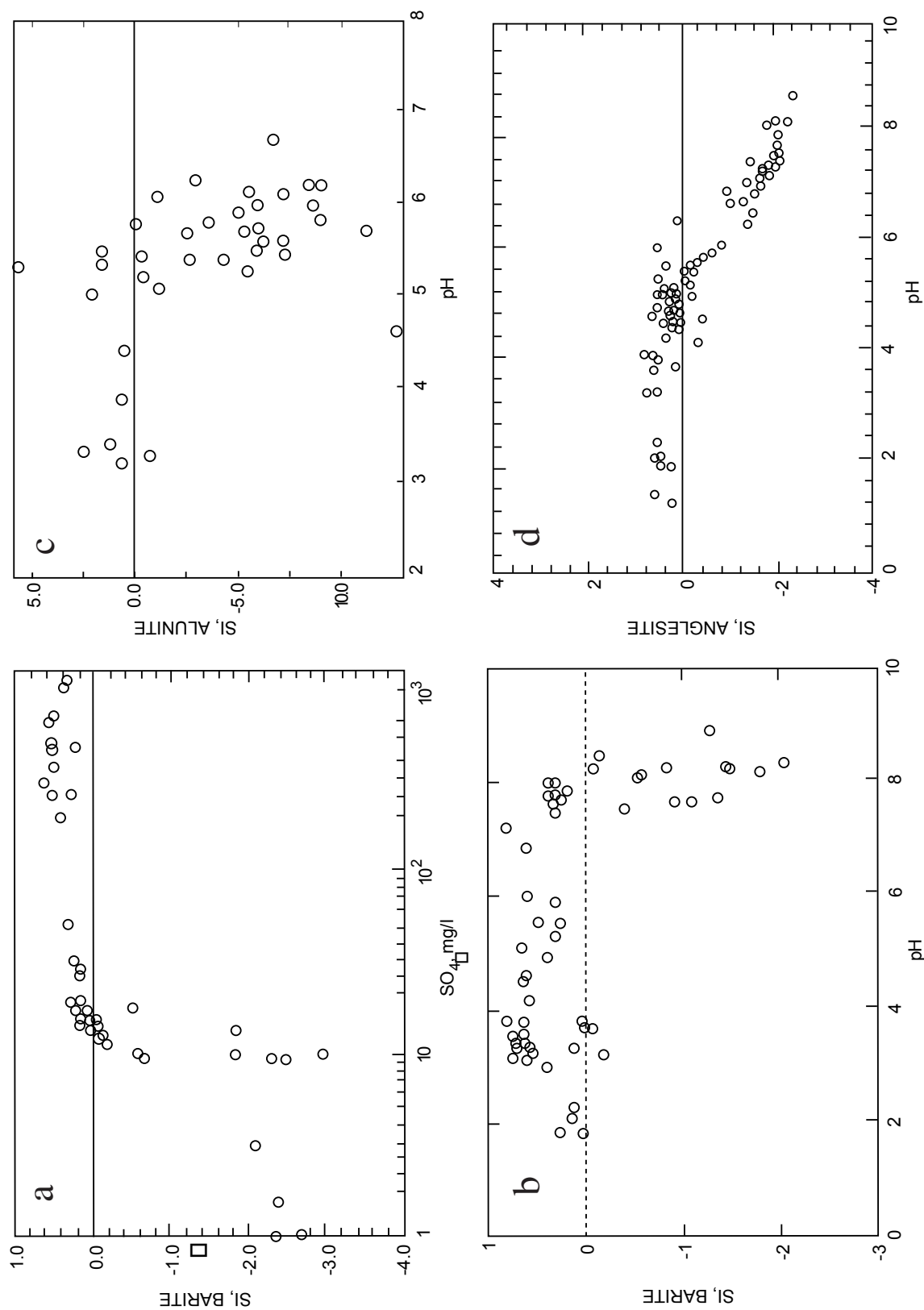


FIGURE 6.4—(a) Saturation indices for barite plotted as a function of sulfate concentration for data from the Osamu Utsumi mine site (Nordstrom et al., 1992). (b) Saturation indices for barite plotted as a function of pH for data from the Leviathan mine site (Ball and Nordstrom, 1989, 1994). (c) Saturation indices for alunite plotted as a function of pH for data from the Osamu Utsumi mine site (Nordstrom et al., 1992). (d) Saturation indices for anglesite plotted as function of pH for mine tailings based on data from Blowes (1990).

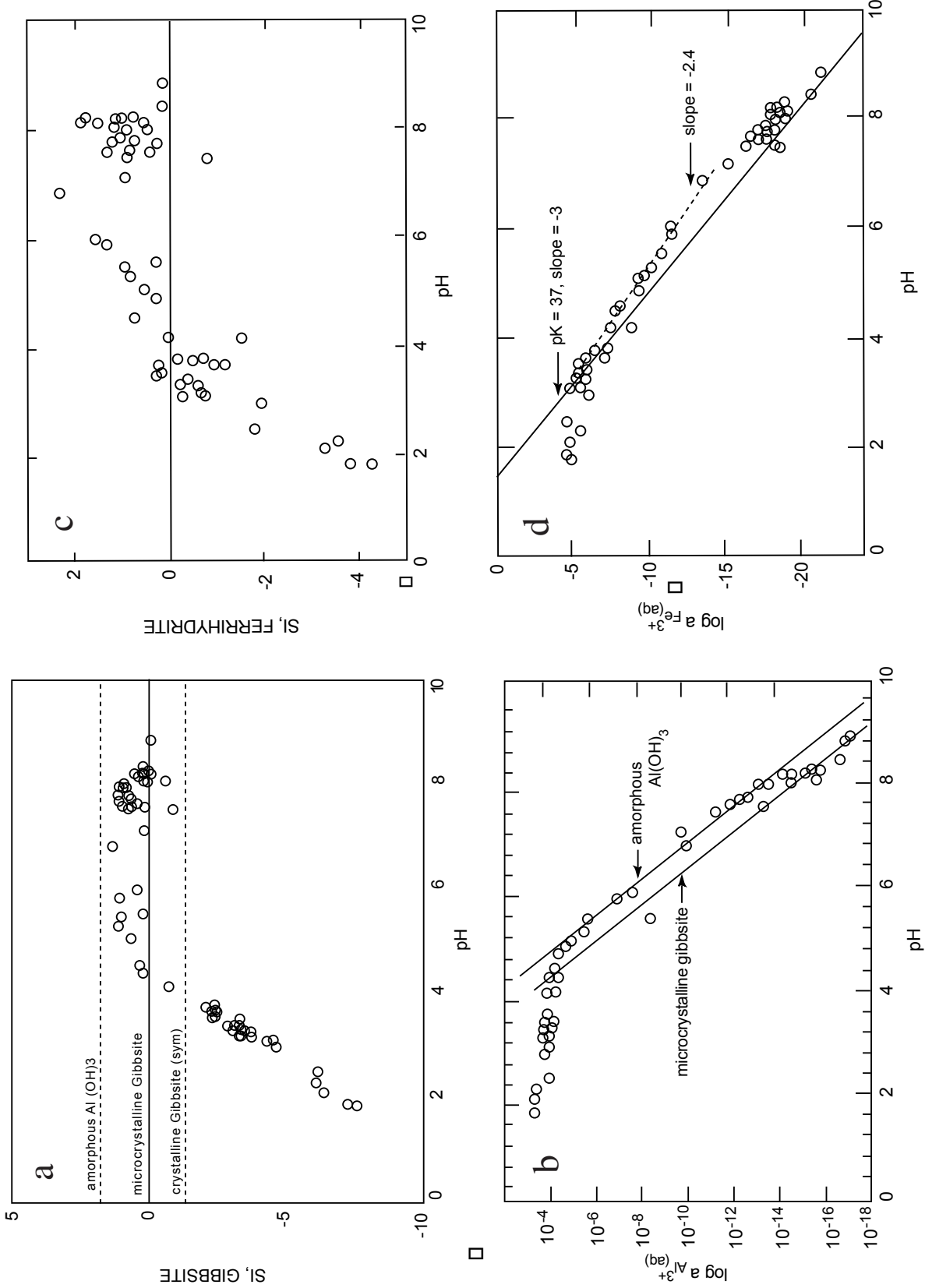
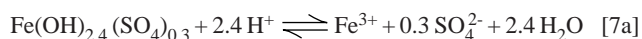


FIGURE 6.5—(a) Saturation indices for gibbsite as a function of pH for data from the Leviathan mine site (Ball and Nordstrom, 1989, 1994). (b) Logarithm of the activity of the aluminum ion plotted against pH with the equilibrium solubility lines for amorphous Al(OH)₃ and microcrystalline gibbsite shown (for 25°C). (c) Saturation indices for ferrrihydrite (≡ Fe(OH)₃) as a function of pH for data from the Leviathan mine site (Ball and Nordstrom, 1989, 1994). (d) Logarithm of the activity of the ferric ion plotted against pH with the equilibrium solubility for freshly precipitated ferrrihydrite at 25°C shown as a solid line and the best fit for data in the pH range of 3.5 to 7 shown as a dashed line (Nordstrom, 1991). The higher slope from the fitted line suggests non-stoichiometric substitution of sulfate for hydroxide in the precipitating ferric phase.

slope of -2.35) in other surface-water environments and in laboratory experiments were interpreted by Fox (1988) to represent a ferric hydroxide in which nitrate has partially substituted for hydroxide, i.e., $\text{Fe}(\text{OH})_{2.35}(\text{NO}_3)_{0.65}$. Kimball et al. (1994) found a regressed slope of -2.23 from iron data on the acid mine waters of St. Kevin Gulch, Colorado during a neutralization experiment.

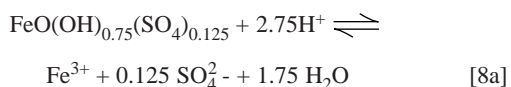
The relation on Figure 6.5d could be caused by a reaction involving a hypothetical sulfate-substituted ferric hydroxide such as



with its log equilibrium constant expression

$$\log K = \log a_{\text{Fe}^{3+}} - 2.4 \log a_{\text{H}^+} + 0.3 \log a_{\text{SO}_4^{2-}} + 2.4 \log a_{\text{H}_2\text{O}} \quad [7b]$$

The data on Figure 6.5d do not indicate solubility with schwertmannite of the composition reported by Bigham (1994). The expected slope on a plot of $a_{\text{Fe}^{3+}}$ vs. pH showing schwertmannite solubility equilibrium would be -2.75, based on the reaction



and its log equilibrium constant expression

$$\log K = \log a_{\text{Fe}^{3+}} - 2.75 \log a_{\text{H}^+} + 0.125 \log a_{\text{SO}_4^{2-}} + 1.75 \log a_{\text{H}_2\text{O}} \quad [8b]$$

Bigham (1994) reported that schwertmannite is associated with mine drainage ranging in pH from about 2.5 to 6, and is most commonly associated with "typical" mine effluents with pH from 3 to 4. Bigham (1994) also noted that ferrihydrite is associated with mine drainage in the pH range of about 5 to 8. The data on Figure 6.5d with slope of -2.4 span from pH of about 4 to about 7. This suggests that the apparent stoichiometry is more likely to represent a sulfate-substituted ferrihydrite, schwertmannite, or other hydrous ferric oxide with a molar Fe:OH ratio of 1:2.4. It is also possible that mixtures of different iron mineral phases are precipitating from these waters over this pH range and the slope is not clearly resolvable into a particular reaction. This complex chemistry needs more detailed work to quantitatively relate water chemistry to iron colloids and other precipitates.

In his thesis work (Blowes, 1990) and in subsequent papers (Blowes and Jambor, 1990; Blowes et al., 1991; Blowes and Ptacek, 1994; Ptacek and Blowes, 1994), Dr. Blowes and his colleagues have mapped the saturation indices for siderite, calcite, goethite, ferrihydrite, gypsum, melanterite, and anglesite with depth in tailings piles at Heath Steele, New Brunswick, and Waite Amulet, Quebec. Similar detailed hydrogeochemical studies are being completed at Kidd Creek and Copper Cliff, Ontario. In some of these studies, two aqueous models are compared: the ion association model and the specific ion interaction (Pitzer) model. For some minerals, the comparisons of saturation indices computed by both models are nearly identical, but for others the Pitzer model gives SI values that are more consistently at equilibrium. The mineralogy at these sites has also been studied in detail and it fully sup-

ports the interpretations based on the Pitzer model saturation index computations, which are more appropriate for solutions of high ionic strength. The strengths and limitations of these aqueous models as applied to acid mine waters are discussed by Alpers and Nordstrom (1999).

SECONDARY MINERALS

Acid mine waters are highly reactive solutions that can dissolve most primary minerals and form a wide variety of secondary minerals. The understanding of secondary mineral formation has important consequences for environmental management of mining wastes. Insoluble secondary minerals with large surface areas can effectively immobilize many of the major contaminants in acid mine waters, providing an important attenuation and detoxifying mechanism. Soluble secondary minerals also slow down toxic metal mobility but only temporarily until the next rainstorm or snowmelt event. Hence, the occurrence and properties of these minerals are equal in importance to the water chemistry and pyrite oxidation rates for the interpretation of chemical processes occurring in mine waste environments.

For the purpose of this discussion, secondary minerals are defined as those that form during weathering. A further distinction can be made between secondary minerals formed by natural processes prior to human disturbance and those formed after the commencement of mining, exploration, or other human activity. In this chapter we refer to these effects as pre-mining and post-mining.

There are clear similarities in the geochemistry of pre- and post-mining weathering processes, as well as in the nature of the associated aqueous solutions and secondary minerals; however, there are also some important differences. Mining tends to cause a dramatic increase in the rate of sulfide oxidation reactions because of rapid exposure of large volumes of reactive material to atmospheric oxygen. Blasting and crushing of ores and waste material leads to a considerable increase in the available surface area of reactive minerals. Hydrologic changes caused by mine dewatering in both underground and open-pit mines may expose large volumes of rock to atmospheric oxygen.

The type of secondary mineral formed depends on the composition of the water, the type and composition of the primary minerals, the temperature, and the moisture content. The initial minerals that precipitate in certain environments tend to be poorly crystalline, metastable phases that may transform to more stable phases over time. Therefore, those secondary minerals that are preserved in the geologic record in leached cappings, gossans, and zones of secondary enrichment may be quite different in their mineralogy compared with the secondary minerals that form over shorter time frames in mine drainage settings.

Four important processes lead to the formation of secondary minerals from acid mine waters: (1) iron oxidation and hydrolysis, (2) reaction of acid solutions with sulfides, gangue minerals, and country rock, (3) mixing of acid mine waters with more dilute waters, and (4) evaporation of acid mine waters.

A suite of Fe(III) minerals can form from iron oxidation and hydrolysis. Many of these phases have very low solubility, fall in the colloidal size range (less than 1.0 micrometer), and can adsorb or coprecipitate significant quantities of trace elements. Reaction of acid mine waters with country rock and some gangue minerals, such as calcite and dolomite, will cause neutralization and precip-

itation of metals. Evaporation concentrates the acid, sulfate, and metals found in acid mine waters until they reach mineral saturation, forming efflorescent sulfate salts, a common feature associated with oxidizing sulfide-bearing mine wastes.

This section describes five categories of secondary minerals:

(1) metal oxides, hydroxides, and hydroxysulfates, (2) soluble sulfates, (3) less-soluble sulfates, (4) carbonates, and (5) secondary sulfides. For each category, one or more lists of mineral formulas are provided (Tables 6.6–6.13). These lists are intended to include the more common secondary minerals in each category, but it should not be inferred that all minerals on the lists have been demonstrated to control metal concentrations in acid mine waters on a large scale. A discussion of the secondary minerals that are likely to control metal concentrations in acid mine waters is included as the final part of this section.

Metal oxides, hydroxides, and hydroxysulfates

Most divalent and trivalent metals exhibit amphotericism, i.e., they produce a solubility minimum at circum-neutral pH values with enhanced solubilities under both acidic and basic conditions. Figure 6.6 shows both the amphoteric solubilities of ferrihydrite, gibbsite, and the hydroxides of Cu, Zn, Fe(II), and Cd at 25°C, as well as the importance of pH in controlling the dissolved concentration of these metals. Different metals reach their minimum solubility at different pH values. This phenomenon provides the basis for the removal of metals during rapid neutralization of acid mine drainage by alkaline treatment (lime, limestone, or sodium hydroxide). The pH-specific solubility minimum varies for each metal, causing a different efficiency of metal removal for neutralization to a given pH (Barton, 1978). At metal concentrations greater than 10^{-6} molar, metal hydroxides should precipitate in the following sequence with increasing pH: Fe(III), Pb, Al, Cu, Zn, Fe(II), and Cd. This sequence is also very closely followed by the pH-dependent sequence of adsorption of metals on hydrated ferric oxide surfaces (Dzombak and Morel, 1990).

Iron—The minerals discussed in this section are ferrous (Fe^{II}) and ferric (Fe^{III}) oxides, hydroxides, and hydroxysulfates. The list of minerals in Table 6.6 includes some that are not observed to form readily during weathering, but are included for completeness and for analogy with other metals, especially aluminum (Table 6.7; discussed in a later subsection).

Ferrous hydroxide is considerably more soluble than its ferric equivalent at a given pH (Fig. 6.6) and the former appears only rarely in nature. $\text{Fe}(\text{OH})_2$, when slightly oxidized, takes on a green appearance and is also known as “green rust.” It occurs when Fe^{II} -rich solutions are mixed with a highly alkaline solution and allowed to oxidize slightly. This material has been prepared in the laboratory and Ponnampetuma et al. (1967) have argued effectively for its occurrence in nature, but it is not credited as a mineral because it is unstable and poorly characterized.

Ferrihydrite is a poorly crystalline form of hydrous ferric oxide/hydroxide that seems to be the first phase to form upon neutralization of Fe(III)-bearing solutions at low temperature, surficial conditions. For many years, this phase was considered to be “amorphous $\text{Fe}^{\text{III}}(\text{OH})_3$.” However, careful examination by X-ray diffraction (XRD) and Mössbauer spectroscopy (e.g., Schwertmann, 1985a) has revealed that this material is commonly a poorly crystalline substance with a range of structural order, yielding an XRD pattern with two to six peaks (Carlson and

Schwertmann, 1981). Ferrihydrite formed in mining environments tends to have two to four XRD peaks, and is associated with waters having pH values of 5 to 8 (Bigham, 1994). The “two-line” ferrihydrite is also referred to as “proto-ferrihydrite” (Chukhrov et al., 1973), although this is not an approved mineral name. At least two formulas for ferrihydrite have been reported: $\text{Fe}_5\text{HO}_8 \cdot 4\text{H}_2\text{O}$ (Towe and Bradley, 1967) and $\text{Fe}_2\text{O}_3 \cdot 2\text{FeO}(\text{OH}) \cdot 2.6\text{H}_2\text{O}$, a structural formula based on infrared spectroscopy (Russell, 1979). The latter formula can also be expressed as $\text{Fe}_2\text{O}_3 \cdot 1.8\text{H}_2\text{O}$.

Hematite (Fe_2O_3) and goethite [$\text{FeO}(\text{OH})$] are the most common and most stable forms of ferric oxide and oxyhydroxide, respectively. The solubility and stability of hematite and goethite are sufficiently close that grain size and surface Gibbs free energy have important influence on the phase relations. With regard to coarse-grained minerals, goethite appears to be stable relative to hematite at temperatures below about 80°C (Langmuir, 1969, 1971, 1972). However, fresh goethite nearly always occurs in a particle size less than 0.1 micrometers in soils and sediments, so it is unstable relative to coarser-grained hematite under the geologic conditions that form sedimentary rocks. This conclusion is supported by both laboratory (Berner, 1969, 1971) and field evidence (Walker, 1967, 1974, 1976). Both goethite and hematite have slow growth kinetics at surficial temperatures, so the initial solid products from the hydrolysis of $\text{Fe}_{(\text{aq})}^{3+}$ are poorly crystalline, metastable phases such as microcrystalline goethite or ferrihydrite. Thus, kinetic factors play an important role in determining the nature of the ferric precipitate(s) that may form as a result of ferrous iron oxidation and hydrolysis. Some progress has been made in understanding these factors and how they influence the distribution of hematite and goethite in soil profiles (Kämpf and Schwertmann, 1982; Schwertmann, 1985a, b). Ferrihydrite is known to convert to hematite if conditions are maintained between pH 5 and 9. Outside of this range, most of the ferrihydrite dissolves and reprecipitates as goethite (Schwertmann and Murad, 1983). Other factors may influence the formation of these phases, such as humidity, Al-content (Tardy and Nahon, 1985), grain size, and the presence of trace elements (Torrent and Guzman, 1982; Thornber, 1975). The preparation and characterization of iron oxides has been reviewed by Schwertmann and Cornell (1991).

Relatively little work has been done to understand the factors that influence the distribution of hematite and goethite in the weathered zone of mineral deposits. Leached cappings and gossans represent the *in situ* oxidized equivalents of porphyry copper and massive sulfide deposits, respectively. The mineralogy of iron in the oxidized zones of these deposits is dominated by hematite, goethite, and jarosite [$(\text{K}, \text{Na}, \text{H}_3\text{O})\text{Fe}^{\text{III}}_3(\text{SO}_4)_2(\text{OH})_6$]. The early literature (e.g., Locke, 1926; Tunell, 1930) documented the observation that “deep maroon to seal brown” hematitic iron oxide tends to remain in rocks after oxidation of supergene chalcocite-bearing ores, which form as the enrichment product of copper-iron sulfide protodes. Increasing amounts of goethite and jarosite relative to hematite correlate with progressively higher ratios of pyrite to chalcocite at depth (Loghry, 1972; Alpers and Brimhall, 1989). The texture of the iron oxides (or “limonites”) also reflects a systematic change from indigenous (in original sulfide cavities) to transported (outside sulfide cavities and in fractures) with increasing relative pyrite content prior to oxidation (Blanchard, 1968; Loghry, 1972).

Aluminum has been observed to substitute into goethite and

TABLE 6.6—Iron oxide, hydroxide, and hydroxysulfate minerals.

Mineral	Formula
Hematite	$\alpha\text{-Fe}_2\text{O}_3$
Maghemite	$\gamma\text{-Fe}_2\text{O}_3$
Magnetite	$\text{FeO}\cdot\text{Fe}_2\text{O}_3$
Goethite	$\alpha\text{-FeO(OH)}$
Akaganéite	$\beta\text{-FeO(OH,Cl)}$
Lepidocrocite	$\gamma\text{-FeO(OH)}$
Feroxyhyte	$\delta'\text{-FeO(OH)}$
Ferrihydrite	$\text{Fe}_5\text{HO}_8\cdot 4\text{H}_2\text{O}$ or $\text{Fe}_2\text{O}_3\cdot 2\text{FeO(OH)}\cdot 2.6\text{H}_2\text{O}$
Schwertmannite	$\text{Fe}^{\text{III}}_8\text{O}_8(\text{SO}_4)(\text{OH})_6$
Fibroferrite	$\text{Fe}^{\text{III}}(\text{SO}_4)(\text{OH})\cdot 5\text{H}_2\text{O}$
Amarantite	$\text{Fe}^{\text{III}}(\text{SO}_4)(\text{OH})\cdot 3\text{H}_2\text{O}$
Jarosite	$\text{KFe}^{\text{III}}_3(\text{SO}_4)_2(\text{OH})_6$
Natrojarosite	$\text{NaFe}^{\text{III}}_3(\text{SO}_4)_2(\text{OH})_6$
Hydronium Jarosite	$(\text{H}_3\text{O})\text{Fe}^{\text{III}}_3(\text{SO}_4)_2(\text{OH})_6$
Ammonium Jarosite	$(\text{NH}_4)\text{Fe}^{\text{III}}_3(\text{SO}_4)_2(\text{OH})_6$
Argentojarosite	$\text{AgFe}^{\text{III}}_3(\text{SO}_4)_2(\text{OH})_6$
Plumbojarosite	$\text{Pb}_{0.5}\text{Fe}^{\text{III}}_3(\text{SO}_4)_2(\text{OH})_6$
Beaverite	$\text{PbCuFe}^{\text{III}}_2(\text{SO}_4)_2(\text{OH})_6$
Chromate jarosite	$\text{KFe}^{\text{III}}_3(\text{CrO}_4)_2(\text{OH})_6$

TABLE 6.7—Aluminum oxide, hydroxide, and hydroxysulfate minerals.

Mineral	Formula
Corundum	$\alpha\text{-Al}_2\text{O}_3$
[γ -Alumina] ¹	$\gamma\text{-Al}_2\text{O}_3$
Diaspore	$\alpha\text{-AlO(OH)}$
Boehmite	$\gamma\text{-AlO(OH)}$
Gibbsite	$\gamma\text{-Al(OH)}_3$
Bayerite	$\alpha\text{-Al(OH)}_3$
Doyleite	Al(OH)_3
Nordstrandite	Al(OH)_3
Alunite	$\text{KAl}_3(\text{SO}_4)_2(\text{OH})_6$
Natroalunite	$\text{NaAl}_3(\text{SO}_4)_2(\text{OH})_6$
[Hydronium Alunite] ²	$(\text{H}_3\text{O})\text{Al}_3(\text{SO}_4)_2(\text{OH})_6$
Ammonium Alunite	$(\text{NH}_4)\text{Al}_3(\text{SO}_4)_2(\text{OH})_6$
Osarizawaite	$\text{PbCuAl}_2(\text{SO}_4)_2(\text{OH})_6$
Jurbanite	$\text{Al}(\text{SO}_4)(\text{OH})\cdot 5\text{H}_2\text{O}$
Basaluminate	$\text{Al}_4(\text{SO}_4)(\text{OH})_{10}\cdot 5\text{H}_2\text{O}$
Hydro-basaluminate	$\text{Al}_4(\text{SO}_4)(\text{OH})_{10}\cdot 12\text{-}36\text{H}_2\text{O}$

¹ γ -Alumina is a synthetic compound, used as a catalyst in industry. Surface properties are reviewed by Goldberg et al. (1995).² Hydronium alunite has not been found in nature and therefore is not considered a mineral.**TABLE 6.8**—Some other oxide and hydroxide minerals and native metals.

Mineral	Formula
Pyrolusite	MnO_2
Hausmannite	Mn_3O_4
Manganite	$\gamma\text{-MnO(OH)}$
Pyrochroite	Mn(OH)_2
Todorokite	$(\text{Mn}^{\text{II}},\text{Ca},\text{Mg})\text{Mn}^{\text{IV}}_3\text{O}_7\cdot \text{H}_2\text{O}$
Takanelite	$(\text{Mn}^{\text{II}},\text{Ca})\text{Mn}^{\text{IV}}_4\text{O}_9\cdot \text{H}_2\text{O}$
Rancieite	$(\text{Ca},\text{Mn}^{\text{II}})\text{Mn}^{\text{IV}}_4\text{O}_9\cdot 3\text{H}_2\text{O}$
Native copper	Cu
Tenorite	CuO
Cuprite	Cu_2O
Delafossite	CuFeO_2
Bunsenite	NiO
Theophrastite	Ni(OH)_2
Jamborite	$(\text{Ni}^{\text{II}},\text{Ni}^{\text{III}},\text{Fe})(\text{OH})^2(\text{OH},\text{S},\text{H}_2\text{O})$
Native silver	Ag
Native gold	Au
Native mercury	Hg
Montroydite	HgO
Massicot litharge	PbO
Plattnerite	PbO_2

TABLE 6.9—Selected soluble iron-sulfate minerals.

Mineral	Formula
Melanterite	$\text{Fe}^{\text{II}}\text{SO}_4\cdot 7\text{H}_2\text{O}$
Siderotil	$\text{Fe}^{\text{II}}\text{SO}_4\cdot 5\text{H}_2\text{O}$
Rozenite	$\text{Fe}^{\text{II}}\text{SO}_4\cdot 4\text{H}_2\text{O}$
Szomolnokite	$\text{Fe}^{\text{II}}\text{SO}_4\cdot \text{H}_2\text{O}$
Halotrichite	$\text{Fe}^{\text{II}}\text{Al}_2(\text{SO}_4)_4\cdot 22\text{H}_2\text{O}$
Roemerite	$\text{Fe}^{\text{II}}\text{Fe}^{\text{III}}_2(\text{SO}_4)_4\cdot 14\text{H}_2\text{O}$
Coquimbite	$\text{Fe}^{\text{III}}_2(\text{SO}_4)_3\cdot 9\text{H}_2\text{O}$
Kornelite	$\text{Fe}^{\text{III}}_2(\text{SO}_4)_3\cdot 7\text{H}_2\text{O}$
Rhombochase	$(\text{H}_3\text{O})\text{Fe}^{\text{III}}(\text{SO}_4)_2\cdot 3\text{H}_2\text{O}$
Ferricopiapite	$\text{Fe}^{\text{III}}_5(\text{SO}_4)_6\text{O(OH)}\cdot 20\text{H}_2\text{O}$
Copiapite	$\text{Fe}^{\text{II}}\text{Fe}^{\text{III}}_4(\text{SO}_4)_6(\text{OH})_2\cdot 20\text{H}_2\text{O}$
Voltaite	$\text{K}_2\text{Fe}^{\text{II}}_5\text{Fe}^{\text{III}}_4(\text{SO}_4)_{12}\cdot 18\text{H}_2\text{O}$

TABLE 6.10—Some other soluble sulfate minerals.

Mineral	Formula
Epsomite	$MgSO_4 \cdot 7H_2O$
Hexahydrate	$MgSO_4 \cdot 6H_2O$
Goslarite	$ZnSO_4 \cdot 7H_2O$
Bianchite	$ZnSO_4 \cdot 6H_2O$
Gunningite	$ZnSO_4 \cdot H_2O$
Zincosite	$ZnSO_4$
Gypsum	$CaSO_4 \cdot 2H_2O$
Anhydrite	$CaSO_4$
Morenosite	$NiSO_4 \cdot 7H_2O$
Retgersite	$NiSO_4 \cdot 6H_2O$
Boothite	$CuSO_4 \cdot 7H_2O$
Chalcanthite	$CuSO_4 \cdot 5H_2O$
Chalcocyanite	$CuSO_4$
Alunogen	$Al_2(SO_4)_3 \cdot 17H_2O$
Mirabilite	$Na_2SO_4 \cdot 10H_2O$
Thenardite	Na_2SO_4

TABLE 6.11—Some less-soluble sulfate and hydroxysulfate minerals.

Mineral	Formula
Celestite	$SrSO_4$
Anglesite	$PbSO_4$
Barite	$BaSO_4$
Radium sulfate	$RaSO_4$
Antlerite	$Cu_3(SO_4)(OH)_4$
Brochantite	$Cu_4(SO_4)(OH)_6$
Langite, Wroewolfeite	$Cu_4(SO_4)(OH)_6 \cdot 2H_2O$
Posnjakite	$Cu_4(SO_4)(OH)_6 \cdot H_2O$

TABLE 6.12—Some carbonate minerals.

Mineral	Formula
Rhombohedral	
Calcite	$CaCO_3$
Magnesite	$MgCO_3$
Siderite	$FeCO_3$
Rhodochrosite	$MnCO_3$
Smithsonite	$ZnCO_3$
Otavite	$CdCO_3$
Gaspéite	$NiCO_3$
Sphaerocobaltite	$CoCO_3$
Orthorhombic	
Aragonite	$CaCO_3$
Strontianite	$SrCO_3$
Witherite	$BaCO_3$
Cerrusite	$PbCO_3$
Double	
Dolomite	$CaMg(CO_3)_2$
Kutnahorite	$Ca(Mn,Mg)(CO_3)_2$
Ankerite	$Ca(Fe^{II},Mg,Mn)(CO_3)_2$
Minrecordite	$CaZn(CO_3)_2$
Hydroxyl	
Malachite	$Cu_2(CO_3)(OH)_2$
Azurite	$Cu_3(CO_3)_2(OH)_2$
Hydrocerussite	$Pb_3(CO_3)_2(OH)_2$
Hydrozincite	$Zn_5(CO_3)_2(OH)_6$
Aurichalcite	$(Zn,Cu)_5(CO_3)_2(OH)_6$

TABLE 6.13—Supergene and diagenetic sulfide minerals.

Mineral	Formula
Supergene sulfide minerals	
Chalcocite	Cu_2S
Djurleite-I	$Cu_{1.965}S$
Djurleite-II	$Cu_{1.934}S$
Digenite	$(Cu,Fe)_9S_5$
Anilite	Cu_7S_4
Geerite	Cu_8S_5
Spionkopite	$Cu_{39}S_{28}$
Yarrowite	Cu_9S_8
Blue-remaining covellite	$Cu_{(1+x)}S$
Covellite	CuS
Violarite	Ni_2FeS_4
Millerite	NiS
Diagenetic sulfide minerals	
Amorphous FeS	FeS with coprecipitated Zn, Cd, Mn, Cu, Ni, As)
Mackinawite	$(Fe,Ni)_9S_8$
Smythite	$(Fe,Ni)_9S_{11}$
Greigite	$Fe^{II}Fe^{III}_2S_4$
Pyrite, marcasite	FeS_2

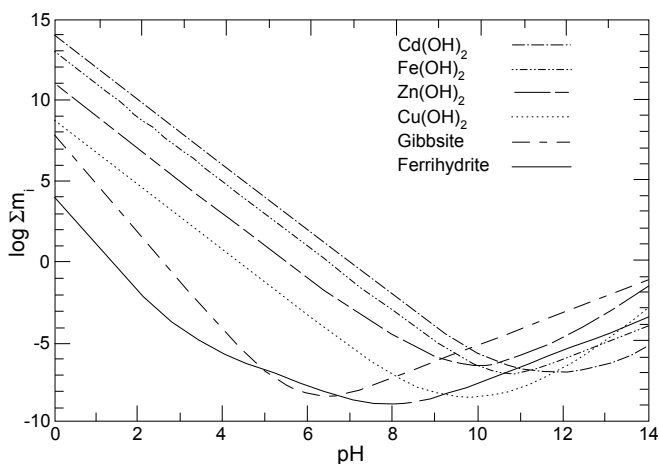


FIGURE 6.6—Solubility curves for gibbsite, ferrihydrite, and the hydroxides of Cu, Zn, Fe (II), and Cd shown as a function of pH.

hematite in certain soils, to maximum concentrations of 33 mole % $\text{AlO}(\text{OH})$ and 14 mole % Al_2O_3 , respectively (Yapp, 1983; Tardy and Nahon, 1985; Schwertmann, 1985a). Although both iron and aluminum are highly soluble in acid mine waters, we are unaware of any data showing significant aluminum substitution in iron oxide minerals formed in mine drainage settings. Adsorption and precipitation of hydrolyzable metal ions tends to take place at pH values near the first hydrolysis pK for that metal. The first pK of hydrolysis for Fe^{III} is 2.2, and for Al is 5.0, so the coprecipitation of Al in hydrous Fe^{III} oxides formed at pH values less than about 4.5 is unlikely. This fundamental difference between iron and aluminum chemistry leads to spatial and temporal separation of precipitating phases of hydrolyzed iron and aluminum in oxidizing mineral deposits and mine waters.

Schwertmannite is a poorly crystalline iron-hydroxysulfate mineral that has recently been discovered to be a fairly common phase in ochres formed in mine drainage environments (Bigham et al., 1990; Bigham, 1994; Murad et al., 1994). The structure of schwertmannite appears to be related to that of akaganéite, an iron oxyhydroxide with essential chloride (Bigham, 1994; Murad et al., 1994). A combination of powder XRD and Mössbauer spectroscopy is necessary for definitive identification of schwertmannite (Murad et al., 1994). Schwertmannite or other sulfate-substituted, hydrous ferric oxides are most likely to control ferric iron solubility in acid mine drainage, as discussed previously (Fig. 6.5d).

Jarosite-alunite—The jarosite-alunite group of minerals shares a common crystal structure and stoichiometry, with many possible compositional substitutions. The general jarosite-alunite formula is $\text{AB}_3(\text{SO}_4)_2(\text{OH})_6$ where the B sites are occupied by Fe^{III} to form jarosites and by Al to form alunites. Endmember formulas for some of the more common jarosite group minerals are given in Table 6.6, and the more common alunite endmember formulas in Table 6.7. The A site is occupied either by a monovalent cation or by a divalent cation alternating with a vacancy to maintain charge balance. The most common occupants of the A site in order of abundance in natural alunites and jarosites are $\text{K}^+ > \text{Na}^+ > \text{H}_3\text{O}^+$ (Kubisz, 1960, 1961, 1964; Brophy and Sheridan, 1965; Scott, 1987). The pure potassium-iron endmember is jarosite and the pure potassium-aluminum endmember is alunite. Pure end-

members are rare; jarosites and alunites formed during weathering and those synthesized at temperatures below 100°C tend to contain considerable hydronium ion in the A site (Dutrizac and Kaiman, 1976; Dutrizac, 1983; Alpers et al., 1989, 1992; Stoffregen and Alpers, 1992). Hydronium jarosite has been reported as a naturally occurring mineral (Kubisz, 1970), whereas hydronium alunite has not yet been found in nature. The hydronium endmembers can be synthesized readily (Ripmeester et al., 1986). Solid solutions between alunite and jarosite have also been synthesized (Parker, 1962; Brophy et al., 1962), but thermodynamic relations for iron-aluminum substitution have not been established and mineral compositions intermediate to alunite and jarosite are not commonly observed. This effect is probably caused by the different first hydrolysis constants for Fe^{III} ($\text{pK}_1 = 2.2$) and Al ($\text{pK}_1 = 5.0$), as discussed earlier regarding hematite and goethite. Further summaries on substitutional properties of the alunite-jarosite group were presented by Scott (1987), Stoffregen and Alpers (1987, 1992), and Alpers et al. (1989). Information on the relation between the crystallographic, chemical, and isotopic properties of alunite and jarosite was reported by Alpers et al. (1992) and by Stoffregen and Alpers (1992).

Aluminum—A list of some aluminum oxide, hydroxide, and hydroxysulfate minerals and their formulas is provided in Table 6.7. Thermodynamic properties of aluminous minerals have been reviewed, evaluated, and tabulated by Hemingway and Sposito (1996). Properties of aqueous aluminum ions and polymers have been reviewed and evaluated by Nordstrom and May (1996) and Bertsch and Parker (1996), respectively.

Solubility and stability relations among gibbsite, alunite, basaluminate, jurbanite, and alunogen were delineated by Nordstrom (1982b). In acid mine waters, aluminum-sulfate and -hydroxysulfate minerals become more stable than common soil minerals such as gibbsite and kaolinite. At pH values less than about 5.5 (depending on sulfate and potassium activities) gibbsite becomes unstable relative to alunite (Nordstrom, 1982b). Below pH values of about 4, jurbanite becomes most stable. Alunogen becomes stable only at pH values below 0 (i.e., hydrogen ion activities greater than 1.0). Some of these stability relationships need to be revised in light of the work by Reardon (1988), who applied the Pitzer approach to aluminum-sulfate solutions, and the recent revisions on thermodynamic properties of aluminum minerals and aqueous species (Hemingway and Sposito, 1996; Nordstrom and May, 1996). Despite its apparent thermodynamic stability, jurbanite tends to occur only rarely as a post-mining efflorescence (Anthony and MacLean, 1976), and has not been found commonly as a mineral precipitate from acid mine waters. We suspect that jurbanite has little significance as a solubility control in spite of the near-zero SI values commonly found, for three reasons:

- 1) recalculation of the solubility field is needed, based on revised thermodynamic properties for auxiliary species that may show the stability field of jurbanite to be at lower pH values,
- 2) jurbanite appears to be an efflorescent salt and most efflorescent salts in mine wastes form at pH values much less than 4,
- 3) other factors seem to govern aluminum and sulfate concentrations in acid mine waters (Nordstrom and Ball, 1986).

The behavior of aluminum in acid mine waters (and stream waters affected by acid rain) has been described by Nordstrom and Ball (1986). For waters with pH values less than 4.5 to 5.0, dissolved aluminum tends to behave as a conservative ion in surface waters, whereas for waters with pH values above 5.0, solubility control of dissolved aluminum by microcrystalline to amorphous

$\text{Al}(\text{OH})_3$ is apparent, as described previously (Figs. 6.5a and 6.5b). Such control may be caused by equilibrium solubility or by a surface reaction involving the exchange of Al^{3+} for 3H^+ on an aluminous surface. May and Nordstrom (1991) showed that a characteristic change of behavior for aluminum from conservative to non-conservative is common for a wide variety of sulfate-acidified waters. When the pH in an acid mine water increases to 5 or higher because of rapid mixing with circumneutral, dilute water, an aluminum-hydroxysulfate compound precipitates immediately. This precipitate is usually white, and is most commonly amorphous to XRD, electron diffraction, transmission electron microscopy, and scanning electron microscopy (Nordstrom et al., 1984). It seems to be of fairly constant composition, similar to the amorphous basaluminite reported by Adams and Rawajfeh (1977). It has been observed many times by people working on acid mine waters and mine wastes. The occurrence of the white, aluminous precipitate at pH values of 5 or above is so consistent that one can frequently use its presence to predict the pH of the water when a pH electrode and meter are unavailable. A classic example is the caved portal at the Gem Mine (often called the Paradise portal), in the San Juan Mountains of southwestern Colorado, which has been discharging mine water continuously with a pH of 5.5 ± 0.3 for more than 30 years. This site has a striking white precipitate, affectionately known as "white death," that consists primarily of aluminum, sulfate, and water (Nordstrom et al., 1984); anomalous concentrations of lanthanide elements have been found in this precipitate (Carlson-Foszcz, 1991; Nordstrom et al., 1995).

As with the iron minerals, thermodynamic stability relations among the aluminum minerals and their kinetic rates of formation can vary greatly, depending upon sulfate concentration, salinity, pH, particle size, and temperature. Precipitation rates for some of these aluminous minerals may be sluggish so that the equilibrium conditions are not often reached in surface waters. In soil and ground waters, longer residence times favor solubility control by mineral-solution equilibria.

Other metals—Native metals, oxides, and hydroxides of several other metals such as copper, nickel, manganese, silver, gold, and mercury may occur from the weathering and oxidation of primary sulfide minerals (Table 6.8). These minerals tend to occur as residual products in oxidized zones (gossans and leached cappings), where many pore volumes of water have reacted with the formerly mineralized rocks. It is unlikely that these phases exert solubility control on large volumes of water, but rather they are likely to form during dry periods when isolated microenvironments may reach saturation with a given native metal, oxide or hydroxide. The absence of discrete trace-metal-bearing oxides and hydroxides in most oxidized mine wastes suggests that other mechanisms, such as adsorption or coprecipitation with hydrous iron oxides, limit the concentrations of dissolved trace metals in mining environments (see Smith, 1999).

The behavior of nickel in tailings impoundments and acid-mine-drainage precipitates illustrates that the fate of trace metals in mine drainage settings is generally tied to that of the major elements, particularly iron. Mineralogical analysis and microanalysis by Jambor and co-workers as part of a study on the Copper Cliff tailings area at Sudbury, Ontario, has indicated that nickel tends to occur dispersed in hydrous iron oxides forming alteration rims on pentlandite and nickeliferous pyrrhotite, rather than as discrete nickel oxide or hydroxide phases (Alpers et al., 1994b). Overall,

the bulk of the nickel liberated by oxidation of these sulfides ends up in goethite, a part of the nickel remains in solution and is transported from the site of oxidation, a small amount is taken up by vermiculite and associated mixed-layer silicates that replace biotite, and some may occur as secondary violarite (see Supergene and Diagenetic Sulfides section, below), which is expected to occur but has not yet been found in the Copper Cliff tailings (Alpers et al., 1994b).

Copper oxides, particularly tenorite and cuprite, are known to form in the oxidized zone of sulfide deposits and are indicative of low pyrite content and/or a high wallrock neutralization capacity (Loghry, 1972; Anderson, 1982). The behavior of copper in tailings impoundments and waste-rock piles is similar to that of nickel in that discrete secondary copper oxides are rarely formed; rather the copper is either transported away from the oxidized zone in solution, is fixed in other secondary phases such as sulfates, carbonates, or silicates, or is coprecipitated and/or adsorbed to hydrous iron oxides.

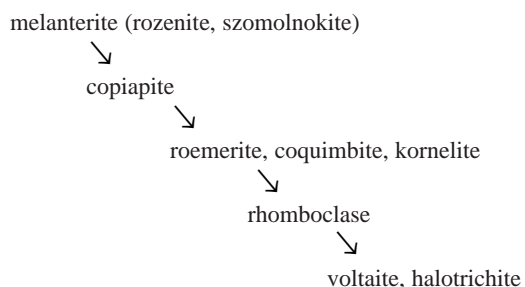
Manganese oxides and hydroxides are known to form from acid mine drainage, often at considerable distance from the source(s) of sulfide oxidation and acid formation. Krauskopf (1957) pointed out that the redox and hydrolysis properties of iron and manganese are such that they sometimes behave differently under changing conditions of oxidation and reduction. Hem (1978, 1980) considered the effects of manganese oxidation and disproportionation on the coprecipitation of other trace metals with manganese oxides. He demonstrated the effect of manganese on the coprecipitation of $\text{CoO}(\text{OH})$ (Hem et al., 1985) and on the precipitation of zinc as hetaerolite, ZnMn_2O_4 , at 25°C (Hem et al., 1987). He further discussed the possibility that low-temperature "ferrite" compounds may be responsible for the low concentrations of trace metals found in uncontaminated natural waters. Hem also made many other significant contributions to our understanding of the hydrolysis and precipitation of trace metals (Hem, 1985).

Manganese oxides are actively precipitating at Pinal Creek, Arizona, in the Globe-Miami mining district, and so provide an opportunity for study of geochemical processes controlling manganese solubility in a mine drainage setting. At Pinal Creek, an alluvial ground-water aquifer was contaminated by acidic recharge (pH about 2.7) from copper mining and smelting activities (Eychaner, 1991). After neutralization by interaction with the alluvial material, the contaminated ground-water emerges at near-neutral pH in a perennial reach of Pinal Creek, about 15 km down-gradient from the acid source, at which point manganese-rich crusts have developed in the streambed. Chemical and XRD analyses (Lind, 1991) suggest that the manganese occurs as a mixture of two related hydrous oxides, takanelite and rancieite (see Table 6.8), plus an Mn-bearing carbonate, probably kutnohorite (see Table 6.12). The overall oxidation state of the manganese in the less-than-75 micrometer size fraction of the Pinal Creek precipitates was 3.65 (Lind, 1991). To test the hypothesis that neutralization of acidic Mn-bearing water would lead to formation of similar Mn-bearing minerals, titrations were made of Mn-rich ground waters from the Pinal Creek area with a 0.1 molar NaOH solution with and without CO_2 present; these experiments yielded hausmannite (which aged to manganite), kutnohorite, and a mixed Ca-Mn species similar to todorokite (Hem and Lind, 1993).

Soluble sulfates

Soluble sulfate minerals, often occurring as efflorescent salts, are common in mines, on mine tailings and waste rock, and on sulfide mineralization exposed to the air. These phases store metals and sulfate during dry periods and dissolve readily during flushing events, a process that has an important influence on temporal variations of metals in surface waters affected by mine wastes.

Iron sulfates—The most common efflorescent minerals are hydrated iron sulfate salts (Table 6.9). Based both on laboratory experiments of evaporating acid mine waters as well as field observations, the hydrated iron sulfate minerals seem to follow a paragenetic sequence as shown below (Buurman, 1975; Nordstrom, 1982a; C. Maenz, written commun., 1995).



The formation of melanterite as the first phase to precipitate from the evaporation of many acid mine waters is consistent with the preponderance of aqueous ferrous iron in these waters. Reactions (2) and (3) indicate that aqueous ferrous iron and sulfate are the initial products of pyrite oxidation, and it is these ions that combine to form melanterite. The remaining iron sulfates in the generalized paragenetic sequence form as the solutions evaporate and the ferrous iron oxidizes to ferric; however, a simple progression from ferrous to ferric salts is not observed because of differences in solubility among the various salts and the influence of other major elements which substitute to a variable degree for divalent and trivalent iron, such as copper and zinc for ferrous iron and aluminum for ferric iron.

Copper tends to partition into melanterite in preference to zinc (Alpers et al., 1994a). The result of this partitioning is a tendency toward higher ratios of zinc/copper in residual solutions as melanterite and related phases form in the dry season, and then lower ratios of zinc/copper as the salts are flushed in the wet season (Alpers et al., 1994a).

Another important role of the soluble iron sulfates is to store acidity and oxidation potential in the form of hydronium and ferric ions. The mineral rhomboclase is essentially a solid form of sulfuric acid plus ferric sulfate. Although generally considered rare, large quantities of rhomboclase and other iron sulfate salts were found at Iron Mountain, California, in inactive underground mine workings within a volcanogenic massive sulfide deposit (Alpers and Nordstrom, 1991). The salts were observed to be actively forming from waters with pH values from 1 to less than -3 (Nordstrom et al., 1991; Alpers et al., 1991; Nordstrom and Alpers, 1999). Rhomboclase may be present in trace amounts in other settings where acid waters evaporate to dryness, providing a storage mechanism for hydronium ions. Other ferric-sulfate and mixed ferrous-ferric-sulfate salts have been found associated with mine wastes and spoils in numerous localities including coal and metal mines (e.g., Zdrov and McCandlish, 1978a, b; Zdrov et

al., 1979; Cravotta, 1994; Plumlee et al., 1995).

Dissolution of these salts can create large quantities of very acid mine waters. Flooding of underground mines and mine wastes as a remedial measure may not result in short-term improvements in water quality because the ferric salts will dissolve and the ferric iron will hydrolyze (if pH is above 2.2), providing an oxidant that will cause continued sulfide oxidation (e.g., Cravotta, 1994).

Other metal sulfates—There are a large number of additional metal sulfates that occur as efflorescent minerals in weathered mineral deposits and mining environments. Some of the more common ones are listed in Table 6.10. One of the important aspects of these salts is that they are a solid form of acid mine drainage that is stored until the next rainstorm event when the salts can quickly dissolve and be transported to a drainage system. Dagenhart (1980) demonstrated that the concentrations of copper, zinc, iron, and aluminum increase sharply during the rising limb of the discharge as rain dissolves and flushes efflorescent salts from oxidizing tailings into a receiving stream. This phenomenon is probably common at mined sites and may be an important factor in the association of fish kills during periods of high runoff, especially after a significant dry period.

Less-soluble sulfates

Although there are a great many metal sulfate minerals of low solubility known to occur, the most common ones are barite, celestite, and anglesite (Table 6.11). These are likely to provide solubility controls for the concentrations of barium, strontium, and lead (see previous section on mineral solubilities, Fig. 6.4). Their low solubilities tend to immobilize these elements in the environment and make them less bioavailable than many of the other hazardous metals at mine sites. In particular, lead concentrations in acid mine drainage and tailings pore waters appear to be controlled at relatively low levels by anglesite solubility (e.g., Blowes and Jambor, 1990).

Carbonates

Many carbonate minerals occur as either primary or secondary minerals in mine wastes. Examples are given in Table 6.12. Carbonates may originate as an accessory gangue mineral that accompanies the mineral deposit and mine waste (mine working residuum, waste piles, tailings), as an amended material for neutralization, or as a secondary product from weathering of wastes or amendments. Carbonate minerals are important as neutralizers of acid in mine drainage (Blowes and Ptacek, 1994). Siderite forms as a secondary phase in tailings impoundments where calcite reacts with Fe(II)-rich solutions (Ptacek and Blowes, 1994). The hydroxyl-bearing carbonates in Table 6.13 form as secondary minerals in the oxidation of Zn-Cu-Pb ores and related mine wastes.

Supergene and diagenetic sulfides

The supergene enrichment process that affects primary sulfide ores may also be a factor in redistribution of metals in mine waste environments, particularly tailings impoundments. Supergene alteration of copper- and nickel-sulfide deposits has resulted in

enrichment of ore grades by oxidation and leaching of metals in the unsaturated zone above the water table followed by transport of metals to a zone of more reducing conditions where secondary sulfide minerals are formed (Anderson, 1982; Alpers and Brimhall, 1989). A list of some supergene copper and nickel minerals is given in Table 6.13. The two compositions for djurleite are based on the investigation by Potter (1977). An example of active supergene enrichment in a tailings impoundment is the presence of secondary covellite near the depth of active oxidation at Waite Amulet, Ontario (Blowes and Jambor, 1990).

Diagenetic processes affect mine drainage geochemistry in areas where reducing conditions can lead to sulfate reduction and the formation of secondary sulfides. The sulfides are generally insoluble, so this represents a plausible geochemical mechanism for metal fixation in mine workings, anoxic wetlands, and lake bottoms, if reducing conditions are maintained. Iron is commonly the most abundant transition metal and therefore is the most likely metal to combine with H_2S to produce secondary sulfides in environments affected by mine drainage. Other divalent metals present will also tend to form secondary sulfides, as indicated in Table 6.13. The relative solubility of metal sulfides, starting from the most soluble, is: $MnS > FeS > NiS \sim ZnS > CdS \sim PbS > CuS > HgS$ (DiToro et al., 1991).

A summary of mineralogic controls on metal concentrations

As a guide to the aqueous geochemistry for acid mine waters, we have compiled a list of minerals in Table 6.14 that might be important in governing metal concentrations. This list is drawn from our experience in modeling and interpreting mine water chemistry and is meant as a guide rather than a strict protocol. The two columns in Table 6.14 show those minerals most likely to have a solubility control and those less likely but possible.

SUMMARY

Physical, chemical, and biological processes all play important roles in the production, release, mobility, and attenuation of contaminants in acid mine waters. Physical aspects include the geology (geomorphology, structure, petrology, geophysical features), the hydrology (water budget, porosity, permeability, flow direction, flow rate, dispersion, mixing, surface transport characteristics), and the effects of mining and mineral processing. The specific processes that have been studied and found to contribute to the overall phenomenon of acid mine water geochemistry are:

- 1) pyrite oxidation
- 2) oxidation of other sulfides
- 3) oxidation and hydrolysis of aqueous iron and other elements
- 4) neutralizing capacity of gangue minerals and country rock
- 5) neutralizing capacity of bicarbonate-buffered waters
- 6) oxygen transport
- 7) fluid transport of water and water vapor
- 8) form and location of permeable zones relative to flow paths
- 9) climatic variations (diel, storm events, seasonal)
- 10) evaporation, efflorescence, redissolution
- 11) heating by conduction and radiation (due to a variety of exothermic reactions including pyrite oxidation, dissolution of soluble salts, and dilution of concentrated acid)

- 12) temperature
- 13) microbial catalysis of reaction rates
- 14) microbial sorption and uptake of metals
- 15) mineral precipitation and dissolution during transport
- 16) adsorption and desorption of metals during transport
- 17) photoreduction of iron
- 18) organic complexing
- 19) microenvironmental processes (surface films, microbial films, mineral coatings)

TABLE 6.14—Minerals whose solubilities might control metal concentrations in mine waters.

Solubility equilibrium likely	Solubility equilibrium difficult but possible
alunogen	alunite
anglesite	ankerite
barite	antlerite
basaluminite (amorphous)	atacamite, paratacamite
calcite	azurite
cerussite	bronchantite
chalcantinite	chrysocolla
epsomite	goethite
ferrhydrite	hemimorphite
gibbsite (amorphous to microcrystalline)	hematite
goslarite	hydrozincite
gypsum	jarosite
halotrichite-pickeringite	kaolinite
manganese oxides	kutnohorite
melanterite	malachite
otavite	natroalunite
rhodochrosite	natrojarosite
schwertmannite	plumbojarosite
scorodite	
siderite	
silica (microcrystalline)	
smithsonite	
witherite	

Many of these processes are represented schematically on Figure 6.7. Perhaps the most important factors affecting the production of acid mine waters are the amount, concentration, grain size, and distribution of pyrite present in a mine, tailings, or waste pile. The rate of oxidation can vary depending on the accessibility of air, moisture, and microbes to the pyrite surfaces and the neutralizing capacity of available buffering materials. These complex geochemical processes can be modeled with either equilibrium or kinetic principles to estimate the result of pyrite oxidation, carbonate buffering, and silicate hydrolysis (see Chapter 14 on geochemical modeling). Modeling calculations of this type have been done for pyritic rocks and waters of different initial compositions (e.g., Lichtner, 1994). Modeling calculations, however, are well-educated guesses. There will always be inadequate data and contentions ambiguities in the conclusions. The advantage of modeling is that it can take into account some of the complex interactions between hydrology, geochemistry, geology, and other site characteristics as well as performing database management. This advantage is a major step beyond various acid-base accounting, static, and kinetic tests for which comparison, evaluation, and agreement is lacking (White and Jeffers, 1994).

The geochemistry of acid mine waters is a complex subject that draws upon many technical disciplines. Although considerable

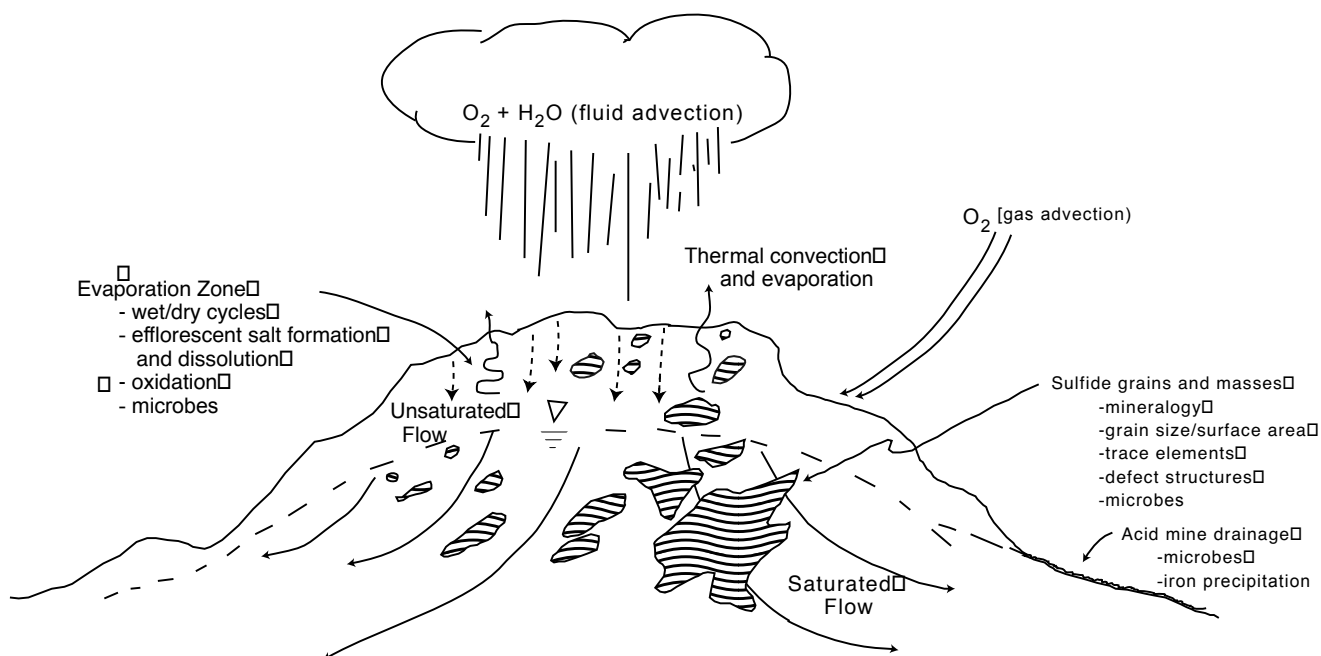


FIGURE 6.7—Schematic diagram depicting a hypothetical tailings or waste pile or mineralized site, showing the various materials and processes involving reaction and flow.

research has been accomplished on this subject, surprises and new challenges continue to appear. Inadequate recognition of the importance of the multi-disciplinary nature of the subject can result in inappropriate or even dangerous remediation measures. In this arena, as with many other environmental problems, the quick fixes are rare; complexity and heterogeneity of this environment along with high-cost, high-risk options are the rule. A cautious, phased, and iterative approach to both site characterization and remediation would seem most warranted.

ACKNOWLEDGMENTS—We are deeply indebted to Geoff Plumlee and the Society of Economic Geologists for inviting us to participate in this short course and for showing enormous patience with our unanticipated delays. The reviewers, David Blowes, Briant Kimball, Geoff Plumlee, Teresa Rogers, and Katie Walton-Day were most helpful in catching errors and mistakes and in asking for important points of clarification. Their comments led to significant improvements in the manuscript. Finally, we would like to acknowledge all the students and colleagues with whom we have shared both sweat and joy in attempting to demystify some of the secrets of mine water geochemistry.

REFERENCES

- Adams, F. and Rawajfih, Z., 1977, Basaluminite and alunite—A possible cause of sulfate retention by acid soils: *Soil Science Society of America Journal*, v. 41, pp. 686–692.
- Agricola, G., 1546, *De Natura Fossilium* (Textbook of Mineralogy), translated by Bandy, M.C., and Bandy, J.A., 1955: Geological Society of America Spec. Pub. No. 63, 240 pp.
- Agricola, G., 1556, *De Re Metallica*, translated by Hoover, H.C., and Hoover, L.H., 1950: Dover Publications, New York, 638 pp.
- Alpers, C.N., and Brimhall, G.H., 1989, Paleohydrologic evolution and geochemical dynamics of cumulative supergene metal enrichment at La Escondida, Atacama Desert, northern Chile: *Economic Geology*, v. 84, pp. 229–255.
- Alpers, C.N., and Nordstrom, D.K., 1991, Geochemical evolution of extremely acid mine waters at Iron Mountain, California—Are there any lower limits to pH?: *in Proceedings, 2nd Internl Conference on the Abatement of Acidic Drainage*, Montreal, Quebec, Canada: CANMET, Ottawa, Sept. 16–18, 1991, v. 2, pp. 324–342.
- Alpers, C.N., and Nordstrom, D.K., 1999, Geochemical modeling of water-rock interactions in mining environments; *in Plumlee, G.S., and Logsdon, M.J. (eds.), The Environmental Geochemistry of Mineral Deposits, Part A. Processes, Techniques, and Health Issues: Society of Economic Geologists, Reviews in Economic Geology*, v. 6A, pp. 289–323.
- Alpers, C.N., Nordstrom, D.K., and Ball, J.W., 1989, Solubility of jarosite solid solutions precipitated from acid mine waters, Iron Mountain, California, U.S.A.: *Sciences Géologiques Bulletin*, v. 42, pp. 281–298.
- Alpers, C.N., Meinz, C., Nordstrom, D.K., Erd, R.C., and Thompson, J.M., 1991, Storage of metals and acidity by iron-sulfate minerals associated with extremely acidic mine waters from Iron Mountain, California [abs.]: *Geological Society of America Annual Meeting, Abstracts with Programs*, v. 23, no. 5, p. A383.
- Alpers, C.N., Rye, R.O., Nordstrom, D.K., White, L.D., and King, B.-S., 1992, Chemical, crystallographic, and isotopic properties of alunite and jarosite from acid hypersaline Australian lakes: *Chemical Geology*, v. 96, pp. 203–226.
- Alpers, C.N., Nordstrom, D.K., and Thompson, J.M., 1994a, Seasonal variations of Zn/Cu ratios in acid mine waters from Iron Mountain, California; *in Alpers, C.N., and Blowes, D.W. (eds.), Environmental Geochemistry of Sulfide Oxidation: American Chemistry Society Symposium Series 550*, Washington, D.C., pp. 324–344.
- Alpers, C.N., Blowes, D.W., Nordstrom, D.K., and Jambor, J.L., 1994b, Secondary minerals and acid mine-water chemistry; *in Jambor, J.L., and Blowes, D.W. (eds.), The Environmental Geochemistry of Sulfide Mine-Wastes: Mineralogical Association of Canada, Nepean, Ontario, Short Course Handbook*, v. 22, pp. 247–270.

- Anderson, J.A., 1982, Characteristics of leached capping and techniques of appraisal; *in* Titley, S.R. (ed.), *Advances in Geology of the Porphyry Copper Deposits, Southwestern North America*, Tucson: University of Arizona Press, Tucson, pp. 275–295.
- Anthony, J.W., and MacLean, W.J., 1976, Jurbanite, a new post-mine aluminum sulfate mineral from San Manuel, Arizona: *American Mineralogist*, v. 61, pp. 1–4.
- Appalachian Regional Commission, 1969, *Acid mine drainage in Appalachia: Report to the President*, 126 pp.
- Ash, S.H., Felegy, E.W., Kennedy, D.O., and Miller, P.S., 1951, *Acid mine drainage problems—Anthracite region of Pennsylvania*: U.S. Bureau of Mines Bulletin 508, 72 pp.
- Ball, J.W., and Nordstrom, D.K., 1989, Final revised analyses of major and trace elements from acid mine waters in the Leviathan mine drainage basin, California and Nevada—October 1981 to October 1982: U. S. Geological Survey Water-Resources Investigations Report 89–4138, 46 pp.
- Ball, J.W., and Nordstrom, D.K., 1991, User's manual for WATEQ4F, with revised thermodynamic data base and test cases for calculating speciation of major, trace, and redox elements in natural waters: U.S. Geological Survey Open-File Report 91–183, 189 pp., plus diskette.
- Ball, J.W., and Nordstrom, D.K., 1994, A comparison of simultaneous plasma, atomic absorption, and iron colorimetric determinations of major and trace constituents in acid mine waters: U.S. Geological Survey Water-Resources Investigations Report 93–4122, 151 pp.
- Barton, P., 1978, The acid mine drainage; *in* Nriagu, J.O. (ed.), *Sulfur in the Environment, Part II. Ecological Impacts*: John Wiley and Sons, New York, pp. 313–358.
- Basolo, F., and Pearson, R.G., 1967, Mechanisms of inorganic reactions—A study of metal complexes in solution, 2nd ed.: John Wiley and Sons, New York, 701 pp.
- Beck, J.V., 1977, Chalcocite oxidation by concentrated cell suspensions of *Thiobacillus ferrooxidans*; *in* Schwartz, W. (ed.), *Conference Bacterial Leaching 1977*: GBF, Verlag Chemie, Weinheim, pp. 119–128.
- Bennett, J.C., and Tributsch, H., 1978, Bacteria leaching patterns on pyrite crystal surface: *Journal of Bacteriology*, v. 134, pp. 310–326.
- Bergholm, A., 1955, Oxidation of pyrite: *Jernkontorets Annalen*, v. 139, pp. 531–549.
- Berner, R.A., 1969, Goethite stability and the origin of red beds: *Geochimica et Cosmochimica Acta*, v. 33, pp. 267–273.
- Berner, R.A., 1971, *Principles of chemical sedimentology*: McGraw-Hill Book Company, New York, 240 pp.
- Berner, R.A., 1981, A new geochemical classification of sedimentary environments: *Journal of Sedimentary Petrology*, v. 51, pp. 359–365.
- Bertsch, P.M. and Parker, D.R., 1996, Aqueous polynuclear aluminum species; *in* Sposito, G., (ed.), *The Environmental Chemistry of Aluminum*, 2nd ed.: CRC Press/Lewis Publishers, Boca Raton, Fla., pp. 117–168.
- Biernacki, A., 1978, Fish kills caused by pollution—Fifteen year summary 1961–1975: U.S. Environmental Protection Agency Report EPA-440/4–78–011, 78 pp.
- Bigham, J.M., 1994, Mineralogy of ochre deposits formed by sulfide oxidation; *in* Jambor J.L., and Blowes, D.W., (eds.), *The Environmental Geochemistry of Sulfide Mine-Wastes: Mineralogical Association of Canada, Nepean, Ontario, Short Course Handbook*, v. 22, pp. 103–132.
- Bigham, J.M., Schwertmann, U., Carlson, L., and Murad, E., 1990, A poorly crystallized oxyhydroxysulfate of iron formed by bacterial oxidation of Fe(II) in acid mine waters: *Geochimica et Cosmochimica Acta*, v. 54, pp. 2743–2758.
- Blanchard, R., 1968, Interpretation of leached outcrops: *Nevada Bureau of Mines Bulletin*, v. 66, 196 pp.
- Blowes, D.W., 1990, The geochemistry, hydrogeology, and mineralogy of decommissioned sulfide tailings—A comparative study: Unpub. Ph.D. thesis, Univ. of Waterloo, Ontario, Canada, 635 pp.
- Blowes, D.W., and Jambor, J.L., 1990, The pore-water geochemistry and the mineralogy of the vadose zone of sulfide tailings, Waite Amulet, Quebec, Canada: *Applied Geochemistry*, v. 5, pp. 327–346.
- Blowes, D.W., and Ptacek, C.J., 1994, Acid-neutralization mechanisms in inactive mine tailings; *in* Jambor, J.L., and Blowes, D.W., (eds.), *The Environmental Geochemistry of Sulfide Mine-Wastes: Mineralogical Association of Canada, Nepean, Ontario, Short Course Handbook*, v. 22, pp. 271–292.
- Blowes, D.W., Reardon, E.J., Jambor, J.L., and Cherry, J.A., 1991, The formation and potential importance of cemented layers in inactive sulfide mine tailings: *Geochimica et Cosmochimica Acta*, v. 55, pp. 965–978.
- Blowes, D.W., Al, T., Lortie, L., Gould, W.D., and Jambor, J.L., 1995, Microbiological, chemical, and mineralogical characterization of the Kidd Creek mine tailings impoundment, Timmins area, Ontario: *Geomicrobiology Journal*, v. 13, pp. 13–31.
- Braeuning, E., 1977, Mine water development in the lead and zinc deposits of Bawdwin, Burma; *in* 2nd Internl Symposium on Water-Rock Interaction: Strasbourg, France, pp. 1237–1245.
- Braley, S.A., 1954, Summary of report of Commonwealth of Pennsylvania, No. 326–B: Department of Health, Industrial Fellowship, Mellon Institute, 279 pp.
- Bricker, O.P., 1982, Redox potential—Its measurement and importance in water systems; *in* Minear, R.A., and Keith, L.H. (eds.), *Water Analysis, v. 1, Inorganic Species, Part 1*: Academic Press, New York, pp. 55–83.
- Brierley, C.L., and Murr, L.E., 1973, Leaching—Use of a thermophilic and chemoautotrophic microbe: *Science*, v. 179, pp. 488–489.
- Brierley, J.A., and Le Roux, N.W., 1977, A facultative thermophilic *Thiobacillus*-like bacterium—Oxidation of iron and pyrite; *in* Schwartz, W. (ed.), *Conference Bacterial Leaching 1977*: GBF, Verlag Chemie, Weinheim, pp. 55–66.
- Brophy, G.P., and Sheridan, M.E., 1965, Sulfate studies IV. The jarosite-natrojarosite-hydronium jarosite solid solution series: *American Mineralogist*, v. 50, pp. 1595–1607.
- Brophy, G.P., Scott, E.S., and Snellgrove, R.A., 1962, Sulfate studies II. Solid solution between alunite and jarosite: *American Mineralogist*, v. 47, pp. 112–126.
- Brown, A.D., and Jurinak, J.J., 1989, Mechanisms of pyrite oxidation in aqueous mixtures: *Journal of Environmental Quality*, v. 18, pp. 545–550.
- Bryner, L.C., Beck, J.F., Davis, D.B., and Wilson, D.G., 1954, Microorganisms in leaching sulfide minerals: *Industrial and Engineering Chemistry*, v. 46, pp. 2587–2592.
- Burke, S.P., and Downs, W.R., 1938, Oxidation of pyrite sulfur in coal mines: *American Institute of Mining, Metallurgical, and Petroleum Engineering*, v. 130, pp. 425–444.
- Buurman, P., 1975, *In vitro* weathering products of pyrite: *Geologie en Mijnbouw*, v. 54, pp. 101–105.
- Burkstaller, J.E., McCarty, P., and Parks, G.A., 1975, Oxidation of cinnabar by Fe(III) in acid mine waters: *Environmental Science and Technology*, v. 9, p. 676–678.
- Carlson, L., and Schwertmann, U., 1981, Natural ferrihydrites in surface deposits from Finland and their association with silica: *Geochimica et Cosmochimica Acta*, v. 4, pp. 421–429.
- Carlson-Foszcz, V., 1991, Rare earth element mobility in acid mine drainage, Ophir region, San Juan Mountains, Colorado: Unpub. M.S. thesis, Dartmouth College, Dartmouth, N.H., 71 pp.
- Carpentor, L.V., and Herndon, L.K., 1933, Acid mine drainage from bituminous coal mines: *West Virginia University Engineering Exploration Station Research Bulletin No. 19*, 38 pp.
- Carrucio, F.T., 1970, The quantification of reactive pyrite by grain size distribution—3rd Symposium on Coal Mine Drainage Research: National Coal Association/Bituminous Coal Research, pp. 123–131.
- Carrucio, F.T., Geidel, G., and Sewell, J. M., 1976, The character of drainage as a function of the occurrence of framboidal pyrite and ground water quality in eastern Kentucky—6th Symposium on Coal Mine Drainage Research: National Coal Association/Bituminous Coal Research, pp. 1–16.
- Carson, C.D., Fanning, D.S., and Dixon, J.B., 1982, Alfisols and ultisols with acid sulfate weathering features in Texas; *in* Kittrick, J.A., Fanning, D.S., and Hossner, L.R. (eds.), *Acid Sulfate Weathering: Soil Science Society of America Spec. Pub. No. 10*, Madison, Wis., pp. 127–146.

- Cathles, L.M., 1994, Attempts to model the industrial-scale leaching of copper-bearing mine waste; *in* Alpers, C.N., and Blowes, D.W. (eds.), *Environmental Geochemistry of Sulfide Oxidation*: American Chemical Society Symposium Series 550, Washington, D.C., pp. 123–131.
- Cathles, L.M., and Apps, J.A., 1975, A model of the dump leaching process that incorporates oxygen balance, heat balance, and air convection: *Metallurgical Transactions B*, v. 6B, p. 617–624.
- Chen, K.Y., and Morris, J.C., 1971, Oxidation of aqueous sulfide by O_2 . 1. General characteristics and catalytic influences: *Proceedings of the 5th Internatl Water Pollution Research Conference*, III–32, pp. 1–17.
- Chen, K.Y., and Morris, J.C., 1972, Kinetics of oxidation of aqueous sulfide by O_2 : *Environmental Science and Technology*, v. 6, pp. 529–537.
- Chukhrov, F., Zvijagin, B.B., Gorshkov, A.I., Erilova, L.P., and Balashova, V.V., 1973, Ferrihydrite: *Izvetzia Akadamiy Nauklady SSSR Series Geology*, v. 4, pp. 23–33.
- Clark, C.S., 1966, Oxidation of coal mine pyrite: *Journal of Sanitary Engineering Division, Proceedings of American Society of Civil Engineers*, v. 92, pp. 127–145.
- Clarke, F.W., 1916, *The data of geochemistry*, 3rd ed.: U.S. Geological Survey Bulletin 616, 821 pp.
- Colmer, A.R., and Hinkle, M.E., 1947, The role of microorganisms in acid mine drainage: *Science*, v. 106, pp. 253–256.
- Colmer, A.R., Temple, K.L., and Hinkle, M.E., 1950, An iron-oxidizing bacterium from the acid drainage of some bituminous coal mines: *Journal of Bacteriology*, v. 59, pp. 317–328.
- Cravotta, C.A. III, 1994, Secondary iron-sulfate minerals as sources of sulfate and acidity; *in* Alpers, C.N., and Blowes, D.W. (eds.), *Environmental Geochemistry of Sulfide Oxidation*: American Chemical Society Symposium Series 550, Washington, D.C., pp. 345–364.
- Dagenhart, T.V., Jr., 1980, The acid mine drainage of Contrary Creek, Louisa County, Virginia: Factors causing variations in stream water chemistry: Unpub. M.S. thesis, Univ. of Virginia, 215 pp.
- Devasia, P., Natarajan, K.A., Sathayanarayana, D.N., and Rao, G.R., 1993, Surface chemistry of *Thiobacillus ferrooxidans* relevant to adhesion on mineral surfaces: *Applied and Environmental Microbiology*, v. 59, pp. 4051–4055.
- DiToro, D.M., Mahony, J.D., Hanson, D.J., Scott, K.J., Hicks, M.B., Mayr, S.M., and Redmond, M.S., 1991, Toxicity of cadmium in sediments: The role of acid volatile sulfide: *Environmental and Toxicological Chemistry*, v. 9, pp. 1487–1502.
- Dugan, P.R., 1972, Biochemistry of acid mine drainage; *in* *Biochemical Ecology of Water Pollution*: Plenum Press, New York, pp. 123–137.
- Dugan, P.R., MacMillan, C.B., and Pfister, R.M., 1970, Aerobic heterotrophic bacteria indigenous to pH 2.8 acid mine water. I. Microscopic examination of acid streamers, II. Predominant slime-producing bacteria in acid streamers: *Journal of Bacteriology*, v. 101, p. 973–988.
- Dutrizac, J.E., 1983, Factors affecting alkali jarosite precipitation: *Metallurgical Transactions B*, v. 14B, p. 531–539.
- Dutrizac, J.E., and Kaiman, S., 1976, Synthesis and properties of jarosite-type compounds: *Canadian Mineralogist*, v. 14, pp. 151–158.
- Dzombak, D.A., and Morel, F.F., 1990, Surface complexation modeling—Hydrous ferric oxide: John Wiley and Sons, New York, 545 pp.
- Ehrlich, H.L., 1963a, Bacterial action on orpiment: *Economic Geology*, v. 58, pp. 991–994.
- Ehrlich, H.L., 1963b, Microorganisms in acid drainage from a copper mine: *Journal of Bacteriology*, v. 86, pp. 350–352.
- Ehrlich, H.L., 1964, Bacterial oxidation of arsenopyrite and enargite: *Economic Geology*, v. 59, p. 1306–1308.
- Elberling, B., Nicholson, R.V., and David, D., 1993, Field evaluation of sulfide oxidation rates: *Nordic Hydrology*, v. 24, p. 323–338.
- Evangelou, V.P. (Bill), 1995, Pyrite oxidation and its control: CRC Press, Boca Raton, Fla., 285 pp.
- Eychaner, J.H., 1991, The Globe, Arizona research site—Contaminants related to copper mining in a hydrologically integrated environment; *in* Mallard, G.E., and Aronson, D.A., (eds.), *Proceedings, U.S. Geological Survey Toxic Substances Hydrology Program*: U.S. Geological Survey Water-Resources Investigations Report 91–4034, pp. 439–447.
- Federal Water Pollution Control Administration, 1968, Pollution caused fish kills—1967: 8th Annual Report, Washington, D.C., 16 pp.
- Fox, L.E., 1988, The solubility of colloidal ferric hydroxide and its relevance to iron concentrations in river water: *Geochimica et Cosmochimica Acta*, v. 52, pp. 771–777.
- Garrels, R.M., 1954, Mineral species as functions of pH and oxidation potentials with special reference to the zone of oxidation and secondary enrichment of sulfide ore deposits: *Geochimica et Cosmochimica Acta*, v. 5, pp. 153–168.
- Garrels, R.M., and Christ, C.M., 1965, *Solutions, minerals, and equilibria*: Freeman and Cooper, New York, 450 pp.
- Garrels, R.M., and Thompson, M.E., 1960, Oxidation of pyrite by iron sulfate solutions: *American Journal of Science*, v. 258A, pp. 57–67.
- Goldberg, S., Davis, J.A., and Hem, J.D., 1995, The surface chemistry of aluminum oxides and hydroxides; *in* Sposito, G., (ed.), *The Environmental Chemistry of Aluminum*, 2nd ed.: CRC Press/Lewis Publishers, Boca Raton, Fla., pp. 271–332.
- Goldhaber, M.B., 1983, Experimental study of metastable sulfur oxyanion formation during pyrite oxidation at pH 6–9 and 30°C: *American Journal of Science*, v. 283, pp. 193–217.
- Goleva, G.A., 1977, Hydrogeochemistry of ore elements: Nedra, Moscow, 215 pp.
- Goleva, G.A., Polyakov, V.A., and Nechayeva, T.P., 1970, Distribution and migration of lead in ground waters: *Geochemistry International*, v. 7, pp. 256–268.
- Gould, W.D., Béchard, G., and Lortie, L., 1994, The nature and role of microorganisms in the tailings environment; *in* Jambor, J.L., and Blowes, D.W. (eds.), *The Environmental Geochemistry of Sulfide Mine-Wastes*: Mineralogical Association of Canada, Short Course Handbook, v. 22, pp. 185–200.
- Granger, H.C., and Warren, C.G., 1969, Unstable sulfur compounds and the origin of roll-type uranium deposits: *Economic Geology*, v. 64, pp. 160–171.
- Harries, J.R., and Ritchie, A.I.M., 1981, The use of temperature profiles to estimate the pyritic oxidation rate in a waste rock dump from an open-cut mine: *Water, Air, and Soil Pollution*, v. 15, pp. 405–423.
- Hem, J.D., 1961, Stability field diagrams as aids in iron chemistry studies: *Journal American Water Works Association*, Feb., 1961, pp. 211–232.
- Hem, J.D., 1978, Redox processes at surfaces of manganese oxide and their effects on aqueous metal ions: *Chemical Geology*, v. 21, pp. 199–218.
- Hem, J.D., 1980, Redox coprecipitation mechanisms of manganese oxide; *in* Kavanaugh, M.C., and Leckie, J.O. (eds.), *Particulates in Water: Advances in Chemistry Series 189*, American Chemical Society, Washington, D.C., pp. 45–72.
- Hem, J.D., 1985, Study and interpretation of the chemical characteristics of natural water, 3rd ed.: U.S. Geological Survey Water-Supply Paper 2254, 264 pp.
- Hem, J.D., and Lind, C., 1993, Chemical processes in manganese oxide and carbonate precipitation in Pinal Creek, Arizona; *in* Morganwalp, D.W., and Aronson, D.A., (eds.), *U.S. Geological Survey Toxic Substances Hydrology Program with Abstracts*: U.S. Geological Survey Open-File Report 93–454, pp. 163.
- Hem, J.D., and Roberson, C.E., 1990, Aluminum hydrolysis reaction and products in mildly acidic aqueous systems; *in* Melchior, D.C., and Bassett, R.L. (eds.), *Chemical Modeling of Aqueous Systems II*: American Chemical Society Symposium Series 416, Washington, D.C., pp. 430–446.
- Hem, J.D., Roberson, C.E., and Lind, C.E., 1985, Thermodynamic stability of $CoOOH$ and its coprecipitation with manganese: *Geochimica et Cosmochimica Acta*, v. 49, pp. 801–810.
- Hem, J.D., Roberson, C.E., and Lind, C.E., 1987, Synthesis and stability of heterolite, $ZnMn_2O_4$, at 25°C: *Geochimica et Cosmochimica Acta*, v. 51, pp. 1539–1547.
- Hemingway, B.S., and Sposito, G., 1996, Inorganic aluminum-bearing solid phases; *in* Sposito, G. (ed.), *The Environmental Chemistry of*

- Aluminum, 2nd ed.: CRC Press/Lewis Publishers, Boca Raton, Fla., pp. 81–116.
- Hostetler, J.D., 1984, Electrode electrons, aqueous electrons, and redox potentials in natural waters: *American Journal of Science*, v. 294, pp. 734–759.
- Joseph, J.M., 1953, Microbiological study of acid mine waters—Preliminary report: *Ohio Journal of Science*, v. 53, pp. 123–127.
- Kämpf, N., and Schwertmann, U., 1982, Goethite and hematite in a clino-sequence in southern Brazil and their application in classification of kaolinitic soils: *Geoderma*, v. 29, pp. 27–39.
- Kelly, D.P., Norris, P.R., and Brierly, C.L., 1979, Microbiological methods for extractions and recovery of metals: *Symposium on Microbial Technology*, Society of General Microbiology, v. 29, pp. 263–308.
- Khalid, A.M., and Ralph, B.J., 1977, The leaching behavior of various zinc sulphide minerals with three *Thiobacillus* species; in Schwartz, W. (ed.), *Conference Bacterial Leaching 1977*: GBF, Verlag Chemie, Weinheim, p. 165–173.
- Kimball, B.A., Broshears, R.A., McKnight, D.M., and Bencala, K.E., 1994, Effects of instream pH modification on transport of sulfide-oxidation products; in Alpers, C.N., and Blowes, D.W. (eds.), *Environmental Geochemistry of Sulfide Oxidation*: American Chemical Society Symposium Series 550, Washington, D.C., pp. 224–243.
- Kleinmann, R.L.P., 1989, Acid mine drainage in the United States—Controlling the impact on streams and rivers: 4th World Congress on the Conservation of the Built and Natural Environments, Univ. of Toronto, pp. 1–10.
- Konishi, Y., Asai, S., and Sakai, H.K., 1990, Bacterial dissolution of pyrite by *Thiobacillus ferrooxidans*: *Bioprocess Engineering*, v. 5, pp. 5–17.
- Krauskopf, K.B., 1957, Separation of iron and manganese in sedimentary processes: *Geochimica et Cosmochimica Acta*, v. 12, pp. 61–84.
- Krauskopf, K.B., 1967, *Introduction to geochemistry*, 1st ed.: McGraw-Hill Book Company, New York, 617 pp.
- Krauskopf, K.B. and Bird, D.K., 1995, *Introduction to geochemistry*, 3rd ed.: McGraw-Hill Book Company, New York, 647 pp.
- Krumbein, W.C., and Garrels, R.M., 1952, Origin and classification of chemical sediments in terms of pH and oxidation-reduction potentials: *Journal of Geology*, v. 60, pp. 1–33.
- Kubisz, J., 1960, Hydronium jarosite— $(\text{H}_3\text{O})\text{Fe}_3(\text{SO}_4)_2(\text{OH})_6$: *Bulletin Academia Polonia, Science, Series Science Geology and Geography*, v. 8, no. 2, pp. 95–99.
- Kubisz, J., 1961, Natural hydronium jarosites: *Bulletin Academia Polonia, Science, Series Science Geology and Geography*, v. 9, no. 4, pp. 195–200.
- Kubisz, J., 1964, Minerals of the alunite-jarosite group: *Polonia Academia Nauk, Prace Geologia*, v. 22, pp. 1–93 (in Polish).
- Kubisz, J., 1970, Studies on synthetic alkali-hydronium jarosites. I. Synthesis of jarosite and natrojarosite: *Mineralogia Polonia*, v. 1, pp. 45–57.
- Kushner, D.J. (ed.), 1978, *Microbial life in extreme environments*: Academic Press, New York, 465 pp.
- Kwong, Y.T.J., 1995, Influence of galvanic sulfide oxidation on mine water chemistry; in Hynes, T.P., and Blanchette, M.C. (eds.), *Proceedings of Sudbury '95—Mining and the Environment*, v. 2, May 28–June 1, Sudbury, Ontario: CANMET, Ottawa, pp. 477–484.
- Lacey, D.T., and Lawson, F., 1977, Kinetics of the liquid-phase oxidation of acid ferrous sulfate by the bacterium *Thiobacillus ferrooxidans*: *Biotechnology and Bioengineering*, v. 12, pp. 29–50.
- Lackey, J.B., 1938, The flora and fauna of surface waters polluted by acid mine drainage: *Public Health Report* 53, pp. 1499–1507.
- Landesman, J., Duncan, D.W., and Walden, C.C., 1966, Oxidation of inorganic sulfur compounds by washed cell suspensions of *Thiobacillus ferrooxidans*: *Canadian Journal of Microbiology*, v. 12, pp. 957–964.
- Langmuir, D., 1969, The Gibbs free energies of substances in the system $\text{Fe}-\text{O}_2-\text{H}_2\text{O}-\text{CO}_2$: U.S. Geological Survey Professional Paper 650-B, pp. 180–184.
- Langmuir, D., 1971, Particle size effect on the reaction goethite = hematite + water: *American Journal of Science*, v. 271, pp. 147–156.
- Langmuir, D., 1972, Correction—Particle size effect on the reaction goethite = hematite + water: *American Journal of Science*, v. 272, pp. 972.
- Le Roux, N.W., and Marshall, V.M., 1977, Effect of light on *Thiobacilli*; in Schwartz, W., (ed.), *Conference Bacterial Leaching 1977*: GBF, Verlag Chemie, Weinheim, pp. 21–35.
- Lichtner, P.C., 1994, Time-space continuum formulation of supergene enrichment and weathering of sulfide-bearing ore deposits; in Alpers, C.N., and Blowes, D.W. (eds.), *Environmental Geochemistry of Sulfide Oxidation*: American Chemical Society Symposium Series 550, Washington, D.C., pp. 153–170.
- Lind, C., 1991, Manganese minerals and associated fine particulates in the Pinal Creek streambed; in Mallard, G.E., and Aronson, D.A. (eds.), *Proceedings, U.S. Geological Survey Toxic Substances Hydrology Program*: U.S. Geological Survey Water-Resources Investigations Report 91–4034, pp. 486–491.
- Lindberg, R.D., and Runnells, D.D., 1984, Ground water redox reactions—An analysis of equilibrium state applied to Eh measurements and geochemical modeling: *Science*, v. 225, pp. 925–927.
- Lindgren, W., 1928, *Mineral deposits*, 3rd ed.: McGraw-Hill, New York, 1049 pp.
- Locke, A., 1926, *Leached outcrops as guides to copper ores*: Williams and Wilkins Co., Baltimore, Md, 166 pp.
- Loghry, J.D., 1972, Characteristics of favorable cappings from several southwestern porphyry copper deposits: Unpub. M.S. thesis, Univ. of Arizona, Tucson, 112 pp.
- Lowson, R.T., 1982, Aqueous oxidation of pyrite by molecular oxygen: *Chemical Reviews*, v. 82, pp. 461–497.
- Lundgren, D.G., Anderson, K.J., Remson, C.C., and Mahoney, R.P., 1964, Culture, structure and physiology of the chemoautotroph *Ferrobacillus ferrooxidans*: *Developments in Industrial Microbiology*, v. 6, pp. 250–259.
- Luther, G.W., II, 1987, Pyrite oxidation and reduction—Molecular orbital theory considerations: *Geochimica et Cosmochimica Acta*, v. 51, pp. 3193–3199.
- Luther, G.W., II, 1990, The frontier-molecular-orbital theory approach in geotechnical processes; in Stumm, W., (ed.), *Aquatic Chemical Kinetics*: John Wiley and Sons, Inc., New York, pp. 173–198.
- Lyon, J.S., Hilliard, T.J., and Bethell, T.N., 1993, *Burden of guilt*: Mineral Policy Center, Washington, D.C., 68 pp.
- Markosyan, G.E., 1972, A new iron-oxidizing bacterium *Leptospirillum ferrooxidans*: gen. et sp. nov. *Biol. Zh. Arm.* v. 25, p. 26 (in Russian).
- Martin, H.W., and Mills, W.R., Jr, 1976, Water pollution caused by inactive ore and mineral mines: USEPA Contract Report 68–03–2212, 184 pp.
- Mathews, C.T., and Robins, R.G., 1972, The oxidation of ferrous disulfide by ferric sulfate: *Australian Chemical Engineering*, v. 47, pp. 21–25.
- Mathews, C.T., and Robins, R.G., 1974, Aqueous oxidation of iron disulfide by molecular oxygen: *Australian Chemical Engineering*, v. 15, pp. 19–24.
- May, H.M., and Nordstrom, D.K., 1991, Assessing the solubilities and reactions kinetics of aluminous minerals in soils; in Ulrich, B., and Sumner, M.E. (eds.), *Soil Acidity*: Springer-Verlag, pp. 125–148.
- McKay, D.R., and Halpern, J., 1958, A kinetic study of the oxidation of pyrite in aqueous suspension: *Transactions of the Metallurgical Society AIME*, v. 121, pp. 301–309.
- McKibben, M.A., and Barnes, H.L., 1986, Oxidation of pyrite in low temperature acidic solutions—Rate laws and surface textures: *Geochimica et Cosmochimica Acta*, v. 50, pp. 1509–1520.
- McKnight, D., and Bencala, K.E., 1988, Diel variations in iron chemistry in an acidic stream in the Colorado Rocky Mountains, U.S.A.: *Arctic and Alpine Research*, v. 20, pp. 492–500.
- McKnight, D.M., and Bencala, K.E., 1989, Reactive iron transport in an acidic mountain stream in Summit County, Colorado—A hydrologic perspective: *Geochimica et Cosmochimica Acta*, v. 53, pp. 2225–2234.
- McKnight, D.M., Kimball, B.A., and Bencala, K.E., 1988, Iron photoreduction and oxidation in an acidic mountain stream: *Science*, v. 240, pp. 637–640.

- Mills, A.L., 1999, The role of bacteria in environmental geochemistry; *in* Plumlee, G.S., and Logsdon, M.J. (eds.), The Environmental Geochemistry of Mineral Deposits, Part A. Processes, Techniques, and Health Issues: Society of Economic Geologists, Reviews in Economic Geology, v. 6A, pp. 125–132.
- Moore, J.N., and Luoma, S.N., 1990, Hazardous wastes from large-scale metal extraction: *Environmental Science and Technology*, v. 24, p. 1278–1285.
- Moses, C.O., and Herman, J.S., 1991, Pyrite oxidation at circumneutral pH: *Geochimica et Cosmochimica Acta*, v. 55, pp. 471–482.
- Moses, C.O., Nordstrom, D.K., and Mills, A.L., 1984, Sampling and analyzing mixtures of sulphate, sulphite, thiosulfate, and polythionate: *Talanta*, v. 31, pp. 331–339.
- Moses, C.O., Nordstrom, D.K., Herman, J.S. and Mills, A.L., 1987, Aqueous pyrite oxidation by dissolved oxygen and by ferric iron: *Geochimica et Cosmochimica Acta*, v. 51, pp. 1561–1571.
- Murad, E., Schwertmann, U., Bigham, J.M., and Carlson, L., 1994, Mineralogical characteristics of poorly crystallized precipitates formed by oxidation of Fe²⁺ in acid mine sulfate waters; *in* Alpers, C.N., and Blowes, D.W. (eds.), Environmental Geochemistry of Sulfide Oxidation: American Chemical Society Symposium Series 550, Washington, D.C., pp. 190–200.
- Nathansohn, A., 1902, Über eine neue Gruppe von Schwefelbakterien und ihren Stoffwechsel: *Mitt. Zool. Staatsmus. Neapel*, v. 15, pp. 655–680.
- Nicholson, R.V., 1994, Iron-sulfide oxidation mechanisms—Laboratory studies; *in* Jambor, J.L., and Blowes, D.W. (eds.), The Environmental Geochemistry of Sulfide Mine-Wastes: Mineralogical Association of Canada, Short Course Handbook, v. 22, pp. 163–183.
- Nicholson, R.V., and Scharer, J.M., 1994, Laboratory studies of pyrrhotite oxidation kinetics; *in* Alpers, C.N., and Blowes, D.W. (eds.), Environmental Geochemistry of Sulfide Oxidation: American Chemical Society Symposium Series 550, Washington, D.C., pp. 14–30.
- Nicholson, R.V., Gillham, R.W., and Reardon, E.J., 1988, Pyrite oxidation in carbonate-buffered solutions, 1. Experimental kinetics: *Geochimica et Cosmochimica Acta*, v. 52, pp. 1077–1085.
- Nor, Y.M., and Tabatai, M.A., 1976, Oxidation of elemental sulfur in soils: *Soil Science Society of America Journal*, v. 41, pp. 736–741.
- Nordstrom, D.K., 1982a, Aqueous pyrite oxidation and the consequent formation of secondary iron minerals; *in* Kittrick, J.A., Fanning, D.S., and Hossner, L.R., (eds.), Acid Sulfate Weathering: Soil Science Society of America Spec. Pub. No. 10, pp. 37–56.
- Nordstrom, D.K., 1982b, The effects of sulfate on aluminum concentrations in natural waters—Some stability relations in the system Al₂O₃–SO₃–H₂O at 298 K: *Geochimica et Cosmochimica Acta*, v. 46, pp. 681–692.
- Nordstrom, D.K., 1985, The rate of ferrous iron oxidation in a stream receiving acid mine effluent; *in* Selected Papers in the Hydrological Sciences: U.S. Geological Survey Water-Supply Paper 2270, pp. 113–119.
- Nordstrom, D.K., 1991, Chemical modeling of acid mine waters in the western United States; *in* Mallard, G.E., and Aronson, D.A. (eds.), Proceedings, U.S. Geological Survey Toxic Substances Hydrology Program: U.S. Geological Survey Water-Resources Investigations Report 91–4034, pp. 534–538.
- Nordstrom, D.K., and Alpers, C.N., 1999, Negative pH, efflorescent mineralogy, and consequences for environmental restoration at the Iron Mountain Superfund site, California: Proceedings of the National Academy of Sciences, v. 96, pp. 3455–3462.
- Nordstrom, D.K., and Ball, J.W., 1985, Toxic element composition of acid mine waters from sulfide ore deposits: 2nd Internatl Mine Water Symposium, Granada, Spain, pp. 749–758.
- Nordstrom, D.K., and Ball, J.W., 1986, The geochemical behavior of aluminum in acidified surface waters: *Science*, v. 232, pp. 54–56.
- Nordstrom, D.K., and May, H.M., 1996, Aqueous equilibrium data for mononuclear aluminum species; *in* Sposito, G. (ed.), The Environmental Chemistry of Aluminum, 2nd ed.: CRC Press/Lewis Publishers, Boca Raton, Fla., pp. 39–80.
- Nordstrom, D.K., and Munoz, J.L., 1994, Geochemical thermodynamics, 2nd ed.: Blackwell Science, 493 pp.
- Nordstrom, D.K., and Southam, G., 1997, Geomicrobiology of sulfide mineral oxidation; *in* Banfield, J.F., and Nealon, K.H. (eds.), Geomicrobiology—Interactions Between Microbes and Minerals: Reviews in Mineralogy, Mineralogical Society of America, Washington, D.C., v. 35, pp. 361–390.
- Nordstrom, D.K., Jenne, E.A., and Averett, R.C., 1977, Heavy metal discharges into Shasta Lake and Keswick Reservoir on the Upper Sacramento River, California—A reconnaissance during low flow: U.S. Geological Survey Open-File Report 76–49, pp. 25.
- Nordstrom, D.K., Jenne, E.A., and Ball, J.W., 1979, Redox equilibria of iron in acid mine waters; *in* Jenne, E.A., (ed.), Chemical Modeling in Aqueous Systems: American Chemical Society Symposium Series 93, Washington, D.C., pp. 51–80.
- Nordstrom, D.K., Ball, J.W., Roberson, C.E., and Hanshaw, B.B., 1984, The effect of sulfate on aluminum concentrations in natural waters, II. Field occurrences and identification of aluminum hydroxysulfate precipitates [abs.]: Geological Society of America Abstracts with Programs, v. 16, no. 6, pp. 611.
- Nordstrom, D.K., Alpers, C.N., and Ball, J.W., 1991, Measurement of negative pH and extremely high metal concentrations in acid mine water from Iron Mountain, California [abs.]: Geological Society of America Annual Meeting, Abstract with Programs, v. 23, no. 5, p. A383.
- Nordstrom, D.K., McNutt, R.H., Puigdomènech, I., Smellie, J.A.T., and Wolf, M., 1992, Ground water chemistry and geochemical modeling of water-rock interactions at the Osamu Utsumi mine and Morro do Ferro analogue study sites, Poços de Caldas, Minas Gerais, Brazil: *Journal of Geochemical Exploration*, v. 45, pp. 249–287.
- Nordstrom, D.K., Carlson-Foszcz, V., and Oreskes, N., 1995, Rare earth element (REE) fractionation during acidic weathering of San Juan tuff, Colorado [abs.]: Geological Society of America Annual Meeting, Abstracts with Programs, v. 27, no. 6, p. A–199.
- Olson, G.J., 1991, Rate of pyrite bioleaching by *Thiobacillus ferrooxidans*—Results of an interlaboratory comparison: *Applied and Environmental Microbiology*, v. 57, pp. 642–644.
- Pabst, A., 1940, Cryptocrystalline pyrite from Alpine County, California: *American Mineralogist*, v. 25, pp. 425–431.
- Parker, R.L., 1962, Isomorphous substitution in natural and synthetic alunite: *American Mineralogist*, v. 47, pp. 127–136.
- Parks, G.A., 1990, Surface energy and adsorption at mineral/water interfaces—An introduction; *in* Hochella, M.F., Jr., and White, A.F. (eds.), Mineral-Water Interface Geochemistry: Reviews in Mineralogy, Mineralogical Society of America, Washington, D.C., v. 23, pp. 133–175.
- Plumlee, G.S., Smith, K.S., Mosier, E.L., Ficklin, W.H., Montour, M., Briggs, P.H., and Meier, A.L., 1995, Geochemical processes controlling acid-drainage generation and cyanide degradation at Summitville; *in* Posey, H.H., Pendleton, J.A., and Van Zyl, D., (eds.), Summitville Forum Proceedings: Colorado Geological Survey Spec. Pub. No. 38, pp. 23–34.
- Ponnampuruma, F.N., Tianco, E.M., and Loy, T., 1967, Redox equilibria in flooded soils, I. The iron hydroxide systems: *Soil Science*, v. 103, pp. 374–382.
- Potter, R.W., II, 1977, An electrochemical investigation of the system copper-sulfur: *Economic Geology*, v. 72, pp. 1524–1542.
- Pourbaix, M., 1945, Thermodynamique des solutions aqueuses diluées—Représentation graphique du pH et du potentiel: Ph.D. thesis, Delft, Beranger, Paris and Liege.
- Pourbaix, M., 1966, Atlas of electrochemical equilibria in aqueous solutions: Pergamon Press, New York, 670 pp.
- Pourbaix, M., and Pourbaix, A., 1992, Potential-pH equilibrium diagrams for the system S–H₂O from 25 to 150°C—Influence of access of oxygen in sulfide solutions: *Geochimica et Cosmochimica Acta*, v. 56, pp. 3157–3178.
- Powell, A.R., and Parr, S.W., 1919, Forms in which sulfur occurs in coal: Bulletin of the American Institute of Mining and Metallurgical Engineering, pp. 2041–2049.

- Ptacek, C.J., and Blowes, D.W., 1994, Influence of siderite on the geochemistry of inactive mine tailings impoundment; *in* Alpers, C.N., and Blowes, D.W. (eds.), *Environmental Geochemistry of Sulfide Oxidation*: American Chemical Society Symposium Series 550, Washington, D.C., pp. 172–189.
- Reardon, E.J., 1988, Ion interaction parameters for Al-SO₄ and application to the prediction of metal sulfate solubility in binary salt systems: *Journal of Physical Chemistry*, v. 42, pp. 6426–6431.
- Rickard, P.A., and Vanselow, D.G., 1978, Investigations into the kinetics and stoichiometry of bacterial oxidation of covellite (CuS) using a polarographic probe: *Canadian Journal of Microbiology*, v. 24, pp. 998–1003.
- Rimstidt, J.D., Chermak, J.A., and Gagen, P.M., 1994, Rates of reaction of galena, sphalerite, chalcopyrite, and arsenopyrite with Fe(III) in acidic solutions; *in* Alpers, C.N., and Blowes, D.W. (eds.), *Environmental Geochemistry of Sulfide Oxidation*: American Chemical Society Symposium Series 550, Washington, D.C., pp. 2–13.
- Ripmeester, J.A., Ratcliffe, C.I., Dutrizac, J.E. and Jambor, J.L., 1986, Hydronium ion in the alunite-jarosite group: *Canadian Mineralogist*, v. 24, pp. 435–447.
- Ritcey, G.M., 1989, Tailings management, problems and solutions in the mining industry: Elsevier Science Publishing Co. Inc., Amsterdam, 970 pp.
- Ritchie, A.I.M., 1994a, Sulfide oxidation mechanisms—Control and rates of oxygen transport; *in* Jambor, J.L., and Blowes, D.W. (eds.), *The Environmental Geochemistry of Sulfide Mine-Wastes*: Mineralogical Association of Canada, Short Course Handbook, v. 22, pp. 201–245.
- Ritchie, A.I.M., 1994b, Rates of mechanisms that govern pollutant generation from pyritic wastes; *in* Alpers, C.N., and Blowes, D.W. (eds.), *Environmental Geochemistry of Sulfide Oxidation*: American Chemical Society Symposium Series 550, Washington, D.C., pp. 108–122.
- Runnells, D.D., Shepard, T.A., and Angino, E.E., 1992, Metals in water—Determining natural background concentrations in mineralized areas: *Environmental Science and Technology*, v. 26, pp. 2316–2322.
- Russell, J.D., 1979, Infrared spectroscopy of ferrihydrite—Evidence for the presence of structural hydroxyl groups: *Clay Minerals*, v. 14, pp. 109–113.
- Sakaguchi, H., Torma, A.E., and Silver, M., 1976, Microbiological oxidation of synthetic chalcocite and covellite by *Thiobacillus ferrooxidans*: *Applied and Environmental Microbiology*, v. 31, pp. 7–10.
- Sand, W., Rhode, K., and Zenneck, C., 1992, Evaluation of *Leptospirillum ferrooxidans* for leaching: *Applied and Environmental Microbiology*, v. 58, pp. 85–92.
- Sato, M., 1992, Persistency-field Eh-pH diagrams for sulfides and their application to supergene oxidation and enrichment of sulfide ore bodies: *Geochimica et Cosmochimica Acta*, v. 56, pp. 3133–3156.
- Scala, G., Mills, A.L., Moses, C.O., and Nordstrom, D.K., 1982, Distribution of autotrophic Fe and sulfur-oxidizing bacteria in mine drainage from sulfide deposits measured with the FAINT assay [abs.]: American Society of Microbiology Annual Meeting.
- Schwertmann, U., 1985a, The effect of pedogenic environments on iron oxide minerals, *in* Stewart, B.A. (ed.), *Advances in Soil Science*, v. 1: Springer-Verlag, New York, pp. 171–200.
- Schwertmann, U., 1985b, Occurrence and formation of iron oxides in various pedoenvironments; *in* Stucki, F.W., Goodman, B.A. and Schwertmann, U. (eds.), *Iron in Soils and Clay Minerals*: D. Reidel Pub. Co., Boston, Mass., NATO Advanced Study Institute Series C, v. 217, pp. 267–308.
- Schwertmann, U., and Cornell, R.M., 1991, Iron oxides in the laboratory—Preparation and characterization: Verlag Chemie, Weinheim, Germany, 137 pp.
- Schwertmann, U., and Murad, E., 1983, The effect of pH on the formation of goethite and hematite from ferrihydrite: *Clays and Clay Minerals*, v. 31, pp. 277–284.
- Scott, K.D., 1987, Solid solution in, and classification of, gossan-derived members of the alunite-jarosite family, Northwest Queensland, Australia: *American Mineralogist*, v. 72, pp. 178–187.
- Silverman, M.P., 1967, Mechanism of bacterial pyrite oxidation: *Journal of Bacteriology*, v. 94, pp. 1046–1051.
- Silverman, M.P., and Lundgren, D.G., 1959, Studies on the chemoautotrophic iron bacterium *Ferrobacillus ferrooxidans*, I. An improved medium and a harvesting procedure for securing high cell yields: *Journal of Bacteriology*, v. 77, pp. 642–647.
- Silverman, M.P., Rogoff, M.H., and Wender, I., 1961, Bacterial oxidation of pyritic materials in coal: *Applied and Environmental Microbiology*, v. 9, pp. 491–496.
- Singer, P.C., and Stumm, W., 1968, Kinetics of the oxidation of ferrous iron, 2nd Symposium on Coal Mine Drainage Research: National Coal Association/Bituminous Coal Research, pp. 12–34.
- Singer, P.C., and Stumm, W., 1970a, Acid mine drainage—The rate-determining step: *Science*, v. 167, pp. 1121–1123.
- Singer, P.C., and Stumm, W., 1970b, Oxygenation of ferrous iron: Federal Water Quality Administration Report 14010–06/69, 198 pp.
- Smith, E.E., and Shumate, K.S., 1970, Sulfide to sulfate reaction mechanism: Federal Water Pollution Control Federation Report, 115 pp.
- Smith, K.S., 1999, Metal sorption on mineral surfaces—An overview with examples relating to mineral deposits; *in* Plumlee, G.S., and Logsdon, M.J. (eds.), *The Environmental Geochemistry of Mineral Deposits, Part A. Processes, Techniques, and Health Issues*: Society of Economic Geologists, Reviews in Economic Geology, v. 6A, pp. 161–182.
- Sokolova, G.A., and Karavaiko, G.I., 1968, Physiology and geochemical activity of *Thiobacilli*: Izdatelstvo “Nauka,” Moscow, 283 pp.
- Southam, G., and Beveridge, T.J., 1992, Enumeration of *Thiobacilli* within pH-neutral and acidic mine tailings and their role in the development of secondary mineral soil: *Applied and Environmental Microbiology*, v. 58, pp. 1904–1912.
- Steger, H.F., and Desjardins, L.E., 1978, Oxidation of sulfide minerals, IV. Pyrite, chalcopyrite, and pyrrhotite: *Chemical Geology*, v. 23, pp. 225–237.
- Stoffregen, R.E., and Alpers, C.N., 1987, Woodhouseite and svanbergite in hydrothermal ore deposits—Products of apatite destruction during advanced argillic alteration: *Canadian Mineralogist*, v. 45, pp. 201–211.
- Stoffregen, R.E., and Alpers, C.N., 1992, Observations on the unit-cell dimensions, H₂O contents, and δD values of natural and synthetic alunite: *American Mineralogist*, v. 77, pp. 1092–1098.
- Stokes, H.N., 1901, On pyrite and marcasite: U.S. Geological Survey Bulletin 186, 50 pp.
- Stumm, W., and Morgan, J.J., 1981, *Aquatic chemistry*, 2nd ed.: Wiley-Interscience, New York, 770 pp.
- Sveshnikov, G.B., and Dobychin, S.L., 1956, Electrochemical solution of sulfides and dispersion aureoles of heavy metals: *Geokhimiya*, no. 4, pp. 413–419.
- Sveshnikov, G.B., and Ryss, Yu.S., 1964, Electrochemical processes in sulfide deposits and their geochemical significance: *Geokhimiya*, v. 3, pp. 208–218.
- Tardy, Y., and Nahon, D., 1985, Geochemistry of laterites, stability of Al-goethite, Al-hematite, and Fe³⁺-kaolinite in bauxites and ferricretes: *American Journal of Science*, v. 285, pp. 865–903.
- Temple, K.L., and Colmer, A.R., 1951, The autotrophic oxidation of iron by a new bacterium—*Thiobacillus ferrooxidans*: *Journal of Bacteriology*, v. 62, pp. 605–611.
- Temple, K.L., and Delchamps, E.W., 1953, Autotrophic bacteria and the formation of acid in bituminous coal mines: *Applied Microbiology*, v. 1, pp. 255–258.
- Tervari, P.H., and Campbell, A.B., 1976, Dissolution of iron sulfide (troilite) in aqueous sulfuric acid: *Journal of Physical Chemistry*, v. 80, pp. 1844–1848.
- Thorber, M.R., 1975, Supergene alteration of sulfides, II. A chemical study of the Kambalda nickel deposits: *Chemical Geology*, v. 15, pp. 117–144.
- Thorstensen, D.C., 1984, The concept of electron activity and its relation to redox potentials in aqueous geochemical systems: U.S. Geological Survey Open-File Report 84–072, 45 pp.
- To, B.T., Nordstrom, D.K., Cunningham, K.M., Ball, J.W., and

- McCleskey, R.B., 1999, New method for the direct determination of dissolved Fe(III) concentration in acid mine waters: *Environmental Science and Technology*, v. 33, pp. 807–813.
- Torma, A.E., and Habashi, F., 1972, Oxidation of copper (II) selenide by *Thiobacillus ferrooxidans*: *Canadian Journal of Microbiology*, v. 18, pp. 1780–1781.
- Torma, A.E., and Subramanian, K.N., 1974, Selective bacterial leaching of a lead sulphide concentrate: *International Journal of Mineral Processing*, v. 1, pp. 125–134.
- Torma, A.E., Walden, C.C., Duncan, D.W., and Branion, R.M., 1972, The effect of carbon dioxide and particle surface area on the microbiological leaching of a zinc sulfide concentrate: *Biotechnology and Bioengineering*, v. 15, pp. 777–786.
- Torma, A.E., Legault, G., Kougiomoutzakis, D., and Ouellet, R., 1974, Kinetics of bio-oxidation of metal sulfides: *Canadian Journal of Chemical Engineering*, v. 52, pp. 515–517.
- Torma, A.E., Gabra, G.G., Guay, R., and Silver, M., 1976, Effects of surface active agents on the oxidation of chalcopyrite by *Thiobacillus ferrooxidans*: *Hydrometallurgy*, v. 1, pp. 301–309.
- Torrent, J., and Guzman, R., 1982, Crystallization of Fe(III)-oxides from ferrihydrite in salt solutions—Osmotic and specific ion effects: *Clays and Clay Minerals*, v. 17, pp. 463–469.
- Towe, K.M., and Bradley, W.F., 1967, Mineralogical constituents of colloidal “hydrous ferric oxides”: *Journal of Colloid and Interface Science*, v. 24, pp. 384–392.
- Tunell, G., 1930, The oxidation of disseminated copper ores in altered porphyry: Unpub. Ph.D. thesis, Harvard Univ., 104 pp.
- Tuovinen, O.H., Niemela, S.I., and Gyllenberg, H.G., 1971, Tolerance of *Thiobacillus ferrooxidans* to some metals: *Antonie van Leeuwenhoek*, v. 37, pp. 489–496.
- Turner, A.W., 1949, Bacterial oxidation of arsenite: *Nature*, v. 164, pp. 76–77.
- U.S. Environmental Protection Agency, 1985, Wastes from the extraction and beneficiation of metallic ores, phosphate rock, asbestos, overburden from uranium mining, and oil shale: Report to Congress, EPA/530-SW-85-033.
- Vairavamurthy, A., Manowitz, B., Zhou, W., and Jeon, Y., 1994, Determination of hydrogen sulfide oxidation products by sulfur K-edge X-ray absorption near-edge structure spectroscopy; *in* Alpers, C.N., and Blowes, D.W. (eds.), *Environmental Geochemistry of Sulfide Oxidation: American Chemical Society Symposium Series 550*, Washington, D.C., pp. 412–430.
- Vranesh, G., 1979, Mine drainage—The common enemy; *in* Argal, G.O., Jr., and Brawner, C.O. (eds.), *Proceedings, 1st Internatl Mine Drainage Symposium: Miller Freeman Publications*, pp. 54–97.
- Waite, T.D., and Morel, F.M.M., 1984, Photoreductive dissolution of colloidal iron oxides in natural waters: *Environmental Science and Technology*, v. 18, pp. 860–868.
- Wakao, N., Sakurai, Y., and Shiota, H., 1977, Microbial oxidation of ferrous iron in acid mine water at sulfur and iron-sulfide mine: *Soil Science and Plant Nutrition*, v. 23, pp. 207–216.
- Wakao, N., Mishina, M., Sakurai, Y., and Shiota, H., 1982, Bacterial pyrite oxidation, I. The effect of pure and mixed cultures of *Thiobacillus ferrooxidans* and *Thiobacillus thiooxidans* on release of iron: *Journal of General and Applied Microbiology*, v. 28, pp. 331–343.
- Wakao, N., Mishina, M., Sakurai, Y., and Shiota, H., 1984, Bacterial pyrite oxidation, III. Adsorption of *Thiobacillus ferrooxidans* cells on solid surfaces and its effect on iron release from pyrite: *Journal of General and Applied Microbiology*, v. 30, pp. 63–77.
- Wakao, N., Koyatsu, H., Komai, Y., Shimokawara, H., Sakurai, Y., and Shiota, H., 1988, Microbial oxidation of arsenite and occurrence of arsenite-oxidizing bacteria in acid mine water from a sulfur-pyrite mine: *Geomicrobiology Journal*, v. 6, pp. 11–24.
- Waksman, S.A., and Jaffe, J.S., 1921, Acid production by a new sulfur-oxidizing bacterium: *Science*, v. 53, pp. 216.
- Waksman, S.A., and Jaffe, J.S., 1922, Microorganisms concerned in the oxidation of sulphur in the soil, II. *Thiobacillus thiooxidans*, a new sulphur-oxidizing organism isolated from the soil: *Journal of Bacteriology*, v. 7, pp. 239–256.
- Walker, T.R., 1967, Formation of red beds in modern and ancient deserts: *Geological Society of America Bulletin*, v. 78, pp. 353–368.
- Walker, T.R., 1974, Formation of red beds in moist tropical climates—A hypothesis: *Geological Society of America Bulletin*, v. 84, pp. 633–638.
- Walker, T.R., 1976, Diagenetic origin of continental red beds; *in* Falke, H. (ed.), *The Continental Permian in Central, West, and South Europe: D. Reidel Publishing Co.*, pp. 241–282.
- Walsh, A.W., and Rimstidt, J.D., 1986, Rates of reaction of covellite and blaubleibender covellite with ferric iron at pH 2.0: *Canadian Mineralogist*, v. 24, pp. 35–44.
- White, A.F., and Brantley, S.L., 1995, Chemical weathering rates of silicate minerals: *Reviews in Mineralogy, Mineralogical Society of America*, Washington, D.C., v. 31, 583 pp.
- White, W.W., III, and Jeffers, T.H., 1994, Chemical predictive modeling of acid mine drainage from metallic sulfide-bearing waste rock; *in* Alpers, C.N., and Blowes, D.W. (eds.), *Environmental Geochemistry of Sulfide Oxidation: American Chemical Society Symposium Series 550*, Washington, D.C., pp. 608–630.
- Wieder, R.K., 1994, Diel changes in iron(III)/iron(II) in effluent from constructed acid mine drainage treatment wetlands: *Journal of Environmental Quality*, v. 23, no. 4, pp. 730–738.
- Wiersma, C.L., and Rimstidt, J.D., 1984, Rates of reactions of pyrite and marcasite with ferric iron at pH 2: *Geochimica et Cosmochimica Acta*, v. 48, pp. 85–92.
- Wilber, C.G., 1969, *The biological aspects of water pollution: C.C. Thomas*, New York, 296 pp.
- Williams, E.G., Rose, A.W., Parizek, R.R., and Waters, S.A., 1982, Factors controlling the generation of acid mine drainage: *Pennsylvania State University Report to the U.S. Bureau of Mines*, 265 pp.
- Williamson, M.A., and Rimstidt, J.D., 1993, The rate of decomposition of the ferric-thiosulfate complex in acidic aqueous solutions: *Geochimica et Cosmochimica Acta*, v. 57, pp. 3555–3561.
- Yakhontova, L. K., Zeman, I., and Nesterovich, L.G., 1980, Oxidation of tetrahedrite: *Doklady, Earth Sciences Section, Akademia Nauk SSSR*, v. 253, pp. 461–464.
- Yapp, C.J., 1983, Stable hydrogen isotopes in iron oxides—Isotope effects associated with the dehydration of a natural goethite: *Geochimica et Cosmochimica Acta*, v. 47, pp. 1277–1287.
- Zhang, J., and Millero, F.J., 1994, Kinetics of oxidation of hydrogen sulfide in natural waters; *in* Alpers, C.N., and Blowes, D.W. (eds.), *Environmental Geochemistry of Sulfide Oxidation: American Chemical Society Symposium Series 550*, Washington, D.C., pp. 393–409.
- Zodrov, E.L., and McCandlish, K., 1978a, Hydrated sulphates in the Sydney Coalfield, Cape Breton, Nova Scotia: *Canadian Mineralogist*, v. 16, pp. 17–22.
- Zodrov, E.L., and McCandlish, K., 1978b, Roof weakness—Fossilization and (cyclic) regenerative hydrated sulphates, Discussion: *Canadian Institute of Mining and Metallurgy Bulletin*, v. 71, pp. 90–91.
- Zodrov, E.L., Wiltshire, J., and McCandlish, E., 1979, Hydrated sulphates in the Sydney Coalfield, Cape Breton, Nova Scotia, II. Pyrite and its alteration products: *Canadian Mineralogist*, v. 17, pp. 63–70.
- Zverev, V.P., Dol'nikov, V.A., Khutorskoy, M.D., Dobrovol'skiy, Ye.V., Lyal'ko, V.I., Mitnik, M.M. and Fotogdinov, R.A., 1983, Sulfide oxidation kinetics and heat effects: *Geochemistry International*, v. 20, pp. 82–90.

Chapter 7

METAL SORPTION ON MINERAL SURFACES: AN OVERVIEW WITH EXAMPLES RELATING TO MINERAL DEPOSITS

Kathleen S. Smith

U.S. Geological Survey, Box 25046, MS 973, Federal Center, Denver, CO 80225-0046

INTRODUCTION

Sorption reactions, involving both inorganic and organic particulates, are an important control on the transport and fate of many trace elements in natural systems. Understanding the controls on trace-element concentrations in waters is critical for a number of applications including the transport of contaminants and nutrients, geochemical prospecting, agriculture, municipal and industrial water treatment, and bioavailability to name a few. This chapter provides an overview of metal sorption on mineral surfaces and gives examples of predictive modeling of metal-sorption reactions in mine-drainage systems.

The word “sorption” is a general term that describes removal of a solute from solution to a contiguous solid phase and is used when the specific removal mechanism is not known. “Sorbate” or “adsorbate” refers to the solute that sorbs on the solid phase. “Sorbent” or “adsorbent” is the solid phase or substrate onto which the sorbate sorbs. “Adsorption” refers to the two-dimensional accumulation of an adsorbate at a solid surface. In the case of “surface precipitation,” there is a three-dimensional accumulation of sorbate at the solid surface. The term “absorption” is used when there is diffusion of the sorbate into the solid phase. Absorption processes usually show a significant time dependency. Sposito (1986) and Jenne (1998) provide a more detailed description of these terms. In this chapter, the term adsorption is used when describing laboratory studies with simple, well-characterized systems, and when discussing models that have been developed to describe adsorption phenomena.

PRINCIPLES OF SORPTION REACTIONS

Trace elements partition between dissolved and particulate phases and this partitioning can influence their transport and bioavailability (Luoma and Davis, 1983; Jenne and Zachara, 1987). Sorption processes probably limit metal mobility in most natural aqueous systems (Jenne, 1968; Hem, 1985). Partitioning of a metal between solid and solution phases is influenced by several factors. Generally, low-pH conditions, reducing conditions, low particulate loads, and/or high dissolved concentrations of a strong complexing agent cause metals to be present in the solution phase. Typically, pH is the most important control of metal partitioning. In general, sorption reactions depend on solution pH, sorbate identity and concentration, presence of competing sorbates, formation of solution complexes, sorbent composition, and the concentration of surface-binding sites on the sorbent.

Properties of important sorbent materials

Often, the most effective sorbent materials are secondary minerals that form from the weathering of primary minerals. Jenne (1968) noted that hydrous oxides of manganese and iron, as well as reactive particulate carbon, appear to be the principal controls on metal sorption in soils and fresh-water sediments. In addition, hydrous oxides of aluminum and silicon, and clay and zeolite minerals may contribute to the sorption potential of a soil or sediment (Jenne, 1977). Hydrous metal oxides and organic matter are ubiquitous in most natural systems and often exist as coatings on clay-size minerals in soils and sediments. These coatings likely give rise to the high metal sorption potential commonly observed for clay-size fractions. Consequently, because clay-size minerals often are coated in natural systems, it is difficult to assess their actual contribution to the metal-sorption potential of soils and sediments. Surface area is another consideration that will be discussed later.

The process of sorption involves interactions between a sorbate and a sorbent at the surface-water interface. Hence, surface properties of the sorbent(s) play an important role in the sorption process. Some earth materials are much better sorbents than others. This is related both to their capacity to bind metals and to the intensity with which they bind metals. A sorbent's capacity to bind metals depends both on the number of metal-binding sites present, “binding-site density,” and on the amount of metal-accessible surface, “specific surface area.” The metal-binding intensity is related to the strength of interaction between the sorbate and sorbent, and can be expressed as a binding constant. The relative importance of various earth materials in sorption reactions is also dependent on their abundance.

Surface functional groups

Functional groups on mineral surfaces are the binding sites for sorption reactions. A surface functional group is “a chemically reactive molecular unit bound into the structure of a solid at its periphery such that the reactive components of the unit can be bathed by a fluid” (Sposito, 1989). Figure 7.1 illustrates the surface layer of a metal-oxide mineral. Metal-oxide minerals comprise some of the most important sorbent minerals in natural systems. Surface molecules have fewer nearest neighbors than bulk molecules and are not fully coordinated. When a metal-oxide mineral comes into contact with water, hydroxyl functional groups (OH⁻) form on the surface. This is due to the chemisorption (Fig. 7.1b) and subsequent hydrolysis (Fig. 7.1c) of water molecules at

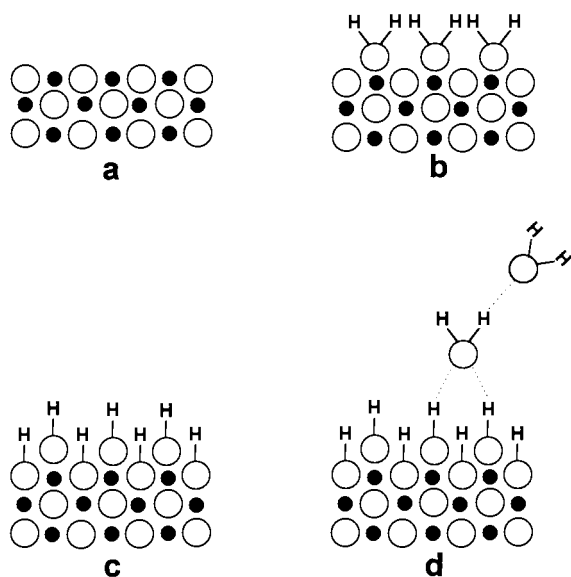


FIGURE 7.1—Cross section of the surface layer of a metal-oxide mineral. Filled circles are structural metal ions, open circles are oxide ions. (a) Unhydrated surface. (b) Surface metal ions coordinated with H₂O molecules. (c) Hydroxylated surface formed from the dissociation of protons from sorbed H₂O molecules. (d) Water sorption on the hydroxylated surface. Modified from Schindler (1981) and Dzombak and Morel (1990).

the mineral surface. Additional water can sorb on the hydroxylated surface. Figure 7.1d shows a hypothetical mechanism to form structured water at the oxide-water interface (McCafferty and Zettlemoyer, 1971). A variety of functional groups may be present on organic compounds including carboxyl (-COO⁻), amine (NH₃⁺), and sulfhydryl (-SH) groups (Macalady and Ranville, 1998).

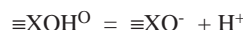
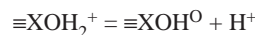
Surface-charge development

Interfacial regions between different phases have unique properties. Forces acting at solid-solution interfaces are extensions of forces within the individual phases. Solid surfaces acquire an electrical charge when in contact with an aqueous phase. This surface charge produces a microenvironment of electrical potential imbalance at the solid-solution interface that influences the distribution of neighboring ions. The charged surface attracts ions of opposite charge, “counterions,” and repels ions of like charge, “coions.” Macroscopically, there must be charge balance between the total net charge of the solid surface and solution to preserve electroneutrality.

Stumm and Morgan (1996) describe three principal origins of surface charge including: (1) chemical reactions at the surface of the particle; (2) crystalline imperfections, broken bonds, and isomorphous replacements within the crystal lattice; and, (3) sorption of a surface-active ion. There are two idealized end members for the origins of surface charge: (1) “variable surface charge” (e.g., hydrous metal oxides, organic matter, edges of clay minerals), where the surface charge is dependent on the composition of the surrounding solution, but the magnitude of the surface potential is not affected by the presence of indifferent electrolytes; and, (2)

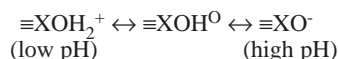
“constant surface charge,” which is approached by layer clay minerals such as smectite, where the surface charge is independent of the surrounding solution composition (van Olphen, 1977; Stumm and Morgan, 1996; Langmuir, 1997). Many minerals exhibit combinations of these idealized end-member types of charge distribution. The type of particulate surface (i.e., variable charge or constant charge) affects the environmental behavior of the particulates. For example, the cation exchange capacity (CEC) of a soil containing variable-charge surfaces increases with increasing pH. Consequently, liming the soil will increase both pH and CEC. However, it is difficult to raise the pH of a variable charge soil above 6.5 because H⁺ ions are released from the hydroxylated soil surfaces, which in turn will neutralize OH⁻ (Singh and Uehara, 1986). The type of surface also influences the stability of suspended particulates (flocculation status). See Ranville and Schmiermund (1999) for discussion of particle stability.

Variable surface charge—Many hydrous metal oxides and organic materials contain ionizable functional groups at their surfaces. Surface charge can develop as a result of the dissociation of these functional groups. The charge on particles is usually expressed as a surface density (units of charge per unit area). Proton exchange reactions for surface functional groups of metal-oxide minerals are expressed as:

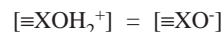


where $\equiv\text{XOH}^0$ is a surface-binding site, and $\equiv\text{XOH}_2^+$ and $\equiv\text{XO}^-$ are proton-exchange surface complexes.

The charge at the surface is dependent on the pH of the surrounding water. Neutral or alkaline pH conditions generally will result in a net negatively charged surface. Conversely, under acidic conditions, excess protons generally are retained at the surface yielding a net positively charged surface as illustrated below:



(Parks, 1990). It is important to keep in mind that at almost any pH there is a distribution of positively, negatively, and neutrally charged species at mineral surfaces. At some intermediate pH, termed the “point of zero charge (PZC),” the net surface charge will be equal to zero such that:



(Lewis-Russ, 1991; Sverjensky, 1994). Table 7.1 lists the PZC for several minerals. The surface charge may have an effect on the distribution of neighboring solutes in that decreasing the pH (more acidic) of the surrounding water will attract anionic species from solution. Conversely, increasing pH (less acidic) will attract cationic species from solution.

Constant surface charge—The constant surface charge or permanent charge case is most applicable to clay minerals that have lattice imperfections and(or) nonstoichiometric isomorphous substitution of cations within their lattice. These clay minerals pos-

sess a net-negative charge deficiency. Sorption of interlayer cations may compensate for this deficiency. Owing to the fact that one ion may be replaced by another ion to compensate for charge imbalances, the term “cation exchange” often is used instead of sorption when speaking of constant surface charge situations.

TABLE 7.1—Point of zero charge (PZC) for a variety of minerals.

Mineral	pH _{PZC} ⁽¹⁾
Fe ₂ O ₃ ·H ₂ O (amorphous) (hydrrous ferric oxide)	8.1
α - FeOOH (goethite)	6–7
α - Fe ₂ O ₃ (hematite)	4.2–6.9
α - Al(OH) ₃ (gibbsite)	10
δ - MnO ₂ (birnessite)	1.5–2.8
SiO ₂ (amorphous)	3.5
Kaolinite	4.6
Montmorillonite	2.5

⁽¹⁾These values were determined by different researchers often using different methods and electrolyte solutions.

Physicochemical properties

Knowledge of sorbent properties such as particle size and shape, particle-size distribution, crystallinity, chemical composition, surface area, porosity, and numbers and types of surface functional groups is necessary for the interpretation and mechanistic modeling of sorption data. James and Parks (1982) review experimental methods and data for the physicochemical characterization of minerals. It is important to keep in mind that the chemical and physical properties of a bulk material are different from the chemical and physical properties of its surface (Hochella, 1990).

Composition and crystallinity—X-ray diffraction, microscopic, and spectroscopic techniques commonly are used to examine the composition and crystallinity of sorbent materials. Generally, the more crystalline a sorbent material, the less sorption capacity it has for metals. Recent advances in several spectroscopic techniques provide opportunities to gain a better understanding of surface composition and microtopography of sorbent materials (Hochella, 1990).

Surface area—Metal sorption by soils and sediments generally increases with decreasing grain size; this relationship is due to increasing surface area with decreasing grain size (Sposito, 1984; Ranville and Schmiermund, 1999). Horowitz and Elrick (1987) report a correlation between sediment surface area and trace-element content indicating that trace element incorporation into sediments may be primarily due to sorption.

Specific surface area is the amount of reactive surface area available for sorbing solutes per unit weight of the sorbent (Davis and Kent, 1990). Knowledge of the specific surface area is necessary for calculation of layer charges and potentials in many surface-complexation models. It can be determined by a number of techniques including gas adsorption, negative adsorption, adsorption from solution, and theoretical calculations (Gregg and Sing, 1982). Surface area measurements frequently are used to estimate adsorption binding site densities of minerals, but there are several potential limitations to this approach (White and Peterson, 1990; Chiou and Rutherford, 1993).

Influence of solution composition

The solution composition can influence sorption reactions on adjacent solid surfaces. For example, dissolved constituents can compete with the solid surface for sorbate ions, compete with sorbate ions for surface-binding sites, and bind to different surface sites and alter the surface properties. Consequently, it is essential to perform thorough chemical analyses to characterize the system and determine the presence and concentration of sorbate solutes and potential complexing species.

pH

For surface-binding reactions of metals on oxide minerals, solution pH is a master variable. Typically, cation adsorption increases with increasing pH from near zero to nearly 100% over a pH range of 1 to 2 units (James and Healy, 1972c; Kinniburgh and Jackson, 1981; Davis and Hayes, 1986). This pH region is termed the “adsorption edge” and its placement seems to be characteristic of the particular adsorbate and, to a lesser extent, to the particular adsorbent as well as to the concentrations of surface binding sites and adsorbate (Spark et al., 1995). The adsorption edge is illustrated on Figure 7.2. Anion adsorption is the mirror image of cation adsorption in that anion adsorption tends to decrease with increasing pH. For a given adsorbate concentration, increasing the amount of adsorbent material will shift down the pH of the adsorption edge for cations and shift up the pH of the adsorption edge for anions (see Fig. 7.2). Conversely, increasing the concentration of a cationic adsorbate for a given amount of adsorbent will shift the adsorption edge to higher pH values. This phenomenon is termed the “loading effect.” The loading effect may be an artifact of diffusion processes and disequilibrium (Axe and Anderson, 1998).

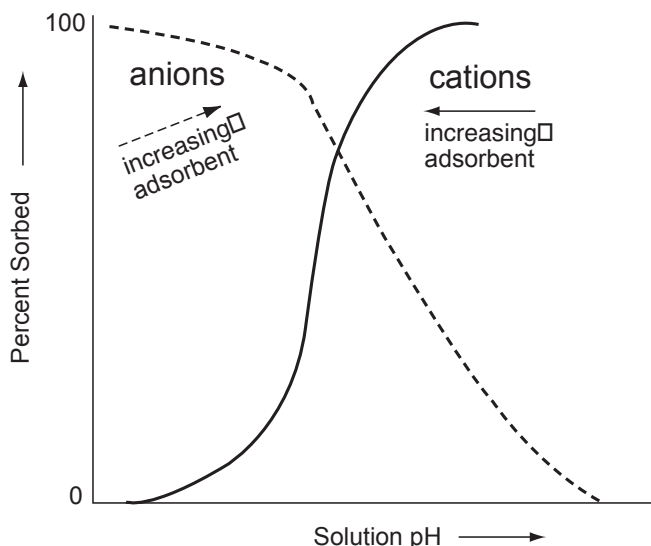


FIGURE 7.2—Generalized adsorption edge for cation (solid curve) and anion (dashed curve) adsorption on a metal-oxide mineral. For a given solute concentration, the adsorption edge will shift in the direction of the arrows with increasing adsorbent content.

Solute speciation

Complexation of metals by dissolved ligands can either enhance or inhibit sorption reactions (Davis and Leckie, 1978a). Generally, metal complexation with inorganic ligands tends to inhibit metal sorption. Zachara et al. (1989) report that surfaces and aqueous carbonate compete for Cr(VI) in soils. Smith and Langmuir (1987) and Smith (1986) observed similar competition between goethite surfaces and aqueous carbonate complexes for Cu and Pb, and Hsi and Langmuir (1985) for uranyl ion. Metal complexation by organic ligands with more than one functional group or by some inorganic ligands (such as SCN^- and $\text{S}_2\text{O}_3^{2-}$) often enhances metal sorption due to bonding of the other functional groups to the solid surface (Benjamin and Leckie, 1982).

Competition effects for surface-binding sites can be important in sorption reactions. Often, competition effects are not observed until one of the sorbates is in large excess (Benjamin et al., 1982). Hence, competition effects are most often noted when the surface-binding sites are nearly saturated.

Different redox states of a metal have different sorption affinities (e.g., As(III) versus As(V) and Se(IV) versus Se(VI)). For example, Howell (1994) notes that reduction of As(V) to As(III) in mine tailings can lead to greater leaching of As due to a reduction in sorption on iron-oxide minerals. Balistrieri and Chao (1990) report stronger sorption of Se(IV) than Se(VI) on amorphous iron oxyhydroxide and manganese dioxide. Consequently, Se(VI) generally is more mobile in natural systems. Davis et al. (1993) discuss redox states and sorption affinities of metals in ground water.

Temperature

Most sorption studies are conducted at room temperature or carefully regulated at 20 or 25°C. Therefore, few studies address the temperature dependence of sorption reactions. Several factors can affect the temperature-dependence of sorption reactions. First, aqueous speciation of the sorbate solutes is temperature dependent, which will in turn affect sorption reactions. Also, the surface charge of the sorbent material is temperature dependent and the point of zero charge of metal-oxide minerals appears to increase as temperature decreases (Machesky, 1990). This has the effect of allowing more positively charged surface-binding sites to be present at a given pH. The degree of hydration of sorbent minerals may change with temperature (Avotins, 1975; Harter, 1991). Observations show that specific sorption of anions tends to increase and that of cations tends to decrease with decreasing temperature (Machesky, 1990). Based on this information, seasonal temperature fluctuations could impact sorption reactions in natural systems. Therefore, sorption studies should be performed over the temperature range of interest.

Sorption on oxide minerals

In addition to surface ionization reactions described previously for variable surface charge systems, there can also be complexation reactions between ions in solution and the ionized surface functional groups. Sorption of cations and anions on oxide minerals is strongly pH dependent. Cations and anions sorb with opposite pH dependence in that sorption of cations increases with increasing pH whereas sorption of anions decreases with increas-

ing pH. An example of predicted relative placements of several metal-adsorption edges on hydrous ferric oxide is given on Figure 7.3a for conditions at a stream that receives mine drainage. In-depth discussions of the sorption of ions on oxide minerals are provided by Hem (1977), Kinniburgh and Jackson (1981), Sposito (1984), Dzombak and Morel (1987), Schindler and Stumm (1987), Parks (1990), and Davis and Kent (1990).

Several generalizations can be made about metal-cation sorption on oxide surfaces:

- 1) Sorption is strongly pH-dependent, increases with increasing pH, and usually occurs over a narrow pH range.
- 2) The pH region of the adsorption edge is usually more characteristic of the sorbing cation than of the sorbent material.
- 3) The relative placement of the adsorption edge for different metals is similar to that for formation of hydrolysis species.
- 4) Protons are released (or OH^- consumed) as a result of sorption reactions.

The mechanism of metal sorption on hydrous ferric oxide has been demonstrated by Gadde and Laitinen (1974) and Hildebrand and Blum (1974) from the example of Pb^{2+} interactions under a variety of conditions. Dzombak and Morel (1990) present some generalizations about cation sorption on hydrous ferric oxide. They state that the larger the cation charge, the more strongly the cation is sorbed. Also, the stronger the tendency of the cation to hydrolyze, the more strongly it is sorbed. Leckie and coworkers have studied metal sorption on hydrous ferric oxide (Davis, 1977; Davis and Leckie, 1978b; Benjamin, 1979; Leckie et al., 1980; Benjamin and Leckie, 1981a, 1981c, 1982; Benjamin et al., 1982; Benjamin, 1983). Benjamin and Leckie (1981c) report that oxide surfaces consist of sites of varying energy and that metals preferentially bind to high-energy sites. Also, Benjamin and Leckie (1981a, b) found that there is little competition among metals for binding sites on hydrous ferric oxide. This indicates that many of the high-energy metal-binding sites on hydrous ferric oxide may be metal specific.

Reviews covering anion sorption include Parfitt (1978), Hingston (1981), Mott (1981), and Barrow (1985). Generally, maximum sorption of anions occurs at pH values near their acidity constants ($\text{p}K_a$) (Hingston et al., 1967). An example of placements of several anion-adsorption edges is given on Figure 7.3b. Smith and Huyck (1999, Table 2.13) list the tendency for various metals to be cationic, anionic, and redox-sensitive in aqueous systems.

Specific and non-specific sorption

Sorption of ions on oxide minerals can involve predominantly electrostatic (non-specific) or predominantly chemical (specific) interactions with the oxide surface. These two types of interactions result in very different sorption behaviors about which some generalizations can be made.

Non-specific sorption:

- 1) Sorption takes place on surfaces of opposite charge, but little sorption takes place on surfaces of neutral or similar charge.
- 2) Sorption density decreases with increasing ionic strength.

Specific sorption:

- 1) Sorption is insensitive to surface charge.
- 2) Sorption is insensitive to ionic strength.

In the case of non-specific sorption, the surface charge of the mineral controls the sorption process and the identity of the sor-

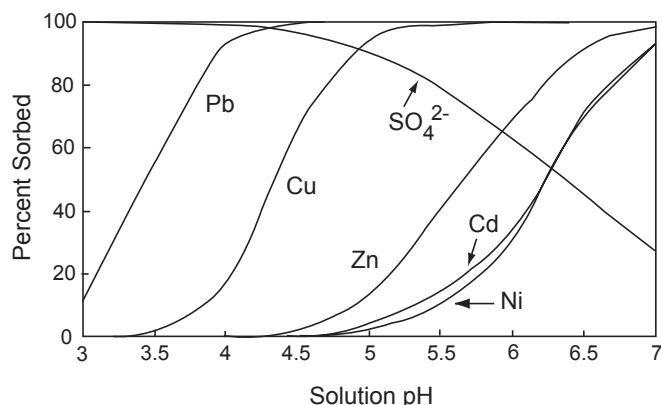


FIGURE 7.3a—Model sorption curves showing relative placement of adsorption edges of selected metals and sulfate on hydrous ferric oxide. Model input was for geochemical conditions from a stream receiving acid-mine drainage. Modified from Smith and Macalady (1991).

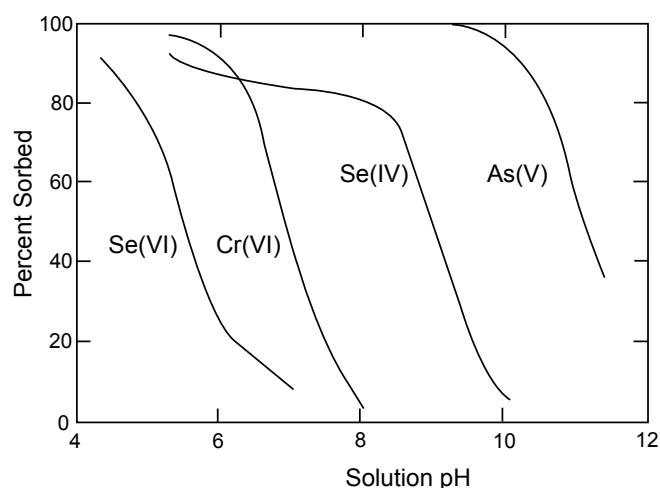


FIGURE 7.3b—Sorption curves showing relative placement of adsorption edges of selected oxyanions on hydrous ferric oxide. Modified from Davis and Kent (1990).

bate is relatively unimportant. Non-specific sorption takes place through coulombic attraction between the charged surface and the oppositely charged sorbate ion. Non-specific sorption is also referred to as physical adsorption, and the sorbates form outer-sphere complexes with the mineral surface.

Specific sorption involves chemical bonding of a particular sorbate to the mineral surface and the identity of the sorbate is often very important. Specific sorption can result in a reversal of surface charge, which implies that specifically sorbed ions are able to overcome electrostatic repulsion. Specific sorption is also referred to as chemical adsorption, and the sorbates form inner-sphere complexes with the mineral surface.

Sorption selectivity

Many studies have demonstrated that pH is a master variable for metal sorption reactions on oxides (Kinniburgh and Jackson, 1981, and references therein). Selectivity is a measure of the relative affinity of a particular ion for a given sorbent. The lower the pH that a cation sorbs on a sorbent, the higher the selectivity. Because sorption of monovalent ions (not including H⁺) is usually non-specific, selectivity differences between monovalent ions is usually small, and monovalent-ion selectivity is generally much lower than that for multivalent ions. Divalent transition-metal cations typically have much higher selectivities than do alkaline-earth cations. It has been noted that there appears to be a broad relationship between selectivity of metal cations and the onset of hydrolysis (James and Healy, 1972c). For alkali and alkaline earth cations, the sorption selectivity increases with the ionic radius of the ion:

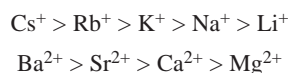


Table 7.2 lists sorption selectivity sequences determined by various researchers for divalent metal cations on a variety of

metal-oxide minerals and organic matter. There is general agreement for selectivity sequences of a given metal oxide, although some differences between phases exist. Several of the sequences are similar between different metal-oxide minerals, but there are some distinct differences (such as the preference of MnO₂ for Co). With few exceptions, the sorption selectivity on most metal-oxide minerals follows the sequence Cr ≥ Pb ≥ Cu > Co ≥ Zn and Ni ≥ Cd (Schultz et al., 1987).

The pH at which metal sorption becomes significant varies with the particular metal cation, the particular sorbent, the solid:solution ratio, the specific surface area of the sorbent, the total metal-cation concentration, and the concentration of other competing or interacting species. Consequently, it is very difficult to make generalizations about metal sorption on different oxide minerals. However, based on synthesis of results from numerous studies reported in the literature, there appears to be specific pH ranges in which adsorption edges occur for metal-cation sorption on oxide minerals. This is discussed in detail in Kinniburgh and Jackson (1981).

Table 7.3 lists the pH ranges that usually approximate observed adsorption edges for divalent metal sorption on iron- and aluminum-oxide minerals. Adsorption edges for metal sorption on silica tend to be at higher pH values than those listed, and edges for sorption on manganese-oxide minerals tend to be at lower pH values (Kinniburgh and Jackson, 1981). Therefore, manganese-oxide minerals generally have higher selectivities, and silica has lower selectivities than do aluminum- and iron-oxide minerals for divalent metal cations. A comparison of metal-binding constants for sorption on iron- and manganese-oxide minerals is given in Smith and Jenne (1991) in the context of a sorption model. In a study by Kinniburgh et al. (1976), it appears that metal cations are more strongly sorbed by iron gel than by aluminum gel.

Sorption rates

The importance of sorption reactions in controlling trace-element concentrations in natural systems is partly due to the initial

TABLE 7.2—Sorption selectivity sequences for divalent metal cations on a variety of metal-oxide minerals and organic matter. (Some data in this table are from Sparks, 1995.)

Cu > Pb > Zn > Ni > Co > Cd	Al gel	Kinniburgh et al., 1976
Cu > Zn > Co > Cd	α -alumina	Spark et al., 1995
Pb >> Cu > Mn > Zn, Cd	natural Al/Fe precipitate	Paulson, 1997
Pb > Cu > Zn > Ni > Cd > Co	Fe gel	Kinniburgh et al., 1976
Zn > Cd > Hg	Fe gel	Brunnix, 1975
Pb > Zn > Cd	Fe gel	Gadde and Laitinen, 1974
Pb > Cu > Zn > Cd	amorphous Fe oxyhydroxide	Benjamin, 1979
Pb > Cu > Zn > Cd ~ Ni	natural Fe precipitate	Smith, 1991
Cu > Zn > Mn	natural Fe-rich sediment	Davis et al., 1991
Pb > Cu > Zn, Cd	natural Fe-rich sediment	Sanden, 1991
Cu > Pb > Zn > Co > Cd	α -FeOOH	Forbes et al., 1976
Cu > Zn > Co > Mn > Cd	α -FeOOH	Grimme, 1968
Cu > Zn > Cd > Co	α -FeOOH	Spark et al., 1995
Cu > Zn > Ni > Mn	Fe ₃ O ₄	Venkataramani et al., 1978
Co > Mn > Zn > Ni	MnO ₂	Murray, 1975b
Pb > Zn > Cd	MnO ₂	Gadde and Laitinen, 1974
Co > Cu > Ni	MnO ₂	Murray et al., 1968
Cu > Co > Zn > Ni	MnO ₂	Kozawa, 1959
Co > Cu > Mn	MnO ₂	Traina and Doner, 1985
Co > Zn	δ -MnO ₂	Loganathan and Burau, 1973
Co > Cu > Zn > Ni	α -MnO ₃	McKenzie, 1972
Cu > Zn > Co > Ni	δ -MnOOH	McKenzie, 1972
Pb > Cu > Mn > Zn > Ni	natural MnO ₂	Eley and Nicholson, 1994
Pb > Cu > Zn	natural MnO ₂	Catts and Langmuir, 1986
Zn > Cu > Ni > Co > Mn	Si gel	Taniguchi et al., 1970
Zn > Cu > Co > Mn > Ni	Si gel	Vydra and Galba, 1969
Cu > Zn > Cd > Co	silica	Spark et al., 1995
Cu > Zn > Co > Fe > Ni > Mn	SnO ₂	Donaldson and Fuller, 1968
Ni > Co > Pb > Cu > Zn	Soil fulvic acid	Schnitzer and Hanson, 1970
Cu > Fe ²⁺ > Ni > Pb > Co > Zn > Mn at pH 3.5	Soil fulvic acid	Schnitzer and Skinner, 1966, 1967
Cu > Pb > Fe ²⁺ > Ni > Mn ~ Co > Zn at pH 5.0	Soil fulvic acid	Schnitzer and Skinner, 1966, 1967
Fe ³⁺ > Al > Cu > Zn > Ni > Co > Mn	Soil humic acid	Khan, 1969

rapid equilibration of most sorption reactions (Ahmed and Maksimov, 1968) in contrast to the often longer periods of time required for precipitation reactions. Mechanisms that control the rate of sorption reactions are poorly understood. Sorption appears to be a two-step process. In the first step, metals sorb to external surface sites and rapidly equilibrate with the surrounding solution. With sufficient mixing, the rates of this reaction are quite fast (generally seconds to minutes; Hachiya et al., 1984; Hayes and Leckie, 1986). In the second step, the metal slowly diffuses to interior sites (e.g., Coughlin and Stone, 1995; Papelis et al., 1995; Axe and Anderson, 1998). This fraction can become isolated from the bulk solution. It is important to recognize that sorption processes may be limited by mass transfer in natural systems (e.g., Stollenwerk and Kipp, 1990; Weber et al., 1991).

TABLE 7.3—Critical pH ranges for sorption of divalent metal cations on hydrous iron and aluminum oxides (after Kinniburgh and Jackson, 1981). Generally, the critical pH range is higher for silica and lower for manganese oxides.

Cation	Critical pH Range
Cu, Pb, Hg	3 - 5
Zn, Co, Ni, Cd	5 - 6.5
Mn	6.5 - 7.5
Mg, Ca, Sr	6.5 - 9

Desorption

Desorption processes can be extremely important in understanding the mobility, bioavailability, and fate of metals in natural systems. The sorbent mineral acts as a sink for sorbed metals. When the metals desorb, the sorbent mineral can act as a constant source of metals to the surrounding solution (e.g., Wanty et al., 1999; Axe and Anderson, 1998). There are relatively few studies of metal desorption from natural materials. It is often observed that sorbed metals are not readily or completely desorbed (i.e., sorption reactions are partially irreversible; e.g., McKenzie, 1967; Gadde and Laitinen, 1974; McLaren et al., 1983, 1986; Padmanabham, 1983; Schultz et al., 1987; Backes et al., 1995). However, completely reversible sorption also has been observed (e.g., Gadde and Laitinen, 1974). Desorption also can be induced by dissolved species.

Barrow (1986) and Hogg et al. (1993) observed that increasing the contact time between soil and sorbed trace metals decreases the desorption of the metals. This may be due to diffusion of the metals into interior sites of the sorbent mineral (Axe and Anderson, 1998).

The reversibility of metal sorption in iron-rich systems can be influenced by the transformation or aging of metastable sorbent phases to more thermodynamically stable phases. Upon aging of metastable sorbent phases, some sorbed metals may be incorporated into the structure and other metals may be excluded from the structure (e.g., Ford et al., 1997).

DESCRIPTION OF SORPTION REACTIONS

Several empirical, semi-empirical, and mechanistic approaches are used to describe sorption reactions. The following brief discussion of several approaches is intended to provide an overview of how sorption reactions are described. More detailed discussions can be found in Sposito (1984), Stumm and Morgan (1996), and Jenne (1998).

Partition coefficients

The partition coefficient or distribution coefficient, K_d , is the ratio of the amount of adsorbate adsorbed per mass of adsorbent solid to the amount of the adsorbate remaining in solution per solution volume. The K_d can be expressed as:

$$K_d = q / C$$

where C is the adsorbate concentration remaining in solution and q is the amount of adsorbate adsorbed on the adsorbent solid. It is generally assumed that available adsorption sites are in ample excess compared with C .

The K_d is valid only under the conditions it is measured and cannot be extrapolated to other adsorbents, adsorbates, or aqueous conditions (e.g., pH, electrolyte concentrations, etc.; Reardon, 1981). Some researchers have normalized K_d values for variables such as surface area (Balistrieri and Murray, 1984) and aqueous speciation (Tessier et al., 1989).

Tabulations of K_d values have been made for use in contaminant transport models. For example, Thibault et al. (1990) tabulate K_d values for soils based on soil texture.

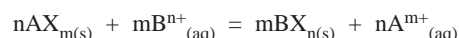
Particle concentration effect

It is commonly observed that K_d decreases with increasing total suspended solids. This effect, termed the particle concentration effect (PCE) or solids concentration effect, can have a substantial influence on solid-solution partitioning (O'Connor and Connolly, 1980; DiToro, 1985; Honeyman and Santschi, 1988). There is some controversy about what causes the PCE. Some possible explanations of the PCE include kinetics, irreversible adsorption, incomplete desorption, variations in surface chemistry, filtration artifacts, particle-particle interactions, and the presence of colloids in the filtrate. Morel and Gschwend (1987) and Benoit (1995) present data indicating that the PCE is due to metals associated with colloidal particles included in the "dissolved" fraction. McKinley and Jenne (1991) found that the PCE could often be attributed to experimental or data interpretation artifacts.

Ion exchange reactions

There are several meanings of ion exchange. The most general meaning is any replacement of an ion in a solid phase in contact with a liquid by another ion. In soil science the term ion exchange often means the replacement of one readily exchangeable ion by another ion. This implies surface phenomena involving outer-sphere complexes or ions in the diffuse layer (Sposito, 1984, 1989).

An ion-exchange reaction on a clay between cations A and B with valences of m and n , respectively, can be expressed as



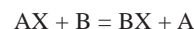
where X is the exchanger surface, $AX_{m(s)}$ and $BX_{n(s)}$ represent the exchanger surface with exchangeable cation A of valence m and exchangeable cation B of valence n , respectively, and $B^{n+}_{(aq)}$ and $A^{m+}_{(aq)}$ are aqueous cations.

As previously mentioned, most clay minerals have a permanently negative charge. This negative charge is compensated for by interlayer cations or accumulation of counterions. Clay minerals generally favor polyvalent cations over monovalent cations. Among the monovalent cations, they prefer the larger, less hydrated cations such as Cs^+ . Usually, clay minerals do not show much selectivity among multivalent cations of the same charge.

Thomas (1977) gives a good overview of historical developments concerning ion exchange in soil chemistry and Dzombak and Hudson (1995) and Mahoney and Langmuir (1991) provide a detailed discussion of electrostatic contributions to ion exchange. The understanding of exchange reactions is a starting point for understanding soil sorption phenomena in general.

Power exchange function

For the exchange reaction



the general power-exchange function can be written as

$$K_{ex} = \frac{[A]}{[B]} \left(\frac{[BX]}{[AX]} \right)^n$$

where the ratio of sorbed cation mole fractions is raised to the n th power (Langmuir, 1981, 1997). When $n \neq 1$ and $K_{ex} \neq 1$, the power exchange function can model trace element adsorption behavior on variable-charge surfaces.

Adsorption isotherms

Adsorption reactions are often described in terms of isotherms that relate the amount of an adsorbate in solution to the amount of adsorbate adsorbed at constant temperature. Adsorption isotherms are empirical and can be used to describe data but cannot be used to define adsorption mechanisms (Veith and Sposito, 1977).

Langmuir isotherm

The Langmuir isotherm can be written as:

$$q = kCb / (1 + kC)$$

where q is the amount of adsorbate adsorbed per unit mass of adsorbent, C is the adsorbate concentration remaining in solution

at equilibrium, b is the maximum adsorption capacity of the adsorbent (monolayer coverage), and k is a constant related to the binding strength. The Langmuir isotherm assumes (1) a finite number of surface sites, (2) no electrostatic or chemical interactions, (3) constant binding energy for all surface sites, (4) that binding energy is independent of the adsorption density, and (5) that maximum amount of adsorption is limited to a monolayer coverage of the surface sites (Adamson, 1990).

When the above equation is rearranged, a plot of C/q against C results in a linear representation of adsorption data with a slope of $1/b$ and an intercept of $1/kb$. In many cases, sorption in natural systems deviates from this linear representation.

Freundlich isotherm

The Freundlich isotherm can be written as:

$$q = KC^{1/n}$$

where q and C are previously defined, and K and n are positive empirical constants. The value of n is generally ≥ 1 ; in dilute solutions $n = 1$ but as the adsorption density increases $n > 1$.

When the above equation is rearranged to the linear form, a plot of $\log q$ against $1/n \log C + \log K$ results in a slope of $1/n$ and an intercept of $\log K$. One drawback of the Freundlich isotherm is that it does not predict an adsorption maximum (Sposito, 1980).

Affinity distributions

Affinity spectrum and log- K models are semi-empirical models to describe metal partitioning reactions in complex systems. For each site i for a one-dimensional case:

$$[C] [X_i] K_{MX_i} = [CX_i]$$

$$T_{X_i} = [X_i] + [CX_i]$$

where $[C]$ is the dissolved metal concentration, $[X_i]$ is the concentration of free binding sites of type i , $[CX_i]$ is the concentration of the bound metal, K_{MX_i} is the stability constant, and T_{X_i} is the total analytical concentration of binding sites of type i . Constants for the model are determined by setting values of K_{MX_i} equal to integral values that span the range of $[C]$ in solution, and then calculating corresponding values for T_{X_i} using a nonlinear least squares optimization procedure (Westall, 1994). A binding curve can be simulated by a distribution of values and thought of as a linear superposition of Langmuir isotherms (Borkovec et al., 1996).

Using empirically derived affinity distribution models, it is possible to quantitatively describe metal-partitioning reactions. This type of an approach may represent a preferred alternative to mechanistic sorption modeling in some heterogeneous natural systems (Westall et al., 1995). These models have interpolative abilities and may have some extrapolative abilities (Westall, 1994; Westall et al., 1995; Cernik et al., 1995, 1996; Borkovec et al., 1996).

Surface-complexation models

A surface complex can be defined as the stable molecular unit formed out of the reaction between a chemical species in aqueous solution and a functional group exposed at the surface of a solid (Sposito, 1995). Table 7.4 illustrates some types of surface complexes that can form on metal-oxide mineral surfaces. In the surface-complexation approach (Stumm et al., 1970, 1976; Schindler and Gamsjager, 1972; Schindler et al., 1976) sorption of ions on surfaces of oxide minerals is treated as analogous to the formation of aqueous complexes. Hence, these surface-complexation reactions can be described by mass-law equations. Surface-complexation reactions have an additional coulombic-correction term incorporated into their mass-law equations that takes into account electrostatic effects due to variable surface charge.

Several surface-complexation models (SCM) exist and have been reviewed and evaluated by Westall and Hohl (1980), Morel et al. (1981), Westall (1986), Davis and Kent (1990), Dzombak and Morel (1990), and Goldberg (1992). Table 7.5 lists some SCM and gives the main references for each model. The models differ in their description of the structure of the electrical double layer, specifically in the number of planes within the interface, the relationships between charge and potential, and the location of surface complexes relative to the surface. These models require knowledge of concentrations of various adsorbing species, intrinsic constants that define the interaction between surface sites and each adsorbing species, and characteristics of the adsorbent surface such as capacitances, specific surface areas, and surface hydroxyl site densities.

The following criteria characterize all surface complexation models (Dzombak and Morel, 1990; Langmuir, 1997):

- 1) Sorption takes place at specific surface coordination sites.
- 2) Sorption reactions can be described by mass law equations.

TABLE 7.4—Surface complexes between metal-oxide functional groups and solutes. X represents a binding site on an oxide-mineral surface, M represents a cationic metal solute, and L represents an anionic solute.

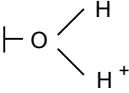
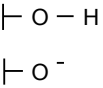
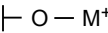
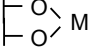
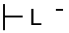
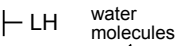
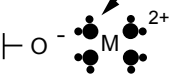
Proton Exchange:	
$XOH_2^+ = XOH + H^+$	
$XOH = XO^- + H^+$	
Cation Complexes:	
$XOH + M^{2+} = XOM^+ + H^+$	
$2XOH + M^{2+} = (XO)_2M + 2H^+$	
Anion Complexes:	
$XOH + L^{2-} + H^+ = XL^- + H_2O$	
$XOH + L^{2-} + 2H^+ = XHL + H_2O$	
Outer-Sphere Complexes:	
$XOH + M^{2+} + H_2O = XO^-(H_2O)M^{2+} + H^+$	

TABLE 7.5—Some types of surface-complexation models with brief descriptions and references. Information from Davis and Kent (1990); Goldberg (1992); and Sposito (1995).

Model	Comments	References
Diffuse Double-Layer Model (DDLDM)	Two interfacial planes; surface plane contains H^+ , OH^- , and inner-sphere complexes; diffuse-layer plane contains outer-sphere complexes	Stumm et al., 1970; Huang and Stumm, 1973
Constant Capacitance Model (CCM)	Special case of DDLDM; all surface complexes are inner sphere; linear relationship between surface charge and surface potential	Schindler and Gamsjager, 1972; Hohl and Stumm, 1976
Generalized Two-Layer Model (GTLM)	Based on DDLDM with additional features; two binding-site types for cations; all surface complexes are inner sphere	Dzombak and Morel, 1990
Triple-Layer Model (TLM)	Two capacitance layers and a diffuse layer; three layers relate potential to charge; H^+ and OH^- are inner sphere; metals and ligands are outer-sphere	Davis and Leckie, 1978b, 1980
Modified Triple-Layer Model (TLM)	Enhancement of original TLM; allows metals and ligands to be inner-sphere	Hayes and Leckie, 1986, 1987
Four-Layer Model (FLM) (a.k.a. Stern Variable Surface Charge-Variation Surface Potential Model (VSC-VSP))	Combines CCM and TLM; H^+ , OH^- , and strongly sorbed ions are inner-sphere; weakly sorbed ions are outer-sphere	Bowden et al., 1977, 1980; Barrow et al., 1980, 1981
One-pK Stern Model	H^+ and OH^- are inner-sphere; metals and ligands are outer-sphere	Bolt and van Riemsdijk, 1982; van Riemsdijk et al., 1986, 1987; Hiemstra et al., 1987

- 3) Surface charge results from the sorption reaction itself.
- 4) The effect of surface charge on sorption can be taken into account by applying a correction factor derived from electric double-layer theory to the mass law constants for surface reactions.

SCM can describe data over a broad range of conditions such as varying pH, ionic strength, adsorbate concentrations, adsorbent concentrations, and solution conditions.

Electrical double-layer theory

The distribution of electrical potential at the solid-solution interface has been envisioned as a double layer of charge, the electrical double layer (EDL), in which one layer of charge is localized next to the surface and the other layer is developed in a diffuse region extending out into the solution (Adamson, 1990; Stumm and Morgan, 1996). Many of the SCM that describe sorption behavior are based on EDL theory developed by Gouy (1910) and Chapman (1913) who mathematically describe the diffuse distribution of ions adjacent to a charged surface. Stern later modified the Gouy-Chapman model to include a layer of counterions (ions of opposite charge to the surface charge) nearest the charged surface. James and Healy (1972a, b), Adamson (1990), Shaw (1980), Stumm and Morgan (1996), and Singh and Uehara (1986) provide a detailed discussion of EDL theory.

Figure 7.4 shows the Gouy-Chapman model of the diffuse double layer (DDL), which illustrates a negatively charged surface and the distribution of cations and anions with distance from the surface. The counterions are most concentrated nearest the surface and decrease exponentially with distance away from the surface. The coions (ions having the same charge as the surface) are depleted nearest the charged surface. Calculations show that for a counterion concentration of 1 mmol/dm^3 , the thickness of the double layer will be 10 nm for monovalent counterions and 5 nm for divalent counterions (van Olphen, 1977).

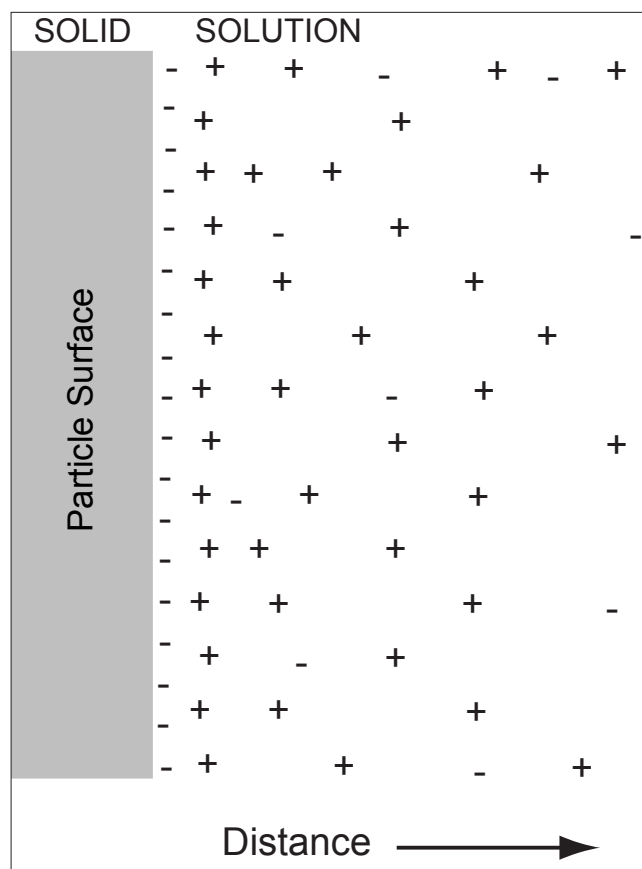


FIGURE 7.4—Cartoon of the diffuse double layer adjacent to a negatively charged surface. Positively charged counterions are most concentrated near the surface with decreasing concentration away from the surface. Modified from van Olphen (1977).

Inner-sphere and outer-sphere complexes

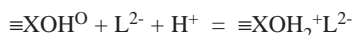
SCM refer to specific and non-specific ion binding on an oxide surface as inner-sphere and outer-sphere complexes, respectively. In the formation of inner-sphere complexes, a largely covalent bond between the surface and the ion is formed. Inner-sphere complexes can affect the reactivity of a surface (Sposito, 1984; Stumm, 1992, 1995, 1998). In the case of an outer-sphere complex, an ion of opposite charge approaches the surface, and the ion and the surface are separated by one or more water molecules (see Table 7.4). These types of bonds are largely electrostatic. Outer-sphere complexation is usually a rapid, reversible process. In contrast, inner-sphere complexation tends to be somewhat slower, and not completely reversible. Adsorption of inner-sphere complexes can occur on a surface regardless of surface charge. The distinction between inner- and outer-sphere is important because the bound species have different chemical properties depending upon how they are bound to the surface.

The presence of inner-sphere complexes has been confirmed by the use of spectroscopy (Hayes et al., 1987; Chisholm-Brause et al., 1990; Roe et al., 1991). Brown (1990) provides an overview of spectroscopic studies. Another method used to distinguish inner-sphere and outer-sphere complexes is to assess the effect of ionic strength on the surface complex. Outer-sphere complexes typically have a strong dependence on ionic strength (Hayes and Leckie, 1987; Hayes et al., 1988).

Ligand exchange: Strongly binding anions sorb on metal-oxide minerals by a ligand exchange mechanism (Stumm et al., 1980; Harrison and Berkheiser, 1982). This mechanism involves the exchange of an anion for a surface hydroxyl group:



where $\equiv\text{XOH}^{\text{O}}$ is a surface binding site, L^{2-} is a divalent anion, and $\equiv\text{XHL}^{\text{O}}$ and $\equiv\text{XL}^-$ are surface complexes. This results in the formation of an inner-sphere complex. In contrast, weaker binding anions sorb through electrostatic interactions with the oxide surface and a water molecule remains between the surface site and the sorbed anion (Hayes et al., 1987):



which results in an outer-sphere complex.

Model parameters

Different surface complexation models require different parameters. The following tabulation lists parameters required for three of the models (Sparks, 1995; Langmuir, 1997).

<u>Diffuse</u>	<u>Constant Capacitance</u>	<u>Triple Layer</u>
Double-Layer		
Specific surface area	Specific surface area	Specific surface area
Total site concentration	Total site concentration	Total site concentration
pK for proton gain	pK for proton gain	pK for proton gain
pK for proton loss	pK for proton loss	pK for proton loss
pK for metal binding	pK for metal binding	pK for metal binding
	1 capacitance	pK for electrolyte
		2 capacitances

These parameters represent fitted or separately determined values. Generally, fitted parameters are determined with the use of numerical optimization techniques. Each of the models contain different parameters or different parameter values because each of the models assumes different geometric features of the oxide-water interface. Westall and Hohl (1980) demonstrated that five different SCM could fit proton adsorption data on Al_2O_3 equally well despite their mutually contradictory underlying molecular hypotheses. This is because of the adjustable parameters that can be employed to fit the data (Dzombak and Morel, 1987).

Literature sorption data have been interpreted with a variety of SCM. Because the parameters for these SCM are different, literature sorption parameter values and surface-complexation constants are not consistent. Parameter values and sorption constants are not interchangeable between SCM.

MODELING METAL-SORPTION REACTIONS IN NATURAL SYSTEMS

Knowing the distribution of metals between dissolved and particulate phases is important in understanding their ecological impact, transport and fate, and infiltration into ground-water systems. Particulates in natural systems consist of mixtures of different organic and inorganic materials, which makes predictive sorption modeling a formidable task. Some attempts have been made to characterize the metal-binding properties of naturally occurring particulates (Vuceta and Morgan, 1978; Balistrieri et al., 1981; Luoma and Bryan, 1981; Lion et al., 1982; Balistrieri and Murray, 1983, 1984; Mouvet and Bourg, 1983; Tessier et al., 1985; Muller and Sigg, 1990; Ali and Dzombak, 1996; Tessier et al., 1996; Wang et al., 1997; Payne et al., 1998; Smith et al., 1998; and Wen et al., 1998).

Although many of the empirical approaches to sorption reactions (e.g., isotherms) are descriptive, they are not predictive, especially beyond the conditions measured. This discussion will emphasize surface-complexation models (SCM) because they have predictive capabilities beyond the measured conditions. Surface complexation reactions and other descriptions of sorption reactions (such as K_d) have been incorporated into several speciation and transport modeling codes.

Modeling difficulties

When modeling sorption reactions in natural systems, an assumption often is made that most of the reactive metal-binding surfaces are natural organic matter, and hydrous oxides of iron, manganese, aluminum, and silica. Crystalline minerals and clay minerals generally are of lesser importance. In natural systems low in organic matter, metal sorption is commonly thought to be controlled by iron- and aluminum-oxide coatings on particle surfaces (Davis and Kent, 1990). Metal sorption by pure oxide phases can be successfully predicted by SCM (e.g., Dzombak and Morel, 1990). Application of SCM to natural systems necessitates detailed characterization of the solid phases and their surface composition. Many of the experimental techniques that are used to characterize sorption and EDL properties in simple mineral-water systems cannot be applied in a straightforward manner to soils and sediments. The real trick is determining the types and concentrations of important surface functional groups and their reactive surface areas.

Incorporation of metal binding on natural organic matter (NOM) into predictive sorption models presents a major challenge (Kinniburgh et al., 1998). Binding site concentrations and constants are not easily determined for NOM. Discussion of metal binding on NOM is beyond the scope of this paper. However, NOM may play an important role in many cases and there are some NOM metal-binding models and approaches that look promising (e.g., Wilson and Kinney, 1977; Cabaniss et al., 1984; Ephraim et al., 1986; de Wit et al., 1991; Bartschat et al., 1992; Tipping and Hurley, 1992; Benedetti et al., 1995; Tipping et al., 1995; and Westall et al., 1995). Future developments may allow incorporation of NOM into predictive sorption models. Metal sorption onto biological surfaces also has been considered (e.g., Beveridge and Murray, 1976; Hudson and Morel, 1990; Sigg, 1994; and Fein et al., 1997). Sorption of dissolved organic carbon onto oxide minerals can be an important mechanism in some systems (e.g., McKnight et al., 1992). Westall et al. (1995) suggest the use of semi-empirical models, instead of mechanistic models, for complex systems. This approach offers an alternative for many applications including the incorporation of metal-partitioning capabilities into transport models.

Langmuir (1997, p. 392–393) suggests several questions be asked when applying adsorption models to natural systems. Among those questions are: (1) when multiple sorbent phases are present, which are most likely to interact with the sorbate species of interest?; (2) when multiple sorbent phases are present, can we simplify the problem and limit our analysis to adsorption by a single sorbent?; (3) what are the absolute and relative abundances of important sorbent phases and what fraction of their surface areas is exposed to flowing water?; and (4) what is the chemical composition of the water?

Additivity and interactive effects between phases

There is an ongoing controversy about whether or not the sorptive properties of minerals are the same in mixtures as they are individually. Honeyman (1984) found differences in sorptive properties when certain minerals were present in mixtures. Anderson and Benjamin (1990) showed that aluminum hydroxide in a binary system altered the surface chemical properties of the other mineral phase. Meng and Letterman (1993) also noted altered sorptive properties due to interference by aluminum hydroxide. Davis (1984) reported that dissolved organic carbon was able to coat metal-oxide minerals in many natural systems. This organic coating interacted strongly with some metals, such as Cu, and did not seem to affect other metals, such as Cd.

On the other side of the sorption additivity controversy, Davies-Colley et al. (1984) found little difference in sorptive properties of a variety of minerals in mixtures. Siegel et al. (1992) successfully modeled sorption in a mixture of goethite and montmorillonite. The compilation of Vandergraaf et al. (1993) assumes additivity of the sorptive properties of minerals. Tessier et al. (1996) modeled sorption reactions in a natural system assuming additivity of sorptive properties.

It appears that some amorphous minerals and dissolved organic carbon are able to alter the sorptive properties of minerals in some mixed systems. Consequently, the assumption of sorptive additivity in natural systems should be made with caution. When possible, empirical observations of sorption reactions on natural materials should be made for the mixture as a whole.

Surface functional groups

As mentioned, one of the most difficult tasks in modeling is the identification and quantification of surface functional groups in heterogeneous mixtures of mineral phases. In many cases the surface chemical properties of natural materials are dominated by secondary minerals and coatings, which usually constitute only a minor fraction of the whole sample (e.g., Davis, 1984). Techniques to measure these parameters must be chosen with care. Balistrieri and Murray (1983) used tritium exchange to estimate the total density of surface sites on marine sediments and noted that these data compared well with those from simpler cation exchange measurements (Balistrieri and Murray, 1984). Zachara et al. (1989) estimated site densities from sorption data by applying the Langmuir isotherm. If a particular mineral phase is thought to dominate sorption processes, site densities can be estimated from the abundance of the mineral phase in the bulk material (e.g., Smith, 1991).

For coatings, abundance can be estimated by partial chemical extractions (e.g., Chao and Zhou, 1983; Chao, 1984; Tessier et al., 1989). For example, Fuller et al. (1996) used partial chemical extractions combined with surface area measurements to estimate metal sorption in a sand and gravel aquifer. Jenne and Creclius (1988) used partial chemical extractions to estimate the quantities of amorphous iron- and manganese-oxide sorbents, reactive particulate organic carbon, and associated sorbed metals in fine-grained sediments.

Iron oxide minerals are generally the primary adsorbent for transition metals in oxic environments unless unusual amounts of other adsorbents exist (Jenne, 1998). In the absence of evidence of sorptive dominance by a particular component, the bulk can be modeled. Davis and Kent (1990) recommend that the reactive surface area be multiplied by an average value for site density of surface hydroxyl groups per unit surface area. They suggest a single value for total surface-site density of 2.31 sites/nm² (or 3.84 $\mu\text{moles/m}^2$; Dzombak and Morel, 1990). In this way a uniform value can be accepted for modeling site density and metal adsorption density.

Several spectroscopic and microscopic techniques, such as scanning Auger microscopy, show promise for the examination and determination of surface functional groups. For example, Hayes et al. (1987) examined surface complexes of SeO_3^{2-} on goethite. Hochella (1990) and Sposito (1995) discuss several of these techniques.

Reactive surface area

One of the most difficult parameters to estimate for model input is the reactive surface area of the various sorbent materials. Surface-area estimates are dependent on the analysis used to determine them. Warren and Zimmerman (1994) found that, in the case of mixed coatings on particulates, the exposed surface area for a given geochemical phase is not well represented by surface areas estimated from single component sediments or by calculated estimates using total surface area measurements and concentration data for suspended particulate matter. Wanty et al. (1991) suggest a method that involves calculating the minimum surface area of a model sorbent required to reduce the sorbate concentration to a value of the difference between the dissolved concentration in equilibrium with saturation indices and the observed value

in natural water. Davis and Kent (1990) state that gas adsorption techniques yield the most useful information, including estimates of external surface area and an evaluation of the extent of microporosity. Gas absorption techniques can be problematic for porous sorbents (White and Peterson, 1990; Chiou and Rutherford, 1993).

Surface-complex data sets

A drawback of SCM is the lack of complete internally consistent data sets of surface complexes. Determining such complexes is cumbersome. Data for several different types of sorption models are in the literature, but surface complexation data are not interchangeable between models. Therefore, it is extremely important to stick with one type of surface complexation model when compiling a data set. Dzombak and Morel (1990) and Smith and Jenne (1991) have published internally consistent data sets for the GTLM and TLM, respectively, and Turner (1995) compiled a data set for radionuclide sorption using the TLM.

MODELING METAL-SORPTION REACTIONS IN MINE-DRAINAGE SYSTEMS

Mine-drainage systems offer a rather unique situation for metal-sorption modeling. Due to the often high levels of iron in these systems, they represent a case in which metal-sorption reactions usually are dominated by a single component, hydrous ferric oxide (HFO). Therefore, the types of functional groups are known, and the quantity of functional groups can be estimated from the bulk iron content.

Role of iron-oxide minerals

Iron-oxide minerals are ubiquitous in the near-surface environment and are common components of natural gossans, soils, and mine waste. Several different iron-oxide minerals have been identified in nature. Hydrous ferric oxide (a.k.a. amorphous ferric hydroxide, amorphous iron oxyhydroxide, and ferrihydrite) is the solid formed upon rapid hydrolysis of ferric Fe solutions at 20–30°C (Dzombak and Morel, 1990). HFO is usually amorphous or nearly amorphous as determined by X-ray diffraction. The stoichiometry is uncertain and is represented by the general formula $\text{Fe}_2\text{O}_3 \cdot n\text{H}_2\text{O}$. Measurements and calculations of associated surface areas vary widely. Upon aging, HFO gradually transforms to a crystalline oxide, usually goethite ($\alpha\text{-FeOOH}$).

Dzombak and Morel (1990) defined properties of HFO in order to extract surface-complexation constants from experimental data using the GTLM. Table 7.6 lists some of those HFO properties. Dzombak and Morel (1990) developed an internally consistent database for metal sorption on HFO for the GTLM. Although the iron-rich precipitates in mine-drainage systems consist of a variety of iron-oxide minerals, it is possible to consider them in bulk and lump them under the “HFO definition.”

Previous studies of metal partitioning in mine-drainage systems

Downstream decreases in dissolved metal concentrations will occur due to oxidation, precipitation, sorption, and dilution

processes. Several researchers have studied metal dispersion and attenuation in acidic, metal-rich drainages. The following discussion covers some representative studies from the literature. There is a wide variety of data in the literature, but no clear-cut picture exists as to how to anticipate metal mobility in mine-drainage systems. Additional studies include Theobald et al. (1963), Collins (1973), Foster et al. (1978), Filipek et al. (1981), Robinson (1981, 1983), Kuwabara et al. (1984), Johnson (1986), Jones (1986), Andrews (1987), Bencala et al. (1987), Karlsson et al. (1987, 1988a, 1988b), Fuller and Davis (1989), Rampe and Runnells (1989), Axtmann and Luoma (1991), Sanden (1991), Winland et al. (1991), Howell (1994), Kimball et al. (1994, 1995), Webster et al. (1994), Benner et al. (1995), Broshears et al. (1996), Levy et al. (1997), and Paulson (1997).

TABLE 7.6—Properties of hydrous ferric oxide used in the extraction of surface-complexation constants from experimental data using the Generalized Two-Layer surface-complexation model (data from Dzombak and Morel, 1990).

Specific Surface Area	=	600 m ² /g
High-Affinity Site Density	=	0.005 moles sites / mole Fe
Low-Affinity Site Density	=	0.2 moles sites / mole Fe
Stoichiometry	=	$\text{Fe}_2\text{O}_3 \cdot \text{H}_2\text{O}$
Molecular Weight	=	89 g HFO/mole Fe
Pristine Point of Zero Charge	=	8.1

Chapman et al. (1983) found that a combination of sorption, precipitation, and dilution processes accounts for the decrease in concentration of dissolved elements in two streams (pH 2.7–3.2 and pH 3.1–6.8) in New South Wales, Australia. In the lower-pH stream, they report that Al, As, Fe, SiO_2 , and SO_4^{2-} are reactive constituents resulting from the precipitation of Fe as amorphous ferric hydroxide and the subsequent sorption of Al, As, SiO_2 , and SO_4^{2-} . They attribute diminished concentrations of Cd, Cu, and Zn to dilution effects. In the higher-pH stream, Chapman and others found that Al, Cu, Fe, and Pb are reactive elements, and that Al, Cu and Fe probably precipitate. They attribute decreased Pb concentrations to sorption reactions and decreased concentrations of Cd, Mn, and Zn to dilution effects.

Filipek et al. (1987) studied confluences of acidic metal-rich waters with West Squaw Creek, California. They found that the ratios of sorbed Cu, Mn, and Zn concentrations to dissolved concentrations are a function of pH with the least amount of sorption taking place at lower pH. They observed that As is quickly scavenged from solution near its source. They calculate that both ferric hydroxides and jarosite are at saturation in these waters.

Davis et al. (1991) examined factors that affect element partitioning between water and suspended sediment in North Clear Creek (pH 5.8–7.4), Colorado. Based on mass balance calculations, they found that Al, Ca, Cl, F, and Zn (and perhaps Cd, K, Mg, and Na) behave conservatively whereas Cu, Fe, Mn, and SO_4^{2-} are reactive. They observed that Al, Cu, and Fe are mainly associated with the suspended sediment, and Cd, Mn, and Zn are present predominantly as dissolved species. They concluded that Al and Fe solubilities are controlled by precipitation and that dissolved Cu is controlled by sorption reactions. Based on batch laboratory desorption studies using sediment collected from North Clear Creek, Davis and others found the affinity sequence of metals for the sediment to be $\text{Al} > \text{Cu} > \text{Zn} > \text{Mn}$.

Webster et al. (1998) studied sorption of metals onto a natural iron(III) oxy hydroxy sulfate mineral precipitated in a mine-drainage system and compared those results with sorption studies using synthetic schwertmannite and pure hydrous iron(III) oxide. They found that Cu and Zn sorption onto the natural precipitate was greater than that onto synthetic schwertmannite, which was in turn greater than that onto hydrous iron oxide. Cadmium sorption was also enhanced onto the natural precipitate. Sorption modeling generally underestimated the degree of metal sorption onto the natural precipitate.

Predictive modeling of metal mobility in mine-drainage systems

Smith and colleagues (Smith et al., 1989, 1991, 1998; Smith and Macalady, 1991; Smith, 1991, 1996) studied metal-sorption reactions between stream water and streambed sediment from St. Kevin Gulch, Colorado, a subalpine stream impacted by mine drainage. They performed batch pH-dependent metal-partitioning experiments (see Smith, 1991 for details) using the natural stream water and streambed sediment, and observed that the metal-partitioning reactions follow previously observed trends (Kinniburgh et al., 1976; Benjamin, 1979) for sorption of metals by synthetic HFO. They successfully used the GTLM surface-complexation model to predictively model metal sorption reactions on natural iron-rich streambed sediment. This work demonstrates that predictive SCM can be used for modeling mine-drainage systems and provides a field validation for the GTLM coupled with the MINTEQA2 computer program (Allison et al., 1991).

The previous studies lay the groundwork for additional metal-sorption studies and predictive modeling in a variety of mine-drainage systems (Smith et al., 1992, 1993, 1994, 1998; Webster et al., 1994). The general approach is briefly outlined below.

General sorption-modeling approach

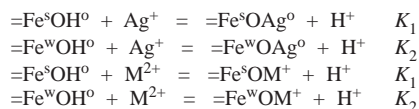
Computer simulations of sorption reactions employ the equilibrium speciation program MINTEQA2 (Allison et al., 1991) coupled with the GTLM and accompanying database of surface-complexation constants for HFO (Dzombak and Morel, 1990). MINTEQA2 computes sorption reactions and solution equilibria simultaneously in a self-consistent manner. The GTLM evokes a two-site model for cation sorption that includes a subset of high-affinity cation-binding sites. It is assumed that M^{2+} is the only metal species that sorbs on HFO. Table 7.7 lists some of the surface-complexation constants for metal sorption on HFO using the GTLM. It is important to note that the parameters and surface-complexation constants listed in Tables 7.6 and 7.7 are specific for HFO and for the GTLM. Consequently, use of these parameters and constants with other sorption models or for other sorbent surfaces is not valid.

Complete analytical data for water composition are input to MINTEQA2. The pH is fixed at desired values with the water in equilibrium with atmospheric carbon dioxide. Neither trace-metal hydroxide phases nor anglesite ($PbSO_4$) exceed saturation in the computer simulations. Only two solid phases, ferrihydrite and amorphous aluminum hydroxide, are allowed to precipitate in the simulations because they are the most likely solids to control Fe and Al solubilities during the 6-hour time frame of the batch experiments (6 hours were determined to be adequate from sorp-

tion-rate experiments; see Smith, 1991; Smith et al., 1998).

TABLE 7.7—Derived and estimated surface-complexation constants for metal-cation sorption on hydrous ferric oxide from the Generalized Two-Layer sorption model (data from Dzombak and Morel, 1990).

Cation	$\log K_1^{int}$	$\log K_2^{int}$
Ag ⁺	-0.72	-5.3
Ba ²⁺	5.46	-7.2
Be ²⁺	5.7	3.3
Cd ²⁺	0.47	-2.90
Co ²⁺	-0.46	-3.01
Cu ²⁺	2.89	0.6
Hg ²⁺	7.76	6.45
Mn ²⁺	-0.4	-3.5
Ni ²⁺	0.37	-2.5
Pb ²⁺	4.65	0.3
Sn ²⁺	8.0	5.9
UO ₂ ²⁺	5.2	2.8
Zn ²⁺	0.99	-1.99



HFO is the sole sorbent material in the model simulations. All of the Fe in the sediment is assumed to be present as HFO and calculations of binding-site concentrations and total amorphous Fe are based on this assumption. As suggested by Dzombak and Morel (1990), for conversions from g/l HFO to mole/l Fe, the stoichiometry $Fe_2O_3 \cdot H_2O$ (89 g HFO/mole Fe) was assumed. In the case of suspended sediment, the difference between filtered and unfiltered Fe values in water is assumed to be the concentration of Fe in the suspended sediment. All of that Fe is assumed to be present as HFO.

All of the model input is derived either from chemical analyses or from information and parameters provided by Dzombak and Morel (1990). None of the model parameters were modified and no fitting of parameters is involved in these model simulations. A similar modeling approach has been used by Loux et al. (1989) and Stollenwerk (1994).

Importance of suspended sediment in sorption reactions

Smith et al. (1992) compared field data with computer-model predictions for metal sorption at ten diverse mine-drainage sites. In the mine-drainage streams they observed that metal sorption on iron-rich suspended sediment appears to regulate dissolved metal concentrations, with bed sediment playing a decidedly lesser role. They achieved good agreement between computer-model predictions and field measurements in mine-drainage streams when they assumed that all metal sorption takes place only on suspended sediment (i.e., no sorption on bed sediment). Therefore, it appears that a limited amount of sorbent material is available for metal-sorption reactions in mine-drainage streams. Figure 7.5 illustrates the consequences of having a limited amount of sorbent available. When there is abundant sorbent material present (Fig. 7.5A), well-defined adsorption edges result. However, when the sorbent material becomes limited and competition for binding sites with major

cations becomes more important (Fig. 7.5B), as is usually the case with metal sorption on suspended sediment in mine-drainage systems, less-defined adsorption edges result, and Zn, Cd, and Ni tend not to sorb at all. Consequently, Zn, Cd, and Ni would be expected to be mobile in many mining areas, which is observed by Plumlee et al. (1999).

SELF-MITIGATING CAPACITY OF MINE WATERS

The self-mitigating capacity of a mine water is the inherent ability of the water to clean itself up by removing dissolved metals from solution. It is related to the amount of dissolved Fe in the water that can precipitate and consequently attenuate dissolved metals by sorption reactions. Dissolved Fe commonly precipitates in response to oxidation or neutralization of mine waters. Self-mitigating capacity depends on the amount of dissolved Fe, the concentration and identity of dissolved metals, and the ratio of precipitated Fe (available surface-binding sites) to dissolved metals at a given pH.

The self-mitigating capacity of a mine water is useful for predicting metal mobility, providing guidance in remediation and planning, estimating pH and optimal conditions for removal of a particular metal, and predicting metal-removal efficiency. Dissolved or particulate Fe in a metal-contaminated watershed can have a positive influence on the attenuation of metals. However, Smith et al. (1992, 1993) observed that it is important to maximize contact between the particulate Fe and dissolved metals.

Method to predict self-mitigating capacity

Computer-model simulations can predict the self-mitigating capacity of a mine water. Smith et al. (1993, 1998) discuss this approach, which is summarized here. The simulations employ the

equilibrium speciation program MINTEQA2 (Allison et al., 1991) coupled with the GTLM as described previously.

To determine the amount of sorbent for the computer simulations, the dissolved Fe is assumed to precipitate and the concentration is converted to HFO. Two site densities are used, 0.005 moles sites per mole Fe for the high-affinity site densities and 0.2 moles sites per mole Fe for the low-affinity site densities as described previously. HFO is the sole sorbent material in the simulations and sorption on HFO is the sole mechanism for removal of trace metals in the simulations.

Examples

We now look at some examples of the use of computer-model simulations to predict the self-mitigating capacity of mine waters. These examples use data from actual mine waters and illustrate several concepts that are important in the self-mitigating capacity of mine waters.

Example 1—Oxygen-deficient mine water from a collapsed adit

Water containing ferrous Fe at pH 5.8 emanates from the collapsed Rawley-12 adit near Bonanza, Colorado. Table 7.8 lists the composition of the mine water. Figure 7.6 shows results from a computer simulation in which the dissolved Fe in the water precipitates and is allowed to sorb metals in the mine water. HFO sorbs most of the As, Cu, and Pb between pH 6 and about 7.5. HFO sorbs little Zn, Cd, or Ni at any pH between 6 and 8. Removal efficiency of Cu and Pb decreases above pH 7.5 due to competition by dissolved hydroxo and carbonato species. Cadmium and Ni concentrations were too low to show on the figure.

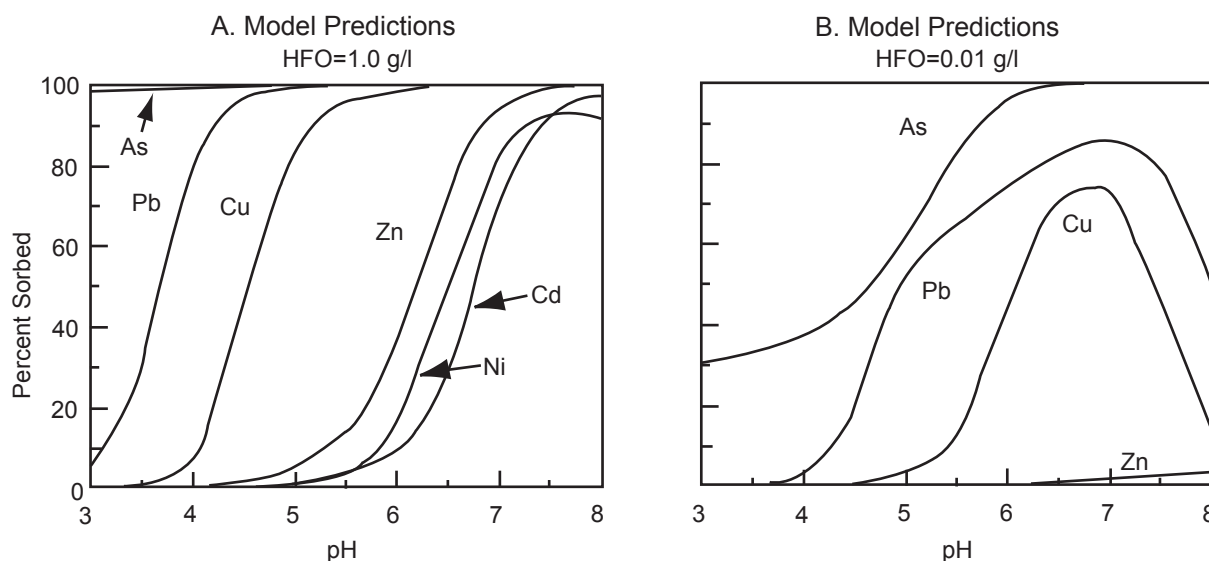


FIGURE 7.5—Model predictions of metal sorption on hydrous ferric oxide (HFO) as a function of pH for two different sorbent concentrations (A and B). After Smith et al. (1992).

This example illustrates that some oxygen-deficient waters can have a relatively good self-mitigating capacity once the Fe is oxidized and precipitated. Also, the computer simulation shows the importance of knowing an optimal pH range in order to maximize the removal efficiency of Cu.

TABLE 7.8—Chemical composition of filtered water from the Rawley-12 adit near Bonanza, Missionary East Seep at Summitville, and Tip Top adit adjacent to Gamble Gulch, Colorado. Samples were filtered through a 0.1 μm filter.

	Rawley-12 Adit	Missionary East Seep	Tip Top Adit
As ($\mu\text{g/l}$)	8.5	200	—
Pb ($\mu\text{g/l}$)	120	210	13
Cu ($\mu\text{g/l}$)	4,900	58,000	100
Zn ($\mu\text{g/l}$)	58,000	6,800	2,500
Cd ($\mu\text{g/l}$)	280	50	11
Ni ($\mu\text{g/l}$)	36	350	38
Fe (mg/l)	42	150	4.7
SO ₄ ²⁻ (mg/l)	700	1,540	300
pH (field)	5.7	3.8	3.8

Example 2—Low pH, high Fe and metals

The Missionary East Seep at Summitville, Colorado, discharges pH 3.8 water containing 150 mg/l of Fe and extremely high concentrations of some metals (see Table 7.8). Figure 7.7 shows computer-simulation results when this 150 mg/l dissolved Fe precipitates as HFO and sorbs dissolved trace metals over the pH range 4 to 8. Sorption of Ni over the pH range 4 to 8 was <1%, and sorption of Cd was <2% (curves not shown on Fig. 7.7). HFO sorbs most of the As and little of the Zn between pH 4 and 8. Removal efficiency of Cu never reaches values above about 40%.

This example illustrates that, even if it contains high Fe concentrations, a water may not have a particularly good self-mitigat-

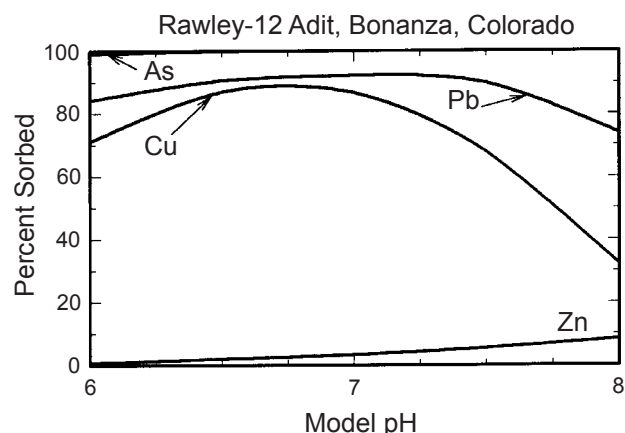


FIGURE 7.6—Computer simulation of metal sorption on hydrous ferric oxide (HFO) as a function of pH for drainage from the Rawley-12 adit, near Bonanza, Colorado. HFO concentration was derived from the precipitation of dissolved Fe originally present in the drainage.

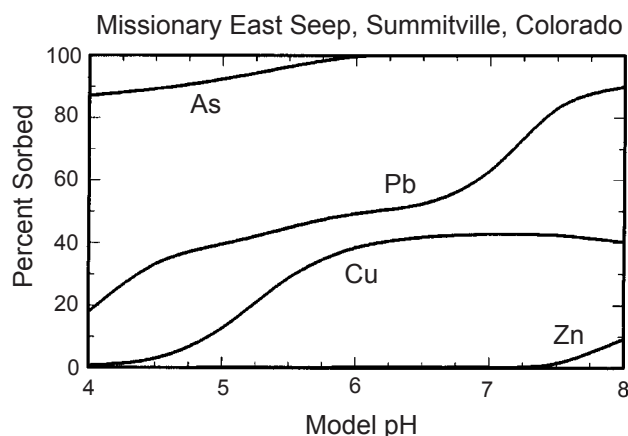


FIGURE 7.7—Computer simulation of metal sorption on hydrous ferric oxide (HFO) as a function of pH for drainage from the Missionary East Seep at Summitville, Colorado. HFO concentration was derived from the precipitation of dissolved Fe originally present in the drainage.

ing capacity. In this case, the extremely high concentration of Cu cannot be self-mitigated by more than about 40%. Dissolved Cu, Zn, Cd, and Ni can remain largely mobile in waters discharging from this site.

Example 3—Low pH, moderate Fe and metals

The Tip Top adit adjacent to Gamble Gulch, Colorado, discharges pH 3.8 water containing 4.7 mg/l of Fe and moderate concentrations of some metals (see Table 7.8). Figure 7.8 shows computer-simulation results when this 4.7 mg/l dissolved Fe precipitates as HFO and sorbs dissolved trace metals over the pH range 4 to 8. Sorption of Ni over the pH range 4 to 8 was <1%, and sorption of Cd was <2% (curves not shown in Fig. 7.8). HFO sorbs most of the Pb between pH 5.5 and 8 and little of the Zn between pH 4 and 8. Removal efficiency of Cu peaks at about 80% at pH values near 7. Removal efficiency of Cu decreases above pH 7.5 due to competition by dissolved hydroxo and carbonate species.

This example illustrates that, even though it contains only moderate Fe concentrations, a water may have a relatively good self-mitigating capacity at some pH values. In this case, HFO sorbs most of the Pb and Cu at around pH 7. However, dissolved Zn, Cd, and Ni can remain mobile in waters discharging from this site.

Applications

Some mine waters have the inherent ability to clean themselves up when discharged into the environment. Computer-model simulations can predict this self-mitigating capacity of mine waters. This approach could provide guidance in mine-drainage remediation and planning efforts.

Zinc, Cd, and Ni are difficult to self-mitigate in mine waters due to their relatively weak sorption on hydrous iron oxides. Consequently, these metals tend to remain mobile in waters discharging from mined lands. Elevated levels of Zn have been documented in numerous mine waters (e.g., Plumlee et al., 1999).

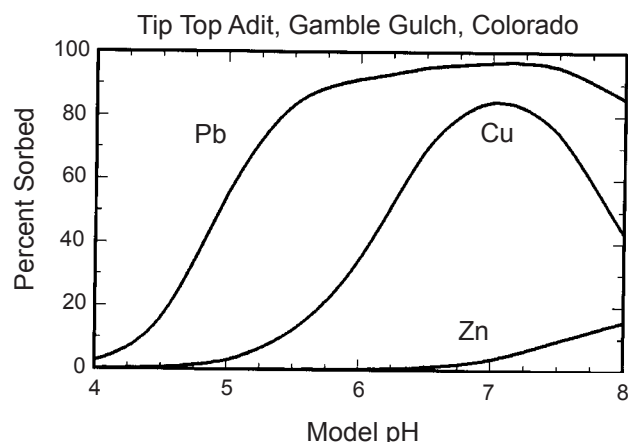
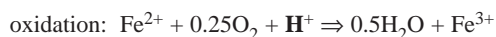


FIGURE 7.8—Computer simulation of metal sorption on hydrous ferric oxide (HFO) as a function of pH for drainage from the Tip Top adit adjacent to Gamble Gulch, Colorado. HFO concentration was derived from the precipitation of dissolved Fe originally present in the drainage.

The concept of self-mitigating capacity can be exploited in remediation activities. Addition of dissolved Fe to mine waters can enhance the eventual attenuation of dissolved metals. Computer simulations can predict the amount of additional Fe necessary to achieve the desired results. Iron and aluminum flocculants often are used in industry to clean up inorganic contaminants (e.g., Clifford et al., 1986).

An important factor to keep in mind with Fe-treatment systems is that, although the oxidation of Fe consumes acid, the precipitation of Fe generates acid as illustrated in the following equations:



When planning for pH adjustment, it is important to add enough base to counteract acidification by hydrolysis and precipitation reactions (not only for Fe but for all metals in the mine water).

Another important factor is that of desorption. Metal sorption may be transitory if conditions change to favor desorption. Change in factors such as pH, dissolved species, and temperature may trigger desorption reactions. Aging of sorbent material may also result in desorption of some metals.

ACKNOWLEDGMENTS—The author would like to thank L. Balistrieri and R. Wanty for their technical reviews of this manuscript and T.T. Chao and H. Huyck for their helpful comments. This work was funded through the Toxic Substances Hydrology and Mineral Resources Programs of the U.S. Geological Survey.

REFERENCES

- Adamson, A.W., 1990, *Physical chemistry of surfaces*, 5th ed.: Wiley, New York, 698 pp.
- Ahmed, S.M., and Maksimov, Dimitry, 1968, *Studies of the oxide surfaces at the liquid-solid interface. Part II. Fe oxides*: Canadian J. of Chemistry, v. 46, pp. 3841–3846.
- Ali, M.A., and Dzombak, D.A., 1996, Interactions of copper, organic acids, and sulfate in goethite suspensions: *Geochimica et Cosmochimica Acta*, v. 60, pp. 5045–5053.
- Allison, J.D., Brown, D.S., and Novo-Gradac, K.J., 1991, MINTEQA2/PRODEFA2, a geochemical assessment model for environmental systems: version 3.0 user's manual: U.S. Environmental Protection Agency Report EPA/600/3–91/021, 106 pp.
- Anderson, P.R., and Benjamin, M.M., 1990, Surface and bulk characteristics of binary oxide suspensions: *Environmental Science and Technology*, v. 24, pp. 692–698.
- Andrews, E.D., 1987, Longitudinal dispersion of trace metals in the Clark Fork River, Montana; in Averett, R.C., and McKnight, D.M. (eds.), *Chemical Quality of Water and the Hydrologic Cycle*: Lewis Pub., Chelsea, Mich., pp. 179–191.
- Avotins, P.V., 1975, Adsorption and coprecipitation studies of mercury on hydrous iron oxide: Ph.D. Thesis, Stanford University, Calif.
- Axe, L., and Anderson, P.R., 1998, Intraparticle diffusion of metal contaminants in amorphous oxide minerals; in Jenne, E.A. (ed.), *Adsorption of Metals by Geomedia*: Academic Press, San Diego, Calif., pp. 193–208.
- Axtmann, E.V., and Luoma, S.N., 1991, Large-scale distribution of metal contamination in the fine-grained sediments of the Clark Fork River, Montana, USA: *Applied Geochemistry*, v. 6, pp. 75–88.
- Backes, C.A., McLaren, R.G., Rate, A.W., and Swift, R.S., 1995, Kinetics of cadmium and cobalt desorption from iron and manganese oxides: *Soil Sci. Soc. Am. J.*, v. 59, pp. 778–785.
- Balistreri, L.S., and Chao, T.T., 1990, Adsorption of selenium by amorphous iron oxyhydroxide and manganese dioxide: *Geochimica et Cosmochimica Acta*, v. 54, pp. 739–752.
- Balistreri, L.S., and Murray, J.W., 1983, Metal-solid interactions in the marine environment: estimating apparent equilibrium binding constants: *Geochimica et Cosmochimica Acta*, v. 47, pp. 1091–1098.
- Balistreri, L.S., and Murray, J.W., 1984, Marine scavenging: trace metal adsorption by interfacial sediment from MANOP site H: *Geochimica et Cosmochimica Acta*, v. 48, pp. 921–929.
- Balistreri, L.S., Brewer, P.G., and Murray, J.W., 1981, Scavenging residence times of trace metals and surface chemistry of sinking particles in the deep ocean: *Deep-Sea Research*, v. 28A, pp. 101–121.
- Barrow, N.J., 1985, Reaction of anions and cations with variable-charge soils: *Advances in Agronomy*, v. 38, pp. 183–230.
- Barrow, N.J., 1986, Testing a mechanistic model. II. The effects of time and temperature on the reaction of zinc with a soil: *J. Soil Sci.*, v. 37, pp. 277–286.
- Barrow, N.J., Bowden, J.W., Posner, A.M., and Quirk, J.P., 1980, An objective method for fitting models of ion adsorption on variable charge surfaces: *Aust. J. Soil Res.*, v. 18, pp. 37–47.
- Barrow, N.J., Bowden, J.W., Posner, A.M., and Quirk, J.P., 1981, Describing the adsorption of copper, zinc and lead on a variable charge mineral surface: *Aust. J. Soil Res.*, v. 19, pp. 309–321.
- Bartschat, B.M., Cabaniss, S.E., and Morel, F.M.M., 1992, Oligoelectrolyte model for cation binding by humic substances: *Environ. Sci. Technol.*, v. 26, pp. 284.
- Bencala, K.E., McKnight, D.M., and Zellweger, G.W., 1987, Evaluation of natural tracers in an acidic and metal-rich stream: *Water Resources Research*, v. 23, pp. 827–836.
- Benedetti, M.F., Milne, C.J., Kinniburgh, D.G., van Riemsdijk, W.H., and Koopal, L.K., 1995, Metal-ion binding to humic substances—application of the nonideal competitive adsorption model: *Environ. Sci. Technol.*, v. 29, pp. 446–457.
- Benjamin, M.M., 1979, Effects of competing metals and complexing ligands on trace metal adsorption at the oxide/solution interface: Ph.D. Dissertation, Stanford University, Calif., 228 pp.
- Benjamin, M.M., 1983, Adsorption and surface precipitation of metals on amorphous iron oxyhydroxide: *Environmental Science and Technology*, v. 17, pp. 686–692.
- Benjamin, M.M., and Leckie, J.O., 1981a, Multiple-site adsorption of Cd, Cu, Zn, and Pb on amorphous iron oxyhydroxide: *Journal of Colloid and Interface Science*, v. 79, pp. 209–221.

- Benjamin, M.M., and Leckie, J.O., 1981b, Competitive adsorption of Cd, Cu, Zn, and Pb on amorphous iron oxyhydroxide: *Journal of Colloid and Interface Science*, v. 83, pp. 410–419.
- Benjamin, M.M., and Leckie, J.O., 1981c, Conceptual model for metal-ligand-surface interactions during adsorption: *Environmental Science and Technology*, v. 15, pp. 1050–1057.
- Benjamin, M.M., and Leckie, J.O., 1982, Effects of complexation by Cl, SO₄, and S₂O₃ on adsorption behavior of Cd on oxide surfaces: *Environmental Science and Technology*, v. 16, pp. 162–170.
- Benjamin, M.M., Hayes, K.F., and Leckie, J.O., 1982, Removal of toxic metals from power-generation waste streams by adsorption and coprecipitation: *Journal of the Water Pollution Control Federation*, v. 54, pp. 1472–1481.
- Benner, S.G., Smart, E.W., and Moore, J.N., 1995, Metal behavior during surface-groundwater interaction, Silver Bow Creek, Montana: *Environ. Sci. Technol.*, v. 29, pp. 1789–1795.
- Benoit, G., 1995, Evidence of the particle concentration effect for lead and other metals in fresh waters based on ultraclean technique analyses: *Geochimica et Cosmochimica Acta*, v. 59, pp. 2677–2687.
- Beveridge, T.J., and Murray, R.G.E., 1976, Uptake and retention of metals by cell walls of *Bacillus subtilis*: *J. Bacteriol.*, v. 127, pp. 1502–1518.
- Bigham, J.M., Schwertmann, U., Carlson, L., and Murad, E., 1990, A poorly crystallized oxyhydroxysulfate of iron formed by bacterial oxidation of Fe(II) in acid mine waters: *Geochimica et Cosmochimica Acta*, v. 54, pp. 2743–2758.
- Bolt, G.H., and van Riemsdijk, W.H., 1982, Ion adsorption on inorganic variable charge constituents; in Bolt, G.H. (ed.), *Soil Chemistry, Part B. Physico-Chemical Models*: Elsevier, Amsterdam, pp. 459–503.
- Borkovec, M., Rusch, U., and Westall, J.C., 1996, Modeling of competitive ion binding to heterogeneous materials with affinity distributions; in Jenne, E.A. (ed.), *Adsorption of Metals by Geomedia*: Academic Press, San Diego, Calif., pp. 467–482.
- Bowden, J.W., Posner, A.M., and Quirk, J.P., 1977, Ionic adsorption on variable charge mineral surfaces—Theoretical charge development and titration curves: *Aust. J. Soil Res.*, v. 15, pp. 121–136.
- Bowden, J.W., Nagarajah, S., Barrow, N.J., Posner, A.M., and Quirk, J.P., 1980, Describing the adsorption of phosphate, citrate and selenite on a variable charge mineral surface: *Aust. J. Soil Res.*, v. 18, pp. 49–60.
- Borkovec, M., Rusch, U., Cernik, M., Koper, G.J.M., and Westall, J.C., 1996, Affinity distributions and acid-base properties of homogeneous and heterogeneous sorbents: exact results versus experimental data inversion: *Colloids and Surfaces A*, v. 107, pp. 285–296.
- Bowell, R.J., 1994, Sorption of arsenic by iron oxides and oxyhydroxides in soils: *Applied Geochemistry*, v. 9, pp. 279–286.
- Broshears, R.E., Runkel, R.L., Kimball, B.A., McKnight, D.M., and Bencala, K.E., 1996, Reactive solute transport in an acidic stream: experimental pH increase and simulation of controls on pH, aluminum, and iron: *Environ. Sci. Technol.*, v. 30, pp. 3016–3024.
- Brown, G.E., Jr., 1990, Spectroscopic studies of chemisorption reaction mechanisms at oxide-water interfaces; in Hochella, M.F., and White, A.F. (eds.), *Mineral-Water Interface Geochemistry: Reviews in Mineralogy, Mineralogical Society of America, Washington, D.C.*, v. 23, pp. 309–363.
- Brunninx, E., 1975, The coprecipitation of Zn, Cd and Hg with ferric hydroxide: *Phillips Research Reports*, v. 30, pp. 177–191.
- Cabaniss, S.E., Shuman, M.S., and Collins, B.J., 1984, Metal-organic binding: a comparison of models; in Kramer, C.J.M., and Duinker, J.C. (eds.), *Complexation of Trace Metals in Natural Waters*: Martinus Nijhoff / Dr. W. Junk Pub., The Hague, pp. 165–179.
- Catts, J.G., and Langmuir, D., 1986, Adsorption of Cu, Pb and Zn by δ-MnO₂—Applicability of the site binding-surface complexation model: *Applied Geochemistry*, v. 1, pp. 255–264.
- Cernik, M., Borkovec, M., and Westall, J.C., 1995, Regularized least-squares methods for the calculation of discrete and continuous affinity distributions for heterogeneous sorbents: *Environ. Sci. Technol.*, v. 29, pp. 413–425.
- Cernik, M., Borkovec, M., and Westall, J.C., 1996, Affinity distribution description of competitive ion binding to heterogeneous materials: *Langmuir*, v. 12, pp. 6127–6137.
- Chao, T.T., 1984, Use of partial dissolution techniques in geochemical exploration: *J. Geochemical Exploration*, v. 20, pp. 101–135.
- Chao, T.T., and Zhou, L., 1983, Extraction techniques for selective dissolution of amorphous iron oxides from soils and sediments: *Soil Science Society America J.*, v. 47, pp. 225–232.
- Chapman, B.M., Jones, D.R., and Jung, R.F., 1983, Processes controlling metal ion attenuation in acid mine drainage streams: *Geochimica et Cosmochimica Acta*, v. 47, pp. 1957–1973.
- Chapman, D.L., 1913, A contribution to the theory of electrocapillarity: *Phil. Mag.*, v. 25, pp. 475–481.
- Chiou, C.T., and Rutherford, D.W., 1993, Sorption of N₂ and EGME vapors on some soils, clays, and mineral oxides and determination of sample surface areas by use of sorption data: *Environmental Science and Technology*, v. 27, pp. 1587–1594.
- Chisholm-Brause, C.J., O'Day, P.A., Brown, G.E., Jr., and Parks, G.A., 1990, Evidence for multinuclear metal-ion complexes at solid/water interfaces from X-ray absorption spectroscopy: *Nature*, v. 348, pp. 528–531.
- Clifford, D., Subramonian, S., and Sorg, T.J., 1986, Removing dissolved inorganic contaminants from water: *Environ. Sci. Technol.*, v. 20, pp. 1072–1080.
- Collins, B.I., 1973, The concentration control of soluble copper in a mine tailings stream: *Geochim. Cosmochim. Acta.*, v. 37, pp. 69–75.
- Coughlin, B.R., and Stone, A.T., 1995, Nonreversible adsorption of divalent metal ions (Mn, Co, Ni, Cu, Pb) onto goethite: effects of acidification, Fe addition, and picolinic acid addition: *Environ. Sci. Technol.*, v. 29, pp. 2445–2455.
- Davies-Colley, R.J., Nelson, P.O., and Williamson, K.J., 1984, Copper and cadmium uptake by estuarine sedimentary phases: *Environ. Sci. Technol.*, v. 18, pp. 491–499.
- Davis, A., Olsen, R.L., and Walker, D.R., 1991, Distribution of metals between water and entrained sediment in streams impacted by acid mine discharge, Clear Creek, Colorado, USA: *Applied Geochemistry*, v. 6, pp. 333–348.
- Davis, J.A., 1977, Adsorption of trace metals and complexing ligands at the oxide/water interface: Ph.D. Dissertation, Stanford University, Calif., 286 pp.
- Davis, J.A., 1984, Complexation of trace metals by adsorbed natural organic matter: *Geochimica et Cosmochimica Acta*, v. 48, pp. 679–691.
- Davis, J.A., and Hayes, K.F., 1986, Geochemical processes at mineral surfaces: an overview; in Davis, J.A., and Hayes, K.F. (eds.), *Geochemical Processes at Mineral Surfaces, American Chemical Society Symposium Series 323*: American Chemical Society, Washington, D.C., pp. 2–18.
- Davis, J.A., and Kent, D.B., 1990, Surface complexation modeling in aqueous geochemistry; in Hochella, M.F., and White, A.F. (eds.), *Mineral-Water Interface Geochemistry: Reviews in Mineralogy, Mineralogical Society of America, Washington, D.C.*, v. 23, pp. 177–260.
- Davis, J.A., and Leckie, J.O., 1978a, Effect of adsorbed complexing ligands on trace metal uptake by hydrous oxides: *Environmental Science and Technology*, v. 12, pp. 1309–1315.
- Davis, J.A., and Leckie, J.O., 1978b, Surface ionization and complexation at the oxide/water interface. 2. Surface properties of amorphous iron oxyhydroxide and adsorption of metal ions: *J. Colloid Interface Sci.*, v. 67, pp. 90–107.
- Davis, J.A., and Leckie, J.O., 1980, Surface ionization and complexation at the oxide/water interface. 3. Adsorption of anions: *J. Colloid Interface Sci.*, v. 74, pp. 32–43.
- Davis, J.A., James, R.O., and Leckie, J.O., 1978, Surface ionization and complexation at the oxide/water interface. I. Computation of electrical double layer properties in simple electrolytes: *Journal of Colloid and Interface Science*, v. 63, pp. 480–499.
- Davis, J.A., Kent, D.B., Rea, B.A., Maest, A.S., and Garabedian, S.P., 1993, Influences of redox environment and aqueous speciation on metal transport in groundwater: preliminary results of trace injection studies; in Allen, H.A., Perdue, E.M., and Brown, D.S. (eds.), *Metals in*

- Groundwater: Lewis Pub., pp. 223–273.
- de Wit, J.C.M., Nederlof, M.N., van Riemsdijk, W.H., and Koopal, L.K., 1991, Determination of proton and metal ion affinity distributions for humic substances: *Water Air Soil Pollut.*, v. 57–58, pp. 339.
- Di Toro, D.M., 1985, A particle interaction model of reversible organic chemical sorption: *Chemosphere*, v. 14, pp. 1503–1538.
- Donaldson, J.D., and Fuller, M.J., 1968, Ion exchange properties of tin (IV) materials, I. Hydrous tin (IV) oxide and its cation exchange properties: *J. Inorg. Nucl. Chem.*, v. 30, pp. 1083–1092.
- Dzombak, D.A., and Hudson, R.J.M., 1995, Ion exchange; *in* Huang, C.P., O'Melia, C.R., and Morgan, J.J. (eds.), *Aquatic Chemistry—Interfacial and Interspecies Processes*, ACS Advances in Chemistry Series No. 244: American Chemical Society, Washington, D.C., pp. 59–94.
- Dzombak, D.A., and Morel, F.M.M., 1986, Sorption of cadmium on hydrous ferric oxide at high sorbate/sorbent ratios: equilibrium, kinetics, and modeling: *J. Colloid Interface Sci.*, v. 112, pp. 588–598.
- Dzombak, D.A., and Morel, F.M.M., 1987, Adsorption of inorganic pollutants in aquatic systems: *Journal of Hydraulic Engineering*, v. 113, pp. 430–475.
- Dzombak, D.A., and Morel, F.M.M., 1990, Surface complexation modeling—hydrous ferric oxide: John Wiley and Sons, New York, 393 pp.
- Dzombak, D.A., Fish, W., and Morel, F.M.M., 1986, Metal-humate interactions. I. Discrete ligand and continuous distribution models: *Environmental Science and Technology*, v. 20, pp. 669–675.
- Eley, M., and Nicholson, K., 1994, Adsorption of metals on manganese oxides—towards an environmental model: *Environmental Geochemistry and Health*, v. 16, pp. 89–90.
- Ephraim, J., Alegret, S., Mathuthu, A., Bicking, M., Malcolm, R.L., and Marinsky, J.A., 1986, A unified physiochemical description of the protonation and metal ion complexation equilibria of natural organic acids (humic and fulvic acids). II. Influence of polyelectrolyte properties and functional group heterogeneity on the protonation equilibria of fulvic acid: *Environmental Science and Technology*, v. 20, pp. 354.
- Fein, J.B., Daughney, C.J., and Davis, T.A., 1997, A chemical equilibrium model for metal adsorption onto bacterial surfaces: *Geochim. Cosmochim. Acta*, v. 61, pp. 3319–3328.
- Filipek, L.H., Chao, T.T., and Carpenter, R.H., 1981, Factors affecting the partitioning of Cu, Zn and Pb in boulder coatings and stream sediments in the vicinity of a polymetallic sulfide deposit: *Chem. Geol.*, v. 33, pp. 45–64.
- Filipek, L.H., Nordstrom, D.K., and Ficklin, W.H., 1987, Interaction of acid mine drainage with waters and sediments of West Squaw Creek in the West Shasta Mining District, California: *Environmental Science and Technology*, v. 21, pp. 388–396.
- Fish, W., Dzombak, D.A., and Morel, F.M.M., 1986, Metal-humate interactions. II. Applications and comparison of models: *Environmental Science and Technology*, v. 20, pp. 676–683.
- Forbes, E.A., Posner, A.M., and Quirk, J.P., 1976, The specific adsorption of divalent Cd, Co, Cu, Pb, and Zn on goethite: *J. Soil Science*, v. 27, pp. 154–166.
- Ford, R.G., Bertsch, P.M., and Farley, K.J., 1997, Changes in transition and heavy metal partitioning during hydrous iron oxide aging: *Environ. Sci. Technol.*, v. 31, pp. 2028–2033.
- Foster, P. Hunt, D.T.E., and Morris, A.W., 1978, Metals in an acid mine stream and estuary: *Sci. Tot. Env.*, v. 9, pp. 75–86.
- Fuller, C.C., and Davis, J.A., 1989, Influence of coupling of sorption and photosynthetic processes on trace element cycles in natural waters: *Nature*, v. 340, pp. 52–54.
- Fuller, C.C., Davis, J.A., Coston, J.A., and Dixon, E., 1996, Characterization of metal adsorption variability in a sand and gravel aquifer, Cape Cod, Massachusetts, U.S.A.: *J. Contaminant Hydrology*, v. 22, pp. 165–187.
- Gadde, R.R., and Laitinen, H.A., 1974, Studies of heavy metal adsorption by hydrous iron and manganese oxides: *Analytical Chemistry*, v. 46, pp. 2022–2031.
- Goldberg, S., 1992, Use of surface complexation models in soil chemical systems: *Advances in Agronomy*, v. 47, pp. 233–329.
- Gouy, G., 1910, Sur la constitution de la charge électrique à la surface d'un électrolyte: *Ann. Phys. (Paris)*, v. 9, pp. 457–468.
- Gregg, S.J., and Sing, K.S.W., 1982, Adsorption, surface area and porosity: Academic Press, London, 303 pp.
- Grimme, H., 1968, Die adsorption von Mn, Co, Cu und Zn durch goethit aus verdünnten lösungen: *Z. Pflanzenernähr. Dung. Bodenkunde*, v. 121, pp. 58–65.
- Hachiya, K., Sasaki, M., Saruta, Y., Mikami, N., and Yasanuga, T., 1984, Static and kinetic studies of adsorption-desorption of metal ions on the α -Al₂O₃ surface: *J. Phys. Chem.*, v. 88, pp. 23–31.
- Harrison, J.B., and Berkheiser, V.E., 1982, Anion interactions with freshly prepared hydrous iron oxides: *Clays Clay Minerals*, v. 30, pp. 97–102.
- Harter, R.D., 1991, Kinetics of sorption/desorption processes in soil; *in* Sparks, D.L., and Suarez, D.L. (eds.), *Rates of Soil Chemical Processes*, Spec. Pub. No. 27: Soil Science Society of America, Madison, Wis., pp. 135–149.
- Hayes, K.F., and Leckie, J.O., 1986, Mechanism of lead ion adsorption at the goethite-water interface; *in* Davis, J.A., and Hayes, K.F. (eds.), *Geochemical Processes at Mineral Surfaces*, ACS Symposium Series 323: American Chemical Society, Washington, D.C., pp. 114–141.
- Hayes, K.F., and Leckie, J.O., 1987, Modeling ionic strength effects on cation adsorption at hydrous oxide/solution interfaces: *J. Colloid Interface Science*, v. 115, pp. 564–572.
- Hayes, K.F., Roe, A.L., Brown, G.E., Jr., Hodgson, K.O., Leckie, J.O., and Parks, G.A., 1987, In-situ X-ray absorption study of surface complexes at oxide-water interfaces: selenium oxyanions on α -FeOOH: *Science*, v. 238, pp. 783–786.
- Hayes, K.F., Papelis, C., and Leckie, J.O., 1988, Modeling ionic strength effects of anion adsorption at hydrous oxide/solution interfaces: *J. Colloid Interface Science*, v. 125, pp. 717–726.
- Hem, J.D., 1977, Reactions of metal ions at surfaces of hydrous iron oxide: *Geochimica et Cosmochimica Acta*, v. 41, pp. 527–538.
- Hem, J.D., 1985, Study and interpretation of the chemical characteristics of natural water, 3rd Edition: U.S. Geological Survey Water-Supply Paper 2254, 263 pp.
- Hering, J.G., and Morel, F.M.M., 1990, Kinetics of trace metal complexation: ligand exchange reactions: *Environmental Science and Technology*, v. 24, pp. 242–252.
- Hiemstra, T., van Riemsdijk, W.H., and Bruggenwert, M.G.M., 1987, Proton adsorption mechanism at the gibbsite and aluminum oxide solid/solution interface: *Neth. J. Agric. Sci.*, v. 35, pp. 281–293.
- Hildebrand, E.E., and Blum, W.E., 1974, Lead fixation by clay minerals: *Naturwissenschaften*, v. 61, pp. 169–170.
- Hingston, F.J., 1981, A review of anion adsorption; *in* Anderson, M.A., and Rubin, A.J. (eds.), *Adsorption of Inorganics at Solid-Liquid Interfaces*: Ann Arbor Science, Ann Arbor, Mich., pp. 51–91.
- Hingston, F.J., Atkinson, R.J., Posner, A.M., and Quirk, J.P., 1967, Specific adsorption of anions: *Nature*, v. 215, pp. 1459–1461.
- Hochella, M.F., Jr., 1990, Atomic structure, microtopography, composition, and reactivity of mineral surfaces; *in* Hochella, M.F., and White, A.F. (eds.), *Mineral-Water Interface Geochemistry: Reviews in Mineralogy*, Mineralogical Society of America, Washington, D.C., v. 23, pp. 87–132.
- Hogg, D.S., McLaren, R.G., and Swift, R.S., 1993, Desorption of copper from some New Zealand soils: *Soil Sci. Soc. Am. J.*, v. 57, pp. 361–366.
- Hohl, H., and Stumm, W., 1976, Interaction of Pb²⁺ with hydrous α -Al₂O₃: *J. Colloid Interface Science*, v. 55, pp. 281–288.
- Honeyman, B.D., 1984, Cation and anion adsorption at the oxide/solution interface in systems containing binary mixtures of adsorbents: an investigation of the concept of adsorptive additivity: Ph.D. Dissertation, Stanford University, Calif.
- Honeyman, B.D., and Santschi, P.H., 1988, Metals in aquatic systems: *Environmental Science and Technology*, v. 22, pp. 862–871.
- Horowitz, A.J., and Elrick, K.A., 1987, The relationship of stream sediment surface area and composition to trace element chemistry: *Applied Geochemistry*, v. 2, pp. 437–451.
- Hsi, C.-K.D., and Langmuir, D., 1985, Adsorption of uranyl onto ferric

- oxyhydroxides: application of the surface complexation site-binding model: *Geochim. Cosmochim. Acta*, v. 49, pp. 1931–1941.
- Huang, C.P., and Stumm, W., 1973, Specific adsorption of cations on hydrous α - Al_2O_3 : *J. Colloid Interface Science*, v. 43, pp. 409–420.
- Hudson, R.J.M., and Morel, F.M.M., 1990, Iron transport in marine phytoplankton—kinetics of cellular and medium coordination reactions: *Limnol. Oceanogr.*, v. 35, pp. 1002–1020.
- James, R.O., and Healy, T.W., 1972a, Adsorption of hydrolyzable metal ions at the oxide-water interface. I. Co(II) adsorption on SiO_2 and TiO_2 as model systems: *Journal of Colloid and Interface Science*, v. 40, pp. 42–52.
- James, R.O., and Healy, T.W., 1972b, Adsorption of hydrolyzable metal ions at the oxide-water interface. II. Charge reversal of SiO_2 and TiO_2 colloids by adsorbed Co(II), La(III), and Th(IV) as model systems: *Journal of Colloid and Interface Science*, v. 40, pp. 53–64.
- James, R.O., and Healy, T.W., 1972c, Adsorption of hydrolyzable metal ions at the oxide-water interface. III. A thermodynamic model of adsorption: *Journal of Colloid and Interface Science*, v. 40, pp. 65–79.
- James, R.O., and Parks, G.A., 1982, Characterization of aqueous colloids by their electrical double-layer and intrinsic surface chemical properties; in Matijevic, E. (ed.), *Surface and Colloid Science*, Vol. 12: Plenum Press, New York, pp. 119–216.
- Jenne, E.A., 1968, Controls on Mn, Fe, Co, Ni, Cu, and Zn concentrations in soils and water—the significant role of hydrous Mn and Fe oxides; in Gould, R.F. (ed.), *Trace Inorganics in Water, Advances in Chemistry Series No. 73*: American Chemical Society, Washington, D.C., pp. 337–387.
- Jenne, E.A., 1977, Trace element sorption by sediments and soils—sites and processes; in Chappell, W.R., and Peterson, K.K. (eds.), *Molybdenum in the Environment*, Vol. 2: Marcel Dekker, New York, pp. 425–553.
- Jenne, E.A., 1998, Adsorption of metals by geomedial: data analysis, modeling, controlling factors, and related issues; in Jenne, E.A. (ed.), *Adsorption of Metals by Geomedial*: Academic Press, San Diego, Calif., pp. 1–73.
- Jenne, E.A., and Crecelius, 1988, Determination of sorbed metals, amorphous Fe, oxidic Mn, and reactive particulate organic carbon in sediments and soils; in Orio, A.A. (ed.), *Environmental Contamination 3rd International Conference*, Sept. 26–29, Venice, Italy, pp. 88–93.
- Jenne, E.A., and Zachara, J.M., 1987, Factors influencing the sorption of metals; in Dickson, K.L., Maki, A.W., and Brungs, W.A. (eds.), *Fate and Effects of Sediment-Bound Chemicals in Aquatic Systems*, SETAC Special Publication Series: Pergamon Press, New York, pp. 83–98.
- Johnson, C.A., 1986, The regulation of trace element concentrations in river and estuarine waters contaminated with acid mine drainage: the adsorption of Cu and Zn on amorphous hydrous oxides-oxyhydroxides: *Geochimica et Cosmochimica Acta*, v. 50, pp. 2433–2438.
- Jones, K.C., 1986, The distribution and partitioning of silver and other heavy metals in sediments associated with an acid mine drainage system: *Env. Pol. (B)*, v. 12, pp. 249–263.
- Karlsson, S., Sanden, P., and Allard, B., 1987, Environmental impacts of an old mine tailings deposit—metal adsorption by particulate matter: *Nordic Hydrology*, v. 18, pp. 313–324.
- Karlsson, S., Allard, B., and Hakansson, K., 1988a, Characterization of suspended solids in a stream receiving acid mine effluents, Bersbo, Sweden: *Applied Geochemistry*, v. 3, pp. 345–356.
- Karlsson, S., Allard, B., and Hakansson, K., 1988b, Chemical characterization of stream-bed sediments receiving high loadings of acid mine effluents: *Chemical Geology*, v. 67, pp. 1–15.
- Khan, S.U., 1969, Interaction between the humic acid fraction of soils and certain metallic cations: *Soil Science Society of America Proc.*, v. 33, pp. 851–854.
- Kimball, B.A., Broshears, R.E., Bencala, K.E., and McKnight, D.M., 1994, Coupling of hydrologic transport and chemical reactions in a stream affected by acid mine drainage: *Environ. Sci. Technol.*, v. 28, pp. 2065–2073.
- Kimball, B.A., Callender, E., and Axtmann, E.V., 1995, Effects of colloids on metal transport in a river receiving acid mine drainage, upper Arkansas River, Colorado, USA: *Applied Geochemistry*, v. 10, pp. 285–306.
- Kinniburgh, D.G., and Jackson, M.L., 1981, Cation adsorption by hydrous metal oxides and clay; in Anderson, M.A., and Rubin, A.J. (eds.), *Adsorption of Inorganics at Solid-Liquid Interfaces*: Ann Arbor Science, Ann Arbor, Mich., pp. 91–160.
- Kinniburgh, D.G., Jackson, M.L., and Syers, J.K., 1976, Adsorption of alkaline earth, transition, and heavy metal cations by hydrous oxide gels of iron and aluminum: *Soil Science Society of America J.*, v. 40, pp. 796–799.
- Kinniburgh, D.G., van Riemsdijk, W.H., Koopal, L.K., and Benedetti, M.F., 1998, Ion binding to humic substances; in Jenne, E.A. (ed.), *Adsorption of Metals by Geomedial*: Academic Press, San Diego, Calif., pp. 483–520.
- Kozawa, A., 1959, On an ion exchange property: *J. Electrochem. Soc.*, v. 106, pp. 552–556.
- Kuwabara, J.S., Leland, H.V., and Bencala, K.E., 1984, Copper transport along a Sierra Nevada stream: *J. Environ. Eng.*, v. 110, pp. 646–655.
- Langmuir, D., 1981, The power exchange function: a general model for metal adsorption onto geological materials; in Tewari, D.H. (ed.), *Adsorption from Aqueous Solutions*: Plenum Press, New York, pp. 1–17.
- Langmuir, D., 1997, *Aqueous environmental geochemistry*: Prentice Hall, Upper Saddle River, N.J.
- Leckie, J.O., Benjamin, M.M., Hayes, K., Kaufman, G., and Altmann, S., 1980, Adsorption/coprecipitation of trace metals from water with iron oxyhydroxide, CS-1513, Research Project 910-1: Electric Power Research Institute, Palo Alto, Calif.
- Levy, D.B., Custis, K.H., Casey, W.H., and Rock, P.A., 1997, A comparison of metal attenuation in mine residue and overburden material from an abandoned copper mine: *Applied Geochemistry*, v. 12, pp. 203–211.
- Lewis-Russ, A., 1991, Measurement of surface charge of inorganic geological materials—techniques and their consequences; in Sparks, D.L. (ed.), *Advances in Agronomy*, v. 46: Academic Press, New York, pp. 199–243.
- Lion, L.W., Altmann, R.S., and Leckie, J.O., 1982, Trace-metal adsorption characteristics of estuarine particulate matter—evaluation of contributions of Fe/Mn oxide and organic surface coatings: *Environmental Science and Technology*, v. 16, pp. 660–666.
- Loganathan, P., and Burau, R.G., 1973, Sorption of heavy metal ions by a hydrous manganese oxide: *Geochim. Cosmochim. Acta*, v. 37, pp. 1277–1293.
- Loux, N.T., Brown, D.S., Chafin, C.R., Allison, J.D., and Hassan, S.M., 1989, Chemical speciation and competitive cationic partitioning on a sandy aquifer material: *Chemical Speciation and Bioavailability*, v. 1, pp. 111–125.
- Luoma, S.N., and Bryan, G.W., 1981, A statistical assessment of the form of trace metals in oxidized estuarine sediments employing chemical extractants: *Science of the Total Environment*, v. 17, pp. 165–196.
- Luoma, S.N., and Davis, J.A., 1983, Requirements for modeling trace metal partitioning in oxidized estuarine sediments: *Marine Chemistry*, v. 12, pp. 159–181.
- Macalady, D.L., and Ranville, J.F., 1998, The chemistry and geochemistry of natural organic matter (NOM); in Macalady, D.L. (ed.), *Perspectives in Environmental Chemistry*: Oxford Univ. Press, New York, pp. 94–137.
- Machesky, M.L., 1990, Influence of temperature on ion adsorption by hydrous metal oxides; in Melchior, D.C., and Bassett, R.L. (eds.), *Chemical Modeling of Aqueous Systems II, ACS Symposium Series 416*: Washington, D.C., American Chemical Society, pp. 282–292.
- Mahoney, J.J., and Langmuir, D., 1991, Adsorption of Sr on kaolinite, illite and montmorillonite at high ionic strengths: *Radiochim. Acta*, v. 54, pp. 139–144.
- Mayer, L.M., and Schinck, L.L., 1981, Removal of hexavalent chromium from estuarine waters by model substrates and natural sediments: *Environmental Science and Technology*, v. 15, pp. 1482–1484.
- McCafferty, E., and Zettlemoyer, A.C., 1971, Adsorption of water vapor on α - Fe_2O_3 : *Discussions Faraday Society*, v. 52, pp. 239–254.

- McKenzie, R.M., 1967, The sorption of cobalt by manganese minerals in soils: *Aust. J. Soil Res.*, v. 5, pp. 235–246.
- McKenzie, R.M., 1972, The sorption of some heavy metals by the lower oxides of manganese: *Geoderma*, v. 8, pp. 29–35.
- McKinley, J.P., and Jenne, E.A., 1991, An experimental investigation and review of the “solids concentration” effect in adsorption studies: *Environ. Sci. Technol.*, v. 25, pp. 2082–2087.
- McKnight, D.M., Bencala, K.E., Zellweger, G.W., Aiken, G.R., Feder, G.L., and Thorn, K.A., 1992, Sorption of dissolved organic carbon by hydrous aluminum and iron oxides occurring at the confluence of Deer Creek with the Snake River, Summit County, Colorado: *Environ. Sci. Technol.*, v. 26, pp. 1388–1396.
- McLaren, R.G., Williams, J.G., and Swift, R.S., 1983, Some observations on the desorption and distribution behaviour of copper with soil components: *J. Soil Sci.*, v. 34, pp. 325–331.
- McLaren, R.G., Lawson, D.M., and Swift, R.S., 1986, Sorption and desorption of cobalt by soils and soil components: *J. Soil Sci.*, v. 37, pp. 413–426.
- Meng, X., and Letterman, R.D., 1993, Effect of component oxide interaction on the adsorption properties of mixed oxides: *Environ. Sci. Technol.*, v. 27, pp. 970–975.
- Morel, F.M.M., and Gschwend, P.M., 1987, The role of colloids in the partitioning of solutes in natural waters; in Stumm, W. (ed.), *Aquatic Surface Chemistry*: John Wiley and Sons, New York, pp. 405–422.
- Morel, F.M.M., Yeasted, J.G., and Westall, J.C., 1981, Adsorption models: a mathematical analysis in the framework of general equilibrium calculations; in Anderson, M.A., and Rubin, A.J. (eds.), *Adsorption of Inorganics at Solid-Liquid Interfaces*: Ann Arbor Science, Ann Arbor, Mich., pp. 263–294.
- Mott, C.J.B., 1981, Anion and ligand exchange; in Greenland, D.J., and Hayes, M.H.B. (eds.), *The Chemistry of Soil Processes*: Wiley, New York, pp. 179–219.
- Mouvet, C., and Bourg, A.C.M., 1983, Speciation (including adsorbed species) of copper, lead, nickel and zinc in the Meuse River: *Water Research*, v. 17, pp. 641–649.
- Muller, B., and Sigg, L., 1990, Interaction of trace metals with natural particle surfaces: comparison between adsorption experiments and field measurements: *Aquatic Sciences*, v. 52, pp. 75–92.
- Murray, J.W., 1975a, The interaction of cobalt with hydrous manganese dioxide: *Geochim. Cosmochim. Acta*, v. 39, pp. 635–647.
- Murray, J.W., 1975b, The interaction of metal ions at the manganese dioxide-solution interface: *Geochim. Cosmochim. Acta*, v. 39, pp. 505–519.
- Murray, D.J., Healy, T.W., and Fuerstenau, D.W., 1968, The adsorption of aqueous metal on colloidal hydrous manganese oxide; in Gould, R.F. (ed.), *Adsorption from Aqueous Solution, Advances in Chemistry Series No. 79*: American Chemical Society, Washington, D.C., pp. 74–81.
- O’Connor, D.J., and Connolly, J.P., 1980, The effect of concentration of adsorbing solids on the partition coefficient: *Water Research*, v. 14, pp. 1517–1526.
- Padmanabham, M., 1983, Comparative study of the adsorption-desorption behaviour of copper(II), zinc(II), cobalt(II) and lead(II) at the goethite-solution interface: *Aust. J. Soil Res.*, v. 21, pp. 515–525.
- Papelis, C., Roberts, P.V., and Leckie, J.O., 1995, Modeling the rate of cadmium and selenite adsorption on micro- and mesoporous transition aluminas: *Environ. Sci. Technol.*, v. 29, pp. 1099–1108.
- Parfitt, R.L., 1978, Anion adsorption by soils and soil materials: *Advances in Agronomy*, v. 30, pp. 1–50.
- Parks, G.A., 1990, Surface energy and adsorption at mineral/water interfaces—an introduction; in Hochella, M.F., and White, A.F. (eds.), *Mineral-Water Interface Geochemistry: Reviews in Mineralogy, Mineralogical Society of America, Washington, D.C.*, v. 23, pp. 133–175.
- Paulson, A.J., 1997, The transport and fate of Fe, Mn, Cu, Zn, Cd, Pb and SO_4 in a groundwater plume and in downstream surface waters in the Coeur d’Alene Mining District, Idaho, USA: *Applied Geochemistry*, v. 12, pp. 447–464.
- Payne, T.E., Lumpkin, G.R., and Waite, T.D., 1998, Uranium VI adsorption on model minerals: controlling factors and surface complexation modeling; in Jenne, E.A. (ed.), *Adsorption of Metals by Geomedia*: Academic Press, San Diego, Calif., pp. 75–97.
- Plumlee, G.S., Smith, K.S., Montour, M.R., Ficklin, W.H., and Mosier, E.L., 1999, Geologic controls on the composition of natural waters and mine waters draining diverse mineral-deposit types; in Filipek, L.H., and Plumlee, G.S. (eds.), *The Environmental Geochemistry of Mineral Deposits, Part B. Case Studies and Research Topics*: Society of Economic Geologists, *Reviews in Economic Geology*, v. 6B, pp. 373–432.
- Rampe, J.J., and Runnells, D.D., 1989, Contamination of water and sediment in a desert stream by metals from an abandoned gold mine and mill, Eureka District, Arizona, USA: *Applied Geochemistry*, v. 4, pp. 445–454.
- Ranville, J.F., and Schmiermund, R.L., 1998, An overview of environmental colloids; in Macalady, D.L. (ed.), *Perspectives in Environmental Chemistry*: Oxford Univ. Press, New York, pp. 25–56.
- Ranville, J.F., and Schmiermund, R.L., 1999, General aspects of aquatic colloids in environmental geochemistry; in Plumlee, G.S., and Logsdon, M.J. (eds.), *The Environmental Geochemistry of Mineral Deposits, Part A. Processes, Techniques, and Health Issues*: Society of Economic Geologists, *Reviews in Economic Geology*, v. 6A, pp. 183–199.
- Reardon, E.J., 1981, Kd’s—Can they be used to describe reversible ion sorption reactions in contaminant transport?: *Ground Water*, v. 19, pp. 279–286.
- Robinson, G.D., 1981, Adsorption of Cu, Zn and Pb near sulfide deposits by hydrous manganese-iron oxide coatings on stream alluvium: *Chemical Geology*, v. 33, pp. 65–79.
- Robinson, G.D., 1983, Heavy metal adsorption by ferromanganese coatings on stream alluvium—natural controls and implications for exploration: *Chemical Geology*, v. 38, pp. 157–174.
- Roe, A.L., Hayes, K.F., Chisholm-Brause, C., Brown, G.E., Jr., Parks, G.A., Hodgston, K.O., and Leckie, J.O., 1991, In-situ X-ray absorption study of lead ion surface complexes at the goethite-water interface: *Langmuir*, v. 7, pp. 367–373.
- Sanden, P., 1991, Estimation and simulation of metal mass transport in an old mining area: *Water, Air, Soil Pollution*, v. 57/58, pp. 387–397.
- Schindler, P.W., 1981, Surface complexes at oxide-water interfaces; in Anderson, M.A., and Rubin, A.J. (eds.), *Adsorption of Inorganics at Solid-Liquid Interfaces*: Ann Arbor Science, Ann Arbor, Mich., pp. 1–49.
- Schindler, P.W., and Gamsjager, H., 1972, Acid-base reactions of the TiO_2 (anatase)-water interface and the point of zero charge of TiO_2 suspensions: *Kolloid-Z.Z. Polym.*, v. 250, pp. 759–763.
- Schindler, P.W., and Stumm, W., 1987, The surface chemistry of oxides, hydroxides, and oxide minerals; in Stumm, W. (ed.), *Aquatic Surface Chemistry*: Wiley-Interscience, New York, pp. 83–110.
- Schindler, P.W., Furst, B., Dick, B., and Wolf, P.U., 1976, Ligand properties of surface silanol groups. I. Surface complex formation with Fe^{3+} , Cu^{2+} , Cd^{2+} , and Pb^{2+} : *J. Colloid Interface Science*, v. 55, pp. 469–475.
- Schnitzer, M., and Hansen, E.H., 1970, Organo-metallic interactions in soils. 8. An evaluation of methods for the determination of stability constants of metal-fulvic acid complexes: *Soil Science*, v. 109, pp. 333–340.
- Schnitzer, M., and Skinner, S.I.M., 1966, Organo-metallic interactions in soils. 5. Stability constants of Cu^{++} , Fe^{++} , and Zn^{++} -fulvic acid complexes: *Soil Science*, v. 102, pp. 361–365.
- Schnitzer, M., and Skinner, S.I.M., 1967, Organo-metallic interactions in soils. 7. Stability constants of Pb^{++} , Ni^{++} , Mn^{++} , Co^{++} , Ca^{++} , and Mg^{++} -fulvic acid complexes: *Soil Science*, v. 103, pp. 247–252.
- Schultz, M.F., Benjamin, M.M., and Ferguson, J.F., 1987, Adsorption and desorption of metals on ferrihydrite: reversibility of the reaction and sorption properties of the regenerated solid: *Environ. Sci. Technol.*, v. 21, pp. 863–869.
- Shaw, D.J., 1980, *Introduction to colloid and surface chemistry*, 3rd ed.: Butterworths.

- Siegel, M.D., Tripathi, V.S., Rao, M.G., and Ward, D.B., 1992, Development and validation of a multi-site model for adsorption of metals by mixtures of minerals: I. Overview and preliminary results; *in* Kharaka, Y.K., and Maest, A.S. (eds.), *Water-Rock Interaction*, 7th Internatl Symposium on Water-Rock Interaction, Park City, Utah, July 13–18, 1992, Proceedings, v. 1: A.A. Balkema, Rotterdam, pp. 63–67.
- Sigg, L., 1987, Surface chemical aspects of the distribution and fate of metal ions in lakes; *in* Stumm, W. (ed.), *Aquatic Surface Chemistry*: Wiley-Interscience, New York, pp. 319–349.
- Sigg, L., 1994, Regulation of trace elements in lakes; *in* Buffle, J., and deVitre, R. (eds.), *Chemical and Biological Regulation of Aquatic Processes*: Lewis Pub., Boca Raton, Fla., pp. 177–197.
- Singh, U., and Uehara, G., 1986, Electrochemistry of the double-layer: principles and applications to soils; *in* Sparks, D.L. (ed.), *Soil Physical Chemistry*: CRC Press, Boca Raton, Fla., pp. 1–38.
- Spark, K.M., Johnson, B.B., and Wells, J.D., 1995, Characterizing heavy-metal adsorption on oxides and oxyhydroxides: *European J. Soil Science*, v. 46, pp. 621–631.
- Smith, K.S., 1986, Adsorption of copper and lead onto goethite as a function of pH, ionic strength, and metal and total carbonate concentrations: M.S. Thesis, Colorado School of Mines, Golden, 177 pp.
- Smith, K.S., 1991, Factors influencing metal sorption onto iron-rich sediment in acid-mine drainage: Ph.D. Dissertation, Colorado School of Mines, Golden, 239 pp.
- Smith, K.S., 1996, Processes controlling dissolved copper concentrations during an instream pH-modification experiment; *in* Morganwalp, D.W., and Aronson, D.A., (eds.), U.S. Geological Survey Toxic Substances Hydrology Program—Proceedings of the Technical Meeting, Colorado Springs, Colorado, Sept. 20–24, 1993: U.S. Geological Survey Water-Resources Investigations Report 94–4015, vol. 2, pp. 769–774.
- Smith, K.S., and Huyck, H.L.O., 1999, An overview of the abundance, relative mobility, bioavailability, and human toxicity of metals; *in* Plumlee, G.S., and Logsdon, M.J. (eds.), *The Environmental Geochemistry of Mineral Deposits, Part A. Processes, Techniques, and Health Issues*: Society of Economic Geologists, Reviews in Economic Geology, v. 6A, pp. 29–70.
- Smith, K.S., and Langmuir, D., 1987, Inhibition of aqueous copper and lead adsorption onto goethite by dissolved carbonate species; *in* Averett, R.C., and McKnight, D.M., (eds.), *Chemical Quality of Water and the Hydrologic Cycle*: Lewis Publishers, Inc., Chelsea, Mich., pp. 351–358.
- Smith, K.S., and Macalady, D.L., 1991, Water/sediment partitioning of trace elements in a stream receiving acid-mine drainage: 2nd Internatl Conference on the Abatement of Acidic Drainage, Montreal, Canada, Sept. 16–18, 1991, Proceedings, v. 3, pp. 435–450.
- Smith, K.S., Macalady, D.L., and Briggs, P.H., 1989, Partitioning of metals between water and flocculated bed material in a stream contaminated by acid mine drainage near Leadville, Colorado; *in* Mallard, G.E., and Ragone, S.E., (eds.), U.S. Geological Survey Toxic Substances Hydrology Program—Proceedings of the Technical Meeting, Phoenix, Arizona, Sept. 26–30, 1988: U.S. Geological Survey Water-Resources Investigations Report 884220, pp. 101–109.
- Smith, K.S., Ranville, J.F., and Macalady, D.L., 1991, Predictive modeling of copper, cadmium, and zinc partitioning between streamwater and bed sediment from a stream receiving acid mine drainage, St. Kevin Gulch, Colorado; *in* Mallard, G.E., and Aronson, D.A., (eds.), U.S. Geological Survey Toxic Substances Hydrology Program—Proceedings of the Technical Meeting, Monterey, California, March 11–15, 1991: U.S. Geological Survey Water-Resources Investigations Report 91–4034, pp. 380–386.
- Smith, K.S., Ficklin, W.H., Plumlee, G.S., and Meier, A.L., 1992, Metal and arsenic partitioning between water and suspended sediment at mine-drainage sites in diverse geologic settings; *in* Kharaka, Y.K., and Maest, A.S., (eds.), *Water-Rock Interaction*: 7th Internatl Symposium on Water-Rock Interaction, Park City, Utah, July 13–18, 1992, Proceedings, v. 1, Rotterdam, A.A. Balkema, pp. 443–447.
- Smith, K.S., Ficklin, W.H., Plumlee, G.S., and Meier, A.L., 1993, Computer simulations of the influence of suspended iron-rich particulates on trace-metal removal from mine-drainage waters: Mined Land Reclamation Symposium, Billings, Montana, March 21–27, 1993, Proceedings, v. 2, pp. 107–115.
- Smith, K.S., Plumlee, G.S., and Ficklin, W.H., 1994, Predicting water contamination from metal mines and mining wastes—notes from a workshop presented at the International Land Reclamation and Mine Drainage Conference and the Third International Conference on the Abatement of Acidic Drainage, Pittsburgh, Pennsylvania, April 24, 1994: U.S. Geological Survey Open-File Report 94–264, 112 pp.
- Smith, K.S., Balistrieri, L.S., Smith, S.M., and Severson, R.C., 1997, Distribution and mobility of molybdenum in the terrestrial environment, Chap. 3; *in* Gupta, U.C., (ed.), *Molybdenum in Agriculture*: Cambridge University Press, New York, pp. 23–46.
- Smith, K.S., Ranville, J.F., Plumlee, G.S., and Macalady, D.L., 1998, Predictive double-layer modeling of metal sorption in mine-drainage systems; *in* Jenne, E.A. (ed.), *Adsorption of Metals by Geomedia*: Academic Press, San Diego, Calif., pp. 521–547.
- Smith, R.W., and Jenne, E.A., 1991, Recalculation, evaluation, and prediction of surface complexation constants for metal adsorption of iron and manganese oxides: *Environmental Science and Technology*, v. 25, pp. 525–531.
- Sparks, D.L., 1995, *Environmental soil chemistry*: Academic Press, San Diego, Calif., 267 pp.
- Sposito, G., 1980, Derivation of the Freundlich equation for ion exchange reactions in soils: *Soil Sci. Soc. Am. J.*, v. 44, pp. 652–654.
- Sposito, G., 1984, *The surface chemistry of soils*: Oxford University Press, New York, 234 pp.
- Sposito, G., 1986, Distinguishing adsorption from surface precipitation; *in* Davis, J.A., and Hayes, K.F. (eds.), *Geochemical Processes at Mineral Surfaces*, ACS Symposium Series 323: American Chemical Society, Washington, D.C., pp. 217–228.
- Sposito, G., 1989, *The chemistry of soils*: Oxford University Press, New York.
- Sposito, G., 1995, Adsorption as a problem in coordination chemistry; *in* Huang, C.P., O'Melia, C.R., and Morgan, J.J. (eds.), *Aquatic Chemistry—Interfacial and Interspecies Processes*, ACS Advances in Chemistry Series No. 244: American Chemical Society, Washington, D.C., pp. 33–57.
- Stollenwerk, K.G., 1994, Geochemical interactions between constituents in acidic ground water and alluvium in an aquifer near Globe, Arizona: *Applied Geochemistry*, v. 9, pp. 353–369.
- Stollenwerk, K.G., and Kipp, K.L., 1990, Simulation of molybdenum transport with different rate-controlled mechanisms; *in* Melchior, D.C., and Bassett, R.L. (eds.), *Chemical Modeling of Aqueous Systems II*, ACS Symposium Series 416: American Chemical Society, Washington, D.C., pp. 243–257.
- Stumm, W., 1992, *Chemistry of the solid-water interface*: Wiley-Interscience, New York, 428 pp.
- Stumm, W., 1995, The inner-sphere surface complex: a key to understanding surface reactivity; *in* Huang, C.P., O'Melia, C.R., and Morgan, J.J. (eds.), *Aquatic Chemistry, Advances in Chemistry Series No. 244*: American Chemical Society, Washington, D.C., pp. 1–32.
- Stumm, W., 1998, The solid-water interface in natural systems; *in* Macalady, D.L. (ed.), *Perspectives in Environmental Chemistry*: Oxford Univ. Press, New York, pp. 3–24.
- Stumm, W., and Morgan, J.J., 1996, *Aquatic chemistry*, 3rd ed.: John Wiley and Sons, New York, 1022 pp.
- Stumm, W., Huang, C.P., and Jenkins, S.R., 1970, Specific chemical interaction affecting the stability of dispersed systems: *Croat. Chem. Acta*, v. 42, pp. 223–245.
- Stumm, W., Hohl, H., and Dalang, F., 1976, Interaction of metal ions with hydrous oxide surface: *Croat. Chem. Acta*, v. 48, pp. 491–504.
- Stumm, W., Kummert, R., and Sigg, L., 1980, A ligand exchange model for the adsorption of inorganic and organic ligands at hydrous oxide interfaces: *Croat. Chem. Acta*, v. 53, pp. 291–312.
- Sverjensky, D.A., 1994, Zero-point-of-charge prediction from crystal chemistry and solvation theory: *Geochim. Cosmochim. Acta*, v. 58, pp. 3123–3129.

- Taniguchi, K., Nakajima, M., Yoshida, S., and Tarama, K., 1970, The exchange of the surface protons in silica gel with some kinds of metal ions: *Nippon Kagaku Zasshi*, v. 91, pp. 525–529.
- Tessier, A., Rapin, F., and Carignan, R., 1985, Trace metals in oxic lake sediments: possible adsorption onto iron oxyhydroxides: *Geochimica et Cosmochimica Acta*, v. 49, pp. 183–194.
- Tessier, A., Carignan, R., Dubreuil, B., and Rapin, F., 1989, Partitioning of zinc between the water column and the oxic sediments in lakes: *Geochimica et Cosmochimica Acta*, v. 53, pp. 1511–1522.
- Tessier, A., Fortin, D., Belzile, N., DeVitre, R.R., and Leppard, G.G., 1996, Metal sorption to diagenetic iron and manganese oxyhydroxides and associated organic matter: Narrowing the gap between field and laboratory measurements: *Geochim. Cosmochim. Acta*, v. 60, pp. 387–404.
- Theobald, P.K., Jr., Lakin, H.W., and Hawkins, D.B., 1963, The precipitation of aluminum, iron and manganese at the junction of Deer Creek with the Snake River in Summit County, Colorado: *Geochimica et Cosmochimica Acta*, v. 27, pp. 121–132.
- Thibault, D.H., Shepard, M.I., and Smith, P.A., 1990, A critical compilation and review of default soil solid/liquid partition coefficients, K_d , for use in environmental assessments, AECL-10125: Atomic Energy Canada Ltd., Pinawa, Manitoba, Canada.
- Thomas, G.W., 1977, Historical developments in soil chemistry: Ion exchange: *Soil Sci. Soc. Am. J.*, v. 41, p. 230–238.
- Tipping, E., 1981, The adsorption of aquatic humic substances by iron oxides: *Geochimica et Cosmochimica Acta*, v. 45, pp. 191–199.
- Tipping, E., and Hurley, M.A., 1992, A unifying model of cation binding by humic substances: *Geochimica et Cosmochimica Acta*, v. 56, pp. 3627–3641.
- Tipping, E., Griffith, J.R., and Hilton, J., 1983, The effect of adsorbed humic substances on the uptake of copper(II) by goethite: *Croatia Chemica Acta*, v. 56, pp. 613–621.
- Tipping, E., Fitch, A., and Stevenson, F.J., 1995, Proton and Cu binding by humic acid: application of a discrete-site/electrostatic ion-binding model: *Eur. J. Soil Sci.*, v. 46, pp. 95–101.
- Traina, S.J., and Doner, H.E., 1985, Co, Cu, Ni, and Ca sorption by a mixed suspension of smectite and hydrous manganese dioxide: *Clays Clay Minerals*, v. 33, pp. 118–122.
- Turner, D.R., 1995, A uniform approach to surface complexation modeling of radionuclide sorption; Report CN-WRA 95-001: Center for Nuclear Waste Regulatory Anal., San Antonio, TX.
- van Olphen, H., 1977, An introduction to clay colloid chemistry: Wiley, New York, 318 pp.
- van Riemsdijk, W.H., Bolt, G.H., Koopal, L.K., and Blaakmeer, J., 1986, Electrolyte adsorption on heterogeneous surfaces: adsorption models: *J. Colloid Interface Sci.*, v. 109, pp. 219–228.
- van Riemsdijk, W.H., de Wit, J.C.M., Koopal, L.K., and Bolt, G.H., 1987, Metal ion adsorption on heterogeneous surfaces: adsorption models: *J. Colloid Interface Sci.*, v. 116, pp. 511–522.
- Vandergraaf, T.T., Ticknor, K.V., and Melnyk, T.W., 1993, The selection of a sorption database for the Geosphere model in the Canadian Nuclear Fuel Waste Management Program: *J. Contaminant Hydrology*, v. 1, pp. 327–345.
- Veith, J.A., and Sposito, G., 1977, On the use of the Langmuir Equation in the interpretation of “adsorption” phenomena: *Soil Sci. Soc. Am. J.*, v. 41, p. 697–702.
- Venkataramani, B., Venkateswarlu, K.S., and Shankar, J., 1978, Sorption properties of oxides. III. Iron oxides: *J. Colloid Interface Sci.*, v. 67, pp. 187–194.
- Vuceta, J., and Morgan, J.J., 1978, Chemical modeling of trace metals in fresh waters: role of complexation and adsorption: *Environ. Sci. Technol.*, v. 12, pp. 1302–1309.
- Vydra, F., and Galba, J., 1969, Sorption von metallkomplexen an silicagel. V. Sorption von hydrolysenprodukten des Co^{2+} , Mn^{2+} , Ni^{2+} , Zn^{2+} an silicagel: *Colln Czech. Chem. Comm.*, v. 34, pp. 3471–3478.
- Wang, F., Chen, J., and Forsling, W., 1997, Modeling sorption of trace metals on natural sediments by surface complexation model: *Environ. Sci. Technol.*, v. 31, pp. 448–453.
- Wanty, R.B., Rice, C.A., Langmuir, D., Briggs, P., and Lawrence, E.P., 1991, Prediction of uranium adsorption by crystalline rocks: the key role of reactive surface area: *Mat. Res. Soc. Symp. Proc.*, v. 212, pp. 695–702.
- Wanty, R.B., Miller, W.R., Briggs, P.H., and McHugh, J.B., 1999, Geochemical processes controlling uranium mobility in mine drainages; *in* Plumlee, G.S., and Logsdon, M.J. (eds.), *The Environmental Geochemistry of Mineral Deposits, Part A. Processes, Techniques, and Health Issues: Society of Economic Geologists, Reviews in Economic Geology*, v. 6A, pp. 201–213.
- Warren, L.A., and Zimmerman, A.P., 1994, The importance of surface area in metal sorption by oxides and organic matter in a heterogeneous natural sediment: *Applied Geochemistry*, v. 9, pp. 245–254.
- Weber, W.J., Jr., McGinley, P.M., and Katz, L.E., 1991, Sorption phenomena in subsurface systems: concepts, models and effects on contaminant fate and transport: *Water Res.*, v. 25, pp. 499–528.
- Webster, J.G., Nordstrom, D.K., and Smith, K.S., 1994, Transport and natural attenuation of Cu, Zn, As, and Fe in the acid mine drainage of Leviathan and Bryant Creeks; *in* Alpers, C.N., and Blowes, D.W., (eds.), *Environmental Geochemistry of Sulfide Oxidation: American Chemical Society Symposium Series 550*, American Chemical Society, Washington, D.C., pp. 244–260.
- Webster, J.G., Swedlund, P.J., and Webster, K.S., 1998, Trace metal adsorption onto an acid mine drainage iron(III) oxy hydroxy sulfate: *Environ. Sci. Technol.*, v. 32, pp. 1361–1368.
- Wen, X., Du, Q., and Tang, H., 1998, Surface complexation model for the heavy metal adsorption on natural sediment: *Environ. Sci. Technol.*, v. 32, pp. 870–875.
- Westall, J.C., 1986, Reactions at the oxide-solution interface—chemical and electrostatic models; *in* Davis, J.A., and Hayes, K.F. (eds.), *Geochemical Processes at Mineral Surfaces, ACS Symposium Series 323*: American Chemical Society, Washington, D.C., pp. 54–78.
- Westall, J.C., 1987, Adsorption mechanisms in aquatic surface chemistry; *in* Stumm, W. (ed.), *Aquatic Surface Chemistry: Wiley-Interscience*, New York, pp. 3–32.
- Westall, J.C., 1994, Modeling of the association of metal ions with heterogeneous environmental sorbents: *Materials Research Society Symposium Proceedings, XVIII International Symposium on the Scientific Basis for Nuclear Waste Management, Kyoto, Japan, October 23–27, 1994*.
- Westall, J., and Hohl, H., 1980, A comparison of electrostatic models for the oxide/solution interface: *Advances in Colloid and Interface Science*, v. 12, pp. 265–294.
- Westall, J.C., Jones, J.D., Turner, G.D., and Zachara, J.M., 1995, Models for association of metal ions with heterogeneous environmental sorbents. 1. Complexation of Co(II) by leonardite humic acid as a function of pH and NaClO_4 concentration: *Environmental Science and Technology*, v. 29, pp. 951–959.
- White, A.F., and Peterson, M.L., 1990, Role of reactive-surface-area characterization in geochemical kinetic models; *in* Melchior, D.C., and Bassett, R.L. (eds.), *Chemical Modeling of Aqueous Systems II, ACS Symposium Series 416*: American Chemical Society, Washington, D.C., pp. 461–475.
- Wilson, D.E., and Kinney, P., 1977, Effects of polymeric charge variations on the proton-metal ion equilibria of humic materials: *Limnol. Oceanogr.*, v. 22, pp. 281.
- Winland, R.L., Traina, S.J., and Bigham, J.M., 1991, Chemical composition of ochreous precipitates from Ohio coal mine drainage: *J. Environ. Quality*, v. 20, pp. 452–460.
- Yates, D.E., Levine, S., and Healy, T.W., 1974, Site-binding model of the electrical double layer at the oxide/water interface: *Journal of the Chemical Society, Faraday Transactions I*, v. 70, pp. 1807–1818.
- Zachara, J.M., Ainsworth, C.C., Cowan, C.E., and Resch, C.T., 1989, Adsorption of chromate by subsurface soil horizons: *Soil Science Society of Am. J.*, v. 53, pp. 418–428.

Chapter 8

GENERAL ASPECTS OF AQUATIC COLLOIDS IN ENVIRONMENTAL GEOCHEMISTRY

J.F. Ranville¹ and R.L. Schmiermund²

¹*Department of Chemistry/Geochemistry, Colorado School of Mines, Golden, CO 80401*

²*Knight Piésold LLC, 1050 17th Street, Suite 500, Denver, CO 80265*

INTRODUCTION

A recent emphasis in society is on conducting mining activities with the least environmental impact possible. A manifestation of this is the cost-effective monitoring of contaminant levels in surface and ground waters, usually in order to meet specific environmental regulations. However the simple collection of monitoring data may not provide understanding of either the actual impact of mining on the environment or suggest the most appropriate treatment processes for specific mining wastes. More detailed information on the chemical and physical forms of contaminants is needed. One aspect of this is that the occurrence and distribution of natural and anthropogenic chemicals in natural water systems is strongly influenced by their partitioning between solid and aqueous phases (Allan, 1986). Therefore contaminant behavior is generally defined in terms of “two-phase” water-rock interactions where metals, for example, are present either in the stationary solid phases of the country rock, ore pad, waste rock pile, tailings empondment, or slag heap or they are present as mobile, aqueous phase solutes. For groundwater the solid phase is considered to be the stationary aquifer material. In surface waters the solid phases generally considered are the sediments in the stream, pond, or lake bottom. Accordingly, computer models have been developed that address dissolution, precipitation, adsorption, and desorption between the solid and aqueous phases as well as the formation of various solute species and complexes.

The reality is, however, that most natural water systems are three-phase systems, the third phase being a mobile solid phase in the form of suspended matter. Turbidity is the macroscopic, visual evidence of suspended matter in a water system. A certain portion of suspended matter, the largest particles first, will settle out over time. However, by some estimates (Moran and Moore, 1989), as much as one half of the suspended matter in natural waters is less than 1 μm (10^{-6} meter) in diameter and does not settle out over even long periods of time. By definition these particles are “colloids” and represent a “permanent” phase, which, of all the solid phases, can potentially exert the most significant control over water-borne chemicals. The small size of colloids results in a very high surface area per unit mass that facilitates all surface area-dependent interactions between solution and solid components. Extensive laboratory studies of contaminant sorption to colloidal phases (i.e., metal oxides, clays, etc.) has resulted in a reliable but evolving physicochemical understanding of this process

(Morel and Geschwend, 1987). However sufficient data are currently lacking on the abundance and chemical nature of colloids in natural waters.

The available evidence clearly shows that significant amounts of certain trace elements in surface waters occur in the colloidal component of suspended solid phases. Interest in the environmental importance of colloids has been further heightened over recent years (McCarthy and Zacara, 1989) as a result of evidence which suggests that colloids can be mobile in porous media and may therefore act as transport phases for colloid-associated contaminants in soils and ground waters. Therefore, ground waters must also be considered intrinsically three-phase systems. This complicates the previously-held view of contaminant transport in groundwater as consisting of a two-phase chromatographic process where solutes are partitioned between solution and an immobile aquifer matrix. Numerous two-phase models for contaminant transport have been devised which include equilibrium adsorption and ion exchange with respect to the stationary matrix (e.g., AGU-10, HST-3D, MOC, ONE-D, SUMATRA-1, and SUTRA etc.; see IGWMC, 1992 for descriptions). Where mobile colloids are present, contaminants having an affinity for interaction with solid surfaces may not be retarded as significantly as predicted by current physicochemical models because part of the sorbent solid phase is also mobile.

It is important for the environmental geochemist to have an understanding of what colloids are, what influences their chemical and physical stability, how they are transported in natural waters, and how contaminants associate with colloids. Both the transport of colloids and their interactions with contaminants are dependent on the physical and surface chemical properties of the colloids; these topics will be addressed in varying depth in this chapter. Emphasis will be given to the basic properties of colloidal systems and how these affect colloid transport. Available data on the occurrence and environmental significance of colloidal particles will also be presented. In this paper, the focus will primarily be on metal and radionuclide contaminants. Transport of biocolloids, bacteria and virus, and interactions of organic contaminants with colloids, while extremely important, are considered outside the scope of this paper and discussion will be limited. Adsorption of metals by solid phases is addressed by Smith (1999) and by colloids specifically by Rees (1991). The reader is referred to other reviews for discussion of organic contaminant interaction with colloids (Morel and Geschwend, 1987; Rees, 1991).

DISSOLVED VERSUS COLLOIDAL PROCESSES

Major processes affecting metal transport in surface waters are illustrated on Figure 8.1 (adapted from Forstner and Salomons; 1983). “Dissolved Processes,” shown on the right, include metal complexation by inorganic and organic ligands, which are quantitatively described by equilibrium-based thermodynamic constants that are well known for a variety of metals and simple ligands. Also included are metal, metal-ligand and ligand sorption reactions with well defined solid components as described by empirical relationships and various physicochemical models. Among the physicochemical models addressing sorption of ionic contaminants to solid surfaces are those that employ conditional surface sorption constants to account for electrostatic and specific chemical interactions (Smith, 1999). These constants are known for many metals and solid phases such as clays and iron, manganese, and aluminum oxides and hydroxides.

In contrast, “Colloidal Processes,” shown on the left side of Figure 8.1, include metal complexation and sorption with less well-defined components, such as complex organic and inorganic colloids. These processes are poorly understood. The limited amount of thermodynamic or even empirical data for such reactions is due mainly to the complexity and heterogeneity of organic colloids and the lack of characterization resulting from the difficulties associated with their collection.

Uncertainty in sorption constants also arises from the practical difficulty in separating colloids from dissolved phases in laboratory experiments. Colloids behave similarly to solutes in that they are not effectively removed by centrifugation or filtration. The

commonly observed apparent decrease in sorption coefficients of organic and inorganic contaminants observed with increasing total solids concentration (Morel and Gschwend, 1987) has been explained by the presence of colloids that were not completely separated from the aqueous phase (Morel and Gschwend, 1987). Contaminants associated with colloids are mistakenly measured as part of the solution phase, therefore reducing the observed sorption coefficient. The amount of colloids present increases with increasing total solids and if colloids are taken into account the partitioning coefficient becomes invariant with suspended solids concentration, as predicted by most sorption models.

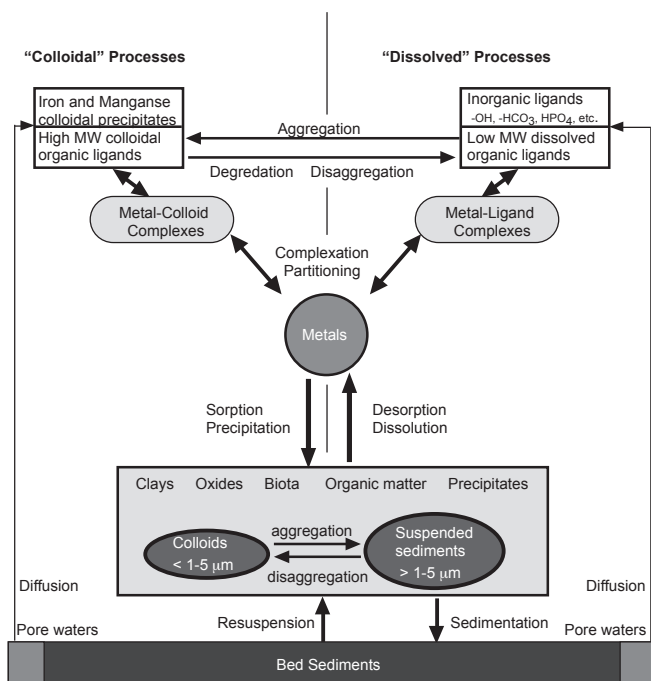
DEFINITIONS OF AQUATIC COLLOIDS

Filtration through a 0.45 μm pore-size membrane, although quite arbitrary, has been widely accepted as a means of separating particulate from “dissolved” species. Such an operational definition ignores the issue of colloids entirely. Chemical species present in whole or raw natural waters may be more accurately considered to physically occur in a variety of modes. These modes of physical occurrence define an essentially continuous series which we will refer to as the solute/colloid/suspended sediment continuum. While the pure end member modes are easily conceptualized as: (a) dissolved ions or molecules; and (b) macroscopic particles with or without associated ions or molecules, the intermediate modes require further explanation. The word “colloid” as used here collectively identifies the intermediate continuum of modes. Chemical species that may be referred to as “colloidal” include: (a) discrete chemical species with sufficient size or mass to behave as colloids (macromolecules); (b) amorphous or crystalline chemical compounds that exist in the solid phase as colloid particles; and (c) chemical species associated with (usually by sorption) compositionally distinct, colloid-size particles and whose mobility is controlled by those particles.

A colloidal system is more easily described than a colloid itself as a two-phase system in which one phase is uniformly and permanently distributed or dispersed in the second phase. This is in contrast with both a true solute/solvent system, which comprises a single phase, and a suspended-sediment/solvent system, which is a two phase system but is typically not uniform and never permanent. Although natural colloidal systems exist for every binary combination (except gas-in-gas) of solid, liquid and gas phases (e.g., fog is a liquid-in-gas colloidal system), our sole focus here is on the most geochemically relevant systems, those with an aqueous dispersing medium, and dispersed solid particles, known as sols. Chemically, colloids behave like solids requiring consideration of surface area and charge and other aspects of heterogeneous reaction theory. Physically or hydrodynamically however, colloids behave somewhat like solutes principally because of their small size.

An exceedingly wide variety of natural colloidal material has been identified in surface and ground waters (Table 8.1). Natural colloids can be subdivided into two main groups, including:

- 1) sparingly soluble, hydrophobic (also termed lyophobic or solvophobic) materials that have an inherent resistance to chemical interactions with water (e.g., insoluble minerals) and;
- 2) hydrophilic (also termed lyophilic or solvophilic) materials that are polar and hence form direct hydrogen bonds with water (e.g., macromolecular organics, polymeric precipitates).



Adapted from Forstner and Salomons (1983)

FIGURE 8.1—Comparison of “dissolved” versus “colloidal” processes which affect the physical and chemical form of pollutants in surface waters.

Long-term kinetic stability as a suspension is a fundamental property a colloid and a colloidal system. For hydrophobic solids, permanent dispersion or suspension is maintained by the random thermal activity of water molecules (Brownian movement). In order for this mechanism to be effective, the particle must be sufficiently small to allow spatially uneven bombardment by water molecules. Evenly distributed bombardment of the surface of a large particle would result in no net displacement and consequently gravity and density differences would ultimately cause the particle to settle (Halliday and Resnick, 1967) or float on the aqueous medium. If not for the presence of ions of like charge on the colloid surface, the hydrophobic nature of these particles would tend to force them together during mutual particle collisions and promote aggregation, which would in turn lead to larger and larger particle sizes and eventual destruction of the colloidal system. These surface ions promote coulombic repulsion between particles and allow interactions with water molecules thus making the particles effectively more hydrophilic. Naturally hydrophilic macromolecules, which more closely approach true solute behavior, maintain their colloidal stability via interactions between charged functional groups and water molecule dipoles. Such large molecules frequently undergo some flexure or folding to best accommodate these interactions. Large molecules that are inherently hydrophobic (e.g., oils and greases) may form stable colloidal systems (an emulsion or liquid-in-liquid colloidal system) through interaction with surfactants, which are large molecules having both hydrophobic and hydrophilic portions. The hydrophobic molecule interacts with the hydrophobic portion of the surfactant while the hydrophilic end of the surfactant interacts with water. A micelle is thus formed and the hydrophobic molecule is stabilized.

TABLE 8.1—Some examples of aquatic colloids (colloidal species of greater importance given in bold).

Hydrophobic colloids	Hydrophilic colloids
Minerals	Macromolecular organic matter
- Phyllosilicates, clays	- Humic and fulvic acids
- Iron, manganese, and aluminum oxides and hydroxides	- Polysaccharides
- Framework silicates	- Proteins
- Carbonates, sulfides, and phosphates	- Polymeric precipitates
Biocolloids (living and non-living)	- Silica gel
- Bacteria	- Alumina gel
- Virus	
- Organic detritus	

Another fundamental property of colloidal systems, in addition to their physical stability, is their ability to scatter light, known as the Tyndall effect. Interactions between a beam of incident light and colloidal particles include refraction, polarization, reflection and adsorption. The collective effect is that some of the incident light is scattered in all directions and the colloidal suspension appears turbid. The light scattering characteristics of a given suspension are complexly related to concentration, size, shapes and molecular weight of the colloidal particles (Moore, 1972). These relationships have led to the development of important tools for the investigation of colloids such as photon-correlation spectroscopy for colloid size determination and electrophoretic light-scattering for surface charge determination (Rees, 1987). Because the overall decreased light transmittance of turbid water can dra-

matically affect biological productivity, turbidity is an important water quality issue (Greenberg et al., 1992).

Although particle size is not part of the technical definition of a colloid, in order for particles to be dispersed by Brownian motion they must be very small but yet not so small that they are actually ions or individual simple molecules (i.e., not part of the aqueous phase). In order to produce the Tyndall effect they must have sufficient size to scatter light. Generally, "colloid" is only operationally defined by environmental scientists, typically in terms of the ability of a particle to pass a certain filter or molecular sieve size. Similarly, it is conceptually convenient to describe the differences between solutes, colloids and suspended solids in terms of particle diameters or molecular weights. However, numerous operational factors, such as filter efficiency, and particle density and surface charge, influence and generally complicate separations based on size. Colloids clearly lie between solutes and suspended solids in the size continuum of water-dispersed particulate matter (Fig. 8.2) but the size cutoffs are a matter of debate (Table 8.2). Generally the size of colloids is quoted as simply being sub-micron or, more specifically, ranging from 0.001 to 1.0 μm (1 to 1000 nm). A slightly larger lower size limit is used by some while others extend the upper range to 2–5 μm to coincide with the classical clay-silt boundary, while still others further extend this range to 10 μm (Stumm and Morgan, 1981). As is generally the case when describing a continuum, intermediate limits and bounds are necessarily arbitrary.

In this paper we assume that the size distinction between solute (i.e., truly dissolved) and colloidal constituents is best drawn at the upper size limit for thermodynamically well defined species (i.e., simple inorganic and organic aquo-ions). The largest hydrated-ion size parameter in Debye-Huckel equations (cf., Nordstrom and

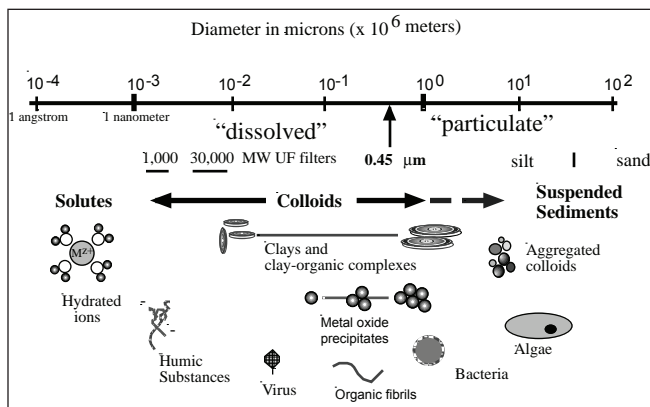


FIGURE 8.2—The solute/colloid/particle size continuum and examples of aquatic colloids.

TABLE 8.2—Generally accepted colloid size limits in microns.

Lower diameter	Upper diameter	Reference
0.0005	5	Driscoll, 1986
0.001	1	Domenico and Schwartz, 1990
		Freeze and Cherry, 1979
		Metcalf and Eddy Inc., 1991
0.003	1	Pankow, 1991
0.005	10	Stumm and Morgan, 1981

Munoz, 1986), of 11 Å or 0.0011 µm, corresponds well to the 0.001 µm lower size limit for colloids accepted by many authors. Examples of inorganic species with these large sizes are some fully hydrated, high-valent actinide (Th⁴⁺), lanthanide (Ce⁴⁺) and transition elements (Zr⁴⁺). It should be pointed out that colloid "sizes" are referenced either to their linear dimensions of length, width or diameter (units of microns or nanometers) or their mass (usually in terms of molecular weights or Daltons). Organic molecules must reach molecular weights of several hundred to a few thousand Daltons in order to reach similar hydrated ion sizes. The relationship between mass and size of organic molecules depends on molecular shape in solution and the compound's density.

The colloid-suspended particle boundary can be based on the wide spread use of 0.45 µm filtration, but larger particles do in fact behave like colloids. An upper size limit of approximately 2 to 5 µm better describes the hydrodynamic behavior of larger colloids that make them mobile in surface and ground waters, as will be discussed shortly.

Colloidal particles in natural waters may be composed of an exceedingly wide variety of natural and synthetic materials ranging from macromolecules (molecular weight >1000) to oxides and phyllosilicates, as shown on Figure 8.2. Obviously the relative importance of various colloids will vary with the environment of the water. For example, it is likely that in biologically productive surface waters, living microorganisms and non-living organic materials will dominate the colloid population. In waters affected by mining operations, iron and aluminum oxides and clays may be the most abundant colloids (see Nordstrom and Alpers, 1999). Bacteria may also be important in these types of waters due to their role in the generation of acid-mine drainage (see Mills, 1999).

Colloids originate in at least three ways:

- 1) They can be acquired from the surrounding environment by disaggregation/dissolution and entrainment. This includes, for example, suspension of primary or authigenic clays, acquisition of atmospheric dust by rain, weathering of framework silicates, suspension of oxides and oxyhydroxides, dissolution of fulvic acids in soil profiles, and washing of mineral and rock fragment fines from tailing piles or soil profiles.
- 2) They can result from *in-situ* aqueous phase precipitation due to changing chemical or physical conditions. This includes, for example, precipitation of calcite due to pH changes, precipitation of iron oxides and(or) sulfides due to redox changes, formation of complex phosphate mineral suspensions at chemical interfaces in lakes, and polymerization of dissolved silica due to pH changes.
- 3) They can result from biological activity, for example, the growth and death of microbes, production of fibrils, organic skeletons and protein-rich cell fragments (Leppard, 1992), and biologically mitigated precipitation or dissolution of minerals.

SIGNIFICANCE OF AQUATIC COLLOIDS

The environmental significance of colloids mainly arises from their very large specific surface areas that facilitate reactions between truly dissolved solutes and the particle surfaces. These heterogeneous reactions include simple electrostatic sorption, chemisorption, coadsorption, catalysis of complexation, redox and hydrolysis reactions among solute species and dissolution, precipitation and leaching. Increased surface area is an express or

implied factor in increasing either the equilibrium capacity, for example, the solubility or sorption capacity of a solid, and(or) the chemical kinetic rates of these reactions. The significance of small particles like colloids in influencing the available surface area can be illustrated in several ways that will be discussed in the following paragraphs.

As particle size decreases, the total surface area per unit mass of suspended material increases dramatically. Since adsorption is, at least in part, a surface area-extensive process it is logical that the total adsorption capacity of a volume of water with suspended matter will be related to the particle size of that suspended matter. A theoretical number of particles, and hence the associated total surface area, is easily calculated for a known concentration of suspended matter with a particular density assuming a uniform particle size (*d*, sphere diameter or cube side length) and regular shape. Gregg and Sing (1982) and Parks (1990) provide formulae for calculating particle number and total areas for different shapes and non-uniform size distributions. For example, 1 µm spheres of quartz would have a specific surface area of 2.26 m²/g. Simple estimates such as these tend to underestimate surface areas of natural materials due to complex shapes, porosity, and surface defects (White and Peterson, 1990; Davis and Kent, 1990). For example, Parks (1990) shows a plot of measured specific surface area as a function of grain size for natural quartz sand and crushed quartz that indicates approximately 10 m²/g is reasonable for 1 µm diameter particles. Figure 8.3 illustrates the effect of dividing a 1 cm cube of hematite into smaller and smaller cubes. Not only does the number of cubes increase tremendously, the total surface area approaches 1000 m²/g at the lower size limit for colloids. Taking this one step further, consider the reactivity of the hematite itself. Obviously any reaction must take place with the surficial atoms of iron and oxygen, for example those within 2 angstroms of the surface. As the particle size decreases below 1 µm, the percentage of atoms near the surface rises dramatically and approaches 100% at 1 nm; thus almost the entire mass of hematite is immediately available for reaction.

Experimental adsorption data is typically reported in the form of isotherms that compare the dissolved concentration of some solute (mass/vol) with the sorbed concentration (mass/mass). The

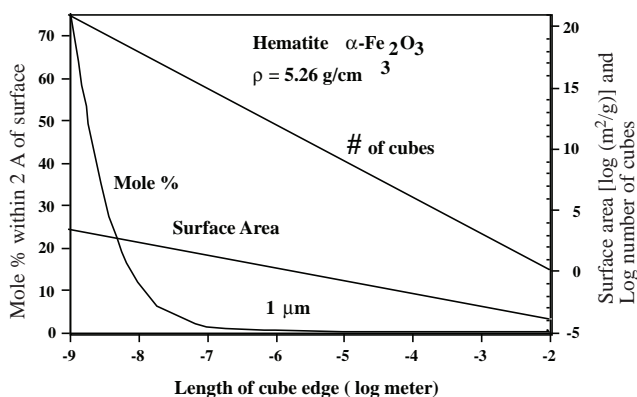


FIGURE 8.3—Plot showing the changes in surface area that would result from progressively dividing a 1 cm cube of hematite into smaller and smaller cubes. For particles of 0.01 µm (1×10^{-8} m), the percentage hematite within 2 Å of the particle surface is approaching 100%. Since Fe and O radii are each on the order of 1 Å this means that a significant number of atoms are subject to reactions that occur at the particle surface.

same experimental data may be normalized to the measured surface area of sorbent and reported as sorption site density for an individual sorbed species (Γ , sites/nm²) or Γ_{\max} for conditions of maximum sorption (see Smith, 1999, for a detailed discussion of adsorption densities). Davis and Kent (1990) report sorption site density data derived from numerous sources for various materials, including α -FeOOH, other iron oxides, titanium oxide polymorphs, aluminum oxides and hydroxides, amorphous silica and kaolinite. Sorption site densities are also reported for α -FeOOH as derived from adsorption experiments involving OH⁻, H⁺, F⁻, SeO₃²⁻, PO₄³⁻, oxalate and Pb²⁺. For the latter data, Γ values vary from 0.8 to 7.3 sites/nm², in part due to intrinsic differences in adsorption mechanisms for different sorbates and in part due to differences in experimental conditions.

Figure 8.4 illustrates the combined effects of particle size and sorption site density on the suspended matter-sorbed versus solute load assuming full saturation of available sorption sites with sorbate ions and 1:1 ratio of sorption sites to sorbed ions. The plot suggests that a water sample with 100 mg/l of some suspended matter (e.g., α -FeOOH having $\Gamma = 2.6$ to 7) and 10⁻⁶ moles/l truly dissolved solute (e.g., 0.2 mg/l dissolved Pb²⁺) could contain significantly greater concentrations of the same solute as a suspended matter-sorbed phase. In this extremely simplistic scenario, as the particle size decreases the moles of metal associated with colloids may equal or exceed the moles of metal actually dissolved. The picture is complicated in natural waters by (1) competition of multiple metals species for the available sites, (2) aqueous complexation of the metal, and (3) variable site densities and variable aqueous concentrations.

Figure 8.5 illustrates the importance of colloid surface area relative to the surface area of solid aquifer material in a groundwater. A cubic meter of hypothetical aquifer composed of 1 mm diameter spherical sand grains ($\rho = 2.5$ g/cm³), and having 30%

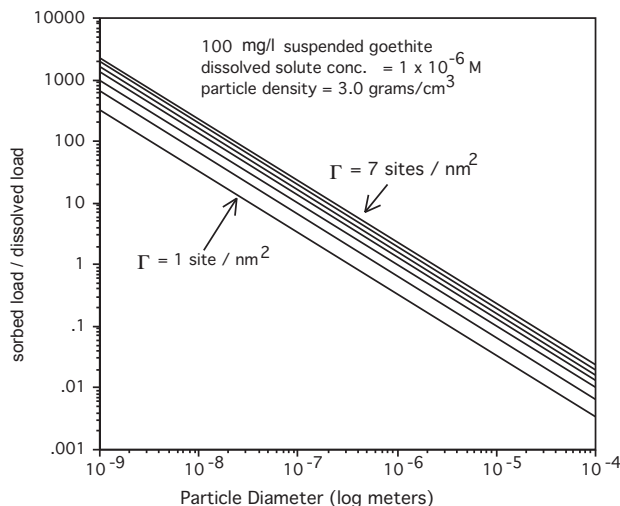


FIGURE 8.4—Theoretical comparison of dissolved and suspended loads as a function of site density and particle size of goethite. Each line represents a different surface sorption site density ranging from 1 to 7 sites/nm². If there is complete occupancy of the surface sites, the suspended load can carry significantly greater amounts of the constituent than the aqueous phase.

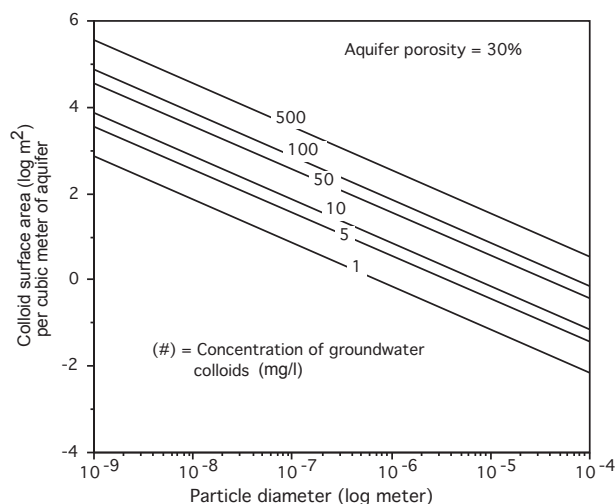


FIGURE 8.5—Particle size dependence of total particulate surface area (m²) available in the liquid phase of 1 m³ of a saturated 30% porosity aquifer. Lines represent different concentrations of suspended matter (mg/l).

porosity, has a computed total surface area of 4200 m² and a specific surface area of 2.4E-3 m²/g. An approximately equivalent total surface area would be available in the liquid phase if the pore water contained 580 mg/l of similar-density, spherical, 0.1 μ m diameter particles or 5.8 mg/l of 0.001 μ m particles. These suspended loads would have calculated specific surface areas of 24 and 2400 m²/g respectively. Assuming the larger particle size (0.1 μ m) and the lower concentration (5.8 mg/l), a groundwater velocity of 1 m/day would result in a surface area equivalent to the aquifer matrix passing through the aquifer volume every 100 days.

These examples, although very simplistic, illustrate the potential importance of colloids to the chemistry of contaminants in groundwater and other natural aqueous systems.

SURFACE CHARGE ASPECTS OF COLLOIDS

A colloid, like any other particle in an aqueous medium, is bounded by an interface that separates the two phases. Such an interface is a region of tremendous complexity, lateral inhomogeneity, and extreme microtopography, and is rarely if ever static (Hochella, 1990). Electrical charges are an integral and ubiquitous characteristic of solid-aqueous phase interfaces and strongly influence the thickness and nature of the transition zone between the two bulk phases. The total amount of electrical charge at the interface is a surface area-intensive function. In the case of colloidal particles, or any suspended particle for that matter, this electrified nature of the interface has three very important consequences:

- 1) Electrical forces of attraction and repulsion control how closely two particles may approach one another and whether or not there will be sufficient tendency for them to remain together if the approach is close enough or forceful enough; this is the basis for coagulation or agglomeration of suspended matter, and controls the stability and transportability of colloids in the aqueous medium. This aspect of surface charge is discussed in following paragraphs.

- 2) Electrical charges associated with particle interfaces influences the processes of adsorption that allow metal ions, anions and organic molecules to become associated with particles. So, electrical forces influence the identity and abundance of sorbed ions and molecules associated with colloids. These ions and molecules may be contaminants of environmental interest. This aspect of surface charge is discussed by Smith (1999).
- 3) By combination of the first two consequences, electrical interfaces influence the physical and chemical transportability of colloid-associated contaminants.

Origin of colloid surface charge

The basic concepts involved in the formation of surface charge are presented in detail by Smith (1999). In the following paragraphs the concepts of surface charge development most relevant to describing the behavior of colloids are reviewed.

“Permanent” (i.e., not affected by the aqueous environment) surface charges have their origin within the bulk solid phase where substitutions of similar-sized but different-charged atoms lead to a net lattice charge imbalance. These charges are typically negative in sign (e.g., substitution of Al^{3+} for Si^{4+} in the tetrahedral layer or Mg^{2+} for Al^{3+} in the octahedral layer of smectite clays). The result of the lattice charge deficiencies is a non point-source electrostatic surface charge which gives rise to such phenomena as cation exchange. Non-stoichiometric substitutions in other minerals such as carbonates can generate similar charges.

Another source of surface charge is located on the actual particle surfaces and occurs due to the amphoteric nature of surface hydroxyl groups. These groups exist as either X-O^- , X-OH^0 , or X-OH_2^+ , where X represents the surface of the particle. The relative abundance of each of these surface groups and therefore the net surface charge, is a function of the pH of the aqueous medium (positively charged at lower pHs and negatively charged at higher pHs). The pH where the surface is neutral is the ZPC or zero point of charge.

Another mechanism for surface charge development is the sorption of ions to the particle surface. In most aquatic environments the sorption of organic matter on suspended particles has been shown to most greatly influence particle surface charge (Tipping and Cooke, 1982; Beckett, 1990). Hunter and Liss (1979) concluded that adsorption of organic matter is responsible for the observation that particles have a net negative charge in almost all natural waters, regardless of the particle mineralogy. Natural organic material is a complex mixture of polyelectrolytes, whose charge primarily results from carboxylic acid functional groups ($-\text{COOH}$) with pK_a values in the range of 3–4. Thus at typical environmental pHs they tend to be negatively charged ($-\text{COO}^-$). Adsorption of organic matter to mineral surfaces is primarily through a ligand exchange mechanism where $-\text{COO}^-$ groups bond directly to the metal (i.e., Al, Fe, Mn) and displace the surface OH group. Not all COO^- groups of the organic matter are involved in sorption to the particle surfaces and those remaining provide the net negative charge shown to occur on particles in natural waters. The sorption of organic matter in turn effects colloid stability (Tipping and Higgins, 1982; Liang and Morgan, 1990) and chemical removal of organic coating has been shown to reduce colloid stability significantly (Gibbs, 1983).

Surface charge and colloid stability

The interactions of colloids with one another and with macroscopic solid phases are governed by hydrodynamic and chemical forces (O’Melia, 1987). The physical stability of colloids (not to be confused with chemical stability with respect to dissolution) refers to their ability to remain in suspension by avoiding aggregation due to particle interactions. Hydrodynamic forces tend to bring suspended particles into contact with one another. Figure 8.6 illustrates the physical processes contributing to particle collisions in surface waters. Gravitational aggregation is caused when colloids collide with larger, rapidly settling particles. Random collisions between colloids due to Brownian motion occur with greater frequency as colloid size decreases and result in what is called perikinetic aggregation. Colloidal particles in lakes are subject to aggregation, via both these processes and is dependent on both particle surface charge and initial particle size (Ali et al., 1985). Aggregated particles are then subject to sedimentation which may act to transport adsorbed metals from the water column to the sediments (Sigg, 1985). The overall result of these two aggregation mechanisms is that particles of intermediate size, on the order of a few μm , tend to be the most stable in non-flowing water bodies. Collisions also occur when particles are being transported in zones of steep fluid velocity profiles (orthokinetic aggregation) such as occur in turbulent rivers. The bulk chemical properties between settling colloidal aggregates and not-settling colloids can be very different, especially in respect to their organic matter and trace metal content (Ranville et al., 1991).

Collision of two particles can have two outcomes, either the particles adhere to each other or they do not (O’Melia, 1992). As two similar, like-charged hydrophobic particles approach each other they begin to experience electrostatic repulsion as the gap between them closes. As the separation decreases the electrostatic repulsive forces increase and more energy is required to continue the approach. However, if the separation can be made sufficiently small, van der Waal’s attractive forces begin to come into play and ultimately overwhelm the repulsive forces and aggregation can take place. The overall surface charge and the thickness of the dif-

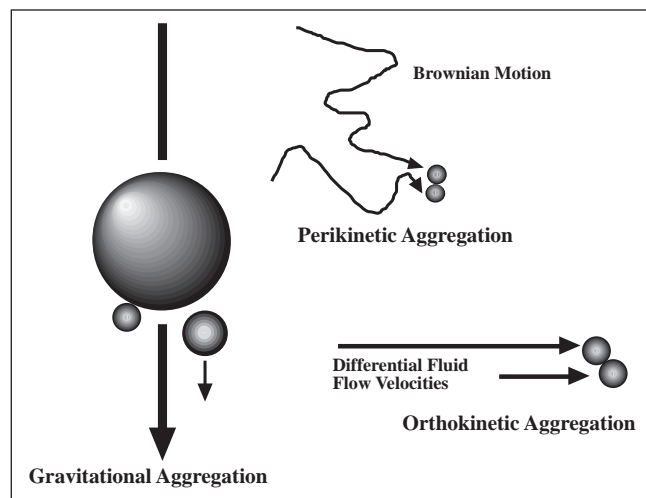


FIGURE 8.6—Physical processes causing particle collisions in surface waters that can lead to particle aggregation.

fuse charge layer surrounding the particle controls the magnitude of the repulsive force. The diffuse layer charge thickness is decreased by the presence of ions, especially multi-valent species, in the aqueous media. Therefore, as ionic strength increases the diffuse charge cloud shrinks and the repulsive force decreases and aggregation is more likely.

An example of this process may be observed in the behavior of iron oxyhydroxide precipitates that form in streams that receive acid-mine drainage. These types of streams often have abundant flocculated iron oxides on the streambed that are easily resuspended. Iron oxides often form as very small colloidal particles with diameters less than about 0.1 μm . These small primary particles have been observed to occur in much larger aggregates that rapidly settle to the streambed, as illustrated on Figure 8.7 (Ranville et al., 1991b). It is likely that the relatively high concentration of sulfate ion that occurs in these streams effectively neutralizes the net positive charge on iron oxyhydroxides that exist at pHs below 7–9 and also reduces the electrical double layer thus promoting particle aggregation.

THEORY OF COLLOID MOBILITY IN POROUS MEDIA

The abundance of colloids in groundwater is a function of their source area and(or) *in-situ* processes. Weathering and disaggregation results in the generation or release of colloids from the grain surface. Movement of colloids in a groundwater aquifer involves all the mechanisms of surface water transport with the added complications of finite pore sizes, very complex flow paths and abundant opportunity to interact with the solid aquifer matrix. This is illustrated in Figure 8.8, is described in detail by McDowell-Boyer et al. (1986) and is summarized here. An exhaustive review of colloid mobilization and transport in ground water is given by Ryan and Elimelech (1996).

Colloids may or may not penetrate an aquifer depending on their relative size compared to the pore size of the porous media.

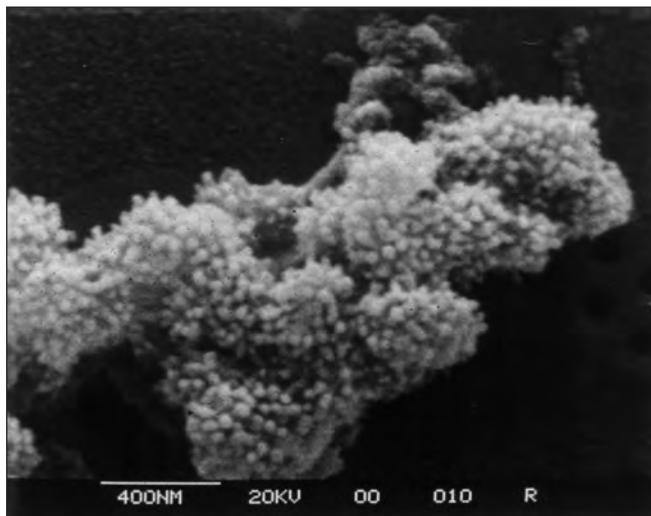


FIGURE 8.7—Scanning electron photomicrograph of a suspended iron oxyhydroxide particle collected from a stream receiving acid-mine drainage. Primary iron oxyhydroxide particles appear as spheres of about 0.05 μm diameter that are aggregated into larger particles with diameters of a few μm .

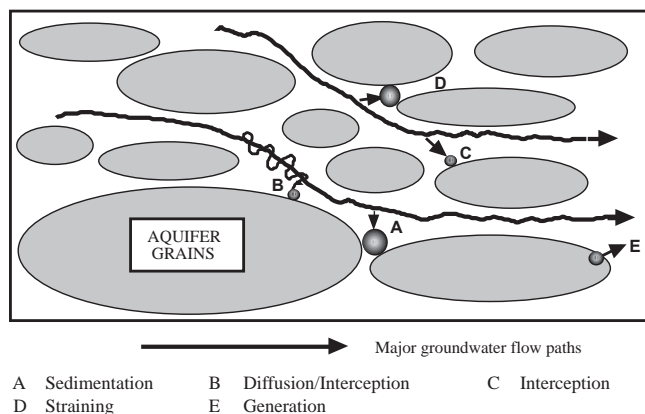


FIGURE 8.8—Processes occurring in a porous medium that affect colloid transport in ground water.

The grain size of the porous media is directly related to pore size, is considerably easier to measure, and therefore the more widely-used parameter. When the particle diameter/media diameter (d_p/d_m) is greater than 0.1, particles are normally excluded from a porous media and form an external cake. Somewhat smaller particles entering the porous media are subject to gravitational settling (depending on the flow velocity) and straining. Straining is the process whereby particles become trapped when they reach constrictions in the pores. Straining appears to be most important when d_p/d_m is between 0.1 and 0.05. Significant losses of porosity may occur due to straining, and the mechanism itself may become more important when either d_p increases, due to colloid agglomeration, and(or) when d_m decreases due to changes in lithology. The combination of these mechanisms probably result in the upper size limit for suspended and(or) mobile particles in porous media. According to these parameters, even the largest colloids (1 μm diameter) could easily enter a fine sand aquifer with uniform spherical grain sizes of 0.1 mm. Assuming clay-sized (0.001 mm) aquifer grains, colloids up to 50 nm could potentially move through the available pore spaces. Obviously these are very conservative estimates and do not take into account irregular grain shapes and non-uniform packing, which would reduce the maximum size of transportable particles.

For particles small enough to penetrate a porous media, the probability that they remain suspended or entrained in the prevailing flow depends in large measure on particle-media interactions. McDowell-Boyer et al. (1986) regard the process as physical-chemical filtration comprised of the initial collision and subsequent attachment mechanisms. A larger suspended particle may collide with a matrix surface as a result of gravitational forces “pulling” it from the flow path, or the trajectory of the flow lines may result in direct interception of the particle by the media surface. For smaller particles and perhaps all colloids, Brownian motion-based diffusion is the predominant collision mechanism. Brownian motion allows colloids to diffuse from the principle flow region within pore spaces and closely approach the aquifer grains where attachment may occur. Attachment is determined by the complex nature of the electrified interface and is a balance between attractive and repulsive forces as previously described. Attractive forces are dependent upon the nature of the particles whereas repulsive forces, due to charge on the surface are also

dependent upon water chemistry. Water chemistry parameters of importance include pH (Kita et al., 1987) and ionic strength (Cerdeira, 1987; McDowell-Boyer, 1992).

The consequence of the processes that remove both large and small particles is an optimum particle size for transport in porous media (Yao et al., 1971). The greatest mobility is shown to occur for particles near 1 μm . This suggests that filtration through 0.45 μm filters may result in under-estimation of colloid-associated contaminant transport. These processes have been most clearly demonstrated by the work of Harvey et al. (1989) with various tracer tests which were conducted between monitoring wells in a glacial aquifer on Cape Cod, MA under conditions of natural and induced flow gradients. Chloride and bromide were used as conservative tracers and fluorescent-labeled bacteria and submicron latex spheres were used to study the mobility of particles. These tests demonstrated that:

- 1) Micron- and submicron-size particles can easily migrate in porous media.
- 2) Average velocities of particles may exceed those of conservative solutes.
- 3) As predicted, submicron-size particles travel more slowly than micron-size particles.
- 4) The chemical functionality of the spheres (carboxyl, carbonyl, uncharged) affects retention and retardation.

The transport of these spheres was successfully modeled by colloid filtration theory (Harvey and Garabedian, 1991).

Additional research reveals the potential impact of colloids on adsorbed contaminant transport in a porous media. Puls and Powell (1992) compared the mobility of arsenic associated with iron oxide colloidal particles to that of truly dissolved arsenic in laboratory columns of natural aquifer material. Tritium was used as conservative tracer. The following was reported; FeOx colloids moved very easily through the columns (shown by the similarity of the tritium and colloid arrival times), colloid-associated As was transported through the columns 21 times faster than dissolved As, and colloid velocity was a function of colloid size and the ionic environment of the solutions.

METHODS OF ANALYSIS OF AQUATIC COLLOIDS

The study of environmental colloids requires special care in their collection and physical, and chemical characterization. The bulk chemical properties of colloids are less sensitive to post-sampling changes than the surface chemical properties and the physical properties of particle size and degree of aggregation. The ease of alteration of a colloid's properties, combined with their low concentrations in most waters, which generally require sample concentration, make these materials extremely difficult to study unambiguously.

Aspects of sample collection

Full understanding of the distribution of dissolved and particulate components in any natural water requires that special care be taken to obtain representative samples and to avoid the creation of sampling artifacts. Artifacts include any result of the sampling process which causes the sample, as presented for analysis, to be physically or chemically different from the water *in situ*. While considerable attention has been given to the impact of sampling

artifacts on dissolved or presumably dissolved components (Barcelona, 1990; Kent and Payne, 1988; Smith et al., 1988; Herzog et al., 1991; Palmer et al., 1987; Barcelona and Helfrich 1986; U.S. EPA, 1986, and many others), less regard has been focused on particles, and especially colloids. It is now clear that the act of sampling, especially of ground waters, can alter suspended particulate populations *in situ* and therefore bias information, not only about the particulates themselves, but also about dissolved constituents (Ryan and Gschwend, 1990; Backhaus et al., 1986).

The problem of artifacts is especially acute in groundwater sampling because:

- 1) Physical and chemical conditions in deep or confined aquifers and even some relatively shallow, unconfined aquifers may be significantly different than those at the surface.
- 2) The act of sampling can impose dramatic changes in the immediate vicinity of the sampling point.

Regarding the first point, differences in total pressure, partial pressures of reactive gases (e.g., CO_2 or H_2S), temperature, and light can affect; composition of dissolved gases and other volatile components, heterogeneous equilibria involving gas phases, and reaction rates. These in turn can alter the redox state, carbonate equilibria, and pH, which can initiate precipitation-dissolution reactions, shifts in aqueous phase speciation, and(or) changes in sorption-desorption equilibria. Many of these potential reactions can affect the identity, quantity, stability, size, and sorbed chemical composition of colloidal phases.

Regarding the second point, well development activities that often induce considerable turbulence, such as purging and sample collection (especially when done with high-volume pumps), can mobilize particles from the aquifer matrix because these actions can impose higher-than-normal piezometric gradients and can result in accelerated flow velocities. This results in the mobilization of particles that might otherwise remain attached to the aquifer media and(or) disturbance of the size distribution of existing suspended matter; either could alter the distribution of analytes in the sample. EPA currently recommends low velocity sampling whenever possible (Puls and Barcelona; 1989).

Only recently have the effects of sampling on groundwater colloids been studied (Backhaus et al., 1986; Puls et al., 1990). Puls et al. (1991) found that bailed samples contained significantly higher concentrations of particulate chromium and arsenic than pumped samples. This presumably was due to turbulence in the well that caused re-suspension of particles from either the bottom of the well or from the surrounding aquifer. Furthermore, Puls et al. (1991) found differences between pump types which related primarily to sampling rate. A bladder pump (flow rate = 0.6–1.1 l/min) produced 13 times less particles than a low speed submersible pump (2.8–3.8 l/min) and 20 times less than a high speed submersible pump (12–92 l/min). Light scattering intensity, a measure of particle concentration, has been shown to decrease as pumping rates decreased (Ryan and Gschwend, 1990) indicating unnatural entrainment of particles by pumping. Light-scattering and turbidity measurements have also shown that in some cases, many more well casing volumes must be purged to reach a stable particulate concentration than for stabilization of dissolved groundwater chemical parameters such as pH, dissolved oxygen, temperature, and Eh (Ryan and Gschwend, 1990; Puls et al., 1991). Gschwend et al. (1990) employed a modified gear pump to obtain groundwater samples at very low rates in order to study colloids. These studies collectively suggest that groundwater samples

should be taken at low pumping rates ($<100 \text{ ml min}^{-1}$) and that particle-sensitive parameters such as turbidity should be monitored to determine purging volumes.

Water should not be withdrawn from a well bore faster than it recharges under normal hydrostatic conditions, so as to not exceed normal interstitial flow velocities. This pertains to purging as well as sampling. To achieve this there should be no drawdown during purging or sampling where a single aquifer is present. Where multiple aquifers are present the individual water producing intervals should be isolated if possible and the *in-situ* pressure monitored during withdrawal. Such practices raise the issue of practicality, particularly in the case of a slowly-recharging monitoring well. Sampling protocol decisions should not be made on the basis of very short term cost analysis but on the long term benefits of accurate baseline data, reproducible values and understanding.

An additional concern for groundwater sampling where colloid-sensitive parameters are concerned is contact with the atmosphere. Formation of ferric oxyhydroxide precipitates and their subsequent flocculation are common occurrences when reduced waters are exposed to air. A study the colloid-facilitated groundwater transport of radionuclides in the Gorleben aquifer (F.D.R.), avoided this problem by transferring samples directly into resin coated aluminum drums equipped with an N_2 atmosphere (Lieser and Hill, 1992; Deerlove et al., 1991; and Kim et al., 1992).

In sampling surface waters, precautions similar to those used in groundwater sampling to exclude exposure to the atmosphere, must be taken when sampling lakes and reservoirs, especially where anaerobic zones exist. Redox-sensitive species such as iron exist as very different phases in oxic and anoxic waters and have been shown to exist in significant amounts as colloids at the oxic-anoxic boundary (Buffle et al., 1989). For flowing surface waters (rivers, canals, etc.) the non-homogenous distribution of particles vertically and horizontally must be taken into account. Techniques to obtain horizontally and vertically integrated, discharge-weighted samples should be used (Meade and Stevens, 1990). Pressure-compensating, isokinetic bag-samplers allow collection of sample volumes at each point which represent the proportion of flow at that point. From this data the mass flux of colloidal particles can be computed. These methods have recently been used to investigate colloidal size distributions in the Mississippi River (Rees and Ranville, 1990).

Current standard filtration practices

Sample filtration is a critical aspect of natural water sampling, both to the geochemist interested in details of solute speciation, modeling and transport mechanisms, and to those concerned with regulatory compliance and/or water facilities operations. Filtration is also a point of considerable disagreement revolving around suspended particles and colloids (Nielsen, 1991). For the geochemist, equilibrium-based solute modeling utilizing analytical data from samples which include particulate-associated cations or anions as a significant portion of the "dissolved" solute is an exercise in futility. For owner/operators of water facilities or environmentally regulated facilities, specified sample filtration practices are mandated for regulatory compliance (even though such practices may produce misleading data); however, additional correct and elective filtration practices may be necessary to obtain an accurate understanding of process control.

Standard practice for filtration of those natural waters intend-

ed for "dissolved" (as opposed to "suspended," "total," or "acid-extractable") species analysis is to filter through a submicron, typically $0.45 \mu\text{m}$, membrane filter. The selection of the $0.45 \mu\text{m}$ pore size appears to have its origin in early bacteriology and the smallest dimensions of some bacteria. It is not apparent that such a size was ever intended to address solutes. Greenberg et al. (1992) suggests either vacuum or pressure filtration through a 0.4 or $0.45 \mu\text{m}$ polycarbonate or cellulose acetate filter for dissolved metals analysis, certain inorganic non-metals like sulfate and phosphate, and waters to be analyzed by ion chromatography, but make no recommendations for other constituents. The U.S. EPA (1986) specifies $0.45 \mu\text{m}$ filtration for metals analysis on one split of the sample and no filtration of the other split. The U.S. Geological Survey (1982) recommends filtration for all dissolved inorganic constituents through a non-metallic $0.45 \mu\text{m}$ filter. Barcelona (1990) cautions that dissolved gases and volatile organic constituents are notable exceptions to the above recommendations and should never be determined in filtered samples. "Dissolved" is thus operationally defined as anything passing a $0.45 \mu\text{m}$ filter but Hem (1985) alludes to the inadequacy of this definition.

Recent studies have revealed the particulate-associated nature of significant portions of ions and molecules in the $<0.45 \mu\text{m}$ fraction of natural waters. These observations obviously compromise the $0.45 \mu\text{m}$ filter pore size-based operational term "dissolved" which clearly ignores colloids. This is further discussed in the "Colloids in Natural Waters" section. Filtration using $0.45 \mu\text{m}$ membranes is also inadequate to determine colloid-associated chemical species as colloid sizes spans a range which encompasses this size.

Particle size analysis

Many techniques exist for the size analysis of colloidal particles, however, the discussion of these methods will be limited in this paper. Methods include those based on light-scattering, microscopy, sedimentation, filtration, and dialysis. Coupling of some size analysis methods with a wide variety of chemical analysis gives additional information of the composition of various sized particles. Since the focus of this discussion is contaminant transport only those methods providing chemical information will be presented.

Scanning electron microscopy and transmission electron microscopy are extremely useful techniques for examining colloids (Nomizu et al., 1988). Microscopy provides the most direct way of sizing particles but is very time consuming and care must be taken to avoid creation of artifacts. Limited chemical information is provided by energy-dispersive X-ray analysis (EDAX) commonly available with SEM instruments. Electron microscope techniques for examining colloids in natural waters have been reviewed by Leppard (1992).

Considerable difficulty exists in differentiating between colloids and dissolved species. Filtration through micro-porous membranes, dialysis, and centrifugation at high gravities have been employed for this separation (Batley, 1990). Obviously the distinction between "colloidal" and "dissolved" is operational and furthermore, many factors affect the actual physical size or molecular weight of particles passing a given nominal filter pore size, especially when membrane filtration is employed. Filtration through successively smaller pore sizes has most commonly been used to give size distributions of colloidal-sized particles and to

ultimately obtain the "dissolved" fraction of natural waters (Kennedy et al., 1974; Wagemann and Brunskill, 1975; Danielsson, 1982; Laxen and Chandler, 1982; Hoffman et al., 1981; Tanizaki et al., 1992).

Factors affecting the results of filtration were carefully examined by Buffle et al. (1992), including such variables as filter type, filter loading, and flow rates. Two major types of commercial filters exist and were examined: (1) depth filters, composed of a complex mat of fibers which retain particles within the matrix of the filter; and (2) screen filters, which consist of non-porous materials containing discrete holes that retain particles on the surface of the filter.

The most important physicochemical processes occurring during filtration were (1) concentration polarization (i.e., buildup of particles) at the membrane surface, which promotes coagulation and alteration of the size distribution, and (2) membrane exclusion effects which inhibit the passage of very small particles through pores with similar diameters. Honeyman and Santschi (1991) documented the failure of $0.25 \mu\text{m}$ ^{59}Fe -hematite particles to pass a $0.40 \mu\text{m}$ membrane filter, apparently as a result of aggregation at the filter surface. The study of Buffle et al. (1992) illustrated how dependent the results of filtration are on procedural technique and suggests that any interpretation of particle size measurements based on filtration must be carefully examined within the context of how the filtration was performed. Often filtration is routinely performed in the field with little control over the methods used. This has ominous consequences as to how valid our current data base is on the "true" distribution of solutes, colloids, and suspended particles in natural waters.

Cross-flow filtration is a very promising filtration method which may overcome some of the aforementioned problems associated with filtration (Gutman, 1987). In tangential or cross-flow filtration, a high flow rate is maintained parallel to the filter membrane while a much lower flow rate of filtrate passes through the membrane. This method induces large shear forces near the membrane surface and thus reduces both the concentration polarization region and membrane fouling. Filtration membranes are generally stacked in order to provide large areas, on the order of a few square meters, to further limit filter fouling. The method allows processing of large volumes of water to isolate colloids in significant quantities without reduced filtration rates. Cross-flow filtration uses systems based on either hollow-fibers ($4\text{--}8 \text{ l min}^{-1}$ @ $0.2 \mu\text{m}$, Kuwabara and Harvey, 1990; Marley et al., 1991) or flat membranes ($10\text{--}12 \text{ l hr}^{-1}$ @ 10000 MW or $\approx 10 \text{ nm}$, Whitehouse et al., 1986, 1990). A number of studies have utilized these techniques with success in producing upwards of gram quantities of material in the colloid size range. Tangential-flow filtration using different sized membranes in series has been used successfully to isolate particles in various colloidal size classes Douglas et al. (1996). The accuracy of the size cutoff for tangential-flow filtration has not as yet been investigated.

Continuous-flow centrifugation is a useful technique for the large scale isolation of suspended particles and larger colloids. In this method a suspension is continuously passed through a spinning centrifuge. Larger particles are retained on the walls of the centrifuge bowl whereas solutes and smaller particles are carried through (Horowitz et al., 1989). Continuous flow centrifugation has been used to separate river water particles down to about $0.3 \mu\text{m}$ (Leenheer et al., 1989; Rees et al., 1991; Douglas et al., 1996). It has been noted that suspended particles retained by continuous flow filtration, when disaggregated, show similar particle size dis-

tributions to the colloids not retained by the centrifuge (Rees et al., 1991). This suggests either the particles occur as aggregates in the sample or aggregation occurs in the centrifuge.

A new and very powerful method of colloid size analysis is field-flow fractionation (Beckett et al., 1988). This method, analogous to chromatography, provides high resolution and a continuous distribution unlike sequential filtration which has low resolution, which is defined by the number of pore sizes used. Various sub-techniques of field-flow fractionation exist which allow analysis of particles ranging in size from 0.001 to $50 \mu\text{m}$. Because this method elutes the fractionated particles, fractions can be further analyzed for their composition. This technique has been shown to be useful to study colloid-pollutant interactions (Beckett et al., 1990), especially with the recent direct coupling of the FFF technique to ICP-MS analysis (Ranville et al., 1998; Taylor et al., 1992; Murphy et al., 1993).

COLLOIDS IN NATURAL WATERS

Colloids occur to varying extents in essentially all aquatic environments. The colloids present in surface waters and ground waters consist of mixtures of generally similar materials. However, the relative abundance of each component can vary from one environment to another. Specific examples of the types and abundances of colloids in various environments are given in the following paragraphs.

Surface water colloids

Most data on the importance of colloids in aquatic systems come from studies of surface waters. Fluvial suspended sediments are generally composed of aggregates and contain variable percentages of particles less than $2 \mu\text{m}$. Walling and Moorehead (1989) found the amount of less than $2 \mu\text{m}$ material ranged from about $10\text{--}30\%$. After disaggregation the amount of less than $2 \mu\text{m}$ material increased to $40\text{--}80\%$, with $5\text{--}30\%$ less than $0.2 \mu\text{m}$.

Some researchers have found little or no differences between $0.45 \mu\text{m}$ filtrates and ultrafiltrates ($10\text{--}100 \text{ K daltons}$) for most elemental concentrations, suggesting little colloidal material less than $0.45 \mu\text{m}$ (Taylor et al., 1990; Waber et al., 1990). In contrast, Hoffman et al. (1981) used an ultrafiltration scheme to investigate trace metal concentrations in sizes ranging from less than $10,000$ to greater than $100,000$ daltons. Their results show significant amounts of trace metal were present as colloidal particles in the upper Mississippi River. Salbu et al. (1985) studied colloidal metals in surface and ground waters using filtration, dialysis, and centrifugation; they found, for example, that the majority of Cd and Cr were present in the $0.1\text{--}0.005 \mu\text{m}$ fraction. Moran and Moore (1989), using cross-flow filtration, found 15% of the $<0.45 \mu\text{m}$ aluminum to be present in the $<10,000$ dalton fraction of open sea water.

The size distribution and concentrations of 46 elements in eight Japanese river waters was determined by Tanizaki et al. (1992) using filtration and ultrafiltration. They were able to divide elements into groups based on their affinities for various size classes, including: suspended sediments ($>0.45 \mu\text{m}$); colloid fractions of $0.45 \mu\text{m}\text{--}10,000$ dalton and $10,000\text{--}500$ daltons; and solutes <500 dalton. Transition elements were largely present in the $>0.45 \mu\text{m}$, $10,000\text{--}500$ dalton, and <500 dalton fractions. The

most dramatic colloidal effects were evident in the trace element determinations, particularly REEs, where typically less than 20% of the <0.45 μm fraction content was present in the <500 dalton fraction (see Table 8.3). These results compare favorably with those of Kim et al. (1992) who studied REE elements in ground waters.

TABLE 8.3—Average percentages of the concentration of 44 chemical species in 0.45 mm filtrate that remain in 500 dalton ultrafiltrate. Data from Tanizaki et. al. (1992).

Species	% remaining	Species	% remaining	Species	% remaining
Cl	98.2	Ca	71.1	Mo	28.0
Na	93.2	Mn	66.9	Ho	20.0
Al	90.2	Ta	65.2	Th	18.0
Rb	89.6	Ni	42.4	Sm	16.0
K	89.5	As	42.0	Ce	13.0
SiO ₂	88.7	Cr	40.5	Eu	11.9
Cs	87.7	SO ₄ ⁼	40.5	Yb	11.7
CO ₃ ⁼	86.3	Co	37.9	La	10.3
Au	84.0	W	37.8	Tb	10.2
V	74.6	U	34.2	Sc	9.6
Sb	74.0	Zn	32.1	Fe	9.3
Ba	72.8	Se	31.9	Lu	8.6
Sr	72.5	Hf	30.6	Tm	7.8
Br	72.1	PO ₄ ⁼	29.9	Ag	5.2
Mg	71.1	Organic C	28.6		

Table 8.4 contains selected results of an exercise using the data of Tanizaki et al. (1992) as input for chemical modeling using PHREEQE (Parkhurst et al., 1980). The results illustrate the potential differences that can arise from the use of chemical data which include some particulate-associated ions in the solute values. Major ion concentrations and the mineral saturation indices solely based on them (e.g., calcite, halite, etc.) are relatively unaffected by filtration. However, minor and trace element concentrations and the predicted thermodynamic solubility of solid phases containing those elements show greater impacts. For example, ferrihydrite (Fe(OH)₃) appears to be slightly supersaturated in the <0.45 μm filtrate ($SI = \log(IAP/K_{sp}) = 0.84$) but is undersaturated ($SI = -0.23$) in the more truly “dissolved” (<500 dalton) fraction. In the case of zinc, results using <0.45 μm indicate supersaturation with a zinc phosphate mineral, whereas <500 dalton data indicate undersaturation with respect to this mineral. More work should prove fruitful in establishing the true nature of transported loads in natural waters. It should, however, already be evident that thermochemical-based modeling of <0.45 μm filtrates should be limited to those constituents not significantly attenuated by such

filters.

Humic substances, which are ubiquitous in surface and ground waters, exist at the boundary between dissolved and colloidal size with molecular weights of about 700 to 2000 daltons, and as such are best considered macromolecules. These materials are excellent complexers of metals and radionuclides in solution (Buffle, 1988). Humic substances sorbed to surfaces generally affect the metal sorption of the particles by increasing sorption at low pH (Davis, 1984; Tipping et al., 1983). Some recent work, however, suggests a lesser role for sorbed organic matter in trace metal partitioning in acid mine drainage (Smith et al., 1992), presumably due to competition from the abundant dissolved iron for binding sites. Humic substances have been demonstrated to influence the transport of organic contaminants in aquatic systems (Enfield and Bengtsson, 1988). The transport of cadmium through soil columns was greatly enhanced by the presence of humic material (Dunnivant et al., 1992).

Higher molecular weight organic colloids have been found to occur in estuarine waters (Sigleo and Helz, 1981) and porewaters at high concentration (Chin and Geschwend, 1992a). These colloids have been shown to affect the partitioning of hydrophobic organic chemicals (Means and Wijayarathne, 1982; Chin and Geschwend, 1992b) and are expected to also bind trace metals. Porewater organic colloids can diffuse into overlying waters and may act to enhance the flux of contaminants from these sediments (Thoma et al., 1991).

Colloidal iron and manganese phases are common in surface waters (Laxen, 1983) and are often present in regions of redox boundaries. These boundaries frequently occur in lakes at the oxycline, where dissolved oxygen disappears due to biological respiration. These particles are generally a few tenths of a micrometer in size and are associated with organic matter and phosphorous (Buffle et al., 1989).

A very important redox-active system is acid-mine drainage. In these systems ferrous iron is oxidized to ferric iron, which then hydrolyzes and subsequently precipitates as colloidal hydrous iron oxides and hydrous iron hydroxysulfates (see Nordstrom and Alpers, 1999; Smith, 1999). Colloidal iron can make up a significant portion of total suspended iron in these systems and can also adsorb and transport trace metals (Smith, 1999). Roughly an order of magnitude difference between 0.45 μm and 0.01 μm filtered iron has been shown to persist in a river for hundreds of kilometers downstream of acid-mine drainage inputs (Kimball et al., 1995). Solubility calculations for iron hydroxides will not only be affected by the enhanced solubility of small particles (Langmuir and Whittemore, 1971) but in a more practical sense by the choice of filter pore size used to determine “dissolved” iron (Kimball et al., 1992). Acid-mine drainage systems are the only environment where positively charged particles have been clearly demonstrated

TABLE 8.4—Selected geochemical modeling (PHREEQE) results of data from Tanizaki et al. (1992) comparing the mineral saturation indices [$SI = \log(IAP/K_{sp})$] obtained by inputting “dissolved” concentrations into the model using either 0.45 μm or 500 dalton filtrate data. IAP is the product of the aqueous ion activities of the species that are formed by dissolution of the mineral and K_{sp} is the minerals solubility product. For a mineral at equilibrium $SI = 0$, for supersaturation $SI > 0$, and for under saturation $SI < 0$.

Mineral	Al(OH) ₃ amorphous	KAl(SO ₄) ₂ (OH) ₆ alunite	CaCO ₃ calcite	Fe(OH) ₃ ferrihydrite	FePO ₄ ·2H ₂ O strengite	Zn ₃ (PO ₄) ₂
SI (<0.45 mm)	-0.005	-0.54	-1.5	0.84	-0.55	1.5
SI (<500 Dalton)	-0.20	-2.1	-1.7	-0.23	-2.1	-0.12

to exist in surface water (Newton and Liss, 1987; Ranville et al., 1991b). This occurs primarily as a result of insufficient organic matter to fully coat the extensive iron hydroxides surfaces formed in these systems. This may affect both metal interaction with iron oxyhydroxide colloids and particle stability, and hence transport.

Soil and groundwater colloids

A significant amount of the mineral and organic components of soils are colloidal in size. These components are bound up in aggregates that make up the "texture" of soils. The properties of some soil colloids were studied by Bremner and Genrich (1990). In a study of ten Iowa Mollisols they found that on average, 30% of the soil mass was less than 2 μm in size. Even more importantly, the <2 μm fraction contained 68, 73, and 80% of the total organic matter, iron and cation exchange capacity respectively. Mobilization of soil colloids can thus carry colloid-associated contaminants vertically into the aquifer. Vertical transport of DDT adsorbed on sewage particles and Paraquat adsorbed to montmorillonite was observed in soil columns by Vinten et al. (1983). The addition of calcium chloride significantly reduced the amount of pesticide transported, presumably either by aggregation and straining in the pores or by sorption of the particles to the soil matrix. The physical structure of soils will greatly influence colloid transport. Macropores, consisting of connected fractures and root channels, have been shown to facilitate the transport of organic and mineral colloids in soils (Chittleborough et al., 1992). The presence of these macropores will complicate transport modeling which is based on flow through porous media, particularly for colloids.

Very few studies have investigated the nature and amount of colloids naturally present in groundwater (Reynolds, 1985). Salbu et al. (1985) used centrifugation, filtration, hollow-fiber ultrafiltration and dialysis to determine colloid concentrations in groundwater. The concentrations of 20 elements were determined in four size fractions: >0.45 μm , 0.45–0.1 μm , 0.1–0.005 μm , <0.005 μm . In the groundwater, iron, zinc, and copper were primarily present as particles >0.45 μm , whereas chromium, cadmium, and manganese showed significant amounts in each of the size fractions. Colloidal particles have been found in deep fractures in granite at a concentration of 10^{10} particles/l (Degueldre et al., 1989); these colloids consisted primarily of small alumino-silicates. Waber et al. (1990) studied the relationship between colloid content of the river Glatt and a shallow aquifer which is continuously recharged by the river. Colloid (<0.45 μm) concentrations in the river were computed to be approximately 2.3 mg/l, of which >90% was composed of organic matter. In contrast, the colloid concentration in the groundwater was an order of magnitude less, thus leading the authors to conclude that transport of colloids from the river to the groundwater was insignificant.

Natural and anthropogenic changes to the chemistry of soil and ground waters can result in the formation or liberation of colloids. This is particularly true for changes that may remove cementing agents, which bind together soil and aquifer matrix colloids. Ryan and Geschwend (1990) found that dissolution of iron hydroxides by infiltration waters with naturally low Eh released colloidal kaolinite and other alumino-silicates. Dissolution of iron hydroxides might also be expected to release organic matter that has been shown to strongly adsorb to iron hydroxides (Tipping and Cooke, 1982). This process might mobi-

lize contaminants associated with the released organic matter. Geschwend et al. (1990) found that perturbation of the carbonate equilibrium of a groundwater near a coal ash disposal site resulted in dissolution of calcite and decementation which released colloids into the groundwater. SEM-EDX analysis suggested these colloids were composed of alumino-silicates and residual carbonate cements. Changes in groundwater conductivity or pH can mobilize otherwise immobile colloids. Significant amounts of colloidal particles have been mobilized by artificial recharge of an aquifer by low conductivity surface water (Nightingale and Bianchi, 1977); from turbidity data, these researchers estimated a groundwater particle concentration of 9.93 mg/l and that approximately 148 metric tons of particles were liberated from the overlying sandy soils during one year of recharge. These colloids appeared to be effectively transported since no decrease in recharge rate was observed. Application of gypsum prevented mobilization of colloids by destabilizing the colloids.

Precipitation of colloids resulting from human-caused perturbations in water chemistry can occur in aquifers. Reaction of phosphorous-rich sewage effluent with aquifer iron resulted in the precipitation of ferrous phosphate colloids in a sand and gravel aquifer at Cape Cod (Geschwend and Reynolds, 1987). These particles were approximately 0.1 μm in size and fairly monodisperse. Particle concentration was estimated at 10^6 particles/liter.

Biocolloids

Much of the information on colloid transport in ground waters comes from work with biocolloids. Bacteria and viruses, have been demonstrated to be transported over significant distances in groundwater (Gerba and Bitton, 1984). Laboratory experiments have shown pH to be a major factor in interaction between bacteria and the aquifer matrix (Scholl and Harvey, 1992). The deposition of bacteria in soil columns can be modeled by using electrical double layer theory (see Smith, 1999) to explain bacterial stability and clean-bed filtration theory to describe the physical processes involved (Martin et al., 1992).

Radionuclides

One of the most important areas for concern over colloid-facilitated transport of contaminants is of that of radionuclide transport. Most radionuclides are considered extremely insoluble or highly sorbing, and hence immobile in the aquatic environment. A number of studies have indicated the radionuclides are indeed mobile in groundwater and this may be attributed to colloid transport. Bates et al. (1992) clearly show the formation of colloids containing radionuclides by the interaction of waste glass with water. These colloids form near the surface of the glass and can be released into solution. Colloid associated radionuclides were found at the Nevada test site, where after a nuclear test, colloid concentrations in the cavity formed were on the order of 10 mg/l (Buddemeier and Hunt, 1988). Hollow-fiber ultrafiltration was used by Lawson and Short (1990) to investigate colloids in groundwater down-gradient from a uranium ore body. These researchers found colloids in the size range of 1.0–0.018 μm were composed of iron and silica, and contained uranium and thorium. Although only a minor proportion of the total uranium was associated with the colloids, a significant amount of ^{230}Th was associ-

ated with the colloid. Enhanced transport of americium and plutonium in an aquifer in an arid climate was demonstrated by Penrose et al. (1990). Predicted transport based on measurements of radionuclide sorption to soil materials were on the order of a few meters, whereas observations showed transport of several kilometers.

Kim et al. (1992), using membrane filtration, determined the abundances of a wide variety of elements in >0.4 , $0.4-0.1$, $0.1-0.002$ and $0.002-0.001$ μm fractions of deep (150–300m) ground waters from a sedimentary sequence overlying a salt dome intended for disposal of radionuclides. Their results showed that 70–87% of REE, selected transition metals, uranium and thorium, 99% of americium (Am^{3+}) and curium (Cm^{3+}) and 90+% of DOC found in the <0.4 μm filtrates were removed by filtration through 0.001 μm filters. Thus the 0.4 μm filtrate provided a significant overestimate of the dissolved content of these constituents. Acidification, however, allowed effectively all Am and Cm to pass the 0.001 μm filter and time resolved laser fluorescence spectroscopy (TRLFS) indicated these elements were bound to fulvic acid colloids. Puls and Barcelona (1989), working with ground waters from the Globe, Arizona area, observed a steady decrease in major, minor and transition elements using 10, 0.4 and 0.1 μm filters respectively.

MODELING COLLOID TRANSPORT

Modeling of colloid-facilitated transport is in its infancy. Various models exist which describe filtration and coagulation effects but few overall transport models for ground waters are available. These are reviewed and classified by Mills et al. (1991). An early one-dimensional colloid transport model was presented by Travis and Nuttal (1987). Mills et al. (1991) developed a conceptual model (COMET, COLLOIDS-METAL Transport) to predict colloidally-facilitated transport of metals in porous media and incorporated it into EPA's CML model for multimedia exposure assessment. Their calculations suggest greatly enhanced transport of contaminants when colloids are present, if the colloid-solute partition coefficient is significantly greater than the immobile aquifer-solute partition coefficient. The incorporation of more sophisticated adsorption models, as opposed to partition coefficients, into a similar framework may provide better results.

CONCLUSIONS

Colloids are recognized as a distinct mobile solid phase in the majority of natural water systems. These particles are capable of hosting heterogeneous reactions typically ascribed to immobile solid phases, but exhibit mobilities similar to those of true solutes and the aqueous media itself. An important role for colloidal particles in facilitating transport of contaminants in surface and ground waters is theoretically reasonable and is supported by a relatively small but rapidly growing number of field and laboratory studies. Interest is strong not only in the area of understanding the existing role of colloids in a given situation but also in the area of manipulating colloids to control contaminant migration (McCarthy and Wobber, 1993).

The mobility of particles in the micron size range, as shown by laboratory studies and limited field data, suggests that standard filtration practices (0.45 μm) may overestimate truly dissolved con-

centrations (including contaminant loads). On the other hand, the use of ultrafilters may result in seriously underestimating the total transported contaminant load, which includes that portion carried by colloids. Furthermore, filtration results are greatly affected by factors such as flow rate through the filter, total volumes filtered through a given filter apparatus, concentration of particles, filter type, and sample storage time. Often these variables are not considered during the design of field sampling schemes and (or) filtering practices are not reproducible from one sampling event to the next. Even if considered, these variables are often not closely controlled in the field due to the pressure to obtain samples in a rapid, cost-effective manner. For this reason, the EPA has suggested the collection of both unfiltered and filtered water samples (Puls et al., 1991). If significant differences are found, further examination is recommended to access the possibility of colloidal transport. It should be pointed out that such a comparison yields little direct evidence about colloid-associated loads if a relatively large pore size filter (e.g., 0.45 μm) is employed.

The magnitude of the general importance of colloids and colloid-facilitated transport is yet to be determined, especially in groundwater systems. In the case of ground waters it appears that the most important factor determining the mobility of natural colloids is the groundwater chemistry. In particular, changes to groundwater chemistry (i.e., pH, ionic strength, redox, and chemical composition) due to human activities can influence colloid stability. Colloids may be formed by *in-situ* precipitation reactions or liberated from aquifer material. Similarly, alterations in the ambient chemistry may result in destabilization of existing colloids through flocculation or adhesion to the matrix. In the course of investigations of groundwater contamination sites, determination of the spatial distributions of colloids may give important clues to understanding the migration of contaminants and the most effective means of remediation.

Various aspects of groundwater sampling protocol, such as pump type, purging schedules, sampling rate, and control of redox and dissolved gases can influence colloid populations and hence the results of chemical analyses. This is particularly true of unfiltered or inadequately filtered samples. Improper sampling techniques which disturb the groundwater in the vicinity of the well bore may result in artificially high levels of particulates. Observed temporal variations in dissolved and particulate concentrations may therefore be as much due to differences in sampling and filtration techniques as due to real physicochemical speciation. It cannot be strongly enough stressed that our understanding of the nature of contaminants in surface and groundwater will be incomplete until uniform sampling protocols, which accurately determine the presence of micrometer and sub-micrometer sized particles are developed.

Particle size and density control the movement of colloids and particles in porous media such as porous sedimentary rock. Surface charge and the nature of specific chemical surface sites are factors that control the attenuation of colloids and particles by porous media. The combination of these factors of particle movement and attenuation determine the mobility of these particles in groundwater. Despite the identification of these factors, transport of colloids and particles is currently only poorly modeled by filtration theory in even simple systems. Much work will be required to develop models for particle transport in soils and aquifers which are heterogeneous in nature.

Despite the current lack of a clear understanding of the role of colloids in contaminant transport, interest in colloids will contin-

ue to grow. It is now necessary for careful work to be done to develop the techniques and data bases which will, in time, provide a clearer picture of what, if any, role colloids play in the overall environmental fate and transport of contaminants in surface and ground waters.

REFERENCES

- Ali, W., O'Melia, C.R., and Edzwald, J.K., 1985, Colloidal stability of particles in lakes—Measurements and significance: *Water Science Technology*, v. 17, pp. 701–712.
- Allan, R.J., 1986, The role of particulate matter in the fate of contaminants in aquatic ecosystems; *in* *Water Quality Management—The Role of Particulate Matter in the Transport and Fate of Pollutants*: Water Studies Centre, Melbourne, Australia, pp. 1–56.
- Backhus, D.A., Geschwend, P.M., and Reynolds, M.D., 1986, Sampling colloids in groundwater [abs.]: EOS, H41D-03 0900H, v. 67, 954 pp.
- Barcelona, M.J., 1990, Uncertainties in ground water chemistry and sampling problems; *in* *Chemical Modeling of Aqueous Systems, II*. ACS Symposium Series: American Chemical Society, Washington, D.C., pp. 310–320.
- Barcelona, M.J., and Helfrich, J.A., 1986, Well construction and purging effects on ground-water samples: *Environmental Science and Technology*, v. 20, no. 11, pp. 1179–1184.
- Bates, J.K., Bradley, J.P., Teetsov, A., Bradley, C.R., and Buchholtz ten Brink, M., 1992, Colloid formation during waste form reaction—Implications for nuclear waste disposal: *Science*, v. 256, pp. 649–651.
- Batley, G.E., 1990, Physicochemical separation methods for trace element speciation in aquatic samples; *in* Batley, G.E., (ed.), *Trace Element Speciation—Analytical Methods and Problems*: CRC Press, Boca Raton, Fla., pp. 43–76.
- Beckett, R., 1990, The surface chemistry of humic substances; *in* Beckett, R., (ed.), *Surface and Colloid Chemistry in Natural Waters and Water Treatment*: Plenum Press, New York, pp. 3–20.
- Beckett, R., Nicholson, G., Hart, B.T., Hansen, M., and Giddings, J.C., 1988, Separation and size characterization of colloidal particles in river water by sedimentation field-flow fractionation: *Water Res.*, v. 22, pp. 1535–1545.
- Beckett, R., Hotchin, D.M., and Hart, B.T., 1990, The use of field-flow fractionation to study pollutant-colloid interactions: *J. Chromatog.*, v. 517, pp. 435–477.
- Bremner, J.M., and Grenrich, D.A., 1990, Characterization of the sand, silt and clay fractions of some Mollisols, *in* DeBoodt, M.F., Hayes, M.H.B., and Herbillon, A., (eds.), *Soil Colloids and Their Association in Aggregates*: Plenum Press, New York, pp. 423–483.
- Buddemeier, R.W., and Hunt, J.R., 1988, Transport of colloidal contaminants in groundwater—Radionuclide migration at the Nevada Test Site: *Applied Geochemistry*, v. 3, pp. 535–548.
- Buffle, J., 1988, Complexation reactions in aquatic systems—An analytical approach: Ellis Horwood, Chichester, UK, 692 pp.
- Buffle, J., DeVitre, R.R., Perret, D., and Leppard, G.G., 1989, Physicochemical characteristics of a colloidal iron phosphate species formed at the oxic-anoxic interface of a eutrophic lake: *Geochimica et Cosmochimica Acta*, v. 53, pp. 399–408.
- Buffle, J., Perret, D., and Newman, M., 1992, The use of filtration and ultrafiltration for size fractionation of aquatic particles, colloids, and macromolecules; *in* Buffle, J., and van Leeuwen, H., (eds.), *Environmental Particles, v. 1*: Lewis Publishers, Boca Raton, Fla., pp. 171–230.
- Cerda, C.M., 1987, Mobilization of kaolinite fines in porous media: *Colloids and Surf.*, v. 27, pp. 219–241.
- Chin, Y.P., and Geschwend, P.M., 1992a, The abundance distribution, and configuration of porewater organic colloids in recent sediments: *Geochimica et Cosmochimica Acta*, v. 55, no. 5, pp. 1309–1318.
- Chin, Y.P., and Geschwend, P.M., 1992b, Partitioning of polycyclic aromatic hydrocarbons to marine porewater colloids: *Environmental Science and Technology*, 26, pp. 1621–1626.
- Chittleborough, D.J., Smettem, K.R., Costaris, E., and Leaney, F.W., 1992, Seasonal changes in pathways of dissolved organic carbon through a hillslope soil (Xeralf) with contrasting texture: *Aust. J. Soil Res.*, v. 30, pp. 465–476.
- Danielsson, L.G., 1982, On the use of filters for distinguishing between dissolved and particulate fractions in natural waters: *Water Res.*, v. 16, pp. 179–182.
- Davis, J.A., 1984, Complexation of trace metals by adsorbed organic matter: *Geochimica et Cosmochimica Acta*, v. 48, pp. 679–691.
- Davis, J.A., and Kent, D.B., 1990, Surface complexation modeling in aqueous geochemistry; *in* Hochella, M.E., Jr., and White, A.F., (eds.), *Mineral-Water Interface Geochemistry: Reviews in Mineralogy*, Mineralogical Society of America, Washington, D.C., v. 23, pp. 177–248.
- Deerlove, J.P.L., Longworth, G., Ivanovich, M.J.I., Delakowitz, B., and Zeh, P., 1991, A study of groundwater-colloids and their geochemical interactions with natural radionuclides in Gorleben aquifer systems: *Radiochimica Acta*, v. 52/53, pp. 83–89.
- Degueldre, C., Baeyens, B., Goerlich, W., Riga, J., Verbist, J., and Stadelmann, P., 1989, Colloids in water from a subsurface fracture in granitic rock, Grimsel Test Site, Switzerland: *Geochimica et Cosmochimica Acta*, v. 53, no. 3, pp. 603–610.
- Domenico, P.A., and Schwartz, F.W., 1990, *Physical and chemical hydrogeology*: John Wiley and Sons, New York, 824 pp.
- Douglas, G.B., Beckett, R., and Hart, B.T., 1996, Fractionation and concentration of suspended particulate matter in natural waters: *Hydrological Processes*, v. 7.
- Driscoll, G.W., 1986, *Ground water and wells*, 2nd ed.: Johnson Division, St. Paul, Minn., 1089 pp.
- Dunnivant, F.M., Jardine, P.M., and Taylor, D.L., 1992, Transport of naturally occurring dissolved organic carbon in laboratory columns containing aquifer material: *Soil Science Society of America Journal*, v. 56, no. 2, pp. 437.
- Enfield, C.G., and Bengtsson, G., 1988, Macromolecular transport of hydrophobic contaminants in aqueous environments: *Groundwater*, v. 26, no. 1, pp. 64–70.
- Forstner, U., and Salomons, W., 1983, Trace element speciation in surface waters—Interactions with particulate matter; *in* Leppard, G.G., (ed.), *Trace Element Speciation in Surface Waters and Its Ecological Implications*: Plenum Press, New York, pp. 245–273.
- Freeze, R.A., and Cherry, J.A., 1979, *Groundwater*: Prentice-Hall, Englewood Cliffs, N.J., 604 pp.
- Gibbs, R.J., 1983, Effect of natural organic coatings on the coagulation of particles: *Environmental Science and Technology*, v. 17, pp. 237–240.
- Gerba, C.P., and Bitton, G., 1984, Microbial pollutants—Their survival and transport pattern to groundwater; *in* Bitton, G., and Gerba, C.P., (eds.), *Groundwater Pollution Microbiology*: Wiley-Interscience, New York, 377 pp.
- Greenberg, A.E., Clesceri, L.S., and Eaton, A.D., (eds.), 1992, *Standard methods for the examination of water and wastewater*: American Public Health Association, American Water Works Association, Water Environment Federation, Washington, D.C.
- Gregg, S.J., and Sing, K.S.W., 1982, *Adsorption, surface area and porosity*, 2nd ed.: Academic Press, London, 303 pp.
- Gschwend, P.M., and Reynolds, M.D., 1987, Monodisperse ferrous phosphate colloids in an anoxic groundwater plume: *J. Contaminant Hydrology*, v. 1, no. 1, pp. 309–327.
- Gschwend, P.M., Backhus, D.A., MacFarlane, J.K., and Page, A.L., 1990, Mobilization of colloids in groundwater due to infiltration of water at a coal ash disposal site: *J. Contaminant Hydrology*, v. 6, pp. 307–320.
- Gutman, R.G., 1987, *Membrane filtration—The technology of pressure driven crossflow processes*: Adam Hilger, Bristol, UK, 210 pp.
- Halliday, D., and Resnick, R., 1967, *Physics*, 2nd ed.: John Wiley, Inc., New York, 1324 pp.
- Harvey, R.W., and Garabedian, S., 1991, Use of colloid filtration theory in modeling movement of bacteria through a contaminated sandy aquifer: *Environmental Science and Technology*, v. 25, no. 1, pp. 178–185.

- Harvey, R.W., George, L.H., Smith, R.L., and Leblanc, D.R., 1989, Transport of microspheres and indigenous bacteria through a sandy aquifer—Results of natural and forced-gradient tracer experiments: *Environmental Science and Technology*, v. 23, pp. 51–56.
- Hem, J.D., 1985, Study and interpretation of the chemical characteristics of natural water: U.S. Geological Survey Water-Supply Paper 2254, Washington, D.C., 263 pp.
- Herzog, B., Pennino, J., and Nielsen, G., 1991, Ground-water sampling; *in* Nielsen, D.M. (ed.), *Practical Handbook of Ground-Water Monitoring*: Lewis Publishers, Chelsea, Mich., pp. 449–499.
- Hochella, M.F., Jr., 1990, Atomic structure, microtopography, composition and reactivity of mineral surfaces; *in* Hochella, M.E., Jr., and White, A.F. (eds.), *Mineral-Water Interface Geochemistry: Reviews in Mineralogy*, Mineralogical Society of America, Washington, D.C., pp. 87–132.
- Hoffmann, M.R., Yost, E.C., Eisenreich, S.J., and Maier, W., 1981, Characterization of soluble and colloidal-phase metal complexes in river water by ultrafiltration—A mass balance approach: *Environmental Science and Technology*, v. 15, pp. 655–661.
- Honeyman, B.D., and Santschi, P.H., 1991, Coupling adsorption and particle aggregation—Laboratory studies of “colloid pumping” using ⁵⁹Fe-labeled hematite: *Environmental Science and Technology*, v. 25, no. 10, pp. 1739–1746.
- Horowitz, A.J., Elrick, K.A., and Hopper, R.C., 1989, A comparison of dewatering methods for the separation and concentration of suspended sediment for sequential trace element analysis: *Hydrological Processes*, v. 2, pp. 163–184.
- Hunter, K.A., and Liss, P.S., 1979, The surface charge of suspended particles in estuarine and coastal waters: *Nature*, v. 282, pp. 823–825.
- IGWMC, 1992, International Groundwater Modeling Center, Software Catalog: Institute for Ground-Water Research and Education, Golden, Colo., 34 pp.
- Kennedy, V.C., Zellweger, G.W., and Jones, B.F., 1974, Filter pore-size effects on the analysis of Al, Fe, Mn, and Ti in water: *Water Resources Research*, v. 10, pp. 785–790.
- Kent, R.T., and Payne, K.E., 1988, Sampling groundwater monitoring wells—Special quality assurance and quality control considerations; *in* *Principles of Environmental Sampling*: American Chemical Society, Washington, D.C., pp. 231–246.
- Kim, J.I., Zeh, P., and Delakowitz, B., 1992, Chemical interactions of actinide ions with groundwater colloids in Gorleben aquifer systems: *Radiochimica Acta*, v. 58/59, pp. 147–154.
- Kimball, B.A., McKnight, D.M., Wetherbee, G.A., and Harnish, R.A., 1992, Mechanisms of iron photoreduction in a metal-rich, acidic stream (St. Kevin Gulch, Colorado, U.S.A.): *Chemical Geology*, v. 96, pp. 227–239.
- Kimball, B.A., Callendar, E.C., and Axtmann, E.V., 1995, Effects of colloids on metal transport in a river receiving acid mine drainage, upper Arkansas River, Colorado, U.S.A.: *Applied Geochemistry* 10, pp. 285–306.
- Kita, S.F., Folger, H.S., and Reed, M.G., 1987, Effect of pH on colloidal induced fines migration: *J. Colloid Interface Sci.*, v. 118, pp. 158–168.
- Kuwabara, J.S., and Harvey, R.W., 1990, Application of hollow fibre, tangential flow device for sampling suspended bacteria and particles from natural waters: *Journal of Environmental Quality*, v. 19, pp. 625–629.
- Langmuir, D., and Whittemore, D.O., 1971, Variations in the stability of precipitated ferric oxyhydroxides; *in* Hem, J., (ed.), *Non-equilibrium Systems in Natural Water Chemistry: Advanced Chemistry Series*, v. 106, American Chemical Society, Washington, D.C., pp. 209–234.
- Laxen, D.P.H., 1983, Size distribution of iron and manganese in freshwaters: *Geochimica et Cosmochimica Acta*, v. 47, pp. 731–741.
- Laxen, D.P.H., and Chandler, I.M., 1982, Comparison of filtration techniques for size distribution in freshwaters: *Analytical Chemistry*, v. 54, pp. 1350–1355.
- Leenheer, J.A., Meade, R.H., Taylor, H.E., and Pereira, W.E., 1989, Sampling, fractionation, and dewatering of suspended sediment from the Mississippi River for geochemical and trace-contaminant analysis; *in* Mallard, G.E., and Ragone, S.E., (eds.), U.S. Geological Survey Toxic Substances Hydrology Program, Proceedings of the Technical Meeting, Phoenix, Arizona, Sept., 26–30, 1988: Water-Resource Investigations Report 88–4220.
- Leppard, G.G., 1992, Evaluation of electron microscope techniques for the description of aquatic colloids; *in* Buffle, J., and van Leeuwen, H.P. (eds.), *Environmental Particles: v. 1*, Lewis Publishers, Boca Raton, Fla., pp. 231–290.
- Liang, L., and Morgan, J.J., 1990, Coagulation of iron oxide particles in the presence of organic materials; *in* Melchior, D., and Bassett, R.L., (eds.), *Chemical Modeling in Aqueous Systems*, II. ACS Symposium Series 416: American Chemical Society, Washington, D.C., pp. 293–309.
- Lieser, K.H., and Hill, R., 1992, Chemistry of thorium in the hydrosphere and in the geosphere: *Radiochimica Acta*, v. 56, no. 3, pp. 141–151.
- Lowson, R.T., and Short, S.A., 1990, Application of the uranium decay series to the study of groundwater colloids; *in* Beckett, R., (ed.), *Surface and Colloid Chemistry in Natural Waters and Water Treatment*: Plenum Press, New York, pp. 71–86.
- Marley, N.A., Gaffney, J.S., Orlandini, K.A., and Dugue, C.P., 1991, An evaluation of an automated hollow-fiber ultrafiltration apparatus for the isolation of colloidal materials in natural waters: *Hydrological Processes*, v. 5, pp. 291–299.
- Martin, R.E., Bouwer, E.J., and Hanna, L.M., 1992, Application of cleaned filtration theory to bacteria deposition in porous media: *Environmental Science and Technology*, v. 26, no. 5, pp. 1053–1058.
- McCarthy, J.F., and Wobber, F.J., (eds.), 1993, *Manipulation of groundwater colloids for environmental restoration*: Lewis Publishers, Boca Raton, Fla., 371 pp.
- McCarthy, J.F., and Zachara, J.M., 1989, Subsurface transport of contaminants: *Environmental Science and Technology*, v. 23, pp. 496–502.
- McDowell-Boyer, L.M., 1992, Chemical mobilization of micron-sized particles in saturated porous media under steady flow conditions: *Environmental Science and Technology*, v. 26, pp. 586–593.
- McDowell-Boyer, L.M., Hunt, J.R., and Sitar, N., 1986, Particle transport through porous media: *Water Resources Research*, v. 22, no. 13, pp. 1901–1921.
- Meade, R.H., and Stevens, H.H., 1990, Strategies and equipment for sampling suspended sediment and associated toxic chemicals in large rivers—with emphasis on the Mississippi River: *The Science of the Total Environment*, v. 97/98, pp. 125–135.
- Means, J.C., and Wijayaratne, R., 1982, Role of natural colloids in the transport of hydrophobic pollutants: *Science*, v. 215, pp. 968–970.
- Metcalf and Eddy Inc., 1991, *Wastewater engineering—Collection, treatment, disposal*: McGraw-Hill, New York, 782 pp.
- Mills, A.L., 1999, The role of bacteria in environmental geochemistry; *in* Plumlee, G.S., and Logsdon, M.J. (eds.), *The Environmental Geochemistry of Mineral Deposits, Part A. Processes, Techniques, and Health Issues*: Society of Economic Geologists, Reviews in Economic Geology, v. 6A, pp. 125–132.
- Mills, W.B., Liu, S., and Fong, F.K., 1991, Literature review and model (COMET) for colloid/metals transport in porous media: *Groundwater*, v. 29, no. 2, pp. 199–208.
- Moore, W.J., 1972, *Physical chemistry*, 4th ed.: Prentice-Hall, Inc., Englewood Cliffs, N.J., 977 pp.
- Moran, S.B., and Moore, R.M., 1989, The distribution of colloidal aluminum and organic carbon in coastal and open waters off Nova Scotia: *Geochimica et Cosmochimica Acta*, v. 53, no. 10, pp. 2519–2527.
- Morel, F.M.M., and Gschwend, P.M., 1987, The role of colloids in the partitioning of solutes in natural waters; *in* Stumm, W., (ed.), *Aquatic Surface Chemistry*: John Wiley and Sons, New York, pp. 405–522.
- Murphy, D.M., Garbarino, J.R., Taylor, H.E., Hart, B.T., and Beckett, R., 1993, Determination of size and element composition distributions of complex colloids using sedimentation field-flow fractionation/inductively coupled plasma-mass spectroscopy: *J. Chromatog.*, v. 642, pp. 459–467.
- Newton, P.P., and Liss, P.S., 1987, Positively charged suspended particles—Studies in an iron-rich river and its estuary: *Limnological*

- Oceanography, v. 32, pp. 1267–1276.
- Nielsen, D.M. (ed.), 1991, Practical handbook of ground-water monitoring: Lewis Publishers, Chelsea, Mich., 717 pp.
- Nightingale, H.I., and Bianchi, W.C., 1977, Groundwater turbidity resulting from artificial recharge: *Groundwater*, v. 15, pp. 146–152.
- Nomizu, T., Goto, K., and Mizuike, A., 1988, Electron microscopy of nanometer particles in freshwater: *Analytical Chemistry*, v. 60, pp. 2653–2656.
- Nordstrom, D.K., and Alpers, C.N., 1999, Geochemistry of acid mine waters; in Plumlee, G.S., and Logsdon, M.J. (eds.), *The Environmental Geochemistry of Mineral Deposits, Part A. Processes, Techniques, and Health Issues*: Society of Economic Geologists, Reviews in Economic Geology, v. 6A, pp. 133–160.
- Nordstrom, D.K., and Munoz, J.L., 1986, Geochemical thermodynamics: Blackwell Scientific Publications, Palo Alto, Calif., 477 pp.
- O'Melia, C.R., 1987, Particle-particle interactions; in Stumm, W. (ed.), *Aquatic Surface Chemistry*: John Wiley and Sons, New York, pp. 385–403.
- O'Melia, C.R., 1992, Kinetics of colloid chemical processes in aquatic systems; in Stumm, W. (ed.), *Aquatic Chemical Kinetics*: John Wiley and Sons, New York, pp. 447–474.
- Palmer, C.D., Keely, J.F., and Fish, W., 1987, Potential for solute retardation on monitoring well sand packs and its effect on purging requirements for ground water sampling: *Ground Water Monitoring Review*, Spring 1987, pp. 40–47.
- Pankow, J.F., 1991, *Aquatic chemistry concepts*: Lewis Publishers, Chelsea, Mich., 673 pp.
- Parkhurst, D., Thorstenson, D.C., and Plummer, L.N., 1980, PHREEQE—A computer program for geochemical calculations: Water Resources Division, U.S. Geological Survey Water Resource Investigations Report 80–96, 146 pp.
- Parks, G.A., 1990, Surface energy and adsorption at mineral/water interfaces—An introduction; in Hochella, M.E., Jr, and White, A.F., (eds.), *Mineral-Water Interface Geochemistry: Reviews in Mineralogy*, Mineralogical Society of America, Washington, D.C., pp. 133–175.
- Penrose, W.R., Polzer, W.L., Essington, E.H., Nelson, D.M., and Orlandini, K.A., 1990, Mobility of plutonium and americium through a shallow aquifer in a semiarid region: *Environmental Science and Technology*, v. 24, pp. 228–234.
- Puls, R.W., and Barcelona, M.J., 1989, Filtration of ground water samples for metals analysis: R.S. Kerr Environmental Research Laboratory, U.S. EPA and Illinois State Water Survey, EPA/600/J–89/278, 10 pp.
- Puls, R., and Powell, R., 1992, Transport of inorganic colloids through natural aquifer material—Implications for contaminant transport: *Environmental Science and Technology*, v. 26, no. 3, pp. 614–621.
- Puls, R.W., Eychaner, J.H., and Powell, R.M., 1990, Colloid-facilitated transport of inorganic contaminants in groundwater, Part I. Sampling considerations: U.S. EPA, Environmental Research Brief, EPA/600/M–90/023.
- Puls, R.W., Powell, R.M., Clark, D.A., and Paul, C.J., 1991, Facilitated transport of inorganic contaminants in ground water, Part II. Colloid transport: Environmental Research Brief, USEPA, EPA/600/M–91/040.
- Ranville, J.F., Harnish, R.A., and McKnight, D.M., 1991a, Particulate and colloidal organic material in Pueblo Reservoir, Colorado—Influence of autochthonous source on chemical composition; in Baker, R., (ed.), *Organic Substances and Sediments in Water*, v. 1: Lewis Publishers, Chelsea, Mich., pp. 47–74.
- Ranville, J.F., Smith, K.S., McKnight, D.M., Macalady, D.L., and Rees, T.F., 1991b, Effect of organic matter coprecipitation and sorption with hydrous iron oxides on electrophoretic mobility of particles in acid mine drainage; in Mallard, G.E., and Aronson, D.A. (eds.), U.S. Geological Survey Toxic Substances Hydrology Program, Proceedings of the Technical Meeting, Monterey, California, March 11–15, 1991: U.S. Geological Survey Water Resources Investigations Report 91–4034, pp. 422–427.
- Ranville, J.F., Chittleborough, D.J., Shanks, F., Morrison, R.J.S., Harris, T., Doss, F., and Beckett, R., 1999, Development of sedimentation field-flow fractionation-inductively coupled plasma mass-spectrometry for the characterization of environmental colloids, *Analytical Chimica Acta*, v. 381, pp. 315–320.
- Rees, T.F., 1987, A review of light-scattering techniques for the study of colloids in natural water: *J. Contam. Hydrology*, v. 1, pp. 425–439.
- Rees, T.F., 1991, Transport of pollutants by colloid-mediated; in Hutzinger, O. (ed.), *The Handbook of Environmental Chemistry, Part 2, Vol. F, Reactions and Processes*: Springer-Verlag, Heidelberg, pp. 165–184.
- Rees, T.F., and Ranville, J.F., 1990, Collection and analysis of colloidal particles transported in the Mississippi River, U.S.A.: *J. Contam. Hydrology*, v. 6, pp. 214–250.
- Rees, T.F., Leenheer, J.A., and Ranville, J.F., 1991, Use of a single-bowl continuous-flow centrifuge for dewatering suspended sediments—Effect on the sediment physical and chemical characteristics: *Hydrological Processes*, v. 5, pp. 201–214.
- Reynolds, M.D., 1985, *Colloids in groundwater*: Unpub. M.S. thesis, Massachusetts Institute of Technology, Cambridge, 92 pp.
- Ryan, J.N., and Elimelech, M., 1996, Colloid mobilization and transport in groundwater. *Colloids and Surfaces A: Physicochem. Eng. Aspects*, 107, pp. 1–56.
- Ryan, J.N., and Gschwend, P.M., 1990, Colloid mobilization in two Atlantic coastal plain aquifers—Field studies: *Water Resources Research*, v. 26, no. 2, pp. 307–322.
- Salbu, B., Bjørnstad, H. E., Lindstrøm, N.S., Lydersen, E., Brevik, E.M., Rambaek, J.P., and Paus, P.E., 1985, Size fractionation techniques in the determination of elements associated with particulate or colloidal material in natural fresh waters: *Talanta*, v. 32, no. 9, pp. 907–913.
- Scholl, M.A., and Harvey, R.W., 1992, Laboratory investigations on the role of sediment surface and groundwater chemistry in the transport of bacteria through a contaminated sandy aquifer: *Environmental Science and Technology*, v. 26, no. 7, pp. 1410–1417.
- Sigg, L., 1985, Metal transfer mechanisms in lakes—The role of settling particles; in Stumm, W. (ed.), *Chemical Processes in Lakes*: John Wiley and Sons, New York, pp. 283–310.
- Sigleo, A.C., and Helz, G.R., 1981, Composition of estuarine colloidal material—Major and trace elements: *Geochimica et Cosmochimica Acta*, v. 45, pp. 283–310.
- Smith, J.S., Steele, D.P., Malley, M.J., and Bryant, M.A., 1988, Groundwater sampling; in *Principles of Environmental Sampling*: American Chemical Society, Washington, D.C., pp. 255–260.
- Smith, K.S., 1999, Metal sorption on mineral surfaces—An overview with examples relating to mineral deposits; in Plumlee, G.S., and Logsdon, M.J. (eds.), *The Environmental Geochemistry of Mineral Deposits, Part A. Processes, Techniques, and Health Issues*: Society of Economic Geologists, Reviews in Economic Geology, v. 6A, pp. 161–182.
- Smith, K.S., Ficklin, W.H., Plumlee, G.S., and Meier, A.L., 1992, Metal and arsenic partitioning between water and suspended sediment at mine-drainage sites in diverse geologic settings; in Kharaka, Y.K., and Maest, A.S., (eds.), *Water-Rock Interactions: Proceedings of the 7th Internat Symposium on Water-Rock Interaction-WRI-7*, Balkema, Rotterdam, pp. 443–447.
- Stumm, W., and Morgan J.J., 1981, *Aquatic chemistry*: John Wiley and Sons, New York, 780 pp.
- Tanizaki, Y., Shimokawa, T., and Nakamura, M., 1992, Physicochemical separation of trace elements in river waters by size fractionation: *Environmental Science and Technology*, v. 26, pp. 1433–1444.
- Taylor, H.E., Garbarino, J.R., and Brinton, T.I., 1990, The occurrence and distribution of trace metals in the Mississippi River and its tributaries: *The Sci. Total Environ.*, v. 97/98, pp. 369–384.
- Taylor, H.E., Garbarino, J.R., Murphy, D.M., and Beckett, R., 1992, Inductively coupled plasma-mass spectrometry as an element-specific detector for field flow fractionation separation: *Analytical Chemistry*, v. 64, pp. 2036–2041.
- Thoma, G.J., Koulermos, A.C., Valsaraj, K.T., Reible, D.D., and Thibodeaux, L.J., 1991, The effects of pore-water colloids on the transport of hydrophobic organic compounds from bed sediments; in Baker, R.A. (ed.), *Organic Substances and Sediments in Water*, v. 1: Lewis

- Publishers, Chelsea, Mich.
- Tipping, E., and Cooke, D.C., 1982, The effects of adsorbed humic substances on the surface charge of goethite (α -FeOOH) in freshwaters: *Geochimica et Cosmochimica Acta*, v. 46, pp. 75–80.
- Tipping, E., and Higgins, D.C., 1982, The effect of adsorbed humic substances on the colloid stability of hematite particles: *Colloids Surf.*, v. 5, pp. 85–92.
- Tipping, E., Griffith, J.R., and Hilton, J., 1983, The effect of adsorbed humic substances on the uptake of copper(II) by goethite: *Croatica. Chimica. Acta*, v. 56, pp. 613–621.
- Travis, B.J., and Nuttal, H.E., 1987, Analysis of colloid transport; *in* Tsang, C. (ed.), *Coupled Processes Associated with Nuclear Waste Repositories*: Academic Press, Ann Arbor, Mich., pp. 453–472.
- U.S. Environmental Protection Agency, 1986, RCRA Ground-Water Monitoring Technical Enforcement Guidance Document (TEGD): OSWER-9950.1, U.S. Government Printing Office, Washington, D.C., 208 pp. plus appendices.
- U.S. Geological Survey, O.o.W.D.C., 1982, National handbook of recommended methods for water-data acquisition: U.S. Department of the Interior, Reston, Va.
- Vinten, A.J.A., Yaron, B., and Nye, P.H., 1983, Vertical transport of pesticides into soil when adsorbed on suspended particles: *J. Agric. Food Chem.*, v. 31, pp. 662–664.
- Waber, U.E., Lienert, C., and Von Gunten, H.R., 1990, Colloid-related infiltration of trace metals from a river to shallow groundwater: *J. Contaminant Hydrology*, v. 6, pp. 251–265.
- Wagemann, R., and Brunskill, G.J., 1975, The effect of filter pore-size on analytical concentrations of some elements in filtrates of natural water: *International Journal of Environmental Analytical Chemistry*, v. 4, pp. 75–84.
- Walling, D.E., and Moorehead, P.W., 1989, The particle size characteristics of fluvial suspended sediment—An overview: *Hydrobiologia*, v. 176/177, pp. 125–149.
- White, A.F., and Peterson, M.L., 1990, Role of reactive-surface-area characterization in geochemical kinetic models; *in* Melchior, D.C., and Bassett, R.L. (eds.), *Chemical Modeling of Aqueous Systems, II*. ACS Symposium Series: American Chemical Society, Washington, D.C., pp. 461–477.
- Whitehouse, B.G., Petrick, G., and Ehrhardt, M., 1986, Crossflow filtration of colloids from Baltic Sea water: *Water Res.*, v. 20, pp. 1599–1601.
- Whitehouse, B.G., Yeats, P.A., and Strain, P.M., 1990, Cross-flow filtration of colloids from aquatic environments: *Limnological Oceanography*, v. 35, pp. 1368–1375.
- Yao, K., Habibian, M.T., and O'Melia, C.R., 1971, Water and wastewater filtration—Concepts and applications: *Environmental Science and Technology*, v. 5, pp. 1105–1112.

Chapter 9

GEOCHEMICAL PROCESSES CONTROLLING URANIUM MOBILITY IN MINE DRAINAGES

R.B. Wanty, W.R. Miller, P.H. Briggs, and J.B. McHugh (retired)

U.S. Geological Survey, Box 25046, MS 973, Federal Center, Denver, CO 80225-0046

INTRODUCTION

Comprehensive models of ore genesis incorporate metal sources, transport and concentration mechanisms, and preservation mechanisms. Analogous concepts apply to the problem of metal migration from mines, mine wastes, and mine tailings, including: the concentrations, mineralogical occurrence, and availability of metals in mineral deposits, host rocks, mine wastes, and tailings (the source); the mechanisms for metal mobilization and transport during weathering; the mechanisms for metal fixation and the permanence of the fixation. Similarly, undisturbed mineral deposits or alteration zones that are exposed at the Earth's surface may be natural sources from which metals can be solubilized during weathering.

Uranium (U), a naturally-occurring radioactive element, may be present in mineral deposits in sufficient concentrations that in itself constitutes ore. It may also be present in ores of other metals at concentrations that exceed average crustal abundances. Any uranium that is not completely removed from these ores in the mining and milling process may be available for mobilization into ground or surface waters via the weathering and oxidation of solid tailings or mine waste piles. This chapter discusses the relative importance of various geochemical processes that control uranium mobility via weathering in both mined and unmined mineralized environments. The data presented in this paper focus on mined areas because the great extent of historic mining in the field areas examined for this study preclude extensive consideration of undisturbed areas.

Uranium is environmentally important because it may be linked to a variety of human health effects, either because of its behavior in the human body as a heavy metal, or because of its radioactivity (cf. Aieta et al., 1987; Wanty and Schoen, 1991). As a heavy metal, chronic ingestion of U may lead to kidney dysfunction. As a radioactive element, U may enter the bone structure where it is a potential carcinogen.

The greatest mobilization of uranium from a mine or mill site will occur if acidic waters develop, and if the uranium occurs in minerals that are readily dissolved in these acidic waters; such conditions would be expected to result from the weathering of sulfide-rich ores, especially in deposits where acid-buffering minerals are scarce or absent (Smith and Huyck, 1999; Plumlee, 1999). Various geochemical processes help maintain uranium transport in solution. Ultimately, other processes serve to remove uranium from solution, and the permanence of this fixation varies depending on the process. Although it is unlikely that acidic drainage waters would be used directly as a drinking-water supply, it is

likely that some drinking-water sources may receive a contribution from waters that have been impacted by such drainage. Therefore, if not properly treated, there exists a potential pathway for uranium to enter drinking-water supplies.

Prior work on U geochemistry in the vicinity of mines or milling sites have focused on U ores directly (White et al., 1984; Morin et al., 1988a; 1988b; Morin and Cherry, 1988) or on broad regions that may contain U mineralization (Wanty et al., 1998). In these cases, significant concentrations of uranium were found in ground-water contaminant plumes migrating from U tailings impoundments. Murray et al. (1993) investigated the migration of natural radionuclides in a tropical river system, presumably under near-neutral pH conditions, and found that a significant fraction of the transported radionuclides were present in suspended form (adsorbed to suspended solids) rather than in the dissolved state. Despite these studies, little is known of the migration of uranium from mine dumps of metal mines that are not U mines. This study therefore fills a gap in the existing literature by examining the concentrations of U in mine drainages and the processes that contribute to or attenuate those concentrations.

URANIUM ABUNDANCES IN ROCKS AND ORES OF OTHER METALS

The concentration of uranium in continental rocks varies widely. Uranium abundances in natural rocks generally range from 1 to 10 ppm (Brownlow, 1979; Henderson, 1982). The average estimated U concentration of continental rocks is between 1 and 4 parts per million (ppm) by mass (Phair and Gottfried, 1964; Rogers and Adams, 1972). In general, the U concentration of magmas increases towards the later, more silica-rich members of the igneous differentiation series; thus, granites and rhyolites tend to have greater U contents than do more mafic rocks. Uranium concentrations of various metalliferous ores may be significantly higher than those of continental rocks. Often, ore-forming solutions are either hydrous residuals of the differentiation process that accompanies the cooling and crystallization of an igneous body, or are fluids that interact with these hydrous residuals. Therefore, ores formed from these fluids tend to be enriched in U.

Uranium concentrations in base and precious metal ores commonly are enriched over average crustal abundances for the reasons cited above. Phair (1952) found U abundances as high as 240 ppm in some intrusive rocks in the Central City district, Colorado. Sims et al. (1963) reported U concentrations between 100 and 10,000 ppm for ores in the Quartz Hill area of the Central City dis-

trict. Lower U grades (mostly 10 to 100 ppm U) were reported for areas south of Central City, including the Idaho Springs district (Sims et al., 1963). Porphyry molybdenum deposits, such as Climax, Colorado, are genetically related to U-enriched high-silica granites and typically have quite anomalous U concentrations as well (Westra and Keith, 1981; White et al., 1981).

In most ore deposits of other metals, as well as their host rocks, unweathered uranium typically occurs as discrete minerals such as uraninite (UO_2), coffinite (ideally USiO_4), pitchblende (an amorphous uranium oxide with the approximate formula UO_2) or as a trace element within other minerals.

URANIUM MOBILITY IN THE ENVIRONMENT

Processes that lead to mobilization and aqueous transport of U

An exhaustive review of U geochemistry is beyond the scope of this paper, but numerous references are available. Langmuir (1978) presents a thorough review of the geochemistry of uranium, with an orientation toward natural ground-water conditions and formation of sandstone-hosted U deposits; much of this discussion is updated in Langmuir (1997). Other reviews of U geochemistry can be found in Hostetler and Garrels (1962), Lemire and Tremaine (1980), Graves (1987), Wanty and Schoen (1991), and Wanty and Nordstrom (1993). Scott and Barker (1962) and Janzer et al. (1991) provide data for U in waters collected from numerous sources around the United States. Because acid-mine-drainage solutions are generated by oxidation of pyrite and other sulfide minerals, the anion compositions of the resultant solutions are dominated by sulfate. Leaching of U in rocks and wastes by these sulfate-rich acid solutions is analogous to the commercial process of leaching uranium ore with sulfuric acid solutions; Riese (1978) and White et al. (1984) provide a thorough description of the chemistry of such fluids in the context of U mobility.

Uranium is present in natural systems in three oxidation states. The most reduced form, U^{IV} , is the oxidation state of U in uraninite and coffinite. This is the least soluble oxidation state for U. The intermediate oxidation state, U^{V} , is stable only at low pH (<6) and in the presence of high total dissolved U (Langmuir, 1978). The most oxidized form, U^{VI} , is also the most soluble. In oxygenated acid-mine drainage systems, most of the dissolved U is expected to be present as U^{VI} or some complex thereof. Minerals containing U^{VI} , such as carnotite ($\text{K}_2(\text{UO}_2)_2(\text{VO}_4)_2$) or tyuyamunite ($\text{Ca}(\text{UO}_2)_2(\text{VO}_4)_2$), are stable only in the presence of unusually high concentrations of dissolved vanadium (Langmuir, 1978). Other U^{VI} minerals, such as schoepite ($\text{UO}_2(\text{OH})_2 \cdot \text{H}_2\text{O}$) or rutherfordine (UO_2CO_3) are so soluble that the aqueous U^{VI} concentration is rarely great enough for these minerals to form.

Uranium^{IV} can be oxidized to U^{VI} in the intense weathering environment of mine-waste or mine-tailings piles. Other reduced minerals in the piles may also be oxidized. A contributing factor which speeds the oxidation process is that mining and milling processes greatly decrease the average particle size, and so increase the amount of exposed surface area; hence, the rates at which reduced minerals can be oxidized increases greatly. If sulfide minerals such as pyrite are present in the mine wastes, infiltrating waters may become quite acidic, especially if they are very poorly buffered such as rain waters (Stumm and Morgan, 1981; Nordstrom, 1982; Nordstrom and Alpers, 1999); these acidic

waters have significantly enhanced capacity for U dissolution. The most acidic conditions develop if the infiltrating waters remain in contact with the atmosphere, thereby allowing oxygen consumed in the sulfide oxidation reactions to be continuously replenished. Thus, the availability of O_2 , as well as both U- and sulfide-bearing minerals, governs the ultimate mobility of U in mine-waste leachates. Plumlee et al. (1992, 1993) arrived at a similar conclusion with respect to oxygen availability and metal mobility.

The predominant U species in acidic oxygenated waters are the uranyl ion (UO_2^{2+}) or uranyl-sulfate complexes ($\text{UO}_2(\text{SO}_4)_n^{2-2n}$, where $n=1$ or 2; Fig. 9.1). The stability of the uranyl-sulfate complexes increases with increasing sulfate concentrations; as a result, these complexes can be quite significant in sulfate-rich waters (commonly with sulfate levels exceeding 1,000 mg/l) generated by oxidation of sulfide minerals. In acidic waters containing fluoride ions, some uranyl-fluoride complexes may also be present; however, at pH values below 2, fluoride is less effective as a complexing agent because greater than 90% of the fluoride is present as HF^0 . At pH values from 4 to 7, uranyl ions form strong complexes with phosphate if phosphate is present in the waters (Fig. 9.2); however, phosphate is usually not present to any appreciable extent in natural waters, in part because it is itself strongly adsorbed onto some particulates. In alkaline solutions, uranyl carbonate com-

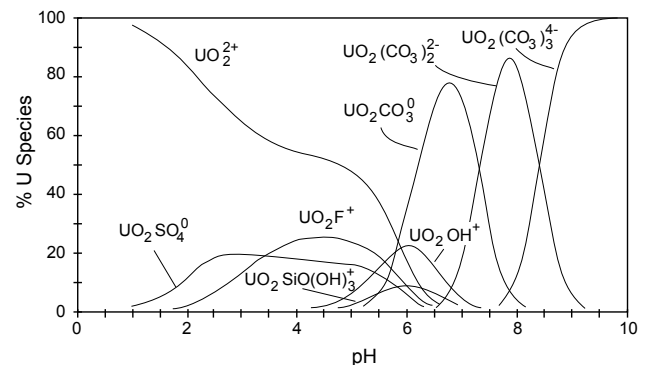


FIGURE 9.1—Calculated speciation of dissolved U as a function of pH, using the computer program PHREEQE. Conditions for this diagram are as follows: 2ppb U, 100 ppm each of SO_4 and Cl, 10 ppm Si, .1 ppm F, $P_{\text{CO}_2}=10^{-3.5}$ atm. The $\text{UO}_2(\text{SO}_4)_2^{2-}$ complex becomes stable only at higher concentrations of SO_4^{2-} .

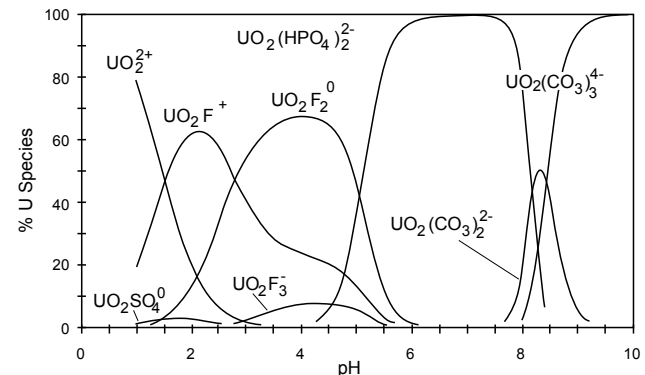


FIGURE 9.2—Calculated speciation of dissolved U as a function of pH. Conditions for this diagram are as follows: 2 ppb U, 100 ppm each of SO_4 and Cl, 10 ppm each of F and Si, .1 ppm PO_4 , $P_{\text{CO}_2}=10^{-3.5}$ atm.

plexes of the form $\text{UO}_2(\text{CO}_3)_n^{2-2n}$, where $n = 1-3$, predominate (Langmuir, 1978); carbonate thus is the most likely complexing agent available for U in alkaline solutions.

Processes that remove uranium from solution

The most important processes that decrease uranium concentrations in mine runoff waters are adsorption, coprecipitation, and dilution. Numerous studies have demonstrated the importance of U adsorption onto various substrates; these studies report that U adsorption is strongest at near-neutral pH values in the absence of complexing agents. Complexing agents such as carbonate compete with adsorbing sites and stabilize U in solution. Adsorbing substrates that have been studied include, among others, iron oxyhydroxides, clay minerals, micas, and organic material. Coprecipitation may occur in one of two fashions: U may substitute for a major component in a growing crystal lattice, or it may be absorbed by a growing mineral onto whose surface it has been adsorbed (Van der Weijden et al., 1985). The latter case is really a special condition of adsorption.

For several reasons, the most likely substrates for U adsorption from mine-drainage waters are Fe-oxyhydroxides, although aluminum oxyhydroxides and clay minerals may also be important in some drainages. First, because of their fine particle size and convoluted surfaces, freshly precipitated Fe-oxyhydroxides have an extremely high specific surface area, on the order of tens to hundreds of square meters per gram (Anderson and Benjamin, 1990; Hsi, 1981; Riese, 1982; Hsi and Langmuir, 1985). Second, oxidation of iron sulfide minerals releases Fe to solution. This Fe (either ferrous or ferric) remains in solution as long as the pH remains low. When the pH increases, ferrous is rapidly oxidized by oxygen to produce ferric iron. Amorphous ferric oxyhydroxides readily precipitate under these conditions. For example, an acid water carrying millimolar (tens of mg/l) levels of dissolved Fe at low pH (<3) will end up with micromolar (tens of $\mu\text{g/l}$) or lower concentrations of dissolved Fe when the pH is neutralized above 6 (Fig. 9.3). Third, the Fe-oxyhydroxides thus produced form coatings on bed and suspended material, or exist as discrete suspended particles. In any of these forms, the particles are in contact with the solution and are able to adsorb metals. Lastly, experimental studies have shown that Fe-oxyhydroxides have a strong tendency to adsorb U.

Adsorption of U onto various Fe oxides and oxyhydroxides has been studied extensively by Hsi (1981) and Hsi and Langmuir (1985). They found that uranyl ion is more strongly adsorbed by amorphous Fe-oxyhydroxide and goethite ($\alpha\text{-FeOOH}$) than by hematite. They also found that carbonate complexing inhibited uranyl adsorption at alkaline pH values, but that phosphate complexing had little or no effect. Competing ions such as Ca^{2+} and Mg^{2+} also had no measurable effect on uranyl adsorption (Hsi, 1981). Hsi and Langmuir (1985) modeled the uranyl adsorption reaction as a series of surface-hydrolysis reactions wherein the hydrolyzed forms of uranyl played an important role. They found that the most likely adsorbed species are UO_2OH^+ and $(\text{UO}_2)_3(\text{OH})_5^+$ and that these species adsorb onto negatively charged sites on the ferric oxyhydroxide surface. Using a rigorous chemical and thermodynamic model, they were able to produce close fits of experimental data. The results of Hsi and Langmuir agree with other studies (Ames et al., 1983a; Koss, 1988; Tolmachev, 1943; Tsunashima et al., 1981; Van der Weijden et al.,

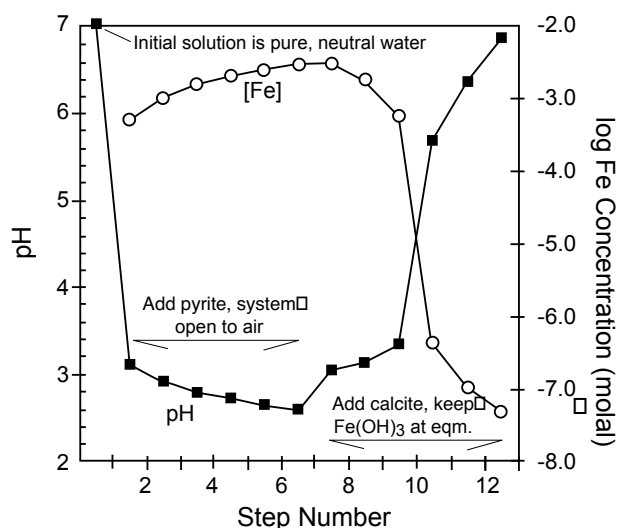


FIGURE 9.3—Calculation of pyrite oxidation in a system open to exchange with oxygen in the atmosphere. In steps 1 through 6, increments of pyrite are added to a solution with 0.1 atm O_2 . In steps 7 through 12, pyrite is no longer added, but calcite is added to neutralize pH. In these last six steps, equilibrium is maintained between the solution and amorphous ferric oxyhydroxide (FeOx) by precipitating FeOx in each step.

1985) that have found strong adsorption of uranyl onto various oxides and silicates under near-natural conditions and decreased adsorption in the presence of carbonate ion. More recently, Waite et al. (1994) studied adsorption of uranyl onto ferrihydrite and suggested a simpler surface speciation, involving only the uranyl ion complexing with two different types of surface sites.

Adsorption of U onto Fe-oxyhydroxides has been discussed here as the major sink for U in systems affected by mine wastes mostly because experimental and field studies are available to demonstrate the affinity of U for those minerals. Another possible adsorbent in acid mine drainage systems may be Al-oxyhydroxides. Most of the reasons enumerated earlier in this section for the importance of U adsorption onto Fe-oxyhydroxides apply equally well to Al-oxyhydroxides. However, the authors are unaware of any experimental studies that have been performed to demonstrate U adsorption onto Al-oxyhydroxides. Several accounts in the literature describe geologic occurrences of U associated with Al-oxyhydroxides or bauxite deposits (Frederickson, 1948; Lovering, 1955; Adams and Richardson, 1960). Some studies have shown that U can be removed from solution by flocculation with freshly precipitated Al-oxyhydroxide minerals (Laskorin et al., 1958; Reid et al., 1985). Nevertheless, more work is needed to characterize the adsorption of U onto aluminum minerals.

MOBILITY OF URANIUM DAUGHTER PRODUCTS IN THE ENVIRONMENT

Daughter products formed by the radioactive decay of uranium may also be present in the same rocks, waste and tailings materials, and drainage waters in which uranium occurs. A detailed discussion of the mobility of these daughter elements is beyond the scope of this chapter. However, based on literature accounts (cf.

Langmuir, 1978; Langmuir and Herman, 1980; Langmuir and Riese, 1985; Wanty and Nordstrom, 1993; Landa, 1999), some brief generalizations can be made about the geochemistry of these daughter elements. Radium (Ra) is probably the element most likely to migrate any distance downstream in all but the most acidic drainages (cf. Landa and Gray, 1995; Landa, 1999). However, due to the characteristically high concentrations of sulfate in acidic mine drainages, Ra mobility may be hindered by the formation of barite (ideally BaSO_4), which, as it forms, incorporates Ra in its crystal structure (Doerner and Hoskins, 1925). Thorium (Th), although generally insoluble at pH values greater than about 5, may be somewhat mobile at lower pH's. Indeed, Th concentrations may be appreciable (>0.05 ppm) in some acidic drainage waters (Plumlee et al., 1993; 1999). Radiogenic (and possibly also radioactive) isotopes of lead may be mobile under acidic conditions; the geochemistry of lead is covered by Smith and Huyck (1999).

A FIELD STUDY OF U MOBILITY FROM METAL-MINE SITES IN COLORADO

To illustrate the above principles, and to determine possible ranges of U concentrations in mine drainages, a field study of mine-drainage chemistry was undertaken at a number of sites throughout Colorado (Fig. 9.4). The drainages chosen for this study represent a variety of metal deposit types within the Colorado Mineral belt, including precious- and base-metal deposits and porphyry molybdenum deposits.

Procedures

Fieldwork involved measurement of unstable parameters, and collection and preservation of water and sediment samples for later laboratory analysis. Unstable parameters, such as temperature, pH, dissolved oxygen, and specific conductance, were analyzed according to techniques outlined in Wood (1976) and Ficklin and Mosier (1999). Dissolved oxygen was determined col-

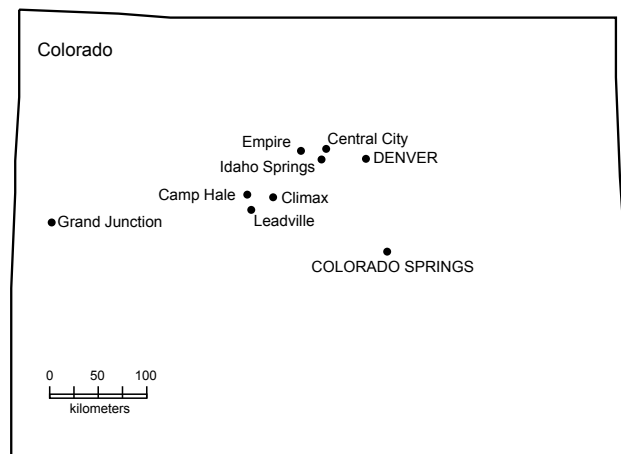


FIGURE 9.4—Sample-site locations in Colorado. Table 9.1 lists sample numbers and localities which can be referenced to this base map.

orimetrically using a Hach DR-2000¹ spectrophotometer with reagent ampoules supplied by that company. Iron (ferrous and total) was analyzed on selected samples using the Hach DR-2000 spectrophotometer with Hach reagent ampoules. Values of pH were measured after calibrating the meter/electrode assembly with at least one and up to three buffers. Extremely low pH values (<3) may be less accurate because only one buffer (at pH 4.00) was used to calibrate the instrument. Higher-pH results (>4) are more reliable as they had a three-buffer calibration (buffers of pH 4.00, 6.86, and 9.18 at 25°C).

Water samples collected in the field were analyzed using various techniques (Crock et al., 1999) for U, anions such as fluoride, chloride, nitrate, phosphate, and sulfate, cations such as Na, K, Ca, Mg, Fe, and a variety of trace metals. Sample preservation techniques were as follows: for U, trace metals and other cations, samples were filtered through 0.45 μm filters and acidified to pH <1 with concentrated HNO_3 ; for anions, samples were filtered and kept cool. For samples with field-pH values greater than about 5 that contain carbonate alkalinity, the alkalinity was determined in the laboratory by titrating a raw, unfiltered 50-ml sample saved in a 125-ml bottle according to the electrometric titration technique described in Skougstad et al. (1979).

Uranium concentrations were determined by laser phosphorimetry using a Scintrex UA-3 U analyzer. Standard additions were performed on every sample to minimize errors due to quenching or enhancing of fluorescence by other constituents in each sample. Cations and trace elements were analyzed by inductively-coupled plasma atomic emission spectroscopy (Lichte et al., 1987). Anions were analyzed within 72 hours of sample collection using a Dionex model 2120i ion chromatograph (Fishman and Pyen, 1979).

At some sample sites, stream sediments were collected for leaching experiments to quantify the amount of labile (adsorbed) U on the sediments. After drying, weighed amounts of the sediments were leached at room temperature (approximately 20°C) for at least 48 hours using a 0.1 M NaHCO_3 solution; Zielinski and Meier (1988) found that this solution was capable of removing $>80\%$ of the labile U from peat samples after leaching for 24 hours. Mohagheghi (1985) used a similar leach solution of 0.02 M NaCO_3 to completely desorb U from kaolinite. In both cases, the leach solution is effective because of the formation of uranyl-carbonate complexes. The pH of the leach solution was about 8.3, so the concentration of carbonate ion was about 0.002 M. Uranium in the leachates was analyzed by laser phosphorimetry with standard additions.

Aqueous speciation and mineral saturation indexes were calculated for the dissolved water samples using the computer program PHREEQE (Parkhurst et al., 1980) which was modified to include U aqueous species and solids using the thermodynamic data of Langmuir (1978). Mass-balance and reaction-path calculations were performed using PHREEQE and BALANCE (Parkhurst et al., 1982). Because redox reactions directly affect the outcome of aqueous speciation calculations for U (as well as other redox-sensitive elements), assignment of a value for Eh (or pE) is critical. In our calculations we tried several approaches. Because of the availability of data, the most consistently applied method was to input concentrations of total dissolved iron into

¹Any use of trade, product, or firm names in this publication is for descriptive purposes only and does not imply endorsement by the U.S. Government.

PHREEQE, then run the program repeatedly while adjusting the value of pE to attain equilibrium with respect to amorphous ferric oxyhydroxide. If field analyses were performed for Fe^{2+} and total Fe, it was also possible to use the Nernst equation to calculate pE based on $\text{Fe}^{2+}/\text{Fe}^{3+}$ ratios (Nordstrom et al., 1979). In every case, the value of pE calculated by either the ferric-oxyhydroxide saturation method or by using $\text{Fe}^{2+}/\text{Fe}^{3+}$ ratios was extremely oxidized. Most of the pE values were at the upper limit for the water-stability boundaries at the pH values of the samples, accurately reflecting the fact that most of the samples were saturated with respect to atmospheric partial pressure of oxygen.

Results of water and sediment sampling

Samples of surface waters, spring waters, and stream sediments were collected from a variety of mining districts in Colorado. Brief descriptions of each sample locality are given in Table 9.1. Analytical results for all water samples are given in Table 9.2.

All waters sampled, except 92CO-502 and -505, had high dissolved oxygen concentrations indicating atmospheric saturation. Thus, most of the mine drainages occur under oxidizing conditions conducive to U mobilization. The low pH values indicate open-system weathering of sulfide minerals as shown previously (Fig. 9.3). This result has important implications on U mobility; open-system weathering of sulfides will result in oxidizing, strongly acidic conditions most favorable for U dissolution. Thus, under these conditions, U mobility is maximized and in fact, high U concentrations commonly were observed in the stream-water samples. Uranium concentrations ranged from 0.3 ppb to 1.9 parts per million (Table 9.2); the mean U concentration was 300 ppb.

The state of saturation of U minerals was evaluated by calculating saturation indexes (SI) using the program PHREEQE. Saturation indexes are calculated using the formula $\text{SI} = \log_{10}(\text{IAP}/K_T)$, where IAP refers to the activity product of the ions produced by dissolution of a mineral and K_T is the temperature-corrected equilibrium constant; positive SI values indicate supersaturation with respect to a mineral, negative values indicate undersaturation, and a value of zero indicates equilibrium. SI values were calculated for the U^{VI} minerals rutherfordine (if pH was greater than about 5 so that carbonate was measurable) and schoepite, and for the U^{IV} -oxide minerals. For schoepite and rutherfordine, the maximum SI values were -3.6 and -3.1, respectively. The greatest SI values for coffinite and uraninite were -3.5 and -3.6. Vanadium was not present in any sample in detectable concentrations, so maximum SI values were calculated for the minerals tyuyamunite and carnotite using the detection-limit V concentration; the greatest SI values thus calculated were +0.43 and -0.79, respectively; the positive tyuyamunite SI value is likely an overestimate of the true SI because V was below detection in all samples. Thus, it is quite likely that all the U minerals are undersaturated in all the samples and some process other than the dissolution/precipitation of these U minerals must be limiting U concentrations in these waters.

In water samples collected for this study, higher U concentrations are observed in lower-pH waters (Fig. 9.5). This trend of decreasing U with increasing pH is not due to dilution. Instead, it is consistent with U adsorption on bed and suspended material, coupled with a lack of carbonate in the waters to form uranyl carbonate complexes; this is consistent with results of the numerous

TABLE 9.1—Description of sample sites from which water samples were collected.

Sample no.	Description
92CO-501	Effluent of Argo tunnel, Idaho Springs, 5/12
92CO-502	Effluent of tunnel approx. 2 km N of Idaho Springs in Virginia Canyon, 5/12
92CO-503	Leavenworth Creek W of Central City, 5/12
92CO-503a	Same site, 5/20
92CO-504	Spring on flank of Quartz Hill W of Central City, 5/12
92CO-505	Effluent of Quito Mine, approx. 2 km SW of Idaho Springs, 5/12
92CO-506	Effluent of mine at the top of Spring Gulch, 10 km SW of Idaho Springs, 5/12
92CO-507	Spring at foot of mine-waste pile at the top of Leavenworth Gulch, 5/20
92CO-508	Spring in Leavenworth Gulch, about 20 m NE of site 507, 5/20
92CO-509	Leavenworth Gulch about 80 m downstream from sites 507 and 508, 5/20
92CO-510	Spring along Leavenworth Gulch, 5/20
92CO-511	Leavenworth Gulch about 0.3 km downstream from site 503, 5/20
92CO-512	Russell Gulch about 2 km downstream from site 511, 5/20
92CO-513	Lake Gulch before it enters as a tributary to Russell Gulch near site 512, 5/20
92CO-514	Russell Gulch just before it empties into the North Fork of Clear Creek, 5/20
92CO-514a	Same site, 10/22
92CO-515	North Fork of Clear Creek upstream of the confluence with Russell Gulch, 5/20
92CO-515a	Same site, 10/22
92CO-516	Spring issuing from pipe at head of Nevada Gulch, W of Central City, 6/3
92CO-517	Nevada Gulch several km downstream from site 516, 6/3
92CO-518	Eureka Gulch, NW of Central City, 6/3
92CO-519	Effluent of Rockford Tunnel W of Idaho Springs, 6/3
92CO-520	Effluent of Lamartine Mine SW of Idaho Springs, 6/3
92CO-521	Arkansas River about 2 km downstream from Climax Mine, 6/24
92CO-522	E. Fork of Arkansas River about 8 km downstream from site 521, 6/24
92CO-523	Evans Gulch near Leadville approx. 2 km downstream from mine dump, 6/24
92CO-524	E. Fork Arkansas River approx. 3 km upstream from Leadville, 6/24
92CO-525	Eagle River at Camp Hale, 6/24
92CO-526	E. Fork of the Eagle River about 2 km upstream from Camp Hale, 6/24
92CO-527	E. Fork of the Eagle River about 1 km downstream from Climax Mine, 6/24
92CO-528	E. Fork of the Eagle River about 0.5 km downstream from Climax Mine, 6/24
92CO-530	Tennmile Creek about 5 km downstream from Climax Mine, 6/24
92CO-531	N. Empire Creek about 1 km N of Empire, 6/24
92CO-532	Leavenworth Gulch about 100m downstream from site 503, 10/22

All samples were collected between 12 May and 22 October, 1992. See Fig. 9.4 for locations on a base map of Colorado.

Dates (in 1992) are shown for each sample.

Sample numbers with the suffix "a" denote a duplicate sample from the same site at a different time.

Analytical results are given in Table 9.2.

TABLE 9.2—Analytical results for samples collected at various mining districts in Colorado. A full suite of cation analyses was run only on samples 501 through 515. For those samples, several elements were never present above analytical detection limits, including: Ti (<1 ppm); Ag (<0.4 ppm); As, Au, Bi (<0.2 ppm); Eu, Mo, Sc, Sn, V (<0.04 ppm); and Ga, Ho, Pb (<0.08 ppm). Phosphate was present only in samples 501 (16 ppm), 506 (0.3 ppm), and 515 (0.8 ppm); all other samples had <0.1 ppm phosphate.

Sample no.	pH	DO ppm	SpC μ mho/cm	F ppm	Cl ppm	NO ₃ ppm	CO ₃ ppm	SO ₄ ppm	T °C	[U] ppb	Si ppm
92CO-501	2.92	6.3	3700	6.6	2.3	<0.1	n.d.	2800	18	150	55
92CO-502	4.81	0.22	3300	<0.1	<0.1	<0.1	n.d.	2400	10	42	45
92CO-503	3.62	8.6	2300	<0.1	<0.1	<0.1	n.d.	1500	8.3	1300	76
92CO-503a	3.59	7	2400	<0.1	<0.1	<0.1	n.d.	1300	9.6	1200	72
92CO-504	4.8	7.8	380	<0.1	<0.1	<0.1	n.d.	140	7	18	24
92CO-505	6.1	1.6	2400	<0.1	37	<0.1	360	330	11	33	36
92CO-506	5.98	10	100	0.2	0.6	<0.1	<10	15	3.2	4	13
92CO-507	3.59	6	2200	<0.1	<0.1	<0.1	n.d.	1100	7.7	630	67
92CO-508	2.85	11	4100	<0.1	<0.1	<0.1	n.d.	2900	7.9	1900	100
92CO-509	2.75	11	2900	<0.1	<0.1	<0.1	n.d.	1600	9.7	800	78
92CO-510	3.4	11	3000	<0.1	<0.1	<0.1	n.d.	1900	9.9	1700	92
92CO-511	3.5	7	2500	<0.1	158	<0.1	n.d.	1200	15	670	79
92CO-512	3.8	8	1100	<0.1	<0.1	<0.1	n.d.	440	12	39	49
92CO-513	4.2	7	2000	<0.1	<0.1	<0.1	n.d.	750	17	11	48
92CO-514	6.0	7	700	<0.1	<0.1	<0.1	<10	280	17	2	31
92CO-514a	5.94		570						10	0.7	
92CO-515	6.62	7	110	0.5	2.7	1.1	<10	29	13	0.6	10
92CO-515a	6.4		540						8.0	0.3	
92CO-516	6.33	7	92	<0.1	0.8	<0.1	<20	10	6	0.4	13
92CO-517	3.98	6	800	<0.1	<0.1	<0.1	n.d.	350	15	10	28
92CO-518	6.4	6	140	<0.1	1.4	<0.1	31	8	10	0.3	12
92CO-519	3.24	6	1600	<0.1	<0.1	<0.1	n.d.	680	8	82	31
92CO-520	6.4	7	330	<0.1	1.5	<0.1	29	150	7	47	24
92CO-521	6.84	7	50	0.1	0.3	1.0	n.d.	5	6	2.0	1
92CO-522	7.65		70	0.1	0.3	0.8	19	6	8	1.7	2
92CO-523	7.86		160	<0.1	<0.1	<0.1	42	8	9	0.7	1
92CO-524	7.55		110	0.2	0.7	0.8	29	8	8	2.0	2
92CO-525	8.13	6	190	0.1	0.6	<0.1	49	11	12	1.3	4
92CO-526	8.07		180	0.1	0.3	<0.1	43	16	10	1.6	5
92CO-527	8.14		250	0.1	0.4	<0.1	64	17	12	3.3	3
92CO-528	8.55		320	0.0	0.4	<0.1	78	38	14	4.7	3
92CO-530	7.02		640	3.2	2.5	4.0	19	280	9	8.9	1
92CO-531	2.65		2700	<0.1	<0.1	<0.1	n.d.	2600	11	78	27
92CO-532	3.4		1900				n.d.		5.5	1400	

Sample no.	Al ppm	Ca ppm	Fe ppm	K ppm	Mg ppm	Na ppm	Ba ppm	Be ppm	Cd ppm	Ce ppm	Co ppm	Cr ppm
92CO-501	31	340	220	3.1	130	22	<0.02	0.02	0.18	0.49	0.22	0.02
92CO-502	5	430	170	8.8	140	34	<0.02	<0.02	0.19	<.08	0.28	<0.02
92CO-503	66	210	<1	5.3	95	8.4	<0.02	<0.02	0.24	1.2	0.15	<0.02
92CO-503a	62	210	2.6	5.6	95	9	<0.02	<0.02	0.24	1.2	0.14	<0.02
92CO-504	60	150	1.9	4.9	70	7	<0.02	<0.02	0.23	0.58	0.12	<0.02
92CO-505	<1	210	25	35	85	270	0.04	<0.02	<.04	<0.08	<.02	<.02
92CO-506	<1	6	<1	<1	2.1	3.1	0.02	<0.02	<.04	<.08	<.02	<.02
92CO-507	<1	42	2.1	2.4	13	5	0.03	<0.02	0.04	<.08	<.02	<.02
92CO-508	240	140	63	<1	140	5.9	<0.02	0.04	0.43	2	0.49	0.07
92CO-509	95	180	14	3.8	96	8	<0.02	0.02	0.25	0.93	0.23	0.02
92CO-510	140	180	<1	4.4	110	7	<0.02	0.02	0.31	1.7	0.27	0.02
92CO-511	40	250	1.4	6.8	93	26	0.02	<0.02	0.18	0.89	0.12	<.02
92CO-512	11	99	1.3	5.6	32	12	<0.02	<0.02	0.04	0.18	0.07	<.02
92CO-513	10	160	<1	6.6	69	8.4	0.02	<0.02	0.12	<.08	0.15	<.02
92CO-514	<1	75	<1	5.9	23	16	0.04	<0.02	<.04	<.08	<.02	<.02
92CO-515	<1	11	2.1	1.3	3	4.1	0.02	<0.02	<.04	<.08	<.02	<.02

Sample no.	Cu ppm	La ppm	Li ppm	Mn ppm	Nd ppm	Ni ppm	Sr ppm	Th ppm	Y ppm	Yb ppm	Zn ppm
92CO-501	8.4	0.27	0.04	110	0.31	0.3	1.5	0.11	0.3	0.03	53
92CO-502	0.25	0.07	<.04	130	0.1	0.4	1.6	0.1	<.04	<.02	75
92CO-503	8.9	0.92	0.06	36	0.78	0.39	0.59	0.1	0.76	0.06	54
92CO-503a	8.7	0.92	0.06	36	0.77	0.4	0.62	0.08	0.75	0.06	53

TABLE 9.2—Continued

Sample no.	Cu ppm	La ppm	Li ppm	Mn ppm	Nd ppm	Ni ppm	Sr ppm	Th ppm	Y ppm	Yb ppm	Zn ppm
92CO-504	7	0.45	0.07	25	0.47	0.32	0.44	0.09	0.5	0.04	48
92CO-505	<.02	<.04	0.33	1.4	<.08	<.04	4.2	0.08	<.04	<.02	<.04
92CO-506	0.03	<.04	<.04	0.21	0.09	<.04	0.03	0.1	<.04	<.02	0.24
92CO-507	0.06	<.04	<.04	1.5	<.08	0.06	0.18	0.09	<.04	<.02	9.1
92CO-508	28	0.92	0.16	58	1.4	0.58	0.15	0.22	1.2	0.1	88
92CO-509	11	0.58	0.08	38	0.7	0.41	0.43	0.12	0.64	0.06	60
92CO-510	15	1.1	0.1	45	1.1	0.47	0.42	0.09	0.96	0.07	68
92CO-511	6.2	0.7	0.06	33	0.58	0.4	0.78	0.09	0.64	0.05	38
92CO-512	1.5	0.11	<.04	7.3	0.15	0.13	0.72	0.09	0.09	<.02	7.1
92CO-513	5.1	0.06	0.04	27	0.08	0.85	0.71	0.08	0.07	<.02	18
92CO-514	0.25	<.04	<.04	1.7	0.08	0.08	0.83	0.1	<.04	<.02	3.5
92CO-515	0.06	<.04	<.04	0.6	<.08	<.04	0.08	<.08	<.04	<.02	0.45

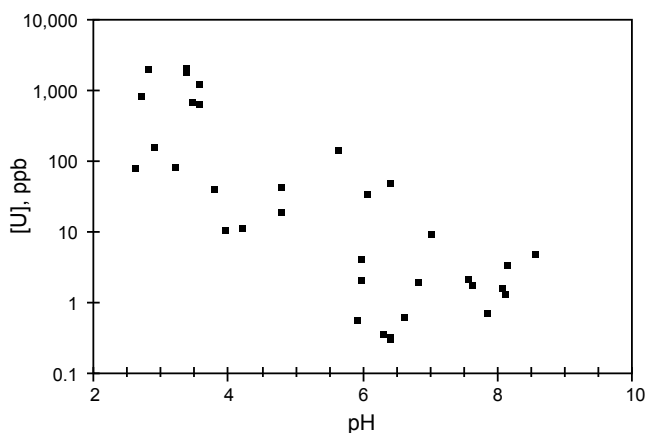


FIGURE 9.5—Dissolved U concentrations in various drainage waters from Colorado, plotted versus pH of the runoff waters. See Table 9.2 for individual analytical results.

experimental studies of U adsorption on mineral surfaces presented in the previous section. The data plotted on Figure 9.5 represent a number of geologic environments and drain a variety of ore-deposit types. The remarkably good correlation between U and pH ($r = -0.6$, significant at $>99.9\%$), despite the geologic variability, demonstrates the effectiveness of adsorption reactions in limiting U concentrations in a variety of environments. The adsorption model is further substantiated by the observation that U minerals are undersaturated in all the samples despite the fact that U is available to be leached from the rocks and bed sediments.

The general trend of decreasing concentration with increasing pH is also observed for other metals besides U. For major elements such as Fe and Al, this trend probably reflects a decrease in oxyhydroxide-controlled solubility as pH increases. A similar argument might be made for the trace metals such as Pb and Cu, but a more likely possibility is that they are adsorbed or coprecipitated with fresh Fe- or Al-oxyhydroxides. Thus, pH-dependent adsorption reactions play an important role in attenuating concentrations of a variety of trace metals (Smith et al., 1992; Smith, 1999).

Based on the discussion so far, a general model can be constructed for U migration from mine wastes. Acid generation by weathering of sulfide minerals results in aggressive dissolution of U from rocks and sediments. Then, a gradual decrease in U con-

centrations occurs downstream as the mine waters are diluted by higher pH surface waters. Uranium dissolution is limited primarily to the zone of acid generation, the mine-waste pile, because the greatest amount of leachable material is present there. To test this model, surface-water and sediment samples were collected along several streams (Leavenworth-Russell Gulches and Nevada Gulch) downstream from mines and mine dumps, whose ores contain enriched but subeconomic concentrations of U, in the Central City mining district west of Denver, Colorado.

U mobility in Leavenworth Gulch and Russell Gulch

The upper part of Leavenworth Gulch drainage basin is underlain by complexly folded Precambrian gneisses and pegmatites intruded by early Eocene bostonite and porphyry dikes (Drake, 1957; Sims and Gable, 1964). All the rocks are cut by east to northeast-trending precious and base metal-bearing veins and mineralized faults (Drake, 1957). The principal vein in the upper Leavenworth Gulch drainage basin is the Calhoun vein. The Calhoun vein ranges from 1 to 45 cm wide and consists of quartz, pyrite, and chalcopyrite. Sphalerite, galena, and pitchblende also occur locally. The pitchblende, which consists of both sooty and hard lustrous varieties, is thought to have been deposited by residual solutions from the quartz-bostonite magma (Drake, 1957). Minimal production of pitchblende has been recorded from the Calhoun vein (Landa, 1987).

The mine dumps in upper Leavenworth Gulch consist of waste rock and gangue minerals, particularly quartz, along with pyrite and other minor minerals found in the Calhoun vein. Much of this material is fine grained. Some pitchblende from the Calhoun vein is undoubtedly present in the waste material, and is thus the likely source for the high U concentrations in water samples collected from Leavenworth Gulch (Table 9.2). The pitchblende is fine-grained and highly susceptible to weathering, so U is readily released to the natural waters of the area as a result of sulfide oxidation, acid-drainage generation and acid-attack on the pitchblende.

At the time of sampling, Leavenworth Gulch was fed by two springs issuing from the base of two separate waste piles (Fig. 9.6). In upstream reaches, flow was very low; visual estimates were on the order of <0.1 liters per second (l/s) at the source to about 0.6 l/s 0.5 km downstream. Leavenworth Gulch flowed intermittently between the surface and underground before flow-

ing into Russell Gulch. At the point where Russell Gulch empties into the North Fork of Clear Creek, flow was approximately 5 l/s. The main branch of the creek was sampled at various points along the way, as were most of the major tributaries.

Significant variations in water chemistry were observed along the creek, especially between the point where the creek leaves the zone of former mining activity and where it empties into Clear Creek. Samples 512 and 513 (Fig. 9.6) were collected near the edge of past mining activity along the Calhoun vein and sample 514 was collected about 5 km downstream. Between the low-pH regime (pH < 4) upstream and the near-neutral pH regime downstream, significant decreases were observed in concentrations of a number of metals. For example, Al decreased from levels mostly greater than 50 ppm upstream to <1 ppm downstream (Fig. 9.7). Similar decreases were measured for Fe and U (Fig. 9.8), among other metals.

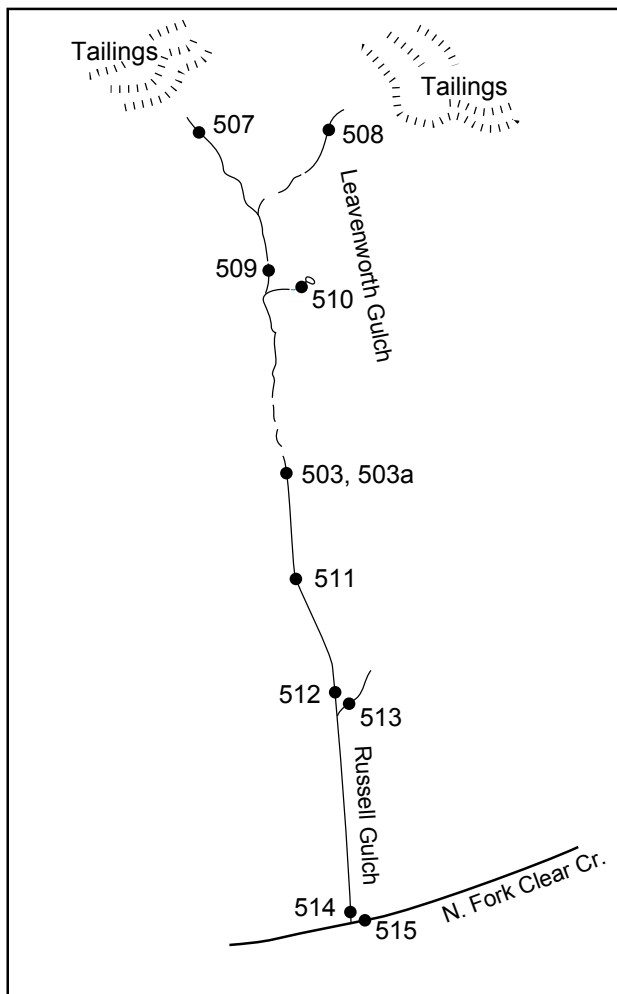


FIGURE 9.6—Schematic map of sample localities from Leavenworth Gulch and Russell Gulch, southwest of Central City, Colorado. This map is drawn to show the spatial relationships of the samples and is not to scale. For instance, the distance between samples 507 and 503 is about 0.5 km; the distance between site 512 and 514 is about 5 km.

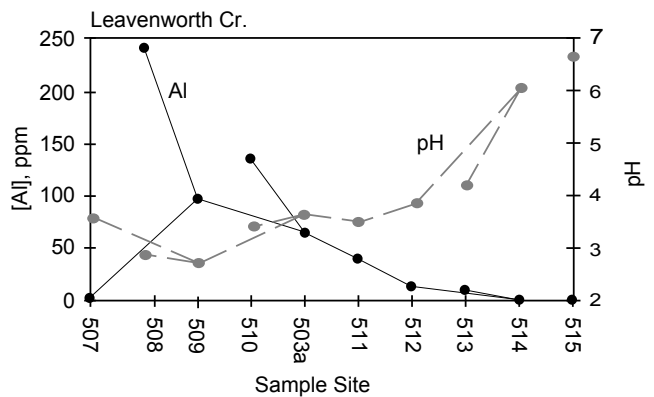


FIGURE 9.7—Variations in Al concentration and pH in Leavenworth Gulch and Russell Gulch. The stream-flow direction is from left to right. Branches represent values of these parameters in tributaries to the stream.

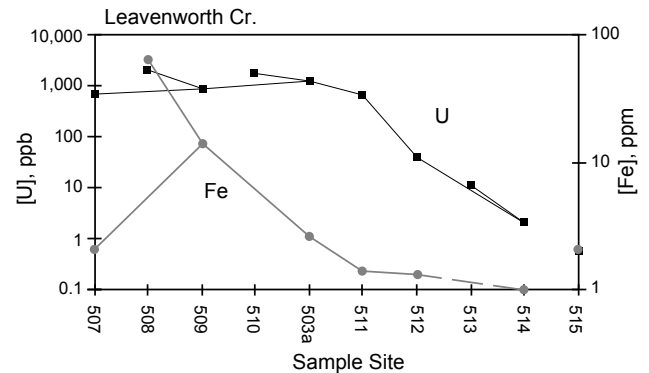


FIGURE 9.8—Concentrations of Fe and U in Leavenworth Gulch and Russell Gulch. The stream-flow direction is from left to right. Branches represent values of these parameters in tributaries to the stream.

Samples were collected along Leavenworth and Russell Gulches in the main stream before and after each tributary, and in the tributaries as well. Estimates of the flow rate at each branch of the stream system were made visually or by using a stopwatch and large beaker. Thus, mixing of tributaries could be calculated as the proportion of the estimated flow rates. Several factors limited this approach: ground-water discharge into the stream could not be accounted for; chemical reactions such as precipitation, dissolution, adsorption, ion exchange, etc., could not be accounted for; and some tributaries were inaccessible.

Despite the problems with quantitative mixing calculations along the length of the stream system, some simple mixing calculations still are possible. To test the hypothesis that U may be attenuated solely by dilution with a higher-pH, U-poor solution, a mixing calculation was performed using PHREEQE (see White et al., 1999, for a summary of the theory and practice of chemical reaction path modeling). The two endmember solutions were an acidic, U-rich water and a near-neutral, U-poor water. For this calculation, sample 507 (see Table 9.2 and Fig. 9.6), with a pH of 3.6 and 630 ppb U, was mixed with sample 514, with a pH of 6.0 and 0.6 ppb U. The former represents the more acid-drainage end-

member; the latter a downstream, more “benign” solution. The mixing was calculated in steps, from one pure endmember solution to the other. The approximate ratio of flow rates at the two sample points was estimated to be 10 to 1. Thus, a 10:1 mixture of sample 514 to 507 would represent a case where 91% of the flow at sample site 514 was contributed by a tributary whose chemistry was essentially the same as that at site 514. Figure 9.9 shows that in the early stages of mixing, pH increases more rapidly than U concentrations decrease. The 10:1 mixture has a U concentration much higher than pure sample 514, but nearly the same pH. Thus, dilution may play only an indirect role in attenuating U concentrations, and adsorption is probably more important. The role of dilution, although indirect, is still important as it is the primary mechanism for increasing pH into the range at which adsorption reactions occur more readily.

The specific behavior of individual elements can be examined by means of congruent element plots (Chapman et al., 1983). Such plots allow for the identification of specific stream reaches where precipitation or dilution may be occurring. According to Chapman et al. (1983), constituents that maintain a ratio near unity are considered conservative, those that are less than unity have been attenuated by some mechanism, and those greater than unity have received some input either from a tributary or from ground-water discharge. An example of such a plot is shown on Figure 9.10 for the Leavenworth-Russell Gulch system. The elemental concentrations are shown as the ratio to site 503a because that is the first sample site downstream of the major inputs of metals and acid

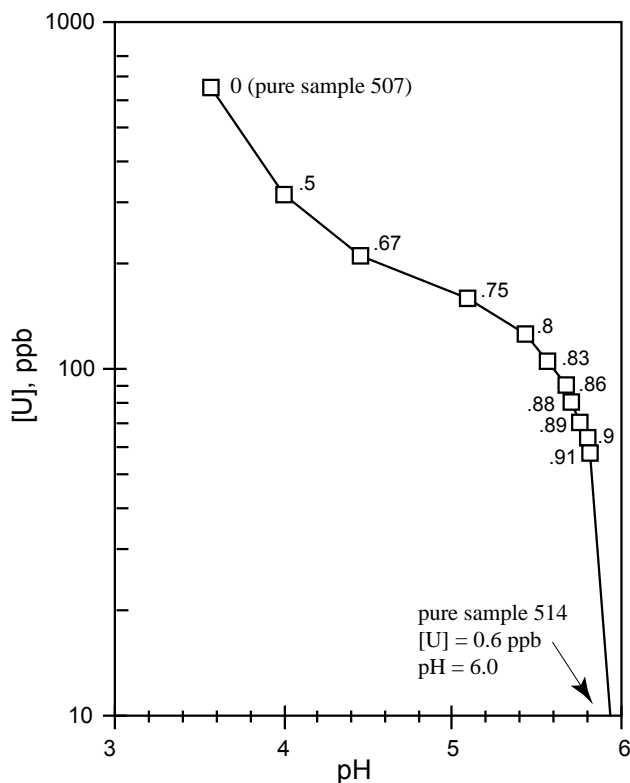


FIGURE 9.9—Hypothetical mixing of sample 507 with sample 514, calculated using PHREEQE. The numbers next to each data point represent the proportion of sample 514 in the mixture.

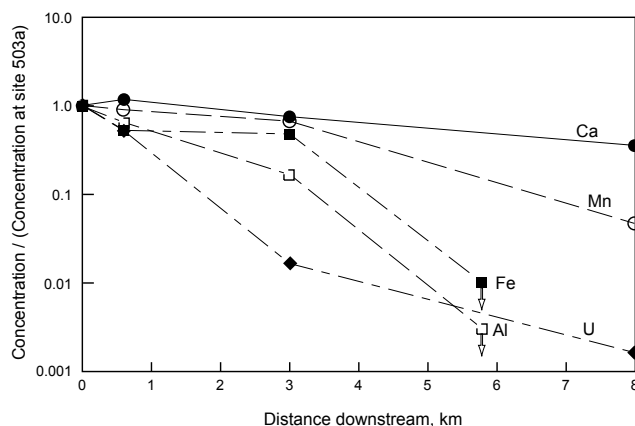


FIGURE 9.10—Congruent-element plot for Leavenworth and Russell Gulches. Elemental concentrations are shown as the ratio of each element at each site to its concentration at site 503a. A value of 1 indicates no change in the concentration of an element. Downward arrows for Fe and Al indicate that beyond 3 km downstream, both elements were below analytical detection limits. See text for further explanation.

water. In Leavenworth and Russell Gulches, conservative constituents include Ca, Mg, Na, Ni, Si, Sr, and SO_4 . Elements attenuated by dilution probably include Cu, Mn, and Zn. Elements affected by precipitation include Al, Fe, Cd, and U. To avoid confusion on Figure 9.10, only Ca, Mn, Al, Fe, and U are shown, but the other elements each plot within their group of congruent constituents. The fact that the major cations and anions act as “conservative” elements actually indicates that the tributaries along the length of the stream have similar concentrations of those constituents so that their concentrations in the mixture are nearly unchanged.

Stream sediments were collected at sites 512 and 514 along Russell Gulch, and from a drainage near Empire, Colorado (site 531 in Table 9.2). At site 512, within the area of mining of the Calhoun vein, the sediments had a slight reddish color, and consisted mostly of fine to medium-grained sand with some pebbles. The sample from site 531 had similar physical characteristics. At site 514, a thick coat (approx. 1 cm) of extremely fine, X-ray amorphous, grayish-white precipitate had formed on the stream bottom. Sediment samples from these locations were leached and the leachates analyzed according to the methods described above. The sediments had a wide variation in leachable U, with sample 514 having the greatest amount of leachable U (470 μg U per gram sediment) and sample 531 the least (0.2 μg U per gram sediment); sample 512 had 1 μg U per gram of sediment.

If the U leached from the sediments represents adsorbed U, then the sediments in contact with the most acidic waters should have the least adsorbed U. This relationship is shown in the leach-experiment results (Fig. 9.11) as square symbols. A second set of stream sediments was collected in October, 1992, following a prolonged dry spell. During the October sampling period, no flow was observed along most of the stream so opportunities to sample water with accompanying sediment were limited. Three pairs of water + sediment samples were collected. The results of leaching these sediment samples are shown on Figure 9.11 as circles. In this case, the amount of U leached from the sediment appears to be independent of the pH of the solution with which it was in con-

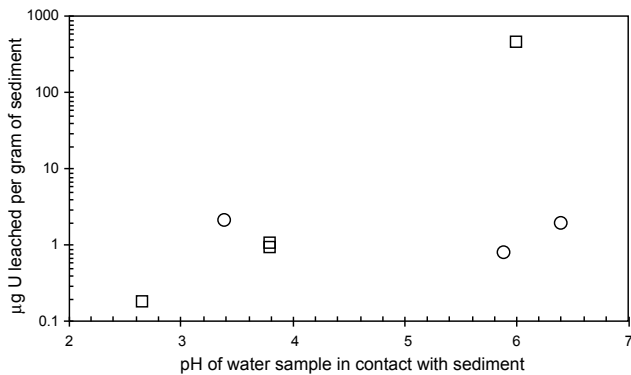


FIGURE 9.11—Results of leaching experiments in which stream-sediment samples were leached with 0.1 M NaHCO_3 solution. Leached U is expressed as ppm by mass of sediment and is plotted against the pH of the stream water at each sediment collection site. Squares represent samples collected on 20 May 92; circles represent samples collected 22 Oct. 92.

tact. In this case, the leached U still represents adsorbed U (because it was readily leached by the carbonate solution), but because of the possible effects of evaporation or intermittent leaching by storm runoff, no relationship between leachable U and pH is observed. Further, the sediments at $\text{pH} \approx 6$ had about three orders of magnitude lower leachable U in October than in May, despite the fact that they were collected from the same site. These results point to the significance of carrying out a multiseason sampling program to fully evaluate the impacts of mine drainage on a stream. Results of stream-sediment sampling programs can vary significantly depending on flow conditions when samples are collected.

The amount of readily leachable U in sample 514 exceeds the average crustal abundance of U by about two orders of magnitude. This amount might be remobilized in the natural system if the water chemistry changed in response to some perturbation in the system (Zielinski and Meier, 1988), such as seasonal variations, long-term climatic variations, or anthropogenic influences. An example of anthropogenic influences is mitigation of the acid mine drainage in upstream reaches of the drainage, thus raising the paradox that upstream cleanup might introduce problems downstream. Dissolved metals in acid waters that have been flowing downstream for decades have contributed to the adsorbed load of metals in the stream sediments. If the upstream waters are mitigated so that virtually no metals leave the mine site(s), metals may be slowly leached from the sediments downstream. The rate and degree of this leaching is unknown, but should be investigated as part of a mitigation plan.

The data shown on Figure 9.11 represent sediment samples which were collected in contact with continuously flowing water, so some statements can be made about the rock-water interactions occurring in the system. However, because of the constraint of collecting sediments in contact with water, within the dry Colorado climate, a limited number of samples was collected. Thus, the data shown should be taken as representing the Leavenworth Creek/Russell Gulch drainage and these results may not be representative of all drainages affected by mining, or of drainages which experience natural acidic conditions. Nevertheless, Figure 9.11 shows that significant amounts of readily leachable U may accumulate on sediment surfaces in these drainages.

Nevada Gulch

Two samples were collected along Nevada Gulch west of Central City to illustrate the impact of mine wastes on relatively pristine water. The first sample (#516 in Table 9.2) was a spring issuing from a pipe protruding from a spring house. The second sample (#517) was collected several kilometers downstream after the water flowed over or around numerous mine dumps. No major tributaries exist between the two sample sites, and flow rates were similar at the two sites. In contrast to the Leavenworth Gulch-Russell Gulch drainage, the source water in Nevada Gulch was originally of excellent quality with low ionic strength: sample 516 had a pH of 6.33, 0.4 ppb U, and total dissolved iron concentration of 0.03 ppm. After flowing over the tailings piles near Nevadaville, the pH had dropped to about 4, U increased to 10 ppb, and total iron was 0.11 ppm. Because no mining has taken place in the Nevadaville area for many decades, these data show that superficial contact of surface water with mine wastes may degrade water quality significantly for historically long periods of time. No samples were collected downstream from site 517 because the stream percolated into the ground, leaving no flow at the surface; however, if the results of Leavenworth Gulch-Russell Gulch are representative of other areas, the U concentration in Nevada Gulch water should decrease as pH rises away from areas of former mining activity.

CONCLUSIONS

In the Introduction, an analogy was made between the formation of ore deposits and the migration of metals from abandoned mines. This analogy considered the source of metals, migration and fixation mechanisms, and the preservation potential of the deposited metals. In that context, the source of U is the mine dump. Significant U concentrations may exist in ores of base and precious metals and in many cases, the milling process does not remove the U. Uranium mobilization from mine-waste and tailings piles begins with sulfide oxidation and acid generation. Under acidic, oxidized conditions present in many mine waste piles and tailings piles, uranium can be effectively leached by weathering of the mine wastes and tailings. The uranium will remain in solution until the pH is neutralized and adsorption reactions occur; in most carbonate-poor waters, uranium adsorption onto particulates is quite effective. How long the uranium remains adsorbed onto the particulates depends on the permanence and reversibility of the adsorption reactions. Because U adsorption is readily reversible (Hsi and Langmuir, 1985), the stability of adsorbed U depends largely on the chemistry of the water in contact with the adsorbing substrate. If the water chemistry does not change over time to a new condition that favors desorption, the U will likely remain adsorbed on the particulates.

This model for uranium mobility was demonstrated by a suite of field samples collected from several mining districts in Colorado. Extremely high concentrations of U (>1 ppm) were found in some acidic water samples draining U-bearing mine dumps. Concentrations of U generally decrease downstream from mine sites as the pH increases: the pH increase may be driven by dilution with tributaries containing uncontaminated water or by reaction with country rock. Although U concentrations are diminished somewhat by dilution, the primary effect of dilution is to increase pH. Thus, the role of dilution is indirect. As pH increases,

es, several processes occur: precipitation of solid oxyhydroxides of metals such as Fe and Al, which may be effective adsorbents for U; adsorption of U onto these fresh mineral surfaces; and fixation (at least temporarily) of the U as new layers of oxyhydroxide form over previously exposed adsorptive surfaces. Precipitation of discrete U minerals is unlikely, as it was shown that all mine-drainage waters collected in this study were undersaturated with respect to common U-bearing minerals.

Adsorption is an important process in limiting U concentrations, but it is also a reversible process. If chemical conditions change in the surface water due to some perturbation, such as seasonal variation, U may be remobilized. This is particularly true if the chemical change leads to a more alkaline, carbonate-rich water capable of complexing U in solution; such waters might be generated, for example, by remediation of acid mine waters at a mine site. Thus, as former mine sites are evaluated for cleanup, it will be necessary to evaluate the potential for remobilization of metals such as uranium from stream sediments in downstream reaches of the drainages fed by the mining districts.

The results of this research suggest that, given enough time, U released during oxidation and leaching of mine wastes will be attenuated to environmentally safe levels by natural processes. The main processes that enhance this "natural remediation" include neutralization of acid mine drainage by interaction with nonsulfide-bearing stream sediments and dilution with neutral-pH waters. It is important that the streambed sediments be relatively free of sulfide minerals so that no further acid generation occurs as a result of oxidation of sulfide minerals.

When preparing a mitigation plan for an area impacted by acid mine drainage, the entire drainage should be considered in the context of these processes. Because of the "natural remediation" just described, the impact of the acid mine drainage may extend far beyond the geographic limits of the mine claim or even beyond the mining district. Further, the sediment may be impacted by its continual adsorption of U, despite the fact that the stream water appears to be of good overall quality. The preservation potential of adsorbed U depends on the constancy of the water chemistry in the stream. If the stream chemistry is altered by anthropogenic effects such as remediation, and if the remediation leads to water chemistry that favors U desorption, then the upstream remediation may ultimately trigger release of U downstream, with subsequent adverse effects.

REFERENCES

- Adams, J.A.S., and Richardson, K.A., 1960, Thorium, uranium, and zirconium concentrations in bauxite: *Economic Geology*, v. 55, pp. 1653–1675.
- Aieta, E.M., Singley, J.E., Trussell, A.R., Thorbjarnarson, K.W., and McGuire, M.J., 1987, Radionuclides in drinking water—An overview: *Journal American Water Works Association*, v. 79, pp. 144–152.
- Ames, L.L., McGarragh, J.E., and Walker, B.A., 1983a, Sorption of trace constituents from aqueous solutions onto secondary minerals. I. Uranium: *Clays and Clay Minerals*, v. 31, pp. 321–334.
- Ames, L.L., McGarragh, J.E., and Walker, B.A., 1983b, Sorption of uranium and radium by biotite, muscovite, and phlogopite: *Clays and Clay Minerals*, v. 31, pp. 343–351.
- Ames, L.L., McGarragh, J.E., Walker, B.A., and Salter, P.F., 1983c, Uranium and radium sorption on amorphous ferric oxyhydroxide: *Chemical Geology*, v. 40, pp. 135–148.
- Anderson, P.R., and Benjamin, M.M., 1990, Constant-capacitance surface complexation model—Adsorption in silica-iron binary oxide suspensions; *in* Melchior, D.C., and Bassett, R.L. (eds.), *Chemical Modeling of Aqueous Systems II: American Chemical Society Symposium Series v. 416*, Washington, D.C., American Chemical Society, pp. 272–281.
- Brownlow, A.H., 1979, *Geochemistry*: Prentice-Hall, Inc., Englewood Cliffs, N.J., 498 pp.
- Chapman, B.M., Jones, D.R., and Jung, R.F., 1983, Processes controlling metal ion attenuation in acid mine drainage streams: *Geochimica et Cosmochimica Acta*, v. 47, pp. 1957–1973.
- Crock, J.G., Arbogast, B.F., and Lamothe, P.J., 1999, Laboratory methods for the analysis of environmental samples; *in* Plumlee, G.S., and Logsdon, M.J. (eds.), *The Environmental Geochemistry of Mineral Deposits, Part A. Processes, Techniques, and Health Issues: Society of Economic Geologists, Reviews in Economic Geology*, v. 6A, pp. 265–287.
- Doerner, H.A., and Hoskins, W.M., 1925, Coprecipitation of radium and barium sulfates: *Journal of the American Chemical Society*, v. 47, pp. 662–75.
- Drake, A.A., 1957, *Geology of the Wood and East Calhoun Mines, Central City district, Gilpin County, Colorado*: U.S. Geological Survey Bulletin 1032-C, pp. 129–170.
- Ficklin, W.H., and Mosier, E.L., 1999, Field methods for sampling and analysis of environmental samples for unstable and selected stable constituents; *in* Plumlee, G.S., and Logsdon, M.J. (eds.), *The Environmental Geochemistry of Mineral Deposits, Part A. Processes, Techniques, and Health Issues: Society of Economic Geologists, Reviews in Economic Geology*, v. 6A, pp. 249–264.
- Fishman, M.J., and Pyen, G., 1979, Determination of selected anions in water by ion chromatography: U.S. Geological Survey Water-Resources Investigations Report 79–101.
- Frederickson, A.F., 1948, Some mechanisms for the fixation of uranium in certain sediments: *Science*, v. 108, pp. 184–185.
- Graves, B., ed., 1987, *Radon, radium, and other radioactivity in ground water*: Lewis Publishers, Chelsea, Mich., 546 pp.
- Henderson, P., 1982, *Inorganic geochemistry*: Pergamon Press, New York, 353 p.
- Hostetler, P.B., and Garrels, R.M., 1962, Transportation and precipitation of uranium and vanadium at low temperatures, with special reference to sandstone-type uranium deposits: *Economic Geology*, v. 57, pp. 137–167.
- Hsi, C.-K.D., 1981, Sorption of uranium (VI) by iron oxides: Unpub. Ph.D. thesis, Colorado School of Mines, Golden, 154 pp.
- Hsi, C.-K.D., and Langmuir, D., 1985, Adsorption of uranyl onto ferric oxyhydroxides—Application of the surface complexation site-binding model: *Geochimica et Cosmochimica Acta*, v. 49, pp. 1931–1941.
- Janzer, V.J., Stanley, G.W., Long, H.K., Farrar, J.W., and Brezina, K.A., 1991, Data for gross-alpha, gross-beta, gross radium as radium-226, and uranium in ground and surface waters in the United States, mid-1954 through 1965: U.S. Geological Survey Open-File Report 91–70, 153 pp.
- Koss, V., 1988, Modeling of uranium (VI) sorption and speciation in a natural sediment-groundwater system: *Radiochimica Acta*, v. 44/45, pp. 403–406.
- Landa, E.R., 1987, Buried treasure to buried waste—The rise and fall of the radium industry: *Colorado School of Mines Quarterly*, v. 82, no. 2, pp. 1–77.
- Landa, E.R., 1999, Geochemical and biogeochemical controls on element mobility in and around uranium mill tailings—Recent studies; *in* Filipek, L.H., and Plumlee, G.S. (eds.), *The Environmental Geochemistry of Mineral Deposits, Part B. Case Studies and Research Topics: Society of Economic Geologists, Reviews in Economic Geology*, v. 6B, pp. 527–538.
- Landa, E.R., and Gray, J.R., 1995, U.S. Geological Survey research on the environmental fate of uranium mining and milling wastes: *Environmental Geology*, v. 26, pp. 19–31.
- Langmuir, D., 1978, Uranium solution-mineral equilibria at low temperatures with applications to sedimentary ore deposits: *Geochimica et Cosmochimica Acta*, v. 42, pp. 547–569.

- Langmuir, D., 1997, *Aqueous environmental geochemistry*: Prentice Hall, Upper Saddle River, New Jersey, 600 pp.
- Langmuir, D., and Herman, J.S., 1980, The mobility of thorium in natural waters at low temperatures: *Geochimica et Cosmochimica Acta*, v. 44, pp. 1753–1766.
- Langmuir, D., and Riese, A.C., 1985, The thermodynamic properties of radium: *Geochimica et Cosmochimica Acta*, v. 49, pp. 1593–1601.
- Laskorin, B.N., Metalnikov, S.S., and Terentiev, A.S., 1958, Extraction of uranium from natural water: 2nd Internat Conference on the Peaceful Uses of Atomic Energy, v. 3., pp. 211–215.
- Lemire, R.J., and Tremaine, P.R., 1980, Uranium and plutonium equilibria in aqueous solutions to 200°C: *Journal of Chemical Engineering Data*, v. 25, no. 4, pp. 361–370.
- Lichte, F.E., Golightly, D.W., and Lamothe, P.J., 1987, Inductively coupled plasma-atomic emission spectrometry; in Baedecker, P.A. (ed.), *Methods for Geochemical Analysis*: U. S. Geological Survey Bulletin 1770, pp. B1–B10.
- Lovering, T.G., 1955, Progress in radioactive iron oxides investigations: *Economic Geology*, v. 50, pp. 186–195.
- Mohagheghi, A., 1985, The role of aqueous sulfide and sulfate-reducing bacteria in the kinetics and mechanisms of the reduction of uranyl ion: Unpub. Ph.D. thesis, Colorado School of Mines, Golden, 300 pp.
- Morin, K.A., and Cherry, J.A., 1988, Migration of acidic groundwater seepage from uranium-tailings impoundments, 3. Simulation of the conceptual model with application to Seepage Area A: *Journal of Contaminant Hydrology*, v. 2, pp. 323–342.
- Morin, K.A., Cherry, J.A., Davé, N.K., Lim, T.P., and Vivuyurka, A.J., 1988a, Migration of acidic groundwater seepage from uranium-tailings impoundments, 1. Field study and conceptual hydrogeochemical model: *Journal of Contaminant Hydrology*, v. 2, pp. 271–303.
- Morin, K.A., Cherry, J.A., Davé, N.K., Lim, T.P., and Vivuyurka, A.J., 1988b, Migration of acidic groundwater seepage from uranium-tailings impoundments, 2. Geochemical behavior of radionuclides in groundwater: *Journal of Contaminant Hydrology*, v. 2, pp. 305–322.
- Murray, A.S., Johnston, A., Martin, P., Hancock, G., Marten, R., and Pfitzner, J., 1993, Transport of naturally occurring radionuclides by a seasonal tropical river, northern Australia: *Journal of Hydrology*, v. 150, pp. 19–39.
- Nordstrom, D.K., 1982, Aqueous pyrite oxidation and the consequent formation of secondary iron minerals; in Kittrick, J.A. (ed.), *Acid Sulfate Weathering*: Soil Science Society of America Spec. Pub. No. 10, pp. 37–56.
- Nordstrom, D.K., and Alpers, C.N., 1999, Geochemistry of acid mine waters; in Plumlee, G.S., and Logsdon, M.J. (eds.), *The Environmental Geochemistry of Mineral Deposits, Part A. Processes, Techniques, and Health Issues*: Society of Economic Geologists, *Reviews in Economic Geology*, v. 6A, pp. 133–160.
- Nordstrom, D.K., Jenne, E.A., and Ball, J.W., 1979, Redox equilibria of iron in acid mine waters; in Jenne, E.A. (ed.), *Chemical Modeling in Aqueous Systems*: American Chemical Society Symposium Series v. 93, Washington, D.C., American Chemical Society, pp. 51–79.
- Parkhurst, D.L., Thorstenson, D.C., and Plummer, L.N., 1980, PHREEQE—A computer program for geochemical calculations: U.S. Geological Survey Water-Resources Investigations 80–96, 210 pp.
- Parkhurst, D.L., Plummer, L.N., and Thorstenson, D.C., 1982, BALANCE—A computer program for calculating mass transfer for geochemical reactions in ground water: U.S. Geological Survey Water-Resources Investigations 82–14, 29 pp.
- Phair, G., 1952, Radioactive tertiary porphyries in the Central City District, Colorado, and their bearing upon pitchblende deposition: U.S. Geological Survey Trace Elements Investigations Report 247, 53 pp.
- Phair, G., and Gottfried, D., 1964, The Colorado Front Range, Colorado, U.S.A., as a uranium and thorium province; in Adams, J.A.S., and Lowder, W.M. (eds.), *The Natural Radiation Environment*: Chicago University Press, Chicago, Ill., pp. 7–38.
- Plumlee, G.S., 1999, The environmental geology of mineral deposits; in Plumlee, G.S., and Logsdon, M.J. (eds.), *The Environmental Geochemistry of Mineral Deposits, Part A. Processes, Techniques, and Health Issues*: Society of Economic Geologists, *Reviews in Economic Geology*, v. 6A, pp. 71–116.
- Plumlee, G.S., Smith, K.S., Ficklin, W.H., and Briggs, P.H., 1992, Geological and geochemical controls on the composition of mine drainages and natural drainages in mineralized areas; in Kharaka, Y.K., and Maest, A.S. (eds.), *Water-Rock Interaction, Proceedings of the 7th Internat Symposium on Water-Rock Interaction*: A.A. Balkema, Rotterdam, pp. 419–422.
- Plumlee, G.S., Smith, K.S., Ficklin, W.H., Briggs, P.H., and McHugh, J.B., 1993, Empirical studies of diverse mine drainages in Colorado—Implications for the prediction of mine-drainage chemistry: *Proceedings, 1993 Mined Land Reclamation Symposium, Billings, Mont.*, v. 1, pp. 176–186.
- Plumlee, G.S., Smith, K.S., Montour, M.R., Ficklin, W.H., and Mosier, E.L., 1999, Geologic controls on the composition of natural waters and mine waters draining diverse mineral-deposit types; in Filipek, L.H., and Plumlee, G.S. (eds.), *The Environmental Geochemistry of Mineral Deposits, Part B. Case Studies and Research Topics*: Society of Economic Geologists, *Reviews in Economic Geology*, v. 6B, pp. 373–432.
- Reid, G.W., Lassovszky, P., and Hathaway, S., 1985, Treatment, waste management and cost for removal of radioactivity from drinking water: *Health Physics*, v. 48, no. 5, pp. 671–694.
- Riese, A.C., 1978, An application of solution mineral equilibrium chemistry to uranium leaching: Unpub. M.S. thesis, New Mexico Institute of Mining and Technology.
- Riese, A.C., 1982, Adsorption of radium and thorium onto quartz and kaolinite—A comparison of solution/surface equilibria models: Unpub. Ph.D. thesis, Colorado School of Mines, Golden, 292 pp.
- Rogers, J.J.W., and Adams, J.A.S., 1972, Uranium; in Wedepohl, K.H. (ed.), *Handbook of Geochemistry*: Springer-Verlag, New York, pp. 92-1–92-O-8.
- Scott, R.C., and Barker, F.B., 1962, Data on uranium and radium in ground water in the United States 1954 to 1957: U.S. Geological Survey Professional Paper 426, 115 pp.
- Sims, P.K., and Gable, D.J., 1964, Geology of Precambrian rocks, Central City district, Colorado: U.S. Geological Survey Bulletin 474–C, 52 p.
- Sims, P.K., Armstrong, F.C., Drake, A.A. Jr., Harrison, J.E., Hawley, C.C., Moench, R.H., Moore, F.B., Tooker, E.W., and Wells, J.D., 1963, Geology of uranium and associated ore deposits, central part of the Front Range Mineral Belt, Colorado: U.S. Geological Survey Professional Paper 371, 119 pp., 9 plates.
- Skougstad, M.W., Fishman, M.J., Friedman, L.C., Erdmann, D.E., and Duncan, S.S., 1979, Methods for determination of inorganic substances in water and fluvial sediments: *Techniques of Water-Resources Investigations of the U.S. Geological Survey*, Book 5, Ch. A5, 626 pp.
- Smith, K.S., 1999, Metal sorption on mineral surfaces—An overview with examples relating to mineral deposits; in Plumlee, G.S., and Logsdon, M.J. (eds.), *The Environmental Geochemistry of Mineral Deposits, Part A. Processes, Techniques, and Health Issues*: Society of Economic Geologists, *Reviews in Economic Geology*, v. 6A, pp. 161–182.
- Smith, K.S., and Huyck, H.L.O., 1999, An overview of the abundance, relative mobility, bioavailability, and human toxicity of metals; in Plumlee, G.S., and Logsdon, M.J. (eds.), *The Environmental Geochemistry of Mineral Deposits, Part A. Processes, Techniques, and Health Issues*: Society of Economic Geologists, *Reviews in Economic Geology*, v. 6A, pp. 29–70.
- Smith, K.S., Ficklin, W.H., Plumlee, G.S., and Meier, A.L., 1992, Metal and arsenic partitioning between water and suspended sediment at mine-drainage sites in diverse geologic settings; in Kharaka, Y.K., and Maest, A.S. (eds.), *Water-Rock Interaction, Proceedings of the 7th Internat Symposium on Water-Rock Interaction*: A.A. Balkema, Rotterdam, pp. 443–447.
- Stumm, W., and Morgan, J.J., 1981, *Aquatic chemistry*, 2nd ed.: John Wiley and Sons, New York, 780 pp.
- Tolmachev, Y.M., 1943, The adsorption of uranyl salts onto solid adsorbents: *Bulletin of the Academy of Sciences, USSR, Chemistry Series*, v. 1, pp. 28.

- Tsunashima, A., Brindley, G.W., and Bastovanov, M., 1981, Adsorption of uranium from solutions by montmorillonite; compositions and properties of uranyl montmorillonites: *Clays and Clay Minerals*, v. 29, no. 1, pp. 10–16.
- Van der Weijden, C.H., Van Leeuwen, M., and Peters, A.F., 1985, The adsorption of U (VI) onto precipitating amorphous ferric hydroxide: *Uranium*, v. 2, pp. 53–58.
- Waite, T.D., Davis, J.A., Payne, T.E., Waychunas, G.A., and Xu, N., 1994, Uranium (VI) adsorption to ferrihydrite—Application of a surface complexation model: *Geochimica et Cosmochimica Acta*, v. 58, pp. 5465–5478.
- Wanty, R.B., and Nordstrom, D.K., 1993, Natural radionuclides; *in* Alley, W.M. (ed.), *Ground-Water Quality Concepts*: VanNostrand Reinhold.
- Wanty, R.B., and Schoen, R., 1991, A review of the chemical processes affecting the mobility of radionuclides in natural waters, with applications; *in* Gundersen, L.C.S., and Wanty, R.B. (eds.), *Field Studies of Radon in Rocks, Soils, and Water*: United States Geological Survey Bulletin 1971, pp. 183–194.
- Wanty, R.B., Miller, W.R., Zielinski, R.A., Plumlee, G.S., Bove, D.J., Lichte, F.E., Meier, A.L., and Smith, K.S., 1998, Uranium mobility in surface waters draining mineralized areas in the western U.S.; *in* Arehart, G.B., and Hulston, J.R. (eds.) *Proceedings of the 9th Internatl Symposium on Water-Rock Interaction*: A.A. Balkema, pp. 1013-1016.
- Westra, G., and Keith, S.B., 1981, Classification and genesis of stockwork molybdenum deposits: *Economic Geology*, v. 76, p. 844–873.
- White, A.F., Delany, J.M., Narasimhan, T.N., and Smith, A., 1984, Groundwater contamination from an inactive uranium mill tailings pile, 1. Application of a chemical mixing model: *Water Resources Research*, v. 20, no. 11, pp. 1743–1752.
- White, W.H., Bookstrom, A.A., Kamilli, R.J., Ganster, M.W., Smith, R.P., Ranta, D.E., and Steininger, R.C., 1981, Character and origin of climax-type molybdenum deposits; *in* Skinner, B.J. (ed.), *Economic Geology 75th Anniversary Volume*: Economic Geology Publishing Company, El Paso, Tex., pp. 270–316.
- White III, W.W., Lapakko, K.A., and Cox, R.L., 1999, Static-test methods most commonly used to predict acid-mine drainage—Practical guidelines for use and interpretation; *in* Plumlee, G.S., and Logsdon, M.J. (eds.), *The Environmental Geochemistry of Mineral Deposits, Part A. Processes, Techniques, and Health Issues*: Society of Economic Geologists, *Reviews in Economic Geology*, v. 6A, pp. 325–338.
- Wood, W.W., 1976, Guidelines for the collection and field analysis of ground-water samples for selected unstable constituents: *Techniques of Water-Resources Investigations of the U.S. Geological Survey*, Book 1, Ch. D2, 24 pp.
- Zielinski, R.A., and Meier, A.L., 1988, The association of uranium with organic matter in Holocene peat—An experimental leaching study: *Applied Geochemistry*, v. 3, pp. 631–643.

Chapter 10

GEOCHEMISTRY OF THE PROCESSES THAT ATTENUATE ACID MINE DRAINAGE IN WETLANDS

Katherine Walton-Day

U.S. Geological Survey, Box 25046, MS 415, Federal Center, Denver, CO 80225-0046

INTRODUCTION

Because conventional treatment of acid-mine drainage (AMD) involves installation and maintenance of water treatment plants, regulators and mine operators have sought lower cost and lower maintenance technologies. One ecological engineering technology that has received increasing research attention is the use of natural and constructed wetlands for remediation of some of the water-quality problems associated with AMD. As surface water flows through a wetland, several processes can occur to decrease the elevated concentrations of sulfate, trace metals, arsenic, and hydrogen ions that characterize AMD. These processes range from precipitation of mineral phases to the active uptake of solutes by vegetation. The relative importance of these processes between different wetlands depends on the hydrologic and geochemical characteristics of the wetlands.

This paper describes the geochemistry of the processes that contribute to AMD attenuation in wetlands and presents some of the case studies that have identified these processes. The attenuation of AMD in wetlands has been studied in natural and in man-made (constructed) wetlands. In this paper, case studies of both are presented. A discussion of some of the general characteristics of wetlands is followed by more detailed discussions of the processes and geochemistry that contribute to the treatment of AMD in wetlands, relevant case studies, and a brief discussion of constructed wetland design. The physical, chemical, and hydrologic characteristics of a wetland that affect its potential for supporting specific types of reactions are also emphasized.

Although mine drainage can have pH values ranging from acid to alkaline (Hedin, personal commun., 1992; Ficklin et al., 1992; Plumlee et al., 1993; Smith et al., 1994; Plumlee et al., 1999), most wetlands that have been studied with respect to their effect on the water quality of mine drainage receive AMD, and the discussion in this paper, therefore, focuses on processes that occur where wetlands interact with AMD. Other recent summaries concerning wetland treatment of AMD are Kleinmann (1990) and Klusman and Machemer (1991). Nordstrom and Alpers (1999) review the formation of AMD.

GENERAL AND GEOCHEMICAL CHARACTERISTICS OF WETLANDS

Wetlands are transitional between terrestrial and aquatic ecosystems. They are characterized by one or more of the following conditions (Cowardin et al., 1979; Hammer and Bastian, 1989):

- 1) They contain hydrophytic vegetation (plants that are adapted to survive in waterlogged soils).
- 2) They contain hydric soils (soils that are wet enough for sufficient time to produce anaerobic conditions which, in turn, limit the types of plants that can grow).
- 3) They contain nonsoil substrate (such as rock or gravel) that is saturated or covered by shallow water at some time during the growing season.

A scientific classification of wetlands has been developed by the U.S. Fish and Wildlife Service (Cowardin et al., 1979) and is being used to map and inventory wetlands in the United States. Currently (as of late 1995), the definition of wetlands for jurisdictional purposes in the United States is a subject of controversy (Kusler, 1992). Studies of natural wetlands presented in this paper have not been examined to determine whether the study areas are scientific or jurisdictional wetlands, or both.

Comprehensive discussions of the geochemistry of wetlands are provided in several publications (Ponnampetuma, 1972; Gambrell and Patrick, 1978; Sikora and Keeney, 1983; Mitsch and Gosselink, 1986; Shotyk, 1988; Faulkner and Richardson, 1989). A general discussion derived from these references and others follows.

A generalized profile of a flooded wetland includes an oxidized water column and oxidized sediment layer that overlie a reduced sediment zone (Fig. 10.1). A relatively uniform level of oxygen exists in the water column and upper sediment layer because of

- 1) The rapid exchange of oxygen across the atmosphere/surface-water interface;
- 2) The limited population of oxygen-consuming organisms present;
- 3) Oxygen production by photosynthetic algae within the water column; and
- 4) Surface-water mixing by convection and wind action (Gambrell and Patrick, 1978).

In saturated sediments, the replenishment of oxygen is limited by the aqueous diffusion of dissolved oxygen into the sediments, which is four orders of magnitude slower than gaseous diffusion (Greenwood, 1961). Therefore, oxygen concentrations in the oxidized sediment zone decrease with depth, and anaerobic (anoxic) conditions develop in the underlying sediment zones (the reduced sediments) where microbial and chemical oxygen demand exceed the rate of resupply by aqueous diffusion. Within the reduced sediments, oxidized microenvironments can exist immediately adjacent to roots that transport oxygen from the atmosphere. The thickness and continuity of the oxidized and reduced soil zones are variable and depend on several factors, including soil permeability, duration and frequency of flooding, and supply of carbon avail-

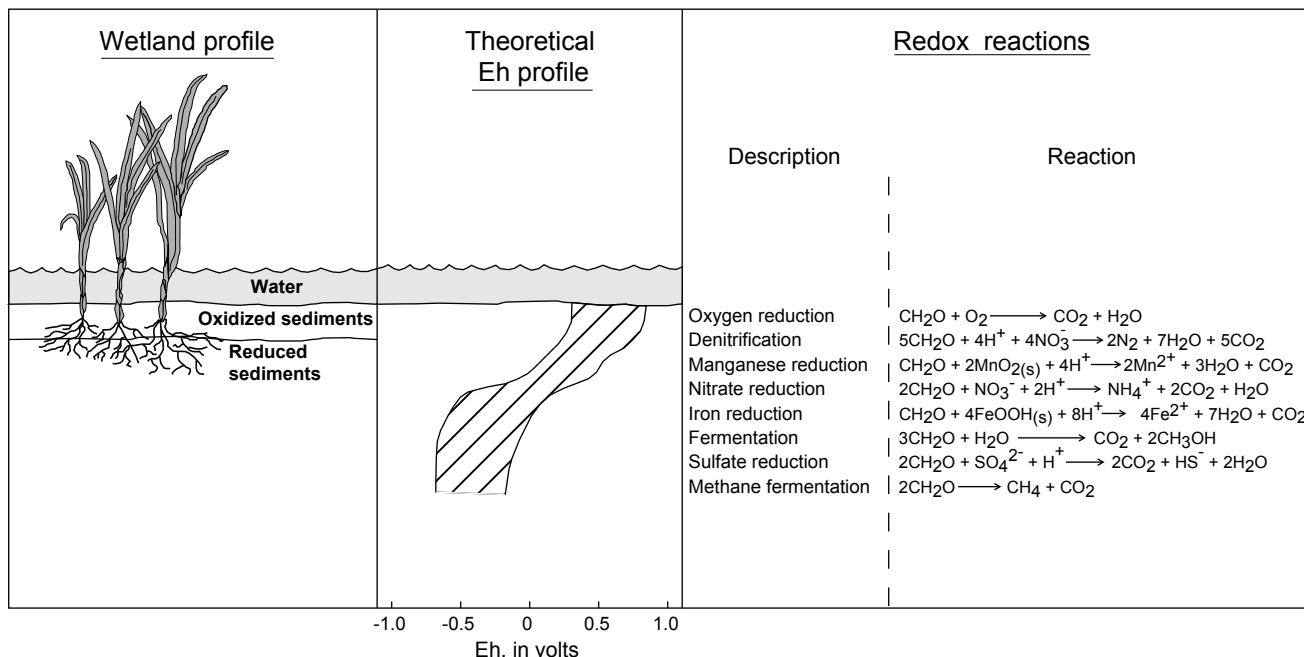


FIGURE 10.1—Generalized profile of wetland soil and some soil chemical parameters (adapted from Gambrell and Patrick, 1978; Stumm and Morgan, 1981).

able for microbial metabolism (Gambrell and Patrick, 1978). This typical wetland redox profile develops independent of wetland hydrology; that is, the profile can develop in flow-through wetlands, in wetlands that recharge adjacent and underlying ground-water systems, and in wetlands that receive discharge from adjacent ground-water systems.

The redox profile that develops in saturated soils results from a sequence of microbially mediated reactions that are thermodynamically controlled: the reactions yield less energy on a molar basis as the redox potential decreases. Respiration is the amalgam of biological processes whereby organisms oxidize organic and inorganic matter to obtain energy. Most organisms oxidize organic matter as a source of energy, but some specialized organisms known as chemoautotrophic bacteria obtain energy from the oxidation of reduced inorganic compounds (Stanier et al., 1986; Mills, 1999). Oxidation releases electrons that must be incorporated into another compound known as the terminal electron acceptor. Oxygen is the optimal terminal electron acceptor because the oxidation of organic matter by oxygen (known as aerobic respiration) yields more energy on a molar basis than any other common oxidant. As aerobic and facultative anaerobic microorganisms deplete oxygen in flooded soils, facultative and obligate anaerobes that use anaerobic respiration to obtain energy begin to dominate. Facultative anaerobes are organisms that can use aerobic or anaerobic respiration, whereas obligate anaerobes use only anaerobic respiration. Inorganic substances other than oxygen are the terminal electron acceptors for oxidation of organic matter in anaerobic respiration. The sequence of reduction reactions proceeds, based on decreasing energy yield, from oxygen reduction to denitrification, manganese reduction, nitrate reduction, iron reduction, fermentation, sulfate reduction, and methane fermentation (Fig. 10.1). Generally, a redox zonation develops in

soils as the supply of an energetically favorable terminal electron acceptor is depleted, and as organisms that use the next most energetically favorable terminal electron acceptor begin to dominate. Most of these reactions generate alkalinity, so that the pH tends to increase with depth in a wetland. Values of pH in peat-dominated wetlands normally range from 4 to 8.5 (Shotyk, 1988).

The differences between aerobic and anaerobic respiration also account for the accumulation of organic matter in wetland soils. Aerobic respiration usually degrades organic materials faster than anaerobic respiration; hence, organic materials are more likely to accumulate in anaerobic settings (Gambrell and Patrick, 1978; Stanier et al., 1986).

PROCESSES THAT CONTRIBUTE TO ATTENUATION OF ACID MINE DRAINAGE IN WETLANDS

Water-quality improvement that occurs as AMD flows through wetlands is caused by the transformation of dissolved and particulate constituents to forms not available for waterborne transport. The constituents of AMD are transferred from the aqueous phase to other phases including inorganic solids, gases, and biomass within the wetland substrate. Specific processes in wetlands that are known to contribute to AMD attenuation are (Fig. 10.2):

- 1) Sedimentation of particulate material;
- 2) Oxidation and precipitation of iron and manganese oxyhydroxides;
- 3) Ion exchange and adsorption of dissolved constituents onto solid components of the wetland substrate;
- 4) Complexation of dissolved constituents with organic matter;
- 5) Sulfate reduction and precipitation of metal sulfides; and
- 6) Plant assimilation of metals.

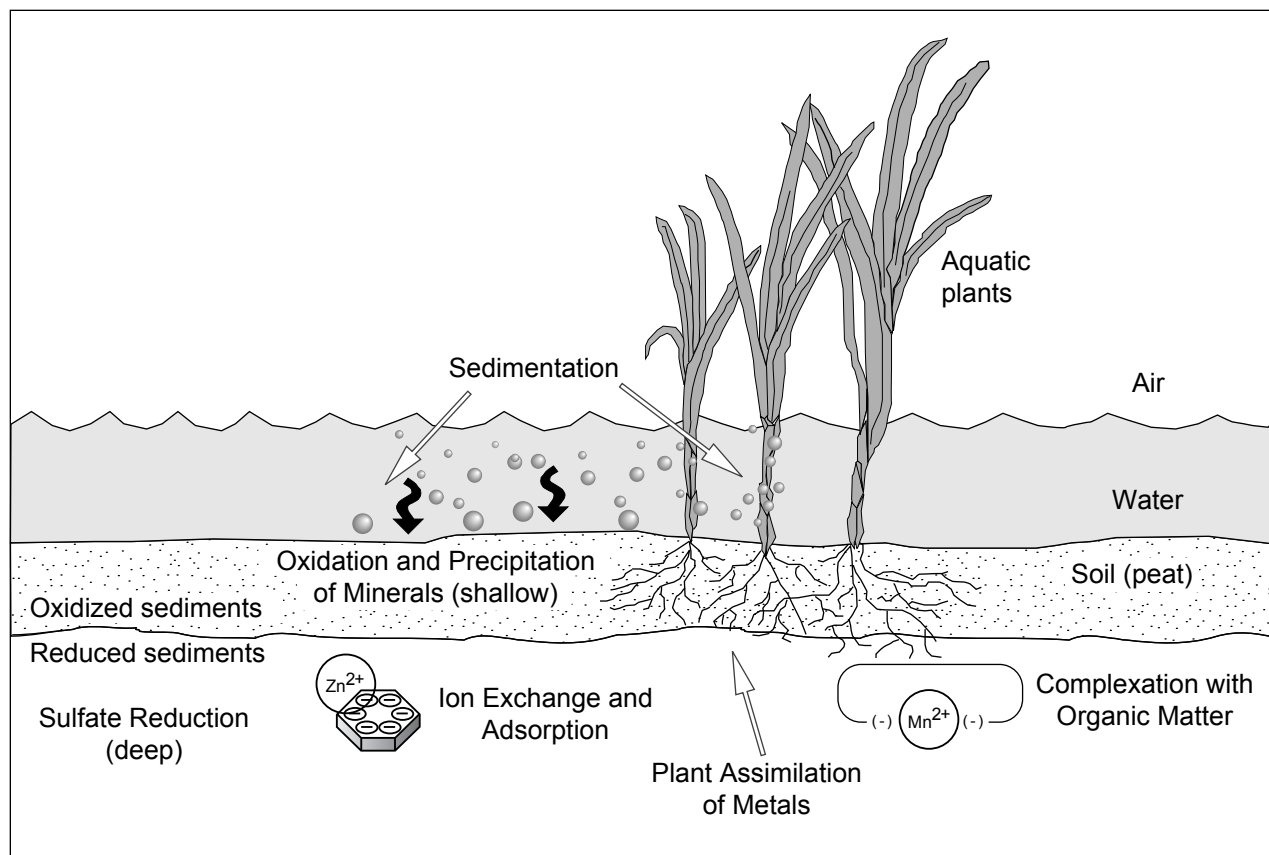


FIGURE 10.2—Geochemical and physical processes that contribute to metal retention in wetlands. Cartoons represent hydrated manganese ion complexing with organic molecule and zinc ion adsorbed to charged surface of a mineral.

Processes 1 and 2 occur primarily in the upper, oxidized zones of wetland sediments. Process 5 is restricted to the reduced zone of the sediment, whereas the other processes occur throughout the soil column or in the plants. The bacterial uptake of metals (Grappelli et al., 1992; Pradhan and Levine, 1992) is another process that may operate in wetlands, but has not been investigated with respect to AMD in wetlands and, therefore is not discussed further. The discussion in this paper of AMD attenuation by wetlands also does not consider the water-quality improvements that occur where additional water sources in the wetland (such as springs, tributary streams, or precipitation onto the wetland) dilute the concentrations of dissolved constituents. Instead, the discussion is concerned with reactions and processes that immobilize or otherwise remove the constituents from the water column so that not only the concentration, but also the mass rate of transport of dissolved constituents, is decreased as AMD flows through the wetland.

Investigators have used several different approaches to quantify constituent removal as water passes through wetland treatment systems. One method defines “treatment efficiency” (TE) as follows:

$$TE = (C_i - C_o)/C_i \quad [1]$$

where C_i and C_o are the inflow and outflow concentrations of the constituent of interest (Girts and Kleinmann, 1986). This method is used most often because it employs concentrations that are the criteria used to determine if a facility has met its regulatory requirements. However TE does not account for wetland hydrology. Therefore, dilution from water sources in the wetlands, such as springs, could cause a positive TE value; whereas, evaporation from the wetland could cause a negative TE value. In addition, TE does not account for the magnitude of inflow versus outflow concentration. For instance, a wetland that has constituent inflow and outflow concentrations of 700 and 500 mg/l has the same TE as a wetland with constituent inflow and outflow concentrations of 7 and 5 mg/l. Obviously, the magnitude of the problem and treatment (200 mg/l removed compared to 2 mg/l removed) is very different in the two wetlands (Wieder, 1989). Finally, TE does not account for size variations between wetlands. In the previous example, the identical TE values are comparable only if the former wetland were 100 times larger than the latter.

Another variable that has been used to describe constituent removal efficiency is area adjusted constituent loading or removal expressed as mass of metal per time per area [e.g., $grams\ day^{-1}\ m^{-2}$ or gdm (Hedin and Nairn, 1990)]. Calculation of this variable is more time consuming and costly than the calculation of TE because it requires measurement of influent and effluent concen-

trations and discharges or flux rates (Wieder, 1988; Wieder, 1989). This variable is superior to TE because it accounts for dilution and evaporation effects and the size of the wetland and, therefore, enables performance comparisons between wetlands. Unfortunately, hydrologic flux data are expensive to obtain and are often not available for a study site, so that this variable cannot readily be calculated (Wieder, 1989).

Sedimentation of particulate material

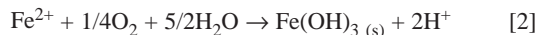
Primary sedimentation in wetlands can remove much of the influent sediment load and, consequently, can remove any chemical constituents associated with the sediments. Sheet flow of water through wetlands decreases the velocity of water and promotes the settling of suspended particles (Boto and Patrick, 1978; Mitsch and Gosselink, 1986). In addition, filtration of sediment by closely spaced plant stems contributes to sediment trapping in wetlands.

Some case studies have reported that sedimentation can be a major contributor to the treatment of AMD in wetlands. Results of a mass-balance study of iron in a constructed wetland that receives AMD indicated that most of the iron removal in the wetland was caused by sedimentation and precipitation of iron hydroxides (Fennessey and Mitsch, 1989). A mass-balance study of iron and trace metals in a subalpine wetland that receives AMD, showed that 60–70% of the iron removal that occurs in the wetland is due to physical settling of iron oxyhydroxide particles greater than 0.1 μm (Walton-Day, 1996).

Oxidation and precipitation of iron and manganese oxyhydroxides

The oxidation of iron and precipitation of iron oxyhydroxides is an important metal removal mechanism in wetlands. Many studies have reported iron removal from mine drainage as a result of this process, and many constructed wetlands have been designed to maximize this process. Theoretically, manganese also ought to precipitate in oxic zones of wetlands by this mechanism.

The oxidation of iron and precipitation of iron oxyhydroxides can be written as a net reaction (Bigham et al., 1990):



In aerated solutions at pH >5, ferrous iron autooxidizes to ferric iron. However, at lower pH values, bacteria such as *Thiobacillus ferrooxidans* catalyze iron oxidation. Because *T. ferrooxidans* are acidophilic (acid-loving), iron oxidation is optimal at pH 3 to 3.6 (Ehrlich, 1981). Although reaction [2] removes iron from solution, the reaction also produces hydrogen ions. The decreased pH that results from this reaction if there is no buffering is undesirable and is one reason other wetland processes have been sought to remove iron from AMD.

The iron hydroxides that can form in AMD and oxic wetlands are complex. Some of the iron hydroxides that form in AMD are actually poorly crystallized oxyhydroxysulfates of iron (Bigham et al., 1990) that have recently been named schwertmannite (Murad et al., 1994). In addition, the types of iron hydroxide material that form in mine drainage can be classified on the basis

of pH and sulfate content of the mine drainage (Bigham et al., 1992; Bigham, 1994): jarosite $[(\text{K},\text{Na})\text{Fe}_3(\text{OH})_6(\text{SO}_4)_2]$ precipitation is favored by very low pH values (1.5–3.0) and elevated sulfate concentrations (>3,000 mg/l); pH values from 3 to 4 and sulfate concentrations ranging from 1000–3000 mg/l favor schwertmannite $[\text{Fe}_8\text{O}_8(\text{OH})_6\text{SO}_4]$; pH values greater than 5 and elevated concentrations of iron favor ferrihydrite $[\text{Fe}_3(\text{OH})_8 \cdot 4\text{H}_2\text{O}]$ formation. Goethite (Alpha $\text{FeO} \cdot \text{OH}$) forms as an alteration product of jarosite, schwertmannite, and ferrihydrite, and can form directly at low pH and low sulfate concentrations and at higher pH in bicarbonate-rich water (Bigham et al., 1992; Bigham, 1994). The results of this classification have not yet been applied to precipitation of iron solids in wetlands, but seem to indicate that precipitation of iron oxides at high pH values and low sulfate concentrations is the most desirable scenario because it produces the most stable precipitate. In addition, alteration of jarosite, schwertmannite, or ferrihydrite to goethite could release metals sorbed to the original mineral phase.

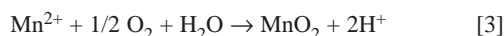
Many case studies of natural, constructed, and laboratory-scale microcosm wetlands have indicated that the formation of iron oxides is an important iron-removal process in wetland treatment systems. Formation of iron oxides was responsible for 73–86% of iron retention that occurred in laboratory-scale constructed wetlands exposed to synthetic acid coal mine drainage (Wieder et al., 1990). Iron oxides accumulated in the oxic zone of a natural wetland (Pennsylvania, U.S.A.) exposed to AMD (Tarutis et al., 1992). Faulkner and Richardson (1990) reported that 80% of the iron accumulating in constructed wetlands in Alabama, U.S.A., was in an oxide form (goethite) and that biological or chemical oxidation, or both, was the dominant removal mechanism.

The acidity produced by oxidation and precipitation of iron hydroxides can exacerbate water-quality problems. In constructed wetlands that receive AMD containing extremely elevated iron concentrations (40–170 mg/l) and pH values less than or equal to 5.6, oxidation of iron and precipitation of iron hydroxides increases acidity and lowers pH in the wetlands necessitating additional water treatment to comply with regulations (Brodie, 1990).

The factors controlling iron mobility in natural systems are complex and include the pH and Eh of the system and the presence of certain types of bacteria, complexing agents, and ligands that combine with iron to form minerals. A process that affects iron speciation in acid streams is the photoreduction of iron. In daylight, sunlight striking an acid stream promotes reductive dissolution of iron hydroxides in the stream. This dissolution results in greater concentrations of dissolved ferrous iron during daylight versus darkness (McKnight et al., 1988). If iron photoreduction occurs in wetland treatment systems where precipitation of iron oxyhydroxides is a major treatment mechanism, the photoreduction could cause less effective removal of iron and dissolution of previously precipitated iron oxides during daylight. Henrot et al. (1989) initially attributed diurnal fluctuations in dissolved iron concentrations exiting a wetland treatment system to iron photoreduction. However, in a subsequent report, Henrot and Wieder (1990) reported that photoreduction caused insignificant iron remobilization in laboratory peat microcosms that were subjected to AMD. Similar results were reported for five pilot-scale constructed wetlands (Wieder, 1992). In addition, Wieder (1992) noted that iron retention effectiveness was greater during the daytime than at night, which he attributed to daytime oxygenation of surface waters by photosynthetic algae.

As with iron, the oxidation of manganese and precipitation of

manganese oxides in wetlands can reduce manganese levels in AMD. The oxidation of manganese can occur as follows (Ehrlich, 1981):



The oxidation of manganese and the precipitation of manganese oxides occurs at greater Eh and pH values than oxidation and precipitation of iron hydroxides (Fig. 10.3). As in the equivalent reactions for iron, reaction [3] produces acidity and can be catalyzed by bacteria.

The removal of manganese by oxidative processes in wetlands is generally less effective than the removal of iron (Gerber et al., 1985; Wieder and Lang, 1986; Henrot and Wieder, 1990). Although manganese-oxidizing bacteria have been identified in wetlands (Batal et al., 1989), failure of wetland treatment systems to remove significant quantities of manganese by oxidative processes has been attributed to low pH values in the wetlands (Henrot and Wieder, 1990; Wildeman et al., 1990). Manganese autooxidizes at pH values of 8.5 or greater. Limited research indicates that manganese-oxidizing bacteria are not active at low pH (Henrot and Wieder, 1990). Removal of manganese by formation of MnCO_3 should proceed at higher pH values (Sikora and Keeney, 1983). This removal process has not been reported in

wetlands that receive AMD, but could be important if wetlands are used to remediate mine drainage that has circumneutral to alkaline pH.

In summary, oxidation and precipitation of oxides, hydroxides, or oxyhydroxides in wetlands remove iron from AMD. However, iron removal by these processes is incomplete and generates acidity. These processes do not seem to remove manganese at the acid to circumneutral pH values that predominate in wetland treatment systems. Other metals, such as copper and aluminum, can also oxidize and/or form metal-oxide precipitates in the Eh and pH ranges where iron and manganese hydroxides and oxides form; however, no case studies of wetlands were found that examined if these processes remove other metals present in AMD. The role of sorption of trace metals to these minerals is described in the section "Ion exchange and adsorption." In addition, in circumneutral-to alkaline-pH mine-drainage/wetland systems, other minerals, such as carbonate minerals, could form and remove metals; however, only limited research has been reported on alkaline mine drainage/wetland systems.

Ion exchange and adsorption

Adsorption and ion exchange contribute to the removal of trace elements from solution in many natural aqueous systems. Similarly, they contribute to metal immobilization in wetlands, but most case studies indicate that their contribution is minor compared to other processes. Detailed geochemical discussions of adsorption are in Stumm and Morgan (1981), Evans (1989), Davis and Kent (1990), and Smith (1999).

Ion exchange and adsorption are processes that occur at the surface of particles in the substrate and between layers in the crystal structures of some clay minerals. Both processes attach dissolved ions or molecules to a pre-existing solid (Drever, 1988). Ion exchange (also referred to as nonspecific adsorption) is a relatively weak interaction between particle surfaces and ions, and most attached ions can be easily removed from the surface under appropriate conditions. It is rapid and usually reversible. In ion exchange a hydrated ion is held against the particle surface primarily by electrostatic attraction. The electrostatic bond is also known as an outer-sphere complex. The sorbed ions will readily exchange for other ions that similarly only form outer-sphere complexes with the surface. In contrast, in adsorption (also referred to as specific adsorption), a covalent bond (or inner-sphere complex) forms between the mineral surface and the adsorbing ion. In this interaction, the adsorbing ion is not readily replaced. The difference between the two processes results from a different degree of interaction between the particle surface and the ion.

In adsorption, elements that form oxyanions, such as arsenic, chromium, and molybdenum bond to variably charged particle surfaces through the process of ligand exchange. Cations also can bond to variably charged surfaces where a hydrolyzed cation forms an inner-sphere complex with a negatively charged, deprotonated surface (Stumm and Morgan, 1981; Evans, 1989).

In wetland systems, hydrous iron oxides and organic matter are probably the two most important substrates for adsorption. The zero point of charge (ZPC) for iron oxyhydroxides has been reported at values of pH ranging from 6.1 to 8.5 (Leckie and James, 1974; Stumm and Morgan, 1981). This result indicates that the net surface charge on iron oxyhydroxide minerals should be positive in the pH range of AMD and of wetlands affected by

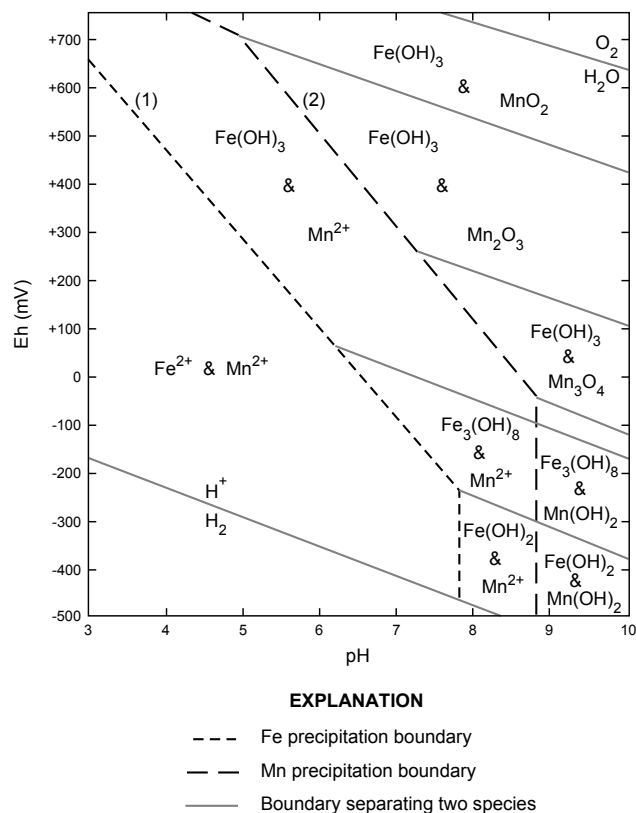


FIGURE 10.3—Eh-pH diagram for Mn and Fe (from Collins and Buol, 1970; Faulkner and Richardson, 1989; reprinted with permission).

AMD. Therefore, based on purely electrostatic considerations, sorption of anions would predominate in wetland treatment systems. Nevertheless, removal of trace-metal cations from AMD has been attributed to adsorption onto hydrous iron oxide minerals (K.S. Smith, U.S. Geological Survey, written commun., 1995). Specific adsorption of trace-metal cations would not be subject to the electrostatic constraints described. It is also possible that the surface charge of the minerals is modified by adsorption of organic or other anions, resulting in (nonspecific) adsorption of cations to the iron oxide surfaces as described by Tipping et al. (1983).

Several studies have cited ion exchange and adsorption as processes contributing to metal retention in wetland treatment systems (Wieder and Lang, 1986; Karathanasis and Thompson, 1991; Machermer and Wildeman, 1992). For some metals such as manganese, ion exchange may be the dominant retention process, but the process does not remove a sufficient amount of metal to be an efficient removal mechanism on its own. In addition, because ion exchange is readily reversible, it is not a reliable treatment process in long-term passive treatment systems; unforeseen changes in environmental conditions could release metals held in exchange positions. In general, ion exchange and adsorption may contribute to metal removal in mine drainage, particularly in the initial stages of a constructed wetland (Kleinmann, 1990; Machermer and Wildeman, 1992). However, the amount of metal removed by these processes in a wetland is limited by the volume of the wetland.

Complexation with organic matter

The complexation of metal ions with organic matter may be an important metal-removal process in wetlands that receive AMD. However, the process also can increase metal mobility in certain situations and has been cited as a reason for incomplete removal of metals in wetland treatment systems.

Organic matter in soils consists of plant and animal products in various stages of decomposition. This material can be divided into humic and nonhumic substances, which, depending on the substance and ambient conditions, can have varying degrees of solubility in water. Humic substances are the most stable compounds in soils and include humic acid, fulvic acid, and humin. Nonhumic

substances include high- and low-molecular-weight organic acids, carbohydrates, proteins, peptides, amino acids, lipids, waxes, polycyclic aromatic hydrocarbons, and lignin fragments (Kabata-Pendias and Pendias, 1984). The source of organic matter in a wetland and its degree of decomposition will affect the properties of the organic matter. For instance, organic matter in a constructed wetland that has a manure substrate might have very different properties than organic matter in a natural wetland that has a substrate consisting primarily of decomposed plant material.

Interactions between metal ions and organic matter help control the mobilities of some metals in organic-rich environments (Fraser, 1961; Theis and Singer, 1974). Metal-organic interactions include ion exchange, surface sorption, complexation and chelation, coagulation, and peptization. Because of the complexity of natural organic matter and the possibility that more than one molecule may interact with a metal ion, identification of the specific process involved may be difficult. The discussion in this section is confined to complexation of metals by organic matter, which is essentially the same as specific adsorption to mineral surfaces that was discussed previously. The discussion is general in nature because many of the specific details of metal-organic interactions are complex, poorly understood, controversial, or all three, and a detailed discussion is beyond the scope of this presentation.

Metal-organic complexes may assume many forms. Two possible complex types are shown on Figure 10.4. The manganese-organic complex (Fig. 10.4a) is termed an outer sphere complex because the organic ligand does not interact directly with the hydrated manganese ion; the hydrated manganese ion is held within the ligand by electrostatic forces. In the inner sphere complex (Fig. 10.4b), the ligand donates electrons to the hydrated metal ion, and a covalent bond forms. The latter is a stronger interaction than the former and more strongly affects the solubility of the metal (Bloom, 1981). Hydroxyl and carboxyl functional groups on organic matter are probably the most important sites for complexation.

Formation of a metal-organic complex may result in increased or decreased mobility of the metal, depending on the solubility of the metal-organic complex. For instance, iron-humic-acid complexes are soluble if the pH ranges from 3 to 9, but precipitate at lower pH values (Elder, 1988); this behavior mimics the behavior of humic acids that are insoluble at low pH values, but soluble at

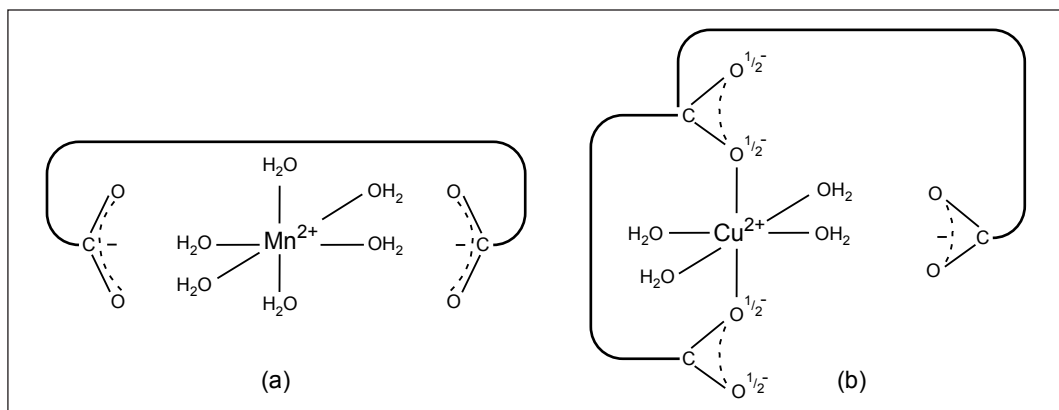


FIGURE 10.4—Generalized chemical structures of outer sphere (a) and inner sphere (b) metal-organic complexes (from Bloom, 1981; Salomons and Förstner, 1984; reprinted with permission).

greater values. In contrast, metal-fulvic-acid complexes and fulvic acids are generally more soluble over a greater pH range (Kabata-Pendias and Pendias, 1984).

The stabilities of metal-organic complexes vary. The Irving-Williams order is probably the most cited, and it indicates the stability of divalent-metal-organic complexes decreasing as follows (Irving and Williams, 1948):



Wieder (1990) reported slightly different orders of stability for metal binding to *Sphagnum* peat and sawdust. As mentioned previously in this section, the study of metal-organic interactions is evolving, and more quantitative descriptions await advances in the science.

Many case studies have cited organic binding of metals as an important metal-retention process in wetland substrates that receive AMD. Wieder and Lang (1986) reported that most of the Al and Fe retained in four natural wetlands that received metal-rich inputs were bound to organic matter in the peat. About 40% of the Al accumulating in a constructed wetland receiving highway runoff was specifically adsorbed (complexed) to organic matter (Wieder et al., 1988). Twenty-two percent of iron retained in peat microcosms that were subjected to applications of synthetic AMD was organic-bound iron (Henrot and Wieder, 1990); however, 62% of the iron was contained in iron oxides. In a case study of metal retention in the substrate of a constructed wetland, Karathanasis and Thompson (1991) reported that Cu and Al were retained by association with organic matter more than other metals. From 20–40% of the two metals were bound to organic matter and the remainder was distributed between exchangeable, adsorbed, and residual forms. However, Karathanasis and Thompson (1991) did not report absolute metal concentrations in the extractions, or pretreatment-substrate-metal concentrations, so it is difficult to evaluate how much of the extracted metal had accumulated in the substrate since the onset of treatment. Other case studies also have indicated the importance of organic-bound metals (such as, Cu, Pb, and U) in wetlands that are metal-rich from sources other than AMD (Walton-Day et al., 1990; Ton et al., 1991; Owen et al., 1992).

In these case studies, the details of the metal-organic interactions are seldom described, and evidence for their existence is based on the results of sequential chemical extraction of sediment samples. In general, the specificity of extractions for sediment phases, such as a specific mineral or organic matter, is operationally defined, often controversial, and depends on:

- 1) The dominant matrix and chemical composition of the sample (Robinson, 1984; Martin et al., 1987);
- 2) The order in which the extractions are applied (Miller et al., 1986); and
- 3) Alteration by mineral dissolution and resorption of elements under certain extraction conditions (Rendell et al., 1980).

Therefore, although evidence gained through sequential chemical extraction of sediments has indicated the phases in which metals may be present in wetlands, much of this evidence has been accumulated using operationally defined, indirect techniques.

Some case studies have attributed poor performance of wetland treatment systems to the formation of metal-organic complexes that have increased metal mobility. For instance, Lapakko

and Eger (1988) attributed limited metal removal observed at low inflow metal concentrations in batch and column experiments with peat and different mine drainage solutions to formation and leaching of dissolved-metal organic complexes. In one study where metal speciation was directly quantified, 40 and 99% of dissolved Al and Cu, respectively, were complexed with organic matter in the effluent of a constructed wetland that receives AMD (Karathanasis and Thompson, 1991). They described low and variable removal of Al in the wetland but did not report the extent of copper removal or the speciation of the metals in the wetland influent.

In summary, the formation of metal-organic complexes can retain metals in wetlands that receive AMD. However, most evidence for this process is somewhat indirect, and details have not been described. Additional research in AMD-wetland systems and in metal-organic interactions in general would remedy this situation.

Sulfate reduction and precipitation of metal sulfides

Microbially mediated reduction of sulfate affects improvement in several water quality parameters. First, sulfate reduction can increase the alkalinity and pH. Second, in the presence of reduced metal species, such as ferrous iron, the reduction of sulfate to sulfide promotes the precipitation of metal sulfide minerals that have low solubilities. This process decreases aqueous concentrations of metals and sulfate. Third, sulfate reduction promotes the formation of volatile, organic and inorganic reduced sulfur species that can diffuse to the atmosphere out of the wetland; through this process, sulfur is transferred from the water to the atmosphere. Fourth, sulfate reduction may result in the incorporation of reduced sulfur into organic sulfur species; this process decreases the concentration of sulfate and sometimes consumes protons depending on the stoichiometry of the organic sulfur compound. Transmission of water down to and through the reducing layers of the substrate must be large relative to the total amount of AMD in a system for the process to operate efficiently. Many case studies have documented the presence of sulfate-reducing bacteria in wetlands and the water-quality improvements attributed to some of these processes.

During microbially mediated sulfate reduction, facultative and obligate anaerobes oxidize organic matter using sulfate as a terminal electron acceptor. In assimilatory sulfate reduction, the microorganisms incorporate the reduced sulfur into biochemical compounds; no extracellular sulfide is produced. In dissimilatory sulfate reduction, the microorganisms use sulfate as a terminal electron acceptor and produce sulfide (Ehrlich, 1981). In the net reaction:



or



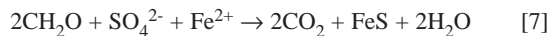
microorganisms oxidize organic matter (CH_2O) to CO_2 and water (or bicarbonate), and SO_4^{2-} is reduced to H_2S . The two reactions are equivalent except that, in reaction [5], the carbonic acid-bicar-

bonate equilibria has been included to show the generation of bicarbonate alkalinity, which is equivalent to the consumption of protons that occurs as reaction [4] proceeds to the right. At pH values less than about 4.5, sulfate reduction tends to cause an increase in pH without generating bicarbonate (reaction [4]). At greater pH values, sulfate reduction also increases bicarbonate concentrations (reaction [5]). In addition, the sulfate-reducing bacteria are reported to be inactive at pH values less than 4.2 (Trudinger, 1979); therefore, the process may have no effect until greater pH is achieved.

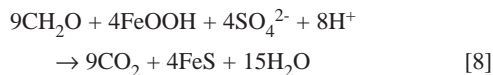
The net consumption of protons or the generation of bicarbonate alkalinity in this reaction depends on interactions of iron and other metals with sulfur in the system. If reduced iron and H₂S combine to form FeS:



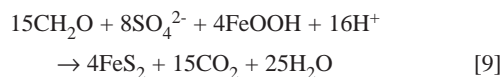
two protons are produced so that when reactions [4] and [6] are combined:



there is no net change in the proton budget. Similarly, protons are not consumed when other metals that occur as free dissolved cations [such as Zn (II)] form sulfides following sulfate reduction (Anderson and Schiff, 1987). However, if oxidized iron in iron oxyhydroxide minerals is dissolved and reduced, then in the net reactions:



and

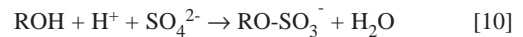


protons are consumed where either iron monosulfide or pyrite is formed. The alkalinity in the iron oxyhydroxides is transferred from the solid to the aqueous phase using reactions [8] and [9] (Anderson and Schiff, 1987). Therefore, if the reduction of a metal and the formation of its sulfide involves consumption of protons, the net result will be an increase in alkalinity and pH. However, if reduction of the metal and the formation of its sulfide does not involve consumption of protons (e.g., reaction [7]), there is no net change in alkalinity and pH.

Reaction [5] indicates that H₂S gas can form during sulfate reduction. If this gas diffuses upward through the sediments and the water column in a wetland without being reoxidized, it can escape to the atmosphere. If the gas escapes, sulfate reduction results in a consumption of hydrogen and sulfate ions, and the loss of hydrogen and sulfur from the sediment/water system into the atmosphere. The evidence that this process occurs is obvious to anyone who has walked across a sulfur-rich wetland and smelled "swamp gas" rich in reduced sulfur compounds. Also, the forma-

tion and loss of organic sulfur gases such as methyl and dimethyl sulfide possibly could contribute to loss of sulfur from mine drainage in wetlands.

Reduced organic sulfur compounds can be formed through assimilatory sulfate reduction, and during diagenesis through reactions between organic matter and H₂S (Anderson and Schiff, 1987). Reactions can be written that indicate consumption of protons during this process:



where ROH is an alcohol, and RO-SO₃⁻ is a sulfate ester. Some case studies have indicated that accumulation of organic sulfur is more important than accumulation of inorganic sulfur in natural wetlands that receive elevated sulfur loadings (e.g., Wieder and Lang, 1986). However, studies investigating the forms of sulfur in lakes and wetlands affected by AMD have shown that organic sulfur formation and accumulation is relatively unimportant compared to formation of inorganic sulfur compounds (Herlihy et al., 1988; Laudon, 1988; Wieder and Lang, 1988). With diagenesis, the fixation of sulfur in organic compounds possibly becomes more important, as evidenced by the amounts of organic sulfur in coal deposits (Davis, 1982; Casagrande, 1987).

Water-quality improvements in lakes and wetlands have been attributed to sulfate reduction and the formation of metal sulfides or both (Herlihy et al., 1987; Hedin et al., 1988; Kleinmann, 1990; McIntyre and Edenborn, 1990; Wildeman et al., 1990; Machermer and Wildeman, 1992). Sulfate reduction seems to be the only wetland process capable of removing significant quantities of some of the metals, such as dissolved Cu, Zn, and Cd, more common in metal-mine drainage than in coal-mine drainage (e.g., Wildeman et al., 1990; Machermer and Wildeman, 1992). Ninety-five percent removal of dissolved Fe, Zn, Mn, Ni, and Cd was attributed to sulfate reduction and precipitation of metal sulfides in pilot-scale bioreactors [barrels loaded with water-saturated mushroom compost (Dvorak et al., 1991)]. A failure of treatment systems dominated by sulfate reduction to remove manganese sulfide has been attributed to the higher solubility of MnS compared to other metal sulfides and to the fact that MnS requires a greater pH to precipitate in anaerobic wetlands than do other metal sulfides (Klusman, 1991). The inability of sulfate reduction to become established in some wetland systems or the reduced performance of sulfate reduction in some wetlands has been attributed to excess acidity (Kuyucak et al., 1991), metal toxicity (Kuyucak et al., 1991), lack of oxidizable organic matter (Dollhopf et al., 1988; Stark et al., 1991; Tarutis et al., 1992), and insufficient flow of water through the substrate (Hedin et al., 1989). In addition, there is some controversy about the source of alkalinity generated in these wetlands. As described previously in this section, sulfate reduction combined with the precipitation of metal sulfides has no net effect on the proton budget; therefore, alkalinity is not generated unless precipitation of sulfides is accompanied by reduction of metal oxyhydroxides. The alkalinity generated in some systems where sulfate reduction occurs may be from dissolution of CaCO₃ or other alkaline materials in the substrate (McIntyre and Edenborn, 1990; T. Wildeman, Colorado School of Mines, written commun., 1995) or from dissolution of ferric iron oxyhydroxides (Wieder, 1992; Vile and Wieder, 1993). However, Dvorak et al. (1992) demonstrated alkalinity generation in substrates where all carbonate

alkalinity was removed by acid-leaching prior to the initiation of sulfate reduction. In addition, Kalin et al. (1991) demonstrated increases in alkalinity attributed to the activity of microorganisms, including sulfate-reducing bacteria.

Only limited research has been conducted on the role of H_2S loss in improving water-quality in wetland treatment systems. Effluent from pilot-scale sulfate-reducing systems that were constructed to treat mine drainage water contained S^{2-} and H_2S (Dvorak et al., 1991). Emission of H_2S accounted for up to only 2% of sulfur accumulation in five wetlands constructed to treat AMD (Wieder, 1992). Studies of a constructed wetland indicated that about 1% of total sulfur input escaped as H_2S gas and dissolved sulfide (Machemer et al., 1993). About 17% of the escaped sulfur, or less than 0.2% of the total sulfur input, escaped as H_2S gas. Based on these case studies, loss of H_2S is not a major process contributing to loss of sulfur and acidity in wetlands that treat AMD.

In summary, sulfate reduction and the precipitation of metal sulfides may have great potential to improve water quality in wetland treatment systems. In fact, treatment designs have been moving away from vegetated wetlands toward unvegetated bioreactors (Dvorak et al., 1991; Dvorak et al., 1992) in order to optimize sulfate reduction. There are, however, some details about the precise controls and mechanisms of the process that need to be clarified. Specifically, the alkalinity controversy and the reduced performance of sulfate-reducing wetlands caused by excess acidity, metal toxicity, lack of oxidizable organic matter, and insufficient flow of water through the wetland substrate need to be resolved to allow optimal performance of wetland treatment systems.

Plant assimilation of metals

Microbially mediated sulfate reduction and the concomitant precipitation of metal sulfides are perhaps the most significant ways that wetland biota contribute to treatment of mine drainage. However, plants also contribute to the immobilization of mine drainage components by accumulating metals within their structures. The general mechanisms and controls on this process are fairly well understood. Several case studies have indicated that elevated metal concentrations are present in plants from wetlands that treat mine drainage. However, plant assimilation of metals does not significantly contribute to metal immobilization in mine drainage and may be undesirable because assimilation makes some toxic metals available to consumers farther up the food chain (Kleinmann, 1990; Kelly, 1999).

Trace elements are termed micronutrients if small amounts are essential for plant nutrition. Macronutrients, such as carbon, sulfur, and nitrogen, are those required by the plant in copious amounts. Examples of micronutrient elements that are present in mine-drainage waters are aluminum, arsenic, cadmium, cobalt, copper, iron, manganese, mercury, molybdenum, nickel, silicon, and zinc. These elements are present in: structural materials (e.g., Fe and Si); small molecules, including antibiotics and porphyrins (e.g., As, Co, Cu, Fe, Hg, Si); large molecules (e.g., Co, Cu, Fe, Mn, Mo, and Zn); large molecules having storage, transport or unknown functions (e.g., Cd, Co, Cu, Fe, Hg, Mn, Ni, and Zn); and organelles or their parts (Cu, Fe, Mn, Mo, and Zn) (Kabata-Pendias and Pendias, 1984). Together, these elements participate in many important metabolic functions such as respiration, photosynthesis, and fixation and assimilation of other essential ele-

ments. Other trace metals that are present in plants, but that have no known physiological function (nonessential trace elements), include lead and silver. Many trace elements, both micronutrient and nonessential, can be toxic to plants where large quantities of the element are present in the environment of the plants.

Trace element uptake by plants can be either passive or active. In passive, or nonmetabolic, uptake, ions of an element diffuse along a chemical gradient from the external soil solution into the root endodermis. Active, or metabolic, uptake, requires metabolic energy and can occur against a chemical gradient (Kabata-Pendias and Pendias, 1984). If metabolic absorption of an element occurs faster than its arrival by mass flow from the soil solution, a concentration gradient develops, and diffusion then assists the absorption process (Loneragan, 1975).

Chemical speciation in the soil limits element availability to plants. Therefore, parameters that affect the speciation of an element and the sorptive capacity of a soil for an element such as pH, Eh, concentrations of complexing ions, organic-matter content of the soil, and clay content and mineralogy of the soil, will in turn affect the availability of an element to a plant. Freely dissolved ions, ions complexed with some forms of dissolved organic matter, and ions held in exchange positions on the surface of clay minerals are most readily available to plants (Kabata-Pendias and Pendias, 1984).

Specific molecular-scale descriptions of trace-element uptake by vegetation are difficult to locate. Kabata-Pendias and Pendias (1984) proposed three mechanisms of trace element uptake by roots: cation exchange by the roots, transport into cells with chelating agents or other carriers, and rhizosphere effects. Excretions of mucilaginous material, organic acids, amino acids, bicarbonate, and protons by the plant may mobilize trace elements (specifically trace metals) that are fixed in the soil, thereby enabling their uptake by the plant (Loneragan, 1975). Dejaegere et al. (1981) proposed a proton pump model wherein cation uptake by plants is promoted by proton extrusion by roots. They used the model to describe the mechanisms of K^+ , NH_4^+ and Ca^{2+} absorption by plants, but the model also could be extended to account for absorption of trace cations.

Many case studies have described trace-metal accumulation by plants in natural and constructed wetlands affected by AMD. Vegetation in a constructed wetland in Colorado had as much as 1% metal content (Howard et al., 1989b). Heavy-metal removal potentials (in kilograms per hectare) have been reported for several types of submerged, emergent, and floating wetland aquatic vegetation (Chan et al., 1982). Concentration decreases of iron and manganese in water have been attributed to uptake of the metals by *Typha* (cattail) species in two wetland systems receiving mine drainage in Pennsylvania (Snyder and Aharrah, 1984). Algae and other aquatic organisms contributed to lead and zinc removal from mining and milling effluents in Missouri (Gale and Wixson, 1979). The ability of *Sphagnum* moss and other bryophytes to accumulate metals has been reported in several case studies (Kleinmann et al., 1983; Burris et al., 1984; Lee et al., 1984; Kelly, 1999). In addition, the U.S. Bureau of Mines developed a product manufactured from *Sphagnum* for use in metal-mine drainage treatment (Bennett et al., 1991).

In most wetlands, the absolute amount of metals removed by the plants is insignificant compared to the amounts accumulating in the substrate. In constructed wetlands in Colorado, plants accumulate metal concentrations of as much as 1%, but the amounts are insignificant compared to metal removal occurring in the sub-

strate (Howard et al., 1989b). Uptake of iron by *Typha* accounted for less than 1% of the iron that was being removed from mine drainage by some natural West Virginia wetlands (Sencindiver and Bhumbala, 1988). However, researchers have hypothesized that the cattails help support the ecological system which functions to remove iron in the substrate (Sencindiver and Bhumbala, 1988; Samuel et al., 1988). Iron uptake by *Sphagnum* was minor in comparison to the binding of iron to organic matter and the formation of iron oxides that together can account for as much as 97% of iron retention in natural and constructed wetlands (Spratt and Wieder, 1988; Wieder, 1988).

The translocation of metals from soils to plants makes the metals available for ingestion by many higher organisms that graze or feed in the wetlands and, thus may be undesirable because the metals then move up the food chain and may cause toxicity problems in higher organisms. In addition, despite the ability of plants to accumulate metals, this process is usually insignificant compared to other accumulation mechanisms occurring in wetlands and may be undesirable from an ecological standpoint.

CONSTRUCTED WETLAND DESIGN

Although natural wetlands have been used to treat AMD either by chance or on purpose, constructed wetlands are becoming the preferred medium for AMD treatment because of the legal problems associated with using natural wetlands, the lack of natural wetlands at sites where treatment is needed, and the need to control and optimize hydraulic and chemical parameters in the treatment system. In addition, ecosystems have been destroyed or severely injured where AMD was introduced into natural wetlands (e.g., Wheeler et al., 1991). The brief discussion of constructed wetland design in this section is intended as a minimal introduction to the topic. The interested reader is referred to the references cited for more detailed information.

A basic design scheme for a constructed wetland includes an excavated or constructed, sealed, shallow pond that

- 1) Is filled with organic substrate (e.g., peat, manure, mushroom compost);
- 2) Supports natural wetland vegetation; and
- 3) Contains discrete, controlled inflow and outflow locations.

Several references describe some of the design criteria including sizing, choices of substrate and vegetation, and optimal pH, flow rates, and mineral loadings (Kleinmann et al., 1986; Howard et al., 1989a; Cohen and Staub, 1992).

Two basic constructed wetland designs have evolved to maximize the aerobic and anaerobic aspects of wetland geochemistry. In aerobic constructed wetlands, water flow is dominantly over the surface of the wetland substrate to maximize oxidation of the water column, and to take advantage of the geochemical processes that occur in the oxidized portions of wetlands. This design requires that sufficient alkalinity be added to the water or substrate to prevent pH from falling due to the precipitation of iron oxyhydroxide minerals. Aerobic constructed wetlands are most often used in coal mine drainage where concentrations of metals other than iron are low. Anaerobic constructed wetlands must be engineered to maximize water flow through the subsurface where anoxic conditions prevail. Typically, these wetlands are designed so that water flows vertically through the substrate. In these wetlands, sulfate reduction is used to precipitate metals as sulfide minerals. Anaerobic constructed wetlands are used to help remove

heavy metals such as zinc and copper that are not efficiently removed in aerobic wetlands (Filipek et al., 1991). Constructed wetland design continues to evolve as the understanding of the dominant processes in wetland treatment systems evolves.

SUMMARY

The processes that occur in wetlands that can improve water quality of AMD with respect to trace metal and sulfate concentrations and pH include: sedimentation of particulate material, oxidation and precipitation of iron and manganese oxyhydroxides and oxides, complexation with organic matter, ion exchange and adsorption, sulfate reduction and formation of metal sulfides, and plant assimilation of metals. The most significant contributors to water-quality improvement are formation of iron hydroxides and metal sulfides. Sulfate reduction is particularly significant because it is the only process to date that is capable of removing significant quantities of trace metals common to metal-mine drainage. Other processes contribute to metal removal but are limited by surface area in the substrate (e.g., ion exchange and adsorption), and by biomass and uptake capacity of biomass (e.g., plant assimilation). In addition, the ability of a given wetland to remove metals by oxide or sulfide formation may be limited by hydrologic and geochemical characteristics of the wetland. For instance, limited residence time in the wetland, insufficient substrate permeability, low pH, or lack of organic material may limit the effectiveness of sulfate reduction. Therefore, the ability of wetlands to treat mine drainage varies between each site. Research continues to define optimal design characteristics for wetland treatment systems; however, some implementation continues on a pilot scale despite the limitations.

REFERENCES

- Anderson, R.F., and Schiff, S.L., 1987, Alkalinity generation and the fate of sulfur in lake sediments: Canadian Journal of Fisheries and Aquatic Sciences, v. 44, supplement no. 1, pp. 188–193.
- Batal, W., Laudon, L.S., Wildeman, T.R., and Mohndnoordin, Noorhanita, 1989, Bacteriological tests from the constructed wetland of the Big Five Tunnel, Idaho Springs, Colorado; in Hammer, D.A. (ed.), Constructed Wetlands for Wastewater Treatment—Municipal, Industrial, and Agricultural: Lewis Publishers, Chelsea, Mich., pp. 550–557.
- Bennett, P.G., Ferguson, C.R., and Jeffers, T.H., 1991, Biological treatment of acid mine waters—case studies: Proceedings, 2nd Internatl Conference on the Abatement of Acidic Drainage, Montreal, 16–18 Sept. 1991, v. 1, pp. 283–299.
- Bigham, J.M., 1994, Mineralogy of ochre deposits formed by sulfide oxidation; in Jambor, J.L., and Blowes, D.W. (eds.), Short Course Handbook on Environmental Geochemistry of Sulfide Mine-Wastes, Waterloo, Ontario, Canada, May 1994: Mineralogical Association of Canada, v. 22, p. 101–132.
- Bigham, J.M., Schwertmann, U., Carlson, L., and Murad, E., 1990, A poorly crystallized oxyhydroxysulfate of iron formed by bacterial oxidation of Fe(II) in acid mine waters: Geochimica et Cosmochimica Acta, v. 54, no. 10, pp. 2743–2758.
- Bigham, J.M., Schwertmann, U., and Carlson, L., 1992, Mineralogy of precipitates formed by the biogeochemical oxidation of Fe(II) in mine drainage; in Skinner, H.C.W., and Fitzpatrick, R.W. (eds.), Biomineralization Processes of Iron and Manganese—Modern and Ancient Environments: Catena Verlag, Cremlingen-Destedt Germany, pp. 219–232.

- Bloom, P.R., 1981, Metal-organic interactions in soil; *in* Chemistry of the soil environment: Soil Science Society of America, Spec. Pub., v. 40, American Society of Agronomy, Madison, Wis., pp. 129–150.
- Boto, K.G., and Patrick, W.H., Jr., 1978, Role of wetlands in the removal of suspended sediments; *in* Greeson, P.E., Clark, J.R., and Clark, J.E. (eds.), Wetlands Functions and Values—The State of Our Understanding: American Water Resources Association, Minneapolis, Minn., pp. 479–489.
- Brodie, G.A., 1990, Constructed wetlands for treating acid drainage at Tennessee Valley Authority coal facilities; *in* Cooper, P.F., and Findlater, B.C. (eds.), Constructed Wetlands in Water Pollution Control, Proceedings of the Internatl Conference on the Use of Constructed Wetlands in Water Pollution Control, Cambridge, U.K., Sept. 24–28, 1990: Pergamon Press, Oxford, England, pp. 461–470.
- Burris, J.E., Gerber, D.W., and McHerron, L.E., 1984, Removal of iron and manganese from water by *Sphagnum* moss; *in* Burris, J.E. (ed.), Treatment of Mine Drainage by Wetlands: The Pennsylvania State Univ., Department of Biology, Contribution 264, pp. 1–13.
- Casagrande, D.J., 1987, Sulfur in peat and coal; *in* Scott, A.C. (ed.), Coal and Coal-bearing—Recent Advances, Keynote addresses and invited papers to a conference held at Royal Holloway and Bedford New College, Univ. of London, April 8–10, 1986: Blackwell Scientific Publications, Oxford, England, pp. 87–105.
- Chan, E., Bursztynsky, T.A., Hantzschke, N., and Litwin, Y.T., 1982, The use of wetlands for water pollution control: U.S. Environmental Protection Agency, Report EPA-600/2-82-086, 276 pp.
- Cohen, R.H., and Staub, M.W., 1992, Technical manual for the design and operation of a passive mine drainage treatment system, Report prepared for the U.S. Bureau of Reclamation: Colorado School of Mines, Department of Environmental Science and Engineering, Golden, Colo., 69 pp.
- Collins, J.F., and Buol, S.W., 1970, Effects of fluctuations in the Eh-pH environment on iron and/or manganese equilibria: Soil Science, v. 110, no. 2, pp. 111–118.
- Cowardin, L.M., Carter, V., Golet, F.C., and LaRoe, E.T., 1979, Classification of wetlands and deepwater habitats of the United States: U.S. Fish and Wildlife Service Report FWS/OBS-79/31, 103 pp.
- Davis, A., 1982, Sulfur in coal: Earth and Mineral Sciences Letters, v. 51, no. 2, pp. 1–18.
- Davis, J.A., and Kent, D.B., 1990, Surface complexation modeling in aqueous geochemistry; *in* Hochella, M.F., and White, A.F. (eds.), Reviews in Mineralogy: Mineralogical Society of America, Washington, D.C., v. 23, pp. 177–260.
- Dejaegere, R., Neirinckx, L., Stassart, J.M., and Deleger, V., 1981, Mechanism of ion uptake across barley roots: Plant and Soil, v. 63, no. 1, pp. 19–24.
- Dollhopf, D.J., Goering, J.D., Rennick, R.B., Morton, R.B., Gauger, W.K., Guckert, J.B., Jones, P.M., Cooksey, K.C., Bucklin, K.E., Weed, R., and Lehman, M.M., 1988, Hydrochemical, vegetational, and microbiological effects of a natural and a constructed wetland on the control of acid mine drainage: Montana State Univ., Bozeman, Reclamation Research Pub. 88-04, 214 pp.
- Drever, J.I., 1988, The geochemistry of natural waters: Prentice-Hall, Englewood Cliffs, N.J., 437 pp.
- Dvorak, D.H., Hedin, R.S., Edenborn, H.M., and Gustafson, S.L., 1991, Treatment of metal-contaminated water using bacterial sulphate reduction—results from pilot-scale reactors: Proceedings, 2nd Internatl Conference on the Abatement of Acidic Drainage, Montreal, Sept. 16–18, 1991, v. 1, pp. 301–314.
- Dvorak, D.H., Hedin, R.S., Edenborn, H.M., and McIntyre, P.E., 1992, Treatment of metal-contaminated water using bacterial sulfate reduction—results from pilot-scale bioreactors: Biotechnology and Bioengineering, v. 40, no. 5, pp. 609–616.
- Ehrlich, H.L., 1981, Geomicrobiology: Marcel Dekker Inc., New York, 393 pp.
- Elder, J.F., 1988, Metal biogeochemistry in surface-water systems—a review of principles and concepts: U.S. Geological Survey Circular 1013, 43 pp.
- Evans, L.J., 1989, Chemistry of metal retention by soils: Environmental Science and Technology, v. 23, no. 9, pp. 1046–1056.
- Faulkner, S.P., and Richardson, C.J., 1989, Physical and chemical characteristics of freshwater wetland soils; *in* Hammer, D.A. (ed.), Constructed Wetlands for Wastewater Treatment—Municipal, Industrial, and Agricultural: Lewis Publishers, Chelsea, Mich., pp. 41–72.
- Faulkner, S.P., and Richardson, C.J., 1990, Iron and manganese fractionation in constructed wetlands receiving acid mine drainage; *in* Cooper, P.F., and Findlater, B.C. (eds.), Constructed Wetlands in Water Pollution Control, Proceedings of the Internatl Conference on the Use of Constructed Wetlands in Water Pollution Control, Cambridge, U.K., Sept. 24–28, 1990: Pergamon Press, Oxford, England, pp. 441–450.
- Fennessey M.S., and Mitsch, W.J., 1989, Design and use of wetlands for renovation of drainage from coal mines; *in* Mitsch, W.J., and Jorgensen, S.E. (eds.), Ecological Engineering, An Introduction to Ecotechnology: John Wiley and Sons, New York, pp. 231–253.
- Ficklin, W.H., Plumlee, G.S., Smith, K.S., and McHugh, J.B., 1992, Geochemical classification of mine drainages and natural drainages in mineralized areas; *in* Kharaka, Y.F., and Maest, A.F. (eds.), Water-Rock Interaction, Proceedings of the 7th Internatl Symposium on Water-Rock Interaction, WRI-7, Park City, Utah, U.S.A., 13–18 July 1992: A.A. Balkema, Rotterdam, pp. 381–384.
- Filipek, L.H., Gusek, J.J., Gormley, J.T., and Wildeman, T.R., 1991, Increasing the lifetime of constructed wetlands to control acid rock drainage [abs.]: Annual Conf. of Rocky Mountain Environmental Professionals, Vail, Colo., May 29–30.
- Fraser, D.C., 1961, Organic sequestration of copper: Economic Geology, v. 56, no. 6, pp. 1063–1078.
- Gale, N.L., and Wixson, B.G., 1979, Removal of heavy metals from industrial effluents by algae: Developments in Industrial Microbiology, v. 20, pp. 259–273.
- Gambrell, R.P., and Patrick, W.H., Jr., 1978, Chemical and microbial properties of anaerobic soils and sediments; *in* Hook, D.D., and Crawford, R.M.M. (eds.), Plant Life in Anaerobic Environments: Ann Arbor Science, Ann Arbor, Mich., pp. 375–423.
- Gerber, D.W., Burris, J.E., and Stone, R.W., 1985, Removal of dissolved iron and manganese ions by a *Sphagnum* moss system; *in* Brooks, R.P., Samuel, D.E., and Hill, J.B. (eds.), Wetlands and Water Management on Mined Lands, Proceedings of a conference, Oct. 23–24, 1985: Pennsylvania State Univ., University Park, School of Forest Resources, pp. 365–372.
- Girts, M.A., and Kleinmann, R.L.P., 1986, Constructed wetlands for treatment of acid mine drainage—a preliminary review: 1986 National Symposium on Mining, Hydrology, Sedimentology, and Reclamation, Univ. of Kentucky, Lexington, Dec. 8–11, 1986, pp. 165–171.
- Grappelli, A., Campanella, L., Cardarelli, E., Mazzei, F., Cordatore, M., and Peitrosanti, W., 1992, Metals removal and recovery by *Arthrobacter* sp. biomass: Water Science and Technology, v. 26, no. 9–11, pp. 2149–2152.
- Greenwood, D.J., 1961, The effect of oxygen concentration on the decomposition of organic materials in soil: Plant and Soil, v. 14, no. 4, pp. 360–376.
- Hammer, D.A., and Bastian, R.K., 1989, Wetlands ecosystems—natural water purifiers?; *in* Hammer, D.A. (ed.), Constructed Wetlands for Wastewater Treatment—Municipal, Industrial, and Agricultural: Lewis Publishers, Chelsea, Mich., pp. 5–19.
- Hedin, R.S., and Nairn, R.W., 1990, Sizing and performance of constructed wetlands—case studies; *in* Skousen, J., Sencindiver, J., and Samuel, D. (eds.), Proceedings of the 1990 Mining and Reclamation Conference and Exhibition, v. 2: West Virginia University Services, Morgantown, W.Va., pp. 385–392.
- Hedin, R.S., Hyman, D.M., and Hammack, R.W., 1988, Implications of sulfate-reduction and pyrite formation processes for water quality in a constructed wetland—preliminary observations; *in* Mine Drainage and Surface Mine Reclamation, Proceedings of a conference, Pittsburgh, Pa., April 19–21, 1988, v. 1, Mine Water and Mine Waste: U.S. Bureau of Mines Information Circular 9183, pp. 382–388.

- Hedin, R.S., Hammack, R., and Hyman, D., 1989, Potential importance of sulfate reduction processes in wetlands constructed to treat mine drainage; *in* Hammer, D.A. (ed.), *Constructed Wetlands for Wastewater Treatment—Municipal, Industrial, and Agricultural*: Lewis Publishers, Chelsea, Mich., pp. 508–514.
- Henrot, J., and Wieder, R.K., 1990, Processes of iron and manganese retention in laboratory peat microcosms subjected to acid mine drainage: *Journal of Environmental Quality*, v. 19, no. 2, pp. 312–320.
- Henrot, J., Wieder, R.K., Heston, K.P., and Nardi, M.P., 1989, Wetland treatment of coal mine drainage—controlled studies of iron retention in model wetland systems; *in* Hammer, D.A. (ed.), *Constructed Wetlands for Wastewater Treatment—Municipal, Industrial, and Agricultural*: Lewis Publishers, Chelsea, Mich., pp. 793–800.
- Herlihy, A.T., Mills, A.L., Hornberger, G.M., and Bruckner, A.E., 1987, Importance of sediment sulfate reduction to the sulfate budget of an impoundment receiving acid mine drainage: *Water Resources Research*, v. 23, no. 2, pp. 287–292.
- Herlihy, A.T., Mills, A.L., and Herman, J.S., 1988, Distribution of reduced inorganic sulfur compounds in lake sediments receiving acid mine drainage: *Applied Geochemistry*, v. 3, no. 3, pp. 333–344.
- Howard, E.A., Emerick, J.C., and Wildeman, T.R., 1989a, Design and construction research for passive mine drainage treatment in Idaho Springs, Colorado; *in* Hammer, D.A. (ed.), *Constructed Wetlands for Wastewater Treatment—Municipal, Industrial, and Agricultural*: Lewis Publishers, Chelsea, Mich., pp. 761–764.
- Howard, E.A., Wildeman, T.R., Laudon, L.S., and Macherer, S.D., 1989b, Design considerations for the passive treatment of acid mine drainage; reclamation, a global perspective; *in* Proceedings of the conference: Alberta Land Conservation and Reclamation Council Report RRTAC89–2, Calgary, Alberta, v. 2, pp. 651–660.
- Irving, H. and Williams, R.J.P., 1948, Order of stability of metal complexes: *Nature*, v. 162, no. 4123, pp. 746–747.
- Kabata-Pendias, A., and Pendias, H., 1984, Trace elements in soils and plants: CRC Press Inc., Boca Raton, Fla., 315 pp.
- Kalin, M., Cairns, J., and McCready, R., 1991, Ecological engineering methods for acid mine drainage treatment of coal wastes: *Resources, Conservation, and Recycling*, v. 5, no. 2–3, pp. 265–275.
- Karathanasis, A.D., and Thompson, Y.L., 1991, Metal speciation and retention patterns in a high metal load acid mine constructed wetland of southeastern Kentucky, Proceedings, 2nd Internatl Conference on the Abatement of Acidic Drainage: Montreal, Sept. 16–18, 1991, v. 2, pp. 485–498.
- Kelly, M.G., 1999, Effects of heavy metals on the aquatic biota; *in* Plumlee, G.S., and Logsdon, M.J. (eds.), *The Environmental Geochemistry of Mineral Deposits, Part A. Processes, Techniques, and Health Issues*: Society of Economic Geologists, Reviews in Economic Geology, v. 6A, pp. 363–371.
- Kleinmann, R.L.P., 1990, Biological treatment of acid mine water using constructed wetlands, Proceedings, 7th U.S.-Korea Joint Workshop of Coal Utilization Technology: Pittsburgh, Pa., PETC-KIER, pp. 251–258.
- Kleinmann, R.L.P., Tiernan, T.O., Solch, J.C., and Harris, R.L., 1983, A low-cost, low-maintenance treatment system for acid mine drainage using *Sphagnum* moss and limestone, Proceedings, 1983 Symposium on Surface Mining, Hydrology, Sedimentology, and Reclamation: Univ. of Kentucky, Lexington, Pub. BU-133, pp. 241–245.
- Kleinmann, R.L.P., Brooks, R., Huntsman, B., and Pesavento, B., 1986, Constructing wetlands for the treatment of mine water: Course notes, U.S. Bureau of Mines paper 12–1986, 25 pp. plus 14 figures.
- Klusman, R.W., 1991, Computer modeling of biogeochemical processes operating in a constructed wetland, Proceedings, 2nd Internatl Conference on the Abatement of Acidic Drainage: Montreal, Canada, Sept. 16–18, 1991, v. 2, pp. 235–255.
- Klusman, R.W., and Macherer, S.D., 1991, Review of processes operating in constructed wetlands to attenuate acid mine drainage; *in* Peters, D.C. (ed.), *Geology in Coal Resource Utilization*: Techbooks, Fairfax, Va., pp. 513–540.
- Kusler, J., 1992, Wetlands delineation—an issue of science or politics?: *Environment*, v. 34, no. 2, pp. 6–37. [The article is not continuous over these pages.]
- Kuyucak, N., Lyew, D., St-Germain, P., and Wheeland, K.G., 1991, In situ bacterial treatment of AMD in open pits: Proceedings, 2nd Internatl Conference on the Abatement of Acidic Drainage, Montreal, Canada, Sept. 16–18, 1991, v. 1, pp. 335–353.
- Lapakko, Kim, and Eger, Paul, 1988, Trace metal removal from stockpile drainage by peat; *in* Mine Drainage and Surface Mine Reclamation, Proceedings of a conference in Pittsburgh, Pa., April 19–21, 1988, v. 1, Mine Water and Mine Waste: U.S. Bureau of Mines Information Circular 9183, pp. 291–300.
- Laudon, L.S., 1988, Sulfur mineralization in a wetland constructed to treat acid mine drainage: Unpub. M.S. thesis, Colorado School of Mines, Golden, Colo., 58 pp.
- Leckie, J.O., and James, R.O., 1974, Control mechanisms for trace metals in natural waters; *in* Rubin, A.J. (ed.), *Aqueous-Environmental Chemistry of Metals*: Ann Arbor Science Publishers, Ann Arbor, Mich., pp. 1–76.
- Lee, J., Jonasson, I.R., and Goodfellow, W.D., 1984, Metal accumulation by bryophytes in some zinc-rich blanket bogs, Selwyn Mountains, Yukon Territory: *Canadian Journal of Botany*, v. 62, no. 4, pp. 722–728.
- Loneragan, J.F., 1975, The availability and absorption of trace-elements in soil-plant systems and their relation to movement and concentrations of trace elements in plants; *in* Nichols, D.J.D., and Egan, A.R. (eds.), *Trace Elements in Soil, Plant, and Animal Systems*: Academic Press Inc., New York, pp. 109–134.
- Macherer, S.D., and Wildeman, T.R., 1992, Adsorption compared with sulfide precipitation as metal removal processes from acid mine drainage in a constructed wetland: *Journal of Contaminant Hydrology*, v. 9, no. 1/2, pp. 115–131.
- Macherer, S.D., Reynolds, J.S., Laudon, L.S., and Wildeman, T.R., 1993, Balance of S in a constructed wetland built to treat acid mine drainage, Idaho Springs, Colorado, U.S.A.: *Applied Geochemistry*, v. 8, no. 6, pp. 587–603.
- Martin, J.M., Nirel, P., and Thomas, A.J., 1987, Sequential extraction techniques—promises and problems: *Marine Chemistry*, v. 22, no. 2–4, pp. 313–341.
- McIntyre, P.E., and Edenborn, H.M., 1990, The use of bacterial sulfate reduction in the treatment of drainage from coal mines; *in* Skousen, J., Sencindiver, J., and Samuel, D. (eds.), Proceedings of the 1990 Mining and Reclamation Conference and Exhibition, v. 2: West Virginia University Services, Morgantown, W. Va., pp. 409–415.
- McKnight, D.M., Kimball, B.A., and Bencala, K.E., 1988, Iron photoreduction and oxidation in an acidic mountain stream: *Science*, v. 240, no. 4852, pp. 637–640.
- Miller, W.P., Martens, D.C., and Zelazny, L.W., 1986, Effect of sequence in extraction of trace metals from soils: *Soil Science Society of America Journal*, v. 50, no. 3, pp. 598–601.
- Mills, A.L., 1999, The role of bacteria in environmental geochemistry; *in* Plumlee, G.S., and Logsdon, M.J. (eds.), *The Environmental Geochemistry of Mineral Deposits, Part A. Processes, Techniques, and Health Issues*: Society of Economic Geologists, Reviews in Economic Geology, v. 6A, pp. 125–132.
- Mitsch, W.J., and Gosselink, J.G., 1986, *Wetlands*: Van Nostrand Reinhold, New York, 539 pp.
- Murad, E., Schwertmann, U., Bigham, J.M., and Carlson, L., 1994, Mineralogical characteristics of poorly crystallized precipitates formed by oxidation of Fe²⁺ in acid sulfate waters; *in* Alpers, C.N., and Blowes, D.W. (eds.), *Environmental Geochemistry of Sulfide Oxidation*: American Chemical Society, Washington, D.C., ACS Symposium Series 550, pp. 190–200.
- Nordstrom, D.K., and Alpers, C.N., 1999, Geochemistry of acid mine waters; *in* Plumlee, G.S., and Logsdon, M.J. (eds.), *The Environmental Geochemistry of Mineral Deposits, Part A. Processes, Techniques, and Health Issues*: Society of Economic Geologists, Reviews in Economic Geology, v. 6A, pp. 133–160.
- Owen, D.E., Otton, J.K., Hills, F.A., and Schumann, R.F., 1992, Uranium

- and other elements in Colorado Rocky Mountain wetlands—a reconnaissance study: U.S. Geological Survey Bulletin 1992, 33 pp. plus 1 plate.
- Plumlee, G.S., Smith, K.S., Ficklin, W.H., Briggs, P.H., and McHugh, J.B., 1993, Empirical studies of diverse mine drainages in Colorado—implications for the prediction of mine drainage chemistry; *in* Proceedings from the 6th Billings Symposium, Planning, Rehabilitation, and Treatment of Disturbed Lands, March 21–27, 1993: Montana State Univ., Bozeman, Reclamation Research Unit Pub. 93-01, pp. 176–186.
- Plumlee, G.S., Smith, K.S., Montour, M.R., Ficklin, W.H., and Mosier, E.L., 1999, Geologic controls on the composition of natural waters and mine waters draining diverse mineral-deposit types; *in* Filipek, L.H., and Plumlee, G.S. (eds.), The Environmental Geochemistry of Mineral Deposits, Part B. Case Studies and Research Topics: Society of Economic Geologists, Reviews in Economic Geology, v. 6B, pp. 373–432.
- Ponnamperuma, F.M., 1972, The chemistry of submerged soils; *in* Brady, N.C. (ed.), Advances in Agronomy, v. 24: Academic Press, New York, pp. 29–96.
- Pradhan, A.A., and Levine, A.D., 1992, Role of extracellular components in microbial biosorption of copper and lead: Water Science and Technology, v. 26, no. 9–11, pp. 2153–2156.
- Rendell, P.S., Batley, G.E., and Cameron, A.J., 1980, Adsorption as a control of metal concentrations in sediment extracts: Environmental Science and Technology, v. 14, no. 3, pp. 314–318.
- Robinson, G.E., 1984, Sequential chemical extractions and metal partitioning in hydrous Mn-Fe oxide coatings—reagent choice and substrate composition affect results: Chemical Geology, v. 47, no. 1/2, pp. 97–112.
- Salomon, W., and Förstner, U., 1984, Metals in the hydrocycle: Springer-Verlag, Berlin, 349 pp.
- Samuel, D.E., Sencindiver, J.C., and Rauch, H.W., 1988, Water and soil parameters affecting growth of cattails—pilot studies in West Virginia mines; *in* Mine Drainage and Surface Mine Reclamation, Proceedings of a conference in Pittsburgh, Pa., April 19–21, 1988, v. 1, Mine Water and Mine Waste: U.S. Bureau of Mines Information Circular 9183, pp. 367–374.
- Sencindiver, J.C., and Bhumbla, D.K., 1988, Effects of cattails (*Typha*) on metal removal from mine drainage; *in* Mine Drainage and Surface Mine Reclamation, Proceedings of a conference in Pittsburgh, Pa., April 19–21, 1988, v. 1, Mine Water and Mine Waste: U.S. Bureau of Mines Information Circular 9183, pp. 359–366.
- Shotyk, W., 1988, Review of the inorganic geochemistry of peats and peatland waters: Earth Science Reviews, v. 25, no. 2, pp. 95–176.
- Sikora, L.J., and Keeney, D.R., 1983, Further aspects of soil chemistry under anaerobic conditions; *in* Gore, A.J.P. (ed.), Mires—Swamp, Bog, Fen, and Moor; Ecosystems of the World 4A: Elsevier Scientific Publishing Company, Amsterdam, pp. 247–256.
- Smith, K.S., 1999, Metal sorption on mineral surfaces—An overview with examples relating to mineral deposits; *in* Plumlee, G.S., and Logsdon, M.J. (eds.), The Environmental Geochemistry of Mineral Deposits, Part A. Processes, Techniques, and Health Issues: Society of Economic Geologists, Reviews in Economic Geology, v. 6A, pp. 161–182.
- Smith, K.S., Plumlee, G.S., and Ficklin, W.H., 1994, Predicting water contamination from metal mines and mining wastes: U. S. Geological Survey Open-File Report 94–264, 112 pp.
- Snyder C.D., and Aharrah, E.C., 1984, The influence of the *Typha* community on mine drainage; *in* Graves, D.H. (ed.), Proceedings, 1984 Symposium on Surface Mining, Hydrology, Sedimentology, and Reclamation: Univ. of Kentucky, Lexington, Pub. BU-136, pp. 149–153.
- Spratt, A.K., and Wieder, R.K., 1988, Growth responses and iron uptake in *Sphagnum* plants and their relation to acid mine drainage treatment; *in* Mine Drainage and Surface Mine Reclamation, Proceedings of a conference in Pittsburgh, Pa., April 19–21, 1988, v. 1, Mine Water and Mine Waste: U.S. Bureau of Mines Information Circular 9183, pp. 279–285.
- Stanier, R.Y., Ingraham, J.L., Wheelis, M.L., and Painter, P.R., 1986, The microbial world: Prentice-Hall, Englewood Cliffs, N.J., 689 pp.
- Stark, L.R., Wenerick, W.R., Wuest, P.J., Williams, F.M., and Stevens, S.E., Jr., 1991, Adding a carbon supplement to simulated treatment wetlands improves mine water quality: Proceedings, 2nd International Conference on the Abatement of Acidic Drainage, Montreal, Sept. 16–18, 1991, v. 2, pp. 465–483.
- Stumm, W., and Morgan, J.J., 1981, Aquatic chemistry—an introduction emphasizing chemical equilibria in natural waters: John Wiley and Sons, New York, 780 pp.
- Tarutis, W.J., Jr., Unz, R.F., and Brooks, R.P., 1992, Behavior of sedimentary Fe and Mn in a natural wetland receiving acidic mine drainage, Pennsylvania, U.S.A.: Applied Geochemistry, v. 7, no. 1, pp. 77–85.
- Theis, T.L., and Singer, P.C., 1974, Complexation of iron (II) by organic matter and its effect on iron (II) oxygenation: Environmental Science and Technology, v. 8, no. 6, pp. 569–573.
- Tipping, E., Griffith, J.R., and Hilton, J., 1983, The effect of adsorbed humic substances on the uptake of copper (II) by goethite: Croatica Chimica Acta, v. 56, no. 4, pp. 613–621.
- Ton, S., Delfino, J.J., and Odum, H.T., 1991, Natural wetland retention of lead from a hazardous waste site: American Chemical Society, Preprints of papers presented at the 201st National Meeting, Atlanta, Ga., April 14–19, 1991, v. 31, no. 1, pp. 94–96.
- Trudinger, P.A., 1979, The biological sulfur cycle; *in* Trudinger, P.A., and Swaine, D.J. (eds.), Biogeochemical Cycling of Mineral-Forming Elements: Elsevier Scientific Publishing Co., Amsterdam, pp. 293–313.
- Vile, M.A., and Wieder, R.K., 1993, Alkalinity generation by Fe(III) reduction versus sulfate reduction in wetlands constructed for acid mine drainage treatment: Water, Air, and Soil Pollution, v. 69, pp. 425–441.
- Walton-Day, K., 1991, Hydrology and geochemistry of a natural wetland impacted by acid mine drainage: Unpub. Ph.D. dissertation #T-4033, Colorado School of Mines, Golden, Colo., 299 pp.
- Walton-Day, K., 1996, Iron and zinc budgets in surface water for a natural wetland affected by acidic mine drainage, St. Kevin Gulch, Lake County, Colorado, *in* Morganwalp, D.W., and Aronson, D.A. (eds.), U.S. Geological Survey Toxic Substances Hydrology Program, Proceedings of the Technical Meeting, Colorado Springs, Colo., Sept. 20–24, 1993: U.S. Geological Survey Water-Resources Investigations Report 94–4015, v. 2, pp. 759–764.
- Walton-Day, K., Filipek, L.H., and Papp, C.S.E., 1990, Mechanisms controlling Cu, Fe, Mn, and Co profiles in peat of the Filson Creek fen, northeastern Minnesota: Geochimica et Cosmochimica Acta, v. 54, no. 11, pp. 2933–2946.
- Wheeler, W.N., Kalin, M., and Cairns, J.E., 1991, The ecological response of a bog to acidic coal mine drainage—deterioration and subsequent initiation of recovery: Proceedings, 2nd International Conference on the Abatement of Acidic Drainage, Montreal, Canada, Sept. 16–18, 1991, v. 2, pp. 449–464.
- Wieder, R.K., 1988, Determining the capacity for metal retention in man-made wetlands constructed for treatment of coal mine drainage; *in* Mine Drainage and Surface Mine Reclamation, Proceedings of a conference in Pittsburgh, Pa., April 19–21, 1988, v. 1, Mine Water and Mine Waste: U.S. Bureau of Mines Information Circular 9183, pp. 375–381.
- Wieder, R.K., 1989, A survey of constructed wetlands for coal mine drainage treatment in the eastern United States: Wetlands, v. 9, no. 2., pp. 299–315.
- Wieder, R.K., 1990, Metal cation binding to *Sphagnum* peat and sawdust—relation to wetland treatment of metal-polluted waters: Water, Air, and Soil Pollution, v. 53, no. 3/4, pp. 391–400.
- Wieder, R.K., 1992, The Kentucky wetlands project—a field study to evaluate man-made wetlands for acid coal mine drainage treatment, Final report, Cooperative agreement GR-896422 between the U.S. Office of Surface Mining, Reclamation and Enforcement and Villanova University: Villanova Univ., Villanova, Pa., 102 pp.
- Wieder R.K., and Lang, G.E., 1986, Fe, Al, Mn, and S chemistry of

- Sphagnum* peat in four peatlands with different metal and sulfur input: *Water, Air, and Soil Pollution*, v. 29, no. 3, pp. 309–320.
- Wieder, R.K., and Lang, G.E., 1988, Cycling of inorganic and organic sulfur in peat from Big Run Bog, West Virginia: *Biogeochemistry*, v. 5, no. 2, pp. 221–242.
- Wieder, R.K., Heston, K.P., O'Hara, E.M., Lang, G.E., Whitehouse, A.E., and Hett, J., 1988, Aluminum retention in a man-made *Sphagnum* wetland: *Water, Air, and Soil Pollution*, v. 37, no. 1/2, pp. 177–191.
- Wieder, R.K., Linton, M.N., and Heston, K.P., 1990, Laboratory meso-cosm studies of Fe, Al, Mn, Ca, and Mg dynamics in wetlands exposed to synthetic acid coal mine drainage: *Water, Air, and Soil Pollution*, v. 51, no. 1/2, pp. 181–196.
- Wildeman, T.R., Macherer, S.D., Klusman, R.W., Cohen, R.H., and Lemke, P., 1990, Metal removal efficiencies from acid mine drainage in the big five constructed wetlands; *in* Skousen, J., Sencindiver, J., and Samuel, D. (eds.), *Proceedings of the 1990 Mining and Reclamation Conference and Exhibition*, v. 2: West Virginia University Services, Morgantown, W.Va., pp. 417–424.

Chapter 11

THE ENVIRONMENTAL GEOCHEMISTRY OF CYANIDE

A.C.S. Smith¹ and T.I. Mudder²

¹*Deceased*

²*TIMES Limited, 1568 Cobb Hill Road, Bozeman, MT 59718*

“His ways precedeth his coming. We speaketh his name in fear and trembling (Anon, circa 451 AD).” Obscure perhaps, but these words of the Roman centurion about his foe Attila the Hun, immediately prior to the defeat of Attila at the Battle of Chalons-sur-Marne in 451 AD, reflect a similar perception within the community of the nature of cyanide. The status of cyanide as a social and environmental pariah is not founded in the technical literature but is emotionally driven, consequent perhaps from the historic use of cyanide by the agencies of law enforcement in the United States and in other jurisdictions to carry out capital punishment.

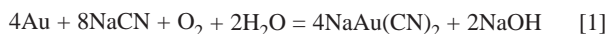
However, a technically based evaluation of the nature and behavior of cyanide in the environment leads to a more sympathetic view of the potential impact of this widely used industrial and mining chemical. In this chapter, we review the environmental geochemistry of cyanide in mining applications. We will first consider the extraction process chemistry for precious metal ores, a chemical process in which cyanide is a vital ingredient. We will then describe fundamental aspects of cyanide chemistry, and translate this chemistry to geochemical reactions and processes. The application of these processes and reactions forms the root of how cyanide migration and attenuation in the natural environment can be evaluated.

Between the basic chemistry of cyanide and final application to cyanide migration, we will insert a caveat by way of a discussion of the widespread difficulties of cyanide analysis and the problem of obtaining reliable data on which sound technical assessment of cyanide behavior can be based.

CYANIDE CHEMISTRY

Extraction and recovery of precious metals

For almost one hundred years, cyanide solutions have been used to extract gold and silver from ores. Gold dissolution using cyanide solutions from ore is a two-stage process, known as cyanidation, which is summarized the reaction described by Elsner's equation:



The reaction with silver is similar. In the absence of other metals that form cyanide complexes, relatively weak cyanide solutions can be used for this process to extract either gold or silver, as they both form strong complexes with cyanide.

However, ores contain many metallic species, particularly from the first transition series of metals in the periodic table, that react with cyanide to form metallo-cyanide complexes; these result in higher cyanide consumption rate and a residual solution bearing a whole range of cyanide species and complexes. For example, Table 11.1 (Scott and Ingles, 1987) gives approximate extraction efficiencies for a range of metals from sulfide ores, many of which are commonly associated with gold mineralization.

TABLE 11.1—Solubility of metal sulfide minerals in cyanide solutions.

Mineral	Formula	Percent extraction of metal
Sphalerite	ZnS	18.4 ⁽¹⁾
Chalcocite	Cu ₂ S	90.2 ⁽²⁾
Chalcopyrite	CuFeS ₂	5.6 (Cu) ⁽²⁾
Bornite	FeS • 2Cu ₂ S • CuS	70.0 (Cu) ⁽²⁾
Enargite	3 CuS • As ₂ S ₅	65.8 (Cu) ⁽²⁾
Tetrahedrite	4 Cu ₂ • Sb ₂ S ₃	21.9(Cu) ⁽²⁾
Metallic copper	Cu	9.0 ⁽²⁾

Source: Scott and Ingles, 1987

Notes: (1) 2.0 g/l NaCN solution (at 45°C)

(2) 1.0 g/l NaCN solution (at 23°C)

Thiocyanate (SCN) and thiocyanate complexes form concurrently with metallo-cyanide complexes. Their formation is enhanced in the presence of free sulfur species or sulfides such as pyrrhotite (FeS) that are relatively reactive.

Gold is recovered from the gold cyanidation solution generally using cementation with zinc (the Merrill-Crowe process) or adsorption on activated carbon; however there are many varieties of each of these two procedures. After gold extraction, a solution remains that contains aqueous cyanide, metallo-cyanide complexes, cyanates, thiocyanates, and other chemical species dissolved from the ores.

Chemistry of cyanidation solutions

Cyanide compounds in cyanidation solutions and mineral processing effluents include free cyanide, the alkali earth salts, and the metal cyanide complexes formed with gold, mercury, zinc, cadmium, silver, copper, nickel, iron, and cobalt. These compounds may be classified into five general categories, as shown in Table 11.2 (Scott and Ingles, 1987). The discussion of cyanidation

solution chemistry is based on the summary by Smith and Mudder (1991).

Free cyanide

The term free cyanide is confined to two species, the cyanide ion (CN^-) and hydrocyanic acid or hydrogen cyanide (HCN). The relative proportion of these two forms depends upon the pH of the system. The reaction between cyanide ion and water is expressed by the following equation:



At any particular pH and temperature, the system is in equilibrium and the relative amounts of each can be determined from the following expression:

$$K_a = \frac{[\text{H}^+][\text{CN}^-]}{[\text{HCN}]} = 2.03 \times 10^{-10}, \text{p}K_a = 9.31 \text{ (at } 20^\circ\text{C)} \quad [3]$$

Figure 11.1 presents this relationship in graphical form. In natural waters with a pH below 8.3, aqueous cyanide is present predominantly as HCN.

Simple cyanide compounds

The simple cyanides are the salts of hydrocyanic acid (i.e., KCN and NaCN), which dissolve completely in solution to produce free alkali earth cations and cyanide anions, for example:



The CN^- then reacts with water to form HCN, the amount of which depends upon the pH of the solution.

The simple cyanides are electrically neutral (the positive charges of the metal ion balance exactly with the negative charges of the cyanide ions) and are capable of existing in solid form. The

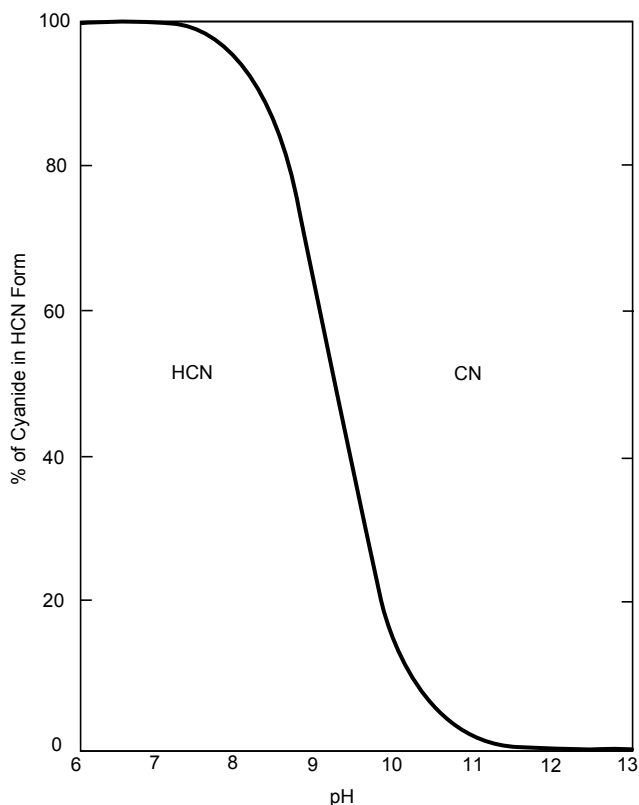


FIGURE 11.1—The relationship between HCN and CN^- with pH.

simple cyanide compounds are water-soluble and dissociate or ionize readily and completely to yield free cyanide (as defined above) and the alkali earth cation.

Cyanide complexes, except strong complexes

These compounds are cyanide complexed with cadmium, copper, nickel, silver and zinc. The complexes form in a step-wise manner, with successively higher cyanide contents as the cyanide concentration of the solution is increased. The stability of these cyanides varies according to the metal ion involved, with zinc and

TABLE 11.2—Classification of cyanide and cyanide compounds in cyanidation solutions on the basis of their stability.

Classification	Compound
1. Free Cyanide	CN^- , HCN
2. Simple Compounds	
a) readily soluble	NaCN, KCN, $\text{Ca}(\text{CN})_2$, $\text{Hg}(\text{CN})_2$
b) neutral insoluble salts	$\text{Zn}(\text{CN})_2$, $\text{Cd}(\text{CN})_2$, CuCN, $\text{Ni}(\text{CN})_2$, AgCN
3. Weak Complexes	$\text{Zn}(\text{CN})_4^{-2}$, $\text{Cd}(\text{CN})_3^{-1}$, $\text{Cd}(\text{CN})_4^{-2}$
4. Moderately Strong Complexes	$\text{Cu}(\text{CN})_2^{-1}$, $\text{Cu}(\text{CN})_3^{-2}$, $\text{Ni}(\text{CN})_4^{-2}$, $\text{Ag}(\text{CN})_2^{-1}$
5. Strong Complexes	$\text{Fe}(\text{CN})_6^{-4}$, $\text{Co}(\text{CN})_6^{-4}$, $\text{Au}(\text{CN})_2^{-1}$, $\text{Fe}(\text{CN})_6^{-3}$

Source: Scott and Ingles, 1987

cadmium forming the weakest complexes. The dissociation constants and order of metal complex stability are presented in Table 11.3 (Caruso, 1975).

TABLE 11.3—Metal-cyanide complex ions in order of decreasing stability in water.

Name ⁽¹⁾	Formula	Dissociation constant
Hexacyanoferrate (III) or Ferricyanide	[Fe(CN) ₆] ⁻³	1.0 x 10 ⁻⁵²
Hexacyanoferrate (II) or Ferrocyanide	[Fe(CN) ₆] ⁻⁴	1.0 x 10 ⁻⁴⁷
Tetracyanomercurate (II)	[Hg(CN) ₄] ⁻²	4.0 x 10 ⁻⁴²
Tricyanocuprate (I)	[Cu(CN) ₃] ⁻²	5.0 x 10 ⁻²⁸
Tetracyanonickelate (II)	[Ni(CN) ₄] ⁻²	1.0 x 10 ⁻²²
Dicyanosilverate (I)	[Ag(CN) ₂] ⁻¹	1.0 x 10 ⁻²¹
Tetracyanocadmate (II)	[Cd(CN) ₄] ⁻²	1.4 x 10 ⁻¹⁷
Tetracyanozincate (II)	[Zn(CN) ₄] ⁻²	1.3 x 10 ⁻¹⁷

Source: Caruso, 1975

Note: (1) The Roman numerals indicate the oxidation state of the metal atom.

The rates of chemical dissociation of cyanide complexes are affected by several factors, including the intensity of light, water temperature, pH, total dissolved solids, and complex concentration. The dissociation constants can be utilized to calculate the concentration of free cyanide present in solution in equilibrium with these complexes. Table 11.4 presents the equilibrium concentrations of free cyanide produced at various complex concentrations dissolved in water at pH 7.0 and 25°C (Caruso, 1975). The very low concentrations of free cyanide produced demonstrate the stability of complexes under ambient conditions.

TABLE 11.4—Free cyanide concentration released at various levels of a metal cyanide complex.

Complex ^(1,2)	1 mg/l	10 mg/l	100 mg/l	1000 mg/l	100,000 mg/l
[Hg(CN) ₄] ⁻²	0.00002	0.00003	0.000045	0.00007	0.00018
[Ag(CN) ₂] ⁻¹	0.00009	0.00002	0.0004	0.0009	0.0041
[Cu(CN) ₃] ⁻²	0.0003	0.000540	0.0097	0.0017	0.0054
[Fe(CN) ₆] ⁻³	0.0002	0.0032	0.0004	0.0006	0.0012
[Fe(CN) ₆] ⁻⁴	0.0012	0.0016	0.0022	0.0031	0.0061
[Ni(CN) ₄] ⁻²	0.135	0.215	0.340	0.539	1.324
[Cd(CN) ₄] ⁻²	(3)	2.30	3.64	5.77	14.49
[Zn(CN) ₄] ⁻²	(3)	2.26	3.59	5.68	14.28

Source: Caruso, 1975

Notes: (1) All values in mg/l.

(2) Free cyanide levels calculated at pH = 7 and 25°C.

(3) Calculations indicate that at this dilution the two complexes are completely ionized.

The metallo-cyanide complexes within this group will generally report in the analysis of weak acid dissociable cyanide (WAD). This means that the cyanide can be liberated from the complex by reflux in a mildly acidic solution buffered at pH 4.5.

Iron cyanide complexes

Cyanide reacts with iron to form stable octahedral complexes including hexacyanoferrate II (or ferrocyanide), in which the iron is in the reduced state with a valence of +2. Ferrocyanide, which is the usual form in solution at ambient redox potentials, is readily oxidized to ferricyanide (or hexacyanoferrate III). In ferricyanide, iron is present in the oxidized ferric form with a valence of +3.

From an environmental viewpoint, iron cyanides (i.e., the hexacyanoferrates) require special attention due to their extreme stability in the absence of light and their tendency to dissociate in its presence. Considerable controversy has evolved concerning the relative toxicity of the iron cyanides due to photolytic degradation. Although these complexes resist natural degradation until free cyanide and the more readily degradable metal cyanides have dissipated, they may be capable of releasing hydrogen cyanide when exposed to intense ultraviolet radiation.

The hexacyanoferrates undergo a much broader range of reactions than do the other metal cyanide complexes, and their solution chemistry has been studied more thoroughly. Ferrocyanide and ferricyanide both form stable salts with other metals without undergoing exchange of the cyanide ligand. Similarly, ferrocyanide is readily and reversibly oxidized to ferricyanide, although the cyanide content remains unaffected.

Ferrocyanide can be formed by addition of a soluble ferrous salt or freshly prepared ferrous hydroxide to a solution containing free cyanide. In practice, the reaction appears to be limited to pH values below about 9.0. There is evidence that dissociation of the complex occurs rapidly above this pH value. The addition of excess ferrous iron increases the amount of complex formed. There is some evidence that a large excess of ferrous, coupled with a pH below 4.0, would precipitate other metal cyanide complexes as well. In spite of its larger stability constant, ferrous iron will not displace zinc, copper, or nickel from their cyanide complexes. Ferricyanide cannot be formed directly in solution from ferric iron and cyanide, probably due to the greater insolubility of ferric hydroxide; its formation of ferricyanide is primarily the result of the oxidation of ferrocyanide.

The hexacyanoferrates are classified as "inert" complexes, in that their chemical stability results from extremely slow rates of dissociation and very low solubilities. Although the precipitated iron cyanides present in mining solutions and wastes are mainly in the mixed fer- and(or) ferri-forms, other relatively insoluble metal iron cyanide compounds do exist. A compilation of the solubilities of various iron cyanide complexes is shown in Table 11.5 (Huiatt et al., 1982).

In the presence of ultraviolet light, photolysis and hydrolysis cause a water molecule to displace one of the cyanide moieties in the complex. On prolonged exposure to ultraviolet light, ferrocyanide and ferricyanide have been shown to release up to 85% and 49% of their cyanide content, respectively (Broderius and Smith, 1980); however, these experiments involved closed systems and very high levels of ultraviolet radiation when compared with natural systems.

The hexacyanoferrate II and III salts are formed by the reactions of the hexacyanoferrate ions and the corresponding cation. In the case of ferrocyanide, if alkali earth metals ions are present, the resulting precipitate will usually contain the alkali as well, often as a double salt. Ferricyanides are less subject to this phenomenon.

The alkali and alkaline earth hexacyanoferrates are all soluble in water, except for barium hexacyanoferrate II, which is only

TABLE 11.5—Solubilities of ferrocyanides and ferricyanides

Name	Formula	Solubility g/l (T°C)
Ammonium Ferricyanide	$(\text{NH}_4)_3 \text{Fe}(\text{CN})_6$	very soluble
Ammonium Ferrocyanide	$(\text{NH}_4)_4 \text{Fe}(\text{CN})_6 \cdot 3 \text{H}_2\text{O}$	soluble
Barium Ferrocyanide	$\text{Ba}_2 \text{Fe}(\text{CN})_6 \cdot 6 \text{H}_2\text{O}$	1.7 g (15°)
Cadmium Ferrocyanide	$\text{Cd}_2 \text{Fe}(\text{CN})_6 \cdot X \text{H}_2\text{O}$	insoluble
Calcium Ferrocyanide	$\text{Ca}_2 \text{Fe}(\text{CN})_6 \cdot 12 \text{H}_2\text{O}$	868 g (25°)
Cobalt Ferrocyanide	$\text{Co}_2 \text{Fe}(\text{CN})_6 \cdot X \text{H}_2\text{O}$	insoluble
Copper (I) Ferricyanide	$\text{Cu}_2 \text{Fe}(\text{CN})_6$	insoluble
Copper (II) Ferricyanide	$\text{Cu}_3 (\text{Fe}(\text{CN})_6)_2 \cdot 14 \text{H}_2\text{O}$	insoluble
Copper (III) Ferrocyanide	$\text{Cu}_2 \text{Fe}(\text{CN})_6 \cdot X \text{H}_2\text{O}$	insoluble
Iron (II) Ferricyanide	$\text{Fe}_3 (\text{Fe}(\text{CN})_6)_2$	insoluble
Iron (III) Ferricyanide	$\text{Fe}_6 \text{Fe}(\text{CN})_6$	===
Iron (II) Ferrocyanide	$\text{Fe}_2 \text{Fe}(\text{CN})_6$	insoluble
Iron (III) Ferrocyanide	$\text{Fe}_4 (\text{Fe}(\text{CN})_6)_3$	insoluble
Lead Ferricyanide	$\text{Pb}_3 (\text{Fe}(\text{CN})_6)_2 \cdot 5 \text{H}_2\text{O}$	slightly soluble
Magnesium Ferrocyanide	$\text{Mg}_2 \text{Fe}(\text{CN})_6 \cdot 12 \text{H}_2\text{O}$	330 g
Manganese (II) Ferrocyanide	$\text{Mn}_2 \text{Fe}(\text{CN})_6 \cdot 7 \text{H}_2\text{O}$	insoluble
Nickel Ferrocyanide	$\text{Ni}_2 \text{Fe}(\text{CN})_6 \cdot X \text{H}_2\text{O}$	insoluble
Potassium Ferricyanide	$\text{K}_3 \text{Fe}(\text{CN})_6$	330 g (4+°)
Potassium Ferrocyanide	$\text{K}_4 \text{Fe}(\text{CN})_6 \cdot 3 \text{H}_2\text{O}$	278 g (12°)
Silver Ferricyanide	$\text{Ag}_3 \text{Fe}(\text{CN})_6$	0.00066 (20°)
Silver Ferrocyanide	$\text{Ag}_4 \text{Fe}(\text{CN})_6 \cdot \text{H}_2\text{O}$	insoluble
Sodium Ferricyanide	$\text{Na}_3 \text{Fe}(\text{CN})_6 \cdot \text{H}_2\text{O}$	189 g (0°)
Sodium Ferrocyanide	$\text{Na}_4 \text{Fe}(\text{CN})_6 \cdot 10 \text{H}_2\text{O}$	318.5 g (20°)
Strontium Ferrocyanide	$\text{Sr}_2 \text{Fe}(\text{CN})_6 \cdot 15 \text{H}_2\text{O}$	500 g
Thallium Ferrocyanide	$\text{Tl}_4 \text{Fe}(\text{CN})_6 \cdot 2 \text{H}_2\text{O}$	3.7 g (18°)
Tin (II) Ferrocyanide	$\text{Sn}_2 \text{Fe}(\text{CN})_6$	insoluble
Tin (VI) Ferrocyanide	$\text{Sn} \text{Fe}(\text{CN})_6$	insoluble
Zinc Ferrocyanide	$\text{Zn}_2 \text{Fe}(\text{CN})_6$	insoluble

moderately soluble. All the alkali and alkaline earth salts of hexacyanoferrate II are insoluble in alcohol.

The heavy metal salts of hexacyanoferrate II (ferrocyanide) are insoluble and precipitate in water. Because the corresponding acid is fairly highly dissociated, the solubility of these precipitates, in the absence of metal-complexing ligands, is not greatly affected by changes in pH over the range pH 2 to pH 11.

In the case of those metals that form strong cyanide or amine complexes such as cadmium, copper, nickel, and silver, the precipitates either dissolve or fail to form in solutions that contain excess cyanide ions or free ammonia. However, the solids can again precipitate if the pH is lowered to a point where the concentrations of these ligands are insufficient to maintain the metal complex.

Hexacyanoferrate II and III form an oxidation-reduction couple. Although the reaction $\text{Fe}(\text{CN})_6^{3-} + e = \text{Fe}(\text{CN})_6^{4-}$ does not itself involve the hydrogen ion, it is nevertheless pH dependent due to the difference in dissociation of the corresponding acids and in the relative proportion of the two free ions at pH values below 7. As a result, hexacyanoferrate II is more easily oxidized in neutral than in acid solutions. Hexacyanoferrate III is reported to be reduced to hexacyanoferrate II by cyanide and would be readily reduced during the Merrill-Crowe precipitation step used for gold recovery (Williams, 1915). Hexacyanoferrate II is not

oxidized by air in alkaline solutions in the absence of light or catalysts.

Other cyanide-related compounds

As a result of cyanidation, a variety of cyanide-related compounds are formed in solution, including thiocyanate, cyanate, and ammonia.

The presence of thiocyanate (i.e., SCN^-) in cyanidation solutions results from the reaction of cyanide with labile sulphur atoms, either during pre-aeration or during leaching. The labile sulphur may originate directly from the attack of lime or cyanide or pyrrhotite, or may be formed by the air-oxidation of sulphide ions released by dissolution of the readily soluble metal-sulphide minerals. The thiocyanate ion and cyanide are classified chemically as pseudohalogens (i.e., they have properties similar to chloride, bromide and iodide), and can form insoluble ionic salts with silver, mercury, lead, copper and zinc. Thiocyanate is chemically and biologically degradable, with the metabolic byproducts being ammonium ion, carbonate and sulphate. The primary environmental concerns associated with thiocyanate include its toxicity and its breakdown products (i.e., ammonia), which may be toxic if present in sufficient levels.

Many oxidants (chlorine, ozone, oxygen and hydrogen peroxide) convert cyanide to cyanate. The mechanisms for the dissolution of gold involves formation of hydrogen peroxide as part of the initial step and it is possible that the cyanate present in the cyanide leach solutions arises as a result of peroxide attack on cyanide. In addition, under acid conditions cyanate slowly hydrolyzes to ammonia and carbonate.

At room temperature cyanide and thiocyanate react slowly with water to form ammonia, formate ion, and (or) carbonate. The reaction rate increases with temperature.

Free ammonia forms soluble amine complexes with many heavy metals, including copper, nickel, silver, and zinc. The hydrolysis constant for the free ammonia-ammonium ion equilibrium is 1.86×10^{-10} at 10°C ($\text{pK}_a = 9.73$). As a result, the presence of ammonia in cyanidation solutions can inhibit the precipitation of these metals at basic pH values above 9.0, the pH range generally chosen for precipitation of metal hydroxides.

CYANIDE ANALYSIS

Despite its critical importance, the analysis for cyanide in mining-related solutions remains a source of concern and confusion to both operators and regulators alike. In the United States, the current status and applicability of methods of cyanide analysis to mining solutions is in a state of flux. Effluent discharge standards for cyanide are being codified in permits at levels below the practical quantitation limits (PQL) of cyanide analysis in mining effluents despite acknowledgment and a considerable database to indicate that there are major problems with the determination of such values. It is imperative that the interpretation of cyanide migration data is tempered with an understanding of the reality of problems of cyanide analysis.

The present state of uncertainty will continue for some time until some fundamental review is made of the practical aspects of cyanide analysis. Rather than being a reiteration of various studies on the analysis of cyanide, for example Conn (1981), the section of the chapter is focused on those methods considered most appropriate for cyanidation solutions. This does not mean that the methods described are without their problems and interferences, nor are they universally applicable. It is that these methods have found successful application in specific cases in a mining environment.

Sample preservation

The preservation and storage of samples is critical to the success of any analytical program and is a concern when dealing with samples for cyanide analysis. Methods of preservation have been developed for most commonly analyzed parameters. However, little information is available to define the effect of preservation on sample integrity, or any interfering effect the preservative may have on a particular analysis.

Immediate analysis of the sample is the most desirable method, followed by refrigeration at 4°C and analysis as soon as possible. All other means are somewhat less appropriate or accurate, but nonetheless are commonly employed. The best approach is to utilize chemical preservatives only when necessary, only when they are known to be compatible with the method of analysis, and only when the preservative has been shown acceptable in the particular application under consideration.

Some of the issues and relationships with respect to sample preservation and cyanide can be illustrated by reference to two recent studies from the United States. In the first example, the results from a comparative evaluation of WAD cyanide analysis on refrigerated, nonpreserved samples and sodium hydroxide stabilized (pH 12 or greater) samples are shown in Table 11.6 (Damon et al., 1991). These data show that nonpreservation was successful in this case in retaining the WAD cyanide components in the sample if the sample was refrigerated and determined in a little over 24 hours (Damon et al., 1991).

TABLE 11.6—Comparison of WAD cyanide values from preserved and unpreserved samples.

Sample no.	WAD cyanide (mg/l)	WAD cyanide (mg/l)
	Unpreserved (held 24 hrs.)*	Preserved (held 6 days)
1	0.04	0.05
2	0.04	0.08
3	0.09	0.09
4	0.11	0.08
5	0.03	0.08
6	0.03	0.05
7	0.02	0.04
8	0.02	0.02
9	0.08	0.09
10	0.48	0.41
11	1.52	1.40
12	1.92	1.81
13	2.30	2.12
14	2.22	2.06
15	1.97	1.41
16	1.80	1.68
17	1.77	1.72

Source: Damon et al., 1991

* Refrigerated at 4°C .

The second example is from an evaluation of the effects of the use of preservatives on total, WAD, and free cyanide analyses using two separate laboratories for quality assurance purposes; the results are given in Table 11.7. The samples were unlikely to have contained any residual oxidants and were shown not to contain any detectable levels of sulphides. The data show considerable variability, with the WAD cyanide samples being most affected by the addition of preservatives. The cumulative affect of adding both the preservatives on the WAD cyanide values is particularly striking. In the case of free cyanide values, it is difficult to assess whether the preservatives skew the analysis, as the replication of the analytical method at this level is poor.

Analytical procedures

Selection of a method of cyanide analysis should involve the following considerations:

- Complete characterization of the solution to be analyzed with particular emphasis on the species of cyanide present and potential interfering components.
- Knowledge of basic chemistry of cyanides.

- Awareness of the method's strengths and weaknesses for a given set of conditions.
- Understanding of the capabilities of equipment and operator expertise and experience.
- Knowledge of the potential treatments to obviate or reduce the effect of interferences.
- Recognition of the fact that treatment to reduce an interference may be an interference itself.

In the context of the above considerations, the following analytical methods require discussion with respect to their use of analysis for cyanidation-solutions:

- Distillation method for total cyanide, U.S. EPA Method 9010/9012 or similar, but including alternative finishes to the colorimetric method;
- Standard method 4500-CN (17th ed., 1989)/ASTM Method C distillation methods for weak acid dissociable cyanide;
- Picric acid colorimetric method for weak acid dissociable cyanide;
- Silver nitrate titrimetric method for free cyanide at levels above 10–20 ppm;
- Ion selective electrode for free cyanide and as a finish to distillation methods;
- Ion chromatographic method for individual cyanide species and complexes; and
- "Reactive" cyanide by U.S. EPA (1986) test method section 7.3.3.2 in support of reactivity criteria for cyanide in waste materials.

A fuller discussion of these methods and their applicability to mining related solutions is given in Smith and Mudder (1991).

TABLE 11.7—Effects of the use of preservatives for oxidants and sulphides on cyanide analysis.

	Laboratory A	Laboratory B
Total Cyanide		
Unfixed	1.80	2.30
Fixed for Sulphide	1.80	2.20
Fixed for Oxidants	1.30	2.30
Fixed for Oxidants and Sulphides	2.00	2.10
WAD Cyanide		
Unfixed 0.10	0.18	
Fixed for Sulphide	0.11	0.22
Fixed for Oxidants	0.35	0.45
Fixed for Oxidants and Sulphides	0.75	0.72
Free Cyanide		
Unfixed 0.03	0.07	
Fixed for Sulphide	0.04	0.04
Fixed for Oxidants	0.11	0.08
Fixed for Oxidants and Sulphides	0.02	0.10

Source: Damon et al., 1991
All values in mg/l.

Total cyanide by distillation

Cyanide, as hydrogen cyanide, is released by reflux distillation for one hour of the sample with a strong acid at a pH value less than pH 2 and the hydrogen cyanide collected in a sodium hydroxide scrubber solution. The cyanide so collected is quantified by titrimetric, colorimetric or ion selective electrode techniques, as for WAD cyanides. The U.S. EPA Method 9010 (manual) and 9012 (autoanalyzer) use a colorimetric finish to the analysis, U.S.

EPA (1986). In this procedure the cyanide is converted to cyanogen chloride with chloramine-T at a pH value of less than pH 8, the color being developed by the addition of pyridine-barbituric acid.

This method is subject to a number of common interferences, notably thiocyanates and sulphides. However, these interferences are treatable to a certain extent and the detection limits under favorable conditions are excellent. The total cyanide method will recover all cyanide species with the exception of cobaltous cyanides. Severe interferences are caused by thiocyanate, sulfide, and other sulfur species. Although these interferences are treatable, the treatment may affect the final result.

Lower limits of detection are reported to be $2.0 \pm 1 \mu\text{g/l}$ (Ingersoll et al., 1981) with a relative standard deviation above 10 $\mu\text{g/l}$ of less than 10%. In a single laboratory, using mixed industrial/domestic waste samples in the range of 0.06 to 0.60 mg/l CN⁻, the respective standard deviations were ± 0.005 to ± 0.094 , U.S. EPA (1986) using concentrations of 0.28 and 0.62 mg/l CN⁻, report recoveries of 85% and 102%, respectively. ASTM (1985) suggests a sensitivity limit of 0.1 mg/l CN⁻.

If performed by skilled personnel, the manual total cyanide method is probably the best of the available methods for cyanide determinations. While the reliability of the autoanalyzer version of the method is accepted by the U.S. EPA, there are cases where the autoanalyzer method has been shown to give erroneous results on samples verified using the manual distillation.

Table 11.8 gives comparative values for total cyanide determinations on effluent from a gold/sulphide project in the United States over a six-month period. With anticipated values of total cyanide being in the 5–20 $\mu\text{g/l}$ range, the manual distillation data are seen to be far more representative than the equivalent autoanalyzer results.

A second example is from a comparative study of three laboratories, two of which used a manual distillation method on samples of effluent from a heap leach project in the United States, Table 11.9. Here the cyanide values are two orders of magnitude higher than the first example, yet the autoanalyzer data are still in error, about three times the values seen in the manually determined samples. These two examples suggest that, if the autoanalyzer technique is proposed for routine determination of total cyanide, a comparative study should be made with manual distillation data to ensure that autoanalyzer method is appropriate for the sample matrix being evaluated.

In research conducted in the Homestake Mine analytical laboratory, it was noted that the total cyanide method using sulphuric acid in the presence of thiocyanate resulted in a positive error, probably due to the breakdown of thiocyanate promoted by the acid (Whitlock et al., 1981). The positive interference resulting from thiocyanate is important when considering low and environmentally important levels of cyanide and monitoring of an effluent for compliance purposes. Although the presence of cyanide may be noted through analysis, resulting in an apparent permit violation, it may not be present in reality.

Cyanide amenable to chlorination

The cyanide amenable to chlorination method was widely used in the past, prior to the development of the WAD cyanide procedures. Both methods measure essentially the same cyanide species, although the cyanide amenable to chlorination method is

more time consuming since it involves two total cyanide determinations (i.e., one before and one after a chlorination step).

In recent years, the WAD cyanide method has superseded the amenable to chlorination method and has become widely accepted by the mining industry and many state regulatory agencies for both monitoring and compliance purposes, due to recognition of the problems with the cyanide amenable to the chlorination method. Unfortunately, the U.S. EPA still only recognizes the cyanide amenable to the chlorination method in discharge permits, although the WAD cyanide method has been submitted on occasion.

TABLE 11.8—Comparison of Tohl Cyanide Analyses by Manual (EPA Method 9010) and Autoanalyzer (EPA Method 9012).

Sample no.	Total cyanide (autoanalyzer)	Total cyanide (manual)
1	90	14
2	80	<5
3	1610	<5
4	2780	13
5	780	<5
6	1200	5
7	560	<5
8	2520	20
9	1900	15
10	1090	<5
11	620	40
12	1550	16
13	1770	<5

Note: (1) All values in µg/l.

TABLE 11.9—Comparison of autoanalyzer and non-autoanalyzer analysis for total cyanide in a mining effluent.

Date		Laboratory A (non-auto)	Laboratory B (non-auto)	Laboratory C (autoanalyzer)
16	Unfixed	1.80	2.30	7.60
	Fixed *	1.80	2.20	7.50
17	Unfixed	2.20	2.10	6.40
	Fixed *	2.00	2.20	6.60
18	Unfixed	2.10	2.50	6.80
	Fixed *	2.30	2.70	6.50

Data in mg/l, the anticipated cyanide value from previous cyanide analysis of this effluent was about 2 mg/l.

**"Fixed," treated to remove sulphide from the sample.

The recoveries of cyanide are incomplete for a number of species and appear to be concentration-dependent (Ingersoll et al., 1981). Ecological Analysts Inc. (1979) reported poor accuracy and precision with the method, with susceptibility to a wide range of interferences.

WAD cyanide by distillation

The two most popular versions of this WAD cyanide method are from the 20th edition of Standard Methods (1998) and the ASTM Method C. The method involves the evolution and collection of hydrogen cyanide by reflux distillation for one hour

with the sample buffered at pH 4.5 using an acetate buffer. This is followed by estimation of the cyanide liberated in the distillation using titrimetric, colorimetric or ion specific electrode techniques.

The method recovers all free cyanide and weakly complexed cyanides, for example cadmium and nickel cyanides, but will not dissociate and recover hydrogen cyanide from strongly complexed forms such as iron and cobalt cyanide. The WAD cyanide method is generally less susceptible to interference by either thiocyanate or sulphides than other cyanide analytical methods.

The overall lower limits of detection are similar to total cyanide methods, although the procedure is more reliable at environmental concentrations of cyanide. Precision is listed as linear, expressed as $0.085 \times \text{cyanide concentration} + 0.0032$ for reagent water. Conn (1981) reported a 7.5% relative standard deviation at the 0.08 mg/l as CN level.

Picric acid method for WAD cyanide

The picric acid colorimetric method for WAD cyanide is included in this section as it has been shown to be a relatively reliable and accurate method down to about 0.5 mg/l cyanide in solution. The method involves developing colour with picric acid in the presence of nickel followed by heating over a water bath for 20 minutes prior to measurement using a visible range spectrophotometer.

As an example of the use of the picric acid method for WAD cyanide, Brohm Mining Corporation, South Dakota, USA evaluated the applicability of the picric acid to solution from their heap leach pads. The data in Table 11.10 show that there is generally little difference between WAD cyanide values determined by the picric acid and ASTM Method C WAD cyanide analytical protocols for these solutions. This is consistent with previous experience which has indicated the picric acid procedure has shown to be a reliable analytical method, capable of providing quantitative evaluations of WAD cyanide down to 0.50 mg/l. Prior to implementing the picric acid method for compliance purposes, its accuracy and reproducibility should be confirmed independently on a site specific basis using an outside commercial laboratory.

Free cyanide by titration with silver nitrate

The silver nitrate titration method is used for the determination of free cyanide or as a finish to the total cyanide distillation method. The process involves titrating a known volume of sample with a standard silver nitrate solution, forming silver cyanide in the process. The end point, the presence of excess silver nitrate when all the free cyanide has reacted, is estimated using a dimethylaminobenzalrhodamine indicator. The solution must be maintained at a high pH value with sodium hydroxide to prevent hydrogen cyanide volatilization.

Ion selective electrode for free cyanide

In a similar manner to the silver nitrate titration, the cyanide ion specific electrode can be used both to determine free cyanide only in solution and as a finish for the distillation method for total cyanide. The method involves the direct measurement, using an expanded scale pH or voltmeter, of the response of the electrode to the cyanide in solution against a reference electrode.

TABLE 11.10—Comparison of leach and rinse effluent WAD cyanide analyses.

Sample date	Sample I.D.	Picric acid WAD cyanide (mg/l)	ASTM method C WAD cyanide (mg/l)
4/11/90	Barren Solution	220	224
4/11/90	Cell #5 Effluent	193	199
4/11/90	Column D Effluent	169	170
4/11/90	Column C Effluent	172	171
4/11/90	Column B Effluent	177	173
5/31/90	Column A Effluent	11.8	11.7
5/31/90	Column B Effluent	11.2	11.2
5/31/90	Column C Effluent	11.5	11.3
5/31/90	Column D Effluent	12.4	12.2
5/31/90	Cell #5 Effluent	16.5	16.5
6/28/90	Column B Effluent	0.25	0.17
6/28/90	Column C Effluent	0.11	0.07
6/28/90	Column D Effluent	0.21	0.13
6/28/90	Cell #5 Effluent	2.7	2.8
6/28/90	Neutralization Pond Effluent	0.13	0.11

Source ASCI/SRK, 1990

Notes: (1) April data: leach cycle
(2) May/June data: rinse cycle

A calibration curve is prepared using standard additions of a known cyanide solution. It is important to match the matrix of the standard solutions with that of the test solution where the presence of potential interfering species is suspected, a common issue with mining-related effluents. The cyanide ion specific electrode itself often becomes "poisoned" in effluent solution bearing sulphide species, with coatings forming on the electrode junction. These coatings require removal in order to attain credible results.

Ion chromatographic method

Ion chromatography has been used by many researchers for the separation of several metal cyanide complexes. Varying methods and conditions give good to poor recovery of the loosely complexed metal cyanides. Indirect determination of cyanide by ion chromatography has been successfully demonstrated by several researchers.

A method developed by Koch (1983) claims detection of trace quantities of free cyanide by electrochemical means at 1 µg/l to 1000 µg/l, and a standard deviation better than 1%. Rocklin and Johnson (1983) have also developed a method using electrochemical detection of free cyanide from easily dissociated metal cyanide complexes. Simultaneous determination of cyanide and sulfide was successfully demonstrated. Pohlandt (1984a, b, 1985) and Pohlandt et al. (1983) have shown good recovery of the easily dissociated metal cyanide complexes as well as complexes of nickel, cobalt, iron, and gold conductometrically. Copper cyanide was detected photometrically along with nickel cyanide. The method distinguishes between the two cobalt and iron forms which is significant in industrial applications. UV irradiation of more refractory metals is also utilized.

"Reactive" cyanide by U.S. EPA test protocol

The U.S. EPA defines the hazardous characteristic of reactivity with respect to cyanide for a waste as "waste that, when exposed to pH conditions between 2 and 12.5, can generate toxic

gases, vapors or fumes to present a danger to human health or the environment." The current action level triggering this classification is 250 mg/kg waste.

The method involves placing a small mass of the sample in sulphuric acid, such that the resultant pH is about 2, and passing a stream of nitrogen over the sample for 30 minutes. The concentration of hydrogen cyanide collected from the nitrogen gas stream in a sodium hydroxide scrubber is determined.

Based on recent experience, it is difficult to know how data obtained by this method equates to other cyanide analytical results. Adding sulphuric acid to the material down to pH 2 will cause precipitation of some metalcyanide complexes over the range pH 2–4.5, which will only redissolve slowly. Cyanide from these complexes will not report to the nitrogen stream. For example, some recent unpublished data indicated that a particular sample with a total cyanide of 900 mg/l, 90 mg/l WAD cyanide and 15 mg/l free cyanide had a reactive cyanide value, when corrected for sample mass and scrubber solution volume, of less than 1 mg/l.

Analytical interferences

Associated with any analytical procedure are interferences, both positive and negative, which affect both the precision and accuracy of that method. All of the methods previously discussed are affected by interferences to varying degrees. This section contains a brief discussion the various interferences, as well a discussion of the research directed towards quantification of various interferences.

In summary, the WAD cyanide procedure which measures the weakly complexed forms of cyanide, is least affected by interferences, while the total cyanide method, the ion selective electrode and the titrimetric method for free cyanide are susceptible to many interferences. The principal species which cause interference in cyanide analyses are:

- oxidizing agents
- sulfides
- thiocyanate

- nitrite and nitrate
- carbonates
- thiosulphates, sulfates and other related sulphur compounds
- metals.

A full discussion of interferences in the analysis of cyanide is given in Smith and Mudder (1991).

CYANIDE GEOCHEMISTRY

Some appreciation of the basic chemistry of cyanide is an important building block in the appreciation of cyanide geochemistry. Next, a solid phase is introduced, either the ore or gauge material leached by cyanide in a tank or on a pad, or the subsite geological material (i.e., soil or aquifer material) for geochemical interaction with the cyanide-bearing solutions.

Therefore, the physical and chemical properties of the natural material are related to the cyanide reactions to elicit potential geochemical reactions. Ores, rocks, and soils contain to a greater or less extent silicates, aluminosilicates, clay minerals, sulfides, carbonates, and oxides (e.g., iron and manganese more commonly) as mineral phases, plus organic matter, water, and gases in some cases. These are the potential reactants with the cyanide solutions in slurry leaching, in the tailings impoundments, in the leaching heap, or in the subsite soils and aquifer materials. The solid components can control the solution chemistry with regard to alkalinity or acidity (pH control), buffering capacity, degree of oxidation or reduction (redox potential), resulting in ion exchange adsorption or chemical reaction in the cyanide solution (i.e., precipitation of insoluble species).

In order to use the knowledge of cyanide chemistry and relate it to the analytical data (total cyanide, WAD cyanide, and free cyanide), one needs to have a concept of their interrelationship. Figure 11.2, modified by Smith (1988) from Simovic et al. (1985), takes a geochemical system, such as found in a tailings/heap leach system, with both "strong" and "weak" metal complexes and relates these complexes to cyanide hydrolysis and HCN volatilization. The contribution of each to the "free" cyanide, WAD cyanide, and total cyanide analysis is shown.

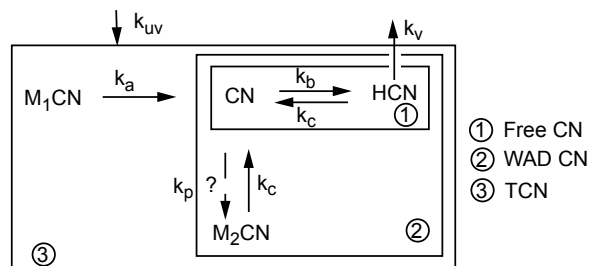
Clearly, this expression of cyanide interrelationships is rather simple, but it is an effective tool for combining the theoretical cyanide chemistry with the actual analytical values used everyday in industry.

Degradation mechanisms of cyanide

There are eight mechanisms of cyanide degradation in natural environments which merit discussions. These are:

- complexation
- cyanide complex precipitation
- adsorption
- oxidation to cyanate
- volatilization
- biodegradation
- formation of thiocyanate
- hydrolysis/saponification.

Conceptualization of FCN, WAD, TCN



where

- M_1 = strong complexing transition metal (TM), e.g., iron
- M_2 = other "weak" TM, e.g., copper, zinc, etc.
- K_{uv} = additional influence of k_{uv} ultraviolet degradation
- K_a, K_b, K_c, K_e, K_f = rate constants transformation
- k_v = volatilization mass transfer coefficient (loss to atmosphere) (L/t)

Now can add, if necessary, cyanate reaction, for example:

1. $HCN \rightarrow CN \rightarrow M_2CN$
2. $2HCN + O_2 (+ catalyst) \rightarrow 2HCNO$
 $2CN + O_2 (+ catalyst) \rightarrow 2CNO$

Mass Balance (MCN, FCN, TCN)

$$1. \frac{d(\overline{MCN})}{dt} = -k_a (MCN) - k_{uv} (MCN) \text{ where } k_{uv} \text{ influenced} \\ \text{or } -k_a (MCN) \text{ where not.}$$

$$2. \frac{d(\overline{FCN})}{dt} = k_a (MCN) + k_{uv} (MCN) - \frac{k_v}{Z} (HCN)$$

where Z is related to volume and area for volatilization

$$Z = \frac{V (m^3)}{A (m^2)} = m$$

$$3. \frac{d(\overline{TCN})}{dt} = -\frac{k_v}{Z} (HCN) \text{ where there is no } k_{uv}, \text{ ultraviolet} \\ \text{degradation of MCN}$$

FIGURE 11.2—Interrelationships in cyanide chemistry.

Complexation

Ford-Smith (1964) reported that 28 elements are capable of forming complexes with cyanide, with 72 metal cyanide complexes possible. The solubilities of these complexes range from very soluble to insoluble. However, some of these compounds are not very stable and will decompose releasing free cyanide. The toxicity of metal cyanide complexes is generally due to the dissociation of the complex into free cyanide.

At a pH of 4.5, some of the metal-cyanide complexes typical found in cyanidation solutions (for example, zinc and copper) may dissociate into free cyanide to varying degrees and at varying

rates. These are the so-called weak acid dissociable metal cyanide complexes.

The tightly bound iron cyanide complexes may produce free cyanide due to photochemical decomposition in favorable conditions. There is some question as to the significance of this decomposition to surface water toxicity under realistic conditions (Doudoroff, 1980). While the formation of metal cyanide complexes does not completely eliminate the toxicity of cyanide, it does effect a substantial reduction in such toxicity. Metal cyanide complexes are also intermediates to formation of more stable compounds that remove free cyanide from the environment (i.e., ferrocyanide precipitates and the oxidation to cyanate). For example, Milne (1950) suggested the use of nickel to form complexes as a method for the disposal of free and complex cyanides in electroplating wastes. Kunz et al., (1979) described a process where copper was complexed with cyanide to enhance the adsorption and oxidation of cyanide on activated carbon. Bishop and Wright (1977) received a patent for an electrochemical cyanide oxidation process using nickel to enhance the process.

The environmental significance of complexation/chelation of cyanide with transition metals is that it is relatively rapid and it occurs wherever soluble species of these metals are present, such as found in soils and ores. It reduces the toxicity of free cyanide and acts as a intermediary to reduce cyanide mobility via adsorption on organic and inorganic surfaces or precipitation of ferrocyanide metal salts. Based on their relative abundance in the soil, it is expected that the majority of metal cyanide reactions occurring in the soil will be with iron.

The complexation of cyanide can have two very diverse affects on cyanide mobility in soils. If cyanide complexes with iron it is less able than free cyanide to adsorb on surfaces; hence, its mobility can be increased as demonstrated by Fuller (1984). However, if free transition metals such as iron, copper, or nickel are present, a ferrocyanide precipitate will cause the cyanide species to be tied-up with the soil. On the other hand, if cyanide chelates as a weak acid dissociable metal complex, it will enhance adsorption of cyanide on organic carbon, metals oxides, feldspar, and clay surfaces.

Cyanide complex precipitation

The ferrocyanide ion ($\text{Fe}(\text{CN})_6^{-4}$) and the ferricyanide ion ($\text{Fe}(\text{CN})_6^{-3}$) form insoluble salts with iron, copper, nickel, manganese, lead, zinc, cadmium, tin, and silver as stated by Weast (1969). Typically within the soil environment, the oxidation potential would result in the formation of ferrocyanide precipitates. In addition, the iron-cyanide complexes can react with thiocyanate to form an even more stable complex, if sulfur is present in the soil.

Hendrickson and Daignault (1973) demonstrated that both ferro- and ferricyanide complexes will precipitate with iron, copper, magnesium, cadmium, and zinc through a broad range of pH's ranging from 2 to 11. However, at higher pH's the precipitation is more complete. Stoichiometric additions of transition materials removed greater than 90% of the ferro- or mixed ferro-ferric complexes. However, at high oxidation potentials where only ferricyanide complexes are present, precipitation only removed about 60 to 90% of the ferricyanide. This indicates that over a broad range of pH and oxidation potentials, iron cyanide metal complexes will precipitate if sufficient free transition metals are available.

Adsorption

Adsorption is another mechanism that attenuates cyanide in soils. Alesii and Fuller (1976) conducted tests with free cyanide in water, potassium ferricyanide in water, and free cyanide in landfill leachate to determine cyanide mobility in various types of soils. The test results indicated that soils having high concentrations of hydrous oxides of iron and manganese retained cyanide best.

Studies conducted for the U.S. EPA in the mid-70s on the leachate pollutant attenuation abilities of soils indicated that soils containing aluminum minerals attenuated cyanide better than other soils (Alesii and Fuller, 1976; Fuller, 1978, 1977, 1980). However, Towill et al. (1978), in reviewing the environmental effects of cyanide, found that free cyanide ions are not strongly adsorbed or retained by soils irrespective of the presence of aluminosilicate minerals (Murrmann and Koutz, 1972).

Based on their tests, Alesii and Fuller (1976) concluded that soils with a high anion exchange capacity would likely attenuate cyanide. Those soils with a high anion exchange capacity typically contain kaolin clay, chlorite, gibbsite clay, and/or iron and aluminum oxides. Conversely, soils containing predominantly strong cation-exchanging materials, (i.e., montmorillonite) were predicted to have a lesser effect.

As is well known in precious metals leaching, organic materials will adsorb or react with cyanide. Carbonaceous materials in ore slurries will adsorb free cyanide and limit precious metal recovery. During this time it has been found that cyanide is first adsorbed, then catalytically oxidized (Bernardin, 1973). The presence of copper, cadmium, zinc, or nickel ions in solution results in the formation of metal cyanide complexes, which enhances the adsorptive capacity of carbon.

Chatwin and Trepanowski (1987) found that the magnitude of cyanide adsorption in subsoils was correlated with the organic carbon content of the soil. It appears that cyanide adsorbs on soil organic matter and becomes bound or is subsequently oxidized to cyanate. Free cyanide as also been found to adsorb on the surface of clays and feldspar (Chatwin and Hendrix, 1988). The results indicate that this mechanism is dependent not only on the mineralogy of the soil but the solution chemistry as well. It was found that metals that form weak acid dissoluble cyanide complexes, such as copper and nickel, enhanced the adsorption process.

Oxidation to cyanate

Cyanide can be converted to cyanate according to the following simplified reaction:



Hydrogen cyanate and cyanate ions are significantly less toxic than HCN. Cyanide conversion to cyanate has been demonstrated when cyanide is in the presence of strong oxidizers (i.e., ozone, hydrogen peroxide, and hypochlorite). Ultraviolet light, in conjunction with catalysts such as titanium dioxide, cadmium sulfide, and zinc oxide, has been shown to convert cyanide to cyanate (Frank and Bard, 1977). It is theorized that the ultraviolet light causes the catalyst to convert oxygen in solution to ozone, which promptly reacts with the cyanide (Miles, 1981). In recent work it has been found that cyanide can be converted to cyanate in the soil

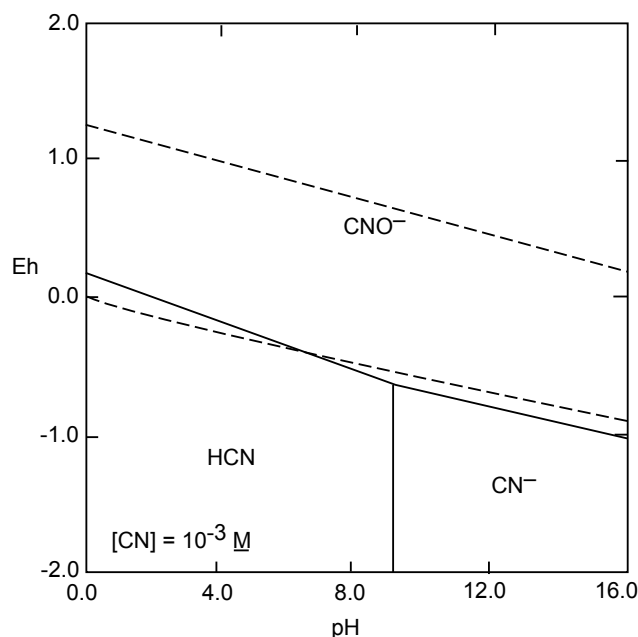


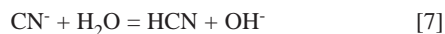
FIGURE 11.3—Eh-pH diagram for the CN^- - H_2O system at 25°C. Source: Smith, 1988.

on the surface of organic and inorganic materials (Chatwin and Hendrix, 1988).

The thermodynamics of the cyanide-cyanate reaction, as seen on Figure 11.3, indicate that cyanate should be the predominant species under natural conditions. However, it has been found difficult to oxidize cyanide to cyanate under natural ambient conditions. A strong oxidant such as ozone, hydrogen peroxide, or chlorine is required to drive this reaction. Bacterial enzymes or catalytic surfaces of titanium dioxide, zinc sulfide, and carbon have been found necessary to promote this oxidation as well.

Volatilization

Hydrogen cyanide (HCN), also known as hydrocyanic acid, is a colorless gas or liquid with a boiling point of 25.7°C and a vapor pressure of 100 pKa at 26°C (Huiatt et al., 1982). The equilibrium hydrolysis reaction between cyanide ion and water occurs according to the following reaction:



At a pH of 9.36, which is the pK value, the concentrations of HCN and CN^- ion are equal as shown on Figure 11.1. At lower pH values and at 20°C, the majority of cyanide exists as HCN (i.e., 69.6% at pH 9; 95.8% at pH 8, and greater than 99% at pH 7). Thus, at neutral pH most of the free cyanide will be in the form HCN. Hence, in soils or other natural geochemical systems, where the pH of cyanide solutions are neutralized to lower pH values, the HCN concentration could be quite high. For example, in tests performed by Chatwin and Hendrix (1988) on a suite of arid subsoil

samples the soil pH ranged from 4.5 to 8.9. Should free cyanide be present in contact with these soils, it would result in solutions where the HCN content would be greater than 70%.

Dodge and Zabbon (1952) and Chester Engineers (TCE, 1977), identified pH, temperature, interfacial surface area, pressure, concentration, and degree of agitation as factors affecting cyanide volatilization. Palaty and Horokova-Jakubu (1959), cited in Simovic et al. (1985), also studied volatilization of cyanide from simple cyanide solutions. They identified the same variables that affected cyanide volatilization as Dodge and Zabbon (1952).

While cyanide volatilization from surface waters is quite well understood, cyanide volatilization from soils is more difficult to understand. However, in work from using unsaturated column tests (Chatwin and Hendrix, 1988) measured HCN volatilizing from soil surfaces.

Biodegradation

Towill et al. (1978) reported that cyanide salts move only a short distance through soil before being biologically converted under aerobic conditions to nitrates (microbial degradation to ammonia, NH_3 , then conversion to nitrate, NO_3^-) or fixed by trace metals through chelation. The vast majority of this attenuation was attributed to biodegradation.

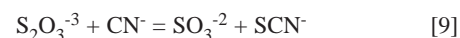
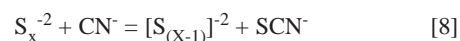
Strobel (1967) tested both sterile and nonsterile soils to determine their effect on cyanide. The nonsterile soil degraded cyanide, while the sterile soil did not appreciably alter cyanide. Fuller (1984) reported that cyanide up to 200 ppm was readily converted to fertilizer nitrogen in the soil. In fact, plants responded to cyanide applications nearly identically as they did to sodium nitrate or ammonium nitrate, both common components of fertilizers.

Cyanide biodegradation is currently being utilized to treat industrial wastewater in two separate processes. Homestake Mining Co. at Lead, South Dakota, utilizes bacteria to treat its wastewater prior to discharge and ICI Bioproducts detoxifies cyanide with a strain of the fungus, *Fusarium lateritium*.

Biodegradation under anaerobic conditions is not nearly as prolific as under aerobic conditions. The limit for effective anaerobic degradation of cyanide was found by Coburn (1949) to be 2 mg/l cyanide. Above this concentration, the cyanide was found to be toxic to the anaerobic microorganisms. Below 2 mg/l, there is evidence that denitrification occurs in certain soluble cyanides, yielding nitrogen gas, N_2 (Huiatt et al., 1982).

Formation of thiocyanate

Free cyanide has been shown to react with various forms of sulfur in the environment to form thiocyanate. Thiocyanate is relatively nontoxic, when compared with cyanide. The two forms of sulfur most likely to react with cyanide are polysulfides (S_2) and thiosulfate (S_2O_3) (IEC 1979). They react according to the following equations.



In neutral to basic solutions, both polysulfides and thiosulfate are oxidation products of sulfides, the latter being abundant in minerals. As such, these products could possibly be present in oxidizing environments, such as the vadose zone in soils. The concentrations of polysulfides and thiosulfate in a soil are strongly dependent on the sulfur content and the Eh-pH conditions in that soil.

McGill et al. (1985) conducted bench tests on various sulfur-bearing ore minerals to determine if they caused the formation of thiocyanate (at a pH of 10). The laboratory results indicated that chalcopyrite, chalcocite, pyrrhotite, and free sulfur contributed a significant portion of their sulfur content to thiocyanate production, while "pure" iron sulfides contributed a lesser yet significant portion. The sulfur contained in sphalerite and pyrite was relatively nonreactive with the cyanide.

Hydrolysis/saponification of HCN

As the system pH falls, HCN can be hydrolyzed by a different route to give formate, as either formic acid or ammonium formate according to the following reactions:



or



The system pH will determine the extent of formation of each compound, a lower pH favoring formic acid formation.

Hoecker and Muir (1987) have tested high temperature hydrolysis of cyanide in autoclaves and have developed kinetic data for this reaction. By extrapolating this data to room temperature, a rate for cyanide hydrolysis to ammonium formate of 4% per month is estimated. This rate is similar to that obtained by DuPont of 2% per month (Longe and DeVries, 1988). Hence, this is not a rapid cyanide degradation mechanism. However, it would be effective under a variety of conditions including those found in saturated aquifers, particularly where the system was relatively anaerobic.

CYANIDE ATTENUATION AND MIGRATION

The natural degradation of cyanide process solutions in ponds, mill tailings, heap leach ore, subsoil fluids and ground water both prior to and after their exit to the environment is an evaluation of five systems, which are strongly affected by the geochemistry of their solid phases (ore, tailings, the subsoil, and the geologic aquifer materials). Each of these systems will be discussed separately, namely:

- Process solution ponds
- The tailings supernatant, pore fluid and tailings system
- The heap leach solution, pore fluid and ore system
- The seepage and subsite soil/geologic materials system
- The ground water/geologic material system

Each system is a truly complex geochemical problem to unravel, but it is possible to produce a quite adequate and workable explanation of each system and how it affects the cyanide chemistry on a general basis it is necessary to construct a working

hypothesis of cyanide chemical behavior for the five geochemical systems.

Surface ponds

The major mechanisms of natural cyanide degradation in surface ponds is volatilization of HCN. The pH of the pond is lowered by uptake of carbon dioxide from the air and from rainwater saturated with carbon dioxide. This drop in pH induces a change in the CN-/HCN balance (Fig. 11.1) increasing HCN volatilization.

Data by Schmidt et al. (1981) illustrate cyanide losses and transformation related to water depth, season, and temperature for two ponds at a mine in northern Canada. Figure 11.4 illustrates:

- Cyanide (total) decay irrespective to pond depth, although there is a slight time lag for the deeper pond section.
- Cyanide transformation to cyanate followed by subsequent cyanate loss from the pool water.
- A slight increase in thiocyanate, followed by substantial decay, particularly in the shallow pond.

At first glance this work appears to disagree with the prior studies by Dodge and Zabbon (1952), who found that cyanide volatilization was dependent upon the ratio of solution area to depth in stagnant solutions. However, in ponds there is a natural mixing caused by the convective currents due to differences in pond temperature with depth and temperature differences between the air and water.

Longe and DeVries (1988) utilized this temperature-induced, convective mixing in their chemical equilibrium pond model, which also assessed the cyanide degradation due to cyanide-copper precipitation. They found that, in an arid location (Yuma, Arizona) at various seasons, the following result were predicted:

- Maximum time for 200 ppm cyanide solution to degrade to 2.6 ppm was 6 months, including 60 days of feeding 1,000 ppm cyanide solution.
- Minimum time for 200 ppm cyanide solution to degrade to 2.6 ppm was 3 months, including 60 days of feeding 1,000 ppm cyanide solution.
- Winter cleanup was more rapid than summer cleanup due to temperature induced convection currents carrying CO₂ rich, cyanide-lean solution to the bottom of the pond.
- Almost all the copper precipitated as CuCN, rather than dissociating, and precipitating as malachite.
- Copper content had little effect on the rate of cyanide loss.
- The chemistry model predicted final pHs approaching 5.0.

Simovic et al. (1985) and Zaidi et al. (1987) have attempted to quantify cyanide losses in process ponds in Canada. They have developed a numerical model that predicts cyanide removal and it has been validated against actual pond data. The volatilization of HCN from surface waters is the dominant mechanism for natural cyanide degradation. Ninety percent of the free cyanide was removed by volatilization and an additional 10% was removed by chemical oxidation (Simovic et al., 1985.) Cyanide degradation was found to follow a first order reaction with respect to free cyanide and cyano-metal complexes of zinc, nickel, copper, and iron. Temperature and aeration have the most significant effect on the volatilization rate of free cyanide and most metal cyanide complexes studied. Simovic et al. (1985) found that UV radiation has a significant effect on the stability and degradation of iron-cyanide complexes in the surface ponds.

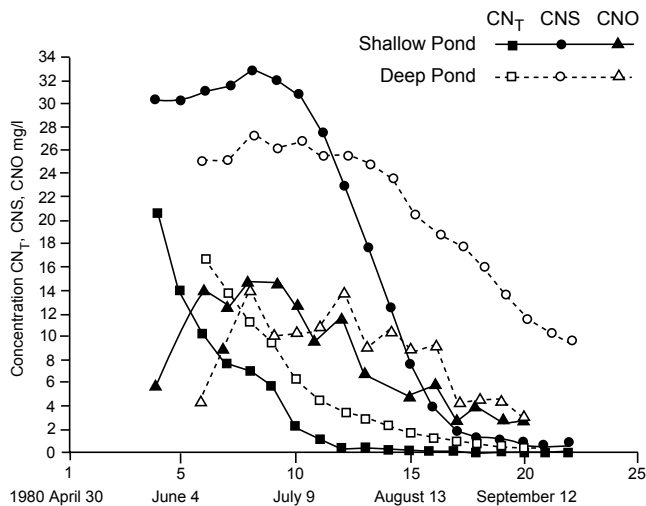


FIGURE 11.4—Concentration of CN_T , CNS, CNO, shallow and deep section of a pond. Source: Schmidt et al., 1981.

Bench-scale laboratory data were fitted to a mathematical model which considered volatilization of free cyanide and dissociation of the metal cyanide complexes. The model fit the experimental data of single metal cyanide complexes quite well with correlation coefficients of 0.93 to 0.99 (Simovic et al., 1985). Validation of the natural degradation model for predicting the degradation of cyanide in impoundments has been performed by Environment Canada. The model has been used to predict the degradation of cyanide in pilot and full-scale batch and dynamic systems.

As the Environment Canada and DuPont models are validated by comparison with measurements from actual field conditions, they will become useful in predicting the rate of natural treatment of process solutions in ponds. They will also be helpful in assessing the potential risk of cyanide release and the monitoring time required for decommissioned and inactive process facilities.

Cyanide in tailings

The objective of this section is to trace the pathways of cyanide through a mill tailings disposal system and evaluate the cyanide behavior in the system. The evaluation of cyanide in mill tailings systems requires a somewhat different approach to that of a heap leach. In the latter case, the heap itself can be almost the entire focus of the assessment. However, for mill tailings, the entire system from thickener to return water facility (where appropriate) bears consideration.

It is possible to track theoretically the behavior of cyanide and its geochemical reactions through a mill with its decant pond and tailings impoundments or a heap leach with its subsystems. By understanding and quantifying the cyanide mechanisms that are significant in each sub system which include the following:

- Mill and thickeners—dilution/concentration/precipitation processes
- Chemical treatment plant (optional)—reagent addition with neutralization/oxidation/precipitation reactions
- Tailings pumping system—oxidation/precipitation/resolubilization reactions

- Discharge onto impoundment (e.g., spigots)—oxidation/precipitation reactions
- Tailings beaches and pool—dilution/concentration/oxidation reactions
- Oxidized tailings zone—precipitation/coprecipitation reactions or solution by acidification due to secondary oxidation
- Reduced tailings zone—resolution due to reduction to lower valency state or precipitation of insoluble phase, i.e., sulfides
- Drains/penstocks/decant—oxidation and precipitation
- Water reclaim facility (where present)—dilution/concentration processes and precipitation

A fundamental question, which is still the subject of debate, is where in such a system are the cyanide “losses” occurring and is there any loss of cyanide within the tailings or heap leach mass? The term “loss” is somewhat of a misnomer in itself. Transformation of cyanide to cyanate or thiocyanate is termed a “loss of cyanide” but large values of cyanate or thiocyanate can be of significance in themselves. Also, the formation of iron cyanide complexes significantly reduces the toxicity of the solutions, and they are still considered in the total cyanide mass balance.

It is worth examining certain practical test and field data dealing with actual tailings and tailings facilities where the behavior of cyanide has been evaluated in various climatic regimes and parts of the world.

Surface effects in tailings ponds

Cyanide degradation mechanisms described in the prior section on surface water ponds is applicable to the surface waters of tailings ponds. Typically the pH of these solutions as they come out of the mill are 10 or above. However, as these solutions “age” in the impoundment, the pH is reduced due to rainfall and carbon dioxide uptake. As the pH is lowered, the HCN concentration in the tailings solution increases and volatilization occurs (see Fig. 11.1).

Surface effects have been shown to contribute to a large proportion of cyanide loss in tailings systems in South Africa (Smith et al., 1985a). Their data show cyanide being decreased from discharge concentrations from a conventional (non-CIP) mill of about 20 mg/l cyanide in the tailings supernatant to less than 2 mg/l in the tailings pore water. Such values are common. Discharge from CIP/CIL plants at 200–250 mg/l free cyanide or more results in pool concentration of cyanide anywhere in the range of 20–50 mg/l or less, throughout the world; (e.g., Australia, Brazil, Canada, New Zealand, South Africa, and the United States).

Reactions in the tailings mass

Residual cyanide values in tailings are a source of substantial (though, perhaps, often somewhat unwarranted) concern to regulatory agencies. They cite lack of data on cyanide “loss” or transformation within the tailings mass itself and there is, in many cases, data which does show the presence of residual cyanide levels after significant time intervals (Hendrix et al., 1987). The extent to which these levels are a real risk to the environment is questionable, however. In this respect, the following work on tailings and tailings impoundments illustrates some of the issues.

The work of Smith et al. (1985a) shows profiles of pore water quality in tailings systems. Table 11.11 shows the variation with depth of total cyanide within a tailings facility yields very low val-

ues of cyanides. Table 11.12 relates concentration to overall chemistry within the tailings, for the oxidized, intermediate, and reduced zones in the tailings mass. It is interesting to note the low values of cyanide in the reduced zone (<1 mg/l total cyanide) and the large number of samples examined, (n = 149).

TABLE 11.11—Cyanide profile in interstitial water in a decommissioned tailings impoundment, Witwatersrand, RSA.

Borehole	Piezometer no.	Depth m ⁽¹⁾	Total CN mg/l ⁽²⁾
A	1	11	0.16
	2	17	0.21
	3	25	0.57
B	1	27	1.54
	2	30	0.16
	3	47	<0.01 ⁽³⁾
C	1	18	0.22
	2	22	2.92
	3	26	0.35
D	1	19	N/S ⁽⁴⁾
	2	24	1.09
	3	28	1.86

Notes: (1) Total height of tailings impoundment, 32 m (104 ft).
 (2) Cyanide discharge concentration varied between 8–19 mg/l during operation.
 (3) Samples taken below 32 m are in the sediments below the impoundments.
 (4) N/S, no sample.

TABLE 11.12—Chemistry of oxidized, intermediate, and reduced zones in tailings impoundments (mean values), Witwatersrand, RSA.^(1,2)

pH ⁽³⁾	TDS	SO ₄	Fe*	Mn	Total	CN ⁽⁴⁾
Oxidized						
Zone 0–3 m	6.6	3350	1850	47	4	0.6
Intermediate						
Zone 3–15 m	6.6	3600	2210	21	11	2.0
Reduced						
Zone 15–35 m	6.6	2850	1600	8	20	0.9

Notes: (1) Two impoundments +20 years old.
 (2) Sample total = 149.
 (3) pH; units otherwise all values in mg/l.
 (4) Total cyanide in near-surface ground water below impoundment was 0.8 mg/l (mean value).
 * Total iron.

Caldwell and Smith (1985) and Smith et al. (1985b) developed their data based on test work from gold tailings for the Cannon Mine, Washington State, USA. The geochemical effects of hydro-geochemical reduction and rainwater leaching of the mixed tailings are shown in Table 11.13. In the chemically reduced case, cyanide levels decreased to <0.05 mg/l, due to thiocyanate formation, and rainwater leaching reduced the total cyanide from >300 mg/l to about 57 mg/l as total cyanide, of which about 2.5 mg/l is free cyanide.

Smith (1987) developed data from test work on the Ridgeway Mine pilot plant tailings in South Carolina. These data show the loss of cyanide levels over time and during leaching with rainwater. The data in Table 11.14 show that copper and cobalt are lost from the aqueous phase of the system at an enhanced rate as compared with their leach rate.

Overall effects in tailings

Kidd (1988) and Burden and Kidd (1987) have developed data on the Golden Cross project, New Zealand, and the Macraes project, New Zealand, showing overall cyanide degradation, both in the tailings pool and in the tailings mass. Mudder and Goldstone (1989) have described and compared cyanide degradation both in tailings decant water and in the entrained tailings pore water from test data at the Golden Cross Mine, New Zealand. In the case of the tailings testing, tailings samples were sealed in canisters and opened sequentially over time. The test results for the decant are given in Table 11.15 and for the tailings pore water in Table 11.16. While the total cyanide levels remained stable, WAD cyanide levels decreased rapidly, particularly in the decant water, (6.8 ppm to 0.33 ppm in 28 days) presumably by precipitation and degradation.

Similar data are given in Smith et al. (1985a), for tailings facilities from South Africa, Smith (1988) for gold tailings projects worldwide, Caldwell and Smith (1985), and Smith (1985), for projects in the United States, specifically.

TABLE 11.13—Cyanide chemistry of “mixed” tailings and flotation tailings liquid, Cannon Mine, Washington State.

Parameter ⁽¹⁾	Mixed tailings supernatant	Flotation tailings supernatant
pH value (units)	7.17	7.30
Total dissolved solids	4230	440
Total cyanide	284	<0.05
Free cyanide	0.35	<0.05
Iron	10	<0.05
Cobalt	0.33	<0.01
Copper	0.03	<0.01
Mercury	0.0024	<0.0003
Silver	<0.01	<0.01

Note: (1) All values in mg/l, except pH.

TABLE 11.14—Time/Cyanide Concentration Dependency of Copper and Cobalt Cyanide in Tailings Interstitial Water Solution Ridgeway Mining Project, South Carolina

Parameter	Original tailings pore water (mg/l)	Leached sample @ time T1 (mg/l)	Leached sample @ time T2 (mg/l)
Total Cyanide	170	2.66	0.90
	408	1.9	0.09
Free Cyanide	170	0.92	0.04
	408	1.4	0.09
Cobalt	0.73	<0.1	<0.1
	2.21	0.05	0.05
Copper	1.81	0.04	<0.01
	6.34	0.04	<0.01

Cyanide in a heap leach

Potential geochemical conditions and cyanide reactions in an abandoned cyanide heap leach operation are presented on Figure

11.5. As with the tailings example, the total system is a continuum, and the separation between the fate of cyanide in the heap itself and the environment becomes somewhat indistinct.

The upper portions of Figure 11.5 (the heap and pad) are essentially in an oxidizing environment. The “high” permeability of the heap itself, a basic requirement so that it will actually leach, ensures a reasonable flow of air. Also, oxygen dissolved in any precipitation which infiltrates the system assist in keeping the geochemical environment oxidized.

TABLE 11.15—Cyanide decay in tailings decant, Golden Cross Project, New Zealand.

Exposure time	pH	Total CN ⁽¹⁾	WAD CN ⁽¹⁾
Initial	10.2	29.4	6.8
1 day	8.0	29.4	--
3 days	8.2	30.0	--
7 days	8.2	30.0	--
14 days	8.0	31.9	--
28 days	7.3	32.0	0.33

Note: (1) All values in mg/l unless otherwise stated.

Cyanide reactions or potential reactions are listed on the left hand side of Figure 11.5. These reactions and their equations (in a somewhat simplified form) are relisted in Table 11.17. These reactions are discussed in more detail by Smith and Struhsacker (1988). In summary, the reactions include: (list of leaching).

There is now a considerable body of data on overall cyanide chemistry of effluent or pregnant solutions from leach operations. Principally, the data are concerned with cyanide losses (consumptive) within the system in terms of additional cyanide makeup requirements during operations, or meeting residual cyanide regulatory levels in a heap either for unloading or for final decommissioning. Aspects of detoxification to meet regulatory requirements are discussed by Smith and Struhsacker (1988) and Smith (1988), while Stotts (1984) gives a useful case history of operations at Stibnite, Idaho, which includes a discussion of their detoxification practices.

Work by Wharf Resources (USA) Inc. at their Annie Creek Mine, South Dakota indicates the general decline of cyanide levels both in terms of consumptive losses in the system and with water/rainfall recharge or decommissioning. Figure 11.6 gives cyanide levels versus pore volumes over time, for a rinse test of the spent ore, in comparison with a theoretical first order decay come for cyanide.

TABLE 11.17—Typical cyanide reactions in a heap leach environment.

a) Hydrolysis	$CN + H_2O = HCN + OH$
b) Oxidation of HCN/CN	$2HCN + O_2 = 2HCNO$ $2CN + O_2 + catalyst = 2CNO$
c) Hydrolysis of CNO	$HCNO + H_2O = NH_{3(8)} + CO_{3(8)}$
d) Hydrolysis/Sponification of HCN	$HC + 2H_2O = NH_4 \cdot COOH$
or	$HCN + 2H_2O = NH_3 + H \cdot COOH$
e) Aerobic Biodegradation	$2HCN + O_2 + enzyme = 2HCNO$
f) Thiocyanate Formation	$S_2 + S_2 + CN = S_{x-1} + CNS$ $S_2O_3 + CN = SO_{32} + CNS$
g) Cyanide Compound Dissociation	$NaCn = Na+ + CN$
h) Metal - Cyanide Complexation	$Zn(CN)_2 + 2CN = Zn(CN)_{24}$
i) Anaerobic Biodegradation	$CN + H_2S_{(80)} = HCNS + H +$ $HCN + HS = HCNS + H+$

From an initial cyanide level of >250 mg/l in the leach solution, the rinsate has a level of about 130 mg/l. This latter value is decreased to 57 mg/l at one pore volume and then follows the “classic” cyanide first order decay, to eventually reach levels below detection. A second cyanide “spike,” common to many rinse and drainage cycles, appears on this graph. This is due to back diffusion into the active, flowing part of the heap void sys-

TABLE 11.16—Cyanide decay in tailings pore water, Golden Cross Project, New Zealand.

Parameter ⁽¹⁾	Initial	1 Week	2 Weeks	4 Weeks	8 Weeks	12 Weeks
pH	10.2	9.7	9.1	9.8	9.8	9.0
SO2	2525	2525	2530	2370	2370	2390
Ca	858	858	858	858	808	805
Total hardness (as CaCO ₃)	2140	2140	2140	2140	2013	2008
Total CN	29.4	29.4	31.3	25.5	27	25
WAD CN	6.8	6.6	5.5	3.8	2.1	1.51
Cd	0.1	<0.01	<0.01	<0.01	<0.01	<0.01
Co	0.33	0.25	0.2	--	--	--
Cu	5	4.3	2.9	2.1	0.53	0.16
Fe	8.7	8.9	9	9.3	9.3	9.5
Zn	0.01	0.03	0.01	<0.01	0.01	0.01
Pb	<0.1	<0.1	<0.1	<0.1	--	--
Mn	0.02	0.02	<0.01	0.01	0.02	0.02
Ag	0.04	0.01	0.01	0.02	0.02	0.02
Cr	0.02	--	--	<0.02	--	--
Hg	0.0002	<0.0001	<0.0001	<0.0001	--	--

Note: (1) All values in mg/l unless otherwise stated.

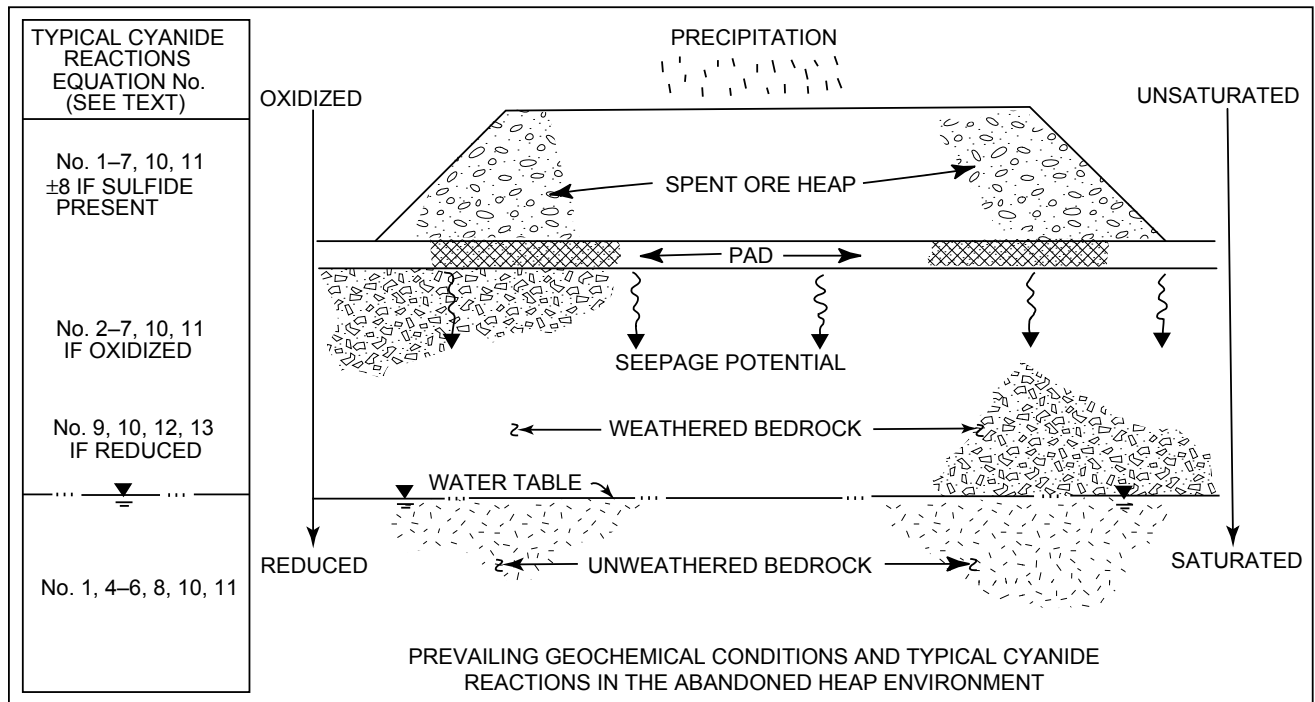


FIGURE 11.5—Prevailing geochemical conditions and typical cyanide reactions in the abandoned heap leach environment. Source: Smith and Struhsacker (1988).

tem, after the first flush of cyanide is removed. It appears to be both a time and concentration gradient-related phenomenon.

Test data from column rinse tests for a heap leach project in the western United States compare the efficiency of the various chemical treatment methods for cyanide destruction, demonstrating the dependence of cyanide chemistry on pH values, Struhsacker and Smith (1990). The data also illustrate the analytical problems associated with free cyanide determinations. Table 11.18 shows the cyanide neutralization levels and pH values achieved in the first pore volume by fresh water rinsing, acidification using sulfuric acid, and acidification coupled with other chemical treatment methods. The cyanide concentrations in the effluent from this test were determined using the total cyanide, the weak acid dissociable cyanide, and the free cyanide analytical methods.

As revealed in Table 11.18, acidification to a target pH of 7.5 in the effluent was the most effective method for reducing cyanide levels, with most of the remaining cyanide existing as free or weak acid dissociable cyanide. However, the free cyanide measurements for this case and the fresh water rinse sample are clearly specious because they exceed the total cyanide and weak acid dissociable cyanide values.

The analytical problems associated with free cyanide analyses have significant implications for projects in which the cyanide neutralization compliance criterion is expressed in terms of free cyanide. Using the pH 7.5 case as an example (Table 11.18), an operator could be deemed grossly out of compliance if free cyanide were the species designated as the neutralization criterion. However, the same effluent would be deemed much closer to compliance based upon either a total or a weak acid dissociable cyanide neutralization standard.

TABLE 11.18—First pore volume effluent pH and cyanide concentration from neutralization testing, Heap Leach Project, United States

Neutralization method ⁽¹⁾	pH achieved	Total CN	WAD CN	Free CN
Fresh water rinsing (control)	11.2	110	110	120
Acidification (pH 9) ⁽²⁾	9.1	77	57	55
Acidification plus peroxide (pH 9) ⁽²⁾	9.5	72	50	37
Acidification plus ferrous sulphate (pH 9) ⁽²⁾	8.4	42	28	38

Notes: (1) pH in standard units, all other values in mg/l
(2) Target pH of effluent

Cyanide migration in soil

In this assessment, Figure 11.5 will be utilized from the discussions on heap leach cyanide geochemistry, since the figure extends below the heap and into the subsoil system to trace cyanide migration through the soil, evaluate cyanide interactions with soil constituents and assess the cyanide degradation mechanisms in soil. As is portrayed on Figure 11.5 there is a continuous increase of the moisture content and a continuous decrease of oxygen potential with soil depth. These two factors have a significant

influence on cyanide degradation in the soil system.

Two cyanide degradation mechanisms are particularly susceptible to changes in soil moisture and oxygen content. They are volatilization and biodegradation. This is significant because these mechanisms have been shown to be the two most effective cyanide degradation mechanisms occurring in the vadose or unsaturated soil (Chatwin and Hendrix, 1988). Hence, the rate of cyanide degradation in the unsaturated or vadose zone is seen to be more rapid than that found in the saturated zone. Cyanide degradation mechanisms effective in soils include:

- volatilization
- biodegradation
- adsorption and precipitation
- hydrolysis.

Cyanide volatilization

Two major factors control volatilization in soils. First is the solution pH, which controls cyanide hydrolysis to HCN and has been discussed previously. The second factor is the availability of continuous vapor path, by which the HCN vapor can migrate from the cyanide solution. Figure 11.6 shows an illustration of an unsaturated zone where continuous vapor phase transport is available, (Chatwin, 1990).

Other properties upon which cyanide volatilization in soils would be dependent are the cyanide solubility in water, HCN vapor pressure, and cyanide concentration in the solution. Soil properties that affect the HCN volatilization include: the soil water content, sorptive and diffusion characteristics of the soil, and bulk properties of the soil such as organic matter content, porosity, density, and clay content. Meteorological parameters that would affect HCN volatilization are airflow rate over the soil, humidity, and temperature.

Cyanide in the soil may be partitioned between the soil water, soil air, and the soil solids. Considered as a whole, the soil represents all three phases of matter rather than one. The atmosphere constitutes another air compartment which is distinct from the soil

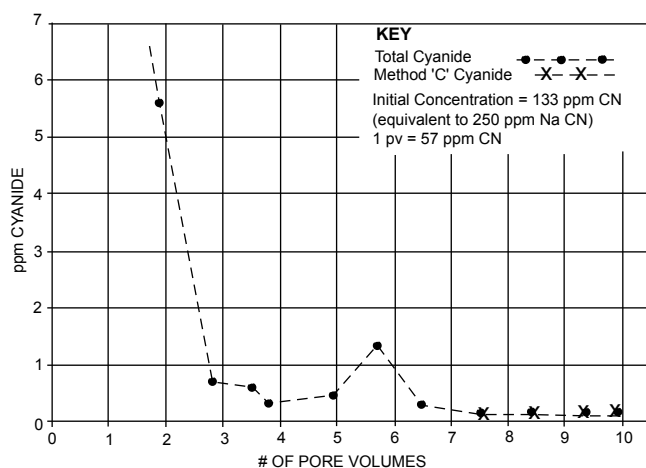


FIGURE 11.6—Reduction of cyanide concentrations versus pore volumes. Source: Smith and Brown (1986), Wharf Resources, Annie Creek Mine, South Dakota.

air. The rate of volatilization of a HCN molecule from a sorption site on the solid phase in the soil (or in solution in the soil water) to the vapor phase in soil air and then to the atmosphere is dependent on the physical and chemical properties of both HCN and the soil, and on the process of moving from one phase to another.

Biological degradation

The upper, oxidized portions of the soil where the conditions are aerobic, biological process may consume cyanide and generate cyanate as shown in Table 11.17 (Towill et al., 1978). The hydrogen cyanide is in turn hydrolyzed into ammonia and carbon dioxide.

From testing of saturated and unsaturated soils, it was found that the oxidation of cyanide is much more effective in the unsaturated zone; almost 25 times more effective in unsaturated soils (Chatwin and Trepanowski, 1987); who showed that the unsaturated soils had substantial bacterial growth (10^9 counts per gram) versus none in the saturated soils. This is consistent with the studies by Fuller (1984) in his comparison of aerobic and anaerobic cyanide removal in soil. Coburn (1949) found the toxic limit for effective anaerobic degradation of cyanide to be about 2 mg/l in a waste stream.

Adsorption and precipitation

Two mechanisms that appear equally effective under both saturated and unsaturated conditions are precipitation and adsorption. These two mechanisms are placed together because it is difficult to separate them. However, in a soil column/cyanide solution system where the cyanide concentration is in hundreds of mg/l it is extremely difficult to determine if the cyanide being removed as a precipitate, an insoluble ferrocyanide, or as cyanide adsorbing on material surfaces in the soil.

In tests with free cyanide solution in soils, it has been found that cyanide attached to soil particles correlates well with soil organic carbon content. Western U.S. subsoils tested showed organic carbon contents ranging from 0.1 to 1.2% with a mean of 0.6% (Chatwin and Trepanowski, 1987). They showed that the organic carbon in the soil could adsorb about 12 ppm cyanide from a 130 ppm solution as it traveled one foot through the soil, or about 0.5 grams of free cyanide adsorbed per gram of contained organic carbon.

Additional studies with pure mineral components (Chatwin and Hendrix, 1988) indicated that free cyanide will also adsorb on inorganic surfaces such as clays and feldspars with a combined removed cyanide in a range from about 20 to 80% of the input concentration of cyanide.

Hydrolysis

As the system pH falls, HCN can be hydrolyzed by a different mechanism to give formate, as either formic acid or ammonium formate. The system pH will determine the extent of formation of each compound, a lower pH favoring formic acid formation.

It is a fact that, in many natural soil environments, cyanide reacts and is "lost" from the solution phase of the system in both field observations and laboratory data. For example, data from Witwatersrand, South Africa given by Smith et al. (1985a), shows

a distinct lack of impact from tailings seepage in terms of cyanide, while the evidence of seepage impact from other species is present in ground water around and below gold tailings facilities.

Glynn (1983), who researched cases of cyanide contamination of ground water from cyanide bearing waste facilities could find few examples of impact. Of the cases located, the effects of subsite hydrogeochemical attenuation were very pronounced. The salient points of this selection of case histories are noted below:

1. Byron, Illinois (Gilkerson et al., 1977)
 - Source: 1500, 30–55 gallon drum of industrial wastes containing metals and cyanide. Many drums punctured
 - Concentration of cyanide up to 10,300 mg/l
 - Cyanide levels detected in ground water at 3 km were at a maximum concentration of 0.02 mg/l, about 10% of the drinking water cyanide criteria
 - No samples in any ground-water sample exceeded the drinking water criterion
2. Cologne Bight, (Effenberger, 1964)
 - Source, gravel pit containing 30,000 m³ of cyanide bearing waste from chemical industry
 - Concentration at 600 meters up to 0.2 mg/l
 - No hazard as cyanide form was as a hexacyanoferrate
3. Flat River Tungsten, NWT, Canada (Sigma Resources Consultants, 1981)
 - Source: cyanide bearing tungsten mill tailings
 - Seepage from tailings into a sand and gravel aquifer and then to river
 - Concentration in ground water less than 0.1 mg/l and no impact on river
 - Cyanide removed due to surface complexing and precipitation
4. Ladybank, Fife, Scotland (Parker and Mather, 1979)
 - Source: cyanide bearing waste from gasworks
 - Cyanide concentration in aquifer immediately below site down to 0.2 mg/l and 0.004 mg/l 200 meters from site

Taken together, these “real-life” examples indicate the fate of cyanide, not only in the ground water itself, but particularly as a result of reactions occurring also in the unsaturated zone between the source of cyanide and the ground water itself.

Quantification of the effects of hydrogeochemical attenuation has been made in overall studies. A detailed study of cyanide “loss” by dilution, degradation (decay), and geochemical attenuation was given by Smith and Brown (1986), for the proposed spent ore disposal site at Wharf Resources, Annie Creek Mine, South Dakota. Table 11.19 illustrates partition coefficients for cyanide attenuation in a variety of subsite materials. There is clearly variation in cyanide reactions with differing types of material, with the weathered materials, (i.e., clay and slate) being better cyanide attenuators than the basal limestone.

The cyanide attenuation and degradation mechanisms that appear to be effective in ground water are adsorption, chelation and precipitation, bacterial degradation, and hydrolysis to formate. Volatilization may also occur but only if there is a pathway by which the HCN can escape from the ground water, Chatwin (1990). The cyanide degradation/attenuation mechanisms listed above are affected by the following parameters: the metal and oxygen content of the ground water, the ground-water pH, and the aquifer mineral content including clay, feldspar, organic carbon, free metals, and (or) metal oxides, based on data from Chatwin and Hendrix, 1988 and Chatwin, 1990. In unconfined aquifers, a capillary fringe would be located above the ground-water table.

The ground-water fringe would be saturated particularly near the aquifer interface and gaseous pathways for HCN migration would be limited or nonexistent. In confined aquifers, the available pathways would be more limited and gaseous migration of HCN from the aquifer would quite small.

TABLE 11.19—Attenuation calculation summary distribution coefficients (ml/g), Wharf Resources Annie Creek Mine, South Dakota.

Material	Sample	Pore volume	Total cyanide	Free cyanide	Arsenic
Clay	1.1	1	1.95	3.42	430
		3	4.0	8.12	--
	1.2	1	1.30	1.48	426
Shale	2.1	3	10.81	33.31	--
		1	0.66	0.69	--
	4	1.93	0.84	667	
Rubble	2.2	1	0.65	0.93	334
		4	1.26	1.04	65.10
	3.1	1	1.25	1.93	98.88
Limestone	3.2	3	0.93	1.33	--
		1	1.60	2.41	98.88
	3	0.83	1.18	--	
	4.1	1	9.06	0.03	--
		3	0.09	0.04	--
4.2	1	0.06	0.03	--	
3	0.07	0.07	--		

While the migration mechanisms for HCN escape from the ground water are slow, it is not necessary for the HCN to leave the soil, but just to leave the aquifer to decrease ground-water concentrations of cyanide. Hence, substantial amounts of HCN can be trapped or isolated in the capillary fringe or soil above the aquifer and not report in an analysis of the ground water. As long as a storm event or precipitation does not drive the isolated cyanide back down into the ground water, it can be slowly removed by biological degradation or hydrolysis to formate in the unsaturated zone.

It should be stressed that there needs to be a distinction made between overall cyanide degradation or decay in soils/rocks and geochemical/hydrogeochemical decay of cyanide. If the decay component of volatilization is removed, some geological material may have little or no capacity for cyanide degradation. For example, geochemical studies on a cemented conglomerate material below a tailings facility in the United States showed that, when tested in an inert (argon-rich) environment with no available pathway for gas losses, there was no appreciable cyanide decay in the system (Smith, 1989, unpub. data).

Cyanide in ground water

The ground-water cyanide geochemical system is similar to that which may be found in saturated soils.

From bench-scale testing of saturated soil columns, Chatwin and Hendrix (1988), found that chelation followed by iron cyanide precipitation is one of the more effective methods of removing free cyanides and this can occur in saturated conditions in ground water. This mechanism requires the formation of a ferrocyanide complex combined with available iron or other transition metals to precipitate the cyanide. The precipitation of insoluble ferro-

cyanide compound occurs over a pH range of 2–11 as demonstrated by Hendrickson and Daignault (1973).

Bacterial degradation in saturated ground water is usually anaerobic due to the low oxygen content of the ground water. However, even in very low oxygen environments (<1 mg/l dissolved oxygen), aerobic degradation will occur. In general, ground-water cyanide bacterial degradation is slower than that found in the vadose or unsaturated soil, due to the lack of nutrients, inadequate mixing, and minimal oxygen.

The process of hydrolysis of cyanide to formate in ground water is slow. The rate of cyanide hydrolysis to formate is about 2 to 4% per month. However, this rate increases with increasing temperature. The activation energy found from an Arrhenius plot was 87 ± 5 kJ per mol (Hoecker and Muir, 1987). At this activation energy the hydrolysis rate would increase by 2.5 times for every 10°C increase in temperature.

There are documented examples of cyanide in ground-water systems, due to waste disposal activities. Braids et al. (1977), Goyal et al. (1981), and Kahar and Bhatragar (1981) have all described case histories of cyanide in ground water due to industrial effluent discharge or by seepage from industrial waste disposal sites. In each case, the apparent source term mass ("major leaks") appear to have overwhelmed the cyanide attenuation capacity of the subsite materials. The absence of impact on ground-water quality from mining waste facilities have already been cited from field case studies in earlier parts of this chapter. For example, the data from the Witwatersrand, South Africa, (Smith et al., 1985a) shows a distinct lack of impact from gold mine tailings seepage in terms of cyanide, while there is evidence of impact from other tailings-related species. Glynn (1983) notes a similar absence of ground-water quality impact from the Flat River Tungsten tailings, NWT, Canada, as well as from two cases of industrial waste disposal and disposal of wastes from coal gas production, the examples coming from Europe and the United States. The evaluations by Smith and Brown (1986) on the Annie Creek Mine, South Dakota and of Smith et al. (1985b) from the Cannon Mine geochemical testing program tend to confirm the field observations.

In addition there are many mine tailings and heap leach facilities in Arizona, California, Nevada, South Dakota, and South Carolina where routine ground-water monitoring program during operations demonstrate no impact of cyanide on ground-water quality. This lack of effect on ground-water quality may well be a function of the low source term concentrations of cyanide, (typically in the range of 100 to 300 ppm cyanide), the relatively low mass loading from the mine waste facilities. In many cases have substantial unsaturated zones below the facilities themselves which have demonstrated abilities to attenuate cyanide.

REFERENCES

- Alesii, B.A., and Fuller, W.H., 1976, The mobility of three cyanide forms in soil: EPA-600/9-76-015, U.S. Environmental Protection Agency, Cincinnati, Ohio.
- ASCI/SRK, 1990, An evaluation of the effectiveness of rinsing procedures on cyanide removal from spent heap leach ore; Brohm Mining Corporation, Lead, SD, USA: for State of South Dakota, September.
- ASTM, 1985, Water and environmental technology, sec. II, v. 11.02.
- Bernardin, F.E., 1973, Cyanide detoxification using adsorption and catalytic oxidation on granular activated carbon: Journal of Water Pollution Control Federation, v. 45, p. 221.
- Bishop, E., and Wright, D.T., 1977, Oxidation of cyanides: U.S. Patent 4,024,037, Chem. Abs. 87:31152b.
- Broderius, S., and Smith, L., 1980, U.S. EPA, Grant No. R805291.
- Burden, R.J., and Kidd, C.H., 1987, The environmental fate of cyanide in gold mine process tailings: Proc. Ann. Conf. AIMM, Nelson, New Zealand.
- Caldwell, J., and Smith, A., 1985, Material considerations in the design of downstream embankments for tailings impoundments: Mining Sci. Tech. No. 3, Elsevier Sci Publ., Amsterdam, Holland.
- Caruso, S.C., 1975, The chemistry of cyanide compounds and their behavior in the aquatic environment: Carnegie Mellon Institute of Research.
- Chatwin, T.D., 1990, Cyanide attenuation/degradation in soil—Final Report: Resource Recovery and Conservation Company, Salt Lake City, Utah.
- Chatwin, T.D., and Hendrix, J., 1988, The fate of cyanide in soils: Randol Gold Forum 88, Scottsdale, Ariz., Feb. 23–24, p. 343.
- Chatwin, T.D., and Trepanowski, J.J., 1987, Utilization of soils to mitigate cyanide releases: Proc. 3rd Western Reg. Conf. on Precious Metals, Coal, and Environment, Rapid City, South Dakota, Sept. 23–26, p. 151.
- Chester Engineers, 1977, Report on the Lower Monongahela River study—Water quality conditions, point and nonpoint source waste loads allocations, Vols. 1 and 2: prepared for the U.S. Steel Corp., Corapolis, Penn.
- Coburn, S.E., 1949, Limits of toxic waste in sewage treatment, Sewage Works Journal, v. 2, p. 522.
- Conn, K., 1981, Cyanide analysis in mine effluents—Cyanide and the gold mining industry: Technical Seminar, Ottawa, Ontario.
- Damon, L., Smith, A., and Mudder, T., 1991, Geochemical study of leach pad cyanide neutralization: Brohm Mining Company, Lead, S. Dakota.
- Dodge, B.F., and Zabbon, W., 1952, Disposal of plating room wastes IV—Batch volatilization of hydrogen cyanide from aqueous solutions of cyanides: Plating, p. 39.
- Doudoroff, P., 1980, A critical review of recent literature on the toxicity of cyanides to fish: American Petroleum Institute, Washington, D.C.
- Ecological Analysts, Inc., 1979, Cyanide—An overview and analysis of the literature on chemistry, fate, toxicity and detection in surface waters: Prepared for inter-industry cyanide group.
- Effenberger, E., 1964, Verunreinigungen eives Grund-wassers durch cyanide Arch. Hyg. Bakteriol.: v. 148, no. 4–5, Munich, pp. 271–287.
- Ford-Smith, M., 1964, The chemistry of complex cyanides—A literature survey: Her Majesty's Stationery Office, London.
- Frank, S.N., and Bard, A.J., 1977, Heterogeneous photocatalytic oxidation of cyanide ion in aqueous solutions with TiO₂ Powder: Journal of the American Chemical Society, v. 99, Jan. 5, pp. 303–304.
- Fuller, W., 1980, Soil modification to minimize movement of pollutants from solid waste operations: CRC Critical Reviews in Environmental Control, March, pp. 213–270.
- Fuller, W., 1984, Cyanides in the environment with particular attention to the soil, cyanide and the environment: v. I, Colorado State Univ., Fort Collins, Colo., pp. 19–46.
- Fuller, W., 1989, Investigation of landfill leachate pollutant attenuation by soils: EPA-600/2-78-158, U.S. EPA, Cincinnati, Ohio, p. 239.
- Gilkerson, R.H., Cartwright, K., Folmer, L.R., and Johnson, R.M., 1977, Contribution of surficial deposits, bedrock, and industrial wastes to certain trace elements in groundwater: Proc. Ann. Eng. Geol. Soils. Eng. Symp., v. 15, pp. 17–38.
- Glynn, P., 1983, Cyanide behaviour in groundwater environments, BSc. Dissertation: Groundwater Research Institute, University of Waterloo, Canada.
- Goyal, M.R., Abrol, O.P., and Vihra, V.K., 1981, Pollution of upper aquifer in Punjab, India: Quality of Groundwater, Proceedings of an Internat Symposium, Noordvijkherhout, Netherlands: Studies in Environmental Science, v. 17.
- Hendrickson, T., and Daignault, L., 1973, Treatment of complex cyanide compounds for reuse or disposal: U.S. Environmental Protection Agency, Report No. EPA R2-73-269, p. 151.
- Hendrix, J., Nelson, J., and Ahmadiantehrani, M., 1987, Cyanide in pre-

- cious metals mill tailings impoundments: AIME Annual Meeting.
- Hoecker, W., and Muir, D., 1987, Degradation of cyanide: The AusIMM Adelaide Branch, Research and Development in Extractive Metallurgy.
- Huiatt, J., Kerrigan, J., Olson, F., and Potter, G., 1982, Cyanide from mineral processing: Proceedings of a Cyanide Workshop, U.S. Bureau of Mines, Salt Lake City, Utah.
- IEC, Ltd., 1979, Polysulphides for conversion of cyanides to thiocyanate in gold mining effluents: Fisheries and Environment Canada, Burlington, Ontario.
- Ingersoll, D., Harris, W., Bomberger, D., and Coulson, D., 1981, Development and evaluation of procedures for the analysis of simple cyanides, total cyanide, and thiocyanate in water and wastewater: U.S. EPA, EPA600/u-83-054.
- Kahar, V.P., and Bhatragar, N.C., 1981, Groundwater pollution due to industrial effluents in Ludiane, India: Quality of Groundwater Proc. International Symposium, Noordwijkerhout, Netherlands, Studies in Environmental Science, v. 17.
- Kidd, C.H., 1988, Prediction of solute transport from gold mine tailings, Coromandel, New Zealand: Proc. 3rd Internat'l Mine Water Conf. Melbourne, Australia.
- Koch, W.M.F., 1983, The determination of trace levels of cyanide by ion chromatography with electrochemical detection: National Bureau of Standards Journal of Research.
- Kunz, R.G., Casey, G., and Huff, J., 1979, Refinery cyanides, a regularity dilemma: *Hydrocarbon Processing*, 57 (10), pp. 98-106.
- Longe, G.K., and DeVries, F.W., 1988, Some recent considerations on the natural disappearance of cyanide, economics and practice of heap leaching in gold mining: Cairns Queensland, Australia.
- McGill, S.L., Hendrix, J., and Nelson, J., 1985, Cyanide/thiocyanate reactions in tailings: Cyanide and the Environment, v. 1, Colorado State Univ., Fort Collins, pp. 143-159.
- Milne, D., 1950, Equilibria in dilute cyanide waste solutions: *Sewage and Industrial Wastes*, v. 22, no. 7, July, pp. 904-911.
- Miles, A.M., 1981, A study of the photocatalytic effects of aqueous suspensions of platinum semiconductor materials on the reactions rates of candidate redox reactions: LAR-12171, National Aeronautics and Space Admin., Hampton, Va.
- Mudder, T.I., and Goldstone, A., 1989, The recovery of cyanide from slurries: Proc. Randol Conference Gold and Silver Recovery Innovations Phase IV Workshop, Sacramento, California.
- Murmann, R.P., and Koutz, F.R., 1972, Role of soil chemical processes in reclamation of wastewater applied to land: *Wastewater Mgmt. by Disposal on the Land, Spec. Report 171*, U.S. Army Cold Regions Research and Engg. Lab., Hanover, N.H., pp. 48-76.
- Palaty, J., and Horokova-Jakubu, M., 1959, The course and rate of removal of cyanides from water under natural conditions: *Faculty of Technology of Fuel and Water*, v. 3, part 1, Prague, Czech.
- Parker, A., and Mather, J.D., 1979, An investigation into pollution from a disused gasworks site near Ladybank, Fife: AERE-R 9213, Harwell, p. 19.
- Pohlandt, C., 1984a, The determination of cyanide in hydrometallurgical process solutions and effluents by ion chromatography: Report No. M128, Council for Mineral Technology, Randburg, South Africa.
- Pohlandt, C., 1984b, The determination of cyanides in the hydrometallurgical processing of gold: Proc. Cyanide and the Environment Conference, Tucson, Ariz.
- Pohlandt, C., 1985, Chromatographic separation and determination of stable metal cyanide complexes in gold processing solution: *South African Journal of Chemistry*, 38 (3), pp. 110-114.
- Pohlandt, C., Jones, E., and Lee, A., 1983, A critical evaluation of methods applicable to the determination of cyanides: *Journal of the South African Institute of Mining and Metallurgy*, pp. 11-19.
- Rocklin, R., and Johnson, E., 1983, Determination of cyanide, sulfide, iodide, and bromide by ion chromatography with electrochemical detection: *Analytical Chemistry* 55, pp. 4-7.
- Schmidt, J.W., Simovic, L., and Shannon, E., 1981, Natural degradation of cyanides in gold milling effluents: Proc. Sem. Cyanide and Gold Mining Industry Seminar, Environment Canada, Jan. 22-23, Ottawa, Ontario.
- Scott, J., and Ingles, J., 1987, State-of-the-art processes for the treatment of gold mill effluents: Mining, Mineral, and Metallurgical Processes Division, Industrial Programs Branch, Environment Canada, Ottawa, Ontario.
- Sigma Resources Consultants Ltd. and Golder Associates Ltd., 1981, Summary Report, Waste Management System: Tungsten, NWT, SRCL 3258, for the Canada Tungsten Mining Corporation.
- Simovic, L., Snodgrass, W., Murphy, K., and Schmidt, J., 1985, Development of a model to describe the natural degradation of cyanide in gold mill effluents: Cyanide and the Environment, v. II, Colorado State Univ., Fort Collins, pp. 413-432.
- Smith, A., 1985, Applied hydrogeochemistry in mining wastes disposal: Proc. of Dunham-Dumam Symposium, Dumam, UK, Pub. Spec. Vol., IMM, London.
- Smith, A., 1987, Testimony to Department of Health and Environmental Control: South Carolina Permit No. SC 0041378 Appeal Hearing, December, Columbia, S.C.
- Smith, A., 1988, The management of cyanide in the gold mining industry: Seminar Proceedings, AGC, November, Australia.
- Smith, A., Unpub. test data, 1989/1990.
- Smith, A., and Brown, A., 1986, The potential for cyanide migration from the Annie Creek Processing Facility: Rept. no. 1086/2 to Wharf Resources (USA), Inc., SRK, Lakewood, Colo.
- Smith, A.C.S., and Mudder, T.I., 1991, Chemistry and treatment of cyanidation wastes: Mining Journal Books, London, England, 365 pp.
- Smith, A., and Struhsacker, D.W., 1988, Cyanide geochemistry in an abandoned heap leach system and regulations for cyanide detoxification—Introduction to evaluation, design, and operation of precious metal heap leaching projects; in Van Zyl, D., Hutchison, I., and Kiel, J. (eds.), *Soc. of Mining Eng./Am. Inst. of Mining and Metallurgical Eng.*
- Smith, A., Dehrmann, A., and Pullen, R., 1985a, The effects of cyanide-bearing, gold tailings disposal on water quality in Witwatersrand, South Africa; in Van Zyl (ed.), *Cyanide and the Environment*, Tucson, Ariz.: Colorado State Univ., Fort Collins, pp. 221-229.
- Smith, A., Moore, D., and Caldwell, J., 1985b, Prediction of groundwater impact of tailings disposal: Proc. 2nd Annual Can/Am Conf. on Hydrogeology, Baniff, Alberta, Canada.
- Standard Methods for the Examination of Water and Wastewater, 1998, 20th ed., APHA-AWWA-WPCF.
- Stotts, W.G., 1984, Handling cyanide at Superior Mining Company's stibrite heap leaching operation: Cyanide and the Environment, Conference, Tucson, Ariz., pp. 231-247.
- Strobel, G.A., 1967, Cyanide utilization in soil: *Soil Science*, v. 103, no. 4, pp. 299-302.
- Struhsacker, D.W., and Smith, A., 1990, Cyanide neutralization and reclamation of heap leach projects: Proc. Planning, Rehabilitation and Treatment of Disturbed Leads, Symposium, Billings, Mont.
- Towill, L., Drury, J., Whitefield, B., Lewis, E., Galyan, E., and Hammons, A., 1978, Reviews of the environmental effects of pollutants: V. Cyanides, EPA-600/1-78-027, U.S. EPA, Cincinnati, Ohio.
- U.S. EPA, 1977, The prevalence of subsurface migration of hazardous chemical substance at selected industrial waste land disposal sites: EPA/530/SW-634.
- U.S. EPA, 1986, Test methods for evaluating solid waste: SW-846, 3rd ed., v. IC, chap. 7, sec. 7.3.
- Weast, R.C. (ed.), 1969, Handbook of chemistry and physics: 50th ed., Chemical Rubber Publishing Co., Cleveland, Ohio.
- Whitlock, J., Sharp, C., and Mudder, T., 1981, Interferences in cyanide analysis—Reflux methods: Homestake Mining Co., unpub. results.
- Williams, H.E., 1915, Cyanide compounds, E. Arnold, London.
- Zaidi, A., Schmidt, J.W., Simovic, L., and Scott, J., 1987, The art and science of treating wastewaters from gold mines: Annual Operator's Conference, Jan. 20-22, Ottawa, Ontario.

Chapter 12

FIELD METHODS FOR SAMPLING AND ANALYSIS OF ENVIRONMENTAL SAMPLES FOR UNSTABLE AND SELECTED STABLE CONSTITUENTS

W.H. Ficklin¹ and E.L. Mosier²

U.S. Geological Survey, Box 25046, MS 973, Federal Center, Denver, CO 80225-0046

¹Deceased; ²Retired

INTRODUCTION

Water is an important agent in the chemical weathering of mineral deposits, mine tailings, waste rock, settling ponds and landfills, and in the dispersion of contaminants from these sources into the aquatic environment. The vast numbers of possible mineral assemblages and the complex chemical reactions that accompany mineral-water interactions result in a limitless variety of fluid compositions. For example, the variability in compositions of mine-drainage waters from a variety of active and inactive metal mines with diverse geologic characteristics are listed in Table 12.1.

In assessing water-quality characteristics, considerable care must be administered during the collection, preservation, and analysis of water samples. Analytical results from an improperly collected sample are at best questionable and at worst worthless. An excellent manual that documents field data collection and analysis procedures used by the U.S. Geological Survey (USGS) for water and fluvial sediments has been published by Fishman and Friedman (1989). Other equally authoritative manuals on

water analysis are available (American Society for Testing and Materials, 1992; American Public Health Association et al., 1992; United States Environmental Protection Agency, 1983). The purpose of this chapter is to describe a number of field sampling and analysis techniques that are commonly used in acid-mine drainage and related mining-environmental water studies. Many of the techniques described here are for on-site measurements; others are for analysis of selected constituents that can be determined in the field, but that are more practically determined in the laboratory. For each method given, the general points covered are application, principle of the method, apparatus and reagents required, and a detailed description of the method including interferences, sample collection and preservation protocol, and reporting units and significant figures.

FIELD ANALYSIS OF AQUEOUS PARAMETERS

Because some dissolved chemical constituents are unstable, their concentrations or intensities must be determined on site.

TABLE 12.1—Selected analytical results for water samples collected from mines and tunnels throughout Colorado (Ficklin et al., 1992). Results for alkalinity and dissolved oxygen are previously unpublished data.

Type of mine mg/l	Cu mg/l	Zn mg/l	Pb	Sp. cond. mS/cm	pH	Sulfate mg/l	Alkalinity mg/l as CaCO ₃	Diss. oxygen mg/l
Pyrite veins, Au Argo Tunnel	4.5	30	0.04	4000	2.9	2100	ND ⁽¹⁾	10
Epithermal Au Blackstrap	500	700	0.06	38000	1.8	128000	ND	ND
Au, Ag, Te veins Carlton Tunnel	0.001	0.11	<0.005	2800	7.7	1200	270	7.5
Fringe of porphyry Mo Chapman Gulch	0.001	0.04	<0.005	1400	7.9	600	66	8.0
Epithermal Ag, Pb, Zn Rawley Tunnel	1.2	33	0.005	900	6.0	600	50	0.3
Epithermal Au Reynolds Tunnel	9.3	18	0.21	3200	2.9	1900	ND	10
Ag-Pb replacement Ruby Mine	<0.001	0.02	<0.005	230	7.8	5	98	6
Epithermal Ag, Pb, Zn Solomon Mine	0.04	26	1.1	790	4.5	310	ND	9
Polymetallic veins and carbonate replacement Yak Tunnel	2.4	69	0.01	980	4.4	640	ND	7.5

⁽¹⁾Not determined.

TABLE 12.2—Table of water parameters that must or can be determined in the field. Those designated by (+) must be determined in the field, those with (-) are optional.

Constituent	Useful range	Method	Alternative	Reference
+ Temperature		Centigrade Thermometer		
+ pH	1 to 11 pH units	Potentiometric	Colorimetric	1
+ Specific Conductance	0 to 5,000 mS/cm	Meter		1
+ Dissolved Oxygen	0 to 12 ppm	Sealed ampoule	Meter; Winkler titration	2
+ Redox Potential		Pt electrode		3
+ Ferrous Iron	0 to 20 mg/l more with dilution	Colorimetric		4
- Total Dissolved Iron	0 to 20 ppm	Colorimetric	AAS, ICP-ASS	3
- Sulfate	50 to 50,000 mg/l more with dilution	Turbidimetric	Ion chromatography	2
- Alkalinity	10 mg/l and up	Titration	Titration cell; CO ₂ gas extraction	1
- Copper	0 to 5 mg/l	Colorimetric	Atomic absorption, ICP-AES	5
- Heavy metals	0 to 5 mg/l	Colorimetric	Atomic absorption, ICP-AES	6

References:

- 1) Fishman and Friedman (1989)
- 2) Commercial kit
- 3) American Public Health Association et al. (1985)
- 4) Canney and Hawkins (1958)
- 5) Bloom (1955)
- 6) Wood (1976)

Table 12.2 lists the determinations that must be made at the sample site along with some other parameters that are easily determined on site. This list is not meant to be restrictive because new field methods are continually being developed and, depending on the equipment available and skill and ingenuity of the field investigator, a broad spectrum of analyses can be made at the sample site. To reduce sampling errors and to minimize sampling-related data variations, all field determinations, site observations, and type of samples collected should be recorded on a field data form similar to the one shown on Figure 12.1. Site observations should include; location, date and time of day, weather and approximate intensity of sunlight, previous weather conditions if known (e.g., recent storms), description of water (e.g., color, odor, turbidity, algae, etc.), topography, type of site (e.g., adit, open pit, waste dump, spring/seep, etc.), description of streambed, and approximate flow rate.

Measurement of flow rates

In order to obtain an estimate of the metal loadings resulting from water draining mine sites or unmined mineralized areas, an estimate of the discharge or flow rate is required. Detailed discussions on stream-flow measurements are given by Brassington (1988, p. 100) and Fetter (1988, p. 54).

For small discharges such as seeps or small springs, a visual estimate or catchment in a quantified container versus a specified period of time (e.g., liters per minute) is generally all that is necessary. To obtain very accurate measurements, it is essential that all the flow goes into the container during the specified period of time.

Estimating the stream-flow rate of larger discharges requires more elaborate procedures that determine water velocity and the

channel cross-sectional area or that involve the installation and use of a weir. When using the velocity-area method, a number of velocity and depth measurements across the stream are required to obtain the most accurate cross sectional area and average velocity; this is because stream velocity and depth vary considerably from bank to bank across the stream. The stream cross section can be divided into subsections, and representative flow and depth measurements can be made at the centroid of each subsection. The cross sectional area of each subsection is calculated from the depth and width of the subsection. Ideally, the velocity of each subsection should be determined by a current meter, a device (similar to an anemometer used to measure wind velocity) that measures flow based on the rotational speed of cups around a central rod; when using a current meter, field studies have shown that the velocity measured at a depth equal to 0.6 times the total stream depth is very close to the average velocity for the entire vertical subsection of stream. If a current meter is not available, a rough estimate of velocity for each stream subsection can be made by timing a small float (e.g., a stick or fishing bobber) over a measured downstream distance of a few meters; because the surface velocity measured by the float is significantly greater than the average stream velocity, it is important to correct the measured value by multiplying it by 0.75. By either method (flow meter versus float) the flow rate (q), as cubic meters per second, for a subsection of stream is calculated from the equation:

$$q = va \quad [1]$$

where v is the average velocity in meters per second and a is the cross-sectional area measured in square meters. To convert to liters per second, simply multiply by 1,000. The total flow for the

USGS FIELD DATA FORM FOR WATER SAMPLING

SITE ID. _____ Lat. _____ Long. _____ Topo. Quad. _____

Site Description: _____ Date: _____ Time: _____

Weather: _____

Air Temp: _____

Measurements	Samples Collected	Corroborated	Isotopes
Water Temp: _____	RU _____	RU _____	H-O _____
	FU.45 _____	FU.45 _____	Pb: _____
pH: _____	FU.2 _____	FU.2 _____	CO ₃ ⁼ _____
Buffers: _____	FU.1 _____	FU.1 _____	SO ₄ _____
pH calibration check:			ml _____
Buff: _____ meas. _____	RA1 _____	RA1 _____	pH _____
Buff: _____ meas. _____	RA2 _____	RA2 _____	ml Ba _____
	RA3 _____	RA3 _____	_____
Spec. cond.: _____			
Diss. Ox.: _____	FA.45 _____	FA.45 _____	Isotopes
Alk: _____	FA.2 _____	FA.2 _____	Corroborated
H ₂ S _____	FA.1 _____	FA.1 _____	H-O: _____
SO ₄ _____			Pb: _____
Thiosulf: _____	Hg F.45 _____	Hg F.45 _____	CO ₃ ⁼ _____
Fe ²⁺ : _____	Hg F.2 _____	Hg F.2 _____	SO ₄ _____
Fe tot: _____	Hg F.1 _____	Hg F.1 _____	_____
Nitrite: _____	HgR _____	Hg R _____	_____
Nitrate: _____	Fe ₂₊ _____	Fe ₂₊ _____	Sediments
CN ⁻ _____	CN FU: _____	CN FU: _____	
SCN ⁻ _____	_____	_____	

Affirmed by: _____ Date: _____

FIGURE 12.1—Example of a field data form that can be used in a study collecting water samples for analysis.

stream can be then calculated by adding the flow for each of the subsections.

A weir is a small dam with a spillway opening of a specified shape and area that restricts the size of the stream channel. These devices provide the most accurate method of measuring the flow of a stream; however, they require significant effort to install and calibrate. The rate at which water flows over the weir (calculated from the weir size and cross sectional area of the weir opening, coupled with the water depth behind the weir) determines the flow rate of the stream.

Temperature

For all sites where water samples (for example, drinking, surface, domestic, saline, waste, mine drainage, and industrial waters) are collected, measurements of water and air temperature should be viewed as essential. Measurements may be made with any good grade of mercury-filled or dial-type centigrade thermometer and are reported to the nearest centigrade degree. Water temperature is determined within the parent body of the system being studied, e.g., stream flow or pond. Air temperature is determined in any shaded area that is representative of the field site. Allow sufficient time for the thermometer to stabilize. To prevent loss or breakage, the thermometer should be equipped with a metal or plastic sheath and a pocket clip for carrying.

pH

The pH of a water sample is an essential measurement in any environmental study, and is applicable for all ground, surface, mine, tailings, and industrial water samples. The pH is defined as the negative logarithm of hydrogen ion activity in a given solution. The quantity of hydrogen or hydroxyl ions in a solution determines whether the solution is acid or alkaline. The scale of ordinary pH values extends from 0 to 14. A 1 N¹ strong acid corresponds approximately to a pH of 0, a 1 N alkali solution to a pH of 14. The pH of a neutral solution is 7. Thus the range of acid pH-values extends from 0 to 7, and that of alkaline values from 7 to 14. In many metal mines, the aqueous oxidation of pyrite produces acid through a complex series of reactions (Nordstrom and Alpers, 1999; Stumm and Morgan, 1981); however, Ritcey (1989, p. 413) lists pH readings from 2 to almost 8 in a variety of Canadian mine-tailings waters.

The most appropriate place to determine pH is at the sample site, perhaps right in the stream or pond. The pH of samples that are stored for any length of time probably have little or no resemblance to the actual pH of the system being studied. For example, dilute waters with near-neutral initial pH values can shift substantially in pH as they equilibrate with atmospheric carbon dioxide. In acid-mine waters containing high levels of iron or aluminum, field-determined pH is generally higher than pH determined later in the laboratory due to the precipitation of iron hydroxides and the resulting production of hydrogen ions (Nordstrom and Alpers, 1999).

All pH values are determined either by:

- 1) some variation of colorimetric methods that use a variety of indicators, or
- 2) the electrometric determination of potentials with the aid of suitable electrodes and a meter.

Colorimetric methods involve the use of indicator dyes that change color at definite pH values. These methods do not require trained staff or expensive instrumentation but do require that the person making the measurements not be color-blind. The most basic colorimetric method is the use of litmus paper. With litmus paper, one can determine whether a solution is acidic or basic. A more accurate means of making pH measurements is with the use of papers impregnated with pH-sensitive dyes. These are made from high-class filter paper impregnated with suitable indicator solutions covering various pH ranges. The paper is dipped into a solution and the color that develops is compared to a color scale supplied with the paper. These measurements are semi-quantitative but, with appropriate papers, pH can be determined to within about 0.5 pH units. The so-called pH indicator papers are fast and simple to use but are probably best used as a quick screening tool for field investigations or as a backup in case of pH meter failure. They can, however, give misleading results if the water sample is highly colored, contains colloids, or reacts with the paper's dye.

The most common method used to determine pH is a potentiometric method using a pH meter and electrode. This method provides accurate and reliable values, provided they have been measured with the aid of a correctly operated and maintained pH meter and electrode.

A short discussion on the theory of pH and use of pH meters can be found in Fishman and Friedman (1989), Van Loon (1982), or in any textbook on instrumental methods of analysis. In principle, pH meters measure the electrical potential between two electrodes immersed in the solution to be tested; the two electrodes are referred to as the reference electrode and the indicating electrode. The reference electrode provides a constant potential for a given temperature, and the indicating electrode assumes a potential dependent on the hydrogen ion concentration of the test solution. Electrode potential is the difference in potential (given in millivolts, mV) between the reference electrode and the indicator electrode. The pH value is then calculated based on the measured electrode potential.

The most convenient and reliable method for pH determination in the field is to use a hand-held, battery-operated pH meter. The meter should have a readout to 0.01 pH units and, because pH varies with temperature, either Automatic Temperature Compensation (ATC) or an adjustment to account for temperature. Most meters are available with automatic buffer recognition (used in meter calibration, discussed below); they sense a mV reading for selected pH buffers when the attached electrode is immersed in the buffer. If that mV reading falls within a specific range, the meter assumes a pH value based on that mV reading and uses that value for calibration. The most useful buffers are pH 4, 7, and 10, and almost all meters with automatic buffer recognition can recognize these buffer values. For acid mine waters the most useful buffers are 1.68, 2.0, 4.0, and 7.0.

Meters are obtainable in numerous varieties with all sorts of sensitivities. Hand-held, battery-operated pH meters are available from all major scientific equipment suppliers. Meters come equipped with either digital or analog readouts. Costs range (1995) from about \$50 for a pH "pen," a pH meter with built in electrode that fits in a shirt pocket, to about \$200 for an analog meter and \$500 to \$800 for a combination digital pH-mV meter with ATC

¹N=normal solution. A normal solution contains one gram molecular weight of the dissolved substance divided by the hydrogen equivalent of the substance per liter of solution.

and at least two-point calibration. Analog readouts are satisfactory but digital readouts remove some of the guesswork of reading a dial. Digital meters with liquid crystal displays (LCD) are much easier to read in the sunlight compared to red light emitting diodes (LED). The more expensive units usually do not come with an electrode, allowing greater selection of electrodes for specific uses. Recommended specifications for purchase of a new meter to be used for mining-environmental applications are:

- 1) automatic buffer recognition of pH 1.68, 2, 4, 7, and 10 buffers,
- 2) automatic temperature compensation,
- 3) readout to 0.01 pH units with auto-read stability indicator,
- 4) mV capability, and
- 5) battery-powered by readily available batteries.

The electrodes used to measure pH should develop steady readings as quickly as possible. Both saturated calomel (Hg/Hg₂Cl₂) electrodes and Ag/AgCl electrodes are the most reliable known and, therefore, are recommended for use as the reference electrode. For measurements at normal room temperature, either of these electrodes is satisfactory. The Ag/AgCl electrode is recommended for measurements at elevated temperatures, where the potential is more stable than that of the saturated calomel electrode. A hydrogen-ion-selective glass electrode is normally used as the indicating electrode. Combination electrodes (e.g., a reference electrode and an indicating electrode contained in one glass or epoxy unit) also are available and are usually the electrode of choice for use with hand-held, battery-operated, field-pH meters or when working with limited volumes of sample. Electrode-pair configuration provides better precision and reproducibility whereas combination electrodes are more convenient and a must for small sample volumes or container sizes. Combination electrodes are available in many configurations that allow placement of the electrode into small containers or small volumes of water. Electrodes are available that are housed in either glass or epoxy bodies and as refillable or gel-filled. Glass body electrodes are easier to clean and less likely to cross contaminate samples. Epoxy bodies may be advantageous in a more rugged field environment. Refillable electrodes provide higher accuracy and longer life; the proper filling solution, as recommended by the manufacturer, is required for refillable electrodes. Gel-filled electrodes are low-maintenance because they require no filling solutions, but generally take longer to obtain a stable pH reading. New electrodes and those that have been stored dry need to be conditioned and maintained as recommended by the manufacturer. Once conditioned, the glass tip of most electrodes should be kept moist to prevent damage to the pH-sensitive membrane.

When calibrating pH meters or when making pH measurements with refillable electrodes, it is necessary to open or uncover the electrode filling hole. The pH meters should be calibrated with at least two buffer solutions that bracket the pH range of the test samples. Certified buffer solutions of known pH are commercially available or buffers can be prepared in the laboratory (see Van Loon, 1982, p. 46 and American Society for Testing and Materials, 1992, p. 276). The measured value of another pH buffer should always be taken to verify the pH calibration. For example, when measuring acidic mine drainage waters, the pH equipment should be calibrated using pH 7 and pH 4 buffers and then verified with either or both pH 6 and pH 3 buffers. Rinse the tip of the pH electrode well with deionized water and blot gently with a tissue between each buffer and before the sample to prevent carry-over of the solutions. If the pH equipment does not have ATC, the

temperature of the pH buffers must be matched to that of the sample (e.g., place the tightly sealed buffer containers in the stream water to be sampled). The verified buffer reading should be within 0.05 units of the true value; if not, the pH meter should be recalibrated. If the pH equipment is working properly and problems are not encountered, one can get by with calibrating only at the first sample site each day and then verify the calibration at subsequent sample sites during the day; however, to rigorously satisfy quality-assurance and quality control protocols likely to be in place at many environmental sites, calibration should be done at every sample site.

If the pH measurement is not made directly in the stream or pond, rinse a clean container in the sample water and collect a representative sample of the water. To make the pH measurement, immerse the pH electrode one inch into the sample water and swirl a few times. Take the pH reading when the electrode and water are still. The pH reading often drifts or takes considerable time to come to a steady or constant value. It is important to wait until the drifting has stopped. This is particularly true in waters that are not well poised (e.g., that have low dissolved solids and specific conductivity). If the pH meter has an automatic stopping feature, take the pH reading at least twice or until the readings are consistent (e.g., within 0.02 pH units). The pH measurement is recorded on the field data form to the nearest hundredth unit, e.g., 5.67, but probably should be rounded to the nearest tenth unit, e.g., 5.7, for scientific publication. Because the pH electrode leaks ions, discard the sample used to measure pH. If the pH measurement is made within the stream or pond, it is important that the pH value obtained is representative of that for the whole stream.

There is an old adage to the effect that if anything can go wrong it will. This seems to be especially so in the case of pH measurements. Batteries have a tendency to fail at the worst possible moment, so it is advisable to have at least one spare set of batteries for any meter. The junction on reference electrodes commonly becomes poisoned and ceases to function. Some meters have built in error messages that will alert the field person when this happens, but reference electrode failure may not be easy to detect. One way to overcome this problem is with frequent calibration. If there is electrode failure, the meter probably will not calibrate. Junction plugging may be encountered when determining the pH of mine waters that carry large amounts of suspended sediments. Some mine waters of low pH may contain dissolved constituents that poison electrodes. It certainly is good practice to have at least one backup electrode as part of the field equipment. New or dried glass electrodes must be soaked in a buffer solution for 24 hours before use. As a consequence, any electrode should be stored in a buffer solution to keep the glass sensing element hydrated.

Specific conductance/total dissolved solids

This method may be applied to all natural, treated, or industrial waters. The term conductance refers to the ability of materials to carry an electric current. Water can conduct a current because of the charged dissolved constituents. The quantities and charges of the dissolved species controls the electrical conductivity. The specific conductance of a solution is defined as the reciprocal of the electrical resistance in ohms, measured between two parallel, 1-cm², non-polarized electrodes immersed 1 cm apart in solution at a specific temperature. By convention the conductivity of a

solution is that which it exhibits at 25.0°C, but other standard temperatures (20.0°C and 18.0°C) are sometimes used (Van Loon, 1982, p. 49). The international unit of measurement is expressed as Siemens/cm (S/cm), milli-Siemens/cm (mS/cm), and micro-siemens/cm ($\mu\text{S/cm}$) at 25.0°C; $1 \mu\text{mho} = 1 \mu\text{S}$.

Specific conductance is an easy measurement to make at a sample site and it provides a very good estimate of the concentration of total dissolved solids (TDS). For most natural waters of mixed type the specific conductance in $\mu\text{S/cm}$ at 25.0°C, multiplied by a factor of 0.65 approximates the TDS in mg/l. The specific conductance in $\mu\text{S/cm}$ at 25.0°C divided by 100 approximates the milliequivalents per liter of either anionic or cationic concentrations. These equations are not exact because the conductance of a solution is dependent on the types and total quantities of ions in solution. However, conductivity measurements serve as a useful indicator of the degree of mineralization in a water sample.

Required equipment consists of a conductivity meter, calibration standard, and, if necessary, a container to hold the sample. Conductivity calibration standards for testing the meter are commercially available. Alternatively, calibration standards can be made in the laboratory by dissolving a suitable salt, e.g., potassium chloride, in deionized water to obtain the desired specific conductivity reading. The actual measurement requires just a few minutes to perform. A sample of the test water is placed in a small container and the probe inserted into the sample. A reading on the meter is rapidly established. Alternatively, the probe can be placed in a quiet part of the stream or pond assuming that the area tested is representative of the whole stream or pond. Specific conductance measurements are an easy way to trace high ionic strength contaminants in a stream or to test how well mixed a stream is at a given location. Depending on the conductivity range, the resultant meter reading is recorded on the field data form as mS/cm or $\mu\text{S/cm}$ at 25°C.

Hand-held portable specific conductance meters are available from major scientific equipment suppliers. Most meters will be equipped with ATC or an adjustable temperature dial; when the meters are so equipped, the conductivity reading is electronically adjusted to reflect specific conductance at 25.0°C. If a meter is used that only determines conductivity, a long and complex conversion to specific conductance at 25.0°C is required. A shortcut is to add 2% to the conductivity reading for each degree below 25.0°C and subtract 2% for each degree above 25.0°C (Van Loon, 1982, p. 52). A fairly good ATC-equipped conductivity meter that fits in a shirt pocket (see pH pen above) is available from many scientific supply companies. Conductivity pens cost about \$50 to \$200 (1995 prices), whereas hand-held meters cost about \$200 to \$500.

Waters from pristine mountain streams will have specific conductance values from about 10 $\mu\text{S/cm}$ to about 100 $\mu\text{S/cm}$. Good quality drinking waters may have specific conductance values of 500 $\mu\text{S/cm}$ or less. The values listed in Table 12.1 show the extreme variability of specific conductance in some mine-drainage waters.

Dissolved oxygen

Oxygen will probably be present in most surficial water samples in sufficient concentrations to be determined. However, waters that have been isolated from the atmosphere (such as ground waters, some wetlands pore waters, or some lake bottom waters) can have very low dissolved oxygen contents. Dissolved

oxygen is vital to aquatic life and aerobic microbes (Mills, 1999), aids in the natural decomposition of organic matter, and is an important geochemical component in the oxidation of sulfide-bearing mineral deposits (Nordstrom and Alpers, 1999).

The concentration of oxygen that is dissolved in water varies with physical, chemical, and biochemical activities in the water body. The solubility of oxygen in water increases with decreasing temperature, decreasing elevation, and increasing atmospheric pressure (Fig. 12.2). Increased concentrations of other dissolved solutes result in a decrease of dissolved oxygen at a given temperature and atmospheric pressure (American Public Health Association et al., 1985, p. 413).

Dissolved oxygen measurements are normally made at the sample site without delay because unsaturated waters (typical of ground waters sampled from many wells, springs, or collapsed mine adits) can rapidly become oxygenated. If at all possible, it is best to make the measurement directly in the stream flow or body of water. Care also must be taken not to introduce atmospheric oxygen into the sample.

The determination of dissolved oxygen is conveniently accomplished using commercially available breakable ampoules (available from some scientific supply companies in kit form) that draw water into a reagent mix. A color develops within the ampoule within a few minutes; the intensity of the color is directly proportional to the dissolved oxygen concentration in the sample. The concentration is obtained by matching the color of the sample ampoule with the corresponding color in a chart or in a set of reference ampoules of specified oxygen contents. The sealed ampoule techniques may not be useful in colored water samples due to interferences. The sealed ampoule kits are available in several ranges covering part per million (ppm) and part per billion (ppb) concentrations. Typical test kits in ppm ranges employ the indigo carmine method and typical test kits in the ppb ranges employ Rhodazine D methodology. The reduced form of indigo carmine reacts with dissolved oxygen to form a blue product and Rhodazine D in reduced form reacts with dissolved oxygen to form a bright pink product. Results are recorded on the field data

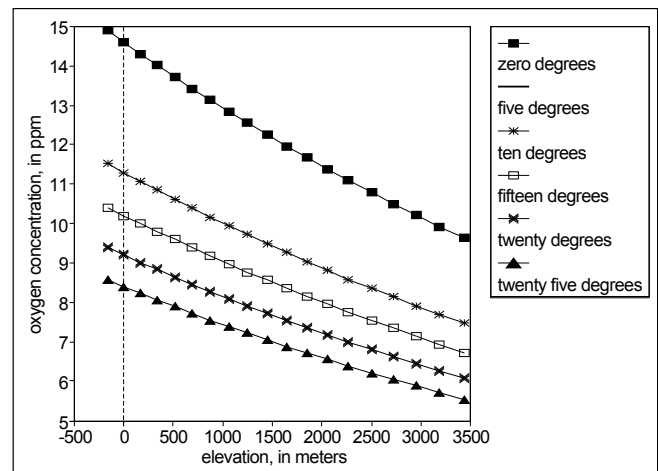


FIGURE 12.2—Dissolved oxygen concentration plotted as a function of altitude (barometric pressure) from 0 to 25°C. Adapted from data listed in Standard Methods for the Examination of Water and Wastewater, American Public Health Association et al. (1985).

form as ppm (mg/l) or ppb ($\mu\text{g/l}$). The price of the oxygen kits containing 30 ampoules range from about \$30 to \$50.

A portable spectrophotometer is commercially available that accepts specially designed ampoules. The ampoule is broken in the sample to draw water into a reagent mix, and the corresponding color develops. The spectrophotometer is used to determine the intensity of the color and from that the concentration of dissolved oxygen. The commercially supplied ampoules come in two concentration ranges; 0 to 800 mg/l and 0 to 13 mg/l. This same meter can be used for a large variety of commonly performed analyses either in the field or in the lab.

Water samples can be collected and fixed for the determination of dissolved oxygen by the idometric method or Winkler method (American Public Health Association et al., 1992, pp. 4–98). The idometric method is a precise and reliable titrimetric procedure based on the addition of divalent manganese solution (e.g., manganous sulfate), followed by strong alkali, to a sample collected in a glass-stoppered bottle. Manganous hydroxide precipitate is formed and the dissolved oxygen rapidly oxidizes an equivalent amount of the manganous hydroxide to manganic hydroxide. Upon acidification in the presence of iodide, the oxidized manganese reverts to the divalent state and iodine is released in a quantity equivalent to the original dissolved oxygen present. The liberated iodine is then titrated with standard sodium thiosulfate solution with use of a starch indicator. The use of this method for acid-mine water samples is limited because of several interferences which include: samples containing more than 1 mg/l ferrous iron; samples containing appreciable quantities of sulfite, thiosulfate, polythionate, hypochlorite, or free chlorine; samples high in suspended material, or; samples containing other oxidizing or reducing materials. A modification of this method applicable to field determinations employing a titration in a syringe is presented by Slack (1968, p. 44).

Dissolved oxygen meters are available from scientific supply companies at a cost of about \$550 to about \$1500. These consist of a meter with a probe and are applicable to waters containing 0.05 to 20 mg/l dissolved oxygen. The probe usually has a membrane through which oxygen passes to react with an inner electrolyte, creating a current that is proportional to the dissolved oxygen concentration. The meters were somewhat bulky and the membrane on the probe is easily damaged, but with newer instrumentation, these problems are minimized. This is also the preferred method for acid mine drainage. The temperature limits are about 0–55°C. The membranes are also difficult to replace, especially so in windy, dusty field conditions.

Redox potential

Oxidation-reduction potential, often referred to as redox, Eh, pe, or ORP, is an indirect measurement of the aqueous equilibrium of some species involved in a redox couple (such as $\text{Fe}^{2+}/\text{Fe}^{3+}$ or $\text{As}^{3+}/\text{As}^{5+}$). It is necessary to determine redox potential at the sample site because, like pH, the results may not be the same after storage. Eh measurements are typically made using a platinum-calomel or platinum-Ag/AgCl electrode system, coupled with a pH meter read in millivolts; the mV reading obtained must be corrected for temperature and adjusted to a potential relative to that of the standard hydrogen electrode (see method in Wood, 1976; Nordstrom, 1977). ZoBell solution, essentially a redox buffer of potassium ferric-ferro-cyanide, can be used as a reference solution to test the functioning of the electrode system; at 25°C,

ZoBell solution should have a potential (measured with a calomel-platinum electrode system) of 183 ± 5 mV (Wood, 1976). For an Eh value measured with a saturated calomel reference electrode the actual mV reading must be corrected by a factor of about +240 mV. Oxidized waters will have a mV reading greater than 400 and this can vary greatly upwards when corrected for the reference electrode. Reduced waters have mV readings from 200 downward. Highly reduced, non-oxygenated waters may have negative redox potentials.

In the past, redox measurements were routinely made as part of water quality studies; however, in recent years, a number of uncertainties have been brought to light that make the validity of Eh measurements questionable. Unfortunately, natural systems are rarely in redox equilibrium; thus, field pe and Eh measurements are often at best qualitative indications of natural redox conditions. Lindberg and Runnels (1984) suggest that redox potential is not a good measurement to make because of a number of uncertainties in what the measurement represents; they suggest that most aqueous systems are at redox disequilibrium and that there is no single true Eh value. On the other hand, Nordstrom et al. (1979) suggest that redox potential measurements may accurately reflect the redox potential in iron-rich waters in which the potential is controlled by the $\text{Fe}^{2+}/\text{Fe}^{3+}$ redox couple (see also Nordstrom and Alpers, 1999). Thus, in natural waters, Eh measurements generally reflect a mixed or aggregate redox potential unless the net exchange current at the electrode surface is dominated by one redox couple, such as $\text{Fe}^{2+}/\text{Fe}^{3+}$.

In addition, there are several common contamination problems with Eh measurements that can compromise their validity, including:

- 1) poisoning of the platinum electrode surface by dissolved oxygen in waters (the electrode becomes coated with a film of platinum oxide or hydroxide),
- 2) poisoning of the platinum electrode surface by sulfur species in anoxic waters (H_2S may complex with the platinum surface), and
- 3) contamination of the platinum electrode surfaces by iron species or organics in some systems (they form a film on the platinum surface).

Thus, field Eh measurements are of questionable meaning and value. Quantitative interpretation of Eh values is not justified unless it is known with certainty that (1) there has been no contamination of the platinum electrode, and (2) one redox couple dominates the system. It can be assumed that electrode contamination probably will occur in oxygenated waters or waters containing reduced sulfur; thus, Eh measurements in these types of waters are highly suspect. The preferred alternative to determining Eh, which is at best qualitative for most samples, is direct determination of the concentrations of redox couples of interest (e.g., $\text{Fe}^{2+}/\text{Fe}^{3+}$ or $\text{As}^{3+}/\text{As}^{5+}$).

Ferrous iron and total iron

Dissolved iron is found in two oxidation states, ferrous (Fe^{2+}) and ferric (Fe^{3+}). Because of the important roles that aqueous iron species play in the generation of acid-mine waters, it is very important to measure the concentration of Fe^{2+} , Fe^{3+} , and total iron. As discussed by Nordstrom and Alpers (1999), and Nordstrom et al. (1979), pyrite oxidation results in the release of ferrous ion and elemental sulfur; the sulfur is then oxidized to sul-

fate (SO_4^{2-}), which results in the release of H^+ . Under abiotic conditions and as long as the pH of the water remains less than about 4 to 4.5, the dissolved iron will remain in the ferrous state because abiotic oxidation of Fe^{2+} to Fe^{3+} is strongly inhibited at $\text{pH} < 4.5$. However, in the presence of the iron-oxidizing bacterium *Thiobacillus ferrooxidans* (which is abundant in oxygenated mine-drainage environments), the oxidation rate of Fe^{2+} to Fe^{3+} is increased by 5 or 6 orders of magnitude over the abiotic rate. Hence, acid mine-drainage waters with pH less than 4.5 can have a mixture of Fe^{2+} and Fe^{3+} . Ferric iron concentrations in solution are controlled by saturation with hydrous ferric oxides above pH values of approximately 2 to 3. Above pH values of 4.5, Fe^{2+} is rapidly oxidized by atmospheric or dissolved oxygen to Fe^{3+} . This rapid oxidation, coupled with the formation of insoluble hydrous ferric oxide minerals, restricts Fe^{3+} concentrations to values that are generally too small to be determined accurately (Langmuir and Whittemore, 1970), except in waters where the ferric iron is complexed by organic species or other effective complexing agents.

Ferrous and total ($\text{Fe}^{2+} + \text{Fe}^{3+}$) iron concentrations in water can be determined in the field. Ferric iron concentration is determined by subtracting Fe^{2+} from total iron. Instructions for preparing reagents and a description of the equipment required to determine Fe^{2+} and total iron in the field is given by Skougstad et al. (1979, p. 387 and p. 373). The methods are applicable to filtered water samples containing between 10 and 4,000 mg/l of Fe^{2+} or total iron. The Fe^{2+} method consists of adding 1 ml of 2,2'-bipyridine solution (0.5 g/l) to a 25-ml sample. The Fe^{2+} reacts immediately to form a red complex. The complex forms when the pH of the test water is between 3 and 10. If the pH of the test solution is not in this range it should be adjusted with a sodium acetate/acetic acid buffer. The colored test solution can be compared to standard solutions of known concentration. A visual comparison can be made for a semi-quantitative estimate of Fe^{2+} concentration or a battery operated spectrophotometer can be used to prepare a calibration curve for absorbance of standard solutions for the quantitative measurement of Fe^{2+} . This analysis must be performed in the field immediately on collecting and filtering the sample. The total iron method is identical to the Fe^{2+} method except Fe^{3+} is first reduced to Fe^{2+} with hydroxylamine hydrochloride to provide a total iron determination.

Colorimetric kits using sealed ampoules are available commercially for total iron and Fe^{2+} . For total iron, the kits are supplied with varying concentration ranges up to 10,000 mg/l. Determinations are made by visual color comparison and provide a fairly good estimate of iron concentrations. For Fe^{2+} , the kits permit determination of concentrations only up to 1 mg/l; hence, mine drainage waters with high Fe^{2+} must be diluted (often significantly) in order to be measured; because the dilution can be a significant source of error, the measurement should be considered qualitative or at best semiquantitative.

The commercially available portable spectrophotometer described above in the dissolved oxygen section also provides methods using sealed ampoules for ferrous and total iron. The disadvantage of these methods is the narrow concentration range provided, 0 to 3.0 mg/l; the high concentration levels of iron in acid-mine waters thus often requires a dilution of the sample and the use of more than one ampoule.

Water samples can be preserved with hydrochloric acid (HCl) and stored for subsequent Fe^{2+} analysis in the laboratory. Hydrochloric acid prevents Fe^{2+} from oxidizing during storage (D.K. Nordstrom, U.S. Geological Survey, personal commun.).

Samples are preserved by adding 0.25 ml (5 drops) of concentrated HCl to 50 ml of sample that has been filtered. Samples must be filtered (0.1 μm) prior to acidification to avoid dissolving particulate iron. The advantage of preservation is that the sample can be analyzed more conveniently and accurately in a laboratory situation.

Alkalinity

Alkalinity is defined as the capacity of water to neutralize a strong acid to a designated pH, usually 4.5. Van Loon (1982, p. 100) gives many reasons why alkalinity is an important constituent to determine. Among them are studying water quality characteristics and their relationship to water hardness or high mineralization, problems with treating waters with excessive alkalinity, and maintenance of healthy aquatic life. Alkalinity in most natural waters is due to bicarbonate, but other salts of weak acids and hydroxide may also contribute to alkalinity. Water samples with a pH between 4.5 and about 8.5 will most likely have only bicarbonate alkalinity. Alkalinity can be stable in water samples for extended periods of time, but in waters that are not in equilibrium, such as mine-drainage waters, irreversible changes may take place during storage. Therefore, alkalinity should be determined as soon as possible after sample collection. Because of time restraints in the field, however, we often refrigerate the water sample and measure alkalinity immediately on returning to the laboratory. If there is any question about the stability of alkalinity, the analysis should be done at the sample site. For water samples in which the pH is less than 4.5, an alkalinity determination is not applicable due to the extremely small concentrations of bicarbonate. Alkalinity is reported as mg/l calcium carbonate (CaCO_3) or mg/l bicarbonate (HCO_3^-).

Alkalinity is determined by titration. An easy field titration can be performed at the sample site in just a few minutes using commercially available titration cells. These cells are supplied in kits of 30 each with analytical ranges of 10 to 100 mg/l, 50 to 500 mg/l, and 100 to 1000 mg/l CaCO_3 . The procedure involves breaking a sealed titration cell immersed in the sample water; then, by means of a squeezable valve on the intake tube, small volumes of sample water are sequentially pulled into the cell and mixed with its contents. An indicator turns red and stays red until the end point of the titration is achieved. At that point the indicator turns clear and finally green. The titration is complete when the indicator turns bright green ($\text{pH} = 4.5$). Total alkalinity is determined by holding the cell in a vertical position and reading the scale opposite the liquid level to obtain the results in mg/l CaCO_3 .

The following is just one of many different potentiometric titration methods for determining total alkalinity. This test is based on the Gran Technique (Gran, 1950) and is particularly applicable, but not restricted, to waters with low alkalinity (0 to about 50 mg/l CaCO_3). Gran's plots are discussed in Stumm and Morgan (1981, p. 144) and Van Loon (1982, p. 106). Titration to a fixed end-point of 4.5 is based on the assumption that total alkalinity is defined only by the carbonate/bicarbonate dissociation. However, the carbonate-bicarbonate components may not be the predominant or only groups in some waters and other buffering species, such as organics and metal ions, may be of major significance. Thomas and Lynch (1960) demonstrated how the error resulting from titration to a fixed end-point pH increases with decreasing alkalinity values, particularly over the lower range of 0 to 50 mg/l CaCO_3 . The Gran procedure is based on the principle that the hydrogen

ion concentration of the sample increases linearly with successive increments of the strong acid added during titration. Thus the inflection point (e.g., the true equivalence point of the bicarbonate-carbonate acid dissociation) is established from a titration curve obtained by plotting the cumulative volume of acid (titrant) added versus the measured pH reading after each successive acid increment. This requires taking a series of pipette and pH meter readings for each sample titrated. Samples are titrated to a final pH of 3.0, because titration of low alkalinity waters to a fixed end point of pH 4.5 may result in total alkalinity results that are biased high.

Total alkalinity by the Gran technique is determined by the following procedure:

Apparatus

- 1) A pH meter capable of reading to 0.01 pH units
- 2) Micro-pipettes (10, 20, 50, and 100 ml or a 0–100 ml digital micro-pipette)
- 3) A 150 ml beaker
- 4) Some means of stirring the sample

Reagent

- 1) Standardized sulfuric acid (H_2SO_4) solution, e.g., 0.18 N.

Procedure

- 1) Measure 50 ml of filtered sample into a 150-ml beaker.
- 2) Measure the pH of the sample while stirring and record.
- 3) Titrate with standard H_2SO_4 while stirring to pH 4.50 and record volume of acid to reach pH 4.50.
- 4) Continue to titrate using small increments of standard H_2SO_4 to a final pH of 3.00. Record the pH after each addition of standard H_2SO_4 .

After addition of each increment of the titrant, the solution pH should become stabilized before it is recorded. In order to ensure accurate identification of the inflection point, enough data points should be obtained around that point by limiting additions to relatively small volumes. Normally a linear least squares analysis of a series of about 5 to 10 data points is adequate, but some samples may require additional data points for a complete analysis of the entire titration curve.

Calculations

The calculations for the Gran technique may be done either graphically or, more conveniently, by linear regression analysis of the titration curve. Figure 12.3 shows a typical spreadsheet layout for a computer generated regression analysis calculation by the Gran technique. By calculating the second order difference coefficient for each successive titration point, the inflection point is denoted by the point at which the coefficient changes sign. The Gran function (F) is determined from the equation:

$$F = (V_s + V) [H] \quad [2]$$

where V_s is the original sample volume, and V is the volume of

titrant added. Then the F values are plotted against V for only the data points that are far enough removed from the inflection (equivalence) point. The volume of titrant corresponding to the equivalence point, and hence the sample alkalinity, is calculated according to the regression coefficients.

Calculations for potentiometric titration to end-point pH 4.5 are made as follows:

$$\text{Alkalinity (mg CaCO}_3\text{/l)} = [A \times N \times 50 \times 1,000] / [\text{ml sample}] \quad [3]$$

where:

A = ml standard acid used and

N = normality of standard acid.

The factor for converting mg $CaCO_3$ to mg HCO_3^- is 1.2193.

Digital titrator

A patented digital titrator is commercially available that makes potentiometric alkalinity titrations in the field a little easier. The equipment consists of the titrator, a titration cartridge with a known concentration of sulfuric acid, and a delivery tube. All that is additionally required is a pH meter and some way to stir the sample, such as a battery powered stirrer. The delivery tube is immersed in the sample and the knob on the titrator is turned to read a few digits. The pH is recorded after each addition. Increments of titrant are added until pH values of 4.5 and 3 are achieved. The volume of titrant can be calculated from the number of digits required to reach the end-point. With practice a titration may be done in about 15 minutes.

Acidity

The acidity of a water is defined as its quantitative capacity to neutralize a strong base to a designated pH and generally is considered with alkalinity because of their interrelationship. There are three general reasons for determining acidity:

- 1) to check the pH;
- 2) to estimate the amount of lime that is required for neutralization; and
- 3) to obtain a parameter to relatively compare water samples. One must beware of the quantitative use of acidity, especially in modeling.

Like alkalinity, acidity is dependent on the pH value and buffering capacity of the water being studied and also is expressed in terms of an equivalent concentration of $CaCO_3$ in mg/l at the designated pH. Acidity also is measured titrimetrically and the end-point can be determined either colorimetrically or with a pH meter. The colorimetric end-point titration method uses methyl orange indicator (color change at approximately pH 3.7) or phenolphthalein indicator (color change at approximately pH 8.3) to denote the equivalence point.

The potentiometric test method described here is modified from the ASTM test method C (1992, p. 191) intended specifically for mine drainage, surface streams receiving mine drainage, industrial waste waters containing waste acids and their salts, and similar waters bearing substantial amounts of ferrous iron or other

	A	B	C	D	E	F	G	H	
1									
2									
3				GRAN TITRATION					
4		94DW W63							
5		9410126							
6									
7	STARTING VOL:		0.00	ACID	0.1657	DILUTE			
8	STARTING PH:	7.67	MEQ	0.5965	0.596				
9	SAMPLE VOLUME:		50	CACO3	29.85	29.851			
10	NORMALITY:	0.18	HCO3	36.40					
11	DILUTION:		1						
12									
13	Enter initial reading and those readings between 4.5 and 3.0.								
14	Check the plot to see if the line is straight.								
15	VOLUME		PH	NETVOL					
16	0.00	7.67		F1					
17	0.178	4.50	50.18	0.00159		Regression Output:			
18	0.180	4.41	50.18	0.00195	Constant	-0.02543			
19	0.200	4.00	50.20	0.00502	Std Err of Y Est	0.000398			
20	0.220	3.79	50.22	0.00814	R Squared	0.999524			
21	0.240	3.64	50.24	0.01151	No. of Observations		13		
22	0.260	3.54	50.26	0.01450	Degrees of Freedom		11		
23	0.280	3.45	50.28	0.01784					
24	0.320	3.32	50.32	0.02408	X Coefficient(s)	0.153454			
25	0.360	3.22	50.36	0.03034	Std Err of Coef.	0.00101			
26	0.400	3.14	50.40	0.03651					
27	0.440	3.08	50.44	0.04195					
28	0.480	3.02	50.48	0.04821					
29	0.500	3.00	50.50	0.05050					

Spreadsheet Explanation:

B4 = Sample ID

B5 = Date

A17 = Volume of acid (titrant) to reach pH 4.50

A18 - A29 = Cumulative volume of acid (titrant) added

B16 & C8 = Original sample pH

B17 - B29 = pH readings

C17 - C29 = Net volume, e.g., C9 + A17

D17 - D29 = Gran function (F1), e.g., (C17)*10^(-1*B17)

F7 = Acid, e.g., (-H18)/G24 (H18 = Constant, G24 = X Coefficient(s))

F8 = Milliequivalents, e.g., 1000/C9*C10*F7

F9 = Total Alkalinity as mg/L Calcium Carbonate, +F8*50.045

F10 = Equivalent Bicarbonate, F9*1.2193

Regression Analysis:

Independent = A17 - A29

Dependent = D17 - D29

FIGURE 12.3—Spreadsheet layout for regression analysis calculation of total alkalinity determination.

polyvalent cations in reduced state. The sample is titrated with standard sodium hydroxide solution to pH 3.7 and 8.3. Because the oxidation and hydrolysis of ferrous iron generates acidity, a reliable measure of acidity or alkalinity is obtained only when complete oxidation of iron is achieved and hydrolysis of ferric and other metal salts is completed. In this method, hydrogen peroxide is added prior to boiling to accelerate the chemical reactions needed for equilibrium.

Apparatus

- 1) A pH meter capable of reading to 0.01 pH units
- 2) Micro pipettes (10, 20, 50, and 100 ml or a 0–100 ml digital micro-pipette)
- 3) A 150 ml beaker
- 4) Some means of stirring the sample
- 5) Hot plate

Reagents

- 1) Hydrogen peroxide (H₂O₂, 30% solution)
- 2) Standardized sodium hydroxide solution, e.g., 0.016 and(or) 0.16 N
- 3) Standardized 0.18 N sulfuric acid (H₂SO₄) solution

Procedure

- 1) Measure 50 ml of filtered sample into a 150-ml beaker.
- 2) Measure the pH of the sample. If the pH is above 4.0, pipette 10 ml increments of 0.18 N standard H₂SO₄ to lower the pH to 4.0 or less. The standard acid added prior to boiling neutralizes volatile components, for example, bicarbonates which contribute to the alkalinity and hence minimizes this source of error. Record volume of acid used.
- 3) Add only 5 drops of H₂O₂.
- 4) Heat the sample to boiling and continue to boil for 2 to 4 minutes.
- 5) Cool to room temperature and, while stirring, titrate with a pH meter using standard NaOH to pH 8.3 (total acidity). Samples with acidity less than 1000 mg/l as CaCO₃ should be titrated with 0.016 N NaOH, while samples with acidity in excess of 1000 mg/l as CaCO₃ are better titrated with 0.16 N NaOH.

Calculations

The acidity of a solution that has been boiled and oxidized can be calculated as follows:

- 1) When no sulfuric acid is added prior to titration:

$$\text{meq/l} = (\text{BN}_b / S) \times 1000 \text{ or mg/l as CaCO}_3 \\ = \text{meq/l} \times 50 \quad [4]$$

- 2) When sulfuric acid is added prior to titration:

$$\text{meq/l} = [(\text{BN}_b - \text{AN}_a) / S] \times 1000 \text{ or mg/l as CaCO}_3 \\ = \text{meq/l} \times 50 \quad [5]$$

where:

A = H₂SO₄ added to sample, ml,
B = NaOH solution required for titration of sample, ml,
N_a = normality of the H₂SO₄,
N_b = normality of the NaOH solution, and
S = volume of sample used, ml
(MW of CaCO₃ = 100)
A negative result is indicative of alkalinity.

Sulfate

Oxidation of sulfide minerals eventually leads to a high concentration of sulfate in mine drainage waters. Pristine alpine waters can contain 10 to 20 mg/l sulfate; however, as seen in Table 12.1, the concentration in mine-drainage waters can be more than several thousand mg/l. Thus, a rapid field method for determination of sulfate in a mine water may be a useful guide, along with pH and specific conductance, in assessing the extent of sulfide oxidation.

A classical reaction of sulfate in water is the precipitation of barium sulfate (BaSO₄) using an acid solution of barium chloride. The reaction is the basis of a field method for turbidimetric determination of sulfate; the necessary reagents are supplied in a commercially available kit. For concentrations from 50 to 200 mg/l the sulfate contained in a specified volume of water is precipitated by addition of a pillow of reagent that contains barium chloride and a suspension agent. The cloudy solution is added in small volumes to a pre-calibrated cylinder until a cross on the bottom of the cylinder disappears. At that point, the concentration is read from a scale on the cylinder. With proper dilution, samples with much greater sulfate concentrations than 200 mg/l can be determined. Results by this field method are compared with results obtained by ion chromatography in the laboratory in Table 12.3. They show reasonable agreement between the two methods. For concentrations below 50 mg/l, the sulfate concentration can be determined using the commercially-available portable spectrophotometer described previously, which provides a method using sealed ampoules for sulfate determination. The concentration range for this method is 0 to 70 mg/l. This method is not especially applicable for acid mine drainage. Ion chromatography or the thorium method is preferred for this type of sample.

Sulfide and hydrogen sulfide

Total dissolved sulfide includes H₂S and HS⁻ after suspended matter has been removed. In highly reduced waters, sulfide minerals can react with the available hydrogen ions to form HS⁻ and H₂S depending on pH. Hydrogen sulfide (H₂S) is the most common form of sulfide and its fumes are noxious and highly toxic. Dissolved H₂S is especially toxic to aquatic life. When escaping from a water supply, the threshold odor concentration of H₂S is between 0.025 and 0.25 µg/l (American Public Health Association et al., 1992, p. 4–123). Under natural conditions, dissolved sulfides can be present in ground water as a result of leaching from sulfur-containing mineral deposits, from the decomposition of organic material, and, under anaerobic conditions, from the reduction of sulfate by bacteria. The presence of dissolved oxygen promotes the oxidation of H₂S to sulfate, thus surface waters normally do not contain high concentrations of H₂S.

TABLE 12.3—Comparison of analytical results for field and laboratory determination of sulfate concentrations in selected mine-water samples.

Sample	Sulfate, mg/l field	Ion chromatography
Alpha-Corsair Mine	320	290
Bandora Mine	210	220
Carlton Tunnel	1400	1230
Chapman Gulch 1	675	615
Chapman Gulch 2	1170	920
Gamble Gulch 1	120	110
Gamble Gulch 2	130	120
Gamble Gulch 3	250	310
Gamble Gulch 4	300	300
Gamble Gulch 5	18	10
Gamble Gulch 6	200	190
Garibaldi Mine	110	80
Leadville Drain	200	250
Unnamed Drainage	90	80
Rawley Tunnel	600	600
Rawley Tunnel 2	620	540
Rawley Tunnel 3	375	340
Solomon Mine 1	330	310
Solomon Mine 2	320	340

Because dissolved sulfides are so extremely volatile, measurements must be made at the sample site to obtain accurate determinations. Commercially available kits for dissolved sulfide determinations make a field analysis feasible. The field determination of dissolved sulfides is based on the methylene blue method (the Hach kit is recommended). Dissolved sulfides react with dimethyl-p-phenylenediamine in the presence of ferric chloride to produce methylene blue. The commercial kit contains self-filling ampoules that are broken in the test solution, to which a few drops of ferric chloride solution has been added. A diagnostic blue color that is directly proportional to the dissolved sulfide concentration in the sample develops in the ampoule. Results are determined by visual comparison with a series of standards supplied with the kit and are expressed as mg/l S. Cline (1969) also has developed a comparatively simple field determination of sulfide based on the methylene blue color reaction using a portable spectrophotometer to determine fairly quantitative results in the 0.03 to 32 mg/l S range.

Heavy metals

Acidic-mine waters may contain dissolved copper and zinc in relatively high concentrations (Table 12.1). They, along with other previously discussed constituents of water, may be diagnostic of sulfide oxidation. Lead, although seldom found in natural waters in concentrations greater than 20 µg/l (ppb), is another important element that could be present at higher levels in acid-mine discharge. High manganese concentrations, often evident from black staining on rocks and boulders in the creek bed, also is characteristic of acid-mine waters. Although these elements are easily determined in a laboratory by a variety of techniques, there are some advantages in detecting them in the field. Some old colorimetric methods for copper and "heavy metals" (most likely zinc) in soil and sediment, which were originally developed for geochemical exploration purposes, can be adapted to acid-mine water and sediments giving immediate semi-quantitative results to guide

additional sampling (see Ward et al., 1963). "Acid-extractable copper" (Canney and Hawkins, 1958) and "citrate-soluble heavy metals" (Bloom, 1955) require readily available reagents and equipment that can be made up in kit form. Commercial kits, based on colorimetric methods, also are available for determining the concentration of copper, lead, manganese, and zinc in water samples by visual color comparisons.

WATER SAMPLING, FILTRATION, PRESERVATION, AND ANALYSIS

Many of the tests described above (temperature, pH/Eh, specific conductance, dissolved oxygen, and sulfide/hydrogen sulfide) should be made as soon as possible after collecting the sample and, if practical, at the sample site. Other tests, such as determining ferrous iron and alkalinity/acidity, are easily performed in the field if time constraint is not a factor; however, if time is a factor, a properly preserved sample can be obtained and the results determined later in the laboratory. It is impractical, however, to perform many of the desired analysis at the time of collection. Therefore, for these analysis, samples must be collected and preserved in such a way so as not to lose their integrity.

The choice of sample container, proper filtration, and sample preservation are factors that determine whether sample integrity is maintained. A general discussion on the collection and preservation of water samples is provided by American Public Health Association et al. (1992 pp. 1–18). It probably is not possible to provide a set of instructions on sample collection and preservation that would cover all situations. In the following section we present as an example a protocol developed for the rapid, reconnaissance sampling of acid-mine waters (Ficklin et al., 1992; Smith et al., 1992). A more rigorous protocol developed for sites where sample contamination during collection is of high potential (i.e., where waters are dilute with very low levels of metals), or for sites where stringent quality-assurance/quality control requirements are in place, is presented by Horowitz et al. (1994).

Sampling protocol

Filtration

Depending on the use of samples, water must be filtered at the time of collection to prevent reactions that may take place between the filterable and non-filterable portions of the sample in the time interval between sample collection and analysis. Filters are available in a large range of pore sizes and the size to use is the subject of a continuing argument. A 0.45 micron (µm) filter required by EPA protocol (U.S. Environmental Protection Agency, 1983) removes most particulate matter, and some bacteria but this pore size is insufficient to remove colloidal matter (Ranville and Schmiermund, 1999). Van Loon (1982) and Fishman and Friedman (1989) make the distinction between dissolved and suspended as that which passes through and retained using a 0.45 µm filter; however, recent work by Wetherbee and Kimball (1991) reports that a pore size of 0.1 µm is still inadequate to remove all colloidal or suspended matter. The pore size of the filtered sample should accompany any reports generated from the analysis of that sample.

The type of filter medium to be used is very important, due to the relative ease with which the various media plug during filter-

ing and their potential to bleed metals into the waters being filtered. For example, some filters claimed by the manufacturer to be certified for trace metals analysis can react with acid waters and bleed low levels of some elements such as Sb into the waters; thus any filter medium to be used should be checked for its contaminating potential by chemical analysis of deionized water (acidified with nitric acid) that has been passed through the filter. For acid-mine water samples, we have found that tortuous filters made from nitrocellulose (also called cellulose nitrate) or nylon provide the best filtration with minimal to no contamination. For dilute waters with very low metal concentrations, polycarbonate filters provide good results with minimal contamination; however, due to the nature of the filters (sub-micron sized holes punched in the medium), they tend to clog very easily, and so are difficult to use in waters with high contents of suspended sediments.

Another consideration is the amount of water to be filtered. If a small volume is all that is needed, the water can be filtered easily using a 60 ml disposable syringe and disposable filters with Luer adapters that are available from most scientific supply companies in various pore sizes. A 13.5 inch caulking gun can be used to facilitate filtering. However, extreme care should be taken not to make contact between the syringe outlet and metal in the gun; the caulking gun should be coated with plastic tape to minimize contact.

Hand filtration becomes impractical when larger volumes of water are needed. Filtering stands of variable sizes using replaceable filters are commercially available. Several liters of water can be filtered this way. However, although filter stands use replaceable filters, the apparatus is hard to decontaminate between samples. An alternative method of filtering large volumes of water is with the use of commercially available, disposable, capsule filters. These are self-contained membrane filter units permanently assembled in a polypropylene housing that can be inserted directly into the flow line. The flow line consists of flexible plastic tubing and the water is driven through the filter with the use of a peristaltic pump, thereby providing positive pressure filtration. To prevent carryover contamination, new tubing and filter are required for each water sample filtered. The filtered water should be stored in clean, unused, high density polyethylene bottles and acidified with concentrated nitric acid (HNO_3) to a pH less than 2 if the water is preserved for metals analysis. It is necessary to rinse the sample container three times with the filtered water prior to collecting the sample. Water for anions should not be acidified but should be filtered, preferably using a 0.1 μm filter pore size. This small size removes bacteria and viruses that might use some of the anions as nutrients and therefore alter the chemistry.

In order to examine the role of colloids, a Millipore Minitan system was used to filter water samples in the acid-mine drainage study mentioned above (Smith et al., 1992). The exact Minitan pore size is hard to determine but the plate used provides filtration through a 10,000 dalton filter (roughly equivalent to a molecular weight of 10,000). This study found that, in the specific mine-drainages sampled, there was little difference in metal concentrations between the 0.45 μm , 0.1 μm , and 10,000 dalton filtered samples. However, other studies (Wetherbee and Kimball, 1991) have documented significant differences in analytical results between the different filter sizes.

Finally, in sampling water, great care must be exercised in the filtering step to avoid contamination of samples. Contamination can be avoided with the use of disposable filters between successive samples, using sterile gloves and changing gloves often,

avoiding contact with metal, and by not touching the syringe outlet or filter inlet and outlet. If two people are available to collect the sample, one person should be designated as the clean hands person (who handles anything such as the syringe that might come in contact with the sample) and the other as the dirty hands person (who handles things such as the sample bottles, etc.); see Horowitz et al. (1994) for further details. Both should wear gloves and the clean hands person performs no function that might possibly contaminate the sample. It is often helpful to put on multiple pairs of gloves prior to initiating the filtration procedure; should the outermost gloves become contaminated, they can easily be stripped off to expose the next inner pair of gloves, and the need for stopping filtration to put on a new pair of gloves is avoided (Horowitz et al., 1994).

Sample preservation

Depending on the types of analyses for which water samples are collected, the samples generally must be preserved in some manner to prevent (or at least minimize) chemical changes that occur in the samples between collection and analysis. The preservation method used for each type of sample collected is discussed in more detail below.

Bulk sample collection

- Use disposable powder free PVC Gloves throughout sampling process.
- Rinse a 1000 ml high-density polyethylene (HDPE) wide-mouth bottle three times with water to be sampled and then collect a full bottle of representative sample water. If more sample is needed, use a one gallon trace-metal certified HDP cubitainer; rinse and collect as above. Mark site ID and date on bottle. If the sample is not filtered immediately after collection, then the bottle should be placed in the shade, and preferably on ice.

Total metals sample

- Total metals are defined as the sum of the concentrations of metals in both dissolved and suspended fractions and are determined on an unfiltered sample subjected to a vigorous digestion (American Public Health Association et al., 1992 p. 3–1). Normally, a slow boil digestion on a hot plate with concentrated HNO_3 is adequate for most samples. Depending on the sample type, e.g., presence of organic material, siliceous material, or interest in specific elements, some samples may require addition of other inorganic acids in conjunction with HNO_3 for complete digestion; see American Public Health Association et al. (1992, p. 3–4) for recommended digestions.
- To collect the sample, shake the bulk sample container to adequately mix any sediments or suspended material. Rinse an acid-washed² 125 ml HDPE wide mouth bottle three times

²To prepare acid-washed bottles, completely fill each bottle with 10% hydrochloric acid, recap bottle, and let stand in an exhaust hood for a minimum of 12 hours. Empty the bottles and thoroughly rinse the bottles with deionized water. Invert bottles and caps on a clean surface and allow to air dry. When dry, cap and mark with blue laboratory tape.

with a few milliliters of sample water before filling bottle with thoroughly mixed sample. Mark site ID, date, and RA (raw-acidified) on bottle. Acidify sample with 10 drops of concentrated HNO_3 .

Preparation of syringe and filter

- Draw 5 to 10 ml of sample into 60 ml disposable syringe and rinse total syringe cylinder three times before starting the filtering process. Place filled syringe in caulking gun, being careful not to make contact between the syringe outlet and metal. Place filter on syringe, being careful not to touch the filter inlet or outlet, e.g., hold filter only on the sides. Force 10 to 20 milliliters of sample through filter before starting to rinse bottles or collect samples. If peristaltic pump and disposable-capsule filters are used, allow water equivalent to three volumes of the capsule filter to pass through the system.

Collection of filtered samples

A variety of filtered samples can be collected. The order in which these samples are collected is designed to minimize potential contamination of the samples from the filter. Before filling bottles, rinse each bottle three times with a few milliliters of the filtered sample.

- **Ferrous iron:** Use a 60 ml acid-washed HDPE narrow mouth bottle for filtered Fe^{2+} samples. Acidify with 10 drops of concentrated HCl (use more acid if pH is above 4, acidified sample should be pH 1–2). Mark site ID, date, and Fe^{2+} on bottle.
- **Dissolved metals:** A 125 ml acid-washed HDPE wide mouth bottle is used for ICP-MS, ICP-AES, and AAS analysis (dissolved metals). Acidify with 10 drops of concentrated HNO_3 (use 20 drops if sample pH is above 4, acidified sample should be pH 1–2). Note on field data form how many drops of acid were used. Mark site ID, date, and FA (Filtered Acidified) on bottle.
- **Anions:** A 125 ml virgin (not acid-washed) HDPE wide mouth bottle is used for anion analysis. If a new filter is needed, be sure to rinse the filter well before collecting this sample. Mark site ID, date, and FU (Filtered Un-acidified) on bottle. This sample needs to be kept cold or refrigerated (4°C) until analyzed.

Total and dissolved mercury samples

- Samples collected for mercury analysis require special storage and preservation techniques to avoid loss of mercury via volatilization. Both the total and dissolved samples should be stored in glass bottles with teflon-lined caps. Both are preserved with the addition of a mixture of nitric acid and sodium (or potassium) dichromate, which oxidizes any mercury to non-volatile mercuric form (see Kennedy and Crock, 1987, and references therein).

Total and dissolved cyanide samples

- Smith and Mudder (1999) recommend that cyanide samples be refrigerated at 4°C and analyzed as soon as possible after collection, with no addition of preservatives.

Acidity and alkalinity samples

- Retain the 1000 ml sample bottle or cubitainer with at least 125 ml of sample for acidity and alkalinity tests to be done later. The bulk sample needs to be refrigerated or placed on ice.

Acid blank, procedural blank, and duplicate samples

- Analytical blanks and duplicate samples are an integral part of the sampling protocol and are essential to ensure the validity of the analytical data. Analytical errors may result from faulty or improperly calibrated instrumentation, or may arise from impurities in reagents, deionized water, or from poor working skills. The validity of the analytical results can be evaluated by several methods that may reveal some dubious results. These include acid blanks, procedural blanks, and duplicate samples.
- Therefore, at the end of each day, prepare an acid blank by filling a 125 ml acid-washed HDPE wide mouth bottle with deionized water and adding 10 or 20 drops of the same concentrated HNO_3 that was used to acidify samples. Note on field sheet how many drops of acid were used. Mark date and acid blank on bottle.
- A set of procedural blanks is required for each field sampling excursion. Procedural blanks are made with deionized water and are meant to duplicate every step or aspect of the sampling protocol. For the above procedure, the following blanks would be collected: deionized water—unwashed bottle; washed bottle; syringe; syringe + syringe filter. Should questions of potential contamination arise, this set of blanks will help identify where in the procedure contamination occurred. Mark date and procedural step on each bottle.
- Duplicate samples are useful in evaluating the overall precision of the collection and analytical procedures. Duplicate samples should be collected from one of every 10 sampling sites.

FIELD SAMPLING AND ANALYSIS OF SOLID MATERIAL

There is a wide variety of solid samples that can be collected and analyzed to help determine metal mobility from mineralized areas and mine sites into the environment. The procedures used to collect these samples vary according to the material being collected, and so are too numerous to discuss here in detail. The interested reader is referred to the references cited in this section for more details on solid sample collection procedures.

Examples of earth materials that can be sampled include:

- 1) the original ore and gangue materials in the deposit,
- 2) minerals that result from pre-mining weathering,
- 3) secondary minerals resulting from the weathering of mine wastes and mineral processing wastes,
- 4) wastes left over from smelting (such as smelter slag),
- 5) soils within and adjacent to mining or mineral processing sites, and
- 6) stream sediments.

For example, secondary salts or minerals are formed during weathering through processes such as oxidation, evaporation of metal-bearing waters, or precipitation as a result of mixing, dilution, and neutralization. Many of these secondary salts are highly soluble sulfate minerals that, in their solid form during dry times,

serve as reservoirs for stored acidity and metals (Nordstrom and Alpers, 1999; Alpers et al., 1994; Plumlee et al., 1995). They are dissolved during periods of rain or snowmelt, thus releasing their load of acid and metal which causes dramatic seasonal fluctuations in surface water that may have hazardous effects on biota. At the Summitville mine in southern Colorado, a U.S. Environmental Protection Agency Superfund site, Plumlee et al. (1995) reported finding secondary salts as surficial coatings on rock materials within the open pit and waste dumps, as coatings on fractures in rocks forming the open-pit walls, and as disseminations within sediments throughout the mine. The collection of secondary salts sometimes can be troublesome because they form as fragile crusts or veneers on surfaces and, because they can lose or gain waters of hydration, their crystallinity changes between the time of collection and laboratory analysis. Storing samples in sealed plastic bags usually is sufficient for chemical analysis, however, for mineral identification, the samples often are immersed in mineral oil upon collection.

In addition to secondary salts, many other types of solid materials may be collected and analyzed to assess environmental impact from surface weathering related to mining activities. Stream-sediment samples are useful in determining the attenuation of elements down stream from a point source such as mining related activities. As water chemistry changes down stream from the point source, dissolved elements either precipitate or are adsorbed onto clays and hydrous oxides. Lake bottom sediments and stream sediments also can be used to evaluate time-integrated effects. Tidball et al. (1995) collected soils, overbank sediments, and eolian deposits in the San Luis Valley to assess the dispersion of elements from the Summitville mine site in the nearby San Juan Mountains and, therefore, any potential impact on valley soils.

Biota also can be sampled to assess environmental impact from anthropogenic activities, including, for example

- 1) crops, trees, and other vegetation,
- 2) fish and other living organisms, and
- 3) hair, blood, and wool of wildlife and livestock.

As part of the Summitville study, Erdman et al. (1995) sampled alfalfa from fields in the San Luis Valley to determine whether significant compositional differences existed between alfalfa grown in fields that were irrigated with water affected by mine-drainage from the Summitville mine site and alfalfa grown in fields that were irrigated with water from the Rio Grande river. Other Summitville studies examined temporal metal distribution in tree rings of trees growing along rivers downstream from Summitville (Gough et al., 1995), and the metal content of hair, blood, and wool samples collected from livestock that had ingested river water affected by acid drainage from Summitville (Brown, 1995). Gray et al. (1994) measured mercury and other heavy-metal concentrations in liver, muscle, and whole-fish samples of Arctic grayling to evaluate mercury contamination downstream from abandoned mercury mines in the Kuskokwim River region of southwest Alaska.

REFERENCES

- Alpers, C.N., Blowes, D.W., Nordstrom, D.K., and Jambor, J.L., 1994, Secondary minerals and acid mine-water chemistry; in Blowes, D.W. and Jambor, J.L. (eds.), *The Environmental Geochemistry of Sulfide Mine-Waste: Short course Handbook v. 22*, Waterloo, Ontario, pp. 247–270.
- American Public Health Association, American Water Works Association, and Water Pollution Control Federation, 1985, *Standard methods for the examination of water and wastewater: 16th ed.*, Washington, D.C., 1268 pp.
- American Public Health Association, American Water Works Association, and Water Pollution Control Federation, 1992, *Standard methods for the examination of water and wastewater: 18th ed.*, Washington, D.C., variable numbers of pages.
- American Society for Testing and Materials, 1992, *Annual book of ASTM Standards*, section 11, water: Philadelphia, American Society for Testing and Materials, v. 11.01, pp. 191–195.
- Bloom, H., 1955, A field method for the determination of ammonium citrate-soluble heavy metals in soil and alluvium: *Economic Geology*, v. 50, no. 5, pp. 533–541.
- Brassington, R., 1988, *Field Hydrology*: Halsted Press, Great Britain, 175 pp.
- Brown, L.N., 1995, Biological concentrations of key elements in blood, hair, and wool of livestock raised in the Alamosa River watershed, Part 1. Veterinary diagnostic analysis; in Posey, H.H., Pendleton, J.A., Van Zyl, Dirk (eds.), *Proceedings, Summitville Forum '95: Colorado Geological Survey Spec. Pub. No. 38*, pp. 304–315.
- Canney, F.C., and Hawkins, D.B., 1958, Cold acid extraction of copper from soils and sediments—A proposed field method: *Economic Geology*, v. 53, no. 7, pp. 877–886.
- Cline, J.D., 1969, Spectrophotometric determination of hydrogen sulfide in natural waters: *Limnology and Oceanography*, v. 14 pp. 454–458.
- Erdman, J.A., Smith, K.S., Dillon, M.A., and ter Kuile, M., 1995, Impact of Alamosa River water on alfalfa, southwestern San Luis Valley, Colorado; in Posey, H.H., Pendleton, J.A., Van Zyl, Dirk (eds.), *Proceedings, Summitville Forum '95: Colorado Geological Survey Spec. Pub. No. 38*, pp. 263–269.
- Fetter, C.W., 1988, *Applied hydrology*, 2nd ed.: Merrill Publishing Co., Columbus, Ohio, 592 pp.
- Ficklin, W.H., Plumlee, G.S., Smith, K.S., and McHugh, J.B., 1992, Geochemical classification of mine drainages and natural drainages in mineralized areas; in Kharaka, Y.K., and Maest, A.S. (eds.), *Proceedings, 7th Internatl Symposium on Water-Rock Interactions: Park City, Utah*, pp. 381–384.
- Fishman, M.J., and Friedman, L.C., 1989, Methods for determination of inorganic substances in water and fluvial sediments; in *Techniques of Water-Resources Investigations of the United States Geological Survey: Book 5, Chapter A1*, 626 pp.
- Gough, L.P., Yanosky, T.M., Lichte, F.E., and Balistrieri, L.S., 1995, Preliminary interpretation of spatial and temporal trends in the chemistry of tree rings downstream from the Summitville Mine; in Posey, H.H., Pendleton, J.A., Van Zyl, Dirk (eds.), *Proceedings, Summitville Forum '95: Colorado Geological Survey Spec. Pub. No. 38*, pp. 236–243.
- Gran, G., 1950, Determination of the equivalence point in potentiometric titrations: *Acta Chimica Scandinavia*, v. 4, pp. 559–577.
- Gray, J.E., Theodorakos, P.M., Budahn, J.R., and O'Leary, R.M., 1994, Mercury in the environment and its implications, Kuskokwim River region, southwestern Alaska; in Till, A.B. and Moore, T.E. (eds.), *Geological Studies in Alaska by the U.S. Geological Survey, 1993: U.S. Geological Survey Bulletin 2107*, pp. 3–13.
- Horowitz, A.J., Demas, C.R., Fitzgerald, K.K., Miller, T.L., and Rickert, D.A., 1994, U.S. Geological Survey protocol for the collection and processing of surface-water samples for the subsequent determination of inorganic constituents in filtered water: U.S. Geological Survey Open-File Report 94–539, 57 pp.
- Kennedy, K.R., and Crock, J.G., 1987, Determination of mercury in geological materials by continuous-flow, cold-vapor, atomic absorption spectrophotometry: *Analytical Letters*, v. 20, pp. 899–908.
- Langmuir, D., and Whittemore, D.C., 1970, Variations in the stability of precipitated ferric oxyhydroxide; in Hem, J.D. (ed.), *Advances in Chemistry Series 106: American Chemical Society, Washington, D.C.*, pp. 209–234.
- Lindberg, R.D., and Runnels, D.D., 1984, Ground water redox reactions—

- An analysis of equilibrium state applied to Eh measurements and geochemical modeling: *Science*, v. 225, pp. 925–927.
- Mills, A.L., 1999, The role of bacteria in environmental geochemistry; *in* Plumlee, G.S., and Logsdon, M.J. (eds.), *The Environmental Geochemistry of Mineral Deposits, Part A. Processes, Techniques, and Health Issues: Society of Economic Geologists, Reviews in Economic Geology*, v. 6A, pp. 125–132.
- Nordstrom, D.K., 1977, Thermochemical redox equilibria of ZoBell's solution, *Geochimica et Cosmochimica Acta*, 41, pp. 1835–1841.
- Nordstrom, D.K., and Alpers, C.N., 1999, Geochemistry of acid mine waters; *in* Plumlee, G.S., and Logsdon, M.J. (eds.), *The Environmental Geochemistry of Mineral Deposits, Part A. Processes, Techniques, and Health Issues: Society of Economic Geologists, Reviews in Economic Geology*, v. 6A, pp. 133–160.
- Nordstrom, D.K., Jenne, E.A. and Ball, J.W., 1979, Redox equilibria of iron in acid mine waters; *in* Jenne, E.A. (ed.), *Chemical Modeling in Aqueous Systems: Symposium Series 93, American Chemical Society, Washington, D.C.* pp. 51–79.
- Plumlee, G.S., Smith, K.S., Ficklin, W.H., and Briggs, P.H., 1992, Geological and geochemical controls on the composition of mine drainages and natural drainages in mineralized areas; *in* Kharaka, Y.K., and Maest, A.S. (eds.), *Proceedings, 7th Internatl Symposium on Water-Rock Interactions: Park City, Utah*, pp. 419–422.
- Plumlee, G.S., Gray, J.E., Roeder, M.M., Coolbaugh, M., and Whitney, G., 1995, The importance of geology in understanding and remediating environmental problems at Summitville; *in* Posey, H.H., Pendleton, J.A., Van Zyl, Dirk (eds.), *Proceedings, Summitville Forum '95: Colorado Geological Survey Spec. Pub. No. 38*, pp. 13–22.
- Ranville, J.F., and Schmiermund, R.L., 1999, General aspects of aquatic colloids in environmental geochemistry; *in* Plumlee, G.S., and Logsdon, M.J. (eds.), *The Environmental Geochemistry of Mineral Deposits, Part A. Processes, Techniques, and Health Issues: Society of Economic Geologists, Reviews in Economic Geology*, v. 6A, pp. 183–199.
- Ritcey, G.M., 1989, *Tailings management problems and solutions in the mining industry: Elsevier, N.Y.*, 970 pp.
- Skougstad, M.W., Fishman, M.J., Friedman, L.C., Erdman, D.E., and Duncan, S.S., 1979, *Methods for determination of inorganic substances in water and fluvial sediments: Techniques of Water Resources Investigations of the United States Geological Survey, Book 5, Chap. 1*, 621 pp.
- Slack, K.V., 1968, A microkit for dissolved oxygen determination; *in* Chase, E.B. and Payne, F.N. (eds.), *Selected Techniques in Water Resources Investigations, 1966–67: U.S. Geological Survey Water-Supply Paper 1892*, pp. 44–54.
- Smith, A.C.S., and Mudder, T.I., 1999, The environmental geochemistry of cyanide; *in* Plumlee, G.S., and Logsdon, M.J. (eds.), *The Environmental Geochemistry of Mineral Deposits, Part A. Processes, Techniques, and Health Issues: Society of Economic Geologists, Reviews in Economic Geology*, v. 6A, pp. 229–248.
- Smith, K.S., Ficklin, W.H., Plumlee, G.S., and Meier, A.L., 1992, Metal and arsenic partitioning between water and suspended sediment at mine-drainage sites in diverse geologic settings; *in* Kharaka, Y.K., and Maest, A.S. (eds.), *Proceedings, 7th Internatl Symposium on Water-Rock Interactions: Park City, Utah*, pp. 443–447.
- Stumm, W., and Morgan, J.J., 1981, *Aquatic chemistry, 2nd ed.: Wiley and Sons, New York*, 796 p.
- Thomas, J.F.J., and Lynch, J.J., 1960, Determination of carbonate alkalinity in natural waters: *Journal of American Water Works Association*, v. 52, pp. 259.
- Tidball, R.R., Stewart, K.C., Tripp, R.B., and Mosier, E.L., 1995, Geochemical mapping of surficial materials in the San Luis Valley, Colorado; *in* Posey, H.H., Pendleton, J.A., Van Zyl, Dirk (eds.), *Proceedings, Summitville Forum '95: Colorado Geological Survey Spec. Pub. No. 38*, pp. 244–262.
- United States Environmental Protection Agency, 1983, *Methods for chemical analysis of water and wastes: Environmental Monitoring and Support Laboratory, EPA-600/4-79-020*, variable pages.
- Van Loon, J.C., 1982, *Chemical analysis of inorganic constituents of water: CRC Press, Boca Raton, Fla.*, 248 pp.
- Ward, F.N., Lakin, H.W., and Canney, F.C., 1963, *Analytical methods used in geochemical exploration by the U.S. Geological Survey: U.S. Geological Survey Bulletin 1152*, 100 pp.
- Wetherbee, G.A., and Kimball, B.A., 1991, Use of environmental variables to estimate metal loads in streams, upper Arkansas River Basin, Colorado; *in* Mallard, G.E., and Aronson, D.A. (eds.), *U.S. Geological Survey Toxic Substances-Hydrology Program, Proceedings of the technical meeting, Monterey, Calif., March 11–15, 1991: U.S. Geological Survey Water Resources Investigation Report 91-4034*, pp. 398–406.
- Wood, W.W., 1976, Guidelines for collection and field analysis of ground-water samples for selected unstable constituents; *in* *Techniques of Water-Resources Investigations of the United States Geological Survey: Book 1, Chapter D2*.

Chapter 13

LABORATORY METHODS FOR THE ANALYSIS OF ENVIRONMENTAL SAMPLES

J.G. Crock, B.F. Arbogast, and P.J. Lamothe

U.S. Geological Survey, Box 25046, MS 973, Federal Center, Denver, CO 80225-0046

INTRODUCTION

The precise, accurate analysis of environmental materials for their total or partial elemental content is anything but a simple or routine task. There are numerous problems that must be addressed to assure a high quality analysis. The first and foremost problem to be addressed is to determine what is the question that the environmental scientist is really trying to answer and how to customize the analysis to meet that need. Is the scientist asking for a given species of an element, the amount of the analyte associated with a certain phase or fraction of the environmental sample, or would a total analysis answer the correct question? The scope of the phrase "Environmental Materials" is where the problems continue. Most naturally occurring materials and some man-made materials can fall into this classification. The concentration of an element of interest commonly ranges from one part per billion (microgram per kilogram or $\mu\text{g}/\text{kg}$) to the tens of weight percent. There are usually sampling problems in the analysis of environmental samples. These problems could include:

- a) Is the sample collected by the environmental scientist truly representative of the population to be studied? (This problem will not be addressed for it is well outside the purpose of this chapter);
- b) Sample homogeneity—is the sample well mixed and ground to a sufficiently small particle size?
- c) Sample size—is the sample too large to handle or is it too small for the required analysis?
- d) Moisture content—do you analyze the sample in its "as-collected-state" or should it be dried to a constant weight?
- e) What is the proper pretreatment of the sample? and,
- f) Sample digestion or dissolution—some samples may completely dissolve in a water leach, whereas others may require a high temperature fusion.

Other problems that often plague the analysis of environmental materials include contamination of the element(s) of interest, spectral or background interferences from concomitant elements for a given method of determination, volatility of the analyte element during the collection, storage, preparation, and digestion of the materials, and lack of a sensitive enough method to determine levels of a given analyte at or below natural background levels.

There are many complete references for the analysis of environmental and geological materials available. Some of the more noteworthy are Carter (1993), Jeffery and Hutchison (1983), Ingamells and Pitard (1986), Potts (1987), Smoley (1992), Stoch (1986), and Westerman (1990). Literature reviews of the analytical chemistry of geological materials (e.g., Jackson et al., 1995) and

of environmental materials (e.g., Clement et al., 1995) offer an updated snapshot of the progress in analytical chemistry for these samples. Fishman and Friedman (1989) and Greenberg et al. (1992) offer an overview of the analytical chemistry of waters. Keith (1988) and LaFleur (1976) present excellent overviews of sampling and how to overcome many of the sampling problems which could render a study invalid. Zief and Mitchell (1976) address the control of contamination in trace analysis and how to minimize it.

One of the most important aspects to the analysis of environmental materials is the digestion/decomposition of the material prior to presenting the sample to the individual instrumental method. Excellent references for the total dissolution of environmental materials include Bock (1979) and Sulcek and Povondra (1989). Chao (1984) addresses in detail the application of partial and sequential dissolution schemes. Chao and Sanzolone (1992) discuss both total and partial dissolution. Often a method of determination is not sensitive enough, either because of the original concentration of the analyte or from the required dilution of the digestion method. This is commonly observed in baseline or background studies. Often the separation and (or) preconcentration of the analyte from the matrix is required. Minczewski et al. (1982) present a comprehensive overview of these useful techniques.

The analytical chemist must also address the mode of occurrence of a given analyte element. Adriano (1986), Greenwood and Earnshaw (1984), Kabata-Pendias and Pendias (1984), and Rose et al. (1979) present comprehensive discussions on the generalized geochemistry and mode of occurrence of most elements. Batley (1989) addresses trace element speciation in environmental samples and the analytical problems associated with different modes of occurrences.

Many of the methods outlined in this chapter are currently in use in the laboratories of the U. S. Geological Survey. The general references for most of these methods are Arbogast (1990, 1996) and Baedeker (1987). These methods will be presented along with an overview to give the reader an introduction to the analytical chemistry of solid and aqueous environmental samples.

TOTAL ANALYSIS OF SOLIDS

Sample preparation

The following is a discussion of the preparation of rock, sediment, soil, and vegetation samples. For an analysis to be of any worth, the sample must first be prepared properly. Sample prepara-

ration is the very important first step to all subsequent analyses.

Most samples of naturally occurring material require some kind of physical preparation prior to chemical analysis. Samples require preparation to effect one or more of the following:

- a) Reduce the sample to a size that is more conveniently transported;
- b) Increase the sample surface area to enhance the efficiency of subsequent chemical attack;
- c) Homogenize the sample to ensure that a subsample is representative of the entire sample; and,
- d) Separate the sample into components based on mineralogy, grain size, or physical and morphological criteria.

Sample preparation is an important step in the analytical process. Without careful preparation, and attention to inter-sample contamination, the worth of the subsequent analyses is significantly diminished.

Rock sample preparation

Rock samples are routinely reduced to ≤ 0.5 -cm fragments in a jaw crusher. The crushed sample is split, if necessary, and fed into an operating and properly adjusted Braun[®] vertical mechanical pulverizer¹ equipped with ceramic plates. The sample is pulverized to approximately minus 100-mesh ($< 150 \mu\text{m}$) and mixed to insure homogeneity for subsequent analysis. Mineral samples with distinctive cleavage planes (i.e., mica or clay minerals) can present a problem in pulverizing due to the crystal structure of the sample. For some methods where the quality of pulverization is critical in obtaining accurate results, the sample or a representative split is placed in either a ceramic or agate SPEX[®] shatterbox and ground until 100% passes an 80-mesh ($< 180 \mu\text{m}$) screen. Ground samples can be stored in cardboard, glass, or plastic containers.

Sediment sample preparation

Dry sediment samples are disaggregated by hand and typically as much organic material as possible, such as leaves, twigs, or roots, is manually removed. The samples are usually sieved to pass an appropriate screen size, usually 80-mesh, and mixed. If the particle size chosen is larger than 80-mesh (particle size $\geq 180 \mu\text{m}$), the sieved fraction is generally ground in a vertical mechanical pulverizer until 100% passes an 80-mesh screen and then mixed.

Soil sample preparation

Dry soil samples are disaggregated, if necessary, in a mechanical, ceramic mortar and pestle. Samples are sieved using a 10-mesh sieve (2 mm) and the plus 10-mesh material is usually discarded. The minus 10-mesh fraction is ground further with vertical mechanical pulverizer until 100% passes an 80-mesh screen. Both sediment and soil samples should be dried only under forced air at ambient temperature to minimize the possible loss of volatile elements, such as mercury, selenium, or sulfur.

Plant material preparation and determination of weight percent ash

The physical preparation of plant material generally consists of washing, drying, and milling, and the subsequent dry ashing of an aliquot, or subsplit of the sample (Peacock, 1992).

Washing of Vegetation Samples—Most plant samples should be washed to eliminate contamination from adhering soil or dust particles. Three common methods for washing plant samples are:

- a) “in the bag” washing by machine;
- b) “beaker soak” hand washing in tap or deionized/demineralized water in plastic beakers, large enough for complete immersion and manual agitation; and the most common,
- c) “colander rinse” with tap or deionized/demineralized water.

For the first method samples are run through at least one complete wash/rinse/spin cycle on gentle mode of a regular commercially-available clothes washing machine using cloth sample bags. All washing must be followed by a deionized/demineralized water rinse to prevent metal uptake from wash water. When the “beaker soak” method is used, water is constantly changed in the beakers since the sample is actually moved from one beaker to another over the course of a few minutes. For the last method the sample is rinsed in a plastic or aluminum colander sequentially with tap and deionized/demineralized water. Samples are transferred to a clean colander for drying. Drying temperatures are held under 40°C, usually under forced air. Material having a resinous coating on stems or leaves is dried without heat to minimize the possibility of its loss through liquification. Samples are dried to brittleness and this usually takes 24–48 hours.

Milling of Vegetation Samples—Dried samples can be put directly into a grinder. It has been found that the Wiley Mill[®] is best for young, woody growth up to a thickness of 5 mm. The Christy/Norris Mill[®] is used for all thicker materials such as twigs, roots, and branches up to about 13 mm in diameter. Mosses and lichens are ground in a blender, Wiley Mill[®], or in a ceramic mortar and pestle after they have been frozen in liquid nitrogen. Larger diameter material must be first cut manually to prevent jamming of the mill. Samples are mixed using a rotary type of tumbling device after grinding.

Dry Ashing of Vegetation and Organic Carbon-Rich Samples—Whenever ashing is required by an analytical technique, a calculation of weight percent ash is required. The analytical results are converted back to a dry-weight basis for comparison with other analytical techniques. Commonly encountered problems for dry ashing include:

- a) contamination from dust or soil from the sampling site which may coat stems and leaves;
- b) loss of volatile elements at the ashing temperature; and,
- c) incomplete ashing of certain species at the prescribed temperature.

Most contamination of vegetation samples is by dust or soil and can be eliminated by washing in deionized/demineralized water. An ashing temperature of 500°C is often chosen because it is the optimum temperature at which most plant materials will lose most of their organic components. This temperature is maintained for at least 12 hours to maximize loss of organic material. Material that does not ash completely at 500°C should remain in the furnace for a second ashing cycle. Volatile elements (i.e., Se, As, Hg, Cl, and P) are commonly determined in unashed subsplits of the sample. Ashing requires only a portion of the sample, but enough to satisfy the analytical needs of the following digestion methods while

¹Any use of trade, product, or firm names in this publication is for descriptive purposes only and does not imply endorsement by the U.S. Government.

remaining representative of the entire sample. The amount of this "aliquot" is also determined by its density, estimated ash yield, and amount of sample available. An aliquot of 10g is usually adequate, although satisfactory results have been obtained from splits of 1 to 24 g. Ashing proceeds with the door of the muffle furnace fully closed. The small amount of oxygen necessary for the oxidizing process enters through the imperfect seal between door and wall bricks. Furnaces are programmed to "ramp" up to the ashing temperature of 500°C over a period of 5 hours. Complete ashing is insured by maintaining this temperature for ≥ 12 hours. The furnaces are allowed to cool for ≥ 8 hours before sample dishes are removed. While cooling, the door should be slightly open but not swung away until the inside temperature dips below 200°C. Sample dishes should remain undisturbed until cooled to $< 100^\circ\text{C}$. The ash must then be mixed and reduced in volume, for it tends to be highly charged with static. This is done through the use of a 5-mm solid-borosilicate bead (placed into a plastic vial prior to addition of the ash), and 10 to 60s of shaking in a mixer/mill. This bead should remain in the plastic vial. The ash is then ready for laboratory analysis.

Total major, minor, and trace metal analyses

Introduction

With advancements in analytical instrumentation over the past three decades, the analyst has a choice of several precise and accurate methods with sufficient sensitivity for most environmental study requirements. Some of the more popular methods of instrumental analysis are: flame atomic absorption spectroscopy (F-AAS), graphite furnace-atomic absorption spectroscopy (GF-AAS), inductively coupled plasma-atomic emission spectroscopy (ICP-AES), and inductively coupled plasma-mass spectrometry (ICP-MS). Table 13.1 lists detection limits for most elements for these four techniques. Each method has its advantages and disadvantages. Table 13.2 summarizes the comparative benefits of these methods. Few laboratories rely on only one of these analytical methods, but often use compatible combinations of these techniques. Other methods of analysis commonly used in the laboratory for environmentally important analytes include X-ray fluorescence, instrumental neutron activation analysis, electrochemical methods (especially specific ion electrode methods), infrared detection of combustion products, ion chromatography, and colorimetry. Colorimetry will not be addressed in this chapter; Sandell (1959) offers a classic overview of this method and many applications. Various manufacturers of colorimeters also offer excellent methods manuals for colorimetry (e.g., Hach® Chemical Company).

Inductively coupled plasma-atomic emission spectroscopy

Since its introduction in the early 1970s, inductively coupled plasma-atomic emission spectroscopy (ICP-AES) has become an important technique for the analysis of environmental and geochemical materials for their trace, minor, and major elemental content (Fassel and Kniseley, 1974). In this technique, element excitation is achieved by an argon plasma sustained by the interaction of ionized argon gas inductively coupled to a radio-frequency energy field. An inductively coupled plasma is an attrac-

tive spectral source because of its high temperatures, as much as 10,000°K, optical transparency, and long-term stability. About three-fourths of the common elements can be determined by this technique, with lower limits of detection in the range of 0.05 to 50 $\mu\text{g/l}$. This technique is noted for linearity of response, often covering four to five orders of magnitude, and relative freedom from matrix effects which often plague other spectroscopic and classical methods. The technique offers excellent measurement precision, usually from 1 to 3% relative standard deviation, and has good accuracy. ICP-AES is a rapid multielement technique, by which 30 to 40 elements can be determined routinely within two minutes (Crock et al., 1983).

Several books and articles on the ICP-AES technique explain in detail the theory and chemistry of the plasma and the analysis of environmental and geological materials. Montaser and Golightly (1992) present the theory and chemistry of the plasma, as well as its general application to analytical chemistry. A handbook of ICP-AES analysis (Thompson and Walsh, 1989) describes the complete and partial analyses of geological materials, water analysis, and the analysis of environmental samples. Winge et al. (1985) present an excellent atlas of ICP-AES spectral information for most elements. This atlas aids in selecting the proper analytical wavelength to maximize sensitivity in a given matrix while minimizing potential spectral overlap interferences. Lichte et al. (1987a) present a condensed handbook of the routine ICP-AES analysis of geochemical materials. Reviews of the current literature on ICP-AES analyses of geological and inorganic materials are published annually or biennially in journals such as the *Journal of Analytical Atomic Spectrometry* and *Analytical Chemistry*.

The most common ICP-AES technique is to analyze an environmental material as an aqueous solution. However, there are techniques in which the elements of interest are extracted into an organic solvent that is aspirated directly (e.g., Motooka, 1988). Limited success has been reported with the direct nebulization of a slurry powder or direct insertion of samples using a graphite cup (Thompson and Walsh, 1989). The most promising solid sampling technique is laser ablation of a solid sample into the plasma (Thompson et al., 1989).

Sample dissolution is usually the most tedious, time-consuming, and limiting factor in chemical analyses. A multiacid digestion, combining hydrofluoric, hydrochloric, nitric, and perchloric acids at low temperatures and pressures (Crock et al., 1983), is a common dissolution method. Most of the common rock-forming aluminosilicate minerals can be dissolved by this method. The advantages of acid digestion are the ease of the method, use of large samples (as much as 2 g, although 0.2 g is more common), low reagent blanks, and low total dissolved salts in the analytical solution. With an acid digestion, the final dilution factor commonly is less than 100, allowing many elements to be determined at or near their crustal abundance. One disadvantage of acid digestion is the volatilization of some elements, such as silicon and boron as fluoride compounds. Commonly, a higher pressure, closed-vessel "bomb" digestion with addition of a complexing agent for the excess fluoride is used to avoid volatilization of silicon and boron.

Some minerals are resistant to routine acid digestions and require a more rigorous digestion. These minerals include spinels, beryl, tourmalines, chromite, zircon, monazite, niobates, tungstates, topaz, and cassiterite. These minerals can be completely dissolved by the proper choice of a sinter or fusion diges-

TABLE 13.1—Atomic spectroscopy detection limits (ppb or micrograms/liter).

Element	Symbol	Method				Symbol	Alternate Method	
		F-AAS	GF-AAS	ICP-AES	ICP-MS			
Aluminum	Al	45	0.3	6	0.006	Al		
Antimony	Sb	45	0.4	90	0.001	Sb	0.15	(HG-AAS)
Arsenic	As	150	0.5	30	0.0006	As	0.03	(HG-AAS)
Barium	Ba	1.5	0.9	0.15	0.002	Ba		
Beryllium	Be	1.5	0.02	0.09	0.03	Be		
Bismuth	Bi	30	0.6	30	0.0005	Bi		
Boron	B	1000	45	3	0.09	B		
Bromine	Br				0.2	Br		
Cadmium	Cd	0.8	0.02	1.5	0.003	Cd		
Calcium	Ca	1.5	0.03	0.15	2	Ca		
Cerium	Ce	100,000		15	0.0004	Ce		
Cesium	Cs	15		3200	0.0005	Cs		
Chlorine	Cl				10	Cl		
Cobalt	Co	9	0.4	3	0.0009	Co		
Chromium	Cr	3	0.08	3	0.02	Cr		
Copper	Cu	1.5	0.25	1.5	0.003	Cu		
Dysprosium	Dy	50		0.3	0.001	Dy		
Erbium	Er	60		0.7	0.0008	Er		
Europium	Eu	30		0.3	0.0007	Eu		
Gadolinium	Gd	1800		2.5	0.002	Gd		
Gallium	Ga	75		15	0.001	Ga		
Germanium	Ge	300		15	0.003	Ge		
Gold	Au	9	0.4	6	0.001	Au		
Hafnium	Hf	300		4	0.0006	Hf		
Holmium	Ho	60		0.5	<0.0005	Ho		
Indium	In	30		45	<0.0005	In		
Iodine	I			60	0.008	I		
Iridium	Ir	900	7	30	0.0006	Ir		
Iron	Fe	5	0.3	1.5	0.4	Fe		
Lanthanum	La	3000		1.5	0.0005	La		
Lead	Pb	15	0.15	30	0.001	Pb		
Lithium	Li	0.8	0.15	1.5	0.03	Li		
Lutetium	Lu	1000		0.05	<0.0005	Lu		
Magnesium	Mg	0.15	0.01	0.15	0.007	Mg		
Manganese	Mn	1.5	0.09	0.6	0.002	Mn		
Mercury	Hg	300	1.5	30	0.004	Hg	0.009	(CV-AAS)
Molybdenum	Mo	45	0.2	7.5	0.003	Mo		
Neodymium	Nd	1500		2	0.002	Nd		
Nickel	Ni	6	0.8	6	0.005	Ni		
Niobium	Nb	1500		5	0.0009	Nb		
Osmium	Os	120		5		Os		
Palladium	Pd	30	2	1.5	0.003	Pd		
Phosphorous	P	75,000	320	45	0.3	P		
Platinum	Pt	60	5	30	0.002	Pt		
Potassium	K	3	0.02	75	1	K		
Praseodymium	Pr	7500		0.8	<0.0005	Pr		
Rhenium	Re	750		30	0.0006	Re		
Rhodium	Rh	6		30	0.0008	Rh		
Rubidium	Rb	3	0.08	37	0.003	Rb		
Ruthenium	Ru	100	3	6	0.002	Ru		
Samarium	Sm	3000		7	0.001	Sm		
Scandium	Sc	30		0.3	0.02	Sc		
Selenium	Se	100	0.7	90	0.06	Se	0.03	(HG-AAS)
Silicon	Si	90	2.5	5	0.7	Si		
Silver	Ag	1.5	0.05	1.5	0.003	Ag		

TABLE 13.1—Continued

Element	Symbol	Method				Symbol	Alternate Method
		F-AAS	GF-AAS	ICP-AES	ICP-MS		
Sodium	Na	0.3	0.05	6	0.05	Na	
Strontium	Sr	3	0.03	0.075	0.0008	Sr	
Tantalum	Ta	1500		30	0.0006	Ta	
Tellurium	Te	30	1	75	0.01	Te	
Terbium	Tb	900		5	<0.0005	Tb	
Thallium	Tl	15	0.4	60	0.0005	Tl	
Thorium	Th			17	<0.0005	Th	
Thulium	Tm	15		1.5	<0.0005	Tm	
Tin	Sn	150	0.5	60	0.002	Sn	
Titanium	Ti	75	0.9	0.75	0.006	Ti	
Tungsten	W	1500		30	0.001	W	
Uranium	U	15,000		15	<0.0005	U	
Vanadium	V	60	0.3	3	0.002	V	
Ytterbium	Yb	8		0.3	0.001	Yb	
Yttrium	Y	75		0.3	0.0009	Y	
Zinc	Zn	15	0.3	1.5	0.003	Zn	
Zirconium	Zr	450		1.5	0.004	Zr	

All detection limits were determined using elemental standards in dilute aqueous solutions under optimized conditions for each individual element. All detection limits are based on a 98% confidence level (3 standard deviations). The actual detection limits observed when analyzing environmental samples will be higher due to concomitant elements and various interferences, depending on the method of choice. These detection limits were determined using Perkin-Elmer® instrumentation (personal commun., L.A. Wegelin, Perkin Elmer Corp., Denver, Colo., 1996).

F-AAS: Flame Atomic Absorption Spectrometry
 GF-AAS: Graphite Furnace Atomic Absorption Spectrometry
 ICP-AES: Inductively Coupled Plasma-Atomic Emission Spectrometry
 ICP-MS: Inductively Coupled Plasma-Mass Spectrometry
 HG-AAS: Hydride Generation-Atomic Absorption Spectrometry
 CV-AAS: Cold Vapor-Atomic Absorption Spectrometry

TABLE 13.2—Relative advantages and disadvantages of the four common spectroscopic methods used in environmental analysis.

Benefit	ICP-MS	ICP-AES	GF-AAS	F-AAS
Multielement characteristics	+	+	-	-
Qualitative analysis	+	+	-	-
Low detection limits	+	-/+	+/-	-/+
Analytical speed	+	+	-	+/-
Precision	-	+	+/-	+
Dynamic range of analysis	+	+	-	-/+
Problems from matrix interferences	-	+	+/-	+
Problems from spectral interferences	-	-	+	+
Ease of use	+/-	+	+/-	+
Small sample volumes	-	-	+	-
Isotopic analysis	+	-	-	-
Purchase price	-	-/+	+	+
Cost per analysis	+	+	-	+

+: Relative advantage for that method when compared to the other methods
 -: Relative disadvantage for that method when compared to the other methods
 +/-: More of an advantage than a disadvantage
 -/+: More of a disadvantage than an advantage

tion procedure. A sodium peroxide sinter will dissolve most resistant minerals. For example, boron and silicon are routinely determined in tourmaline by ICP-AES following a sodium peroxide sinter in a zirconium crucible at 445°C. Lithium metaborate, sodium and (or) potassium hydroxide, sodium carbonate, and the alkali persulfates are commonly used as fusion reagents. However, there are drawbacks to the use of fusions or sinters. They introduce a much higher total salt content into the analytical solution, which can clog the nebulizer and torch assembly. These fusions and sinters also tend to have long-term memory effects and higher reagent blanks. A larger dilution factor is used because of the smaller sample size (10 to 100 mg is common) in a larger final solution volume. The final dilution factor is commonly 200 to 400, making the determination of some trace elements impossible by ICP-AES direct aspiration without subsequent separation and preconcentration. Also, at least one element common to the reagent is not determinable, such as lithium and boron from a lithium metaborate fusion.

To minimize matrix and spectral interference problems, and to bring elemental concentrations into the range of ICP-AES, chemical separation and preconcentration steps are sometimes used. An example is the analysis of geological materials for their rare-earth-element (REE) content at or below their chondritic abundance levels. This method uses a lithium metaborate fusion or an acid digestion of the sample and subsequent separation and preconcentration of the REE by sequential-acid ion chromatography (Crock et al., 1986). The method has a final dilution factor as small as 5 (1 g sample in 5 ml final solution).

ICP-AES is subject to spectral interferences, background shifts, and matrix effects (Thompson and Walsh, 1989). An internal standard, e.g. lutetium (Crock et al., 1983), should be used to help minimize these problems. Interelement correction factors and background corrections are applied routinely. Further corrections are made when an element influences other elements beyond the "normal correction." It is common to not report an effected element due to the extraordinary interference of the affecting element. Matrix effects can generally be negated by proper matching of standard and sample matrices.

Analysis by ICP-AES for major, minor, and trace elements is useful for a variety of geochemical and environmental investigations. The lower and upper reporting limits used for this method following an acid digestion are shown in Table 13.3 (Arbogast, 1996).

As an example of ICP-AES analysis of environmental solid materials, a method where forty major, minor, and trace elements are determined in environmental materials ICP-AES is described here. The sample is decomposed using a mixture of hydrochloric, nitric, perchloric, and hydrofluoric acids at low temperature (Crock et al., 1983). The digested sample is aspirated into the ICP-AES discharge where the elemental emission signal is measured simultaneously for the forty elements. Calibration is performed using digested rock reference materials and a series of multielement solution standards (Lichte et al., 1987a).

Typically a 0.200 g sample, to which 50 µg lutetium has been added as an internal standard, is digested to incipient dryness with 3 ml concentrated (conc) HCl, 2 ml conc HNO₃, 1 ml conc HClO₄, and 2 ml conc HF at 110°C. If the sample contains high concentrations of organic carbon, the sample must be ashed prior to analysis by ICP-AES. Additional conc HClO₄ and water are added to the residue and taken to dryness at 150°C. One ml aqua regia is added and the sample is brought to 10.00 g with 1% (v/v) HNO₃. The solution is heated at 95°C for 1 hour after which it is analyzed by ICP-AES.

Another typical method for the dissolution of more refractory materials is a sodium peroxide sinter. The resulting solution is compatible with both ICP-AES and ICP-MS instruments. Typically a 0.100 g sample is weighed into a graphite or zirconium crucible and 0.50 g of dry, fine-grained sodium peroxide is added, and mixed with the sample. The mixture is heated at 450°C for 30 minutes. The sinter cake is dissolved in 20 ml deionized/demineralized water, then 200 µg lutetium and 20 ml of 15% (v/v) HNO₃ are added, and the solution is cooled.

The ICP-AES instrument is typically calibrated at the start of each day using established geological reference materials (e.g., USGS basalt BHVO-1 and Canadian Certified Reference Materials Project syenite SY-3) and four multielement solutions. The major and trace elements are determined by comparing the element intensities obtained from the standards to those obtained from the samples. Three method preparation blanks should be digested with each sample set of 40–50 samples. A blank subtraction is performed to minimize the effect of the reagents. Table 13.4 shows typical element wavelengths for this method.

The following equation is routinely used to calculate the element concentration in the environmental sample:

$$\text{Element concentration} = (\text{IRU/IRS} \times \text{CONSTD} \times \text{WT SOLN/WT SAMPLE}) + \text{IEC} \quad [1]$$

where:

IRU = intensity of element/intensity of Lu
 IRS = intensity of calibration standard/intensity of Lu
 CONSTD = conc of calibration standard
 WT SOLN = weight of final solution
 WT SAMPLE = weight of sample
 IEC = interelement corrections

TABLE 13.3—Reporting limits for 40 elements by ICP-AES after an acid digestion.

Element	Concentration range		Element	Concentration range	
Aluminum, Al	0.005	50%	Gallium, Ga	4	50,000 mg/kg
Calcium, Ca	0.005	50%	Holmium, Ho	4	5000 mg/kg
Iron, Fe	0.02	25%	Lanthanum, La	2	50,000 mg/kg
Potassium, K	0.01	50%	Lithium, Li	2	50,000 mg/kg
Magnesium, Mg	0.005	5%	Manganese, Mn	4	50,000 mg/kg
Sodium, Na	0.006	50%	Molybdenum, Mo	2	50,000 mg/kg
Phosphorous, P	0.005	50%	Niobium, Nb	4	50,000 mg/kg
Titanium, Ti	0.005	25%	Neodymium, Nd	9	50,000 mg/kg
Silver, Ag	2	10,000 mg/kg	Nickel, Ni	3	50,000 mg/kg
Arsenic, As	10	50,000 mg/kg	Lead, Pb	4	50,000 mg/kg
Gold, Au	8	50,000 mg/kg	Scandium, Sc	2	50,000 mg/kg
Barium, Ba	1	35,000 mg/kg	Tin, Sn	5	50,000 mg/kg
Beryllium, Be	1	5000 mg/kg	Strontium, Sr	2	15,000 mg/kg
Bismuth, Bi	10	50,000 mg/kg	Tantalum, Ta	40	50,000 mg/kg
Cadmium, Cd	2	25,000 mg/kg	Thorium, Th	6	50,000 mg/kg
Cerium, Ce	5	50,000 mg/kg	Uranium, U	100	100,000 mg/kg
Cobalt, Co	2	25,000 mg/kg	Vanadium, V	2	30,000 mg/kg
Chromium, Cr	2	50,000 mg/kg	Yttrium, Y	2	25,000 mg/kg
Copper, Cu	2	15,000 mg/kg	Ytterbium, Yb	1	5000 mg/kg
Europium, Eu	2	5000 mg/kg	Zinc, Zn	2	15,000 mg/kg

TABLE 13.4—Common wavelengths used for the analysis of environmental samples by ICP-AES.

Element	Wavelength, nm	Element	Wavelength, nm
Ag	328.0	Mg	285.2 or 279.0
Al	309.2	Mn	257.6
As	189.0	Mo	202.0
Au	242.7	Na	588.9
Ba	455.4	Nb	309.4
Be	313.0	Nd	430.3
Bi	223.0	Ni	231.6
Ca	317.9	P	213.6
Cd	226.5	Pb	220.3
Ce	418.6 or 413.7	Sc	424.6
Co	228.6	Sn	189.9
Cr	267.7	Sr	421.5
Cu	324.7	Ta	240.0
Eu	381.9	Th	401.9
Fe	271.4 or 273.9	Ti	334.9
Ga	294.3	U	409.0
Ho	345.6	V	292.4
K	766.4	Y	321.6 or 371.0
La	298.8 or 408.6	Yb	328.9
Li	670.7	Zn	213.8

Inductively coupled plasma-mass spectrometry

Inductively coupled plasma-mass spectrometry (ICP-MS) has recently become an important tool in the environmental laboratory despite its relative youth in terms of commercial instrumentation. ICP-MS has gained the U.S. Environmental Protection Agency (U.S. EPA) approval for trace metal determinations, both in water and solids. This approval comes in the wake of lower detection limits required for the lower safe levels of various contaminants in drinking water. U.S. EPA methods 1638, 1640, and 200.8 are a few examples of where ICP-MS is the accepted method of analysis. It has many of the attributes and capabilities of its companion technique, ICP-AES, namely the ability to simultaneously determine a variety of elements over a wide dynamic concentration range. However the primary reasons for the popularity of ICP-MS are its great sensitivity and general lack of interferences for elements with masses greater than 70. In contrast to ICP-AES, ICP-MS is slower, less durable, and prone to drift. Thus, in practice the major use of ICP-MS in environmental analysis has been for the determination of toxic elements such as As, Cd, Mo, Pb, Sb, Th, Tl, and U, as well as precious metals, REE, and refractory elements, all at crustal abundance levels and below (sub mg/kg). The ICP-MS uses an argon plasma to generate ions of the trace elements for analysis by mass spectrometry, usually a quadrupole mass spectrometer. ICP-MS tends to have excellent detection limits, equal to or even better than GF-AAS, typically <0.0001 to 0.2 µg/l. Although a sequential method, ICP-MS can perform a rapid, complete elemental analysis in a single aspiration and has the ability to determine isotopic ratios and therefore, to perform isotopic dilution-type determinations. The analytical benefits of ICP-MS include very low detection limits, rapid multielemental analysis, (both qualitative and quantitative), spectral simplicity (especially when compared to ICP-AES), a wide dynamic

analytical range, isotopic analysis capability, and a variety of sample introduction systems.

Environmental applications of ICP-MS include the analysis of natural waters, marine and river sediments, soils, and toxic wastes. It been applied to drinking water, food, air-borne particulates, and human and animal fluids and tissues for a large variety of major, minor, and trace elements. Due to its accuracy using isotopic dilution methods, ICP-MS finds a valuable application in the certification of reference materials. The benefits of ICP-MS in environmental applications include the best features of both ICP-AES and AAS, with the high sensitivity of GF-AAS and the rapid multielement throughput of ICP-AES. The semiquantitative mode of ICP-MS can estimate concentrations of over 80 elements in a few minutes.

ICP-MS interferences come from matrix effects, instrumental drift, and isobaric overlap of some elemental isotopes by molecular ions formed in the plasma. For alumino-silicate analysis, a glass standard is used so samples and standards are matrix matched. Internal standards are added to compensate for matrix effects and instrumental drift. A standard solution should be analyzed every 15 samples, drift calculated, and drift corrections applied. The isotopes measured are selected to minimize isobaric overlap from other elements and from molecular species that might be present.

ICP-MS is compatible with a variety of sampling devices for the introduction of the sample into the plasma. These include direct laser ablation (LA) sampling (Lichte, 1995; Thompson et al., 1989). The benefits of LA-ICP-MS include minimized sample preparation, reduction of contamination, reduced spectral interferences, the ability to analyze very small solid samples, and the ability to perform spot analyses on a given sample. Sample preparation for LA-ICP-MS can be as simple as combining a finely ground sample with a suitable binding agent, such as paraffin or cellulose, and pressing it into a pellet at high pressure. Alternatively, the sample can be fused with a suitable flux and then the fusion bead analyzed directly. Flow injection (FI) is also available as a sample introduction technique. The benefits of FI-ICP-MS include practical automation of on-line pretreatment procedures (including preconcentration with ion exchange), low sample and reagent volume usage, high sample throughput, improved stability with harsh sample matrices, and protection from contamination. FI-ICP-MS can be applied in micro sampling, on-line dilutions, hydride generation, solvent extraction preconcentration, and matrix modification. Electro-thermal vaporization (ETV), or graphite furnace technology, is also applicable for ICP-MS. With ETV-ICP-MS even better detection limits are achieved. For example, using a 50 µl sample, 0.00002 µg/l (1x10⁻¹⁵g) of uranium can be determined. ETV also permits the analysis of slurries and selected solids. For multielement analysis, compromise conditions, similar to GF-AAS, must be used for the temperature program, gas flows, and matrix modifiers. The benefits of ETV-ICP-MS include reduced sample volume requirements (usually less than 100 µL) and reduced polyatomic matrix and background interferences. Difficult samples can also be analyzed. These include solutions with high salt concentrations, high concentrations of mineral acids, viscous or organic samples, or volatile solids. ET-ICP-MS has multielement capability with extremely low detection limits.

Rare Earth Elements By ICP-MS—The REE (La, Ce, Pr, Nd, Sm, Eu, Gd, Tb, Dy, Ho, Er, Tm, and Yb; Lu is excluded since it is added as the internal standard) are determined by ICP-MS in geologic materials (Lichte, et al., 1987b) and this method is pre-

sented here as an example of the usefulness of ICP-MS. The REE are made soluble by sintering the sample with sodium peroxide, leaching with water, and acidifying with nitric acid. Lutetium is added as an internal standard to correct for instrument drift. Calibration for each of the REE is made by using the average intensity of five blanks taken through the entire procedure and the intensities acquired on a solution of a glass standard containing a known concentration of each REE. Rocks and sediments can be analyzed by this method from lower reporting limits of 1.0 La, 2.0 Ce, 0.2 Pr, 1.0 Nd, 0.4 Sm, 0.1 Eu, 0.5 Gd, 0.1 Tb, 0.5 Dy, 0.1 Ho, 0.4 Er, 0.1 Tm, and 0.4 Yb mg/kg, to approximately 500 mg/kg in the sample. Samples that contain higher concentrations of REE must be diluted before analysis.

Atomic absorption spectroscopy

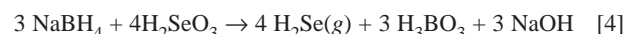
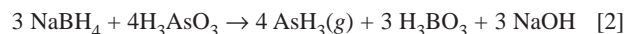
Atomic absorption spectrometry (AAS) became the backbone of many of the environmental and geochemical laboratories by the mid 1970s and continues today to be a very important technique for the determination of many environmentally important elements. Among the reasons for AAS popularity are its relative low purchase price and maintenance cost, abundant literature and applications, acceptance by many regulatory agencies, capability of determining about 70 elements, sensitivity and detection limits which satisfy many studies, speed of analysis, relative freedom from interferences, reasonable precision and accuracy, simplicity, and its field portability. But AAS also has its limitations. AAS is not useful for determining nonmetals such as sulfur, or refractory elements (e.g., the REE) at useful levels. AAS also tends to be a sequential method of analysis. Simultaneous multielement AAS determinations have not yet proven to be practical. There are several excellent comprehensive discussions of AAS, including Varma (1984) and Welz (1985). Viets and O'Leary (1992) present an overview of AAS and its application to geochemical exploration. This discussion also applies to environmental analysis.

AAS has been subdivided into four main categories. These categories are based on the method of sample introduction and the absorption cell. These include flame-AAS (F-AAS), graphite furnace-AAS (GF-AAS), hydride generation-AAS (HG-AAS), both continuous flow and flow injection HG-AAS, and cold vapor-AAS (CV-AAS). F-AAS has seen great application over the years as the method of choice for trace element analysis, replacing many of the colorimetric methods. A sample is first dissolved, diluted to an appropriate concentration level, and then aspirated into the flame of the AAS instrument. There are different flames available, dependent on the temperature required to desolvate and atomize the analyte of concern. These flames include an air/acetylene flame for most nonrefractory elements, a nitrous oxide/acetylene flame for the more refractory elements, and an air/hydrogen flame for the easily atomized elements, such as arsenic or selenium. F-AAS is simple to perform and has few spectral interferences and minimal chemical interferences. However, F-AAS is not always sensitive enough for the levels of analytes found in environmental samples. (For comparison of detection limits of the four common spectroscopic techniques, consult Table 13.1). To increase sensitivity and to make the analysis of small volumes possible, GF-AAS was developed. Here the flame has been replaced with a heated graphite tube and the sample injected into this tube for a more complete and efficient atomization of the sample. GF-AAS however, tends to be a very tedious, slow method. It also suffers from more chemical and spectral interferences,

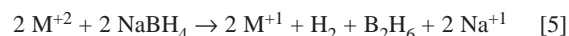
often giving the illusion that GF-AAS is to be considered more art than science. For the hydride-forming elements, such as As, Sb, Se, Bi, Sn, and Pb, the introduction of continuous flow HG-AAS offered a reduction in both chemical and spectral interferences while offering increased automation with the sensitivities of the GF-AAS methods (e.g., Crock and Lichte, 1982; Sanzalone and Chao, 1987). Burguera (1989) discusses flow injection AAS and its relationship to both flame and hydride generation AAS. CV-AAS remains the chosen method of analysis for mercury in most matrices (Crock, 1996) and follows the principles that were first given by Hatch and Ott (1968).

HG-AAS methods for As, Sb, and Se will be summarized here as an example of hydride generation. The determination of Ag and Cd after a separation and preconcentration will serve as an example of F-AAS. A standard CV-AAS method is presented for the determination of mercury in environmental samples. For more methods commonly used for F-AAS and GF-AAS, the analyst should consult the AAS methods books listed earlier or the "Methods Manuals" supplied by most commercial companies with their instruments.

Arsenic, Antimony, and Selenium By Flow Injection or Continuous Flow-HG-AAS—The determinations of arsenic, antimony, and selenium by flow injection or continuous flow-hydride generation-AAS are presented here as examples of the usefulness of HG-AAS in the modern environmental laboratory. Environmental samples are digested using a multiacid procedure in an open Teflon[®] vessel. At the end of the digestion period, arsenic, antimony, and selenium are reduced to oxidation states, +3, +3, and +4, respectively. Sodium borohydride is added to the solution resulting in rapid formation of the hydrides as illustrated by the following equations:



The gaseous hydrides are stripped from the analytical stream and transported with inert gas to the atomizer (a heated quartz furnace) of the atomic absorption spectrophotometer. For selenium, the quartz furnace is heated by an air/acetylene flame to 2000°C; the arsenic and antimony furnace is electrically heated to 900° and 1000°C respectively. Concentrations of the elements are determined using calibration standards in solutions of similar matrix. Interferences usually associated with atomic absorption analysis are negligible, but incomplete recoveries of the elements from the digest solution may yield low analytical results. Incomplete recoveries are principally due to concentration of certain transition and heavy metals (e.g., Cu, Fe, Ni, and Sn) of more than 500 mg/l in the sample digest competing with As, Sb, and Se, for available NaBH₄ according to equation 5:



This competition results in insufficient NaBH₄ for completion of the hydride-forming reaction. Other interferences occur when concentrations of one or more of the hydride forming elements are

present in excess of 1,000 mg/kg in the original sample. Competing hydride elements deplete the oxygen supply in the furnace which is needed to convert hydrides to ground state elements. Interference of hydride formation by incompletely digested organic material, possible volatility losses of the analyte in an organic rich matrix due to organometallic compounds, and coprecipitation of the hydride elements if a metal is reduced to the metallic form, (as is seen with Ag or Au) all will lead to low recoveries of the hydride analyte.

Problems from the first two are generally of minimal concern in environmental samples because the probability of high interference element concentrations are quite low. More often, interference problems occur in mineralized samples, but they can be resolved by dilution of the sample solution. Special care should be taken to ensure that all the organic material in an organic-rich sample is thoroughly and rapidly digested (i.e., oxidized) to enable the reaction to reach completion and to avoid loss through volatilization.

The digestion procedure for rock, soil, and sediment is as follows: Weigh 0.250 g sample (<80-mesh) into a 30-ml Teflon[®] vessel, add 9 ml conc HNO₃ and 0.25 ml of 10% (v/v) HCl. Allow to stand for 3 hours. Add 2 ml conc HClO₄, 2 ml conc H₂SO₄, 10 ml conc HF and heat overnight at 125°C. Cool, add 25 ml 50% (v/v) HCl and let stand for half an hour. Transfer the sample solution to a 60-ml polyethylene bottle and bring up to 55.0 g with deionized/demineralized water. Approximately 8 ml of the solution is decanted into a test tube for selenium analysis and another 8 ml is mixed with 2 ml of a potassium-ascorbic acid solution in a test tube and allowed to stand for 1 hour prior to arsenic or antimony analysis. Arsenic and antimony are measured using a flow injection hydride generation-AAS method modified from the continuous flow hydride generation-AAS (CF-HG-AAS) method as given in Crock and Lichte (1982) using pre-reduced solutions. Samples are analyzed for their Se content using the CF-HG-AAS method as given in Briggs and Crock (1986) and Sanzalone and Chao (1987) on a separate aliquot of the digest. Routinely 0.2 mg/kg As, Sb, and Se can be determined in most solid matrices, and 0.1 µg/l can be determined in most waters and extracts.

The digestion procedure for coal and vegetation is as follows: Weigh a 0.100 g sample of coal or a 1.00 g sample of plant material into a 125 ml Erlenmeyer flask. Add 20 ml conc HNO₃, 2 ml conc H₂SO₄, and let stand overnight. Then add 3 ml of conc HClO₄, insert claw refluxers, and heat at about 175°C for 30 minutes. Remove refluxers and continue to heat to dense white fumes. Cool, and 25 ml 50% (v/v) HCl and continue as above. Aruscavage (1977) presents a GF-AAS method for the determination of arsenic, antimony, and selenium in coal and offers a reasonable alternative HG-AAS method.

The digestion procedure for water and extracts is as follows: Weigh 10.0 g liquid sample into a 30-ml Teflon[®] vessel. Add 1 ml of aqueous saturated potassium persulfate and let stand for 1 hour. Add 1 ml conc HCl and heat at 110°C with watch glass in place. Remove watch glass after 1 hour and continue heating for roughly 2½ to 3 hours or until the volume is reduced to somewhere between 2 and 5 ml. Then add another 2 ml conc HCl, replace the watch glass, and heat for another hour. Cool, add 25 ml 50% (v/v) HCl and let stand for half an hour. Transfer to 60-ml polyethylene bottles with deionized/demineralized water, bring to a final weight of 55.0 g, and analyze as given above.

Mercury in Water, Geologic Materials, and Vegetation By Continuous Flow-CV-AAS—The most widely accepted method

of analysis for mercury is the cold vapor method first described by Hatch and Ott (1968). Over the years many modifications have been made to this method, but it still remains the method of choice for environmental samples. To determine mercury in water, geologic, and plant materials, samples are digested with nitric acid and sodium dichromate in a disposable test tube. After digestion, samples are diluted with water to a constant volume. To determine mercury in water, samples must be preserved upon collection in glass bottles with a 1% sodium dichromate (w/v) and conc nitric acid solution (1 part preserving solution to 19 parts water sample). All samples are mixed with air and a sodium chloride-hydroxyl amine hydrochloride-sulfuric acid solution and then Hg (II) is reduced to Hg with stannous chloride in a continuous flow manifold. The mercury vapor is separated and measured using continuous-flow CV-AAS. This method is a variation of Kennedy and Crock (1987).

Samples containing high concentrations of Ag, Au, Pt, Te, and Se may diminish the extraction efficiency of the Hg in environmental samples (Bartha and Ikrenyi, 1982). Of these elements, only selenium poses a significant problem for nonmineralized geologic or environmental materials. Although a 1 mg/l solution of the other elements causes greater than a 90% suppression of a 0.01 mg/l Hg solution, these elements either will not be dissolved (Au, Pt) or are normally present at low concentrations (Ag, Te). Silver does not become a problem until its concentration exceeds 10 mg/kg in sample. Samples containing silver above 10 mg/kg need to be diluted. Concentrations above 25 mg/kg Se suppress recovery of Hg and should also be diluted or a smaller sample size used. The CV-AAS method offers a lower reporting limit of 0.02 mg/kg mercury in solid-phase samples. Samples exceeding the working range of 0.02–1.8 mg/kg mercury require dilution. For water samples or extracts, the method offers a lower reporting limit of 0.1 µg/l. Samples exceeding the working range of 0.1–1.5 µg/l mercury must be diluted.

Mercury in Whole Coal or Biological Tissue By Continuous Flow-CV-AAS—To determine mercury, weigh 0.150 g of whole coal or dried biological tissue (0.75 to 1.5 g raw, as received, biological tissue) into a 16 x 150-mm disposable flint glass test tube. Then add approximately 0.1 g vanadium pentoxide, 3.5 ml conc HNO₃, and 1.5 ml conc H₂SO₄ to the sample. Vortex to wet the entire sample. Place test tube in an aluminum heating block, cover with watch glass, and ramp gradually to 150°C over a 2-hour period. Heat overnight at this temperature. Remove the tube, allow to cool and dilute sample solution to 15.0 ml with deionized/demineralized water, cap and shake for 5 minutes. Centrifuge at 1,000 rpm for 5 minutes. Analyze the solutions as given above.

Mercury by Atomic Fluorescence Detection—The determination of mercury can be broken into four basic steps: sample decomposition, reduction of the mercuric ion into metallic mercury, phase separation of the metallic mercury vapor from the aqueous matrix, and the measurement of the mercury. The latest innovations in the determination of mercury in environmental samples have focused on using atomic fluorescence as the method of detection after standard digestion and separation procedures. Mercury both absorbs and fluoresces at 254 nm. Atomic fluorescence inherently has a much larger dynamic analytical range and tends to be at least two orders of magnitude more sensitive than the CV-AAS method. Cold vapor-atomic fluorescence spectrometry (CV-AFS) offers the ability to determine mercury at or below the part per trillion levels (ng/l) in water. CV-AFS tends to be relatively interference free when compared to the CV-AAS method,

but the analyst must be very careful of sample contamination and reagent purity. The U.S. EPA has recently proposed a CV-AFS method for the determination of mercury in water (U.S. EPA, 1995).

Cadmium and Silver By F-AAS—Cadmium and silver are determined by a modified F-AAS method developed by O'Leary and Viets (1986) and this method is presented here as an example of F-AAS. The sample is decomposed by hydrofluoric acid and the residue is treated with hydrochloric acid and hydrogen peroxide. Cadmium and silver are selectively extracted into a 10% (v/v) Aliquat 336®-MIBK organic phase in the presence of ascorbic acid and potassium iodide. The organic solution is atomized by F-AAS for determination of silver and cadmium concentrations.

Calcium and iron are major interfering elements in the determination of cadmium and silver in environmental materials by F-AAS. However, these interferences are eliminated by use of 10% (v/v) Aliquat 336®-MIBK which will not extract calcium, and will not extract iron in the presence of ascorbic acid and potassium iodide.

A 0.50 g sample is digested in 50-ml Teflon beakers with 5-ml conc HF at 110°C and taken to dryness. The residue is treated with 5-ml conc HCl and 1-ml 30% H₂O₂ and heated until the remaining hydrogen peroxide and chlorine gas are evolved. The mixture and a 4-ml ascorbic acid-potassium iodide solution (30%–15% w/v) rinse are transferred to disposable test tubes and mixed. After 20 minutes, 3 ml Aliquat 336-MIBK are added to the tubes. The tubes are then capped, shaken for 5 minutes, and centrifuged. The organic layer is then atomized in the flame AA. The reporting limits for cadmium are 0.1 to 10 mg/kg and 0.2 to 10 mg/kg for silver. The upper limit can be extended by diluting an aliquot of the organic layer.

Instrumental neutron activation analysis

Instrumental neutron activation analysis (INAA) selectively measures radioactive nuclide activity produced by nuclear reactions on naturally occurring isotopes. The activity of the indicator radionuclide produced during irradiation is directly proportional to the amount of the element in the sample. The analytical determination is made by comparing the induced activity in the sample with well-characterized standards activated under identical conditions of neutron flux. The activities of the samples and standards are measured using gamma-ray spectroscopy. Gamma-ray radiation emitted by a radionuclide is converted into an electrical signal by a semiconductor detector. The electrical signal is analyzed by a multichannel analyzer. Semiconductor detectors, such as high-purity and lithium-drifted germanium detectors, are used to exploit their high resolution. Spectra produced are analyzed by software which locates peaks, identifies peaks, and calculates the area of each peak. Refer to Gordon et al. (1968), Baedecker and McKown (1987), and Laul (1979) for more detailed descriptions of the principles of INAA.

Neutron activation analysis tends to be matrix dependent. Uranium concentrations higher than 100 ppm increase the detection limits for select REE, Mo, and Zr from the generation of fission products. Detection limits are also effected by samples with high REE abundances, and ore-type samples. Ore-type samples require special counting and computer analysis for accurate determinations. Metamorphic marbles/limestones and quartzites, because of their very low abundances of most trace elements also require special handling and analysis. Samples that have low

abundances of elements, such as Fe, Co, and Sc, will normally decrease the detection limits for other determined elements. INAA also has other factors effecting its precision and accuracy. The factors effecting precision include:

- a) weighing errors;
- b) nonreproducible positioning of the sample during counting;
- c) nonuniform distribution of the neutron flux across the sample irradiation position;
- d) errors due to poor counting statistics and to photopeak baseline selection during photopeak integration; and,
- e) sampling errors.

To help minimize these problems, duplicate analysis should be done and the results averaged. The factors effecting accuracy include:

- a) interfering nuclear reactions on the other elements that yield the same indicator radionuclide, especially for high U samples;
- b) gamma-ray spectral interferences;
- c) self shielding, especially for samples high in the REE;
- d) dead-time errors, especially for the short-lived half lives;
- e) differences in the powder density of the samples and the standards; and,
- f) errors in the preparation or calibration of the standards.

A detailed discussion of these and other known interferences on specific elements can be found in Baedecker and McKown (1987).

Not all elements will be detectable for all matrixes. Samples having unusual matrixes will require adjustments to the counting protocol. A minimum of 4 months is required for completion of the analysis. The technique is "nondestructive" and sample may, with some restrictions, be analyzed by other methods if the amount of a sample is limited. A lower limit on the concentration of an element is calculated by estimating the minimum detectable peak area above the observed background using a peak detection criteria used in a peak fitting algorithm. The minimum detectable peak is determined by 3 sigma of the blank. Reporting limits are matrix dependent and may be higher for routine analysis. The following are two examples of INAA useful for the nondestructive analysis of environmental samples. By measuring only long-lived nuclides, i.e., nuclides with a half life of greater than one day, 24 elements can routinely be determined in most environmental samples. For coals or other carbonaceous samples, up to 29 elements can be determined. If the analyst is able to measure the shorter-lived half lives, using better automation with rapid sample transfer and handling systems and shorter counting times, up to an additional 7 elements can be determined.

INAA Short Count (24 Elements)—Sample aliquots of 0.5 to 1.0 g each are irradiated in a neutron flux for 6 to 8 hours. Standards for most elements are aliquots of a prepared natural obsidian or high purity quartz spiked with primary solutions for selected elements, taken to dryness and homogenized. Standards for Au are homogeneous low-Au quartz. Samples are counted twice on co-axial Ge and (or) Ge(Li) detectors using 1-hour counts after 6 to 8 days of decay, and 2-hour counts approximately 50 days after irradiation. Computerized data reduction procedures are used to measure the activities of the following indicator radio nuclides in the acquired spectra: ²⁴Na, ⁴²K, ⁴⁶Sc, ⁵¹Cr, ⁵⁹Fe, ⁶⁰Co, ⁵⁸Co, ⁶⁵Zn, ⁷⁶As, ⁸⁶Rb, ⁸⁵Sr, ^{99m}Tc, ¹²²Sb, ¹³⁴Cs, ¹³¹Ba, ¹⁴⁰La, ¹⁴¹Ce, ¹⁴⁷Nd, ¹⁵³Sm, ¹⁵²Eu, ¹⁶⁰Tb, ¹⁷⁵Yb, ¹⁷⁷Lu, ¹⁸¹Hf, ¹⁸²Ta, ¹⁹⁸Au, ²³³Pa, and ²³⁹Np. Corrections are made for spectral interferences and interfering nuclear reactions. Table 13.5 lists the lower limits of determination for the abbreviated INAA method (Arbogast, 1996).

TABLE 13.5—Lower limits of determination for abbreviated-count INAA.

Element	Lower reporting limit
Ba	100 ppm
Na, Fe, Ni, Sr	10 ppm
Zn, Rb, Nd	1 ppm
Cr, Co, Sb, Cs, Ce, Sm, Yb, Th, U	0.1 ppm
Sc, La, Eu, Tb, Lu, Hf, Ta	0.01 ppm

The determination of several elements, particularly Cr, Ni, Zn, Ba, Ce, Sm, Tb, Yb, Lu, Hf, Au, and U may be subject to spectroscopic interferences. Corrections must also be made for interferences on the determination of Mo, Ba, La, Ce, and Nd from the products of 235-U fission produced in the sample during neutron irradiation. Special handling is required for the analysis of samples with >100 ppm Gd, >500 ppm As or U, >1% B₂O₅ or Pb, or >5% P₂O₅ due to a variety of analytical problems associated with high concentrations of these elements.

INAA Long Count (40 Elements)—Sample aliquots of 0.5 to 1.0 g each are irradiated in a neutron flux for 6 to 8 hours. Standards for most elements are aliquots of a powdered natural obsidian or high purity quartz spiked with primary solutions, taken to dryness and homogenized. Standards for Ca, Ti, and Au are powdered CaCO₃, TiO₂, and a homogeneous low-Au quartz standard reference material, respectively. At least one replicate sample and one USGS rock standard are irradiated together with the samples and standards. Samples are counted three times on co-axial Ge and (or) Ge(Li) detectors as follows: 1-hour counts after 6 to 8 days of decay, 2-hour counts after 14 to 17 days of decay, and 2 to 4 hour counts approximately 50 days after irradiation. In addition, one or more counts are taken on intrinsic Ge, low-energy photon detectors for the determination of selected elements. Computerized data reduction procedures are used to measure the activities of the following indicator radionuclides in the acquired spectra: ²⁴Na, ⁴²K, ⁴⁷Ca, ⁴⁶Sc, ⁴⁸Sc, ⁵¹Cr, ⁵⁹Fe, ⁶⁰Co, ⁵⁸Co, ⁶⁵Zn, ⁷⁶As, ⁷⁵Se, ⁸²Br, ⁸⁶Rb, ⁸⁵Sr, ⁹⁵Zr, ^{99m}Tc, ^{110m}Ag, ¹¹⁵Cd, ¹²²Sb, ¹³⁴Cs, ¹³¹Ba, ¹⁴⁰La, ¹⁴¹Ce, ¹⁴⁷Nd, ¹⁵³Sm, ¹⁵²Eu, ¹⁵³Gd, ¹⁶⁰Tb, ¹⁷⁰Tm, ¹⁷⁵Yb, ¹⁷⁷Lu, ¹⁸¹Hf, ¹⁸²Ta, ¹⁸⁷W, ¹⁹²Ir, ¹⁹⁸Au, ²⁰³Hg, ²³³Pa, and ²³⁹Np. Corrections are made for spectral interferences and interfering nuclear reactions. Reporting limits are matrix dependent and these approximate lower limits are given in Table 13.6 (Arbogast, 1996).

TABLE 13.6—Approximate lower limits for long count INAA.

Element	Lower limit (ppm)		
K, Ca, Ti, Zr, Cd, Ba, Hg	100	—	1,000
Na, Fe, Ni, Sr, Mo, Ag	10	—	100
Zn, Rb, Nd, Gd, Tm, W	1	—	10
Cr, Co, As, Se, Br, Sb, Cs, Ce, Sm, Yb, W, Th, U	0.1	—	1
Sc, La, Eu, Tb, Lu, Hf, Ta	0.01	—	0.1
Ir, Au	0.001	—	0.01

The determination of several elements, particularly Ca, Cr, Ni, Zn, Se, Zr, Ba, Ce, Sm, Tb, Yb, Lu, Hf, Au, and U may be subject to spectroscopic interferences. Corrections must also be made for

interferences on the determination of Zr, Mo, Ba, La, Ce, and Nd from the products of 235-U fission produced in the sample during neutron irradiation. Special handling is required for the analysis of samples with >100 ppm Gd, >500 ppm As or U, >1% B₂O₅ or Pb, or >5% P₂O₅ due to a variety of analytical problems associated with high concentrations of these elements.

X-ray fluorescence spectrometry

X-ray fluorescence spectrometry is commonly applied to the nondestructive analysis of environmental samples, both in the laboratory and in the field for many major, minor, and trace elements. There are basically two different types of X-ray fluorescence analysis: wavelength dispersive X-ray fluorescence (WDXRF) and energy dispersive X-ray fluorescence (EDXRF). Both techniques entail the excitation of characteristic X-rays within a sample followed by their subsequent detection and measurement. WDXRF is very precise and accurate for major and selected trace constituents in a silicate matrix. EDXRF finds applications for minor and trace element determinations and is field portable. EDXRF is also a very fast and nondestructive qualitative and quantitative tool for measuring samples of unknown composition. It is however, not as precise as some of the other trace element methods. In general, if an element has a lower atomic number than Fe (26), WDXRF is the preferred method for its determination. Whereas if an element has an atomic number larger than Fe, EDXRF is the method of choice. Both methods are matrix dependent for their respective sensitivities and detection limits. An example of each X-ray method follows.

Twelve Selected Trace Elements By EDXRF—Energy-dispersive X-ray fluorescence spectrometry (EDXRF) is a method for the qualitative and quantitative analysis of elemental composition in solid or liquid samples. It is based on the instantaneous generation, detection, and measurement of characteristic X-rays emitted by the elements in a sample, when the sample is bombarded with high energy X-rays. This is a nondestructive analytical process that requires little or no sample preparation. With this method, 12 selected trace elements, Cr, Ni, Cu, Zn, Rb, Sr, Y, Zr, Nb, Ba, La, and Ce can be determined routinely. The analyst is referred to the literature (e.g., Bertin, 1975; Johnson and King, 1987) for more details on the use of EDXRF for geological and environmental applications.

Spectral-line interferences include line overlap and absorption/enhancement effects (matrix effects). The problem of spectral-line overlap is shared by all emission and fluorescence methods. It is due to the incomplete resolution of two or more spectral lines or peaks. There are two types of spectral line overlaps in routine EDXRF analysis. The first is a K β line from one element overlaps the K α line from the adjacent heavier element in the periodic table (e.g., Ni K β overlaps Cu K α). The second is L-series lines from one element interfere with K lines from another element (e.g., Ba L γ 1 with Cr K α). All these interferences can be removed by peak stripping or peak deconvolution techniques using computer algorithms.

Matrix effects (absorption/enhancement) occur when radiation emitted by the analyte interacts with other components in the sample before it reaches the detector. The effects are corrected by a scattered radiation method which has been widely used for routine trace-element analysis of various geologic materials (Johnson, 1984; Burkhalter, 1971; and King, 1987). This correction method is based on the fact that the analyte-line intensity and Compton-

scatter intensity are affected in the same way by differences in mass absorption coefficients from one sample to another. Although the scatter line and the analyte line intensities vary with the matrix, their ratio is constant over a wide range of matrix compositions. Furthermore, if the energy the Compton-scatter peak lies close to the analyte line, the absorption, particle size, packing density, and instrumental effects are more effectively corrected. The matrix effect of secondary enhancement is not corrected by this method, but is usually negligible for elements with an atomic number greater than 26 (Fe).

This method is applicable to the analysis of the above-mentioned 12 trace elements in rocks, stream sediments, and soils samples in loose powder form (minus 200-mesh or $\leq 75\mu\text{m}$). Because this method is nondestructive, the sample can be used for other chemical and instrumental analyses after EDXRF analysis. The detection limits and upper limit of calibration concentrations of the method are summarized in Table 13.7.

TABLE 13.7—Lower limit of detection and upper limit of calibration for the EDXRF method.

Element	Lower limit, mg/kg*	Upper limit, mg/kg
Cr	20	4200
Ni	10	3000
Cu	10	1000
Zn	10	1300
Rb	10	2000
Sr	10	2000
Y	10	200
Zr	10	2000
Nb	10	500
Ba	30	4700
La	30	1300
Ce	30	500

*Represents the highest LOD observed; limits may vary with a calibration.

Other elements can be determined with similar lower limits of detection (LOD) for nonmineralized samples, but tend to be subject to matrix problems. Elements of environmental interest and their respective LOD include Bi (40 mg/kg), Cl (50 mg/kg), Mn (15 mg/kg), Se (10 mg/kg), and Te (10 mg/kg).

Major Elements as Oxides By WDXRF—The following WDXRF method is fully described by Taggart et al. (1987). Exactly 0.8000 g of powdered sample is ignited in a tared platinum crucible at 925°C for 45 minutes. The weight loss is reported as percent loss on ignition (LOI). An 8.000 g charge of lithium tetraborate is added to the sample and thoroughly mixed. A 0.250 ml aliquot of a 50% (w/v) lithium bromide solution is added as a nonwetting agent. The crucible is placed in a muffle furnace on an "automatic fluxer." The combined sample and flux is melted at 1120°C. The melt is maintained in the furnace at this temperature for 40 minutes while it is simultaneously homogenized through the rocking motion of the fluxer. The molten homogenous mixture is poured into a specially designed platinum mold. When cool, the resulting glass disk is inspected and, if acceptable, introduced into the wavelength dispersive X-ray fluorescence spectrometer. The major element concentrations are determined by comparing the fluorescence intensities obtained from standards to those obtained from the sample. Table 13.8 lists the concentration range for LOI and the 10 common rock-forming oxides determined by this technique.

TABLE 13.8—Concentration range for LOI and the 10 common rock forming oxides determined by WDXRF.

Constituent	Range (percent)
SiO ₂	0.10 – 99.0
Al ₂ O ₃	0.10 – 28.0
Fe ₂ O ₃	0.04 – 28.0
MgO	0.10 – 60.0
CaO	0.02 – 60.0
Na ₂ O	0.15 – 30.0
K ₂ O	0.02 – 30.0
TiO ₂	0.02 – 10.0
P ₂ O ₅	0.05 – 50.0
MnO	0.01 – 15.0
LOI (925°C)	0.01 – 100

Interferences may result from mineralogical or other structural effects, spectral line overlaps, and other matrix effects. The structure of the sample is eliminated through fusion with a suitable flux. Fusion of the sample also diminishes matrix effects and produces a stable, flat, homogeneous sample for presentation to the X-ray spectrometer. Maximizing the efficiency of the optics of the spectrometer and selecting certain types of crystal monochrometers eliminates many of the overlap and multiorder line interferences. A deJongh (deJongh, 1973) mathematical correction procedure is used to correct for the absorption and enhancement matrix effects.

Ion selective electrode methods and others

Ion selective electrode (ISE) methods are widely applicable in the modern environmental laboratory, from measuring liquid and solid pH to Eh and various free, uncomplexed cations and anions. The voltage difference developed between a sensing electrode, an electrode usually very specific for a given species, and an appropriate reference electrode is a measure of the activity of that specific analyte in solution. The voltage developed is governed by the Nerst Equation. Table 13.9 lists the common electrodes available, the analyte measured, and the common concentration range measurable. As is seen, the ISE methods offer a large range of concentrations for some very important environmental species. Several of the more common ISE methods are presented here as examples of the applicability of ISE methods to environmental studies in the laboratory.

Chloride By ISE Following a KMnO₄-H₂SO₄-HF Dissolution—Chlorine in environmental materials is determined as chloride by the ion-selective electrode (ISE) potentiometric method. The sample is digested in the outer compartment of a sealed Conway diffusion cell with KMnO₄, H₂SO₄, and HF. Chlorine is distilled from the outer chamber and reduced to chloride in the inner chamber, which contains Na₂SO₃, and KOH. The chloride is measured directly in the inner chamber with a chloride ion-selective electrode (Aruscavage and Campbell, 1983; Elsheimer, 1987).

High concentrations of ions which form insoluble silver salts (bromide, iodide, and hydroxide) could deposit on the membrane surface, causing a malfunction. The diffusion of chloride ions between the outer and inner compartments of the Conway cell separates chloride from other interfering ions. The hydroxide

molar concentration is constant from sample to sample, iodide is not oxidized in an acidic permanganate solution, and bromide is generally much lower in concentration than chloride for a given sample so that its molar ratio to that of chloride is not a problem. The only other type of interference is caused by high concentrations of sulfur, ferrous iron, or other oxidizable components which would compete with chloride for the oxidizing power of the rock digestion solution. In such cases the sample size taken for analysis can be reduced to as little as 50 mg. Results are satisfactorily reproducible at this sample level, even with considerable competition from reducing species. The operating range for chlorine in geologic and environmental materials is 0.01 to 2.0%.

TABLE 13.9—Ion-selective electrode applications to environmental analyses.

Electrode	Analyte measured	Concentration range (mg/l)
Ammonia	NH ₃ or NH ₄ ⁺	0.01 – 17,000
Bromide	Br ⁻	0.4 – 79,900
Cadmium	Cd ²⁺	0.01 – 11,200
Calcium	Ca ²⁺	0.02 – 40,100
Carbon dioxide	CO ₂ /CO ₃ ²⁻	4.4 – 440
Chloride	Cl ⁻	1.8 – 35,500
Cupric	Cu ²⁺	0.0006 – 6,350
Cyanide	CN ⁻	0.000008 – 0.01
Fluoride	F ⁻	0.02 – Saturated Solution
Fluoroborate	BF ⁻	0.61 – 86,800
Iodide	I ⁻	0.005 – 127,000
Lead	Pb ²⁺	0.2 – 20,700
Nitrate	NO ₃ ⁻	0.1 – 14,000
Nitrite	NO ₂ ⁻	0.02 – 100
Nitrogen oxide	NO _x	0.18 – 230
Oxygen	O ₂	0 – 14 (nominal)
Perchlorate	ClO ₄ ⁻	0.7 – 99,500
Potassium	K ⁺	0.04 – 39,000
Silver/Sulfide	Ag ⁺	0.01 – 107,900
	S ²⁻	0.003 – 32,100
Sodium	Na ⁺	0.02 – Saturated
Thiocyanate	SCN ⁻	0.29 – 58,100
Water hardness	X ²⁺	1 – 6 x 10 ⁻⁶ molar

Fluoride By ISE Following a LiBO₂ Fusion and HNO₃ Dissolution—Fluorine in silicate rocks and minerals is determined as fluoride by the ISE method (Bodkin, 1977; Cremer et al., 1984). Samples are fused with lithium metaborate and dissolved in nitric acid. A complexing buffer is added, and the potential of the solution is determined with a millivolt meter. A known volume of standard fluoride solution is added and the potential is again checked. The concentration of fluoride in the sample is computed using the potential difference and the Nernst equation.

1,2-diaminocyclohexane-NNN'-tetra-acetic acid (DCTA) buffers the solution to pH 5.5. At a pH below 5, hydrogen complexes fluoride as the undissociated acid HF and the ion HF₂⁻. At a pH greater than seven, hydroxide ion interferes when the level of hydroxide is greater than one-tenth the level of fluoride ion present. DCTA also controls aluminum and iron interferences.

Fluoride can be determined in silicate rocks and minerals with a lower reporting limit of 100 mg/kg and an upper limit of 2.7% without modification of this procedure. If a sample is suspected of having a fluoride concentration greater than 2.7%, another fusion should be made and a suitable aliquot diluted with an appropriate

volume of DCTA buffer prior to measurement.

Soil pH By ISE—A 20.0 g sample of minus 10-mesh (≤2 mm) soil is mixed with 20 ml deionized/demineralized water for about 1 minute, remixed after 10 minutes two additional times, left to rest for 1 hour, and then the pH of the suspension determined using a combination pH electrode (Crock and Severson, 1980). Soil pH values are normally reported for pH 0–12 using conventional electrodes without acid or alkaline error corrections. Soil pH is usually reported to the nearest 0.1 unit, but may be read to 0.01 unit, depending on the buffering capacity of the soil. The procedure must be followed exactly to obtain comparable results. Factors that must be standardized include: size and shape of the extraction vessel, extraction time, mixing method, sample/water ratio, and temperature. If a sample contains a high percentage of clay or organic matter, the resulting suspension may be very viscous.

Redox-sensitive species

Many elements in nature can occur in more than one oxidation state and tend to be very sensitive to Eh/pH conditions. It is often desired to have information concerning the relative abundances of each oxidation state. Most commonly, separation methods or sequential extractions will help define this relationship (e.g., Chao and Sanzalone, 1989). The following include several methods of analysis for a given oxidation state of an element. Also as mentioned above, ISE technology is extremely valuable for the determination of a given species in solution.

Ferrous Oxide By Potentiometric Titration—A 0.500-g sample is decomposed in a platinum crucible with a gently boiling mixture of sulfuric and hydrofluoric acids. The crucible and digestate are immersed in a solution containing boric, sulfuric, and phosphoric acids. The solution is titrated electrochemically with potassium dichromate to determine FeO.

The range covered by this method is from 0.01% to 10.0% FeO. Several treatments with the mixed-acid digestion solution are necessary to entirely solubilize more-resistant minerals such as garnet. Similarly, repeated treatments are necessary for complete dissolution of ilmenite and magnetite. Pyrite is not appreciably attacked but if pyrite is the only sulfur-bearing mineral in the sample, a correction can be calculated based on the sulfur content. For other insoluble minerals, such as staurolite and tourmaline, alternative digestion techniques which may not be entirely effective, are required. The presence of oxidizing or reducing agents in the sample such as manganese dioxide, trivalent vanadium, or organic matter will adversely effect determination of FeO (Jackson et al., 1987).

Forms of Arsenic in Sediments By Ion Exchange—The chemical speciation of any element in solid environmental materials requires an extraction procedure in which the extractant does not alter the form of the element of interest. This is especially true for elements occurring in more than one oxidation state, such as arsenic. Arsenic can be present as As(III) and As(V). Ficklin (1990) presents a method to extract and speciate the forms of arsenic in lacustrine sediments. To minimize the rapid air oxidation of As(III) to As(V), the sample must be frozen immediately after collection and stored frozen in an air-tight container. The samples are rapidly defrosted under cold water when the extraction is to be performed. A small representative sample is taken for extraction, total moisture (for correction to a dry-weight basis reporting of the results), and for total arsenic determination. It is usually very difficult to obtain a representative sample of muddy,

wet material, especially if there is a range of grain sizes present. Sampling tends to be the limiting factor for this method's precision.

Arsenic is extracted from a subsample (0.50–0.70 g wet material) of the thawed, frozen material with 4N HCl and heated to 90°C for 5 minutes. The separation of As(III) from As(V) is accomplished by ion exchange on the acetate form of Dowex® I-X8 ion exchange resin with 0.12 N HCl eluent. The As content of the eluent can be determined using GF-AAS with standard conditions or with HG-AAS as described earlier. The arsenic remaining in the solid after HCl extraction is reacted with potassium chlorate and conc HCl to dissolve sulfides. The arsenic determined from this extraction is assumed to be sulfide-bound arsenic. The lower reporting limit is 0.5 mg/kg for each of the three species, As(III), As(V), and sulfide-bound As.

Carbon species

Total Carbon By Combustion—Total carbon in geologic materials is most commonly determined by the use of an automated carbon analyzer (Jackson et al., 1987). A weighed sample (approximately 0.25g) is combusted in an oxygen atmosphere at 1370°C to oxidize all forms of carbon to carbon dioxide (CO₂). Moisture and dust are removed and the carbon dioxide gas is measured by a solid state infrared detector. High concentrations of fluorine and molybdenum will interfere with the detection of CO₂ by coating the cell walls and the detector of the carbon analyzer. Samples suspected to contain molybdenum in the range of 0.2 to 1% are analyzed using a reduced sample weight and a halogen trap is installed in the flow system when high concentrations of fluorine are present in the samples. Another problem may be encountered due to abnormally rapid combustion of organic-rich materials. This problem can be corrected by the addition of a retardant (COM-AID®) to the sample.

Carbonate Carbon By Coulometric Titration—Carbonate carbon in geologic material is determined as carbon dioxide, CO₂, by coulometric titration. The sample is treated with hot 2 N perchloric acid and the evolved CO₂ is passed into a cell containing a solution of monoethanolamine. The CO₂, quantitatively absorbed by the monoethanolamine, is coulometrically titrated using platinum and silver/potassium iodide electrodes (Jackson et al., 1987). Processing samples containing high concentrations of sulfur quickly exhausts the sample prescrubber. The analyst must give close attention to the build-up of black sulfide precipitate in the prescrubber solution. The lower reporting limit is 0.01% CO₂ and samples containing up to 50.0% CO₂ may be analyzed. Sample size is adjusted from 0.5 g for the range 0.01 to 5% CO₂, 0.1 g for the range 5 to 10% CO₂, and 0.02 g for greater than 10% CO₂.

Total Organic Carbon (TOC)—Total organic carbon is not determined directly but is computed from the difference between total carbon and carbonate carbon determinations. A variety of procedures have been used to determine organic carbon directly. However, many of these procedures use an acid-leached sample that may have significant loss of soluble, hydrolyzable, or volatile organic compounds due to leaching. Thus organic carbon determined by difference includes all forms of carbonaceous matter, including graphite.

Carbon, Hydrogen, and Nitrogen By a CHN Elemental Analyzer—Carbon, hydrogen, and nitrogen can be determined in geologic materials by a commercial gas chromatography/thermal

conductive analyzer. A 1 to 20-mg sample (depending on concentration and (or) sample type) is combusted in a pure oxygen environment in the CHN elemental analyzer. Carbon, hydrogen, and nitrogen present in the material are converted to CO₂, H₂O, and N₂, respectively, and separated by a frontal gas chromatograph. Concentrations of these gases are determined by thermal conductivity detectors. Acetanilide is commonly used as a calibration standard.

The combination of reagents used in the combustion zone provide both efficient oxidative properties and a high-capacity scrubbing efficiency, insuring the complete oxidation of volatile products and the effective removal of common interferences.

The range of concentration covered is from 0.01% for carbon, hydrogen, and nitrogen to an upper limit of a 100% for each element; although, concentrations for carbon greater than 90%, hydrogen greater than 10%, and nitrogen greater than 15% are not usually observed.

Sulfur species

Total Sulfur By Combustion—Total sulfur in geologic materials is most commonly determined by the use of an automated sulfur analyzer (Jackson et al., 1985, 1987). Approximately 0.25 g sample is weighed and mixed with 1 g vanadium pentoxide flux. The sample is combusted in an oxygen atmosphere at 1370°C where the sulfur oxidizes to sulfur dioxide. Moisture and dust are removed and the sulfur dioxide gas is then measured by a solid state infrared detector. Possible interfering elements are fluorine and molybdenum, both of which can coat the cell walls and the detector. Samples suspected to contain greater than 0.2% F or 1% Mo should be analyzed using a reduced sample weight. Also, a halogen trap must be installed in the flow system when higher concentrations of fluorine are present in the samples. A problem may be encountered due to abnormally rapid combustion of organic-rich materials. This problem can usually be corrected by the addition of a retardant (COM-AID®) to the sample. It may be necessary to cover some samples completely with vanadium pentoxide to assure complete conversion of the sulfur to the dioxide. The reporting range for total sulfur is from 0.05% to about 35.0% sulfur. Samples containing more than 0.2% halogens or molybdenum may be harmful to the detector. Samples suspected to contain high concentrations of these elements will be analyzed using a reduced sample weight.

Acid-Soluble Sulfate, Sulfide, and Organic Sulfur—Total sulfur is first determined on the sample to be analyzed for sulfur species. A separately weighed split of the sample is leached with 0.1 N HCl and the leached sample is analyzed for its sulfur content (residue #1). Another separately weighed split is sequentially extracted with 0.1 N HCl and 0.1 M sodium pyrophosphate to remove the acid-soluble sulfate and the organic sulfur leaving the sulfide behind (residue #2), which is then analyzed for its sulfur content. The acid-soluble sulfate is determined as the difference between the total sulfur and residue #1. The organic sulfur is determined as the difference between residue #1 and residue #2. The method is subjected to the same interferences as the method for the determination of total sulfur, such as fluorine greater than 0.2%, or molybdenum greater than 1%. These interferences can be minimized by reducing the sample size or by using a halogen trap for the sulfur instrument. This method is summarized from Arbogast (1996).

The separation of the sulfur species is operationally defined

and is dependent on the parameters used. The operating range for this method is from 0.05% to about 35.0% sulfur. If the total sulfur in the sample is lower than 0.1%, species of sulfur should not be determined. This method is applicable to the dissolution of the acid-soluble sulfates but is not suitable for coal-like materials. The acid-insoluble sulfates such as barite or alunite will be included with the sulfide fraction.

Laboratory experiments using mixtures of elemental sulfur and quartz, and also standards with known amounts of elemental sulfur, indicate elemental sulfur is not extracted with either the 0.1 N HCl or the 0.1 M sodium pyrophosphate. If elemental sulfur is present in the sample, it will be included with the sulfide fraction. Laboratory experiments on standards with known amounts of sulfides indicate that the best acid concentration for removing the acid-soluble sulfates without dissolving monosulfides is the cold 0.1 N HCl leach. Higher concentrations of the acid and heat dissolve part or all of the monosulfides. Laboratory experiments on monosulfide minerals show only negligible amounts of monosulfides are dissolved by the 0.1 M sodium pyrophosphate.

PARTIAL ANALYSES OF SOLIDS

Introduction

Partial dissolution or sequential partial dissolution techniques are developed to partition sample constituents into associations with operationally defined solid phases. These dissolution techniques provide information on the association or "mode of occurrence" of elements which leads to greater insight into controls on the dispersion of elements. The type of dissolution and the dissolution parameters are customized taking into account the goals of the study, the concentration of the constituents of interest, and the matrix of the sample.

These techniques have application in both environmental and geochemical studies. The use of these techniques in geochemical exploration for concealed deposits is influenced by the observation that ore elements, or associated pathfinder elements, when released from buried deposits to the surficial environment, are held in relatively labile forms. These labile forms can be brought into solution by extractions less drastic in chemical action than total decomposition. Case histories have shown that this approach results in greater geochemical contrast between background and anomalous values.

Environmental applications of these techniques provide information as to the potential availability of constituents to the environment as well as possible sources of enrichment. Chao (1984) presents an excellent discussion of partial and sequential dissolution/analysis methods.

Trace element concentrations in the mg/kg range are typically determined. However, the lower reporting limit depends on dissolution parameters as well as method of detection. The dissolution parameters (including the number of steps in sequential schemes) and the method of detection can be modified to maximize the number of values above the lower reporting limit.

Element phase associations or forms of elements are operationally defined (e.g., see Chao and Sanzalone (1989) for selenium). Development of such techniques requires a thorough knowledge of the matrix of the sample and the concentration level of constituents of interest. Partial dissolution techniques may produce solution matrices that create severe instrumental interference problems, especially with high total dissolved salts. Pilot studies

are usually necessary to develop the appropriate technique and parameters.

Attaining acceptable precision and accuracy in sequential extractions or extractable elemental determinations is much more difficult than in total elemental determinations. For total elemental determinations, decomposition of the sample is qualitatively monitored by the clarity of the resulting solution and by the absence of residues in the final solution. These criteria do not apply to extracts or leaches. Possibilities for error are introduced in virtually every step of an extraction procedure. Variations in elemental extractability can result from vessel size, shape, or composition differences, changes in temperature, method of mixing or shaking, speed of centrifuging, or porosity of the filter paper used, strength of the vacuum used, grain size of the material used for the extraction, extraction time, and even the original matrix composition. To obtain reasonable precision the analyst must standardize as many of the variables as possible in an extraction procedure. No detail is too small to standardize. Accuracy for sequential extractions can be estimated if all the parts are summed to the whole, total element. For extractable determinations standard reference materials do not exist. The analyst must use a secondary reference material to monitor both precision and accuracy of the extraction method. The following are commonly used partial analysis schemes.

Organometallic halide extraction for 10 elements by ICP-AES

A widely used extraction technique has been modified and adapted for use with ICP-AES for the analysis of geologic and environmental materials. A hydrochloric acid-hydrogen peroxide digestion (Viets, 1978; O'Leary and Viets, 1986; Motooka, 1988) dissolves metals not tightly bound in the silicate lattice of rocks, soils, and stream sediments. The metals are extracted as organic halides by a 10% Aliquat 336-diisobutylketone solution. The separated organic phase is pneumatically aspirated into a multichannel ICP-AES instrument where the concentrations of the extracted metals (Ag, As, Au, Bi, Cd, Cu, Mo, Pb, Sb, Zn) are determined simultaneously. It is important to note that this procedure is a partial digestion and depending on an element's availability, results may be biased low when compared to other methods of analyses.

Organic solvent extraction provides preconcentration of the analyte species and when used in conjunction with ICP-AES virtually eliminates the need for complex interference corrections. There are, however, some spectral interferences that must be considered, particularly where very high concentrations of iron and extracted metals (Cu, Mo, and Pb) are encountered. Correction coefficients are determined and computer calculations made to compensate for these interferences. The technique is especially useful in environmental studies where the need to determine trace metals at or near their crustal abundance level is of great importance. Suggested wavelengths and reporting concentration range are listed in Table 13.10.

A 1.50 g sample is treated with 5.0 ml conc HCl and 1.0 ml 30% H₂O₂. After one hour, the digest is placed in a boiling water bath for 20 minutes. The digest is cooled and 4.0 ml ascorbic acid/potassium iodide solution added. The sample solution is mixed and allowed to stand 20 minutes. Three ml diisobutylketone containing a tertiary amine hydrochloride (Aliquat 336®) are added and the combined components are shaken for 5 minutes. Following centrifugation, the separated organic phase is analyzed for 10 elements by ICP-AES.

TABLE 13.10—Wavelength and operating range for 10 elements by ICP-AES.

Element	Wavelength, nm	Lower reporting limit (mg/kg)	Upper reporting limit (mg/kg)
Ag	328.0	0.08	400
As	193.7	1.0	6000
Au	242.8	0.10	1500
Bi	223.0	1.0	6000
Cd	226.5	0.05	500
Cu	324.7	0.05	500
Mo	202.0	0.10	900
Pb	220.3	1.0	6000
Sb	217.6	1.0	6000
Zn	213.8	0.05	500

Metal availability indices by ICP-AES or AAS

A 15.0-g sample of minus 10-mesh soil is extracted with 30 ml DTPA-ABC (diethylene triamine pentacetic acid-ammonium bicarbonate) extracting solution for 2 hours on an oscillating shaker. The resulting solution is centrifuged, filtered, acidified with nitric acid, and the elements of concern determined by either ICP-AES or AAS. Most elements can be determined by ICP-AES or by F-AAS. ICP-AES is the preferred method because of its multielemental capabilities and because it is less prone to matrix problems. If lower limits of detection are required, one can use either GF-AAS or ICP-MS. See Table 13.1 for relative lower limits of determination.

Since this is not a total method of analysis, the given procedure must be followed exactly to obtain comparable results. Factors that must be standardized include: size and shape of the extraction vessel, extraction time and temperature, shaking method and speed, and reagent makeup. This procedure was developed for western U.S. soils. It therefore is most applicable to neutral to basic, oxidized soils. If a sample contains a high percentage of clay, the sample will be difficult to centrifuge and filter (Crock and Severson, 1980; Soltanpour, 1991).

Water-extractable constituents in soil

Water extraction is a commonly used preparation procedure for analysis of soil extractable constituents by ICP-AES, HG-AAS (As, Se), CV-AAS (Hg), and ion chromatography (F, Cl, SO₄). Generally, ICP-AES reports only the major element and transition elements, including boron. For this extraction, a 20.0 g soil sample and 100 g water are weighed into a 125-ml wide-mouth polyethylene bottle. The type of water used for extraction varies with the individual study needs. The water may be simulated rain water, irrigation water, or deionized/demineralized water. The bottle is sealed and transferred to a Erbach[®] horizontal shaker and the contents shaken overnight. The next day the bottle is centrifuged at 1500 rpm for 20 minutes. After centrifugation, the supernatant is decanted and filtered using a 5 ml disposable syringe equipped with a 0.45 micron filter. The filtered solution is transferred to a 60-ml polyethylene bottle and preserved for ICP analysis by spiking the solution with 200 µl conc nitric acid. If samples require anion analysis by ion chromatography a separate aliquot is prepared and left unpreserved, but must be refrigerated.

If the supernatant contains significant quantities of suspended clay material, filtration may be difficult and a second centrifugation is recommended using a high speed (10,000 rpm) centrifuge. Special 50 ml centrifuge tubes are required for this operation. It is also important that each pair of tubes be balanced in order to minimize damage to the centrifuge.

The 1:5 extraction procedure is designed to provide sufficient solution for a multitechnique analysis. If preconcentration is needed prior to ICP-AES or F-AAS analysis, replicate extractions may be necessary. Caution is advised when preconcentrating extraction solution, as elevated salt concentrations (sodium greater than 5,000 mg/kg) will cause nebulization problems during ICP-AES analysis. If soils are extremely absorbent, sufficient mixing of the soil and water may not occur. If this condition is observed, then a 1:10 soil to water is suggested.

VEGETATION

The use of vegetation as biomonitors for environmental studies is growing in acceptance and popularity. With this growth, the analysis of vegetation materials for environmental studies is an increasing need. Huckaby (1993) discusses the use of lichens as biomonitors of contamination, especially aerial. Crock et al. (1992a, b, 1993) have successfully used moss, lichens, and spruce in environmental studies of national parks and preserves in Alaska. Crock et al. (1994) and Wilson et al. (1991) have used alfalfa and other vegetation to monitor the effects of irrigation in the Western United States. In general, the most direct measurement of an element's bioavailability in a given environment is the total element content of the vegetation growing on the soil or the vegetation exposed to the aerial deposition in question (Williams and Funston, 1987). There is abundant literature on partial leaching procedures used to approximate bioavailability, but uptake by the vegetation itself remains the best measure.

Many of the methods used for vegetation analysis are adaptations of those used for soil or rock analysis. Specific questions must be asked prior to plant analysis. Should the sample be washed or not? Should the sample be ashed for preconcentration or matrix volatilization? Which elements are susceptible to loss via volatilization at the ashing temperature? Is the analytical method sensitive enough to measure the element of concern? Is the level of contamination from reagents low enough to determine baseline levels? Are there reference materials available? Which method of digestion (wet oxidation, fusion, or acid digestion) should be used on the raw material or on the ash?

ICP-MS is becoming the method of choice for most trace elements in vegetation following a multiacid digestion of the ash or the raw material. Both F-AAS and GF-AAS are still widely applicable. INAA also is used successfully, but is considered more exotic due to the limited availability of reactor facilities. Whenever possible, the analyst should use a plant ash for analysis. This eliminates most of the organic matrix of the vegetation. The ash content of plant usually ranges from 1–15% and therefore ashing will commonly preconcentrate the analyte of interest from 7 to 100 fold. Also, an acid digestion of the ash keeps the total salt level of the digest low and also minimizes contamination. Typically a 1:100 dilution of (ash):(final fluid volume) is reasonable for most methods. From the values given in Table 13.1, it can be seen that with ash preconcentration most elements can be quantified at or below the sub mg/kg level.

Volatile elements can be lost during the dry ashing procedures. Therefore for their determination, the analyst must use a wet oxidation method employing strong acids and auxiliary oxidizing agents, such as hydrogen peroxide or vanadium pentoxide. Elements of concern include mercury, arsenic, selenium, antimony, and cadmium and are typically determined on the air-dried, raw material.

There are not as many standard reference materials available for vegetation as there are for solids. Gladney et al. (1987) give a compilation of commonly available standards, some of which are available from the National Institute of Standards and Technology. For a particular study of a given species, the analyst should develop an in-house reference material to use to confirm the quality of data, since there is a great variability of matrices and elemental content between plant species.

STANDARD REFERENCE MATERIALS

The analysis of homogeneous, well-characterized geochemical reference materials provide the backbone for the data quality of the modern environmental laboratory. Numerous agencies from around the world have prepared, characterized, and issued reference materials in a multitude of rock, ore, soil, sediment, and coal matrix types. Despite the more than 380 reference materials (Potts et al., 1992; Govindaraju, 1994) that have been generated, the number of geochemical reference materials of a specific sample class is limited, as is the number of high-quality analyses. Nevertheless, the analysis of reference materials in method validation, instrument calibration, and quality control is essential to ensure the reliability of geochemical analyses and this fact cannot be emphasized too greatly.

Accuracy of an analytical method is both a difficult and required measurement in the establishment of an analytical method. To measure accuracy, standard reference materials (SRMs) whose elemental content has been established by several independent methods are essential. Standard reference materials are intended as a control to ensure that different laboratories are analyzing the same homogeneous, well-characterized material. Several SRMs need to be analyzed to establish the complete working range of a method, both in sample matrix composition and level of the analyte. Accuracy assessments are required to establish both quality control and quality assurance for the data produced.

A wide variety of SRMs for the determination of Hg in environmental materials is available (Crock, 1996). Roelandts (1989) presents a compilation of environmental SRMs, data compilation, and suppliers. Table 13.11 presents some available mercury SRMs and their recommended or proposed mercury content [modified from Govindaraju (1989)]. This table also demonstrates the wide range of values available for a given element over a range of environmental materials. Also the diversity of issuing agencies is shown.

ANALYSIS OF WATERS

Introduction

The collection, preparation, and preservation of water samples is given in Ficklin and Mosier (1999). Excellent overviews of the analytical chemistry and methods of analysis of drinking and

waste water are given in Fishman and Friedman (1989) and Greenberg et al. (1992). In general, F-AAS, GF-AAS, ICP-AES, and ICP-MS are the methods of choice for total analysis of cations. Most commonly, anions or complexed species are determined using ion chromatography (IC) (Fishman and Pyen, 1979 and Joyce and Schein, 1989) or by specific ion electrodes (Table 13.6). There is considerable literature available for any given species using alternative methods such as colorimetry or electrochemical methods. The following discussions are selected methods that find wide application to environmental water samples.

Anions

Fluoride, chloride, nitrate, and sulfate in aqueous solution by IC

Four common anions (fluoride, chloride, nitrate, and sulfate) are determined in aqueous solution by ion chromatography (IC). In addition, bromide, nitrite, and phosphate may be determined at the same time. The anions are separated based on their relative affinity for a low capacity, strongly basic anion exchange resin (Small et al., 1975). Each anion elutes from the column with a characteristic retention time in the order of fluoride, chloride, nitrite, nitrate, phosphate, and sulfate when using the described conditions.

Chemically suppressed IC employs a suppressor that reacts with the carbonate eluent to reduce the background conductivity, thus providing greater sensitivity. The separated anions pass through a semi-permeable membrane bathed in dilute sulfuric acid. Each analyte is converted to the highly conductive acid form, while the eluent is converted to weakly conducting carbonic acid. The liquid phase goes into a conductivity cell for detection.

Interferences can be caused by substances with retention times that are similar to and overlap those of the anion of interest. Large amounts of an anion can interfere with the peak resolution of an adjacent anion. Sample dilution and (or) fortification can be used to solve most interference problems. The water dip, or negative peak, that elutes near the fluoride peak and can usually be eliminated by the addition of the equivalent of 1 ml of concentrated (100×) eluent to 100 ml of each standard and sample. Method interferences may be caused by contamination in the reagent water, reagents, glassware, and other sample processing apparatus that lead to discrete artifacts or elevated baseline in ion chromatograms. Any anion that is not retained by the column, or only slightly retained, will elute in the area of fluoride and interfere. Known co-elution is caused by carbonate and other small organic anions. At concentrations of fluoride above 1.5 mg/l this interference may not be significant, however, it is the responsibility of the user to generate precision and accuracy information in each sample matrix. The acetate anion elutes early during the chromatographic run. The retention times of the anions also seem to differ when large amounts of acetate are present. Therefore, this method is not recommended for leachates of solid samples when acetate is used for pH adjustment (Pfaff et al., 1989). Samples that contain particles larger than 0.45 μm and reagent solutions that contain particles larger than 0.20 μm require filtration to prevent damage to instrument columns and flow systems.

Ion chromatography is applicable to the analysis of natural waters and leachate solutions. It can be extended to include the analysis of solid samples that are water soluble. Liquid phase samples should be refrigerated at 4°C and stored no longer than 28

TABLE 13.11—Recommended (*) and proposed values for mercury in selected standard reference materials.

Hg ($\mu\text{g}/\text{kg}$)	Reference material	Sample description	Source
15 \pm 2*	GSS-2	soil	IGGE (Certificate)
16 \pm 1	GSR-6	limestone	IGGE (Certificate)
16*	JG-1	granodiorite	GSI
16.6 \pm 1.7*	GSS-8	soil	IGGE (Certificate)
17 \pm 7	SO-3	soil	CCRMP (Certificate)
18 \pm 2*	GSD-1	stream sediment	IGGE (Certificate)
20 \pm 9	AGV-1	andesite	USGS (Gladney et al., 1983)
20	FER-2	iron formation	CCRMP
21 \pm 3*	SO-1	soil	CCRMP (Gladney et al., 1985)
28*	JB-1	basalt	GSI
32 \pm 3*	GSS-1	soil	IGGE (Certificate)
32 \pm 6	SO-4	soil	CCRMP (Certificate)
40 \pm 5*	GSD-2	stream sediment	IGGE (Certificate)
42 \pm 3*	GSD-8	stream sediment	IGGE (Certificate)
44 \pm 5*	GSD-4	stream sediment	IGGE (Certificate)
45 \pm 5*	GSD-6	stream sediment	IGGE (Certificate)
49 \pm 13	G-2	granite	USGS (Gladney et al., 1983)
53 \pm 9*	GSD-7	stream sediment	IGGE (Certificate)
56 \pm 4*	GSD-12	sediment	IGGE (Certificate)
60 \pm 3*	GSS-3	soil	IGGE (Certificate)
61 \pm 4*	GSS-7	soil	IGGE (Certificate)
63 \pm 12	NBS1646	estuarine sediment	NBS (Certificate)
68 \pm 14	GXR6	soil	USGS (Gladney and Roelandts, 1990)
72 \pm 5*	GSS-6	soil	IGGE (Certificate)
72 \pm 6*	GSD-11	sediment	IGGE (Certificate)
82 \pm 9*	SO-2	soil	CCRMP (Certificate)
83 \pm 6*	GSD-9	granite	USGS (Gladney et al., 1983)
100 \pm 10	GSD-5	stream sediment	IGGE (Certificate)
110 \pm 30	GXR-4	sediment	IGGE (Certificate)
90 \pm 30	G-1	coppermill head	USGS (Gladney and Roelandts, 1990)
129*	BCSS-1	marine sediment	NRCC
140 \pm 40*	MRG-1	gabbro	CCRMP (Certificate)
158 \pm 17*	GXR-5	soil	USGS (Gladney and Roelandts, 1990)
171*	MESS-1	marine sediment	NRCC
190	SDO-1	marine sediment	USGS (Certificate)
210 \pm 70	W-1	diabase	USGS (Gladney et al., 1983)
280 \pm 18*	GSD-10	sediment	IGGE (Certificate)
294 \pm 19*	GSS-5	soil	IGGE (Certificate)
330 \pm 40*	GXR-3	deposit	USGS (Gladney and Roelandts, 1990)
590 \pm 34*	GSS-4	soil	IGGE (Certificate)
1100	NBS1645	river sediment	NBS
1440	NBS1646	estuarine sediment	NBS
2900 \pm 700	GXR-2	soil	USGS (Gladney and Roelandts, 1990)
3900 \pm 600	GXR-1	jasperoid	USGS (Gladney and Roelandts, 1990)
4570	PACS-1	marine sediment	NRCC

Mercury values are from Govindaraju (1989), except for data which includes standard deviation. The reference for confidence intervals are in parenthesis under the sample source.

- GSI: Geological Survey of Japan, 1-1-3 Higashi, Yatabe, Tuskuba, Ibaraki, 305 Japan
IAEA: International Atomic Energy Agency, Analytical Quality Control Central Services, P.O. Box 100 A-1400, Vienna, Austria
ASK: Analytisk Sporelement Komite, Rogalandforskning, Postboks 2503, Ullandhaug, 4001 Stavanger, Norway
IGGE: Institute of Geophysical and Geochemical Prospecting, Ministry of Geology, Peoples Republic of China
CCRMP: Canadian Certified Reference Materials Project, Canada Center for Mineral and Energy Technology, Mines and Resources, 555 Booth Street, Ottawa, Canada K1A 0G1
NBS: National Bureau of Standards (currently NIST, National Institute of Standards and Technology), Office of Standard Reference Materials, NIST, Gaithersburg, Md. 20899
NRCC: National Research Council of Canada, Chemistry Division, National Research Council, Montreal Road, Ottawa, Canada
USGS: United States Geological Survey, Denver Federal Center, Mail Stop 973, Box 25046, Denver, Colorado 80225

days when sulfate and nitrate are to be analyzed. For fluoride, chloride, and bromide, no refrigeration is required. If nitrite or phosphate are to be analyzed, the samples must be refrigerated and analyzed within 48 hours. In a given sample, the anion that requires the shortest holding time will determine the preservation treatment (Pfaff et al., 1989).

Depending on the detector range used, fluoride can be determined from 0.01 to 5 mg/l, chloride from 0.07 to 10 mg/l, nitrate from 0.1 to 30 mg/l, and sulfate from 0.1 to 50 mg/l. Solutions with higher concentrations can be diluted to the appropriate calibration range. Analytical problems may arise if one constituent is present at significantly higher concentrations than the others. This occurs most often with chloride and sulfate and may lead to elevated reporting units for fluoride (Cl interference) or phosphate (SO₄ interference).

Forms of arsenic in waters by ion exchange

This analytical method (Ficklin, 1983) has been successfully applied to determination of As(III) and As(V) in ground and surface water, and interstitial water in sediment columns at the µg/l level. Five ml of filtered (0.45 micron) and acidified (approximately 0.12N HCl) is loaded onto a column (0.7X 10 cm) of Dowex® 1X8 anion exchange resin that has been made into the acetate form. Three or more successive 5-ml volumes of 0.12N HCl are added to the column and allowed to drip through. As(III) passes through the column and is found in the first two 5-ml volumes of solution that pass through the column. As the HCl passes through the column, the acetate form of the resin is converted to the chloride form. Arsenic (V) is not retained by the chloride form and comes out of the column at the point when all of the resin has been converted to the chloride form. Arsenic (V) is found in the 3rd and 4th of the 5-ml volumes that come out of the column. Determination of the concentration can be done by any suitable method for arsenic method, e.g., GF-AAS using standard conditions as given by the instrument manufacturer or HG-AAS as described earlier.

Water samples must be preserved so that As(III) does not oxidize to As(V) during sample storage. One of the best ways to overcome this problem is to do the species separation at the time of sample collection or as soon as possible following collection. Acidification with HCl to about a strength of 0.12N also slows down but does not stop the rate of oxidation for most types of samples.

Cations

Inductively Coupled Plasma-Mass Spectrometry—As mentioned earlier in this chapter, ICP-MS has become one of the most important analytical tools available for measuring trace elements in environmental samples. This is because it is a multielement technique that is capable of simultaneously determining over 80 elements at µg/l (ppb) concentration levels. Late in 1995, ICP-MS was approved by the U.S. EPA as SW846 method 6020 for the determination of Ag, Al, As, Ba, Be, Cd, Co, Cr, Cu, Mn, Ni, Pb, Sb, Tl, and Zn in both liquid and solid waste samples. ICP-MS has also received U.S. EPA approval as method 200.8 for the determination of trace elements in ground waters, surface waters and drinking water, and it is rapidly replacing more time consum-

ing analytical techniques such as GF-AAS and hydride generation AAS. Method 200.8 is applicable to the determination of the following elements in waters: Ag, Al, As, Ba, Be, Cd, Co, Cr, Cu, Hg, Mn, Mo, Ni, Pb, Sb, Se, Th, Tl, U, V, and Zn. The method detection limits for the direct analysis (no sample pretreatment) of water and for the total recoverable (acid digestion) analysis of aqueous samples are given in Table 13.12.

Another distinctive feature of ICP-MS is its ability to measure isotopes and isotopic ratios. Therefore, for elements that have unique isotopic signatures, such as Pb, it is possible to trace these contaminants in natural systems back to their point of origin.

TABLE 13.12—Detection Limits for ICP-MS (µg/l) for water samples.

^a muElement	Total recoverable aqueous	Direct analysis aqueous
²⁷ Al	1.7	0.04
¹²³ Sb	0.04	0.02
⁷⁵ As	0.4	0.1
¹³⁷ Ba	0.04	0.04
⁹ Be	0.03	0.03
¹¹¹ Cd	0.03	0.03
⁵² Cr	0.08	0.08
⁵⁹ Co	0.004	0.003
⁶³ Cu	0.02	0.01
²⁰⁸ Pb	0.05	0.02
⁵⁵ Mn	0.02	0.04
²⁰² Hg	n.a.	0.2
⁹⁸ Mo	0.01	0.01
⁶⁰ Ni	0.06	0.03
⁸² Se	2.1	0.5
¹⁰⁷ Ag	0.005	0.005
²⁰⁵ Tl	0.02	0.01
²³² Th	0.02	0.01
²³⁸ U	0.01	0.01
⁵¹ V	0.9	0.05
Zn	0.1	0.2

Atomic absorption spectroscopy

Although the techniques of ICP-AES and ICP-MS are rapidly replacing F-AAS for the determination of trace elements in aqueous system, a few of the specialized AAS techniques, such as GF-AAS, HG-AAS, and CV-AAS, are still used by some environmental laboratories when only a limited number of elements need to be determined in a particular suite of samples. For example, if a particular study is concerned with the occurrence of As, Sb, or Se, then any one of these elements can be determined very efficiently at the 1–10 µg/l level using HG-AAS. Similarly, GF-AAS is an appropriate choice for the sequential determination of Al, Cd, Cr, Cu, Mn, Mo, Ni, Pb, V, or Zn at low concentrations in aqueous systems. The universal availability of low cost AAS instrumentation and an abundance of well-documented methods have been key factors in the continued use of this technique for environmental applications requiring single-element determinations.

Historically, AAS techniques have been popular with environmental laboratories because the U.S. EPA has mandated the use of

specific analytical techniques, such as GF-AAS, in the text of regulations associated with legislation such as the Safe Drinking Water Act. However, the U.S. EPA is moving in the direction of specifying performance-based analytical protocols rather than technique-based protocols for future regulations. This fact, coupled with U.S. EPA's approval of the more cost-efficient multielement techniques, will undoubtedly lead to diminished use of AAS by most environmental laboratories.

Inductively coupled plasma-atomic emission spectrometry

Twenty-Four Elements in Natural and Acid Mine Waters By ICP-AES—The twenty-four elements shown in Table 13.13 are determined in natural and acid mine waters by ICP-AES. In order to detect the trace constituents in water a preconcentration by evaporation (Thompson and Walsh, 1989) is necessary. Only samples with specific conductivities less than 2,000 microsiemens per centimeter ($\mu\text{S}/\text{cm}$) are preconcentrated. Each sample is analyzed twice in order to report the required elements. A split of the original solution is made for the analysis of Si. A second split is made by preconcentrating the sample 20:1 for the remaining elements. If the specific conductivity is greater than 2000 $\mu\text{S}/\text{cm}$ the sample is analyzed as received with no preconcentration. The solution is then analyzed by ICP-AES (Arbogast, 1996).

ICP-AES interferences may result from spectral interferences, background shifts and matrix effects. Interelement correction factors and background corrections are applied using proprietary data system software. Matrix effects can generally be negated by proper matching of standard and sample matrices.

All samples must be filtered and acidified prior to analysis. In order to be preconcentrated, a minimum of 100 ml of solution is required. Samples with specific conductivities greater than 2000

$\mu\text{S}/\text{cm}$ are analyzed as received and require a minimum of 10 ml of solution. The elements determined, wavelengths used, and operating ranges for this method are shown in Table 13.13. Higher concentrations may be obtained by dilution of the sample.

For the "No preconcentration" procedure, weigh 4.00 g sample into a 13 x 100 mm polypropylene test tube. Then add 40 μl Lu as the internal standard and analyze for 24 elements by ICP-AES. For the "Preconcentration" procedure weigh 80.00 g sample into a 250-ml Teflon beaker. Evaporate to dryness on a hot plate set at 100°C. Cool and then dissolve residue in beaker with 2 ml 50% (v/v) HNO_3 and mix by swirling solution in beaker. Add 2 ml 15% (v/v) HNO_3 and mix by swirling solution in beaker. Add 40 μl Lu as the internal standard and analyze for 24 elements by ICP-AES.

Dissolved organic carbon species

Organic compounds by GC-MS

Two of the major methods for the analysis of organic compounds in solid, liquid, or gaseous materials are gas chromatography (GC) and gas chromatography combined with mass spectrometry (GC-MS). Detectors available for GC are flame ionization, nitrogen-phosphorous, and flame photometric. Typically, screening and quantitative analyses are performed by GC and confirmation of identity of molecules is carried out by GC-MS. Element selective GC detectors allow for high sensitivity analysis of nitrogen, phosphorus, and sulfur-containing organic compounds. Bulk or macromolecule organic compositional information can be provided using elemental analysis (C, H, N, and O) and C-13 nuclear magnetic resonance spectroscopy. GC methods permit detection in the low $\mu\text{g}/\text{kg}$ levels. Element selective detectors are capable of detection in the sub- $\mu\text{g}/\text{kg}$ range. GC-MS

TABLE 13.13—ICP-AES elements, wavelengths, and operating ranges for natural and mine waters.

Element	Wavelength (nm)	Range #1		Range #2	
Al (mg/l)	309.2	0.5	—	1000	0.025
Ba ($\mu\text{g}/\text{l}$)	455.4	20	—	10,000	1
Be ($\mu\text{g}/\text{l}$)	313.0	20	—	10,000	1
B ($\mu\text{g}/\text{l}$)	249.7	50	—	10,000	2.5
Cd ($\mu\text{g}/\text{l}$)	226.5	20	—	10,000	1
Ca (mg/l)	317.9	1	—	1000	0.05
Cr ($\mu\text{g}/\text{l}$)	267.7	40	—	10,000	2
Co ($\mu\text{g}/\text{l}$)	228.6	80	—	10,000	4
Fe (mg/l)	259.9	0.5	—	1000	0.025
Pb ($\mu\text{g}/\text{l}$)	220.3	100	—	10,000	5
Li ($\mu\text{g}/\text{l}$)	670.7	100	—	10,000	5
Mg (mg/l)	285.2	1	—	1000	0.05
Mn ($\mu\text{g}/\text{l}$)	257.6	40	—	10,000	2
Mo ($\mu\text{g}/\text{l}$)	202.0	80	—	10,000	4
Ni ($\mu\text{g}/\text{l}$)	231.6	80	—	10,000	4
Na (mg/l)	588.9	1	—	1000	0.05
P (mg/l)	213.6	0.5	—	1000	0.025
K (mg/l)	766.4	1	—	1000	0.05
Si (mg/l)	251.6	1	—	1000	0.05
Sr ($\mu\text{g}/\text{l}$)	421.5	20	—	10,000	1
Ti ($\mu\text{g}/\text{l}$)	334.9	200	—	10,000	10
V ($\mu\text{g}/\text{l}$)	292.4	40	—	10,000	2
Zn ($\mu\text{g}/\text{l}$)	213.8	40	—	10,000	2

Range #1 dilution factor = 1 (no preconcentration); Range #2 dilution factor = 0.05 (preconcentrated)

methods can identify individual molecules at 1 µg/kg level in the full-scan mode and at lower levels in the selected ion monitoring mode.

SUMMARY

ICP-AES and ICP-MS as a complimentary pair, have few equals for a rapid, precise, and accurate analysis of environmental and geological materials, including minerals, whole rocks, vegetation, waters, soils, and sediments, for their major, minor, and trace inorganic elemental content. There are adequate supplementary techniques for most elemental determinations in the sequential analysis of environmental materials. Proper standards, either single-element solutions and (or) digested reference materials, an understanding of the matrix and elements of concern, a proper and complete digestion, and modern instrumentation are all required for the analysis of environmental materials in the modern laboratory.

REFERENCES

- Adriano, D.C., 1986, Trace elements in the terrestrial environment: Springer-Verlag, New York, pp. 298–328.
- Arbogast, B.F. (ed.), 1990, Quality assurance manual for the Branch of Geochemistry, U.S. Geological Survey: U.S. Geological Survey Open-File Report 90–688, 176 pp.
- Arbogast, B.F. (ed.), 1996, Analytical methods manual for the Branch of Geochemistry, U.S. Geological Survey: U.S. Geological Survey Open-File Report 96–525, 248 pp.
- Aruscavage, P.J., 1977, Determination of arsenic, antimony, and selenium in coal by atomic absorption spectrometry with a graphite tube atomizer: U.S. Geological Survey, Journal of Research, v. 5, no. 4, pp. 405–408.
- Aruscavage, P.J., and Campbell, E.Y., 1983, An ion-selective electrode method for determination of chlorine in geological materials: *Talanta*, v. 30, no. 10, pp. 745–749.
- Baedecker, P.A. (ed.), 1987, Methods for geochemical analysis: U.S. Geological Survey Bulletin 1770.
- Baedecker, P.A., and McKown, D.M., 1987, Instrumental neutron activation analysis of geochemical samples; *in* Baedecker, P.A. (ed.), Methods for Geochemical Analysis: U.S. Geological Survey Bulletin 1770, pp. H1–H14.
- Bartha, A., and Ikrenyi, K., 1982, Interfering effects on the determination of low concentrations of mercury in geological materials by cold-vapour atomic absorption spectrometry: *Analytica Chimica Acta*, v. 139, pp. 329–332.
- Batley, G.E., 1989, Trace element speciation—Analytical methods and problems: CRC Press Inc., Boca Raton, Fla., 350 pp.
- Bertin, E.P., 1975, Principles and practice of X-ray spectrometric analysis: Plenum Press, New York.
- Bock, R., 1979, A handbook of decomposition methods in analytical chemistry: International Textbook Company, London, 444 pp.
- Bodkin, J.B., 1977, Determination of fluorine in silicates by use of an ion-selective electrode following fusion with lithium metaborate: *The Analyst*, v. 102, no. 1215, pp. 409–413.
- Briggs, P.H., and Crock, J.G., 1986, Automated determination of total selenium in rocks, soils, and plants: U.S. Geological Survey Open-File Report 86–40.
- Burguera, J.L., 1989, Flow injection atomic spectroscopy: Marcell-Decker, Inc., New York, pp. 139–142.
- Burkhalter, P.G., 1971, Radioisotopic X-ray analysis of silver ores using Compton scatter for matrix correction: *Analytical Chemistry*, v. 43, no. 1, pp. 10–17.
- Carter, M.R. (ed.), 1993, Soil sampling and methods of analysis: Canadian Society of Soil Science, Lewis Publishers, Boca Raton, Fla., 823 pp.
- Chao, T.T., 1984, Use of partial dissolution techniques in geochemical exploration: *Journal of Geochemical Exploration*, v. 20, pp. 101–135.
- Chao, T.T., and Sanzolone, R.F., 1989, Fractionation of soil selenium by sequential partial dissolution: *Soil Science Society of America Journal*, v. 53, no. 2, pp. 385–392.
- Chao, T.T., and Sanzolone, R.F., 1992, Decomposition techniques: *Journal of Geochemical Exploration*, v. 44, pp. 65–106.
- Clement, R.E., Eiceman, G.A., and Koester, C.J., 1995, Environmental analysis: *Analytical Chemistry*, v. 67 pp. 221R–255R.
- Cremer, M.J., Klock, P.R., Neil, S.T., and Riviello, J.M., 1984, Chemical methods for analysis of rocks and minerals: U.S. Geological Survey Open-File Report 84–565, pp. 111–120.
- Crock, J.G., 1996, Mercury, *in* Sparks, D.L. (ed.), Methods of soil analysis—Chemical properties, Ch. 29, Part 1, 3rd ed.: American Society of Agronomy, Inc., Madison, Wis., pp. 769–791.
- Crock, J.G., and Lichte, F.E., 1982, An improved method for the determination of arsenic and antimony in geologic materials by automated hydride generation-atomic absorption spectroscopy: *Analytica Chimica Acta*, v. 144, pp. 223–233.
- Crock, J.G., and Severson, R.C., 1980, Four reference soil and rock samples for measuring element availability in the western energy regions: U.S. Geological Survey Circular 841, 16 pp.
- Crock, J.G., Lichte, F.E., and Briggs, P.H., 1983, Determination of elements in National Bureau of Standards' geological reference materials SRM 278 obsidian and SRM 688 basalt by inductively coupled argon plasma-atomic emission spectrometry: *Geostandards Newsletter*, v. 7, pp. 335–340.
- Crock, J.G., Lichte, F.E., Riddle, G.O., and Beech, C.L., 1986, Separation and preconcentration of the rare earth elements and yttrium from geological materials by ion-exchange and sequential acid elution: *Talanta*, v. 33, pp. 601–606.
- Crock, J.G., Gough, L.P., Mangis, D.R., Curry, K.L., Fey, D.L., Hageman, P.L., and Welsch, E.P., 1992a, Element concentrations and trends for moss, lichen, and surface soils in and near Denali National Park and Preserve, Alaska: U.S. Geological Survey Open-File Report 92–323, 164 pp.
- Crock, J.G., Severson, R.C., and Gough, L.P., 1992b, Determining baselines and variability of elements in plants and soils near the Kenai National Wildlife Refuge, Alaska: *Water, Air, and Soil Pollution*, v. 63, pp. 253–271.
- Crock, J.G., Beck, K., Fey, D.L., Hageman, P.L., Papp, C.S., and Peacock, T.R., 1993, Element concentrations and baselines for moss, lichen, spruce, and surface soils, in and near Wrangell-Saint Elias National Park and Preserve, Alaska: U.S. Geological Survey Open-File Report 93–14, 98 pp.
- Crock, J.G., Stewart, K.C., and Severson, R.C., 1994, Listing of geochemical data and assessment of variability for soils and alfalfa of the Uncompahgre Project Area, Colorado: U.S. Geological Survey Open-File Report 94–580, 83 pp.
- deJongh, W.K., 1973, X-ray fluorescence analysis applying theoretical matrix correction—stainless steel: *X-ray Spectroscopy*, v. 2, pp. 151–158.
- Elsheimer, H.N., 1987, Application of an ion-selective electrode method to the determination of chloride in 41 international geochemical reference materials: *Geostandards Newsletter*, v. 11, no. 1, pp. 115–122.
- Fassel, V.A., and Kniseley, R., 1974, Inductively coupled plasma-optical emission spectroscopy: *Analytical Chemistry*, v. 46, pp. 1110A–1120A.
- Ficklin, W.H., 1983, Separation of Arsenic (III) and Arsenic (V) in ground waters by ion-exchange: *Talanta*, v. 30, pp. 371–374.
- Ficklin, W.H., 1990, Extraction and speciation of arsenic in lacustrine sediments: *Talanta*, v. 37, no. 8, pp. 831–834.
- Ficklin, W.H., and Mosier, E.L., 1999, Field methods for sampling and analysis of environmental samples for unstable and selected stable constituents; *in* Plumlee, G.S., and Logsdon, M.J. (eds.), *The Environmental Geochemistry of Mineral Deposits, Part A. Processes*,

- Techniques, and Health Issues: Society of Economic Geologists, *Reviews in Economic Geology*, v. 6A, pp. 249–264.
- Fishman, M.J., and Friedman, L.C. (ed.), 1989, Methods for determination of inorganic substances in water and fluvial sediments: Chapter A1, Book 5, Laboratory analysis, *Techniques of Water-Resources Investigations of the United States Geological Survey*, 545 pp.
- Fishman, M., and Pyen, G., 1979, Determination of selected anions in water by ion chromatograph: U.S. Geological Survey Water Resources Investigation Report 79–101.
- Gladney, E.S., and Roelandts, I., 1990, 1988 Compilation of elemental concentration data for CCRMP reference rock sample SY–2, SY–3, and MRG–1: *Geostandards Newsletter*, v. 14, pp. 373–458.
- Gladney, E.S., Burns C.E., and Roelandts, I., 1983, 1982 Compilation of elemental concentrations in eleven United States Geological Survey rock standards: *Geostandards Newsletter*, v. 7, pp. 3–226.
- Gladney, E.S., Burns, C.E., and Roelandts, I., 1985, 1983 Compilation of elemental concentrations data for samples SO-1 to SO-4: *Geostandards Newsletter*, v. 9, 35 pp.
- Gladney, E.S., O'Malley, B.T., Roelandts, I., and Gills, T.E., 1987, Compilation of elemental concentration data for NBS clinical, biological, geological, and environmental standard reference materials: U.S. Department of Commerce, NBS Spec. Pub. No. 260–111, pp. 185, 186, 414.
- Gordon, G.E., Randle, K., Goles, G.G., Corliss, J.B., Besson, M.H., and Oxley, S.S., 1968, Instrumental activation analysis of standard rocks with high-resolution X-ray detectors: *Geochimica et Cosmochimica Acta*, v. 32, pp. 369–396.
- Govindaraju, K., 1989, 1989 Compilation of working values and sample description for 272 geostandards: *Geostandards Newsletter*, v. 13 (Special Issue), pp. 1–67.
- Govindaraju, K., 1994, 1994 Compilation of working values and sample description for 383 geostandards: *Geostandards Newsletter*, v. 18 (Special Issue), pp. 1–158.
- Greenberg, A.E., Clesceri, L.S., and Eaton, A.D. (ed.), 1992, Standard methods for the examination of water and wastewater, 18th ed.: American Public Health Association, Washington, D.C.
- Greenwood, N.N., and Earnshaw, A., 1984, *Chemistry of the elements*: Pergamon Press, New York, pp. 1395–1422.
- Hatch, W.R., and Ott, W.L., 1968, Determination of sub-microgram quantities of mercury by atomic absorption spectrophotometry: *Analytical Chemistry*, v. 40, pp. 2085–2087.
- Huckaby, L.S. (ed.), 1993, Lichens as biomonitors of air quality: USDA Forest Service General Technical Report RM-224, Fort Collins, CO: U.S. Department of Agriculture, Forest Service, Rocky Mountain Forest and Range Experiment Station, 131 pp.
- Ingamells, C.O., and Pitard, F.F., 1986, *Applied geochemical analysis*: John Wiley and Sons, New York, 733 pp.
- Jackson, L.L., Engleman, E.E., and Peard, J.L., 1985, Determination of total sulfur in lichens and plants by combustion-infrared analysis: *Environmental Science and Technology*, v. 19, pp. 437–441.
- Jackson, L.L., Brown, F.W., and Neil, S.T., 1987, Major and minor elements requiring individual determination, classical whole rock analysis, and rapid rock analysis, in Baedecker, P.A. (ed.), *Methods for Geochemical Analysis*: U.S. Geological Survey Bulletin 1770, pp. G1–G11.
- Jackson, L.L., Baedecker, P.A., Fries, T.L., and Lamothe, P.J., 1995, Geological and inorganic materials: *Analytical Chemistry*, v. 67, pp. 71R–85R.
- Jeffery, P.G., and Hutchison, D., 1983, *Chemical methods of rock analysis*, 3rd ed.: Pergamon Press, Oxford, 379 pp.
- Johnson, R.G., 1984, Trace element analysis of silicates by means of energy-dispersive X-ray spectrometry: *X-ray Spectrometry*, v. 13, no. 2, pp. 64–68.
- Johnson, R.G., and King, B-S.L., 1987, Energy-dispersive X-ray fluorescence spectrometry, in Baedecker, P.A. (ed.), *Methods for Geochemical Analysis*: U.S. Geological Survey Bulletin 1770, pp. F1–F5.
- Joyce, R.J., and Schein, A., 1989, IC—A powerful analytical tool for environmental laboratories: American Laboratory, Nov. 1989, pp. 46–54.
- Kabata-Pendias, A., and Pendias, H.K., 1984, *Trace elements in soils and plants*: CRC Press, Inc., Boca Raton, Fla., pp. 116–125.
- Keith, L.H. (ed.), 1988, *Principles of environmental sampling*: ACS Professional Reference Book, American Chemical Society, Washington, D.C., 458 pp.
- Kennedy, K.R., and Crock, J.G., 1987, Determination of mercury in geological materials by continuous-flow, cold-vapor, atomic absorption spectrophotometry: *Analytical Letters*, v. 20, pp. 899–908.
- King, B.W., 1987, Determination of trace elements in eight Chinese stream-sediment reference samples by energy-dispersive X-ray spectrometry: *Geostandards Newsletter*, v. 11, no. 2, pp. 193–195.
- LaFleur, P.D. (ed.), 1976, *Accuracy in trace analysis: Sampling, sample handling, analysis, v. I and II*: National Bureau of Standards (currently the National Institute of Standard Technology), Gaithersburg, Md., 1304 pp.
- Laul, J.C., 1979, Neutron activation analysis of geological materials: *Atomic Energy Review*, v. 17, pp. 93–114.
- Lichte, F.E., 1995, Determination of elemental content of rocks by laser ablation inductively coupled plasma mass spectrometry: *Analytical Chemistry*, 67, pp. 2479–2485.
- Lichte, F.E., Golightly, D.W., and Lamothe, P.J., 1987a, Inductively coupled plasma—atomic emission spectrometry, in Baedecker, P.A. (ed.), *Methods for Geochemical Analysis*: U.S. Geological Survey Bulletin 1770, pp. B1–B10.
- Lichte, F.E., Meier, A.L., and Crock, J.G., 1987b, Determination of the rare earth elements in geological materials by inductively coupled plasma mass spectrometry: *Analytical Chemistry*, v. 59, no. 8, pp. 1150–1157.
- Minczewski, J., Chwastowska, J., and Dybczynski, R., 1982, Separation and preconcentration methods in inorganic trace analysis: Ellis Horwood Limited, Chichester, England, 543 pp.
- Montaser, A. and Golightly, D.W., 1992, Inductively coupled plasmas in analytical atomic spectroscopy: VCH Publishing, Inc., New York, 1017 pp.
- Motooka, J.M., 1988, An exploration geochemical technique for the determination of preconcentrated organometallic halides by ICP-AES: *Applied Spectroscopy*, v. 42, pp. 1293–1296.
- O'Leary, R.M., and Viets, J.G., 1986, Determination of antimony, arsenic, bismuth, cadmium, copper, lead, molybdenum, silver, and zinc in geological materials by atomic absorption spectrometry using a hydrochloric acid-hydrogen peroxide digestion: *Atomic Spectroscopy*, v. 7, pp. 4–8.
- Peacock, T.R., 1992, The preparation of plant material and determination of weight percent ash: U.S. Geological Survey Open-File Report 92–345, 9 pp.
- Pfaff, J.D., Brockoff, C.A., and O'Dell, J.W., 1989, The determination of inorganic ions in water by ion chromatography-method 300.0: U.S. Environmental Protection Agency, p. 300.0.
- Potts, P.J., 1987, *A handbook of silicate rock analysis*: Blackie and Son Ltd., London, 622 pp.
- Potts, P.J., Tindle, A.G., and Webb, P.C., 1992, *Geochemical reference materials compositions*: CRC Press Inc., Boca Raton, Fla., 313 pp.
- Roelandts, I., 1989, Environmental reference materials: *Spectrochimica Acta*, v. 44B, pp. 925–934.
- Rose, A.W., Hawkes, H.E., and Webb, J.S., 1979, *Geochemistry in mineral exploration*: Academic Press, New York, 657 pp.
- Sandell, E.B., 1959, *Colorimetric determinations of traces of metals*: Interscience Publishers, Inc., New York, 1032 pp.
- Sanzolone, R.F., and Chao, T.T., 1987, Determination of selenium in thirty-two geochemical reference materials by continuous-flow hydride generation atomic absorption spectrophotometry: *Geostandards Newsletter*, v. 11, pp. 81–85.
- Small, H., Stevens, T.S., and Bauman, W.C., 1975, Novel ion exchange chromatographic method using conductimetric detection: *Analytical Chemistry*, v. 47, pp. 1801–1809.
- Smoley, C.K., 1992, Methods for the determination of metals in environmental samples: Environmental Monitoring Systems Laboratory,

- Office of Research and Development, U.S. Environmental Protection Agency, Cincinnati, Ohio, 305 pp.
- Soltanpour, P.N. 1991. Determination of nutrient availability and elemental toxicity by AB-DTPA soil test and ICPS; *in* Stewart, B.A. (ed.), *Advances in Soil Science*, v. 16: Springer-Verlag, New York, pp. 165–190.
- Stoch, H., 1986, A manual of analytical methods used at Mintek: Council for Mineral Technology (MINTEK), Spec. Pub. No. 7, Private Bag X3015, Randburg, 2125 South Africa, 426 pp.
- Sulcek, Z., and Povondra, P., 1989, Methods of decomposition in inorganic analysis: CRC Press, Inc., Boca Raton, Fla., 325 pp.
- Taggart, J.E., Jr., Lindsey, J.R., Scott, B.A., Vivit, D.V., Bartel, A.J., Stewart, K.C., 1987, Analysis of geologic materials by wavelength-dispersive X-ray fluorescence spectrometry; *in* Baedeker, P.A. (ed.), *Methods for Geochemical Analyses*: U.S. Geological Survey Professional Paper 1770, pp. E1–E19
- Thompson, M., and Walsh, J.N., 1989, A handbook of inductively coupled plasma spectrometry, 2nd ed.: Blackie, London, 316 pp.
- Thompson, M., Simon, C., and Bret, L., 1989, Calibration studies in laser ablation microprobe-inductively coupled plasma atomic emission spectrometry: *Journal of Atomic Spectroscopy*, v. 4, pp. 11–16.
- U.S. Environmental Protection Agency, 1995, Draft method 1631—Mercury in water by oxidation, purge and trap, and cold vapor atomic fluorescence spectrometry: U.S. EPA, Office of Water, Engineering, and Analysis Division (4303), Washington, D.C. 20460.
- Varma, A., 1984, CRC handbook of atomic absorption analysis, v. I and II: CRC Press, Inc., Boca Raton, Fla., 510 pp. (v. I), 444 pp. (v. II).
- Viets, J.G., 1978, Determination of silver, bismuth, cadmium, copper, lead, and zinc in geologic materials by atomic absorption spectrometry with tricaprilmethylammonium chloride: *Analytical Chemistry*, v. 50, no. 8, pp. 1097–1101.
- Viets, J.G., and O'Leary, R.M., 1992, The role of atomic absorption spectrometry in geochemical exploration: *Journal of Geochemical Exploration*, v. 44, pp. 107–138.
- Welz, B., 1985, Atomic absorption spectrometry: VCH Publishers, Deerfield Beach, Fla., 506 pp.
- Westerman, R.I. (ed.), 1990, Soil testing and plant analysis: Soil Science Society of America, Inc., Madison, Wis., 784 pp.
- Williams, S.E., and Funston, R.S., 1987, Mercury; *in* Williams, R.D., and Schuman, G.E. (eds.), *Reclaiming Mine Soils and Overburden in the Western United States—Analytical Parameters and Procedures*: Soil Conservation Society of America, Ankeny, Iowa, pp. 313–323.
- Wilson, S.A., Tidball, R., Kennedy, K., Briggs, P., Hageman, P., and Cappalucci, T., 1991, Assessment of geochemical variability and a listing of geochemical data for soils, drain sediments, alfalfa, greasewood, ground water and water extractable soil constituents from the TJ-Drain Study Area, Nevada: U.S. Geological Survey Open-File Report 91–581.
- Winge, R.K., Fassel, V.A., Peterson, V.J., and Floyd, M.A., 1985, Inductively coupled plasma-atomic emission spectrometry—An atlas of spectral information: Elsevier, N.Y., 584 pp.
- Zief, M., and Mitchell, J.W., 1976, Contamination control in trace element analysis: John Wiley and Sons, New York, 262 pp.

Chapter 14

GEOCHEMICAL MODELING OF WATER-ROCK INTERACTIONS IN MINING ENVIRONMENTS

C.N. Alpers¹ and D. Kirk Nordstrom²

¹*U.S. Geological Survey, Placer Hall, 6000 J Street, Sacramento, CA 95819-6129*

²*U.S. Geological Survey, 3215 Marine Street, Boulder, CO 80303-1066*

INTRODUCTION

Geochemical modeling is a powerful tool for evaluating geochemical processes in mining environments. Properly constrained and judiciously applied, modeling can provide valuable insights into processes controlling the release, transport, and fate of contaminants in mine drainage. This chapter contains

- 1) an overview of geochemical modeling,
- 2) discussion of the types of models and computer programs used,
- 3) description of a procedure for screening water analyses for modeling input, and
- 4) examples of the application of modeling for interpreting geochemical processes in mining environments.

Three general strategies in current use to interpret water-rock interactions are statistical analysis, “inverse” modeling, and “forward” modeling. Multivariate correlation analysis, factor analysis, cluster analysis, and other statistical techniques can group water-chemistry data into sets that may relate to hydrogeochemical processes (Drever, 1988; Puckett and Bricker, 1992). In the field of geochemical exploration, statistical analysis is used widely to treat large data sets of rock and sediment chemistry (e.g., Garrett, 1989). No physical or chemical principles are involved directly in these statistical treatments, hence they are not considered further in this chapter. Nevertheless, statistical analysis can be a useful tool in organizing complex geochemical data for interpretation.

Inverse modeling uses field data to interpret water analyses in terms of water-rock interactions. Chemical and isotopic data for water and rocks along a known flow path are used to test hypotheses regarding geochemical processes by mass-balance considerations. Several possible combinations of geochemical reactions are considered simultaneously to narrow the choice to a minimum number of feasible reactions. Although inverse modeling is based primarily on mass balance and mineral compositions without any thermodynamic or kinetic data, it can be further constrained by detailed mineralogic information, by mineral saturation states determined with speciation calculations, and by a general knowledge of kinetic rates of mineral dissolution and precipitation.

Forward modeling predicts or simulates the consequences of particular geochemical reactions given assumptions regarding the initial state of a system and its boundary conditions. Forward models attempt to answer questions such as “What would be the result if a rock of composition A were to react with a water of composition B?” From user-supplied reactions with associated thermodynamic data and assumptions regarding equilibrium, the consequences of specific geochemical reactions can be computed.

Reactions that may be modeled include mineral dissolution and precipitation, oxidation-reduction, gas evolution, and sorption. Forward geochemical models have been combined with hydrologic models that incorporate physical transport processes to create “coupled reaction-transport” models. Forward geochemical models can be used in mining environments for a variety of applications. Examples include estimating pre-mining water-quality conditions (Runnells et al., 1992), determining optimal conditions and reagent requirements for water treatment, predicting consequences of remediation alternatives, and predicting downstream water-quality conditions resulting from mining and remediation.

Modeling is not an exact science and its application has numerous pitfalls, uncertainties, and limitations. As a precautionary note we first discuss the philosophy behind modeling, a theme to which we return at the end of the chapter. Next, we describe the screening of water analyses and the formulation of preliminary hypotheses using ion plots. A fundamental aspect of most modeling computations is the aqueous speciation calculation, which should be done only with water analyses that survive the scrutiny of the screening procedures. Following a section on aqueous speciation, we describe inverse modeling and forward modeling, with brief discussions of advanced forward models that simulate sorption, solid solutions, and coupled reaction-transport.

MODELING PHILOSOPHY AND PERSPECTIVES

Scientific models are evolving ideas, ways of capturing into communicable language certain aspects of physical reality, embodiments of hypotheses (Konikow and Bredehoeft, 1992), and ways of looking at the world; they are best thought of as guides to our thinking. We adopt the following definition for a model: “a *testable* idea, hypothesis, theory, or combination of theories that provides...insight or a new interpretation of an old problem.” (Nordstrom, 1994). A chemical model is a theoretical construct that permits the calculation of physicochemical processes and properties of substances (such as thermodynamic, kinetic, and quantum mechanical properties); a geochemical model is a chemical model developed for geologic systems (Nordstrom, 1994).

The goals of modeling are to improve and refine a conceptual model (Greenwood, 1989). A model is not reality, nor is it a reliable, correct, or valid representation of reality. A model is not a computer code, *per se*. A conceptual model begins as an idea that has logical and testable consequences. It can sometimes be translated into a mathematical model; mathematical models can usually be converted into numerical models which can then be pro-

grammed as computer codes. The resulting computer programs may include chemical and numerical models, but are not considered geochemical models until applied to a specific geologic or geochemical system. Hence, we have come full circle back to a revised conceptual model after a formal translation (mathematics), and an approximate solving routine (numerical methods), using an electronic managing and accounting device (the computer).

The geochemical model itself can never be proven to be true nor shown to be valid in an absolute sense; the computed results are only valuable insofar as they improve or disprove the original conceptual model (Nordstrom, 1994). Hazardous waste engineers, managers, and regulators need to know about the reliability of models and use the term "model validation" to refer to provisional acceptance according to predefined criteria. However, the concept of "model validation" remains a highly controversial and contentious area of debate. Recent discussions (e.g., Konikow and Bredehoeft, 1992; Oreskes et al., 1994; Nordstrom, 1994) contend that both hydrologic and geochemical models cannot be validated (i.e., proven to be true or valid) *per se* because the models are merely approximations of reality intended to test the implications of hypotheses. The term "model verification" is most often used in the sense of comparing the results of complex numerical codes to analytical solutions (e.g., Lichtner, 1993) and does not relate to the issue of whether or not the model or analytical expression provides an adequate description of the system under consideration. Models can disprove but never prove hypotheses. Even when a prediction by a model is shown later by independent means to have been correct, this does not indicate that the model (or set of hypotheses) will be correct when applied to other systems; it may have been right for the wrong reasons, or somehow incomplete or inadequate in ways that were not tested.

Why do earth scientists make models? Models help guide our thinking, opening up new possibilities, insights, and hypotheses that might not have been possible without them. Models are tools that increase our understanding and are not ends in themselves. Models are necessarily limited and approximate. In science, they are often on the forefront of knowledge and may contain huge uncertainties. They are continually revised and updated as more information becomes available and as more ideas are tested. Consequently, the knowledge a person brings to bear on a problem is far more important than the sophistication of a certain computer program in determining the usefulness of a modeling result. Knowledge and experience with both practical and theoretical hydrogeochemistry as well as general knowledge of hydrologic and geologic processes are essential for successful geochemical modeling.

With an appropriate sensitivity to the inherent limitations and uncertainties of geochemical models and modeling, it is possible to use the modeling approach to gain considerable insight into processes that may be occurring at a contaminated mine site, to test hypotheses regarding major controls on the mobility of selected contaminants, and to assess the probable consequences of various remediation strategies without costly field experiments.

DATA SCREENING AND ION PLOTS

When using water analyses as a basis for geochemical modeling, the data must be carefully screened. Major ion concentrations should be determined well enough that electrical charge imbalances are minimized. One method for computing charge imbalance

(CI) is the following formula (modified from Ball and Nordstrom, 1991):

$$CI (\%) = \frac{[\sum_i m_i^+ z_i^+ - \sum_i m_i^- z_i^-] * 100}{[\sum_i m_i^+ z_i^+ + \sum_i m_i^- z_i^-] / 2} \quad [1]$$

where m_i^+ and m_i^- are the molalities of cation and anion species, respectively, and z_i^+ and z_i^- represent the charge on each species. Water samples with CI values less than 10% are preferred as input for geochemical modeling.

Several other tests of analytical quality should have been completed by the analysts in the laboratory according to accepted quality assurance/quality control (QA/QC) procedures, including spiked recoveries, standard additions, replicate analyses to determine precision, alternate standards, alternate methods, standard reference materials, tests for matrix interferences, and relevant statistical tests (Elving and Kienitz, 1978). Numerous standard reference materials that have undergone interlaboratory comparisons are available to provide the basis for accuracy estimates. From these results, analytical errors on individual constituents can be derived for error propagation and sensitivity analysis as part of geochemical modeling (e.g., Nordstrom and Ball, 1989).

Less common but very useful techniques for screening water analyses include comparisons of measured with calculated total dissolved solids (TDS) and measured with calculated specific conductance. Furthermore, because sulfate is usually the dominant anion in acid mine waters, sulfate concentrations should correlate very well with both TDS and specific conductance. Ball and Nordstrom (1989) used this technique to evaluate mine water analyses from the Leviathan mine, California. Because sulfate analyses are often the least precise and least accurate of the major ions, these correlation tests can be very useful in identifying erroneous data. In areas where multiple samples have been taken over a period of time, time-series plots of concentrations and of ratios of certain constituents can be useful in identifying erroneous data or contaminated samples.

Analytical data for water samples used in speciation or mass-balance computations must be of high accuracy and precision. Relatively small errors in the analytical data can be exaggerated when propagated to produce results such as saturation indices or mass-balance coefficients. Errors in analytical data can be minimized by several procedures:

- 1) careful attention to water sample acquisition, field measurements, and proper filtration and preservation procedures,
- 2) appropriate choice of analytical procedures for the particular sample compositions, including correction or prevention of interferences, and
- 3) appropriate tests of analytical accuracy and precision by standard additions, alternative methods, and analysis of blanks, duplicates, and replicate samples according to standard QA/QC protocols.

It is important to choose analytical methods with sufficiently low detection limits for dissolved constituents. This is especially true for constituents that can be important complexing agents for trace elements despite low concentrations, e.g., PO_4 and F if concerned with controls on Al or U solubility.

Standard errors in analytical data should be clearly identified for purposes of error propagation when performing a sensitivity analysis. The appropriate number of significant figures should be

used for each analytical result, and the uncertainty in each analysis should be known, including errors introduced by dilution. The uncertainty on pH measurements should be based on the success in reproducing expected values for standard buffers that bracket the unknown pH value. Field values of pH are often reported with three significant figures; however, this level of precision can be obtained only if a check of standards is made both before and after the unknown measurement, and the standard buffers are within 0.05 units of the expected values. Uncertainties on laboratory analytical data range generally between 2 and 25% of the amount present, depending on numerous factors including the method used, the amount and number of dilutions, and proximity to the detection limit.

Iron species are commonly the dominant cations in acid mine waters. Therefore, analytical determinations of Fe(II) and Fe(III) as distinct constituents must be obtained on acid mine waters so that the charge balance and speciation calculations are reasonable. Standard methods for this procedure involve analysis of Fe(II) and Fe(total) by spectrophotometry using a ferroin complexing agent such as ferrozine (Stookey, 1970) or dipyridine (Brown et al., 1970), with calculation of Fe(III) by difference. It is strongly recommended that the same analytical method be used for both Fe(II) and Fe(total) so that analytical errors are minimized; in this way, systematic errors should cancel out in computation of Fe(III) concentrations. A new method (To et al., 1999) allows direct determination of Fe(III). There is often an excellent correlation between the activity ratio of Fe(III)/Fe(II) and the reduction-oxidation (redox) potential (Eh or pe) in iron-rich acid mine waters (e.g., Nordstrom et al., 1979a; Ball and Nordstrom, 1989). However, the field measurement of redox potential should be used as a check, rather than as a substitute, for analytical determination of both Fe(II) and Fe(III).

After the data are screened, simple ion plots are often helpful in formulating hypotheses concerning geochemical processes. For example, in a drainage system containing acid mine waters, any constituent which correlates strongly with sulfate is likely to be transported as a relatively conservative or nonreacting solute, analogous to chloride in most circum-neutral waters. Therefore, a plot of different constituents against sulfate may help to distinguish conservative from nonconservative constituents during downstream transport. Dissolved aluminum is a constituent which may exhibit either conservative or nonconservative behavior, depending on pH (Nordstrom and Ball, 1986). Other examples of the use of ion plots can be found in papers by Nordstrom et al. (1989, 1992) and by Plummer et al. (1990).

AQUEOUS SPECIATION MODELING

Aqueous speciation is the distribution of dissolved constituents among various aqueous complexes and individual free ions. The calculation of speciation is fundamental to most geochemical models and is used routinely to interpret water analyses for which all major ions have been determined. The speciation results are needed to compute the degree of saturation of an aqueous solution with respect to various minerals.

Speciation calculations can provide some bounding constraints on water-rock interactions but mostly they indicate which reactions are possible thermodynamically, not necessarily which reactions are likely to occur. Kinetic barriers may inhibit many mineral precipitation or dissolution reactions from taking place. For example, many surface waters and most shallow ground waters

have concentrations of $\text{SiO}_{2(\text{aq})}$ more than 6.3 mg/l, which is the equilibrium solubility of quartz at 25°C (Fournier and Potter, 1982). Despite quartz supersaturation for these waters, quartz does not form readily below 100°C (Fournier and Potter, 1982) because of very slow precipitation rates. Amorphous silica, which has an equilibrium silica solubility of about 120 mg/l at 25°C (Fournier and Rowe, 1977), tends to provide an upper limit to aqueous silica concentrations in natural waters; however, most low-temperature, non-geothermal waters have dissolved silica concentrations less than about 30 mg/l (Hem, 1985), suggesting control by other forms of crystalline silica such as chalcedony or cristobalite, or by a poorly-crystalline-to-amorphous clay mineral such as halloysite (Hem et al., 1973). The relations in the $\text{SiO}_2\text{-H}_2\text{O}$ system illustrate the complexity of low-temperature water-rock interactions, in which metastable phases may control or influence solubility because of kinetic barriers affecting thermodynamically stable phases.

Numerous minerals simply do not reach solubility equilibrium in natural waters at temperatures of 0–100°C. Minerals with slow precipitation rates are unlikely to control the aqueous concentrations of the relevant ions. Some knowledge of mineral reaction rates can be very helpful in the interpretation of the chemistry of natural waters using aqueous speciation and mineral saturation calculations (see Nordstrom and Alpers, 1999).

Quantitative knowledge of aqueous speciation is important for evaluating bioavailability and toxicity because certain aqueous species of a given element are much more toxic than others (see Smith and Huyck, 1999). For example, $\text{Cu}^{2+}_{(\text{aq})}$ is considered more toxic to fish than $\text{CuCO}_3^0_{(\text{aq})}$ or other complexed forms of copper (Hodson et al., 1979). Other useful results from speciation modeling include the elemental molalities needed as input for mass-balance and reaction-path models and the aqueous activities of individual ions. Correlation plots of aqueous activity values and activity ratios can be used to evaluate the stoichiometry of a precipitating phase that controls solubility (see Nordstrom and Alpers, 1999).

Speciation calculation

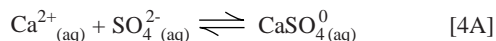
Speciation and mineral saturation are calculated by a sequence of steps containing both thermodynamic quantities and numerical approximations. The overall calculation seeks a minimum in the Gibbs free energy of the system. Although several techniques have been used to solve free energy minimization, they all seek a numerical solution for the combined non-linear set of mass-balance and mass-action equations that define the problem. Mass-balance equations of the form

$$m_{T(A)} = \sum_i m_{i(A)} \quad [2]$$

express the conservation of mass for all species that have a common component, where $m_{T(A)}$ is the total dissolved molality of a component A, and $m_{i(A)}$ is the molality of the i^{th} species containing the Ath component. For example, the mass-balance equation for calcium might be

$$m_{\text{Ca}_T} = m_{\text{Ca}^{2+}_{(\text{aq})}} + m_{\text{CaHCO}_3^+_{(\text{aq})}} + m_{\text{CaCO}_3^0_{(\text{aq})}} + m_{\text{CaSO}_4^0_{(\text{aq})}} \quad [3]$$

The mass-action equations express the equilibrium established among species by the equilibrium constant, K . For example, the association reaction for the CaSO_4^0 ion pair is



for which the mass-action equation is:

$$K_{\text{CaSO}_4^0}^{25^\circ\text{C}} = \frac{a_{\text{CaSO}_4^0_{(\text{aq})}}}{a_{\text{Ca}^{2+}_{(\text{aq})}} a_{\text{SO}_4^{2-}_{(\text{aq})}}} = 10^{2.30} \quad [4B]$$

The mass-balance and mass-action equations contain known quantities, and the condition of electroneutrality (charge balance) represents a known quantity, leaving the concentrations and activities of the individual aqueous species as the unknown quantities. For aqueous speciation calculations, the system is usually overdetermined by one degree of freedom (Merino, 1979), so that finding a solution is a tractable problem. The distribution of aqueous species among free ions and complexes in the aqueous phase is assumed to be at homogeneous equilibrium.

Most (but not all) geochemical modeling codes assume at the start of the calculation that the total dissolved concentration is equivalent to the free ion concentration, i.e., for calcium

$$m_{\text{Ca}_{\text{T}(\text{aq})}} = m_{\text{Ca}^{2+}_{(\text{aq})}} \quad [5]$$

For ion association models, the ionic strength, I , is computed from

$$I = \frac{1}{2} \sum_i m_i z_i^2 \quad [6]$$

where m_i and z_i are the molality and charge, respectively, of the i^{th} ion. The ionic strength is then used to calculate the activity coefficient of each ion, γ_i , according to the extended Debye-Hückel equation, the Davies equation, or a Brønsted-Guggenheim equation (e.g., Nordstrom and Munoz, 1994). The activity of each ion is then computed with the equation

$$a_i = \gamma_i m_i \quad [7]$$

After one iteration through a numerical approximation, a first estimate of speciation is made. The Newton-Raphson and continued-fraction methods are commonly used to find a numerical solution. An application using each of these methods is described by Nordstrom and Munoz (1994).

An alternative approach to calculating activity coefficients is with the Pitzer equations (Pitzer, 1973, 1979, 1987). This approach is known as the specific-ion interaction method because all ions are assumed to interact to some degree and these interactions are incorporated into terms that are added to an electrostatic Debye-Hückel term. The power of this approach is that activity coefficients can be fit to experimental data for ionic strengths up to 10 molal and higher in some chemical systems, whereas with the ion-association model, good fits to experimental data are limited to considerably lower ionic strengths.

Application of ion-association models to solutions with ionic strengths greater than about 0.1 molal can only be obtained with a linear term added on to the extended Debye-Hückel equation, i.e., a Brønsted-Guggenheim model. Such an expression can be considered a hybrid between the extended Debye-Hückel equation and the Pitzer approach. The hybrid model has been used in Sweden for many years with considerable success in the interpretation of aqueous electrolyte data (Grenthe et al., 1992).

There are two main drawbacks with application of the Pitzer approach to acid mine waters. One is that insufficient data are available to model the activity coefficients for all the principal trace elements found in acid mine waters. Considerable progress has been made on deriving the interaction parameters for some constituents in acid mine waters, specifically for the systems Fe(II)- H_2SO_4 - H_2O (Reardon and Beckie, 1987), Al- SO_4 - H_2O (Reardon, 1988), Ni- H_2SO_4 - H_2O (Reardon, 1989), and Pb- SO_4 - H_2SO_4 - H_2O (Paige et al., 1992). However, interaction parameters for systems with Fe(III), As(III/V), Cu, and Zn are needed for a complete description of highly concentrated acid mine waters, and the temperature dependence of some interaction parameters remain uncertain or unknown (C. Ptacek and D. Blowes, written commun., 1995). The other drawback to the Pitzer method is the necessity to refit the interaction parameters for all elements whenever new data are added, so that consistency is maintained.

Redox reactions are important in the geochemistry of acid mine waters, yet most geochemical modeling codes assume erroneously that redox equilibrium is maintained. The redox chemistry must be determined by analyzing water samples for the individual redox states of elements such as Fe (II and III) and As (III and V). Aqueous redox reactions and their rates are not understood well enough to assume any particular ratio of redox species based on platinum electrode measurements. Disequilibrium among redox couples is the rule not the exception (e.g., Lindberg and Runnells, 1984).

Once the speciation calculation has been made then the ion activity product (IAP) can be compared to the solubility product constant (K_{sp}) to test for mineral saturation. The saturation index, SI, is computed for each mineral in the data base from

$$\text{SI} = \log \left(\frac{\text{IAP}}{K_{\text{sp}}} \right) \quad [8]$$

The SI for an aqueous solution with respect to a particular mineral describes the thermodynamic tendency of that solution to precipitate or to dissolve that mineral. Positive values of SI indicate supersaturation and the tendency of the water to precipitate that mineral. Negative values of SI indicate undersaturation and the tendency of the water to dissolve a certain mineral. A value of SI = 0 indicates apparent equilibrium, a balance between the thermodynamic driving forces of dissolution and precipitation. Examples of SI values and their interpretation for various minerals in mine drainage environments are given in a later section of this chapter and in the chapter by Nordstrom and Alpers (1999).

Input data

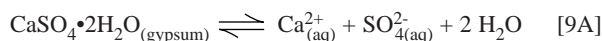
Two types of input data are used with computer codes that compute aqueous speciation: (1) analytical data on the water com-

position, and (2) thermodynamic data for aqueous species and minerals. Some computer programs have the thermodynamic data resident in the code or in an accessible data table; other programs require the thermodynamic data to be user-supplied. Regardless of the format, the thermodynamic data should always be considered as input data for which the reliability is the responsibility of the user.

Most computer programs that perform speciation modeling require input data for pH, temperature, and major ion concentrations as minimum parameters. For acid mine waters, dissolved oxygen, alkalinity (for samples with pH > 4.2), specific conductance, liquid density, and Eh (or pe) are also important input parameters, along with trace element concentrations of interest. Other aspects of analytical data evaluation were discussed in the previous section on Data Screening and Ion Plots.

Thermodynamic input data can be in the form of Gibbs free energies, enthalpies, entropies, heat capacities, and molar volumes for individual species that participate in a given reaction, or can be in the form of an equilibrium constant for the reaction (K) along with values or expressions for computing the enthalpy and heat capacity of reaction for determining the temperature dependence of K, and molar volumes of reaction for determining the pressure dependence. Some codes accept data in both forms. Some codes contain analytical expressions for log Ks of reactions as a function of temperature.

For example, the dissolution of gypsum in pure water is described by the reaction:



$$K_{\text{sp,gypsum}}^{25^\circ\text{C}} = \frac{a_{\text{Ca}^{2+}(\text{aq})} a_{\text{SO}_4^{2-}(\text{aq})} a_{\text{H}_2\text{O}}^2}{a_{\text{CaSO}_4 \cdot 2\text{H}_2\text{O}_{(\text{gypsum})}}} = 10^{-4.58} \quad [9B]$$

For solids close to end-member composition, the solid activity term in the denominator can be set equal to 1. This approximation has been shown to be reasonable for gypsum from a field site in Arizona (Glynn, 1991a) but is not generally applicable to other solids of variable composition, as discussed in a later section on solid solutions. Setting the activity of $\text{CaSO}_4 \cdot 2\text{H}_2\text{O}$ in gypsum equal to 1 and taking the logarithm of equation [9B] gives

$$\log K_{\text{sp,gypsum}}^{25^\circ\text{C}} = \log a_{\text{Ca}^{2+}(\text{aq})} + \log a_{\text{SO}_4^{2-}(\text{aq})} + 2 \log a_{\text{H}_2\text{O}} = -4.58 \quad [9C]$$

The association reaction for the $\text{CaSO}_4^0_{(\text{aq})}$ ion pair was given in equation [4A] and the corresponding mass action equation in equation [4B]. Taking the logarithm of equation [4B],

$$\log K_{\text{CaSO}_4^0}^{25^\circ\text{C}} = \log a_{\text{CaSO}_4^0_{(\text{aq})}} - \log a_{\text{Ca}^{2+}(\text{aq})} - \log a_{\text{SO}_4^{2-}(\text{aq})} = 2.30 \quad [10]$$

For gypsum dissolution (equations [9A], [9B], and [9C]) in program WATEQ4F (Ball and Nordstrom, 1991), the temperature dependence of the equilibrium constant is calculated by the equation

$$\log K_{\text{sp,gypsum}} = 68.2401 - \frac{3221.51}{T} - 25.0627T \quad [11]$$

where T is temperature in Kelvins. For the ion association reaction (equations [4A], [4B], and [10]) the temperature dependence of the equilibrium constant is calculated using a value for $\Delta H_r^0 = 5.50 \text{ kJ} \cdot \text{mol}^{-1}$ in the Van't Hoff equation

$$\frac{-2.303 \, d(\log K_r)}{dT} = \frac{\Delta H_r^0}{RT^2} \quad [12]$$

Finding thermodynamic data for all water-mineral reactions of interest is a considerable challenge. Ideally, an internally consistent set of thermodynamic data would be preferred but this is not likely to be available. It is possible, however, to have a limited set of tolerably inconsistent thermodynamic data, in other words, a set in which the propagated errors in thermodynamic data do not significantly affect the speciation calculations or the resulting mineral saturation indices. The beginning of such a set can be found in Appendix D of Nordstrom and Munoz (1994). Programs that use the Pitzer equations tend to have a higher degree of internal consistency because it is a necessary consequence of deriving the fitting parameters. Thermodynamic data may not exist for many species of interest, especially trace-element association constants and mineral solubility constants. Sometimes these can be estimated (see Langmuir, 1979; Helgeson et al., 1981; Sverjensky, 1987; Shock and Helgeson, 1988, 1990; Shock et al., 1989, 1992; Shock and Koretsky, 1993). With or without estimation, the modeler is responsible for checking the adequacy of the critical stability constants for the geochemical system being studied.

Even if internal consistency were achieved, it would not be a guarantee of reliable data. Internal consistency simply refers to a consistent set of data according to the following criteria (Stipp et al., 1993; Nordstrom and Munoz, 1994):

- 1) Fundamental thermodynamic relationships (the basic laws and their consequences) are obeyed.
- 2) Common scales are used for temperature, energy, atomic mass, and fundamental physical constants.
- 3) Conflicts and inconsistencies among measurements are resolved.
- 4) An appropriate mathematical model is chosen to fit all temperature- and pressure-dependent data.
- 5) An appropriate aqueous chemical model is chosen to fit all aqueous solution data.
- 6) An appropriate choice of standard states is made and applied to all similar substances.
- 7) An appropriate starting point is selected for the development of a thermodynamic network.

As more of these criteria are met, greater consistency is achieved. With greater consistency, the probability that the data are reliable becomes greater, but there is still a finite probability that the data are incorrect.

The general absence of a sufficiently consistent and comprehensive thermodynamic data base increases the need for sensitivity analyses to be performed for those data that are critical to a geochemical interpretation. This aspect will be discussed further in the next section.

Interpretation of output

Aqueous speciation calculations for acid mine waters commonly reveal considerable complexation of metals with sulfate. For examples, we consider four acid mine water analyses that cover a range in pH values from about 5.0 to 0.5, with concentrations of sulfate from 206 to 118,000 mg/l and of iron from 4.7 to 20,300 mg/l. Complete analyses of the four samples are given in Table 14.1.

Analyses AMD-A and -B in Table 14.1 are for water samples from the Leviathan mine, which exploited an epithermal deposit containing elemental sulfur and cryptocrystalline pyrite located in Alpine County, California, near the Nevada border (Ball and Nordstrom, 1989). Analysis AMD-C is for combined discharge from the Hornet and Richmond mines, at Iron Mountain, in Shasta County, California (Nordstrom, 1977). At Iron Mountain, the oxidation of massive pyrite at or above the water table within a rhyolitic country rock having little neutralizing capacity has produced a concentrated acid mine water in which iron (II) is the dominant cation followed by iron (III), aluminum, zinc, magnesium, and copper. Analysis AMD-D in Table 14.1 represents an extreme case of "ultra-acid" water that flows from the Richmond mine at Iron Mountain, California (Alpers and Nordstrom, 1991); such extreme metal and sulfate concentrations are encountered only rarely, but serve to demonstrate the compositional limits of the ion-association modeling method.

Speciation of copper, sulfate, aluminum, and iron for samples AMD-A, -B, -C, and -D, computed with the computer program WATEQ4F (Ball and Nordstrom, 1991), is shown graphically as pie charts on Figure 14.1. With decreasing pH and increasing sulfate concentration, the degree of metal complexation with sulfate increases even though the ratio of sulfate to metals decreases. For the simple case of copper, the proportion of free $\text{Cu}^{2+}_{(\text{aq})}$ decreases from 85.5% in AMD-A to 43.4% in AMD-D because of the formation of the $\text{CuSO}_4^0_{(\text{aq})}$ ion pair. Similarly, the distribution of the free $\text{SO}_4^{2-}_{(\text{aq})}$ ion changes from 83.4% in AMD-A to 8.3% in AMD-D, with numerous metal-sulfate complexes competing for sulfate at the higher concentrations; the bisulfate ion ($\text{HSO}_4^-_{(\text{aq})}$) and metal-bisulfate complexes also compete for sulfate at pH values less than about 2. In addition to simple metal-sulfate ion pairs, double-sulfate complexes such as $\text{Zn}(\text{SO}_4)_2^{2-}_{(\text{aq})}$, $\text{Al}(\text{SO}_4)_2^-_{(\text{aq})}$ and $\text{Fe}(\text{SO}_4)_2^-_{(\text{aq})}$ become more abundant with higher sulfate concentrations.

Chemical equilibrium between sulfate and bisulfate ions is expressed by the reaction



The log K for reaction [13] is 1.99 at 25°C (Nordstrom et al., 1990), indicating that activities of sulfate and bisulfate are equal at pH values of about 2.0. At pH values less than 2.0, the bisulfate ion dominates sulfate equilibria, as in samples AMD-C and -D.

Although metal-bisulfate complexes for aluminum, zinc, and magnesium are in the database of WATEQ4F used in the computations, only the iron-bisulfate species $\text{Fe}^{\text{II}}\text{HSO}_4^+$ and $\text{Fe}^{\text{III}}\text{HSO}_4^{2+}$ are significant contributors to sulfate speciation in these samples (Fig. 14.1).

TABLE 14.1—Chemical data for four acid mine water samples. [Samples AMD-A and AMD-B correspond respectively to samples 82WA109 and 82WA110 from the Leviathan mine, Alpine County, California (Ball and Nordstrom, 1989); sample AMD-C corresponds to sample 76WA103 from the Hornet and Richmond mines, Iron Mountain, Shasta County, California (Nordstrom, 1977); sample AMD-D corresponds to sample 90WA103 from the Richmond mine at Iron Mountain (Alpers and Nordstrom, 1991).]

	AMD-A	AMD-B	AMD-C	AMD-D
Sample number	82WA109	82WA110	76WA103	90WA103
Water temperature (°C)	16.0	19.5	24.0	34.8
pH (field)	4.9	3.25	1.10	0.48
Constituent	(mg/l)			
Ca	44.7	82.2	240	183
Mg	13.5	23.6	720	821
Na	8.6	11.8	79.0	251
K	3.21	4.57	107	261
Cl	1.0	1.1	2.0	---1
SO ₄	206	483	50,000	118,000
HCO ₃	---	0	0	0
SiO ₂	42.6	46.4	140	165
Ba	0.042	0.048	---	0.068
Al	5.06	19.8	1,410	2,210
F	0.30	0.52	2.0	---
Fe (total)	4.72	18.4	11,000 ³	20,300
Fe (II)	4.44	9.01	7,820	18,100
Fe (III) ²	0.28	9.39	3,180	2,200
Mn	1.26	3.04	11.0	17.1
Cu	0.09	0.23	360	290
Zn	0.04	0.15	1,860	2,010
Cd	.004	0.01	14.0	15.9
As (total)	0.01	0.02	---	56.4
As (III)	---	---	---	8.14
As (V) ⁴	---	---	---	48.3

¹---, not determined.

²Fe (III) computed as difference of Fe (total) and Fe (II).

³Value uncertain by up to 15%.

⁴As (V) computed as difference of As (total) and As (III).

Ferric iron and aluminum are similar in that both substances form trivalent free cations. However, iron and aluminum speciation differ to a large degree because the hydrolysis of ferric iron takes place at a much lower pH than that of aluminum. As discussed by Nordstrom and Alpers (1999), the first hydrolysis reactions for aluminum and iron can be expressed as follows:



$$K_{\text{Al}(\text{OH})^{2+}}^{25^\circ\text{C}} = \frac{a_{\text{Al}(\text{OH})^{2+}} a_{\text{H}^+}}{a_{\text{Al}^{3+}} a_{\text{H}_2\text{O}}} = 10^{-5.0} \quad [14B]$$

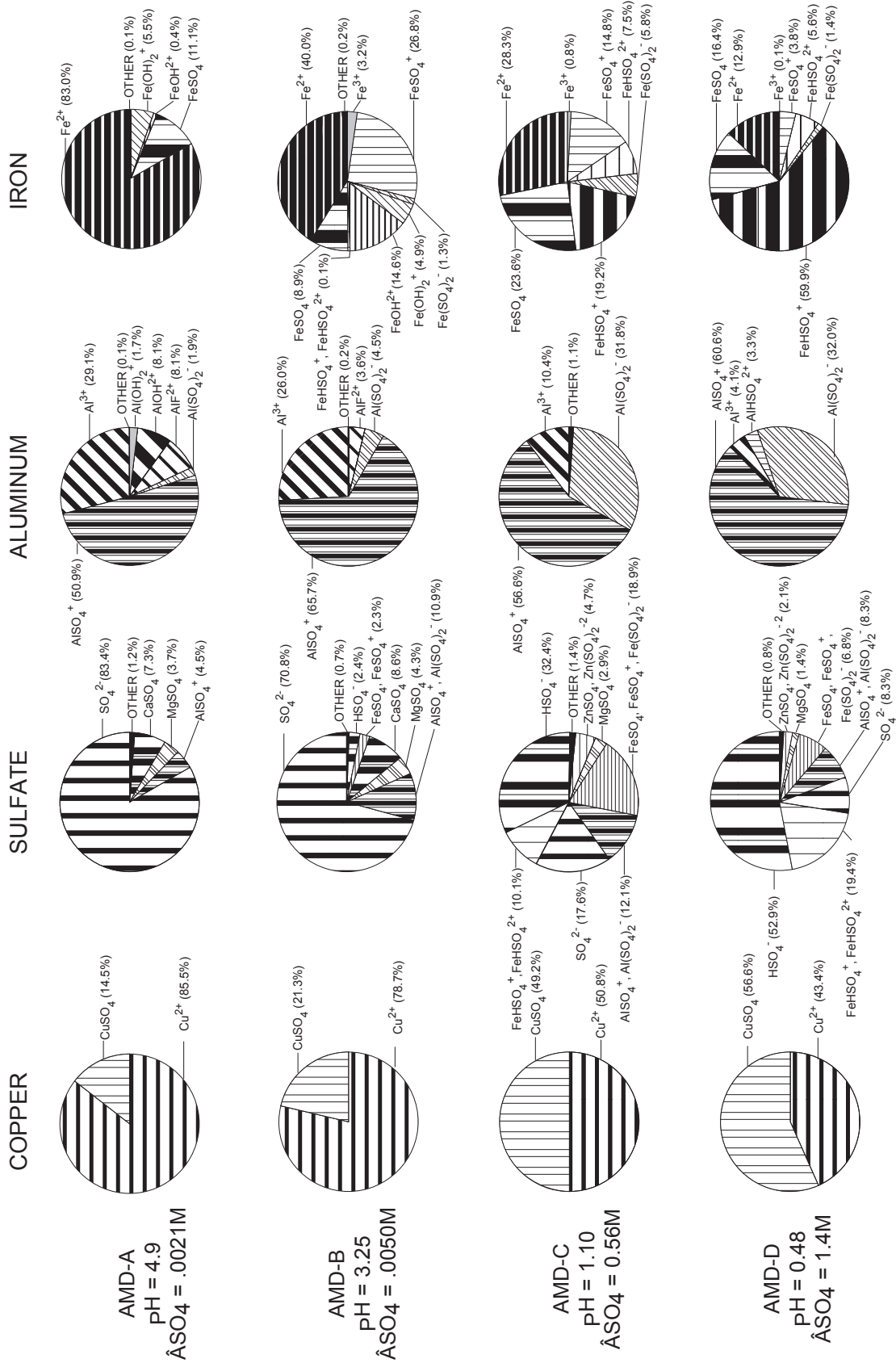


FIGURE 14.1—Pie charts showing results of aqueous speciation calculations in terms of relative molalities of copper, sulfate, aluminum, and iron species, using program WATEQ4F (Ball and Nordstrom, 1991) for acid mine water compositions in Table 14.1.

$$\log K_{\text{Al(OH)}_2^{2+}}^{25^\circ\text{C}} = \log a_{\text{Al(OH)}_2^{2+}} - \log a_{\text{Al}^{3+}} + \log a_{\text{H}^+} - \log a_{\text{H}_2\text{O}} = -5.0 \quad [14\text{C}]$$



$$K_{\text{Fe(OH)}^{2+}}^{25^\circ\text{C}} = \frac{a_{\text{Fe(OH)}^{2+}} a_{\text{H}^+}}{a_{\text{Fe}^{3+}} a_{\text{H}_2\text{O}}} = 10^{-2.2} \quad [15\text{B}]$$

$$\log K_{\text{Fe(OH)}^{2+}}^{25^\circ\text{C}} = \log a_{\text{Fe(OH)}^{2+}} - \log a_{\text{Fe}^{3+}} + \log a_{\text{H}^+} - \log a_{\text{H}_2\text{O}} = -2.2 \quad [15\text{C}]$$

The values of log K in equations [14C] and [15C] contribute to a sharp decrease in abundance of Al-hydroxide complexes at pH values below 5 (e.g., samples AMD-B, -C, and -D) and a similar decrease in Fe^{III}-hydroxide complexes at pH values below 2.2 (AMD-C and -D). The relation of these pH values to the log K values for the hydrolysis reactions can be seen by rearranging equations [14C] and [15C], while setting $a_{\text{H}_2\text{O}}$ equal to 1 ($\log a_{\text{H}_2\text{O}} = 0$) and using the definition $\text{pH} \equiv -\log a_{\text{H}^+}$ to yield

$$\log a_{\text{Al}^{3+}} - \log a_{\text{Al(OH)}_2^{2+}} + \text{pH} = 5.0 \quad [14\text{D}]$$

$$\log a_{\text{Fe}^{3+}} - \log a_{\text{Fe(OH)}^{2+}} + \text{pH} = 2.2 \quad [15\text{D}]$$

The value on the right hand side of equation [14D], equal to -log K for reaction [14A], corresponds to the pH value at which an equal activity of the free aluminum ion and the aluminum-hydroxide ion pair will coexist; the analogous relation for ferric iron is shown in equation [15D].

Hydrolysis of Fe²⁺ and other divalent metals (e.g., Cu, Zn, Cd, Pb, Co, Ni) is not a significant factor in the speciation of acid mine waters with pH values less than about 5. However, hydroxide complexes can be extremely important in speciation analysis of divalent metals in waters with circum-neutral pH. Significant uncertainties remain with regard to thermodynamic data for critical species such as Cu(OH)_{2(aq)}⁰. This underscores the need for users of speciation computer codes to use caution with regard to the quality, uncertainty, and internal consistency of thermodynamic data, as discussed earlier in this chapter.

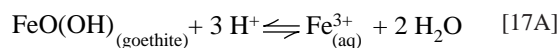
Table 14.2 contains computed molalities and activities for free ions in the four acid mine waters described in Table 14.1 and Figure 14.1, as well as saturation indices for several common secondary minerals, computed using program WATEQ4F (Ball and Nordstrom, 1991). Note that the difference between the logarithms of molality and activity for a given ion is represented by the logarithm of the individual ion activity coefficient, γ_i . Taking the logarithm of equation [7] yields

$$\log a_i = \log \gamma_i + \log m_i \quad [16]$$

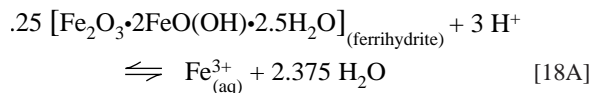
Values of γ_i deviate from 1 to a greater degree for more highly charged species and for solutions of high ionic strength (Garrels and Christ, 1965).

Mineral saturation indices in Table 14.2 indicate the thermodynamic tendency of the four water samples to precipitate or to dissolve certain minerals. All four samples show undersaturation with respect to gypsum. Supersaturation with respect to barite is evident in the three samples for which dissolved Ba data are available. Note that detection of Ba in samples with very high sulfate is problematic because of the low solubility of barite.

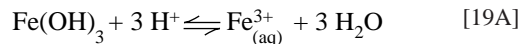
Interpretation of saturation indices for hydrous ferric oxides such as goethite, ferrihydrite, and ferric hydroxide is facilitated by writing the dissolution reactions for these phases in such a way that the K_{sp} expressions share the same exponents for the ferric and hydrogen ions.



$$K_{\text{sp,goethite}} = \frac{a_{\text{Fe}_{(\text{aq})}^{3+}} a_{\text{H}_2\text{O}}^2}{a_{\text{H}^+}^3} \quad [17\text{B}]$$



$$K_{\text{sp,ferrihydrite}} = \frac{a_{\text{Fe}_{(\text{aq})}^{3+}} a_{\text{H}_2\text{O}}^{2.375}}{a_{\text{H}^+}^3} \quad [18\text{B}]$$



$$K_{\text{sp,Fe(OH)}_3} = \frac{a_{\text{Fe}_{(\text{aq})}^{3+}} a_{\text{H}_2\text{O}}^3}{a_{\text{H}^+}^3} \quad [19\text{B}]$$

The only differences between the mass-action expressions in equations [17B], [18B], and [19B] are the values of the exponent applied to the activity of water (a quantity usually very close to unity) and the values of the equilibrium solubility constants. For goethite (equations [17A],[B]) and ferric hydroxide (equations [19A],[B]), the K_{sp} values differ by about 5.8 log units, which is the approximate difference between the SIs of these two phases for the four water samples shown in Table 14.2. As pointed out by Bigham (1994), "Ferrihydrite has become a popular but often misused synonym for 'amorphous' ferric hydroxide." Because goethite is less soluble than ferrihydrite or ferric hydroxide, it will always appear to be supersaturated in a low-temperature solution

TABLE 14.2—Molalities, activities, and saturation indices for four acid mine waters, computed using program WATEQ4F (Ball and Nordstrom, 1991) with chemical data in Table 14.1.

pH (field)	AMD-A		AMD-B		AMD-C		AMD-D	
	4.9		3.25		1.10		0.48	
Species	log m _i	log a _i	log m _i	log a _i	log m _i	log a _i	log m _i	log a _i
H ⁺	-4.87	-4.9	-3.21	-3.25	-0.98	-1.10	-0.35	-0.48
SO ₄ ²⁻	-2.74	-2.90	-2.45	-2.65	-1.01	-1.75	-0.92	-1.80
Cu ²⁺	-14.8	-14.9	-11.8	-11.8	-2.51	-3.02	-2.64	-2.93
Zn ²⁺	-6.26	-6.41	-5.77	-5.98	-1.95	-2.46	-1.92	-2.53
Cd ²⁺	-7.55	-7.70	-7.30	-7.51	-4.40	-4.91	-4.34	-4.64
Fe ²⁺	-4.15	-4.31	-3.88	-4.09	-1.22	-1.73	-1.26	-1.55
Fe ³⁺	-8.77	-9.11	-4.97	-5.44	-2.78	-3.91	-3.54	-4.20
Al ³⁺	-4.26	-4.61	-3.72	-4.19	-2.23	-3.37	-2.40	-3.07
Mineral	Formula	SI ²	SI	SI	SI	SI	SI	SI
		AMD-A	AMD-B	AMD-C	AMD-D			
Gypsum	CaSO ₄ •2H ₂ O	-1.48	-1.06	-0.33	-0.71			
Barite	BaSO ₄	0.40	0.52	---3	0.90			
Melanterite	FeSO ₄ •7H ₂ O	-4.88	-4.46	---	---			
Goethite	FeO(OH)	6.59	5.31	0.38	-1.79			
Ferric hydroxide [ferrihydrite ¹]	Fe(OH) ₃ ¹	0.70	-0.58	-5.52	-7.70			
Jarosite	KFe ₃ (SO ₄) ₂ (OH) ₆	0.64	2.66	-2.32	-5.85			
Alunite	KAl ₃ (SO ₄) ₂ (OH) ₆	5.91	-1.64	-8.55	-9.81			
Kaolinite	Al ₂ Si ₂ O ₅ (OH) ₄	5.65	-3.01	-12.74	-14.61			
Gibbsite	Al(OH) ₃	1.46	-2.86	-8.25	-9.25			
Amorphous Al(OH) ₃	Al(OH) ₃	-1.31	-5.60	-10.95	-11.85			

¹For discussion of ferric hydroxide and ferrihydrite formulas, see Nordstrom and Alpers (1999).

²SI, saturation index.

³---, not computed.

that is saturated with respect to poorly crystalline, metastable hydrous ferric oxide such as ferric hydroxide, ferrihydrite, or schwertmannite, a sulfate-bearing ferric oxyhydroxide (see Nordstrom and Alpers, 1999).

Most other SI values in Table 14.2 are either greater than 1.0 or less than -1.0, indicating that solubility control by the listed phases is unlikely for the water samples under consideration. Other aspects of solubility control on acid mine water composition are discussed by Nordstrom and Alpers (1999).

In summary, the effect of sulfate complexing on metal concentrations is to decrease the free ion concentrations of metals and sulfate. These trends greatly affect saturation index calculations. Therefore it is critical to incorporate speciation analysis into any computations of mineral saturation or equilibrium with sulfate-rich waters common in mining environments.

Available programs and their evolution

The diagram on Figure 14.2 shows the evolution of selected aqueous speciation modeling programs. Figure 14.2 is not intended to be a comprehensive survey of available programs, but rather to provide a framework for understanding the origin of some of the programs in current usage. For more information on programs of this type, the reader is referred to the comparison of chemical models by Nordstrom et al. (1979b) and to the reviews by Waite (1989), Yeh and Tripathi (1989a), Bassett and Melchior (1990), Mangold and Tsang (1991), Plummer (1992), Wolery (1992a), and Nordstrom and Munoz (1994).

An early example of speciation calculations applied to natural waters was the pioneering work of Garrels and Thompson (1962) on the speciation of ocean water. One of the first available speciation computer codes was the HALTAFALL program, based on a successive-approximation algorithm (in ALGOL) developed by Ingri et al. (1967). This program was originally intended to simulate laboratory mixing procedures including titrations, precipitation separations, and solvent extractions. Other uses of the HALTAFALL program have been for the speciation of seawater (Dyrssen and Wedborg, 1974) and of estuarine waters (Dyrssen and Wedborg, 1980). Eriksson (1971, 1979) modified HALTAFALL to compute high-temperature equilibria and produced the new program SOLGASWATER (originally SOLGAS), which uses a Gibbs free energy minimization technique with Gaussian elimination. SOLGASWATER has been applied, primarily in Sweden, to both laboratory and field problems (Öhman, 1983; Lidén, 1983).

The REDEQL program was first described by Morel and Morgan (1972) as a speciation and phase-distribution program using a Newton-Raphson iteration. Numerous improvements and modifications have been made to this program, including REDEQL2 (McDuff and Morel, 1973), MINEQL (Westall et al., 1976), MICROQL (Westall, 1979), REDEQL.EPA (Ingle et al., 1978), and REDEQL.UMD (Harriss et al., 1984). MINTEQ (Felmy et al., 1984) combined MINEQL and the data base from WATEQ3 (Ball et al., 1981). Subsequent versions of MINTEQ include MINTEQA1 (Brown and Allison, 1987) and MINTEQA2 (Allison et al., 1991), which are products of the U.S. Environmental Protection Agency and are widely used for interpretation of exper-

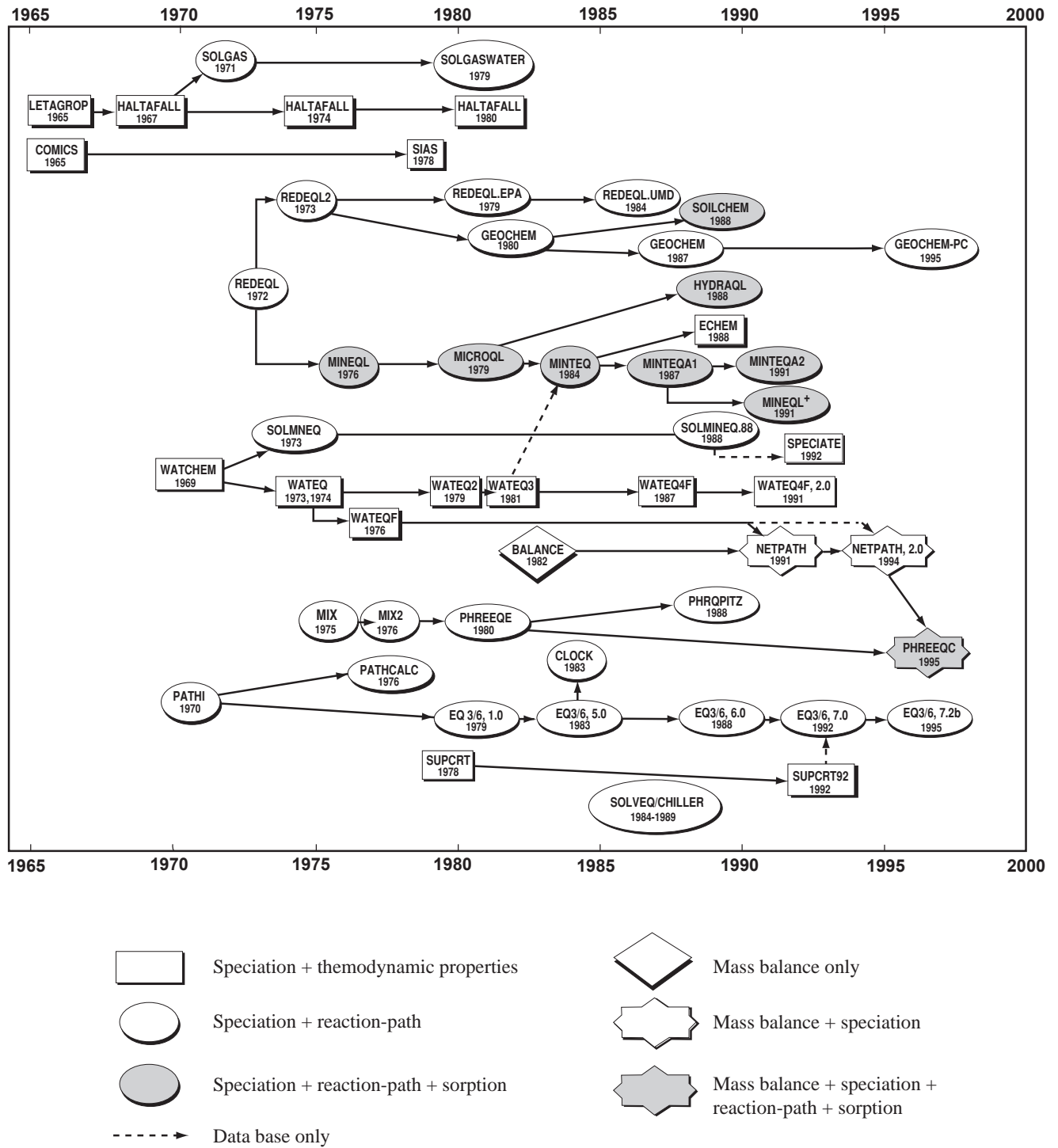


FIGURE 14.2—Evolution of selected geochemical modeling programs.

imental and field data. Other related programs are GEOCHEM for soil-water interactions (Sposito and Mattigod, 1980; Parker et al., 1987), updated as GEOCHEM-PC (Parker et al., 1995), SOILCHEM which includes a large number of organic species (Sposito and Coves, 1988), HYDRAQL (Papelis et al., 1988), ECHEM (Morrey, 1988), and MINEQL+, an interactive version of MINTEQA1 (Schecher and McAvoy, 1991). In addition to capabilities for computing aqueous speciation and mineral saturation indices, the MINTEQ series of programs can compute mass transfer (forward modeling) and can model adsorption, as discussed in later sections of this chapter and in the chapter by Smith (1999). MINTEQA2 is written in FORTRAN and runs on IBM-type personal computers. MacuQL (Muller, 1993) is a version of MICROQL that runs on Macintosh-type personal computers.

Another widely used series of speciation programs that compute mineral saturation indices is the WATEQ series developed by the U.S. Geological Survey, including WATEQ (Truesdell and Jones, 1973, 1974), WATEQF (Plummer et al., 1976), WATEQ2 (Ball et al., 1979, 1980), WATEQ3 (Ball et al., 1981), and WATEQ4F (Ball et al., 1987; Ball and Nordstrom, 1991). The latest version, WATEQ4F, v. 2.3 for IBM-type PC's, has an updated data base (Nordstrom et al., 1990) and was developed with an emphasis on trace metals and redox-sensitive species; the user may designate redox disequilibrium among the redox-sensitive elements, if desired.

The PHREEQE (pronounced "freak") program (Parkhurst et al., 1980) incorporates an aqueous model similar to programs in the WATEQ series. As in WATEQF and WATEQ4F, the user can choose between the Truesdell-Jones and the Davies models for computing aqueous activity coefficients. PHREEQE uses a dual-algorithm method that computes speciation with a continued fraction algorithm; forward modeling (mass transfer) is computed using a Newton-Raphson iteration. An advantage of the PHREEQE program relative to the WATEQ codes is the ease with which the user can add aqueous species, elements, and minerals to the model as part of the input file. This feature can facilitate the job of sensitivity analysis with regard to the thermodynamic data for individual minerals and aqueous species. The PHREEQC program (Parkhurst, 1995), written in C, is a recent update of PHREEQE that eliminates many of the deficiencies and limitations of the original code, such as the lack of mass balance on hydrogen and oxygen, and adds new capabilities including surface-complexation, ion-exchange, one-dimensional reactive transport, and inverse modeling (Parkhurst, 1995, 1997, 1998); several of these new capabilities are discussed in later sections of this chapter.

PHRQPITZ (pronounced "freak-pitz"; Plummer et al., 1988; Plummer and Parkhurst, 1990) is a version of the PHREEQE program that incorporates Pitzer's equations for analysis of solutions with high ionic strength. As with PHREEQE, the PHRQPITZ program can compute reaction paths (forward modeling) as well as aqueous speciation. A limitation of PHRQPITZ is that specific interaction parameters must be in the data base for all elements considered, which limits analysis to the system Na-K-Ca-Mg-H-Cl-CO₃-HCO₃-CO₂-SO₄-OH-H₂O. The PHRQPITZ data base has been extended to include parameters for the subsystems Fe^{II}SO₄-H₂SO₄-H₂O (Reardon and Beckie, 1987), Al-SO₄-H₂O (Reardon, 1988), and NiSO₄-H₂SO₄-H₂O (Reardon, 1989), although some problems remain with temperature coefficients (C. Ptacek and D. Blowes, written commun., 1995).

The EQ3NR program (Wolery, 1983; Wolery et al., 1990;

Wolery, 1992b) is another speciation program in wide use by geochemists. Its origin stems from the PATHI (pronounced "path-one") program of Helgeson et al. (1970) which was the first reaction-path (forward modeling) program in geochemistry. Output from EQ3 (Wolery, 1979) and the revised EQ3NR (Wolery, 1983, 1992b) can be used as input to the EQ6 program (Wolery and Daveler, 1992), which has forward modeling capabilities discussed in a later section of this chapter. A recent version of EQ3NR (v. 7.0, Wolery, 1992a, b) includes a hybrid Newton-Raphson solving algorithm that allows equilibrium and disequilibrium calculations, and five supporting data files that allow a choice between various applications of ion association and specific-ion interaction (Pitzer's equations) for the aqueous model, over a temperature range of 0–300°C. The EQ3/6 package of programs was developed at the Lawrence Livermore National Laboratory, and is distributed by the U.S. Department of Energy. Updates (v. 7.1 in 1993 and v. 7.2b in 1995; T. Wolery, written commun., 1995) have fixed bugs identified in earlier versions, and include a data base compatible with that from SUPCRT92 (Johnson et al., 1992), a program which facilitates computation of mineral-fluid equilibria over a temperature range of 0–1000°C and a pressure range of 0–5,000 bars. EQ3NR is written in FORTRAN and runs most easily on UNIX-based mainframe computers or workstations, although an earlier version (v. 6.0) was adapted to run on an IBM-type 486-based PC (S. McCauley, A. Williams-Jones, and C. Alpers, written commun., 1991). Updated versions (v. 7.2b and v. 8) were designed to run on Pentium-based PC's (Wolery, 1994; T. Wolery, written commun., 1995).

The program SOLMNEQ (Kharaka and Barnes, 1973) was developed at the U.S. Geological Survey concurrently with WATEQ and performs similar computations, with the additional capability to compute equilibria and mass transfer for geothermal waters at elevated temperature and pressure. An update, SOLMINEQ.88 (Kharaka and other, 1988; Perkins et al., 1990) was developed jointly by the U.S. Geological Survey and the Alberta Research Council. Several features are designed for analysis of geothermal fluids and oil-field brines, including fluid geothermometers, gas mixing and unmixing, and mineral-water mass transfers, discussed in a later section of this chapter. SOLMINEQ.88 has an option to use Pitzer's equations for brines, and several organic ligands are included in the data base. SPECIATE (Nesbitt et al., 1992) is a spreadsheet-based program that uses the SOLMINEQ.88 data base to calculate the aqueous speciation of radionuclides, organics, and major elements.

SOLVEQ (Reed, 1982; Spycher and Reed, 1989a) is a speciation program able to compute mineral-gas-solution equilibria. It was developed for hydrothermal conditions, particularly with regard to deposition of ore minerals by boiling and condensing processes, but is applicable also to low-temperature conditions. As with EQ3 and EQ6, the output from SOLVEQ can be used as input to CHILLER (Reed and Spycher, 1984), a forward modeling program discussed in a later section of this chapter.

"The Geochemist's Workbench™" is a proprietary package of geochemical modeling software developed by Bethke (1992a, 1998) at the University of Illinois, Hydrogeology Program. The code "React," successor to an earlier code known as "Gt," has the capability to compute aqueous speciation as well as mass transfer (forward modeling), with an option for using a Pitzer-based aqueous model. Other programs in the package include "Act2" and "Tact," which plot various types of stability diagrams, and "Rxn," which manipulates chemical reactions. An update to program

React has added the capability to decouple redox reactions and to compute sorption equilibria. Other capabilities of the package are discussed in later sections of this chapter.

Uncertainties and limitations

The use of speciation modeling programs can provide useful information concerning the geochemistry of water samples. Provided that a complete analysis of the water is available and that errors in analytical and thermodynamic data are minimal, it may be possible to determine which minerals are likely to dissolve or to precipitate in water of a given composition. Analysis of several water samples from one field area may provide support for a hypothesis that the solubility of a certain mineral or group of minerals controls the concentrations of certain metals. However, the correctness of such an interpretation depends in large part on the knowledge and experience of the modeler, especially his/her knowledge of hydrogeochemical processes.

The application of chemical models and their computer codes is limited to a range of water compositions. Waters with high ionic strength such as brines should be modeled where possible with the specific-ion interaction (Pitzer) approach, however critical data are not yet available for certain trace elements or for Fe(III), a major constituent of many acid mine waters with pH values below 3.

Redox disequilibrium is common in acid mine waters, but is often ignored in aqueous speciation calculations. Most commonly, this is due to a lack of analytical data for individual redox-active species. Individual redox species should be measured if at all possible, and a modeling program that can handle independent couples (e.g., WATEQ4F v. 2.0 or EQ3NR, v. 7.0 or later) should be used. Otherwise, interpretations concerning the geochemistry of redox-active metals such as Fe, As, and Mn are subject to extreme uncertainty and error.

INVERSE MODELING—MASS BALANCE

Inverse modeling using the mass-balance approach is one of the most powerful tools available for identifying the processes responsible for the chemistry of surface and ground water. Inverse modeling as a general approach to problem-solving refers to a problem where final results of a process are known and it is either the initial conditions or the nature of the processes themselves that are unknown. The mass-balance approach to geochemical modeling of water-rock interactions described here is based strictly on the compositions of water and of possible reactant and product minerals. The basic goal of mass-balance modeling is to determine one (or more) set(s) of reactions that are sufficient to account for known changes in water composition caused by mineral-water interactions. If water samples are available at two or more points along a flow path, then differences in concentration of various dissolved constituents can be used to determine possible sets of water-rock reactions that may have caused the changes in chemistry.

Compositional parameters may include elements, electrons (redox state) and stable isotopes. The mass-balance approach does not depend on thermodynamics or kinetics, *per se*. However, the user must be prepared to rule out unreasonable models that are inconsistent with the thermodynamics or kinetics of hydrogeochemical processes. For example, one should use the results of

speciation modeling (as discussed in the previous section of this chapter) to ensure that one does not hypothesize dissolution of a mineral into a solution supersaturated with that mineral; conversely, one should not hypothesize the precipitation of a mineral from a solution undersaturated with respect to that mineral. With regard to kinetics, it is necessary to use caution when invoking the participation of phases with very slow rates of precipitation or dissolution under the conditions being considered. In addition, one must consider the possibility that temperature and/or pressure conditions in the middle of a flow path may differ from those at the sampling points.

Theoretical basis and input data

A pioneering application of mass-balance principles to the geochemistry of weathering was the work of Garrels and McKenzie (1967) who used spring compositions to infer the relative reaction rates and stoichiometry of silicate mineral dissolution reactions in the granitic batholith of the Sierra Nevada, California. Other workers have used chemical mass-balance methods to derive elemental fluxes and rate constants for mineral dissolution using changes in water composition along flow paths in small watersheds and in aquifers, including Pačes (1983), Velbel (1985), Kenoyer and Bowser (1992), and Rowe and Brantley (1993).

The conceptual basis for computing net mass transfer to and from an aqueous solution between two points along a flow path was elucidated by researchers in the Water Resources Division of the U.S. Geological Survey, who applied the inverse modeling approach using the computer codes BALANCE (Parkhurst et al., 1982) and NETPATH (Plummer et al., 1991, 1992; Parkhurst and Plummer, 1993). The conceptual formulation of this approach is to find solutions to the following overall reaction (Plummer et al., 1983, 1991):



The initial and final water compositions, if known, are first converted to units of molality (moles per kg H₂O). A convenient way to compute molalities is to use a speciation program. Density data for the aqueous solutions must be known or estimated so that conversion to the molality scale can be made for the mass-balance computations to follow. The density correction can be important for some mine waters, which may have density values as high as 1.36 g/cm³ (Alpers et al., 1994). An approximate density for sulfate-rich waters can be estimated using data for mixtures of sulfuric acid and water. The next step is to compute values of Δ , the difference in concentration between the two water samples, for each element or compositional parameter of interest.

Other input data needed are the stoichiometric formulas of all minerals possibly interacting with the water along the flow path. For solid phases of variable composition (i.e., solid solutions) such as certain sulfides, feldspars, micas, and other rock-forming silicates and carbonates, compositional data from electron microprobe analysis, petrography, X-ray diffraction, energy dispersive analysis, or other means can provide an advantage during inverse modeling by allowing a solid-solution composition (e.g., Na_{0.96}Ca_{0.04}Al_{1.04}Si_{2.96}O₈ for albite feldspar) to take the place of

two or more end members. If significant variation of a solid-solution composition is observed or expected in the field, then input of two distinct compositions would allow the overall average composition to be determined by weighted average of the resulting mass-transfer coefficients. Ion-exchange and stable-isotope exchange reactions may also be included. Ion exchange reactions can be specified as simple exchange reactions, such as $\text{Ca}^{2+} \leftrightarrow \text{Mg}^{2+}$, or $\text{Ca}^{2+} \leftrightarrow 2 \text{K}^+$ without regard for the substrate; for example, cation exchange taking place on either phyllosilicate interlayer sites or on ferric hydroxide surfaces would be represented by a simple exchange reaction of the same form. Another type of mass transfer for which reaction coefficients may be computed is the flux of gasses in and out of solution.

Evaporation is an important process affecting water compositions in many environments, and can be considered in mass balance computations either explicitly or implicitly. Even if the hydrogen and oxygen in water are not considered as part of the mass balance, evaporation can be modeled as mixing with a solution of pure water with a negative mass transfer coefficient.

The mass-balance computation follows a simple matrix equation of the form $\mathbf{A} \cdot \mathbf{x} = \mathbf{B}$, where \mathbf{A} is a matrix with the stoichiometric coefficients of the possible reactant and product minerals and exchange reactions, \mathbf{B} is a column vector with the Δ values for each element, and \mathbf{x} is a column vector of unknown values corresponding to coefficients for the reactions represented by each row in matrix \mathbf{A} , in units of moles of reaction per kg H_2O (Fig. 14.3). To solve this matrix equation, the number of rows in column vectors \mathbf{B} and \mathbf{x} and in matrix \mathbf{A} must be equal; this corresponds to having the same number of equations as unknowns. So, the number of reactions among solid phases and gasses that can be considered at any one time is equal to the number of known compositional parameters in the Δ column vector (\mathbf{B}). In addition to major constituents in most waters, such as Ca, Mg, Na, K, Si, Cl, HCO_3 , and SO_4 , the elements abundant in most acid mine waters such as Fe, Al, Cu, Zn, and Mn can provide useful constraints. A redox parameter, such as the parameter RS of Parkhurst et al. (1982), should be included as a way of conserving electrons in any redox reactions to be considered. Stable and radiogenic isotopes of

hydrogen (δD and tritium) and of oxygen ($\delta^{18}\text{O}$) in water as well as isotopes of dissolved constituents such as carbon ($\delta^{13}\text{C}$ and ^{14}C), nitrogen ($\delta^{15}\text{N}$), sulfur ($\delta^{34}\text{S}$), and strontium ($^{87}\text{Sr}/^{86}\text{Sr}$) can also help to constrain the mass balance (e.g., Plummer et al., 1990, 1994). A similar mass-balance formulation may be derived for mixing of two or more water compositions, in combination with other water-rock reactions.

An inverse “model” is considered to be “a subset of the selected phases (and the computed mass-transfer coefficients) that satisfies all the selected constraints” (Plummer et al., 1991). This is consistent with the distinction made earlier between the conceptual model of a system and the computer code(s) used to test it.

Interpretation of output

In general, the output from inverse modeling will consist of one or more sets of reaction coefficients for the input hypothesized water-mineral reactions. It is important to realize that, although “models” derived by the inverse method may be exact, they are usually non-unique. Depending on the nature of the hypothesized reactions, the output from an inverse modeling program may consist of reaction coefficients for the moles of minerals dissolved and (or) precipitated, moles of gases in-gassed or out-gassed, moles of ion-exchange reactions, and (or) proportions of mixed solutions. Inverse models are subject to uncertainties from analytical data and from the underlying assumption of steady-state conditions.

Given multiple mass-balance models that are consistent with the input data, the choice of the most appropriate set of reactions and reaction coefficients should be based on consideration of questions such as the following:

- 1) Are the hypothesized reactant phases present in sufficient amounts in the host material?
- 2) Are the relative reaction coefficients consistent with relative kinetics of the hypothesized reactions?
- 3) Are the results compatible with the hydrogeologic setting?
- 4) Is the system open or closed with respect to gas fluxes?

$$\begin{matrix}
 & \mathbf{A} & & \cdot & \mathbf{x} & = & \mathbf{B} \\
 \left[\begin{array}{cc}
 \text{moles Si} & \text{moles Si} \\
 \text{mole albite} & \text{mole sericite} \\
 \\
 \text{moles Al} & \text{moles Al} \\
 \text{mole albite} & \text{mole sericite} \\
 \cdot & \cdot \\
 \cdot & \cdot \\
 \cdot & \cdot
 \end{array} \right] & & & & \left[\begin{array}{c}
 \text{moles albite} \\
 \text{kg H}_2\text{O} \\
 \\
 \text{moles sericite} \\
 \text{kg H}_2\text{O} \\
 \cdot \\
 \cdot \\
 \cdot
 \end{array} \right] & & & & \left[\begin{array}{c}
 \text{moles Si} \\
 \text{kg H}_2\text{O} \\
 \\
 \text{moles Al} \\
 \text{kg H}_2\text{O} \\
 \cdot \\
 \cdot \\
 \cdot
 \end{array} \right]
 \end{matrix}$$

FIGURE 14.3—Matrix for mass-balance computations.

Available programs and their application

The program BALANCE (Parkhurst et al., 1982) was the first inverse geochemical modeling program to be applied widely to ground water problems. The original BALANCE program was limited to consideration of one combination at a time of possible reactions involving reactants and products, although the user could run multiple combinations sequentially by using an appropriately edited input file. It was also incumbent upon the BALANCE user to compute separately the saturation indices for water samples used in the modeling, so that thermodynamic constraints on mineral dissolution and precipitation were known.

The program NETPATH (Plummer et al., 1991, 1992, 1994) represents a significant enhancement of BALANCE (Fig. 14.2). The NETPATH program allows the user to consider more phases than the number of known compositional parameters by computing every possible combination of the correct number of phases. For example, if ten compositional parameters are known and there are eleven possible reactant and product minerals, then eleven different combinations of the compositional parameters will be tried, each combination leaving out one of the eleven possible reactant or product phases in turn. The user can streamline the process by indicating that certain phases should be allowed only to dissolve or precipitate, and can force the model to include certain phases in all possible solutions which can reduce considerably the number of possible combinations. Early versions of NETPATH had a companion program DB (Plummer et al., 1991) incorporating the speciation-saturation program WATEQF (Plummer et al., 1976) which can be used to compute elemental molalities for input to the mass-balance calculations and to compute saturation indices. A more recent version of NETPATH (v. 2.0, Plummer et al., 1994) includes a new speciation code, using the thermodynamic data base from PHREEQE, a subset of that from WATEQF. The revised version of NETPATH (Plummer et al., 1994) has the capability of mixing up to five waters and performing isotope mass balances and Rayleigh fractionation calculations for ^2H , ^{13}C , ^{14}C , ^{15}N , ^{18}O , ^{34}S , and ^{86}Sr . The program PHREEQC (Parkhurst, 1995) also has inverse modeling capabilities similar to those in NETPATH, v. 2.0. The most recent version of PHREEQC (v. 1.6) does not handle isotope mass balance; however, this capability is planned for later versions (v. 2.0; D. Parkhurst, written commun., 1998). Another improvement to the inverse modeling capability of PHREEQC is the consideration of analytical uncertainties (Parkhurst, 1995, 1998).

Example: Mass balance for Richmond mine water

An example follows of a relatively simple application of mass-balance modeling to a severe acid mine drainage problem. In this example, the goal of the modeling is to determine one or more sets of geochemical reactions that are responsible for the formation of a very concentrated mine water emanating from the Richmond mine at Iron Mountain, in the West Shasta mining district of northern California (Nordstrom, 1977; Alpers and Nordstrom, 1991; Alpers et al., 1992a). The composition of the mine water is given as sample AMD-D in Table 14.1; molalities were computed using the program WATEQ4F. At the Richmond mine, rainwater infiltrates through the mineralized zone, which consists of massive sulfide and stringer sulfide mineralization in an altered keratophytic (meta-dacitic) wall rock. The mine workings contain at

least 6 million tons of unmined pyritic Cu-Zn massive sulfide ore which remains above the water table, allowing ready access of oxygen by air convection and advection. The haulage level of the Richmond mine (2600 level) acts as an effective drain for the mine workings. The hydrogeologic setting is described further by Alpers et al. (1994). The concentrations of elements of interest in the initial rainwater solution are insignificant compared with those which leave the Richmond mine workings, so the water composition in Table 14.1 can be used as the Δ values.

The compositions of mineral phases likely to be dissolving and precipitating in the Richmond mine at Iron Mountain are given in Table 14.3. Compositions of chlorite, muscovite, epidote, and sphalerite determined by electron microprobe for samples from other mines in the West Shasta mining district (Reed, 1984) were used. Feldspar compositions were determined optically (Kinkel et al., 1956). The dacitic wall rock was metasomatized on the ocean floor prior to or during mineralization, so the majority of the feldspar is close to albite ($\text{Ab}_{.96}\text{An}_{.04}$) in composition. Because a range of feldspar compositions ($\text{Ab}_{1.00}$ to $\text{Ab}_{.80}\text{An}_{.20}$) was observed (Kinkel et al., 1956), sensitivity of the BALANCE model to the feldspar composition was tested, and was found to have little influence on computed reaction coefficients.

TABLE 14.3—Minerals considered in mass-balance computation for Richmond mine water.

Mineral	Formula	Source ¹
Albite	$\text{Na}_{.96}\text{Ca}_{.04}\text{Al}_{1.04}\text{Si}_{2.96}\text{O}_8$	1
Sericite	$\text{K}_{.70}\text{Na}_{.12}(\text{H}_3\text{O})_{.16}\text{Al}_{1.91}\text{Mg}_{.06}\text{Fe}_{.02}^{\text{II}}(\text{Al}_{.9}\text{Si}_{3.1})\text{O}_{10}(\text{OH})_2$	2
Kaolinite	$\text{Al}_2\text{Si}_2\text{O}_5(\text{OH})_4$	
Epidote ²	$\text{Ca}_{1.96}\text{Fe}_{.88}^{\text{II}}\text{Mg}_{.05}\text{Al}_{2.05}\text{Si}_{3.04}\text{O}_{12}(\text{OH})$	2
Chlorite	$\text{Mg}_{2.95}\text{Fe}_{.88}^{\text{II}}\text{Al}_{1.82}^{\text{Oct}}\text{Al}_{.81}^{\text{tet}}\text{Si}_{2.82}\text{O}_{10}(\text{OH})_8$	2
Quartz	SiO_2	
Calcite	CaCO_3	
Pyrite	FeS_2	
Chalcopyrite	CuFeS_2	
Sphalerite	$\text{Zn}_{.933}\text{Fe}_{.062}^{\text{II}}\text{Cu}_{.005}\text{S}$	2
Melanterite	$\text{Fe}^{\text{II}}\text{SO}_4 \cdot 7\text{H}_2\text{O}$	

¹Sources: (1) Kinkel et al. (1956); (2) Reed (1984).

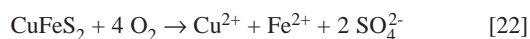
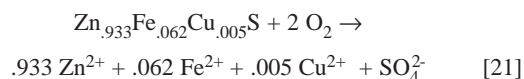
²Epidote formula included for reference only; phase not included in preferred mass-balance solution for water sample AMD-D.

Results from the mass-balance analysis for Richmond mine portal effluent, using input data from Tables 14.1 and 14.3, are shown in Table 14.4. Nearly one mole of pyrite has oxidized per kg of H_2O , along with much smaller amounts of sphalerite and chalcopyrite. The relative amounts of gangue minerals dissolved are also shown in Table 14.4; the largest contribution is from chlorite (0.013 mol/kg H_2O , equal to 7.5 g/kg H_2O), followed by sericite (0.011 moles or 4.3 g/kg H_2O) and albite (0.012 moles or 3.1 g/kg H_2O). In addition, dissolution of relatively small amounts of kaolinite (0.0063 mol/kg H_2O) and calcite (0.0047 mol/kg H_2O) is also indicated. Epidote (formula in Table 14.3) was included as a potential reactant, but no model solutions were found in which its dissolution was indicated. This result is consistent with slow kinetics of dissolution for epidote relative to the other gangue minerals considered.

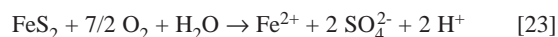
The principal reaction products indicated by the mass-balance solution are melanterite ($\text{Fe}^{\text{II}}\text{SO}_4 \cdot 7\text{H}_2\text{O}$) and amorphous silica ($\text{SiO}_2 \cdot n\text{H}_2\text{O}$). An exceptionally large amount of melanterite precipitation (0.576 moles/kg H_2O) is indicated. An earlier attempt at mass balance for the Richmond portal effluent (Alpers and Nordstrom, 1989) used goethite (FeOOH) as the secondary iron phase, which seemed reasonable at the time given the abundance of this mineral in the gossan on top of Iron Mountain (Kinkel et al., 1956). However, renovation of the Richmond mine workings by the U.S. Environmental Protection Agency as part of a Superfund remediation program during 1989–90 made it possible to observe directly the secondary iron minerals forming in the underground mine workings (Alpers and Nordstrom, 1991; Alpers et al., 1991). It was found that melanterite ($\text{Fe}^{\text{II}}\text{SO}_4 \cdot 7\text{H}_2\text{O}$) is the most abundant precipitate in areas of active mine-water flow during low-flow conditions, and that this and other Fe-sulfate minerals are likely to be dissolved during periods of high flow, including an annual flushing after the onset of the wet season (Alpers et al., 1991, 1992a, 1994). Thus, we expect that an inverse model based on water samples taken during a period of flushing would indicate dissolution of melanterite and (or) other soluble salts in contrast to the melanterite precipitation during the dry season indicated by the model shown in Table 14.4. Alpers et al. (1994) showed that melanterite formed in the Richmond mine has significant quantities of copper and zinc substituting for iron in solid solution. Although pure melanterite was used in the model shown in Table 14.4, a further refinement of the model would include a Cu-Zn-bearing melanterite as a reaction product, which would have the effect of requiring the oxidation of relatively more chalcocopyrite and sphalerite than shown in Table 14.4.

Note that water of hydration for the product phases is not considered in the mass balance because the programs BALANCE and NETPATH do not account explicitly for H or O. However, evaporative concentration can be modeled by expanding the model to include mixing with pure water in addition to the mineral dissolution and precipitation and gas flux reactions. If evaporative concentration is indicated, the pure water component will receive a negative coefficient, corresponding to the subtraction of pure water from the system.

The amount of gaseous oxygen that has combined with pyrite in the overall oxidation reaction represented by the mass-balance model in Table 14.4 can be estimated by subtracting the amount associated with oxidation of other sulfides from the total O_2 coefficient. For the purpose of this discussion it is assumed that sphalerite and chalcocopyrite have oxidized by the following overall reactions:



The corresponding amount of O_2 consumed by reactions [21] and [22] is 0.0872 moles/kg H_2O , which leaves 3.45 moles/kg H_2O associated with pyrite oxidation. Dividing 3.45 by the moles of pyrite consumed (.982) gives a molar ratio of 3.51, which is in excellent agreement with the coefficient of O_2 in the following pyrite oxidation reaction:



Given that about 90% of the dissolved iron in water sample AMD-D was Fe(II), it is assumed that the consumption of oxygen by oxidation of Fe(II) from sulfides and silicate gangue minerals is negligible. Thus, nearly all of the oxygen consumed has contributed to the oxidation of reduced sulfur (in pyrite and other sulfide minerals) to sulfate.

TABLE 14.4—Reaction coefficients for mineral dissolution and precipitation, and gas fluxes for the formation of water sample AMD-D (data in Table 14.1), based on mass-balance computations using mineral formulas in Table 14.3.

	Reaction coefficient (mol/kg H_2O)	Formula weight (g/mole)	Reactive mass (g/kg H_2O)	Percent of total reactants (wt%)
Reactants				
Pyrite	.9816	120	117.8	
Chalcocopyrite	.0051	184	0.9	
Sphalerite	.0385	96	3.7	
Total Sulfides			122.4	48
Calcite	.0047	100	0.5	
Albite	.0119	263	3.1	
Sericite	.0111	389	4.3	
Chlorite	.0132	567	7.5	
Kaolinite	.0063	258	1.6	
Total Gangue			17.0	7
O_2 gas	3.5421	32	113.3	45
Total Reactants			252.7	100
Products				
Melanterite	.5759	152 ¹	87.5	
Silica (amorphous)	.1162	60 ¹	7.0	
CO_2 gas	.0047	40	0.2	
Total Products			94.7	37
Net Total (reactants-products)			158.0	63

¹Melanterite and amorphous silica formula weights without waters of hydration; H and O not included in mass balance.

Other examples

Examples of the application of inverse modeling to regional ground-water flow systems are provided by Denver (1989) and Plummer et al. (1990), and are discussed by Parkhurst and Plummer (1993) and Parkhurst (1997). Other examples of NETPATH applications, including the incorporation of stable isotope data, are given in the user's manual (Plummer et al., 1994). An application of BALANCE and WATEQ4F to an acid mine drainage problem at an abandoned and partially reclaimed coal mine is given by Cravotta (1994). Rowe and Brantley (1993) describe the application of NETPATH to reactions between acidic ground water and fresh volcanic rocks on the flank of the Poás Volcano, Costa Rica.

FORWARD MODELING—REACTION-PATH AND REACTION-TRANSPORT MODELS

Forward models generally describe geochemical and hydrogeologic systems with sets of initial and boundary conditions and march forward either with respect to time or reaction progress, resulting in a predicted future state. As applied to geochemical systems, the progress of a chemical reaction is often used instead of time as the progress variable in the absence of quantitative information on the rates of many geochemical processes.

There is a fundamental distinction between the forward geochemical models that have a spatial component and those that do not. In this section, we first describe models without a spatial component, and refer to them collectively as “reaction-path” models. Then, the discussion turns to models with a spatial component, referred to as “reactive-transport” models. Some additional capabilities of the forward models are also discussed in this section, including the abilities to compute sorption equilibria, to consider solid-solution/aqueous-solution interactions, and to incorporate kinetic rate expressions for mineral dissolution and precipitation.

Reaction-path models

Models describing the transfer of mass and the distribution of elements between aqueous solution, solids, and gases by geochemical processes are often described as reaction-path models. The geochemical processes that are modeled include mineral dissolution and precipitation, fluid mixing, sorption, and ion exchange. The “path” refers to evolutionary changes in the composition and abundance of modeled phases, including the aqueous phase, through the course of the simulation. In most cases, it is the composition of the aqueous solution that is the frame of reference used to follow reaction progress in geochemical reaction-path models.

There are numerous examples in the geochemical literature of the application of reaction-path modeling to the genesis of hydrothermal ore deposits and accompanying wallrock alteration (e.g., Helgeson, 1970; Villas and Norton, 1977; Brimhall, 1980; Garven, 1982; Brimhall and Ghiorso, 1983; Janecky and Seyfried, 1984; Reed and Spycher, 1984; Bowers and Taylor, 1985; Spycher and Reed, 1989b; Plumlee et al., 1994, 1995) and to the formation of weathering products (e.g., Helgeson et al., 1969, 1970; Bladh, 1982). However, relatively few applications of reaction-path modeling have been made to environmental aspects of mineral deposits; contributions of this kind by Runnells et al. (1992) and by Parkhurst and Plummer (1993) are discussed later in this section.

Theoretical basis

Reaction-path models predict the results of hypothetical, irreversible water-rock-gas reactions applied to an initial solution, usually 1 kg of H₂O with known amounts of dissolved constituents. An initial analysis of aqueous speciation and mineral saturation is performed, and any supersaturated phases are either brought into equilibrium (saturation) or suppressed from the calculation if known to have slow kinetics relative to the time scale of interest (e.g., quartz at low temperature). The irreversible reaction products are then added to the initial solution in very small increments. A reaction progress variable ξ is defined most com-

monly as total moles of specific reactant(s) consumed. At each step of reaction progress, another speciation calculation is carried out, supersaturated phases are again brought to equilibrium, and the quantities of any minerals precipitated or dissolved are tallied. The reaction may be allowed to continue until either the aqueous solution comes to equilibrium with all reactants, or the reactants are consumed.

An important consideration in reaction-path modeling is whether to treat a system as open or closed. A closed-system model allows newly formed reaction products to participate as reactants and to be redissolved if the aqueous solution becomes undersaturated with respect to them at a later point of reaction progress. A variation of the closed-system model is a titration model, which can be used to simulate mineral dissolution or fluid mixing (Wolery and Daveler, 1992). In contrast, an open-system model assumes that the reaction products from each step of reaction progress are removed from contact with the aqueous solution and are not available for subsequent dissolution. A subset of open-system models is the situation where a system is in contact with a large external gas reservoir, such as would pertain to weathering at the earth's surface, in the hydrologically unsaturated zone, and in certain types of experimental conditions where gas fugacities are fixed (Delany and Wolery, 1984; Wolery and Daveler, 1992). The distinction between closed and open systems has important consequences for determining the compositional path that aqueous solutions follow during irreversible reactions. In general, fluid compositions resulting from mineral-solution reactions in a closed system follow phase boundaries on activity diagrams, whereas open systems allow solution compositions to cross activity boundaries between mineral stability, as illustrated in the following example.

Reaction-path models describing the titration of orthoclase (KAlSi₃O₈) into pure water are shown on Figure 14.4. Starting with 1 kg of pure water, the feldspar is titrated into the water a little at a time. In each increment, the additional reactant mineral is dissolved completely prior to the next reaction step, releasing the constituent cations (K⁺, Al³⁺, and Si⁴⁺) to the aqueous solution in their stoichiometric (molar) proportions within the feldspar (K:Al:Si = 1:1:3). After each increment of dissolution, the next step is to check for saturation with all mineral phases in the data base; if any phase becomes supersaturated in the newly created aqueous solution and is not suppressed in the calculation, then that phase precipitates from solution. Some examples of reaction-path calculations involving K-feldspar dissolution with quartz suppressed are shown on Figure 14.4 (from Helgeson, 1974, 1979). In an open system (path A'B'D' on Fig. 14.4), the first phase to become saturated is gibbsite, then kaolinite, and finally the solution comes to equilibrium with K-feldspar. In comparison, two closed-system models for K-feldspar dissolution yield different reaction paths (A'B'C'D' and ABCDE on Fig. 14.4), depending on initial water composition (see discussions by Helgeson, 1979, and by Parkhurst et al., 1980). Path A'B'C'D' indicates a solution composition that traverses the gibbsite field, precipitating gibbsite until reaching the kaolinite phase boundary. The aqueous solution composition then tracks along the gibbsite-kaolinite boundary, precipitating kaolinite and dissolving gibbsite, until all gibbsite is dissolved. Then, the closed-system model tracks across the kaolinite field until reaching equilibrium with K-feldspar. Path ABCDE differs from path A'B'C'D' in that a different starting composition leads to intersection of the K-mica stability field and a final stable assemblage of K-feldspar plus K-mica. In the exam-

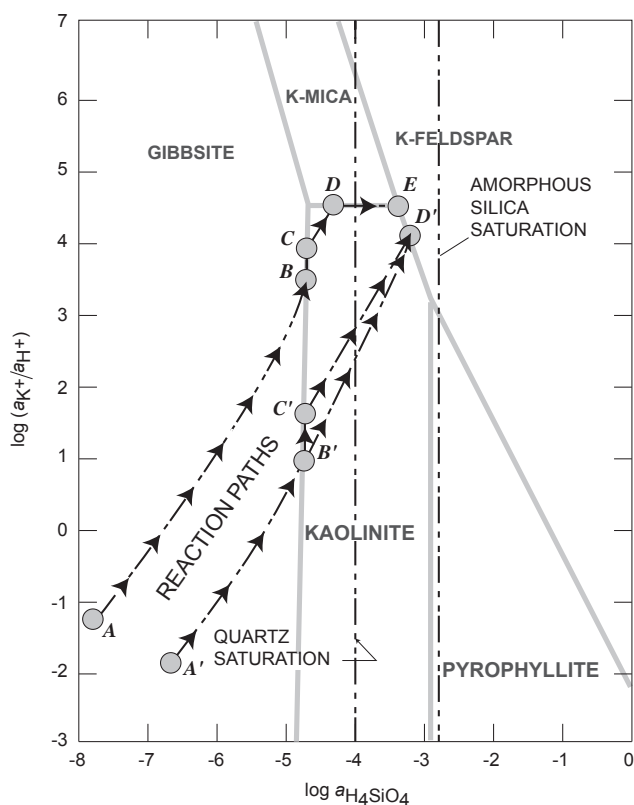


FIGURE 14.4—Equilibrium aqueous activity diagram for potassium versus silica at 25°C and 1 bar, showing a comparison of closed-system reaction paths (ABCDE and A'B'C'D') and an open-system path (A'B'D') for the dissolution of K-feldspar; after Helgeson (1974) and reproduced with permission from Manchester University Press.

ple shown on Figure 14.4, K-mica can be best thought of as a proxy for illite, hydromica or another similar phase that would be more likely to form than muscovite at the low temperature (25°C) of this simulation.

Input data and data base requirements

The necessary input data for a reaction-path model are a starting fluid composition and a set of reactants to be interacted irreversibly with that fluid. The reactants can take the form of a single mineral or gas, a group of minerals or gasses, a whole rock composition (e.g., volcanic glass), or another fluid composition. If a group of minerals is chosen, the user must define the relative kinetic rates of dissolution among these reactant phases. An arbitrary choice often made is to assume equal rates of dissolution based on volume percent, mole percent (e.g., Brimhall, 1980), or relative surface area in the reactant assemblage, however the rapidly accumulating data on low-temperature mineral dissolution kinetics (e.g., Petrovich, 1976, 1981a,b; Petrovich et al., 1976; Berner 1978, 1980, 1981; Berner and Holdren, 1979; Lasaga, 1981a,b; Aagard and Helgeson, 1982; Wood and Walther, 1983; Chou and Wollast, 1984, 1985; Wollast and Chou, 1985; Holdren

and Speyer, 1985a,b, 1986, 1987; Knauss and Wolery, 1986, 1988; Murphy and Helgeson, 1987, 1989; Murphy, 1989; Carroll-Webb and Walther, 1988; Dove and Crerar, 1990; Blum and Lasaga, 1991; Casey et al., 1991; Nagy et al., 1991; Rose, 1991; Nagy and Lasaga, 1992; Amrhein and Suarez, 1992; Murphy et al., 1992; Burch et al., 1993; Brady and Carroll, 1994; Brantley and Stillings, 1994; Oxburgh et al., 1994; Stillings and Brantley, 1995; Oelkers and Schott, 1995; White and Brantley, 1995) indicate that better approximations can and should be made for modeling weathering reactions. In using kinetic rate data from the literature it is important to realize that sample preparation techniques and fluid/mineral ratios can have a large influence on laboratory rates, and can explain in part the discrepancies of three orders of magnitude or more between rates observed in the laboratory and the field (e.g., Brantley and Velbel, 1993; Casey et al., 1993; Drever et al., 1994). Swoboda-Colberg and Drever (1993) and Velbel (1993) suggest that such discrepancies are due to physical differences involving spatially heterogeneous flow in field settings such that a small proportion of potentially available mineral surfaces actually participate in reactions with pore fluids at a given point in time.

Some of the more sophisticated reaction-path programs (e.g., CLOCK: Helgeson and Murphy, 1983; EQ6: Delany et al., 1986; Wolery and Daveler, 1992; KINDIS: Madé, 1991; Madé and Fritz, 1992) include kinetic rate laws for mineral dissolution and (or) precipitation. These expressions allow kinetic rates to change with solution composition and distance from equilibrium. Kinetic rate laws based on transition-state theory (Lasaga, 1981a,b) include terms for concentrations or activities of reactants (e.g., H^+) in the rate-limiting reaction that produce an activated complex, as well as a chemical-affinity or free-energy term (similar to the saturation index) that defines proximity to equilibrium. It is well known that mineral dissolution and precipitation reactions slow down near equilibrium, and this should be reflected in the kinetic rate expressions. In the absence of a rate expression based on transition-state theory, estimates of relative rates of mineral dissolution from experimental or field observations can also be used, providing better approximations than the relative amounts of minerals present in the starting assemblage. For most common sulfide minerals, empirical rate constants based on experimental studies are available (e.g., Wiersma and Rimstidt, 1984; McKibben and Barnes, 1986; Moses et al., 1987; Nicholson et al., 1988; Moses and Herman, 1991; Nicholson and Scharer, 1994; Rimstidt et al., 1994; see Nordstrom and Alpers, 1999). Sulfide minerals undergoing oxidation generally remain far from thermodynamic equilibrium, so it is less important to have a chemical affinity term in these rate expressions.

Data base requirements for reaction-path modeling are essentially the same as for aqueous speciation calculations, discussed previously. As with speciation modeling, the user must be diligent to use minerals and aqueous species for which data are available in the appropriate temperature range, and to use an appropriate expression for aqueous activity coefficients. For high ionic strength solutions ($I > 0.7$) it is generally recommended that a specific ion interaction (Pitzer) model be used. At least three computer programs are now available which incorporate the Pitzer equations into reaction-path modeling: EQ6 (Wolery and Daveler, 1992), PHRQPITZ (Plummer et al., 1988), and SOLMINEQ.88 (Kharaka et al., 1988). However, the Pitzer data bases are presently limited to a relatively small number of major ions, as discussed in the earlier section of this chapter on speciation modeling.

Output data and interpretation

The output from reaction-path modeling programs generally consists of predicted changes in solution composition and mineral assemblages as a function of reaction progress, including quantities of primary minerals dissolved and secondary minerals formed. If kinetic rate expressions are used, the time of reaction will also be computed.

Results from reaction-path modeling in terms of aqueous constituents and product-mineral abundances are commonly plotted as a function of reaction progress on a logarithmic scale (for example, see Brimhall, 1980; Brimhall and Ghiorso, 1983). Although results of the modeling are quantitative, interpretation in terms of comparison with field occurrences is often qualitative, and is considered successful if a certain sequence of reaction or weathering products is reproduced, with some agreement as to relative abundances of product phases. For simulation of laboratory experiments, one should demand much better agreement between a forward reaction-path model and actual observations, as the boundary conditions are much better defined, although equilibrium may be difficult to obtain depending on reaction kinetics.

A common technique used to visualize the results of such modeling is to trace the composition of the aqueous phase on activity-activity diagrams, which indicate the minerals predicted to dissolve or precipitate at different stages of the reaction path. Caution must be used with this approach, however, as two-dimensional representations can be misleading in systems with many chemical components and inspection of saturation indexes is required.

Available programs and their evolution

Figure 14.2 indicates the evolution of selected reaction-path modeling programs, and shows their relationship to other modeling programs, particularly the speciation programs with which they are intimately associated. The pioneering work on reaction-path modeling by Helgeson and coworkers (Helgeson, 1968; Helgeson et al., 1969, 1970), produced the PATHI (pronounced "path-one") program. During the 1970s, PATHI was modified by several different research groups, resulting in programs known as PATH+ and FASTPATH (not shown on Fig. 14.2).

A distinction can be made between reaction-path modeling programs in which the user must define the reaction path and those which are truly "path-finding." An example of a "user-defined" reaction-path modeling program is PHREEQE (Parkhurst et al., 1980), with which the user must indicate the stoichiometry of each phase to be dissolved or precipitated. The quantity of phases to be dissolved or precipitated with PHREEQE must also be specified, except in cases where the program is instructed to carry out sufficient reaction to reach a specified phase boundary, saturation, or supersaturation condition. In contrast, the "path-finding" modeling programs such as EQ6 (Wolery, 1979, 1992a), CHILLER (Reed and Spycher, 1984; Spycher and Reed, 1989a) and React (Bethke, 1992a, 1998) determine the identity and quantity of the phase(s) to be transferred into or out of solution by minimizing the Gibbs free energy of the system after each step of reaction progress. A useful computational tool which is available in some reaction-path modeling programs is an algorithm that automatically reverses and takes smaller progress variable steps if two or more potential product phases become supersaturated after a single increment of reaction progress.

Without this feature, one risks a situation where the computed reaction path could differ depending on the chosen step size for the progress variable, and risks violation of the phase rule. With a user-defined-path modeling program, one must manually control the step size so that only one additional phase becomes supersaturated at a time.

Applications of reaction-path modeling

Example: pyrite oxidation—An example of reaction-path modeling using the PHRQPITZ program (Plummer et al., 1988) is taken from Alpers and Nordstrom (1991), whose objective was to explore the origin of negative pH values observed in drip waters in underground mine workings of the Richmond mine at Iron Mountain (Nordstrom et al., 1991). In this example, pyrite is reacted with oxygen gas and initially pure water to yield aqueous ferrous iron, sulfate and hydrogen ions (see reaction [23]). In this simulation, all the iron remains ferrous; there is no oxidation of ferrous iron to ferric and subsequent oxidation of pyrite by ferric iron, as is thought to occur in nature. The reason for this simplification is the unavailability of Pitzer coefficients for ferric iron solutions. Results are plotted on Figure 14.5. A very small amount of reaction (0.0001 moles) is required to achieve a pH of 3.7, and a pH value of about 2 is reached after 0.01 moles of reaction, corresponding to only 1.2 grams of pyrite per kg of H₂O. Continued oxidative dissolution of pyrite leads to a pH value less than 1.0 after 0.17 moles of reaction, and finally to a pH value just below zero (-0.02) after 1.5485 moles of reaction [23], at which point the solution reaches saturation with respect to melanterite (Fe^{II}SO₄•7H₂O). The reaction continues, with essentially all of the iron going into melanterite:



A plot of pH versus the logarithm of the progress variable, in this case moles of pyrite oxidized, is shown on Figure 14.5b. The curvature on Figure 14.5b can be attributed to changes in the activity coefficient of H⁺ as the solutions become progressively non-ideal at higher sulfuric acid concentrations.

Other examples of reaction-path modeling—An example of reaction-path modeling applied to mining environments is the paper by Runnells et al. (1992), in which forward modeling was used to estimate ground-water compositions prior to mining by assuming equilibrium between water and various mineral assemblages. As stated earlier, a model is not useful if it cannot be tested. Thus, it is necessary to be able to confirm such predictions with field data for such an approach to be considered useful. However, in the absence of such data from mineralized but undisturbed areas, which are increasingly difficult to find, this sort of predictive effort can provide order-of-magnitude estimates for solubility constraints on metal compositions, provided that reasonable assumptions are used regarding the reactivity of the chosen phases.

Another example of forward modeling is the paper by Parkhurst and Plummer (1993), which used the PHREEQE model to predict *a priori* the evolution of water chemistry as an acid mine water is removed from contact with the atmosphere and migrates into the anoxic environment of a carbonate aquifer. The simulation

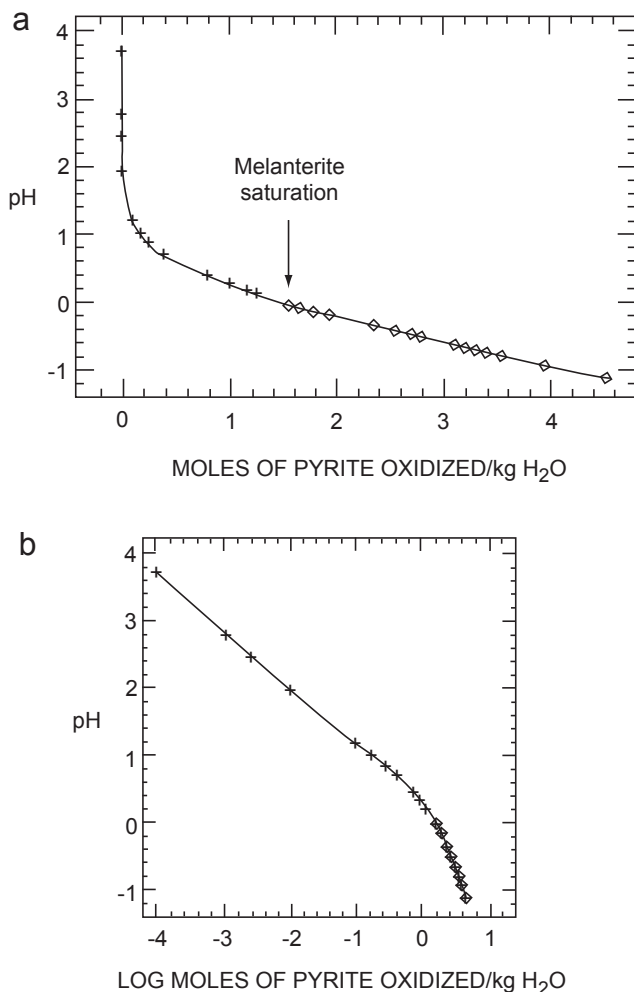


FIGURE 14.5—Forward simulation using program PHRQPITZ of pyrite oxidation, with melanterite precipitation at negative pH; from Alpers and Nordstrom (1991). (a) Linear horizontal scale; (b) Logarithmic horizontal scale, showing non-ideal solution behavior at negative pH values.

was purposely based on limited data from the Picher Pb-Zn mining area of northeastern Oklahoma and southeastern Kansas (Parkhurst, 1987; Playton et al., 1980) as a starting point for forward simulations, and was not intended to reproduce the exact chemical compositions found in those studies (Parkhurst and Plummer, 1993). Three different environments were simulated:

- 1) an oxic environment in which the mine waters were in contact with the mineralized zone (sphalerite, galena, pyrite, calcite, dolomite) and the atmosphere;
- 2) an anoxic environment in which contact with the atmosphere was cut off, but where sulfide oxidation continued with dissolved Fe^{3+} as the oxidant; and
- 3) the interaction of an anoxic mine water created in environment (2) with an unmineralized part of the carbonate aquifer (Parkhurst and Plummer, 1993).

With reaction progress from environment (1) to (3), the pH values rose from about 3 to about 6, and several minerals became supersaturated and were assumed to precipitate, in the following order:

gypsum, sphalerite, goethite, and smithsonite (ZnCO_3). The simulation was ended as the solution became saturated with dolomite, a constituent of the aquifer. As pointed out by the authors:

“...care must be taken not to over-estimate the value of these calculations. Many assumptions about equilibrium with phases and the amounts and relative rates of reactions were used to arrive at these results. Data provide the necessary information to test assumptions, but the most efficient use of that data would be to calculate saturation indices with a speciation code to determine which minerals are indeed in equilibrium and to calculate mass transfers using the mass-balance approach to determine the amounts and relative rates of reactions.” (Parkhurst and Plummer, 1993).

Reaction-path vs. mass-balance modeling

The choice of using reaction-path (forward) modeling rather than mass-balance (inverse) modeling should be based on one's objectives and the available data. If the system is sufficiently well constrained and has attained an approximate steady-state condition, and water chemistry data are available for at least two points along a flow path, then the mass-balance approach is preferred because it results in one or more exact solutions that provide possible explanations of the available data. However, many situations do not present sufficient data or knowledge of the system for this approach, or are sufficiently transient in nature that the mass-balance approach is inappropriate; in these cases the predictive, reaction-path approach can be a useful alternative. Table 14.5 provides a summary comparison between various aspects of the two approaches.

Combining reaction-path and mass-balance modeling

There are some advantages to combining the forward and inverse modeling approaches. An example is the study of the Madison aquifer in parts of Montana, South Dakota, and Wyoming (Plummer, 1985; Plummer et al., 1990; Parkhurst and Plummer, 1993), in which inverse modeling was used to determine the relative reaction rates of irreversible reactions, and then forward modeling was used to make predictions of various dissolved constituents, including dissolved Ca, Mg, inorganic C, pH, and CO_2 partial pressure. It was concluded that a relatively simple set of geochemical reactions, including dedolomitization and sulfate reduction, could explain the observed ranges in water composition and stable isotopes throughout the regional Madison aquifer system, if changes were allowed from place to place in relative rates and reaction extent (Plummer et al., 1990; Parkhurst and Plummer, 1993).

Example: Richmond Mine water

Another example combining the forward and inverse approaches is illustrated using the mass-balance example described in a previous section of this chapter for Richmond portal effluent at Iron Mountain, California. Using the results of the mass-balance calculations shown in Table 14.4, the PHREEQE program was used to simulate the formation of the mine water, starting from pure water. Rather than react all minerals at the same time, each mineral is reacted individually, so the contribution of each mineral to changes in pH and solution composition can be assessed. Results of the PHREEQE forward modeling are shown on Figure 14.6. First, the sulfide minerals are reacted with the appropriate amount of $\text{O}_{2(g)}$

TABLE 14.5—Comparison of features, inverse and forward modeling.

	Inverse modeling	Forward modeling
Theoretical basis	Mass balance, Stoichiometry, Consistency with saturation indices ensures thermodynamic reasonableness	Mass transfer, Irreversible thermodynamics
Role of kinetics	Implicit in choice of phases, No time scale	Can test assumed relative reaction rates, Computes time of reaction with rate laws, Simulates experiments
Input data (known or assumed)	Initial and final water compositions, Composition of possible reactants and products	Initial water composition only, Composition of reactants and products, Thermodynamic properties of products
Output	Proportions of reactants and products, accounting for observed changes in water chemistry along flow path	Predicts consequences of hypothesized reactions, Reaction paths
Applications	Can determine: geochemical processes in aquifers and surface waters, mixing proportions in ground waters	Designing experiments, Inaccessible systems, Ore deposit genesis, Predicts consequences of remedial alternatives

according to reaction coefficients in reactions [21], [22], and [23]. Reaction of 0.01 moles of pyrite per kg H₂O by reaction [23] results in a pH value of about 2.0; further reaction to a total of 0.1 moles results in a pH value of about 1.2. The full amount of pyrite (.982 moles) results in a pH value of about 0.5, which happens to be nearly identical to the actual pH of water sample 90WA103 (AMD-D, Tables 14.1 and 14.2). Additional reactions with sphalerite and chalcopyrite by reactions [21] and [22] have little effect on pH, as would be expected. Next, the gangue minerals are added to solution in the following arbitrary sequence: calcite, albite, sericite, chlorite, and kaolinite. As plotted on Figure 14.6, the total effect of all the gangue minerals is to raise pH by about 0.2 units, actually a large amount of neutralizing capacity given the logarithmic scale and the predicted pH value of about 0.5. Precipitation of amorphous silica has no effect on pH; the final step is precipitation of 0.576 moles of melanterite (Fe^{II}SO₄·7H₂O), which causes pH to drop by about 0.2 units because of the liberation of H⁺ ions from HSO₄⁻ and HFe^{II}SO₄⁺ aqueous complexes. The final computed pH value is 0.46, in excellent agreement with the measured value of 0.48.

The programs BALANCE and PHREEQE do not explicitly inventory moles of H and O, a deficiency corrected by PHREEQC (Parkhurst, 1995); however, in BALANCE and PHREEQE, the calculation of pH is made implicitly by charge and electron balance (Parkhurst et al., 1980, 1982). This means that the observed agreement in pH in the present example does not provide an independent confirmation of the validity of either the inverse or the forward modeling result. However it does give us some confidence in the robustness of these codes, and their ability to handle a very concentrated water composition without Pitzer parameters.

Surface chemistry models

A small, but increasing number of geochemical modeling programs have the capability to simulate the processes of adsorption and coprecipitation of inorganic aqueous species onto solid phases. A full review of the theory and application of sorption and coprecipitation modeling is beyond the scope of this chapter. The

interested reader is referred to reviews by Davis and Kent (1990) and by Dzombak and Morel (1990). The discussion in this chapter is limited to a brief summary of the capabilities and application of the modeling programs mentioned in the context of other modeling capabilities. More detail on this subject can be found in Smith (1999).

Available programs

The most widely used group of geochemical modeling programs with surface chemistry capabilities is the MINTEQ series. As indicated on Figure 14.2, and described in the earlier section on Aqueous Speciation Modeling, the original MINTEQ model-

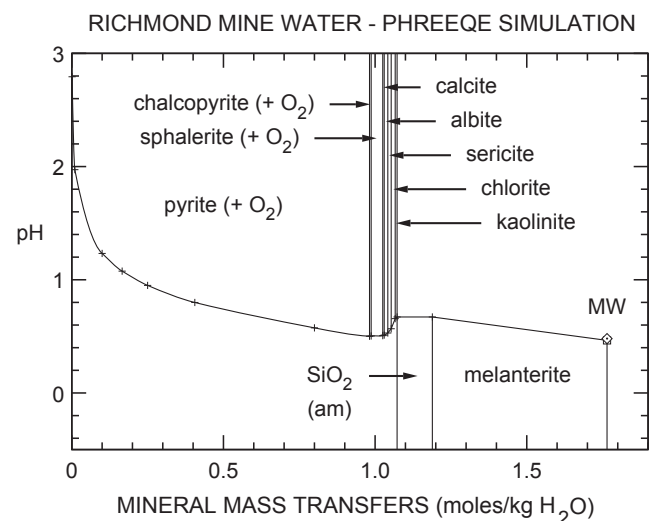


FIGURE 14.6—Forward simulation using program PHREEQE of mineral dissolution using reaction coefficients in Table 14.4; from Alpers and Nordstrom (1991).

ing program (Felmy et al., 1984) resulted from combination of the fundamental structure of the MINEQL program (Westall et al., 1976), which was in turn based on the sorption modeling capabilities of the REDEQL program of Morel and Morgan (1972), with the thermodynamic data base of WATEQ3 (Ball et al., 1981). The MINTEQA2 modeling program (Allison et al., 1991) has incorporated considerable changes from the original MINTEQ in terms of features and options available, the manner in which calculations are performed, and the thermodynamic data base.

The MINTEQA2 program has seven options regarding the modeling of surface reactions:

- 1) the activity K_d model,
- 2) the activity Langmuir model,
- 3) the activity Freundlich model,
- 4) the ion exchange model,
- 5) the constant capacitance model,
- 6) the triple-layer model, and
- 7) the diffuse-layer model (Allison et al., 1991).

The user defines surface properties for up to five minerals, each with up to two types of reactive sites. Reactions pertaining to each of the surface-reaction models are included with the aqueous speciation expressions, and the equilibrium distribution of aqueous species is determined among dissolved, sorbed, and solid phases. The surface complexes considered in the constant capacitance, diffuse-layer, and triple-layer models are analogous to complexes formed in aqueous solution, whereas the other four adsorption models neglect the electrostatic interactions of charged surfaces with solution composition (Allison et al., 1991).

Some examples of the application of MINTEQA2 to mining environments include the work of Webster et al. (1994) on transport of Zn, Cu, Fe, and As at the Leviathan mine, California, the work on arsenic sorption on ferrihydrite (Fuller et al., 1993; Waychunas et al., 1993), and the work of Stollenwerk (1994) simulating field and laboratory data on the interactions between acidic ground water and an alluvial aquifer near Globe, Arizona; see also Smith (1999).

Other geochemical modeling programs with sorption capabilities include HYDRAQL (Papelis et al., 1988), HYDRO-GEOCHEM (Yeh and Tripathi, 1989b) with its EQMOD subroutine (Siegel et al., 1992), and PHREEQC (Parkhurst, 1995), which includes a double-layer model based on Dzombak and Morel (1990) and a non-electrostatic model for surface-complexation reactions. The React program (Bethke, 1992a) has also been upgraded to include sorption modeling capabilities (Bethke, 1998).

Solid-solution/aqueous-solution modeling

There is no such thing in nature as a pure mineral. However, many phases approach a pure composition, and for the purposes of understanding the distribution of major elements in geologic systems, it is sufficient to approximate these solid phases as pure end members. For example, quartz is essentially SiO_2 , and in most applications one need not be concerned with trace amounts of Ti, Fe, Al, Li, and Na that may occur in it (Deer et al., 1966). However, there are numerous other minerals which display considerable variations in composition, and accounting for these variations can have an important effect on modeling some hydrogeochemical systems. The correct application of inverse models depends on knowledge of the possible compositions of solid phas-

es in the system, and compositional variations in minerals may correspond to significant shifts in both thermodynamic and kinetic properties, affecting the predictions of forward models. Therefore, solid solution effects have a potential impact on all types of geochemical modeling involving solid phases.

Some well known examples of minerals exhibiting a large degree of solid solution are silicates and aluminosilicates (feldspar, mica, amphibole, pyroxene, olivine), carbonates (Mg-rich calcite, ankerite, ferroan dolomite, siderite-rhodochrosite-magnesite), sulfates (e.g., barite-celestite and many others), sulfides (e.g., sphalerite), and sulfosalts (e.g., tennantite-tetrahedrite). As advances in analytical technology allow compositional information to be gathered from increasingly small volumes of material, we shall learn increasingly more about compositional variations in minerals at the microscopic and sub-microscopic scale. Thermodynamic principles for dealing with ideal and non-ideal solid solutions are relatively straightforward; however, there are large gaps in our ability to quantify non-ideality in specific binary and multi-component mineral systems, in many cases because of sparse experimental data.

Theoretical basis

Thermodynamic modeling of solid solutions among petrologists and mineralogists has focused on quantitative descriptions of departures from ideality. An ideal solution, whether gas, liquid, or solid, is one in which the different molecular species do not interact. Another way to express this is to say that an ideal solution obeys Raoult's law for all compositions (see Nordstrom and Munoz, 1994). The fundamental relationship of concentration to activity for solid phases can be expressed as:

$$a_i = X_i \cdot \lambda_i \quad [25]$$

where a_i represents the activity of the i^{th} component, X_i signifies the mole fraction of that component in the mineral, and λ_i is the rational activity coefficient. The partial molal Gibbs free energy, or chemical potential, of an ideal solid solution can be expressed as (Nordstrom and Munoz, 1994):

$$\bar{G}_{\text{ideal}} = \sum X_i \mu_i^0 + RT \sum X_i \ln X_i, \quad [26]$$

where μ_i^0 is the standard state chemical potential of the i^{th} component and the bar over G signifies a partial molal property. In non-ideal ("real") solutions, the departure from ideality, or excess Gibbs free energy is defined as $\bar{G}_{\text{excess}} = \bar{G}_{\text{real}} - \bar{G}_{\text{ideal}}$. The non-ideal component of the chemical potential is $\bar{G}_{\text{excess}} = RT \sum X_i \ln \lambda_i$, also known as \bar{G}^{XS} . The total free energy of the system can be expressed as the sum of the chemical potentials of all components in the system multiplied by their respective mole fractions, giving:

$$\bar{G}_{\text{real}} = \bar{G}_{\text{ideal}} + \bar{G}_{\text{excess}}$$

$$\bar{G}_{\text{real}} = \sum X_i \mu_i = \sum X_i \mu_i^0 + RT \sum X_i \ln X_i + RT \sum X_i \ln \lambda_i \quad [27]$$

Several chemical models have been developed to compute solid-phase activity coefficients for binary and ternary mineral systems. Margules-type formulations (Thompson, 1967; Mukhopadhyay et al., 1993) have been used extensively in the petrologic literature. Within the context of ideal site-mixing, vacancies can be considered, as has been done for zeolites (Viani and Bruton, 1992). Other models for binary solutions include the regular solution model (Saxena, 1973, p. 11–12), the third-order Maclaurin model (Helgeson et al., 1970), the cubic Maclaurin model (Saxena, 1973, p. 16) and the Guggenheim polynomial model (Saxena, 1973, p. 14–15). All of the above solid-solution models are programmed in a general form into the EQ3/6 software package (Daveler and Wolery, 1992), which allows the user to select the appropriate model for any minerals for which the user provides appropriate fit parameters; a limited number of fit parameters, mostly for the ideal site-mixing model, are distributed with EQ3/6 (Daveler and Wolery, 1992).

A convenient formulation for solid-solution activity coefficients is the truncated Guggenheim series (sub-regular model) for the excess Gibbs free energy of mixing (Glynn, 1990):

$$\ln \lambda_1 = X_{1,i}^2 [a_0 - a_1(3X_i - X_{1,i}) + \dots] \quad [28]$$

Equation [28] can be used to fit values of λ_1 from solubility data for solid solutions. Glynn (1990) has compiled available mixing data for binary sulfate and carbonate mineral solid solutions at 25°C in terms of values for the fit parameters a_0 and a_1 . These data can be used for predictive modeling of mineral compositions likely to form from aqueous solutions of variable composition.

The literature on non-ideal mixing in silicate minerals formed at high temperatures is voluminous (e.g., reviews by Ghiorso, 1987; Ganguly and Saxena, 1987). However, these data generally involve phases that form at elevated temperature and pressure, and are not particularly relevant to geochemical modeling at surficial temperatures. Only phases that are likely to form at low temperatures (i.e., less than 100°C) are likely to play an important role in controlling the composition of non-hydrothermal solutions. Nevertheless, an understanding of solid-solution compositions among these minerals is of importance for the reasons stated above, i.e., proper use of mass-balance models and proper application of kinetic data for mineral dissolution and precipitation.

Available programs: Evolution and application

Glynn (1990, 1991b) developed the program MBSSAS to facilitate modeling of solid-solution/aqueous-solution interactions. This program allows the user to predict the thermodynamically stable composition of both solid and aqueous phases during hypothetical dissolution and precipitation reactions. In addition, MBSSAS can be used to construct phase diagrams and to calculate the stable intermediate compositions (i.e., miscibility and spinodal gaps) for binary series that are not stable at all compositions (Glynn, 1991b). Comparisons of modeling predictions with data generated from laboratory studies (Glynn and Reardon, 1990; Glynn et al., 1990) have shown that a non-equilibrium aqueous composition known as “stoichiometric saturation” is approached during the dissolution of relatively insoluble solid solutions that behave as single-component solids of invariant composition. For example, Mg-calcite, Sr-aragonite, and (Ba,Sr)SO₄ rarely achieve

thermodynamic equilibrium with the contacting aqueous solution in an observable time frame because of slow rates of solid diffusion and solid recrystallization kinetics. In contrast, thermodynamic equilibrium between the aqueous and solid phases is approached for more soluble solid solutions such as alkali halides (Glynn, 1991b).

Glynn and Parkhurst (1992) modified the PHREEQE reaction-path program to include solid-solution thermodynamics for any binary solid solution series. The resulting program allows the user to predict the composition of a solid solution forming in thermodynamic equilibrium with a given water composition, which itself may be evolving during reaction progress. Similar capabilities for prediction of the solid-solution composition of reaction products were incorporated into the EQ3/6 software package (Bourcier, 1986). A more recent version of EQ3/6 (Wolery, 1992a) gives the user a choice of several formulations to describe G^{XS} , as described earlier in this section.

In general, the application of solid-solution modeling to mining environments has been quite limited, however there are certain environments where the formation and dissolution of phases with variable composition can have important effects on water chemistry. For example, Alpers et al. (1994) have described a setting where the formation and dissolution of Zn-Cu-bearing melanterite [(Fe^{II},Zn,Cu)SO₄•7H₂O] appears to influence seasonal variations in the Zn/Cu ratio in effluent from an underground mine.

Another group of minerals, common in mining environments, that exhibits extensive solid solution is the alunite-jarosite group (Scott, 1987; Stoffregen and Alpers, 1987, 1992). The jarosite formula can be written as [K_xNa_y(H₃O)_{1-x-y}]₃Fe^{III}(SO₄)₂(OH)₆. The mole fraction of hydronium (H₃O⁺) commonly ranges from 10 to 20% in jarosites formed at temperatures below 100°C (Kubisz, 1970; Ripmeester et al., 1986; Alpers et al., 1992b). Alpers et al. (1989) showed that the solubility of jarosite solid solutions with about 20 mole percent hydronium are consistent with an ideal solid solution between K and H₃O components. A value for the solubility product of jarosite solid solution with the composition [K_{0.77}Na_{0.03}(H₃O)_{0.20}]₃Fe^{III}(SO₄)₂(OH)₆ has been incorporated in the data base for WATEQ4F (Ball and Nordstrom, 1991); the saturation index for this phase should be evaluated along with that of the end members when dealing with mine waters for which data are available for Fe(II) and Fe(total). If jarosite is thought to be actively forming or recently formed, then the composition of the solid solution should be determined using chemical or X-ray diffraction methods (e.g., Alpers et al., 1992b) and a solubility product for the appropriate composition should be computed for comparison with the aqueous data. Use of the appropriate solid-solution composition can in some cases explain apparent supersaturation of water samples with respect to end-member compositions, where the solid solution represents the thermodynamically stable phase (e.g., Baron and Palmer, 1996).

Reaction-transport models

The coupling of hydrologic models with geochemical models results in models referred to as reaction-transport models. These models are fundamentally different than reaction-path models because they have a spatial component. The phenomena which can be simulated by reaction-transport modeling include advective

tion (the physical transport of fluid), molecular diffusion (the movement of dissolved species in response to concentration gradients), dispersion (the physical spreading of solutes caused by tortuous flow paths), decay (radioactive and biological), ion exchange, adsorption, oxidation-reduction, and mineral dissolution-precipitation. Space limitations preclude discussions of the theoretical basis of hydrologic transport modeling or the various strategies employed for improving the efficiency of numerical computation. The interested reader is referred to reviews and discussions by Rubin (1983), Cederberg (1985), Cederberg et al. (1985), Lichtner (1985), Yeh and Tripathi (1989a), Bahr (1990), Mangold and Tsang (1991), Apps (1992), and Dzombak and Ali (1993). The focus of this section is to describe the evolution of several reaction-transport modeling programs that are in current use and to discuss recent applications of this modeling approach to mining environments.

Available programs—their evolution and application

In several cases, existing geochemical models have been coupled explicitly with existing hydrologic models, resulting in a reaction-transport model. The mechanics of this coupling can be as straightforward as the calling of the chemical modeling program as a subroutine from the hydrologic program for each time increment and for each spatial node or element of the model. An example of this “brute force” method of coupling is the program DYNAMIX (Narasimhan et al., 1986; Liu, 1988; Liu and Narasimhan, 1989a,b), which coupled the saturated-unsaturated flow program TRUMP (Edwards, 1972) with the reaction-path program PHREEQE (Parkhurst et al., 1980). Many geochemical transport models, including TRUMP and DYNAMIX, take advantage of the fact that chemical transport and heat transport are described by equations of the same form (Narasimhan et al., 1986).

The evolution of selected reaction-transport modeling programs is outlined on Figure 14.7. An earlier attempt at explicit coupling involving the TRUMP and EQ3/6 programs resulted in the METASOM program (Cunningham, 1984; Ague and Brimhall, 1989). Both DYNAMIX and METASOM have been applied (Liu, 1988; Ague and Brimhall, 1989) to the problem of one-dimensional (vertical) transport and enrichment of copper in supergene weathering profiles, a setting which is similar to sulfide weathering in mining wastes. Another application of DYNAMIX to mining environments include a pseudo-three-dimensional model of ground-water contamination from a pyritic uranium mill tailings pile in Riverton, Wyoming (Narasimhan et al., 1986). DYNAMIX was also applied to selenium contamination at Kesterson Reservoir, California (Liu, 1988).

An approach to reaction-transport modeling based on the quasi-stationary-state approximation (Lichtner, 1985, 1988, 1992, 1993, 1994) has computational advantages over the explicit coupling techniques described earlier. Lichtner's approach makes use of the observation that most elements are much more concentrated in solid minerals than in the aqueous solution, which facilitates the solution of reaction-transport equations over geologic time spans. For very long time spans, Lichtner (1993) has shown that reaction-transport equations describing advection, diffusion, and dispersion approach asymptotically the pure advective local-equilibrium limit. The program MPATH (Lichtner, 1988, 1993) is based on the idea of multiple reaction paths, in which each reac-

tion path corresponds to a stationary state. Lichtner has applied MPATH to the problems of bauxite and laterite formation (Lichtner, 1988; Lichtner and Waber, 1992), uranium transport at a site that represents a natural analogue to a high-level nuclear waste depository (Lichtner and Waber, 1992), and supergene copper enrichment (Lichtner and Biino, 1992; Lichtner, 1994). This modeling approach was developed to simulate the geochemical evolution of weathering profiles over geologic time spans, rather than to determine geochemical processes in active weathering environments.

Two other reaction-transport modeling programs which make use of the PHREEQE program are PHREEQM (Appelo and Willemssen, 1987; Appelo et al., 1990, 1992; Appelo and Postma, 1993) and MST1D (Engesgaard, 1989; Engesgaard and Kipp, 1992). The PHREEQM modeling program uses a mixing cell approach, where the processes of advection and dispersion are simulated separately. In the PHREEQM code, advection is simulated by transferring water from one cell volume to the next at each time step. Ground-water velocity in the model is determined by an appropriate choice of cell size and time step. Dispersion and molecular diffusion are simulated by mixing the contents of adjacent cells at each time step, with chemical equilibration computed by the PHREEQE code between advection and dispersion steps (Appelo and Postma, 1993). In contrast, the MST1D code, which was developed by combining aspects of the three-dimensional transport program HST3D (Kipp, 1987) with PHREEQE, solves the transport equations (by a finite-difference approximation) without decoupling advection and dispersion, and iterates sequentially between the solution of the partial-differential transport equations and that of the algebraic chemical-reaction equations in the PHREEQE geochemical code. Glynn et al. (1991) compared the application of PHREEQM and MST1D to one-dimensional transport of acid mine drainage in an alluvial aquifer at Pinal Creek, a contaminant study site in the Globe-Miami mining district of Arizona.

Two other relatively new programs, MINTRAN and OTEQ, have coupled the MINTEQA2 program (Allison et al., 1991) to physically based flow models. The MINTRAN program (Walter et al., 1994a,b) resulted from coupling MINTEQA2 with PLUME2D, a two-dimensional flow model (Frind et al., 1990), for application to multicomponent reactive transport in ground water at mill-tailings environments. Frind and Molson (1994) describe the application of MINTRAN to a generic tailings impoundment with similarities to the Nordic deposit near Elliot Lake, Ontario, expanding on the work of Morin et al. (1988a,b) and Morin and Cherry (1988). The oxidation of pyrite and the diffusion of oxygen in waste dumps described in an algorithm by Davis et al. (1986) provided the basis for the numerical model PYROX (Wunderly et al., 1995, 1996). PYROX and MINTRAN have been coupled to produce the program MINTOX (Wunderly et al., 1995, 1996), a three-dimensional reaction-transport program that can be used to simulate pyrite oxidation, gas diffusion, and the formation of oxidation products in mining waste environments.

The OTEQ program (Runkel et al., 1996) combines one-dimensional in-stream solute transport with stream-bank storage from program OTIS (Runkel and Broshears, 1991) with MINTEQA2, resulting in a coupled reaction-transport code that can simulate redox chemistry and sorption processes. The OTEQ program has been applied to the simulation of solute transport during a pH-modification experiment in a stream affected by

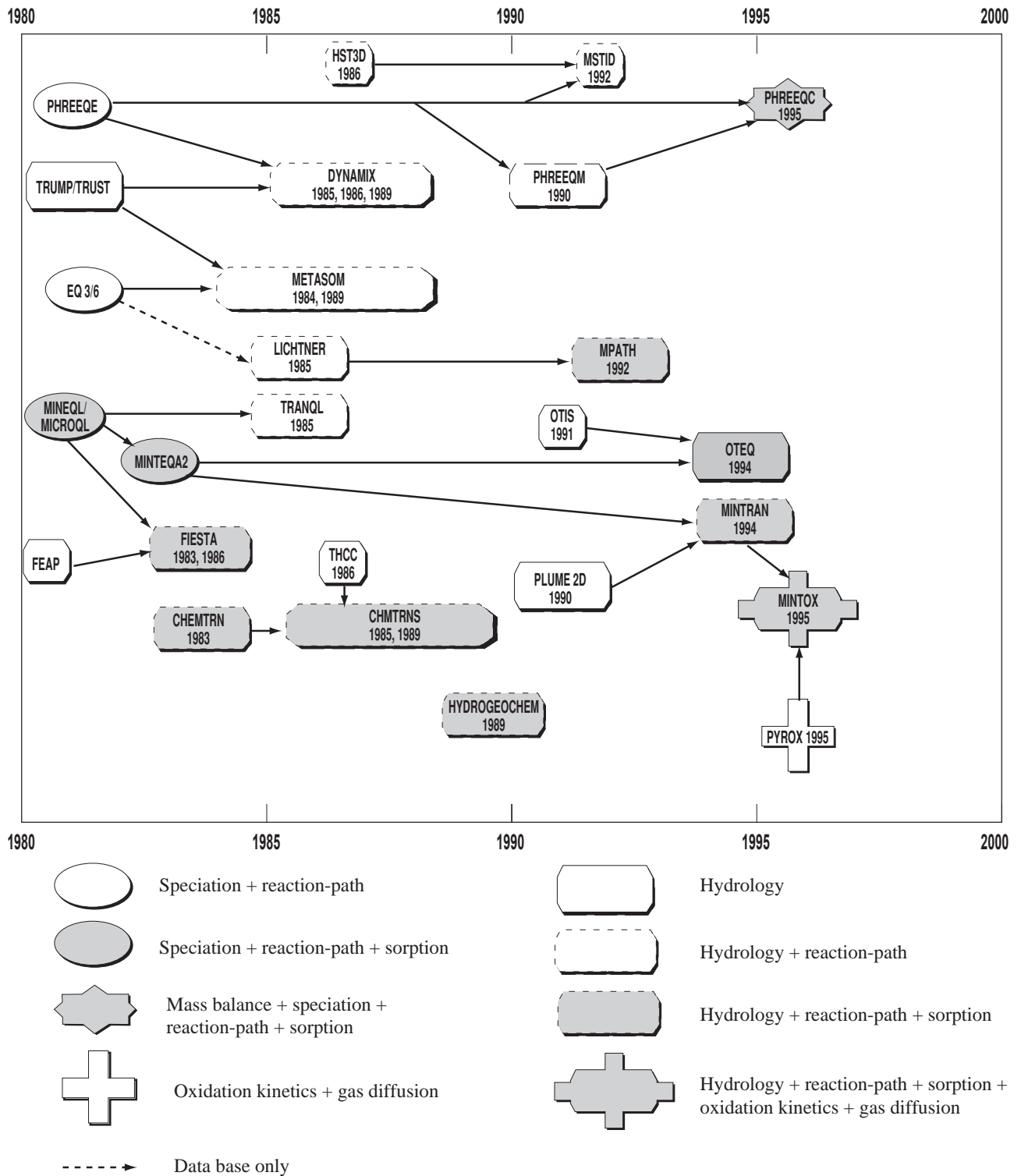


FIGURE 14.7—Evolution of selected coupled chemical-hydrologic modeling programs.

acid mine drainage in Colorado (Broshears et al., 1994, 1996; Kimball et al., 1994).

Other coupled chemical-hydrologic modeling programs include CHEMTRN (Miller and Benson, 1983), TRANQL (Cederberg, 1985), THCC (Carnahan, 1986), CHMTRNS (Noorishad et al., 1987), HYDROGEOCHEM (Yeh and Tripathi, 1989b) (Fig. 14.7). A comparison of features of these and other reaction-transport models was provided by Mangold and Tsang (1991).

Reaction-transport modeling is a rapidly evolving field of study, and the present review is far from complete. Many of the existing reaction-transport models are prone to problems with numerical dispersion and failure to converge, especially when modeling redox-sensitive reactions and sharp-front transport problems, which are poorly suited to finite-element and finite-difference approximations. Accordingly, the user should exercise considerable caution in the selection and application of existing reaction-transport programs for geochemical modeling, or in the development of new modeling programs.

UNCERTAINTIES AND LIMITATIONS OF GEOCHEMICAL MODELING

It is important to emphasize the critical assumptions that go into geochemical modeling, because careless application may lead to erroneous results and unreasonable models. For example, a central assumption in applying inverse modeling to ground-water compositions is that both initial and final water samples are along a single flow path. The best way to be assured of this would be to conduct a tracer injection test in which 100% of the tracer is recovered from the "final" well; however, this is not always practical because of limitations of budget and hydrogeologic settings. In the absence of such information, one must consider the apparent success of a mass-balance model to be qualitative or semi-quantitative at best, despite its exactness.

Another critical assumption with inverse modeling is that the chemistry of the system being modeled is in a steady-state condition. Transient behavior of either flow or chemistry, if not recognized, can cause erroneous results in mass-balance modeling. Consider, for example, a pyritic tailings impoundment overlying an permeable alluvial aquifer, with two monitoring wells (A and B) placed as shown on Figure 14.8. Depending on the hydrologic boundary conditions and in particular on the fluctuations of the water table, the flux rate of sulfide oxidation products to the ground water may vary considerably with time. For a constant water-table elevation, one might expect the fluxes to decrease with time exponentially as the reactant sulfides are consumed (Davis and Ritchie, 1986; Blowes, 1990). Therefore, if one were to attempt to use inverse modeling to derive the water-rock reactions affecting the ground-water composition between wells A and B, one must first determine that steady-state chemical conditions have been established. The transient nature of contaminant plumes and the other processes affecting hydrochemical transport (e.g., dispersion, diffusion) that are not considered in the mass-balance approach make the application of inverse modeling to this type of setting problematic. However, the mass-balance approach should be applicable in some special cases of this type of setting. For example a relatively permeable aquifer from which data are available over a long period of time could be shown to be in steady-state chemical condition if the travel time between sam-

pling points is short relative to the period for which data are available.

It must also be stressed that reactions hypothesized in mass-balance models must be feasible, both thermodynamically and kinetically. Thermodynamic feasibility can be established with saturation indices, by ensuring that only phases that are saturated or supersaturated are allowed to precipitate, and that only phases that are undersaturated are allowed to dissolve. It is also up to the user to determine independently whether or not there are any kinetic barriers to hypothesized reactions, including mineral precipitation and dissolution, ion exchange, and isotope exchange. Wherever possible, mass-balance modeling should be accompanied by detailed mineralogical and geochemical characterization of aquifer material.

Knowledge of the flow system and the effects of sampling on the system are important with regard to interpreting the chemistry of ground-water samples and using this type of data to determine boundary conditions for geochemical models, both inverse and forward. In some heterogeneous systems, especially fractured-rock aquifers, drilling and sampling cause drastic disruption of the natural flow system. Extensive well purging is often carried out with pumping rates substantially higher than natural flow rates, and the water sampled may represent water from the most hydraulically conductive zones or fractures and may not represent the bulk of water actually resident in the system before sampling.

Many of the limitations and uncertainties described with regard to inverse modeling also pertain to forward modeling. Assumptions are often made as to what are the reactive minerals, which minerals reach equilibrium and which do not, and what the relative reaction rates are. Detailed mineralogical characterization can provide valuable constraints on forward modeling (e.g., Lichtner and Waber, 1992), but even the most sophisticated of the models presently available will only approximate the complexity of the natural system. Forward modeling, by its very nature, puts much more responsibility on the user to make appropriate choices with regard to phases, components, and reaction equilibria. The major constraints on the usefulness and accuracy of the model come from the user's knowledge of hydrogeochemical processes.

Another important limitation, emphasized by Bethke (1992b), is that geochemical computations may be non-unique in the sense that a particular geochemical condition may be achieved by more than one possible equilibrium system. Computations that appear to be adequately specified may still contain ambiguities leading to non-unique solutions that are not obvious from code outputs. Also, models can be correct for incorrect reasons, i.e., two "wrongs" can sometimes appear to make a "right." Although a geochemical model may be based on sound principles, its application to real systems will usually result in large uncertainties because the real systems can only rarely be characterized in sufficient detail for the critical hydrogeochemical processes to be completely understood.

All of these limitations to geochemical modeling can be reduced to two main sources of uncertainty: (a) the input data (thermodynamic data, kinetic data, water compositions, mineral compositions, surface areas) and (b) the user's knowledge of hydrogeochemical processes, both in general and with specific reference to the real system being modeled. Future research in three areas will help to reduce these uncertainties. The first is to conduct basic research on thermodynamic, electrolyte, and kinetic properties of relevant geochemical substances and processes. The second is to carry out more research on applying the inverse

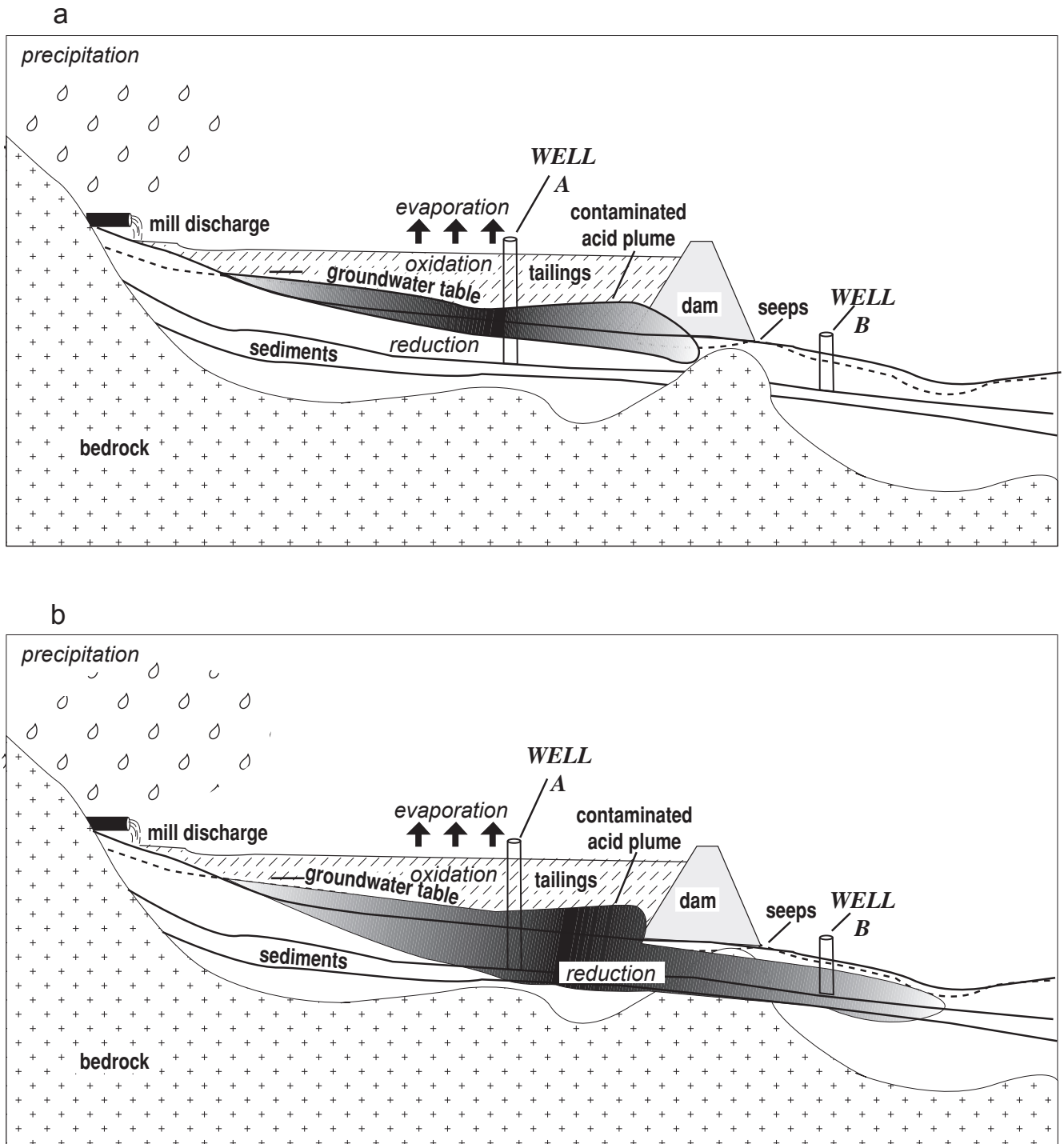


FIGURE 14.8—Schematic cross-section through a tailings impoundment at two points in time showing the evolution of a contaminant acid plume, to illustrate pitfalls of inverse modeling in transient systems.

modeling approach to water-rock interactions. The third is to apply systematic sensitivity analyses to modeling computations.

CONCLUSIONS

If used with proper caution and care, geochemical models can be powerful tools for interpreting the processes that affect water quality. However, as with any tool, the potential for misuse is high and it is the responsibility of the user to bring to each modeling application an adequate knowledge of the thermodynamic and kinetic behavior of phases to be modeled, as well as an appreciation of uncertainties in the input data.

Assumptions made in the construction of geochemical models must always be clear to users and clearly stated to readers of published results. For example, significant errors may result from the use of models that assume fully coupled aqueous redox conditions at low temperatures, where redox equilibrium is seldom attained. Anticipated improvements in modeling capabilities include the incorporation and quantification of redox disequilibrium (decoupled systems).

Inverse modeling of hydrochemical systems should be done where the data allow it; then forward modeling can be used to extend the analysis to parts of time and space where constraints are not available, i.e., to fill in the gaps. The inverse modeling is thus a type of calibration; if done properly, complementary forward modeling could provide a prediction of the inverse model's implications, which could be tested should more data become available.

There are numerous examples in the literature of the successful application of geochemical models to mining environments, several of which are mentioned and described in this chapter. Existing computer programs should be adequate for most mine drainage problems involving ground and surface waters. The aqueous models based on ion association (extended Debye-Hückel expressions) are adequate for mine waters with ionic strength less than about 1.0 for the speciated solution. The application of geochemical models to the formation of efflorescent sulfate salts from highly concentrated sulfate brines with ionic strengths greater than 1.0 is limited by the lack of specific-ion-interaction (Pitzer) parameters for Al, Fe(III), Cu, Zn, SO_4 and other constituents reaching high concentrations in some acid mine waters. However, the existing inverse and forward modeling programs are adequate for modeling the dissolution of such salts, allowing determination of their effects on water quality in various environments.

REFERENCES

- Aagard, P. and Helgeson, H.C., 1982, Thermodynamic and kinetic constraints on reaction rates among minerals and aqueous solutions, I. Theoretical considerations: *American Journal of Science*, v. 282, pp. 237–285.
- Ague, J.J., and Brimhall, G.H., 1989, Geochemical modeling of steady state fluid flow and chemical reaction during supergene enrichment of porphyry copper deposits: *Economic Geology*, v. 84, pp. 506–528.
- Allison, J.D., Brown, D.S., and Novo-Gradac, K.J., 1991, MINTEQA2/PRODEFA2, A geochemical assessment model for environmental systems: Version 3.0 user's manual, EPA/600/3–91/021, U.S. Environmental Protection Agency, Environ. Res. Lab., Athens, Ga.
- Alpers, C.N., and Nordstrom, D.K., 1989, Stoichiometry of mineral reactions from mass balance computations of acid mine waters, Iron Mountain, California; *in* Gadsby, J.W., Malick, J.A., and Day, S.J. (eds.), *Acid Mine Drainage—Designing for Closure*: BiTech Publishers Ltd., Vancouver, British Columbia, pp. 23–33.
- Alpers, C.N., and Nordstrom, D.K., 1991, Evolution of extremely acid mine waters at Iron Mountain, California—Are there any lower limits to pH?; *in* Proceedings, 2nd Internat Conference on the Abatement of Acidic Drainage, MEND (Mine Environment Neutral Drainage): Ottawa, Canada, v. 2, pp. 321–342.
- Alpers, C.N., Nordstrom, D.K., and Ball, J.W., 1989, Solubility of jarosite solid solutions precipitated from acid mine waters, Iron Mountain, California, U.S.A.: *Sciences Géologiques Bulletin*, v. 42, pp. 281–298.
- Alpers, C.N., Maenz, C., Nordstrom, D.K., Erd, R.C., and Thompson, J.M., 1991, Storage of metals and acidity by iron-sulfate minerals associated with extremely acidic mine waters, Iron Mountain, California [abs.]: *Geological Society of America, Abstracts with Programs*, v. 23, no. 5, p. A382.
- Alpers, C.N., Nordstrom, D.K., and Burchard, J.M., 1992a, Compilation and interpretation of water-quality and discharge data for acidic mine waters at Iron Mountain, Shasta County, California, 1940–1991: *U.S. Geological Survey Water-Resources Investigations Report 91–4160*, 173 pp.
- Alpers, C.N., Rye, R.O., Nordstrom, D.K., White, L.D., and King, B-Shia, 1992b, Chemical, crystallographic, and isotopic properties of alunite and jarosite from acid hypersaline Australian lakes: *Chemical Geology*, v. 96, p. 203–226.
- Alpers, C.N., Nordstrom, D.K., and Thompson, J.M., 1994, Seasonal variations of Zn/Cu ratios in acid mine water from Iron Mountain, California; *in* Alpers, C.N., and Blowes, D.W. (eds.), *Environmental Geochemistry of Sulfide Oxidation*: ACS Symposium Series 550, American Chemical Society, Washington, D.C., pp. 324–344.
- Amrhein, C., and Suarez, D.L., 1992, Some factors affecting the dissolution kinetics of anorthite at 25°C: *Geochimica et Cosmochimica Acta*, v. 56, pp. 1815–1826.
- Appelo, C.A.J., and Postma, D., 1993, *Geochemistry, groundwater, and pollution*: A. A. Balkema, Rotterdam, 536 pp.
- Appelo, C.A.J., and Willemsen, A., 1987, Geochemical calculations and observations on salt water intrusion, I. A combined geochemical mixing cell model: *Journal of Hydrology*, v. 94, pp. 313–330.
- Appelo, C.A.J., Willemsen, A., Beekman, H.E., and Griffioen, J., 1990, Geochemical calculations and observations on salt water intrusions, II. Validation of a geochemical transport model with column experiments: *Journal of Hydrology*, v. 120, pp. 225–250.
- Appelo, C.A.J., Nienhuis, P.R., and Willemsen, A., 1992, PHREEQM—PHREEQE in a mixing cell flowtube; *in* Kharaka, Y.K., and Maest, A.S. (eds.), *Water-Rock Interaction: Proceedings of the 7th International Symposium on Water-Rock Interaction*, A.A. Balkema, Brookfield, Vt., v. 1, pp. 201–204.
- Apps, J.A., 1992, Current geochemical models to predict the fate of hazardous wastes in the injection cones of deep disposal wells: Report LBL–26007, Lawrence Berkeley Laboratory, Berkeley, Calif., 140 pp.
- Bahr, J.M., 1990, Kinetically influenced terms for solute transport affected by heterogeneous and homogeneous classical reactions: *Water Resources Research*, v. 26, pp. 21–34.
- Ball, J.W., and Nordstrom, D.K., 1989, Final revised analyses of major and trace elements from acid mine waters in the Leviathan Mine drainage basin, California and Nevada—October 1981 to October 1982: *U.S. Geological Survey Water-Resources Investigations Report*, 89–4138, 46 pp.
- Ball, J.W., and Nordstrom, D.K., 1991, User's Manual for WATEQ4F, with revised thermodynamic data base and test cases for calculating speciation of major, trace, and redox elements in natural waters: *U.S. Geological Survey Open-File Report 91–183*, 189 pp.
- Ball, J.W., Jenne, E.A., and Nordstrom, D.K., 1979, WATEQ2—A computerized chemical model for trace and major element speciation and mineral equilibria of natural waters; *in* Jenne, E.A. (ed.), *Chemical Modeling in Aqueous Systems*, ACS Symposium Series 93, American Chemical Society: Washington, D.C., pp. 815–835.
- Ball, J.W., Nordstrom, D.K., and Jenne, E.A., 1980, Additional and

- revised thermodynamic data and computer code for WATEQ2—A computerized chemical model for trace and major element speciation and mineral equilibria of natural waters: U.S. Geological Survey Water-Resources Investigations Report, 78–116, 109 pp.
- Ball, J.W., Jenne, E.A., and Cantrell, M.W., 1981, WATEQ3—A geochemical model with uranium added: U.S. Geological Survey Open-File Report 81–1183, 81 pp.
- Ball, J.W., Nordstrom, D.K., and Zachmann, D.W., 1987, WATEQ4F—A personal computer FORTRAN translation of the geochemical model WATEQ2 with revised data base: U.S. Geological Survey Open-File Report 87–50, 108 pp.
- Baron, D., and Palmer, C.D., 1996, Solubility of jarosite at 4–35°C: *Geochimica et Cosmochimica Acta*, v. 60, pp. 185–195.
- Bassett, R.L., and Melchior, D.C., 1990, Chemical modeling of aqueous systems—An overview; *in* Melchior, D.C., and Bassett, R.L. (eds.), *Chemical Modeling of Aqueous Systems II: ACS Symposium Series 416*, American Chemical Society, Washington, D.C., pp. 1–14.
- Berner, R.A., 1978, Rate control of mineral dissolution under earth surface conditions: *American Journal of Science*, v. 278, pp. 1235–1252.
- Berner, R.A., 1980, Dissolution of pyroxenes and amphiboles during weathering: *Science*, v. 207, pp. 1205–1206.
- Berner, R.A., 1981, Kinetics of weathering and diagenesis; *in* Lasaga, A.C., and Kirkpatrick, R.J. (eds.), *Kinetics of Geochemical Processes: Reviews in Mineralogy*, Mineralogical Society of America, Washington, D.C., v. 8, pp. 111–134.
- Berner, R.A., and Holdren, G.R., Jr., 1979, Mechanism of feldspar weathering. II. Observations of feldspars from soils: *Geochimica et Cosmochimica Acta*, v. 43, pp. 1173–1186.
- Bethke, C., 1992a, The Geochemist's Workbench™—A user's guide to Rxn, Act2, Tact, React, and Gtplot: Hydrogeology Program, Univ. of Illinois, Urbana, Ill., 174 pp. (Revised 1994; software copyrights 1993, 1994).
- Bethke, C., 1992b, The question of uniqueness in geochemical modeling: *Geochimica et Cosmochimica Acta*, v. 56, pp. 4315–4320.
- Bethke, C., 1998, The geochemist's workbench, ver. 3.0—A user's guide to Rxn, Act2, Tact, React, and Gtplot: Hydrogeology Program, Univ. of Illinois, Urbana, Ill., 184 pp.
- Bigham, J.M., 1994, Mineralogy of ochre deposits formed by sulfide oxidation; *in* Jambor, J.L., and Blowes, D.W. (eds.), *The Environmental Geochemistry of Sulfide Mine-Wastes: Mineralogical Association of Canada, Short Course Handbook*, v. 22, pp. 103–132.
- Bladh, K.W., 1982, The formation of goethite, jarosite, and alunite during the weathering of sulfide-bearing felsic rocks: *Economic Geology*, v. 77, pp. 176–184.
- Blowes, D.W., 1990, The geochemistry, hydrogeology, and mineralogy of decommissioned sulfide tailings—A comparative study: Unpub. Ph.D. thesis, Univ. of Waterloo, Waterloo, Ontario, Canada, 637 pp.
- Blum, A.E., and Lasaga, A.C., 1991, The role of surface speciation in the dissolution of albite: *Geochimica et Cosmochimica Acta*, v. 55, pp. 2193–2201.
- Bourcier, W.L., 1986, Improvements in the solid solution modeling capabilities of EQ3/6; *in* Jackson, K.J., and Bourcier, W.L. (eds.), *Proceedings of the Workshop on Geochemical Modeling: CONF-8609134*, Lawrence Livermore National Laboratory, Livermore, Calif., pp. 41–48.
- Bowers, T.S., and Taylor, H.P., Jr., 1985, An integrated chemical and stable isotope model of the origin of midocean ridge hot spring systems: *Journal of Geophysical Research*, v. 90, pp. 12,583–12,606.
- Brady, P.V., and Carroll, S.A., 1994, Direct effects of CO₂ and temperature on silicate weathering—Possible implications for climate control: *Geochimica et Cosmochimica Acta*, v. 58, pp. 1853–1856.
- Brantley, S.L., and Stillings, L., 1994, An integrated model for feldspar dissolution under acid conditions: *Mineralogical Magazine*, v. 58A, pp. 117–118.
- Brantley, S.L., and Velbel, M.A., 1993, Preface; *in* Brantley, S.L., and Velbel, M.A. (eds.), *Geochemical Kinetics of Mineral-Water Reactions in the Field and the Laboratory: Chemical Geology*, v. 105, pp. vii–ix.
- Brimhall, G.H., Jr., 1980, Deep hypogene oxidation of porphyry copper potassium-silicate protore at Butte, Montana—A theoretical evaluation of the copper remobilization hypothesis: *Economic Geology*, v. 75, pp. 384–409.
- Brimhall, G.H., Jr., and Ghiorsio, M.S., 1983, Origin and ore-forming consequences of the advanced argillic alteration process in hypogene environments by magmatic gas contamination of meteoric fluids: *Economic Geology*, v. 78, pp. 73–90.
- Broshears, R.E., Runkel, R.L., and Kimball, B.A., 1994, Development and application of a reactive solute transport model for trace metals in mountain streams: *Toxic Substances and the Hydrologic Sciences, American Institute of Hydrology*, pp. 19–34.
- Broshears, R.E., Kimball, B.A., and Runkel, R.L., 1996, Simulation of reactive transport during a pH modification experiment in a mountain stream affected by acid mine drainage; *in* Morganwalp, D.W., and Aronson, D.A. (eds.), *U.S. Geological Survey Toxic Substances Hydrology Program, Proceedings of the Technical Meeting*, Colorado Springs, Colorado, Sept. 20–24, 1993: U.S. Geological Survey Water-Resources Investigations Report 94–4014, pp. 781–788.
- Brown, D.S., and Allison, J.D., 1987, MINTEQA1, An equilibrium metal speciation model: User's Manual, EPA/600/3–87/012, U.S. Environmental Protection Agency, Athens, Ga.
- Brown, E., Shougstad, M.W., and Fishman, M.J., 1970, Methods for collection and analysis of water samples for dissolved minerals and gases—Techniques for water resources investigations of the United States Geological Survey: Book 5, Chap. A1, U.S. Geological Survey, Washington, D.C., pp. 101–105.
- Burch, T.E., Nagy, K.L., and Lasaga, A.C., 1993, Free energy dependence of albite dissolution kinetics at 80°C and pH 8.8; *in* Brantley, S.L., and Velbel, M.A. (eds.), *Geochemical Kinetics of Mineral-Water Reactions in the Field and the Laboratory: Chemical Geology*, v. 105, pp. 137–162.
- Carnahan, C.L., 1986, Simulation of uranium transport with variable temperature and oxidation potential—The computer program THCC: Report LBL–21639, Lawrence Berkeley Laboratory, Berkeley, Calif., 10 pp.
- Carroll-Webb, S.A., and Walther, J.V., 1988, A surface complex reaction model for the pH-dependence of corundum and kaolinite dissolution rates: *Geochimica et Cosmochimica Acta*, v. 52, pp. 2609–2623.
- Casey, W.H., Westrich, H.R., and Holdren, G.R., 1991, Dissolution rates of plagioclase at pH = 2 and 3: *American Mineralogist*, v. 76, pp. 211–217.
- Casey, W.H., Banfield, J.F., Westrich, H.R., and McLaughlin, L., 1993, What do dissolution experiments tell us about natural weathering?: *Chemical Geology*, v. 105, pp. 1–15.
- Cederberg, G.A., 1985, TRANQL—A groundwater mass-transport and equilibrium chemistry model for multicomponent systems: Unpub. Ph.D. thesis, Stanford Univ., Stanford, Calif., 117 pp.
- Cederberg, G.A., Street, R.L., and Leckie, J.O., 1985, A groundwater mass transport and equilibrium chemistry model for multicomponent systems: *Water Resources Research*, v. 21, pp. 1095–1104.
- Chou, L., and Wollast, R., 1984, Study of the weathering of albite at room temperature and pressure with a fluidized bed reactor: *Geochimica et Cosmochimica Acta*, v. 48, pp. 2205–2217.
- Chou, L., and Wollast, R., 1985, Steady-state kinetics and dissolution mechanisms of albite: *American Journal of Science*, v. 285, pp. 963–993.
- Cravotta, C.A., III, 1994, Secondary iron-sulfate minerals as sources of sulfate and acidity—The geochemical evolution of acidic ground water at a reclaimed surface coal mine in Pennsylvania; *in* Alpers, C.N., and Blowes, D.W. (eds.), *Environmental Geochemistry of Sulfide Oxidation: ACS Symposium Series 550*, American Chemical Society, Washington, D.C., pp. 345–364.
- Cunningham, A.B., 1984, Geologically constrained hydrologic and geochemical modeling of supergene weathering processes using physical and modal data: Unpub. M.S. thesis, Univ. of California, Berkeley, Calif., 122 pp.
- Daveler, S.A., and Wolery, T.J., 1992, EQPT, A data file preprocessor for the EQ3/6 software package—User's guide and related documentation (version 7.0): Report UCRL–MA–110662 PT II, Lawrence Livermore National Laboratory, Livermore, Calif., 89 pp.

- Davis, G.B., and Ritchie, A.I.M., 1986, A model of oxidation in pyritic mine wastes, I. Equations and approximate solutions: *Applied Mathematics Modelling*, v. 10, pp. 314–322.
- Davis, G.B., Doherty, G., and Ritchie, A.I.M., 1986, A model of pyrite oxidation in mine wastes, II. Comparison of numerical and approximate solutions: *Applied Mathematics Modelling*, v. 10, pp. 323–329.
- Davis, J.A., and Kent, D.B., 1990, Surface complexation modeling in aqueous geochemistry; in Hochella, M.F., Jr., and White, A.F. (eds.), *Mineral-Water Interface Geochemistry: Reviews in Mineralogy*, Mineralogical Society of America, v. 23, pp. 177–260.
- Deer, W.A., Howie, R.A., and Zussman, J., 1966, An introduction to the rock-forming minerals: Longman Group Ltd., Burnt Mill, U.K., 528 pp.
- Delany, J.M., Puigdomenech, I., and Wolery, T.J., 1986, Precipitation kinetics option for the EQ6 geochemical reaction path code: UCRL-53642, Lawrence Livermore National Laboratory, Livermore, Calif., 44 pp.
- Delany, J.M., and Wolery, T.J., 1984, Fixed fugacity option for the EQ6 geochemical reaction path code: UCRL-53598, Lawrence Livermore National Laboratory, Livermore, Calif., 20 pp.
- Denver, J.M., 1989, Effects of agricultural practices and septic-system effluent on the quality of water in the unconfined aquifer in parts of eastern Sussex County, Delaware: Delaware Geological Survey Report of Investigations no. 45, 66 pp.
- Dove, P.M., and Crerar, D.A., 1990, Kinetics of quartz dissolution in electrolyte solutions using a hydrothermal mixed flow reactor: *Geochimica et Cosmochimica Acta*, v. 54, pp. 955–969.
- Drever, J.I., 1988, *The geochemistry of natural waters*: 2nd ed., Prentice Hall, Englewood Cliffs, N.J., 437 pp.
- Drever, J.I., Murphy, K.M., and Clow, D.W., 1994, Field weathering rates versus laboratory dissolution rates—An update: *Mineralogical Magazine*, v. 58A, pp. 239–240.
- Dyrssen, D., and Wedborg, M., 1974, Equilibrium calculations of the speciation of elements in seawater; in Goldberg, E.D. (ed.), *The Sea: v. 5, Marine Chemistry*, John Wiley and Sons, New York, pp. 181–195.
- Dyrssen, D., and Wedborg, M., 1980, Major and minor elements, chemical speciation in estuarine waters; in Olausson, E., and Cato, I. (eds.), *Chemistry and Biogeochemistry of Estuaries*: John Wiley and Sons, New York, pp. 71–119.
- Dzombak, D.A., and Ali, M.A., 1993, Hydrochemical modeling of metal fate and transport in freshwater environments: *Water Pollution Research Journal, Canada*, v. 28, pp. 7–50.
- Dzombak, D.A., and Morel, F.M.M., 1990, *Surface complexation modeling—Hydrous ferric oxide*: John Wiley and Sons, New York, 393 pp.
- Edwards, A.L., 1972, TRUMP—A computer program for transient and steady state temperature distributions in multi-dimensional systems: Report 14754, Rev. 3, Lawrence Livermore National Laboratory, Livermore, Calif.
- Elving, P.J., and Kienitz, H., 1978, *Methodology of analytical chemistry*; in Kolthoff, I.M., and Elving, P.J. (eds.), *Treatise on Analytical Chemistry, Part I: v. I, Sect. B*, John Wiley and Sons, New York, pp. 53–94.
- Engesgaard, P., 1989, Multicomponent solute transport with equilibrium chemistry—Tracking a dissolution front: Progress Report 69, August 1989, Institute of Hydrodynamics and Hydraulic Engineering, Technical Univ. of Denmark, pp. 61–77.
- Engesgaard, P., and Kipp, K.L., 1992, A geochemical transport model for redox-controlled movement of mineral fronts in groundwater flow systems—A case of nitrate removed by oxidation of pyrite: *Water Resources Research*, v. 28, pp. 2829–2843.
- Eriksson, G., 1971, Thermodynamic studies of high temperature equilibria: *Acta Chemica Scandinavica*, v. 25, pp. 2651–2658.
- Eriksson, G., 1979, An algorithm for the computation of aqueous multi-component, multiphase equilibria: *Analytica Chimica Acta*, v. 112, pp. 375–383.
- Felmy, A.R., Girvin, D.C., and Jenne, E.A., 1984, MINTEQA—A computer program for calculating aqueous geochemical equilibria: EPA-600/3-84-032, U.S. Environmental Protection Agency, Athens, Ga.
- Fournier, R.O., and Potter, R.W., II, 1982, An equation correlating the solubility of quartz in water from 25° to 900°C at pressures up to 10,000 bars: *Geochimica et Cosmochimica Acta*, v. 46, p. 1969–1973.
- Fournier, R.O., and Rowe, J.J., 1977, The solubility of amorphous silica in water at high temperatures and high pressures: *American Mineralogist*, v. 62, p. 1052–1056.
- Frind, E.O., and Molson, J.W., 1994, Modelling of mill-tailings impoundments; in Jambor, J.L., and Blowes, D.W. (eds.), *The Environmental Geochemistry of Sulfide Mine-Wastes: Short Course Handbook*, v. 22, Mineralogical Association of Canada, Nepean, Ontario, pp. 19–58.
- Frind, E.O., Duynisveld, W.H.M., Strelbel, O., and Boettcher, J., 1990, Modeling of multicomponent transport with microbial transformation in groundwater—The Fuhrberg case: *Water Resources Research*, v. 26, pp. 1707–1719.
- Fuller, C.C., Davis, J.A., and Waychunas, G.A., 1993, Surface chemistry of ferrihydrite, Part 2. Kinetics of arsenate adsorption and coprecipitation: *Geochimica et Cosmochimica Acta*, v. 57, pp. 2271–2282.
- Ganguly, J., and Saxena, S.K., 1987, *Mixtures and mineral reactions*: Minerals and Rocks Series, v. 19, Springer-Verlag, New York, N.Y., 291 pp.
- Garrels, R.M., and Christ, C.L., 1965, *Solutions, minerals, and equilibria*: Freeman, Cooper and Co., San Francisco, Calif., 450 pp.
- Garrels, R.M., and MacKenzie, F.T., 1967, Origin of the chemical composition of some springs and lakes; in *Equilibrium Concepts in Natural Waters: Advances in Chemistry Series 67*, American Chemical Society, pp. 222–242.
- Garrels, R.M., and Thompson, M.E., 1962, A chemical model for seawater at 25°C and one atmosphere total pressure: *American Journal of Science*, v. 260, pp. 57–66.
- Garrett, R.G., 1989, The chi-squared plot, a tool for multivariate outlier regression: *Journal of Geochemical Exploration*, v. 32, pp. 319–342.
- Garven, G., 1982, The role of groundwater flow in the genesis of stratabound ore deposits—A quantitative analysis: Unpub. Ph.D. thesis, Univ. of British Columbia, Vancouver, B.C., Canada, 304 pp.
- Ghiorso, M.S., 1987, Thermodynamics of minerals and melts: *Reviews of Geophysics*, v. 25, pp. 1054–1064.
- Glynn, P.D., 1990, Modeling solid-solution reactions in low-temperature aqueous systems; in Melchior, D.C., and Bassett, R.L. (eds.), *Chemical Modeling of Aqueous Systems II: ACS Symposium Series 416*, American Chemical Society, Washington, D.C., pp. 74–86.
- Glynn, P.D., 1991a, Effects of impurities in gypsum on contaminant transport at Pinal Creek, Arizona; in Mallard, G.E., and Aronson, D.A. (eds.), *Proceedings of the Technical Meeting, U.S. Geological Survey Toxic Substances Hydrology Program, Monterey, Calif., March 11–15, 1991: Water-Resources Investigations Report 91-4034*, pp. 466–474.
- Glynn, P.D., 1991b, MBSSAS—A code for the computation of Margules parameters and equilibrium relations in binary solid-solution aqueous-solution systems: *Computers and Geoscience*, v. 17, pp. 907–966.
- Glynn, P.D., and Parkhurst, D.L., 1992, Modeling non-ideal solid-solution aqueous-solution reactions in mass-transfer computer codes; in Kharaka, Y.K., and Maest, A.S. (eds.), *Water-Rock Interaction, Proceedings, 7th Internat. Symposium on Water-Rock Interaction: A.A. Balkema, Brookfield, Vt.*, v. 1, pp. 175–179.
- Glynn, P.D., and Reardon, E.J., 1990, Solid-solution aqueous-solution equilibria—Thermodynamic theory and representation: *American Journal of Science*, v. 290, pp. 164–201.
- Glynn, P.D., Reardon, E.J., Plummer, L.N., and Busenberg, E., 1990, Reaction paths and equilibrium end-points in solid-solution aqueous-solution systems: *Geochimica et Cosmochimica Acta*, v. 54, pp. 267–282.
- Glynn, P.D., Engesgaard, P., and Kipp, K.L., 1991, Use and limitations of two computer codes for simulating geochemical mass transport at the Pinal Creek toxic-waste site; in Mallard, G.E., and Aronson, D.A. (eds.), *U.S. Geological Survey Toxic Substances Hydrology Program, Proceedings of the Technical Meeting, Monterey, Calif., March 11–15, 1991: Water-Resources Investigations Report 91-4034*, pp. 454–460.
- Greenwood, H.J., 1989, On models and modeling: *Canadian Mineralogist*, v. 27, pp. 1–14.
- Grenthe, I., Fuger, J., Lemire, R.J., et al., 1992, *Chemical thermodynamics*

- of uranium: Elsevier, N.Y., 715 pp.
- Harriss, D.K., Ingle, S.E., Magnuson, V.R., and Taylor, D.K., 1984, Programmer's manual for REDEQL.UMD: Univ. of Minnesota, Duluth, Minn. (unreleased preliminary document).
- Helgeson, H.C., 1968, Evaluation of irreversible reactions in geochemical processes involving minerals and aqueous solutions, I. Thermodynamic relations: *Geochimica et Cosmochimica Acta*, v. 32, pp. 853–877.
- Helgeson, H.C., 1970, A chemical and thermodynamic model of ore deposition in hydrothermal systems: Mineralogical Society of America Spec. Paper No. 3, pp. 155–186.
- Helgeson, H.C., 1974, Chemical interaction of feldspars and aqueous solutions; in MacKenzie, W.S., and Zussman, J. (eds.), *The Feldspars*: Manchester University Press, pp. 184–217.
- Helgeson, H.C., 1979, Mass transfer among minerals and hydrothermal solutions; in Barnes, H.L. (ed.), *The Geochemistry of Hydrothermal Ore Deposits*: 2nd ed., John Wiley and Sons, New York, pp. 568–610.
- Helgeson, H.C., and Murphy, W.M., 1983, Calculation of mass transfer among minerals and aqueous solutions as a function of time and surface area in geochemical processes, I. Computational approach: *Mathematical Geology*, v. 15, pp. 109–130.
- Helgeson, H.C., Garrels, R.M., and MacKenzie, F.T., 1969, Evaluation of irreversible reactions in geochemical processes involving minerals and aqueous solutions, II. Applications: *Geochimica et Cosmochimica Acta*, v. 33, pp. 455–481.
- Helgeson, H.C., Brown, T.H., Nigrini, A., and Jones, T.A., 1970, Calculation of mass transfer in geochemical processes involving aqueous solutions: *Geochimica et Cosmochimica Acta*, v. 34, pp. 569–592.
- Helgeson, H.C., Kirkham, D.H., and Flowers, G.C., 1981, Theoretical prediction of the thermodynamic behavior of aqueous electrolytes at high pressures and temperatures, IV. Calculation of activity coefficients, osmotic coefficients, and apparent molal and standard and relative partial molal properties to 600°C and 5 kb: *American Journal of Science*, v. 281, pp. 1249–1516.
- Hem, J.D., 1985, Study and interpretation of the chemical characteristics of natural water: 3rd ed., U.S. Geological Survey Water-Supply Paper 2254, 264 pp.
- Hem, J.D., Roberson, C.E., Lind, C.J., and Polzer, W.L., 1973, Chemical interactions of aluminum with aqueous silica at 25°C: U.S. Geological Survey Water-Supply Paper 1827-E, 57 pp.
- Hodson, P.V., Borgmann, U., and Shear, H., 1979, Toxicity of copper to aquatic biota; in Nriagu, J.O. (ed.), *Copper in the Environment, Part 2, Health effects*: Wiley Interscience, New York, pp. 307–372.
- Holdren, G.R., Jr., and Speyer, P.M., 1985a, Reaction rate-surface area relationships during the early stages of weathering, I. Initial observations: *Geochimica et Cosmochimica Acta*, v. 49, pp. 675–681.
- Holdren, G.R., Jr., and Speyer, P.M., 1985b, pH dependent changes in the rates and stoichiometry of dissolution of an alkali feldspar at room temperature: *American Journal of Science*, v. 285, pp. 994–1026.
- Holdren, G.R., Jr., and Speyer, P.M., 1986, Stoichiometry of alkali feldspar dissolution at room temperature and various pH values; in Colman, S.M., and Dethier, D.P. (eds.), *Rates of Chemical Weathering of Rocks and Minerals*: Academic Press, Orlando, Fla., pp. 61–81.
- Holdren, G.R., Jr., and Speyer, P.M., 1987, Reaction rate-surface area relationships during the early stages of weathering, II. Data on eight additional feldspars: *Geochimica et Cosmochimica Acta*, v. 51, pp. 2311–2318.
- Ingle, S.E., Schuldt, M.D., and Shults, D.W., 1978, A user's guide for REDEQL.EPA—A computer program for chemical equilibria in aqueous systems: U.S. Environmental Protection Agency Report EPA600/3-78-024, Corvallis, Ore.
- Ingrì, N., Kakolowicz, W., Sillen, L.G., and Warnquist, B., 1967, High-speed computers as a supplement of graphical methods, V. HALTAFALL, a general program for calculating the composition of equilibrium mixtures: *Talanta*, v. 14, pp. 1261–1286.
- Janecky, D.R., and Seyfried, W.E., Jr., 1984, Formation of massive sulfide deposits on oceanic ridge crests—Incremental reaction models for mixing between hydrothermal solutions and seawater: *Geochimica et Cosmochimica Acta*, v. 48, pp. 2723–2738.
- Johnson, J.W., Oelkers, E.H., and Helgeson, H.C., 1992, SUPCRT92—A software package for calculating the standard molal thermodynamic properties of minerals, gases, aqueous species, and reactions from 1 to 5000 bars and 0° to 1000°C: *Computers and Geosciences*, v. 18, pp. 899–947.
- Kenoyer, G.J., and Bowser, C.J., 1992, Groundwater chemical evolution in a sandy silicate aquifer in northern Wisconsin, 2. Reaction modeling: *Water Resources Research*, v. 28, pp. 591–600.
- Kharaka, Y.K., and Barnes, I., 1973, SOLMNEQ—Solution-mineral equilibrium computations: U.S. Geological Survey Computer Contribution, National Technical Information Service, NTIS PB 215–899, 81 pp.
- Kharaka, Y.K., Gunter, W.D., Aggarwal, P.K., Perkins, E.H., and DeBraal, J.D., 1988, SOLMINEQ.88—A computer program for geochemical modeling of water-rock interactions: U.S. Geological Survey Water-Resources Investigations Report 88-4227, 420 pp.
- Kimball, B.A., Broshears, R.E., McKnight, D.M., and Bencala, K.E., 1994, Effects of instream pH modification on transport of sulfide-oxidation products; in Alpers, C.N., and Blowes, D.W. (eds.), *Environmental Geochemistry of Sulfide Oxidation*: ACS Symposium Series 550, American Chemical Society, Washington, D.C., pp. 224–243.
- Kinkel, A.R., Jr., Hall, W.E., and Albers, J.P., 1956, Geology and base-metal deposits of the West Shasta copper-zinc district: U.S. Geological Survey Professional Paper 285, 156 pp.
- Kipp, K.L., Jr., 1987, HST3D—A computer code for simulation of heat and solute transport in three-dimensional ground-water flow systems: U.S. Geological Survey Water-Resources Investigations Report 86-4095, 517 pp.
- Knauss, K.G., and Wolery, T.J., 1986, Dependence of albite dissolution kinetics on pH and time at 25°C and 70°C: *Geochimica et Cosmochimica Acta*, v. 50, pp. 2481–2497.
- Knauss, K.G., and Wolery, T.J., 1988, The dissolution kinetics of quartz as a function of pH and time at 70°C: *Geochimica et Cosmochimica Acta*, v. 52, pp. 43–53.
- Konikow, L., and Bredehoeft, J., 1992, Ground-water models cannot be validated: *Advances in Water Resources*, v. 15, pp. 75–83.
- Kubisz, J., 1970, Studies on synthetic alkali-hydronium jarosites, I. Synthesis of jarosite and natrojarosite: *Mineralogia Polonica*, v. 1, pp. 47–57.
- Langmuir, D., 1979, Techniques of estimating thermodynamic properties for some aqueous complexes of geochemical interest; in Jenne, E.A. (ed.), *Chemical Modeling in Aqueous Systems*: ACS Symposium Series 93, American Chemical Society, Washington, D.C., pp. 353–387.
- Lasaga, A.C., 1981a, Rate laws of chemical reactions; in Lasaga, A.C., and Kirkpatrick, R.J. (eds.), *Kinetics of Geochemical Processes: Reviews in Mineralogy*, Mineralogical Society of America, Washington, D.C., v. 8, pp. 1–68.
- Lasaga, A.C., 1981b, Transition state theory; in Lasaga, A.C., and Kirkpatrick, R.J. (eds.), *Kinetics of Geochemical Processes: Reviews in Mineralogy*, Mineralogical Society of America, Washington, D.C., v. 8, pp. 135–169.
- Lichtner, P.C., 1985, Continuum model for simultaneous chemical reactions and mass transport in hydrothermal systems: *Geochimica et Cosmochimica Acta*, v. 49, pp. 779–800.
- Lichtner, P.C., 1988, The quasi-stationary state approximation to coupled mass transport and fluid-rock interaction in a porous medium: *Geochimica et Cosmochimica Acta*, v. 52, pp. 143–165.
- Lichtner, P.C., 1992, Time-space description of fluid/rock interaction in permeable media: *Water Resources Research*, v. 28, pp. 3135–3155.
- Lichtner, P.C., 1993, Scaling properties of time-space kinetic mass transport equations and the local equilibrium limit: *American Journal of Science*, v. 293, pp. 257–296.
- Lichtner, P.C., 1994, Time-space continuum formulation of supergene enrichment and weathering of sulfide-bearing ore deposits; in Alpers, C.N., and Blowes, D.W. (eds.), *Environmental Geochemistry of Sulfide Oxidation*: ACS Symposium Series 550, American Chemical Society, Washington, D.C., pp. 153–170.
- Lichtner, P.C., and Biino, G.G., 1992, A first principles approach to super-

- gene enrichment of a porphyry copper protore, I. Cu-Fe-S subsystem: *Geochimica et Cosmochimica Acta*, v. 56, pp. 3987–4013.
- Lichtner, P.C., and Waber, N., 1992, Redox front geochemistry and weathering—Theory with application to the Osamu Utsumi uranium mine, Poços de Caldas, Brazil: *Journal of Geochemical Exploration*, v. 45, p. 521–564.
- Lidén, J., 1983, Equilibrium approaches to natural water systems—A study of anoxic- and ground-waters based on *in situ* data acquisition: Ph.D. thesis, Univ. of Umeå, Sweden, 52 pp. (plus 7 appendices).
- Lindberg, R.D., and Runnells, D.D., 1984, Ground water redox reactions—An analysis of equilibrium state applied to Eh measurements and geochemical modeling: *Science*, v. 225, pp. 925–927.
- Liu, Chen-Wuing, 1988, Multiple-species chemical transport involving oxidation/reduction reactions in geological media: Unpub. Ph.D. thesis, Univ. of California, Berkeley, Calif., 257 pp.
- Liu, C.-W., and Narasimhan, T.J., 1989a, Redox-controlled multiple-species reactive chemical transport, I. Model development: *Water Resources Research*, v. 25, pp. 869–882.
- Liu, C.-W., and Narasimhan, T.J., 1989b, Redox-controlled multiple-species reactive chemical transport, II. Verification and application: *Water Resources Research*, v. 25, pp. 883–910.
- Madé, B., 1991, Modélisation thermodynamique et cinétique des réactions géochimiques dans les interactions eau-roche: Thesis ULP, Strasbourg, France, 308 pp.
- Madé, B., and Fritz, B., 1992, Theoretical approach and modelling of the dissolution and precipitation of minerals under kinetic control; *in* Kharaka, Y.K., and Maest, A.S. (eds.), *Water-Rock Interaction, Proceedings, 7th Internat Symposium on Water-Rock Interaction*: A.A. Balkema, Brookfield, Vt., v. 1, pp. 101–105.
- Mangold, D.C., and Tsang, C.-F., 1991, A summary of subsurface hydrological and hydrochemical models: *Review of Geophysics*, v. 29, pp. 51–79.
- McDuff, R.E., and Morel, F.M.M., 1973, Description and use of the chemical equilibrium program REDEQL2: Technical Report EQ-73-02, Keck Laboratory, California Institute of Technology, Pasadena, Calif., 75 pp.
- McKibben, M.A., and Barnes, H.L., 1986, Oxidation of pyrite in low temperature acidic solutions—Rate laws and surface textures: *Geochimica et Cosmochimica Acta*, v. 50, pp. 1509–1520.
- Merino, E., 1979, Internal consistency of a water analysis and uncertainty of the calculated distribution of aqueous species at 25°C: *Geochimica et Cosmochimica Acta*, v. 43, pp. 1533–1542.
- Miller, C., and Benson, L., 1983, Simulation of solute transport in a chemically reactive heterogeneous system—Model development and application: *Water Resources Research*, v. 19, pp. 381–391.
- Morel, F.M.M., and Morgan, J.J., 1972, A numerical method for computing equilibria in aqueous chemical systems: *Environmental Science and Technology*, v. 6, pp. 58–67.
- Morin, K.A., and Cherry, J.A., 1988, Migration of acid groundwater seepage from uranium tailings impoundments, 3. Simulation of the conceptual model with application to seepage area A: *Journal of Contaminated Hydrology*, v. 2, pp. 323–342.
- Morin, K.A., Cherry, J.A., Dave, N.K., Lim, T.P., and Vivuyurka, A.J., 1988a, Migration of acidic groundwater seepage from uranium-tailings impoundments, 1. Field study and conceptual hydrogeochemical model: *Journal of Contaminated Hydrology*, v. 2, pp. 271–303.
- Morin, K.A., Cherry, J.A., Dave, N.K., Lim, T.P., and Vivuyurka, A.J., 1988b, Migration of acidic groundwater seepage from uranium-tailings impoundments, 2. Behavior of radionuclides in water: *Journal of Contaminated Hydrology*, v. 2, pp. 305–322.
- Morrey, J.R., 1988, User's guide to the ECHEM equilibrium geochemistry code: FASTCHEM™ Package, EPRI Report EA-5870-CCM, v. 4, Prepared by Battelle, Pacific Northwest Laboratories, for Electric Power Research Institute, Palo Alto, Calif., 218 pp.
- Moses, C.O., and Herman, J.S., 1991, Pyrite oxidation at circumneutral pH: *Geochimica et Cosmochimica Acta*, v. 55, pp. 471–482.
- Moses, C.O., Nordstrom, D.K., Herman, J.S., and Mills, A.L., 1987, Pyrite oxidation by dissolved oxygen and by ferric iron: *Geochimica et Cosmochimica Acta*, v. 51, pp. 1561–1571.
- Mukhopadhyay, B., Basu, S., and Holdaway, M.J., 1993, A discussion of Margules-type formulations for multicomponent solutions with a generalized approach: *Geochimica et Cosmochimica Acta*, v. 57, pp. 277–284.
- Muller, B., 1993, MacqQL v. 1.1—A program to calculate chemical speciation and adsorption: EAWAG/ETH, Limnological Research Center, Kasteneinboum, Switzerland.
- Murphy, W.M., 1989, Dislocations and feldspar dissolution: *European Journal of Mineralogy*, v. 1, pp. 315–326.
- Murphy, W.M., and Helgeson, H.C., 1987, Thermodynamic and kinetic constraints on reaction rates among minerals and aqueous solutions, III. Activated complexes and the pH-dependence of the rates of feldspar, pyroxene, wollastonite, and olivine hydrolysis: *Geochimica et Cosmochimica Acta*, v. 51, pp. 3137–3153.
- Murphy, W.M., and Helgeson, H.C., 1989, Thermodynamic and kinetic constraints on reaction rates among minerals and aqueous solutions, IV. Retrieval of rate constants and activation parameters for the hydrolysis of pyroxene, wollastonite, olivine, andalusite, quartz, and nepheline: *American Journal of Science*, v. 289, pp. 17–101.
- Murphy, W.M., Pabalan, R.T., Prikryl, J.D., and Goulet, C.J., 1992, Dissolution rate and solubility of analcime at 25°C; *in* Kharaka, Y.K. and Maest, A.S. (eds.), *Water-Rock Interaction, Proceedings of the 7th Internat Symposium on Water-Rock Interaction*: A.A. Balkema, Brookfield, Vt., v. 1, pp. 107–110.
- Nagy, K.L., and Lasaga, A.C., 1992, Dissolution and precipitation kinetics of gibbsite at 80°C and pH 3—The dependence on solution saturation state: *Geochimica et Cosmochimica Acta*, v. 56, pp. 3093–3111.
- Nagy, K.L., Blum, A.E., and Lasaga, A.C., 1991, Dissolution and precipitation kinetics of kaolinite at 80°C and pH 3—The dependence on solution saturation state: *American Journal of Science*, v. 291, pp. 649–686.
- Narasimhan, T.N., White, A.F., and Tokunaga, T., 1986, Groundwater contamination from an inactive uranium mill tailings pile, 2. Application of a dynamic mixing model: *Water Resources Research*, v. 22, pp. 1820–1834.
- Nesbitt, H.W., Kettlewell, D., and Cramer, J.J., 1992, SPECIATE—A spreadsheet-based speciation program for aqueous radionuclides; *in* Kharaka, Y.K., and Maest, A.S. (eds.), *Water-Rock Interaction, Proceedings, 7th Internat Symposium on Water-Rock Interaction*: A.A. Balkema, Brookfield, Vt., v. 1, pp. 237–238.
- Nicholson, R.V., and Scharer, J.M., 1994, Laboratory studies of pyrrhotite oxidation; *in* Alpers, C.N., and Blowes, D.W. (eds.), *Environmental Geochemistry of Sulfide Oxidation*: ACS Symposium Series 550, American Chemical Society, Washington, D.C., pp. 14–30.
- Nicholson, R.V., Gillham, R.W., and Reardon, E.J., 1988, Pyrite oxidation in carbonate buffered solutions, I. Experimental kinetics: *Geochimica et Cosmochimica Acta*, v. 52, p. 1077–1085.
- Noorishad, J., Carnahan, C.L., and Benson, L.V., 1987, Development of the non-equilibrium chemical transport code CHMTRNS: Lawrence Berkeley Laboratory Pub. LBL-22361, Livermore, Calif., 231 pp.
- Nordstrom, D.K., 1977, Hydrogeochemical and microbiological factors affecting the heavy metal chemistry of an acid mine drainage system: Unpub. Ph.D. thesis, Stanford Univ., Stanford, Calif., 210 pp.
- Nordstrom, D.K., 1994, On the evaluation and application of geochemical models; *in* von Maravic, H., and Smellie, J. (eds.), *Proceedings of the 5th CEC (Commission of the European Community) Natural Analogue Working Group Meeting and Alligator Rivers Analogue Project: Final Workshop, Toledo, Spain, Oct. 5–9, 1992, EUR 15176 EN, appendix 2*, pp. 375–386.
- Nordstrom, D.K., and Alpers, C.N., 1999, Geochemistry of acid mine waters; *in* Plumlee, G.S., and Logsdon, M.J. (eds.), *The Environmental Geochemistry of Mineral Deposits, Part A. Processes, Techniques, and Health Issues*: Society of Economic Geologists, Reviews in Economic Geology, v. 6A, pp. 133–160.
- Nordstrom, D.K., and Ball, J.W., 1986, The geochemical behavior of aluminum in acidified surface waters: *Science*, v. 232, p. 54–56.
- Nordstrom, D.K., and Ball, J.W., 1989, Mineral saturation states in natural waters and their sensitivity to thermodynamic and analytical errors: *Sciences Géologiques Bulletin*, v. 42, pp. 269–280.

- Nordstrom, D.K., and Munoz, J.L., 1994, *Geochemical thermodynamics*: 2nd ed., Blackwell Scientific, Palo Alto, Calif., 493 pp.
- Nordstrom, D.K., Jenne, E.A., and Ball, J.W., 1979a, Redox equilibria of iron in acid mine waters; *in* Jenne, E.A. (ed.), *Chemical Modeling in Aqueous Systems*: ACS Symposium Series 93, American Chemical Society, Washington, D.C., pp. 51–80.
- Nordstrom, D.K., Plummer, L.N., Wigley, T.M.L., Wolery, T.J., Ball, J.W., Jenne, E.A., Bassett, R.L., Crerar, D.A., Florence, T.M., Fritz, B., Hoffman, M., Holdren, G.R., Jr., Lafon, G.M., Mattigod, S.V., McDuff, R.E., Morel, F.M.M., Reddy, M.M., Sposito, G., and Thraillkill, J., 1979b, A comparison of computerized chemical models for equilibrium calculations in aqueous systems; *in* Jenne, E.A. (ed.), *Chemical Modeling in Aqueous Systems*: ACS Symposium Series 93, American Chemical Society, Washington, D.C., pp. 857–892.
- Nordstrom, D.K., Ball, J.W., Donahoe, R.J., and Whittemore, D., 1989, Groundwater chemistry and water-rock interactions at Stripa: *Geochimica et Cosmochimica Acta*, v. 53, pp. 1727–1740.
- Nordstrom, D.K., Plummer, L.N., Langmuir, D., Busenberg, E., May, H.M., Jones, B.F., and Parkhurst, D.L., 1990, Revised chemical equilibrium data for major water-mineral reactions and their limitations; *in* Melchior, D.C., and Bassett, R.L. (eds.), *Chemical Modeling in Aqueous Systems II*: ACS Symposium Series 416, American Chemical Society, Washington, D.C., pp. 398–413.
- Nordstrom, D.K., Alpers, C.N., and Ball, J.W., 1991, Measurement of negative pH and extremely high metal concentrations in acid mine water from Iron Mountain, California: *Geological Society of America Abstracts with Programs*, v. 23, no. 5, pp. A383.
- Nordstrom, D.K., McNutt, R.H., Puigdomènech, I., Smellie, J.A.T., and Wolf, M., 1992, Ground water chemistry and geochemical modeling of water-rock interactions at the Osamu Utsumi mine and the Morro do Ferro analogue study sites, Poços de Caldas, Minas Gerais, Brazil: *Journal of Geochemical Exploration*, v. 45, pp. 249–287.
- Oelkers, E.H., and Schott, J., 1995, Experimental study of anorthite dissolution and the relative mechanism of feldspar hydrolysis: *Geochimica et Cosmochimica Acta*, v. 59, pp. 5039–5053.
- Öhman, L.-O., 1983, Equilibrium studies of ternary aluminum (III) complexes: Ph.D. thesis, Univ. of Umeå, Sweden, 74 pp. (plus 8 appendices).
- Oreskes, N., Shrader-Frechette, K., and Belitz, K., 1994, Verification, validation, and confirmation of numerical models in the earth sciences: *Science*, v. 263, pp. 641–646.
- Oxburgh, R., Drever, J.I., and Sun, Y.-T., 1994, Mechanism of plagioclase dissolution in acid solution at 25°C: *Geochimica et Cosmochimica Acta*, v. 58, pp. 661–669.
- Pačes, T., 1983, Rate constants of dissolution derived from the measurements of mass balance in hydrological catchments: *Geochimica et Cosmochimica Acta*, v. 37, pp. 2641–2663.
- Paige, C.R., Kornicker, W.A., Hileman, O.E., Jr., and Snodgrass, W.J., 1992, Modelling solution equilibria for uranium ore processing—The $\text{PbSO}_4\text{-H}_2\text{SO}_4\text{-H}_2\text{O}$ and $\text{PbSO}_4\text{-Na}_2\text{SO}_4\text{-H}_2\text{O}$ systems: *Geochimica et Cosmochimica Acta*, v. 56, pp. 1165–1173.
- Papelis, C., Hayes, K.F., and Leckie, J.O., 1988, HYDRAQL—A program for the computation of chemical equilibrium composition of aqueous batch systems including surface-complexation modeling of ion adsorption and the oxide/solution interface: Department of Civil Engineering Technical Report 306, Stanford Univ., Stanford, Calif., 130 pp.
- Parker, D.R., Zelazny, L.W., and Kinraide, T.B., 1987, Improvements to the program GEOCHEM: Soil Science Society of America Journal, v. 51, no. 2, pp. 488–491 (plus errata sheet).
- Parker, D.R., Norvell, W.A., and Chaney, R.L., 1995, GEOCHEM-PC—A chemical speciation program for IBM and compatible personal computers; *in* Loepfert, R.H. et al. (eds.), *Chemical Equilibrium and Reaction Models*: Soil Science Society of America, Spec. Pub. No. 42, ASA and SSSA, Madison, Wis., pp. 253–269.
- Parkhurst, D.L., 1987, Chemical analysis of water samples from the Picher mining area, northeast Oklahoma and southeast Kansas: U.S. Geological Survey Open-File Report 87–453, 43 pp.
- Parkhurst, D.L., 1995, User's guide to PHREEQC—A computer program for speciation, reaction-path, advective-transport, and inverse geochemical calculations: U.S. Geological Survey Water-Resources Investigations Report 95–4227, 143 pp.
- Parkhurst, D.L., 1997, Geochemical mole-balance modeling with uncertain data: *Water Resources Research*, v. 33, pp. 1957–1970.
- Parkhurst, D.L., 1998, PHREEQC website (http://www.wbrr.cr.usgs.gov/projects/GWC_coupled/phreeqc/)
- Parkhurst, D.L., and Plummer, L.N., 1993, *Geochemical models*; *in* Alley, W.M. (ed.), *Regional Ground-Water Quality*: Van Nostrand Reinhold, New York, pp. 199–225.
- Parkhurst, D.L., Thorstenson, D.C., and Plummer, L.N., 1980, PHREEQE—A computer program for geochemical calculations: U.S. Geological Survey Water-Resources Investigations Report 80–96, 210 pp. (Reprinted with corrections, 1985, 1990).
- Parkhurst, D.L., Plummer, L.N., and Thorstenson, D.C., 1982, BALANCE—A computer program for calculating mass transfer for geochemical reactions in ground water: U.S. Geological Survey Water-Resources Investigations Report 82–14, 29 pp.
- Perkins, E.H., Kharaka, Y.K., Gunter, W.D., and DeBraul, J.D., 1990, Geochemical modeling of water-rock interactions using SOLMINEQ.88; *in* Melchior, D.C., and Bassett, R.L. (eds.), *Chemical Modeling of Aqueous Systems II*: ACS Symposium Series 416, American Chemical Society, Washington, D.C., pp. 117–127.
- Petrovich, R., 1976, Rate control in feldspar dissolution. II. The protective effect of precipitates: *Geochimica et Cosmochimica Acta*, v. 40, pp. 1665–1674.
- Petrovich, R., 1981a, Kinetics of dissolution of mechanically comminuted rock-forming oxides and silicates, I. Deformation and dissolution of quartz under laboratory conditions: *Geochimica et Cosmochimica Acta*, v. 45, pp. 1665–1674.
- Petrovich, R., 1981b, Kinetics of dissolution of mechanically comminuted rock-forming oxides and silicates, I. Deformation and dissolution of oxides and silicates in the laboratory and at the Earth's surface: *Geochimica et Cosmochimica Acta*, v. 45, pp. 1675–1686.
- Petrovich, R., Berner, R.A., and Goldhaber, M.B., 1976, Rate control in dissolution of alkali feldspar, I. Studies of residual feldspar grains by X-ray photoelectron spectroscopy: *Geochimica et Cosmochimica Acta*, v. 40, pp. 537–548.
- Pitzer, K.S., 1973, Thermodynamics of electrolytes, I. Theoretical basis and general equations: *Journal of Phys. Chemistry*, v. 77, pp. 268–277.
- Pitzer, K.S., 1979, Theory—Ion interaction approach; *in* Pytkowicz, R.M. (ed.), *Activity Coefficients in Aqueous Solutions*: v. 1, CRC Press, Inc., Boca Raton, Fla., pp. 157–208.
- Pitzer, K.S., 1987, Thermodynamic model for aqueous solutions of liquid-like density; *in* Charmichael, I.S.E., and Eugster, H.P. (eds.), *Thermodynamic Modeling of Geological Materials—Minerals, Fluids, and Melts*: Reviews in Mineralogy, Mineralogical Society of America, Washington, D.C., v. 17, pp. 97–142.
- Playton, S.J., Davis, R.E., and McClafflin, R.G., 1980, Chemical quality of water in abandoned zinc mines in northeastern Oklahoma and southeastern Kansas: *Oklahoma Geological Survey Circular* 82, 49 pp.
- Plumlee, G.S., Leach, D.L., Hofstra, A.H., Landis, G.P., Rowan, E.L., and Viets, J.G., 1994, Chemical reaction path modeling of ore deposition in Mississippi Valley-type Pb-Zn deposits of the Ozark Region, U.S. Midcontinent: *Economic Geology*, v. 89, p. 1361–1383.
- Plumlee, G.S., Goldhaber, M.B., and Rowan, E.L., 1995, The potential role of magmatic gases in the genesis of Illinois-Kentucky fluorspar deposits—Implications from chemical reaction path modeling: *Economic Geology*, v. 90, p. 999–1011.
- Plummer, L.N., 1985, Geochemical modeling—A comparison of forward and inverse methods; *in* Proceedings, First Canadian/American Conference on Hydrogeology: Practical Applications of Ground Water Geochemistry, National Water Well Association, Worthington, Ohio, pp. 149–177.
- Plummer, L.N., 1992, Geochemical modeling of water-rock interaction—Past, present, future; *in* Kharaka, Y.K., and Maest, A.S. (eds.), *Water-Rock Interaction*, Proceedings of the 7th Internatl Symposium on Water-Rock Interaction, v. 1: A.A. Balkema, Brookfield, Vt., pp. 23–33.
- Plummer, L.N., and Parkhurst, D.L., 1990, Application of the Pitzer equa-

- tions to the PHREEQE geochemical model; *in* Melchior, D.C., and Bassett, R.L. (eds.), *Chemical Modeling of Aqueous Systems II: ACS Symposium Series 416*, American Chemical Society, Washington, D.C., pp. 128–137.
- Plummer, L.N., Jones, B.F., and Truesdell, A.H., 1976, WATEQF—A FORTRAN IV version of WATEQ, a computer program for calculating chemical equilibria of natural waters: U.S. Geological Survey Water-Resources Investigations Report 76–13, 61 pp.
- Plummer, L.N., Parkhurst, D.L., and Thorstenson, D.C., 1983, The development of reaction models for ground-water systems: *Geochimica et Cosmochimica Acta*, v. 47, pp. 665–686.
- Plummer, L.N., Parkhurst, D.L., Fleming, G.W., and Dunkle, S.A., 1988, PHRQPITZ—A computer program incorporating Pitzer's equations for calculation of geochemical reactions in brines: U.S. Geological Survey Water-Resources Investigations Report 88–4153, 310 pp.
- Plummer, L.N., Busby, J.F., Lee, R.W., and Hanshaw, B.B., 1990, Geochemical modeling of the Madison aquifer in parts of Montana, Wyoming, and South Dakota: *Water Resources Research*, v. 26, pp. 1981–2014.
- Plummer, L.N., Prestemon, E.C., and Parkhurst, D.L., 1991, An interactive code (NETPATH) for modeling net geochemical reactions along a flow path: U.S. Geological Survey Water-Resources Investigations Report 91–4078, 227 pp.
- Plummer, L.N., Prestemon, E.C., and Parkhurst, D.L., 1992, NETPATH—An interactive code for interpreting NET geochemical reactions from chemical and isotopic data along a flow PATH; *in* Kharaka, Y.K., and Maest, A.S. (eds.), *Water-Rock Interaction, Proceedings, 7th International Symposium on Water-Rock Interaction: A.A. Balkema, Brookfield, Vt.*, v. 1, pp. 239–242.
- Plummer, L.N., Prestemon, E.C., and Parkhurst, D.L., 1994, An interactive code (NETPATH) for modeling net geochemical reactions along a flow path, version 2.0: U.S. Geological Survey Water-Resources Investigations Report 94–4169, 130 pp.
- Ptacek, C.J., and Blowes, D.W., 1994, Influence of siderite on the pore-water chemistry of inactive mine tailings impoundments; *in* Alpers, C.N., and Blowes, D.W. (eds.), *Environmental Geochemistry of Sulfide Oxidation: ACS Symposium Series 550*, American Chemical Society, Washington, D.C., pp. 172–189.
- Puckett, L.J., and Bricker, O.P., 1992, Factors controlling the major ion chemistry of streams in the Blue Ridge and valley and ridge physiographic provinces of Virginia and Maryland: *Hydrologic Processes*, v. 6, pp. 79–98.
- Reardon, E.J., 1988, Ion interaction parameters for $Al-SO_4$ and their application to the prediction of metal sulfate solubility in binary salt systems: *Journal of Physical Chemistry*, v. 92, pp. 6426–6431.
- Reardon, E.J., 1989, Ion interaction model applied to equilibria in the $NiSO_4-H_2SO_4-H_2O$ system: *Journal of Physical Chemistry*, v. 93, pp. 4630–4636.
- Reardon, E.J., and Beckie, R.D., 1987, Modelling chemical equilibria in acid mine drainage—The $FeSO_4-H_2SO_4-H_2O$ system: *Geochimica et Cosmochimica Acta*, v. 51, pp. 2355–2368.
- Reed, M.H., 1982, Calculation of multicomponent chemical equilibria and reaction processes in systems involving mineral, gases, and an aqueous phase: *Geochimica et Cosmochimica Acta*, v. 46, pp. 513–528.
- Reed, M.H., 1984, Geology, wall-rock alteration, and massive sulfide mineralization in a portion of the West Shasta mining district, California: *Economic Geology*, v. 79, pp. 1299–1318.
- Reed, M.H., and Spycher, N., 1984, Calculation of pH and mineral equilibria in hydrothermal waters with application to geothermometry and studies of boiling and dilution: *Geochimica et Cosmochimica Acta*, v. 48, pp. 1479–1492.
- Rimstidt, J.D., Chermak, J.A., and Gagen, P.M., 1994, Rates of reaction of galena, sphalerite, chalcopyrite, and arsenopyrite, with Fe(III) in acidic solution; *in* Alpers, C.N., and Blowes, D.W. (eds.), *Environmental Geochemistry of Sulfide Oxidation: ACS Symposium Series 550*, American Chemical Society, Washington, D.C., pp. 2–13.
- Ripmeester, J.A., Ratcliffe, C.I., Dutrizac, J.E., and Jambor, J.L., 1986, Hydronium ion in the alunite-jarosite group: *Canadian Mineralogy*, v. 24, p. 435–447.
- Rose, N. M., 1991, Dissolution rates of prehnite, epidote, and albite: *Geochimica et Cosmochimica Acta*, v. 55, pp. 3273–3286.
- Rowe, G.L., Jr., and Brantley, S.L., 1993, Estimation of the dissolution rates of andesitic glass, plagioclase, and pyroxene in a flank aquifer of Poás Volcano, Costa Rica; *in* Brantley, S.L., and Velbel, M.A. (eds.), *Geochemical Kinetics of Mineral-Water Reactions in the Field and the Laboratory: Chemical Geology*, v. 105, pp. 71–87.
- Rubin, J., 1983, Transport of reacting solutes in porous media—Relation between mathematical nature of problem formulation and chemical nature of reactions: *Water Resources Research*, v. 19, pp. 1231–1252.
- Runkel, R.L., and Broshears, R.E., 1991, One-dimensional transport with inflow and storage (OTIS)—A solute transport model for small streams: Technical Report 91–01, CADSWES (Center for Advanced Decision Support for Water and Environmental Systems), Univ. of Colorado, Boulder, Colo., 85 pp.
- Runkel, R.L., Bencala, K.E., and Broshears, R.E., 1996, An equilibrium-based simulation model for reactive solute transport in small streams; *in* Morganwalp, D.W., and Aronson, D.A. (eds.), *U.S. Geological Survey Toxic Substances Hydrology Program, Proceedings of the Technical Meeting, Colorado Springs, Colo., Sept. 20–24, 1993: U.S. Geological Survey Water-Resources Investigations Report 94–4014*, pp. 775–780.
- Runnells, D.D., Shepherd, T.A., and Angino, E.E., 1992, Metals in water—Determining natural background concentrations in mineralized areas: *Environmental Science and Technology*, v. 26, pp. 2316–2323.
- Saxena, S.R., 1973, *Thermodynamics of rock-forming crystalline solutions: Springer-Verlag, New York.*
- Schecher, W.D., and McAvoy, D.C., 1991, MINEQL+—A chemical equilibrium program for personal computers, User's manual, version 2.1: Proctor and Gamble Company, Cincinnati, Ohio (version 2.23 available since November 1992).
- Scott, K., 1987, Solid solution in, and classification of, gossan-derived members of the alunite-jarosite family, Northwest Queensland, Australia: *American Mineralogy*, v. 72, pp. 178–187.
- Shock, E.L., and Helgeson, H.C., 1988, Calculation of the thermodynamic and transport properties of aqueous species at high pressures and temperatures—Correlation algorithms for ionic species and equation of state predictions to 5 kb and 1000°C: *Geochimica et Cosmochimica Acta*, v. 52, pp. 2009–2036.
- Shock, E.L., and Helgeson, H.C., 1990, Calculation of the thermodynamic and transport properties of aqueous species at high pressures and temperatures—Standard partial molal properties of organic species: *Geochimica et Cosmochimica Acta*, v. 54, pp. 915–945.
- Shock, E.L., and Koretsky, C.M., 1993, Metal-organic complexes in geochemical processes—Calculation of standard partial molal thermodynamic properties of aqueous acetate complexes at high pressures and temperatures: *Geochimica et Cosmochimica Acta*, v. 57, pp. 4899–4922.
- Shock, E.L., Helgeson, H.C., and Sverjensky, 1989, Calculation of the thermodynamic and transport properties of aqueous species at high pressures and temperatures—Standard partial molal properties of inorganic neutral species: *Geochimica et Cosmochimica Acta*, v. 53, pp. 2157–2183.
- Shock, E.L., Oelkers, E.H., Johnson, J.W., Sverjensky, D.A., and Helgeson, H.C., 1992, Calculation of the thermodynamic properties of aqueous species at high pressures and temperatures—Effective electrostatic radii, dissociation constants, and standard partial molal properties to 1000°C and 5 kb: *Journal of Chemical Society, Faraday Transactions*, v. 88, pp. 803–826.
- Siegel, M.D., Tripathi, V.S., Rao, M.G., and Ward, D.B., 1992, Development and validation of a multi-site model for adsorption of metals by mixtures of minerals, 1. Overview and preliminary results; *in* Kharaka, Y.K., and Maest, A.S. (eds.), *Water-Rock Interaction, Proceedings of the 7th International Symposium on Water-Rock Interaction: A.A. Balkema, Brookfield, Vt.*, v. 1, pp. 63–67.
- Smith, K.S., 1999, Metal sorption on mineral surfaces—An overview with examples relating to mineral deposits; *in* Plumlee, G.S., and Logsdon, M.J. (eds.), *The Environmental Geochemistry of Mineral Deposits, Part A. Processes, Techniques, and Health Issues: Society of*

- Economic Geologists, *Reviews in Economic Geology*, v. 6A, pp. 161–182.
- Smith, K.S., and Huyck, H.L.O., 1999, An overview of the abundance, relative mobility, bioavailability, and human toxicity of metals; *in* Plumlee, G.S., and Logsdon, M.J. (eds.), *The Environmental Geochemistry of Mineral Deposits, Part A. Processes, Techniques, and Health Issues: Society of Economic Geologists, Reviews in Economic Geology*, v. 6A, pp. 29–70.
- Sposito, G., and Coves, J., 1988, SOILCHEM—A computer program for the calculation of chemical speciation in soils: Report, Kearny Foundation, Univ. of California, Riverside and Berkeley, Calif.
- Sposito, G., and Mattigod, S.V., 1980, GEOCHEM—A computer program for the calculation of chemical equilibria in soil solutions and other natural water systems: Report, Kearny Foundation, Univ. of California, Riverside and Berkeley, Calif., 92 pp.
- Spycher, N.F., and Reed, M.H., 1989a, CHILLER—A program for computing water-rock reactions, boiling, mixing, and other reaction processes in aqueous-mineral-gas systems: Manual, Univ. of Oregon, Eugene, Oreg.
- Spycher, N.F., and Reed, M.H., 1989b, Evolution of a Broadlands-type epithermal ore fluid along alternative P-T paths—Implications for the transport and deposition of base, precious, and volatile metals: *Economic Geology*, v. 84, pp. 328–359.
- Stillings, L.L., and Brantley, S.L., 1995, Feldspar dissolution at 25°C and pH 3—Reaction stoichiometry and the effect of ionic strength: *Geochimica et Cosmochimica Acta*, v. 59, pp. 1483–1496.
- Stipp, S.L.S., Parks, G.A., Nordstrom, D.K., and Leckie, J.O., 1993, Solubility-product constant and thermodynamic properties for synthetic otavite, $\text{CdCO}_3(\text{s})$ and aqueous association constants for the $\text{Cd}(\text{II})\text{-CO}_2\text{-H}_2\text{O}$ system: *Geochimica et Cosmochimica Acta*, v. 57, pp. 2699–2713.
- Stoffregen, R.E., and Alpers, C.N., 1987, Woodhouseite and svanbergite in hydrothermal ore deposits—Products of apatite destruction during advanced argillic alteration: *Canadian Mineralogist*, v. 45, pp. 201–211.
- Stoffregen, R.E., and Alpers, C.N., 1992, Observations on the unit-cell dimensions, H_2O contents, and δD of natural and synthetic alunite: *American Mineralogist*, v. 77, pp. 1092–1098.
- Stollenwerk, K.G., 1994, Geochemical interactions between constituents in acidic groundwater and alluvium in an aquifer near Globe, Arizona: *Applied Geochemistry*, v. 9, pp. 353–369.
- Stookey, L.L., 1970, Ferrozine—A new spectrophotometric reagent for iron: *Analytical Chemistry*, v. 42, pp. 779–781.
- Sverjensky, D.A., 1987, Calculation of the thermodynamic properties of aqueous species and the solubilities of minerals in supercritical electrolyte solutions; *in* Carmichael, I.S.E., and Eugster, H.P. (eds.), *Thermodynamic Modeling of Geological Materials—Minerals, Fluids, and Melts: Reviews in Mineralogy, Mineralogy Society of America, Washington, D.C.*, v. 17, pp. 97–142.
- Swoboda-Colberg, N.G., and Drever, J.I., 1993, Mineral dissolution rates in plot-scale field and laboratory experiments; *in* Brantley, S.L., and Velbel, M.A. (eds.), *Geochemical Kinetics of Mineral-Water Reactions in the Field and the Laboratory: Chemical Geology*, v. 105, pp. 51–69.
- Thompson, J.B., Jr., 1967, Thermodynamic properties of simple solutions; *in* Abelson, P.H. (ed.), *Researches in Geochemistry II: John Wiley and Sons, New York*, pp. 340–361.
- To, B.T., Nordstrom, D.K., Cunningham, K.M., Ball, J.W., and McCleskey, R.B., 1999, New method for the direct determination of dissolved Fe(III) concentration in acid mine waters: *Environmental Science and Technology*, v. 33, pp. 807–813.
- Truesdell, A.H., and Jones, B.F., 1973, WATEQ, A computer program for calculating chemical equilibria of natural waters: National Technical Information Service, NTIS PB 220-464, Springfield, Va., 77 pp.
- Truesdell, A.H., and Jones, B.F., 1974, A computer program for calculating chemical equilibria of natural waters: *U.S. Geological Survey Journal of Research*, v. 2, pp. 233–248.
- Velbel, M.A., 1985, Geochemical mass balances and weathering rates in forested watersheds of the southern Blue Ridge: *American Journal of Science*, v. 285, pp. 904–930.
- Velbel, M.A., 1993, Constancy of silicate-mineral weathering-rate ratios between natural and experimental weathering—Implications for hydrologic control of differences in absolute rates; *in* Brantley, S.L., and Velbel, M.A. (eds.), *Geochemical Kinetics of Mineral-Water Reactions in the Field and the Laboratory: Chemical Geology*, v. 105, pp. 89–99.
- Viani, B.E., and Bruton, C.J., 1992, Modeling fluid-rock interaction at Yucca Mountain, Nevada—A progress report: UCRL-ID-109921, Lawrence Livermore National Laboratory, Livermore, Calif.
- Villas, R.N., and Norton, D., 1977, Irreversible mass transfer between circulating hydrothermal fluids and the Mayflower stock: *Economic Geology*, v. 72, pp. 1471–1504.
- Waite, T.D., 1989, Mathematical modeling of trace element speciation; *in* Batley, G.E. (ed.), *Trace Element Speciation—Analytical Methods and Problems: CRC Press, Boca Raton, Fla.*, pp. 117–184.
- Walter, A.L., Frind, E.O., Blowes, D.W., Ptacek, C.J., and Molson, J.W., 1994a, Modeling of multicomponent reactive transport in groundwater, 1. Model development and evaluation: *Water Resources Research*, v. 30, 3137–3148.
- Walter, A.L., Frind, E.O., Blowes, D.W., Ptacek, C.J., and Molson, J.W., 1994b, Modeling of multicomponent reactive transport in groundwater, 2. Metal mobility in aquifers impacted by acidic mine tailings discharge: *Water Resources Research*, v. 30, pp. 3149–3158.
- Waychunas, G.A., Rea, B.A., Fuller, C.C., and Davis, J.A., 1993, Surface chemistry of ferrihydrite, Part I. EXAFS studies of the geometry of coprecipitated and adsorbed arsenate: *Geochimica et Cosmochimica Acta*, v. 57, pp. 2251–2270.
- Webster, J.G., Nordstrom, D.K., and Smith, K.S., 1994, Transport and natural attenuation of Cu, Zn, As, and Fe in the acid mine drainage of Leviathan and Bryant Creeks; *in* Alpers, C.N., and Blowes, D.W. (eds.), *Environmental Geochemistry of Sulfide Oxidation: ACS Symposium Series 550, American Chemical Society, Washington, D.C.*, pp. 244–260.
- Westall, J.C., 1979, MICROQL, I. A chemical equilibrium program in BASIC; II. Computation of adsorption equilibria in BASIC: Swiss Institute of Technology, EAWAG, 77 pp.
- Westall, J.C., Zachary, J.L., and Morel, F.M.M., 1976, MINEQL, A computer program for the calculation of chemical equilibrium composition of aqueous systems: Technical note no. 18, Massachusetts Institute of Technology, Cambridge, Mass., 91 pp.
- White, A.F., and Brantley, S.L., (eds.), 1995, Chemical weathering rates of silicate minerals: *Reviews in Mineralogy, Mineralogical Society of America, Washington, D.C.*, v. 31, 583 pp.
- Wiersma, C.L., and Rimstidt, J.D., 1984, Rates of reaction of pyrite and marcasite with ferric iron at pH 2: *Geochimica et Cosmochimica Acta*, v. 48, pp. 85–92.
- Wolery, T.J., 1979, Calculation of chemical equilibrium between aqueous solution and minerals—The EQ3/6 software package: Lawrence Livermore National Laboratory Report UCRL-52658, Livermore, Calif., 41 pp.
- Wolery, T.J., 1983, EQ3NR, a computer program for geochemical aqueous speciation-solubility calculations—User's guide and documentation: Lawrence Livermore National Laboratory Report UCRL-53414, Livermore, Calif., 191 pp.
- Wolery, T.J., 1992a, EQ3/6, A software package for geochemical modeling of aqueous systems—Package overview and installation guide, version 7.0: Lawrence Livermore National Laboratory Report UCRL-MA-110662 PT I, Livermore, Calif., 66 pp.
- Wolery, T.J., 1992b, EQ3NR, A computer program for geochemical aqueous speciation solubility calculations—Theoretical manual, user's guide, and related documentation, version 7.0: Lawrence Livermore National Laboratory Report UCRL-MA-110662 PT III, Livermore, Calif., 246 pp.
- Wolery, T.J., 1994, Letter report: EQ 3/6 version 8—Differences from version 7: Lawrence Livermore National Laboratory Report UCRL-ID-129749, 26 pp.
- Wolery, T.J., and Daveler, S.A., 1992, EQ6, A computer program for reaction path modeling of aqueous geochemical systems—Theoretical manual, user's guide, and related documentation, version 7.0: Lawrence Livermore National Laboratory Report UCRL-MA-110662

- PT IV, Livermore, Calif., 338 pp.
- Wolery, T.J., Jackson, K.J., Bourcier, W.L., Bruton, C.J., Viani, B.E., Knauss, K.G., and Delany, J.M., 1990, Current status of the EQ3/6 software package for geochemical modeling; *in* Melchior, D.C., and Bassett, R.L. (eds.), *Chemical Modeling of Aqueous Systems II: ACS Symposium Series 416*, American Chemical Society, Washington, D.C., pp. 104–116.
- Wollast, R., and Chou, L., 1985, Kinetic study of the dissolution of albite with a continuous flow-through fluidized bed reactor; *in* Drever, J.I. (ed.), *The Chemistry of Weathering*: D. Reidel Publishing Co., pp. 75–96.
- Wood, B.J., and Walther, J.V., 1983, Rates of hydrothermal reactions: *Science*, v. 222, pp. 413–415.
- Wunderly, M.D., Blowes, D.W., Frind, E.O., Ptacek, C.J., and Al, T.A., 1995, A multicomponent reactive transport model incorporating kinetically controlled pyrite oxidation; *in* Hynes, T.P., and Blanchette, M.C. (eds.), *Proceedings of Sudbury '95, Mining and the Environment*, May 28–June 1, 1995: Sudbury, Ontario, Canada, v. 3, pp. 989–997.
- Wunderly, M.D., Blowes, D.W., Frind, E.O., and Ptacek, C.J., 1996, Sulfide mineral oxidation and subsequent reactive transport of oxidation products in mine tailings impoundments—A numerical model: *Water Resources Research*, v. 32, pp. 3173–3187.
- Yeh, G.T., and Tripathi, V.S., 1989a, A critical evaluation of recent developments in hydrogeochemical transport models of reactive multicomponent systems: *Water Resources Research*, v. 25, pp. 93–108.
- Yeh, G.T., and Tripathi, V.S., 1989b, HYDROGEOCHEM, A coupled model of hydrologic transport and geochemical equilibria of reactive multicomponent systems: Oak Ridge National Laboratory Report ORNL-6371, Oak Ridge, Tenn.
- Following the preparation of this chapter, several books and research papers have been published on the topic of geochemical modeling of water-rock reactions, with reference to the formation of acid mine drainage and other environmental aspects of mining. The supplemental list of references provided below is not intended to be a comprehensive update, but rather a guide to some of the more significant recent publications in this expanding area of research.
- Bethke, C.M., 1996, *Geochemical reaction modeling—Concepts and applications*: Oxford University Press, New York, 397 pp.
- Bigham, J.M., Schwertmann, U., Traina, S.J., Winland, R.L., and Wolf, M., 1996, Schwertmannite and the chemical modeling of iron in acid sulfate waters: *Geochimica et Cosmochimica Acta*, v. 60, pp. 2111–2121.
- Brown, J.G., Bassett, R.L., and Glynn, P.D., 1998, Analysis and simulation of reactive transport of metal contaminants in ground water in Pinal Creek Basin, Arizona: *Journal of Hydrology*, v. 209, pp. 225–250.
- Gerke, H.H., Molson, J.W., and Frind, E.O., 1998, Modelling the effect of chemical heterogeneity of acidification and solute leaching in overburden mine spoils: *Journal of Hydrology*, v. 209, pp. 166–185.
- Glynn, P., and Brown, J., 1996, Reactive transport modeling of acidic metal-contaminated ground water at a site with sparse spatial information; *in* Lichtner, P.C., Steefel, C.I., and Oelkers, E.H., (eds.), *Reactive Transport in Porous Media: Reviews in Mineralogy, Mineralogical Society of America*, v. 34, pp. 377–438.
- Grenthe, I., and Puigdomenech, I. (eds.), 1997, *Modelling in aquatic geochemistry*: Nuclear Energy Agency, Organization for Economic Cooperation and Development, Paris, France, 726 pp.
- Kaszuba, J.P., Harrison, W.J., and Wendlandt, R.F., 1995, Geochemical modeling of waste rock leachate generated in precious metal mines; *in* *Tailings and Mine Waste '95*: Balkema, Rotterdam, pp. 23–34.
- Langmuir, D., 1997, *Aqueous environmental geochemistry*: Prentice Hall, Upper Saddle River, N.J., 576 pp.
- Lichtner, P.C., Steefel, C.I., and Oelkers, E.H., (eds.), 1996, *Reactive Transport in Porous Media: Reviews in Mineralogy, Mineralogical Society of America*, Washington, D.C., v. 34, 438 pp.
- Perkins, E.H., Nesbitt, H.W., Gunter, W.D., St-Arnaud, L.C., and Mycroft, J.R., 1995, Critical review of geochemical models adaptable for prediction of acidic drainage from waste rock: MEND (Mine Environment Neutral Drainage Program) Project 1.42.1, MEND Secretariat, CANMET (Canadian Centre for Mineral and Energy Technology), Ottawa, Ontario, Canada, 265 pp.
- Perkins, E.H., Gunter, W.D., Nesbitt, H.W., and St-Arnaud, L.C., 1997, Critical review of classes of geochemical computer models adaptable for prediction of acidic drainage from mine waste rock; *in* *Proceedings, 4th Internatl Conference on Acid Rock Drainage*: Vancouver, B.C., Canada, May 31–June 6, 1997, pp. 587–601.
- Runkel, R.L., Bencala, K.E., Broshears, R.E., and Chapra, S.C., 1996, Reactive solute transport in streams, I. Development of an equilibrium-based model: *Water Resources Research*, v. 32, pp. 409–418.
- Runkel, R.L., McKnight, D.M., Bencala, K.E., and Chapra, S.C., 1996, Reactive solute transport in streams, II. Simulation of a pH-modification experiment: *Water Resources Research*, v. 32, pp. 419–430.
- Schnoor, J.L., 1996, *Environmental modeling—Fate and transport of pollutants in air, water, and soil*: Wiley-Interscience, New York, 682 pp.
- Steefel, C.I., and Van Cappellen, P., 1998, Reactive transport modeling of natural systems: *Journal of Hydrology*, v. 209, pp. 1–7.

Chapter 15

STATIC-TEST METHODS MOST COMMONLY USED TO PREDICT ACID-MINE DRAINAGE: PRACTICAL GUIDELINES FOR USE AND INTERPRETATION

W.W. White III,¹ K.A. Lapakko,² and R.L. Cox³

¹*U.S. Department of the Interior, Research Center, Bureau of Mines, Salt Lake City, UT 84108**

²*Division of Minerals, Minnesota Department of Natural Resources, St. Paul, MN 55155*

³*2329 West Henry Alice Circle, West Jordan, UT 84084*

INTRODUCTION

Acid mine drainage (AMD) is contaminated effluent from mines and mining wastes that results from the oxidation of iron-sulfide minerals exposed to air and water. The intensity and duration of AMD formation are complex functions of deposit geology, mineralogy, and hydrology, and the subsequent interaction of climatic conditions upon ore and waste when exposed by various mining methods. Because AMD can produce effluent containing acid- and heavy-metal concentrations that exceed water quality standards and is perceived as irreversible once started, it is one of the more vexing environmental problems facing land-managing agencies and the minerals industry today. Consequently, reliable prediction tools that quantify the risk for a particular mine waste to produce AMD are actively sought by the minerals industry and regulators.

Today numerous tools in the form of various laboratory "static"- and "kinetic"-predictive tests are available for fees that range from \$35 to as much as \$5,200 per sample. Static tests are short term (usually measured in hours or days) and relatively low cost per sample (from \$35 to \$135). Their objective is to provide an estimate of a mine waste's capacity to produce acid and its capacity to neutralize acid. One shortcoming of static tests is that they measure only the capacities for acid production and consumption and do not consider the differences between the respective dissolution rates of acid-producing and acid-consuming minerals. Another potential source of error inherent to static-test-data interpretation is the assumption that all acid-producing and acid-consuming minerals present will react completely, an assumption which ignores the influence of acid-producing and acid-consuming mineral particle-size and morphology.

Kinetic tests are long term (usually measured in months and sometimes years) and expensive per sample (from \$500 to as much as \$5,200). Their objectives are to confirm or reduce uncertainty in static-test classifications (i.e., the sample is either acid- or non-acid producing), identify dominant chemical-weathering reactions, and determine acid-generation rates and temporal variations in leachate water quality. This is accomplished by accelerating the natural weathering rate of a mine-waste sample under closely controlled laboratory conditions (Lapakko, 1988; Lawrence, 1990; White and Jeffers, 1994). One shortcoming of kinetic tests is the extended amount of time required to perform the tests, as it is not uncommon for these tests to continue for at least 20 weeks (e.g., Lapakko and Wessels, 1995).

As state and federal land-managing agencies have become aware of these predictive tests, they have required operators to subject larger populations of mine-waste samples to a variety of predictive tests as part of the permitting process. Because several different kinds of laboratory-predictive tests are now available, both operator and regulator have asked similar questions such as:

- 1) which tests are most commonly used today,
- 2) how are these tests performed, and
- 3) how accurate are these tests?

These questions are partially addressed by the objectives of this paper, which are to:

- 1) summarize mine-waste dissolution chemistry and its relationship to data produced by laboratory-predictive tests,
- 2) identify the static-test methods most commonly used in the United States and Canada,
- 3) summarize their protocols,
- 4) identify sources of error in neutralization potential (NP) determinations and quantify their influence on selected samples, and
- 5) suggest measures to improve NP determination accuracy.

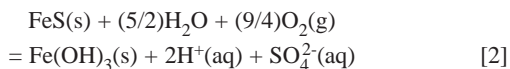
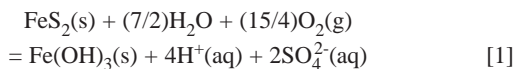
Previous analyses of predictive tests have been presented by Perry (1985), Ferguson (1985), Ferguson and Mehling (1986), Ferguson and Erickson (1988), Coastech Research Inc. (1989), Bradham and Caruccio (1991), and Lapakko (1992a, 1993, 1994a). This report includes relevant questions and conclusions from the more recent literature. It elucidates these points and draws additional conclusions based on data generated by selected static tests on mine-waste samples obtained from a variety of metal-mine settings. These tests were performed from 1991 through 1995 in the course of cooperative AMD-related studies by Minnesota Department of Natural Resources (MDNR) and the U.S. Bureau of Mines (USBM).

MINE WASTE DISSOLUTION

Sources of acid

The dissolution of iron sulfide minerals such as pyrite and pyrrhotite is responsible for the majority of mine-waste acid production (Stumm and Morgan, 1981). Equations [1] and [2] are commonly published reactions believed to represent typical pyrite and pyrrhotite chemical-weathering products (after Stumm and Morgan, 1981; Nelson, 1978):

*currently with Bureau of Land Management, Salt Lake Field Office, 2370 South 2300 West, Salt Lake City, UT 84119



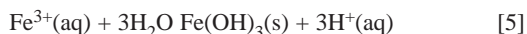
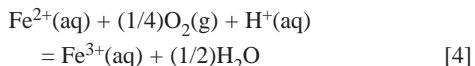
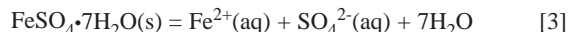
These weathering reactions produce acidic, iron- and sulfate-rich aqueous water which can

- 1) contact sulfide minerals and accelerate their oxidation,
- 2) evaporate partially or totally to precipitate hydrated iron-sulfate and other minerals and (or)
- 3) contact host rock minerals which react to neutralize some or all of the acid.

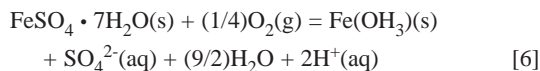
Acidic flow which migrates through the mine waste will exit as AMD.

Hydrated iron-sulfate minerals precipitate during the evaporation of acidic, iron- and sulfate-rich water within mine-waste materials and store (for potential subsequent release) acid generated by iron sulfide mineral oxidation. The more common hydrated iron-sulfate minerals that occur as efflorescent salts on the surfaces of weathering pyrite include melanterite, rozenite, szomolnokite, romerite and copiapite ($\text{FeSO}_4 \cdot 7\text{H}_2\text{O}$, $\text{FeSO}_4 \cdot 4\text{H}_2\text{O}$, $\text{FeSO}_4 \cdot \text{H}_2\text{O}$, $\text{Fe}^{2+}\text{Fe}_2^{3+}(\text{SO}_4)_4 \cdot 14\text{H}_2\text{O}$, and $\text{Fe}^{2+}\text{Fe}_4^{3+}(\text{SO}_4)_6(\text{OH})_2 \cdot 20\text{H}_2\text{O}$, respectively) (Alpers et al., 1994). According to Nordstrom (1982) and Cravotta (1994), these sulfate salts are highly soluble and provide an instantaneous source of acidic water upon dissolution and hydrolysis. They are partially responsible for increased acidity and metals loadings in the receiving environment during rainstorm events.

As an example, equations [3], [4], and [5] summarize the stepwise dissolution of melanterite.

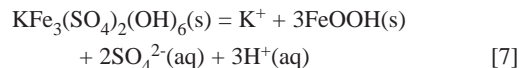


The net result of equations [3] through [5] is summarized in equation [6], which shows a net production of two moles, acid produced for each mole of melanterite dissolved.



Cravotta (1994) showed that a similar aqueous dissolution of romerite produced six moles of acid for each mole of romerite dissolved. The cumulative storage and incremental release of acid from these salts may help explain the lag from mine-waste placement to AMD-formation particularly in arid climates.

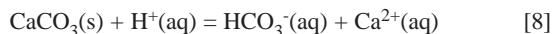
According to Nordstrom (1982), the formation of hydrated iron sulfates is an important intermediate step that precedes the precipitation of the more common insoluble iron minerals such as goethite and jarosite. However, jarosite is slightly soluble (Alpers et al., 1994) and can, therefore, contribute acid according to equation [7]. For example, recent preliminary leach studies



on natural and synthetic jarosites conducted by USBM showed a drop in pH from 6 in the deionized water leachate to 3 or 4 after contact with the jarosites. Because of its relatively low solubility, the acid contributed by jarosite dissolution is probably small relative to that by dissolution of more soluble hydrated iron sulfates.

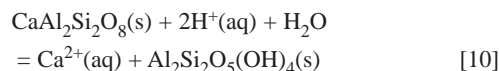
Sources of neutralization

The balance between the rates of acid production by iron-sulfide mineral oxidation and host rock buffering will determine the acidity of mine-waste drainage. The most effective minerals for neutralizing acid are those containing calcium carbonate and magnesium carbonate. Examples include calcite, magnesite, dolomite, and ankerite (CaCO_3 , MgCO_3 , $\text{CaMg}(\text{CO}_3)_2$, and $\text{CaFe}(\text{CO}_3)_2$, respectively). Equation [8] represents the dominant dissolution reaction of calcite (CaCO_3) with iron-sulfide-generated acid (H^+) above pH 6.4, while equation [9] is the dominant reaction below pH 6.4 (Drever, 1988):



The dissolution rates for the calcite reactions shown in equations [8] and [9] are relatively rapid. However, dissolution rates are not the same for all carbonates; for example, Rauch and White (1977) and Busenberg and Plummer (1986) have reported that the rates of magnesium carbonate and calcium-magnesium carbonate (i.e., magnesite and dolomite) dissolution are substantially slower than that of calcium carbonate. Additionally, iron carbonates do not provide for net acid neutralization under oxidizing conditions, due to oxidation of the ferrous iron released, subsequent precipitation of ferric hydroxide, and the consequent acid production (reactions 4, 5).

Dissolution of silicates such as plagioclase-feldspar minerals (e.g., anorthite in equation [10], Busenberg and Clemency, 1976) and olivine minerals (e.g., forsterite in equation [11], Hem, 1970) can also neutralize acid under acidic conditions, but their dissolution rates (and subsequent acid neutralization) are slow relative to the carbonate minerals.





The effectiveness of silicate-mineral neutralization is thought to be optimized by these factors:

- 1) the acid-production rate is relatively slow,
- 2) feldspar minerals comprise a significant percentage of the overall mineralogy, and
- 3) the available silicate-mineral surface area is large (Morin and Hutt, 1994).

STATIC TEST METHODS

The most commonly-used static test is known as acid-base accounting (ABA; Ferguson and Erickson, 1988). Several variations of ABA are in use in the United States and Canada (Lapakko, 1992a); they include standard ABA (Sobek et al., 1978), modified ABA (Coastech Research Inc., 1989; Lawrence, 1990; Reclamation Research Unit and Schafer and Associates, 1987), the B.C. Research Initial Test (BCRI, Bruynesteyn and Duncan, 1979), and the NP(pH6) Test (Lapakko, 1994a). This report will focus on these tests.

The Net Acid Production (NAP) (Coastech Research Inc., 1989) and Net Acid Generation (NAG) (Miller et al., 1990) tests are based on the principle that hydrogen peroxide accelerates the oxidation of iron sulfide minerals. The acid consequently produced dissolves neutralizing minerals present, and the net result of the acid production and neutralization can be measured directly. This test does not require sulfur determinations and is, therefore, more readily conducted in a field laboratory than other static tests. Problems associated with this type of test and a modification of the protocol are presented elsewhere (Lapakko, 1992a, 1993; Lapakko and Lawrence, 1993). Hydrogen peroxide based tests are not discussed here. Likewise, the paste pH test (Sobek et al., 1978) and the acid concentration present test (Bucknam, personal commun., 1994), which measure the acid present on mine-waste particles, are not addressed in this report.

Acid-base accounting

Principles

The acid-base accounting (ABA) test was originally designed to evaluate the acid-producing capability of coal-mine wastes. It is now used to evaluate both coal- and metal-mine wastes. ABA measures the balance between the acid-producing potential (AP) and acid-neutralizing potential (NP) of each mine-waste sample. AP is determined by sulfur assay and represents the sulfur contained in acid-generating iron-sulfide minerals present in the sample. The AP value is calculated based on the assumption that two moles of acid will be produced for each mole of sulfur present (equations [1] and [2]). Because one mole of calcium carbonate will neutralize the two moles of acid (equation [9]), the percent sulfur obtained from the sulfur assay is multiplied by 31.25¹ to yield AP in units of tons calcium carbonate equivalent per thousand tons mine waste. NP is determined by subjecting the mine-waste sample to some form of acid digestion and represents the amount of acid-neutralizing carbonate minerals present in the sample. NP value is also reported in units of tons calcium carbonate per thou-

sand tons of mine waste. This report expresses AP and NP in equivalent and more concise units of kg calcium carbonate per ton of mine waste or kg/t CaCO₃.

Net-neutralizing potential (NNP), which is the difference between these values (NP - AP = NNP), is one of the measurements used to classify a mine-waste sample as potentially acid or non-acid producing. The NNP is often called the "acid-base account" of the sample. If NP is greater than AP, NNP is positive; conversely, if NP is less than AP, NNP is negative.

The question of how positive or negative the NNP must be for a sample to be considered safely non-acid producing (or conversely, definitely acid producing) has been a source of classification controversy. Recent ABA classifications for mine-waste samples are based on both NNP and the NP/AP ratio (i.e., if NP > AP, then NP/AP > 1; conversely, if NP < AP, then NP/AP < 1). Three categories comprise the ABA classification ("high," "uncertain," and "low" acid-producing potential). The ranges of NNP and NP/AP values included in each of the three categories have been described by Brodie et al. (1991), Day (1989), Ferguson and Morin (1991), and Morin and Hutt (1994) and are shown in Table 15.1. Note the variability in the NNP values for each category as compared with the more consistent corresponding NP/AP values. Also note that NNP values have not been defined for the "non acid" category. Samples classified in the "uncertain" category are typically subjected to kinetic testing (Ferguson and Morin, 1991).

TABLE 15.1—Interpretation of acid-producing potential for samples subjected to ABA static tests, based on NNP (kg/t CaCO₃) and NP/AP ratio.

Acid-Base Account	Acid	Uncertain	Non-Acid
NNP:			
Appalachian coal-mine criterion ¹	<-5	ND	ND
B.C. metal-mine criterion ²	≤ 0	ND	ND
Ferguson & Morin, 1991, p. 86	ND	-20 < NNP < +20	ND
Day, 1989	< +10	ND	ND
NP/AP:			
Brodie et al., 1991, p. 121	< 1	1 < NP/AP < 3	> 3
Morin & Hutt, 1994, p. 148	< 1	1 < NP/AP < 1.3 to 4.0	> 1.3 to 4.0

¹Sobek, et al., 1978, p. 3.

²Ferguson and Morin, 1991, p. 86.

ND, not defined in reference.

K.A. Morin (1989, oral commun.) observed threshold NNP values for acid production of -15, +10, and +20 kg/t CaCO₃ for a modified procedure on various sets of samples.

The ABA classification that requires a mine-waste sample to meet or exceed an NP/AP ratio of 3 to 1 to be considered non-acid producing has interesting ramifications when sample sulfide content approaches 9%. If the sulfide is present as pyrite, the pyrite would represent about 17% of the sample mass; and, if the sulfide is present as pyrrhotite, the pyrrhotite would make up about 21% of the sample mass. In either case, all of the remaining sample

¹A 1 to 1 mole ratio of S to CaCO₃ (32 g/mole and 100 g/mole, respectively) is equal to a weight ratio of 1:3.125. Multiplying the weight-percent sulfur contained in the sample by 3.125 converts the sulfur to weight percent calcium carbonate required to neutralize the produced acid; multiplying by 31.25 yields the required amount of calcium carbonate in parts per thousand.

mass would have to be calcium carbonate to meet the 3 to 1 criterion. Therefore, mine-waste samples containing more than 9% sulfide would be classified as acid producers during the initial sample screening process (Lapakko, 1992a). Table 15.2 compares percent sulfide (converted to percent pyrite and pyrrhotite) with the corresponding percent of calcium carbonate required to be present in the sample to meet 3 to 1 criterion proposed by California and Montana, and 1.2 to 1 criterion required by Nevada (U.S. EPA, 1994, Table 7).

TABLE 15.2—Percent sulfide converted to percent pyrite and pyrrhotite, and compared with corresponding percent calcium carbonate required to meet NP/AP 3:1 and 1.2:1 criteria.

Sulfide (S ²⁻)	Weight Percent		NP/AP	
	Pyrite (FeS ₂)	Pyrrhotite (Fe ₅ S ₆ - Fe ₁₆ S ₁₇) ¹	3:1 ² % CaCO ₃	1.2:1 ³ (% CaCO ₃)
0.25	0.47	0.61 – 0.66	2.34	0.94
0.50	0.94	1.23 – 1.32	4.69	1.87
1.00	1.88	2.46 – 2.65	9.38	3.75
3.00	5.63	7.38 – 7.94	28.13	11.25
5.00	9.38	12.29 – 13.24	46.88	18.75
7.00	13.13	17.21 – 18.53	65.63	26.25
8.50	15.94	20.90 – 22.50	79.69	31.88
8.89	16.67	NAP	83.34	33.34

¹Range of compositional variation (Dana, 1963, p. 428).

²California and Montana (% S²⁻ × 3.125 × 3 = % CaCO₃).

³% S²⁻ × 3.125 × 1.2 = % CaCO₃.

NAP, not applicable.

Protocols

Standard ABA Method—This method was developed by Smith et al. (1974) and later modified by Sobek et al. (1978); it is often referred to as the standard Sobek method. The AP is determined based on the total sulfur content obtained by sulfur assay and assumes that all sulfur is present as sulfide.

The first step in determining the NP is a “fizz” test which is designed to estimate the calcium carbonate and magnesium carbonate content of the sample. An acid solution comprised of one part concentrated hydrochloric acid to three parts water is applied dropwise to 0.5g of sample, and the extent of “fizzing” is observed (the “fizzing” is the result of the reaction of the acid and carbonate present in the sample—equation [9]). Based on the vigor of this reaction, the volume and concentration of hydrochloric acid to be added to 2g of minus 60-mesh mine-waste sample are determined (“no fizz,” 20 ml 0.1N; “slight fizz,” 40 ml 0.1 N; “moderate fizz,” 40 ml 0.5 N; “strong fizz,” 80 ml 0.5 N). The mixture of acid and mine-waste sample is then boiled until the reaction has ceased (as indicated by cessation of bubble production). After the boiling step, the mixture is cooled and titrated to pH 7.0 with sodium hydroxide (NaOH) to measure the amount of acid consumed during its reaction with the sample.

Modified ABA Method—This method, which is also known as the modified Sobek method was developed by Coastech Research Inc. (1989) and described by Lawrence (1990). While similar to the Standard ABA Method in sample mass and acid concentration and volume used, the modified ABA method bases the AP on sulfide content rather than total sulfur. This requires additional steps during analysis to speciate the dominant sulfur forms

present in the sample. This speciation can be accomplished with either a combustion-infrared spectrophotometer (e.g., a LECO furnace), or a sequential, wet-chemical leach (Sobek et al., 1978; see “Carbon-Sulfur Analysis” for details). Basing the AP on the sulfide-sulfur content assumes that sulfur present as sulfate is not acid producing (e.g., sulfate minerals such as gypsum and barite, which are common to some western U.S. metal mines). In place of a heated acid digestion, the modified ABA uses a 24-hour, ambient temperature, agitated acid digestion to determine the NP. At the completion of the 24-hour digestion, the mixture of acid and mine-waste sample is required to have a pH range of 1.5 to 2.0 (if not, the test is re-run with an acid addition that is adjusted based on the previous test’s final pH). A titration endpoint of pH 8.3 is used rather than the reportedly unstable pH 7.0 value used in the standard ABA method (Coastech Research Inc., 1989).

B.C. Research Initial Method—(BCRI, Duncan and Walden, 1975; Bruynesteyn and Duncan, 1979). Although this method uses different terminology and different units of quantification, the terminology and units are translated to be consistent with those of the ABA methods for ease of presentation. As with the standard ABA, AP is based on total sulfur content. NP is determined by titrating, with 10N sulfuric acid, a stirred mixture of 10g mine waste (70% minus 325 mesh or, equivalently, 70% of the particles having diameter less than 0.044 mm) and 100 ml distilled water. The titration is continued until pH 3.5 is reached and less than 0.1 ml of acid is added over a period of 4 hours. More recently, a 1.0N sulfuric acid titrant has been used (O’Hearn, personal commun., 1996).

NP(pH6) Method—The NP(pH6) is the same as the B.C. Research Initial method except for the strength of acid and the endpoint used. Specifically, a slurry comprised of 10g solid and 100 ml deionized water is titrated with 1N sulfuric acid until pH 6.0 is reached, and less than 0.1 ml of acid is added over a period of 4 hours. The resulting volumes of acid for the respective endpoints are then converted to parts per thousand calcium carbonate equivalent (NP). The NP obtained at pH 6 is termed the “effective” NP, or the calcium carbonate equivalent available in the sample to maintain the pH above 6 (Lapakko, 1992b). The NP(pH6) method differs significantly from the previously mentioned tests in that the “digestion” occurs at pH 6 rather than in a more acidic environment.

Modified NP (pH6) Method—A modification of the NP (pH6) method was necessary to evaluate mine-waste samples that contained only traces of actual calcium- or magnesium-carbonate mineral NP, or whose carbonate minerals were mainly iron carbonate (e.g., siderite, ankerite, and ferroan dolomite). These conditions caused titration endpoints to be exceeded with addition of the first drop of titrant during BCRI and NP (pH6) titration methods. The problem was resolved by distributing six to eight 10-g aliquots of the solid sample to separate 400-ml beakers where each sample was slurried with 100 ml of deionized water. No sulfuric acid was added to the slurried sample in the first beaker which served as a control. Pre-selected, progressively-increasing volumes of acid were added to each of the sample slurries contained in their respective beakers (numbered 2 through 6 or 8). All of the sample beakers were then placed on an orbital shaker and agitated for a total of 4 hours. After the first and second 0.5-hour periods, and after three subsequent 1-hour increments, agitation was stopped and pH measurements were taken and recorded for each sample. Recorded pH obtained at specified time intervals from each sample was converted to corresponding hydrogen ion

concentration. Hydrogen ion concentration representing pH 6 and its corresponding acid volume was estimated by interpolation for each sample. The estimated acid volume at pH 6 was converted to calcium-carbonate equivalent NP. The NP obtained at pH 6 is termed the “effective” NP, or the calcium carbonate equivalent available in the sample to maintain the pH above 6 (Lapakko, 1992b).

Carbon-Sulfur (C-S) Analysis—Bucknam (1995a) is developing a consensus-based ASTM-standard method for total carbon and sulfur determination to estimate carbonate, sulfide, and subsequent acid-base account in metal-mine ore, concentrate, tailings and waste-rock samples. The approach is predicated on the concept that all sulfide present is associated with iron (and therefore can be used to quantify acid production potential) and all carbonate is associated with calcium and magnesium (and therefore can be used to quantify acid neutralization potential). Total carbon and sulfur analyses for these samples are determined by a combustion-infrared spectrophotometer (e.g., a LECO furnace). Carbonate and sulfide are determined from sample duplicates through partial-decomposition procedures, followed by combustion-infrared spectrophotometer C-S analysis. The partial-decomposition procedures include pyrolysis (muffle roast at 550°C) and chemical decomposition (individual hydrochloric-acid, nitric-acid, and sodium-carbonate leaches).

The muffle-furnace roast at 550°C drives off sulfide sulfur as sulfur dioxide, and organic carbon as carbon dioxide. The pretreated sample is then analyzed for carbon and sulfur, and the results are subtracted from the total carbon and sulfur results of a non-pretreated sample split. The remaining sulfur determined in the pretreated split is assumed to be sulfate sulfur, and the remaining carbon is considered to be carbonate.

Chemical decomposition using hydrochloric acid is intended to solubilize carbonate minerals. Total carbon and sulfur values from the hydrochloric-acid pretreated sample represent organic carbon, pyritic sulfur, some trace-metal sulfides, and organic sulfur; carbonate carbon is estimated by difference. The purpose of nitric acid decomposition is to oxidize sulfides to sulfate. Sulfate reports to the acid leachate and consequently is separated from the solid phase. The sodium carbonate leach is intended to solubilize all sulfates (with the exception of barite—BaSO₄) while most sulfides are unaffected and remain in the solid phase. When samples are subjected to chemical decomposition, their sulfide-sulfur contents are estimated by subtracting the nitric-acid residual-sulfur value from the sodium-carbonate residual-sulfur value.

This proposed ASTM method for ABA by C-S analysis has been distributed for interlaboratory testing. It will be available

after tests are completed and the method has received the required ASTM-committee approvals (Bucknam, 1995b, written commun.).

An alternative sulfur-speciation method to the C-S analysis method is the sequential, wet-chemical-leach speciation method for sulfur forms (total, sulfide, and sulfate) described in Sobek et al. (1978).

Protocol modifications for this study—Three modifications of standard protocols were made in USBM methods used for the present study. First, a standard minus 150 mesh particle size was used for the standard ABA, modified ABA, and modified NP(pH6) tests. This was done to normalize for particle size effects. The minus 150 mesh fraction was selected since it was used by USBM to prepare samples for chemical analysis. Two additional changes were made to the standard ABA method:

- 1) the titration endpoint of pH 7.0 was changed to the more stable endpoint of pH 8.4, and
- 2) the qualitative “near boiling” temperature for the acid leach was modified to heat the sample pulp for 1 hour in a water bath maintained at 85°C.

RESULTS AND DISCUSSION

Sources of error from protocol variables

Static tests quantify the potential of mine waste samples to produce and neutralize acid. The commonly used static tests quantify acid producing potential (AP) using either total sulfur or sulfide-sulfur content to estimate the quantity of acid-producing minerals present (Table 15.3). The total sulfur content will overestimate the actual AP of samples containing substantial non acid producing sulfate minerals (e.g., barite or gypsum). On the other hand, the sulfide-sulfur measurement will underestimate the actual AP of samples containing substantial acid-producing sulfate minerals (e.g., melanterite or jarosite, reactions 6, 7). Knowledge of the mine waste sulfate mineralogy will indicate if the sulfate minerals present, if any, are acid producing and, thereby, allow selection of the more appropriate AP quantification. Existing techniques, such as those using a combustion furnace with subsequent quantification of the sulfur dioxide evolved (e.g., LECO furnace, as applied in ASTM E-1019, ASTM E-395, ASTM D-4239), are capable of accurately determining either total sulfur or sulfide-sulfur and, thereby, the AP.

Different static-test methods can produce markedly different NP values for the same sample (Lapakko, 1992a, 1992b, 1994a).

TABLE 15.3—Standard and modified ABA, BCRI, and NP(pH6) static test methods.

ABA method	Particle size (mesh) ¹	AP Sulfur form	NP-Determination Acid Leach			
			(Acid, and N)	pH (range)	Duration (hours)	Temperature (°C)
ABA, standard	-60	Total	HCl, 0.1–0.5	0.5–7.0 ²	1	85
ABA, modified	-200	Sulfide	HCl, 0.1–0.5	1.5–2.0 ³	24	25
BCRI	-100 to -400	Total	H ₂ SO ₄ , 1.0	3.5	4+	25
NP(pH6)	-150 to -325	Sulfide	H ₂ SO ₄ , 0.1–1.0	6.0	4–120	25

¹Particle size for the BCRI test was reported as -100 mesh by Bruynesteyn and Duncan (1979) and -400 mesh by Bruynesteyn and Hackl (1982). 75% passing 325 mesh has been used by industry laboratories (Lapakko 1994a).

²pH is not controlled with this method.

³This range was used by Lawrence Consulting LTD. (1991); a range of 1.0 to 1.6 was reported in an earlier publication (Lawrence 1990).

Protocol variables which may contribute to these differences include mine-waste particle size (tailings are typically run "as received"); "digestion" variables such as the acid used, amount of acid added (i.e., digestion pH), temperature, and duration; and the endpoint pH of the "back titration," if a back titration is used (Table 15.3). The most influential of the protocol variables are particle size, extent of acid addition, and the back titration endpoint. The extent to which protocol variables will affect the measured NP is dependent on the sample mineralogy.

Particle size—To examine the effect of particle size on NP, the standard ABA method was used to determine the NP of the -1/4 inch, -60 mesh, -150 mesh, and -325 mesh fractions of three rock samples (Table 15.4). The minus 1/4-inch size was included because it is commonly used in humidity-cell accelerated-weathering tests, such as those described in White and Jeffers (1994). For each of the rock types, NP increased as particle size decreased. This trend reflects increasing dissolution of acid-neutralizing minerals, due to increasing mineral surface area with decreasing particle size (e.g., Lapakko and Antonson, 1991). Thus, the reduction of particle size in neutralization potential determinations increases the dissolution of acid-neutralizing minerals which, in turn, leads to overestimation of the NP of the larger particles. The extent of this overestimation would tend to be greater for the BCRI and NP(pH6) tests, in which finer particle size fractions are used (Table 15.3).

TABLE 15.4—Standard-ABA NP increased as particle size decreased.

Sample size (mesh)	Sample NP (kg/t CaCO ₃)		
	1-C	MN-4	3-A
-325 ¹	8	15	943
-150 ¹	6	12	915
-60 ¹	6	11	900
-1/4 inch ²	0.09	2	ND

¹2-g sample mass.

²20-g sample mass.

ND, not determined.

Amount of acid added—The amount of acid added during the digestion can have a substantial influence on the NP value determined. As the acid addition increases, pH tends to decrease. This, in turn, leads to increased dissolution of acid-neutralizing minerals and a consequent increase in the NP measured. Indeed, the general approach for determining NP has been criticized since the low pH in the strongly acidic digestions may dissolve minerals, with consequent acid neutralization, which would not dissolve (and neutralize acid) at circumneutral pH (Lutwick, 1986). That is, minerals which dissolve to neutralize acid at low pH in NP digestions may not dissolve fast enough (at higher pH) to maintain neutral pH conditions in the environment. Consequently, NP digestions have been reported to generally overestimate the environmentally practical capacity of mine wastes to neutralize acid (Lapakko, 1994a). One example of such overestimation is reported for Duluth Complex rock, in which silicate mineral dissolution contributed to the standard ABA NP. In both laboratory and field tests, this dissolution neutralized acid produced by oxidation of sulfide minerals present in the rock. However, the rate of dissolution was not fast enough to maintain drainage pH above 6.0 even for rock of moderate sulfide mineral content (Lapakko, 1988, 1990; Lapakko and Antonson, 1994; Lapakko, 1994b).

To illustrate this phenomenon, the standard ABA NP of 14 samples was compared to the amount of acid neutralized by the samples prior to drainage pH decreasing below 6.0 in laboratory tests. This observed neutralization potential has been referred to as the "empirical NP" (Lapakko, 1994b). In all 14 cases the standard ABA NP overestimated the empirical NP by 5 to 21 kg/t CaCO₃ (Table 15.5). Even after drainage from these rocks had acidified (decreased below pH 6.0), indicating that no neutralization potential remained, the standard ABA tests conducted on the leached solids indicated a residual NP. Examination of the unleached, empirical, and leached NP values clearly indicates that the standard ABA NP overestimates the actual capacity of these mine wastes to neutralize acid while maintaining drainage pH above 6.0.

TABLE 15.5—Standard ABA NP (kg/t CaCO₃) of fresh and leached Duluth Complex drill core samples.

Sample	PCT S	Unleached NP	Empirical NP ¹	Minimum pH	Leached NP	Change in NP
G	0.92	21.8	0.40	4.20	13.9	-7.9
H	0.92	21.8	0.41	4.55	20.8	-1.0
K	1.24	12.6	0.61	4.20	11.8	-0.8
L	1.24	12.6	0.58	4.15	12.9	+0.3
C	1.35	10.5	0	3.75	10.2	-0.3
Q	1.74	9.1	0	4.05	5.9	-3.2
R	1.74	9.1	0	4.00	7.2	-1.9
S	1.87	23.7 ²	2.0	4.50	8.3	-15.4
T	1.87	23.7 ²	1.8	4.20	7.8	-15.9
B	2.01	7.9	0	3.70	8.3	+0.4
U	2.17	7.9	0.22	3.90	35.1 ³	+27.2
V	2.17	7.9	0	4.55	35.1 ³	+27.2
W	2.57	5.1	0	3.95	2.4	-2.7
X	2.57	5.1	0	3.95	3.7	-1.4

¹Neutralization potential above pH 6 observed in laboratory dissolution test.

²Average of duplicate values: 20.4, 27.1 kg/t CaCO₃.

³One sample of U, V combined. The reason for the increase in NP after leaching is unknown.

This error can be exacerbated and reproducibility hindered due to the potential for variable acid addition in the standard ABA and modified ABA NP digestions. Acid addition can vary with the standard ABA and modified ABA (although to a lesser degree) but not with the BCRI "titration" of a mine waste sample, during which mineral dissolution and neutralization occurs at pH greater than or equal to 3.5. This is higher than the typical pH range in the ABA test and the prescribed modified ABA test range (1.5–2.0) and, consequently, acid neutralization due to the dissolution of relatively unreactive minerals would contribute less "false NP" in the BCRI test. Nonetheless, mineral dissolution and acid neutralization can occur in the BCRI test at lower pH values, and may not be rapid enough to maintain mine waste drainage pH above 6.0. Contributions from low pH mineral dissolution and acid neutralization are eliminated in the NP(pH6) test.

The acid added in the standard ABA digestion varies from 20 ml 0.1N to 80 ml 0.5 N hydrochloric acid, a twenty-fold variation, based on a subjective interpretation of the "fizz" test. This range of acid addition can produce a digestion pH ranging from 0.5 to 7. In the modified ABA the amount of acid added is based on the "fizz" test, but is also limited by requiring a pH range of 1.5 to 2.0 at the end of the digestion. During the BCRI and NP(pH6) "titrations" of a mine waste sample, mineral dissolution and neutraliza-

tion occurs at pH greater than or equal to 3.5 and 6, respectively.

Lapakko (1992b) reported that increasing H⁺ additions for the modified ABA digestion by factors of 1.25 to 5 increased the resultant NP by an average of 27 kg/t CaCO₃, with a maximum increase of 76 kg/t CaCO₃ (Table 15.6). These values demonstrate graphically the influence of the digestion acid strength on NP. However, the actual impact on modified ABA values is limited since the protocol requires a digestion pH in the range of 1.5 to 2.0. Thus, the potential range of the acid addition is limited by the objective criterion of the target pH range rather than the subjective interpretation of the “fizz” test (Lapakko, 1992b).

TABLE 15.6—Effect of acid addition on NP (pH 8.3 titration endpoint) determined by modified ABA method (Lapakko, 1992b). pH₀ = pH at beginning of titration. NP in kg/t CaCO₃.

Sample	ml HCl	N HCl	H ⁺ equivalents	pH ₀	NP
T1	40	0.100	0.004	4.83	200
	40	0.300	0.012	1.37	187
	40	0.500	0.020	0.65	205
T2	30	0.300	0.009	2.09	170
	40	0.500	0.020	0.64	200
T3	40	0.100	0.004	4.39	78
	20	0.527	0.010	1.20	146
	40	0.500	0.020	0.81	148
T4	40	0.100	0.004	4.39	76
	20	0.527	0.010	1.14	144
	40	0.500	0.020	0.62	152
T5	40	0.100	0.004	2.14	69
	60	0.105	0.006	1.65	92
	40	0.500	0.020	0.51	88
T6	40	0.100	0.004	2.14	41
	60	0.105	0.006	1.76	62
	30	0.527	0.016	1.28	219
T7	40	0.500	0.020	0.74	226
	40	0.100	0.004	4.59	69
T8	20	0.527	0.010	2.18	109
	20	0.105	0.002	1.85	22
T9	40	0.100	0.004	0.51	16
	35	0.527	0.018	1.22	204
T10	40	0.500	0.020	1.00	210

In contrast, the impact in the standard ABA test can be substantial, since the acid addition is based strictly on a subjective evaluation of the “fizz” test by the laboratory technician. Differing evaluations of this test lead to different acid additions and, consequently, variations in the NP determined. Lapakko (1991) reported that increasing the acid addition to a hydrothermal-quartz-carbonate gold tailing sample from 40 ml 0.1N HCl to 40 ml 0.5N HCl, increased the resultant ABA NP from 80 to 174 kg/t CaCO₃. The initial digestion pH values for the two acid additions were 4.87 and 1.17, respectively.

Back titration endpoint—The ABA and modified ABA tests use back titrations, to respective endpoints of 7.0 and 8.3, following the digestion step to determine the amount of acid remaining in solution. With hydrothermal quartz-carbonate hosted gold tailings, modified ABA NP values using a pH 7.0 endpoint were typically 20 to 30 kg/t CaCO₃ higher than those for the pH 8.3 endpoint, with a maximum increase of 165 kg/t CaCO₃ (Table 15.7). This suggests that the pH 7.0 titration endpoint did not account for all of the acidity in solution. In particular, the lower titration end-

point did not allow for the oxidation of ferrous iron (released from iron carbonate minerals, for example) and subsequent precipitation of iron hydroxide (Lapakko, 1992b). The contribution of iron and other metals in solution can be accounted for by peroxide addition, as described in methods for determination of mineral acidity (ASTM Method D1067 or American Public Health Association et al., 1992). Since the BCRI and NP(pH6) methods do not include a back titration, acidity released during the digestion step (e.g., iron) is not accounted for.

TABLE 15.7—Comparison of ABA NP values determined at pH endpoints of 7.0 and 8.3. Acid addition for ABA was 40 ml of 0.5 N HCl unless otherwise noted (Lapakko, 1992b).

Sample	Standard ABA NP, kg/t CaCO ₃	
	pH 7.0 endpoint	pH 8.3 endpoint
T1	231	205
	228	208
T2	202	173
T3	202	173
	188	163
T4	190	162
	178	156
T5	106	98
	91	85
T6 ¹	69	48
T7	270	241
T8	174	142
T8 ¹	80	74
T9 ¹	18	17
T10	373	208

¹Acid addition 40 ml of 0.1 N HCl.

Acid type—Except for the influence of digestion duration on the NP(pH6), there is little evidence to indicate the influences of the remaining digestion variables (acid type, temperature, duration) are substantial. Standard and modified ABA digestions use hydrochloric acid, while the BCRI and NP(pH6) tests use sulfuric acid. Pyrrhotite is more soluble in hydrochloric than sulfuric acid and, therefore, might be expected to contribute more false NP in the standard and modified ABA tests than the BCRI and NP(pH 6) tests. Jennings and Dollhopf (1995) reported an average of 80% of three pyrrhotite samples was solubilized by treatment with 4.91 M HCl (approximately 150 ml HCl/g -100-mesh pyrrhotite).

However, solubilization of pyrrhotite under the conditions of the ABA NP determination appears to be slight. No increase in ABA NP values was observed as the pyrrhotite content of Duluth Complex rocks increased from 1.2% to 6.5% (Lapakko, 1995). To further examine this phenomenon, the USBM subjected pyrrhotite-bearing samples of Duluth Complex rock to a procedure similar to the ABA neutralization-potential determination. Samples of 80% passing 150 mesh were subjected to 40 ml 0.1 N HCl (plus 60 ml E-pure water) for one hour at 80°C. The pyrrhotite dissolution during this digestion was minimal. The average sulfur content (LECO furnace) of the three samples was 1.50±0.10% after the test as compared to 1.60±0.03% before the digestion. Thus, it is concluded that little false NP would be contributed by pyrrhotite dissolution in the presence of hydrochloric acid in the standard and modified ABA static tests. Apparently either 1) pyrrhotite was solubilized by the more concentrated hydrochloric acid used by Jennings and Dollhopf (1995) but not by lower

concentrations in the standard ABA, or
 2) there was some difference between the pyrrhotite present in the samples examined in the two studies.

Digestion temperature and duration—Relative to the modified ABA, the elevated temperature used in the standard ABA digestion may enhance the dissolution of host rock minerals. On the other hand, a greater degree of neutralizing mineral dissolution would be expected with the longer digestion duration of the modified ABA test. However, previous research indicated that, within the ranges typical of standard and modified ABA testing, the influence of elevated temperature and test duration on 12 mine waste samples of variable composition (Coastech Research Inc., 1989) and 10 hydrothermal-quartz-carbonate-hosted-gold tailings was negligible (Lapakko, 1992b).

To examine the effect of modified NP(pH6) digestion duration on NP results, USBM subjected five samples to this test. Sample 3-A is nearly 100% calcite; 3-B is comprised of 60% carbonate as dolomite/ankerite; sample 3-D contains approximately 5% carbonate as ankerite and dolomite; and the final two samples were purchased specimens of calcite and siderite. With this digestion the NP values after 120 hours of digestion were typically 1.1 to 2.3 times those after a 4-hour digestion (Table 15.8). The increase for samples dominated by calcite (3-A and calcite sample) was small relative to that for samples dominated by magnesium and iron carbonates, reflecting the relatively rapid dissolution of calcite. That is, the most of the calcite dissolved within the first four hours of digestion, while the majority of magnesium carbonate dissolved between 4 and 120 hours. Thus, for this test, measurement of NP contributions from magnesium carbonates requires a longer duration than those from calcium carbonate.

TABLE 15.8—Successive NP results from 4-, 24-, and 120-h modified NP(pH6) leaches of two mineral specimens and three carbonate-rock samples.

Sample	Neutralization potential (kg/t CaCO ₃)		
	4 hours	24 hours	120 hours
3-A ¹	737	790	864
3-B ²	105	204	250
3-D ³	10	19	32
Calcite	859	ND	945
Siderite	2	ND	9

ND, not determined.

¹Approximately 100% calcite.

²60% carbonate as dolomite and ankerite.

³Approximately 5% dolomite.

Effect of sample mineralogy

The extent to which protocol variables will affect the NP determined by various tests is dependent upon the mineralogy of the sample under examination. Tests were conducted on carbonate and feldspar minerals to assess their contribution to measured NP.

Carbonate minerals—Two relatively pure carbonate minerals (“Iceland-spar” calcite and siderite) were purchased from a commercial supplier. Their X-ray-diffraction (XRD) patterns were nearly perfect matches with respective patterns of their corresponding XRD-reference samples. XRD analysis detected some MnCO₃ in the calcite sample, and some mixed carbonates of cal-

cium, magnesium, iron, and manganese in the siderite sample. X-ray fluorescence analysis of the samples indicated traces of manganese, iron, and strontium in the calcite sample and traces of manganese and calcium in the siderite sample. The purchased samples were pulverized to 80% passing 150 mesh and, along with mixtures of the two samples, subjected to four different NP procedures (C-S analysis, standard ABA, modified ABA, modified NP(pH6)).

The C-S method determined the “calcite” sample was 57% carbonate (CO₃) which, assuming none of the carbonate was associated with iron or manganese, implies an NP of 950 tons CaCO₃/1000 tons rock. This value yields an upper bound for the NP present with calcium and magnesium carbonates, assuming the technique accurately determined the carbonate content of the sample. Furthermore, it indicates that approximately five percent of the sample was comprised of noncarbonate minerals. The agreement among the three remaining static tests was good, and the values determined were roughly 90% of the maximum calcium/magnesium carbonate content indicated by the C-S method (Table 15.9). The difference between the results of these three tests and the C-S determination may be due to (1) the presence of some iron and (or) manganese carbonate (approximately 10% of the entire sample) or (2) incomplete digestion of the sample by the standard and modified ABA and modified NP(pH6) methods.

TABLE 15.9—Neutralization potential (NP) of calcite and siderite using four different techniques (kg/t CaCO₃).

Sample	Expected value ¹	NP-determination methods			NP(pH6), modified ²
		C-S analysis	ABA, standard	ABA, modified	
Calcite	1000	948	863	858	859
Siderite	0	772	763	632	2
5:5:90 ³	50	86 ⁴	89.5	NA	35.2
10:10:80 ³	100	172 ⁴	165	NA	86.5
10:20:70 ³	100	249 ⁴	241	NA	94.9
20:10:70 ³	200	267 ⁴	254	NA	178

NA, not analyzed.

¹Expected NP = percent calcite x 10.

²4-h test duration.

³Ratio of calcite: siderite: quartz.

⁴Calculated based on values from “pure” samples.

Underestimation of the total calcium/magnesium carbonate content is atypical of static test NP determinations in general, but may have resulted from the extremely high calcite content of the sample. The amount of acid added in the standard and modified ABA was precisely that required to dissolve a sample of pure calcite. In other words the acid added in these two tests was only slightly in excess of the carbonate mineral content and, consequently, the digestion of the calcite may have been incomplete due to slow reaction at higher pH. Similarly, the modified NP(pH6) digestion of calcite may have been incomplete due to the near neutral conditions of this test.

For the siderite sample the C-S method yielded a carbonate (CO₃) content of 46.3% which implies an NP of 772 tons CaCO₃/1000 tons rock, assuming none of the carbonate was associated with iron. Based on the XRD analysis of the sample it is more reasonable to assume the carbonate was associated with iron, which yields a siderite content of 89% and a noncarbonate mineral content of about 11% for the sample. This further implies a cal-

cium/magnesium carbonate NP of 0. The standard and modified ABA techniques both yielded NP values well above the expected value of 0 kg/t CaCO₃ (Table 15.9). This indicates that the digestions dissolved the siderite, but that the oxidation of ferrous iron and subsequent precipitation of ferric oxyhydroxide in the back titration was incomplete (see also Lapakko, 1992b, 1994a). The modified ABA technique yielded a lower NP, indicating a lesser attack of the siderite during the digestion (Table 15.9).

The modified NP(pH6) was in excellent agreement with the expected value, and indicated that the dissolution of siderite was minimal at the higher digestion pH of this test. That is, only a small amount of acid could be added to the mixture of water and siderite sample and still maintain a pH of 6. Apparently the dissolution of siderite was minimal in the less acidic NP(pH6) digestion. If significant siderite dissolution did occur, the ferrous iron released was oxidized and precipitated as ferric hydroxide with the consequent acid production (equations [4] and [5]). Thus, this acidity would be accounted for in this test rather than being neglected due to its presence as aqueous ferrous iron, which can occur in other static tests.

The trends observed for the calcite: siderite: quartz mixtures semi-quantitatively reflected the analyses of the “pure” samples. The standard ABA NP values exceeded the expected values by an average of almost 80%, further supporting a substantial contribution of “false” NP by siderite in the standard ABA. In contrast, the modified NP(pH6) values were an average of 14% below the expected values, suggesting an incomplete digestion of the calcite. These errors were calculated assuming both the “calcite” and “siderite” samples were pure mineral phases. Since the C-S analysis indicates the “calcite” sample was less than pure, it is likely that the actual errors in the ABA NP values were slightly higher, while those for the modified NP(pH6) method were slightly lower.

Feldspar minerals—To determine the extent to which various feldspar minerals contribute to the NP determined by standard ABA, three different specimen-grade feldspars were subjected to a standard-ABA NP digestion. Acid additions for this test produce a calculated pH range of 0.5 to 1.8, prior to mine waste sample addition. Under these low pH conditions, a reaction similar to equation [10] occurs. Potassic feldspar (microcline), and the calcic and sodic end members of the plagioclase feldspars (bytownite-AN70–90 and oligoclase-AN10–30, respectively) were selected because they are common mineral constituents of rock types common to mine waste from metal mines. After completion of the acid leach, the leach mixture was filtered and the filtrate analyzed for potential feldspar-dissolution products (Al, Ca, K, Na, Si).

Table 15.10 shows that bytownite is solubilized to a much greater extent than either oligoclase or microcline. Concentrations of selected cations from bytownite dissolution are one to two orders of magnitude greater than corresponding cation concentrations for oligoclase and microcline. Cation concentrations for oligoclase and microcline were nearly identical. Additionally, bytownite dissolution has a buffering effect on the acid leach that is not demonstrated by either oligoclase or microcline (pH 3.5 versus pH 2.0).

A second standard-ABA NP-determination acid leach was conducted on splits of the same bytownite and oligoclase samples to determine if measurable NP would result from the rigorous leach conditions. Because the previous microcline and oligoclase acid-leach results were nearly identical (Table 15.10), NP was not determined for microcline. Resulting NPs are listed in Table 15.11. Results are consistent with the acid-leach results summa-

rized in Table 15.10; bytownite NP ranged from 12 to 24, while oligoclase NP ranged from 0.0 to 0.4. Although calcium carbonate was totally absent from the specimen-grade feldspars, bytownite dissolution resulting from the standard-ABA acid leach produced measurable NP and erroneously suggested the presence of more than 2% calcium carbonate. The significance of the tests summarized in Tables 15.4, 15.10, and 15.11 is that NP can be overestimated by tens of parts per thousand due to differences in sample-size reduction and unanticipated dissolution of silicate gangue minerals.

TABLE 15.10—Filtrate analyses¹ after acid leaches (standard ABA method) of three non-carbonate-bearing specimen-grade feldspars

Sample	Oligoclase (sodic)	Bytownite (calcic)	Microcline (potassic)
pH	2.02	3.46	1.99
Na	4.30	31.40	4.30
Ca	5.19	66.10	5.26
K	1.40	4.60	2.10
Si	1.50	128.00	<1
Al	2.04	99.40	2.04

¹Cation concentrations in mg/l (parts per million)

TABLE 15.11—Comparison of average pH and range of NP values determined from acid leaches (standard ABA method) of specimen-grade bytownite and oligoclase feldspars.

Sample	pH	NP ¹
Bytownite (calcium feldspar)	2.6	12–24
Oligoclase (sodium feldspar)	1.9	0.0–0.4

¹Expressed as kg/t CaCO₃.

It should, however, be noted that feldspars can provide practical acid neutralization. Morin and Hutt (1994) reported that for more than a decade of weathering in the field, the 50% calcium feldspar present in tailings neutralized the acid produced by the oxidation of pyrite present in a concentration of 1.9%. Factors which enhanced the effectiveness of feldspar neutralization in this case were

- 1) the relatively fine particles and consequent high specific surface area of the feldspar,
- 2) the feldspar was largely calcium feldspar, which is more reactive than sodium or potassium feldspar (Table 15.10), and
- 3) possible subaqueous conditions which would limit the rate of pyrite oxidation and consequent acid production.

Comparison of NP determinations on various mine waste samples

The extent to which various NP methods will differ for a given mine waste sample is dependent upon the sample composition. Lapakko (1992b, 1994a) compared various static test NP values to each other and to the total calcium carbonate and magnesium carbonate content, or mineralogic NP (equation [12]). The mineralogic NP was used to estimate the actual neutralization potential of mine waste samples, assuming that calcium carbonate and

magnesium carbonate present in the mine waste samples, and only these minerals, would dissolve to maintain a pH of at least 6.0. *The mineralogic NP allows estimation of Static-test NP accuracy in the absence of adequate laboratory or field data required to determine the empirical NP (see definition of “empirical NP” on page 330 under the heading “Amount of acid added”).*

$$\text{Mineralogic NP} = 10 \times (\% \text{CaCO}_3) + 11.9 \times (\% \text{MgCO}_3) \quad [12]$$

For 10 hydrothermal quartz-carbonate tailings Lapakko (1992b) reported that, relative to the standard ABA method, the NP determined by the modified ABA method was lower, and more closely approximated the mineralogic NP (Table 15.12). The combined quartz and carbonate mineral content of the tailings averaged about 50%, with feldspar, chlorite, and mica constituting an average of 42%. *The partial dissolution of some or all of these silicate minerals during standard and modified ABA NP-test digestions resulted in test NP values that exceeded corresponding mineralogic NP values. Modified ABA NP values that were less than mineralogic NP values suggest incomplete dissolution of the calcium and magnesium carbonates during the 24-hour digestion period.*

TABLE 15.12—Comparison of neutralization potentials of hydrothermal quartz-carbonate hosted gold tailings as determined by standard ABA, modified ABA, and calcium carbonate plus magnesium carbonate content.

Sample	Neutralization potential, kg/t CaCO ₃		
	ABA, standard	ABA, modified	CaCO ₃ + MgCO ₃
T1	230	200	207
T2	230	180	189
T3	195	130	163
T4	184	130	147
T5	98	92	65
T6	69	64	45
T7	270	220	229
T8	174	120	110
T9	18	16	14
T10	373	200	200

Lapakko (1994a) used a similar approach to evaluate standard ABA, modified ABA, and B.C. Research Initial neutralization potentials of ten mine waste samples of varying mineralogy. The standard ABA and modified ABA produced similar NP values on most samples. For four of the samples the standard ABA and modified ABA NP values were not significantly different from the mineralogic NP of four samples, and were within 10 kg/t CaCO₃ of the mineralogic NP of an additional three samples (Table 15.13). The major minerals in these seven samples were quartz, potassium feldspar, and mica. However, for the remaining three samples NP values from these two static tests exceeded the mineralogic NP by 13 to 47 kg/t CaCO₃. The mineralogic components contributing to the excessive static test values for these three samples were calcium feldspar (and perhaps pyroxene and olivine), clinopyroxene, and iron carbonates.

The B.C. Research Initial NP values were slightly higher than those for the standard and modified ABA, perhaps due to the smaller particle size used in the BCRI. Nonetheless, the BCRI NP

values for eight of the samples were within 10 kg/t CaCO₃ of the corresponding mineralogic NP. The BCRI NP values for the remaining two samples were 15 and 49 kg/t CaCO₃ higher than the corresponding mineralogic neutralization potentials. Both of these samples contained iron carbonates, which were identified as responsible for the excessively high BCRI NP values. The NP(pH6), similar to the BCRI but using an endpoint of pH 6.0, was proposed as an alternative for NP determination. This method was within 3 kg/t CaCO₃ of the mineralogic NP of all ten samples.

TABLE 15.13—Neutralization potential (kg/t CaCO₃) of mine waste samples from various rock types.

Sample	Standard ABA	Modified ABA	B.C. Research	NP(pH6)	Mineralogic NP
RK1	12	9.6	7.7	3.0	0 (0–2.9) ¹
RK2	35	33	11	2.8	1 (0–2.3)
RK3	15	14	25	3.3	5 (1.9–9.7)
RK4	28	28	33	28	32 (28–37)
TL1	27	27	30	24	19 (17–23)
TL2	18	20	25	16	16 (13–21)
TL3	46	61	82	30	19 (8.1–33)
TL4	3.8	2.9	15	3.8	5 (3.7–6.6)
TL5	7.5	3.2	20	15	12 (9.8–17)
TL6	99	72	58	55	46 (35–52)

¹Error bar in parenthesis.

To further illustrate the difference among static test neutralization potentials, the USBM subjected samples from four different rock-type groups to four different methods of NP determination (C-S analysis, standard ABA, modified ABA, and modified NP(pH6)). The four rock-type groups tested were latite porphyry, mudstone, carbonate, and gabbro. Major mineral constituents for each rock-type group and a range of corresponding weight-percent estimates for each mineral are listed in Table 15.14. Mineral weight-percent ranges for latite porphyry, mudstone, and carbonate were estimated using X-ray diffraction (XRD), while estimates for gabbro were made using point counts from thin sections. Table 15.15 shows the response of the four rock-type groups (as influenced by their respective mineralogies) to the four NP-determination methods.

General gangue mineralogy for the latite porphyry and mudstone samples are similar. More importantly, XRD-determined carbonate content for both rock types is low (3 to 5%, and 4%, respectively), and the carbonate mineralogy is dominated by iron-carbonate species such as ankerite, siderite, and ferroan dolomite/magnesite (Table 15.14). C-S analysis of the latite porphyry suggests that less than 1% (expressed as CaCO₃) is actually present, whereas C-S analysis results of 4 to 6% for the mudstone samples are in good agreement with the XRD estimate of about 4%.

Insufficient acid addition to the latite porphyry and mudstone samples was first thought to be a plausible explanation for underestimated NP by the standard and modified ABA methods. However, when ABA acid-leach solutions from latite porphyry and mudstone samples were titrated (to a pH 8.4 endpoint) at the end of their respective leaches, between 85 and 100% of the original acid volume had not reacted with the rock samples. It was concluded instead that the carbonate present was predominantly associated with iron and, for these solids, the standard and modified ABA methods did not greatly overestimate the calcium and

TABLE 15.14—Range of weight-percent estimates for major mineral constituents comprising the four rock-type groups.

Major Mineral Constituents	Rock-Type Group			
	Latite porphyry	Mudstone	Carbonate	Gabbro
Iron sulfide	Py (6)	Py (3–24), Po (0–5)	ND	Po (0.6–3)
Base-metal sulfide	ND	Tetra (tr.)	ND	Cp (1.5–3)
Carbonate	Ankerite ¹ (3–5)	Siderite ² (1–2) Kutnohorite ³ (1–2) Dolomite, ferroan ⁴ (tr.) Magnesite, ferroan ⁵ (tr.) Ankerite ¹ (tr.)	Calcite (10–90) Dolomite (5–20) Ankerite ¹ (3–4)	ND
Silicate	Microcline (20) Albite (15) Quartz (50)	Microcline (5–10) Albite (5–10) Quartz (45–50)	Quartz	Labradorite (60–65) Pyrox/amphib (14–19) Olivine (5–7)

NOTE: values in parentheses represent percent of minerals present
 ND, Not detected
 Po, pyrrhotite
 Py, pyrite
 Cp, chalcopyrite
 Tetra, tetrahedrite

¹Ca(Fe,Mg)(CO₃)²
²FeCO₃
³Ca(Mn,Mg)(CO₃)²
⁴Ca(Mg,Fe)(CO₃)²
⁵(Mg,Fe)CO₃

magnesium carbonate content. That is, the iron carbonate present did not contribute NP at the low pH digestions in these tests. A second explanation is that calcium and magnesium carbonates were present and of low reactivity (due perhaps, to iron oxyhydroxide coatings on their surface) and did not dissolve in the ABA digestions. Preliminary USBM scanning-electron microscopy (SEM) studies of related mudstone samples documented presence of rhombohedral carbonate occurrences rimmed with higher-density iron-calcium-manganese carbonate (Chirban, unpub. laboratory notes, 1991).

TABLE 15.15—Neutralization potential (NP) of four different waste-rock groups by NP-determination method (NP expressed as kg/t CaCO₃).

Waste-rock group	Sample	NP-determination methods			
		C-S analysis	ABA, standard	ABA, modified	NP(pH6), modified ¹
Latite porphyry	1-B	5.8 ²	0.0	0.0	0.1
	1-C	59 ²	4.4 ²	3.9 ²	1.9
Mudstone	1-D	40 ²	6.9 ²	2.9 ²	2.3
	3-A	919 ²	885	872 ²	737
	3-B	369 ²	263 ²	294 ²	105
Carbonate	3-D	36	40 ²	59	10
	MN-2	7.9	29	10	2.8
	MN-4	8.3	28	7.8	0.2
Gabbro	MN-6	6.5	21	16	7.4

¹4-hour test duration
²Average of two tests

Carbonate sample NP-determination test results are in good agreement with respective sample mineralogy. According to C-S analysis, sample 3-A contains 90% calcium carbonate equivalent which has been identified by XRD as calcite. Standard and modified ABA NP values were 95% of the C-S NP value, and modified NP(pH6) was 80% of C-S NP. These results are consistent with calcite's rapid reaction rate and subsequent nearly-complete digestion when subjected to excess acid. Sample 3-B contains about 40% calcium carbonate equivalent which has been identified by XRD as dolomite. Standard and modified ABA NP values

for sample 3-B were 70 and 80% of the C-S value, respectively. The underestimated ABA NPs may be due to insufficient acid addition; minimal titrant was required during the back titration to reach a pH 8.4 endpoint because 80 to 90% of the acid was consumed during its neutralization by the sample. The modified NP(pH6) value was only 28% of C-S NP, and is believed to be a result of insufficient leach time (4 hours). Dolomite has a slower dissolution rate compared with that of calcite; when sample 3-B was allowed to leach for a 120-hour period, an NP of 250 or 68% of C-S NP was achieved, which was more than twice the NP obtained by the 4-hour leach (see Table 15.8). Sample 3-D contains only about 4% calcium carbonate equivalent which has been identified by XRD as ankerite. Standard and modified ABA NP values are 100+% of C-S NP. This is consistent with the amount of excess acid present at the completion of the respective leaches (about 50 to 80% of the original volume was neutralized during the back titration). However, modified NP(Ph6) value was only 28% of C-S NP, but again this was believed to be a function of insufficient leach time (4 hours). When sample 3-D was leached for a 120-hour period, an NP(pH6) value of 32 or 89% of C-S NP resulted.

Gabbro sample mineralogy is dominated by calcium, magnesium, and iron-magnesium silicates, and contains less than 1% carbonate (identified by C-S analysis as calcium-carbonate equivalent). Standard ABA NP values for all three gabbro samples were three times larger than their respective C-S NPs, while modified ABA NP values were only slightly higher for two of three samples. Overestimation of gabbro-sample NP by the standard ABA method is most likely caused by dissolution of calcic plagioclase which is the dominant gangue mineral in each of the three samples (MN-2, 4, and 6). Standard ABA NP values obtained for the gabbro samples are consistent with observed dissolution of pure calcic plagioclase samples when subjected to the same test (see Table 15.10). Modified NP(pH6) results are one and two orders of magnitude lower for gabbro samples MN-2 and MN-4, compared with their corresponding standard ABA NPs. These results are consistent with the higher pH conditions of the modified NP(pH6) test (pH > 6.0), which would be less likely to solubilize much calcic plagioclase.

SUGGESTIONS FOR IMPROVING STATIC-TEST ACCURACY

The following suggestions are offered to help solve specific problems with NP-determination tests that were identified in the previous section.

- The method of determining acid production potential should be based on the sulfur-bearing minerals present. If only iron sulfide is present, the AP can be based on total sulfur determination. If other sulfur-bearing minerals are present in substantial quantities, it may be necessary to determine their abundance to accurately quantify the AP.
- Know the carbonate mineralogy and major host rock minerals present in samples being tested.
- If iron carbonates are present, care should be taken to allow for iron precipitation in the back titration of the standard and modified ABA tests. This precipitation can be enhanced by use of an endpoint of 8.3 rather than 7.0 and allowing additional time for endpoint pH stabilization. It can be essentially eliminated by the addition of hydrogen peroxide, as used for mineral acidity determination (ASTM method D-1067 or American Public Health Association et al., 1992).
- If no iron carbonates are present, measurement of carbon dioxide evolved from the sample will accurately quantify the calcium/magnesium carbonate content of the mine waste. Errors from commonly used static tests will be limited to those introduced by dissolution of noncarbonate host rock minerals during the NP digestion and the attendant low-pH acid neutralization.
- The presence of minerals such as calcium-rich plagioclase should be noted. The possible contribution of false NP by dissolution of these minerals in low-pH digestions must be considered. Only if the rate of acid production is quite slow, will these minerals neutralize acid while maintaining a neutral pH in the environment. Their practical neutralization potential is severely limited if they are present in waste rock.
- The NP(pH6) test will probably be more accurate than the standard ABA, modified ABA, and BCRI initial tests in quantifying the NP present as calcium carbonate and magnesium carbonate for samples containing elevated levels of siderite (iron carbonate) or calcic plagioclase (e.g., labradorite). This test, however, is often more time consuming than the more commonly used NP determinations.
- For waste rock samples, NP digestions should be conducted on larger size fractions in addition to the recommended size reduction, in order to better quantify the influence of particle size on the available NP. Testing minus 1/4-inch samples will further benefit interpretation of humidity cell data from waste rock samples.

SUMMARY

Static tests conducted on a variety of metal-mine-waste samples showed that neutralization potential (NP) variability for a given sample was (1) most strongly influenced by differences in sample particle size, amount of acid addition, back-titration endpoint, and sample mineralogy; (2) influenced in one test by digestion duration; and (3) virtually unaffected by acid type and temperature of digestion:

- Reducing particle size of three samples from minus 1/4 inch to

minus 325 mesh increased NP by 8- to 43-kg/t CaCO_3 (increases of 98% and 5%, respectively).

- Increasing acid strength by up to five times increased the NP of ten samples by 5 to 76 kg/t CaCO_3 (increases of 3 to 50%, respectively).
- Changing the back-titration endpoint from pH 7 to pH 8.3 decreased NP by 20 to 30 kg/t CaCO_3 (decreases of 11 to 15%, respectively).
- The influences of temperature (25 vs 85°C) and digestion duration (1 vs 24 hours) on standard and modified ABA NP values for 12 mine-waste samples of variable composition and for 10 hydrothermal-quartz-carbonate-hosted gold-tailings samples were negligible.
- When digestion duration of the modified NP(pH6) test was increased from 4 to 120 hours for 5 carbonate-rock samples, NP increased by 1.1 to 2.3 times.

The extent to which protocol variables affect NP is a function of sample mineralogy:

- Standard ABA digestions performed on specimen-grade sodic- and calcic-end member feldspars produced NP ranges of 0.0-0.4 and 12-24 kg/t CaCO_3 , respectively. Although carbonate was not present in the feldspar samples, resulting calcic feldspar dissolution by the acidic ABA digestion produced an NP that is equivalent to the presence of as much as 2.4% CaCO_3 .
- For mudstone and carbonate rocks, standard ABA, modified ABA, and modified NP(pH6) determinations yielded lower NP values than that indicated by the total carbonate content of the rock (carbonate content was determined by speciating sample total-carbon content into carbonate- and organic-carbon components). The difference was attributed to:
 - the presence of some iron or manganese carbonate and (or),
 - the inability of static-test digestions to dissolve calcium and magnesium carbonate which were coated with iron and manganese precipitates.
- For Duluth Complex rock the standard and modified ABA NP values were typically two to three times those estimated based on the carbonate content of the rock, apparently due to acid neutralization by calcic plagioclase dissolution in the static test digestions. In contrast, the modified NP(pH6) values were less than or equal to estimates based on the carbonate content of the rock, reflecting the less acidic (and more conservative) conditions of this digestion.

ACKNOWLEDGMENTS—The following U.S. Bureau of Mines personnel contributed significantly to the study: Nathan A. Spencer conducted the early standard and modified ABA tests, and helped establish the USBM's modified NP(pH6) protocol; Denise Chirban and Jeff Vandell performed the mineral characterization studies, and Ferril Jacobson prepared the samples and produced the screen fraction analysis; chemical characterization was provided by Kim Harbaugh, Marta Limberg, Fern Stones, William Lockman, and Dwight Hammargren. Anne Jagunich and Jean Matthew determined neutralization potentials of Duluth Complex rocks for the Minnesota Department of Natural Resources (MDNR). Studies conducted by the MDNR were funded by the U.S. Environmental Protection Agency (administered by the Western Governor's Association) and the Minnesota Minerals Coordinating Committee. In addition, the authors thank the participating mining companies who provided the mine-waste samples; without their participation, this study would not have been possible.

REFERENCES

- Alpers, C.N., Blowes, D.W., Nordstrom, D.K., and Jambor, J.L., 1994, Secondary minerals and acid-mine water chemistry; *in* Short Course Handbook on Environmental Geochemistry of Sulfide Mine Wastes, Waterloo, Ontario: May 1994, Mineralogical Association of Canada, pp. 247–270.
- American Public Health Association, American Water Works Associations and Water Environment Federation, 1992, Standard methods for the examination of water and wastewater, 18th ed.: American Public Health Association, Washington D.C., 981 pp.
- ASTM Method D 1067–92, 1995, Standard test methods for acidity or alkalinity of water: American Society for Testing and Materials Annual Book of ASTM Standards, Sec. 11, v. 11.01, Water (I), pp. 82–88.
- ASTM Method D 4239–85, 1988, Standard test methods for sulfur in the analysis sample of coal and coke using high temperature tube furnace combustion methods: American Society for Testing and Materials Annual Book of ASTM Standards, Sec. 5, v. 05.05, pp. 385–390.
- ASTM Method E 395–95A, 1995, Test method for determination of total sulfur in iron ores and related materials by combustion-iodate titration, Sec. 3, v. 03.06, pp. 62–64.
- ASTM Method E 1019–94, 1994, Methods for determination of carbon, sulfur, nitrogen, and oxygen in steel and in iron, nickel, and cobalt alloys, Sec. 3, v. 03.06, pp. 286–304.
- Bradham, W.S., and Caruccio, F.T., 1991, A comparative study of tailings analysis using acid/base accounting, cells, columns, and soxhlets; *in* Proceedings of the 2nd Internat Conference on the Abatement of Acidic Drainage: Sept. 16–18, 1991, Montreal, Canada, pp. 157–173.
- Brodie, M.J., Broughton, L.M., and Robertson, A.M., 1991, A conceptual rock classification system for waste management and a laboratory method for ARD prediction from rock piles; *in* Proceedings of the 2nd Internat Conference on the Abatement of Acidic Drainage: Sept. 16–18, 1991, Montreal, Canada, Tome 3, pp. 119–135.
- Bruynesteyn, A., and Duncan, D.W., 1979, Determination of acid production potential of waste materials: Met. Soc. AIME, paper A–79–29, 10 pp.
- Bruynesteyn, A., and Hackl, R.P., 1982, Evaluation of acid production potential of mining waste materials: Minerals and the Environment, v. 4 (1), pp. 5–8.
- Bucknam, C.H., 1995a, Test method for the analysis of metal bearing ores and related materials by combustion infrared adsorption spectrometry, Unpub. draft standard #7 (Oct. 7, 1995) under jurisdiction and consideration by American Society for Testing and Materials (ASTM) Committee E–01, Available upon request from Charles Bucknam, (801) 583–8974, 13 pp.
- Bucknam, C.H., 1995b, Invitation to participate in an interlaboratory study to develop standard methods for the carbon-sulfur analysis of ores and related materials, Written commun., Dec. 4, 1995, Available upon request from Charles Bucknam, (801) 583–8974.
- Busenberg, E., and Clemency, C., 1976, The dissolution kinetics of feldspars at 25°C and 1 atmosphere CO₂ partial pressure: *Geochimica et Cosmochimica Acta* 40, pp. 41–49.
- Busenberg, E., and Plummer, L.N., 1986, A comparative study of the dissolution and crystal growth kinetics of calcite and aragonite: *U.S. Geological Survey Bulletin* 1578, pp. 139–168.
- Chirban, D.D., 1991, Scanning electron microscopy (SEM) studies of waste rock associated with western United States metal mines: Unpub. laboratory notes accompanied by photomicrographs and EDS plots (currently archived with U.S. Bureau of Land Management, Utah State Office, Salt Lake City, UT 85145-0155).
- Coastech Research Inc., 1989, Investigation of prediction techniques for acid mine drainage: MEND Project 1.16.1 a. Canada Centre for Mineral and Energy Technology, Energy, Mines and Resources, Canada, 61 pp. plus appendices.
- Cravotta, C.A., 1994, Secondary iron-sulfate minerals as sources of sulfate and acidity—Geochemical evolution of acidic ground water at a reclaimed surface coal mine in Pennsylvania; *in* Environmental Geochemistry of Sulfide Oxidation: ACS Symposium Series 550, American Chemical Society, Washington, D.C., 1993, pp. 343–364.
- Dana, E.S., 1963, A textbook of mineralogy with an extended treatise on crystallography and physical mineralogy, 4th ed.: John Wiley and Sons, New York, 851 pp.
- Day, S.J., 1989, Comments after presentation of—A practical approach to testing for acid mine drainage in the mine planning and approval process: 13th Annual British Columbia Mine Reclamation Symposium, June 7–8, 1989, Vernon, B.C.
- Drever, J.I., 1988, The geochemistry of natural waters: Prentice Hall, Englewood Cliffs, N.J., 437 pp.
- Duncan, D.W., and Walden, C.C., 1975, Prediction of acid generation potential: Report to Water Pollution Control Directorate, Environmental Protection Service, Environment Canada, Nov. 1975, 18 pp.
- Ferguson, K.D., 1985, Static and kinetic methods to predict acid mine drainage; *in* International Symposium Biohydrometallurgy: Aug. 22–24, 1985, Vancouver, B.C., 37 pp.
- Ferguson, K.D., and Erickson, P.M., 1988, Pre-mine prediction of acid mine drainage; *in* Salomons, W., and Forstner, U. (eds.), Environmental Management of Solid Waste—Dredged Material and Mine Tailings: Springer-Verlag, N.Y., pp. 24–43.
- Ferguson, K.D., and Mehling, P.E., 1986, Acid mine drainage in B.C.—The problem and search for solutions: Presented at 10th CIM Meeting, Oct. 2–4, Victoria, B.C., 21 pp.
- Ferguson, K.D., and Morin, K.A., 1991, The prediction of acid rock drainage—Lessons from the data base; *in* Proceedings of the 2nd Internat Conference on the Abatement of Acidic Drainage: Sept. 16–18, Montreal, Canada, Tome 3, pp. 83–106.
- Hem, J.D., 1970, Study and interpretation of the chemical characteristics of natural water: U.S. Geological Survey Water-Supply Paper 1473, Washington, D.C., 363 pp.
- Jennings, S.R., and Dollhopf, D.J., 1995, Acid-base account effectiveness for determination of mine waste potential acidity: *Journal of Hazardous Materials* 41, pp. 161–175.
- Lapakko, K.A., 1988, Prediction of acid mine drainage from Duluth Complex mining wastes in northeastern Minnesota; *in* Mine Drainage and Surface Mine Reclamation, v. 1: Mine Water and Mine Waste. Proceedings of the 1988 Mine Drainage and Surface Mine Reclamation Conference, Bureau of Mines IC 9183, pp. 180–190.
- Lapakko, K.A., 1990, Solid phase characterization in conjunction with dissolution experiments for prediction of drainage quality; *in* Doyle, F. (ed.), Proceedings of the Western Regional Symposium on Mining and Mineral Processing Wastes: Society for Mining, Metallurgy, and Exploration, Inc., Littleton, Colo., pp. 31–39.
- Lapakko, K.A., 1991, Non-ferrous mine waste characterization project: Minnesota Dept. of Natural Resources, Div. of Minerals, St. Paul, 68 pp. plus appendices.
- Lapakko, K.A., 1992a, Recent literature on static predictive tests; *in* Chander, S. (ed.), Emerging Process Technologies for a Cleaner Environment: Proceedings of the Symposium on Emerging Processing Technologies for a Cleaner Environment, Feb. 24–27, Phoenix, Ariz., Society for Mining, Metallurgy, and Exploration, Inc., Littleton, Colo. pp. 109–119.
- Lapakko, K.A., 1992b, Characterization and static testing of ten gold mine tailings; *in* Proceedings of the 1992 American Society for Surface Mining and Reclamation Meeting: June 14–18, Duluth, Minn., pp. 370–384.
- Lapakko, K.A., 1993, Evaluation of tests for predicting mine waste drainage pH: Report to the Western Governors’ Association, 76 pp. plus appendices.
- Lapakko, K.A., 1994a, Evaluation of neutralization potential determinations for metal mine waste and a proposed alternative; *in* Proceedings of the International Land Reclamation and Mine Drainage Conference on the Abatement of Acidic Drainage: April 24–29, Pittsburgh, Pa., pp. 129–137.
- Lapakko, K.A., 1994b, Comparison of Duluth Complex rock dissolution in the laboratory and field; *in* Proceedings of the International Land Reclamation and Mine Drainage Conference on the Abatement of

- Acidic Drainage: April 24–29, Pittsburgh, Pa., pp. 419–428.
- Lapakko, K.A., 1995, Unpub. data from Minnesota Department of Natural Resources, Division of Minerals, St. Paul, Minn.
- Lapakko, K.A., and Antonson, D.A., 1991, The mixing of limestone with acid producing rock; *in* Proceedings of the 2nd Internatl Conference on the Abatement of Acidic Drainage: Sept. 16–18, Montreal, Canada, pp. 343–358.
- Lapakko, K.A., and Antonson, D.A., 1994, Oxidation of sulfide minerals present in Duluth Complex rock—A laboratory study; *in* Environmental Geochemistry of Sulfide Oxidation: ACS Symposium Series 550, American Chemical Society, Washington, D.C., pp. 593–607.
- Lapakko, K.A., and Lawrence, R.W., 1993, Modification of the net acid production (NAP) test; *in* Proceedings of the 17th Annual British Columbia Mine Reclamation Symposium: May 4–7, Port Hardy, B.C. pp. 145–159.
- Lapakko, K.A., and Wessels, J.N., 1995, Release of acid from hydrothermal quartz-carbonate hosted gold-mine tailings; *in* Proceedings of Sudbury '95: May 28–June 1, Conference on Mining and the Environment, Sudbury, Ontario, pp. 139–148.
- Lawrence, R.W., 1990, Prediction of the behavior of mining and processing wastes in the environment; *in* Doyle, F. (ed.), Proceedings of the Western Regional Symposium on Mining and Mineral Processing Wastes: Society for Mining, Metallurgy, and Exploration, Inc., Littleton, Colo., pp. 115–121.
- Lawrence Consulting LTD, 1991, Final Report—Acid mine drainage prediction testing: Western Governors' Association Program, Prepared for Minnesota Department of Natural Resources, St. Paul, 19 pp. plus appendices.
- Lutwick, G.D., 1986, Mineral composition and acid consuming potential of Nova Scotia shales: Nova Scotia Research Foundation Corporation, Halifax, Nova Scotia, 32 pp.
- Miller, S.D., Jeffery, J.J., and Murray, G.S.C., 1990, Identification and management of acid generating mine wastes—Procedures and practices in Southeast Asia and the Pacific Regions; *in* Gadsby, J.W., Malick, J.A., and Day, S.J. (eds.), Acid Mine Drainage Designing for Closure: BiTech Publishers Ltd., Vancouver, B.C., pp. 1–11.
- Morin, K.A., and Hutt, N.M., 1994, Observed preferential depletion of neutralization potential over sulfide minerals in kinetic tests—Site specific criteria for safe NP/AP ratios; *in* Proceedings of the Internatl Land Reclamation and Mine Drainage Conference on the Abatement of Acidic Drainage: April 24–29, Pittsburgh, Pa., pp. 148–156.
- Nelson, M.B., 1978, Kinetics and mechanisms of the oxidation of ferrous sulfide: Ph.D. thesis, Stanford Univ., Palo Alto, Calif., 286 pp.
- Nordstrom, D.K., 1982, Aqueous pyrite oxidation and the consequent formation of secondary iron minerals; *in* Kittrick, J.A., Fanning, D.S., and Hossner, L.R. (eds.), Acid Sulfate Weathering: Soil Science Society of America Spec. Pub. No. 10, pp. 37–56.
- O'Hearn, T., 1996, Unpub. laboratory notes: B.C. Research Corporation, Vancouver, B.C. Personal commun. with K.A. Lapakko.
- Perry, E.F., 1985, Overburden analysis—An evaluation of methods; *in* Proceedings of the Symposium on Surface Mining, Hydrology, Sedimentology, and Reclamation: Univ. of Kentucky, Lexington, Ky., pp. 369–375.
- Rauch, H.W., and White, W.B., 1977, Dissolution kinetics of carbonate rocks, 1. Effects of lithology on dissolution rate: Water Resource Research, v. 13, no. 2, pp. 381–394.
- Reclamation Research Unit and Schafer and Associates, 1987, Laboratory analytical protocol for the streambank tailings and revegetation studies, Silver Bow Creek RI/FX: EPA Region 8, App. 16, Acid-Base Account, Montana State Univ., Bozeman, Mont., pp. A-108–A-131.
- Scharer, J.M., Garga, V., Smith, R., and Halbert, B.E., 1991, Use of steady state models for assessing acid generation in pyritic mine tailings; *in* Proceedings of the 2nd Internatl Conference on the Abatement of Acidic Drainage: Sept. 16–18, Montreal, Canada, pp. 211–230.
- Smith, R.M., Grube, W.E., Jr., Arkele, T., Jr., and Sobek, A.A., 1974, Mine spoil potentials for soil and water quality: West Virginia Univ., EPQ-670/2-74-070.
- Sobek, A.A., Schuller, W.A., Freeman, J.R., and Smith, R.M., 1978, Field and laboratory methods applicable to overburden and minesoils: EPA 600/2-78-054, 203 pp.
- Stumm, W., and Morgan, J.J., 1981, Aquatic chemistry—An introduction emphasizing chemical equilibria in natural waters: John Wiley and Sons, New York, 470 pp.
- U.S. Environmental Protection Agency, 1994, Technical document—Acid mine drainage prediction: Office of Solid Waste, Special Waste Branch, EPA 530-R-94-036, Washington, D.C., 49 pp.
- White, W.W., III, and Jeffers, T.H., 1994, Chemical predictive modeling of acid mine drainage from metallic sulfide-bearing waste rock; *in* Environmental Geochemistry of Sulfide Oxidation: ACS Symposium Series 550, American Chemical Society, Washington, D.C., pp. 608–630.

Chapter 16

THE HEALTH EFFECTS OF MINERAL DUSTS

Malcolm Ross

U.S. Geological Survey, 12201 Sunrise Valley Drive, MS 954, Reston, VA 20192

PROLOGUE

“Everything is a poison, nothing is a poison, the dose alone makes the poison.” (Paracelsus 1493–1541).

As a consequence of environmental and health consciousness that began in the 1970s and continues unabated to this day, several common minerals have become suspect as agents of cancer and other diseases. Many mine dumps have been placed on the Environmental Protection Agency’s (EPA) Superfund list for future cleanup, because some of the minerals contained in these dumps are assumed to be hazardous to human health. Better environmental controls were certainly needed in many of our basic mining, smelting, steel, and chemical industries, and much progress has been made in recent years in reducing industrial emissions. However, some of the newly instituted (and excessively restrictive in the view of many) regulatory controls are the result of an extreme overreaction to perceived health risks that are in fact insignificant or nonexistent.

The very stringent Federal regulations promulgated in the United States are based on a health policy that appears to require a risk-free living environment. The prevailing cancer dogma in the United States espouses the “no threshold” theory of cancer induction. It is stated repeatedly by influential health specialists that, since no one knows the minimum amount of a carcinogen required to initiate the growth of a tumor, it must be assumed that any amount of a carcinogen is unsafe. Thus, the public is led to believe that exposure to just one molecule of a chemical carcinogen can cause cancer. In regard to exposure to asbestos and other mineral dusts, this paradigm becomes “one mineral fiber or particle can kill.” What the public has not been told is that simply living on Earth exposes us to innumerable naturally-occurring carcinogens. It should be recognized that naturally occurring carcinogens (as defined by animal experiments) are ubiquitous in foods we eat; we ingest at least 10,000 times more of nature’s carcinogens than of man-made carcinogens (Ames et al., 1987). For example, in California’s Silicon Valley, 35 water wells were shut down because the water contains concentrations as high as 2,800 parts per billion (ppb) of trichloroethylene (a man-made organic solvent that causes cancer in animals when administered in large doses), even though this water is at least 1,000 times **less** carcinogenic than an equal volume of cola, beer, coffee, or wine; these beverages contain animal carcinogens such as hydrogen peroxide, methylglyoxal, formaldehyde, nitrosamines, and ethyl alcohol. Naturally occurring chemical carcinogens at concentrations of 50,000 ppb or greater are found in such common foods as apples, strawberries, cauliflower, cabbage, peaches, celery, lettuce, pota-

toes, bananas, carrots, nutmeg, broccoli, and mushrooms (Ames et al., 1987; 1990a). In summary, an extraordinary variety of chemicals, many proven to be animal carcinogens, are found in edible plants; they are part of the plant’s natural defense mechanism against pests such as fungi, bacteria, and insects. The same can be said about mineral carcinogens, for we are exposed to asbestos and other mineral-bearing dusts in the ambient environment every day of our lives; some of these dusts can cause lung disease after heavy exposure of long duration in the work place but seldom affect those experiencing low workplace exposure or exposure outside the occupational setting. As we shall see, *the dose makes the poison*.

INTRODUCTION

Ore and gangue minerals that are presently classified by world health organizations as human carcinogens include chrysotile, amosite, crocidolite, anthophyllite, tremolite, and actinolite asbestos; minerals containing arsenic, cadmium, chromium, nickel, and beryllium; radioactive minerals; quartz; tridymite; and cristobalite. Many workers, including asbestos workers, miners, millers, quarry workers, sandblasters, stone masons, tunnel drivers, and agricultural workers, are exposed to mineral dusts from a variety of sources, but particularly through the inhalation of powders arising from the fragmentation of rocks and their constituent minerals in the mine and mill. These workers may develop pneumoconiosis (a disease of the lung caused by the inhalation of foreign particles) and, in some instances, malignant neoplasms (new tissue not serving any necessary physiologic function), particularly lung cancer, as a result of such exposures. These diseases are also found in working populations which process or handle rock and mineral products in secondary capacities, for example in the smelter, foundry, and construction environments (note that workers in these occupations are also exposed to other toxic agents, such as, various metals and synthetic compounds). Although mankind has been exposed to many different types of mineral dusts, there are only a few minerals to which exposure was of sufficient density and duration that definitive medical evidence of injury is documented. In addition to defining the nature of the disease or lesion in the exposed worker through the practice of clinical medicine, epidemiological studies of a group (cohort) of workers exposed to the same type or types of mineral dust should be made so as to clearly describe the causative agent(s) and to define a “dose-response” relationship between the amount of exposure and degree of injury. The basic principles of the science of epi-

demiology are given by Morris (1975) and Shy (1986).

Miners are generally exposed to rock dusts containing several minerals. For example, granite workers are exposed to large amounts of quartz, feldspars, amphiboles, pyroxenes, and micas; coal miners are exposed to quartz, carbonaceous material, and small amounts of other minerals including various clays, carbonates, sulfides, and silicates; taconite iron ore miners are exposed to quartz, iron oxides, carbonates, amphiboles, and various layer silicates; and chrysotile asbestos miners are exposed to the three serpentine minerals (chrysotile, and asbestiform lizardite and antigorite) and to minor amounts of other minerals. These multiple exposures often make it difficult to describe the exact etiology (cause) of a worker's disease. For example, there is still disagreement as to the relative importance of quartz versus carbonaceous compounds to the development of coal worker's pneumoconiosis (black lung) and quartz versus layer silicates (micas, chlorites, etc.) to the origin of slateworkers' pneumoconiosis. In the following I will give a general review of the health effects from occupational exposure to mineral dusts where there is definite clinical evidence of disease that is supported by some epidemiological data defining the origin of the disease. Since workers are often exposed to more than one type of dust, comparative epidemiology and pathology are necessary to isolate the dust or dusts responsible for injury. For example, if workers such as the Gauley Bridge tunnel drivers who were exposed to sandstone dusts composed almost entirely of quartz (Cherniack, 1986) show the same health effects as granite workers, then quartz can be considered to be the important contributor to disease, with the other minerals in the granite (feldspars, amphiboles, micas, etc.) being much less important. As another example, asbestos workers exposed to amphibole asbestos show much greater amount of disease than do those exposed only to chrysotile asbestos.

The health effects of the following mineral and rock dusts will be reviewed: the three commercially important asbestos minerals (chrysotile, amosite, and crocidolite), three polymorphs of silica (quartz, cristobalite, and tridymite), coal (predominantly carbonaceous material plus minor amounts of other minerals), and several silicate minerals (including talc, pyrophyllite, sepiolite, kaolinite, bentonite, attapulgite, sepiolite, palygorskite, mica, vermiculite, and erionite).

THE ASBESTOS MINERALS

Mineralogy of asbestos

Standard references published over the last 50 years list six forms of asbestos (all belonging to the "silicate" group of minerals) that are used in commerce: the serpentine variety is chrysotile, and the amphibole varieties are amosite, crocidolite, anthophyllite, actinolite, and tremolite. Detailed understanding of the structure and chemistry of these minerals came later than their discovery, thus some of the older literature can be confusing with regard to mineral identifications.

Chrysotile $[\text{Mg}_3\text{Si}_2\text{O}_5(\text{OH})_4]$, one of the three polymorphs of serpentine, is generally fibrous and is found in serpentinites and kindred rocks; the two other serpentine minerals, lizardite and antigorite, are nonfibrous. About 90 to 95% of the past and present world production of asbestos was or is of the chrysotile type. Amosite $[(\text{Fe},\text{Mg})_7\text{Si}_8\text{O}_{22}(\text{OH})_2]$ is the very rare asbestiform variety of grunerite amphibole. It is mined only in South Africa in

metamorphosed banded iron formations and in the past comprised 2 to 3% of the total world production of asbestos. Crocidolite $[\text{Na}_2(\text{Fe}^{2+},\text{Mg})_3\text{Fe}_2^{3+}\text{Si}_8\text{O}_{22}(\text{OH})_2]$ is the asbestiform variety of riebeckite amphibole, and has been mined in only four localities: (1 and 2) in the banded iron formations of the Transvaal and Cape Provinces of South Africa, (3) in the iron formations of the Hammersley Range of Western Australia, and (4) in the Cochabamba area of Bolivia. Only the South African mines are still active. Crocidolite composes about 3% of the world asbestos production. The only other form of asbestos that has been mined on a significant scale is anthophyllite $[(\text{Mg},\text{Fe})_7\text{Si}_8\text{O}_{22}(\text{OH})_2]$ from the Paakkila area of East Finland. With the Finnish mines closed, there is now very little anthophyllite mined anywhere in the world. Minor amounts of tremolite $[\text{Ca}_2\text{Mg}_5\text{Si}_8\text{O}_{22}(\text{OH})_2]$ and actinolite $[\text{Ca}_2(\text{Mg},\text{Fe})_5\text{Si}_8\text{O}_{22}(\text{OH})_2]$ asbestos have been mined but were of little economic importance. However, these two forms of asbestos may be associated as minor contaminants in chrysotile-bearing rocks and other types of ores and as such have been of some concern to those studying the health effects of miners and other workers.

Deposits of asbestos are found in four types of rocks: (a) Type I—alpine-type ultramafic rocks, including ophiolites and serpentinites (chrysotile, anthophyllite, actinolite, and tremolite); (b) Type II—stratiform ultramafic intrusions (chrysotile, actinolite, and tremolite); Type III—serpentinized limestone (chrysotile); and Type IV—banded iron formations (amosite and crocidolite). Type I deposits are by far the most important and account for approximately 90% of the asbestos ever mined. Reviews of asbestos mineralogy and the geological occurrences of commercial asbestos are given by Ross (1978, 1981).

Diseases related to exposure to asbestos fibers

Three principal diseases are related to exposure to one or more of the asbestos minerals. These are: (1) *lung cancer*, which includes cancer of the trachea, bronchus, and lung proper; (2) *mesothelioma*, a cancer of the pleural and peritoneal membranes, which invests the lung and abdominal cavities, respectively; and (3) *asbestosis*, a nonmalignant diffuse interstitial fibrosis of the lung tissue, often leading after long exposure to severe loss of lung function and respiratory failure. The occurrence of lung cancer in asbestos workers is complicated by its strong association with use of tobacco, which leads to considerable difficulty in assigning the relative risks of asbestos exposure to smokers. For complete reviews of asbestos-related disease, the reader is referred to Craighead et al. (1982), Dement et al. (1986), and Skinner et al. (1988).

Lung cancer

There are four major histological types of lung cancer, all of which are prevalent in asbestos workers: *squamous cell carcinoma* is the most prevalent lung tumor followed by *adenocarcinoma*, *small cell carcinoma*, and *large cell carcinoma*, respectively (Skinner et al., 1988, p. 138). These four tumors account for approximately 85% of all primary neoplasms of the lung. The lung cancers may be generally classified as hilar types (presumed to originate within the bronchial wall) or peripheral types (presumed to originate in the small airways of the lung). Squamous cell carcinomas are of the hilar type, arising from the major and segmen-

tal bronchi. Adenocarcinomas may arise in the hilar or peripheral region of the lung, the latter arising from cells lying distal to the terminal bronchioles. The small cell carcinomas arise in both major bronchi and in the lung periphery. Microscopically, the small cell type may be divided into oat cell and intermediate cell carcinomas, or a combination of the two. Large cell carcinomas are composed of undifferentiated malignant cells showing no special features. Included in this category are tumors showing clear cells or giant cells that tend to arise from the more distal bronchi (Green and Vallyathan, 1986). The prognosis for bronchial carcinoma is poor and survival rates have changed little over the last 30 years. Overall, 5-year survival rates are less than 10%, but those asymptomatic patients who undergo surgical resection of small peripheral carcinoma can expect a 5-year survival rate of 50% (Hodous and Melius, 1986). The distribution of the four main types of lung cancer among asbestos workers is similar to that found in lung cancer patients who were unexposed to asbestos, the only difference is that the cancer tends to appear in the lower lobes of the lung in the asbestos workers (Skinner et al., 1988). In asbestos worker cohorts a significant increase of lung cancer death rate appears 10 to 14 years after first exposure to asbestos and the rate peaks 20 to 25 years later (Selikoff et al., 1980).

Mesothelioma

Mesothelioma is a rare tumor that arises from the mesothelial membrane that lines the pleural, peritoneal, and pericardial cavities. The tumor is usually, but not always, associated with exposure to asbestos, and particularly to crocidolite asbestos. The macroscopic features of pleural mesothelioma are those of a gray-white mass or yellow-gray mass that may cover part of the lung surface, or may completely encase the lung. Microscopically, the mesothelioma tumor can be classified into tubo-papillary, sarcomatous, and mixed types. The tumor spreads along the interlobar fissures and often invades the superpleural portions of the lungs. Direct invasion of adjacent organs, such as the heart, diaphragm, and liver often occur, as well as metastases to local lymph nodes. Peritoneal mesothelioma tends to spread along the peritoneal cavity and to invade the abdominal organs, becoming so widespread that surgery is ineffective in controlling it (Brenner et al., 1981). Mesothelioma generally appears 20 to 40 years after first exposure to asbestos, but once it appears there is a very rapid growth. Death usually occurs within a year after the first symptoms appear. Mesothelioma is difficult to diagnose for the nature of the clinical course of this disease and its location mimics peripheral bronchogenic carcinoma of the lung parenchyma, a tumor that may spread to the pleura. Pleural mesothelioma is approximately five times more common than peritoneal mesothelioma, except in some of the cohorts exposed to asbestos (HEI.AR, 1991).

Asbestosis

Asbestosis, a nonmalignant disease, is a diffuse interstitial fibrosis of the lung tissue resulting from the inhalation of large amounts of asbestos fibers, often leading after long exposure to severe loss of lung function and respiratory or cardiac failure. The disease is often associated with thickening of the pleura (pleural fibrosis), pleural calcification, and the appearance of asbestos bodies (asbestos fibers that are coated with collagen and ferritin). The earliest lesion related to asbestos exposure involves the respi-

ratory bronchioles where deposition of asbestos fibers on the walls of the bronchioles and adjacent air sacs (the alveoli) stimulate macrophage response that promotes deposition of reticulin and collagen in the walls of the bronchioles. As the disease progresses, the fibrosis extends to the walls of the alveoli and eventually the fibrosis leads to the destruction of the alveolar spaces. This fibrous scar tissue causes the lung tissue to stiffen, narrows the airways, and causes reduced efficiency of gas exchange resulting in shortness of breath (dyspnea) and requiring the patient to expend more effort in breathing. Pulmonary hypertension is frequently associated with advanced asbestosis, and resultant *cor pulmonale* (right-sided heart failure) may be the cause of death.

Epidemiological studies of occupational cohorts exposed to asbestos

Three common forms of asbestos, chrysotile, amosite, and crocidolite, were used extensively throughout the industrialized world from the late 1800s to the present. Ross (1984, pp. 58–60) gives historical data on asbestos use in the United States in terms of tonnages imported of the three common forms of asbestos and the commercial applications of each type. The specific use of chrysotile, amosite, and crocidolite is of great importance in understanding the health history of specific asbestos worker cohorts.

The asbestos trades-workers

A very significant increased incidence, in relation to the general male population, of lung cancer, mesothelioma, and asbestosis is found in men who were employed in the “asbestos trades”—the asbestos insulation of pipes, steam boilers, and buildings and the production of asbestos textiles, roofing materials, friction materials, tiles, wall boards, packings, gaskets, etc. These “trades” workers generally worked with chrysotile, amosite, and crocidolite during their working careers. Ross (1984, Tables 3a,b) gives the observed and expected mortality of 21 cohorts of asbestos trades workers. Of these epidemiological studies, 12 are of asbestos factory workers, 8 are of insulation workers, and 1 of asbestos construction workers. These 21 cohorts comprised 50,143 individuals and of these 7,166 were deceased. Death due to lung cancer was reported for 1,198 (16.7%) workers and 402 (5.61%) deaths were reported as due to mesothelioma. There was also very large excess of mortality (over the control cohorts) due to nonmalignant respiratory disease, including asbestosis. These epidemiological studies show that most asbestos trades worker cohorts showed a large excess death due to lung cancer, mesothelioma, and asbestosis. Lung cancer mortality was much greater for smokers than for nonsmokers, but there appeared to be no relationship between smoking and mesothelioma mortality. Of the 21 trades cohorts reported by Ross (1984) two were exposed to mostly crocidolite asbestos and one was exposed only to chrysotile asbestos. The mortality picture of these three cohorts is quite different; a large excess of mesothelioma and lung cancer appeared on the crocidolite-exposed cohorts, whereas in the chrysotile-exposed cohort, lung cancer mortality was similar to the control cohort and there were no mesothelioma deaths. In addition to the studies of cited by Ross (1984), there are additional health reports on workers who produced chrysotile-bearing friction materials and cement products, for example see Newhouse and Sullivan

(1989), Thomas et al. (1982), Gardner et al. (1986), and Ohlson and Hogstedt (1985). These four studies show no significant excess asbestos-related disease in workers exposed only to chrysotile. Table 16.1 gives mortality data for the cohort of Swedish chrysotile asbestos cement workers studied by Ohlson and Hogstedt (1985). An explanation of epidemiological nomenclature and data tabulation, as presented in Tables 16.1, 16.4, 16.5, 16.6, 16.7, and 16.8, is given in the appendix.

TABLE 16.1—Observed (Obs.) and expected (Exp.) number of deaths 1951-58 for the total cohort of 1,176 Swedish asbestos cement workers, exposed only to chrysotile asbestos. Table adapted from Ohlson and Hogstedt (1985).

Cause of death*	Obs.	Exp.	SMR*
All causes	220	214	103
Malignant tumors	44	50	88
Lung cancer	11	9	123
Gastric cancer	1	5.9	17
Intestinal cancer	11	5.9	186
Cancer of the pancreas	2	2.2	90
Diseases of the circulatory system	103	98	105
Diseases of the respiratory tract	13	8.5	153
Violent death	34	27	125

*Standardized Mortality Ratio. $SMR = 100(\text{Obs.})/(\text{Exp.})$.
An SMR of 100 indicates there is no increased risk of disease.

The asbestos miners and millers

Unlike the trades workers, the men working in the mining and milling of asbestos are generally exposed to only one type of fiber; a few exceptions occur in the mining regions of South Africa where some workers were employed in crocidolite, amosite, and chrysotile mines. Epidemiological studies of miners and millers exposed to only one type of fiber permit one to ascertain the human health effects of the different forms of asbestos. Ross (1984, Table 4—Studies A, F, G, H, and J) gives mortality data for the five major epidemiological studies of asbestos miners and millers; one is a cohort of anthophyllite asbestos miners, one is a cohort of crocidolite miners, and three are cohorts of chrysotile miners. The mortality patterns noted on comparing the trades and mines cohorts makes it clear that there are very significant differences in the human health effects of the different asbestos minerals.

Comparative epidemiology of the asbestos-exposed cohorts

Those groups exposed only to chrysotile asbestos experienced much less disease than those who were exposed to amphibole asbestos (most of the trades cohorts were exposed to amphibole as well as chrysotile asbestos). The long term studies of chrysotile miners and millers from the asbestos mining towns of Québec, Canada (McDonald et al., 1980; Ross, 1984, pp. 72–77) show that those experiencing exposures of less than 20 fibers/cm³ for a working lifetime are not at increased risk of developing asbestos-related disease. A similar mortality profile is reported for the Italian chrysotile miners (Ross, 1984, Table 4). In contrast, epi-

demiological studies of crocidolite miners and trades workers show that short term heavy exposure or long term moderate-to-light exposure to this type of fiber causes excessive mortality due to lung cancer, mesothelioma, and asbestosis. There are only two mining regions of the world where mesothelioma is a statistically significant cause of death—the crocidolite mining districts of the Cape Province of South Africa and Wittenoom, Western Australia. Study of the trades workers exposed mostly to amosite asbestos show that this fiber too can cause severe disease. In contrast to chrysotile, where exposure thresholds can be prescribed to prevent disease (<10 fibers/cm³), there is little exposure data to make a similar estimate to protect the crocidolite or amosite worker. Mossman et al. (1990) present data that shows that exposure to chrysotile asbestos in buildings, schools, and homes (including structures with spray-on chrysotile asbestos coatings) is not a health risk. They state “clearly, the asbestos panic in the U.S. must be curtailed.”

THE SILICA MINERALS AND AMORPHOUS SILICA

Mineralogy of silica

The six naturally occurring crystalline silica minerals are composed mostly of silicon and oxygen (SiO₂); only small amounts of Al, Fe, Mn, Mg, Ca, and Na are contained in the crystal structures of these minerals. These minerals (generally referred to in the mineralogical literature as the *silica minerals*) are quartz, cristobalite, tridymite, melanophlogite, coesite, and stishovite. Micro-crystalline varieties of quartz include chalcedony, chert, jasper, agate, prase, onyx, and flint. The silica minerals are all composed of SiO₄ tetrahedra, each linked to four like tetrahedra to form the three-dimensional crystal structure. However, the orientation of the tetrahedra are different in each of these six minerals. Quartz is the second most common mineral (after feldspar) in the Earth's crust; for example, common rocks such as granite rocks contain 25 to 40% quartz, shales average 22% quartz, and sandstones 67% quartz (Clark, 1924). Cristobalite and tridymite are much less common than quartz and occur in cavities in volcanic rocks and as products of devitrification of volcanic glasses. Melanophlogite, coesite, and stishovite are very rare minerals and need not be considered here. General reviews on the nature of the crystalline silica minerals are given by Frondel (1962), Ampian and Virta (1992), and USBM (1992a).

In the health reports of SiO₂-exposed workers the mineral names quartz, cristobalite, etc. are seldom used. Instead the term *silica*, *crystalline silica*, or less often (and improperly) *free silica* is substituted for the correct mineral name. In most of the health studies of silica-exposed workers the exposure has been to quartz, but since the mineral name is often not explicitly stated in the reports, we must in this review continue to use the term *silica*. There are very few studies of workers exposed to cristobalite and there are no studies of workers exposed only to tridymite.

The noncrystalline forms of silica (*amorphous silica*) include natural glasses found in various volcanic rocks and synthetic glasses such as fume silica, fiber glass, and mineral wool. Opal is a natural occurring hydrated form of silica; it may be amorphous or nearly amorphous and appears in a variety of geologic localities, especially in hot spring deposits. Opaline materials are also found in diatomaceous earth deposits and in bentonite clays. Many opals have no crystallinity (amorphous) and are sometimes

referred to as amorphous silica or as opal A. Devitrification in some opals may produce very small inclusions of poorly crystallized cristobalite; such material is sometimes referred to as opal C or opal CT. Some crystallites in opal may be disordered structures composed of domains of cristobalite mixed with domains of tridymite. Amorphous silica may, when heated to high temperature, be converted to cristobalite. Dusts composed of amorphous silica (with the exception of fiber glass) have not been implicated with human disease and thus will not be considered further in this review.

Diseases related to exposure to silica dust

Silicosis

Three types of silicosis are defined.

- 1) *Chronic silicosis* (also referred to as *classical* or *nodular silicosis*) is a progressive obstructive lung disease characterized by the development of fibrogenic tissue. In response to inhalation of quartz particles (and perhaps other forms of crystalline silica) in the median size range of 0.5 to 0.7 μm , macrophages (the cells that scavenge and ingest foreign particulate matter in the lung) generate fibrogenic proteins and growth factors that stimulate the formation of collagen (Craighead, 1988). The hilar lymph nodes tend to be enlarged and silica-containing fibrotic nodules (which form confluent masses 2 to 3 mm in diameter) appear in large numbers in the apical and posterior regions of the upper and lower lobes of the lung. As the silicosis disease progresses, the fibrotic nodules coalesce into larger masses and these may contain the remnants of blood vessels and bronchi. These lesions may vary in size from about 3 mm to a size involving one-third of the lung (Lapp, 1981). Heart or respiratory failure is the ultimate consequence of silicosis.
- 2) *Acute silicosis* (also referred to as *silicotic alveolar proteinosis*) develops in workers exposed to exceptionally high concentrations of fine particles of silica, usually quartz dust. Here the lining of the airways are damaged and a lipid-rich protein accumulates, obliterating the air spaces. Progressive massive fibrosis appears, usually in the upper regions of the lung, and superinfection by mycobacterial organisms generally occurs. In acute silicosis the lungs are often very heavy and semisolid and microscopic examination on autopsy shows that the air spaces are filled with an amorphous finely granular substance (Craighead, 1988).
- 3) *Accelerated silicosis* is a condition whereby the progression of disease is intermediate between chronic and acute silicosis. This form of silicosis develops after 5 to 10 years of heavy exposure to crystalline silica dust and is especially seen in sandblasters who were exposed to fine particulates of almost pure quartz. The victim of accelerated silicosis often shows no clinical abnormalities other than breathlessness, but X-ray shows irregular upper zone fibrosis associated with numerous nodules. This form of silicosis is progressive with a continuing decrease of lung function even in the absence of further dust exposure. Death by cardiopulmonary failure within 10 years of onset of symptoms is often the outcome of this form of silicosis (Craighead, 1988).

Silicotuberculosis

There has long been noted an association between silicosis and *tuberculosis* and in the past tuberculosis was a major cause of death of those with silica-damaged lungs; death certificates often listed the cause of death as due to *silicotuberculosis*. For example, in the 1976 *Vital Statistics of the United States*, it is reported that there were 215 silicosis deaths (ICD.8, 515.0) and 92 silicotuberculosis deaths (ICD.8, 010); in contrast, only 54 *asbestosis* (ICD.8, 515.2) deaths were listed for 1976. More recently, due to better dust control and chemotherapy, tuberculosis associated with silicosis has much decreased except in the less developed areas of the world. Experimental evidence shows that the presence of silica promotes the growth of *M. tuberculosis* in macrophage cultures. Silicosis appears to modify the progress of tuberculosis but may also change the character of the tuberculosis lesions. Epithelioid cell proliferation, Langhan's giant cell formation, and the lymphocytic reaction seen in the usual tuberculosis patient may be suppressed by the silicosis (Lapp, 1981).

Cancer

Recently, the crystalline silica minerals have been implicated in the pathogenesis of bronchogenic carcinoma. In 1986 a working group of the International Agency for Research on Cancer (IARC) reviewed the scientific data that suggested a relationship between exposure to crystalline silica dust and cancer induction. They published their findings in IARC Monograph 42 (IARC, 1987a), concluding that there was sufficient evidence for carcinogenicity in experimental animals and limited evidence for carcinogenicity in humans. Monograph 42 was followed by IARC's 1987 publication of Supplement 7 (IARC, 1987b) which, upon review of 628 substances, placed the crystalline silica minerals into Group 2A as **probably carcinogenic to humans**. As a result of this IARC decision, the United States Occupational Safety and Health Administration (OSHA) invoked the OSHA Hazard Communication Standard of 1983 to require that **any product** containing any of the crystalline silica minerals in amounts greater than 0.1 wt% be labeled as a possible human carcinogen.

The fibrogenic effects of crystalline silica in animal models are well known (Saffiotti, 1960, 1962, 1986; Reiser and Last, 1979), but there are also a significant number of experimental studies that show that tumors can be produced in rats through the inhalation and intrapleural or intratracheal injection of silica dusts (usually quartz is used in animal experiments). Wagner (1966) and Wagner and Wagner (1972) produced tumors in Alderly Park rats through single intrapleural inoculations of silica. These tumors consisted of malignant histiocytic lymphomas, reticulum cell sarcomas, and lymphoblastic and lymphocytic lymphomas. Holland et al. (1983) noted squamous cell carcinomas and adenocarcinomas in Fischer-344 rats after silica inhalation and in Sprague-Dawley rats after intratracheal instillation of silica.

Saffiotti (1986) in a review of the fibrogenic and carcinogenic activity of silica-bearing dusts on experimental animals, noted that there were significant differences in the pathogenic effects on different animal species. Saffiotti states "the response of the Syrian golden hamster to the introduction of crystalline silica in the respiratory tract (either by inhalation or by intratracheal instillation) is altogether different from that in the rat. In the hamster no respiratory tumors were induced under exposure conditions compara-

ble to those for rats. A consistent association was observed in these two species between the induction of fibrosis and the induction of tumors of the lung." As shown in Table 16.2, the same types of silica that were effectively fibrogenic and carcinogenic in rats failed to produce either type of response in the hamsters.

TABLE 16.2—Tumorigenic and fibrogenic effects of quartz dust on rats and hamsters. Table adapted from Saffiotti (1986).

Test material	Animal species	Route	Tumors	Fibrosis
Quartz (Min-U-Sil)	Rat (Sprague-Dawley)	i.t.* (10 doses, 7 mg each)	yes	yes
Quartz (Min-U-Sil)	Rat (F-344)	Inhalation (24 mos.)	yes	yes
Raw shale (12% quartz)	Rat (F-344)	Inhalation (24 mos.)	yes	yes
Spent shale (8% quartz)	Rat (F-344)	Inhalation (24 mos.)	yes	yes
Quartz (Min-U-Sil)	Rat (F-344)	i.t. (20 mg, once)	yes	yes
Quartz (novaculite)	Rat (F-344)	i.t. (20 mg, once)	yes	yes
Quartz (Min-U-Sil)	Rat (F-344)	Inhalation (24 mos.)	yes	yes
Quartz (Min-U-Sil)	Syrian golden hamster	i.t. (10 doses, 7 mg each)	no	no
Quartz (Min-U-Sil)	Syrian golden hamster	i.t. (3 mg each)	no	no
Raw shale (12% quartz)	Syrian golden hamster	Inhalation (24 mos.)	no	no
Spent shale (8% quartz)	Syrian golden hamster	Inhalation (24 mos.)	no	no
Quartz (Min-U-Sil)	Syrian golden hamster	i.t. (15 doses, 0.7 mg each)	no	no

* i.t., intratracheal instillation

Craighead (1992) questions the validity of such animal experiments in predicting silica induction of cancer in humans. He asks—"Are the neoplasms that develop in rats exposed to silica and asbestos analogous to bronchogenic carcinomas in humans, or are they unique to the laboratory animal and a reaction to chronic irritation and scarring of tissue rather than a neoplastic response to a carcinogen?" But in view of the rat and hamster experiments discussed by Saffiotti, we might ask a question corollary to that of Craighead's: If silica dust levels are reduced to a point where chronic disease (e.g., fibrosis) disappears in a group of workers, will cancer also disappear? Some further insight into this question can be obtained from an epidemiological review of silica-exposed workers.

Epidemiological studies of occupational cohorts exposed to crystalline silica dust

Compared to asbestos workers and coal miners, relatively few epidemiological studies of workers exposed to silica dusts have been completed. However, in the 1980s, perhaps due to the suggestion that silicosis may increase the risk of lung cancer, many new studies were initiated. Early prevalence studies initiated by the U.S. Public Health Service and the U.S. Bureau of Mines (Lanza and Higgins, 1915; Higgins et al., 1917) showed that many miners in the Joplin District of Missouri, who were exposed to

high levels of quartz-bearing dusts, suffered from very high rates of nonmalignant lung disease. The first very large and comprehensive study of U.S. hard rock miners exposed to quartz dusts was accomplished by Flinn et al. (1963). This study included over 14,000 employees working at 50 metal mines. The mine dust concentrations (based on 14,480 impinger sample measurements) varied from 0 to 50 million particles per cubic foot (mppcf) and quartz content of the dust varied from 2 to 95%. The medical history, lung function, chest X-rays, occupational histories, and mine dust control methods, were recorded. A strong relationship was found between duration of exposure to silica and prevalence of silicosis. The health of those having less than 5 years exposure was unaffected whereas 60% of those exposed for 30 or more years showed evidence of silicosis. These and earlier studies clearly demonstrated the need to limit exposure to silica-bearing dust and were the basis to institute more comprehensive state and federal regulations to protect the worker.

One of the problems of measuring the effects of silica dusts is that miners, millers, foundry workers, etc. are exposed to a variety of dusts, both natural and man made. Thus, it has been very difficult to mount an epidemiological study of such workers where the degree and types of exposure to dusts, chemicals, radon, etc. are accurately evaluated. More recently, as funds became more readily available and epidemiological techniques greatly improved, scientists have made progress in defining the effects of these more complex workplace exposures. In the following we will review some of the newer studies of silica exposure in specific occupational groups provided below.

Minnesota iron ore miners (magnetite-bearing rock)

Taconite is a term used particularly in the Lake Superior region of Minnesota for certain rock from the Biwabik Iron-formation. A high-grade iron ore concentrate is obtained from commercial grade taconite that contains enough magnetite (Fe_3O_4) to be economically processed by fine grinding and magnetic separation. During the period from 1989 to 1991 about 43 million metric tons of taconite iron ore concentrate were processed each year in Minnesota (USBM, 1992). Taconite is a hard, dense, fine-grained metamorphic rock that contains major amounts of quartz (20–50%) and magnetite (10–20%), in addition to various other mineral constituents including hematite, carbonate minerals, amphiboles (of the cummingtonite-grunerite series), greenalite, chamosite, minnesotaite, and stilpnomelane (French, 1968). The average mineral composition the Biwabik Iron-formation taconite is: quartz (31.9%), minnesotaite (19.3%), magnetite (18.4%), siderite (9.3%), stilpnomelane (8.7%), plus minor amounts of other silicates and carbonates (Lepp, 1972, p. 275).

The mineral content of the dusts emitted from the mining and milling of taconite rock collected at the mine and mill sites of the Reserve Mining Company, near Babbitt and Silver Bay, Minnesota, respectively, are given in Table 16.3. Clark et al. (1980) report that the quartz content of the rock dust for two groups of Reserve miners varied from 0.21 million to 7.74 million particles per cubic foot with a mean of 2.7 mppcf. Based on the quartz content of the rock, the threshold limit value (TLV) for total dust in the work area is given as 5 mppcf. The TLV is the maximum number of airborne quartz particles allowable in the work place by state or federal regulations. The Minnesota taconite miners work in open pits, thus there should be no health effects due to inhalation of radon gas.

TABLE 16.3—Cohort categories by job and extent of exposure to mineral dust at the mine and mill sites of the Reserve Mining Company, Babbitt and Silver Bay, Minnesota. Table adapted from Clark et al. (1980).

Group	Processing activity	Dust composition*		
		Quartz (wt%)	Silicates (wt%)	Magnetite (wt%)
1	Mining, crushing	25–40	25–35	25–40
2	Pelletizing, shipping	2–5	6–25	65–90
3	Railroad, power plant	0	0	0
4	None, school system employees	0	0	0

*Percentages based on total airborne dust data obtained from industrial hygiene surveys conducted by the Trudeau Institute, Saranac Lake, New York.

Analysis of the mortality among men who were employed by the Reserve Mining Company from 1952 to 1976 has been reported by Higgins et al. (1983). This study was initiated in the 1970s in response to suggestions that “asbestos” was released into the air and water during processing of the taconite rock and posed a risk to the miners as well as to the general public. The town and city drinking water (obtained from Lake Superior and into which Reserve had deposited the pulverized waste rock from the mill) was thought to be a particular hazard to the residents. It was alleged that the amphibole in the waste rock (cummingtonite-grunerite series) was “asbestos” and this asbestos would cause gastrointestinal-intestinal cancer through ingestion and lung cancer from inhalation of the air-borne particles (a complete review of this controversy and the ensuing court case is given by Schaumburg, 1976; see also Ross, 1984, p. 72–78). The Reserve cohort consisted of 5,751 men, of whom 298 were deceased and 907 had worked for the company for more than 20 years. The men were exposed to respirable dust concentrations from a low of 0.02 mg/m³ to a high of 2.75 mg/m³, the modal range being 0.2 to 0.6 mg/m³. The mineral “fiber” content of the dust was occasionally higher than 0.5 “fibers”/ml in the crushing department, but usually concentrations were much lower (these “fibers” were actually cleavage fragments of cummingtonite and grunerite amphibole). The observed and expected deaths and standardized mortality ratios (SMRs) for all men who had worked more than one year or longer from 1952 to 1976 are given in Table 16.4. Overall mortality was less than expected (SMR=87) when compared to the male mortality in Minnesota, as was mortality from cardiovascular disease, all cancer, respiratory cancer, and selected nonmalignant respiratory diseases including pneumoconiosis. There was no relationship between mortality and lifetime exposure to silica dust, nor was there any suggestion that deaths from cancer increased after 15 to 20 years of latency. No mesothelioma or asbestosis cases that might be suggestive of a risk from asbestos were recorded (it is clear that the amphibole in the taconite rock is **not asbestos**).

A second epidemiological study of Minnesota taconite miners and millers, who were employed by the Erie Mining Company (Erie mine) and the U.S. Steel Corporation (Minntac mine), is reported by Cooper et al. (1992). This study cohort, followed from 1947 through 1988 with a minimum observation period of 30 years for all participants, was composed of 3,431 men of which 1,058 were deceased. Dust levels in the two mines are reported as containing 28 to 40% crystalline silica in one and 20% in the other (Sheehy and McJilton, 1987). Mineral “fiber” counts at the two mines were nearly all below 2 fibers/ml and nearly all fibers were shorter than 5 µm in length (Wylie, 1990). Note that fibers less

than 5 µm in length are not considered hazardous and thus are not included in the total count. The total number of deaths (Table 16.5) of these taconite workers was significantly less than expected, SMR=83 (based on U.S. male rates) and 91 (based on Minnesota male rates). SMRs for all cancer, respiratory cancer, diseases of the circulatory system, and nonmalignant respiratory disease were also fewer than expected when compared to both control groups. Slightly elevated, but not statistically significant, SMRs were found for colon cancer, cancer of the kidney, and lymphopoietic cancer. There was one reported case of mesothelioma in a 62-year old worker whose exposure to taconite had begun only 11 years before his death. He had previously been employed as a locomotive fireman and engineer, an occupation where he may have been exposed to amosite or crocidolite asbestos that was used as boiler insulation. Analyses of mortality of the Minnesota iron ore workers with varying lengths of service, exposure to varying amounts of dust, and with a minimum potential latency period of 30 years, provide no evidence to indicate an increased risk of lung cancer or nonmalignant respiratory disease. Thus, there is no evidence to suggest that exposure to quartz, amphibole “fibers,” or any other agent has affected the health of these miners.

TABLE 16.4—Selected causes of mortality for men who worked one year or longer for the Reserve Mining Company. Table adapted from Higgins et al. (1983).

Cause of death	ICD, 8th*	Deaths		
		Observed	Expected	SMR**
All causes	000-E999	298	343.65	87
Cardiovascular disease	402, 404, 410–429	112	123.79	90
All cancer	140–209	58	63.38	92
Respiratory cancer	160–163	15	17.94	84
Digestive cancer	150–159	20	17.57	114
Urinary cancer	188–189	3	2.97	101
Genital cancer	180–187	3	3.31	91
Selected nonmalignant respiratory diseases	470–474, 480–486, 490, 491, 493, 510–519	4	6.80	59
Most trauma	E800–E978	76	72.76	104
Motor vehicle accidents	E810–E823	38	31.12	122

*International Classification of Diseases, Eighth Revision.

**Standardized Mortality Ratio, based on white male mortality in Minnesota, 1952–1976.

Iron ore miners (hematite-bearing rock)

The Biwabik iron formation of Minnesota is composed of both hard rock taconite (the present source of most Minnesota iron ore and discussed above) and soft rock iron ore, which formed by late-stage alteration of the primary taconite. Oxidation changed the iron-bearing minerals of the taconite to hematite (Fe₂O₃) and goethite [FeO(OH)]. This soft ore was a primary source of U.S. iron ore in the past and was mined in the area of the Mesabi Range located between the towns of Hibbing and Mesaba. At present only a small amount of the soft ore is mined. The Mesabi ore contains major amounts of iron oxides, and several percent fine-grained quartz as well as minor amounts of other minerals, including kaolinite, sulfides, residual carbonates, and silicates (Gruner, 1946). Lawler et al. (1985) studied a population of 10,403 workers employed by a large steel company engaged in mining hematite

iron ore in St. Louis County, Minnesota. Of these, 4,708 worked under ground and 5,695 worked above ground. The interval of follow-up was from 1937 through 1978 and at the end of this period 2,642 under ground and 2,057 above ground workers were deceased. Quartz content of the ore was 7 to 10% and radon daughter levels were low (<60 pCi/L or 0.3 working levels). This mortality study (Table 16.6) found no excess risk of lung cancer in the total cohort (SMR=94), in the under ground miners (SMR=100), or in the above ground miners (SMR=88), contrary to the reports of excess of this disease in hematite miners from Sweden, France and England. In the Minnesota hematite miners, there was also a deficiency of nonmalignant respiratory disease (SMR=79, total cohort; 72, under ground; 89, above ground). Significant excess mortality due to stomach cancer was observed in both groups of miners when compared to U.S. males, but this excess disappeared, except for Finnish-born miners, when comparison was made to local county rates. Lawler et al. (1985) suggest that the apparent lack of significant radon exposure, under ground smoking prohibition, and absence of under ground diesel fuel may explain why the under ground miners do not show the cancer risk seen in hematite miners of Europe. However, since both groups of miners have very similar health histories (Table 16.6), any additional health effects of under ground mining are not apparent.

TABLE 16.5—Observed and expected deaths by major causes (1948-1988) in taconite miners and millers employed by the Erie Mining Company and the U.S. Steel Corporation who were exposed to taconite mineral dusts for 3 months or more prior to January 1, 1959. Table adapted from Cooper et al. (1992).

Cause of Death (ICD, 7th Revision, 1955)	Deaths		SMR*
	Observed	Expected	
All causes (001-998)	1058	1272.5	83
All malignant neoplasms (140-205)	232	267.7	87
Digestive organs and peritoneum (150-159)	66	70.5	94
Stomach (151)	11	12.0	92
Large intestine (153)	26	23.9	109
Respiratory system (160-164)	65	97.0	67
Bronchus, trachea, lung (162-163)	62	92.2	67
Kidney (180)	12	6.8	177
Lymphopoietic (200-205)	29	25.8	112
All diseases of circulatory system (400-468)	477	575.1	83
Arteriosclerotic heart disease (420)	368	481.8	76
Cirrhosis of liver (581)	24	35.5	68
Nonmalignant respiratory disease (470-527)	55	77.2	71
All external causes of death (800-998)	114	112.3	102
All accidents (800-962)	79	74.4	106
Motor vehicle accidents (810-835)	32	33.4	96
Suicides (963, 970-979)	32	27.3	117
Cause unknown	19		
Number of workers	3,431		
Number of person-years	101,055		
Deaths per 1,000 person-years	10.5		
Adjustment of cause-specific SMRs for missing certificates	+1.8%		

*Standardized mortality ratio.

TABLE 16.6—Observed and expected deaths of total cohort of St. Louis County, Minnesota iron ore (hematite) miners, 1937 to 1978. Table adapted from Lawler et al. (1985).

Cause of death	ICD*	Obs.	Exp.	SMR**
All causes	001-999	4,699	5,058.6	93
All cancers	140-209	854	879.1	97
Respiratory system	160-163	230	242.3	95
Larynx	161	12	13.7	88
Lung	162-163	212	225.8	94
Digestive organs	150-159	329	295.5	111
Tuberculosis	010-019	33	74.0	45
Arteriosclerotic heart disease	410-413	1,783	1,743.3	102
Vascular lesions of CNS	430-438	405	444.7	91
Respiratory disease	460-519	234	295.5	79
Pneumonia	480-486	95	133.1	71
Emphysema	492	59	63.4	93
Asthma	493	8	13.5	59
Digestive system	520-577	178	228.8	78
Cirrhosis	571	69	92.2	75
Genitourinary system	580-629	46	118.9	39
Chronic nephritis	582	19	39.9	48
Symptoms, senility, and ill-defined	780-799	17	43.0	40
Accidents	800-949	297	274.9	108
Motor vehicle	810-827	97	112.2	86
Suicide	950-959	102	87.4	117

*International Classification of Diseases (8th revision).

**Standardized Mortality Ratio.

European iron ore miners

Epidemiological studies have reported excess malignant and nonmalignant lung disease in European iron ore miners—for example, the studies of the iron ore miners of Kiruna, Sweden (Jørgensen, 1984); Kiruna and Gällivare, Sweden (Damber and Larsson, 1985); Cumberland, England (Boyd et al., 1970); and Lorraine, France (Pham et al., 1983). The excess disease in the English and French studies was variously attributed to radon, silica, and iron oxides, but the quality of the studies was not sufficient to define the etiology of the miners' diseases. The recent Swedish reports, however, implicate radon exposure and tobacco use as the important factors in causing excess lung cancer in the Swedish under ground iron ore miners. There were 15 cases of lung cancer (4.6 expected) among the Kiruna miners who were in the past exposed to radon concentration greater than 60 pCi/L or 0.3 working levels (Jørgensen, 1984). The average radon level reported in the study of Damber and Larsson (1985) was 50 pCi/liter. There were 42 lung cancer cases (38 were smokers); the lung cancer risk was calculated by Damber and Larsson to be about 45% from radon exposure during under ground mining and about 80% from smoking. Possible effect of mineral dusts to both cohorts of Swedish miners was not mentioned. Stokinger (1984), in a review of the world literature on exposure to iron oxides in the under ground mining environment, finds that ionizing radiation "might be an etiological factor." He exonerates iron oxides as carcinogenic, both in the mine and factory workplace. Stokinger also brings to question the nature of the disease "siderosis," a pneumoconiosis thought to be caused by inhalation of iron oxide dusts. Nonmalignant disease attributed to these dusts may be due to

exposure to other mineral dusts, especially quartz dusts. Iron oxide particles, being opaque to X-rays, are prominent in chest X-ray photographs of iron ore workers and produce a picture of reticulation without the presence of fibrosis; the patients are essentially symptom free (Stokinger, 1984, p. 129). Among underground iron ore miners of Cumberland, England there were, over a 20 year period, 42 deaths attributed to lung cancer; 21 deaths from this disease were expected. There was a substantial radon hazard associated with mining of the hematite-bearing ore in Cumberland, for radon in the mine air averaged 100 pCi/liter. In addition, some of the miners developed silicosis, indicating that quartz dust was an etiological factor, as was tobacco use, in promoting disease. It would appear that a combination of high radon levels, cigarette smoking, and quartz-bearing mine dust were cofactors in the increased health risks to these miners.

Granite workers (Vermont)

The granite industry located in the Barre area of central Vermont includes 60 quarrying and manufacturing companies employing more than 1,700 workers (USBM, 1989, p. 490). The average mineral composition (mineral mode) of the Barre granite is as follows (Chayes, 1952): quartz (27.2 vol%), potash feldspar (19.1%), plagioclase (35.2%), biotite (8.1%), muscovite (8.3%), opaque accessories (metal oxides and sulfides, 0.2%), and non opaque accessories (0.8%). This area has a long history of granite quarrying, milling, and carving—occupations that have employed a large portion of the residents of Barre township. For many years, especially in the 1920s and 1930s, there was a great prevalence of silicosis and tuberculosis among the Vermont granite workers. Dust control measures were instituted between 1937 and 1940, so that granite dust levels were reduced from average values of 40 to 60 mppcf to levels below 10 mppcf (Russell, 1941).

Costello and Graham (1986) followed a cohort of 5,414 Vermont granite workers from 1950 through 1982 to determine the causes of mortality. Many of these workers were employed well prior to 1940 when dust levels were very high. Of the total cohort of 5,414 workers, 1,532 were deceased by 1982.

Preliminary results show that silicosis, tuberculosis, and lung cancer accounted for 24.4% of the deaths, with silicosis alone accounting for 8% of the deaths. Lung cancer was the cause of death for 102 workers, with an additional 25 lung cancers cited as an “additional cause of death.” The Standard Mortality Ratio (SMR) for the total cohort is: silicosis (586.6), tuberculosis (473.8), and lung cancer (104.9). High quartz dust levels did not appear to be a significant factor in the induction of lung cancer in these workers. Costello and Graham (1986) also examined the mortality data for those employed after 1940 when dust levels were greatly reduced. As can be seen in Table 16.7, the health experience for post-1940 workers is superior to that of the control group (SMR<100). The SMRs for silicosis, tuberculosis, and lung cancer are all less than 100 indicating that dust control was effective in minimizing these diseases as important causes of death.

Slateworkers (Vermont and North Wales)

Slate is a compact, fine-grained metamorphic rock and is particularly characterized by a well-defined cleavage—thus its usefulness for such purposes as roofing shingles. The two most important minerals contained in slate are mica (usually muscovite or sericite) and quartz; lesser amounts of chlorite, hematite, carbonates, rutile, pyrite, magnetite, and carbonaceous matter are often found in slate. Dale (1914) gives the following percentages for slate from Ardennes, France: muscovite (38–40%), quartz (31–45%), Chlorite (6–18%), hematite (3–6%), and rutile (1–1.5%). In the United States slate is quarried particularly in Virginia, Maryland, Pennsylvania, New York, and Vermont. About 35% of the total work force of the U.S. slate industry is employed in a 10 x 25 mile area of western Vermont and adjacent New York. Black slate from Benson, Vermont has the following mineral constituents in order of abundance: muscovite, quartz, chlorite, carbonate, rutile, pyrite, and magnetite (Dale, 1914, p. 144). The quartz in this slate is very fine-grained with particles varying in width from 0.013 mm to 0.03 mm. The workers who quarry and process this slate are thus exposed to very fine dust particles.

Craighead et al. (1992) made a detailed mineralogical and patho-

TABLE 16.7—Selected causes of death and Standard Mortality Ratios (SMR) for Vermont granite workers by date of first employment. Table adapted from Costello and Graham (1986).

Cause of death*	Year of first employment									
	Before 1930		1930–1939		1940–1949		1950–1959		1960–1969	
	Obs.	SMR	Obs.	SMR	Obs.	SMR	Obs.	SMR	Obs.	SMR
All causes of death	891	96	209	78	250	70	135	54	38	42
All tuberculosis	116	764	6	137	2	40	0	-	0	-
All malignant neoplasms	152	96	54	105	49	73	28	58	9	54
Respiratory cancer	53	128	21	124	20	89	9	54	5	88
Lung cancer	49	128	20	125	20	95	8	51	5	91
All circulatory system diseases	399	75	83	58	120	66	37	31	9	25
Arterial and coronary heart diseases	266	80	63	64	82	64	25	29	6	22
All respiratory diseases	86	147	17	102	10	49	7	53	1	24
All pneumonia	10	38	2	32	3	38	1	21	0	-
Emphysema	19	166	4	97	5	104	2	60	0	-
Silicosis	34	919	4	421	1	90	0	-	0	-
Suicide	16	132	7	133	7	83	10	129	2	45

*International Classification of Diseases (ICD, 8th revision).

logic examination of lung tissue of 12 western Vermont slateworkers who had developed pneumoconiosis while employed in their trade. Lung tissue study revealed vascular and bronchial lesions, interstitial fibrosis, and macules, the latter scattered diffusely in the lung tissue. These lesions were associated with a variable number of silicotic nodules. X-ray diffraction analysis of four lung tissue residues from low temperature ashing show the ash to be composed mostly of quartz and muscovite. Energy dispersive X-ray spectrographic analysis of the inorganic residues of the other tissue samples showed the presence of major amounts of various aluminum silicates and silica, consistent with the X-ray diffraction results.

Pneumoconiosis in slateworkers has been reported sporadically in many parts of the world. Many of these cases were diagnosed as silicosis clinically; histologic examination of lung tissue revealed a large number of silicotic lesions. In a comparative study, however, Craighead et al. (1992) found that silicotic lesions were more prominent in the lungs of the Welsh slateworkers (Glover et al., 1980) than in those of the Vermont slateworkers. In addition, chest X-rays of the Vermont slateworkers reveal a diffuse interstitial pulmonary disease, not the nodular lesions characteristic of silicosis. Concluding, Craighead et al. (1992) state "slateworkers are exposed to respirable airborne dust that has the capacity to produce a pneumoconiosis that differs from the classic silicosis." It appears that excessive exposure to mica dusts can cause a pneumoconiosis that is somewhat different from silicosis.

Sandblasting

The occupation of sand blasting exposes the worker, unless carefully protected, to large quantities of quartz dust. The health danger of this trade was particularly brought to the attention of medical scientists in the Gulf Coast area of Louisiana when the emerging petrochemical and ship building industries required a large increase in sandblasting to protect metal surfaces. Respirable quartz dust levels were measured at 318 times the threshold limit value (TLV) in samples taken outside protective hoods during sandblasting (Samimi et al., 1974). Hughes et al. (1982) described the health history of a cohort of silicotic sandblasters. There were 83 patients with a mean age of 44 years and an average silica exposure of 11.3 years. Complicated disease, as defined by the presence of large opacities in the lung and distortion of the intrathoracic organs, sometimes accompanied by tuberculosis, was present in 64% of the cohort. By 1982, 11 members of the cohort had died. They further state that accelerated silicosis and the now rare acute silicosis kills many Gulf Coast sandblasters in the 30–40 year age group. In a review of several health studies of those in the sandblasting trades, Jones et al. (1986) state that this occupation can be extremely hazardous, in theory it could be safe, but in practice it is unsafe and should be stopped unless the workers can be adequately protected.

Cohort studies of certified silicotics

The classification of the crystalline silica minerals as "probably carcinogenic to humans" presented in a report of the International Agency for Research on Cancer (IARC, 1987b) has generated much additional concern about the health effects of these minerals. Conventional epidemiological studies of occupational cohorts, such as those presented above, do not show that

workers exposed to silica dust have a significantly increased risk of dying of lung cancer. However, in the last 6 years there have been fifteen or more studies of "certified silicotics"—groups of workers within a specific regional area who were occupationally exposed to silica and are or were drawing workers' compensation for diagnosed silicosis. For example, Kurppa et al. (1986) reported on 961 diagnosed cases of silicosis in Finnish men for the period 1935 and 1977. In this Finnish cohort, as expected, there was a very significant excess of nonmalignant respiratory disease (silicosis, tuberculosis, bronchitis, etc.), but there was also a 3-fold excess of lung cancer. Mortality data for this cohort is given in Table 16.8. In a similar study of 2,399 certified silicotics in Switzerland it was estimated that the risk of lung cancer was 2.2 times that expected from national mortality statistics (Schüler and Rüttner, 1986). In addition, Westerholm et al. (1986) found a 2- to 5-fold risk of lung cancer in Swedish silicotics, Zambon et al. (1986) reported a 2-fold risk of lung cancer in silicotics from the Veneto region of Italy, and a 2-fold risk of this disease was reported by Finkelstein et al. (1986) for miners from Ontario, Canada. However, Hessel and Sluis-Cremer (1986) reported on a case-control study of 127 pairs of South African gold miners; the cases were miners who died of lung cancer and the controls were miners who died of some other cause. A carefully documented history of smoking habits for cases and controls was made. The results of this study indicated that there was no association between lung cancer and silicosis.

TABLE 16.8—Mortality data for 961 Finnish men diagnosed as having silicosis. Table adapted from Kurppa et al. (1986).

Cause of death	Obs.	Exp.	SMR*
Total deaths, all causes	667	335.2	199
Cancer, all sites (ICD 140–209)	122	68.9	177
Lung (trachea, bronchus, pleura) (ICD 162)	80	25.6	312
Esophagus, stomach, colon-rectum (ICD 150–154)	21	19.9	106
Larynx (ICD 161)	-	1.4	-
Oropharynx (ICD 140–149)	1	0.8	128
Leukemia, lymphosarcoma and other neoplasms of lymphatic and haemopoietic system (ICD 200–207)	6	3.7	161
All other sites	20	19.5	103
All cardiovascular disease (ICD 390–458)	203	183.1	111
All pulmonary disease (ICD 460–519)	165	23.4	704
Pneumoconiosis (silicosis) (ICD 515)	120	0.0	infinity
Pneumonia, influenza (ICD 470–474, 480–486)	13	10.2	127
Chronic bronchitis, emphysema, and asthma (ICD 490–493)	27	5.6	478
Other respiratory disease	5	7.5	66
All renal disease (ICD 580–593)	7	5.9	117
Accidents, violent deaths (ICD800–999)	20	23.9	84
Tuberculosis (ICD 010–012)	130	17.6	738
All other causes	20	24.2	83

*Standardized Mortality Ratio

Because many of the conventional cohort studies do not show a statistically strong risk of lung cancer in silica-exposed workers, it is difficult to interpret the studies of silicotics that do suggest a relationship between silicosis and lung cancer. There is a difficulty in properly evaluating the contribution of tobacco use to disease within an occupational cohort if smoking habits are unknown or if the regional or national populations used as controls do not have the same smoking habits as the occupational cohort. For example, cigarette smoking was prevalent among the U.S. male blue collar trades workers and commonly 75 to 85% of the workers smoked. On the other hand, only about 50% of the total male population of the United States were smokers. If 80% of the men in a particular occupational cohort smoke, but who have no other health risks, on the average 8.5% will die of lung cancer. For a "control" cohort in which 50% smoke, on the average 5.5% will die of this disease (Ross, 1984, fig. 2). If the occupational cohort of 80% smokers is erroneously assumed to be composed of 50% smokers, as in the control cohort, an over estimate of lung cancer mortality for smoking habits would be calculated ($8.5 \times 100 / 5.5 = 155$). The 55% excess lung cancer would thus be attributed to some type of occupational hazard rather than to smoking habits.

Other problems with interpreting the studies of silicotics is that they are not true cohorts; that is, they are not well defined occupational groups because the men usually come from several industries. Also, the types and lengths of exposure to dusts, chemicals, radon, etc. were generally unknown in these studies. Craighead (1992) makes the important observation that cancer in silicotics may be a tissue response to lung fibrosis. This is exactly what Hughes and Weill (1991) observed in their study of 839 men employed in the manufacture of asbestos cement products. They reported that no excess of lung cancer was found among workers without radiographically detectable lung fibrosis, whereas those with positive X-ray evidence of fibrosis had a significantly increased risk of lung cancer. Hughes and Weill conclude, "because detectable asbestosis is not likely to result from current occupational and general environmental asbestos exposures, the prevention of the effect of exposure on lung fibrosis is likely also to prevent the excess risk of lung cancer."

COAL

Mineralogy

Several dozen minerals are reported to occur in coals, although most occur only sporadically or in trace amounts. Most of the minerals in coal fall into four groups: (1) aluminum silicates, (2) carbonates, (3) sulfides, and (4) silica, mainly quartz. Aluminum silicates commonly found in coal are clay minerals, including montmorillonite, illite-sericite, kaolinite, halloysite, chlorite, and mixed-layer clays. Principle sulfide minerals are: pyrite, marcasite, galena, chalcopyrite, pyrrotite, arsenopyrite, and millerite. Carbonate minerals include calcite, dolomite, siderite, ankerite, and witherite. In a study of 65 Illinois coals, Rao and Gluskoter (1973) found the mineral matter content to vary from 9.4 to 22.3 wt%, with 15% being an average value. Harvey and Ruch (1986) give the following variation in mineral content of Illinois Basin coals: quartz (1.2 to 3.1 wt%), calcite (0.9 to 2.3%), pyrite (2.8 to 5.9%), and clay minerals (6.6 to 11.2%). Extensive reviews of the mineralogy and petrology of coal are given by Gluskoter et al. (1981) and Stach et al. (1982).

Diseases related to exposure to coal dust

Coal workers' pneumoconiosis

Coal workers' pneumoconiosis is caused, most importantly, by fine-grained coal dust composed of carbonaceous material. One form of this disease, *simple coal workers' pneumoconiosis*, is characterized by the coal macule, a lesion 1–4 mm in diameter and composed of dust laden macrophages that form a mantle around the first and second order respiratory bronchioli. In lung sections the macules appear as black areas; the smaller macules are usually circular, the larger ones are more irregular and often stellate. The cause of simple pneumoconiosis is considered to be an overwhelming of normal lung particle clearance mechanisms by the large amounts of coal dust entering the respiratory passages. The fibrosis and emphysema may be due to the damaging effects of enzymes released by the macrophages (Merchant et al., 1986; Lapp, 1981).

A second type of lesion, a nodular lesion similar to that seen in the chronic silicotic, also occurs in coal workers' pneumoconiosis. These nodules are gray or black in color, are often rounded, but may have irregular prolongations penetrating the surrounding tissue and may be associated with scar emphysema. The major difference between the macular and nodular lesions is that the fibrous protein collagen is present in the latter. The nodular lesions, which are thought to have developed from the macules, contain bundles of collagen that are usually arranged in an irregular pattern. This arrangement of collagen is useful for distinguishing these lesions, formed by an accumulation of carbonaceous particles, from the fibrotic nodules of the silicotic where the collagen is concentrically arranged. Merchant et al. (1986, p. 354–361) present optical photomicrographs of lung sections that contain macules and nodules caused by the inhalation of carbonaceous dust and sections that contain silicotic nodules caused by inhalation of quartz dust. *Complicated coal workers' pneumoconiosis* or *progressive massive fibrosis* is characterized by extensive fibrosis of the lung tissue; often the nodular lesions coalesce so as to replace a major portion of the upper lobes of the lung. There is a strong association between tuberculosis and progressive massive fibrosis, particularly in the coal miners of South Wales (Merchant et al., 1986).

The onset of simple coal workers' pneumoconiosis, which takes many years to develop, is related to the amount and duration of coal dust exposure; however, unlike silicosis there is no convincing evidence of progression of this disease in the absence of further exposure (Lapp, 1981). Complicated coal workers' pneumoconiosis is a more serious condition in that it is generally progressive even after exposure to coal dust ceases. Severe cases of "black lung" disease lead to airway obstruction, the coughing of large volumes of inky black sputum; death occurs in about 10 to 15 years as a result of cardiopulmonary failure.

Coal workers' silicosis

Coal workers' lung disease may be complicated by exposure to other minerals associated with coal, but particularly from exposure to quartz dust in coal and (more importantly) from quartz in the country rock enclosing the coal beds. Evidence for silicosis has been found particularly in those who are primarily engaged in surface drilling of quartz-bearing country rock (Lapp, 1981). Merchant et al. (1986) observed silicotic nodules in the lungs of

some coal workers (their fig. II-29), but they state that good evidence is lacking that quartz dust plays a significant role in coal miners' disease.

Epidemiological studies of occupational cohorts exposed to coal dust

Historical accounts of miners' "black lung" were reported as early as 1831 and since then many studies have been published which described coal workers' pneumoconiosis and its associated morbidity and mortality. Merchant et al. (1986) review twenty-five of the mortality studies and thirteen morbidity studies of coal miner cohorts which were published between 1936 and 1981.

Pneumoconiosis mortality and morbidity

Coal workers' pneumoconiosis (CWP), often referred to as "black lung" or "anthracosilicosis," is prevalent in coal miners as presented in a vast literature. This is a chronic and incapacitating disease due to progressive loss of lung function. There is a clear dose-response relationship between the severity of lung disease and the number of years working under ground—the surrogate for dose. Jacobsen et al. (1971) give the probability of developing simple CWP over a 35 year working life with mine dust levels varying from an average of 1 to 7 mg/m³. For a dust level of 6 mg/m³ the probability of developing simple to more severe pneumoconiosis is approximately 10%. Bronchitis and associated respiratory infections are associated with CWP and seriously impaired lung function is often found in coal workers who have advanced pneumoconiosis, especially progressive massive fibrosis. One of the largest and most extensive mortality studies of coal miners is that of Rockette (1977). He examined a cohort of 22,998 miners, a 10% sample of the qualified members of the United Mine Workers of America Health and Retirement Fund (UMWA cohort). The major findings of the study are given in Table 16.9. The overall Standard Mortality Ratio (SMR) is 101.6 and is not significantly different from the control value of 100. The SMR's for influenza (189.6), emphysema (143.7), asthma (174.9), and tuberculosis (145.5) were significantly elevated. However, major cardiovascular diseases were not elevated in this cohort (SMR=95.2).

Cancer mortality

Overall cancer mortality in the UMWA cohort of Rockette (1977) was slightly less than that of the control (the 1965 total male U.S. population) with an SMR of 97.7. There was a small but statistically insignificant increase in stomach cancer and lung cancer. A study by Enterline (1964) of U.S. coal miners gives an elevated SMR for lung cancer (1.92), however many other health studies of coal miners do not demonstrate that lung cancer is a significant factor in coal miner mortality (Merchant et al., 1986, Table II-20; Bridbord et al., 1979, Table 1). The report by Bridbord et al. (1979) reviews nine epidemiological studies of coal miners; four cohorts show an increased risk of stomach cancer, one shows an increased risk of prostate cancer, one shows an increased risk of lung cancer (Enterline, 1964, cited above) and six show a decreased risk of lung cancer. Rosmanith and Schimanski (1986) report that bronchial cancer seldom develops

in cases of severe coal workers' pneumoconiosis in coal miners from the Czechoslovakian and West German coalfields (Ostrava and Ruhr). Breining (1986) reports that during the last 10 years he examined the lung tissue of more than 1,000 diseased coal workers from the Ruhr area of West Germany who had anthracosilicosis; only five cases were found with silicotic scar carcinomas. As yet, there does not appear to be compelling evidence that coal workers have a significant risk for increased lung cancer incidence.

TABLE 16.9—Observed and expected deaths for cohort of 22,998 U.S. coal miners for selected causes. Data from Rockette (1977).

Cause of death	Observed	Expected	SMR*
All causes	7,628	7,506.1	101.6
All malignant neoplasms	1,223	1,252.2	97.7
Benign and unspecified neoplasms	14	14.4	97.5
Major cardiovascular diseases	4,285	4,501.2	95.2
Bronchitis	27	31.5	84.8
Influenza	28	14.8	189.6
Pneumonia	217	232.3	93.4
Emphysema	170	118.3	143.7
Asthma	32	18.3	174.9
Tuberculosis	63	43.3	145.5
Syphilis	16	13.1	122.3
Other infective and parasitic disease	13	17.6	74.1
Diabetes mellitus	64	110.2	58.1
Peptic ulcer	42	58.7	71.6
Cirrhosis of the liver	64	104.9	61.0
Cholelithiasis, cholecystitis, and cholangitis	22	16.7	132.0
Nephritis and nephrosis	42	46.2	91.0
Accidents	408	283.0	144.2
Suicides	81	81.3	99.6
Homicides	30	26.1	115.1
Ill-defined causes	162	86.2	187.9
All other causes	625	459.5	136.0

*Standardized Mortality Ratio.

THE SILICATE MINERALS (OTHER THAN ASBESTOS)

Mineralogy of the silicates

Silicates form the largest chemical class in the mineral system and they comprise a large portion of the Earth's crust. The silicates are structurally and chemically complex and are characterized by the presence of essential amounts of tetrahedrally coordinated silicon. These minerals also have essential amounts of one or more other elements that are found in various coordination schemes within the crystal structures. In addition to Si, the most common elements found in the silicates are Na, K, Ca, Al, Mg, and Fe. Important mineral groups within the silicate class include feldspars, pyroxenes, amphiboles (including amphibole asbestos), micas, chlorites, serpentines (including chrysotile asbestos), the aluminum silicates (sillimanite, kyanite, andalusite), talcs, clay minerals, zeolites, nephelines, garnets, humites, olivines, and epidotes. Workers, particularly miners and millers, are exposed to the dusts of many of these minerals as they process various types of rocks to extract particular mineral commodities. Some of these silicate minerals are mined for a particular use; examples are talc,

wollastonite, kaolinite, attapulgite, amphibole and serpentine asbestos, bentonite, mica, vermiculite, and zeolites. Exposure to a few of the silicates (especially to asbestos) by occupational groups has been great enough to produce clinical evidence of disease and to permit epidemiological studies to be made. The silicates most implicated with disease (chrysotile and amphibole asbestos have already been discussed) are reviewed below.

Health effects of selected silicate minerals

Talc and pyrophyllite

Talc [$\text{Mg}_3\text{Si}_4\text{O}_{10}(\text{OH})_2$], which commonly forms by hydrothermal alteration of ultrabasic rocks rich in magnesium, is mined in many countries and processed in numerous manufacturing industries for use in paints, ceramics, rubber products, roofing materials, paper, insecticides, cosmetics, and pharmaceuticals. In the United States 1,172,000 metric tons of talc was mined in 1989 (Virta, 1991). There have been numerous health studies of talc workers (Gamble, 1986; IARC, 1987a,b), but the results of these studies have often been ambiguous. Talc workers exposed to talc dust may exhibit symptoms of *talc pneumoconiosis*, sometimes referred to as *talcosis*, as well as bronchitis, emphysema, abnormal chest X-rays, and increased risk of tuberculosis. Clinically, talc workers' pneumoconiosis resembles silicosis or asbestosis and since the talc exposed worker may have been exposed to quartz and other silicates, including chrysotile, anthophyllite, and (or) tremolite asbestos, the true etiology of this disease is difficult to describe. One study (Hogue and Mallette, 1949) reported that rubber workers exposed to high levels of talc dust show no disease and thus they concluded that talc dust was benign. However, examination of lung tissues of some of the persons exposed to talc show diffuse pleural thickening, fibrous adhesions, pleural plaques, and large fibrotic masses (Gamble, 1986). The several epidemiological studies of talc workers are in disagreement over whether talc causes lung cancer. Excess cancer may be related to underestimation of smoking habits or to previous exposure to commercial asbestos. Rubino et al. (1976) studied 1,514 miners and millers from the Piedmont in Italy who were exposed to asbestos-free quartz-bearing talc dust and found elevated pneumoconiosis (described as silicosis) and associated tuberculosis. Lung cancer mortality was much less than expected. A study of New York talc miners and millers (Brown et al., 1979) indicated that there was excessive lung cancer (SMR=270); the SMR for nonmalignant lung disease was 277. Stille and Tabershaw (1982) studied nearly the same cohort of New York miners and millers as examined by Brown et al. (1979) and found a lesser risk of lung cancer (SMR=157). The epidemiological studies of talc workers thus far completed have not proven that talc is a human carcinogen, because the cohorts studied were not large enough to produce statistically significant data, smoking habits are not well defined, and the workers were often exposed to other mineral dusts that could produce disease. There is no doubt, however, that heavy exposure to talc dust can cause nonmalignant respiratory disease.

Pyrophyllite [$\text{Al}_2\text{Si}_4\text{O}_{10}(\text{OH})_2$] has similar uses as talc but is produced in much smaller quantities (U.S. production was 81,000 metric tons in 1989; Virta, 1991). Little health data have been obtained on pyrophyllite workers. Hogue and Mallette (1949) report no apparent disease in pyrophyllite-exposed rubber workers.

The clay minerals, micas, and vermiculite

Kaolinite [$\text{Al}_2\text{Si}_2\text{O}_5(\text{OH})_4$], a common clay mineral (also known as "china clay"), is mined for many uses and particularly for ceramics and filler in papers, paints, and plastics. The kaolinite-bearing rock (referred to as "kaolin") generally contains variable amounts of other minerals including quartz. In 1989 the United States produced 8,973,669 metric tons of this mineral (Ampian, 1991). Kaolinite workers who have been heavily exposed to kaolinite dust may develop pneumoconiosis—sometimes referred to as *kaolinitis*. Simple kaolinitis is similar to other mineral dust pneumoconiosis that are characterized by the presence of rounded opacities in the lung. Complicated kaolinitis is similar to progressive massive pneumoconiosis of the coal worker (Gamble, 1986). If the kaolinite worker is also exposed to silica dust, as often may be the case, his lung disease may appear to be typical silicosis. An increased lung cancer risk has not been reported in kaolinite worker cohorts.

Bentonite is a soft plastic rock composed primarily of silicates belonging to the montmorillonite group of clay minerals having the general composition $[(\text{Na,Ca})_{0.33}(\text{Al,Mg})_2\text{Si}_4\text{O}_{10}(\text{OH})_2 \cdot n\text{H}_2\text{O}]$. Bentonite deposits are generally associated with other minerals including very fine-grained quartz and amorphous silica. Bentonite is used as drilling mud, as a bleaching clay, as a foundry sand bond, as an iron ore pelletizer, and for many other uses. In 1989 the United States mined 3,112,365 metric tons of bentonite (Ampian, 1991). A study of a random sample of Wyoming bentonite workers revealed that 44% had silicosis, including 2 cases of progressive massive fibrosis (Phibbs et al., 1971). Silica content (which included both quartz and cristobalite) of the Wyoming bentonite clays ranged from 0 to 24%. Surveys of bentonite processing plants showed that silica comprised between 5 and 10% of the mineral matter in the airborne dust, and the TLV for silica was exceeded 3 to 10 times (Gamble, 1986).

Fuller's earth is a general term for a soft fine-grained earthy rock that contains large amounts of hydrous aluminum silicates belonging to the montmorillonite and (or) palygorskite clay mineral group as well as quartz and other minerals. Palygorskite has the composition $[(\text{Mg,Al})_2\text{Si}_4\text{O}_{10}(\text{OH}) \cdot n\text{H}_2\text{O}]$ and is chemically and structurally similar to attapulgite and sepiolite. Fuller's earth has many uses, for example, in drilling mud, as an adsorbent and bleach, and as a paint thickener. In 1989 the U.S. production of fuller's earth was 1,881,511 metric tons (Ampian, 1991). There have been a few reports of pneumoconiosis among fuller's earth workers.

The common minerals of the mica group are muscovite [$\text{KAl}_2(\text{AlSi}_3\text{O}_{10}(\text{OH})_2$] and phlogopite and biotite [$\text{K}(\text{Mg,Fe})_3\text{AlSi}_3\text{O}_{10}(\text{OH})_2$]. The micas have numerous uses, particularly in electrical devices and as fillers in plastics, tiles, etc. Mica can cause pneumoconiosis in workers exposed to mica dust from various occupational categories. However, health studies are confounded by the fact that the mica dusts often contain other minerals including quartz.

Vermiculite $[(\text{Mg,Ca})_{0.35}(\text{Mg,Fe,Al})_3(\text{Al,Si})_4\text{O}_{10}(\text{OH})_2 \cdot n\text{H}_2\text{O}]$ is essentially a hydrated mica with water molecules located between the silicate layers. On heating, this mineral expands to form a light weight product so useful as insulation, a soil conditioner, and filler for many products. Vermiculite workers, particularly those working in the enclosed areas where the product is expanded and in loading areas, were exposed to elevated dust levels. Pulmonary effusions have been reported in some workers. At

the Libby, Montana vermiculite mine and mill an excess of lung cancer (SMR=2.45) and 4 deaths from mesothelioma were reported among the workers (McDonald et al., 1986). The excess lung cancer and mesothelioma incidence at Libby may be related to the fibrous amphibole that is associated with the vermiculite ore. McDonald et al. (1988) studied the health history of South Carolina vermiculite miners and millers who had a low exposure to fibrous amphiboles. They report that there was no evidence for excess respiratory cancer or any cases of mesothelioma, but there was a slightly elevated incidence of nonmalignant disease.

Zeolites

Among this large group of hydrated aluminum silicates there are several fibrous varieties, one of which (erionite) is implicated in respiratory disease in residents of the towns of Karain and Tuzköy located in the Cappadocia region of Turkey. Erionite [$\text{NaK}_2\text{MgCa}_{1.5}(\text{Al}_8\text{Si}_{28}\text{O}_{72}) \cdot 28\text{H}_2\text{O}$] is prevalent in the local ash-flow tuffs and interbedded lacustrine deposits that contain reworked tuffs. Mesothelioma is a very common disease in these towns and is practically unknown in other areas of Turkey. In Karain, over the period 1970 to 1978, there were 76 deaths, of which 50 were due to pleural mesothelioma (Saracci et al., 1982). The mineral implicated in this epidemic is extremely thin and fibrous (comparable to crocidolite asbestos in dimensions) and is found in the rocks, soils, and air samples of the two towns. Such fibers have also been reported in the lung tissues of the diseased residents (Rohl et al., 1982). Wagner et al. (1985) report that intrapleural inoculation of rats with fine-fibered erionite from Oregon produced mesothelial tumors in 100% of the animals, a much larger percentage than found in rats similarly treated with crocidolite asbestos. A second group of rats inoculated with "Karain rock fiber" from Turkey showed a 95% tumor incidence. There is good reason to believe that very thin (<0.5 μm) and long (>10 μm) fibers of some of the silicate minerals and certain inorganic compounds have the potential to cause mesothelioma, lung cancer, and asbestosis when exposures are significantly elevated.

DISCUSSION

In reviewing the health effects of a large variety of mineral dusts, we have seen examples of extreme injury to workers exposed to high levels of certain mineral dusts. Crocidolite asbestos and erionite appear to be particularly potent in inducing mesothelioma both in man and animals. Very high dust levels of all forms of asbestos cause excessive respiratory cancer and non-malignant lung diseases, although chrysotile asbestos is much less potent in this respect than amphibole asbestos. Quartz, one of the most common minerals in the crust of the Earth, has probably during the course of human existence caused more morbidity and mortality than any other mineral species, including the asbestos minerals; and yet most people are exposed to this substance everyday of their lives without measurable effect. Those living in dry desert-like areas of the world and those employed in agricultural activities are exposed to relatively high levels of mineral dusts including quartz-bearing dust. Do these people suffer from lung disease? From a review of the literature, apparently not much, although there are scattered references in the medical literature for "silicate pneumoconiosis" in the agricultural occupations.

Sherwin et al. (1979) report of lung inflammation and fibrosis in California farm vineyard workers and Zolov et al. (1967) noted "pleural asbestosis" in Bulgarian farmers, although these farmers may have been exposed to asbestos-containing soils. Bazas et al. (1985) report of pleural calcification in the lungs of rural villagers living in northwest Greece, but state that there was no evidence of any lung dysfunction; the agent responsible for this apparently benign condition was not identified. We also have good scientific evidence that lower exposure to mineral dusts that are dangerous at high levels, does not cause significant disease. For example, moderate exposures to chrysotile asbestos (<20 fibers/cm³) by Québec miners and millers show no increased risk of cancer or respiratory disease. Minnesota taconite miners and millers, after exposure to mine dust averaging 2.7 mppcf or 0.2 to 0.6 mg/m³, did not experience any silica related disease even though the dust contained significant amounts of quartz. However, there is ample reason to believe that **any mineral dust** when inhaled in large enough doses will cause nonmalignant respiratory disease and in some instances cancer. Thus, one should not be surprised that workers heavily exposed to dusts from serpentinite, granite, taconite, slate, coal, bentonite, fuller's earth, diatomaceous earth, and so forth may show a greater than expected morbidity and mortality.

The causes of cancer

In context with the above review of mineral-related disease, it is informative to discuss the work of Bruce Ames and coworkers. They studied the toxic nature of synthetic chemicals as compared to that of natural chemicals, the latter representing the vast bulk of chemicals to which humans are exposed. They find that in high-dose animal tests, a large proportion of both natural and synthetic chemicals are carcinogens, mutagens, teratogens, and clastogens (Ames et al., 1990a). About 50% of the chemicals tested, both natural and synthetic in origin, are carcinogenic in high-dose animal tests. For example, of the 52 natural pesticides that occur in plants and which were tested in animals, 27 were proven to be carcinogenic (Ames et al., 1990b). Ames and Gold (1990) consider why so many animal tests are positive for cancer induction. They postulate that the administration of chemicals at the maximum tolerated dose (MTD), as is done in standard animal cancer tests, causes increased cell death that in turn promotes increased cell division and thus increases cell proliferation (mitogenesis). Mitogenesis in turn increases the rates of mutagenesis, the process of producing mutations in genetic material (DNA) that is particularly enhanced during cell division (see also, Cohen and Ellwein, 1990). An increased rate of mitogenesis and mutagenesis causes an increased rate of carcinogenesis in the test animals. Ethyl alcohol is a human carcinogen and if it were invented today the Food and Drug Administration would never allow it to be marketed. However, epidemiological studies show that alcoholic drinks cause an increased risk of liver cancer only if enough is consumed over the years to so damage the liver that cirrhosis develops. Alcohol is not a significant human carcinogen provided one keeps consumption low enough to prevent liver disease. A similar observation is noted with viral infections. For example, hepatitis B virus can produce chronic hepatitis causing massive liver cell damage and much increased cell division, thus promoting an increased risk of liver cancer. Human papilloma virus 16 is a major risk factor for cervical cancer whose main effect on cells is to increase cell division (Ames and Gold, 1990, p. 7775).

Human cohorts that are exposed to mineral dusts but are free of non malignant lung disease (as noted in the Minnesota iron ore miners exposed to quartz-bearing dusts and the chrysotile asbestos-exposed cement workers) do not show an increased risk of lung cancer. In fact, the epidemiological data of Hughes and Weill (1991) indicate that asbestosis is the **precursor** to lung cancer. Similarly, silicosis may also be a precursor to respiratory cancer, for it is observed that some silicotic cohorts have an increased risk of this disease (Kurppa et al., 1986). As mentioned above, in studies of asbestos-induced lung disease in animals after long term exposure to high concentrations of asbestos dusts, it is observed that cancer appears only in those animals that first develop lung fibrosis. Craighead (1992) suggests that the formation of lung tumors in mineral dust-exposed animals is a reaction to the chronic irritation and scarring of tissue. In a review of inhalation experiments on animals exposed to quartz dust, Saffiotti (1986) states "if the fibrogenesis mechanisms observed in rats are indeed linked to the carcinogenic response in that species, it is interesting to consider that the human lung produces a marked fibrogenic response to silica comparable to rats." It thus appears that the mechanisms of cancer induction by high dose exposure to chemicals, as proposed by Ames and Gold (1990), can be extended to high dose exposure to mineral dusts.

In 1959 U.S. congressman Delaney introduced an amendment to the "Food, Drug and Cosmetics Act" that in part requires that food not contain **any amount** of a carcinogen. At the time this amendment was passed, naturally occurring carcinogens were not known to exist, but now through the work of Ames and many others we know that naturally formed carcinogens are ubiquitous in our environment. If the Delaney amendment is applied to all chemical carcinogens, natural and synthetic, little food could be sold legally. With respect to minerals, we are now in the unfortunate position of having to label **anything** that contains more than 0.1% quartz (rock products, beach sand, cement, fillers, etc.) as a possible human carcinogen. If the Delaney amendment is applied to mineral dusts we might be hard pressed to mine anything for a myriad of minerals and inorganic substances are proven to be carcinogenic when administered to animals in high doses. Common sense requires us to discard the idea of a "no threshold" for cancer induction and look for another way to control materials that may cause human disease. In examining the epidemiological studies of those exposed to mineral dusts, it is noted that if there is no significant evidence of nonmalignant respiratory disease, cancer risk is very low. In cohorts where there is significant excess of nonmalignant lung disease there is often observed an elevation in respiratory cancer mortality. If nonmalignant respiratory disease is eliminated from the workplace through adequate dust control, then lung cancer will become an insignificant health problem. We do see that *the dose does make the poison*.

APPENDIX (EPIDEMIOLOGY)

Epidemiological mortality studies involved the determination of the cause of death of a specially selected group of individuals—the "exposed cohort." Such cohorts are generally composed of workers who were exposed to a substance that presents a particular health risk—for example, asbestos trades workers exposed to asbestos and miners exposed to quartz dust. Cause of death must be determined by accurate death certificates, ideally based on autopsy. The specific disease is numerically coded to the specifi-

cations of a particular revision of the *International Classification of Diseases (ICD)*. For example, mortality due to respiratory cancer (includes cancer of the trachea, bronchus, and lung) is coded as 162; death due to silicosis is coded as 515.0 (ICD, 8th Revision). Not all epidemiological studies report the codes in addition to the disease type. The mortality profile of the exposed cohort must then be compared to a second group, the "control cohort." Ideally, the control cohort should be as nearly identical to the research cohort as possible—in age distribution, ethnicity, sex, dietary and smoking habits, and other social characteristics, but with the exception that the control group was not exposed to the risk factor under study. Generally, however, the control cohort is not specially selected on these criteria, but rather is composed of the total male (or female) county, state, or national population. Use of such a control cohort can introduce significant error, particularly in the case of lung cancer, if the smoking habits of the control cohort differ from those of the exposed cohort. A *Standardized Mortality Ratio (SMR)* is calculated for each particular cause of death by the relation $SMR = 100 \times (\text{observed deaths in the exposed cohort}) / (\text{expected deaths in the control cohort})$, with suitable statistical adjustments for age distribution and age at death. The statistical accuracy of a particular mortality study is of course dependent on the number of deaths within each disease category; SMRs for small numbers of deaths have little meaning. Generally, SMRs less than 150 are not considered as significant. SMRs greater than 200, especially when there are a large number of deaths in a particular category, show that the workers were at significant risk to some substance. As an example, a cohort of North American asbestos trades workers exposed to three types of asbestos dust has a respiratory cancer SMR (ICD 162) of 452, indicating an extreme occupational risk (Ross, 1984, Table 3a, study, IV).

REFERENCES

- Ames, B.N., and Gold, L.S., 1990, Chemical carcinogenesis—Too many rodent carcinogens: Proceedings of the National Academy of Sciences, v. 87, pp. 7772–7776.
- Ames, B.N., MaGaw, R., and Gold, L.S., 1987, Ranking possible carcinogenic hazards: Science, v. 236, pp. 271–280.
- Ames, B.N., Profet, M., and Gold, L.S., 1990a, Nature's chemicals and synthetic chemicals—comparative toxicology: Proceedings of the National Academy of Sciences, v. 87, pp. 7782–7786.
- Ames, B.N., Profet, M., and Gold, L.S., 1990b, Dietary pesticides (99.99% all natural): Proceedings of the National Academy of Sciences, v. 87, pp. 7777–7781.
- Ampian, S.G., 1991, Clays; in Minerals Yearbook, v. 1, Metals and Minerals: U.S. Department of the Interior, Bureau of Mines, pp. 271–304.
- Ampian, S.G., and Virta, R.L., 1992, Crystalline silica overview—Occurrence and analysis: U.S. Department of the Interior, Bureau of Mines Information Circular IC 9317, Washington, D.C., 27 pp.
- Bazas, T., Oakes, D., Gilson, J.C., Bazas, B., and McDonald, J.C., 1985, Pleural calcification in northwest Greece: Environmental Research, v. 38, pp. 239–247.
- Boyd, J.T., Doll, R., Faulds, J.S., and Leiper, J., 1970, Cancer of the lung in iron ore (haematite) miners: British Journal of Industrial Medicine, v. 27, pp. 97–105.
- Breining, H., 1986, Pneumoconiosis and lung cancer—A review of 5 cases [abs.]; in Goldsmith, D.F., Winn, D.M., and Shy, C.M. (eds.), Silica, Silicosis, and Cancer: Praeger Publishers, New York, 533 pp.
- Brenner, J., Sordillo, P.P., Magill, G.B., and Golbey, R.B., 1981, Malignant peritoneal mesothelioma: American Journal of

- Gastroenterology, v. 75, pp. 311–313.
- Bridbord, K., Costello, J., Gamble, J., Groce, D., Hutchison, M., Jones, W., Merchant, J., Ortmeier, C., Reger, R., and Wagner, W.L., 1979, Occupational safety and health implications of increased coal utilization: *Environmental Health Perspectives*, v. 33, pp. 285–302.
- Brown, D.P., Dement, J.M., and Wagoner, J.K., 1979, Mortality patterns among miners and millers occupationally exposed to asbestiform talc; *in* Dement, J.M. and Lemen, R. (eds.), *Dusts and Disease: Pathtox*, Park and Forest South, Ill., pp. 317–324.
- Chayes, F., 1952, The finer grained calc-alkaline granites of New England: *Journal of Geology*, v. 60, pp. 207–254.
- Cherniack, M., 1986, The Hawk's Nest incident—America's worst industrial disaster: Yale Univ. Press, New Haven, Conn., 194 pp.
- Clark, F.W., 1924, The data of geochemistry: U.S. Geological Survey Bulletin 770, 841 pp.
- Clark, T.C., Harrington, V.A., Asta, J., Morgan, W.K.C., and Sargent, E.N., 1980, Respiratory effects of exposure to dust in taconite mining and processing: *American Review of Respiratory Disease*, v. 121, pp. 959–966.
- Cohen, S.M., and Ellwein, L.B., 1990, Cell proliferation in carcinogenesis: *Science*, v. 249, pp. 1007–1011.
- Cooper, W.C., Wong, O., Trent, L.S., and Harris, F., 1992, An updated study of taconite miners and millers exposed to silica and non-asbestiform amphiboles: *Journal of Occupational Medicine*, v. 34, pp. 1173–1180.
- Costello, J., and Graham, W.G.B., 1986, Vermont granite workers' mortality; *in* Goldsmith, D.F., Winn, D.M., and Shy, C.M. (eds.), *Silica, Silicosis, and Cancer*: Praeger Publishers, New York, pp. 437–438.
- Craighead, J.E., 1988, Diseases associated with exposure to silica and nonfibrous silicate minerals: (Report of the Silicosis and Silicate Disease Committee, J.E. Craighead, Chairman) *Archives of Pathology and Laboratory Medicine*, v. 112, pp. 673–720.
- Craighead, J.E., 1992, Do silica and asbestos cause lung cancer?: *Archives of Pathology and Laboratory Medicine*, v. 116, pp. 16–20.
- Craighead, J.E., Abraham, J.L., Churg, A., Green, F.H.Y., Kleinerman, J., Pratt, P.C., Seemayer, T.A., Vallyathan, V., and Weill, H., 1982, The pathology of asbestos-associated diseases of the lungs and pleural cavities—Diagnostic criteria and proposed grading schema: *Archives of Pathology and Laboratory Medicine*, v. 106, pp. 542–597.
- Craighead, J.E., Emerson, R.J., and Stanley, D.E., 1992, Slateworker's pneumoconiosis: *Human Pathology*, v. 23, pp. 1098–1105.
- Dale, T.N., 1914, Slate in the United States: U.S. Geological Survey Bulletin 586, 220 pp.
- Damber, L., and Larsson, L-G., 1985, Underground mining, smoking, and lung cancer—a case-control study in the iron ore municipalities in Northern Sweden: *Journal of the National Cancer Institute*, v. 74, pp. 1207–1213.
- Dement, J.M., Merchant, J.A., and Green, F.H.Y., 1986, Asbestosis; *in* Merchant, J.A. (ed.), *Occupational Respiratory Diseases: DHHS (NIOSH) Publication 86–102*, U.S. Department of Health and Human Services, Washington, D.C., pp. 287–327.
- Enterline, P.E., 1964, Mortality rates among coal miners: *American Journal of Public Health*, v. 54, pp. 758–768.
- Finkelstein, M.M., Muller, J., Kusiak, R., and Suranyi, G., 1986, Follow-up of miners and silicotics in Ontario; *in* Goldsmith, D.F., Winn, D.M., and Shy, C.M. (eds.), *Silica, Silicosis, and Cancer*: Praeger Publishers, New York, pp. 321–325.
- Flinn, R.H., Brinton, H.P., Doyle, H.N., Cralley, L.J., Harris, R.L., Westfield, J., Bird, J.H., and Berger, L.B., 1963, Silicosis in the metal mining industry—A reevaluation 1958–1961: U.S. Department of Health Education and Welfare, Public Health Service, and U.S. Department of the Interior, Bureau of Mines, Washington, D.C., 238 pp.
- French, B.M., 1968, Progressive contact metamorphism of the Biwabik iron formation, Mesabi Range, Minnesota: *Minnesota Geological Survey Bulletin 45*, Univ. of Minnesota Press, Minneapolis, Minn., 103 pp.
- Frondel, C., 1962, Silica minerals, v. 3, *The System of Mineralogy*: John Wiley, New York, 334 pp.
- Gamble, J.F., 1986, Silicate pneumoconiosis; *in* Merchant, J.A. (ed.), *Occupational Respiratory Diseases: DHHS (NIOSH) Publication 86–102*, U.S. Department of Health and Human Services, Washington, D.C., pp. 243–285.
- Gardner, M.J., Winter, P.D., Pannett, B., and Powell, C.A., 1986, Follow up study of workers manufacturing chrysotile asbestos cement products: *British Journal of Industrial Medicine*, v. 43, pp. 726–732.
- Glover, J.R., Bevan, C., and Cotes, J.E., 1980, Effects of exposure to slate dust in North Wales: *British Journal of Industrial Medicine*, v. 37, pp. 152–162.
- Gluskoter, H.J., Shimp, N.F., and Ruch, R.R., 1981, Coal analysis, trace elements and mineral matter; *in* Elliot, M.A. (ed.), *Chemistry of Coal Utilization, 2nd Supplementary Vol.*: John Wiley and Sons, New York, pp. 369–422.
- Green, F.H.Y., and Vallyathan, V., 1986, Pathology of occupational lung cancer; *in* Merchant, J.A. (ed.), *Occupational Respiratory Diseases: DHHS (NIOSH) Publication 86–102*, U.S. Department of Health and Human Services, Washington, D.C., pp. 657–668.
- Gruner, J.W., 1946, Mineralogy and geology of the Mesabi Range: *Iron Range Resources and Rehabilitation*, State Office Bldg., St. Paul, Minn., 127 pp.
- Harvey, R.D., and Ruch, R.R., 1986, Mineral matter in Illinois and other U.S. coals; *in* Vorres, K.S. (ed.), *Mineral Matter and Ash in Coal: ACS Symposium Series 301*, American Chemical Society, Washington, D.C., pp. 10–40.
- HEIAR, 1991, Asbestos in public buildings and commercial buildings—a literature review and synthesis of current knowledge: Cox, A. (chairman), Health Effects Institute-Asbestos Research (HEIAR), Cambridge, Mass., p. 6–3.
- Hessel, P.A., and Sluis-Cremer, G.K., 1986, Case-control study of lung cancer and silicosis; *in* Goldsmith, D.F., Winn, D.M., and Shy, C.M. (eds.), *Silica, Silicosis, and Cancer*: Praeger Publishers, New York, pp. 351–355.
- Higgins, E., Lanza, A.J., Laney, F.B., and Rice, G.S., 1917, Siliceous dust in relation to pulmonary disease among miners in the Joplin District, Missouri: *Bulletin No. 132*, U.S. Department of the Interior, Bureau of Mines, Washington, D.C., 116 pp.
- Higgins, I.T.T., Glassman, J.H., Oh, M.S., and Cornell, R.G., 1983, Mortality of Reserve Mining Company employees in relation to taconite dust exposure: *American Journal of Epidemiology*, v. 118, pp. 710–719.
- Hodous, T.K., and Melius, J.M., 1986, Clinical presentation; *in* Merchant, J.A. (ed.), *Occupational Respiratory Diseases: DHHS (NIOSH) Publication 86–102*, U.S. Department of Health and Human Services, Washington, D.C., pp. 669–670.
- Hogue, W.L., and Mallette, F.S., 1949, A study of workers exposed to talc and other dusting compounds in the rubber industry: *Journal of Industrial Hygiene and Toxicology*, v. 31, pp. 359–364.
- Holland, L.M., Gonzales, M., Wilson, J.S., and Tillery, M.I., 1983, Pulmonary effects of shale dusts in experimental animals; *in* Wagner, W.L., Rom, W.N., and Merchant, J.A. (eds.), *Health Issues Related to Metal and Nonmetallic Mining*: Butterworth Publishers, Boston, Mass., pp. 485–496.
- Hughes, J.M., and Weill, H., 1991, Asbestosis as a precursor of lung cancer—a prospective mortality study: *British Journal of Industrial Medicine*, v. 48, pp. 229–233.
- Hughes, J.M., Jones, R.N., Gilson, J.C., Hammad, Y.Y., Samimi, B., Hendrick, D.J., Turner-Warwick, M., Doll, N.J., and Weill, H., 1982, Determinants of progression in sandblasters silicosis: *Annals of Occupational Hygiene*, v. 26, pp. 701–712.
- IARC, 1987a, IARC Monographs on the evaluation of the carcinogenic risk of chemicals to humans—Silica and some silicates, v. 42: World Health Organization, International Agency for Research on Cancer, Lyon, France, 289 pp.
- IARC, 1987b, IARC Monographs on the evaluation of the carcinogenic risk of chemicals to humans—Overall evaluations of carcinogenicity: An Updating of IARC Monographs 1 to 42, Supplement 7, World

- Health Organization, International Agency for Research on Cancer, Lyon, France, 440 pp.
- Jacobsen, M., Rae, S., Walton, W.H., and Rogan, J.H., 1971, The relation between pneumoconiosis and dust-exposure in British coal mines; *in* Walton, W.H. (ed.), *Inhaled Particles III*, v. 2: Unwin Brothers, London, pp. 903–917.
- Jones, R.N., Hughes, J.M., Hammad, Y.Y., and Weill, H., 1986, Sandblasting and silicosis; *in* Goldsmith, D.F., Winn, D.M., and Shy, C.M. (eds.), *Silica, Silicosis, and Cancer*: Praeger Publishers, New York, pp. 71–75.
- Jørgensen, H.S., 1984, Lung cancer among underground workers in the iron ore in Kiruna on the basis of 30 years of observation [abs.]; *Scandinavian Journal Work Environmental Health*, v. 21, p. 128.
- Kurppa, K., Gudbergsson, H., Hannunkari, I., Koskinen, H., Hernberg, S., Koskela, R.-S., and Ahlman, K., 1986, Lung cancer among silicotics in Finland [abs.]; *in* Goldsmith, D.F., Winn, D.M., and Shy, C.M. (eds.), *Silica, Silicosis, and Cancer*: Praeger Publishers, New York, pp. 311–319.
- Lanza, A.J., and Higgins, E., 1915, Pulmonary disease among miners in the Joplin District, Missouri and its relation to rock dust in the mines—A preliminary report: Technical Paper 105, U.S. Department of the Interior, Bureau of Mines, Washington, D.C., 48 pp.
- Lapp, N.L., 1981, Lung disease secondary to inhalation of nonfibrous minerals: *Clinics in Chest Medicine*, v. 2, pp. 219–233.
- Lawler, A.B., Mandel, J.S., Schuman, L.M., and Lubin, J.H., 1985, A retrospective cohort mortality study of iron ore (hematite) miners in Minnesota: *Journal of Occupational Medicine*, v. 27, pp. 507–517.
- Lepp, H., 1972, Normative mineral composition of the Biwabik formation—a first approach; *in* Doe, B.R., and Smith, D.K. (eds.), *Studies in Mineralogy and Precambrian Geology*: Geological Society of America Memoir 135, pp. 265–278.
- McDonald, J.C., Liddell, F.D.K., Gibbs, G.W., Eyssen, G.E., and McDonald, A.D., 1980, Dust exposure and mortality in chrysotile mining, 1910–75: *British Journal of Industrial Medicine*, v. 37, pp. 11–24.
- McDonald, J.C., McDonald, A.D., Armstrong, B., and Sébastien, P., 1986, Cohort study of mortality of vermiculite miners exposed to tremolite: *British Journal of Industrial Medicine*, v. 43, pp. 436–444.
- McDonald, J.C., McDonald, A.D., Sébastien, P., and Moy, K., 1988, Health of vermiculite miners exposed to trace amounts of fibrous tremolite: *British Journal of Industrial Medicine*, v. 45, pp. 630–634.
- Merchant, J.A., Taylor, G., and Hodous, T.K., 1986, Coal workers' pneumoconiosis and exposure to other carbonaceous dusts; *in* Merchant, J.A. (ed.), *Occupational Respiratory Diseases*: DHHS (NIOSH) Publication 86–102, U.S. Department of Health and Human Services, Washington, D.C., pp. 329–384.
- Morris, J.N., 1975, *Uses of epidemiology*, 3rd ed.: Churchill Livingstone, New York, 318 pp.
- Mossman, B.T., Bignon, J., Corn, M., Seaton, A., and Gee, J.B.L., 1990, Asbestos—scientific developments and implications for public policy: *Science*, v. 247, pp. 294–301.
- Newhouse, M.L., and Sullivan, K.R., 1989, A mortality study of workers manufacturing friction materials—1941–86: *British Journal of Industrial Medicine*, v. 46, pp. 176–179.
- Ohlson, C.-G., and Hogstedt, C., 1985, Lung cancer among asbestos cement workers—A Swedish cohort study and a review: *British Journal of Industrial Medicine*, v. 42, pp. 397–402.
- Pham, Q.T., Gaertner, M., Mur, J.M., Braun, P., Gabiano, M., and Sadoul, P., 1983, Incidence of lung cancer among iron miners: *European Journal of Respiratory Disease*, v. 64, pp. 534–540.
- Phibbs, B.P., Sundin, R.E., and Mitchell, R.S., 1971, Silicosis in Wyoming bentonite workers: *American Review of Respiratory Disease*, v. 103, pp. 1–17.
- Rao, C.P., and Gluskoter, H.J., 1973, Occurrence and distribution of minerals in Illinois coals: Illinois State Geological Survey Circular 476, 56 pp.
- Reiser, K.M., and Last, J.A., 1979, Silicosis and fibrogenesis—Fact and artifact: *Toxicology*, v. 13, pp. 51–72.
- Rockette, H., 1977, Mortality among coal miners by the UMAW Health and Retirement Funds: DHEW NIOSH Publication No. 77–155, U.S. Department of Health, Education, and Welfare, Washington, D.C.
- Rohl, A.N., Langer, A.M., Moncure, G., Selikoff, I.J., and Fischbein, A., 1982, Endemic pleural disease associated with exposure to mixed fibrous dust in Turkey: *Science*, v. 216, pp. 518–520.
- Rosmanith, J., and Schimanski, P., 1986, Epidemiological studies on the relationship between coal workers pneumoconiosis and lung cancer; [abs.]; *in* Goldsmith, D.F., Winn, D.M., and Shy, C.M. (eds.), *Silica, Silicosis, and Cancer*: Praeger Publishers, New York, p. 535.
- Ross, M., 1978, The “asbestos” minerals—definitions, description, mode of formation, physical and chemical properties, and risk to the mining community; *in* Gravatt, C.C., LaFleur, P.D., and Heinrich, K.F.J. (eds.), *Proceedings of Workshop on Asbestos—Definitions and Measurement Methods*: NBS Spec. Pub. No. 506, U.S. Department of Commerce, National Bureau of Standards, Washington, D.C., pp. 49–63.
- Ross, M., 1981, The geologic occurrences and health hazards of asbestos; *in* Veblen, D.R. (ed.), *Amphiboles and Other Hydrous Pyriboles—Mineralogy*, v. 9A: Mineralogical Society of America, Washington, D.C., pp. 279–323.
- Ross, M., 1984, A survey of asbestos-related disease in trades and mining occupations and factory and mining communities as a means of predicting health risks of nonoccupational exposure to fibrous minerals; *in* Levadie, B. (ed.), *Definitions for Asbestos and Other Health-Related Silicates*: ASTM STP 834, American Society for Testing Materials, Philadelphia, Pa., pp. 51–104.
- Rubino, G.F., Scansetti, G., Piolatto, G., and Romano, C.A., 1976, Mortality of talc miners and millers: *Journal of Occupational Medicine*, v. 18, pp. 186–193.
- Russell, A.E., 1941, The health of workers in dusty trades—restudy of a group of granite workers: U.S. Public Health Service Bulletin 269, Washington, D.C.
- Saffiotti, U., 1960, The histogenesis of experimental silicosis, I. Methods for the Histological Evaluation of Experimentally Induced Dust Lesions: *Medicina del Lavoro*, v. 51, pp. 11–18.
- Saffiotti, U., 1962, The histogenesis of experimental silicosis, III. Early Cellular Reactions and the Role of Necrosis: *Medicina del Lavoro*, v. 53, pp. 5–18.
- Saffiotti, U., 1986, The pathology induced by silica in relation to fibrogenesis and carcinogenesis; *in* Goldsmith, D.F., Winn, D.M., and Shy, C.M. (eds.), *Silica, Silicosis, and Cancer*: Praeger Publishers, New York, pp. 287–307.
- Samimi, B., Weill, H., and Ziskind, M., 1974, Respirable silica dust exposure of sandblasters and associated workers in steel fabrication yards: *Archives of Environmental Health*, v. 29, pp. 61–66.
- Saracci, R., Simonato, L., Baris, Y., Artvinli, M., and Skidmore, J., 1982, The age-mortality curve of endemic pleural mesothelioma in Karain, Central Turkey: *British Journal of Cancer*, v. 45, pp. 147–149.
- Schaumburg, F.D., 1976, *Judgment reserved*: Reston Publishing Company, Reston, Va., 265 pp.
- Schüler, G. and Rüttner, J.R., 1986, Silicosis and lung cancer in Switzerland; *in* Goldsmith, D.F., Winn, D.M., and Shy, C.M. (eds.), *Silica, Silicosis, and Cancer*: Praeger Publishers, New York, pp. 357–366.
- Selikoff, I.J., Hammond, E.C., and Seidman, H., 1980, Latency of asbestos disease among insulation workers in the United States and Canada: *Cancer*, v. 46, pp. 2736–2740.
- Sheehy, J.W. and McJilton, C.E., 1987, Development of a model to aid in reconstruction of historical silica dust exposures in the taconite industry: *American Industrial Hygiene Journal*, v. 48, pp. 914–918.
- Sherwin, R.P., Barman, M.L., and Abraham, J.L., 1979, Silicate pneumoconiosis of farm workers: *Laboratory Investigation*, v. 40, pp. 576–582.
- Shy, C.M., 1986, Epidemiologic principles and methods for occupational health studies; *in* Merchant, J.A. (ed.), *Occupational Respiratory Diseases*: DHHS (NIOSH) Publication 86–102, U.S. Department of Health and Human Services, Washington, D.C., pp. 103–136.
- Skinner, H.C.W., Ross, M., and Frondel, C., 1988, *Asbestos and other fibrous minerals*: Oxford Univ. Press, New York, 204 pp.

- Stach, E., Mackowsky, M.-TH., Teichmüller, M., Taylor, G.H., Chandra, D., and Teichmüller, R., 1982, Coal petrology: Gebrüder Borntraeger, Berlin, 535 pp.
- Stille, W.T., and Tabershaw, I.R., 1982, The mortality experience of upstate New York talc workers: *Journal of Occupational Medicine*, v. 24, pp. 480–484.
- Stokinger, H.E., 1984, A review of world literature finds iron oxides non-carcinogenic: *American Industrial Hygiene Association Journal*, v. 45, pp. 127–133.
- Thomas, H.F., Benjamin, I.T., Elwood, P.C., and Sweetman, P.M., 1982, Further follow-up of workers from an asbestos cement factory: *British Journal of Industrial Medicine*, v. 39, pp. 273–276.
- USBM, 1989, Minerals yearbook, v. II, Area Reports—Domestic: U.S. Department of the Interior, Bureau of Mines, Washington, D.C., 533 pp.
- USBM, 1992a, Crystalline silica primer: U.S. Department of the Interior, Bureau of Mines, Washington, D.C., 49 pp.
- USBM, 1992b, State mineral summaries 1992: U.S. Department of the Interior, Bureau of Mines, Washington, D.C., pp. 69–71.
- Virta, R.L., 1991, Talc and pyrophyllite; *in* Minerals Yearbook, v. 1, Metals and Minerals: U.S. Department of the Interior, Bureau of Mines, pp. 1053–1059.
- Wagner, J.C., 1966, The induction of tumors by the intrapleural inoculations of various types of asbestos dust; *in* Severi, L. (ed.), Proceedings of the 3rd Quadrennial International Conference on Cancer: Perugia, Italy, pp. 589–606.
- Wagner, J.C., Skidmore, J.W., Hill, R.J., and Griffiths, D.M., 1985, Erionite exposure and mesothelioma in rats: *British Journal of Cancer*, v. 51, pp. 727–730.
- Wagner, M.M.F., and Wagner, J.C., 1972, Lymphomas in the Wistar rat after intrapleural inoculation of silica: *Journal of the National Cancer Institute*, v. 49, pp. 81–91.
- Westerholm, P., Ahlmark, A., Maasing, R., and Segelberg, I., 1986, Silicosis and lung cancer—a cohort study; *in* Goldsmith, D.F., Winn, D.M., and Shy, C.M. (eds.), *Silica, Silicosis, and Cancer*: Praeger Publishers, New York, pp. 327–333.
- Wylie, A.G., 1990, Discriminating amphibole cleavage fragments from asbestos—rationale and methodology: Proceedings, 7th International Pneumoconiosis Conference, 2, pp. 1065–1069.
- Zambon, P., Simonato, L., Mastrangelo, G., Winkelmann, R., Saia, B., and Crept, M., 1986, A mortality study of workers compensated for silicosis during 1959 to 1963 in the Veneto region of Italy; *in* Goldsmith, D.F., Winn, D.M., and Shy, C.M. (eds.), *Silica, Silicosis, and Cancer*: Praeger Publishers, New York, pp. 367–374.
- Zolov, C., Bourilkov, T., and Babadjov, L., 1967, Pleural asbestosis in agricultural workers: *Environmental Research*, v. 1, pp. 287–292.

Chapter 17

BIOAVAILABILITY OF METALS IN THE ENVIRONMENT: IMPLICATIONS FOR HEALTH RISK ASSESSMENT

G.R. Krieger, H.A. Hattemer-Frey, and J.E. Kester
Dames and Moore, 633 17th Street, Suite 2500, Denver, CO 80202

INTRODUCTION

The bioavailability of environmental contaminants, including heavy metals, is an important issue in assessing exposure and resultant risk to human and ecological receptors that contact these chemicals in the environment. Risk assessment at hazardous waste sites consists of two major elements: exposure assessment (estimation of chemical intake) and toxicity assessment (estimation of the chemical dose-response relationship). These two elements are combined in the process of risk characterization to provide risk managers with as complete and accurate a projection of site risks, including uncertainties, as possible. Chemical exposure is estimated by use of standard intake equations. For example, chemical intake via contaminated soil is modeled as (U.S. EPA, 1989):

$$\text{Intake (mg/kg-day)} = \frac{(\text{ABS}) (C_S) (\text{IR}) (\text{CF}) (\text{EF}) (\text{ED})}{(\text{BW}) (\text{AT})}$$

where

C_S = Soil concentration of chemical (mg/kg)

IR = Soil ingestion rate (mg/day)

ABS = Percent of administered dose that is absorbed (i.e., bioavailable)

BW = body weight

EF = Exposure frequency (days/year)

ED = Exposure duration (years)

AT = Averaging time (years)

CF = 10^{-6} Conversion factor (kg/mg)

365 = Conversion factor (days/year)

Inputs for this and other intake equations usually consist of measured or modeled contaminant concentrations in soil, and various default values.

Because risk is a function of dose, the probability of adverse effects on any organism depends in large part on the dose of toxicant it absorbs. The toxicological significance of exposure to any metal is therefore dependent on its bioavailability, here defined as the percentage of a metal in a given medium (e.g., water, soil, sediment, food) that is absorbed following exposure via various pathways. Thus the health risks posed by metals in the environment are not determined solely by their quantity; indeed, measured concentration is often a poor predictor of toxicity.

Risk assessments for metals typically rely on toxicity studies in which metals are administered as soluble salts. On the basis of such studies, high percentages (greater than 60%) have been assumed to be bioavailable. Use of these default absorption

assumptions may significantly overestimate risks, since lead and arsenic found in soils are generally much less soluble than metal salts (e.g., Davis et al., 1992). Since the bioavailability of heavy metals is highly variable, use of conservative default absorption assumptions may result in significant overestimation of risk.

This paper presents a brief review of available information on the bioavailability of the ubiquitous metals arsenic, cadmium, and lead via the three main routes of exposure (ingestion, inhalation, and dermal contact). Evidence from risk assessments at several mine sites is also discussed which suggests that the bioavailability of lead in mining waste soils may be significantly lower than the default assumption.

FACTORS INFLUENCING THE ABSORPTION AND BIOAVAILABILITY OF METALS IN THE ENVIRONMENT

A number of chemical, environmental and biological conditions and processes influence the bioavailability of metals, and hence their toxicological significance, to organisms. For most terrestrial vertebrates, including humans, the diet is the primary route of exposure to metals in the environment. Chemicals can enter the tissues of edible plants via deposition, transpiration, and uptake from the soil. Animals can be exposed through inhalation of vapors and contaminated dust, ingestion of contaminated feeds and soil, and dermal exposure to soil. Humans in turn derive their body burdens through consumption of these plants and animals, as well as from ingestion, inhalation, and dermal exposure to contaminated soils.

Factors influencing the absorption of bioavailable metals include (1) the characteristics of the interface (e.g., lung, skin, intestine), (2) the reactivity of the metal species with the interface, and (3) the concurrent presence of other metals or other substances that may stimulate or inhibit metal uptake. Insoluble metal salts may aggregate and thereby reduce absorption. Soluble salts dissociate in aqueous environments to release metal ions that are usually absorbed readily. However, soluble salts may react with endogenous anions present at body interfaces, forming insoluble salts.

Soils can represent a highly concentrated source of metals in the environment. The distribution coefficient between soil and water (K_d) governs the bioavailability of a metal to organisms contacting the soil, with weakly bound metals being highly bioavailable and more strongly bound metals less bioavailable. The value of this coefficient depends upon both the properties of the metal species and the composition of the soil. The strongest

adsorption generally occurs in soils with high cation exchange capacity (CEC), highest pH, highest organic and clay content, and largest particle size (see also Smith, 1999).

ARSENIC

Elevated levels of arsenic can be found near smelters and refineries, and in areas where arsenical sprays are used to control pests. Arsenic is designated a class A carcinogen on the basis of human epidemiological studies. It causes lung cancer when inhaled and skin cancer when ingested in drinking water (U.S. EPA, 1993b). It is well known that arsenic toxicity varies significantly with oxidation state and compound. However, as the study used to determine the cancer potency did not distinguish As species present in drinking water, it is unknown which species/compounds may be carcinogenic. The calculated carcinogenic slope factors for both oral and inhalation exposures are controversial and the subject of several recent reviews (Chappell et al., 1997; Carlson-Lynch et al., 1994).

Ingestion

The degree of absorption of arsenic by the gastrointestinal (GI) tract depends upon the specific form of the metal and the dosing rate (U.S. EPA, 1984b). Two recent studies of the oral bioavailability of soil-associated As compounds yielded different estimates of bioavailability. Griffin and Turck (1991) reported similar bioavailability of dissolved and soil-adsorbed sodium arsenite in rabbits. However, as this compound is highly water-soluble and soil "adsorption" consisted only of making a slurry of soil and sodium arsenite solution, the compound was likely not truly associated with the soil matrix. A marked dose- and sex-dependence in uptake was observed.

In a study examining the oral bioavailability of arsenic present in mining waste soil, Freeman et al. (1991) found 60% absorption of sodium arsenate solution administered by gavage and 30% absorption of soil-associated arsenic. Similarly, arsenic in soil was shown to be five times less soluble than arsenic salts (Davis et al., 1992). Casteel et al. (1997) have performed an extensive series of studies looking at arsenic bioavailability in the swine model.

Inhalation

Absorption of arsenic via inhalation depends on arsenic species and particle size. Particles greater than 2 μm in diameter are largely deposited in the upper respiratory tract, expelled, and then swallowed, while those less than 1–2 μm in diameter can penetrate to the alveoli, where they may be absorbed through across the pulmonary epithelium (U.S. EPA, 1984a). Again, arsenic form influences absorption. Inamasu et al. (1982) observed greater uptake of arsenic trioxide than calcium arsenate following single inhalation exposures in rats.

CADMIUM

Cadmium is designated a class B1 carcinogen on the basis of animal studies in which the metal was administered via inhalation or intramuscular or subcutaneous injection. However, seven stud-

ies in rats and mice have shown no evidence of carcinogenic response upon oral administration of cadmium acetate, sulfate, and chloride (U.S. EPA, 1993b). Thus the health risks posed by this element differ with route of exposure: the target organ in chronic oral exposure is the renal proximal tubule, while inhalation exposure can result in lung cancer.

Ingestion

Exposure to cadmium by nonsmoking, nonindustrially-exposed individuals is largely via ingestion of contaminated food items. In the past, the oral reference dose (RfD) was based on a toxicokinetic model that predicts the medium-specific intake resulting in a level of 200 $\mu\text{g/g}$ wet weight in the human renal cortex (the highest concentration not associated with significant proteinuria) (U.S. EPA, 1985). Current research and proposed regulatory guidance indicates that the critical concentration of 200 $\mu\text{g/g}$ in kidney should be lowered to 50 $\mu\text{g/g}$ (Järup, 1998; U.S. EPA, 1999). The RfD, as recently evaluated by ATSDR (1997), has a 10-fold safety factor included in the final calculated value, which translates into an effective critical concentration below 50 $\mu\text{g/g}$. Clearly reflecting differences in bioavailability from different media, the model assumes 2.5% absorption of Cd from food and 5% from water. Food is a highly variable source of cadmium intake.

Inhalation

Absorption of cadmium through the GI tract is considerably less than through the lungs (Friberg et al., 1974). Systemic absorption of the amount deposited in the lungs appears to range from 20% to 25%. The amount of cadmium absorbed from inhaling cigarette smoke is substantially higher. Smokers typically have higher body burdens (approximately two-fold) than non-smokers.

Dermal contact

Wester et al. (1991) reported that absorption across human cadaver skin of cadmium chloride from soil is less than that from water (arithmetic mean for two different skins was 0.045% of dose in soil absorbed into plasma vs. 0.55% of dose in water absorbed into plasma). In general, cadmium is poorly dermally absorbed.

LEAD

Lead is considered to be a class B2 carcinogen, but the EPA has declined to set RfD or cancer potency factor estimates. Estimates of blood lead levels are calculated to evaluate exposure to lead at hazardous waste sites, as these are considered to provide the best measure of the external dose of lead. The EPA has developed the Integrated Uptake/Biokinetic (IUBK) model for this purpose (version 99d). This model is for children 0–6 years of age and other models must be utilized for adults and industrial workers.

Ingestion

The oral bioavailability of lead in soil is influenced by the species and chemical form of the lead incorporated into the soil (which is in turn dependent upon the source of lead), the size of the

lead-containing soil particles, the matrix incorporating the lead species, nutritional status, body burden of iron, and the presence of metals and other compounds ingested with the lead. Forbes and Reina (1974) found that infant rats absorb considerably more lead than adults. The absorption of lead is enhanced by low dietary levels of calcium and iron and high levels of fat and protein (U.S. EPA, 1984b).

The EPA currently assumes that percent bioavailability of lead to infants and young children is approximately 42–53% from the diet and 30% from soil. Adults absorb approximately 10% of ingested lead (Sedman, 1989). However, several epidemiological studies have indicated that exposure to mine waste-associated lead in soils (usually lead sulfide, or galena) results in lower blood lead levels than soil-associated lead from other sources (e.g., smelters, paint, vehicles) (reviewed by Steele et al., 1990). Laboratory studies of relative bioavailability have supported these observations. Rats fed urban soils (collected adjacent to lead-painted houses or along roadsides) accumulated about 70–80% of the body burden measured in lead acetate-fed controls (Dacre and Ter Haar, 1977; Chaney et al., 1984). In contrast, rats fed mining waste soil along with diet accumulated only 8%, 9% and 20% of lead acetate-fed control levels in liver, bone and blood, respectively (Johnson et al., 1991). Further, blood lead levels were significantly lower (about 4 µg/dl) in individuals living near a mining area than in individuals living near a smelter (about 12 µg/dl) or in two urban areas impacted by automobile emissions (15–28 µg/dl) (Davis et al., 1992).

Inhalation

Lead inhaled from automobile emissions is approximately 35% absorbed (Chamberlain et al., 1975). Like intestinal absorption, respiratory uptake seems to be greater in children than adults (U.S. EPA, 1984b). The solubility and bioavailability of lead sulfide are greatly influenced by particle size. Larger particles do not remain airborne as long as smaller particles and are therefore not as widely dispersed or inhaled as readily. Since absorption of lead is greater from the respiratory tract than from the GI tract, reduced inhalation of lead-containing particles will result in lower total body burdens.

BIOAVAILABILITY OF LEAD IN MINING WASTE SOILS

As mentioned above, recent work at a variety of old mining sites clearly demonstrates that the bioavailability of lead associated with mine-related soils is substantially less than 30% (Chaney, et al., 1988; Karem, 1990; Mushak, 1991; Steele et al., 1990; Davis et al., 1991, 1992; Freeman et al., 1992a, b; Schoof et al., 1993; U.S. EPA, 1993a; and Casteel, 1997). Old mine sites are associated with several factors that clearly militate against high default levels of lead bioavailability:

- Mine waste materials are typically associated with large particles (≥ 250 µm) and are less likely to be inhaled or inadvertently ingested.
- Large particles release less of their lead content per unit time than smaller particles (Bornschein et al., 1990, and Freeman et al., 1992a).
- Mine waste leads are typically lead sulfides imbedded in a quartz matrix (galena ore tailings) that are not readily dissolv-

able at normal human stomach pH's.

- Detailed blood lead studies in vivo and in vitro assays at Butte, Montana clearly demonstrate that mine waste materials have significantly lower bioavailability than standard default assumptions (U.S. EPA, 1983, and Freeman et al., 1992b).

The bioavailability of lead and arsenic in copper mining waste material from Butte, Montana has been studied in detail (Davis et al., 1992; Freeman et al., 1992a, b; Ruby et al., 1992; U.S. EPA, 1993a). Waste rock from previous underground mining activities is scattered throughout the Butte area. Use of material from these piles for residential fill material has resulted in its incorporation into residential soils. Measures of the oral bioavailability of lead in these waste materials have ranged from 2–12% (Freeman et al., 1992b, and U.S. EPA, 1993a).

The relationship between blood lead levels in children and soil lead concentrations was investigated during risk assessments at six mining sites in the U.S. In June 1998, as part of the proposed rulemaking under TSCA section 403, the EPA has extensively reviewed lead issues including level modeling. Results from studies conducted at each of these sites are discussed below.

Skagway, Alaska

In Skagway, Alaska, ore is processed into a substance the consistency of gritty talcum powder to concentrate the available lead. The resulting product contains primarily lead sulfide. This concentrated powder was transported through town and stored in a large warehouse on the edge of town. This powder was frequently blown from the warehouse area to the adjacent commercial/residential area, which as a result became heavily contaminated. Environmental sampling done in 1988 showed that the concentration of lead in soils taken from the warehouse and commercial/residential areas contained as much as 60,000 ppm lead. Arsenic, cadmium, and mercury were also found at levels of 160 ppm, 300 ppm, and 122 ppm, respectively. Most soil samples taken from residential lots contained less than 500 ppm lead.

Blood lead levels were measured in 13 children less than five years old in 1988 and 1989. The arithmetic mean blood lead level of the children was 7.8 µg/dl in 1988, and the geometric mean level was 8.3 µg/dl in 1989. The state concluded that there was "no significant difference" in blood lead measured in 1988 versus 1989 and that although lead contamination in and around the town seems to be high, actual body burdens of lead were minimal. Mean blood lead levels in children living in Skagway were "similar" to those measured in children living in "pristine, rural communities." The Centers for Disease Control (CDC) and the Alaska Health Department concluded that the reason for the low blood lead levels, despite the long-term, chronic exposure to lead, was "the low bioavailability and relatively large particle size of the ore concentrate. Lead sulfide has poor solubility and bioavailability, making it relatively nontoxic. Even if ore is ingested, most of it will be excreted in the feces. Only a tiny amount of the lead in the ore in Skagway, if any, gets absorbed through the intestine."

Silver Creek, Utah

Approximately 46,000 tons of silver and lead mill tailings were deposited in the Silver Creek, Utah area from 1900 to 1930. In 1983, soils were found to contain lead, arsenic, and cadmium at concentrations up to 8,000 ppm, 400 ppm, and 89 ppm, respec-

tively. Mean levels of lead in household dust were 1,732 ppm with a high of 8,267 ppm. In 1984, the Utah Department of Health measured blood lead levels in 49 exposed and 19 unexposed children. Survey results showed no significant differences in blood lead levels between the two groups. The mean blood level in exposed children was 11.5 µg/dl, whereas the mean level in unexposed children was 9.5 µg/dl.

In 1987, the Agency for Toxic Substance and Disease Registry (ATSDR) monitored blood lead levels in children 9 to 71 months old living in the affected area and compared those data to levels measured in children from a control area. Arsenic, cadmium, and beta-2-microglobulin (a biomarker for cadmium exposure), were measured in urine samples taken from the two groups. Although the geometric mean blood lead level in children from the affected area (7.8 µg/dl) was statistically higher than the mean level in children from the control area (4.0 µg/dl), both values were lower than the national average and lower than levels of public health concern. Cadmium and arsenic levels in all urine samples tested were within established reference limits, and urine cadmium levels were actually lower in individual living in the affected versus the control area.

Midvale, Utah

Midvale was the site of a former lead, copper, and zinc milling and smelter operation. Approximately 1,400 people live within one-quarter mile of the site, and about 8,200 people live within a half mile. The geometric mean concentration of lead in residential soils was 399 ppm (the range was from 58 ppm to 6,665 ppm). Thirteen percent of the soil/dust samples had a concentration greater than 1,000 ppm and 2% exceeded 2,000 ppm. Thirty-six percent of the homes contained lead paint. The geometric mean blood lead level for all children six to 72 months old was 5.2 µg/dl. For children living closer to the site, the mean level was 5.9 µg/dl, which is similar to the U.S. background level. The authors of the study concluded that the low blood levels were most likely due to the low bioavailability of lead in the larger particles that were typical of the site. The authors also hypothesized that high levels of zinc in site soil and (or) other soil factors may offer some protective effect by reducing the amount of absorbed lead.

Telluride, Colorado

Soil samples taken in Telluride (a small resort community in the southwestern Colorado Rocky Mountains) following the closure of a local crushing and concentration mill showed that 30% of the town was built on soils that contained more than 500 ppm lead and 17% contained more than 1,000 ppm lead. Investigators from the University of Cincinnati conducted a blood lead study in children less than 72 months old in 1986. Results showed that none of the 258 individuals monitored had excessive blood lead levels. A significant correlation was found between blood lead levels and lead levels in household dust but not in outdoor soil. The investigators concluded that the low blood levels were probably due to the "low transfer from the environment to the child and the low bioavailability of soil lead." Most of the lead was associated with large particles (i.e., those greater than 150 microns in diameter). As the diameter of particles most likely to adhere to a child's hand is 10 microns (Duggan and Inskip, 1985), the particles associated with lead in Telluride soils are not likely to be

ingested during hand-to-mouth activity. Furthermore, most of the lead measured in Telluride soils was in the form of lead sulfide, which is not likely to dissolve in and be absorbed by the gut (Bartrop and Meek, 1975). Finally, much of the soil in the area was covered by grass, which reduced exposures via direct contact.

Leadville, Colorado

Extensive mining, milling, and smelting operations took place in Leadville from 1860 to 1966. These operations were located on the edge of and within the community of Leadville. Lead sulfide and oxidized forms of lead, such as lead carbonate, lead sulfate, and lead oxide, were all found in the area. Environmental sampling of Leadville was initiated in 1986. Results showed soil concentrations of lead greater than 1,000 ppm throughout most of the town. More than 60% of the surface soil samples contained lead levels greater than 1,000 ppm, and 80% had lead levels greater than 500 ppm. The geometric mean concentration of lead in dust samples was 969 ppm. In 1987, blood lead levels were measured in 239 children aged 6 to 71 months old. The geometric mean blood lead level was 8.7 µg/dl, while 23 children had blood lead levels greater than 15 µg/dl. The authors hypothesized that the presence of more soluble forms of lead (the oxidized forms) and the relatively small particle size of the waste probably enhanced the bioavailability of lead and may account for the wide range of blood lead levels observed. The authors were not able to isolate the cause of the elevated blood lead levels or determine if they were due to exposure to mine waste or household exposures.

Smuggler's Mountain, Aspen, Colorado

Smuggler's Mountain, located near Aspen, Colorado, was extensively mined for silver, lead, and zinc between 1879 and 1920. In the 1960s, the mine wastes were reprocessed and dispersed throughout the area. Tailings were mixed with soil and left exposed or used for residential development. Some people now live directly on tailings. The mean concentration of lead in backyard soils was 4,060 ppm, with some residential soils having concentrations up to 21,000 ppm. Blood lead levels were measured in 22 individuals, 15 of whom were less than 12 years old. None of these individuals had blood lead levels above the normal range.

CONCLUSIONS

The toxicological significance of exposure to metals in the environment is a function of their absorption into the body, which is in turn governed by the chemical species and bioavailability of the metals. Because the factors controlling metal speciation and interaction with environmental media are complex and as yet poorly understood, regulatory agencies recommend use of conservative estimates of absorption to ensure that risk assessment results are protective of human health. However, risk assessors and managers should be aware that the rates of lead absorption from urban soils (Dacre and Ter Haar, 1977; Chaney et al., 1984) and the default assumption of 30% absorption from dust and soils used in the lead IUBK model are significantly greater than those observed in either laboratory studies with mining waste soils (Johnson et al., 1991; Davis et al., 1992; Freeman et al., 1992a, b) or the mining site investigations discussed in this paper. Similarly,

absorption of soil-associated arsenic appears to be considerably less than the default assumption of 60%–100% (Freeman et al., 1991). Thus, recent evidence indicates that use of default assumptions may result in unnecessary overestimation of exposure and risk at mining sites.

REFERENCES

- ATSOR, 1997, Agency for Toxic Substances and Disease Registry, Toxicology profile for cadmium (draft).
- Bartrop, D., and Meek, F., 1975, Absorption of different lead compounds: *Postgrad. Med. J.*, v. 51, pp. 805–809.
- Bornschein, R.L., Clark, S., and Pan, W., 1990, Midvale community lead study final report: Univ. of Cincinnati, July 1990.
- Carlson-Lynch, H., Beck, B.D., Boardman, P.D., 1994, Arsenic risk assessment: *Environ. Health Perspect.*, v. 102, pp. 354–356.
- Casteel, S.W., Brown, L.D., and Dunsmore, M.E., 1997, Relative bioavailability of arsenic in mining wastes: Document Control No. 4500–88–AORH, Dec. 1997.
- Chamberlain, A.C., Clough, W.S., Heard, M.J., Newton, D., Stoth, A.N.B., and Wells, A.C., 1975, Uptake of lead by inhalation of motor exhaust: *Proceedings of the Royal Society of London*, v. B192, pp. 77–110.
- Chaney, R.L., Sterrett, S.B., and Mielke, H.W., 1984, The potential for heavy metal exposure from urban gardens and soils; *in* Preer, J. (ed.), *Proceedings of the Symposium on Heavy Metals in Urban Gardens*: Agriculture Experimental Station, Univ. of the District of Columbia, Washington, D.C.
- Chaney, R.L., Mielke, H.W., and Sterrett, S.B., 1988, Speciation, mobility, and bioavailability of soil lead; *in* *Lead in Soil—Issues and Guidelines*: Environmental Geochemistry and Health Monograph, supplement to v. 9, pp. 105–129.
- Chappell, W.R., Beck, B.D., Brown, K.G., 1997, Inorganic arsenic—A need and an opportunity to improve risk assessment: *Environ. Health Perspect.*, v. 105, no. 10, Oct. 1997, pp. 1060–1067.
- Dacre, J.C., and Ter Haar, 1977, Lead levels in tissues from rats fed soils containing lead: *Arch. Environ. Contam. Toxicol.*, v. 6, pp. 111–120.
- Davis, A., Ruby, M.V., and Bergstrom, P.D., 1991, Geochemical controls on the bioavailability of lead from mine waste impacted soils, *Proceedings of the Hazardous Materials Conference*: Hazardous Materials Control Institute, Greenbelt, Md., pp. 514–569.
- Davis, A., Ruby, M.V., and Bergstrom, P.D., 1992, Bioavailability of arsenic and lead in soils from the Butte, Montana, mining district: *Environmental Science and Technology*, v. 23, pp. 461–468.
- Duggan, M.J., and Inskip, M.J., 1985, Childhood exposure to lead in surface dust and soil—A community health problem: *Public Health Review*, v. 13, pp. 31–54.
- Forbes, G.B., and Reina, J.C., 1974, Effect of age on gastrointestinal absorption (Fe, Sr, Pb) in the rat: *Journal of Nutrition*, v. 102, pp. 647–652.
- Freeman, G.B., Johnson, J.D., Killinger, J.M., Liao, S.C., Garvey, E.E., Chaney, R.L., and Bergstrom, P.D., 1991, Bioavailability of arsenic in mining waste using New Zealand White rabbits: *The Toxicologist*, v. 11, 59 pp.
- Freeman, G.B., Johnson, J.D., Killinger, J.M., Liao, S.C., Feder, P.I., Davis, A., Ruby, M.V., Chaney, R.L., and Bergstrom, P.D., 1992a, Relative bioavailability of lead from mining waste soil in rats: *Fundamentals of Applied Toxicology*, v. 19, pp. 388–398.
- Freeman, G.B., Liao, S.C., Feder, P.I., and Johnson, J.D., 1992b, Absolute bioavailability of lead following intravenous and dosed feed administration using Sprague-Dawley rats: Prepared for Atlantic Richfield Company, Denver, Colo., Battelle Columbus Operation, Columbus, Ohio.
- Friberg, L., Piscator, M., Nordberg, G.F., and Kellstrom, T., 1974, *Cadmium in the environment*: CRC Press, Boca Raton, Fla.
- Griffin, S., and Turck, P., 1991, Bioavailability in rabbits of sodium arsenite adsorbed to soils: *The Toxicologist*, v. 11, pp. 718.
- Inamasu, T., Hisanaga, A., and Ishinaihi, N., 1982, Comparison of arsenic trioxide and calcium arsenate retention in the rat lung after intratracheal instillation: *Toxicology Letters*, v. 12, pp. 1–5.
- Järup, L. (ed.), 1998, Health effects of cadmium exposure—A review of the literature and risk estimate: *Scand. J. Work, Envir. Health*, v. 24, Suppl. 1, pp. 1–51.
- Johnson, J.D., Freeman, G.B., Liao, S.-C., Feder, P.I., and Killinger, J.M., 1991, Bioavailability of lead in mining waste soil—A dosed feed study using Sprague-Dawley rats: Battelle Columbus Operations, Laboratory ID #SC9000006.
- Karem, H.S., and Beck, B.D., 1990, Current issues in determining acceptable lead concentrations in soils: *Comments on Toxicology*, v. 3, pp. 509–529.
- Mushak, P., 1991, Gastro-intestinal absorption of lead in children and adults—Overview of biological and biophysico-chemical aspects: *Chemical Speciation and Bioavailability*, v. 3, pp. 87–104.
- Ruby, M.V., Davis, A., Kempton, J.H., Drexler, J.W., and Bergstrom, P.D., 1992, Lead bioavailability, dissolution kinetics under simulated gastric conditions: *Environmental Science and Technology*, v. 26, pp. 1242–1248.
- Schoof, R.A., Steele, M.J., Whittaker, S.G., and Butcher, M.K., 1993, Assessing the validity of lead bioavailability estimates from animal studies: *The Toxicologist*, v. 13, p. 478.
- Sedman, R.M., 1989, The development of applied action levels for soil contact—A scenario for the exposure of humans to soil in a residential setting: *Environmental Health Perspectives*, v. 79, pp. 291–313.
- Smith, K.S., 1999, Metal sorption on mineral surfaces—An overview with examples relating to mineral deposits; *in* Plumlee, G.S., and Logsdon, M.J. (eds.), *The Environmental Geochemistry of Mineral Deposits, Part A. Processes, Techniques, and Health Issues*: Society of Economic Geologists, Reviews in Economic Geology, v. 6A, pp. 161–182.
- Steele, M.J., Beck, B.D., Murphy, B.L., and Strauss, H.S., 1990, Assessing the contribution from lead in mining wastes to blood lead: *Regul. Toxicol. Pharmacol.*, v. 11, pp. 158–190.
- U.S. Environmental Protection Agency (EPA), 1984a, Health effects assessment for arsenic: EPA540/8–86–020, Office of Research and Development, Environmental Criteria and Assessment Office, Cincinnati, Ohio.
- U.S. Environmental Protection Agency (EPA), 1984b, Health effects assessment for lead: EPA–540/1–86–055, Office of Research and Development, Environmental Criteria and Assessment Office, Cincinnati, Ohio.
- U.S. Environmental Protection Agency (EPA), 1985, Drinking water criteria document for cadmium, Office of Drinking Water, Washington, D.C.
- U.S. Environmental Protection Agency (EPA), 1989, Risk assessment guidance for Superfund, Vol. 1—Human Health Evaluation Manual (Part A), Interim Final: EPA/540/1–89/002, Office of Emergency and Remedial Response, Washington, D.C.
- U.S. Environmental Protection Agency (EPA), 1992, A SAB Report: Review of the Uptake Biokinetic (UBK) Model for lead: Review by the Indoor Air Quality and Total Human Exposure Committee of the OSWER Model to Assess Total Lead Exposure and to Aid in Developing Soil Lead Cleanup Levels at Residential CERCLA/RCRA Sites: Science Advisory Board (A–101). EPA–SAB–LAQC–92L016.
- U.S. Environmental Protection Agency (EPA), 1993a, Butte priority soils: Development of Preliminary Remediation Goals (PRGs) for Lead in Soils.
- U.S. Environmental Protection Agency (EPA), 1993b, Integrated Risk Information System (IRIS).
- U.S. Environmental Protection Agency (EPA), 1999, Toxicological review—Cadmium and compound integrated risk information system (IRIS): March 4 (also available online at <http://www.epa.gov/ncea>).
- Wester, R.C., Maibach, H.I., Sedik, L., Melendres, J., DiZio, S., Jamall, I., and Wade, M., 1991, In vitro percutaneous absorption of cadmium from water and soil into human skin: *The Toxicologist*, v. 11, pp. 11–15.

Chapter 18

EFFECTS OF HEAVY METALS ON THE AQUATIC BIOTA

M.G. Kelly

Bowburn Consultancy, 11 Montaigne Drive, Bowburn, Durham DH6 5QB, UK

INTRODUCTION

This review focuses on the effects of heavy metals on the aquatic (primarily freshwater) biota. During the 1970s and 1980s there was intense research interest in the biological effects of heavy metals. While this has provided a firm foundation for the interpretation of toxic effects associated with metalliferous mining in particular, many other aspects of mining, with potentially adverse effects on the biota, have received less attention. In particular, physical factors, such as those associated with high suspended solid loads, for example, are studied comparatively rarely, although for many deposits of insoluble metals (e.g., gold, tin) such factors may be more significant than toxicity (LaPerriere et al., 1985; Van Nieuwenhuysse and LaPerriere, 1986; Briones, 1987). Moreover, discovery of a valuable mineral may lead to large increases in population. The town of Jos in Nigeria, for example, owes its existence to the tin mines in the region and the main water quality problem in the Delimi river downstream of the town is due to sewage pollution rather than to mining (Kelly and Ali, 1993). Further environmental impacts can include clearing land for agriculture to feed the growing population (Livett et al., 1979). It would be wrong to consider the potential impact of a new development without considering these aspects as well.

Toxic effects of mining wastes, however, remain the prime subject of concern, particularly because of potential impacts on human health due to the movement of heavy metals through food-webs and into organisms consumed by human populations. The ecological impact depends upon the particular metal, or cocktail of metals, in question. This can be further modified by other factors related to the background geology (acidity, water hardness, etc.) which affect the speciation of the metal. The biological environment can also affect toxicity: of particular note is the methylation of some metals (particularly Hg) under anaerobic conditions to form extremely toxic compounds (Moore and Ramamoorthy, 1984). Bioaccumulation of methylated Hg was responsible for the outbreaks of "Minamata disease" in areas of Japan, where humans consumed diets rich in Hg-contaminated fish (Clark, 1986; Honma, 1988).

The term "heavy metal" is traditionally reserved for metals with a density >5 (e.g., Passow et al., 1961) although lighter metals (e.g., Al) have often been included as well. However, toxic effects within this group are not constant and attempts have been made to abandon the term heavy metal in favor of a more biologically-relevant classification (Nieboer and Richardson, 1980). In

this classification, metal ions are grouped into three groups based upon their affinity for different ligands. Class A metals (e.g., K, Ca, Ba) tend to seek oxygen-containing ligands while Class B metals (e.g., Cu(I), Ag, Au, Hg) seek nitrogen- and sulphur-containing ligands; Borderline metals (e.g., Ni, Cu(II), Zn, Cd, Pb) with intermediate properties are grouped with the Class B metals, as they have similar toxic effects. Although unsuccessful in displacing the term "heavy metal" from the public imagination, this classification does provide a set of criteria by which metals may be compared toxicologically.

The purpose of this review is to draw generalizations about the toxic effects on the aquatic biota of metals associated with mining activities. For a detailed review of this sizeable and complex subject, the reader is referred to general references such as Kelly (1988) and references contained therein.

UNDERLYING ECOLOGICAL CONCEPTS

Central to an understanding of the ecological effects of pollution is the concept of "stress," defined as "external constraints limiting the rate of resource acquisition, growth or reproduction of organisms" (Grime, 1989) or "an environmental condition that, when first applied, impairs Darwinian fitness" (Sibley and Calow, 1989). These definitions apply principally to individual organisms; however, the integrated effects on individuals may ultimately affect community structure. Although the concepts of succession (the natural sequence of changes in an ecosystem over time), and climax (the equilibrium community at the end of a succession) are difficult to apply in flowing waters, biologists recognize, implicitly or explicitly, an "expected" or "ideal" community that should be present for a given river type. Departures from this suggest that some form of external stress is acting on the system, although it is important to recognize that many forms of stress are natural (i.e., extremes of temperature, tidal movements, etc.) and, indeed, stress is the driving force behind natural selection and evolution (Hoffman and Parsons, 1993).

Early studies on the ecological effects of heavy metals noted changes in distributions of plants and animals downstream of mines. Implicit were the assumptions that the mines were responsible for some degree of ecological perturbation, and that the expected range of species present at those sites had changed in direct response to the mining. For example, Carpenter (1924, 1926) noted an impoverished fauna immediately downstream of a

Pb mine in Mid Wales that she attributed to the toxic effect of Pb in the water, although it is now considered that the observed effects were more likely to have been caused by Zn. When mining ceased, the fauna recovered from 14 species in 1920 to 130 species in 1949 (Fig. 18.1; Jones, 1949) and appears to have remained at this state subsequently. Recovery, therefore, is a relatively slow process limited, perhaps, by the rate at which individuals from new species are able to immigrate to the river, although evidence for this is largely circumstantial.

The "struggle for existence," first described by Darwin (1859), occurs primarily within populations of the same species, rather than between communities of many different species. For any particular population exposed to heavy metal toxicity downstream of a mine, some individuals may prove more tolerant than others and these will survive and, possibly thrive in the absence of competition. It is a classic case of natural selection: successful (i.e., tolerant) individuals pass their genotypes onto the next generation which therefore contains a greater proportion of the genes responsible for tolerance. Over time, populations come to be composed almost entirely of tolerant individuals. This has been shown particularly clearly in the algae (see below) and some grasses (Bradshaw and McNeilly, 1981).

However, particular species within a community will also vary in the extent to which they are affected by a toxin. This may be due partly to physiological differences between species but also to ecological or behavioral factors: plants may vary in the proportion of their surface area that is exposed to the water, while invertebrates that ingest large quantities of sediment may accumulate higher concentrations of toxin than species that ingest leaf material. Thus, the interrelationships between organisms in a stream will change. A species that is particularly sensitive may decline in abundance while one that is more tolerant will increase. As the

concentration of the toxin increases, so some species may disappear altogether while at very high concentrations, conditions may approach those of biologically "extreme" environments such as saline lakes and thermal springs. However, while these "extreme" environments tend to be dominated by microorganisms (Brock, 1969), all groups of photosynthetic taxa of any quantitative importance in freshwaters have a few representatives that are tolerant of elevated metals (Whitton, 1980). When the level of environmental stress is particularly high, then it becomes the principal determinant of species numbers at a site. At lower stress levels, however, other factors (e.g., diversity of habitats, nutrients) may also affect species numbers (Fryer, 1980). This was particularly clearly illustrated for heavy metals in a study by Whitton and Diaz (1980) who plotted the number of photosynthetic organisms found in 10-m lengths (termed "reaches") of an enormous number of sites in the U.K., Europe, and the United States against the concentration of Zn in the water (Fig. 18.2). The number of taxa at sites with low Zn concentrations is highly variable, but at sites with high Zn concentrations it is always low.

The reduction in competition from less tolerant individuals at high concentrations of heavy metals may enable the few species that are tolerant to thrive. Thus, mine adits are often characterized by lush growths of algae (Armitage, 1979; Patterson and Whitton, 1981) possibly due to a lack of competing algae (Leland and Carter, 1984) or invertebrate grazers (Klotz, 1981). The massive growths themselves can change conditions within the stream, either by smothering the substrate (Armitage, 1979) or causing deoxygenation of the water at night, so interpretation of these effects is not necessarily straightforward.

The relationship between primary producers and grazers introduces a further ecological concept necessary to understand the effects of heavy metals on the biota. This is "bioaccumulation," derived from the fundamental ecological idea of biogeochemical cycles in which the environment and different trophic levels (feeding strata in a food chain) are represented stochastically as compartments, between which elements are transferred over time. Organisms have well-developed mechanisms for absorbing, metabolizing and excreting nutrients such as nitrogen and phosphorus. Indeed, they can even absorb, metabolize, and excrete metals at concentrations that are encountered naturally. These mecha-

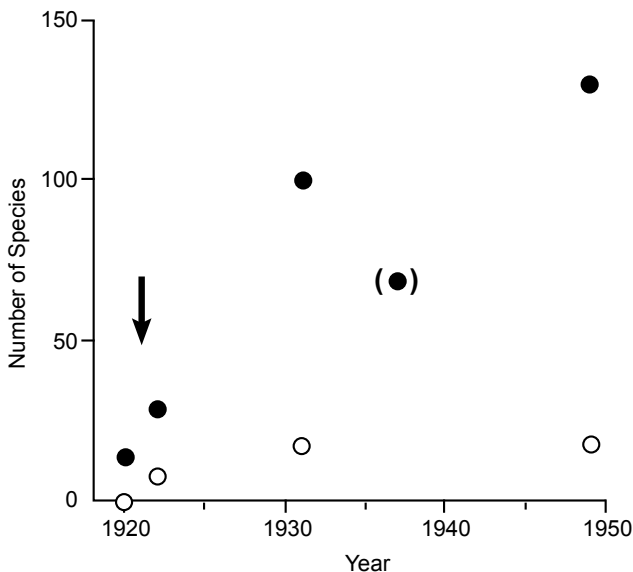


FIGURE 18.1—The recovery of the invertebrate fauna in the River Rheidol, Mid Wales, following the cessation of lead mining (arrowed). Closed circles = all invertebrates; open circles = Trichoptera species only; bracketed circle = sample collected after period of heavy rain. Compiled from published sources by Kelly (1988).

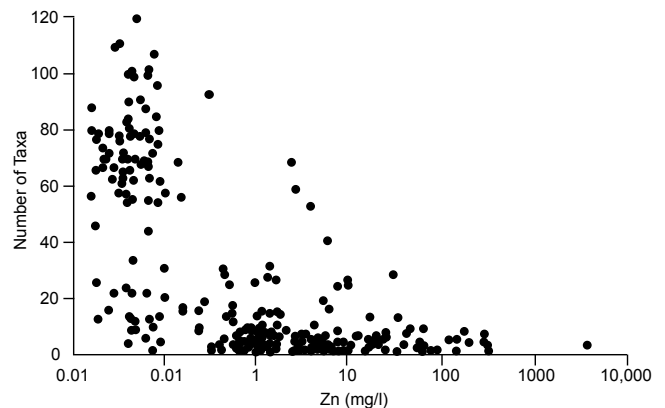


FIGURE 18.2—Relationship between Zn in water and number of species in 10-m lengths of streams and rivers in U.K., Western Europe and U.S.A. Adapted from Whitton and Diaz (1980).

nisms, however, can become saturated at high concentrations of metals, and the rate of uptake can exceed the rate of loss, a more energetically demanding process. For this reason, organisms can accumulate high concentrations of heavy metals in their tissues. During its lifetime a predator will consume many times its own body weight of prey and if this prey has high concentrations of metals, then the predator, similarly unable to metabolize and excrete the metals, will accumulate yet higher concentrations in its tissues. This idea of "biomagnification" along a food chain was famously studied for pesticides (Carson, 1963) and is relevant to studies of heavy metals as well (Anderson, 1977), although the evidence is often equivocal (Kelly, 1988 and see below).

ACCUMULATION OF HEAVY METALS

It has been understood for about thirty years that organisms can accumulate heavy metals to much greater concentrations than those found in their environment. "Enrichment ratios" (concentration in organism/concentration in water, also known as "concentration factors") are typically in the range 10^3 – 10^4 , although these tend to decrease as the aqueous concentration increases (Kelly, 1988). However, concentrations within organisms at any site can vary considerably, depending upon growth strategies (in plants), feeding strategies (in animals) and basic physiological differences. In general, there is a good relationship between the aqueous concentration of a metal and its concentration found in plants (Fig. 18.3). Deviations from this trend can be partly explained by environmental factors such as low pH, which limits metal accu-

mulation, and the use of metal exclusion by some algae as a tolerance mechanism (Kelly, 1988).

Similar relationships can be established for individual species; a number of plants have been studied in this way (Wehr and Whitton, 1983; Whitton et al., 1989; Kelly and Whitton, 1989a and b). A comparison of metal concentrations in three algae and four bryophytes as a function of metal concentrations in water (Fig. 18.4) indicated that the bryophytes accumulated more Zn, Cd and Pb than the algae, although the green algae (*Cladophora glomerata*, *Stigeoclonium tenue*) had steeper slopes, indicating a greater change in accumulated concentrations for the same change in aqueous concentrations (Kelly and Whitton, 1989a); the red alga *Lemanea* had a similar slope to the bryophytes but contained lower overall concentrations. In rooted vascular plants, metals also enter the plants via the sediments and, in general, higher concentrations are found in roots than shoots (Fig. 18.3). In *Potamogeton crispus* and *P. pectinatus*, Cu, an essential trace element, was translocated from the roots to the shoots while Pb, which is not essential, was retained in the roots (Welsh and Denny, 1979).

The sediments are also a major pathway for uptake of metals by animals, with species living in close proximity to sediments (e.g., burrowing mayflies, Ephemeridae and some Chironomidae) having higher concentrations. Filter feeders, detritivores, algal grazers, carnivores, and surface feeding species have progressively lower concentrations (Smock, 1983a). Metals in the gut may represent a major proportion of the total body load (Ellwood et al., 1976) and, as a result, many workers keep invertebrates alive but unfed for 2–4 days prior to analysis to allow purging of the gut

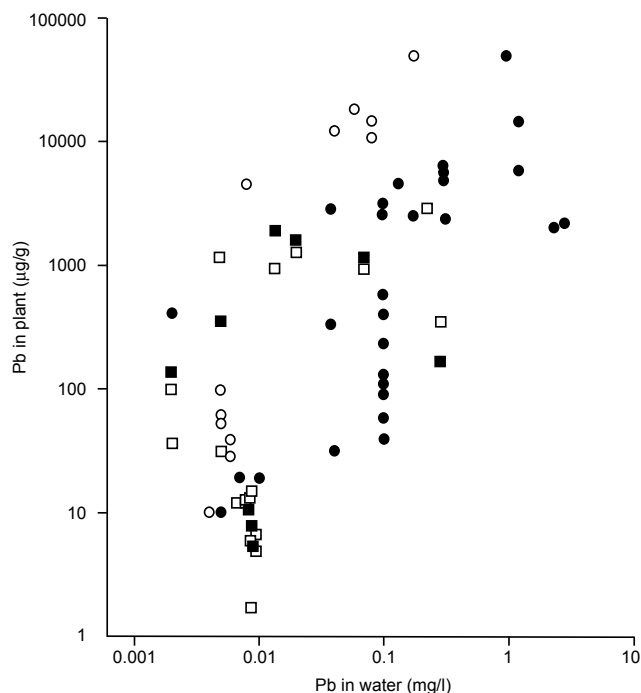


FIGURE 18.3—Accumulation of Pb from water by: algae (closed circles); bryophytes, or mosses (open circles); and angiosperms, or flowering plants (roots, closed squares; shoots, open squares). Compiled from published and unpublished sources by Kelly (1988).

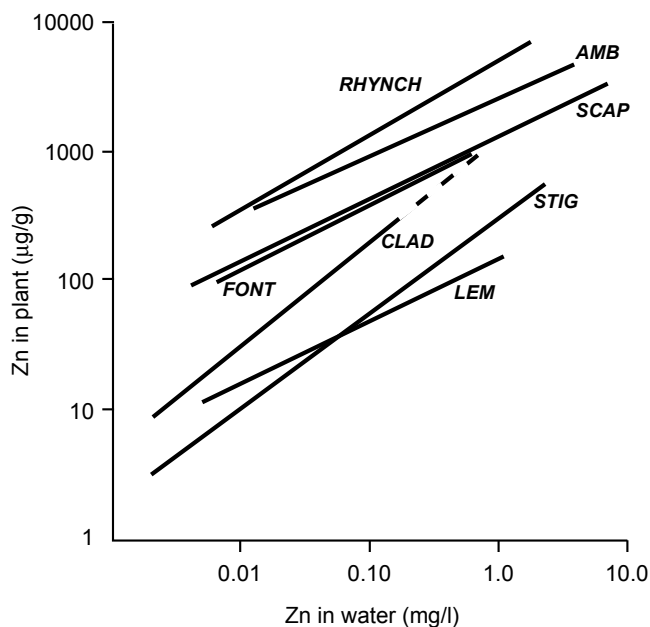


FIGURE 18.4—Influence of aqueous Zn on Zn concentration in plants. Algae: LEM, *Lemanea fluviatilis*; CLAD, *Cladophora glomerata*; STIG, *Stigeoclonium tenue*. Bryophytes: SCAP, *Scapania undulata*; AMB, *Amblystegium riparium*; FONT, *Fontinalis antipyretica*; RHYNCH, *Rhynchostegium riparioides*. After Kelly and Whitton (1989a).

contents. The unselective ingestion of sediment (which masks the biological “signal”) by many aquatic animals may be one reason why clear relationships between organismic and environmental concentrations of metals are harder to find in the literature compared with similar studies on plants. Other factors that complicate determination of metal uptake from sediments are direct accumulation from the water itself (Smock, 1983b; Rainbow and Moore, 1986) and the localization of metals within particular organs. Fish muscle tissue, in particular, often contains low concentrations compared to organs such as the liver and kidney (Murphy et al., 1978; Cowx, 1982; Bendell-Young et al., 1986). Thus, piscivorous (fish-eating) species such as perch (*Perca fluviatilis*) and pike (*Esox lucius*) have lower concentrations of Zn, Cd and Pb than bottom-feeding species such as roach (*Rutilus rutilus*) and bream (*Abramis brama*; Badsha and Goldspink, 1982) although at high metal concentrations, susceptible prey species may be eliminated and replaced by metal tolerant species. The effect on predators will depend upon whether tolerance is due to an ability to accumulate and detoxify a metal, or exclude it from cells. This will act either as a positive or negative feedback mechanism to enhance or weaken the transfer of metals through the food chain (Dallinger et al., 1987).

TOXICITY AND TOLERANCE

Toxicity of materials to aquatic populations has traditionally been expressed as “LC₅₀”: the concentration that would kill (“lethal concentration”) 50% of a batch of organisms within a specified time period (usually 48–96 h). Although this toxicity measurement is used widely for fish and invertebrates, unicellular algae present particular problems for the test, as a concentration that inhibits growth might not necessarily kill the cells outright.

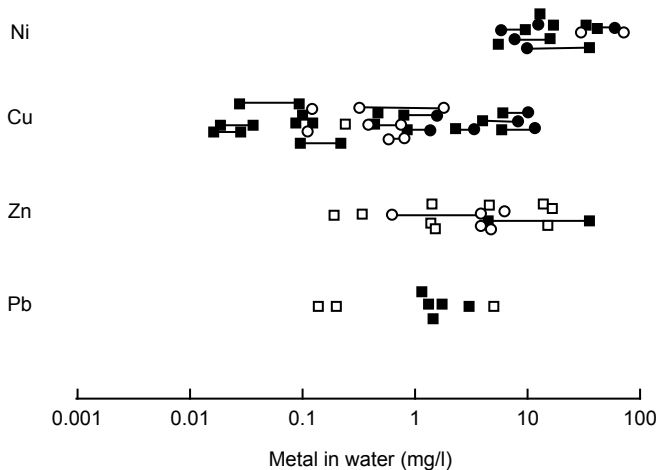


FIGURE 18.5—Effect of nickel, copper, zinc, and lead on freshwater fish, expressed as LC₅₀. No attempt is made to distinguish different taxa; however, distinctions have been drawn between 24-h LC₅₀ (closed circles), 48-h LC₅₀ (open circles), 96-h LC₅₀ (closed squares) and LC₅₀ values based on incubation times in excess of 10 days (open squares). Solid lines indicate range of effects obtained from different treatments. Compiled from published sources by Kelly (1988).

For this reason, the term LC₅₀ is often replaced by “EC₅₀”: the effective concentration required to reduce a particular parameter (usually growth) by 50%. In both cases, physical, chemical and biological aspects of the test can have major effects on results (Mance, 1987) although compilations of data are still useful for making comparisons between metals (Fig. 18.5) and between taxonomic groups (Fig. 18.6).

Although measurement of acute toxic effects is still valuable for some purposes, the emphasis in recent years, however, has moved to an understanding of the various components of environmental stress and their effects on ecological fitness (see above). Environmental effects on ecological fitness can take many forms. For example, juvenile life-stages are often more susceptible to heavy metals than adult stages (Watton and Hawkes, 1984; Nicola Giudici et al., 1987), reproduction may be impaired (Brungs et al., 1976; Sehgal and Saxena, 1986) and both invertebrates (McMurtry, 1984) and fish (Atchinson et al., 1987) show avoidance behavior when exposed to heavy metals.

To put this into context, the “Maximum Acceptable Toxicant Concentration,” assessed with reference to effects on reproduction and fecundity (fertility), for copper and lead was determined to be between two and three orders of magnitude lower than LC₅₀ values for these metals (Brungs et al., 1976). Moreover, molecular biological studies are now able to detect the “switching on” of genes coding for cellular systems involved in detoxification and metabolism of metals at even lower concentrations (Roch et al., 1986; George and Langston, 1994).

Plants

Many physiological processes have been shown to be disrupted by heavy metals and it is likely that there are cascades of toxic effects within cells. For example, many studies have shown photosynthesis to be reduced (Fångstrom, 1972; Brown and Rattigan, 1979; Rabe et al., 1982), possibly as the central Mg atom of the chlorophyll molecule is replaced by the heavy metal (Arndt, 1974). Other studies have shown respiration to be reduced (Bonaly et al., 1986) and photorespiration to increase (Filbrin and Hough, 1979). If such basic metabolic processes are damaged, then many

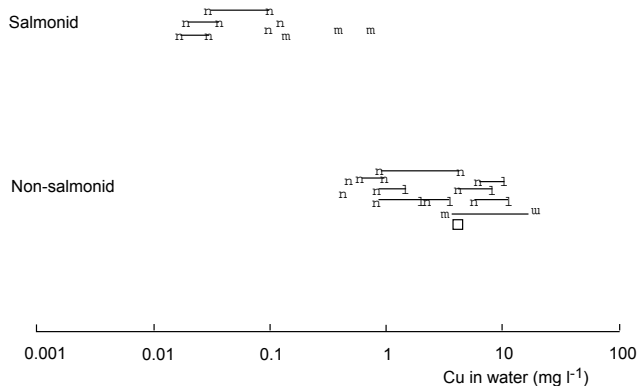


FIGURE 18.6—Comparative effects of copper on Salmonidae and other fish, expressed as LC₅₀. Details as for Figure 18.5. Compiled from published sources by Kelly (1988).

other cellular processes will also be affected, for example, breakdown of membrane integrity (Singh and Yadava, 1986) and inhibition of nutrient uptake (Kashyap and Gupta, 1982; Peterson and Healey, 1985). The result of these effects are illustrated by an unpublished study on *Chlorella* sp. (Fig. 18.7), which shows slower growth at higher Zn concentrations, leading to lower overall yields as cellular processes are disrupted by higher and higher concentrations of metal. At very high concentrations, cell numbers decline.

Tolerance can be induced in algae by sub-culturing in successively higher concentrations of metals (Stokes, 1975; Shehata and Whitton, 1982). As algal cultures tend to have very little genetic variability, it is assumed that such tolerance is due to the selection of spontaneous mutants. Tolerance has also been observed in field populations of green algae, where there tends to be a clear relationship with aqueous metal concentrations along with morphological changes (Harding and Whitton, 1976; Say et al., 1977).

Given the ease with which tolerance can be induced in the laboratory in a range of organisms, it seems likely that selective pressures will work simultaneously on many cellular processes, leading to many possible "solutions" to the problem of toxicity. Thus, Foster (1977) observed Cu-tolerant varieties of *Chlorella* sp. in the R. Hayle, Cornwall, that appeared to exclude Cu from the cell, whereas tolerant strains of *Stigeoclonium tenue*, another green alga, appear to accumulate much higher concentrations than non-tolerant ones (Kelly and Whitton, 1989b). Other common tolerance mechanisms include the production of extracellular products to "bind" metals into complexes (Clarke et al., 1987) and the production of metallothioneins (see below). The former have been studied particularly in the Cyanobacteria, where they are thought to be produced naturally in response to Fe starvation, but to have a secondary role protecting against elevated metal concentrations.

Animals

The literature on the physiological effects of heavy metals on animals is enormous and, at times contradictory, although the consensus seems to be that hypoxia (a deficiency in the amount of oxygen reaching bodily tissues) is the prime manifestation of

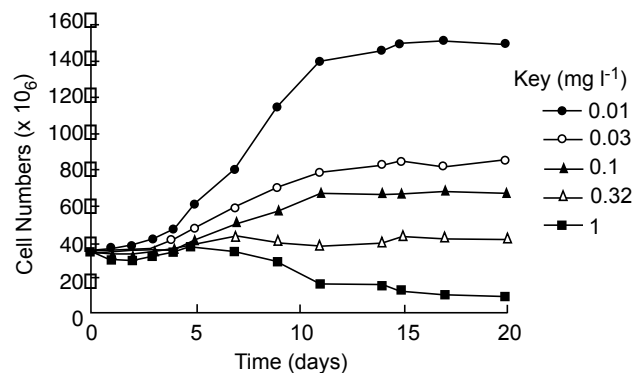


FIGURE 18.7—The effect of Zn on growth of *Chlorella* sp. Unpublished data of S.J. Oluwatoyin and M.G. Kelly. Rate of growth and yield are both negatively correlated with \log_{10} Zn concentration, whilst the length of the lag phase (the period between inoculation and start of exponential phase) is positively correlated.

metal toxicity (Burton et al., 1972). This is caused by a breakdown in gas exchange either from coagulation and precipitation of mucus or from cytological (cell) damage. Hypoxia is manifested in many ways, including increased heart rate, ventilation and coughing (Hughes and Tort, 1985), anemia (Tewari et al., 1987; Hughes, 1988) and oxygen dissociation (Hughes, 1988). The latter two may be related to changes in the hemoglobin molecule itself (due to displacement of the central Fe atoms), or changes in the synthesis of the hemoglobin (Jackim, 1973). Effects on respiration have also been observed in invertebrates (Hubschman, 1967; Correa, 1987). One consequence of these effects is a steady metabolic cost from exposure to sub-lethal concentrations of metals (Collvin, 1985). This becomes more pronounced when the organism has been starved prior to exposure (Segner, 1987) although a certain amount of acclimation has been noted when organisms are pre-exposed to the metal in question (Laurén and McDonald, 1987). The longer lifecycles of fish and benthic invertebrates, when compared with the microscopic algae discussed above, means that the development of tolerance over several generations has not been studied in the same detail. There is, however, a considerable literature on the role of metallothioneins (see below) in fish.

Effects on behavior and reproduction were mentioned above. One particularly bizarre cause of reproductive failure amongst marine invertebrates (Dog-whelks, *Nucella lapillus*) is due to "imposex," the development of male characters, notably a penis, on females, caused by tributyltin (a tin-containing organic compound used in antifouling paints (Gibbs and Bryan, 1986; Gibbs et al., 1987).

Environmental factors affecting toxicity

Toxicity of a metal can vary over several orders of magnitude (Figs. 18.5 and 18.6) depending upon a number of factors, most notably pH and water hardness. These can affect the speciation of the metal in solution, the rate that it is accumulated by an organism and the organism's response. In particular, pH has a pronounced effect on speciation of some metals (e.g., Al, Cu, Mn and Pb; Campbell and Stokes, 1985), with the proportion present as free ions (generally regarded as the most toxic form) increasing as pH falls. For many other metals, however, pH-induced changes in toxicity are more likely to be due to the organisms response to the metals. Metal accumulation is much reduced at low pH (Satake et al., 1984; Harrison et al., 1986). However, the amelioration caused by less metal being accumulated at low pH values has to be considered alongside the increased physiological stress caused by low pH. This is well illustrated by a study on *Salmo gairdneri* (rainbow trout) in which Cu uptake at pH 5.0 was half that at pH 7.0 while toxicity increased between four and ten times (Laurén and McDonald, 1986).

These effects are particularly pronounced in "soft" water with low buffering capacity. Water hardness is defined as the sum of concentrations of Ca and Mg salts; increased concentrations of these salts have been shown to decrease metal uptake by aquatic bryophytes both in the field (Wehr and Whitton, 1983) and the laboratory (Wehr et al., 1987). Many studies have demonstrated reduced toxicity in hard water (Winner and Gauss, 1986; Mance, 1987) although the scale of the effect varies depending upon the metal in question. A likely explanation for these effects is increased competition for metal binding sites in the cell (Stokes, 1983).

Conversely, field (Harding and Whitton, 1976; Say et al., 1977) and laboratory (Harding and Whitton, 1977; Say and Whitton, 1977) studies have shown that algal populations from hard water are generally less tolerant to a particular Zn concentration than populations from soft water sites. This is presumably because the natural "protection" offered by Ca and Mg (which competes with the metals for binding sites and so reduces uptake) reduces the need for genetic tolerance mechanisms.

An external factor that might reduce the concentration of free metal ions is the presence of natural chelating agents such as humic acids and polypeptides, which have been shown to markedly increase LC₅₀ concentrations of metals to invertebrates (Winner, 1984; Winner and Gauss, 1986). EDTA is often used in the laboratory as an artificial chelating agent and it appears to mask the toxic effects of metals up to the point where the concentration of metal exceeds the binding capacity of the EDTA (Stokes, 1983; Schreinemakers and Dorhout, 1985). Chelating agents occur naturally, for example from the breakdown of plant products, but many algae also appear to produce their own chelating agents in response to elevated metal concentrations (see above; Jardim and Pearson, 1984; Starodub et al., 1987)

Phosphorus is an important factor determining toxicity of metals to algae and other plants. As the major nutrient limiting growth in freshwaters, P can have a marked effect on algae quite separate to any alleviation of metal toxicity (Say and Whitton, 1977): for example, phosphate-starved populations of '*Anacystis nidulans*' (\equiv *Synechococcus* sp.) have been shown to be more sensitive to Zn than phosphate-rich populations (Shehata and Whitton, 1982). However, interpretation of these results is difficult as high concentrations of phosphates (as found in recipes for many growth media) tend to form insoluble complexes with metals (Stumm and Morgan, 1981), rendering the metal unavailable to organisms, while other studies have shown metals to inhibit P uptake (Peterson and Healey, 1985) and/or metabolism (Kuwabara, 1985).

Synergism, additivity, and antagonism

Where two or more metals are found together, the combined toxic effect may: (1) equal the sum of the toxicities of the constituents ("additive" behavior); (2) exceed the sum of the toxicities of the individual metals ("synergistic" behavior); or (3) be less than the sum of the individual toxicities ("antagonistic" behavior). In practice, results are strongly affected by experimental protocols (Wong and Beaver, 1981; Kelly, 1988): for example, mixtures of Zn and Cd have behaved synergistically to algae (Say and Whitton, 1977) and higher plants (Hutchinson and Czyska, 1975), additively to some higher plants (Nasu et al., 1984) and invertebrates (Thorp and Lake, 1973), and antagonistically to some algae (Shehata and Whitton, 1982) and invertebrates (Thorp and Lake, 1973). By contrast, Cu and Zn appear to always act additively (algae: Petersen, 1982; invertebrates: McMurtry, 1984; fish: Thompson et al., 1980).

Metallothioneins: a unifying hypothesis for metal toxicity?

Metallothioneins are a group of proteins with molecular weight between 6000–7000 Daltons and 60–62 amino acids,

including about 20 cysteine residues (Robinson et al., 1993; George and Langston, 1994). Their original function remains the subject of debate, although it seems likely that they may bind surplus quantities of potentially toxic metals such as Cu and Zn which are essential for life processes, in order to maintain a small "store" (George and Langston, 1994). Under normal (i.e., unpolluted) conditions, metal accumulation works to an organism's advantage, permitting trace metals that might otherwise limit growth to be scavenged from the environment. Once inside a cell, however, they need to be stored in a non-toxic state until required for growth. However, where concentrations of Cu and Zn—or chemically similar metals such as Cd and Hg—are elevated, the capacity of the metallothioneins is exceeded and life processes will be inhibited. Organisms can, to some extent overcome this by increasing the amount of metallothionein in a tissue, and correlations have been demonstrated in fish between metallothionein concentrations and hepatic (George and Langston, 1994) and ambient (Roch and McCarter, 1984) metal concentrations.

Metallothionein-like compounds have been found in virtually all groups of organisms, with particularly strong homology (i.e., similar protein and DNA sequences) amongst the vertebrates (George and Langston, 1994) for which a vast literature exists. However, studies on fast-growing lower organisms such as fungi and algae which are easily manipulated in culture have provided several insights into the evolutionary and ecological significance of these compounds. It has been shown, for example, that the metallothionein gene can be deleted from fungi and cyanobacteria using molecular biological techniques, with little effect on growth or reproduction but with reduced tolerance to metals (Hamer, 1986; Turner et al., 1993). In other words, where metal concentrations are low and constant, then organisms do not need metallothioneins for maintaining a constant internal environment (homeostasis). When metal concentrations increase, however, then "normal" cells are able to increase the quantity of metallothionein by increased gene transcription (Hamer, 1986).

Where lines of cyanobacteria tolerant to Cd have been induced by sub-culturing into successively higher concentrations of metals, an increase in the gene copy number has been observed (Gupta et al., 1992), permitting more Cd to be bound within the cell. This was accompanied by the deletion of the repressor which normally controlled metallothionein synthesis (Gupta et al., 1993), which meant that the gene was permanently "switched-on" in Cd-tolerant cells.

Metallothioneins—and metallothionein-like compounds—are clearly widespread and may partly explain why organisms can accumulate relatively high concentrations of metals. To date, however, there have been few studies synthesizing these molecular studies with ecological and ecotoxicological observations. There appear to be, for example, no studies in which the effect on metallothioneins of environmental factors such as pH and hardness are evaluated. What follows is, therefore, speculative.

Many of the environmental factors which protect against toxic metals do so outside the cell, either by affecting the chemical speciation of the metal or by competing with the metal either for binding sites on the cell wall (Kelly, 1988) or for uptake sites on the cell membrane (see above). It might be postulated that they are acting in series with the metallothioneins, insofar as metals that are not trapped either outside the cell or (in the case of plants) in the cell wall, are absorbed and so will provoke metallothionein synthesis. Selective pressures will therefore work on all stages contributing to metal tolerance, and a study demonstrating metal

exclusion as a tolerance mechanism (e.g., Foster, 1977) does not necessarily invalidate hypotheses concerning metallothioneins. Indeed, in groups such as the aquatic bryophytes with thick cell walls rich in cation-exchange sites (Wehr et al., 1987), only 2% or less of metal was estimated to be bound to metallothionein-like compounds (Jackson et al., 1991).

CONCLUDING COMMENTS

It has been my intention in this review to identify some of the common strands from an enormous literature covering both a large number of metals and a huge variety of organisms. It should be apparent from what I have written that several factors are common, relating to broad chemical similarities between metals and common physiological mechanisms at the cellular level. These two factors form a contrapuntal theme around which infinite variations can be woven.

REFERENCES

- Anderson, R.V., 1977, Concentration of cadmium, copper, lead and zinc in thirty-five genera of freshwater macroinvertebrates from the Fox River, Illinois and Wisconsin: *Bulletin of Environmental Contamination and Toxicology*, v. 18, pp. 345–349.
- Armitage, P.D., 1979, The effects of mine drainage and organic enrichment on benthos in the River Nent system, Northern Pennines: *Hydrobiologia*, v. 74, pp. 119–128.
- Arndt, U., 1974, The Kautsky-effect—A method for the investigation of the actions of air pollutants in chloroplasts: *Environmental Pollution*, v. 6, pp. 181–194.
- Atchinson, G.J., Henry, M.G., and Sandheinrich, M.B., 1987, Effects of metals on fish behavior—A review: *Environmental Biology of Fishes*, v. 18, pp. 11–25.
- Badsha, K.S., and Goldspink, C.R., 1982, Preliminary observations on the heavy metal content of four species of freshwater fish in north-west England: *Journal of Fish Biology*, v. 21, pp. 251–267.
- Bendell-Young, L.I., Harvey, H.H., and Young, J.F., 1986, Accumulation of cadmium by White Suckers (*Catostomus commersoni*) in relation to fish growth and lake acidification: *Canadian Journal of Fisheries and Aquatic Science*, v. 43, pp. 806–811.
- Bonaly, J., Miginiac-Maslow, M., Brochiero, E., Hoarau, A., and Mestre, J.C., 1986, Cadmium effects on the energetics of *Euglena* during the development of cadmium resistance: *Journal of Plant Physiology*, v. 123, pp. 349–358.
- Bradshaw, A.D., and McNeilly, T., 1981, *Evolution and pollution*: Edward Arnold, London, 76 pp.
- Briones, N.D., 1987, Mining pollution—The case of the Baguio Mining District, the Philippines: *Environmental Management*, v. 11, pp. 335–344.
- Brock, T.D., 1969, Microbial growth under extreme conditions: *Symposia of the Society for General Microbiology*, v. 19, pp. 15–41.
- Brown, B.T., and Rattigan, B.M., 1979, Toxicity of soluble copper and other ions to *Elodea canadensis*: *Environmental Pollution*, v. 20, pp. 303–314.
- Brungs, W.A., Geckler, J.R., and Gast, M., 1976, Acute and chronic toxicity of copper to the fathead minnow in a surface water of variable quality: *Water Research*, v. 10, pp. 37–43.
- Burton, D.T., Jones, A.H., and Cairns, J., 1972, Acute zinc toxicity to rainbow trout (*Salmo gairdneri*)—confirmation of the hypothesis that death is related to tissue hypoxia: *Journal of the Fisheries Research Board of Canada*, v. 29, pp. 1463–1466.
- Campbell, P.G.C., and Stokes, P.M., 1985, Acidification and toxicity of metals to aquatic biota: *Canadian Journal of Fisheries and Aquatic Science*, v. 42, pp. 2034–2049.
- Carpenter, K.E., 1924, A study of the fauna of rivers polluted by lead mining in the Aberystwyth District of Cardiganshire: *Annals of Applied Biology*, v. 11, pp. 1–23.
- Carpenter, K.E., 1926, The lead mine as an active agent in river pollution: *Annals of Applied Biology*, v. 13, pp. 395–401.
- Carson, R., 1963, *Silent spring*: Hamish Hamilton, London, 304 pp.
- Clark, R.B., 1986, *Marine pollution*: Clarendon Press, Oxford, 215 pp.
- Clarke, S.E., Stuart, J., and Sanders-Loehr, J., 1987, Induction of siderophore activity in *Anabanea* spp. and its moderation of copper toxicity: *Applied and Environmental Microbiology*, v. 53, pp. 917–922.
- Collvin, L., 1985, The effect of copper on growth, food consumption and food conversion of perch *Perca fluviatilis* L. offered maximal food rations: *Aquatic Toxicology*, v. 6, pp. 105–113.
- Correa, M., 1987, Physiological effects of metal toxicity on the tropical freshwater shrimp *Macrobrachium carcinus* (Linnaeus, 1758): *Environmental Pollution*, v. 45, pp. 149–155.
- Cowx, I.G., 1982, Concentrations of heavy metals in the tissues of trout *Salmo trutta* and char *Salvelinus alpinus* from two lakes in North Wales: *Environmental Pollution Series A*, v. 29, pp. 101–110.
- Dallinger, R., Prosi, F., Segner, H., and Back, H., 1987, Contaminated food and uptake of heavy metals by fish—a review and a proposal for future research: *Oecologia* (Berlin), v. 73, pp. 91–98.
- Darwin, C., 1859, *On the origin of species by means of natural selection*: Murray, London, 240 pp.
- Ellwood, J.W., Hildebrand, S.G., and Beauchamp, J.J., 1976, Contributions of gut contents to the concentration and body burden of elements in *Tipula* spp. from a spring-fed stream: *Journal of the Fisheries Research Board of Canada*, v. 33, pp. 1930–1938.
- Fängström, I., 1972, The effects of some chelating agents and their copper complexes on photosynthesis in *Scenedesmus quadricauda*: *Physiologia Plantarum*, v. 27, pp. 389–397.
- Filbrin, G.J., and Hough, R.A., 1979, The effects of excess copper sulphate on the metabolism of the duckweed *Lemna minor*: *Aquatic Botany*, v. 7, pp. 79–86.
- Foster, P.L., 1977, Copper exclusion as a mechanism of tolerance in a green alga: *Nature* (London), v. 269, pp. 322–323.
- Fryer, G., 1980, Acidity and species diversity in freshwater crustacean faunas: *Freshwater Biology*, v. 10, pp. 41–45.
- George, S.G., and Langston, W.J., 1994, Metallothionein as an indicator of water quality assessment of the bioavailability of cadmium, copper, mercury and zinc in aquatic animals at the cellular level; in Sutcliffe, D.W. (ed.), *Water Quality and Stress Indicators in Marine and Freshwater Systems—Linking Levels of Organization*: Freshwater Biological Association, Ambleside, pp. 138–153.
- Gibbs, P.E., and Bryan, G.W., 1986, Reproductive failure in populations of the dog-whelk, *Nucella lapillus*, caused by imposex induced by tributyltin from antifouling paints: *Journal of the Marine Biological Association of the U.K.*, v. 66, pp. 767–777.
- Gibbs, P.E., Bryan, G.W., Pascoe, P.L., and Burt, G.R., 1987, The use of the dog-whelk, *Nucella lapillus*, as an indicator of tributyltin (TBT) contamination: *Journal of the Marine Biological Association of the U.K.*, v. 67, pp. 507–523.
- Grime, J.P., 1989, The stress debate—symptoms of impending synthesis?: *Biological Journal of the Linnean Society*, v. 37, pp. 3–17.
- Gupta, A., Whitton, B.A., Morby, A.P., Huckle, J.W., Robinson, N.J., 1992, Amplification and rearrangement of a prokaryotic metallothionein locus *smt* in *Synechococcus* PC 6301 selected for tolerance to Cd: *Proceedings of the Royal Society of London Series B*, v. 248, pp. 273–281.
- Gupta, A., Morby, A.P., Turner, J.S., Whitton, B.A., and Robinson, N.J., 1993, Deletion within the metallothionein locus of Cd-tolerant *Synechococcus* PCC 6301 involving a highly iterated palindrome: *Molecular Microbiology*, v. 7, pp. 189–195.
- Hamer, D.H., 1986, Metallothionein: *Annual Review of Biochemistry*, v. 55, pp. 913–951.
- Harding, J.P.C., and Whitton, B.A., 1976, Resistance to zinc of *Stigeoclonium tenue* in the field and the laboratory: *British*

- Phycological Journal, v. 11, pp. 417–426.
- Harding, J.P.C., and Whitton, B.A., 1977, Environmental factors reducing the toxicity of Zn to *Stigeoclonium tenue*: British Phycological Journal, v. 12, pp. 17–21.
- Harrison, G.I., Campbell, P.G.C., and Tessier, A., 1986, Effects of pH changes on zinc uptake by *Chlamydomonas variabilis* grown in batch culture: Canadian Journal of Fisheries and Aquatic Science, v. 43, pp. 687–693.
- Hoffman, A.A., and Parsons, P.A., 1993, Evolutionary genetics and environmental stress: Oxford University Press, Oxford, 284 pp.
- Honma, Y., 1988, Dace (*Leuciscus* spp.) and other cyprinid fish as biological indicators of Hg pollution; in Yasuno, M., and Whitton, B.A. (eds.), Biological Monitors of Environmental Pollution: Tokai University Press, Tokai, pp. 49–84.
- Hubschman, J.H., 1967, Effects of copper on the crayfish *Orconectes rusticus*, II. Mode of toxic action: Crustaceana, v. 12, pp. 141–150.
- Hughes, G.M., 1988, Changes in blood of fish following exposure to heavy metals and acid; in Yasuno, M., and Whitton, B.A. (eds.), Biological Monitors of Environmental Pollution: Tokai University Press, Tokai, pp. 11–17.
- Hughes, G.M., and Tort, L., 1985, Cardio-respiratory responses of rainbow trout during recovery from zinc treatment: Environmental Pollution Series A, v. 37, pp. 255–266.
- Hutchinson, T.C., and Czyska, H., 1975, Heavy metal toxicity and synergism to floating aquatic plants: Verhandlungen, Internationale Vereinigung für Theoretische und Angewandte Limnologie, v. 19, pp. 2102–2111.
- Jackim, E., 1973, Influence of lead and other metals on fish alpha-aminolevulinic dehydrase activity: Journal of the Fisheries Research Board of Canada, v. 30, pp. 560–562.
- Jackson, P.P., Robinson, N.J., and Whitton, B.A., 1991, Low molecular weight metal complexes in the freshwater moss *Rhynchosstegium riparioides* exposed to elevated concentrations of Zn, Cu, Cd and Pb in the laboratory and field: Environmental and Experimental Botany, v. 31, pp. 359–366.
- Jardim, W.F., and Pearson, H.W., 1984, A study of the copper-complexing compounds released by some species of cyanobacteria: Water Research, v. 18, pp. 985–989.
- Jones, J.R.E., 1949, An ecological study of the River Rheidol, North Cardiganshire, Wales: Journal of Animal Ecology, v. 18, pp. 67–88.
- Kashyap, A.K., and Gupta, S.L., 1982, Effect of lethal copper concentrations on nitrate uptake, reduction and nitrate release in *Anacystis nidulans*: Zeitschrift für Pflanzenphysiologie, v. 107, pp. 289–294.
- Kelly, M.G., 1988, Mining and the freshwater environment: Elsevier Applied Science Publishers, London, 231 pp.
- Kelly, M.G., and Ali, A.D., 1993, The effect of organic pollution on algal communities in a tropical stream: Tropical Freshwater Biology, v. 3, pp. 353–370.
- Kelly, M.G., and Whitton, B.A., 1989a, Interspecific differences in Zn, Cd and Pb accumulation by freshwater algae and bryophytes: Hydrobiologia, v. 175, pp. 1–11.
- Kelly, M.G., and Whitton, B.A., 1989b, Relationship between accumulation and toxicity of zinc in *Stigeoclonium* (Chaetophorales, Chlorophyta): Phycologia v. 28, pp. 512–517.
- Klotz, R.L., 1981, Algal response to copper under riverine conditions: Environmental Pollution Series A, v. 24, pp. 1–19.
- Kuwabara, J.S., 1985, Phosphorus-zinc interactive effects on growth by *Selanastrum capricornutum* (Chlorophyceae) to copper: Environmental Science and Technology, v. 19, pp. 417–421.
- LaPerriere, J.D., Wagener, S.M., and Bjerklie, D.M., 1985, Gold mining effects on heavy metals in streams, Circle Quadrangle, Alaska: Water Resources Bulletin, v. 21, pp. 245–252.
- Laurén, D.J., and McDonald, D.G., 1986, Influence of water hardness, pH, and alkalinity on the mechanisms of copper toxicity in juvenile rainbow trout, *Salmo gairdneri*: Canadian Journal of Fisheries and Aquatic Science, v. 43, pp. 1488–1496.
- Laurén, D.J., and McDonald, D.G., 1987, Acclimation to copper by rainbow trout, *Salmo gairdneri*—physiology: Canadian Journal of Fisheries and Aquatic Science, v. 44, pp. 99–104.
- Leland, H.V., and Carter, J.J., 1984, Effects of copper on species composition of periphyton in a Sierra Nevada, California, stream: Freshwater Biology, v. 14, pp. 281–296.
- Livett, E.A., Lee, J.A., and Tallis, J.H., 1979, Lead, zinc and copper analyses of British blanket peats: Journal of Ecology, v. 67, pp. 865–891.
- Mance, G., 1987, Pollution threat of heavy metals in the aquatic environment: Elsevier Applied Science Publishers, London, 372 pp.
- McMurtry, M.J., 1984, Avoidance of sublethal doses of copper and zinc by tubificid oligochaetes: Journal of Great Lakes Research, v. 10, pp. 267–272.
- Moore, J.W., and Ramamoorthy, S., 1984, Heavy metals in natural waters—Applied monitoring and impact assessment: Springer-Verlag, New York, 268 pp.
- Murphy, B.R., Atchinson, G.J., and McIntosh, A.W., 1978, Cd and Zn in muscle of bluegill (*Lepomis macrochirus*) and largemouth Bass (*Micropterus salmoides*) from an industrially contaminated lake: Environmental Pollution, v. 17, pp. 253–257.
- Nasu, Y., Kugimoto, M., Tanaka, O., and Takimoto, A., 1984, *Lemna* as an indicator of water pollution and the absorption of heavy metals by *Lemna*; in Pascoe, D., and Edwards, R.W. (eds.), Freshwater Biological Monitoring: Pergamon Press, Oxford, pp. 113–120.
- Nicola Giudici, M., Migliore, L., and Guarino, S.M., 1987, Sensitivity of *Asellus aquaticus* (L.) and *Proasellus coxalis* Dollf. (Crustacea, Isopoda) to copper: Hydrobiologia, v. 146, pp. 63–69.
- Nieboer, E., and Richardson, D.H.S., 1980, The replacement of the non-descript term ‘heavy metals’ by a biologically and chemically significant classification of metal ions: Environmental Pollution Series B, v. 1, pp. 3–26.
- Passow, H., Rothstein, A., and Clarkson, T.W., 1961, The general pharmacology of heavy metals: Pharmacological Review, v. 13, pp. 18–25.
- Patterson, G., and Whitton, B.A., 1981, Chemistry of waters, sediments and algal filaments in groundwater draining an old lead-zinc mine; in Say, P.J., and Whitton, B.A. (eds.), Heavy Metals in Northern England—Environmental and Biological Aspects: Department of Botany, Univ. of Durham, pp. 65–81.
- Petersen, R., 1982, Influence of copper and zinc on the growth of a freshwater alga, *Scenedesmus quadricauda*—the significance of chemical speciation: Environmental Science and Technology, v. 16, pp. 443–447.
- Peterson, H.G., and Healy, F.P., 1985, Comparative pH dependent metal inhibition of nutrient uptake by *Scenedesmus quadricauda* (Chlorophyceae): Journal of Phycology, v. 21, pp. 217–222.
- Rabe, R., Schuster, H., and Kohler, A., 1982, Effects of copper chelate on photosynthesis and some enzyme activities of *Elodea canadensis*: Aquatic Botany, v. 14, pp. 167–175.
- Rainbow, P.S., and Moore, P.G., 1986, Comparative metal analyses in amphipod crustaceans: Hydrobiologia, v. 141, pp. 273–289.
- Robinson, N.J., Tommey, A.M., Kuske, C., and Jackson, P.J., 1993, Plant metallothioneins: Biochemical Journal, v. 295, pp. 1–10.
- Roch, M., and McCarter, J.A., 1984, Metallothionein induction, growth and survival of chinook salmon exposed to zinc, copper, and cadmium: Bulletin of Environmental Contamination and Toxicology, v. 32, pp. 478–485.
- Roch, M., Noonan, P., and McCarter, J.A., 1986, Determination of no effect levels of heavy metals for rainbow trout using hepatic metallothionein: Water Research, v. 20, pp. 771–774.
- Satake, K., Shimizu, H., and Nishikawa, M., 1984, Elemental composition of the aquatic liverwort *Jungermannia vulcanicola* Steph. in acid streams: Journal of the Hattori Botanical Laboratory, v. 56, pp. 241–248.
- Say, P.J., and Whitton, B.A., 1977, Influence of zinc on lotic plants, II. Environmental effects of toxicity of Zn to *Hormidium rivulare*: Freshwater Biology, v. 7, pp. 377–384.
- Say, P.J., Diaz, B.M., and Whitton, B.A., 1977, Influence of zinc on lotic plants, I. Tolerance of *Hormidium* species to zinc: Freshwater Biology, v. 7, pp. 357–376.
- Schreinemakers, W.A.C., and Dorhout, R., 1985, Effects of copper ions on

- growth and ion absorption by *Spirodela polyrrhiza* (L.) Schleiden: *Journal of Plant Physiology*, v. 121, pp. 343–351.
- Segner, H., 1987, Response of fed and starved roach, *Rutilus rutilus*, to sublethal copper contamination: *Journal of Fish Biology*, v. 10, pp. 141–162.
- Sehgal, R., and Saxena, A.B., 1986, Toxicity of zinc to a viviparous fish, *Lebistes reticulatus* (Peters): *Bulletin of Environmental Contamination and Toxicology*, v. 36, pp. 888–894.
- Shehata, F.H.A., and Whitton, B.A., 1982, Zinc tolerance in strains of the blue green alga *Anacystis nidulans*: *British Phycological Journal*, v. 17, pp. 5–12.
- Sibley, R.M., and Calow, P., 1989, A life-cycle theory of responses to stress: *Biological Journal of the Linnaean Society*, v. 37, pp. 101–116.
- Singh, S.P., and Yadava, V., 1986, Cadmium tolerance in the cyanobacterium *Anacystis nidulans*: *Biologisches Zentralblatt*, v. 105, pp. 539–542.
- Smock, L.A., 1983a, Relationships between metal concentrations and organism size in aquatic insects: *Freshwater Biology*, v. 13, pp. 313–321.
- Smock, L.A., 1983b, The influence of feeding habits on whole-body metal concentrations in aquatic insects: *Freshwater Biology*, v. 13, pp. 301–311.
- Starodub, M.E., Wong, P.T.S., Mayfield, C.I., and Chau, Y.K., 1987, Influence of complexation and pH on individual and combined heavy metal toxicity to a freshwater green alga: *Canadian Journal of Fisheries and Aquatic Science*, v. 44, pp. 1173–1180.
- Stokes, P.M., 1975, Adaptation of green algae to high levels of copper and nickel in aquatic environments; in Hutchinson, T.C. (ed.), *Symposium Proceedings of the Internatl Conference on Heavy Metals in the Environment Vol. II Part I. Pathways and Cycling*: Toronto, Canada, pp. 137–154.
- Stokes, P.M., 1983, Responses of freshwater algae to metals; in Round, F.E., and Chapman, D.J. (eds.), *Progress in Phycological Research II*, Elsevier, Amsterdam, pp. 87–112.
- Stumm, W., and Morgan, J.J., 1981, *Aquatic chemistry—An introduction emphasizing chemical equilibria in natural waters*: 2nd ed., Wiley-Interscience, New York, 780 pp.
- Tewari, H., Gill, T.S., and Pant, J., 1987, Impact of chronic lead poisoning on the haematological and biochemical profiles of a fish, *Barbus conchoniis*: *Bulletin of Environmental Contamination and Toxicology*, v. 38, pp. 748–752.
- Thompson, K.W., Hendricks, A.C., and Cairns, J., 1980, Acute toxicity of zinc and copper singly and in combination to the Bluegill (*Lepomis macrochirus*): *Bulletin of Environmental Contamination and Toxicology*, v. 25, pp. 122–129.
- Thorp, V.J., and Lake, P.S., 1973, Pollution of a Tasmanian river by mine effluents, II. Distribution of macroinvertebrates: *Internationale Revue der Gesamten Hydrobiologie*, v. 58, pp. 885–892.
- Turner, J.S., Morby, A.P., Whitton, B.A., Gupta, A., and Robinson, N.J., 1993, Construction of Zn²⁺/Cd²⁺ hypersensitive cyanobacterial mutants lacking a functional metallothionein locus: *Journal of Biological Chemistry*, v. 268, pp. 4494–4498.
- Van Nieuwenhuysse, E.E., and LaPerriere, J.D., 1986, Effects of placer gold mining on primary production in subarctic streams in Alaska: *Water Resources Bulletin*, v. 22, pp. 91–99.
- Watton, A.J., and Hawkes, H.A., 1984, The acute toxicity of ammonia and copper to the gastropod *Potamopyrgus jenkinsi* (Smith): *Environmental Pollution Series A*, v. 36, pp. 17–29.
- Wehr, J.D., and Whitton, B.A., 1983, Accumulation of heavy metals by aquatic mosses. 2. *Rhynchostegium riparioides*: *Hydrobiologia*, v. 100, pp. 261–284.
- Wehr, J.D., Kelly, M.G., and Whitton, B.A., 1987, Factors affecting accumulation and loss of zinc by the aquatic moss *Rhynchostegium riparioides*: *Aquatic Botany*, v. 29, pp. 261–274.
- Welsh, R.P.H., and Denny, P., 1979, The translocation of lead and copper in two submerged angiosperm species: *Journal of Experimental Botany*, v. 30, pp. 339–345.
- Whitton, B.A., 1980, Zinc and plants in rivers and streams; in Nriagu, J.O. (ed.), *Zinc in the Environment Part II—Health Effects*: Wiley-Interscience, New York, pp. 363–400.
- Whitton, B.A., and Diaz, B.M., 1980, Chemistry and plants of streams and rivers with elevated Zn: *Trace Substances in Environmental Health - XIV*, Univ. of Missouri, Columbia, pp. 457–463.
- Whitton, B.A., Gale, N.L., and Wixson, B.G., 1981, Chemistry and plant ecology of zinc-rich wastes dominated by blue-green algae: *Hydrobiologia*, v. 83, pp. 331–341.
- Whitton, B.A., Burrows, I.G., and Kelly, M.G., 1989, Use of *Cladophora glomerata* to monitor heavy metals in rivers: *Journal of Applied Phycology*, v. 1, pp. 293–299.
- Winner, R.W., 1984, The toxicity and bioaccumulation of cadmium and copper as affected by humic acid: *Aquatic Toxicology*, v. 5, pp. 267–274.
- Winner, R.W., and Gauss, J.D., 1986, Relationship between chronic toxicity and bioaccumulation of copper, cadmium and zinc as affected by water hardness and humic acid: *Aquatic Toxicology*, v. 8, pp. 149–161.
- Wong, S.L., and Beaver, J.L., 1981, Metal interactions in algal toxicology, conventional versus in vivo tests: *Hydrobiologia*, v. 85, pp. 65–71.

Chapter 19

GEOLOGIC CONTROLS ON THE COMPOSITION OF NATURAL WATERS AND MINE WATERS DRAINING DIVERSE MINERAL-DEPOSIT TYPES

G.S. Plumlee,¹ K.S. Smith,¹ M.R. Montour,¹ W.H. Ficklin,² and E.L. Mosier³

¹*U.S. Geological Survey, Box 25046, MS 973, Federal Center, Denver, CO 80225-0046*

²*Deceased;* ³*Retired*

INTRODUCTION

Sulfide-bearing mineral deposits formed in reduced conditions out of contact with an oxygenated atmosphere. When sulfides in the deposits are exposed by natural erosion or by mining to atmospheric oxygen and water, weathering of the sulfides can produce natural or mining-related acid-rock drainage. The prediction of water quality that results from mining and mineral processing activities has therefore become a high priority in the permitting of mining activities worldwide, in order to prevent the formation of or mitigate the environmental effects of deleterious drainage waters. In addition, estimating the compositions of natural waters that drained mineral deposits prior to mining is crucial to establish appropriate baseline environmental standards at mine sites.

There are a variety of techniques currently in use to predict the acidity or metal content of mine-drainage waters, most common of which are static and kinetic testing procedures. In static procedures such as acid-base accounting (White et al., 1997, 1999), the contents of acid-generating sulfide minerals from ores and wastes from a proposed mine are measured and balanced against the measured contents of acid-consuming minerals such as carbonates; based on this balance, the materials are determined to be acid generating or non-acid-generating. In kinetic tests such as column or humidity-cell tests (ASTM, 1996), samples of ores and wastes are allowed to react over a period of time under laboratory conditions with oxidized waters or moist air, and the pH and metal contents of the resulting leachates are then measured.

Although both static and kinetic methods are widely used to help predict the compositions of mine waters, they have several potential limitations. Most important of these are (1) whether the samples used in the tests adequately represent the range of mineralogic characteristics commonly present in complex mineral deposits, (2) whether the time scale and laboratory conditions of kinetic tests adequately reproduce the time scales and physical, geochemical, and biological conditions actually present in the mine, mine dump, or tailings impoundment environment, and (3) whether kinetic test leachate compositions accurately reproduce actual drainage quality.

Another approach to mine-drainage prediction that can be used to supplement the static and kinetic engineering tests is one in which the compositions of existing mine waters draining geologically similar deposit types in similar climates are measured empirically and then interpreted in a geologic and geochemical context. By evaluating the compositions of waters draining geologically comparable deposits in comparable climates, it is possible to place constraints on the potential ranges in composition of

waters that might result from the development of a particular ore deposit. Such empirical examinations of existing drainage waters help overcome the issues of sample representation, adequacy of time scales, and accuracy of reproduction of natural conditions by laboratory experiments—the waters already are draining larger, more representative volumes of rock, and they are generated under field conditions and time scales.

Past studies that demonstrated the importance of geologic controls on mine-drainage compositions include those of Wildeman et al. (1974) in the Central City mining district, Colorado, and those of Wai et al. (1980) in the Bunker Hill mine, Coeur d'Alene district, Idaho. Results of both these studies showed that drainage compositions vary predictably within a mine (Wai et al., 1980) and across a district (Wildeman et al., 1974) as a function of deposit geology. However, in the time since these studies were carried out and prior to the early 1990s, a systematic examination of mine-drainage compositions across a spectrum of mineral deposit types, and within different ore types of given deposit types was generally lacking. Since the early 1990s, a number of studies have begun to examine both natural- and mine-drainage water compositions in the context of mineral-deposit geology (Ficklin et al., 1992; Plumlee et al., 1992, 1993a, b; Runnells et al., 1992; Smith et al., 1994; Price et al., 1995; studies in du Bray, 1995; Goldfarb et al., 1996, 1997; Eppinger et al., 1997; Kelley and Taylor, 1997).

This paper summarizes results to date of an ongoing empirical study examining the composition of mine waters and natural waters draining a broad spectrum of mineral deposit types, mineralogic zones within deposit types, and geologically similar mineral deposit types in different climates (Ficklin et al., 1992; Plumlee et al., 1992, 1993a; Smith et al., 1994). We include in this study data that we have collected and data compiled from the literature.

The results to date of this empirical study illustrate the many fundamental controls that mineral-deposit geology exerts, in combination with geochemical processes and biogeochemical processes, on the compositions of mine-drainage waters and natural waters draining unmined mineral deposits. Other important controls, such as climate, mining method used, and mineral processing method used, modify the effects mandated by deposit geology, geochemical, and biogeochemical processes. Our results show that, by interpreting empirical drainage data in a geologic context, it is possible to constrain the potential ranges in pH and ranges in metal concentrations of mine- and natural-drainage waters that may develop within different mineralogic zones, ore types, or alteration types in a given mineral deposit. Our results are not sufficiently precise that they can be used to quantitatively predict the exact compositions of water that will develop in a particular mine,

mine dump, or tailings impoundment at a particular mineral deposit. Instead, the predictive capabilities provided by such an empirical approach should be only part of a comprehensive risk-based approach to environmentally responsible mineral-resource development employed by industry and regulators alike.

For general references on the geology of mineral deposits, the reader is referred to economic geology textbooks such as Guilbert and Park (1986), and to other compilations such as Cox and Singer (1986), Kirkham et al. (1993), du Bray (1995), and references contained therein. For a summary of the environmental geology characteristics of mineral deposits, see Plumlee (1999) and references therein.

SUMMARY OF DATA AND METHODS

Data on the compositions of mine- and natural-drainage water samples determined in this study and gathered from the literature are summarized by mineral-deposit type in the Appendix, and depicted graphically on Figure 19.1.

For the samples collected in this study, a detailed summary of the field sampling protocols is presented by Ficklin and Mosier (1999). For samples summarized from the literature, we primarily included in the Appendix data for samples that had been collected using generally similar methodologies to those we used. The pH values listed in the Appendix are field pH values, due to the potentially large shifts in pH that can occur between field collection and lab analysis. For chemical constituents, the Appendix generally lists samples that were filtered to at least 0.45 μm (and for some samples, to 0.1 μm) prior to chemical analysis. Based on results of sampling done early in this study (Smith et al., 1992) we concluded that, for most mine-drainage samples, the analytical results varied little between samples filtered to 0.45 μm and those filtered to 0.1 μm ; hence, the inclusion of samples in the Appendix having different filter sizes imparts relatively little in the way of overall interpretational uncertainty.

Information on water types is also included in the Appendix. In compiling these data, we focused wherever possible on waters collected at adit openings, springs, open pit lakes, etc., in order not to introduce downstream or down-gradient compositional modifications such as dilution or oxidation. This way, we could examine as closely as possible the effects of deposit geology on drainage composition.

For a summary of environmental water analysis methods, the reader is referred to Crock et al. (1999). For nearly all samples included in the Appendix, ion chromatography was used to determine the concentration of sulfate and (where done) other anions. For cations and trace metals, the data in the Appendix reflect a variety of methods, including flame and (or) graphite furnace atomic absorption spectrophotometry (AA), inductively coupled-plasma atomic emission spectroscopy (ICP-AES), and inductively coupled-plasma mass spectrometry (ICP-MS). Based on the results of data collected in our study, we have found general reproducibility (to within approximately ± 10 –25%) between the different analytical methods we used (K. Smith, G. Plumlee, unpub. data).

Another challenge in interpreting data collected by multiple studies is presented by the concentration units used by the different studies. For the data we collected as part of this study, sulfate, fluoride, chloride, alkalinity, and ferrous iron concentrations were determined in mg/l concentration units; all other major cations,

trace metals, and metalloids were measured in parts per million (ppm) or parts per billion (ppb) units. In contrast, the concentrations of major cations, trace metals and metalloids were measured in some other studies (such as Alpers and Nordstrom, 1991) on a volume basis and presented in mg/l or $\mu\text{g/l}$ units; we have noted in the Appendix all samples measured in these units. For the graphically-based interpretations used in this study (such as Fig. 19.1), we have assumed that mg/l units are equivalent to ppm, and that $\mu\text{g/l}$ units are equivalent to ppb. Although this assumption is appropriate for relatively dilute waters, it becomes less so for the more concentrated waters such as those from Summitville, Colorado or Iron Mountain, California (Alpers and Nordstrom, 1991). However, given the log scale used in all of the plots, the uncertainties introduced by our assumption does not make a substantial difference in our results or interpretation. Nonetheless, given the potential uncertainties introduced by differences in analytical methodologies and concentration units, we will restrict our interpretation of compositional differences between samples to the $\pm 50\%$ level.

The data on both mine-drainage and natural-drainage waters compiled to date span a broad range of pH values (from less than zero to greater than 8) and a broad range in content of a variety of dissolved metals and other species (depending upon the element, levels from $< 1 \mu\text{g/l}$ to tens of thousands of mg/l; Fig. 19.1). In order to help interpret variations in drainage water chemistry between different deposit types, we have developed a classification scheme based on the pH and the sum of the base metals Zn, Cu, Pb, Cd, Co, and Ni (Fig. 19.2; Plumlee et al., 1992). Although Fe, Al, and Mn are typically the most abundant metals in the majority of mine- and natural-drainage waters, differences in the sum of base metals allow us to differentiate between different geologic controls on water composition that we would otherwise not be able to differentiate on the basis of concentrational variations in Fe, Al, or major cations. We have termed such plots Ficklin diagrams in honor of our late colleague, Walter Ficklin. As can be seen from the plots on Figures 19.1 and 19.2: acid-rock drainage can be entirely natural and not related to mining activities; not all natural or mining-related rock drainage is acidic; and not all natural- or mine-drainage waters must be acidic to transport significant quantities of some dissolved metals.

SUMMARY OF IMPORTANT CONTROLS ON DRAINAGE COMPOSITION

Geochemical and biogeochemical controls

In order to understand the controls of mineral-deposit geology on drainage composition, it is first necessary to discuss briefly the geochemical and biogeochemical processes that generate and neutralize acid drainage (summarized by Nordstrom and Alpers, 1999, and references therein). Microbially mediated pyrite oxidation is generally the initial step in the process, and results in the formation of sulfuric acid and ferrous iron. At pH values greater than approximately 6, ferrous iron oxidizes very rapidly to ferric iron; at lower pH values, bacterial catalysis is required for this reaction to proceed. If the waters move out of contact with atmospheric oxygen or oxygenated ground waters, then the bacterial oxidation of iron can still occur only as long as limited concentrations of dissolved oxygen remain in the waters. Ferric iron is a very effective oxidant, and when it reacts with iron sulfides and a

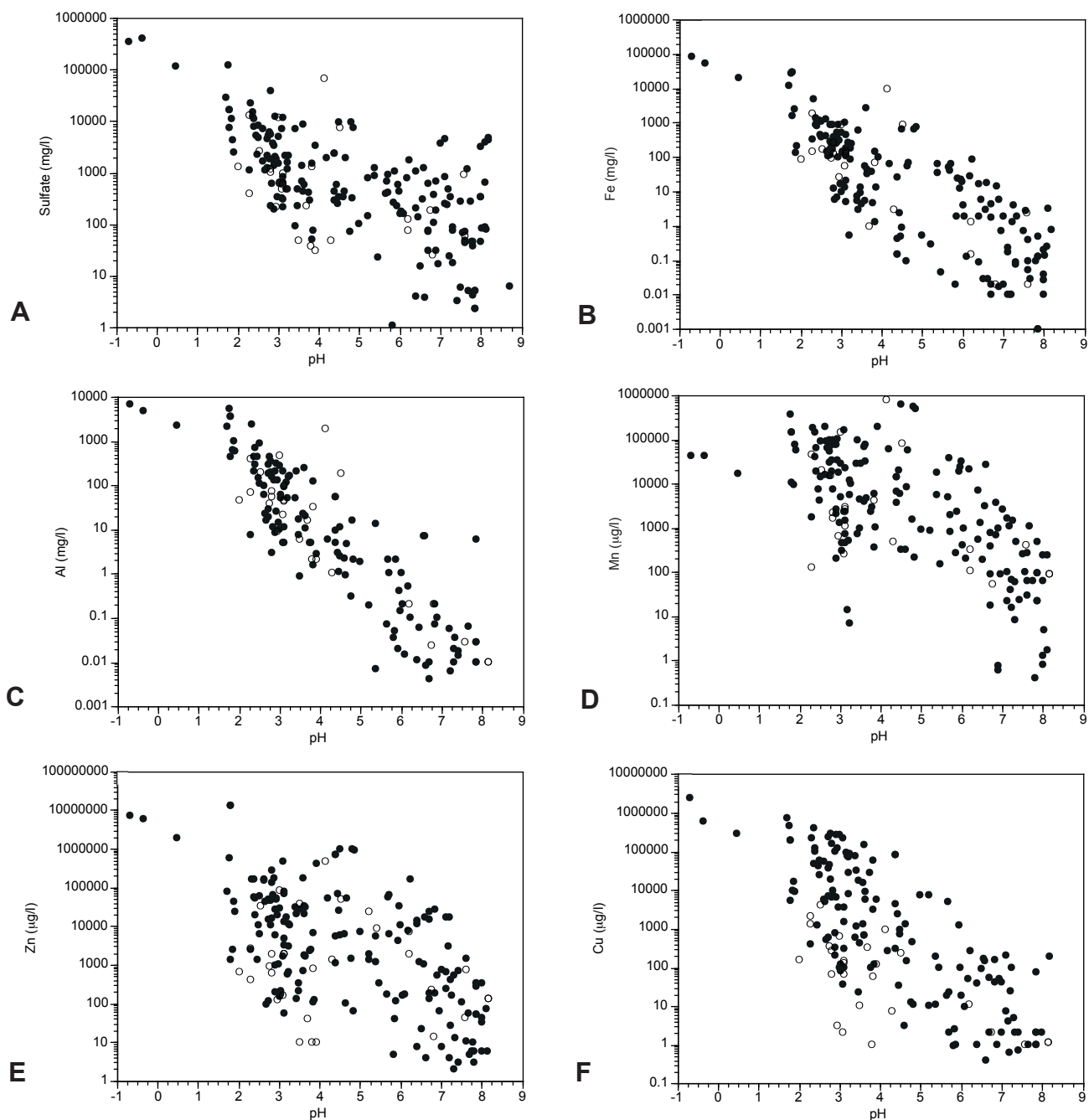


FIGURE 19.1—Plots of dissolved species concentrations of mine-drainage waters (solid circles) and natural waters draining unmineralized areas (open circles) as a function of pH. Data used to construct the plots are summarized in the Appendix. For the metal-pH plots, and all subsequent plots in this paper showing metal concentrations, we assume that ppm and mg/l concentration units are equivalent, and that ppb and $\mu\text{g/l}$ concentration units are equivalent; see Summary of Data and Methods section for discussion. A. Sulfate; B. Total iron; C. Aluminum; D. Manganese; E. Zinc; F. Copper. Note differences in scale of the concentration axis between the plots.

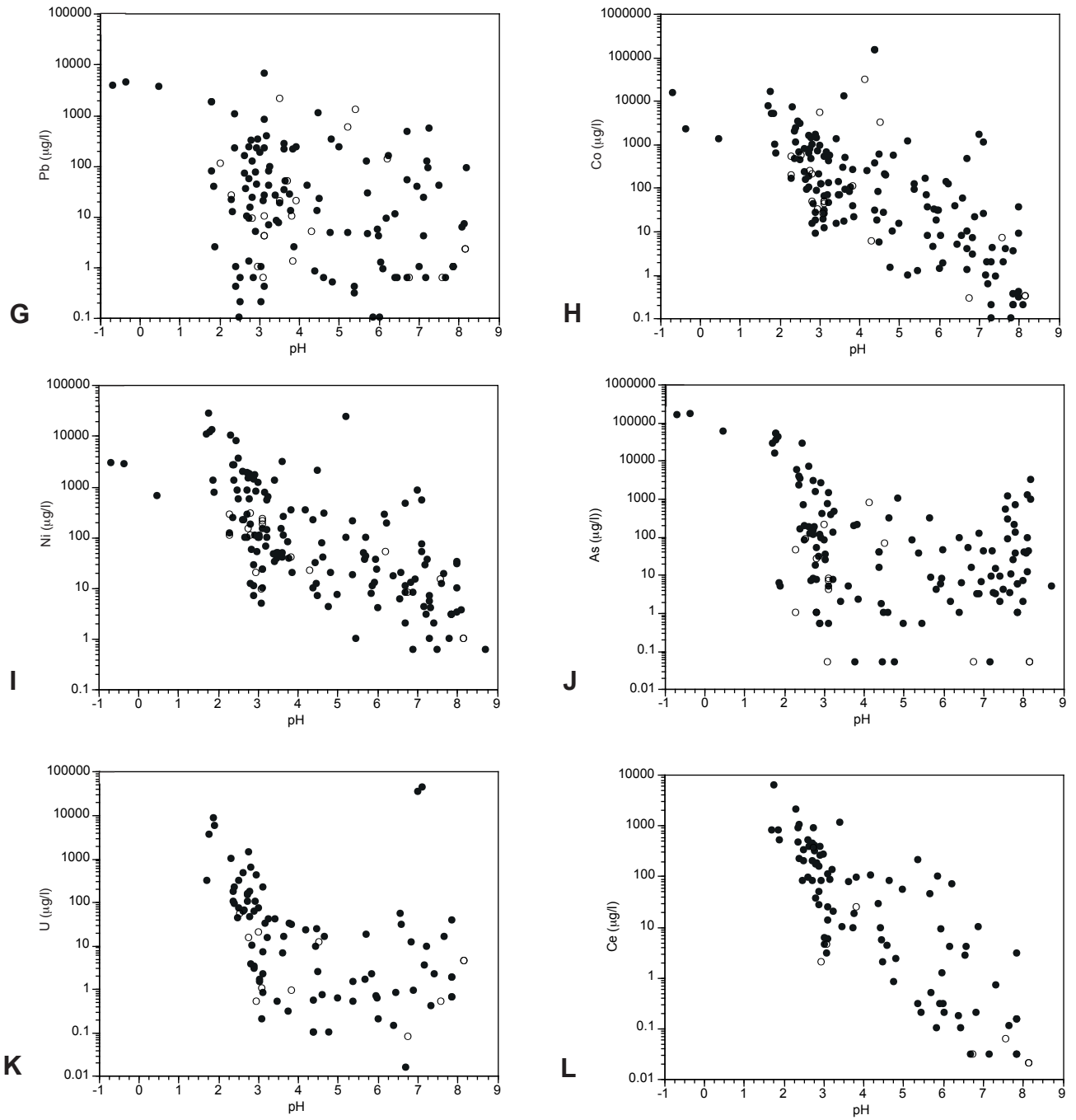


FIGURE 19.1 Continued—Plots of dissolved species concentrations of mine-drainage waters (solid circles) and natural waters draining unmined mineralized areas (open circles) as a function of pH. Data used to construct the plots are summarized in the Appendix. G. Lead; H. Cobalt; I. Nickel; J. Arsenic; K. Uranium; L. Cerium.

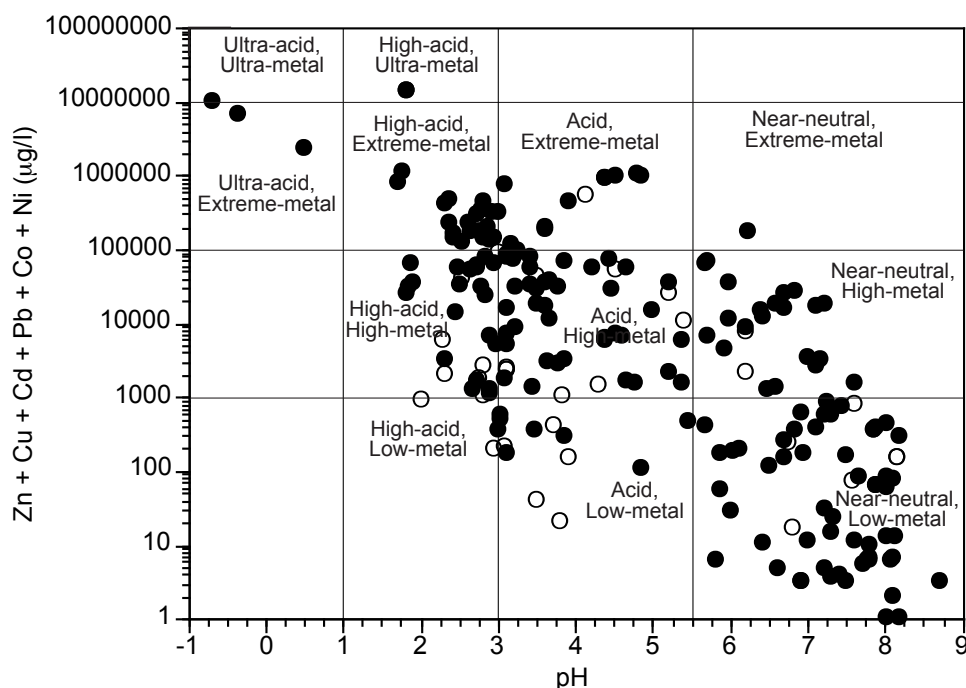


FIGURE 19.2—Ficklin diagram showing the sum of dissolved base metals Zn, Cu, Cd, Pb, Co, and Ni in mine (closed circle) and natural (open circle) waters draining diverse mineral-deposit types. The boundaries and names of metal bins were originally proposed by Plumlee et al. (1992) to help classify different drainage compositions. For the plot, we assume that that ppb and µg/l concentration units are equivalent; see discussion in Summary of Data and Methods section.

variety of other sulfides, it can generate significant quantities of acid plus reduced iron, which is then reoxidized by bacterial catalysis. Metal sulfides with a metal:sulfur ratio ≤ 1 (such as galena, sphalerite, and covellite) do not generate acid when they are oxidized by atmospheric oxygen, but do when they are oxidized by ferric iron (Smith et al., 1994; Nordstrom and Alpers, 1999; Plumlee, 1999).

Once acid drainage waters form, there are a variety of processes that affect their compositions. The acid waters can react with carbonate or some aluminosilicate minerals in the deposit or its host rocks, which can shift pH to less acidic values. Typically, calcite and aragonite are the most reactive carbonate minerals, and therefore are most effective at consuming acid. Other carbonates such as rhodochrosite, dolomite, and magnesite are much less reactive, as are most aluminosilicates, and therefore are much less effective at neutralizing acid in drainage waters. If the waters move out of contact with atmospheric oxygen, they can build up elevated levels of ferrous iron; when they reach the ground surface again, oxidation of the ferrous iron to ferric iron will result.

Saturation with various amorphous or crystalline phases can limit concentrations of some major constituents in the drainage waters. Studies of diverse mine drainages (see Nordstrom and Alpers, 1999) have shown that, at pH values above approximately 2–3, ferric iron concentrations are restricted by the formation of poorly crystalline to amorphous iron phases such as ferrihydrite (a hydrous ferric oxide), jarosite (a potassium-iron hydroxysulfate), or schwertmannite (a ferric hydroxysulfate) (Nordstrom and Alpers, 1999; Smith, 1999); these are the orange to yellow to brown precipitates that commonly line mine-drainage stream beds. Similarly, studies have shown that, at pH values above

4.5–5, aluminum concentrations are limited by the formation of aluminum oxyhydroxysulfates such as basaluminite (Nordstrom and Alpers, 1999); these minerals (typically seen as white coatings on stream beds) most commonly precipitate via pH increases resulting from dilution by non-acidic ground or surface waters. At pH values greater than 5, dissolved ferric iron concentrations are held at very low levels by the ferric phases mentioned previously. However, in less acidic to near-neutral pH waters with low dissolved oxygen, ferrous iron can reach relatively high levels in solution; when the waters come into contact with the atmosphere, the ferrous iron oxidizes rapidly to ferric iron, leading to the precipitation of one of the ferric phases mentioned previously. Hydrous manganese oxide minerals tend to form at quite high pH values (typically > 8); however, bacterial mediation can lead to precipitation of manganese phases at pH values below 6–7. Precipitation of hydrous oxide minerals in mine-drainage streams produces hydrogen ions as a result of metal hydrolysis reactions (Garrels and Christ, 1965; Nordstrom and Alpers, 1999). As a result pH decreases of as much as several pH units downstream from springs or adits can be quite common. Hence, mine- and natural-drainage waters can have near-neutral pH values but can still generate acid once they are liberated into the environment.

Chemical speciation programs such as WATEQ4F (Ball and Nordstrom, 1991; summary in Alpers and Nordstrom, 1999) can be used to calculate mineral saturation indices, which can be used to help constrain the mineral phases that may be controlling drainage compositions. Waters have a thermodynamic tendency to precipitate phases with calculated saturation indices greater than 0, and a thermodynamic tendency to dissolve phases with calculated saturation indices less than 0. Other factors, such as kinetics, or the

presence or absence of the mineral in contact with the water will also influence whether a mineral dissolves or precipitates. We used WATEQ4F to calculate the chemical speciation and solid-phase saturation indices of a number of drainage compositions (see Appendix) spanning much of the spectrum of pH values shown on Figures 19.1 and 19.2; some results of these calculations are shown on Figure 19.3. All but the highest-pH waters (from the Carlton Tunnel, pH 7.7; see Appendix) are calculated to be near saturation or supersaturated with one or more of the jarosite solid-solution end members, indicating that jarosite may be an important phase influencing iron concentrations in these waters. Ferrihydrite, in contrast, is undersaturated in the most acidic waters, suggesting that it is not influencing ferric iron concentrations at pH values below approximately 3–4. All but the Carlton Tunnel waters are very close to saturation with jurbanite (Fig. 19.3), an aluminum hydroxysulfate; these calculations suggest that aluminum concentrations in solution may be influenced by aluminum-bearing phases at pH values even lower than 4.5–5, as is commonly presumed (Filipek et al., 1987; Nordstrom and Alpers, 1999). Silica concentrations are likely to be limited by one of the silica phases, although the calculated saturation indices indicate that the concentration-limiting phase may change with pH (Fig. 19.3). Although not shown on Figure 19.3, the calculations indicate that at least some drainage waters with pH values greater than 6 are calculated to be near saturation or supersaturated with rhodochrosite (the calculations assume that concentrations of dissolved Mn^{2+} and Mn^{3+} are in equilibrium with measured dissolved oxygen concentrations). In addition, the Carlton Tunnel waters are calculated to be near saturation with a variety of aluminosilicate phases such as zeolites or feldspars. Carbonates such as calcite, aragonite, or rhodochrosite may play a role in influencing water compositions; however, zeolites and feldspars are unlikely to influence solution compositions in higher-pH drainage waters (D.K. Nordstrom, written commun., 1998).

The concentrations of metals such as lead, copper, zinc, cadmium, and nickel, and metalloids such as arsenic are variably controlled by aqueous complexation (Fig. 19.4), coupled with sorption onto particulates (most commonly the hydrous ferric or hydrous aluminum oxides; Smith, 1999). In the acidic drainage waters, the speciation calculations indicate most metals occur as the simple metal ions or as sulfate complexes (Fig. 19.4). In near-neutral pH waters, carbonate and hydroxide metal complexes are calculated to become more important than the metal ions or sulfate complexes. Precipitation of carbonate minerals such as cerussite (Pb) and smithsonite (Zn), or malachite and azurite (hydrous Cu-carbonates) may limit concentrations of these metals in near-neutral to alkaline waters. Arsenic and some metals such as molybdenum are commonly present as oxyanion species.

The extent of sorption onto particulates is a function of the pH of the waters, the particular metal, the concentrations of aqueous complexing agents (which compete for the metals with the sorption sites on the particulates), and the concentrations of the metals relative to the amounts of particulates. Smith et al. (1992, 1993) demonstrated that sorption is largely mediated by particulates suspended in the water column, and not by bed sediments. In general, the effectiveness of sorption with increasing pH is $As > Pb > Cu > Zn > Cd, Ni$ (Fig. 19.5). Arsenic and lead are most effectively sorbed at quite acidic pH values (in addition to Fig. 19.5, note the precipitous drop in arsenic in all drainages at pH 2–3 shown on Fig. 19.1J), whereas Zn, Cd, and Ni are partially to minimally sorbed only at near-neutral pH values in waters with small to moderate amounts of suspended particulates. Some ele-

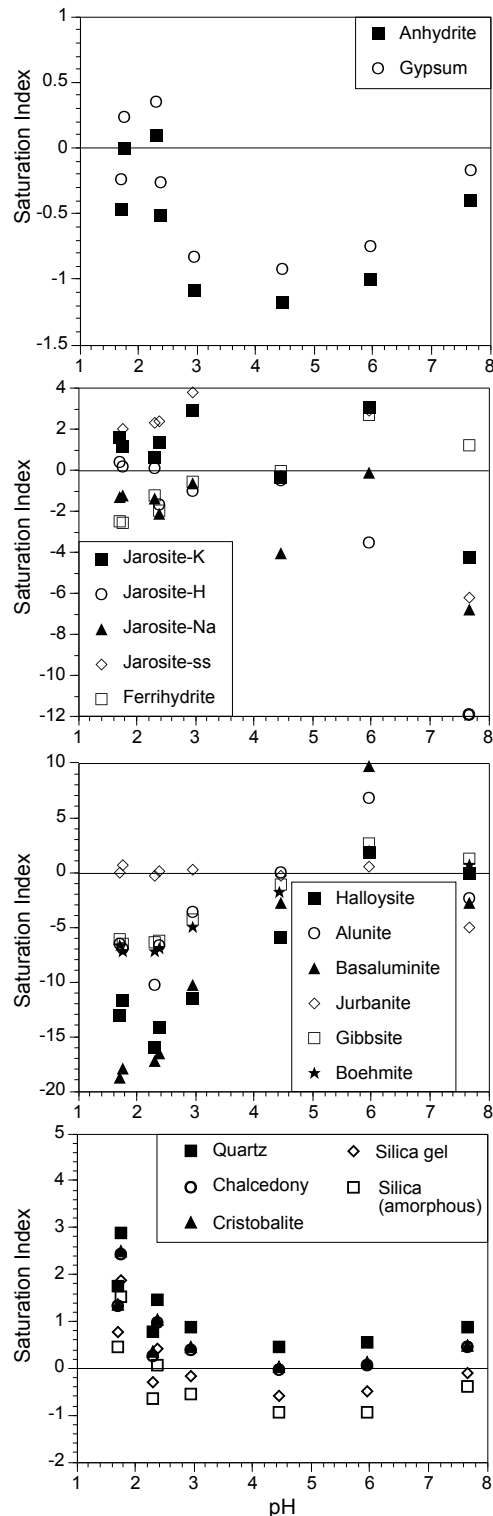


FIGURE 19.3—Calculated saturation indices for various Colorado mine-drainage waters sampled as part of this study. Samples include, in order of increasing pH: Blackstrap, Son-of-Blackstrap, Reynolds adit, Chandler Adit (all from Summitville); Yak Tunnel (Leadville); Bandora (Silverton); and Carlton Tunnel (Cripple Creek). See sample descriptions in the Appendix for the mineral deposits drained by these waters.

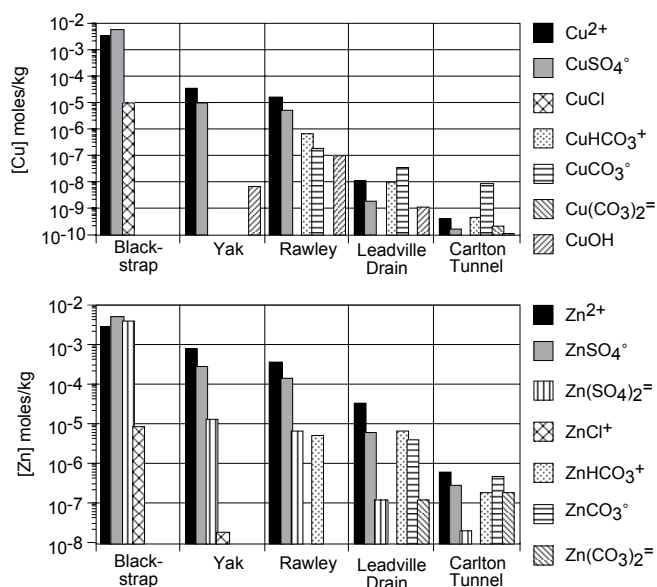


FIGURE 19.4—Calculated concentrations (using WATEQ4F) of copper (upper) and zinc (lower) complexes for several Colorado mine-drainage waters sampled as part of this study (Appendix). pH values increase from left to right: Blackstrap—pH 1.8; Yak—4.4; Rawley—6.0; Leadville Drain—pH 7.2; Carlton—pH 7.7.

ments such as As, and Mo tend to desorb at near-neutral or higher pH values due to their presence as oxyanions, although As desorption in higher-pH drainage waters is not observed in the samples shown on Figure 19.5, it is indicated by the elevated dissolved As concentrations in samples with pH values greater than ~ 7 shown on Figure 19.1. Metals such as U, Cu, and Pb also tend to desorb at near-neutral or higher pH values due to increased competition from complexing agents such as aqueous carbonates, which help keep the elements in solution. For example, the spread of Pb concentrations with increasing pH shown on Figure 19.1G and the increase in U concentrations with increasing pH above 5–6 (Fig. 19.1K) likely reflect desorption due to lack of particulates or increased competition from complexing agents.

Other geochemical processes that affect drainage composition include evaporation and, should sufficient evaporation occur, precipitation of secondary sulfate salts (Nordstrom and Alpers, 1999). Evaporation can be important in open-pit mines, mine dumps, tailings, and underground mine workings. It can lead to increased metal concentrations and, in acid waters, decreased pH. Secondary salts that form from evaporation (Nordstrom and Alpers, 1999) are typically soluble hydrous sulfates of a variety of metals, including iron (melanterite, römerite, and rhomboclase), aluminum (halotrichite), calcium (gypsum), magnesium (pickeringite), copper (chalcantite, brochantite), and zinc (goslarite). A variety of salts can also form directly on sulfides in mine workings and mine dumps through the attack of humid air on the sulfides. No matter how they form, these metal salts can store acid and metals in the solid form, and dissolve readily during the next wet period such as snow-melt or rainstorm runoff.

Geologic controls

When grouped according to the geologic characteristics of the deposits they drain, the water compositions depicted on Figures 19.1 and 19.2 generally span a much smaller range of pH values and metal contents (Fig. 19.6). As will be demonstrated in the discussions that follow, there are a variety of geological features of mineral deposits that control the composition of natural- and mine-drainage waters, including: the content of acid-generating pyrite and other iron sulfides; the content of sulfides other than iron sulfides; the content of carbonates and other acid-consuming minerals in the deposit; the rock types hosting the deposit; the types of alteration present in the deposit host rocks; the nature of the ores (vein, disseminated, massive); the reactivity of both acid-generating and acid-consuming minerals (a function of grain size and trace-element content of the minerals); the trace-element content of the deposit and host rocks; and, the extent of pre-mining oxidation. In general, the trend of increasing metal content with decreasing pH depicted on Figure 19.6 reflects greater amounts of pyrite and other sulfide minerals associated with the deposit, and a smaller content of carbonates and other minerals that consume acid. Some deposits can be carbonate-rich but can still generate acidic waters (see, for example the acidic waters draining carbonate-rich deposits on Fig. 19.6) if the acid-buffering carbonates are physically separate from the acid-generating sulfides so that the waters interact with the sulfides and not the carbonates, or if a reaction barrier of iron hydroxides or other minerals protects the carbonates from reaction with the acid waters. Greater amounts of pyrite or base-metal sulfides (such as chalcopyrite and sphalerite)

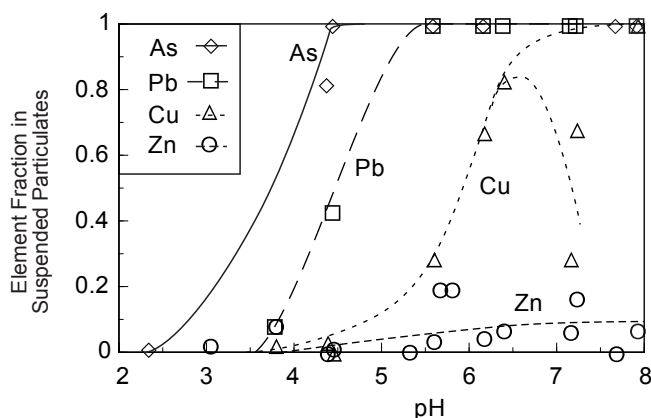


FIGURE 19.5—Plot showing fraction of As, Pb, Cu, and Zn associated with suspended particulates as a function of pH of selected mine-drainage waters sampled in the early phases of this study. A fraction of 1 means that the element is entirely associated with particulates greater than 0.1 μm in size, whereas a fraction value of 0 means that the element is not associated with particulates greater than 0.1 μm . Cadmium and nickel are essentially in solution (not associated with particulates) in all drainage waters shown on the plot. Figure modified from Smith et al. (1992)

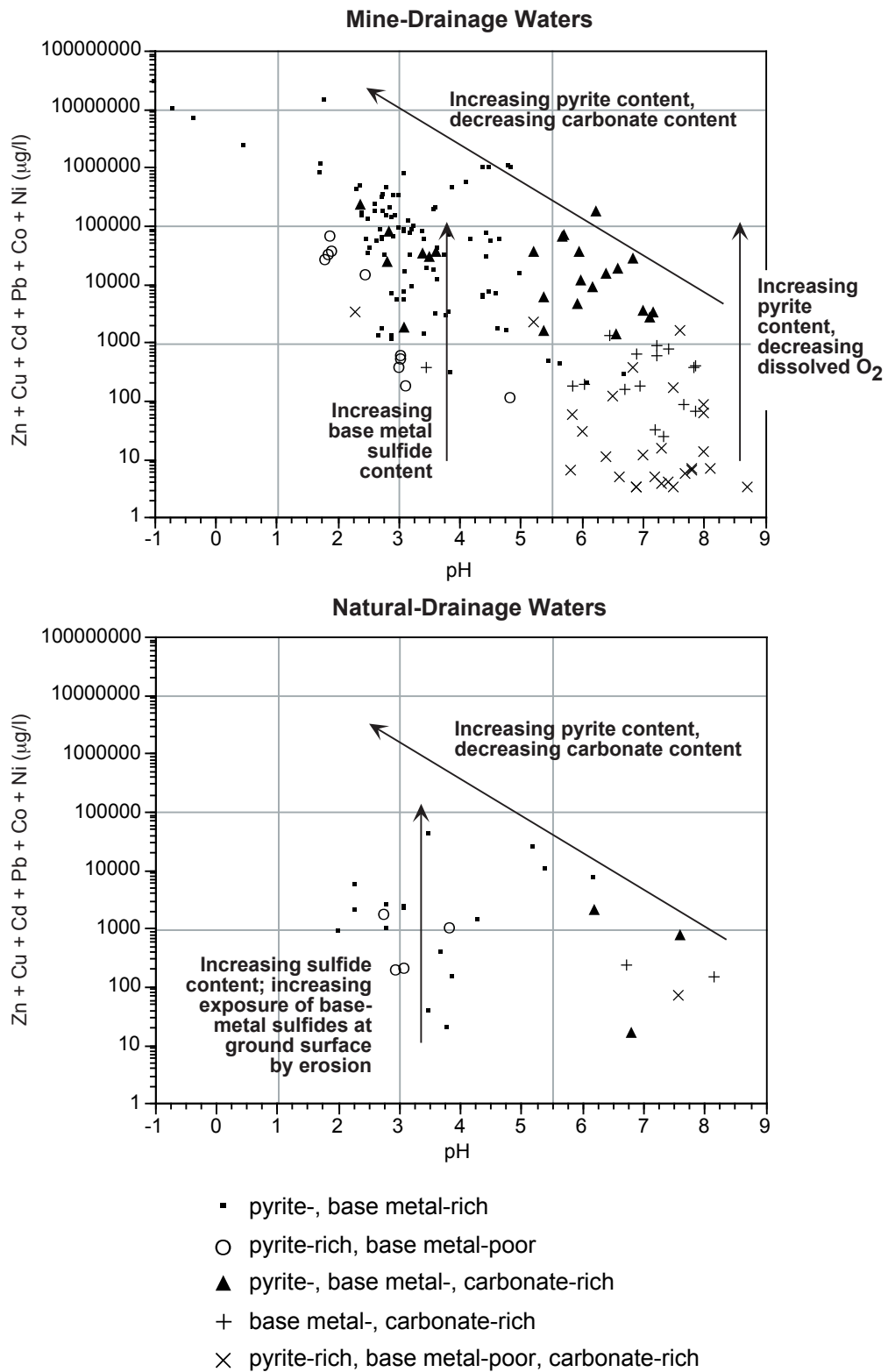


FIGURE 19.6—Ficklin diagrams showing groupings of mine-drainage (upper) and natural-drainage (lower) samples listed in the Appendix according to pyrite content, base-metal sulfide content, and carbonate content of the mineral deposits drained by the waters.

also led to greater dissolved base-metal contents in waters draining deposits with generally similar acid-neutralizing capacities.

Concentrations of individual elements in the drainage waters in part reflect the elements' abundances in the deposits drained by the waters. Due to the abundance of sphalerite in many metal deposits, zinc is the predominant metal (other than Fe, Al, and Mn) in most drainage waters; however, copper-rich, sphalerite-poor deposits tend to have copper-dominant drainage waters, arsenic-rich deposits have arsenic-rich waters, and so on. Due to its limited tendency to sorb onto particulates, zinc is generally the predominant metal in drainage waters with near-neutral pH values. The greatest dissolved zinc values we have measured in near-neutral drainage waters occur in waters draining pyrite- and sphalerite-rich ores with abundant carbonate minerals to buffer pH, but that have limited dissolved oxygen (which prevents the formation of iron particulates that would otherwise sorb more of the dissolved zinc).

For natural waters that drain unmined mineral deposits, the content of dissolved base metals increases at a given pH with increasing base-metal sulfide content of the deposit. In addition, deposits with base-metal sulfides exposed at the ground surface by rapid erosion or glaciation (the natural analogs to the exposure of fresh sulfides by mining activity) commonly have natural-drainage waters with similar pH values but greater dissolved base-metal concentrations than natural waters draining deposits with no sulfides exposed at the ground surface.

A number of mines that are currently in production are developed in mineral deposits that have undergone extensive to complete oxidation during weathering prior to mining. Especially common in dry climates where water tables are deep, this oxidation removes the acid-generating sulfide minerals and leaves behind non-acid-generating oxides, hydroxides, and carbonates. Thus, all deposit types, regardless of their original sulfide content, that have been completely oxidized during pre-mining weathering will most likely generate non-acidic waters with generally low concentrations of metals. However, even small pockets of sulfide-rich, carbonate-poor rocks that remain after weathering can be sufficient to generate acid-mine waters in an otherwise oxidized deposit.

Climate and mining method controls

As can be seen from the Appendix, and as will be shown in the following discussions, climate and the methods used during mining and mineral processing can affect drainage compositions, though mostly within the compositional ranges mandated by geologic characteristics. For example, waters draining mine dumps and those that form in open pits tend to have somewhat more acidic and metalliferous compositions than those draining mine workings, due to the increased surface area of sulfides exposed to weathering and increased opportunities for (a) atmospheric oxygen access to the sulfides and (b) evaporative concentration. Waters draining sulfide-rich tailings impoundments can be quite acidic and metal-bearing even in deposit types with high carbonate contents (see Fig. 19.6, acidic waters draining pyrite- and carbonate-rich deposits). The milling and tailings disposal process can concentrate the pyrite sufficiently that acid generated by sulfide oxidation overwhelms the acid-neutralizing capacity of carbonates in the tailings; for example, physical sorting of dense sulfides from less dense carbonates may create sulfide-rich zones in the tailings that have high acid-generating potential. Similarly,

storm waters draining sulfide-rich, carbonate-bearing mine waste dumps may potentially be acidic, if the acid waters formed by the dissolution of soluble salts growing on sulfide surfaces flush so rapidly from the dumps as to not have time to react with carbonate minerals in the dumps.

Mineral deposits commonly generate less drainage in arid and semi-arid climates than in wet climates. For example, in arid climates, many mines are developed above deep water tables, and many mine dumps may not drain except for short periods after storms. The data in the Appendix indicate that, for acid-generating deposit types, those drainage waters that do occur in arid climates tend to be more acidic and metalliferous than those in wetter climates due to the effects of increased evaporation and the decreased potential to be diluted by non-mineralized ground and surface waters.

MINE- AND NATURAL-DRAINAGE SIGNATURES OF DIVERSE MINERAL-DEPOSIT TYPES

Although mineral deposits can be typed according to overall similarities in their geologic characteristics, geologic setting, and mode of formation, they typically have complex variations in mineralogy, alteration, and (or) wallrock within a given deposit. Thus, the grouping of mine- and natural-drainage waters based on similar geologic characteristics alone (Fig. 19.6) is insufficient to characterize the possible range of drainage compositions that can occur within a geologically complex deposit type. Instead, drainage compositions must be measured and summarized for each ore type, mineralogic zone, alteration type, and (or) host rock type for a given mineral deposit type. In the following discussion, we will use Ficklin plots to show how drainage compositions vary as a predictable function of deposit type and location within a deposit type. We will start our discussion with the deposit types having geologic characteristics in their main ore zones that are favorable for the generation of the most acidic waters, and shift progressively to those deposits having ores that are likely to generate less acidic and metal-bearing waters. However, even in the deposit types most likely to generate highly acidic waters, we will show that a variety of drainage compositions, including those that are less acidic and metalliferous, can occur within different parts of the deposits.

Volcanogenic massive sulfide (VMS) deposits

Syngenetic VMS deposits result from the discharge of hydrothermal mineralizing fluids onto the ocean floor, a process analogous to that observed today where sub-oceanic hot spring systems, known as "black smokers," form chimneys and other sulfide deposits on the ocean floor. For summaries of the geologic characteristics of this type, the reader is referred to reviews such as Franklin (1993), Slack (1993), Taylor et al. (1995), Evans et al. (1995), and references contained therein.

The deposits form in or near areas of subaqueous volcanism, which provides the heat source for the hydrothermal systems, and are commonly associated with volcanic or metamorphosed volcanic rocks. Volcanic-hosted VMS deposits include Cyprus-type, which occur in basaltic volcanic rocks, and Kuroko-type, which occur in andesitic to rhyolitic volcanic rocks (Franklin, 1993). In contrast, Besshi-type VMS deposits occur in sequences of predominantly sedimentary rocks such as turbidites and black shales

(or their metamorphosed equivalents, graphitic schists), with some interbedded volcanic rocks such as basalts or intrusive rocks such as diabase sills.

Variations in metal contents permit further differentiation of VMS deposits. Franklin (1993) differentiates copper-zinc (Cu > Zn content) and zinc-lead-copper (Zn > Pb > Cu content) subtypes. Deposits of the zinc-lead-copper subtype are associated with silicic volcanic rocks. Blackbird-type deposits (named after the Blackbird mining district, Idaho) are cobalt- and arsenic-rich Besshi-type deposits.

VMS deposits are typically zoned, with pyrite, pyrrhotite, and chalcopyrite forming in the hotter, sub-seafloor and near-vent portions of the deposits. These “yellow ores” grade upward and outward into sphalerite- and (in the case of the zinc-lead-copper-subtype deposits) galena-rich ores (“black ores”) that were deposited on the ocean floor. As implied by their name, VMS deposits can consist of massive ore lenses that are predominantly to nearly entirely composed of sulfides. The wallrocks present around the sub-seafloor feeder zones of the deposits are typically altered to chlorite-sericite-pyrite or chlorite-rich assemblages. Some carbonate minerals may be present in the surrounding host rocks, especially in sediment-hosted Besshi-type deposits.

Drainage-water compositions

Geologic controls on the composition of mine drainage waters from VMS deposits are summarized by Taylor et al. (1995) and Goldfarb et al. (1996). As shown on Figure 19.7A, mine-drainage compositions measured in VMS deposits span a large range in pH and metal contents, reflecting geologic controls, the effects of evaporation, and climate. Mine waters from the Iron Mountain, California, Kuroko-type deposit are the most acidic and metalliferous ever measured (Alpers and Nordstrom, 1991; Nordstrom and Alpers, 1999), with field pH values as low as -3.5 and dissolved contents of Fe, Al, Zn, and Cu as high as tens of grams per liter. These extreme compositions most likely reflect several factors. First, the mine waters likely flow through the massive sulfide lenses and do not interact with any potentially acid-consuming wallrock minerals. Second, the temperatures in the mine stopes are very hot (possibly as high as 60–70°C) and water temperatures reach as high as 46–47°C (D.K. Nordstrom, written commun., 1998), due to heat generated by exothermic pyrite oxidation. Thus evaporative concentration of the mine waters is likely to be important (Alpers and Nordstrom, 1991). Third, the climate at the West Shasta district is relatively dry, but with a distinct annual wet-dry

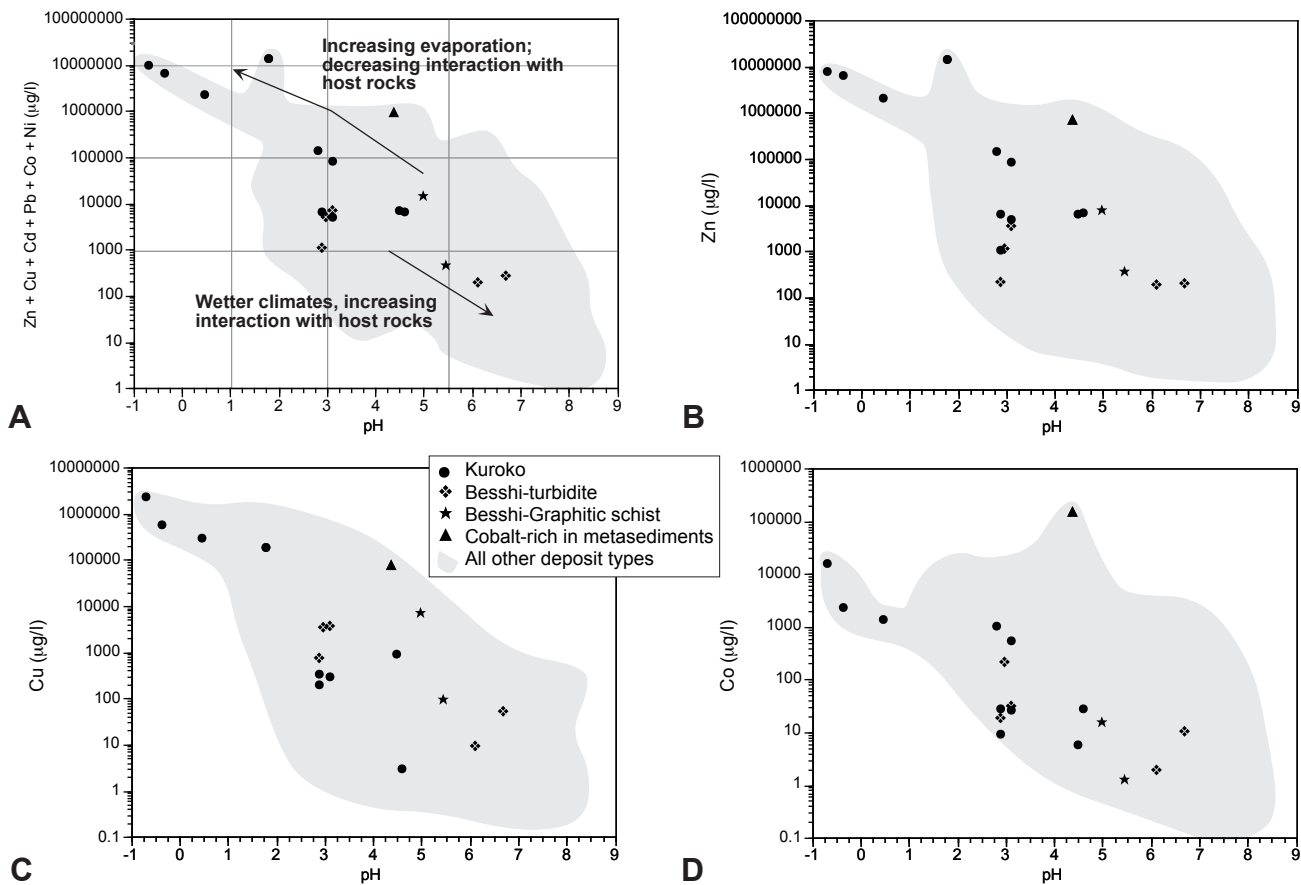


FIGURE 19.7—Plots of mine-drainage compositions for volcanogenic massive sulfide (VMS) deposits: A. Ficklin diagram; B. Zinc; C. Copper; D. Cobalt. Note differences in scale of the concentration axis between the plots. Shaded areas enclose all data points on corresponding Figures 19.1, 19.2.

cycle, which also enhances periodic evaporative concentration of the mine waters.

Mine-water compositions measured in some portions of Iron Mountain (C.N. Alpers, oral commun., 1994), as well as in other Kuroko-type VMS deposits such as Holden, Washington (Kilburn and Sutley, 1997) are typically quite acidic and metalliferous, although less so than the extremely acid waters at Iron Mountain (Appendix). The waters with less extreme acid pH values likely reflect buffering by reactions with aluminosilicate minerals in the deposit host rocks. The Holden mine site is also located in a wetter climate than Iron Mountain, which may lead to greater recharge of ground waters into the mine workings, and may preclude high amounts of evaporation that would lead to extreme concentrations of acid and metals in solution.

Although we have not included in our summary mine-drainage data for Cyprus-type VMS deposits, it is likely that the water compositions are generally similar to those of Kuroko-type VMS deposits. Waters that interact with the intermediate to basaltic-composition rocks hosting Cyprus deposits may be somewhat less acidic than those draining Kuroko-type deposits, due to the increased reactivity and acid-buffering capacity of the basaltic host rocks.

The limited data we have collected on waters draining Besshi-type deposits hosted by graphitic schists in the Great Smoky Mountains of Tennessee indicate a somewhat higher pH and lower overall metal content than for waters draining Kuroko-type deposits. This may result from both the partly disseminated nature of the ore within the graphitic schists and the wetter climate. The data collected by Goldfarb et al. (1996) for turbidite-hosted, Besshi-type VMS deposits in Prince William Sound, Alaska, show a trend to significantly higher pH values and lower metal contents than for waters draining the Kuroko-type VMS deposits. Goldfarb et al. (1996) attributed the higher pH and lower metal contents to the significantly wetter and lower-temperature climate of the area.

Another factor that may affect drainage pH in some VMS deposits is the presence of carbonate minerals in the deposit host rocks. In such deposits, mine waters that interacted significantly with carbonate-bearing host rocks might be expected to have near-neutral pH values but elevated levels of zinc, copper, and cadmium (see for example the distribution of data points marked by triangles on Figure 19.6, which depict drainage compositions of pyrite-rich, base metal-rich and carbonate-rich deposit types).

The relative abundances of metals such as Zn and Cu in the VMS drainage waters in part reflect (1) the overall chemical composition and mineralogy of the deposits, (2) the mineralogic zones within the deposits, and (or) (3) seasonal variations stemming from flushing of salts from the mine workings. For example, the Co- and Cu-rich massive sulfides of the Blackbird mine, Idaho (data summarized by Evans et al., 1995, and McHugh et al., 1987), have exceptionally high levels of Co in the drainage waters (Fig. 19.7D). Copper-rich stockwork feeder zones of VMS deposits generate drainage waters that are enriched in Cu relative to Zn, whereas waters that drain the overlying sphalerite-rich ore zones of the deposits likely have enrichments of Zn over Cu in the waters. Alpers et al. (1994) have shown that seasonal flushing of soluble salts from the mine workings at Iron Mountain results in significant decreases in Zn/Cu due to the selective dissolution of copper-bearing melanterite during the flush.

High sulfidation epithermal (quartz alunite epithermal) deposits

High-sulfidation epithermal, or quartz-alunite epithermal, deposits are Au-Cu-Ag deposits that form in close spatial and temporal association with shallow (within the upper several km of the Earth's crust) silicic volcanic or intrusive centers (Fig. 19.8). At Summitville, Colorado, for example, the deposits are hosted by a 22 Ma quartz latite volcanic dome, and were formed during the late stages of the dome-forming cycle of volcanism. Other examples include Red Mountain Pass, Colorado; Goldfield and Paradise Peak, Nevada; Mount Macintosh, British Columbia, Canada; and Julcani, Peru (see references to studies of these deposits contained in Plumlee et al., 1995c). The deposits are characterized by intense acid leaching and alteration of the deposit host rocks that were generated by magmatic gas condensates prior to ore-stage mineralization. In general, the cores of the deposits are characterized by intersecting zones of silica alteration (where all constituents of the host rock except silica were removed by the leaching), flanked by thin zones of quartz-alunite-pyrite and quartz-kaolinite alteration. In some of these deposits such as Summitville, the silica alteration is vuggy, due to the complete acid leaching of original feldspar phenocrysts from the volcanic host rock. The core of intensely altered rock is surrounded proximally by large volumes of argillically altered rock (the rock is altered to clays and pyrite), and a distal zone of propylitically altered rock (altered to contain epidote, chlorite, some pyrite, and calcite) (Fig. 19.8). Subsequent to the intense acid alteration, hydrothermal fluids, whose flow was focused primarily along the higher-permeability vuggy silica zones, deposited sulfide-rich assemblages containing pyrite, native sulfur, enargite (a copper-arsenic sulfosalt), chalcocite and covellite (copper sulfides), and native gold in the central portions of the deposits, grading upward and outward into sphalerite-, galena-, and barite-rich assemblages in some deposits. At depth beneath the acid-altered rocks, the hydrothermal fluids typically deposited chalcopyrite (a copper-iron sulfide) and tennantite-tetrahedrite (copper-arsenic sulfosalts) in rocks altered to quartz sericite-pyrite assemblages.

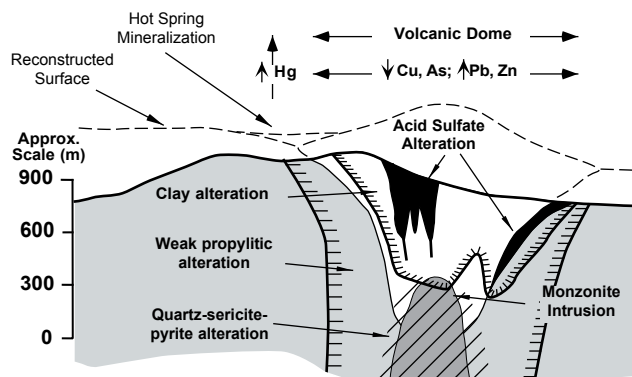


FIGURE 19.8—Generalized cross-section of a high-sulfidation deposit, based primarily on zoning relationships observed at Summitville, Colorado, and Julcani, Peru. Figure from Plumlee et al. (1995c), based on references contained therein.

Post-mineralization oxidation of these deposits typically occurs to great depths (more than 100 m deep at Summitville) along the permeable silica zones. This oxidation commonly removes the sulfides and concomitantly enriches the silica in gold. In contrast, the surrounding argillically altered rock is oxidized to very shallow depths (only several meters at Summitville), due to the low permeability created by the clay minerals.

Other deposit types that are commonly spatially and temporally associated with high sulfidation deposits include: porphyry Cu deposits, which form in the intrusive rocks at depth beneath the high sulfidation deposits; hot-spring Au/Hg deposits, which are the very near-surface manifestations of the high sulfidation system; and adularia-sericite epithermal deposits.

Drainage-water compositions

Intense acid leaching of the deposit host rocks, coupled with the high acid-generating potential of the sulfide minerals, are a geologic formula for extremely acidic and metal-bearing mine-drainage waters (Appendix, Fig. 19.9). The data compiled here were primarily collected as part of our ongoing geoenvironmental studies at Summitville, Colorado (Plumlee et al., 1995a, b; Plumlee and Edelmann, 1995). However, as part of this study, we

have also collected limited data on mine waters from Red Mountain Pass, Colorado, and the 3R Mine, SE Arizona. We have also included here data on natural spring compositions draining unmined high sulfidation deposits at Mount Macintosh/Pemberton Hills, Vancouver Island, British Columbia, Canada (collected by Koyanagi and Panteleyev, 1993).

The most acidic and metalliferous waters are mine waters draining the acid-sulfate alteration portions of the deposits (Figs. 19.9, 19.10), due to the prior removal of nearly all buffering capacity of the rocks during intense, pre-ore, acid-sulfate alteration. Natural waters draining the acid-sulfate-altered portions of the unmined Mount Macintosh deposit (open circles on Fig. 19.9) have the same general range in pH as the mine-drainage waters, but have lower concentrations of Fe, Al, Cu, Zn, As, and other metals. This may reflect the lack of exposure of the base metal sulfides at the ground surface, a lower content of base metal sulfides, or lower permeability in the Mount Macintosh deposit.

Waters draining propylitically altered rocks at Summitville (triangular symbols, Fig. 19.9) have considerably higher pH values and correspondingly lower metal contents than those draining the acid-sulfate alteration zones. This is due to the presence of calcite in the propylitic alteration assemblage, which consumes acid generated by sulfide oxidation,

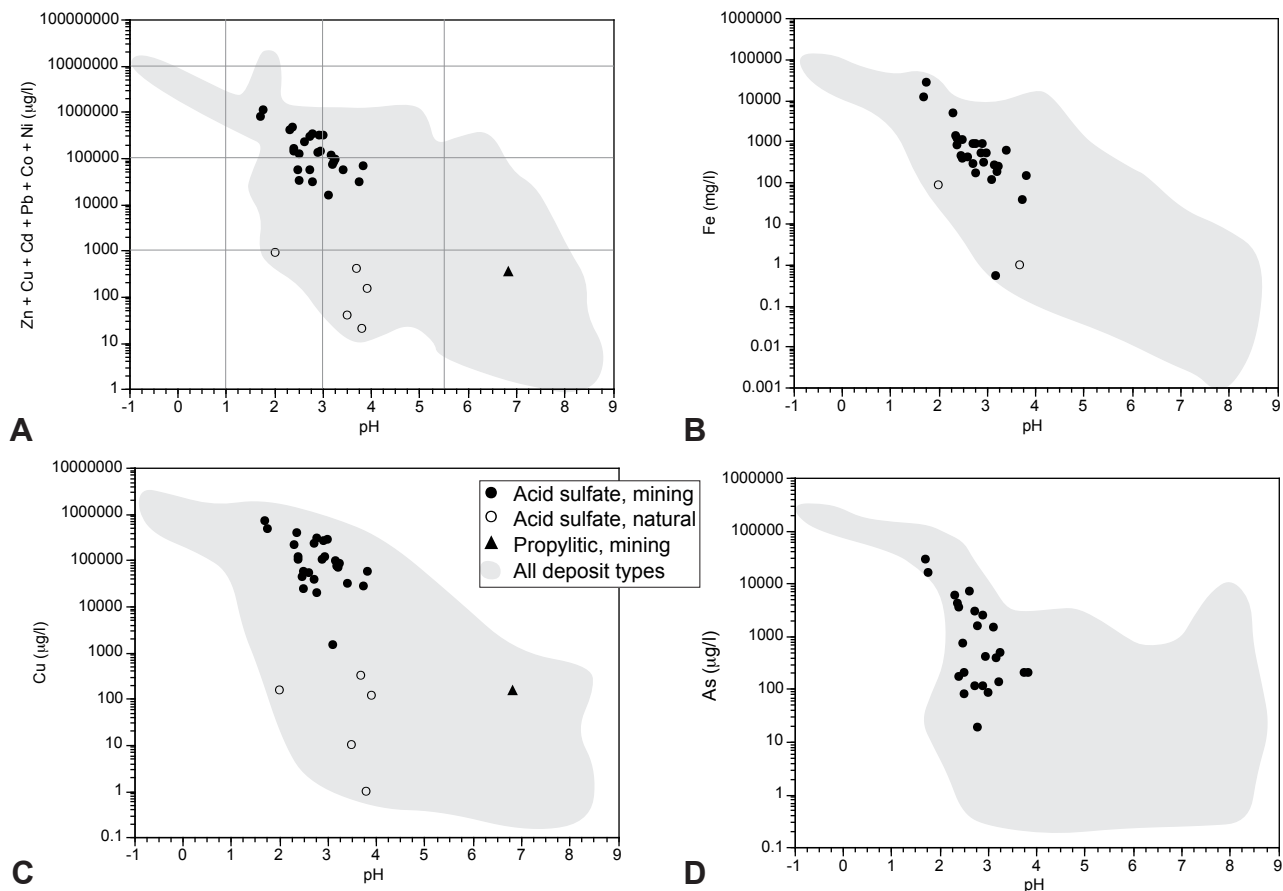


FIGURE 19.9—Plots of mine- and natural-drainage compositions for high sulfidation epithermal deposits: A. Ficklin diagram; B. Iron; C. Copper; D. Arsenic. Note differences in scale of the concentration axis between the plots. Shaded areas enclose all data points on corresponding Figures 19.1, 19.2.

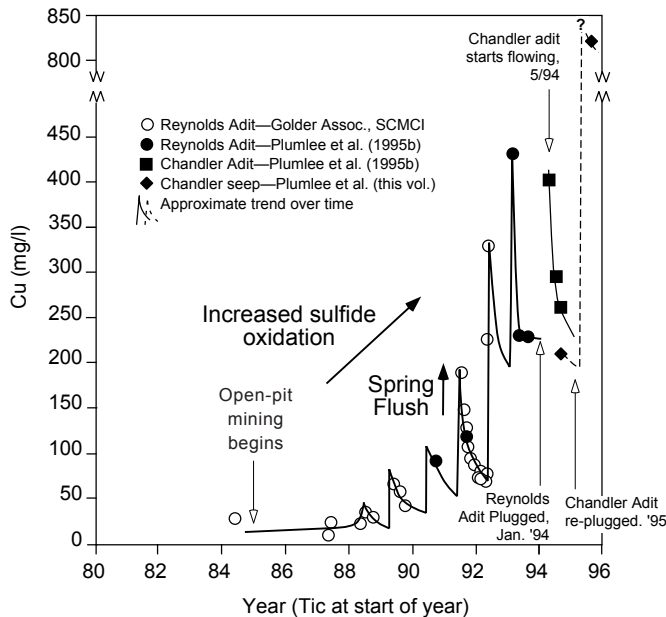


FIGURE 19.10—Plot of copper concentrations in adit outflows from the area beneath the Summitville open pit since the start of open-pit mining in 1985. The general increase in copper content over time reflects the increased exposure of sulfides as a result of mining, whereas the spikes in concentration each spring represent the flush of soluble salts from the mine workings during spring snowmelt. Figure from Plumlee et al. (1995b). The hollow symbols show data collected by Golder and Associates for the mining company, Summitville Consolidated Mining Co., Inc. (SCMCI on figure) prior to the bankruptcy of the company in 1992.

The mine waters draining high sulfidation deposits are generally enriched in copper relative to zinc and are relatively enriched in arsenic, due to the abundance of Cu-sulfides and Cu-As sulfosalts such as enargite in the deposits. Due to their highly acid pH, the waters also react readily with the surrounding wallrocks, and so can contain very high concentrations (Appendix) of a variety of elements leached from the wallrocks and ore minerals such as aluminum (several thousands of mg/l), rare earth elements (from several to tens of mg/l each of cerium, lanthanum, etc.), and cobalt, nickel, chromium, uranium, thorium, and beryllium (hundreds of $\mu\text{g/l}$ up to several mg/l).

Soluble metal sulfate salts also play a key role in the generation of acid-mine drainage at Summitville and other high sulfidation deposits. Plots of copper concentrations in waters draining Summitville's Reynolds and Chandler adits over time since the beginning of open-pit mining show spikes in copper concentrations each spring, reflecting the snowmelt-triggered flush of soluble salts from the mine workings (Fig. 19.10). These adit waters are bright green, have a high ferrous iron content, and most likely reflect the dissolution of salts such as melanterite (a ferrous sulfate) and chalcantite (a copper sulfate) from the mine workings. In addition, highly acidic, bright red puddles form within the open pit and on top of mine waste materials immediately after summer thundershowers, reflecting the dissolution of secondary salts. Evaporation of the acid waters during dry periods results in the reprecipitation of the salts, and, as a result, stores acid and metals until the next period of rain or snowmelt. Mineralogic studies of

the salts in and around the Summitville open pit (Flohr et al., 1995) collected during dry season have identified a variety of salts, including chalcantite and brochantite (Cu sulfates), jarosite (Fe-K hydroxysulfate), halotrichite (Fe-Al sulfate), and others.

Figure 19.11 is a Ficklin diagram comparing the compositions of the Summitville mine-drainage waters to those of waters derived by leaching of Summitville mine waste samples with deionized water, followed by evaporation of the leachate waters (Plumlee et al., 1995a). We interpreted the steep trend of metal content with pH shown by the leachate samples to reflect a short-term salt-dissolution trend. Evaporation of these samples led to shifts to lower pH and higher metal contents. The waters draining mine dumps, waters that collect in ponds during wet seasons, and adit waters collected during spring flush plot at the upper end of the salt dissolution trend. In contrast, adit waters collected during dry periods and waters from seeps outside the open pit area plot along a trend of shallower metal-pH slope, which merges at low pH with the salt dissolution trend. We interpreted this as a longer-term sulfide oxidation and water-rock interaction trend. Two low-volume seeps within the Summitville open pit, Blackstrap and Son-of-Blackstrap (Appendix) are the most acidic and metalliferous of all the drainage waters at Summitville; we interpreted these waters to result from the extreme evaporation of seep water that was ultimately derived from oxidation of sulfides and dissolution of secondary salts in the rocks around the open-pit.

Porphyry Cu and Cu-Mo deposits

Porphyry Cu and Cu-Mo deposits are large deposits characterized by disseminated to veinlet-controlled mineralization deposited throughout large volumes of altered, intermediate-composition intrusive rocks (see geologic summaries by Cox, 1986; Cox and

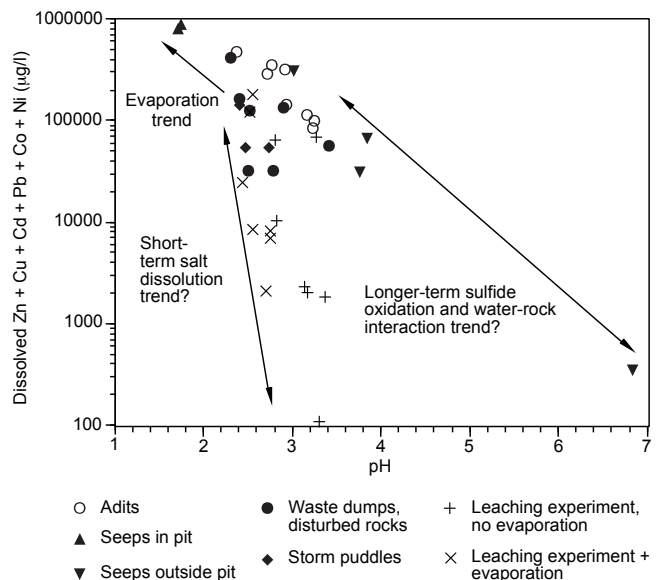


FIGURE 19.11—Ficklin diagram comparing mine-drainage compositions from Summitville, Colorado, with compositions of waters collected from leach studies using mine wastes from Summitville (Figure modified from Plumlee et al., 1995b).

Singer, 1986; Sillitoe, 1993; Cox et al., 1995; and references therein). The deposits formed from magmatic-hydrothermal fluids that were expelled during the crystallization of magmatic intrusions. A schematic cross section of a porphyry copper deposit showing distribution of mineralogic zones and wallrock alteration types (modified from Lowell and Guilbert, 1970) is shown in Filipek et al. (1999). The deposits are characterized by a central core of potassic alteration, where the intrusive rocks are altered to coarse potassium feldspar, biotite, and anhydrite. The core of potassically altered intrusive rocks is surrounded by a much broader phyllic alteration zone, where the intrusive rocks are altered to quartz-sericite-pyrite assemblages. The lateral fringes of the deposits are characterized by propylitic alteration of the rocks surrounding the intrusions to an assemblage containing epidote, chlorite, pyrite, and calcite. The upper portions of the deposits may be altered to clays, and in some deposits are overlain by advanced-argillic or acid-sulfate alteration with associated high-sulfidation or Cordilleran-lode deposits. Where the porphyry-forming magmas intruded into carbonate-bearing sedimentary host rocks, the disseminated and veinlet intrusive-hosted ores are mantled by skarn ores, where the sedimentary rocks as well as the outermost intrusive rocks are typically altered to calc-silicate, sulfide, and oxide mineral assemblages containing pyroxenes, garnets, wollastonite, epidote, magnetite, pyrite, chalcocopyrite, and other sulfides.

Primary ore minerals that typically occur in porphyry-Cu deposits include pyrite, chalcocopyrite, and variable but lesser amounts of bornite, enargite, and molybdenite. Porphyry molybdenum deposits contain molybdenite, lesser chalcocopyrite, and typically do not contain enargite or bornite.

Post mineralization weathering of the deposits leads to a variety of minerals in the oxidized zone above the water table, including iron oxides (goethite, hematite, jarosite), copper oxides (such as tenorite and cuprite), and copper carbonates (malachite, azurite), copper silicates (chrysocolla, turquoise). During weathering,

oxidized ground waters descend through the unsaturated portions of the deposits and leach copper, sulfur, iron, and other metals. When the descending waters reach the reducing conditions below the water table, the copper in the waters reacts with primary iron sulfides and chalcocopyrite to produce supergene Cu-rich sulfide minerals such as chalcocite, covellite, bornite, digenite, djurleite, and others. In many porphyry deposits, significant copper grades occur in, and copper production comes from, these supergene enrichment ores.

Drainage-water compositions

The mine-drainage data that we have compiled from the literature (Appendix; Fig. 19.12) are from Globe, Arizona (Eychaner, 1988), and Mt. Washington, British Columbia (Kwong, 1991), and natural drainage data (open circles) are from the Alamosa River stock, a sub-economic Mo±Cu deposit south of Summitville, Colorado (Barry, 1996). Data for stream waters draining unmined porphyry-Cu deposits in Puerto Rico are summarized by Miller et al. (1982) and shown on Figure 19.12, but are not included in the Appendix.

Mine waters that drain the core potassic and quartz-sericite-pyrite alteration zones of porphyry copper deposits are quite acidic, with pH values as low as 2–3, and metalliferous, with total base metals from several mg/l to hundreds of mg/l (Fig. 19.12). As with the high-sulfidation epithermal and Cordilleran lode deposits, the copper-rich porphyry Cu deposits produce waters with Cu>Zn. Porphyry Mo deposits, on the other hand, tend to produce waters with relatively low base metal contents due to the generally lower abundances of base metal sulfides such as chalcocopyrite and sphalerite. The natural drainage waters from the Alamosa River stock area (Barry, 1996) shown on Figure 19.12 have lower Cu and Zn concentrations because the mineralization is relatively Mo-rich, and Cu- and Zn-poor. Natural drainage

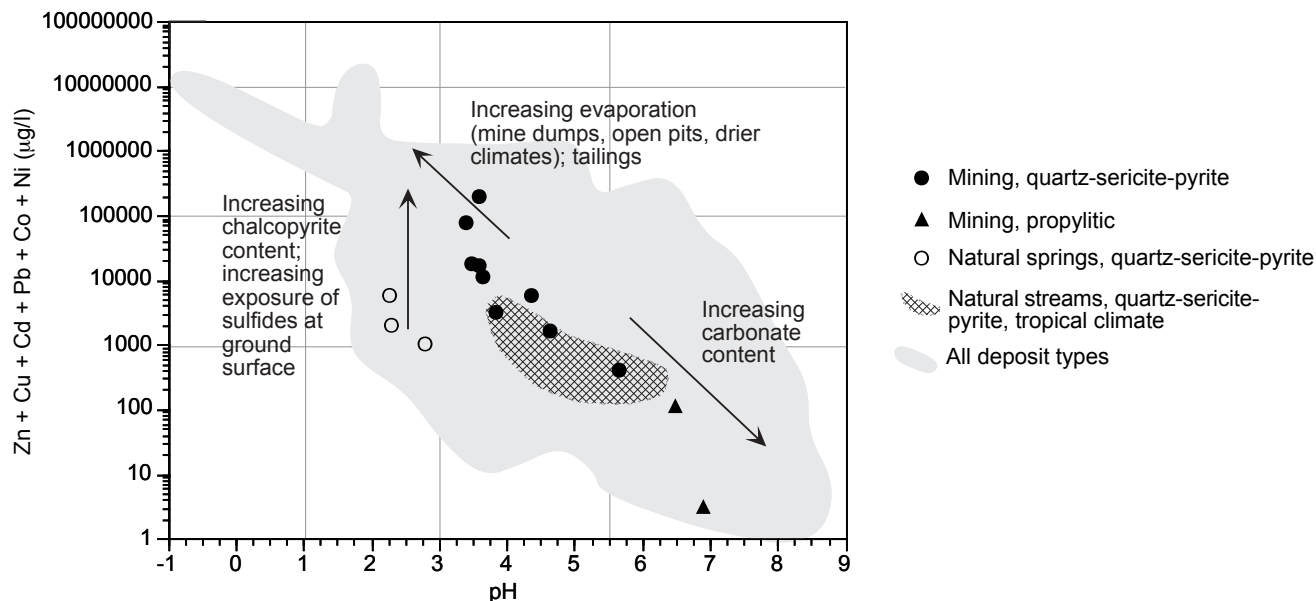


FIGURE 19.12—Ficklin Plot showing sum of dissolved base metals for mine- and natural-waters draining central quartz-sericite-pyrite and potassic alteration zones and peripheral propylitic alteration zones of porphyry Cu and Cu-Mo deposits. Shaded area encloses all data points on Figure 19.2.

waters collected from springs and streams within and near porphyry-Cu deposits in Puerto Rico (Miller et al., 1982) demonstrate that acidic (pH between 4 and 5) waters with elevated base metal concentrations (Cu as high as 4100 µg/l) can be produced, even in warm, wet, tropical climates where rainfall and dilution are substantial.

The role of drier climate in shifting drainage waters to somewhat lower pH values and higher dissolved metal concentrations can be seen by comparing the mine-drainage compositions (Appendix) from Globe, Arizona (Eychaner, 1988), with those from Mt. Washington, B.C. (Kwong, 1991) for similar alteration zones. The Globe waters are more acidic and metal-rich due to the drier climate of the Arizona desert versus the much wetter, cooler climate of British Columbia, shifts similar to those noted previously for VMS deposits.

Mine-drainage data from Mt. Washington (Kwong, 1991) also demonstrate the shifts to much higher pH values and lower metal contents in waters draining carbonate-bearing and (or) propylitically-altered rocks.

Cordilleran lode deposits

Cordilleran lode deposits (Bartos, 1987) are geologically similar to high sulfidation epithermal deposits, with the exception that they form at somewhat greater depths (4–5 km) in the Earth's crust. Instead of occurring within shallow volcanic centers, they form just above or in the upper levels of magmatic intrusions and their associated porphyry-copper deposits. Examples include Butte, Montana; Magma, Arizona; and Quiruvilca, Peru (Guilbert and Park, 1986; Bartos, 1987). These deposits are characterized by high contents of pyrite, enargite, chalcocite, covellite, bornite, and native sulfur. The sulfides occur in pipes or veins within wallrocks that were intensely altered prior to mineralization to advanced argillic assemblages containing kaolinite, pyrophyllite, ± alunite. The deposits are also typically zoned with increasing contents of sphalerite, galena, and carbonates (such as rhodochrosite) toward their peripheries. At Butte and other Cordilleran lode deposits, the high sulfidation veins and advanced argillic alteration crosscut earlier porphyry Cu or Mo mineralization; as a result, many economic geologists consider these deposits to be a variation of porphyry mineralization (Guilbert and Park, 1986). In addition, similar high-sulfidation mineralization may occur as a component of some polymetallic vein and replacement deposits associated with igneous intrusions into carbonate-rich sedimentary rocks (Morris, 1986).

Drainage-water compositions

The mine and natural waters draining Cordilleran lode deposits are likely to have compositions generally similar to those draining high sulfidation epithermal deposits, such as Summitville, with highly acidic, metal-rich waters having enrichments of copper relative to zinc, and enrichments of arsenic relative to other deposits with lesser amounts of arsenic-bearing sulfides. Limited water data are available for the open pit lake at Butte, Montana (Davis and Ashenberg, 1989) (Fig. 19.13). Because the "Main-stage" cordilleran lode deposits at Butte overprint an earlier porphyry Cu-Mo system, the mine waters are probably compositional hybrids reflecting both the lode veins and advanced-argillic alteration in the core of the deposit, and the earlier porphyry mineral-

ization (see above for porphyry Cu/Mo water compositions); hence, their arsenic contents are somewhat elevated, but are lower than those of the waters draining Summitville. The Butte waters are among the most metal-rich of mine waters having similar pH values, in spite of the relatively wet climate; these enrichments presumably reflect evaporative concentration of the open-pit waters during dry periods. Although no drainage data are available for deposits on the carbonate-rich fringes of Cordilleran lode systems, it is likely that the pH values of waters draining the fringes are substantially higher, and metal contents are lower (with higher Zn/Cu) than those of waters draining the cores of the deposits.

Climax-type porphyry Mo deposits

Climax-type porphyry Mo deposits are geologically similar to the porphyry Mo deposits discussed previously, with the exception that they are genetically related to magmas enriched in silica, fluorine, and elements such as uranium and thorium (White et al., 1981). As a result, the deposits are hosted by silica- and uranium-rich granitic or rhyolitic intrusions, have abundant fluorite, and contain fluorine-rich alteration assemblages. The main orebodies consist of stockwork veinlets of quartz and molybdenite with lesser amounts of fluorite and pyrite. Late-stage fluorite (± manganiferous carbonate) veins also cross-cut the orebodies. The central portions of the deposits are generally lacking in base metal sulfides such as chalcopyrite, sphalerite, and galena; however, sphalerite and galena increase in abundance, along with calcite and rhodochrosite, toward the lateral fringes of the deposits. The wallrocks hosting the deposit are altered to the same potassic (cores of the deposits), phyllic (intermediate portions), argillic (upper levels), and propylitic (lateral edges of the deposits) assemblages seen in porphyry Cu and Cu-Mo deposits. In addition, in the deeper levels of the deposits, the wallrocks are altered to so-called "greisen" assemblages containing quartz, topaz, and muscovite (White et al., 1981). Garnet is a common alteration mineral in some portions of the deposits. Examples of Climax-type deposits include Climax, Henderson, and Mt. Emmons, Colorado (White et al., 1981).

Drainage-water compositions

Limited mine-drainage data collected as part of this study from Climax, Colorado (Appendix, Fig. 19.14), show that waters draining mine waste material from the potassic and phyllic alteration zones can be highly acidic (pH < 2). The rates at which feldspars, sericite, and biotite weather are apparently sufficiently slow compared to rates of sulfide oxidation that they do not readily neutralize acid generated by sulfide oxidation. Due to the general lack of Cu, Zn, and Pb sulfides in the potassic and phyllic alteration zones, the mine waters may have slightly lower dissolved concentrations of Cu, Zn, and Pb than waters of equivalent acid pH values that drain other deposit types (Fig. 19.14). Due to the abundance of fluorine in the ores, wallrock alteration, and host rocks, the mine waters are exceptionally enriched in fluoride, with concentrations as high as 710 mg/l (Appendix). As a result of the uranium enrichments in the deposit host rocks, coupled with the low pH and high fluoride concentrations (uranyl fluoride complexes are very stable), the mine waters from Climax also have among the highest levels of dissolved uranium (8–9 mg/l; Fig. 19.14B) of mine waters we have measured in this study or noted in the litera-

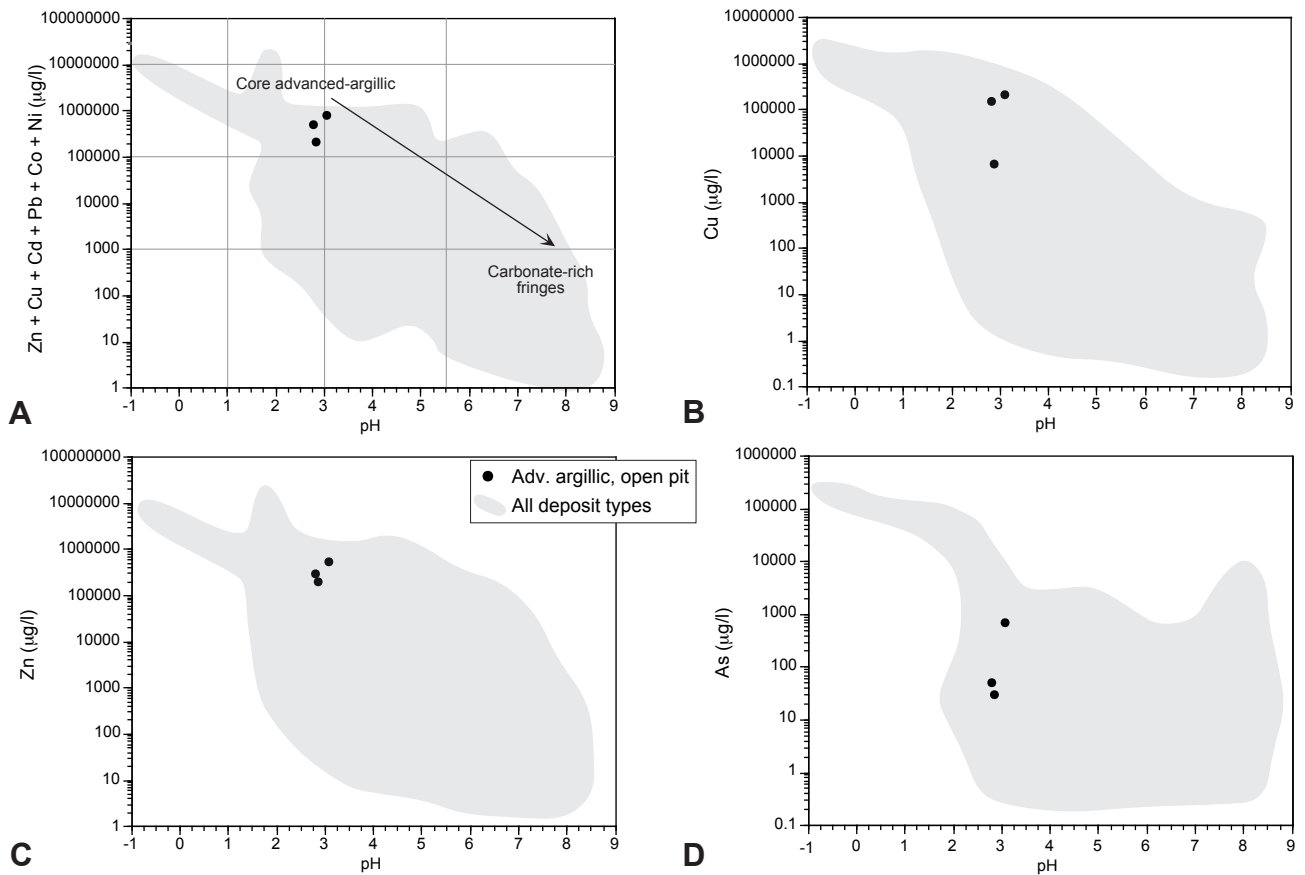


FIGURE 19.13—Plots of open-pit water compositions at Butte, Montana. The deposits at Butte include Cordilleran lodes (veins) superimposed on earlier porphyry-Cu-Mo mineralization: A. Ficklin diagram; B. Copper; C. Zinc; D. Arsenic. Note differences in scale of the concentration axis between the plots. Shaded areas enclose all data points on corresponding Figures 19.1, 19.2.

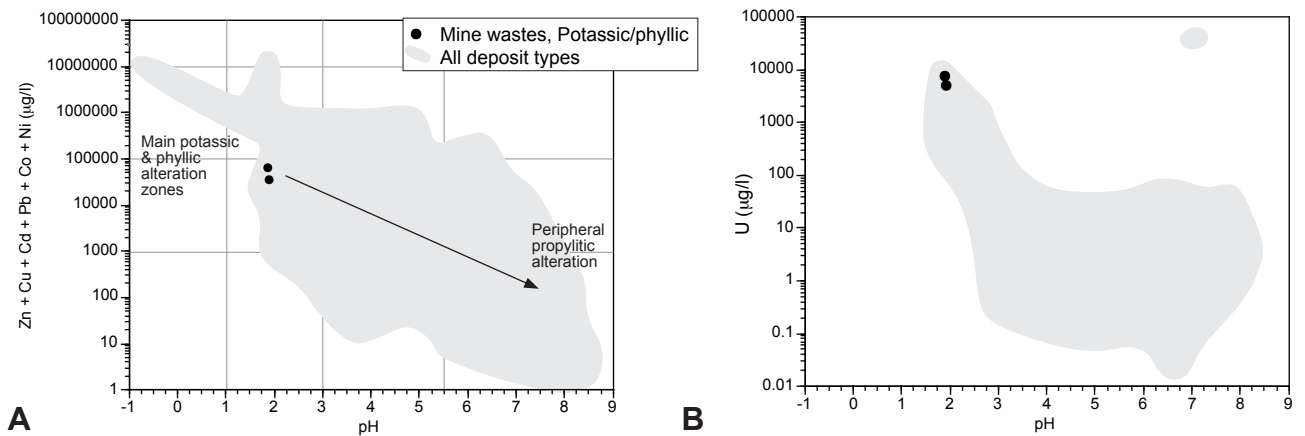


FIGURE 19.14—Plots of mine-drainage compositions for waters draining the central quartz-sericite-pyrite and potassic alteration zones of Climax-type porphyry Mo deposits. A. Ficklin diagram; B. Dissolved uranium. Note differences in scale of the concentration axis between the plots. Shaded areas enclose all data points on corresponding Figures 19.1, 19.2.

ture. The acidic waters from Climax also have the highest molybdenum concentrations (several hundred $\mu\text{g/l}$) among acid-mine water compositions we have measured in this study; however, these concentrations are substantially lower than those measured in alkaline mine waters (up to 42 mg/l) draining sandstone uranium deposits from the southwestern U.S. (Appendix; Longworth, 1994). The mine waters at Climax are currently being treated to neutralize acid and precipitate metals.

Polymetallic vein deposits and adularia-sericite epithermal vein deposits

We have discussed in previous sections deposit types in which the predominant ore zones or ore types are likely to produce acidic, metal-bearing waters. We will now discuss deposit types with major ore zones or ore types that can produce waters with variable pH but generally high levels of dissolved metals.

Polymetallic vein systems and adularia-sericite epithermal vein deposits are deposited from convectively circulating meteoric hydrothermal systems similar to the present-day geothermal systems at Yellowstone, USA, and the North Island of New Zealand (Berger and Eimon, 1983; Heald et al., 1987; Sillitoe, 1993). The deposits are often genetically and spatially related to igneous intrusions at depth, which provide the heat source for the hydrothermal systems, and possibly also fluids, gases, metals, and other constituents carried upward by the fluids and incorporated into the ores. The epithermal deposits form in the upper 1–2 km of the crust, and are characterized by veins, stockwork veins, and mineralized breccias in mostly volcanic host rocks. Polymetallic vein deposits form at slightly greater depths (several km) than epithermal veins, and typically are composed of veins and stockworks hosted by a variety of rock types such as granites and metamorphic rocks.

Both types of deposits can be quite variable and complex from a mineralogical standpoint, depending upon the compositions of the hydrothermal fluids which formed the deposits, the ore deposition mechanism(s), the wallrocks, and the chemical evolution of the hydrothermal fluids during mineralization. Both types of deposits can also show very strong spatial variations in mineralogy within an ore shoot, within a vein or vein system, and across entire districts.

Polymetallic vein deposits (such as Central City, Colorado; Sims et al., 1963) are often characterized by large-scale, district-wide zoning patterns. Mineralogically, they are relatively similar to the Cordilleran lode deposits discussed earlier, with the exception that they do not have the well-developed advanced-argillic alteration assemblages typical of the central portions of the Cordilleran lode deposits. The central portions of polymetallic districts (which form closest to the igneous heat source) are typically Au-rich and characterized by a relatively simple assemblage of quartz and pyrite, with lesser chalcopyrite, galena, and sphalerite (\pm enargite, arsenopyrite). Sphalerite, galena, and carbonates such as rhodochrosite and calcite increase in abundance, toward the outer portions of the districts. Quartz-sericite-pyrite alteration of the wallrocks is common in the central portions of the districts, whereas propylitic alteration of the wallrocks to carbonate, epidote, chlorite, and pyrite is most abundant on the fringes of the district.

The adularia-sericite epithermal deposits (examples include Creede and Bonanza, Colorado; Comstock, Nevada; and Sado, Japan) are so-named due to the abundance of these minerals as

vein fill and alteration minerals (Berger and Eimon, 1983; Heald et al., 1987; Sillitoe, 1993); however several different subtypes have been identified, including Creede-, Comstock-, and Sado-type (all named after their characteristic mining districts). All are characterized by simple sulfides (such as sphalerite, galena, and chalcopyrite), sulfosalts (sulfides containing significant As, Sb, \pm Bi), gold, electrum, silver, \pm tellurides as important ore minerals. Quartz, carbonates, and adularia (\pm barite, chalcedony, and fluorite) are important gangue minerals. Creede-type veins are typically silver-rich, and are dominated by pyrite, sphalerite, galena, and chalcopyrite, with variable but lesser amounts of carbonates, quartz, and barite. Comstock-type veins are typically gold-rich, and are dominated by quartz and adularia, \pm carbonates, with pyrite, sphalerite, galena, and other sulfides comprising less than several percent of the vein material. Sado-type veins are Cu-rich equivalents of Comstock-type veins, with quartz, adularia, and carbonates predominating over chalcopyrite. Strong lateral and vertical variations in vein mineralogy may be present in all three epithermal deposit types, and are especially common in the Creede type. An example of mineral zoning along one vein in the Bulldog Mountain Mine at Creede is shown in Plumlee (1999). Strong lateral and vertical variations in wallrock alteration assemblages (silicification, propylitic, argillic, advanced argillic) are also typical in all three epithermal vein deposit types, with intense silicification, and pervasive argillic and advanced argillic alteration common adjacent to shallow portions of the veins, moderate silicification (\pm potassic alteration) close to veins in the deeper levels, and propylitic alteration away from the veins.

Drainage-water compositions

Both polymetallic vein and adularia-sericite epithermal vein deposits can exhibit a wide spectrum of mine- and natural drainage compositions (Appendix, Figs. 19.15 and 19.16), depending upon the base-metal sulfide and pyrite content of the veins, the carbonate content of the veins and wallrock alteration, and the extent of interaction between the drainage waters and the carbonates. Mine and natural waters for polymetallic vein deposits include those collected as part of this study from the Central City and other districts in Colorado, and those collected by Smith (1991) from the St. Kevins Gulch district, Colorado. Waters draining adularia-sericite epithermal deposits include those collected as part of this study from the Creede, Bonanza, and Silverton, Colorado, districts; the Appendix also includes data collected by Moran (1974) from Bonanza, Colorado. The drainage data listed in the Appendix are primarily from the Rocky Mountains of Colorado, but also include two samples collected from the World's Fair district in Arizona. Price et al. (1995) summarize mine water data from several polymetallic vein deposits and adularia-sericite epithermal vein deposits in Nevada.

In general, the most acidic, metal-rich underground mine waters are those that drain pyrite- and base-metal-sulfide-rich ores in sericitically altered igneous rocks, carbonate-poor metamorphic rocks, or highly welded volcanic rocks (polymetallic—Druid, Idaho, and St. Kevins Gulch, Colorado; epithermal—Solomon and Alpha Corsair, Creede district, Colorado). Deposits that are pyrite-rich but that contain significant carbonate minerals in their gangue or wallrock alteration (such as the American Tunnel, Silverton, Colorado) tend to have mine waters with near-neutral pH values but elevated levels of dissolved zinc (as high as many tens of mg/l) and copper (as high as several mg/l). As discussed previously the

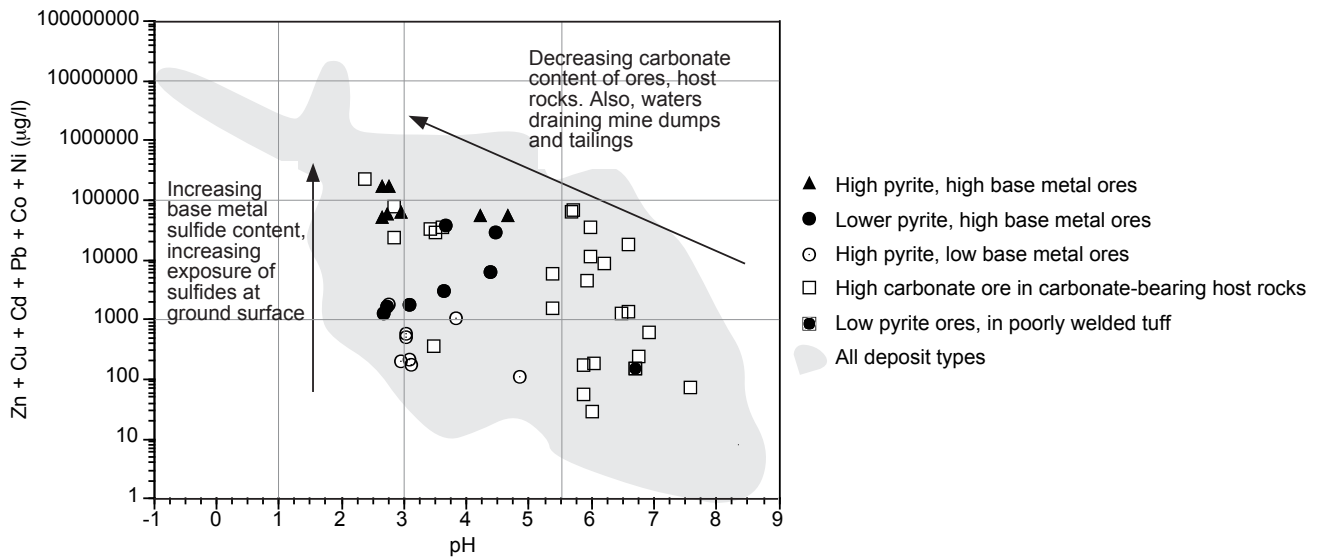


FIGURE 19.15—Ficklin plot showing the dissolved sum of base metals in mine and natural waters draining polymetallic vein and adularia-sericite epithermal vein deposits. Due to general similarities in the geologic characteristics of the deposits, the waters are not grouped according to deposit type. Shaded area encloses all data points on Figure 19.2.

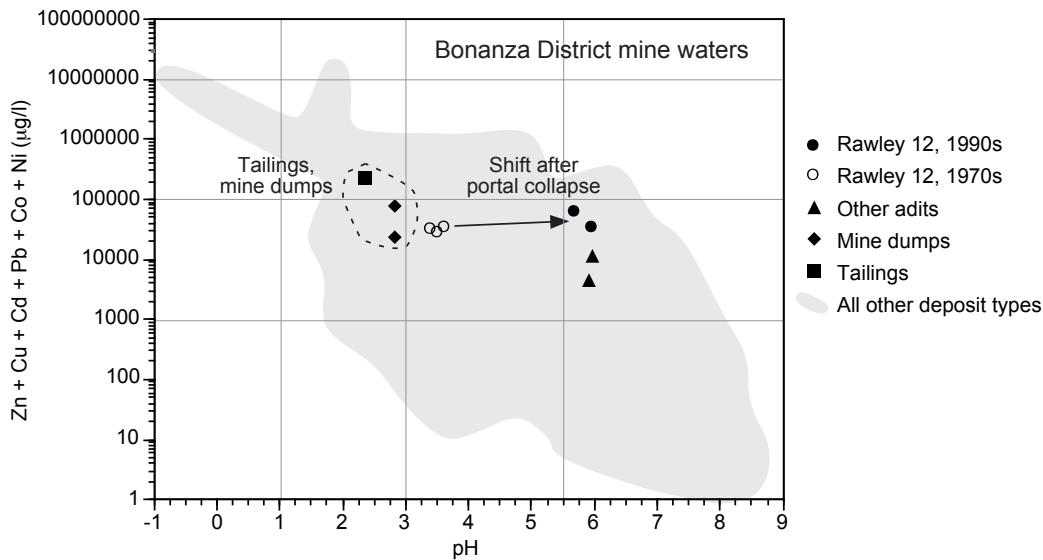


FIGURE 19.16—Ficklin plot showing the dissolved sum of base metals in mine waters draining adularia-sericite epithermal vein deposits in the Bonanza district, Colorado. The veins contain abundant pyrite, sphalerite, galena, and chalcocopyrite, and very little carbonate. The volcanic host rocks, however, are variably propylitized to contain carbonate. See text for explanation of different water compositions. Shaded area encloses all data points on Figure 19.2.

elevated dissolved zinc levels reflect zinc’s tendency to not sorb onto particulates at near-neutral pH values, and the elevated dissolved copper levels reflect copper’s tendency to desorb from particulates due to competition from copper carbonate complexes (Smith, 1999). If oxygenated, the near-neutral waters can also carry substantial amounts of zinc, lead, copper, and other metals in suspended hydrous ferric oxide particulates.

Compositions of waters draining underground mine workings in the Central City district, Colorado, illustrate the substantial

variations in composition that can occur across a district as a result of large-scale zoning of the vein mineral assemblages. As initially pointed out by Wildeman et al. (1974), waters draining quartz-pyrite veins in the central portions of the district (see Druid seep and Idaho adit water compositions in Appendix) are highly acidic and metal-rich. In contrast, increasing carbonate content and decreasing pyrite content of the veins toward the lateral portions of the district results in mine waters that have progressively higher pH and lower base metal contents (e.g., the National

Tunnel water compositions in the Appendix). Plumlee (1999) includes figures showing both the Central City district mineral zoning patterns and variations in mine-water composition across the district.

As demonstrated by mine, waste, and tailings waters in the Bonanza district, Colorado (Fig. 19.16), substantial ranges in drainage pH and metal content can occur in a given deposit where pyrite-rich, carbonate-poor veins are hosted by propylitically altered wallrock (Fig. 19.16). Waters flowing primarily along the veins are typically quite acidic and metal-bearing, because they interact little with the carbonate minerals in the wallrock alteration. If fracture systems or mine workings route the waters through the altered rock, or if the acidic waters from the veins mix with waters from unmineralized fractures in the altered wallrock, then higher pH values result. Highly acidic waters may occur in tailings due to the selective concentration of pyrite by depositional winnowing within the tailings impoundments. Mine dump waters may also be acidic if the dumps have large amounts of pyritic vein or wallrock materials. Dissolution of soluble salts in the dumps by storm or snowmelt waters can generate acid that is not buffered due to lack of time or opportunity to react with carbonate minerals in the dumps.

Compositional shifts of the waters draining the Rawley adit, Bonanza, Colorado, from the 1970s (Moran, 1974) to the 1990s (this study) illustrate the complex interactions between hydrology, geology, and geochemistry that can take place in pyritic veins hosted by propylitically altered wallrock (see data in Appendix and Fig. 19.16). In the early 1970s, the adit was open to at least 700 m in from its portal (R. Moran, oral commun., 1995). At some point during the mid to late 1970s, the portal collapsed, leaving only a small, several-cm opening at the top of the portal from which the waters flowed. In 1973 and 1974, the adit waters were quite acidic (pH 3.7) (Moran, 1974). The adit waters we measured in this study in 1992 and 1993 had much higher pH (around 6) and very low dissolved oxygen. The dissolved concentrations of the predominant metals (Fe, Al, Zn, Cu, Pb) are substantially greater in the higher-pH 1990s waters than in the more acidic 1970s waters. Our interpretation of these compositional shifts is that the ponding of the waters behind the collapsed portal (1) allowed the waters to interact more with the propylitically altered wallrock (thereby helping to maintain a near-neutral pH), and (2) allowed the waters to remain unoxidized until they flowed out the portal opening (presumably, this inhibited the formation of hydrous ferric oxide particulates, a resulting drop in pH, and sorption of metals onto the particulates).

Hot-spring Au-Ag and Hg deposits

Hot spring deposits form where hydrothermal systems flow near to, and (or) discharge onto the Earth's surface; they are commonly associated with epithermal vein deposits at depth, as both may form from the same meteoric-hydrothermal systems. Two dominant types are noted, depending upon the dominant metal of value: hot-spring Au-Ag (Berger, 1986), and hot-spring Hg (Rytuba, 1986). Both types of hot spring deposits are enriched in the suite of trace elements commonly referred to as "mobile epithermal," which includes As, Sb, Hg, Tl, and Au. The deposits consist of chalcedony- and opal-bearing sinter terraces that formed where hydrothermal fluids discharged onto the Earth's surface. The deposits are underlain by stockwork vein systems

that contain silica minerals (quartz, chalcedony, opal), adularia, carbonates (such as calcite), sulfides (including pyrite, marcasite, stibnite, realgar, cinnabar), \pm native sulfur, \pm native mercury. Ore deposition resulted from boiling and cooling of the hydrothermal fluids, and mixing of the hydrothermal fluids with shallow ground waters. Near-surface condensation and oxidation of H_2S boiled from the hydrothermal fluids produces shallow acid-sulfate alteration of the wallrock to alunite, kaolinite, and clays. With increasing depth, the rocks are variably silicified and altered to contain adularia, carbonates, and chlorite. Examples of hot spring deposits include Leviathan, Sulphur Bank, and McLaughlin, California, and Round Mountain, Nevada (Tingley and Bonham, 1986).

Drainage-water compositions

Selected mine drainage data exist. Those available are from the hot-spring deposit at the Leviathan mine, California, (Ball and Nordstrom, 1989) are included in the Appendix and shown on Figure 19.17. The Leviathan waters are highly acidic, and drain wallrocks that have been altered to an acid sulfate assemblage containing alunite, kaolinite, clays, native sulfur, pyrite, marcasite, and chalcocopyrite. Due to the general lack of base metal sulfides in the ores, the Leviathan mine waters have a lower sum of base metal concentrations than most other highly acidic mine waters. As a result of the presence of chalcocopyrite in the ores and the lack of sphalerite, dissolved copper levels exceed those of zinc. The waters also contain relatively high concentrations of dissolved Co, Ni, and Cr (1–14 mg/l), which may have ultimately been derived from the host andesite volcanics. The arsenic-rich nature of the ores is manifested in the arsenic-rich mine water compositions, which are exceptionally enriched in arsenic and have the highest arsenic concentrations (as high as 45 mg/l) of all similarly acidic waters draining all deposit types. Thallium concentrations are also exceptionally high (near 1 mg/l; Ball and Nordstrom, 1989), again reflecting the enrichments of this "mobile epithermal" element in this type of deposit.

The Leviathan data reflect waters draining the most acid-generating portions of hot spring deposits. We have not sampled or seen data in the literature for mine waters draining stockwork ores, although a broad range in possible pH values and metal contents is possible given the mineralogy of the stockwork ores. If carbonate minerals are abundant, as at McLaughlin, California, it can be inferred (based on analogies with other deposits containing arsenic sulfides and carbonates for which drainage data are available) that drainage waters may have near-neutral pH values and somewhat elevated concentrations of arsenic (as high as several hundred $\mu\text{g/l}$?). In stockwork ores with lower carbonate mineral contents and high contents of pyrite and marcasite, it is possible that the drainage waters could be more acidic, with correspondingly higher concentrations of arsenic. Dissolved anion concentrations could also be elevated, especially in acidic waters.

The data available from the literature do not include analyses for mercury. However, unpublished drainage data recently collected by J. Rytuba for several mercury deposit types indicate that the greatest concentrations of Hg in drainage waters arise due to the dissolution of soluble Hg salts from wastes left over after the roast-processing of the ores (J. Rytuba, oral commun., 1997). Concentrations of mercury in the most acid waters may reach as high as several mg/l Hg total, and several hundred $\mu\text{g/l}$ methyl mercury, its most toxic form (J. Rytuba, oral commun., 1997).

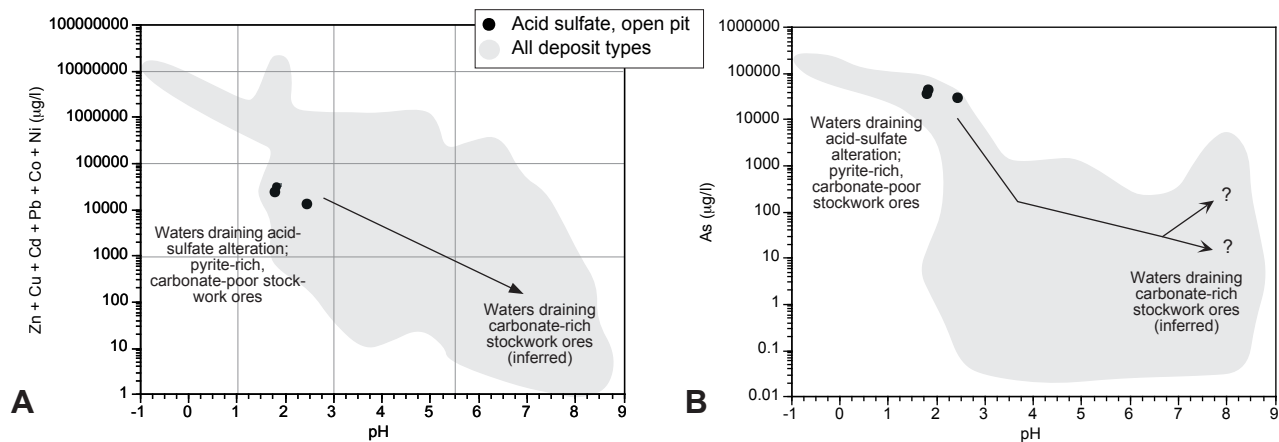


FIGURE 19.17—Plots of mine-drainage compositions for waters draining quartz alunite alteration in the Leviathan, California, hot spring deposit. A. Ficklin diagram; B. Dissolved arsenic. Note differences in scale of the concentration axis between the plots. Shaded areas enclose all data points on corresponding Figures 19.1, 19.2.

Skarn and polymetallic replacement deposits

Skarn and polymetallic replacement deposits are genetically related to magmas that intrude into sedimentary rock sequences; they form when magmatic-hydrothermal fluids are expelled from the magmas and react chemically with the sedimentary rocks. Both types of deposits may therefore be spatially associated with and genetically related to porphyry-Cu, -Cu-Mo, or -Climax-Mo deposits (Fig. 19.18). Examples of polymetallic replacement deposits include: Leadville, Gilman, and Rico, Colorado; New World, Montana; and Park City and Tintic, Utah. Skarn ores are relatively minor ore types in districts with major replacement deposits; however, the New World district does have important skarn and replacement ores. There are skarn deposits associated with a number of porphyry-Mo, -Cu-Mo, and -Cu deposits worldwide, such as Yerington, Nevada; Chino district, New Mexico (the Groundhog deposit), and others.

Skarn deposits typically occur on the outermost portions of their associated intrusions (endoskarn) or in the sediments adjacent to the intrusions (exoskarn) (Hammarstrom et al., 1995). Both the sedimentary and igneous host rocks are intensely altered to a mineral assemblage dominated by carbonate minerals and calc-silicate minerals such as diopside-hedenbergite, wollastonite, tremolite-actinolite, and garnets. Ore minerals in the skarns typically include chalcopyrite, sphalerite, and galena, and are commonly related to carbonate-rich alteration assemblages. Common iron minerals include pyrite, magnetite, and hematite. The skarn ores typically occur as veins, massive lenses, or disseminations within the calc-silicate-altered host rocks.

Polymetallic replacement deposits may be Pb-Zn-rich or Cu (\pm Au-) rich. In general, the replacement deposits that are deeper and proximal to the intrusive stock are Cu-rich, with increasing Pb and Zn and decreasing Cu with increasing distance from the stock (Morris, 1986; Titley, 1993). In addition, polymetallic replacement deposits that are associated with porphyry-Mo deposits have higher Pb and Zn than those that are associated with porphyry-Cu deposits. Several different ore types are typical of the polymetallic deposits, and may include: massive sulfide lenses and veins occurring within and (or) replacing sedimentary host rocks; mineralized breccias within the sedimentary rocks, and;

veins within associated igneous sills and dikes (Fig. 19.18). The deposits typically consist of Fe-rich sphalerite, galena, pyrite, marcasite, chalcopyrite, argentite, \pm tetrahedrite, \pm enargite, \pm digenite, and native Au (Morris, 1986; Titley, 1993). Chalcopyrite, enargite, and native gold are more abundant in replacement deposits that are proximal to the igneous intrusions. Quartz and carbonate minerals such as calcite also are present as gangue minerals. Some calc-silicate alteration of the sedimentary host rocks, as well as alteration of carbonate sedimentary rocks to jasperoid may also be present. The igneous host rocks are typically altered to quartz-sericite-pyrite assemblages.

Drainage-water compositions

We have collected mine-water samples from several polymetallic replacement districts in Colorado (Leadville; Bandora, near Silverton) and Utah (mines unidentified at property owner's request). We have also included in our database (Appendix) published mine-water compositions from polymetallic replacement deposits at Gilman, Colorado, and from polymetallic replacement and skarn deposits from New World, Montana (Pioneer Technical Services, 1994). The mine water compositions show a broad range in pH and metal content that can be ascribed to differences in ore types (Fig. 19.19).

Mine-waters draining the skarn deposits at New World are quite acidic and have relatively high levels of dissolved metals (Fig. 19.19). We interpret this to reflect the lack of neutralizing reactions between the acid waters and the calc-silicate alteration minerals in the skarns, and the lack of reactions with any carbonate minerals that may remain in the original sedimentary host rocks. The interpreted lack of reactivity of the calc-silicate skarn minerals is intriguing, given that these minerals have been noted to be more reactive than many of the rock-forming silicate minerals (Kwong, 1993). The copper-rich nature of the New World skarn ores is reflected in the higher levels of Cu relative to Zn in the waters.

In contrast to the acidic waters draining the New World skarn ores, Eppinger et al. (1997) found that spring waters draining Au-skarn ores of the Nabesna district, Alaska, have near-neutral pH

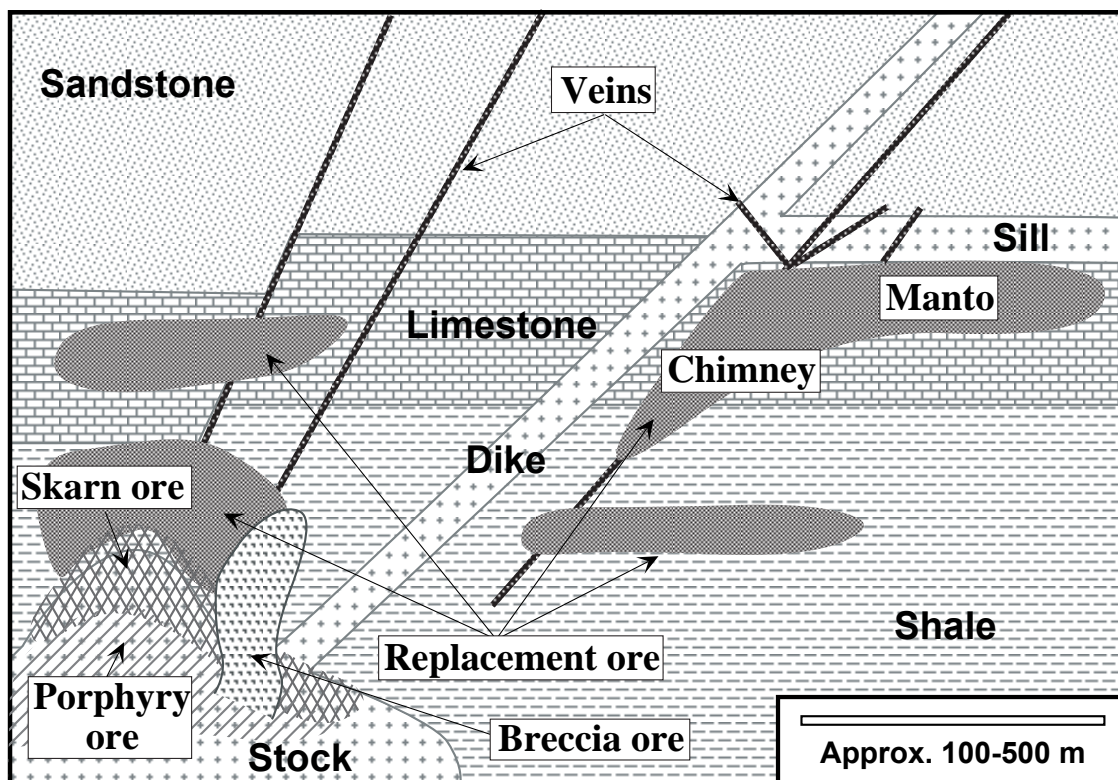


FIGURE 19.18—Conceptual cross section showing mineral-deposit types that are commonly associated with intrusions of magma into sedimentary rock sequences.

values with low dissolved metal concentrations (data are not included in the Appendix, but their compositional ranges are shown on Fig. 19.19). These differences presumably reflect a much greater proportion of acid-buffering carbonate minerals in the Nabesna deposit. However, leach studies of Nabesna tailings and mine waste samples collected during a dry period showed that quite acidic and metal-rich waters may form during rainfall or snow melt events due to the dissolution of soluble secondary salts in the tailings and mine waste materials (Eppinger et al., 1997).

Polymetallic replacement ores hosted by carbonate sedimentary rocks tend to have mine-drainage water compositions that are relatively near-neutral pH (due to the acid-buffering capacity of the host rocks), but that can carry quite high levels of zinc (as high as 170 mg/l) and some copper (as high as several mg/l in waters draining copper-rich orebodies). In general, the highest Zn and Cu concentrations (several mg/l to tens of mg/l Zn and up to several mg/l Cu) occur in waters that drain pyrite-rich ore bodies and that contain low dissolved oxygen; the low oxygen levels prevent hydrous ferric oxides from precipitating and then sorbing the Zn and Cu. Where the near-neutral waters are oxidized, the amount of iron precipitates that form are generally small, and therefore do not serve as a ready sorption sink for the Zn. We do not currently have drainage data for waters draining carbonate-rich mine waste piles and tailings from polymetallic replacement deposits. It is possible that storm or snow-melt waters draining mine wastes and tailings may be quite acidic and metal-bearing if acid generated by dissolution of acid-storing soluble salts does not react sufficiently with the carbonates, either because of rapid runoff rates from the

wastes or the armoring of the carbonate rock surfaces by hydrous iron or aluminum oxides.

Mine waters draining polymetallic veins hosted by igneous dikes and sills, such as the Yak Tunnel waters (Appendix), are acidic and metal-rich (Fig. 19.19), due to the lack of acid-neutralizing capacity of the sericitically altered igneous host rocks, and are similar in composition to waters draining polymetallic veins in districts (such as Central City, Colorado) without carbonate rocks.

Stratiform shale-hosted (SEDEX) deposits

Shale-hosted massive sulfide deposits (also termed sedimentary-exhalative, or SEDEX) are characterized by massive beds of sulfides within black shale and chert-bearing host rocks (Large, 1980; Goodfellow et al., 1993; Kelley et al., 1995). These syngenetic deposits are similar in some respects to the volcanogenic massive sulfide deposits discussed earlier, in that they are thought to have formed through the discharge of hydrothermal fluids onto the sea floor, and are somewhat similar in ore mineralogy and texture. They are different from the VMS deposits, however, in their predominantly black shale and chert host rocks, lesser carbonate host rocks, and in their geologic occurrence in failed continental rifts. The deposits can be very extensive laterally, from hundreds of meters to kilometers (Kelley et al., 1995). Examples include: Red Dog, Lik, and Drenchwater, Alaska; Sullivan, British Columbia; and Mt. Isa and Broken Hill, Australia.

Strong primary mineral zoning is common in SEDEX deposits.

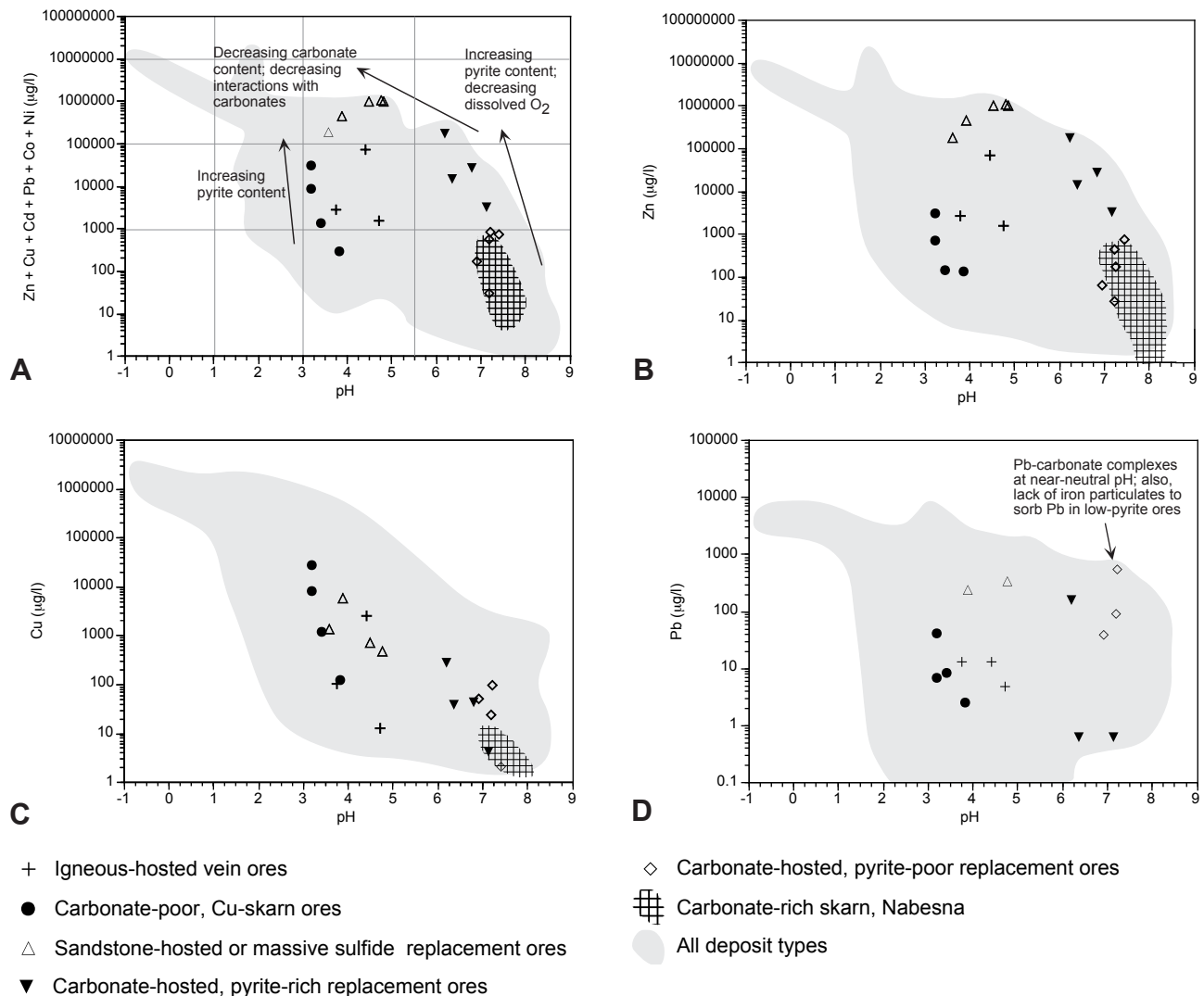


FIGURE 19.19—Plots of mine-drainage compositions for waters draining skarn and polymetallic vein and replacement deposits. A. Ficklin diagram; B. Dissolved Zn. C. Dissolved Cu. D. Dissolved Pb (Nabesna skarn waters had Pb concentrations below 0.1 µg/l). Note differences in scale of the concentration axis between the plots. Shaded areas enclose all data points on corresponding Figures 19.1, 19.2.

The feeder system for the hydrothermal fluids (which is generally linked to a syn-sedimentary fault) is characterized by high degrees of alteration of the host cherts and carbonates to quartz, muscovite, chlorite, siderite, ankerite, tourmaline, and lesser chalcopyrite, pyrrhotite, pyrite, galena, sphalerite, tetrahedrite, and arsenopyrite (Goodfellow et al., 1993). Overlying the feeder zone is the vent complex, where the hydrothermal fluids discharged onto the ocean floor. This is marked by massive, vein, and replacement sulfides such as pyrite, pyrrhotite, marcasite, galena, and sphalerite, with lesser chalcopyrite, arsenopyrite, and sulfosalts. Carbonates may also be in the vent complex. The vent complex mineralization grades laterally into bedded ore facies sediments, with hydrothermal mineral beds (containing pyrite, pyrrhotite, marcasite, sphalerite, galena, barite, calcite, witherite, siderite, and ankerite) interlayered with beds of the host cherts,

shales, or carbonates. Distal sedimentary facies occur lateral to the bedded ore facies, and are marked by low-grade hydrothermal barite, ± pyrite, ± phosphatic chert beds interlayered with the host rock beds.

Sulfides in the bedded portions of the deposits are typically very fine grained (Goodfellow et al., 1993; Kelley et al., 1995). Framboidal and botryoidal textures in the sulfides are common. Crustiform textures and coarser grain sizes are more common in the feeder zones.

Other than the predominant Pb, Zn, and Cu, trace elements that are variably enriched in SEDEX deposits are cadmium (in sphalerite); silver, arsenic, and antimony (in sulfosalts and possibly in botryoidal pyrite/marcasite); and mercury (which can reach quite high levels in pyrite, sphalerite, and sulfosalts) (Kelley et al., 1995).

Drainage-water compositions

Although there are probably mine-drainage data available for SEDEX deposits, we have not yet encountered any in the literature. Several studies have examined natural pre-mining drainage signatures of SEDEX deposits in the Alaskan Brooks Range, and representative data from these studies are included in the Appendix and shown graphically on Figure 19.20.

Kelley and Taylor (1997) compared the compositions of natural stream waters draining several unmined SEDEX deposits in Alaska, including the Lik, Red Dog, and Drenchwater deposits. They demonstrated that the compositions of spring and stream waters are strongly dependent upon the geologic characteristics of the deposits and their host rocks (grade of mineralization, proportion of iron sulfides in the ore, carbonate content of rocks in the watershed) and the extent of exposure of the deposits at the ground surface. Waters that drained Red Dog prior to mining were quite metal-rich (sum of dissolved base metals greater than 10 mg/l, and had variable pH values ranging from less than 4 to near 7. The reddish iron precipitates that form in streams in the area were partly responsible for the discovery of the deposit. The most acidic and metal-rich waters most likely reflect the abundance of base-metal sulfides in the ores (Kelley and Taylor, 1997). The high metal levels may also in part reflect the results of glaciation in the area within the last several thousand years, which exposed fresh, unweathered sulfides at the ground surface. Higher pH stream waters may reflect variable amounts of dilution by waters draining unmineralized rocks outside the main deposit (Kelley and Taylor, 1997), or variable amounts of carbonates in the ores or adjacent wallrocks. In contrast to Red Dog, the Lik deposit occurs in a watershed with abundant carbonate sedimentary rocks. As a result the natural stream waters have generally near-neutral pH values with relatively low to moderate metal concentrations. The Drenchwater deposit waters primarily drain pyrite-rich mineralization exposed at the surface. Due to the relatively low abundances of sulfide minerals other than pyrite in the Drenchwater rocks, the natural drainage waters, although acidic, have general-

ly lower dissolved concentrations of Zn, Cu, and other metals than waters of similar pH draining sphalerite-, chalcopyrite-, and galena-rich mineral deposits (Kelley and Taylor, 1997).

W.R. Miller (unpub. data) has analyzed water samples collected from natural springs draining unmined SEDEX deposits in the Alaskan Brooks Range. Several of these samples are listed in the Appendix and shown on Figure 19.20. Miller (oral commun., 1996) attributes the extremely high dissolved metal concentrations of these waters to the exposure of the unweathered sulfides at the ground surface by glaciation, slow rates of weathering in the cold Arctic climate since the last glaciers retreated, and the residual concentration of the waters by partial freezing in the wintertime. The lower pH and higher metal concentrations of these spring waters compared to those of the stream waters (Fig. 19.20) suggests that dilution by surface waters draining unmineralized areas may be important in producing the range in pH of the stream waters.

Mississippi-Valley-Type (MVT) deposits

MVT deposits are lead- or zinc-rich deposits that are hosted by dolostones (predominant), limestones (less common) and sandstones (much less common) within continental sedimentary basins (see Leach and Sangster, 1993; Leach et al., 1995; and references therein). The deposits formed from heated basinal brines that migrate regionally away from mountain uplifts on basin edges (Leach and Sangster, 1993). The basinal brines deposit small amounts of sulfide minerals (iron sulfides, sphalerite, galena) regionally in the sedimentary aquifers through which they flow. The ore-grade mineral deposits form where zones of permeability allow focused mixing of brines from different aquifers, or flow of brines from one aquifer (such as a dolostone) into a chemically reactive different aquifer (such as a limestone) (Fig. 19.21). Although individual deposits are generally small, they occur in deposit clusters or districts that constitute world-class resources of lead and (or) zinc (Leach and Sangster, 1993). Examples

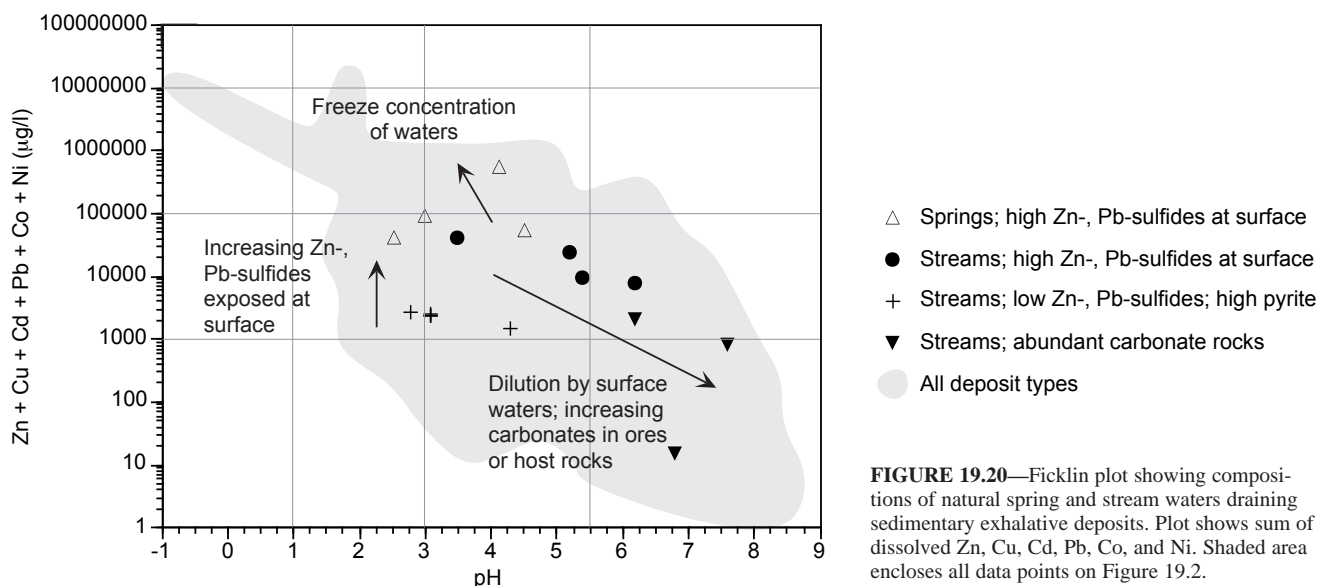


FIGURE 19.20—Ficklin plot showing compositions of natural spring and stream waters draining sedimentary exhalative deposits. Plot shows sum of dissolved Zn, Cu, Cd, Pb, Co, and Ni. Shaded area encloses all data points on Figure 19.2.

include the Old Lead Belt and Viburnum Trend (southeast Missouri), Tri-State (Missouri, Kansas and Oklahoma), Northern Arkansas, Upper Mississippi (Wisconsin), and Central Tennessee districts in the United States; Pine Point, Polaris, and Nanisivik in Canada; and, Silesia in Poland. Many of the deposits are zinc-rich with lesser lead; however, some deposits, such as the Viburnum Trend and Old Lead Belt districts in SE Missouri are predominantly lead-rich. Commodities other than lead and zinc which are variably produced from the deposits include silver, cadmium, germanium, barite, fluorite, and, rarely, nickel.

The ore and gangue mineralogy of the deposits is generally simple (Leach and Sangster, 1993; Leach et al., 1995), with predominant sphalerite, galena, pyrite, marcasite, dolomite, calcite, and quartz, and variable but lesser barite, chalcopyrite, bornite, enargite, and other sulfides. Ore mineral zoning is variable within individual deposits. Mineralogical variations within districts or deposits may reflect lack of occurrence of particular generations of mineralization; for example, some deposits in the Silesian MVT district contain a major late-stage botryoidal marcasite generation, whereas others do not (Viets et al., 1996).

Silicification (replacement of the dolostones and limestones by massive silica to form jasperoids), dolomitization (replacement of limestones by dolomite), and dissolution of the host carbonates (leading to large-scale solution collapse breccias) are the predominant alteration types in these deposits. In addition, formation of authigenic clay and feldspar minerals and destruction of detrital potassium-silicate minerals occurs in some districts.

The ores occur as open-space fillings in veins and breccias, and as replacements of the carbonate host rocks. The breccias may either be pre-mineralization karst breccias, or breccias created by

carbonate dissolution during mineralization. Textures may vary substantially within a deposit, and include massive, fine-grained, very coarse grained (well-formed single crystals up to more than a meter in size), botryoidal, colloidal, and skeletal (Leach and Sangster, 1993).

In addition to the metals discussed previously, copper, nickel, cobalt, arsenic, and thallium are also enriched in some MVT deposits. For example, copper sulfides (bornite, chalcopyrite), and nickel and cobalt sulfides (such as millerite and vaesite) are relatively abundant in the SE Missouri districts, and are common as trace minerals in other MVT districts (Leach et al., 1995). The Silesian MVT deposits have strong enrichments of arsenic (as high as several percent) and thallium (as high as several thousands of ppm) in sphalerite and marcasite (Viets et al., 1996).

Predominant secondary minerals formed during pre-mining weathering of the deposits include iron oxides, cerussite (lead carbonate), anglesite (lead sulfate), smithsonite (zinc carbonate), and goslarite (zinc sulfate) (Leach et al., 1995). The reactivity of sulfides during post-mining weathering of MVT deposits is related to the sulfide mineralogy, texture, and trace-element content. Coarse-grained sphalerite and galena weather relatively slowly (galena to anglesite; sphalerite to goslarite), whereas botryoidal, arsenic-rich marcasite that occurs in a number of deposits weathers quite rapidly to a variety of secondary iron sulfates such as melanterite, copiapite, and others. For example, horn-shaped crystals of melanterite up to several cm long grow directly on As-rich marcasite in humid underground workings in a Silesian MVT deposit; the melanterite forms by the reaction of the As-rich marcasite with water vapor in the air. Acid generated by marcasite weathering may also enhance the reactivity of sulfides intergrown

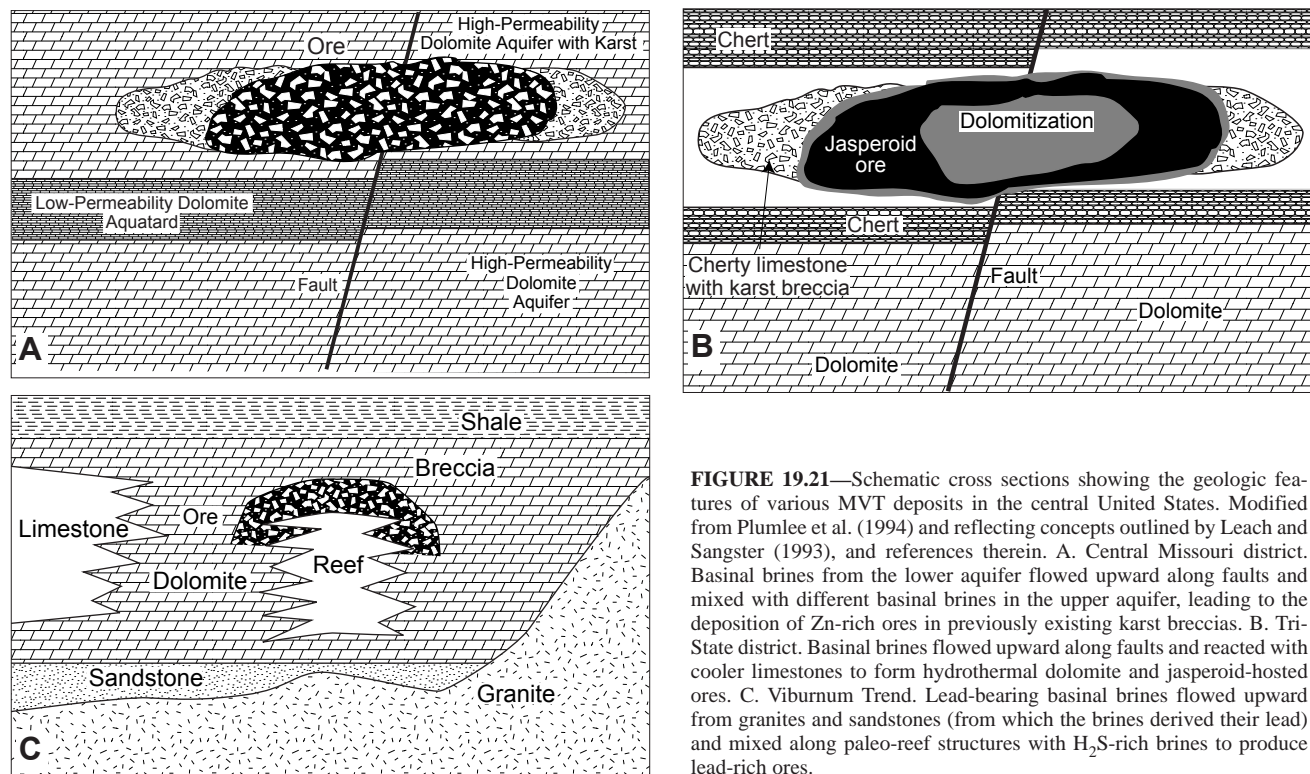


FIGURE 19.21—Schematic cross sections showing the geologic features of various MVT deposits in the central United States. Modified from Plumlee et al. (1994) and reflecting concepts outlined by Leach and Sangster (1993), and references therein. A. Central Missouri district. Basinal brines from the lower aquifer flowed upward along faults and mixed with different basinal brines in the upper aquifer, leading to the deposition of Zn-rich ores in previously existing karst breccias. B. Tri-State district. Basinal brines flowed upward along faults and reacted with cooler limestones to form hydrothermal dolomite and jasperoid-hosted ores. C. Viburnum Trend. Lead-bearing basinal brines flowed upward from granites and sandstones (from which the brines derived their lead) and mixed along paleo-reef structures with H_2S -rich brines to produce lead-rich ores.

with the marcasite. In humid underground stopes in the Viburnum trend, bornite without intergrown marcasite is quite unreactive, whereas bornite with intergrown marcasite weathers extensively to secondary copper sulfate salts.

Drainage-water compositions

Drainage waters listed in the Appendix include several collected from small, MVT deposits near Leadville, Colorado, as part of this study, and waters sampled by Barks (1977) from MVT tailings impoundments in the Old Lead Belt, SE Missouri. The Appendix also includes mine and tailings waters from the jasperoid-rich Tri-State, Missouri deposits (Smith and Schumaker, 1993). Although not included in the Appendix, a study currently underway is comparing mine waters from the Viburnum Trend with mine waters in the Polish Silesian deposits (D. Leach, J. Viets, oral commun., 1998).

From an environmental standpoint, the geology and mineralogy of MVT deposits are generally conducive to the formation of near-neutral drainage waters with generally low metal contents (Fig. 19.22). This is especially true in deposits with low iron-sulfide contents and (or) low amounts of jasperoid. In several MVT districts with low iron-sulfide and jasperoid contents, such as portions of the Viburnum Trend, mine waters are of sufficiently high quality that they are used as sources of potable waters for the mines and nearby towns (Leach et al., 1995); some near-neutral waters may have elevated lead concentrations as high as several hundred $\mu\text{g/l}$ due to formation of lead-carbonate complexes. Moderately acidic and quite metalliferous (primarily zinc-rich) waters may form in iron-sulfide-rich ore bodies, in jasperoid ores, or in tailings impoundments where physical separation of sulfides from carbonates has occurred (Fig. 19.22). Near-neutral waters with elevated concentrations of dissolved Zn (as high as 100 mg/l) and Pb and Cd (several hundred $\mu\text{g/l}$) may form in mine workings

with high iron sulfide contents; the iron sulfides generate acid waters, but the acid waters then are diluted by high-alkalinity waters draining the surrounding carbonate host rocks.

Preliminary water data collected from the As- and Tl-rich Silesian MVT deposits indicate that, although these trace metals occur in high levels in quite reactive marcasite and in sphalerite, their concentrations are very low in the mine waters (D. Leach, J. Viets, oral commun., 1997). Presumably, both the arsenic and thallium released by weathering of the sulfides form insoluble secondary minerals or are sorbed onto particulates.

Sediment-hosted (Carlin-type) Au deposits

Sediment-hosted Au deposits (also known as Carlin-type Au deposits) are large tonnage, low-grade deposits characterized by the occurrence of microscopic Au disseminated through large volumes of predominantly carbonate-rich, carbonaceous sedimentary host rocks (see Guilbert and Park, 1986; Hofstra et al., 1995; and references therein). Examples of sediment-hosted Au deposits include the Carlin, Jerritt Canyon, and Getchell trends in Nevada; within each trend, several major deposits are present.

Host rocks of the deposits are primarily carbonate sedimentary rocks, although in some deposits, such as Twin Creeks in the Getchell trend, the ores are hosted by cherty marine sediments and marine volcanics. Many of the deposits are localized beneath major thrust faults; black shales above the faults tended to serve as aquitards, and focused fluid flow in the underlying reactive carbonates.

The gold occurs primarily within arsenic-rich pyrite and marcasite, which commonly occur as microscopic overgrowths over diagenetic sulfides or as replacements of sedimentary iron oxides. Lesser amounts of gold occur in primary orpiment or realgar, in organic carbon, or in quartz (Hofstra et al., 1995). The realgar and orpiment can be quite coarse-grained, and are the most readily vis-

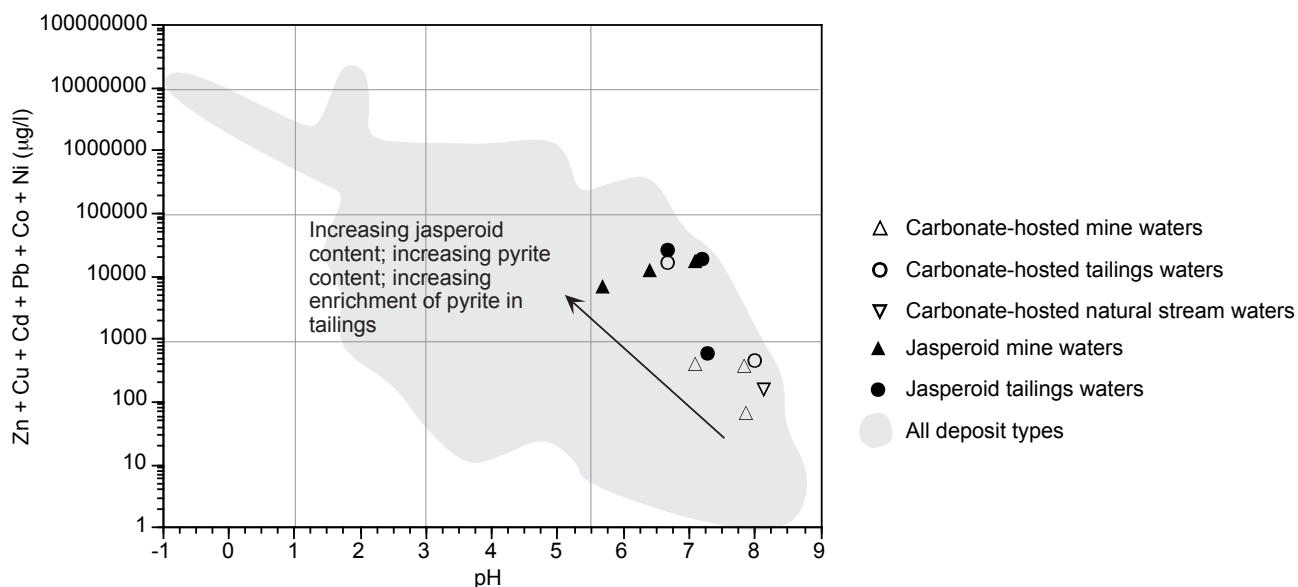


FIGURE 19.22—Ficklin plot showing compositions of mine waters, tailings waters, and a natural water draining carbonate-hosted and jasperoid-rich MVT deposits. Plot shows sum of dissolved Zn, Cu, Cd, Pb, Co, and Ni. Shaded areas encloses all data points on Figure 19.2.

ible ore minerals. Other primary hydrothermal minerals include calcite, dolomite, quartz, barite, cinnabar, and clays. In some deposits, late-stage, coarse grained botryoidal pyrite and marcasite are present.

As indicated by their primary mineralogy, sediment-hosted Au deposits are noted for their strong enrichments in arsenic. Other trace elements include many other of the “mobile epithermal” suite, including Hg, Sb, and Tl. Tungsten and selenium are also present. Base metals such as Zn, Cu, and Pb are conspicuously low in abundance. In deposits where black shales serve as aquitards, metals contained in the shales such as Mo, Co, Ni, U, and Se, may be environmentally important.

Hofstra et al. (1991) concluded that the Jerritt Canyon sediment-hosted Au deposits formed from moderately acidic, H₂S- and As-rich hydrothermal fluids that mixed with cooler, dilute, oxidized ground waters and reacted with Fe-bearing carbonate rocks. In the cores of the Jerritt Canyon deposits, where hydrothermal fluids flowed into the carbonate rocks from feeder fractures, extensive to complete decarbonatization (decalcification) of the host rocks and residual enrichment of silica occurred; this led to significant volume loss in the host rocks. Contemporaneous with the decarbonatization, deposition of hydrothermal quartz and realgar-orpiment veins, as well as sulfidation of Fe minerals in the host rocks occurred to produce the gold-bearing disseminated arsenian pyrite. Grading outward from the feeder zones, the extent of decarbonatization, realgar-orpiment veining, disseminated pyrite, and gold grades progressively decrease; this is accompanied by a progressive increase in the amount of carbonate remaining in the wallrock, as well as an increase in the amounts of pre-ore and ore-stage calcite veins (Hofstra et al., 1991; Hofstra et al., 1995). In deposits (such as Twin Creeks in the Getchell trend) where the ores occur within marine volcanic and siliceous sedimentary rocks, evidence of acid leaching and residual silica enrichment is also present.

Much of the sediment-hosted Au production to date in Nevada has come from the oxide ores. The dry climates in Nevada led to deep weathering of the ore bodies to produce secondary oxides such as hematite, goethite, and limonite, sulfates such as gypsum and celestite, and oxides of arsenic (scorodite, an Fe-As oxide) and antimony (stibiconite) (Hofstra et al., 1995). In these oxide

ores, gold occurs in the iron oxides, in quartz, and on clay minerals. The occurrence of Au in the oxide ores makes them quite amenable to cyanide-heap leaching, a very cost-effective processing method. Increasingly, many deposits are producing gold from the non-oxidized ores (also known as refractory ores) that have high sulfide contents. These ores require special treatment such as roasting or biologically-enhanced oxidation in order to remove the sulfides and organic matter, followed by cyanidation.

Drainage-water compositions

Limited natural- and mine-drainage data are available for sediment-hosted Au deposits from a variety of literature sources. The Appendix includes data for several open-pit lakes (collected or compiled by Price et al., 1995) and ground water pumped from beneath and up hydrologic gradient from the Twin Creeks pits in the Getchell Trend (BLM, 1996). In addition to the data listed in the Appendix, Grimes et al. (1995) collected data from exploration drill holes along the Getchell trend in Nevada. Environmental impact statements submitted to agencies such as the Bureau of Land Management (BLM) are additional sources of natural ground water and mine-drainage data for a number of sediment-hosted deposits.

The data listed in the Appendix and shown on Figure 19.23 illustrate several important aspects of mine waters not only from these deposits, but also other deposits which have been completely oxidized prior to mining. Due to the acid-buffering effects of carbonate-rich host rocks and the low acid-generating potential of the oxide ores, all of the mine waters included in the Appendix have near-neutral pH values. However, unoxidized pyrite- and sulfide-rich ores in zones of intense decarbonatization may generate locally quite acidic waters. As would be expected from the major- and trace-element geochemistry of the deposits, the mine waters from sediment-hosted Au deposits generally have low concentrations of the base metals (Fig. 19.23), but relatively high concentrations of As (Fig. 19.23B). In addition to the data listed in the Appendix, several of the sediment-hosted pit waters have extremely high concentrations of Sb (as high as several mg/l) (BLM, 1996), and relatively high concentrations of Se (several

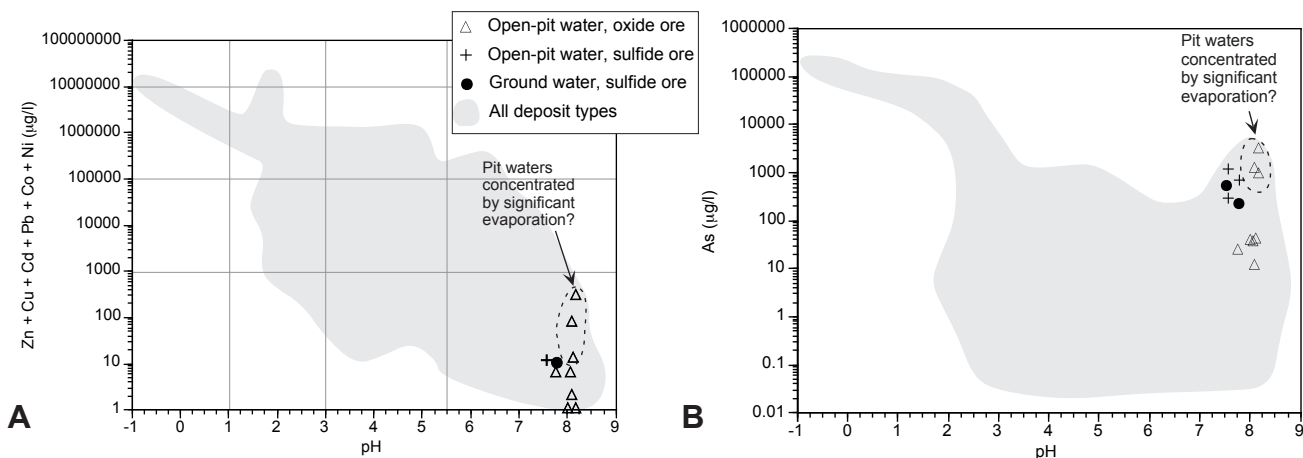


FIGURE 19.23—Plots of mine-water compositions for some sediment-hosted Au deposits. A. Ficklin diagram; B. Dissolved arsenic. Note differences in scale of the concentration axis between the plots. Shaded areas enclose all data points on corresponding Figures 19.1, 19.2.

tens of $\mu\text{g/l}$) (Price et al., 1995). At present, analytical data showing the concentrations of metals such as Mo, Co, Ni, and U in sediment-hosted Au deposit waters are quite sparse. However, these metals are relatively mobile in near-neutral pH waters, and may have source rocks in the black shales overlying many of the Nevada deposits. Hence, these metals may be present in measurable, possibly significant concentrations, and may have a source from outside the deposits themselves.

The arsenic concentrations measured in these deposits are among the highest measured in near-neutral waters draining all mineral deposit types. They likely reflect the desorption of arsenate species from particulates at higher pH in oxidized pit waters, and the high mobility of reduced arsenite species in reduced ground waters.

In general, waters in oxidized ores have lower metal and As concentrations than those in sulfide ores. The exceptions to this in the Appendix are the open pit waters from the oxide Boss deposit, Nevada, which have some of the highest concentrations of base metals (Cu, Pb in hundreds of $\mu\text{g/l}$) and As (as high as several mg/l) in mine water data we have compiled to date for this deposit type. The extreme chloride concentrations in the Boss waters (as high as 4300 mg/l) suggest that the Boss pit waters have undergone extensive evaporative concentration, which may be an explanation for the anomalously high As and base metal concentrations. However, leaching of Cl from the shales may have also contributed to the extreme chloride concentrations.

Magmatic sulfide deposits

Magmatic sulfide deposits are a subset of a broader class of mineral deposits known as magmatic segregation deposits. They are somewhat unusual among sulfide ore deposits in that they form by the segregation and crystallization of sulfide- and metal-rich immiscible liquids from crystallizing mafic magmas (Guilbert and Park, 1986; Cox and Singer, 1986; Foose et al., 1995; and references therein). The largest of these deposits are associated with layered mafic intrusions such as the Sudbury Complex, Ontario, Canada, the Duluth Complex, Minnesota, the Stillwater Complex, Montana, and the Bushveld Complex, South Africa. However, a number of smaller deposits can occur related to ultramafic volcanic rocks or ultramafic accumulations in Alpine ophiolite complexes (packages of sea floor rocks accreted to continents).

These deposits are characterized by massive lenses or bodies of sulfides; in some deposits, the sulfides fill in spaces around crystals of the associated host rock minerals. The mineralogy reflects the enrichments of S, Fe, Ni, Cu, Co, and platinum-group elements in the ores, and lesser enrichments of As, Pb, Zn, Te, and other trace elements. Pyrrhotite, pentlandite (a Fe-Ni sulfide), and chalcopyrite, are the dominant sulfides. Other sulfides include other Ni-sulfides (such as millerite), Ni- and Co- arsenides (such as gersdorffite), sphalerite, galena, and various gold-, silver-, and lead-telluride minerals (Foose et al., 1995).

The mafic and ultramafic host rocks of the deposits are characterized by coarse crystals of ferromagnesian minerals such as pyroxenes and olivine, and calcic plagioclase. Minor primary minerals include amphiboles, biotite, and magnetite. Other minerals such as talc, serpentine, actinolite, tremolite, calcite, epidote, and clays probably reflect hydrothermal alteration of the primary host rock minerals (Foose et al., 1995).

Drainage-water compositions

Foose et al. (1995) summarize mine-drainage compositions from the Duluth, Minnesota, and Stillwater Complex, Montana, collected from several sources, including SCS Engineers (1984), Feltis and Litke (1987), and Ritchie (1988). We have listed in the Appendix a sample collected by Eger (1992) from water draining a sulfide ore stockpile from the Duluth Complex. These data are summarized on Figure 19.24. In addition, Blowes and Ptacek (1994) list ranges of pH, Ni, and Al in the Nickel Rim tailings impoundment, Sudbury, Canada.

The range in pH of the drainage waters shown on Figure 19.24, from 4.5 to 7.7 (with most having pH greater than 6), is probably due to variations in the extent of interactions between acid waters generated by oxidation of sulfides and the reactive mafic and ultramafic host rock minerals such as olivine, pyroxenes, and plagioclase. The metal concentrations of the waters, especially those draining sulfide-rich Duluth Complex deposits, show enrichments of Ni (as high as 38 mg/l) and Cu (as high as 22 mg/l), reflecting the enrichments of Ni- and Cu-sulfides in the ores. Zinc concentrations are also high (up to several mg/l). The high concentrations of these metals in near-neutral pH waters most likely reflect the tendency of Ni and Zn not to sorb onto suspended particulates, and the formation of Cu-carbonate complexes that diminish the amounts of Cu that sorb onto particulates. Although no data are available, we speculate that other elements that are possibly enriched in the waters include Fe (in acidic or reduced waters), Mg, Ca, Co, and As, based on the abundance of these elements in the ores or host rocks. Waters that flow within massive sulfide lenses and that do not interact extensively with the surrounding host rocks most likely can generate highly acidic waters with extreme metal concentrations.

In their study of the Nickel Rim tailings impoundment, Blowes and Ptacek (1994) showed that pore waters in the vadose zone of the impoundment develop quite acidic pH values (as low as 2.1), but shift to higher pH with depth in the impoundment due to reactions with carbonate minerals that presumably are from the deposit host rocks. Dissolved nickel concentrations in the more acidic tailings waters are extreme (greater than 250 mg/l), but decrease to less than 10 mg/l at depth in the impoundment where the pH of the waters rises above 5.8. They attributed this to the sorption of the Ni onto secondary iron-hydroxide minerals in the impoundment. This indicates that sorption of Ni by secondary iron oxide coatings is more effective in the rock-dominated tailings environment than by suspended particulates in the water-dominated environment of mine-drainage streams (Smith et al., 1993).

Banded-iron formation (BIF) deposits

Banded-iron formations are the predominant source of iron worldwide. They are chemical sediments precipitated from ocean water, in which iron oxides (hematite, magnetite, limonite), iron carbonate (siderite), iron silicates (chlorite, greenalite, chamosite, grunerite, stilpnomelane), or iron sulfides (pyrite) are finely inter-laminated or interbedded with chert or jasper (a ferruginous chert) (Guilbert and Park, 1986).

Two major types are recognized. Superior-type deposits do not have a clear link to submarine volcanism. In Superior deposits (such as the Mesabi Iron Range, Minnesota, the Marquette Iron Range, Michigan, and Minas Gerais, Brazil), the iron formation is

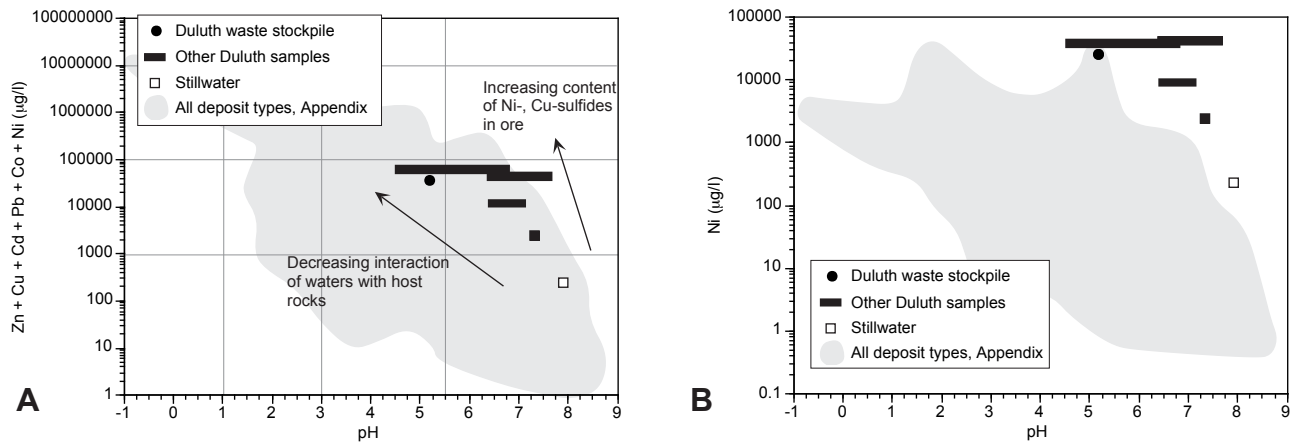


FIGURE 19.24—Plots of mine-drainage compositions for waters draining magmatic sulfide deposits. A. Ficklin diagram; B. Dissolved nickel. Note differences in scale of the concentration axis between the plots. Shaded areas enclose all data points on corresponding Figures 19.1, 19.2.

interbedded with shallow marine sedimentary rocks indicative of deposition on continental shelves (Guilbert and Park, 1986; Cannon et al., 1995a; and references therein). In contrast, Algoma-type BIF deposits (such as the Vermillion Iron Formation, Minnesota, and Sherman Mine, Temagami, Ontario, Canada) are associated with marine volcanic rocks and are therefore likely related genetically to submarine volcanic-hydrothermal processes such as those that produced volcanogenic massive sulfide deposits (Guilbert and Park, 1986; Cannon et al., 1995b; and references therein). Both types of deposits are laterally extensive, extending for many kilometers along strike, and up to tens of hundreds of meters thick.

In many deposits a characteristic zoning in the iron minerals is present reflecting location in the ocean basin, and hence oxidation conditions of the ocean waters at time of formation (James, 1954). Oxide facies were deposited in the near-shore environment, with hematite closest to shore. Toward progressively deeper water, first magnetite and then iron silicates (in the form of amorphous iron silicates) and iron carbonate facies were deposited. In the deepest portions of the basin, sulfide facies iron formation was deposited in areas where the ocean waters became anoxic. Subsequent metamorphism has led to the recrystallization of the ores, with the biggest effect being the formation of fibrous iron silicates such as greenalite, amosite, and minnesotaite.

Weathering of the BIF deposits resulted in leaching of the silica and residual enrichment of the iron. The bulk of the world's BIF iron production has come first from weathered oxide and silicate facies ores, and subsequently from the unweathered, oxide and silicate facies (or taconite) ores (Guilbert and Park, 1986; Cannon et al., 1995b). Relatively little production has come from the carbonate facies or sulfide facies, except where weathering has left behind only secondary iron oxides; however, all facies may be present in a given deposit.

Drainage-water compositions

We have seen only rare mention in the literature of mine-drainage waters from BIF deposits. To date, we have only found one partial analysis of mine waters from Algoma-type BIF

deposits in the Sherman Mine, Temagami, Ontario, Canada (Shelp et al., 1994). The open pit water sampled by Shelp et al. (1994) is clearly from sulfide facies rocks, given the low pH (3.0) of the waters. Given its low pH, the water contains relatively low concentrations of dissolved iron (10 mg/l), manganese (4 mg/l), and the base metals Ni, Cu, and Zn (hundreds of µg/l). These metal variations presumably reflect the abundance of pyrite with low trace metals in the sulfide facies rocks. Trace metal contents of waters draining sulfide facies in Superior-type deposits may have even lower base metal concentrations than those measured by Shelp et al. (1994), due to the generally lower contents of these trace metals in Superior-type deposits. Although generally a minor component of the producing BIF deposits, sulfide facies ores, where present, may pose a potential source of acid-rock drainage.

In general, mine waters draining the much more prevalent oxide, silicate, and carbonate facies BIF ores are likely to have near neutral pH with very low concentrations of metals. This is due to the non-acid-generating nature of the ore and gangue minerals. Pit waters from an oxide-facies iron formation deposit are of sufficiently high quality that they are used as for municipal water supply (W. Day, written commun., 1998).

Low-sulfide, gold-quartz vein deposits

Low-sulfide, gold-quartz vein deposits (also known as mesothermal lode gold and Mother-Lode-type deposits) have been an important source for gold historically, and continue to be explored for and produced in many geologically favorable parts of the world. Examples include the Juneau Gold Belt and Fairbanks, Alaska; Mother Lode, California; Abitibi Belt, Superior Province, Canada; Yellowknife, Northwest Territories, Canada; Kalgoorlie, Australia; and Muruntau, Uzbekistan (see summaries in Guilbert and Park, 1986; Hodgson, 1993; Goldfarb et al., 1995; and references therein).

The ore occurs as native Au in quartz veins in medium-grade greenstone metamorphic rocks (usually metamorphosed basalts, but metamorphosed sediments, ultramafic or felsic volcanic rocks, or granitic intrusive rocks may also host deposits). The veins contain less than 2–3 volume percent sulfides (typically pyrite and

(or) arsenopyrite, with variable but lesser stibnite, chalcopyrite, pyrrhotite, sphalerite, galena, and tetrahedrite). Carbonate minerals, including siderite, ankerite, calcite, or iron-rich dolomite, may be present in the veins.

Wallrock alteration away from the veins is extensive, and includes abundant silicification, carbonatization, and sulfidation; the same sulfide and carbonate minerals present in the veins are introduced as alteration minerals into the surrounding host rocks. Sericite alteration may be also present adjacent to some veins, and grades laterally outward into propylitic alteration containing chlorite and epidote (Goldfarb et al., 1995).

Mineral zoning is generally uncommon. Sulfides in the wall-rock are generally fine-grained, although large arsenopyrite masses may be locally present.

The deposits weather to limonite, leaving behind the quartz. Scorodite, an Fe-As oxide, may also form locally (Goldfarb et al., 1995).

Drainage-water compositions

Goldfarb et al. (1997), Cieutat et al. (1994), and Trainor et al. (1996) present excellent summaries of the geologic controls on mine-drainage compositions from Alaska mesothermal Au deposits. A subset of their data are included in the Appendix.

As with other deposit types having abundant carbonate gangue or carbonate alteration, these vein deposits typically generate mine waters with near-neutral pH values (Fig. 19.25). However, quite acidic pH waters can develop in mine tailings or ore stockpiles, presumably due to the physical enrichment of pyrite and other sulfides. Due to the low base metal sulfide contents of the veins, the near-neutral-pH waters typically have relatively low dissolved base metal concentrations, although vein ores with high pyrite contents and sphalerite contents may generate waters with higher dissolved Zn concentrations of several mg/l. Due to the abundance of arsenopyrite, As is present in mine waters, typically in elevated concentrations ranging from several $\mu\text{g/l}$ to 100 $\mu\text{g/l}$.

Alkalic Au-Ag-Te vein deposits

Alkalic Au-Ag-Te vein deposits have provided significant gold production historically and continue to be the focus of exploration and development. They are spatially and genetically associated with explosive magmatic features (such as diatremes or breccia pipes) in alkalic igneous intrusive complexes. Very large, high grade deposits (such as Cripple Creek, Colorado) may occur; lower-grade vein or disseminated deposits are also common. Other examples include Ladolam, Lihir Island; Emperor, Fiji; Boulder County, Colorado; Ortiz, New Mexico; and Zortman Landusky, Montana. See references such as Thompson et al. (1985), Cox and Bagby (1986), Ahmad et al. (1987), Kelley et al. (1995), and references therein for detailed discussions of the geology of these deposits.

The deposits are characterized by high-grade quartz dominant veins, and low-grade disseminations surrounding the veins (Kelley et al., 1995). Important vein ore minerals include Au- and Ag-telluride minerals such as calaverite and sylvanite, native Au and native Te, and other tellurides; other sulfides include fine-grained pyrite, chalcopyrite, sphalerite, galena, tetrahedrite, stibnite, and occasional cinnabar. Vein gangue minerals include fluorite, adularia, chlorite, calcite, dolomite, barite, celestite (a strontium sulfate), hematite, magnetite, and roscoelite (a vanadium mica).

The disseminated deposits contain native Au, fine-grained auriferous pyrite, occasional telluride minerals, quartz, abundant fine-grained adularia, and fluorite (Kelley et al., 1995).

Wallrocks adjacent to veins are altered to a variable mixture of dolomite, adularia, sericite, roscoelite, magnetite and pyrite. The disseminated deposits are characterized by intense, pervasive alteration of the host rocks to very fine-grained adularia, sanidine, orthoclase, pyrite, \pm sericite.

Drainage-water compositions

The Appendix contains limited data collected in this study from the Cripple Creek and Eldora, Colorado districts. The Carlton

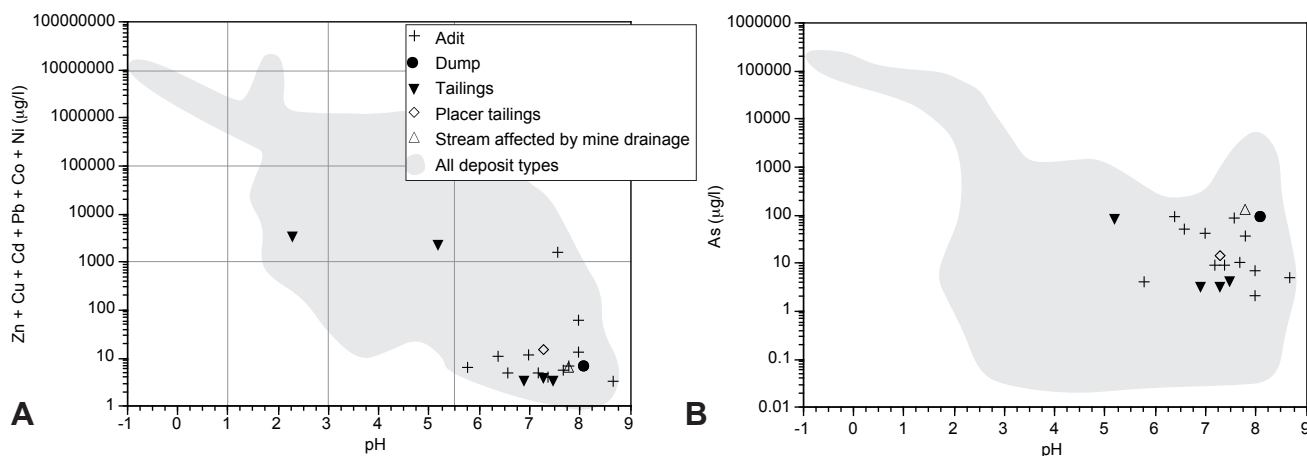


FIGURE 19.25—Plots of mine-drainage and stream compositions for waters draining low-sulfide, Au quartz vein deposits. A. Ficklin diagram; B. Dissolved arsenic. Note differences in scale of the concentration axis between the plots. Shaded areas enclose all data points on corresponding Figures 19.1, 19.2.

Tunnel drains all of the underground workings in the central Cripple Creek district, and so reflects an integrated drainage signature for much of the deposit.

As a result of their generally low sulfide contents and high carbonate contents, these deposits tend to generate near-neutral pH waters with low dissolved base-metal concentrations (Fig. 19.26). It is possible that pyrite-rich ore zones may generate locally acidic waters. However, these disseminated pyrite zones are commonly associated with flooding of the host rocks by fine-grained potassium feldspar. It is interesting to note that acid-base accounting tests of pyrite-rich disseminated ores at Cripple Creek showed that these pyrite- and feldspar-rich ores are non-acid generating, possibly due to the acid-neutralizing capacity and reactivity of the fine-grained feldspars (Cripple Creek mine geologist, oral commun., 1994).

The Carlton Tunnel waters draining Cripple Creek are rather unusual in their chemistry and physical characteristics. They are unusually warm (23°C) and have very high chloride concentrations (22 mg/l) compared to most other mine-adit waters we have measured. As the tunnel drains more than 1000 m vertical extent of mine workings, the warmer water temperatures presumably reflect the geothermal gradient of rocks within the mine. The warmer temperatures of the waters, coupled with their elevated chloride concentrations suggest that the waters may have undergone evaporative concentration in the underground mine workings. The Carlton Tunnel waters, as discussed previously in the section on geochemical controls, are calculated to be at, or above, saturation with a variety of carbonates, zeolites, and feldspars. All of these minerals are noted to form in evaporative playa-lake deposits. Although the carbonates are likely influencing some aspects of the water chemistry, further studies of the suspended particulates are needed to investigate whether zeolites and feldspars are present, and, if they are, whether or not they are influencing the water chemistry. Further studies are also warranted to determine if evaporative concentration is occurring within the underground workings. Although the Carlton Tunnel waters have very low dissolved metals, their volume is sufficiently large (in excess of several million gallons per day) that the total metal loadings leaving the tunnel are substantial.

Sandstone U deposits

Sandstone U deposits include both tabular and roll-front types. As the name implies, they are typically hosted by continental sandstones, which are frequently interbedded with or form channels within redbed shales. Both types of deposits form by the leaching of uranium from U-rich source rocks (such as volcanic rocks or sediments derived from granites) by oxidizing ground waters in the vadose zone, followed by precipitation of the uranium and other elements when the ground waters encounter either organic matter or reduced ground waters at the water table. Repeated oxidation, dissolution, and re-precipitation of the reduced ores by successive volumes of ground waters leads to the formation of ore grade deposits. For details, see several papers on sandstone deposits of the western United States in Ridge (1968), summaries such as Fischer (1974) and Turner-Peterson and Hodges (1986), and references therein. Related deposit types that form by similar processes include redbed Cu deposits (Lindsey et al., 1995) and solution-collapse breccia pipe U deposits (Wenrich et al., 1995).

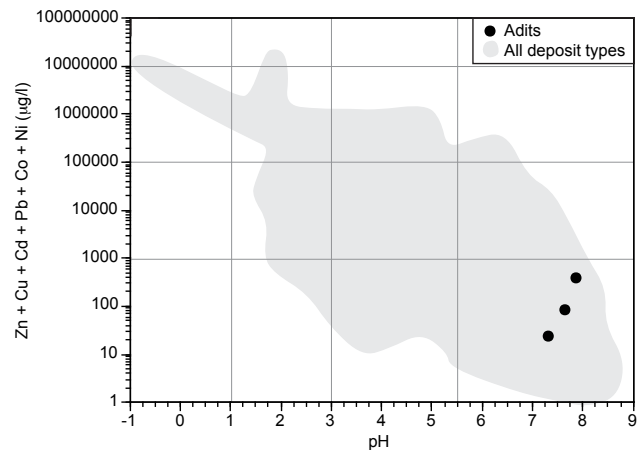


FIGURE 19.26—Ficklin plot showing sum of dissolved Zn, Cu, Cd, Pb, Co, and Ni in adit waters draining Au-Ag-Te vein deposits. Shaded area encloses all data points on Figure 19.2.

In addition to U, other elements typically but variably enriched in sandstone U deposits include V, Mo, Se, Cu, Ag, Ni, Co, Cr, As, and Pb. In the tabular deposits, primary uranium minerals (uraninite, coffinite), Fe-sulfides (pyrite, marcasite), reduced vanadium minerals (such as montroseite, doloresite, corvusite), \pm Cu-sulfides (primarily chalcocite), \pm Ag sulfides replace detrital organic matter within the sandstones; minor sphalerite, galena, and other sulfides may also be present locally. In the roll-front deposits, the oxidized ground waters travel down dip through the vadose zone; upon reaching the reduced conditions of the water table they precipitate reduced uranium minerals (uraninite, coffinite) and iron sulfides, with lesser amounts of Cu- and Ag-sulfides. The roll-front deposits derive their name from the u-shaped cross sections of the deposits, with the round part of the u pointing down dip in the direction of ground-water flow. Calcium carbonate is common in both deposit types as a cement in the host sandstones. Redbed Cu deposits (Lindsey et al., 1995) form in much the same way as sandstone U deposits, except that the source-rock materials leached by the ground waters are Cu-rich rather than U-rich.

Minerals formed in the oxidized zones of these deposits include a complex assemblage of oxidized uranium and vanadium minerals (such as carnotite, tyuyamunite, torbernite, uranophane, hewettite, and many others), copper carbonates (malachite and azurite), hydrous Cu- and Fe-sulfates, and Fe oxides.

Drainage-water compositions

The Appendix summarizes limited mine water data from the Monument Valley and Cameron districts, Arizona (Longworth, 1994). In both these districts, the ore deposits are hosted by sandstone channels within redbed shales, and the ore minerals replace organic detritus within the sandstones (Malan, 1968). The Monument Valley and Cameron district water compositions (Longworth, 1994) reflect the deposit geology and the dry climate and alkaline ground waters typical of the southwestern U.S. desert. The open pit waters and ground waters affected by open pit mining (Fig. 19.27) have quite high pH values (from 6.5–9.5), high chloride contents indicative of evaporative concentration,

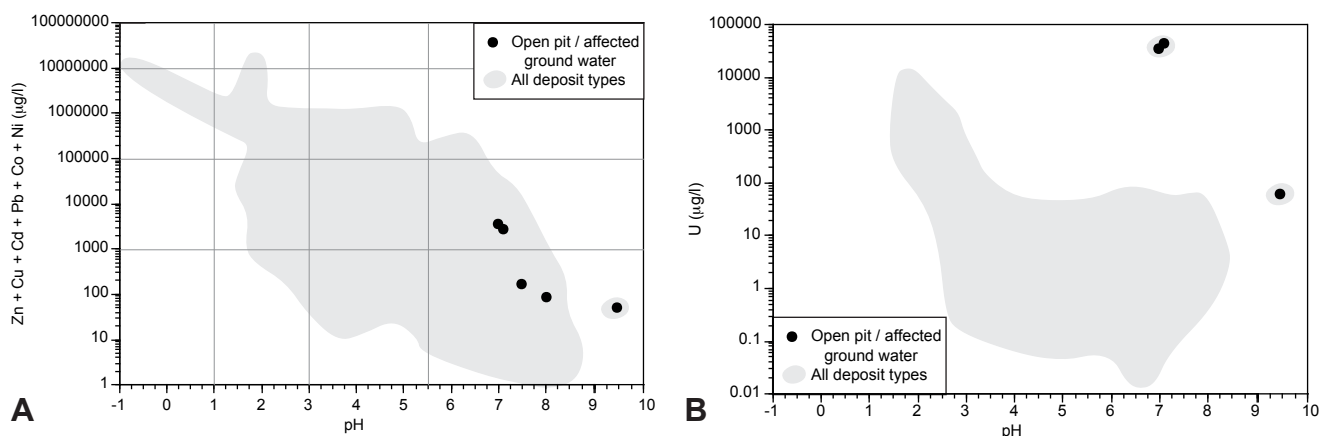


FIGURE 19.27—Compositions of open pit waters and ground waters affected by open-pit mining for sediment-hosted U deposits. A. Ficklin diagram; B. Dissolved uranium. Note differences in scale of the concentration axis between the plots. Shaded areas enclose all data points on corresponding Figures 19.1, 19.2.

and can have exceptionally high concentrations of dissolved U (as high as several tens of mg/l) and other metals that are both enriched in the deposits and mobile in near-neutral to alkaline waters, such as Ni (hundreds of µg/l), Co (1–2 mg/l), Mo (several mg/l), and Zn (1 mg/l). Although not measured, Se and As concentrations in the waters are probably elevated as well.

SUMMARY

The empirical data that we have collected and compiled for waters draining diverse mineral-deposit types underscore the roles that deposit geology, climate, mining- and mineral-processing method, geochemical processes, and other factors play in controlling the compositions of mine waters, tailings waters, and natural waters draining unmined mineral deposits.

The geologic characteristics of a mineral deposit ultimately set the stage for the compositions of waters that drain the deposit both prior to mining and as a result of mining and mineral processing if appropriate remedial practices were not followed. Important geologic characteristics that influence drainage compositions include:

- The amounts of iron sulfides in the deposit, alteration and host rocks, and their reactivities to near-surface weathering processes.
- The amounts of other sulfides in the deposit, wallrock alteration, and host rocks.
- The amounts and reactivities of acid-buffering carbonates and other minerals in the deposit, wallrock alteration, and host rocks, and their reactivities to near-surface weathering processes.
- The textures and trace-element contents of the ore, gangue, alteration, and host rock minerals, which influence their reactivities.
- The trace-element content of the deposit, wallrock alteration, and host rocks. The same trace elements that are enriched in the deposit, alteration, or host rocks are typically enriched in the drainage waters if the elements occur in readily-weathered mineral phases.
- The ore type (vein, massive, disseminated) and hydrogeologic

characteristics of the deposit and host U rocks (structures, permeability of host rocks), which control the access of ground water and atmospheric oxygen to the deposit.

- The spatial distribution of ore types, mineralogic zones, alteration zones, rock types, or other geologic characteristics within a mineral deposit, each of which may produce drainage waters with characteristic ranges in pH and metal concentration.
- The extent of pre-mining oxidation, which converts acid-generating iron sulfide minerals to a variety of non-acid-generating secondary minerals.

Geochemical processes (such as sulfide oxidation, mineral precipitation, and sorption), biogeochemical processes (such as bacterially catalyzed oxidation of aqueous iron), physical processes (such as evaporation) and hydrologic processes (such as dilution by non-mineralized ground or surface waters) play crucial roles in determining the composition of mine- and natural-drainage waters.

Climate, mining method, and mineral processing method also influence drainage compositions, although generally to a lesser extent than deposit geology or geochemical, biogeochemical, physical, and hydrologic processes. Climate influences include the extent of pre-mining oxidation of sulfides, the extent and periodicity of evaporation of drainage waters, and the amounts of ground and surface waters with which the drainage waters mix. The mining method used influences the extent to which the ores and wastes interact with atmospheric oxygen and ground or surface waters. The mineral processing method further influences the accessibility of weathering agents to mine wastes. For example, the higher acidities and metal contents of waters collected from tailings impoundments compared with those of mine waters has been demonstrated for several mineral-deposit types.

Empirical studies as a predictive tool

Our study has compiled empirical data for natural- and mine-drainage waters spanning only a portion of the potential deposit types and climates that are present worldwide. Some inferences about potential compositions of natural and mine-drainage waters

in deposit types and climates for which data are not available may be made by drawing analogies to the most geologically similar deposit types and climates for which drainage data are available. However, further data compilations are clearly necessary, both within deposit types and climates covered by this study, as well as those not covered by this study.

Nonetheless, our results show that, by understanding the geology of a mineral deposit and the other factors that influence mine-drainage compositions, it is possible to constrain the potential ranges in pH and ranges in metal concentrations of mine- and natural-drainage waters that may develop within different mineralogic zones, ore types, or alteration types in a given mineral deposit. Our results are not sufficiently precise, however, that they can be used to quantitatively predict the exact compositions of water that will develop in a particular mine, mine dump, or tailings impoundment at a particular mineral deposit. Instead, results of geologically constrained empirical studies such as ours can be used to help anticipate the potential formation of problematic mine-drainage waters before they develop, so that they can be prevented or mitigated with appropriate engineered solutions (thereby helping active and proposed mines and mineral processing facilities meet regulations requiring zero or minimal discharge of metals into the environment). Empirical studies of waters draining unmined mineral deposits are also useful to help constrain drainage compositions that were present in geologically and climatically similar mineralized areas prior to mining, thereby providing another tool for estimating pre-mining environmental baseline conditions.

The results of this study also suggest that some geologic features of mineral deposits, such as carbonate-bearing rocks or wall-rock alteration, may be potentially useful in the development of lower-cost mine-drainage remediation technologies.

Our study does not address in detail the possible downstream impacts of drainage waters if they are released into the environment from naturally weathering mineral deposits, from past producing mines, or accidentally from active mines or mineral processing facilities. These effects are a complex function of

- The relative volumes of the drainage waters compared to the volumes of stream or ground waters with which they mix.
- The compositions of the drainage waters relative to those of the waters with which they mix (a function of the climate and geology of the watershed surrounding the deposit).
- Geochemical, biogeochemical, and physical processes that occur downstream or down hydrologic gradient from the deposit, such as formation of particulates, sorption of metals onto (or desorption from) particulates, settling of particulates, photolytic reactions, and reactions of waters with bed sediments or aquifer minerals.

Empirical studies of mineral deposits in the context of their surrounding watersheds are thus an important and needed next step in the development of improved predictive methods to help anticipate, mitigate, and remediate the potential environmental effects of mineral-resource development.

REFERENCES

- Ahmad, M., Solomon, M., and Walshe, J.L., 1987, Mineralogical and geochemical studies of the Emperor gold telluride deposit, Fiji: *Economic Geology*, v. 82, pp. 345-370.
- Alpers, C.N., and Nordstrom, D.K., 1991, Geochemical evolution of extremely acid mine waters at Iron Mountain, California—Are there any lower limits to pH?: *in* Proceedings, 2nd International Conference on the Abatement of Acidic Drainage: MEND (Mine Environment Neutral Drainage), Ottawa, Canada, v. 2., pp. 321-342.
- Alpers, C.N., and Nordstrom, D.K., 1999, Geochemical modeling of water-rock interactions in mining environments; *in* Plumlee, G.S. and Logsdon, M.J. (eds.), *The Environmental Geochemistry of Mineral Deposits, Part A. Processes, Techniques, and Health Issues: Society of Economic Geologists, Reviews in Economic Geology*, v. 6A, pp. 289-323.
- Alpers, C.N., Nordstrom, D.K., and Thompson, J.M., 1994, Seasonal variations in copper and zinc concentrations from Iron Mountain, California; *in* Alpers, C.N., and Blowes, D.W. (eds.), *Environmental Geochemistry of Sulfide Oxidation: American Chemical Society Symposium Series 550*, pp. 324-344.
- ASTM, 1996, Standard test method for accelerated weathering of solid materials using a modified humidity cell: ASTM D5744-96, 13 pp.
- Ball, J.W., and Nordstrom, D.K., 1989, Final revised analyses of major and trace elements from acid mine waters in the Leviathan mine drainage basin, California and Nevada—October 1981 to October 1982: U.S. Geological Survey Water-Resources Investigations Report 89-4138, 46 pp.
- Ball, J.W., and Nordstrom, D.K., 1991, User's manual for WATEQ4F with revised thermodynamic data base and test cases for calculating speciation of major, trace, and redox elements in natural waters: U.S. Geological Survey Open-File Report 91-183, 189 pp.
- Barks, J.H., 1977, Effects of abandoned lead and zinc mines and tailings piles on water quality in the Joplin area, Missouri: U.S. Geological Survey Water Resources Investigations 77-75, 49 pp.
- Barry, T.H., 1996, The geochemistry of natural waters draining hydrothermally altered and mineralized terrains in the upper Alamosa River basin, Colorado: Unpub. M.S. thesis, Auburn Univ., 220 pp.
- Bartos, P.J., 1987, Quiruvilca, Peru—mineral zoning and timing of wall-rock alteration relative to Cu-Pb-Zn-Ag vein-fill deposition: *Economic Geology*, v. 82, no. 6, pp. 1431-1452.
- Berger, B.R., 1986, Descriptive model of hot-spring Au-Ag; *in* Cox, D.P., and Singer, D.A. (eds.), *Mineral Deposit Models: U.S. Geological Survey Bulletin 1693*, pp. 143-144.
- Berger, B.R., and Eimon, P.I., 1983, Conceptual models of epithermal metal deposits; *in* Shanks, W.C. (ed.), *Cameron Volume on Unconventional Mineral Deposits: Society of Mining Engineers*, New York, pp. 191-205.
- BLM, 1996, Draft Environmental Impact Statement, Twin Creeks Mine: Bureau of Land Management, Winnemucca, Nev., 469 pp.
- Blowes, D.W., and Ptacek, C.J., 1994, Acid-neutralization mechanisms in inactive mine tailings; *in* Jambor, J.L., and Blowes, D.W. (eds.), *Short Course on Environmental Geochemistry of Sulfide-Mine Wastes: Mineralogical Association of Canada, Short Course Handbook*, v. 22, pp. 271-292.
- Cannon, W.F., Hadley, D.G., and Horton, R.J., 1995a, Superior Fe deposits; *in* du Bray, E.A. (ed.), *Preliminary compilation of descriptive geoenvironmental mineral deposit models: U.S. Geological Survey Open-File Report 95-831*, pp. 256.
- Cannon, W.F., Hadley, D.G., and Horton, R.J., 1995b, Algoma Fe deposits; *in* du Bray, E.A. (ed.), *Preliminary compilation of descriptive geoenvironmental mineral deposit models: U.S. Geological Survey Open-File Report 95-831*, pp. 209-213.
- Cieutat, B.H., Goldfarb, R.J., Borden, J.C., McHugh, J., and Taylor, C.D., 1994, Environmental geochemistry of mesothermal gold deposits, Kenai Fjords National Park, south-central Alaska; *in* Till, A.B., and Moore, T.E. (eds.), *Geological studies in Alaska by the U.S. Geological Survey*, 1993: U.S. Geological Survey Bulletin 2107, pp. 21-25.
- Cox, D.P., 1986, Descriptive model of porphyry copper; *in* Cox, D.P., and Singer, D.A., (eds.), *Mineral deposit models: U.S. Geological Survey Bulletin 1693*, p. 76.
- Cox, D.P., and Bagby, W.C., 1986, Descriptive model of Au-Ag-Te veins; *in* Cox, D.P., and Singer, D.A. (eds.), *Mineral deposit models: U.S. Geological Survey Bulletin 1693*, p. 124.
- Cox, D.P., and Singer, D.A. (eds.), 1986, *Mineral deposit models: U.S.*

- Geological Survey Bulletin 1693, 379 pp.
- Cox, L.J., Chaffee, M.A., Cox, D.P., and Klein, D.P., 1995, Porphyry Cu deposits; *in* du Bray, E.A. (ed.), Preliminary compilation of descriptive geoenvironmental mineral deposit models: U.S. Geological Survey Open-File Report 95-831, pp. 75-89.
- Crock, J.G., Arbogast, B.F., and Lamothe, P.J., 1999, Laboratory methods for the analysis of environmental samples; *in* Plumlee, G.S., and Logsdon, M.J., (eds.), The Environmental Geochemistry of Mineral Deposits, Part A. Processes, Techniques, and Health Issues: Society of Economic Geologists, Reviews in Economic Geology, v. 6A, pp. 265-287.
- Davis, A., and Ashenberg, D., 1989, The aqueous geochemistry of the Berkeley Pit, Butte, Montana, U.S.A.: Applied Geochemistry, v. 4, pp. 23-26.
- du Bray, E.A. (ed.), 1995, Preliminary compilation of descriptive geoenvironmental mineral deposit models: U.S. Geological Survey Open-File Report 95-831, 272 pp. (also available online at <http://minerals.cr.usgs.gov>).
- Eger, P., 1992, The use of sulfate reduction to remove metals from acid mine drainage: Paper presented at 1992 American Society for Surface Mining and Reclamation Meeting, Duluth, Minn., June 14-18, 1992, 13 pp.
- Engineering Science, Inc., 1985, Eagle Mine remedial investigation: prepared for Colorado Department of Law, 237 pp.
- Eppinger, R.G., Sutley, S.J., and McHugh, J.B., 1997, Environmental geochemical study of the Nabesna gold skarn and Kennecott strata-bound copper deposits, Alaska; *in* Dumoulin, J.A., and Gray, J.G. (eds.), Geologic Studies in Alaska by the U.S. Geological Survey, 1995: U.S. Geological Survey Professional Paper 1574, pp. 19-40.
- Evans, K.V., Nash, J.T., Miller, W.R., Kleinkopf, M.D., and Campbell, D.L., 1995, Blackbird Co-Cu deposits; *in* duBray, E.A. (ed.), Preliminary compilation of descriptive geoenvironmental mineral deposit models: U.S. Geological Survey Open-File Report 95-831, pp. 145-151.
- Eychaner, J.H., 1988, Movement of inorganic contaminants in acidic water near Globe, Arizona; *in* Mallard, G.E., and Ragone, S.E. (eds.), U.S. Geological Survey Toxic Substances Hydrology Program—Proceedings of the Technical Meeting, Phoenix, Arizona, September 26-30, 1988: U.S. Geological Survey Water-Resources Investigations Report 88-4220, pp. 567-576.
- Feltis, R.D., and Litke, D.W., 1987, Appraisal of water resources of the Boulder and Stillwater basin, including the Stillwater Complex, south-central Montana: Montana Bureau of Mines and Geology Memoir 60, 121 pp.
- Ficklin, W.H., and Mosier, E.L., 1999, Field methods for sampling and analysis of environmental samples for unstable and selected stable constituents; *in* Plumlee, G.S., and Logsdon, M.J. (eds.), The Environmental Geochemistry of Mineral Deposits, Part A. Processes, Techniques, and Health Issues: Society of Economic Geologists, Reviews in Economic Geology, v. 6A, pp. 249-264.
- Ficklin, W.H., Plumlee, G.S., Smith, K.S., and McHugh, J.B., 1992, Geochemical classification of mine drainages and natural drainages in mineralized areas: Proceedings, 7th Internal Water-Rock Interaction Conference, Park City, Utah, 1992, pp. 381-384.
- Filipek, L.H., Nordstrom, D.K., and Ficklin, W.H., 1987, Interactions of acid mine drainage with waters and sediments of West Squaw Creek in the West Shasta mining district, California: Environmental Science and Technology, v. 21, pp. 388-396.
- Filipek, L.H., VanWynyarden, T.J., Papp, C.S.E., and Curry, J., 1999, A multi-phased approach to predict acid production from porphyry copper-gold waste rock in an arid montane environment; *in* Filipek, L.H., and Plumlee, G.S. (eds.), The Environmental Geochemistry of Mineral Deposits, Part B. Case Studies and Research Topics: Society of Economic Geologists, Reviews in Economic Geology, v. 6B, pp. 433-445.
- Fischer, R.P., 1974, Exploration guides to new uranium districts and belts: Economic Geology, v. 69, pp. 362-376.
- Flohr, M.J.K., Dillenburg, R.G., Nord, G.L., and Plumlee, G.S., 1995, Secondary mineralogy of altered rocks, Summitville Mine, Colorado: U.S. Geological Survey Open-File Report 95-808, 27 pp.
- Foose, M.P., Zientek, M.L., and Klein, D.P., 1995, Magmatic sulfide deposits; *in* du Bray, E.A. (ed.), Preliminary compilation of descriptive geoenvironmental mineral deposit models: U.S. Geological Survey Open-File Report 95-831, pp. 28-38.
- Franklin, J.M., 1993, Volcanic-associated massive sulphide deposits; *in* Kirkham, R.V., Sinclair, W.D., Thorpe, R.I., and Duke, J.M. (eds.), Mineral deposit modeling: Geological Association of Canada Special Paper No. 40, pp. 315-334.
- Garrells, R.M., and Christ, C.L., 1965, Solutions, Minerals, and Equilibria: Freeman, Cooper & Co., San Francisco, 450 p.
- Goldfarb, R.J., Berger, B.R., Klein, T.L., Pickthorn, W.J., and Klein, D.P., 1995, Low sulfide Au quartz veins; *in* du Bray, E.A. (ed.), Preliminary compilation of descriptive geoenvironmental mineral deposit models: U.S. Geological Survey Open-File Report 95-831, pp.261-267.
- Goldfarb, R.J., Nelson, S.W., Taylor, C.D., d'Angelo, W.M., and Meier, A.M., 1996, Acid mine drainage associated with volcanogenic massive sulfide deposits, Prince William Sound, Alaska; *in* Moore, T.E., and Dumoulin, J.A. (eds.), Geologic studies in Alaska by the U.S. Geological Survey during 1994: U.S. Geological Survey Bulletin 2152, pp. 3-15.
- Goldfarb, R.J., Taylor, C.D., Meier, A.L., d'Angelo, W.M., and O'Leary, R.M., 1997, Hydrogeochemistry of mine-drainage waters associated with low-sulfide, gold-quartz veins in Alaska; *in* Dumoulin, J.A., and Gray, J.E. (eds.), Geologic Studies in Alaska by the U.S. Geological Survey, 1995: U.S. Geological Survey Professional Paper 1574, pp. 3-18.
- Goodfellow, W.D., Lydon, J.W., and Turner, R.J.W., 1993, Geology and genesis of stratiform sediment-hosted (SEDEX) zinc-lead-silver sulphide deposits; *in* Kirkham, R.V., Sinclair, W.D., Thorpe, R.I., and Duke, J.M. (eds.), 1995, Mineral deposit modeling: Geological Association of Canada Special Paper No. 40, pp. 201-252.
- Grimes, D.J., Ficklin, W.H., Meier, A.L., and McHugh, J.B., 1995, Anomalous gold antimony, arsenic, and tungsten in ground water and alluvium around disseminated gold deposits along the Getchell Trend, Humboldt County, Nevada: Journal of Geochemical Exploration, v. 52, pp. 351-371.
- Guilbert, J.M., and Park, C.F., Jr., 1986, The geology of ore deposits: W.H. Freeman and Company, New York, 985 pp.
- Hammarstrom, J.M., Kotlyar, B.B., Theodore, T.G., Elliott, J.E., John, D.A., Doebrich, J.L., Nash, J.T., Carlson, R.R., Lee, G.K., Livo, E., an Klein, D.P., 1995, Cu, Au, and Zn-Pb skarn deposits; *in* du Bray, E.A. (ed.), Preliminary compilation of descriptive geoenvironmental mineral deposit models: U.S. Geological Survey Open-File Report 95-831, pp. 90-111.
- Heald, P., Foley, N.K., and Hayba, D.O., 1987, Comparative anatomy of volcanic-hosted epithermal deposits, acid-sulfate and adularia-sericite types: Economic Geology, v. 82, pp. 1-26.
- Hodgson, C.J., 1993, Mesothermal lode-gold deposits; *in* Kirkham, R.V., Sinclair, W.D., Thorpe, R.I., and Duke, J.M. (eds.), 1995, Mineral deposit modeling: Geological Association of Canada Special Paper No. 40, pp. 635-678.
- Hofstra, A.H., Leventhal, J.S., Northrop, H.R., L:and is, G.P., Rye, R.O., Birak, D.J., and Dahl, A.R., 1991, Genesis of sediment-hosted disseminated gold deposits by fluid mixing and sulfidization—chemical-reaction-path modeling of ore depositional processes documented in the Jerritt Canyon district, Nevada: Geology, v. 19, pp. 36-40.
- Hofstra, A.H., Leventhal, J.S., Grimes, D.J., and Heran, W.D., 1995, Sediment-hosted Au deposits; *in* du Bray, E.A. (ed.), Preliminary compilation of descriptive geoenvironmental mineral deposit models: U.S. Geological Survey Open-File Report 95-831, pp. 184-192.
- James, H.L., 1954, Sedimentary facies of iron formation: Economic Geology, v. 49, pp. 235-293.
- Kelley, K.D., and Taylor, C.D., 1997, Environmental geochemistry of shale-hosted Ag-Pb-Zn massive sulfide deposits in northwest Alaska—Natural background concentrations of metals in water from mineralized areas: Applied Geochemistry, v. 12, pp 397-409.

- Kelley, K.D., Seal, R.R., II, Schmidt, J.M., Hoover, D.B., and Klein, D.P., 1995, Sedimentary exhalative Zn-Pb-Ag deposits; *in* du Bray, E.A. (ed.), Preliminary compilation of descriptive geoenvironmental mineral deposit models: U.S. Geological Survey Open-File Report 95-831, pp. 225-233.
- Kilburn, J.E., and Sutley, S.J., 1997, Analytical results and comparative overview of geochemical studies conducted at the Holden Mine, spring, 1996: U.S. Geological Survey Open-File Report 97-128, 38 pp.
- Kirkham, R.V., Sinclair, W.D., Thorpe, R.I., and Duke, J.M. (eds.), 1993, Mineral deposit modeling: Geological Association of Canada Special Paper No. 40, 770 pp.
- Koyanagi, V.M., and Panteleyev, A., 1993, Natural acid-drainage in the Mount Macintosh/Pemberton Hills area, northern Vancouver Island (92L/12); *in* Grant, B. et al. (eds.), Geological fieldwork 1992—a summary of field activities and current research: Ministry of Energy, Mines, and Petroleum Resources, Report 1993-1, pp. 445-450.
- Kwong, Y.T.J., 1991, Acid generation in waste rock as exemplified by the Mount Washington minesite, British Columbia, Canada, Proceedings, 2nd International Conference on the Abatement of Acidic Drainage: MEND (Mine Environment Neutral Drainage), Ottawa, Canada, v. 1., pp. 175-190.
- Kwong, Y.T.J., 1993, Prediction and prevention of acid rock drainage from a geological and mineralogical perspective: MEND Project 1.32.1, 47 pp.
- Large, D.E., 1980, Geologic parameters associated with sediment-hosted, submarine exhalative Pb-Zn deposits: An empirical model for mineral exploration; *in* Stratiform Cu-Pb-Zn deposits: Geologisches Jahrbuch, series D, v. 40, pp. 59-129.
- Leach, D.L., and Sangster, D.F., 1993, Mississippi Valley-type lead-zinc-silver deposits; *in* Kirkham, R.V., Sinclair, W.D., Thorpe, R.I., and Duke, J.M. (eds.), Mineral deposit modeling: Geological Association of Canada Special Paper No. 40, pp. 289-314.
- Leach, D.L., Viets, J.G., Foley-Ayuso, N., and Klein, D.P., 1995, Mississippi Valley-type Pb-Zn deposits; *in* du Bray, E.A. (ed.), Preliminary compilation of descriptive geoenvironmental mineral deposit models: U.S. Geological Survey Open-File Report 95-831, pp. 234-243.
- Lindsey, D.A., Woodruff, L.G., Cannon, W.F., Cox, D.P., and Heran, W.D., 1995, Sediment-hosted Cu deposits; *in* du Bray, E.A. (ed.), Preliminary compilation of descriptive geoenvironmental mineral deposit models: U.S. Geological Survey Open-File Report 95-831, pp. 214-224.
- Longworth, S.A., 1994, Geohydrology and water chemistry of abandoned uranium mines and radiochemistry of spoil-material leachate, Monument Valley and Cameron areas, Arizona and Utah: U.S. Geological Survey Water-Resources Investigations Report 93-4226, 43 pp.
- Lowell, J.D., and Guilbert, J.M., 1970, Lateral and vertical alteration-mineralization zoning in porphyry copper deposits: *Economic Geology*, v. 65, pp. 363-408.
- Malan, R.C., 1968, The uranium mining industry and geology of the Monument Valley and White Canyon districts, Arizona and Utah; *in* Ridge, J.D. (ed.), Ore Deposits of the United States, 1933-1967—The Graton-Sales Volume: American Institute of Mining, Metallurgical, and Petroleum Engineers, Inc., New York, pp. 790-804.
- McHugh, J.B., Tucker, R.E., and Ficklin, W.H., 1987, Analytical results for 46 water samples from a hydrogeochemical survey of the Blackbird Mine area, Idaho: U.S. Geological Survey Open-File Report 87-260.
- Miller, W.R., Ficklin, W.H., and Learned, R.E., 1982, Hydrogeochemical prospecting for porphyry copper deposits in the tropical-marine climate of Puerto Rico: *Journal of Geochemical Exploration*, v. 16, pp. 217-233.
- Moran, R.E., 1974, Trace element content of a stream affected by metal-mine drainage, Bonanza, Colorado: Unpub. Ph.D. dissertation, Univ. of Texas at Austin, 167 pp.
- Morris, H.T., 1986, Descriptive model of polymetallic replacement deposits; *in* Cox, D.P., and Singer, D.A. (eds.), Mineral Deposit Models: U.S. Geological Survey Bulletin 1693, pp. 99-100.
- Nordstrom, D.K., and Alpers, C.N., 1999, Geochemistry of acid mine waters; *in* Plumlee, G.S., and Logsdon, M.J. (eds.), The Environmental Geochemistry of Mineral Deposits, Part A. Processes, Techniques, and Health Issues: Society of Economic Geologists, Reviews in Economic Geology, v. 6A, pp. 133-160.
- Pioneer Technical Services, 1994, Abandoned hardrock mine priority sites, summary report: Montana Department of State Lands, Abandoned Mines and Reclamation Bureau, Engineering Services Agreement DSL-AMRB No. 004, 314 pp.
- Plumlee, G.S., 1999, The environmental geology of mineral deposits; *in* Plumlee, G.S., and Logsdon, M.J. (eds.), The Environmental Geochemistry of Mineral Deposits, Part A. Processes, Techniques, and Health Issues: Society of Economic Geologists, Reviews in Economic Geology, v. 6A, pp. 71-116.
- Plumlee, G.S., and Edelmann, P., 1995, An update on USGS studies of the Summitville Mine and its downstream environmental effects: U.S. Geological Survey Open-File Report 95-23, 9 pp.
- Plumlee, G.S., Smith, K.S., Ficklin, W.H., and Briggs, P.H., 1992, Geological and geochemical controls on the composition of mine drainages and natural drainages in mineralized areas: Proceedings, 7th Internat. Water-Rock Interaction Conference, Park City, Utah, July 1992, pp. 419-422.
- Plumlee, G.S., Smith, K.S., Ficklin, W.H., Briggs, P.H., and McHugh, J.B., 1993a, Empirical studies of diverse mine drainages in Colorado—implications for the prediction of mine-drainage chemistry: Proceedings, 1993 Mined Land Reclamation Symposium, Billings, Mont., v. 1, pp. 176-186.
- Plumlee, G.S., Smith, S.M., Toth, M.I., and Marsh, S.P., 1993b, Integrated mineral-resource and mineral-environmental assessments of public lands—applications for land management and resource planning: U.S. Geological Survey Open-File Report 93-571, 18 pp.
- Plumlee, G.S., Leach, D.L., Hofstra, A.H., Landis, G.P., Rowan, E.L., and Viets, J.G., 1994, Chemical reaction path modeling of ore deposition in Mississippi-Valley-Type Pb-Zn deposits of the Ozark region, U. S. midcontinent: *Economic Geology*, v. 89, no. 6, pp. 1361-1383.
- Plumlee, G.S., Gray, J.E., Roeber, M.M., Jr., Coolbaugh, M., Flohr, M., and Whitney, G., 1995a, The importance of geology in understanding and remediating environmental problems at Summitville; *in* Posey, H.H., Pendleton, J.A., and Van Zyl, D. (eds.), Summitville Forum Proceedings: Colorado Geological Survey Spec. Pub. No. 38, pp. 13-22.
- Plumlee, G.S., Smith, K.S., Mosier, E.L., Ficklin, W.H., Montour, M., Briggs, P.H., and Meier, A.L., 1995b, Geochemical processes controlling acid-drainage generation and cyanide degradation at Summitville; *in* Posey, H.H., Pendleton, J.A., and Van Zyl, D. (eds.), Summitville Forum Proceedings: Colorado Geological Survey Spec. Pub. No. 38, pp. 23-34.
- Plumlee, G.S., Smith, K.S., Gray, J.E., and Hoover, D.B., 1995c, Epithermal quartz-alunite deposits; *in* du Bray, E.A. (ed.), Preliminary compilation of descriptive geoenvironmental mineral deposit models: U.S. Geological Survey Open-File Report 95-831, pp. 162-169.
- Price, J.G., Shevenell, L., Henry, C.D., Rigby, J.G., Christensen, L.G., Lechler, P.J., and Desilets, M.O., 1995, Water quality at inactive and abandoned mines in Nevada: Nevada Bureau of Mines and Geology Open-File Report 95-4, 73 pp.
- Rao, S.R., Kuyucak, N., Sheremata, T., Laeroux, M., Finch, J.A., and Wheeland, K.G., 1994, Prospect of metal recovery/recycle from acid mine drainage, Proceedings, International Land Reclamation and Mine Drainage Conference and 3rd International Conference on the Abatement of Acid Drainage: U.S. Bureau of Mines Spec. Pub. No. SP 06B-94, v. 1, pp. 223-232.
- Ridge, J.D. (ed.), 1968, Ore Deposits of the United States, 1933-1967—The Graton-Sales Volume: American Institute of Mining, Metallurgical, and Petroleum Engineers, Inc., New York, 991 pp.
- Ritchie, I.M., 1988, Environmental management of new mining operations in developed countries—The regional copper-nickel study; *in* Salomons, W., and Forster, U. (eds.), Environmental management of solid waste dredged material and mine tailings: Springer-Verlag,

- Berlin, pp. 182–323.
- Runnells, D.D., Shepherd, T.A., and Angino, E.E., 1992, Metals in water—determining natural background concentrations in mineralized areas: *Environmental Science and Technology*, v. 26, pp. 2316–2323.
- Rytuba, J.J., 1986, Descriptive model of hot-spring Hg; *in* Cox, D.P., and Singer, D.A. (eds.), *Mineral Deposit Models*: U.S. Geological Survey Bulletin 1693, pp. 178–179.
- SCS Engineers, 1984, Summary of damage cases from the disposal of mining wastes: Report prepared for the Environmental Protection Agency under Contract 68–02–3179, 596 pp.
- Shelp, G., Chesworth, W., Spiers, G., and Liu, L., 1994, A demonstration of the feasibility of treating acid mine drainage by an in situ electrochemical method, *Proceedings, International Land Reclamation and Mine Drainage Conference and 3rd Internatl Conference on the Abatement of Acid Drainage*: U.S. Bureau of Mines Special Publication No. SP 06B–94, v. 2, pp. 348–355.
- Sillitoe, R.H., 1993, Epithermal models—genetic types, geometrical controls, and shallow features; *in* Kirkham, R.V., Sinclair, W.D., Thorpe, R.I., and Duke, J.M. (eds.), *Mineral deposit modeling*: Geological Association of Canada Special Paper No. 40, pp. 403–418.
- Sims, P.K., Drake, A.A., and Tooker, E.W., 1963, Geology and ore deposits of the Central City district, Gilpin County, Colorado: U.S. Geological Survey Professional Paper 359, 231 pp.
- Slack, J.F., 1993, Descriptive and grade-tonnage models for Besshi-type massive sulphide deposits; *in* Kirkham, R.V., Sinclair, W.D., Thorpe, R.I., and Duke, J.M. (eds.), *Mineral deposit modeling*: Geological Association of Canada Special Paper No. 40, pp. 343–372.
- Smith, B.J., and Schumacher, J.G., 1993, Surface-water and sediment quality in the Old Lead Belt, southeastern Missouri—1988–89: U.S. Geological Survey Water Resources Investigations Report 93–4012, 92 pp.
- Smith, K.S., 1991, Factors influencing metal sorption onto iron-rich sediment in acid-mine drainage: Ph.D. thesis, Colorado School of Mines, Golden, Colo.
- Smith, K.S., 1999, Sorption of trace elements by earth materials—an overview with examples relating to mineral deposits; *in* Plumlee, G.S., and Logsdon, M.J. (eds.), *The Environmental Geochemistry of Mineral Deposits, Part A. Processes, Techniques, and Health Issues*: Society of Economic Geologists, *Reviews in Economic Geology*, v. 6A, pp. 161–182.
- Smith, K.S., Ficklin, W.H., Plumlee, G.S., and Meier, A.L., 1992, Metal and arsenic partitioning between water and suspended sediment at mine-drainage sites in diverse geologic settings: *Proceedings, 7th Internatl Water-Rock Interaction Conference*, Park City, Utah, July 1992, pp. 443–447.
- Smith, K.S., Ficklin, W.H., Plumlee, G.S., and Meier, A.L., 1993, Computer simulations of the influence of suspended iron-rich particulates on trace metal-removal from mine-drainage waters: *Proceedings, 1993 Mined Land Reclamation Symposium*, Billings, Mont., v. 2, pp. 107–115.
- Smith, K.S., Plumlee, G.S., and Ficklin, W.H., 1994, Predicting water contamination from metal mines and mining waste: Notes, Workshop #2, *International Land Reclamation and Mine Drainage Conference and Third International Conference on the Abatement of Acidic Drainage*: U.S. Geological Survey Open-File Report 94–264, 112 pp.
- Taylor, C.D., Zierenberg, R.A., Goldfarb, R.J., Kilburn, J.E., Seal, R.R., II, and Kleinkopf, M.D., 1995, Volcanic-associated massive sulfide deposits; *in* du Bray, E.A. (ed.), *Preliminary compilation of descriptive geoenvironmental mineral deposit models*: U.S. Geological Survey Open-File Report 95–831, pp. 137–144.
- Thompson, T.B., Trippel, A.D., and Dwelley, P.C., 1985, Mineralized veins and breccias of the Cripple Creek district, Colorado: *Economic Geology*, v. 80, pp. 1669–1688.
- Tingley, J.V., and Bonham, H.F., Jr. (eds.), 1986, *Precious metal mineralization in hot springs systems, Nevada-California*: Nevada Bureau of Mines and Geology, Report 41.
- Titley, S.R., 1993, Characteristics of high-temperature, carbonate-hosted massive sulphide ores in the United States, Mexico, and Peru; *in* Kirkham, R.V., Sinclair, W.D., Thorpe, R.I., and Duke, J.M. (eds.), *Mineral deposit modeling*: Geological Association of Canada Special Paper No. 40, pp. 585–614.
- Trainor, T.P., Fleisher, S., Wildeman, T.R., Goldfarb, R.J., and Huber, C.S., 1996, Environmental geochemistry of the McKinley Lake gold mining district, Chugach National Forest, Alaska; *in* Moore, T.E., and Dumoulin, J.A. (eds.), *Geologic Studies in Alaska by the U.S. Geological Survey, 1994*: U.S. Geological Survey Bulletin 2152, pp. 47–57.
- Turner-Peterson, C., and Hodges, C.A., 1986, Descriptive model of sandstone U; *in* Cox, D.P., and Singer, D.A. (eds.), *Mineral deposit models*: U.S. Geological Survey Bulletin 1693, pp. 209–210.
- Viets, J.G., Leach, D.L., Lichte, F.E., Hopkins, R.T., Gent, C.A., and Powell, J.W., 1996, Paragenetic and minor- and trace-elements studies of Mississippi Valley-Type ore deposits of the Silesian-Cracow district, Poland; *in* Górccka, E., Leach, D.L., and Kozłowski, A. (eds.), *Carbonate-hosted zinc-lead deposits in the Silesian-Cracow area, Poland*: Prace Panstowowego Instytutu Geologicznego, Warsaw, Poland, pp. 37–50.
- Wai, C.M., Reece, D.E., Trexler, B.D., Ralston, D.R., and Williams, R.E., 1980, Production of acid water in a lead-zinc mine, Coeur d’Alene, Idaho: *Environmental Geology*, v. 3, pp. 159–162.
- Wenrich, K.J., Van Gosen, B.S., and Finch, W.I., 1995, Solution-collapse breccia pipe U deposits; *in* du Bray, E.A. (ed.), *Preliminary compilation of descriptive geoenvironmental mineral deposit models*: U.S. Geological Survey Open-File Report 95–831, pp. 244–251.
- White, W.H., Bookstrom, A.A., Kamilli, R.J., Ganster, M.W., Smith, R.P., Ranta, D.E., and Steininger, R.C., 1981, Character and origin of Climax-type molybdenum deposits; *in* Skinner, B. (ed.), *Economic Geology 75th Anniversary Volume, 1905–1980*: pp. 270–316.
- White, W.W., III, Lapakko, K.A., and Cox, R.L., 1997, Effects of protocol variables and sample mineralogy on static-test NP: *Proceedings, Eleventh Annual Conference of the Society of Mineral Analysts*, Elko, Nev., April 7–10, 1997.
- White, W.W., III, Cox, R.L., and Lapakko, K.A., 1999, Static-test methods most commonly used to predict acid-mine drainage—Practical guidelines for use and interpretation; *in* Plumlee, G.S., and Logsdon, M.J. (eds.), *The Environmental Geochemistry of Mineral Deposits, Part A. Processes, Techniques, and Health Issues*: Society of Economic Geologists, *Reviews in Economic Geology*, v. 6A, pp. 325–338.
- Wildeman, T.R., Cain, D., and Ramiriz, R.A.J., 1974, The relation between water chemistry and mineral zonation in the Central City Mining district, Colorado; *in* Hadley, R.F., Snow, D.T. (eds.), *Water Resources Problems Related to Mining*: American Water Resources Association Proc. No. 18, pp. 219–229.

APPENDIX

This appendix is a compilation of dissolved compositions of mine waters and natural waters draining diverse mineral deposit types. Most mine, mine-dump, and tailings data were collected from past producing sites. The data included were either collected during this study, or were compiled from data published in the literature. The data are grouped according to deposit type and, for a given deposit type, further grouped according to ore zone, alteration zone, or mineralogic zone within the deposit.

Abbreviations for water type are as follows: a-adit; mg-groundwater from underground mine; d-mine dump; ms-seep affected by mining activity; t-tailings water; ts-seep affected by tailings waters; op-pond or lake in open pit; os-seep affected by open-pit waters; og-ground water affected by open-pit mining; mst-stream affected by mine drainage waters; ns-natural seep; nst-stream affected by natural drainage waters. Sites we know to be currently under remediation are noted by "r". Tailings water compositions listed here do not include measured concentrations of

cyanide and organic chemicals.

The data contained in this compilation were determined by a variety of analytical methods, which we have indicated whenever possible using different type styles. Anions were determined using ion chromatography. Major cations and trace metals were determined by a variety of techniques, including flame or graphite furnace AA (shown in plain type), ICP-AES (bold type), or ICP-MS (italic type). In a few data sets compiled from the literature, no analytical methods were documented; in these cases, plain type was used for all elements listed. Negative concentration values indicate that the species or element was present in the sample, but in concentrations below the analytical detection limit. Samples marked with an asterisk have metal concentrations measured in mg/l or µg/l units; those without asterisks were measured in generally equivalent ppm or ppb units. These and other sources of uncertainty in the data and interpretations are discussed in the Summary of Data and Methods section.

Deposit type Ore / alteration type Sample	Description	Water Type	Reference
Volcanogenic massive sulfide (VMS)			
<i>Kuroko-type, hosted by volcanic rocks</i>			
*Rich-90WA103	Richmond Mine, Iron Mtn., California	a, r	Alpers and Nordstrom (1991)
*Rich-90WA108	Richmond Mine, Iron Mtn., California	a, r	Alpers and Nordstrom (1991)
*Rich-90WA109	Richmond Mine, Iron Mtn., California	a, r	Alpers and Nordstrom (1991)
*Rich-90WA110A	Richmond Mine, Iron Mtn., California	a, r	Alpers and Nordstrom (1991)
*LMG	Les Mines Gallen, Rouyn Noranda, Quebec	ms	Rao et al. (1994)
Hol-511	Holden, Washington, USA	t	Kilburn and Sutley (1997)
Hol-528	Holden, Washington, USA	t	Kilburn and Sutley (1997)
Hol-529	Holden, Washington, USA	t	Kilburn and Sutley (1997)
Hol-534	Holden, Washington, USA	a	Kilburn and Sutley (1997)
Hol-548	Holden, Washington, USA	d	Kilburn and Sutley (1997)
Hol-549A	Holden, Washington, USA	t	Kilburn and Sutley (1997)
Hol-549B	Holden, Washington, USA	t	Kilburn and Sutley (1997)
<i>Besshi-type, hosted by sedimentary and intermediate submarine volcanic host rocks</i>			
Duch-1	Duchess Mine, Latouche Island, Alaska	a	Goldfarb et al. (1996)
Duch-2	Duchess Mine, Latouche Island, Alaska	t	Goldfarb et al. (1996)
Black-18A	Blackbird Mine, Latouche Island, Alaska	t	Goldfarb et al. (1996)
Beat-16	Beatson Mine, Latouche Island, Alaska	t	Goldfarb et al. (1996)
V-Ely-1	Creek downstream from Ely Mine, Vermont	mst	This study
<i>Besshi-type, hosted by graphitic schists</i>			
FC-3	Adit, Fontana Creek, Tennessee	a	This study
SUG-1 0.2	Sugar Mine, Tennessee	a	This study
<i>Cobalt-rich, hosted by metamorphosed sediments</i>			
*BB25	Cobalt, Idaho	os, r	McHugh et al. (1987)
High sulfidation (quartz alunite epithermal)			
<i>Acid-sulfate alteration</i>			
AD-3	Reynolds Adit, Summitville, Colorado	a, r	This study; Plumlee et al. (1995b)
AD-3	Reynolds Adit, Summitville, Colorado	a, r	This study; Plumlee et al. (1995b)
AD-3	Reynolds Adit, Summitville, Colorado	a, r	This study; Plumlee et al. (1995b)
AD-3	Reynolds Adit, Summitville, Colorado	a, r	This study; Plumlee et al. (1995b)
AD-3	Reynolds Adit, Summitville, Colorado	a, r	This study; Plumlee et al. (1995b)
AD-1435C	Reynolds Adit, Summitville, Colorado	a, r	This study; Plumlee et al. (1995b)

Deposit type			
<i>Ore / alteration type</i>	Description	Water	Reference
Sample		Type	
Chand-1	Chandler Adit, Summitville, Colorado	a, r	This study; Plumlee et al. (1995b)
Chand-1	Chandler Adit, Summitville, Colorado	a, r	This study; Plumlee et al. (1995b)
Chand-1	Chandler Adit, Summitville, Colorado	a, r	This study; Plumlee et al. (1995b)
Dike 2	Cropsy Waste Dump, Summitville, Colorado	d, r	This study; Plumlee et al. (1995b)
550D-R	Cropsy Waste Dump, Summitville, Colorado	d, r	This study; Plumlee et al. (1995b)
North Dump	North Waste Dump, Summitville, Colorado	d, r	This study; Plumlee et al. (1995b)
N Dump S Seep	North Waste Dump, Summitville, Colorado	d, r	This study; Plumlee et al. (1995b)
SC12	Tailings impoundment, Summitville, Colorado	t, r	This study; Plumlee et al. (1995b)
Blackstrap	Seep in open pit, Summitville, Colorado	o, r	This study; Plumlee et al. (1995b)
SOB-1 Seep	Seep in open pit, Summitville, Colorado	o, r	This study; Plumlee et al. (1995b)
IOWA-1	Seep below Iowa Adit, Summitville, Colorado	a, r	This study; Plumlee et al. (1995b)
SPIT-1 Pond	Snowmelt pond in South Pit, Summitville, Colorado	o, r	This study; Plumlee et al. (1995b)
SPIT-2 Pond	Snowmelt pond in South Pit, Summitville, Colorado	o, r	This study; Plumlee et al. (1995b)
NPIT-1 Pond	Snowmelt pond in North Pit, Summitville, Colorado	o, r	This study; Plumlee et al. (1995b)
Ch Seep	Seep near Chandler Adit, Summitville, Colorado	ms	This study; Plumlee et al. (1995b)
Missionary East	Seep near Reynolds Adit, Summitville, Colorado	ms	This study; Plumlee et al. (1995b)
Sh-1	Seep in mine waste pile, Summitville, Colorado	d, r	This study; Plumlee et al. (1995b)
TD Seep	Seep, Summitville, Colorado	ms	This study; Plumlee et al. (1995b)
AREA L	Seep in mine waste pile, Summitville, Colorado	d, r	This study; Plumlee et al. (1995b)
lkp fa	Longfellow-Kohler pond, Red Mtn. Pass, Colorado	a	This study
long 1 fa	Longfellow Tunnel, Red Mtn. Pass, Colorado	a	This study
3R-1	Stream below 3R Mine, Patagonia Mtns., Arizona	ms	This study
*EC91AP16	Mt. Macintosh, Vancouver, British Columbia	nst	Koyanagi and Panteleyev (1994)
*EC91AP19	Mt. Macintosh, Vancouver, British Columbia	nst	Koyanagi and Panteleyev (1994)
*EC91AP22	Mt. Macintosh, Vancouver, British Columbia	nst	Koyanagi and Panteleyev (1994)
*EC91AP24	Mt. Macintosh, Vancouver, British Columbia	nst	Koyanagi and Panteleyev (1994)
*EC92AP-21	Mt. Macintosh, Vancouver, British Columbia	nst	Koyanagi and Panteleyev (1994)
<i>Propylitic alteration</i>			
Missionary West	Seep near Reynolds Adit, Summitville, Colorado	ms	This study
Cordilleran Lode			
<i>Advanced-argillic to quartz-sericite-pyrite alteration</i>			
*Berkeley Pit Surface	Butte, Montana	op	Davis and Ashenberg (1989)
*Berkeley Pit 3 meters	Butte, Montana	op	Davis and Ashenberg (1989)
*Berkeley Pit 100 meters	Butte, Montana	op	Davis and Ashenberg (1989)
Hot Spring S-Au			
<i>Shallow acid-sulfate alteration</i>			
*82WA119	Leviathan, California	a	Ball and Nordstrom (1989)
*81WA132C	Leviathan, California	a	Ball and Nordstrom (1989)
*82WA118	Leviathan, California	a	Ball and Nordstrom (1989)
Climax-type Porphyry Mo			
<i>Potassic, quartz-sericite-pyrite, greisen alteration</i>			
mcn 1 fa	McNulty Dump, Climax, Colorado	d, r	This study
mcn 2 fa	McNulty Dump, Climax, Colorado	d, r	This study
Porphyry Cu, Cu-Mo			
<i>Quartz-sericite-pyrite alteration</i>			
*MW Weir 3	Mt. Washington, British Columbia	op	Kwong (1991)
*MW Weir 1	Mt. Washington, British Columbia	op	Kwong (1991)

Deposit type			
<i>Ore / alteration type</i>	Description	Water	Reference
Sample		Type	
*MW BH89-14	Mt. Washington, British Columbia	og	Kwong (1991)
*MW BH89-4	Mt. Washington, British Columbia	og	Kwong (1991)
*MW BH89-3	Mt. Washington, British Columbia	og	Kwong (1991)
*MW BH89-10	Mt. Washington, British Columbia	og	Kwong (1991)
*MW BH89-8	Mt. Washington, British Columbia	og	Kwong (1991)
*MP1W1, Globe	Globe, Arizona	og	Eychaner (1988)
TMT-29	Alamosa River basin, Colorado	ns	Barry (1996)
TMT-28	Alamosa River basin, Colorado	ns	Barry (1996)
TMT-38	Alamosa River basin, Colorado	ns	Barry (1996)
<i>Propylitic alteration</i>			
*MW BH89-2	Mount Washington, British Columbia	og	Kwong (1991)
*MW BH89-13	Mount Washington, British Columbia	og	Kwong (1991)
Algoma Banded Fe Formation			
<i>Sulfide-facies</i>			
*Sherman S Pit	South Pit, Sherman Mine, Temagami, Ontario	op	Shelp et al. (1994)
Polymetallic veins			
<i>Zn, Pb, ± Cu-rich</i>			
St.KeV	St. Kevin's Gulch, Colorado	a	Smith (1991)
St.KeV	St. Kevin's Gulch, Colorado	a	Smith (1991)
PENN1.1	Pennsylvania Mine, Summit County, Colorado	a	This study
SHO1.1	Shoe Basin Mine, Summit County, Colorado	a	This study
<i>Au-quartz-pyrite</i>			
DRUID1FA.45	Druid Mine, Central City, Colorado	ms	This study
Druid shaft	Druid Mine, Central City, Colorado	a	This study
Argo 1 fa	Argo Tunnel, Central City, Colorado	a, r	This study
Argo 1 fa.1	Argo Tunnel, Central City, Colorado	a, r	This study
ARGO1.1	Argo Tunnel, Central City, Colorado	a, r	This study
VC1A.1	Idaho Mine, Central City, Colorado	a	This study
VC1B.1	Idaho Mine, Central City, Colorado	a	This study
<i>Pyrite-rich; Zn, Pb, Cu-poor</i>			
PMB193 FA .2	Pass Me By Mine, Alamosa River, Colorado	a	This study
PMB1FA.1	Pass Me By Mine, Alamosa River, Colorado	a	This study
Burnt Adit	Burnt Creek Mine, Alamosa River basin, Colorado	a	This study
Burnt Dump	Burnt Creek Mine, Alamosa River Basin, Colorado	d	This study
ARC FA .2	Alamosa River Canyon, Colorado	ns	This study
Fe Spring, Fe Crk	Iron Creek, Alamosa River Basin, Colorado	ns	This study
Burnt Spring	Burnt Creek, Alamosa River Basin, Colorado	ns	This study
SMCB1FA.1	Unnamed adit, South Mineral Creek, Creede, Colorado	ns	This study
<i>Carbonate-rich, or in rocks altered to contain carbonate</i>			
CHAP3FA.45	Chapman Gulch, Ophir, Colorado	a	This study
CHAP2FA.1	Seep, Chapman Gulch, Ophir, Colorado	ns	This study
bon 1 fa	Bonner Mine, Mineral Creek Basin, Colorado	a	This study
MIZ FA .2	Mizer Mine, Alamosa River Basin, Colorado	a	This study
ASIA FA .2	Asiatic Mine, Alamosa River Basin, Colorado	a	This study
CARC-1 FA .2	Unnamed adit 1, Carson Camp, Colorado	a	This study
CARC-3 FA .2	Unnamed adit 3, Carson Camp, Colorado	a	This study
CARC-2 FA .2	Unnamed adit 2, Carson Camp, Colorado	a	This study
ns1 fa	North Star Mine, Silverton, Colorado	a	This study
para up fa	Paradise Portal, Ophir Pass., Colorado	a	This study

Deposit type			
<i>Ore / alteration type</i>	Description	Water	Reference
Sample		Type	
Para 1 fa	Adit near Paradise Portal, Ophir Pass., Colorado		a This study
BUR FA .2 8/1	Burley Tunnel, Silver Plume, Colorado		a, r This study
NATL FA .2 8/	National Tunnel, Blackhawk, Colorado		a This study
NTUN1.1	National Tunnel, Blackhawk, Colorado		a This study
GAM6FA.1	Gamble Gulch, Gilpin County, Colorado		ns This study
MC1FA.1	Unnamed adit, Miners Creek, Creede, Colorado		a This study
Creede-type epithermal			
<i>Carbonate-poor</i>			
AL1FA.1	Alpha Corsair, Creede, Colorado		a This study
SOL1FA.1	Solomon, Creede, Colorado		a This study
<i>Carbonate-rich, or in propylitically altered rocks</i>			
RAW1FA.1	Rawley 12 Adit, Bonanza, Colorado		a This study
*Rawley	Rawley 12 Adit, prior to collapse, Bonanza, Colorado		a Moran (1973)
*Rawley	Rawley 12 Adit, prior to collapse, Bonanza, Colorado		a Moran (1973)
*Rawley	Rawley 12 Adit, prior to collapse, Bonanza, Colorado		a Moran (1973)
Raw1 (Rawley 12)	Rawley 12 Adit, Bonanza, Colorado		a This study
ML-ad	Minnie Lynch Mine, Bonanza, Colorado		a This study
ML-FP	Minnie Lynch Mine, Bonanza, Colorado		a This study
ML-1	Minnie Lynch Mine, Bonanza, Colorado		d This study
Rawley 3 seep	Rawley 3 Adit, Bonanza, Colorado		d This study
KC tail	Kerber Creek Tailings, Bonanza, Colorado		t, r This study
Am 1 fa	American Tunnel, Silverton, Colorado		a, r This study
Magmatic sulfide			
<i>Massive iron-, nickel-, and copper-sulfide lenses in ultramafic rocks</i>			
*DUL	Waste stockpile, Duluth Complex, Minnesota		d Eger (1992)
Polymetallic replacement and skarns			
<i>Sandstones and other carbonate-poor host rocks</i>			
*Eagle 1610	Eagle Mine, Gilman District, Colorado		a, r Engineering Science, Inc. (1985)
*Eagle 1610	Eagle Mine, Gilman District, Colorado		a, r Engineering Science, Inc. (1985)
*Eagle 1610	Eagle Mine, Gilman District, Colorado		a, r Engineering Science, Inc. (1985)
*Eagle Chief	Eagle Mine, Gilman District, Colorado		a, r Engineering Science, Inc. (1985)
*Eagle Chief	Eagle Mine, Gilman District, Colorado		a, r Engineering Science, Inc. (1985)
<i>Igneous-hosted ores</i>			
GAM4FA.1	Tip Top, Gilpin County, Colorado		a This study
YAK1FA.1	Yak Tunnel, Leadville, Colorado		a, r This study
GAR1FA.1	Garibaldi Mine, Leadville, Colorado		a This study
<i>Calc-silicate skarns</i>			
*Glngar GW-1	Glengarry Mine, New World, Montana		a Pioneer Technical Services (1994)
*Glngar GW-2	Glengarry Mine, New World, Montana		a Pioneer Technical Services (1994)
*Glngar SW-2	Glengarry Mine, New World, Montana		d Pioneer Technical Services (1994)
*McLar	McLaren Mine, New World, Montana		d Pioneer Technical Services (1994)
<i>Carbonate-hosted, pyrite-rich</i>			
BAN1FA.1	Bandora Mine, Silverton, Colorado		a This study
LD1FA.1	Leadville Drain, Leadville, Colorado		a This study
FG1.1	French Gulch, Breckenridge, Colorado		ms This study
kok fa	Kokomo Mine, Climax, Colorado		a This study
<i>Carbonate-hosted, pyrite-poor</i>			
Anon1 fa.1	Anonymous mine #1, Park City, Utah		a This study

Deposit type			
<i>Ore / alteration type</i>	Description	Water	Reference
Sample		Type	
Anon2 fa	Anonymous Mine #2, Park City, Utah	a	This study
*FishCk1	Fisher Creek Adit, New World, Montana	a	Pioneer Technical Services (1994)
*Blkwar	Black Warrior Mine, New World, Montana	a	Pioneer Technical Services (1994)
*LilDaisy	Little Daisy Mine, New World, Montana	a	Pioneer Technical Services (1994)
Sedimentary-exhalative (SEDEX)			
<i>Hosted by shales and cherts with no carbonates</i>			
*#2016, Alaska (natural)	Unnamed deposit, Alaska	ns	W. R. Miller, unpub. data
*#2019, Alaska (natural)	Unnamed deposit, Alaska	ns	W. R. Miller, unpub. data
*#2015, Alaska (natural)	Unnamed deposit, Alaska	ns	W. R. Miller, unpub. data
*#2021, Alaska (natural)	Unnamed deposit, Alaska	ns	W. R. Miller, unpub. data
DW010	Drenchwater Creek deposit, Brooks Range, Alaska	nst	Kelley and Taylor (1997)
DW017	Drenchwater Creek deposit, Brooks Range, Alaska	nst	Kelley and Taylor (1997)
DW018	Drenchwater Creek deposit, Brooks Range, Alaska	nst	Kelley and Taylor (1997)
DW024	Drenchwater Creek deposit, Brooks Range, Alaska	nst	Kelley and Taylor (1997)
DW026	Drenchwater Creek deposit, Brooks Range, Alaska	nst	Kelley and Taylor (1997)
RD 23	Red Dog deposit, Brooks Range, Alaska	nst	Kelley and Taylor (1997)
RD33	Red Dog deposit, Brooks Range, Alaska	nst	Kelley and Taylor (1997)
RD42	Red Dog deposit, Brooks Range, Alaska	nst	Kelley and Taylor (1997)
RD44	Red Dog deposit, Brooks Range, Alaska	nst	Kelley and Taylor (1997)
<i>Hosted by shales, cherts, and carbonates</i>			
LK57	Lik Deposit, Brooks Range, Alaska	nst	Kelley and Taylor (1997)
LK61	Lik Deposit, Brooks Range, Alaska	nst	Kelley and Taylor (1997)
LK62	Lik Deposit, Brooks Range, Alaska	nst	Kelley and Taylor (1997)
Mississippi-Valley-Type (MVT)			
<i>Jasperoid-poor</i>			
*Site 4-Drill (mean)	Bonehole, Old Lead Belt, SE Missouri	ms	Smith and Schumacher (1993)
*Site 5 (mean)	Desloge, Old Lead Belt, SE Missouri	ts	Smith and Schumacher (1993)
*Site 8 (mean)	Elvins, Old Lead Belt, SE Missouri	ts	Smith and Schumacher (1993)
DAU1.FA.1	Dauntless Mine, Mt. Sherman, Colorado	a	This study
RUB1.RA	Ruby Mine, Weston Pass, Colorado	a	This study
WP2FA.1	Weston Pass, Colorado	nst	This study
<i>Abundant jasperoid</i>			
*Map # 101	St. Regis Mine, Tri-State District, Missouri	mg	Barks (1977)
*Map #105	Vogey Mine, Tri-State District, Missouri	mg	Barks (1977)
*Map # 109	Sunset Mine, Tri-State District, Missouri	mg	Barks (1977)
*Map # 14	Orongo, Tri-State District, Missouri	ts	Barks (1977)
*Map #16	Orongo, Tri-State District, Missouri	ts	Barks (1977)
*Map # 17	Webb City, Tri-State District, Missouri	ts	Barks (1977)
Sediment-hosted Au			
<i>Primarily oxide ore</i>			
*Boss 4/1/94	Boss Pit, Esmerelda County, Nevada	o	Price et al. (1995)
*Boss Pit 7/1/94	Boss Pit, Esmerelda County, Nevada	o	Price et al. (1995)
*Boss Pit 12/26/94	Boss Pit, Esmerelda County, Nevada	o	Price et al. (1995)
*Cortez East, 6/15/92	Cortez Pit, Carlin, Nevada	o	Price et al. (1995)
*Cortez Middle, 6/15/92	Cortez Pit, Carlin, Nevada	o	Price et al. (1995)
*Cortez West, 6/15/92	Cortez Pit, Carlin, Nevada	o	Price et al. (1995)
*Big Springs 5/30/95	Big Springs Pit, Jerritt Canyon, Nevada	o	Price et al. (1995)
*Big Springs 4/13/95	Big Springs Pit, Jerritt Canyon, Nevada	o	Price et al. (1995)

Deposit type			
<i>Ore / alteration type</i>	Description	Water	Reference
Sample		Type	
<i>Primarily sulfide ore, carbonate-poor host rocks</i>			
*DW-06, 12/22/94	South Pit, Twin Creeks, Nevada	og-ng?	BLM (1996)
*DW-06, 12/22/94	South Pit, Twin Creeks, Nevada	og-ng?	BLM (1996)
*DW-07, 12/22/94	South Pit, Twin Creeks, Nevada	og-ng?	BLM (1996)
*394318-1, 6/14/95	near West Pit, Twin Creeks, Nevada	ng-og?	BLM (1996)
*394319-2, 8/17/95	near South Pit, Twin Creeks, Nevada	ng-og?	BLM (1996)
Low-sulfide Au-quartz veins			
LCK2	Little Creek Prospect, Kenai Fjords Natl. Park, Alaska	mst	Cieutat et al. (1994)
SF6	Sonny Fox Mine, Kenai Fjords Natl. Park, Alaska	a	Cieutat et al. (1994)
Goy13	Goyne Prospect, Kenai Fjords Natl. Park, Alaska	a	Cieutat et al. (1994)
McKin2	McKinley Lake Dist., Chugach Natl. Forest, Alaska	a	Trainor et al. (1996)
McKin5	McKinley Lake Dist., Chugach Natl. Forest, Alaska	a	Trainor et al. (1996)
McKin11	McKinley Lake Dist., Chugach Natl. Forest, Alaska	a	Trainor et al. (1996)
McKin13	McKinley Lake Dist., Chugach Natl. Forest, Alaska	a	Trainor et al. (1996)
McKin19	McKinley Lake Dist., Chugach Natl. Forest, Alaska	a	Trainor et al. (1996)
Ind1	Independence Mine, Willow Creek District, Alaska	t	Goldfarb et al. (1996)
Ind2	Independence Mine, Willow Creek District, Alaska	a	Goldfarb et al. (1996)
GC4	Gold Cord Mine, Willow Creek District, Alaska	t	Goldfarb et al. (1996)
HG6	High Grade Mine, Willow Creek District, Alaska	a	Goldfarb et al. (1996)
HG7	High Grade Mine, Willow Creek District, Alaska	t	Goldfarb et al. (1996)
HY16	Hi-Yu tailings, Fairbanks District, Alaska	t	Goldfarb et al. (1996)
Ch21	Christina Mine, Fairbanks District, Alaska	a	Goldfarb et al. (1996)
Pt22	Placer Tailings, Cleary Crk., Fairbanks, Alaska	pt	Goldfarb et al. (1996)
Sc23	Scrafford mine, Fairbanks district, Alaska	d	Goldfarb et al. (1996)
M27	Mexican mill tailings, Juneau District, Alaska	t	Goldfarb et al. (1996)
Eb28	Ebner Mine, Juneau District, Alaska	a	Goldfarb et al. (1996)
AJ29	Alaska-Juneau Mine, Juneau District, Alaska	a	Goldfarb et al. (1996)
Alkalic Au-Ag-Te veins			
CAR1FA.1	Carlton Tunnel, Cripple Creek, Colorado	a	This study
hur 1 fa	Huron Adit, Eldora, Colorado	a	This study
swa 1 fa	Swathmore Adit, Eldora, Colorado	a	This study
Sediment-hosted U			
*MVD-1	Moonlight Mine, Monument Valley district, Arizona	og	Longsworth (1994)
*MVD-2	Moonlight Mine, Monument Valley district, Arizona	og	Longsworth (1994)
*MVSW-1	Moonlight Mine, Monument Valley district, Arizona	op	Longsworth (1994)
*3T-529	Manuel Denetstone #3 Mine, Cameron district, Arizona	og	Longsworth (1994)
*JSW-1	Jeepster #1 Mine, Cameron district, Arizona	op	Longsworth (1994)

Deposit type <i>Ore / alteration type</i> Sample	Temp. °C	Spec. Cond. µS/cm	Alk. mg/l CaCO ₃	pH	Diss. O ₂ ppm	SO ₄ mg/l	F mg/l	Cl mg/l	Al mg/l	As µg/l
Volcanogenic massive sulfide (VMS)										
<i>Kuroko-type, hosted by volcanic rocks</i>										
*Rich-90WA103	35			0.48		118000			2210	56400
*Rich-90WA108	42			-0.35		420000			4710	169000
*Rich-90WA109	32			-0.7		360000			6680	154000
*Rich-90WA110A	42			-1		760000			1420	340000
*LMG				1.8					3520	50000
Hol-511	15	4420		2.9		1400	1		8.4	-1
Hol-528	8	5600		2.9		1700	2	2	>10	-1
Hol-529	5	2680		3.1		860		1	>10	-1
Hol-534	4.5	840		4.5		340	0.6	3	2.4	-1
Hol-548	3	960		4.6		340	0.7	1.7	2.2	1
Hol-549A	16	16000		3.1		12000	7		>10	1
Hol-549B	18	37500		2.8		39700	60		>10	1
<i>Besshi-type, hosted by sedimentary and intermediate submarine volcanic host rock</i>										
Duch-1	7	320	20	6.1	9.5	166	0.07	3.8	0.015	
Duch-2	12	790		2.9	9	197	0.07	4	>3	
Black-18A	10	822	-10	3.1	8	311	0.4	3.7	>3	
Beat-16	7	146	38	6.7	5	31	0.07	3.4	0.004	
V-Ely-1	21.5	1046		2.98	9	352	0.16	0.51	14	
<i>Besshi-type, hosted by graphitic schist</i>										
FC-3	14	73.2		5.45	6.5	23	0.06	0.48	-0.5	-1
SUG-1 0.2	13	286		4.98	6	103	0.16	0.55	1.8	-1
<i>Cobalt-rich, hosted by metamorphosed sediments</i>										
*BB25				4.38		2400	2.4	21	54	39
High sulfidation (quartz alunite epithermal)										
<i>Acid sulfate alteration</i>										
AD-3	4	2100		3.16		2200			112	360
AD-3	4.5	3200		2.94	10	1920		4.7	130	400
AD-3	4	5400		2.72	10	4530			290	2900
AD-3						4510	-0.5	2.2	230	790
AD-3	4	1800		3.23	10	1650	0.67	6.5	150	130
AD-1435C	4	10		3.25	-	2133			160	460
Chand-1	4	7110		2.37	10	15000	3.7	1.0	430	3900
Chand-1	6	5530		2.77	12	6250	0.99	1.5	340	1500
Chand-1	4	5820		2.92	12	12600	1.6	1.3	310	2500
Dike 2	6	10300		2.31	10	23000		26	2350	5700
550D-R	13.5	7650		2.52	10	8370			890	190
North Dump						3800	1.7	2	260	-40
N Dump S Seep	7.5	7500		2.41	10	11300	3.3	2.5	710	160
SC12	14.5	4100		2.9	10	3360			200	110
Blackstrap	~14	38000		1.75		125800		240	5380	15000
SOB-1 Seep	18	19500		1.71	10	29850			2100	28000
IOWA-1	5	2800		2.79	10	1900	-0.5	2.0	190	18
SPIT-1 Pond	19	3300		2.48	10	2320	0.70	1.3	140	690
SPIT-2 Pond	19	4600		2.41	10	7890	-0.25	2.2	290	3400
NPIT-1 Pond	14	2510		2.73		2140	1.1	0.59	180	110
Ch Seep	3	3670		3.01	10	5000	-0.5	0.51	280	82
Missionary East	5	1450		3.84	4.5	1540	0.51	1.1	120	200
Sh-1	8	5090		3.41	6	7310	1.2	27	210	-20

Deposit type <i>Ore / alteration type</i> Sample	Temp. °C	Spec. Cond. µS/cm	Alk. mg/l CaCO ₃	pH	Diss. O ₂ ppm	SO ₄ mg/l	F mg/l	Cl mg/l	Al mg/l	As µg/l
TD Seep	4	858		3.76	3	425	0.23	10	5	190
AREA L	10	3090		2.51	10	4820	1.2	2.4	110	78
lkp fa	16	3600		2.61	10	1740			60	6700
long 1 fa	3.5	1900		3.11	5	660	2.9		11	1400
3R-1	20.3	971		3.2	12	489	0.48	5.8	52	
*EC91AP16	13.1	163.2		3.9		31			2	
*EC91AP19	13.7	176.5		3.8		39			2	
*EC91AP22	9.4	244		3.5		50			6	
*EC91AP24	9.1	53.9		3.7		228			16	
*EC92AP-21	28.9	2400		2		1300			46	
<i>Propylitic alteration</i>										
Missionary West	5	374	100	6.84	1	110	0.41	0.52	0.07	-20
Cordilleran Lode										
<i>Advanced-argillic to quartz-sericite-pyrite alteration</i>										
*Berkeley Pit Surface				2.86		3850		12	126	30
*Berkeley Pit 3 meters				2.8		5740		9	152	50
*Berkeley Pit 100 meter				3.08		7060		20	206	700
Hot Spring S/Au										
<i>Shallow acid-sulfate alteration</i>										
*82WA119				1.85		11200	5.1	9.2	623	41000
*81WA132C				2.45		5400			440	27100
*82WA118				1.8		7540	3.4	8.4	438	35000
Climax-type Porphyry Mo										
<i>Potassic, quartz-sericite-pyrite, greisen alteration</i>										
mcn 1 fa	4	6800		1.86	10	4340	710		960	6
mcn 2 fa	5	4700		1.9	10	2570	379		590	5
Porphyry Cu, Cu/Mo										
<i>Quartz-sericite-pyrite alteration</i>										
*MW Weir 3	8.3			3.48		226			7.2	-50
*MW Weir 1	4.8			3.59		696			22	-50
*MW BH89-14	7.9			3.84		50.9			1.5	-50
*MW BH89-4	5.4			3.65		608			10.7	-50
*MW BH89-3	5			4.37		445			9.3	-50
*MW BH89-10	5.8			5.66		406			0.07	310
*MW BH89-8	6.6			4.64		452			0.93	310
*MP1W1, Globe				3.6		8800	0.3	340	250	-5
TMT-29	6.4	2540		2.3	12	407	0.9	1.1	66	1
TMT-28	5.4	1430		2.8	4	1010	1.8	0.1	70	1
TMT-38	8.9	10860		2.28	12	13400	8.4	3.6	390	44
<i>Propylitic alteration</i>										
*MW BH89-2	3.6		11.3	6.5		15.9			-0.05	-50
*MW BH89-13	5.4		172	6.9		192			-0.05	120
Algoma Banded Fe Formation										
<i>Sulfide-facies</i>										
*Sherman S Pit				3		1500	1.4	7	10	

Deposit type <i>Ore / alteration type</i> Sample	Temp. °C	Spec. Cond. µS/cm	Alk. mg/l CaCO ₃	pH	Diss. O ₂ ppm	SO ₄ mg/l	F mg/l	Cl mg/l	Al mg/l	As µg/l
Polymetallic veins										
<i>Zn, Pb, ± Cu-rich</i>										
St.Kev				2.72		1290			19	8
St.Kev				2.67		1150			16	7
PENN1.1	5	1300		3.65	6				20	-20
SHO1.1	2.5	770		3.62	10	440	1	0.5		-20
<i>Au-quartz-pyrite</i>										
DRUID1FA.45	10	6000		2.75	9.5	5300	-0.5	10	430	180
Druid shaft	14	6660		2.63	8	7200	5.5	8.3	98	180
Argo 1 fa				2.72	10				29	150
Argo 1 fa.1				2.65					23	120
ARGO1.1	17	4000		2.93	10	2100			25	91
VC1A.1	10	3300		4.65	0.078	2000	3.1	7.2	4.7	-20
VC1B.1	9	3300		4.2	2	1980	2.9	4.7	5.8	-20
<i>Pyrite-rich; Zn, Pb, Cu-poor</i>										
PMB193 FA .2	6	1100		3.02	0.1	630	0.38	0.75	59	33
PMB1FA.1	4.5	1200		3.02	0.075	660	0.3	1.1	51	24
Burnt Adit				3.1		220	0.55	0.56	5	-3
Burnt Dump				4.83		320	1.1	0.33	2	-3
ARC FA .2	9	2600		2.75	11.8				38	-1
Fe Spring, Fe Crk				2.94		220	0.2	0.48	9	-3
Burnt Spring				3.82		1300	5.3	1.6	31	-3
SMCB1FA.1	11.5	750		3.09	4	490	0.01	0.51	21	0.05
<i>Carbonate-rich, or in rocks altered to contain carbonate</i>										
CHAP3FA.45		1000		6.9	0.1	700	-0.1	0.9	0.1	-1
CHAP2FA.1	8	2000	62	7.58	0.1	920	0.01	2.1	0.028	-2
bon 1 fa	5.5	920		3.09	8	330	0.6	0.7	5	-2
MIZ FA .2	7.5	620		5.85	3.6	264	0.6	0.39	0.05	-1
ASIA FA .2	9	480		6	10	163	0.25	0.33	1	-1
CARC-1 FA .2	4	840		3.47	1.5	500	0.54	0.43	17	-3
CARC-3 FA .2	5	400		6.46	0.6	140	0.26	0.35	0.06	6
CARC-2 FA .2		410		6.04	9	180	0.3	0.18	0.2	-3
ns1 fa	8	860		6.57	9	310	1.5	1.9	7	-2
para up fa	6	2000		5.86	0.002	1110			2	-2
Para 1 fa	5	2200		5.37	0.002	1270	5.1	1.4	13	36
BUR FA .2 8/1	8	1000		5.7	7.5	430	1.1	18	1	-3
NATL FA .2 8/	8	1500		5.36	6	900	-0.05	2.4	0.007	-3
NTUN1.1	6	1400		6.18	5	810			0.5	2
GAM6FA.1	5.5	470		6.74	8.0	185	-0.1	0.5	0.02	0.05
MC1FA.1	12	340	58	6.7	7	75	0.01	1.05	0.01	15
Creede-type epithermal										
<i>Carbonate-poor</i>										
AL1FA.1	10	730		4.37	10	290	-0.1	2	5	15.4
SOL1FA.1	7.5	790		4.45	9	260	-0.1	0.6	1.1	0.05
<i>Carbonate-rich, or in propylitically altered rocks</i>										
RAW1FA.1	9.5	1100	61	5.96	0.1	600	0.7	-0.1	0.4	8
*Rawley			0	3.6						5
*Rawley		900	0	3.4						

Deposit type <i>Ore / alteration type</i> Sample	Temp. °C	Spec. Cond. µS/cm	Alk. mg/l CaCO ₃	pH	Diss. O ₂ ppm	SO ₄ mg/l	F mg/l	Cl mg/l	Al mg/l	As µg/l
*Rawley	9.5	1050	0	3.5					0.88	
Raw1 (Rawley 12)	9.5	1200		5.67	1	700	1.3	0.54	2	8.5
ML-ad	7	840		5.97	-1	440	1.1	0.84	0.14	44
ML-FP	5	700		5.93	-1	230	1.5	0.86	0.02	5.5
ML-1	11	1100		2.84	10	620	1.2	0.8	11.00	-1
Rawley 3 seep	6.5	820		2.82	10	230	0.6	0.36	3	7.4
KC tail	22	4890		2.37	10	12200	6.7	1.3	200	2300
Am 1 fa	12	2400		6.59	10	1270	5.7		7	-2
Magmatic sulfide										
<i>Massive iron-, nickel-, and copper-sulfide lenses in ultramafic rocks</i>										
*DUL			3	5.2		820				
Polymetallic replacement and skarns										
<i>Sandstones and other carbonate-poor host rocks</i>										
*Eagle 1610	20.9	5400		4.84		7770		9.5		1000
*Eagle 1610		9300		4.8		9530		7.8	16	
*Eagle 1610		8880	-5	4.5		9600		6.8	11	-1250
*Eagle Chief	10.3	1290		3.59		1405		5.7		-2500
*Eagle Chief		4370		3.9		3340		5.4	2.8	
<i>Igneous-hosted ores</i>										
GAM4FA.1	8	880		3.78	7.5	300	-0.1	2.7	5	0.05
YAK1FA.1	9	980		4.44	7.5	593	1.3	1.1	3	1.7
GAR1FA.1	4.5			4.76	5	75	0.2	0.24	0.3	0.05
<i>Calc-silicate skarns</i>										
*Glngar GW-1				3.23		489		10		7.31
*Glngar GW-2				3.85		77		<5		2.27
*Glngar SW-2				3.43		94		-5		1.89
*McLar				3.21		1210		55		-1.1
<i>Carbonate-hosted, pyrite-rich</i>										
BAN1FA.1	8	660	41	6.38	7.5	210	0.01	2.1	-0.1	1
LD1FA.1	7	700	155	7.15	7.5	246	1.4	1.2	-0.1	0.05
FG1.1	7	4000		6.23	0.15	1800	3.3	1.4	0.1	-20
kok fa	4	820		6.83	0.3	380			0.2	3
<i>Carbonate-hosted, pyrite-poor</i>										
Anon1 fa.1	4.5	390		7.42	8				0.017	2
Anon2 fa	8	970		7.21	7.5				0.006	42
*FishCk1				6.95		17		5		6.5
*Blkwar				7.22		25		7		-1.1
*LilDaisy				7.24		341		6		3.2
Sedimentary-exhalative (SEDEX)										
<i>Hosted by shales and cherts with no carbonates</i>										
*#2016, Alaska (nat.)				4.12		69000	129	354	1900	750
*#2019, Alaska (nat.)				3		11900	30	383	460	205
*#2015, Alaska (nat.)				4.52		7645	14	19	180	65
*#2021, Alaska (nat.)				2.54		2658	4.2	23	190	86
DW010	3	129		4.3		49	0.2	0.1	1	-0.9
DW017	4	2150		2.8		1180	0.5	-0.4	53	26
DW018	3	1410		3.1		964	0.55	1	95	4

Deposit type <i>Ore / alteration type</i> Sample	Temp. °C	Spec. Cond. µS/cm	Alk. mg/l CaCO ₃	pH	Diss. O ₂ ppm	SO ₄ mg/l	F mg/l	Cl mg/l	Al mg/l	As µg/l
DW024	8	1269		3.1		629	0.5	0.3	44	8
DW026	8	1242		3.1		610	0.5	0.3	43	7
RD 23	8.6	195		5.2						
RD33	6.9	192		6.2		75.4				
RD42	6.5	488		3.5						
RD44	3.6	386		5.4						
<i>Hosted by shales, cherts, and carbonates</i>										
LK57	5	127		6.2		127	0.2	0.6	0.2	
LK61	6	190		6.8		26	0.2	0.4	0.2	
LK62	5	320		7.6		60	0.3	0.4	-0.1	
Mississippi-Valley-Type (MVT)										
<i>Jasperoid-poor</i>										
*Site 4-Drill (mean)	14	946	296	7.1		260		10.6		
*Site 5 (mean)	11	998	240	8		340		15.1		
*Site 8 (mean)	15.4	1199	129	6.7		612		5.7		
DAU1.FA.1	1.5	90		7.86	9.5	2.3	-0.2	0.21	0.01	1
RUB1.RA	5	260		7.84	6	5.1	0.02	0.25	0.027	5.6
WP2FA.1	8		207	8.16	10				0.01	0.05
<i>Abundant jasperoid</i>										
*Map # 101	16	1730	53	5.7	0.5	940	0.5	4.9		
*Map #105	16.5	1530	80	7.1	9	830	0.6	3.1		
*Map # 109		2100	126	6.4		1100				
*Map # 14	10.5	386	90	7.3	9	88	0.5	4.3	0.02	
*Map #16	10	234	11	6.7	9.7	79	0.2			
*Map # 17	16.5	1100	69	7.2	8.5	490	0.5	3.6		
Sediment-hosted Au										
<i>Primarily oxide ore</i>										
*Boss 4/1/94			102	8.18		4860	4.3	4310		3100
*Boss Pit 7/1/94			100	8.19		4330	4.3	2740		920
*Boss Pit 12/26/94			102	8.1		4040	4.5	2580		1200
*Cortez East, 6/15/92				8.02		86.5	1.8	24.8		38
*Cortez Middle, 6/15/92			228	8.07		86	1.8	27.8		37
*Cortez West, 6/15/92			225	8.13		81.9	1.8	26.9		40
*Big Springs 5/30/95		1200	127	8.1		646	0.44	-1.5	-0.2	12
*Big Springs 4/13/95		656	80.7	7.75		283	0.15	1.6	-0.2	24
<i>Primarily sulfide ore, carbonate-poor host rocks</i>										
DW-06, 12/22/94	20.6		177	7.6		48.6	0.6	12.5		1180
DW-06, 12/22/94	24		172	7.8		48	0.6	12		680
DW-07,12/22/94	19.4		168	7.6		45.3	0.6	18.3		280
394318-1,6/14/95	17.9		189	7.55		68.3	0.5	15.3		510
394319-2,8/17/95	18		199	7.78		47.7	0.5	13.9		210
Low-sulfide Au-quartz veins										
LCk2	12	85	19	7.8		4.2		2		130
SF6	4	64	40	7.7		5.3		1.4		10
Goy13	8	19	13	7		0.8		0.4		40
McKin2	6	56	22.8	7.2					0.055	9

Deposit type <i>Ore / alteration type</i> Sample	Temp. °C	Spec. Cond. µS/cm	Alk. mg/l CaCO ₃	pH	Diss. O ₂ ppm	SO ₄ mg/l	F mg/l	Cl mg/l	Al mg/l	As µg/l
McKin5	8	19	14.8	7.4		3.4		1	0.014	9
McKin11	8.5	61	34.8	6.6		3.9		1.6	0.008	51
McKin13	11.5	17	3.6	5.8		1.1		1.1	0.036	4
McKin19	8	46	18.2	6.4		4		1.9	0.011	94
Ind1	4	127	34	6.9		32	-0.05	0.12	-0.01	3
Ind2	2	249	75	7.8		38	0.11	0.27	-0.01	37
GC4	4	166	48	7.3		18	-0.05	0.12	-0.01	3
HG6	7	82	27	8.7		6.3	-0.05	0.17	-0.01	5
HG7	4	66	21	7.5		6.2	-0.05	0.17	-0.01	4
HY16	9	339	-10	5.2		150	0.17	0.18	0.19	80
Ch21	3	324	105	7.6		72	0.16	0.29	-0.01	84
Pt22	5	383	155	7.3		77	0.07	0.29	0.01	14
Sc23	6	532	250	8.1		91	0.14	0.19	-0.01	92
M27	11	2350	-10	2.3		1130	0.33	2.2	7.5	-2
Eb28	7	384	170	8		48	0.33	2.1	-0.01	7
AJ29	6	897	160	8		349	-0.05	0.53	-0.01	2
Alkalic Au-Ag-Te veins										
CAR1FA.1	23.5	2800	331	7.66	7.5	1225	3.8	22	0.061	3.4
hur 1 fa	4.5	300	79	7.86	8				6	-2
swa 1 fa	6	520	160	7.33	7.5				0.036	-2
Sediment-hosted U										
*MVD-1	14	5950	336	7	0.4	3700	1.8	65		
*MVD-2	15	7200	406	7.1	0.4	4500	0.5	15		
*MVSU-1	15	5440	324	8	6.2	3300	2.6	51		
*3T-529	16	4200	264	7.5		280	1.3	1000		
*JSW-1	10.5	20300	63	9.5	11.2	12000	3.8	310		

Deposit type	Ca	Cd	Ce	Co	Cu	Fe tot	Fe ⁺⁺	Mg	Mn	Ni
<i>Ore /alteration type</i>	mg/l	µg/l	µg/l	µg/l	µg/l	mg/l	mg/l	mg/l	µg/l	µg/l
Sample										
Volcanogenic massive sulfide (VMS)										
<i>Kuroko-type, hosted by volcanic rocks</i>										
*Rich-90WA103	183	15900		1300	290000	20300	18100	821	17100	660
*Rich-90WA108	424	43000		2200	578000	55600	50800	1380	41800	2800
*Rich-90WA109	330	48300		15500	2340000	86200	79700	1450	42100	2900
*Rich-90WA110A	279	211000		5300	4760000	111000	34500	437	22900	3700
*LMG	5	45300			191000	29800	16700	2790	146000	
Hol-511	130	5.9	27	9	200	270		27	2100	11
Hol-528	130	22	48	27	330	390		44	2700	28
Hol-529	84	28	24	25	300	110		28	1500	23
Hol-534	94	29	2	5.6	900	0.94		8.8	320	7.2
Hol-548	78	62	4.2	27	3	-0.2		9.6	320	78
Hol-549A	160	1500	110	510	>40000	440		>100	>6000	150
Hol-549B	130	2300	170	970	>40000	>500		>100	>6000	180
<i>Besshi-type, hosted by sedimentary and intermediate submarine volcanic host rocks</i>										
Duch-1	42	0.8		1.8	9.5	0.13		4	200	-6
Duch-2	18	0.9		18	760	7.1		5.7	200	7
Black-18A	10	9.6		30	3600	21		36	750	10
Beat-16	12	-0.7		10	52	4.5		2.9	390	8
V-Ely-1	42	-10		210	3500	17		14	1300	52
<i>Besshi-type, hosted by graphitic schists</i>										
FC-3	6.9	0.7	0.2	1.2	97	0.047		2.4	150	1.0
SUG-1 0.2	9.9	18	54	15	7200	0.55		7.1	940	7.4
<i>Cobalt-rich, hosted by metamorphosed sediments</i>										
*BB25	140			150000	78000	0.15		115	14000	
High sulfidation (quartz alunite epithermal)										
<i>Acid sulfate alteration</i>										
AD-3	80	180	84	670	93000	260		25	14	760
AD-3	93	200	80	700	120000	310		34	18000	800
AD-3	120	330	80	1600	234000	920		51	31000	1900
AD-3	110	300	180	950	230000	570		45	23000	1200
AD-3	69	72	130	420	70000	190	177	20	12000	550
AD-1435C	48	70	20	540	84000	250		18	10000	640
Chand-1	150	440	450	2000	400000	1400	196	87	40000	2600
Chand-1	160	380	390	1400	290000	910	985	71	34000	1800
Chand-1	160	430	380	1400	260000	880	760	65	35000	1700
Dike 2	360	1000	2000	7000	220000	5010		380	180000	10000
550D-R	220	360	200	3000	56000	1100		150	92000	3600
North Dump	130	140	70	1000	39000	320		46	40000	1100
N Dump S Seep	310	400	1000	2400	100000	1200	635	100	65000	2600
SC12	250	180	150	1700	100000	540		58	77000	1400
Blackstrap	380	3000	6000	16000	460000	27900		840	370000	28000
SOB-1 Seep	480	460	780	7700	706000	12000		190	> 100000	11000
IOWA-1	82	81	300	460	19000	170		29	19000	580
SPIT-1 Pond	15	73	78	670	42000	470		9	4200	860
SPIT-2 Pond	30	110	220	1100	120000	840		23	19000	1300
NPIT-1 Pond	60	120	200	630	37000	280	79	29	15000	830
Ch Seep	69	220	260	950	270000	540	338	31	28000	1200
Missionary East	59	50	94	260	58000	150	169	15	5800	350
Sh-1	560	130	1100	1300	32000	600	223	140	100000	1300

Deposit type	Ca	Cd	Ce	Co	Cu	Fe tot	Fe ⁺⁺	Mg	Mn	Ni
<i>Ore /alteration type</i>	mg/l	µg/l	µg/l	µg/l	µg/l	mg/l	mg/l	mg/l	µg/l	µg/l
Sample										
TD Seep	87	7	9.3	80	28000	39	35	13	2400	82
AREA L	77	39	330	440	24000	390	102	24	14000	570
lkp fa	100	600	92	230	54000	420		24	16000	220
long 1 fa	66	63	13	63	1500	120		12	2400	23
3R-1	10	41		67	73000	0.54		6	520	65
*EC91AP16	5				120	0		2		
*EC91AP19	4				1	0		2		
*EC91AP22	0				10	0		1		
*EC91AP24	23				320	1		11		
*EC92AP-21	165				150	89		10		
<i>Propylitic alteration</i>										
Missionary West	73	-20	-1	3	150	-0.4	nm	11	700	-30
Cordilleran Lode										
<i>Advanced-argillic to quartz-sericite-pyrite alteration</i>										
*Berkeley Pit Surf. 453		1300			6900	250		194	79000	
*Berkeley Pit 3 m 462		1300			156000	386		201	95000	
*Berkeley Pit 100 m506		1900			218000	1040		272	162000	
Hot Spring S/Au										
<i>Shallow acid-sulfate alteration</i>										
*82WA119	266	338		5070	9640	2510		97	9320	13000
*81WA132C	110	150		3300	1200	1160		42	7600	8000
*82WA118	131	282		5110	5320	1570		53.8	10500	11900
Climax-type Porphyry Mo										
<i>Potassic, quartz-sericite-pyrite, greisen alteration</i>										
mcn 1 fa	420	520	800	1000	16000	140		260	79000	1300
mcn 2 fa	220	290	500	610	8700	210		110	59000	770
Porphyry Cu, Cu/Mo										
<i>Quartz-sericite-pyrite alteration</i>										
*MW Weir 3	31.6			138	16800	9.6		4.4	954	50
*MW Weir 1	156			295	15000	5.6		13	4070	150
*MW BH89-14	5.2			38	3050	1.29		1.3	368	-20
*MW BH89-4	128			483	9050	45.5		19	4760	260
*MW BH89-3	109			370	4200	26.8		14	6770	220
*MW BH89-10	91.1			163	18	53.4		11.2	5000	50
*MW BH89-8	97.8			205	1300	56.2		13.8	8410	40
*MP1W1, Globe	440	600		13000	150000	2800		390	75000	3100
TMT-29	4.3	14.0		200	1300	150	5	3	130	110
TMT-28	13.0	15.0		210	65	130	135	11	1700	110
TMT-38	150.0	29.0		530	2000	1900	1590	130	45000	280
<i>Propylitic alteration</i>										
*MW BH89-2	7.6			-5	91	0.03		1.4	189	-20
*MW BH89-13	105			-5	-5	0.017		24.5	0.75	-20
Algoma Banded Fe Formation										
<i>Sulfide-facies</i>										
*Sherman S Pit					100	10			5000	100

Deposit type <i>Ore /alteration type</i> Sample	Ca mg/l	Cd µg/l	Ce µg/l	Co µg/l	Cu µg/l	Fe tot mg/l	Fe ⁺⁺ mg/l	Mg mg/l	Mn µg/l	Ni µg/l
Polymetallic veins										
<i>Zn, Pb, ± Cu-rich</i>										
St.Kev	80.7	670		100	600	120		25.5	55600	100
St.Kev	80.2	430		90	500	111		26.7	62900	100
PENN1.1		180	76	92	5700	34	35			110
SHO1.1		80	-10	17	680		2			40
<i>Au-quartz-pyrite</i>										
DRUID1FA.45	190	840	870	780	44000	248		200	74000	1500
Druid shaft	430	960	510	780	5700	1300		170	190000	2000
Argo 1 fa	290	170	430	180	6700	170	3000	110	95000	280
Argo 1 fa.1	280	140	370	150	4900	150		100	90000	220
ARGO1.1	340	120	250	88	6400	99	30	130	101000	110
VC1A.1		240	81	200	140	72	160		57000	300
VC1B.1		250	100	240	260	65	140		62000	340
<i>Pyrite-rich; Zn, Pb, Cu-poor</i>										
PMB193 FA .2	7	2	6.1	120	78	150	120	2	310	100
PMB1FA.1	5.5	3	4.4	120	120	140	200	1.7	470	110
Burnt Adit	33	1	5.6	12	100	5		7	460	-10
Burnt Dump	81	-1	2.3	10	11	-1		15	220	20
ARC FA .2	150	4.7	360	240	350	92		100	15000	150
Fe Spring, Fe Crk	7	-1	2.0	33	3	26		2	650	20
Burnt Spring	320	2	24	110	58	72		42	4200	40
SMCB1FA.1	30	1.1	4.4	25	2	55	100	9	260	9.6
<i>Carbonate-rich, or in rocks altered to contain carbonate</i>										
CHAP3FA.45	270	1	9.8	21	1	6.03	5	8	1000	8.2
CHAP2FA.1	470	0.3	0.06	7.2	1	2.48	3	7	420	15
bon 1 fa	83	6	3	19	36	14		6	2400	5
MIZ FA .2	130	-1	0.1	4.5	2.5	2		13	280	7.7
ASIA FA .2	92	-1	0.3	1.4	18	4		11	420	4
CARC-1 FA .2	100	2	10	70	22	14		29	4400	39
CARC-3 FA .2	64	1	0.1	5.0	-2	6		17	1300	-10
CARC-2 FA .2	75	-1	0.2	8.0	-2	2		11	1000	-10
ns1 fa	130	5	2.7	8	170	3		19	3200	6
para up fa	350	-1	99	33	1	24		16	2400	11
Para 1 fa	390	3	210	120	190	67		35	5600	18
BUR FA .2 8/1	93	140	0.5	8.0	23	-1		48	2000	43
NATL FA .2 8/	190	3	0.3	93	11	35		56	18000	210
NTUN1.1	222	28	4	140	50	29		65	21000	280
GAM6FA.1	54	0.72	0.03	0.29	2	-0.01	0.01	14	54	8.1
MC1FA.1	30	0.2	0.03	1.3	2	1.74	2.5	2	760	2
Creede-type epithermal										
<i>Carbonate-poor</i>										
AL1FA.1	91	44	27.8	30	290	0.42	0.5	10	3700	9.8
SOL1FA.1	62	160	5.4	82	33	0.5	0.8	17	6000	12
<i>Carbonate-rich, or in propylitically altered rocks</i>										
RAW1FA.1	130	140	9	30	1200	23.3	32	18	24000	36
*Rawley	130	200			670			15	32000	50
*Rawley	130	13			570	5.4		15	29000	48
*Rawley	120	110		70	420	4.3		15	29000	50

Deposit type	Ca	Cd	Ce	Co	Cu	Fe tot	Fe ⁺⁺	Mg	Mn	Ni
<i>Ore /alteration type</i>	mg/l	µg/l	µg/l	µg/l	µg/l	mg/l	mg/l	mg/l	µg/l	µg/l
Sample										
Raw1 (Rawley 12)	160	280	44	69	4900	42.00	3.2	22.00	38000	36
ML-ad	140	80	1.2	31	98	19.00		22.00	32000	23
ML-FP	76	4.3	0.3	18	-2	13.00		10.00	19000	13
ML-1	50	350	180	44	9800	6.00		11.00	89000	58
Rawley 3 seep	18	66	36	15	6400	13.00		5.00	7300	12
KC tail	420	620	890	470	48000	890	900	78	150000	240
Am 1 fa	400	61	4	58	140	18		14	27000	20

Magmatic sulfide*Massive iron-, nickel-, and copper-sulfide lenses in ultramafic rocks*

*DUL 1200 7300 24500

Polymetallic replacement and skarns*Sandstones and other carbonate-poor host rocks*

*Eagle 1610	507	250		570	-150	741		840	493000	
*Eagle 1610	435	300			450	670		1030	560000	
*Eagle 1610	460	500		600	700	660		1160	610000	2100
*Eagle Chief		640		-150	1280	56			69000	
*Eagle Chief	270	1060			5500	103		329	190000	

Igneous-hosted ores

GAM4FA.1	85	11	18	100	100	4.67	2	17	3000	38
YAK1FA.1	91	290	9.2	18	2400	2.42	3	53	20000	31
GAR1FA.1	21	12	0.81	1.5	12	-0.01	0.1	4	1600	4.2

Calc-silicate skarns

*Glngar GW-1		3		46.1	7730	86			5610	99.2
*Glngar GW-2		3		21.4	121	14			1020	20.5
*Glngar SW-2		3		15.4	1170	3			722	32.5
*McLar		20		133	26700	192			7	141

Carbonate-hosted, pyrite-rich

BAN1FA.1	89	61	0.17	38	38	2	1.5	8	7200	17
LD1FA.1	87	12	0.03	1	4	0.01	0.2	37	1100	4.3
FG1.1		0.5	69	120	270	86	500			190
kok fa	110	44	0.2	7	41	15		28	3800	13

Carbonate-hosted, pyrite-poor

Anon1 fa.1	48	2	-0.1	0.9	2	-0.005		8	23	2
Anon2 fa	99	-1	-0.1	0.6	-1	-0.005	0.1	34	16	3
*FishCk1		-2.6		-9.7	51.1	0.756			91.6	14.8
*Blkwar		-2.6		-9.7	23.4	1.3			65.8	-12.7
*LilDaisy		-2.6		-9.7	96.1	4.15			1460	37.2

Sedimentary-exhalative (SEDEX)*Hosted by shales and cherts with no carbonates*

*#2016, Alaska	210			30000	900	10000		9800	800000	
*#2019, Alaska	275			5500	620	870		2000	145000	
*#2015, Alaska	250			3100	230	920		1200	80000	
*#2021, Alaska	155			540	4000	170		245	20000	
DW010	11	6		6	7	3		1	480	22
DW017	21	6		48	260	270		5	2200	290
DW018	19	5		47	67	150		3	1100	180
DW024	19	6		48	140	130		7	2900	230

Deposit type	Ca	Cd	Ce	Co	Cu	Fe tot	Fe ⁺⁺	Mg	Mn	Ni
<i>Ore /alteration type</i>	mg/l	µg/l	µg/l	µg/l	µg/l	mg/l	mg/l	mg/l	µg/l	µg/l
Sample										
DW026	19	6		43	130	130		7	2700	210
RD 23	13	78								
RD33	15	79		-7	11	1.3		6.6	106	-5
RD42	35	396								
RD44	54	105								
<i>Hosted by shales, cherts, and carbonates</i>										
LK57	27	5		-3	-10	0.15		4	330	51
LK61	32	-1		-3	-10	-0.05		2	-1	-5
LK62	53	-1		-3	-10	-0.05		6	-1	-5
Mississippi-Valley-type (MVT)										
<i>Jasperoid-poor</i>										
*Site 4-Drill (mean)	113	1		26		0.01		63	22	73
*Site 5 (mean)	124	1		37		0.01		65	242	33
*Site 8 (mean)	190	21		460		0.02		64	18	462
DAU1.FA.1	11	0.44	0.03	0.2	1	0.001	0.1	5	22	3
RUB1.RA	41	0.4	0.15	0.36	2	0.13	0.1	14	94	3
*WP2FA.1	58	0.76	0.02	0.33	1.1	-0.01		28	90	1
<i>Abundant jasperoid</i>										
*Map # 101	290	30		37	2	67		19	800	98
*Map #105	360	31			7	0.17		6.9	100	52
*Map # 109	530	2				17		8	550	
*Map # 14	63	1		2		0.08		3.5	60	7
*Map #16	20	27		4		0.01		0.8	90	11
*Map # 17	230	60		2		0.01		5.5	40	29
Sediment-hosted Au										
<i>Primarily oxide ore</i>										
*Boss 4/1/94	150	-10			190	0.81		66	-50	
*Boss Pit 7/1/94	190	-10			-50	-0.05		110	-50	
*Boss Pit 12/26/94	340	-10			-50	3.2		65	-500	
*Cortez E., 6/15/92	44.2	-7			-7	0.145		18	5	
*Cortez M., 6/15/92	43.1	-7			-7	0.257		17.7	-3	
*Cortez W., 6/15/92	43.1	-7			-7	-0.05		17.7	-3	
*Big Spr. 5/30/95	107	-5			-5	-0.05		130	243	
*Big Spr. 4/13/95	72.9	-5			-5	-0.05		42.6	63	
<i>Primarily sulfide ore, carbonate-poor host rocks</i>										
DW-06, 12/22/94	51.3	-2			-2	0.4		19.3	64	
DW-06, 12/22/94	46	-0.2			-100	0.1		18	-100	
DW-07,12/22/94	50	-2			-2	0.055		20.5	30	
394318-1,6/14/95	55.2	-2			-3	2.74		21.7	102	
394319-2,8/17/95	42.1	-2			-3	-0.017		22	-1	
Low-sulfide Au-quartz veins										
LCk2	15				-1	-0.01		0.3		
SF6	15				-1	-0.01		-0.1		
Goy13	2.9				2	0.02		-0.1		
McKin2	2	-0.7			0.6	-0.02		0.1		
McKin5	5.5	-0.7			0.7	-0.02		0.35		
McKin11	13	-0.7			0.4	0.03		0.6		

Deposit type	Ca	Cd	Ce	Co	Cu	Fe tot	Fe ⁺⁺	Mg	Mn	Ni
<i>Ore /alteration type</i>	mg/l	µg/l	µg/l	µg/l	µg/l	mg/l	mg/l	mg/l	µg/l	µg/l
Sample										
McKin13	0.7	-0.7			0.9	0.02		0.1		
McKin19	6.6	1			1	0.09		0.46		
Ind1	14	2		-0.1	-2	-0.04		6.2	0.6	0.6
Ind2	25	2		0.1	-2	-0.04		9.6	0.4	1
GC4	20	2		0.1	-2	-0.04		5	-0.3	1
HG6	12	2		-0.1	-2	-0.04		0.63	-0.3	0.6
HG7	9.3	2		-0.1	-2	-0.04		0.49	-0.3	0.6
HY16	31	20		1	10	0.3		13	860	100
Ch21	49	3		2	-2	0.1		9.4	280	12
Pt22	57	2		0.2	5	0.09		14	8.3	5.5
Sc23	74	2		0.2	-2	-0.04		30	1.7	3.7
M27	93	32		160	380	330		20	1800	120
Eb28	34	1		0.3	2	0.2		11	1.3	3.4
AJ29	120	2		0.4	-2	0.04		37	0.8	10
Alkalic Au-Ag-Te veins										
CAR1FA.1	490	1	0.11	4	1	0.03	0.2	36	1100	19
hur 1 fa	42	2	3	3.5	75	0.5	0.8	9	500	3
swa 1 fa	66	-1	0.7	4.3	2	2	1.5	16	500	4
Sediment-hosted U										
*MVD-1	440	4		1700	40	1.9		540	2700	850
*MVD-2	430	4		1100	200	0.24		640	1700	540
*MVSU-1	430	-3		9	-30	0.028		430	65	30
*3T-529	82	-3		-9	-30	0.73		31	250	-30
*JSW-1	620	2		-4	-10	0.043		130	-10	-1

Deposit type <i>Ore / alteration type</i> Sample	Pb µg/l	Si mg/l	U µg/l	Zn µg/l	Zn+Cu+Cd+ Co+Ni+Pb µg/l
Volcanogenic massive sulfide (VMS)					
<i>Kuroko-type, hosted by volcanic rocks</i>					
*Rich-90WA103	3600			2010000	2321460
*Rich-90WA108	4300			6150000	6780300
*Rich-90WA109	3800			7650000	10060500
*Rich-90WA110A	11900			23500000	28491900
*LMG	1800			13800000	14038100
Hol-511	-0.3		3.2	1000	1226
Hol-528	-0.3		2.9	6000	6407
Hol-529	-0.3		2.2	4800	5176
Hol-534	22		2.5	6000	6964
Hol-548	0.6		0.7	6500	6671
Hol-549A	26		210	81000	83246
Hol-549B	23		600	140000	143533
<i>Besshi-type, hosted by sedimentary and intermediate submarine volcanic host rocks</i>					
Duch-1	0.9			180	194
Duch-2	74			200	1060
Black-18A	220			3300	7170
Beat-16	-0.5			190	260
V-Ely-1	-50	24		1100	4868
<i>Besshi-type, hosted by graphitic schists</i>					
FC-3	-0.6	5.8	-0.1	350	450
SUG-1 0.2	230	7.4	0.6	7400	14870
<i>Cobalt-rich, hosted by metamorphosed sediments</i>					
*BB25			0.1	700000	928000
High sulfidation (quartz alunite epithermal)					
<i>Acid sulfate alteration</i>					
AD-3	370	30	31	18000	112980
AD-3	320	31	410	20000	142020
AD-3	230	30	140	47000	285060
AD-3	320	32	38	31000	263770
AD-3	75	27	15	12000	83117
AD-1435C	92	28	40	11000	96342
Chand-1	220	37	170	57000	462260
Chand-1	310	39	170	47000	340890
Chand-1	220	42	100	49000	312750
Dike 2	12	83	1000	170000	408012
550D-R	0.2	43	310	61000	123960
North Dump	6.3	30	60	23000	64246
N Dump S Seep	0.4	60	210	55000	160400
SC12	5	27	60	28000	131285
Blackstrap	-200	84	36000	610000	1117020
SOB-1 Seep	-2	110	300	82000	807160
IOWA-1	-0.1	35	44	11000	31121
SPIT-1 Pond	0.1	1	42	11000	54603
SPIT-2 Pond	1.0	1	90	20000	142511
NPIT-1 Pond	1.3	11	150	15000	53581
Ch Seep	180	27	72	29000	301550
Missionary East	210	19	29	6800	65670

Deposit type	Pb	Si	U	Zn	Zn+Cu+Cd+
<i>Ore / alteration type</i>	µg/l	mg/l	µg/l	µg/l	Co+Ni+Pb
Sample					µg/l
Sh-1	-2	36	39	21000	55730
TD Seep	27	12	0.3	2300	30496
AREA L	0.6	15	72	6600	31650
lkp fa	150	16	61	170000	225200
long 1 fa	800	8	7	13000	15449
3R-1	-50	44		580	73758
*EC91AP16	20	7		10	150
*EC91AP19	10	9		10	21
*EC91AP22	20	9		10	40
*EC91AP24	50	21		40	410
*EC92AP-21	110	37		650	910
<i>Propylitic alteration</i>					
Missionary West	-2	12	-1	190	348
Cordilleran Lode					
<i>Advanced-argillic to quartz-sericite-pyrite alteration</i>					
*Berkeley Pit Surface				184000	192200
*Berkeley Pit 3 meters				280000	437300
*Berkeley Pit 100 meters				496000	715900
Hot Spring S/Au					
<i>Shallow acid-sulfate alteration</i>					
*82WA119	38			2620	30706
*81WA132C	-20			1400	14052
*82WA118	75			1390	24077
Climax-type Porphyry Mo					
<i>Potassic, quartz-sericite-pyrite, greisen alteration</i>					
mcn 1 fa	2.4	27	8400	43000	61822
mcn 2 fa	-0.3	23	5500	24000	34370
Porphyry Cu, Cu/Mo					
<i>Quartz-sericite-pyrite alteration</i>					
*MW Weir 3		7.07		346	17334
*MW Weir 1		13.5		738	16183
*MW BH89-14		3.02		109	3199
*MW BH89-4		14		1650	11443
*MW BH89-3		15.8		1120	5910
*MW BH89-10		11.9		181	412
*MW BH89-8		9.7		106	1651
*MP1W1, Globe	210			22000	188910
TMT-29	0.03	38		420	2044
TMT-28	0.04	41		610	1010
TMT-38	26	39		2700	5565
<i>Propylitic alteration</i>					
*MW BH89-2		2.54		22	116
*MW BH89-13		5.3		-2	3

Deposit type <i>Ore / alteration type</i> Sample	Pb µg/l	Si mg/l	U µg/l	Zn µg/l	Zn+Cu+Cd+ Co+Ni+Pb µg/l
Algoma Banded Fe Formation					
<i>Sulfide-facies</i>					
*Sherman S Pit				160	360
Polymetallic veins					
<i>Zn, Pb, ± Cu-rich</i>					
St.Kev	9	22.9		117	1596
St.Kev	10	22.9		99.6	1230
PENN1.1	50		16	32000	38132
SHO1.1	260		6.4	1800	2877
<i>Au-quartz-pyrite</i>					
DRUID1FA.45	15	65	1400	> 100000	167135
Druid shaft	68	45	460	160000	169508
Argo 1 fa	55	23	100	51000	58385
Argo 1 fa.1	34	19	64	45000	50444
ARGO1.1	42	9.7	-100	54000	60760
VC1A.1	-20		16	53000	53882
VC1B.1	40		22	55000	56130
<i>Pyrite-rich; Zn, Pb, Cu-poor</i>					
PMB193 FA .2	0.2	33	1.4	180	480
PMB1FA.1	1	>2	1.6	210	564
Burnt Adit	0.4	14	0.8	58	172
Burnt Dump	0.5	14	-0.1	67	109
ARC FA .2	-0.1	22	15	930	1675
Fe Spring, Fe Crk	1.0	11	0.5	130	187
Burnt Spring	1.3	21	0.9	810	1021
SMCB1FA.1	0.6	36	1	170	208
<i>Carbonate-rich, or in rocks altered to contain carbonate</i>					
CHAP3FA.45	-0.6	15	0.88	560	591
CHAP2FA.1	0.6	14	0.5	45	69
bon 1 fa	20	21	0.2	1700	1786
MIZ FA .2	0.1	5	2.1	41	56
ASIA FA .2	0.1	7	0.2	-40	28
CARC-1 FA .2	7.4	14	0.5	220	360
CARC-3 FA .2	0.6	5	0.8	1200	1208
CARC-2 FA .2	1.2	5	-0.1	170	181
ns1 fa	-0.3	7	54	1100	1289
para up fa	-0.3	9	-2	120	165
Para 1 fa	0.4	11	0.5	1200	1531
BUR FA .2 8/1	4.5	3	18	68000	68219
NATL FA .2 8/	0.3	17	1.4	5500	5817
NTUN1.1	9		-1	8100	8607
GAM6FA.1	0.6	11	0.08	230	242
MC1FA.1	0.6	11	0.015	140	146
Creede-type epithermal					
<i>Carbonate-poor</i>					
AL1FA.1	0.8	18	0.54	5600	5975
SOL1FA.1	1100	16	24	26000	27387

Deposit type	Pb	Si	U	Zn	Zn+Cu+Cd+
<i>Ore / alteration type</i>	µg/l	mg/l	µg/l	µg/l	Co+Ni+Pb
Sample					µg/l
<i>Carbonate-rich, or in propylitically altered rocks</i>					
RAW1FA.1	5.4	8	0.68	34000	35411
*Rawley	32			34000	34952
*Rawley	26			32000	32657
*Rawley	18			28000	28668
Raw1 (Rawley 12)	120	10	1.6	58000	63405
ML-ad	4	11	0.6	11000	11236
ML-FP	-0.6	10	-0.1	4300	4336
ML-1	0.6	25	9.8	67000	77253
Rawley 3 seep	120	10	3.6	16000	22613
KC tail	1000	3	100	170000	220330
Am 1 fa	-0.3	8	29	18000	18279
Magmatic sulfide					
<i>Massive iron-, nickel-, and copper-sulfide lenses in ultramafic rocks</i>					
*DUL				1400	34400
Polymetallic replacement and skarns					
<i>Sandstones and other carbonate-poor host rocks</i>					
*Eagle 1610	-1250			932000	932960
*Eagle 1610	330	5		1020000	1021080
*Eagle 1610	-625	-13		980000	983963
*Eagle Chief	-1250			175000	177060
*Eagle Chief	230	5		430000	436790
<i>Igneous-hosted ores</i>					
GAM4FA.1	13	18	31	2500	2762
YAK1FA.1	13	8	9	69000	71752
GAR1FA.1	4.7	5	0.1	1500	1534
<i>Calc-silicate skarns</i>					
*Glngar GW-1	40.1			671	8589
*Glngar GW-2	2.5			127	295
*Glngar SW-2	8.2			137	1366
*McLar	6.5			3000	30001
<i>Carbonate-hosted, pyrite-rich</i>					
BAN1FA.1	0.6	6	0.14	14000	14155
LD1FA.1	0.6	5	3.5	3100	3122
FG1.1	150		-1	170000	170731
kok fa	-0.3	3	12	27000	27105
<i>Carbonate-hosted, pyrite-poor</i>					
Anon1 fa.1	-0.3	8	2.1	710	717
Anon2 fa	-0.3	7	9.2	27	31
*FishCk1	38.1			64	169
*Blkwar	89.8			430	546
*LilDaisy	526			167	828
Sedimentary-exhalative (SEDEX)					
<i>Hosted by shales and cherts with no carbonates</i>					
*#2016, Alaska (natural)			-0.1	500000	530900
*#2019, Alaska (natural)			20	84000	90120
*#2015, Alaska (natural)			12	49000	52330
*#2021, Alaska (natural)			52	35000	39540

Deposit type <i>Ore / alteration type</i> Sample	Pb µg/l	Si mg/l	U µg/l	Zn µg/l	Zn+Cu+Cd+ Co+Ni+Pb µg/l
DW010	5	-1		1400	1446
DW017	9	2		2000	2613
DW018	10	2		1900	2209
DW024	4	2		2000	2428
DW026	4	2		1900	2293
RD 23	554			23700	24332
RD33	132	4		7480	7703
RD42	2100			40000	42496
RD44	1260			8900	10265
<i>Hosted by shales, cherts, and carbonates</i>					
LK57	-10	8		2000	2058
LK61	-10	1		14	17
LK62	-10	1		780	783
Mississippi-Valley-Type (MVT)					
<i>Jasperoid-poor</i>					
*Site 4-Drill (mean)	23	9.7		243	366
*Site 5 (mean)		6.2		346	417
*Site 8 (mean)	51	5.4		15000	15994
DAU1.FA.1	1	1	0.62	55	61
RUB1.RA	1	1	1.8	350	357
WP2FA.1	2.2	3	4.4	140	145
<i>Abundant jasperoid</i>					
*Map # 101	28	23		6300	6495
*Map #105	4	13		17000	17094
*Map # 109	11			12000	12013
*Map # 14		7.6		540	550
*Map #16	450	11		24000	24492
*Map # 17	120	7.4		18000	18211
Sediment-hosted Au					
<i>Primarily oxide ore</i>					
*Boss 4/1/94	90			-50	190
*Boss Pit 7/1/94	-50			-50	
*Boss Pit 12/26/94	-50			-50	
*Cortez East, 6/15/92	-5			-5	
*Cortez Middle, 6/15/92	6			-5	
*Cortez West, 6/15/92	7			6	
*Big Springs 5/30/95	-5			76	
*Big Springs 4/13/95	-5			6	
<i>Primarily sulfide ore, carbonate-poor host rocks</i>					
DW-06, 12/22/94	-40			11	11
DW-06, 12/22/94	-2			-100	
DW-07,12/22/94	-40			-4	
394318-1,6/14/95	-40			-2	
394319-2,8/17/95	-1			10	10

Deposit type	Pb	Si	U	Zn	Zn+Cu+Cd+
<i>Ore / alteration type</i>	$\mu\text{g/l}$	mg/l	$\mu\text{g/l}$	$\mu\text{g/l}$	Co+Ni+Pb
Sample					$\mu\text{g/l}$
Low-sulfide Au-quartz veins					
LCK2	-1			6	6
SF6	-1			5	5
Goy13	1			8	11
McKin2	-0.5			4	5
McKin5	-0.5			3	4
McKin11	-0.5			4	5
McKin13	-0.5			5	6
McKin19	-0.5			8	10
Ind1	-0.6			-2	3
Ind2	-0.6			3	6
GC4	-0.6			-2	4
HG6	-0.6			-2	3
HG7	-0.6			-2	3
HY16	4.8			2000	2136
Ch21	-0.6			1500	1517
Pt22	-0.6			2	15
Sc23	-0.6			-2	6
M27	21			2500	3213
Eb28	-0.6			6	13
AJ29	-0.6			44	57
Alkalic Au-Ag-Te veins					
CAR1FA.1	0.6	30	16	57	83
hur 1 fa	-0.3	5	37	290	374
swa 1 fa	-0.3	9	0.4	13	23
Sediment-hosted U					
*MVD-1	-1	3.6	33200	770	3364
*MVD-2	-1	3.7	42250	690	2534
*MVSW-1	-30	0.03		34	79
*3T-529	40	3.8		110	157
*JSW-1	-1	0.7	6	44	48

Chapter 20

A MULTI-PHASED APPROACH TO PREDICT ACID PRODUCTION FROM PORPHYRY COPPER-GOLD WASTE ROCK IN AN ARID MONTANE ENVIRONMENT

L.H. Filipek,¹ T.J. VanWyngarden,² C.S.E. Papp,³ and J. Curry³

¹5061 Indiana Street, Golden, CO 80403-1743

²ACZ Laboratories, Inc., 30400 Downhill Drive, Steamboat Springs, CO 80487

³U.S. Geological Survey, Retired

INTRODUCTION

Acid rock drainage (ARD) is a solution of sulfuric acid and iron sulfate, formed mainly by the exposure of pyrite to oxygen and water. ARD typically has high concentrations of other heavy metals that are toxic to wildlife and is the single most significant environmental problem associated with mining of ore deposits containing sulfide minerals. Understanding the processes that produce ARD and developing accurate methods to predict and prevent it are therefore key to environmentally conscious mining of such deposits.

The chemical reactions involved in pyrite oxidation are discussed in detail by Nordstrom and Alpers (1999). Several factors affect the kinetics of pyrite oxidation and, thus, the formation of ARD. They include the rate of transportation of oxidant (oxygen or iron (III)) to the surface of the pyrite grain; the chemistry of any solution in contact with the pyrite; the presence of oxidizing bacteria; the morphology, crystallinity, and trace-element content of the pyrite; and the mineralogy of neighboring grains. Once pyrite has been oxidized, reaction with calcium and magnesium carbonates or with rapidly weathering basic silicates can neutralize the acid produced. The interplay of the factors that control the oxidation and neutralization processes ultimately determines whether ARD will occur.

Several categories of methods have been developed to predict ARD. They include geographical comparison (e.g., Brady, personal commun., 1994), geologic models (e.g., Plumlee, 1999), static acid-base geochemical tests (e.g., Sobek et al., 1978), laboratory and field kinetic geochemical tests (e.g., White et al., 1999), and mathematical models (e.g., Scharer et al., 1994). No one of these methods has proven completely accurate when used alone, because of the complexity of the physical, chemical, and biological processes involved in producing and neutralizing ARD.

In this chapter, potential acid production is investigated in an arid montane environment in waste rock from Bajo de la Alumbrera, a porphyry copper/gold deposit located in Catamarca Province, northwest Argentina. A variety of complementary techniques is used, including acid-base accounting to determine the static net acid producing potential, and column and humidity-cell geochemical kinetic tests to simulate weathering for 35 weeks. Sulfur speciation and X-ray diffraction analyses of unweathered and laboratory-weathered waste rock, chemical analyses of leachate solutions from the weathering tests, and thermodynamic equilibrium models are used to determine which minerals have reacted during the 35-week simulated weathering period. Scanning electron microscopy (SEM) and qualitative energy-dis-

persive X-ray emission (EDX) spectrometry of pyrite grains in waste rock samples are used to examine the extent of oxidation and the purity of the pyrite grains in the unweathered waste rock. The results show that pyrite oxidation in the waste rock from this deposit is significantly more complicated than would be predicted using only the standard acid-base accounting methods required by most regulatory agencies.

BACKGROUND

Summary of factors affecting acid rock drainage

The climate and hydrogeology of the site affect the rate of transportation of oxygen to pyrite. Oxygen can attain much higher concentrations in air than in water. In addition, the diffusion coefficient of oxygen in air is nearly five orders of magnitude greater than in water. Thus, pyrite tends to weather significantly faster in an unsaturated environment. However, a very dry environment may decrease the oxidation rate. In laboratory tests, Borek (1994) found that pyrite weathered faster in higher humidity environments.

When water is in contact with the pyrite, constituents other than oxygen affect the oxidation rate. For example, Brown and Jurinak (1989) found that chloride or sulfate tend to inhibit abiotic pyrite oxidation, presumably by decreasing the ability of iron (III) to react with the pyrite surface. The pyrite oxidation rate decreases as the concentration of chloride or sulfate increases at constant pH, with a fractional reaction rate of about 0.1. With inert salt, the reaction is zero order with respect to salt concentration; in other words, there is no significant rate change with increases in ionic strength. Concentrations of test solutions used by Brown and Jurinak ranged from 5 to 500 mmol/l (480 to 48,000 mg SO₄/l). This result suggests that aqueous pyrite oxidation may be self-inhibited. In contrast, neither calcium carbonate nor sodium bicarbonate solutions at the same pH has any effect on pyrite oxidation rate. Carbonate and bicarbonate can, however, increase the pyrite oxidation rate by increasing the pH of the solution, because pyrite oxidation increases rapidly with pH above 7.

Microbes, principally *Thiobacillus ferrooxidans* and *Thiobacillus thiooxidans*, can greatly accelerate pyrite oxidation over abiotic processes. The *T. ferrooxidans* are most active at oxidizing iron and sulfur at a pH of about 2. Above a pH of about 4, they can only oxidize sulfur. They use atmospheric carbon dioxide as a carbon source (e.g., Mills, 1999). A more detailed discussion of the role of bacteria in pyrite oxidation is given in Mills (1999).

The morphology, crystallinity, and trace-element composition of the pyrite and the proximity of the pyrite grain to grains of other metal sulfides also affect the oxidation rate of pyrite. Borek (1994) found that pyrite from different sedimentary and hydrothermal deposits weather at different rates and produce different products under similar weathering conditions. Kwong (1993), using intensity of tarnishing and pitting density as indicators of weatherability, showed that the more heterogeneous the pyrite grain, the faster it tends to oxidize. When the impurities within the pyrite grain occur as separate mineral phases, such as sphalerite or chalcopyrite, or as interstitial impurities, such as gold or silver, they cause local strain in the crystal structure. The strain increases susceptibility to weathering in its vicinity. For substitutional impurities in the pyrite, arsenic appears to enhance the oxidation process, whereas cobalt and nickel appears to protect the pyrite from oxidation. Kwong (1993) noted that this pattern of mineral response to element substitution agrees with Shuey (1975), who found consistent differences in behavior of minerals after substitutions from the right in the periodic table (such as cobalt for iron) compared with substitutions from the left (such as arsenic for sulfur).

Calcite and dolomite are the principal minerals that neutralize acid, because they dissolve rapidly. Certain rapidly weathering basic-silicate minerals such as anorthite and olivine can also provide some buffering capacity. Sverdrup (1990) classified common soil minerals into six groups based on their dissolution rate and its dependency on pH. These groupings and their reactivities relative to calcite are given in Table 20.1. Fast weathering-rate minerals such as anorthite and olivine have a relative reactivity of 0.6 and intermediate weathering-rate minerals such as serpentine and chlorite have a relative reactivity of 0.4. Most other types of minerals react too slowly to provide significant buffering capacity. For example, slow weathering-rate minerals such as albite and kaolinite have a relative reactivity of 0.02 and quartz has a relative reactivity of 0.004.

Static and kinetic geochemical tests

Most states regulating mining activities require that potential mining waste be tested geochemically to determine whether it has the potential to produce acid. If a potential exists, then a mitigation plan must be developed to minimize acid production. Acid-base accounting (Sobek et al., 1978) is the most common geochemical test required by regulators. The test is based on the assumption that the acid production potential (APP) is a function of the concentration of iron sulfides, especially pyrite, because such sulfides produce sulfuric acid when they oxidize. It also assumes that the acid neutralization potential (ANP) consists entirely of calcium carbonate. In calculating APP, a conversion factor of 31.25 is typically used to convert weight-percent sulfur to the equivalent weight of calcium carbonate needed to neutralize the acid, in g/kg (sometimes referred to as tons/1000 tons), assuming one mole of pyrite is neutralized by two moles of calcium carbonate. This conversion allows a direct comparison between APP and ANP values.

The APP based on total sulfur gives a conservative estimate, because some of the sulfur may be in a form such as gypsum that is not acid generating. Therefore, sulfur speciation schemes have been developed to isolate sulfide sulfur. For example, the modified Sobek acid-base accounting method (Sobek et al., 1978) is a series of extractions to separate sulfate (hydrochloric acid-extractable),

pyrite (nitric acid-extractable), and organic (residual) sulfur, where it is typically assumed that the nitric acid-extractable sulfur is the only sulfur form that produces acid. This scheme was designed for analysis of sulfur in coals. In studies of igneous or metamorphic ore deposits, the Sobek sulfur-speciation scheme is typically modified in that the sum of the fractions designated "nitric acid-extractable sulfur" and "residual sulfur" is considered the acid-producing component of sulfur, labeled "sulfide sulfur," because little or no organic sulfur is expected in these types of rocks.

TABLE 20.1—Grouping of minerals according to their acid-neutralization capacity (after Sverdrup, 1990; Kwong, 1993).

Group	Typical minerals	Relative reactivity
Dissolving	calcite, aragonite, dolomite, magnesite, brucite	1.0
Fast weathering	anorthite, nepheline, olivine, garnet, jadeite, leucite, spodumene, diopside, wollastonite	0.6
Intermediate weathering	epidote, zoisite, enstatite, hypersthene, augite, hedenbergite, hornblende, glaucophane, tremolite, actinolite, anthophyllite, serpentine, chrysotile, talc, chlorite, biotite	0.4
Slow weathering	albite, oligoclase, labradorite, vermiculite, montmorillonite, gibbsite, kaolinite	0.02
Very slow weathering	K feldspar, muscovite	0.01
Inert	quartz, rutile, zircon	0.004

Different criteria have been suggested as limits beyond which a rock is considered an acid producer. Lapakko (1992) gives a summary and discussion of the most common of these. One common approach is to calculate the net acid neutralization potential (NANP = ANP - APP). For example, certain researchers (Lapakko, 1992) suggest that rocks with NANP values greater than +20g CaCO₃/kg consistently do not produce acid, whereas those with NANP values less than -20 g/kg consistently do. The behavior of rocks with NANP values between -20 and +20 is considered unpredictable. Another common approach is to calculate the ANP/APP ratio (with either APP_{tot} or APP_{sulf}). For example, the State of Nevada uses an ANP/APP_{tot} or ANP/APP_{sulf} ratio of 1.2 as a threshold value below which a rock is considered an acid producer. Idaho uses a ratio of 2; California uses a ratio of 3.

Acid-base accounting is a "static" test in that it measures the total amount of acid producing material and acid neutralizing material and assumes that both react to completion. It gives no indication of reaction rates. In order to investigate relative reaction rates, "kinetic" geochemical tests are often run. Many states require these tests if the NANP is between -20 and 20, or if the ratio of ANP/APP is close to one.

The most frequently used kinetic test for waste rock has been the EPA humidity-cell test (Sobek et al., 1978: Method 4.1.5), which is conducted in a shoe box-shaped container with waste rock ground to ≤2 mm. The humidity-cell test is typically run for 10 to 20 weeks, with a weekly weathering cycle. In each cycle, dry air is passed through the cell for three days, followed by three days of humid air. On the seventh day, the cell is saturated at a 1:1 weight

ratio with distilled water and allowed to soak for one hour. The leachate from the cell is typically analyzed for pH, conductivity, sulfate, iron, calcium, acidity, and alkalinity. Sulfate in the leachate typically is interpreted as an indicator of pyrite oxidation; whereas calcium is interpreted as an indicator of carbonate dissolution. If the pH decreases to 3.5 or less during the course of the test, the waste rock is considered an acid producer.

Recently, columns of various sizes have been used in place of the humidity cell. The column typically contains waste rock of larger and more variable particle size than the humidity cell and the water added on the seventh day of a weekly cycle flows through the column. These changes from the humidity cell were designed to better simulate the variability in rock size and water flow through a waste rock pile.

SITE CHARACTERISTICS

Material for this study came from Bajo de la Alumbrera, a large porphyry copper/gold deposit in an arid region of the Andes at an altitude of about 2600 m. The annual precipitation in the area averages about 16 cm per year, with most (about 85%) of the moisture produced during a few storms in the summer. Typically, little or no snow falls in the winter, so a snow pack does not accumulate. The soils are typical for arid climates. They tend to be shallow and alkaline, composed mainly of sand or sandy loam. Stream water in the vicinity is typically alkaline. It has a sodium-sulfate composition with substantial hardness and alkalinity.

The deposit is exposed at the surface. (A photograph and conceptual model of the deposit are shown on the front and back cov-

ers, respectively, of *The Geology of Ore Deposits*, 1986, by J.M. Guilbert.) It consists of two hydrothermal dacitic intrusions hosted in andesite. A single set of concentric alteration zoning typical of porphyry systems is visible, which consists of a central potassic core grading outward to phyllic, argillic, and propylitic alteration. Figure 20.1, from Lowell and Guilbert (1970), shows the typical zonation of a porphyry system, along with the mineralogy typically found within each zone. The ore is located in the outer portion of the potassic zone, and is surrounded by a pyrite-rich zone.

In the Bajo de la Alumbrera deposit, phyllic alteration overprints earlier potassic alteration along the fringes of the deposit. Most of the copper mineralization is hypogene chalcopyrite. Minor oxidation and supergene enrichment of copper sulfides have occurred in isolated, structurally-controlled areas.

Four major rock types have been differentiated geochemically at the site. Three relate to a combination of the hydrothermal events and alteration states; they are designated P1, P2, and P3 by the geologists on site. The most common waste-rock type, P1, is from the fringe of the potassic zone and has a phyllic overprint. The fourth rock type is fractured andesite host rock, labeled FA. A dike crossing the system makes up a fifth, very minor rock type.

METHODS

Fifty-seven samples of waste rock were obtained mainly from drill holes. The samples were selected based on pit design and oxidation state to represent each waste rock type expected to be produced during mining operations in its relative amount. Most of the

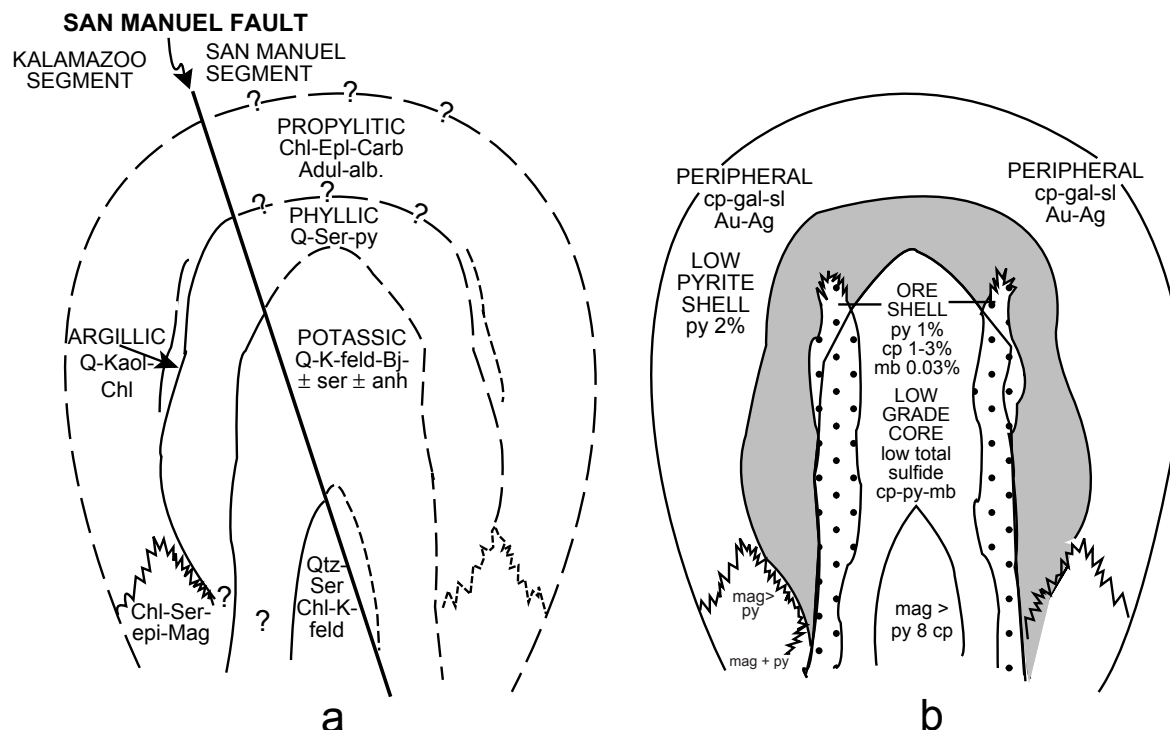


FIGURE 20.1—Schematic drawing of (a) alteration zones and (b) mineralization zones at the San Manuel-Kalamazoo deposit, which is typical of porphyry copper deposits (after Lowell and Guilbert, 1970).

anticipated waste rock is comprised of P1 rock. All but four of the samples came from parts of the deposit that were considered "primary" and appeared relatively unoxidized (or "unweathered"), based on visual inspection. The individual samples were crushed in a jaw crusher to 5 cm or less in diameter. Equal weights (500 g) of each sample were composited and blended in a large plastic barrel for use in the simulated weathering studies.

Acid-base accounting and sulfur speciation

Acid-base accounting using total sulfur was used to determine the APP, ANP, and net acid neutralization potential (NANP = ANP - APP) on the 57 individual waste rock samples. The modified Sobek acid-base accounting scheme (Sobek et al., 1978) and a second recently developed sulfur speciation scheme (Curry and Papp, 1996) were used to estimate the sulfide sulfur-based acid production potential (APP_{sulf}) of composites of the unweathered waste rock and the waste rock after 35 weeks of simulated weathering.

Sulfide sulfur was determined in the modified Sobek scheme by adding the values for nitric acid-extractable sulfur and residual sulfur. The Curry and Papp sulfur speciation method is designed specifically for non-coal rocks. It uses a 0.1N hydrochloric acid leach to remove sulfate and a sodium pyrophosphate solution to extract the organic sulfur fraction. The residual sulfur from these two leaches is considered pyrite sulfur.

The ANP was determined for individual samples using 0.2N hydrochloric acid, which dissolves mainly carbonates. The normality of the acid was increased to 0.5N for analysis of the composite samples used in the kinetic tests in order to better measure the contribution of the basic silicates. Carbonate carbon in the composite samples was also determined by coulometry for comparison with the ANP analyses.

Weathering studies

Two weathering studies were conducted, one in a standard EPA humidity cell and the other in a PVC column. The particle size distribution and amount of sample used were the two major variables between the cell and the column. The two studies were conducted in parallel to determine the effect of particle size and size distribution on the rate of acid generation.

The EPA humidity cell had a standard plastic shoe-box design. The box dimensions were 25 cm x 15 cm x 10 cm with plastic air-flow holes on both ends. The air inlet hole was centered on one end; the air exit hole was located in the lower corner of the opposite end about 1.3 cm from the bottom. The exit hole was also used to drain the leachate of the cell after soaking. The cell used 250 g of composited waste rock ground to ≤ 2.0 mm.

The PVC column was 10 cm in diameter and 30 cm long. The top and bottom of the column were capped with PVC joints sealed with O-rings. Tygon tubing was attached to openings on the top and bottom of the column. A 2-cm thick layer of glass beads was placed inside the column on the bottom and a plastic mesh screen was placed on top of the beads to keep any fine material from exiting the column. The column was filled with 1500 g of composited waste rock, leaving enough room to saturate the column at a 1:1 water-to-rock ratio by weight. The size of the composited waste rock varied from fine material to particles 5 cm in length to better represent the heterogeneous nature of a waste-rock pile.

Once the column was sealed, it was thoroughly moistened with distilled water. An air line was attached to the top of the column.

Both the cell and the column used a graphite compressor as an air source. A needle valve was attached to the air line allowing for constant air flow. The humid air was supplied by running the same air line to a 50-l Nalgene carboy, which was modified with an aerating stone and inlet/outlet line attachments.

The two weathering tests used the standard weekly weathering cycles, which were repeated for 35 weeks. The leachate from the cell was drained out through the tubing into a 250 ml beaker. The leachate from the column was allowed to drain through tubing attached to the bottom, and collected in a 2000 ml beaker.

Once the leachate was drained, its volume, pH, and electrical conductivity (EC) were measured. The leachate was then vacuum filtered through a 0.45 μ m membrane filter and aliquoted for analysis of dissolved metals, acidity, alkalinity, and sulfate. Standard EPA methods were used, including titration for acidity (Method 305.1) and alkalinity (Method 310.1), inductively coupled plasma spectroscopy (Method 200.7) for cations, and ion chromatography (Method 300.0) for sulfate.

Mineralogy

The materials in the column and the humidity cell were removed and ground after they had been weathered for 35 weeks. A split of waste rock was also taken from the unweathered composite and ground. These ground samples were subjected to semi-quantitative X-ray diffraction (XRD) on a Philips X-ray diffractometer to determine the mineralogy before and after weathering.

Three pieces of waste rock were selected at random from the unweathered composite for observation using scanning electron microscopy (SEM) on a Cambridge instrument. The pieces were broken and freshly exposed surfaces were investigated. Photomicrographs and qualitative energy-dispersive X-ray (EDX) analyses were made of pyrite grains and observed alteration rinds.

Thermodynamic modeling

The MINTQA2 code (Allison et al., 1991) was used to determine the saturation state of relevant minerals using concentrations of elements in leachate from the humidity cell and column. Leachates from the first, fifth, tenth, twenty-fifth, and thirty-fifth weeks of weathering were used. The chemical data for week 25 included all major and minor elements except silicon; the data for the remaining weeks included calcium, magnesium, iron, sulfate, and inorganic carbon. The Eh was set at 400 mV to simulate oxidizing conditions.

The PHREEQE code (Parkhurst et al., 1980), with subsequent revisions summarized by Nordstrom et al. (1991), was used in two sets of computer experiments. In the first experiment, distilled water was equilibrated with individual minerals determined by XRD to make up the major components of the waste rock. The purpose was to calculate the pH and water chemistry expected during the weathering tests if the pH were controlled by equilibrium with a single mineral. The second computer experiment involved adding oxygen to two mineral systems: (1) gypsum-pyrite-goethite, and (2) gypsum-pyrite-amorphous iron hydroxide. The computer experiments were run for both an open system exposed to an atmospheric partial pressure of carbon dioxide ($p\text{CO}_2 = -3.5$) and for a system with no carbon dioxide.

RESULTS

Acid-base accounting and sulfur speciation

The acid-base accounting results for the individual samples are given in Table 20.2. Total sulfur averaged 6.1% ($APP_{tot} = 192$ g $CaCO_3/kg$) and ranged from 0.40 to 10.6% on the individual samples. The P1 unweathered (primary) rock type, which experienced both potassic and phyllic alteration, had the highest total sulfur, averaging 7.7% ($APP_{tot} = 241$) and ranging from 0.97 to 10.6%. Total sulfur in the four oxidized and partly oxidized samples ranged from 0.43 to 2.67%.

The ANP for the individual samples averaged 9 g $CaCO_3/kg$ and ranged from 0 to 50. The primary P1 rock type had an average ANP of 7, whereas the primary P3 rock type had an average ANP of 15. The average NANP for the individual samples was -182, indicating that the rock has a significant potential to produce acid.

The modified acid-base accounting and sulfur speciation results for the composite unweathered and simulated weathered samples are given in Table 20.3. The two sulfur speciation methods gave similar results for the sulfur species. In the unweathered rock, total sulfur averaged 7.7%. About 53% of the sulfur appears to be in the form of sulfides, whereas the remaining 47% is in the form of sulfate. The ANP determined with the more concentrated acid was about 24 g $CaCO_3/kg$. Very little carbonate was detected by coulometry, averaging less than 0.1% carbon, which translated into an ANP of about 8. Thus, most of the ANP appears to be due to other minerals. This result will be discussed in more detail in a following section.

The waste rock had a $NANP_{sulf}$ of about -100 to -120 g $CaCO_3/kg$, which indicates a significant potential to produce acid, even using only sulfide sulfur. After 35 weeks of simulated weathering, neither weathered composite was significantly different from the unweathered composite in terms of APP_{sulf} , ANP, or $NANP_{sulf}$, which suggests that neither pyrite nor carbonate or other neutralizing minerals dissolved to any significant extent (Table 20.3).

Weathering studies

The leachate from each weekly cycle of the weathering studies was analyzed for pH, conductivity, alkalinity, acidity, and content of calcium, magnesium, iron, and sulfate. The results for pH, conductivity, calcium, magnesium, and sulfate are shown on Figures 20.2 through 20.8. During the 35 week time period, the pH of the column leachate remained about 4.5, while that of the humidity cell varied between 6.4 and 7.1 (Fig. 20.2). The conductivity of leachate from the humidity cell tended to decrease with time from about 1900 to about 1200 $\mu\text{mhos/cm}$, whereas that of the column increased slightly with time from about 1200 to about 1500 $\mu\text{mhos/cm}$ (Fig. 20.3).

Very little iron was carried in solution during the tests, ranging from less than 0.01 to 0.98 mg/l in the humidity cell tests and from less than 0.01 to 1.67 mg/l in the column tests (not shown). No pattern was evident in the iron leached over time for the humidity cell. However, for the column test, the maximum iron (1.67 mg/l) was leached in the first week, and the concentration declined steadily thereafter. Minor orange staining indicative of iron oxyhydroxide or jarosite was observed on some of the rocks and the PVC column during the course of the column test.

The solutions from both sets of tests were poorly buffered solutions of calcium sulfate with minor magnesium. The cumulative leaching curves for sulfate (Fig. 20.4) and calcium (Fig. 20.5) in both tests increase linearly over the 35 weeks; whereas most of the magnesium leaching occurred over the first 15 to 20 weeks (Fig. 20.6). Initially, the mole ratio of calcium/sulfate in the leachate from the humidity cell was about 0.8 (Fig. 20.7) and that from the column was 0.6 (Fig. 20.8). The ratio gradually increased to the one-to-one molar ratio of gypsum in both tests.

Mineralogy

The ground samples of unweathered and simulated weathered waste rock were indistinguishable based on color. All were a pale gray, indicating that the amount of iron oxyhydroxide or jarosite formed in the column during the weathering process was minor. Quartz, gypsum, mica, plagioclase, pyrite, chlorite, and potassium feldspar were identified by semiquantitative XRD analysis; no carbonate minerals were detected. Table 20.4 gives the approximate percentages of each mineral in the unweathered and simulated weathered composites. Gypsum estimated from XRD, at 38% in the unweathered rock, is higher than the approximately 19% calculated using the sulfur-speciation results, which indicates the semiquantitative nature of the XRD analysis. However, the XRD results indicate that the ratio of gypsum to pyrite in the weathered waste-rock composites is lower than in the unweathered rock, and corroborates sulfur speciation results that indicate the source of the leached sulfate is gypsum.

The SEM photomicrographs, shown on Figures 20.9 through 20.11, indicated that the pyrite grains from samples of unweathered waste rock had both primary hydrothermal-alteration rinds and supergene alteration. The EDX spectral plots, such as those shown on Figures 20.12 through 20.14, indicated that the rinds were composed of platy aluminosilicate and iron-rich material. The alteration material on Figure 20.9 is probably muscovite and an iron oxysulfate or potassium jarosite, based on the qualitative spectral plot shown on Figure 20.12a. The material on Figure 20.10 is probably chlorite and an iron oxysulfate alteration product of pyrite, based on the spectral plot on Figure 20.12b. The boxwork alteration material on Figure 20.11 appears to grade from iron oxyhydroxides with minor sulfate in the upper part of the photomicrograph to more sulfate-rich material in the lower part, based on changes in the ratio of peak heights of iron, sulfur, and oxygen in the spectral plots on Figures 20.13a and 20.13b. The pyrite crystals themselves had few etch pits and appeared to be chemically quite pure in that no heavy metals were observed in EDX spectra of pyrite (for example, Fig. 20.14). No non-pyrite sulfide minerals were detected in association with the pyrite. Gypsum crystals tended to be associated with aluminosilicate material, based on EDX spectra (Fig. 20.15), and were not observed in association with pyrite.

Thermodynamic modeling

Table 20.5 shows the saturation indices of selected minerals in the humidity-cell and column leachates for weeks 1, 5, 10, 25, and 35, calculated using MINTQA2. Calcite was undersaturated in all leachates. In the humidity-cell leachate, gypsum was slightly supersaturated ($SI = 0.13$) in week 1. The saturation index decreased with time and, by week 35, gypsum was slightly under-

TABLE 20.2—Acid-base accounting data for individual samples of expected waste rock.¹

Rock type Drill Hole: Depth (m)	% Total sulfur	APP ²	ANP ³	NANP (ANP- APP)	ANP APP
P1 Oxidized					
44-54:15.1-18.1	2.39	75	33	-42	0.44
P1 Partly Oxidized					
42-58:7.5-10.5	2.64	82	1	-81	0.01
42-58:18-21	2.67	83	2	-81	0.02
P1 Primary					
46-46:45-46.5	2.54	79	2	-77	0.03
50-62:12-15	8.38	262	11	-251	0.04
50-62:63-66	9.10	284	6	-278	0.02
50-62:81-84	7.28	228	25	-203	0.11
54-50:0-03	10.35	323	1	-322	0.00
54-50:21-22.5	8.12	254	3	-251	0.01
54-50:42-43.5	10.41	325	2	-323	0.01
54-50:78-79.5	10.65	333	1	-332	0.00
54-50:90-91.5	8.83	276	3	-273	0.01
54-50:114-117	8.28	259	7	-252	0.03
54-56:18.-21	8.24	258	3	-255	0.01
56-50:12-15	8.87	277	0	-277	0.00
56-50:87-90	10.53	329	1	-328	0.00
56-50:102-105	9.26	289	6	-283	0.02
42-46:03-04.5	10.14	317	3	-314	0.01
42-46:15-16.5	6.09	190	6	-184	0.03
42-46:54-55.5	7.87	246	14	-232	0.06
42-56:21-23.5	0.97	30	2	-28	0.07
44-54:57.1-58.6	2.98	93	50	-43	0.54
52-46:27-30	7.91	247	1	-246	0.00
52-46:36-39	6.20	194	1	-193	0.01
52-46:63-66	8.60	269	3	-266	0.01
52-46:103.5-106.5	6.14	192	6	-186	0.03
56-56:12-13.5	10.54	329	0	-329	0.00
56-56:79.5-81	10.45	327	3	-324	0.01
56-56:30-33	7.78	243	2	-241	0.01
56-56:94-97.5	9.50	297	2	-295	0.01
56-60:9.55-12.55	9.61	300	3	-297	0.01

TABLE 20.2—Continued

Rock type Drill Hole: Depth (m)	% Total sulfur	APP ²	ANP ³	NANP (ANP- APP)	ANP APP
P1 Primary (continued)					
56-60:39.55-42.55	8.20	256	12	-244	0.05
56-60:67-69.55	3.80	119	4	-115	0.03
44-60:51-52.5	7.08	221	9	-212	0.04
46-62:12-15	5.30	166	5	-161	0.03
46-62:22.5-24	9.02	282	6	-276	0.02
46-62:42-43.5	7.48	234	9	-225	0.04
46-62:84-87	9.31	291	6	-285	0.02
46-62:123-126	6.58	206	19	-187	0.09
48-46:9-12	8.92	279	4	-275	0.01
48-46:66-69	8.59	268	10	-258	0.04
50-54:13.5-15	3.10	97	13	-84	0.13
40-46:13-16	8.59	268	8	-260	0.03
44-44:17-20	9.79	306	6	-300	0.02
P2 Primary					
50-54:273-276	1.08	34	6	-28	0.18
P3 Oxidized					
46-54:03-09	0.43	13	4	-9	0.31
P3 Primary					
46-54:15-18	3.73	117	10	-107	0.09
46-54:21-24	3.11	97	13	-84	0.13
46-54:45-48	1.86	58	45	-13	0.78
44-48:36-39	1.45	45	2	-43	0.04
44-48:48-51	1.30	41	1	-40	0.02
42-52:0.06-0.3	3.65	114	13	-101	0.11
42-52:15-16.5	3.99	125	13	-112	0.10
42-52:60-63	2.93	92	6	-86	0.07
48-54:258-261	0.40	12	25	13	2.1
50-54:27-28.5	1.47	46	25	-21	0.54
P4 (Dike)					
	<0.01	<0.03	15	15	500

¹All values in tons CaCO₃ equivalent/1000 tons rock except total sulfur in percent
²APP = Acid Producing Potential
³ANP = Acid Neutralizing Potential

TABLE 20.3—Chemical and mineralogical characteristics of unweathered and weathered waste rock. [From sulfur forms, acid production potential (APP), acid neutralization potential (ANP), calcium carbonate, chlorite, and net acid neutralization potential (NANP). Sulfur forms in percent, others in g of CaCO₃ equivalent per kg rock.]

	Test ¹	Total	Sulfate	Sulfide	APP _{sulf}	ANP	CaCO ₃	Chlorite ²	NANP _{sulf}
Unweathered	EPA	7.3	3.4	3.9	123	24			-99
	C & P	8.1	3.8	4.2	132		8		-108
	Sverdrup ²							11	
Humidity Cell	EPA	5.7	1.9	3.8	119	20			-99
	C & P	6.2	1.8	4.4	138		7		-118
	Sverdrup ²							16	
Column	EPA	5.7	0.8	4.6	145	23			-122
	C & P	5.8	1.2	4.6	143		8		-120
	Sverdrup ²							16	

¹Sulfur speciation was determined by two different test methods: EPA = Sobek et al. (1978) and C & P = Curry and Papp (1994)
²Based on semiquantitative XRD, assuming a relative reactivity compared with calcium carbonate of 0.4 (Sverdrup, 1990)

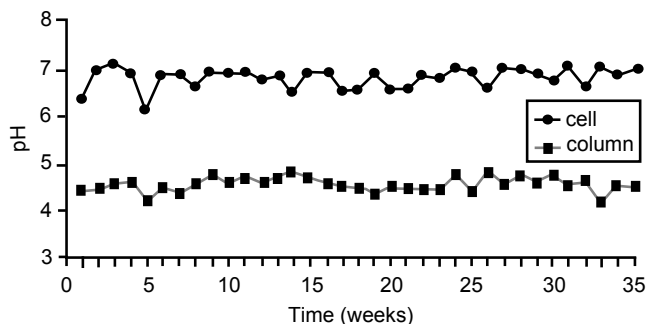


FIGURE 20.2—Plot of pH as a function of time in leachate collected weekly during the humidity-cell and column weathering tests.

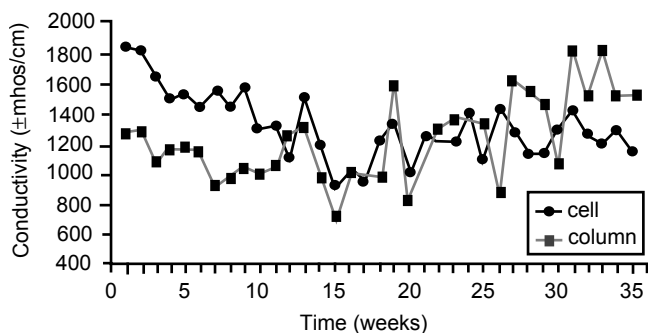


FIGURE 20.3—Plot of conductivity (in $\mu\text{mhos/cm}$) as a function of time in leachate collected weekly during the humidity-cell and column weathering tests.

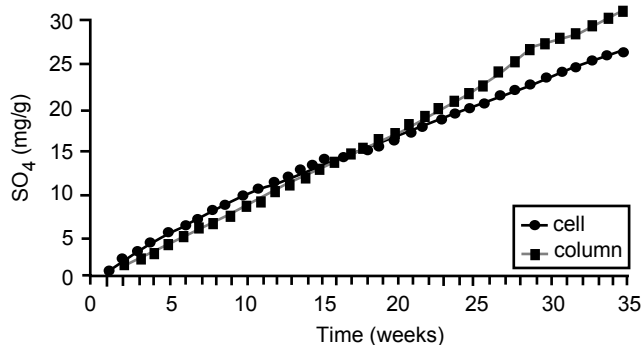


FIGURE 20.4—Plot of cumulative sulfate dissolved (in mg/g of waste rock) as a function of time in leachate collected weekly during the humidity-cell and column weathering tests.

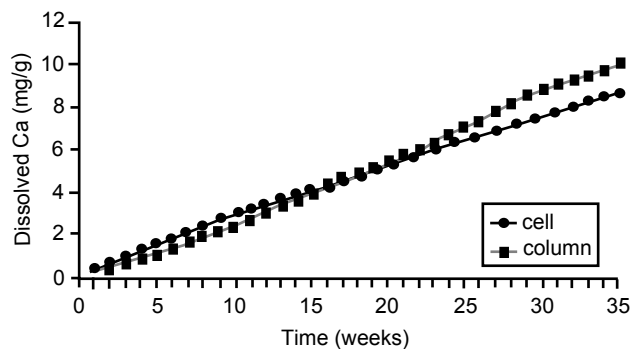


FIGURE 20.5—Plot of cumulative calcium dissolved (in mg/g of waste rock) as a function of time in leachate collected weekly during the humidity-cell and column weathering tests.

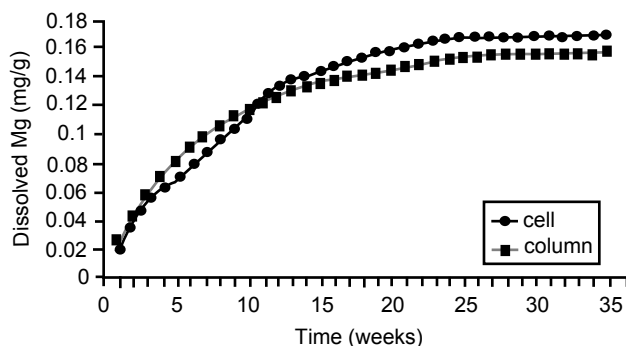


FIGURE 20.6—Plot of cumulative magnesium dissolved (in mg/g of waste rock) as a function of time in leachate collected weekly during the humidity-cell and column weathering tests.

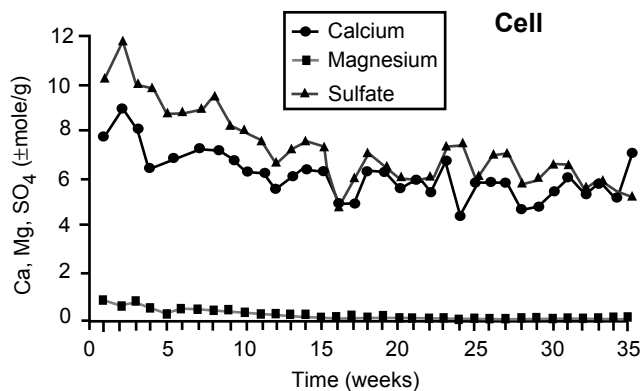


FIGURE 20.7—Plot of dissolved calcium, magnesium, and sulfate (in $\mu\text{moles/g}$ of waste rock) as a function of time in leachate collected weekly during the humidity-cell weathering tests.

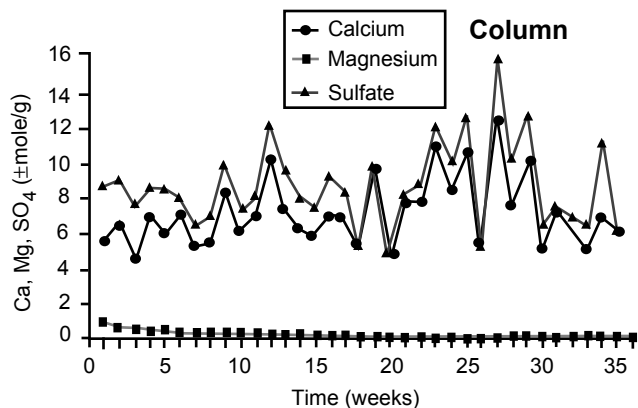


FIGURE 20.8—Plot of dissolved calcium, magnesium, and sulfate (in $\mu\text{moles/g}$ of waste rock) as a function of time in leachate collected weekly during the column weathering tests.

saturated ($SI = -0.18$). In the column leachate, gypsum was slightly undersaturated at all times except week 25, when it was about at saturation ($SI = 0.09$).

Ferrihydrite was supersaturated in the humidity cell ($SI = 1.38$ to 1.94). In the column leachate, ferrihydrite was slightly supersaturated in week 1 ($SI = 0.50$) and became increasingly undersaturated with time. Goethite was supersaturated in all leachates. Hydrogen jarosite began slightly supersaturated ($SI = 0.76$) in the humidity-cell leachate, but became slightly undersaturated ($SI = -0.48$) by week 35. In the column leachate, hydrogen jarosite started out quite supersaturated ($SI = 5.90$) in week 1 and became undersaturated ($SI = -2.02$) by week 35. Potassium jarosite was supersaturated in week 25 (the only week potassium was measured) in both the humidity cell and the column.

Table 20.6 shows the PHREEQE-calculated pH and the concentration of the major cation dissolved when individual minerals found in the waste rock were equilibrated with distilled water. Melantherite was also included to represent dissolution of a potential trace oxidation product in the waste rock. Most of the equilibrations were made at atmospheric partial pressure of carbon dioxide. Equilibration with chlorite produced a pH of 7.58, the highest

pH calculated. Of the major minerals, equilibrium with gypsum produced the lowest pH, at 5.74. When atmospheric carbon dioxide was excluded, gypsum equilibrated with water at a pH of 7.07. Except for gypsum, the major minerals produced very low concentrations of dissolved cations, in the range of 0.03 mg/l (potassium from muscovite) to 3.5 mg/l (magnesium from chlorite). Gypsum produced 630 mg/l of calcium on equilibration. Melantherite dissolution was a function of Eh. At 470 mV, equilibration with melantherite produced a pH of 4.40. However, it also produced an extremely high concentration of dissolved iron, at 73,000 mg/l.

Table 20.7 gives the results of a series of computer experiments in which oxygen was reacted with a system of distilled water and three minerals: pyrite, gypsum, and either goethite or amorphous iron hydroxide. For both mineral suites, the behavior was similar. As oxygen was progressively added, pH and the concentration of calcium decreased, whereas the concentrations of iron and sulfate increased. For a given amount of oxygen, the concentrations of calcium, iron, and sulfate were similar in both sets of experiments, but the pH was lower and the Eh higher in the set with goethite.

DISCUSSION

Initial information collected to develop geologic ARD-prediction models on porphyry copper-gold deposits suggests that such deposits are variable in their tendency to produce ARD. Kwong (1993) investigated certain porphyry deposits in the Canadian Cordillera that were hosted by rocks ranging from diorite to syenite. He found that these deposits tended to have carbonate alteration and no ARD. On the other hand, the copper porphyry deposits at Butte and Bingham in the western U.S. are known for their ARD.

The deposit investigated in the present study does not have significant carbonate alteration, but is hosted by andesite, a fairly basic rock type. The standard acid-base accounting procedures typically required for mine permitting gave a value of NANP for the waste rock of about $-100 \text{ g CaCO}_3/\text{kg}$. The standard interpretation of this result is that this porphyry copper-gold deposit would be a significant acid producer. However, evidence from the site suggests that the waste rock might not produce significant ARD. For example, the soil over the exposed potassic core of the deposit was somewhat acid, but all ground- and surface-water samples collected in and near the deposit were neutral to basic.

Three factors could account for this neutral to basic water. First, the arid conditions likely evaporate most of the water moving through the soil (or a waste rock facility) so that little actually reaches the underlying bedrock aquifer or surface drainages. Second, drainage that does reach ground or surface water has minimal acidity and is neutralized by the greater alkalinity of the rock and water it contacts. Finally, the ground water within the deposit is likely too reducing to sustain pyrite oxidation because the bedrock aquifers are confined and relatively static.

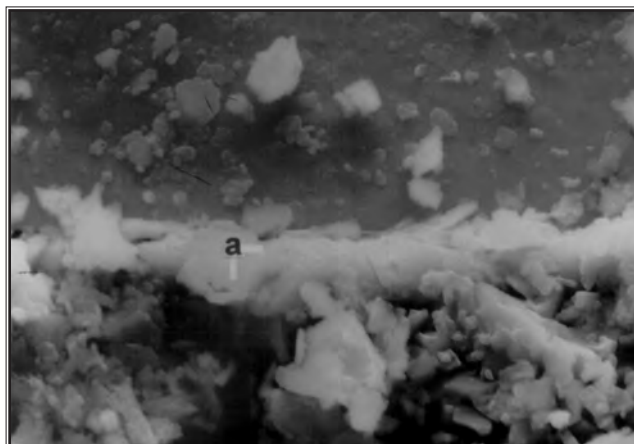
The waste rock would be exposed to minimal water in the proposed waste-rock facility and might behave like the soil formed from the exposed potassic core. For these reasons, it was suspected that the waste rock might be slow to produce acid, despite the negative NANP. Therefore, two types of simulated weathering kinetic tests were conducted. As shown in the RESULTS section, the pHs remained constant at about 7 for the humidity cell and 4.5

TABLE 20.4—Semi-quantitative X-ray diffraction analyses of unweathered and simulated weathered waste rock.

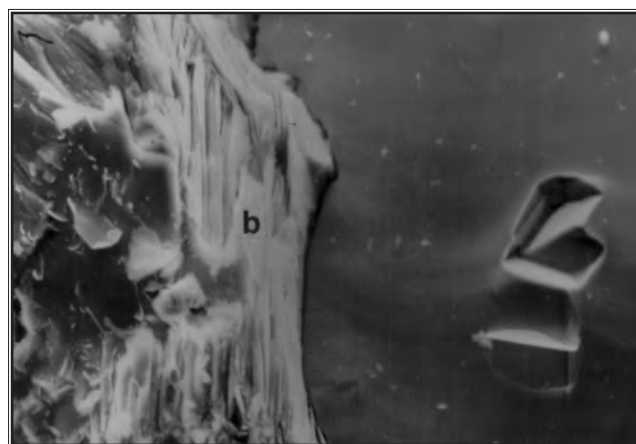
	Quartz	Gypsum	Muscovite	Plagioclase	Pyrite	Chlorite	Potassium Feldspar	Other
Unweathered	23	38	9	7	5	4	3	10
Humidity Cell	28	25	10	8	6	6	4	10
Column	34	13	14	10	6	6	6	10

TABLE 20.5—MINTEQA2-calculated saturation indices for selected minerals in the humidity cell and column leachates.

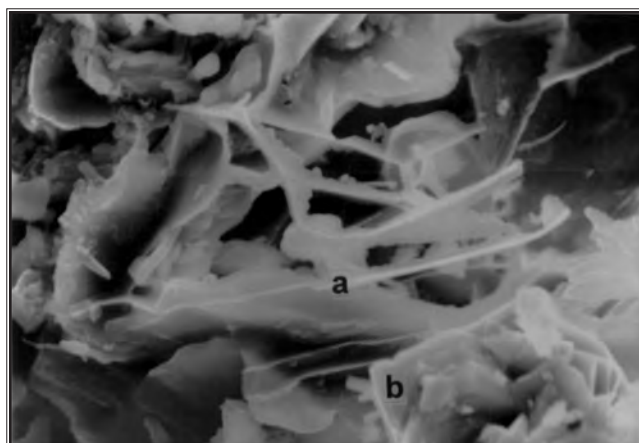
	Humidity Cell					Column				
	Week 1	Week 5	Week 10	Week 25	Week 35	Week 1	Week 5	Week 10	Week 25	Week 35
Calcite	-1.97	-2.56	-1.45	-1.21	-1.45	-5.41	-6.24	-5.58	-5.66	-5.87
Ferrihydrite	1.38	1.38	1.90	1.94	1.92	0.50	-0.18	-0.37	-1.43	-1.89
Goethite	5.78	5.77	6.30	6.33	6.31	4.89	4.21	4.02	2.96	2.50
Gypsum	0.13	0.04	0.02	-0.11	-0.18	-0.18	-0.18	-0.21	0.09	-0.28
H Jarosite	0.76	1.44	0.16	0.04	-0.48	5.90	4.60	2.29	0.20	-2.02
K Jarosite				4.98					2.62	
Na Jarosite				1.91					-0.75	
Alunite				2.54					0.45	



▲ **FIGURE 20.9**—SEM photomicrograph of a pyrite grain (top half of photo) and primary hydrothermal-alteration rind (bottom half) in waste-rock piece no. 1. The small platy particles on the pyrite are aluminosilicates, based on EDX spectral analyses. Point a referenced on Figure 20.12.



▲ **FIGURE 20.10**—SEM photomicrograph of a pyrite grain with etch pit (right half of photo) and alteration rind (left half) on a freshly broken face of waste-rock piece no. 2. Point b referenced on Figure 20.12.



◀ **FIGURE 20.11**—SEM photomicrograph of boxwork alteration rind found along edge of large pyrite grain (not shown) on waste-rock piece no. 3. Points a and b referenced on Figure 20.13.

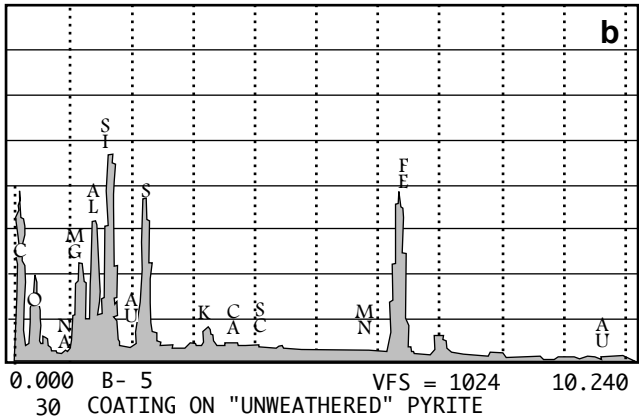
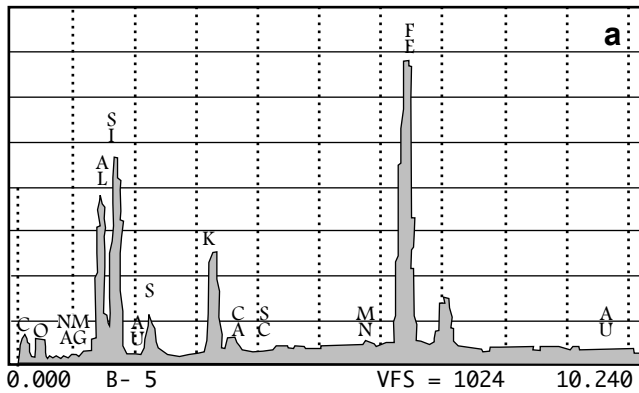


FIGURE 20.12—EDX spectral plots of marked points on alteration rinds from (a) Figure 20.9 and (b) Figure 20.10.

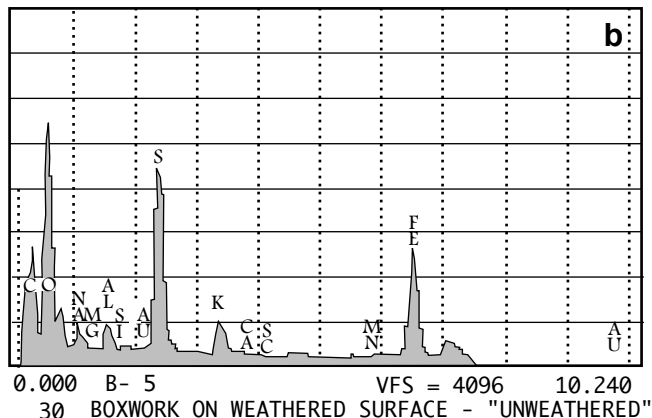
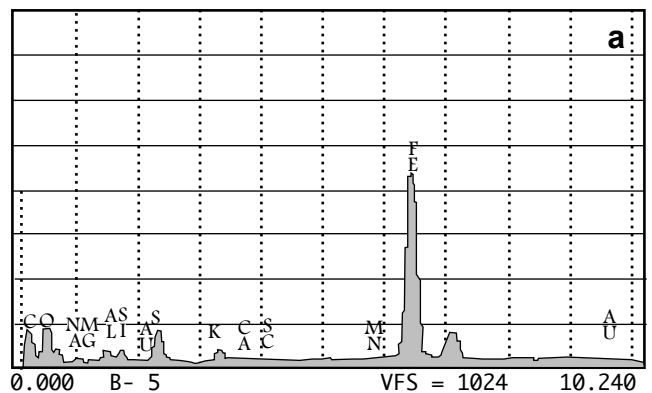


FIGURE 20.13—EDX spectral plots of points "a" and "b" on boxwork alteration on Figure 20.11.

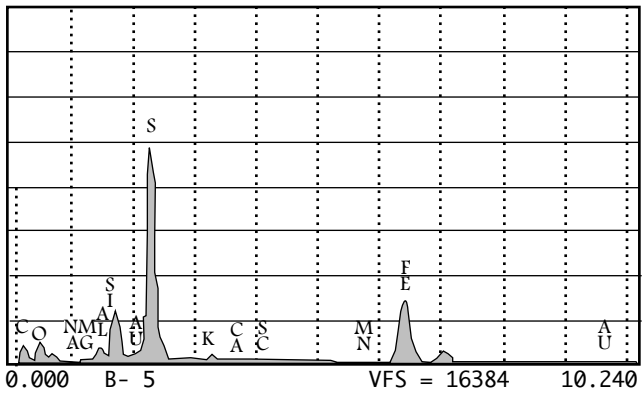


FIGURE 20.14—EDX spectral plot of a point on a pyrite grain from waste-rock piece no. 1.

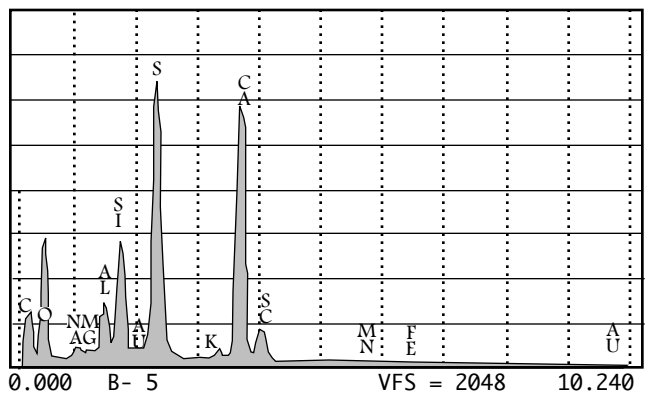


FIGURE 20.15—EDX spectral plot of a point on a gypsum grain from waste-rock piece no. 3.

for the column, indicating that no significant acid production occurred over the 35 weeks of testing.

TABLE 20.6—PHREEQE-calculated pH and major cation concentration (in mg/l) for distilled water equilibrated with selected minerals. Equilibrated at atmospheric $p\text{CO}_2 = -3.5$, except as noted.

Mineral	pH	Cation	Concentration
Chlorite	7.68	Mg	3.5
Albite	6.80	Na	3.1
Quartz	6.80	Si	2.9
Microcline	6.50	K	1.0
Muscovite	5.88	K	0.03
Gypsum	5.74	Ca	630
	7.07 ¹	Ca ¹	630 ¹
Melanterite			
Eh = 235 mV	5.48	Fe ⁺²	73,700
Eh = 470 mV	4.40	Fe ⁺²	73,700

¹Closed system with no carbon dioxide

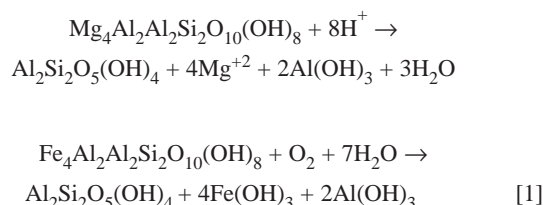
Both sets of tests also produced significant concentrations of dissolved calcium and sulfate in the leachate. Traditionally, the sulfate would be interpreted as evidence of pyrite oxidation and the calcium as evidence of calcium carbonate dissolution. The different pH's of the two sets of test leachates would be interpreted as due to different relative reaction rates of the two minerals due to the different particle sizes and flow paths in the two test vessels.

This traditional interpretation might have stood unquestioned, except for calculations indicating that the amounts of calcium carbonate which would have had to dissolve during the course of the tests far exceeded the initial calcium carbonate contents. In addition, the ANP results for the waste rock after 35 weeks of weathering indicated that no calcium carbonate had dissolved and the APP_{surf} results indicated that no pyrite had oxidized. These results led to an investigation of the mineralogy of the waste rock (Table 20.4), with the conclusion that gypsum was dissolving, rather than calcium carbonate and pyrite.

Gypsum was found to be a major mineral in the waste rock, even though it does not typically occur in porphyry systems. On the other hand, anhydrite is commonly found in the central, potassic alteration zone of porphyry systems (Lowell and Gulbert, 1970). Thus, the gypsum could be a hydrated product of anhydrite. It is more likely, however, that the gypsum was deposited along fractures from evaporated saline ground water. Gypsum commonly occurs as an evaporation product within soils in this type of climate. The gypsum could also have been the result of

oxidation of near-surface pyrite from the deposit itself. The yellow soil typical of an oxidizing potassic core indicated that jarosite and/or iron oxyhydroxide was present in these soils, as would be expected if the gypsum came from near-surface pyrite oxidation.

Based on the XRD analyses (Table 20.4), the only mineral in the unweathered and weathered waste rock with significant neutralizing capability, other than the minor calcium carbonate, is chlorite (Table 20.3). Sverdrup (1990) classified chlorite within the group of minerals considered to have an intermediate weathering rate (Table 20.1), with a reactivity relative to calcite of about 40%. The weathering of chlorite can neutralize significant acidity, depending on its cation composition. Weathering reactions for magnesium chlorite and iron chlorite, two compositional end members, are as follows:



Based on these reactions, the weathering of magnesium chlorite consumes eight moles of acid per mole of chlorite. Weathering of the iron end member produces no net acid neutralization, because the acidity consumed is balanced by the acidity produced by the oxidation and hydrolysis of the iron. Based on the EDX spectral plot shown on Figure 20.12b, the chlorite in the present study is likely a mixed magnesium-iron chlorite with an acid neutralization potential between the two end members.

The maximum ANP produced by chlorite in the waste rock is about 15 g CaCO_3/kg , assuming the mineral is pure magnesium chlorite and has a relative reactivity of 0.4. The total ANP calculated by adding calcium carbonate plus magnesium chlorite is between 19 and 24, which compares well with the ANP of 20 to 24 measured using the more concentrated acid in the acid-base accounting tests (Table 20.3). Essentially all of this neutralization potential remained in the waste rock after 35 weeks of weathering.

The consistent difference in pH of the leachate from the two sets of weathering tests does not appear to be due to differences in pyrite oxidation rate. Other potential causes include consistent differences in the method of pH measurement of leachate from the

TABLE 20.7—PHREEQE Experiment: Adding oxygen to a system of distilled water, gypsum, pyrite, and goethite or $\text{Fe}(\text{OH})_3$ at atmospheric $p\text{CO}_2 = -3.5$. Concentrations in mg/l.

O ₂ added (mole/l)	pH	Eh	Ca	Fe	SO ₄	C (as CaCO ₃)	Goethite	Fe(OH) ₃
0	6.49	-120	628	0.6	1,510	3.0	X	
0	8.47	-245	644	88.7	1,560	231		X
0.001	5.48	-45	622	31.0	1,640	1.3	X	
0.01	4.92	0	580	343	1,990	1.1	X	
0.01	8.07	-215	584	386	2,000	107		X
0.1	4.44	38	443	3,430	6,970	1.1	X	
0.1	7.61	-175	443	3,470	6,980	67.4		X
1	7.11	-135	299	34,400	59,800	75.1		X
10	6.54	-90	228	343,000	591,000	109		X

humidity cell and column or differential dissolution of minerals other than pyrite due to the different particle sizes of material in the two sets of tests. Differences in the method of pH measurement are unlikely to be the cause of the consistent pH differences, because leachates from both tests were collected and measured at the same time by a single analyst using the same equipment and a single set of techniques and buffer solutions.

Differential dissolution of minerals in the two sets of tests was investigated indirectly by geochemical modeling of the pH at saturation for a number of individual minerals found in the waste rock. Silicon was not measured in the leachates, so saturation calculations could not be made of the silicate minerals. Modeling with PHREEQE (Table 20.6) showed that several of the minerals could have produced the circumneutral pH found in the humidity cell tests and that saturation with any of these minerals would produce relatively low cation concentrations similar to those observed in leachates. Gypsum saturation by itself would produce a pH of 5.7 under atmospheric carbon dioxide conditions and a pH of 7.1 if carbon dioxide is excluded. None of the major minerals in the waste rock could account for the pH of about 4.5 that was observed in column leachates.

Dissolution of melanterite or similar ferrous sulfate minerals could lower the pH. However, much higher dissolved iron concentrations would have been expected than were actually observed, assuming the water was at saturation with the sulfate mineral. It is possible that minor amounts of ferrous or ferric sulfate salts were dissolved in both sets of tests and that other more neutralizing minerals, such as calcium carbonate or chlorite, dissolved slightly in the humidity cell tests, which used finer particle sizes than the column tests. As shown in Table 20.3, the ANP of weathered waste rock from the humidity cell tests (ANP = 20 g CaCO₃/kg) was slightly lower than that of the column tests (ANP = 23 g/kg), suggesting that a minor amount of neutralizing material may have dissolved during the course of the humidity cell tests.

Geochemical modeling also was used to investigate whether gypsum solubility controlled the dissolution of calcite or the oxidative dissolution of pyrite. The MINTEQA2 calculations (Table 20.5) showed that calcite was undersaturated in both the humidity cell and column tests, and thus should have dissolved. The total measured carbonate was at the lower limit of detection of the coulometric method used, so the precision of the resulting values is low. It is possible that some of this small amount of carbonate did dissolve during the testing, especially in the humidity cell tests, as mentioned above.

The PHREEQE experiment of adding oxygen to a system of distilled water, gypsum, pyrite, and goethite or amorphous iron hydroxide (Table 20.7) indicated that saturation with gypsum would not keep the pyrite from oxidizing, based on thermodynamic considerations alone. However, the work by Brown and Jurinak (1989), discussed previously in the BACKGROUND section, suggests that the dissolved sulfate produced by dissolution of gypsum would tend to inhibit abiotic pyrite-oxidation kinetics. Abiotic kinetics are expected to prevail at pHs above about 4.

The SEM investigations were conducted to investigate whether gypsum or some other mineral was actually coating pyrite grains and acting as a physical barrier to pyrite oxidation. The SEM results indicated that an alteration rind of iron sulfate-rich material was present on pyrite in samples of presumably primary waste rock. However, fresh pyrite faces on euhedral grains made up much of the pyrite on freshly broken samples, suggesting that

most of the pyrite surface was exposed during the weathering tests. The pyrite surfaces were typically smooth, with few etch pits, and no other sulfide minerals were observed as inclusions. These observations suggest that the nature of the pyrite itself made it relatively unsusceptible to weathering.

CONCLUSIONS

A number of complementary techniques were used to investigate potential acid production in waste rock from Bajo de la Alumbrera, a porphyry copper-gold deposit in an arid montane environment. The results show that pyrite oxidation of the waste rock from this deposit is significantly more complicated than would have been predicted by using only the standard acid-base accounting methods required by most regulatory agencies. It appears that the combination of the physical nature of the pyrite itself and the presence of sulfate in the leachate due to gypsum dissolution combine to inhibit pyrite oxidation. These results provide geochemical mechanisms other than calcium-carbonate neutralization that may play a role in lowering the rate of ARD production for this deposit type, especially in an arid climate where gypsum is present. Finally, the arid conditions at this site should produce only a minimal volume of water entering the waste rock pile and solution formed within the waste rock pile would likely evaporate during the course of its excursion through the pile.

ACKNOWLEDGMENTS—This research was funded in part by International Musto Ltd. while the first author was at Knight Piesold and Co. The authors also wish to acknowledge Mineral Alumbrera Ltd. for permission to publish this paper. We thank T.T. Chao for helpful discussions and reviews; Marty Goldhaber and Scott Effner for their constructive reviews; Steve Sutley and Jim Cathcart, Jr. for conducting the XRD analyses; and Mick Brownfield for training the first author in SEM and EDX techniques.

REFERENCES

- Allison, J.D., Brown, D.S., Novo-Gradac, K.J., 1991, MINTEQA2/PRODEFA2, a geochemical assessment model for environmental systems, Version 3.0 user's manual: EPA/600/3-91/021, U.S. Environmental Protection Agency, Athens, Ga., 106 pp.
- Borek, S.L., 1994, Effect of humidity on pyrite oxidation; *in* Alpers, C.N., and Blowes, D.W. (eds.), *Environmental Geochemistry of Sulfide Oxidation*: ACS Symposium Series 550, Washington, D.C., pp. 31-44.
- Brown, A.D., and Jurinak, J.J., 1989, Mechanism of pyrite oxidation in aqueous mixtures: *Journal of Environmental Quality*, v. 18, pp. 545-550.
- Curry, K.J., and Papp, C.S.C., 1996, Acid-soluble sulfate, sulfide, and organic sulfur; *in* Arbogast, B.F. (ed.), *Quality Assurance Manual for the Branch of Geochemistry*: U.S. Geological Survey Open-File Report 96-525, pp. 182-185.
- Guilbert, J.M., 1986, *The geology of ore deposits*: W.H. Freeman and Company, New York, 985 pp.
- Kwong, Y.T.J., 1993, Prediction and prevention of acidic rock drainage from a geological and mineralogical perspective: MEND Project 1.32.1, CANMET, Ottawa, Ontario, 47 pp.
- Lapakko, K.A., 1992, Recent literature on static predictive tests; *in* *Emerging Process Technologies for a Cleaner Environment*: Society for Mining, Metallurgy, and Exploration, Littleton, Colo., pp. 109-119.
- Lowell, J.D., and Guilbert, J.M., 1970, Lateral and vertical alteration-mineralization zoning in porphyry ore deposits: *Economic Geology*, v. 65,

- pp. 373–408.
- Mills, A.L., 1999, The role of bacteria in environmental geochemistry; *in* Plumlee, G.S., and Logsdon, M.J. (eds.), *The Environmental Geochemistry of Mineral Deposits, Part A. Processes, Techniques, and Health Issues: Society of Economic Geologists, Reviews in Economic Geology*, v. 6A, pp. 125–132.
- Nordstrom, D.K., and Alpers, C.N., 1999, Geochemistry of acid mine waters; *in* Plumlee, G.S., and Logsdon, M.J. (eds.), *The Environmental Geochemistry of Mineral Deposits, Part A. Processes, Techniques, and Health Issues: Society of Economic Geologists, Reviews in Economic Geology*, v. 6A, pp. 133–160.
- Nordstrom, D.K., Plummer, L.N., Langmuir, D., Busenberg, E., May, H.M., Jones, B.F., and Parkhurst, D.L., 1991, Revised chemical equilibrium data for major water-mineral reactions and their limitations; *in* Melchior, D.C., and Bassett, R.L. (eds.), *Chemical Modeling of Aqueous Systems II: ACS Symposium Series 416*, Washington, D.C., pp. 398–413.
- Parkhurst, D.L., Thorstenson, D.C., and Plummer, L.N., 1980, PHREEQE—A computerized program for geochemical calculations: U.S. Geological Survey Water Resources Investigation 80–96, 210 pp.
- Plumlee, G.S., 1999, The environmental geology of mineral deposits; *in* Plumlee, G.S., and Logsdon, M.J. (eds.), *The Environmental Geochemistry of Mineral Deposits, Part A. Processes, Techniques, and Health Issues: Society of Economic Geologists, Reviews in Economic Geology*, v. 6A, pp. 71–116.
- Scharer, J.M., Pettit, C.M., Chambers, D.B., and Kwong, E.C., 1994, Mathematical simulation of a waste rock heap: Proceedings, International Land Reclamation and Mine Drainage Conference and 3rd International Conference on the Abatement of Acidic Drainage, v. 1, pp. 30–39.
- Shuey, R.T., 1975, *Semiconducting ore minerals*: Elsevier Scientific Publishing Company, Amsterdam, 415 pp.
- Sobek, A.A., Shuller, W.A., Freeman, J.R., and Smith, R.M., 1978, *Field and laboratory methods applicable to overburdens and minesoils*: EPA 600/2–78–054, U.S. Environmental Protection Agency, Cincinnati, Ohio, 203 pp.
- Sverdrup, H.U., 1990, *The kinetics of base cation release due to chemical weathering*: Lund University Press, Lund, Sweden, 246 pp.
- White III, W.W., Lapakko, K.A., and Cox, R.L., 1999, Static-test methods most commonly used to predict acid-mine drainage—Practical guidelines for use and interpretation; *in* Plumlee, G.S., and Logsdon, M.J. (eds.), *The Environmental Geochemistry of Mineral Deposits, Part A. Processes, Techniques, and Health Issues: Society of Economic Geologists, Reviews in Economic Geology*, v. 6A, pp. 325–338.

Chapter 21

THE HYDROGEOCHEMISTRY OF A NICKEL-MINE TAILINGS IMPOUNDMENT— COPPER CLIFF, ONTARIO

C.J. Coggans,¹ D.W. Blowes,¹ W.D. Robertson,¹ and J.L. Jambor²

¹*CH2M Gore & Storrie Limited, 600-180 King Street South, Suite 600
Waterloo, Ontario N2J 1P8 Canada*

²*Environmental Laboratory, Ottawa, Ontario, K1A 0G1 Canada*

The tailings impoundments of the Sudbury operation of INCO Ltd., one of the largest mining complexes in the world, cover 21 km² and constitute in excess of 10% of all mine tailings areas in Canada. These tailings are oxidizing within the shallow vadose zone, generating low pH pore waters with high concentrations of dissolved constituents. The impoundments are a local recharge area, with water-table elevations in the impoundments 20–30 m higher than in the surrounding area. Ground-water recharge rate estimates, including age-dating the recharge water with tritium concentrations, indicate that precipitation infiltrates the tailings at 0.24 to 0.28 m/a. The modeled flow system along a 3 km cross section through tailings deposited from 1940 to 1960 suggests that precipitation on the impoundments will recharge the bedrock aquifer to a minor extent, but will also travel laterally from the tailings disposal area toward Finlander Creek, immediately to the east of the impoundments. Infiltrating recharge water is affected by sulfide-oxidation reactions within the vadose zone. Maximum concentrations of 1060 mg/l Fe, 8700 mg/l SO₄, 641 mg/l Ni, and 23.3 mg/l Co are observed in the shallow tailings. The Ni and Co concentrations are probably representative of tailings in the Sudbury area. Sulfide oxidation is complete in the upper 0.10 to 0.25 m of the tailings along the cross section, but is still occurring 1 to 2 m beneath that zone. Unoxidized tailings within the unsaturated zones of the impoundments are evidence of the potential for further sulfide oxidation to occur should the water-table elevation be maintained at its present level. Modeled simulations suggest that the sulfide-oxidation reactions will continue for 5 to 400 years, depending on the thickness of the vadose zone and the sulfide content of the tailings. Jarosite, gypsum, and goethite are the abundant precipitates in the impoundments and are effective solid-phase controls on dissolved concentrations of Fe, SO₄, and Ca. Precipitation of these minerals is cementing the tailings at or near the depth of active oxidation. The hardpan layers act as diffusion barriers to O₂ and CO₂, prolonging the time required to completely oxidize the tailings, but also slowing the downward displacement of the low-pH waters. A sequence of carbonate, aluminum-hydroxide, aluminosilicate, and ferrihydrite dissolution reactions, similar to that observed in other sulfide tailings impoundments, buffer the low pH conditions and retard by a factor of 3.6 to 4.2 the movement of low pH waters. Iron, Ni, and Co exhibit similar mobilities within the impoundments; however, Zn, Cr, Pb, and Cu are less mobile and their transport is strongly dependent upon pH, and precipitation, dissolution, adsorption, and desorption reactions. Anglesite, cerussite, and covellite may be acting as solid-phase controls of Pb and Cu. Manganese and As were observed at

much lower concentrations and seem to migrate through the tailings at the same velocity as Fe, SO₄, and Co.

INTRODUCTION

The Copper Cliff tailings disposal area near the town of Copper Cliff, Ontario (Fig. 21.1) has been used continuously since 1936 and constitutes one of the largest mine disposal areas in the world. The six tailings impoundments within the disposal area cover 21 km², accounting for more than 10% of all sulfide mine tailings in Canada (Feasby et al., 1991).

Approximately 35,000 t/day of ore from the Sudbury Igneous Complex, a fine-to-medium-grained noritic to gabbroic rock locally containing up to 60 wt% sulfides, is mined by INCO Ltd. and processed at the Copper Cliff mill. Monoclinic and hexagonal pyrrhotite (Fe_{1-x}S), pentlandite ((Ni,Fe)₉S₈), chalcopyrite (CuFeS₂), pyrite (FeS₂), and cubanite (CuFe₂S₃) comprise the bulk of the sulfides. Minor concentrations of cobaltite (CoAsS), nickelite (NiAs), galena (PbS), and millerite (NiS) are present (Hawley and Stanton, 1962; Naldrett, 1984). Approximately 95% of the copper and 80% of the nickel are recovered in the milling process, and the remainder is discharged to the impoundments with the bulk tailings (INCO Ltd. staff, personal commun., 1991).

The Copper Cliff tailings disposal area consists of several valleys filled to depths of up to 45 m with silty tailings that have been deposited sequentially since 1936 (Table 21.1). Tailings deposited within the impoundments average 6 wt% total sulfides, predominantly pyrrhotite. Where exposed to oxygen in the unsaturated zone, these sulfide minerals oxidize, generating low-pH conditions and releasing high concentrations of dissolved constituents to the tailings pore water. The reaction products are gradually displaced downward and outward from the tailings area.

A vegetation program, initiated in 1957, has developed self-sustaining grass covers on the C-D, M, and M1 tailings areas. This program required the use of large amounts of agricultural limestone (>8.8 t/ha) and fertilizer (0.45 t/ha); details are provided by Peters (1984). Revegetation has not measurably lessened the oxidation of sulfide minerals or the transport of dissolved constituents within the tailings (Coggans et al., 1991).

The tailings at the Copper Cliff impoundments are representative of tailings generated from the mining and milling of the nickel-rich sulfide ores of the Sudbury area. The mechanisms resulting in the release and movement of sulfide-oxidation products of these tailings were studied at the INCO Ltd. impoundments. This paper

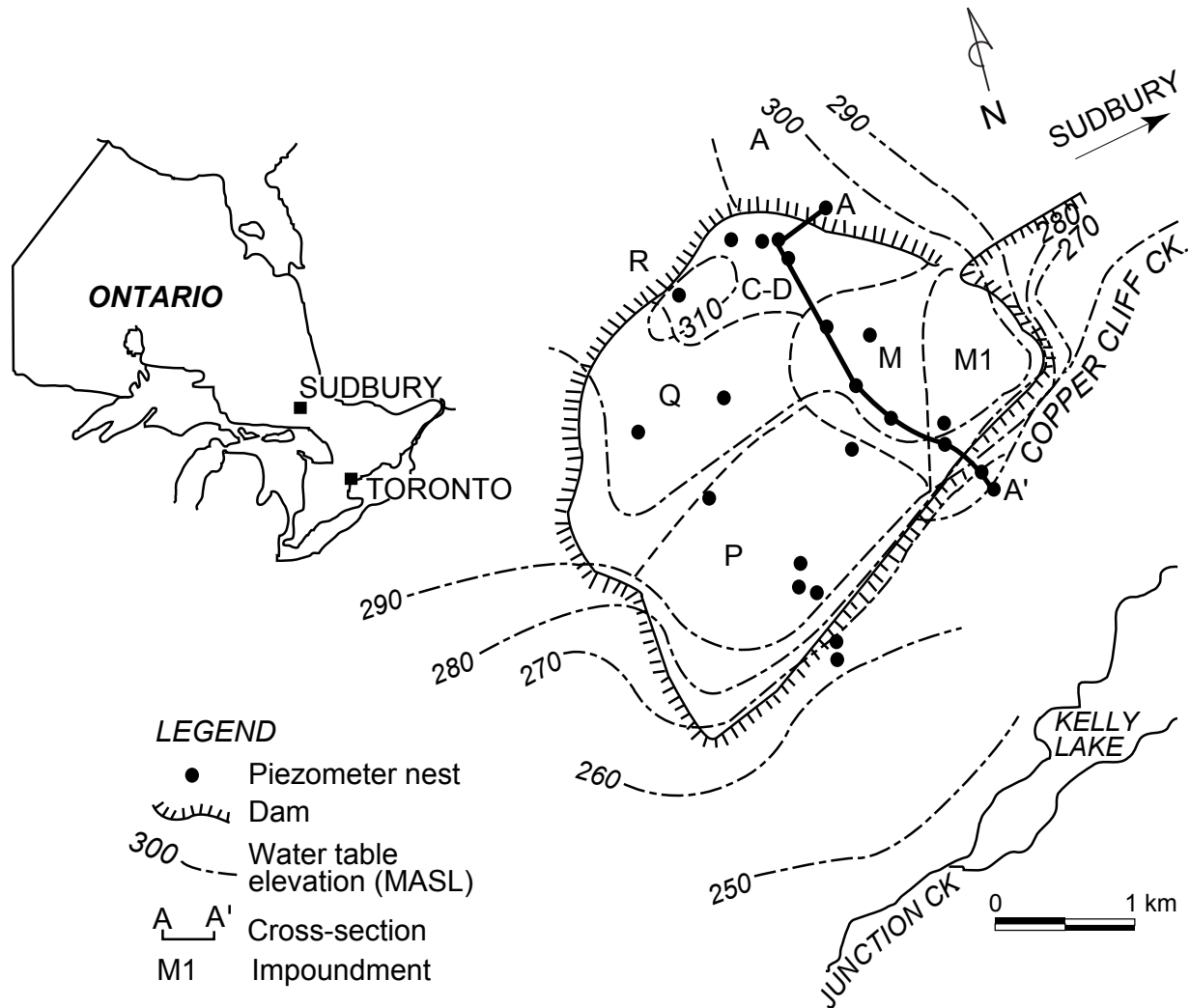


FIGURE 21.1—Location of INCO Ltd. Copper Cliff tailings impoundments and water table configuration.

describes the hydrogeochemistry of the tailings water along a cross section of tailings deposited between 1940 and 1960, paralleling one of the major ground-water flowpaths within the impoundments (cross section A-A': Fig. 21.1).

TABLE 21.1—Characteristics of the INCO Ltd. Copper Cliff, Ontario mine-tailings impoundments.

Impoundment	Disposal	Development	Area (hectares)
A	Tailings	1937–1940	32
C-D	Tailings	1940–1945	150
M	Tailings + Pyrrhotite*	1945–1960	280
P	Tailings	1960–1988	380
Q	Tailings	1960–1988	250
R	Tailings + Pyrrhotite*	1988–present	1000

*Pyrrhotite concentrates that were subsequently deposited in the impoundment.

METHOD OF INVESTIGATION

Data collection

The methods used in this study are similar to those used by Blowes (1990). Samples were collected and analyzed at 10 piezometer nests (IN1, IN2, IN4, IN10, IN11, IN12, IN13, IN16, IN17, and IN18) in June, 1989. Each nest contained four to seven piezometers along a 3 km cross section (A-A': plan view, Fig. 21.1; cross section, Fig. 21.2). Fifty-eight piezometers were driven with a vibrating hammer to depths of up to 25 m throughout the impoundments (Fig. 21.2). The piezometers were a modified Casagrande drive-point type (Starr and Ingleton, 1992), with exact piezometer construction varying, depending on the required depth of penetration.

At each piezometer nest, the O₂ and CO₂ concentrations of the pore gas in the vadose zone were determined using a portable gas analyzer (NOVA Instruments, 305 LBD) following the technique described by Blowes et al. (1991). Samples were collected at 10 cm increments, to a maximum depth of 1.4 m.

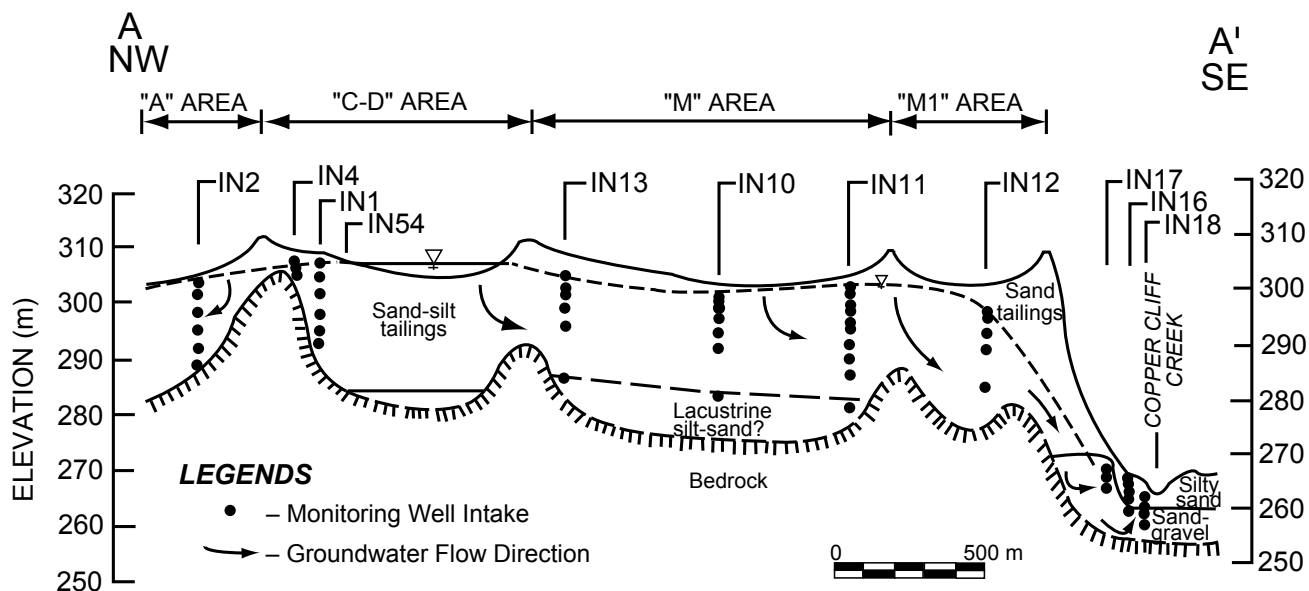


FIGURE 21.2—Cross section along A-A' (Fig. 21.1) showing stratigraphy, ground-water flow direction, and piezometer network.

Water samples from the vadose zone of the tailings were extracted from core samples in the field using the technique described by Smyth (1981). Measurements of pH (with a combination pH electrode: ORION ROSS model 815600), Eh (with a platinum combination Redox electrode: ORION ROSS model 96-7800), specific conductance, and temperature were made immediately after sample extraction. The pH electrode was calibrated before and after each reading using NBS Standard (pH = 4.00 and 7.00) and prepared (pH = 1.68, A.W.W.A. Standard Methods) buffers, maintained at ground-water temperatures. Measurements of the Eh of Zobell's solution (Nordstrom, 1977) were made before and after each reading to assess the response of the electrode. Separate samples were passed through filters of 0.45 μm pore size. Samples for cation analyses were preserved with 12 N HCl; samples for anion analyses were untreated. All samples were refrigerated until analyzed, generally within one to two months after collection.

Water samples from the saturated zone of the tailings were collected from the piezometers using a peristaltic pump. Samples were filtered in-line using 0.45 μm filters and passed through a closed flow-through cell maintained at ground-water temperature. The pH, Eh, and temperature were measured in the cell, isolated from atmospheric gases. The pore water was collected as it passed out of the flow-through cell and Fe^{2+} and alkalinity concentrations were determined. Specific conductivity measurements were made on separate samples. Additional samples were collected separately and stored in the same manner as the vadose-zone water samples.

Ground-water samples were analyzed for Al, Ca, Cd, Co, Cr, Cu, Fe, K, Mg, Mn, Na, Ni, Pb, Si, and Zn concentrations by atomic absorption spectrophotometry (AAS) and Cl, NO_3^- , and SO_4^{2-} concentrations by ion chromatography (IC) at the Water Quality Laboratory at the University of Waterloo. Concentrations of As were determined by AAS after hydride generation using the technique of Shaikh and Tallman (1979). The accuracy of the

results from the laboratory were assessed by analyzing blanks and comparing replicate samples analyzed by external laboratories, and performing charge balance calculations for all samples (Coggans, 1992).

Core samples were retrieved to depths of up to 5.5 m along cross section A-A' (Figs. 21.1 and 21.2). Porosity determinations were made on the core in 10 cm increments. Grain-size distributions were determined at 1 m intervals at IN11 by sieve and hydrometer analyses at the Analytical Services Laboratory, University of Guelph (Fig. 21.3). The total sulfur content of the tailings was measured using the method of Barker and Chatten (1982).

Polished thin sections were prepared from tailings samples collected to 5.5 m depth at IN12 and 2.0 m depth at IN13 by the Thin Section Preparation Laboratory at the University of Toronto. Tailings samples from IN13 and all polished thin sections were sent to the Environmental Laboratory, CANMET for mineralogical examination.

Data interpretation

The geochemical data were interpreted with the aid of MINTQA2 (Felmy et al., 1983; Allison et al., 1990), a geochemical speciation/mass transfer model. Modifications were made to the MINTQA2 database to make it consistent with the WATEQ4F database (Ball and Nordstrom, 1991). The revised database also includes calculated or estimated ion-association constants for Fe^{2+} , Fe^{3+} , Ca^{2+} , and Al^{3+} bisulfate complexes, which were not included in the original MINTQA2 database. The solubility constants for K, Na, and H_3O jarosite were modified to the values recommended by Alpers et al. (1989), which were determined using thermodynamic data in the WATEQ4F database. The rate of sulfate production was estimated using the approximate analytical solution of Davis and Ritchie (1986).

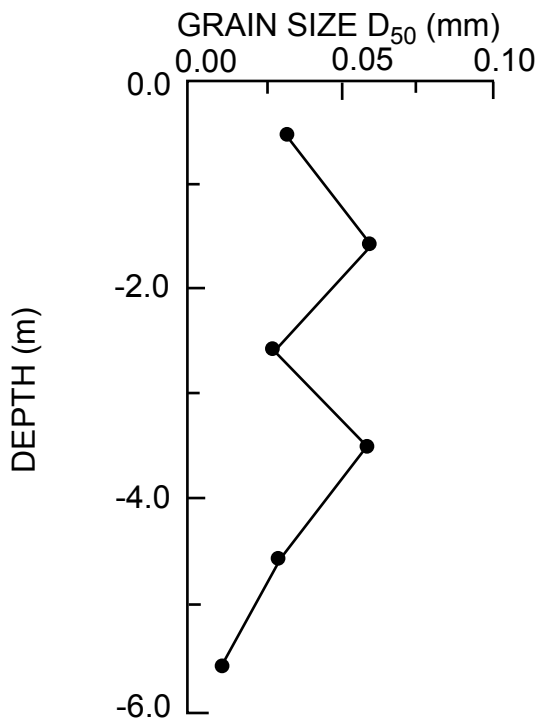


FIGURE 21.3—Grain-size analyses of tailings at piezometer nest IN11 within the M impoundment.

RESULTS AND DISCUSSION

The water table at the piezometer nests along cross section A-A' (Fig. 21.2) varied between 0.7 and 5.1 m below ground surface and the vadose zone increased in thickness near the southeast edge of the impoundments. Within the vadose zone, the pore water pH ranges from pH <3 near the tailings surface to pH >7 at depths greater than 3 m. The oxidation reduction potential (Eh) is 400–500 mV near the tailings surface, indicating oxidized conditions, but decreases to approximately 100 mV below 3 m at all piezometer nests. The alkalinity measurements made in the field vary from nest to nest, but maximum concentrations generally are observed at depths of 3–5 m, ranging from non-detectable at surface to 818 mg/l (as HCO₃⁻) at 3.24 m depth at piezometer nest IN12. The results of ground-water sampling at IN12 and IN13 are plotted on Figures 21.4 and 21.5.

Hydrogeological setting

The Copper Cliff area in Northern Ontario has a cool, humid climate that averages 78.2 cm of annual precipitation (van der Leeden et al., 1991). The elevated tailings impoundments are a regional ground-water recharge zone where precipitation infiltrates downward through the tailings and migrates radially away from the impoundments (Coggans et al., 1991). The elevated water table in the CD and M impoundments is maintained, in part, by continued pumping of water into ponds within the impoundment. The water table slopes gently to the southeast, but hydraulic gradients increase sharply near the tailings dam (Fig. 21.2).

The tailings deposited in the CD and M impoundments along cross section A-A' (Fig. 21.1) are typically a mixture of silt to medium-grained sand (Fig. 21.3). Porosity values of tailings below 0.35 m, where the tailings are not disturbed by vegetation, average 0.50 ($n = 18$, $2\sigma = 0.08$). Hydraulic conductivities of the tailings, determined from piezometer response tests using the method of Chapuis (1988) and modified to account for the anisotropy of the tailings using the technique of Hvorslev (1951), range from 4×10^{-6} cm/s to 4×10^{-5} cm/s. Hydraulic conductivities were also derived from grain-size analyses using the relationship derived by Hazen (Freeze and Cherry, 1979). The K_{HAZEN} calculations indicate an average conductivity of 3×10^{-5} cm/s, similar to that obtained from the response tests.

The tailings are underlain by an estimated 0–10 m of locally derived lacustrine sediments and till in the buried valleys, which are underlain by gneissic and granitic bedrock of the Whitewater Group (Dressler et al., 1991). Hydrogeologic parameters measured adjacent to the impoundment (at IN18 and IN19; Fig. 21.2) indicate a hydraulic conductivity of approximately 1×10^{-5} cm/s for the sediments.

Estimates of ground-water recharge rates, including the method of age-dating the recharge water by means of tritium (³H) concentrations, indicate that precipitation infiltrates the tailings at 0.24 to 0.28 m/a (Coggans et al., 1991). Recharge rates in vegetated and barren tailings ponds vary seasonally, but no significant differences in annual recharge were noted (Coggans et al., 1991). Using the calculated porosity value of 0.5, an average downward ground-water velocity of about 0.5 m/a was determined. Data collected by Morton (1983) from 1964 to 1969 suggest that approximately 0.5 m/a, or 64% of annual precipitation in this area, is prevented from recharging the water table because of evapotranspiration. Thus, these values suggest that approximately 3% of precipitation leaves the Copper Cliff impoundments as surface runoff. Finlander Creek, which is at the base of the impoundments, intercepts surface runoff as well as seepage through the impoundment dikes and directs this water to the INCO Ltd. Copper Cliff Water Pollution Control Facility. Mathematical modeling of the flow system suggests that recharge water infiltrating the central area of the M impoundment takes approximately 40 years to reach Copper Cliff Creek, whereas infiltrating precipitation at the western edge of the CD impoundment takes nearly 400 years (Coggans, 1992).

Identification of process water

When deposition of tailings and discharge of mill water ceased in the impoundments along the cross section A-A' (Fig. 21.1), the rate of downward drainage of tailings water exceeded the rate of recharge of water into the impoundment surface. The position of the water table fell and a vadose zone developed near the tailings surface. Atmospheric oxygen diffused into the tailings, reacting with the sulfide minerals. The sulfide oxidation products SO₄²⁻, Fe²⁺ and other metals were transported downward with the infiltrating precipitation, which gradually displaced the process water.

The process water can be distinguished from recharge water using the chemical characteristics of the water, a method described by Dubrovsky et al. (1984). Chloride concentrations are less than 50 mg/l in the upper 6–12 m of the tailings (Fig. 21.6a). Below these depths, Cl concentrations increase to an average of

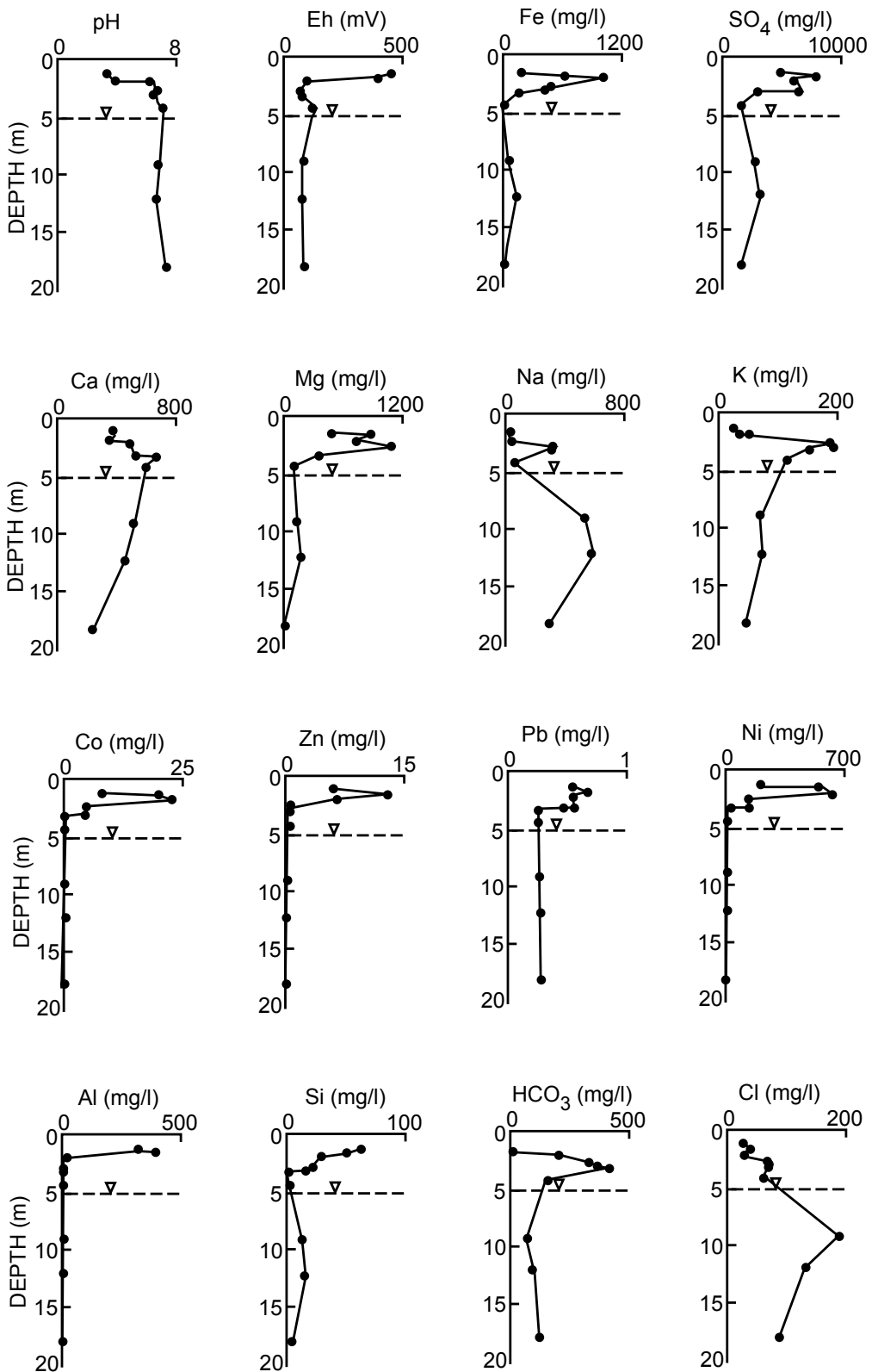


FIGURE 21.4—Water chemistry profile at IN12.

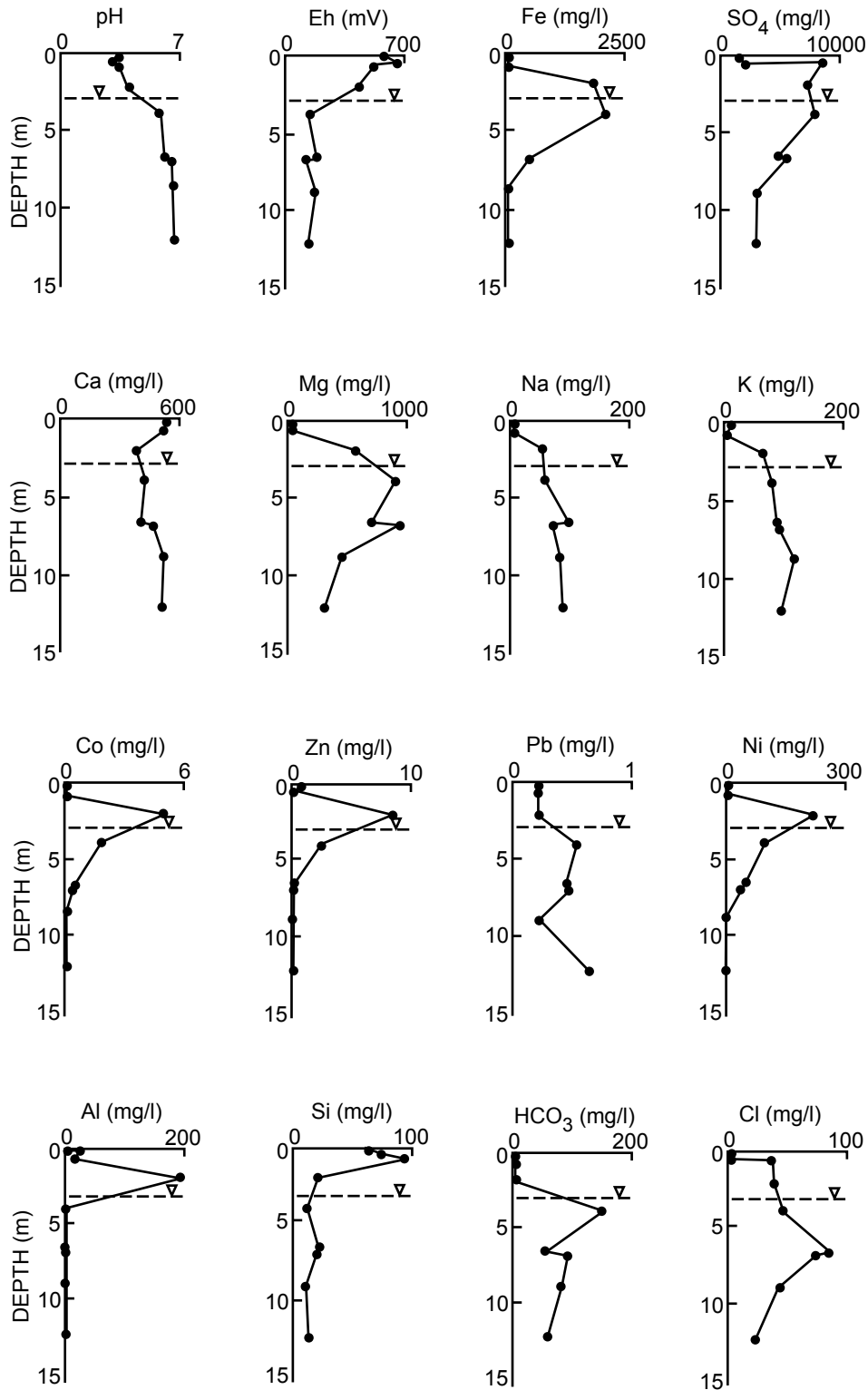


FIGURE 21.5—Water chemistry profile at IN13.

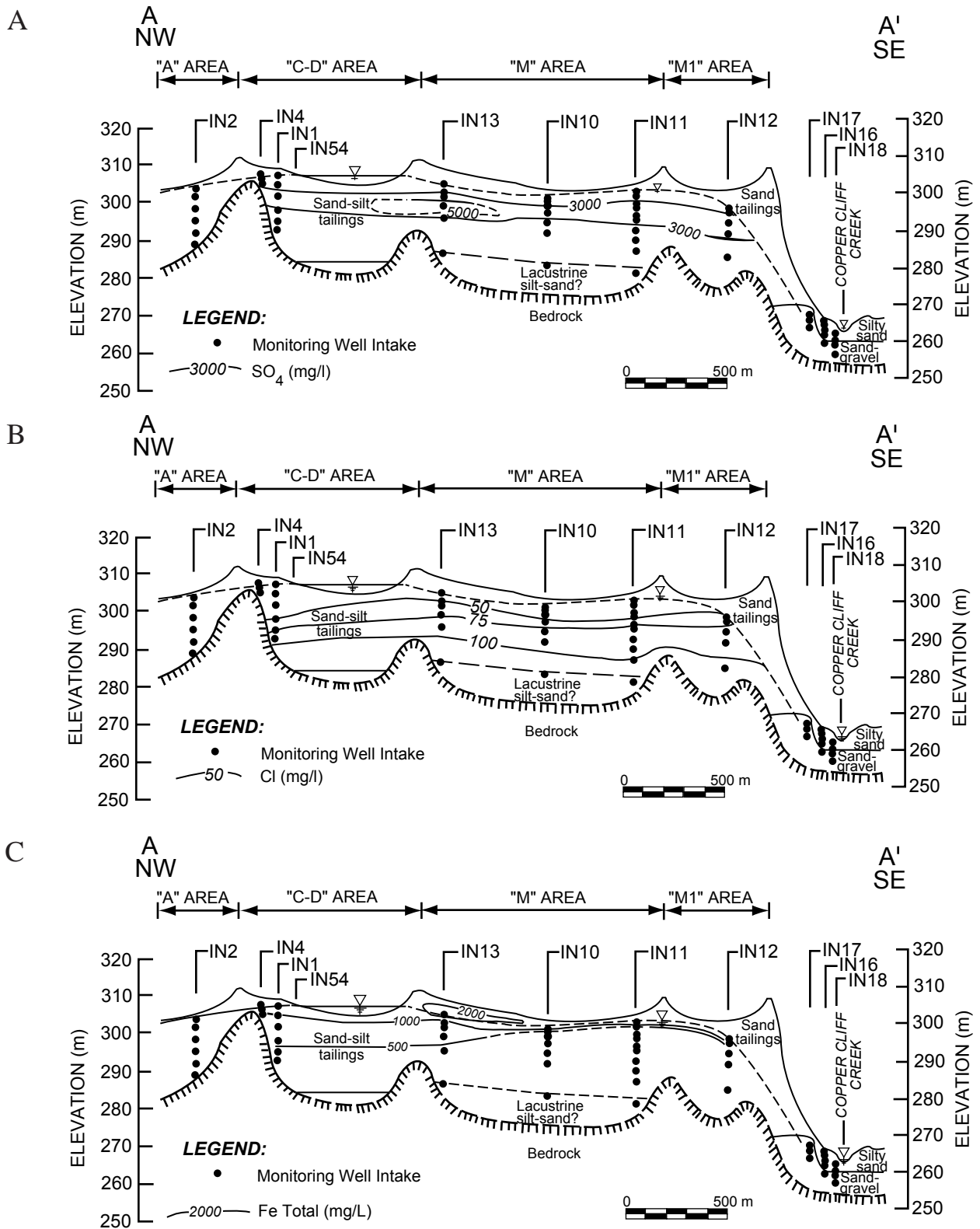


FIGURE 21.6—(A) Cl concentrations along cross section A-A' (Fig. 21.1). (B) SO₄ concentrations along cross section A-A' (Fig. 21.1). (C) Fe concentrations along cross section A-A' (Fig. 21.1).

77.8 mg/l ($n = 13$, $2\sigma = 46.3$ mg/l), similar to the concentration of Cl measured in a process water sample collected from an active pumping station (73.3 mg/l). The tailings material is low in Cl. It is inferred, therefore, that nearly all the Cl present in the deeper tailings water was derived from the milling reagents. Chloride in shallow ground water may have been derived from fertilizer applied in the revegetation program. Because Cl is generally assumed to be a conservative constituent in ground water (Freeze and Cherry, 1979), tailings water at depths greater than 12 m at each piezometer nest is inferred to represent water that originated as process water.

Tailings water with concentrations of SO_4 greater than 3000 mg/l were found to depths of 12 m at piezometers along the cross section (Fig. 21.6b). The distributions of Cl and SO_4 in the M impoundments suggest that the interface between the recharge and process waters ranges from 6.9 to 12.0 m below the surface. Because deposition of tailings in these impoundments ended in 1960, the chemical profiles suggest that the ground-water recharge rate is from 0.11 m/a to 0.19 m/a (calculated using measured porosities of 42% and 47% at each location in the M impoundment). These values are lower than the rate determined from the tritium profiles (0.24 to 0.28 m/a) (Coggans et al., 1991). The nested piezometers along the cross section are spaced at 3 to 6 m intervals at the depth of the process-water/recharge-water interface. Refinement of this spacing would improve the precision of the determination of the interface and resolve the apparent differences between the two calculations.

Sulfide oxidation

The cores from IN13 and IN11 are visibly oxidized to a depth of about 1 m. The tailings are a 10YR 6/8 (Munsell Soil-Colour Chart) brownish yellow in the zone of oxidation and deepen to a 10YR 2/1 black with increasing depth. Oxidized tailings were observed to approximately 2.25 m depth at IN12. The water table is 2 to 5 m below ground surface at this location, indicating that there is a significant potential for continued oxidation of the tailings.

The results of a pore gas survey at each piezometer nest indicate that the pore gas O_2 values range from 20.9% (atmospheric concentrations) at the tailings surface to 0.2% at 1 m depth at piezometer nest IN13. The O_2 concentrations decrease steadily with depth at all piezometer nests except IN11, at which very little change was noted (Fig. 21.7).

Total sulfur contents (measured as FeS) at IN1, IN4, IN11, IN12, and IN13 are below detection in the near-surface tailings and are approximately 3 wt% FeS in the unaltered tailings at IN12 and IN13 (Fig. 21.7). The unoxidized tailings at IN11 are consistently lower, averaging about 1.8 wt% FeS. The tailings deposited in the M impoundment (where IN11 is located) have less iron than other impoundments along the cross section, because this material was subjected to extraction of a pyrrhotite-rich concentrate at the mill (Peters, 1971). The visual evidence of oxidation, the depletion of pore gas O_2 , and the corresponding increase in solid phase sulfur content indicate that sulfide oxidation is active in the upper 1 to 2.5 m of the tailings along cross section A-A'.

Mineral observations of sulfide oxidation

Pyrrhotite is the principal sulfide mineral in the Copper Cliff

tailings; lesser amounts of pentlandite, chalcopyrite, and marcasite are also present. Mineralogical analyses of core samples indicate that the tailings are almost completely depleted of sulfides in the upper 80 cm of the tailings at IN13 and in the upper 224 cm at IN12. The occurrence of sulfide minerals increases with depth to about 4 vol% in the unoxidized tailings.

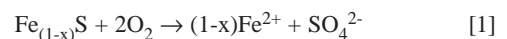
The degree of alteration of the sulfides increases upwards from the depth of active oxidation. Thin, discontinuous oxidation rims surround some of the anhedral to subhedral, primary sulfide grains where sulfide oxidation is active. The alteration rims are thicker and become increasingly common in tailings closer to the impoundment surface. Near the surface, pyrrhotite and pyrite grains are almost completely altered; tiny, anhedral chalcopyrite grains are the most common primary sulfides. The alteration rims are composed mainly of ferric oxyhydroxides, primarily goethite αFeOOH . Native sulfur S^0 is also present.

At IN12, marcasite (FeS_2), a dimorph of pyrite, is present as a supergene alteration over a 0.6 m interval (3.0 and 3.6 m below ground surface) just below the zone of visibly oxidized tailings. At 3.6 m depth, marcasite appears in trace amounts as alteration rims around some pyrrhotite grains. Marcasite increases in abundance towards the surface where it occurs as distinct grains and reaction rims at 3.0 m depth. Marcasite grains are absent from samples collected from above 2.0 m depth. In the shallow samples, the rims around pyrrhotite grains appear to have been altered to ferric oxyhydroxides.

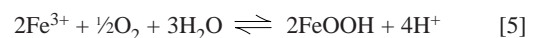
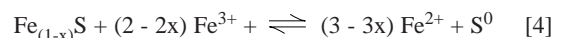
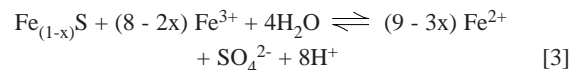
Marcasite forms as a supergene mineral from acid solutions under surface conditions (Hurlbut and Klein, 1977). It appears to be a metastable alteration product of pyrite that further alters to ferric oxyhydroxides within the Copper Cliff tailings.

Sulfide-oxidation reactions

Mineralogical analyses indicate that pyrrhotite is oxidizing within the upper 1.0 to 2.5 m of the tailings. The oxidation of pyrrhotite can be described as:



The Fe^{2+} produced in reaction [1] can be oxidized by O_2 (Nordstrom, 1982) to Fe^{3+} (reaction [2]) and may hydrolyze to precipitate as goethite (reaction [3]). This Fe^{3+} may further react with pyrrhotite through reactions [4] and [5]:



Combined, reactions [1] through [5] produce varying amounts of H^+ and decrease pH. Under low-pH conditions, the oxidation of

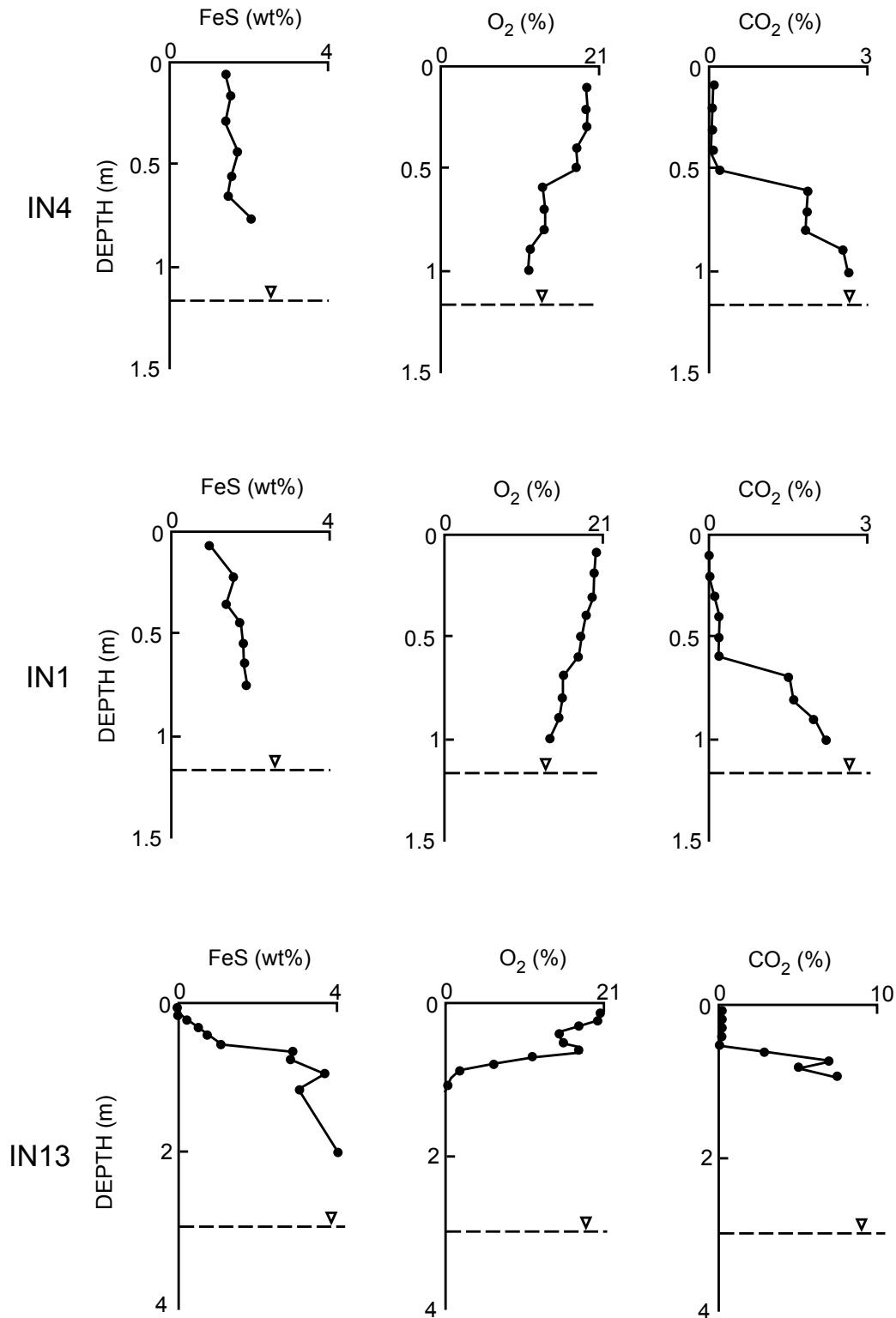


FIGURE 21.7—Total sulfur content expressed as wt% FeS and pore gas oxygen and carbon dioxide concentrations at IN4, IN1, IN13, IN10, IN11, and IN12.

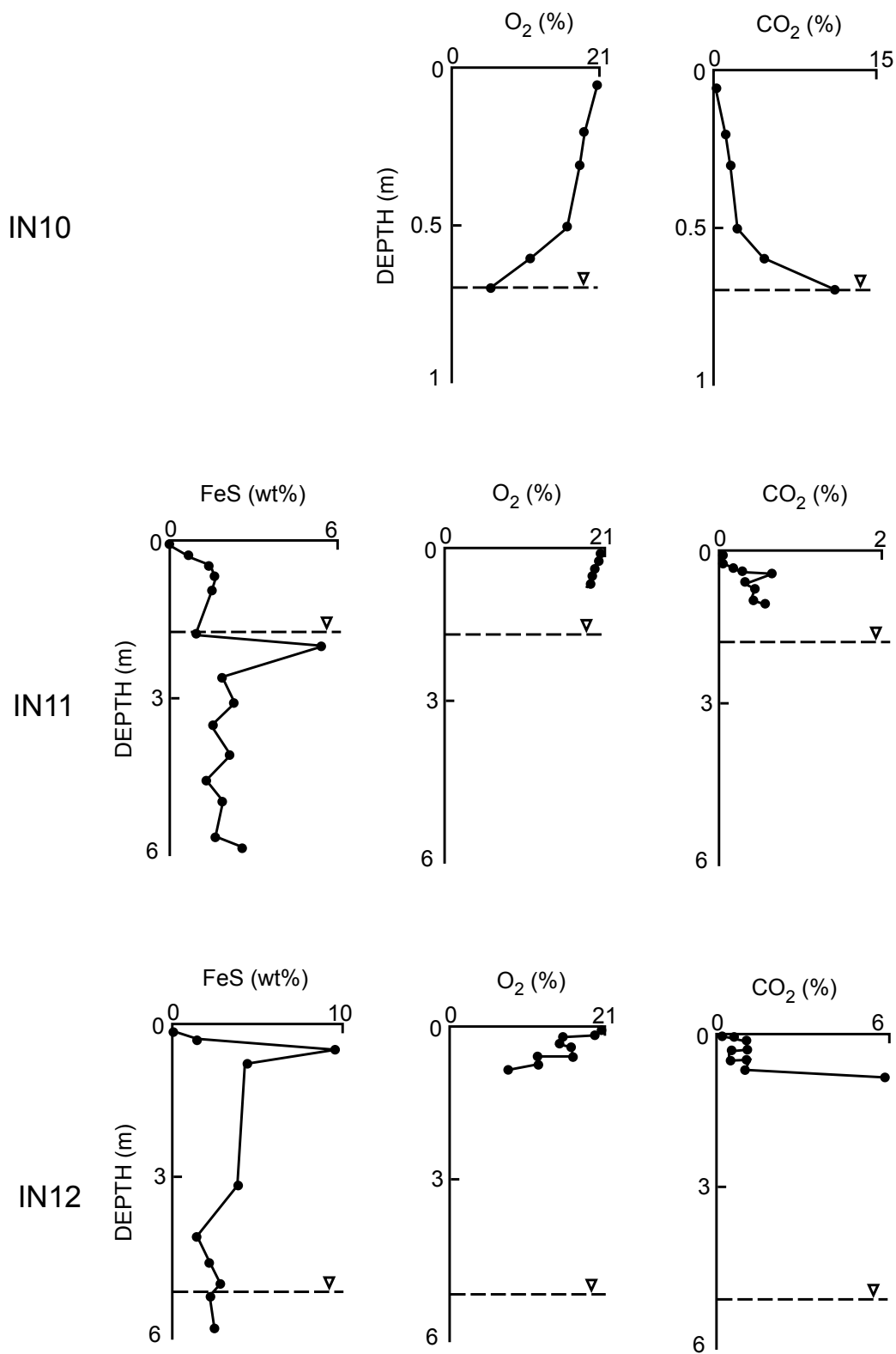


FIGURE 21.7—Continued

pyrrhotite by Fe³⁺ proceeds at a significantly faster rate than with O₂ (Nordstrom, 1982). The rims of goethite coating primary sulfide grains within the oxidation zone, the presence of native sulfur, and the low-pH pore waters observed in the unsaturated zone, suggest that pyrrhotite is being oxidized by Fe³⁺.

The oxidation of Fe²⁺ to Fe³⁺ is extremely slow if pH < 4.5, under which conditions reaction [2] could control the rate of pyrrhotite oxidation in acidic pore waters. However, the presence of chemolithotrophic microorganisms such as *Thiobacillus ferrooxidans*, found in iron sulfide tailings environments (Boorman and Watson, 1976; McCready, 1976), can catalyze the oxidation of Fe²⁺, causing the oxidation of the iron sulfide to proceed at a much greater rate as long as O₂ is present (McCready, 1976). Experimental work by Norris and Parrott (1985) indicated that *T. ferrooxidans* can catalyze the oxidation of pentlandite and nickel-rich pyrrhotite.

No bacterial analyses were conducted on the Copper Cliff tailings. The common occurrence of *T. ferrooxidans* in other sulfide tailings environments, however, suggests that these bacteria are likely to be present in the Copper Cliff tailings.

Modeling of sulfide oxidation

Davis and Ritchie (1986) developed an approximate analytical solution to determine the rate of sulfate production in waste-rock piles. This model was used by Blowes and Jambor (1990) and by Blowes et al. (1991) to simulate sulfide oxidation in mine-tailings impoundments. The model is based on the assumption that the rate of sulfide oxidation is controlled by:

- 1) the diffusion of O₂ in the pore spaces of the tailings and
- 2) the diffusion of O₂ into the reaction sites within the tailings grains.

Further assumptions are that the sulfide grains are evenly distributed throughout the tailings and that the grains are spherical and of one size. Because water is also required, a thin film of water is assumed to coat each grain and the model describes transport of oxygen from the pore space across the film.

Using the model of Davis and Ritchie (1986), O₂ concentrations throughout the thickness of the vadose zone at any time can be determined through equations [6], [7], and [8].

$$X(t) = (2t_d - t_c)^{1/2} - (t_c)^{1/2} \quad [6]$$

where: X(t) = dimensionless depth of planar moving front
= X*/L

t_d = dimensionless time

= t D₁ u₀ / L² ε ρ_s

t_c = dimensionless time for a particle to react at surface of the tailings impoundment

= a² D₁ / 6 D₂ (1 - θ)

X* = position of planar moving front in vadose zone (m)

L = thickness of vadose zone (m)

t = time (s)

D₁ = diffusion coefficient of oxygen in pore space of tailings (m²/s)

D₂ = diffusion coefficient of oxygen in water (m²/s)

u₀ = concentration of oxygen in air (kg/m³)

ε = mass of oxygen used per mass of sulfur in oxidation reaction

ρ_s = density of sulfur within fresh tailings (kg/m₃)

a = radius of particles (m)

θ = porosity of tailings

λ = a proportionality constant encompassing both Henry's Law and the gas law,

$$\text{where } u(x, t) = 1 - x \left[\frac{(\beta)^{1/2}}{(1 + (\beta)^{1/2} X(t))} \right] \quad 0 \leq x \leq X(t) \quad [7]$$

$$\text{where } u(x, t) = \exp(-(\beta)^{1/2} (x - X(t))) / (1 + (\beta)^{1/2} X(t)) \quad X(t) \leq x \leq 1 \quad [8]$$

where: u(x, t) = dimensionless oxygen concentration

= u*/u₀

x = dimensionless spatial coordinate

= x*/L

β = 6L²λD₂(1 - θ) / D₁a²

u* = oxygen concentration within a pore space of the vadose zone (kg/m³)

x* = vertical spatial coordinate (m)

Parameters used in the development of these equations (Table 21.2) and parameter values estimated for, or measured at, the Copper Cliff site were used in the model. The number of moles of S released per O_{2(g)} consumed was set at 1.995, based on equation [6] because pyrrhotite is the dominant sulfide mineral at the Copper Cliff site. The bulk diffusion coefficient (D₁ measured in m²/s) was calculated using a semi-empirical equation derived by Reardon and Moddle (1985):

$$D_1 = 3.98 \times 10^{-5} \left[\frac{(\phi - 0.05)}{0.95} \right]^{1.7} T^{1.5} \quad [9]$$

where φ = air-filled porosity (m³/m³), and T = temperature (K). This equation is applicable where φ is greater than 0.05. A moisture-content value, averaged throughout the depth of pore-gas sampling (usually to 1 m depth), was used to calculate the D₁ term at each piezometer nest. Averaged D₁ values ranged from 6 x 10⁻⁷ m²/s to 4 x 10⁻⁶ m²/s. The modeled O_{2(g)} concentrations are dependent on the source concentration of sulfur in the fresh tailings. For the model calculations, the density of sulfur in the tailings (ρ_s) at IN4, IN1, IN13, IN10, and IN12 was assumed to be 169 kg/m³ as FeS, based on an average total wt% sulfur measured on samples collected below the zone of oxidation total. At IN11, the average total wt% sulfur of samples was 23 kg/m³ as FeS.

The modeled O₂ concentrations are also strongly dependent on the value selected for the bulk diffusion coefficient (D₁). For locations IN1, IN4, IN10, IN11, IN12, and IN13, values were adjusted to obtain the best fit with measured O₂ profiles (Fig. 21.8; Table 21.3). The modeled bulk diffusion coefficients were 7 to 30 times larger than the D₁ values calculated using field-measured moisture contents (Table 21.3). Because the diffusion coefficient is dependent upon the moisture content of the unsaturated tailings, the calculated value is only representative of the vadose zone conditions

of September 1989, when the moisture content of the tailings was measured. The measured O₂ profiles and the sulfide-content measurements of the tailings reflect an averaging of the rates of sulfide oxidation within the tailings over the history of each impoundment, as affected by the naturally varying moisture conditions. The water table was raised along the cross section when water collection ponds were established on the surface of the older impoundments after they were filled with tailings. The moisture content of the unsaturated tailings increased as the water table rose, and reached the tailings surface at the pond locations. Thus, the D₁ values calculated using the long-term moisture contents of September 1989 can be expected to be lower than the average D₁ values present since decommissioning of the impoundments. The D₁ values estimated from the modeled O₂ concentration profiles also represent a range of conditions including drier periods in the impoundment histories. If the water table remains at its present elevation, the measured D₁ values will be more suitable for predicting times required to completely oxidize the sulfides in the unsaturated tailings at each location.

TABLE 21.2—Parameters used in the sulfide-oxidation model.

Parameter	Value	Units	Source
u ₀	0.265	kg/m ³	measured
ε	1.995	—	calculated
λ	0.03	—	measured
θ	0.47–0.59	—	measured
L	2–6	m	measured
a	0.00002	m	measured
D ₁	4.0x10 ⁻⁶ –4.0x10 ⁻⁵	m ² /s	calculated
D ₂	2.6 x 10 ⁻¹²	m ² /s	estimated*
ρ _s	169 (23 at IN11)	kg/m ³	measured

*Estimated value obtained from Davis and Ritchie (1986)

The model describes the depth, X(t), to which sulfide oxidation has advanced, through the solution of equation [6] (Davis and Ritchie, 1986). When the vadose zone is meters thick and the tailings are millimeters in diameter, the t_c term in equation [6] becomes insignificant. The depth of active oxidation predicted using the measured D₁ values at each nest agrees well with the profiles of wt% sulfur (as FeS) for IN12 and IN13 (Fig. 21.8). Although the modeled depth of active oxidation at IN12 is below the zone of measured solid-phase sulfur depletion, core samples collected from this location were visibly oxidized for an additional 0.83 m depth (to 2.2 m below the surface), which is the approximate depth of oxidation indicated by the model calculations. The largest difference between calculated and modeled D₁ terms was found at IN12 (Table 21.3). Ground-water flow modeling predicted that the water table elevation, and hence the moisture contents in the vadose zone at IN12, is strongly influenced by a pond located 300 m to the north of cross section A-A', which was created after decommissioning of the impoundment. The additional ground-water recharge from the pond probably accounts for the difference between the calculated and measured D₁ terms at IN12.

By rearranging equation [6], the time required to completely oxidize the sulfides in the entire vadose zone can be determined. The predicted oxidation time is sensitive to the thickness of the vadose zone (Table 21.3). Where the vadose zone is less than 2 m thick (i.e., IN1, IN10, and IN11), the time required for complete oxidation ranges from 5 to 13 years, using the measured D₁ values

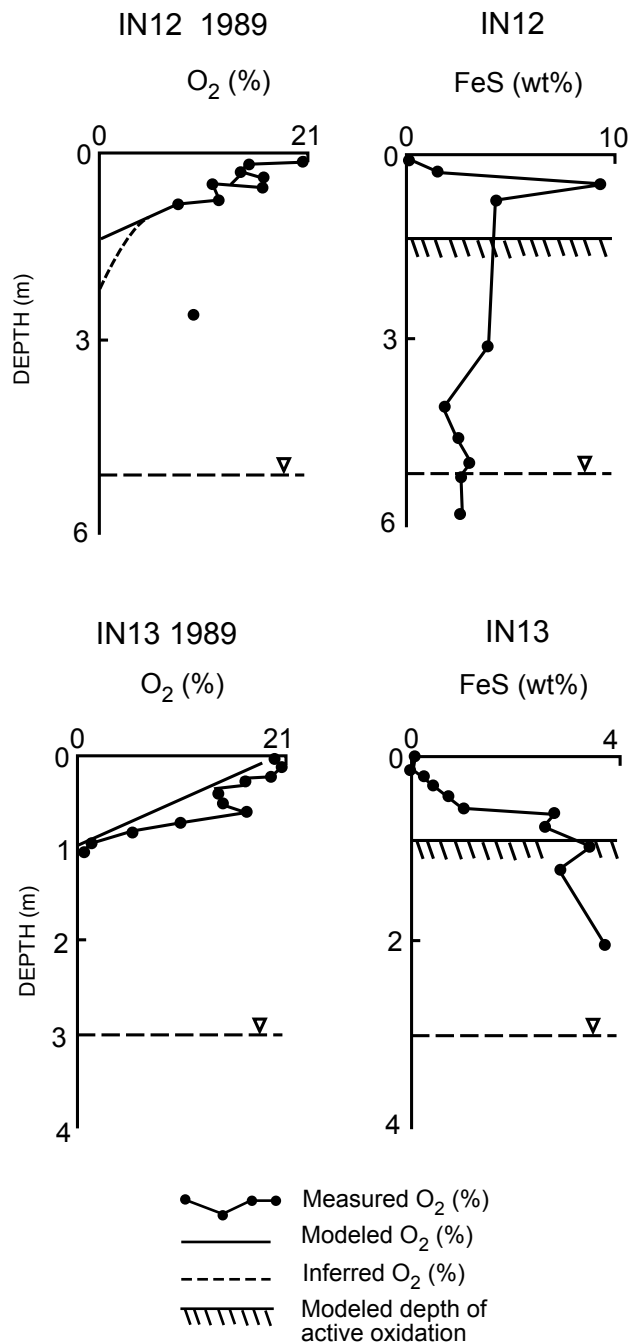


FIGURE 21.8—Comparison of measured and modeled oxygen pore gas concentrations with measured total sulfur concentrations (as FeS). The modeled depth of active oxidation, determined using the method of Davis and Ritchie (1986), is included for reference.

TABLE 21.3—Measured and best-fit D_1 values and the resulting time predictions to completely oxidize the unsaturated tailings (using the measured D_1).

Location	Thickness of oxidized tailings (m)	Thickness of unsaturated tailings (m)	D_1		Time required for complete oxidation of unsaturated tailings (years)
			Calculated (m^2/s)	Modeled (m^2/s)	
IN1	1.16	1.16	2.1×10^{-6}	4×10^{-5}	23
IN4	2.17	2.17	4.1×10^{-6}	4×10^{-5}	13
IN13	0.92	2.97	5.9×10^{-7}	4×10^{-6}	303
IN10	0.70	0.70	-	9×10^{-6}	5
IN11	1.71	1.71	1.5×10^{-7}	4×10^{-5}	5
IN12	2.24	5.14	1.4×10^{-6}	4×10^{-5}	386

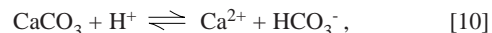
and the total wt% S at each nest. At IN12, however, where the vadose zone is more than 5 m thick, the time required for complete oxidation is estimated to be nearly 400 years (assuming that the water table is maintained at its present elevation over this time). The moisture content values used in the calculations are the mean values from the upper 1 m of the tailings. The moisture content increases with increasing depth and proximity of the water table, lessening the rate of downward O_2 diffusion, and resulting in longer times for complete oxidation of the sulfides in the unsaturated zone. In addition, sulfide oxidation rates will decrease as the active oxidation front continues to travel downward.

pH buffering reactions

The pH of the pore water in the upper 1.5 m of the tailings at all piezometer nests along the cross section is less than 4.0. At all these locations the pH increases to greater than 7.0 at 5.4 m depth. High concentrations of SO_4 are present to depths of up to 12 m. In the 29 years since decommissioning, the front of low-pH water, defined as tailings water with pH <4.5, has moved downward approximately 0.8 to 4.6 m at an average velocity of 0.03 m/a to 0.16 m/a. The average downward velocity of the tailings water was calculated to be 0.47 to 0.55 m/a using the results of 3H analyses (Coggans et al., 1991). The ratio of the velocities shows that the advancement of the low pH water through the flow system is thus retarded by a factor of 2.9 to 18.3. The retardation of the downward migration of the low-pH front is attributed to pH-buffering reactions occurring in the shallow tailings. Similar increases in pH within zones of high concentrations of dissolved Fe and SO_4 observed at other tailings impoundments have been attributed to a series of pH-buffering reactions that include calcite dissolution, dolomite dissolution, siderite dissolution, Al-silicate and -hydroxide dissolution, and Fe-hydroxide dissolution (Dubrovsky, 1986; Morin et al., 1988; Blowes and Jambor, 1990; Blowes, 1990).

The results of total carbonate analyses indicate that, except for the upper 25 cm of the tailings in which agricultural limestone was harrowed into the tailings as part of the revegetation program, the upper 1 m of the tailings is deficient in carbonates. Dolomite $CaMg(CO_3)_2$, but not calcite $CaCO_3$, has been identified in tailings samples from the Copper Cliff impoundments. Pore-gas sampling in the upper 1 m of the vadose zone shows atmospheric CO_2 concentrations (<0.01 vol%) in the upper 5–25 cm. With increasing depth, the CO_2 concentrations increase up to 6.0 vol% at the

deepest sampling point (1.0 m) at IN12. The results of total carbonate analyses indicate that the carbonate content of the shallow tailings has been depleted. This observation, combined with the CO_2 -gas measurements suggest that carbonate dissolution is occurring below 1 m depth and that the resultant CO_2 is diffusing upward. The dissolution of calcite at pH <6.35 can be described as (Dubrovsky et al., 1984):



Reactions [10] through [12] show that for every mole of calcite consumed, two moles of H^+ are consumed and one mole of CO_2 gas and Ca^{2+} are produced.

Equilibrium calculations conducted using MINTEQA2 indicate that pore water within the shallow vadose zone is strongly undersaturated with respect to calcite, dolomite, and siderite $FeCO_3$. These calculations indicate a tendency for any carbonate minerals in the shallow tailings to dissolve, until completely depleted or until saturation is attained.

Calculations using MINTEQA2 also suggest that the tailings water reaches saturation with respect to siderite and approaches saturation with respect to calcite and dolomite at a pH range of 6.0 to 6.7 at IN13, IN10, IN11, and IN12. The pH of water samples collected from IN1 and IN4 were consistently below 5.8. These results suggest that where siderite is present, its dissolution is an important pH-buffering reaction between pH of 6.0–6.7.

Unaltered tailings contain about 15 vol% pyroxene, primarily as augite ((Ca,Na)(Mg,Fe,Al,Ti)(Si,Al) $_2O_6$) and hypersthene ((Mg,Fe) $_2Si_2O_6$). Pyroxenes become less abundant towards the surface in the upper 2.0 m at piezometer nest IN12 and the upper 0.70 m at IN13, suggesting that the pyroxenes are leached in the vadose zone of the impoundments. Alteration of pyroxene releases Fe, Mg, Mn, Si, and Al to the pore water (Deer et al., 1966). Biotite $(K(Mg,Fe)_3(AlFe)Si_3O_{10}(OH,F)_2)$ shows about a 50 vol% depletion (from approximately 7 vol% to 3 vol%) with increasing oxidation of the tailings. The alteration of biotite consumes H^+ and releases K, Fe, Mg, Si, and Al into the tailings pore water. Electron-microprobe and X-ray studies indicate that initial alter-

ation of the biotite is marked by the loss of K and that advanced alteration leads to the progressive loss of other elements and eventual pseudomorphism by cristobalite.

A comparison of the geochemistry of the process water entering the impoundments and the shallow-tailings pore water shows the effect of the dissolution of the aluminosilicates in the oxidation zone. The process water contains 7 mg/l of dissolved silica and <1 mg/l of dissolved aluminum. The shallow-tailings water samples contain 50 to 100 mg/l of dissolved silica and several hundred mg/l of dissolved aluminum (Figs. 21.4 and 21.5). Aluminum concentrations in excess of 400 mg/l were measured in the oxidized zone, decreasing sharply to below detection limits with increasing depth.

The Al concentrations decrease abruptly in tailings water collected below the zone of oxidized tailings, where pH is greater than 6. Geochemical calculations, conducted using MINTEQA2, suggest that at pH >6, the tailing water is supersaturated with respect to amorphous aluminum hydroxide Al(OH)₃, at all piezometer nests. The precipitation of Al(OH)₃ produces H⁺, as shown below:



Possibly because of low quantities and lack of crystallinity, no secondary aluminum-bearing hydroxide minerals were identified in the mineralogical study. Equilibrium calculations indicate that the pore water from near the tailings surface, where pH ranges from 5 to 6, either approaches or attains saturation with respect to amorphous Al(OH)₃. Tailings-water samples are undersaturated with respect to all carbonate minerals within this pH range. Conditions near equilibrium with respect to Al(OH)₃ in this zone suggests that precipitation and dissolution of amorphous Al(OH)₃ are probably important pH-buffering reactions in the absence of carbonate minerals.

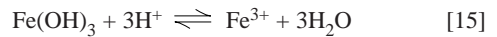
Iron-oxide precipitates were observed on the surfaces of tailings particles in the oxidized zone and the presence of goethite (α-FeOOH) was confirmed by X-ray diffraction. Lepidocrocite (σ-FeOOH) was not detected. Concentrations of goethite and iron oxide precipitates decrease with decreasing depth from the zone of active oxidation, suggesting that dissolution of these phases may be occurring within the shallow oxidized zone.

With the measurements of Eh made in the field, MINTEQA2 was used to calculate the activities of Fe²⁺ and Fe³⁺, using the Nernst Equation:

$$E_H = E^0 - \frac{RT}{nF} \ln \frac{[\text{Fe}^{2+}]}{[\text{Fe}^{3+}]} \quad [14]$$

The Fe³⁺ activities were found to range from 10⁻⁹ molal, within the oxidized zone, to 10⁻¹⁶ molal deeper within the tailings. The Fe²⁺ activities were consistently between 10⁻⁵ to 10⁻³ molal in tailings water at all depths within the impoundments.

Calculations using MINTEQA2 suggest that water samples from within the oxidized zone at all piezometer nests, where pH is less than 5, are supersaturated with respect to goethite and lepidocrocite while approaching or attaining saturation with respect to amorphous Fe(OH)₃. The dissolution and precipitation of Fe(OH)₃ is dependent on the pore-water pH through the relation-



Plots of saturation indices for Fe(OH)₃, goethite, and lepidocrocite versus depth at piezometer nests IN13 and IN12 (Fig. 21.9), at which dissolved iron concentrations were greater, show that tailing water within the zone of oxidized tailings is undersaturated with respect to amorphous Fe(OH)₃ and is supersaturated with respect to the crystalline ferric oxyhydroxides. Mineralogical analyses of the alteration rims surrounding the sulfide grains indicated that the rims consist mainly of goethite. With greater depth and increasing pH, the tailings water reaches equilibrium with respect to Fe(OH)₃.

In the shallow tailings, in the absence of carbonate minerals or Al-hydroxides, the dissolution of amorphous Fe(OH)₃ may be an important pH-buffering mechanism. Deeper in the tailings, where pH is greater than 6.0, geochemical calculations with MINTEQA2 suggest that the tailings water becomes supersaturated with respect to amorphous Fe(OH)₃ and remains supersaturated with respect to goethite. The precipitation of these ferric oxyhydroxide phases releases H⁺ into the tailings water, further affecting the pore water pH.

With decreasing pH at the Copper Cliff tailings impoundments, therefore, sequential carbonate, aluminum hydroxide, aluminosil-

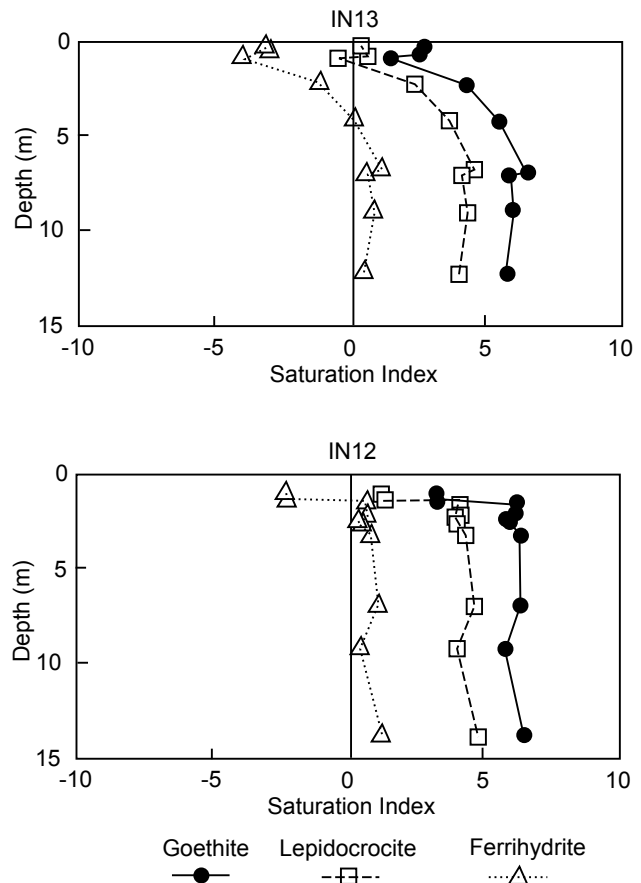


FIGURE 21.9—Calculated saturation indices of the major ferric hydroxide minerals plotted versus depth of piezometer nests IN13 and IN12.

icate, and ferrihydrite dissolution reactions may control the pH of the tailings ground water. With the exception of the aluminosilicate dissolution reactions, which are not equilibrium controlled, the dissolution reactions are reversible and precipitation of these minerals releases H^+ into the tailings water. Thus, while the initial members of the sequence (i.e., the carbonates) are dissolving and consuming H^+ , precipitation of the other members (i.e., the aluminum and ferric oxyhydroxides) may be precipitating, resulting in the formation of secondary, pH-buffering minerals.

Hardpan formation

An 8 cm thick lens of cemented tailings occurs at the depth of active oxidation (0.6 m below ground surface) at IN13. Thin, discontinuous lenses of cemented tailings occur near the base of the oxidized tailings (1.8 to 2.0 m below ground surface) in core from IN12 and in piezometer installations at other locations. X-ray diffractometer analyses indicate the presence of jarosite ($KFe_3(SO_4)_2(OH)_6$) always with goethite and gypsum ($CaSO_4 \cdot H_2O$) within the zone of oxidized tailings and within the hardpan layers at IN12 and IN13. Jarosite has been reported at several locations where sulfide oxidation is active (Van Breeman, 1973; Miller, 1980; Dubrovsky et al., 1984; Blowes and Jambor, 1990; Blowes et al., 1991).

The solubility constants for K, Na, and H jarosite were evaluated by Alpers et al. (1989), who recommended the thermodynamic data summarized in Table 21.4. MINTEQA2 calculations indicate that the tailings water at IN13 approaches saturation with respect to jarosite with increasing depth, attaining saturation just below the depth of active oxidation. The tailings water then becomes increasingly undersaturated deeper within the tailings. Additional calculations at IN12 yielded a similar trend, except that saturation with respect to jarosite is not attained. These calculations indicate a tendency for the jarosite previously precipitated in the shallow vadose zone at IN12 to dissolve.

Unlike O_2 concentrations, the pore gas CO_2 concentrations decrease sharply from a maximum concentration of 12 vol% beneath the hardpan layer (where carbonates are being consumed) to below the detection limit of 0.1 vol% above the hardpan layer (where carbonates have been virtually eliminated). The decline in CO_2 concentrations with decreasing depth is more gradual above the cemented tailings. Thus, the hardpan layer seems to be acting as a diffusion barrier to pore gas CO_2 . It is probable that the hardpan layers in the vadose zone also act as diffusion barriers for O_2 . Similar O_2 profiles were observed in the mine tailings at Waite Amulet, Quebec, and Heath Steele, New Brunswick (Blowes et al., 1991), where hardpan layers are also inferred to inhibit O_2 and CO_2 gas diffusion.

If the hardpan layers are extensive and significantly retard the downward diffusion of O_2 , the rate of sulfide oxidation may

decrease more rapidly than predicted by the model of Davis and Ritchie (1986). The decrease will prolong the time required to completely oxidize the vadose zone of the tailings, but will also lessen the concentration of sulfide oxidation products in the tailings water, and may slow the downward displacement of low pH waters.

Iron, nickel, and cobalt

Maximum observed concentrations of Ni and Co in the Copper Cliff tailings water are higher than those found at several other tailings impoundments (Dubrovsky, 1986; Blowes, 1990). These high Ni concentrations may be representative of tailings derived from ore from the Sudbury Igneous Complex. Iron, Ni, and Co appear to be equally mobile and more so than other trace metals (e.g., Zn, Pb, and Cu) in the Copper Cliff tailings (Figs. 21.4 and 21.5). The simultaneous release of Fe, Ni, and Co into the tailings water, without significant attenuation in the shallow tailings, would explain the similarities in concentration profiles of these metals.

Iron is the dominant cation on a molar basis in the C-D and M impoundments, with measured dissolved concentrations up to 2190 mg/l and 1060 mg/l (4 m at IN13 and 2 m at IN12) (Fig. 21.6c). Because of changes in the milling process, tailings discharged into the M1 impoundment (Peters, 1971) contain lower concentrations of Fe than the other impoundments. The maximum concentration of Fe observed in the M1 impoundment is 76.6 mg/l at 3.2 m at IN11. Iron (oxy)hydroxides, principally goethite, and jarosite are the most abundant precipitates within the Copper Cliff tailings, suggesting that precipitation of these minerals limit the Fe_{TOTAL} concentrations in the tailings ground water.

Nickel is second in abundance on a molar basis among the heavy metals derived from sulfide oxidation reactions in the tailings pore water. Nickel occurs in concentrations of up to 641 mg/l (at 1.98 m, IN12). Nickel speciation is dependent upon the pH of the tailings water and on the presence of complexing ligands such as SO_4^{2-} , Cl^- , and CO_3^{2-} . Geochemical calculations suggest that at all pH values found within the tailings environment, the free ion, Ni^{2+} , predominates. MINTEQA2 calculations indicate that Ni complexes strongly with SO_4 and $NiSO_4$, comprising approximately 35% of the total concentration of dissolved Ni at low pH. This decreases to 20% at near-neutral pH. Under these pH conditions, $NiCO_3$ complexes account for up to 60% of the total dissolved Ni concentration.

The $pNi + 2pOH$ activities at all piezometers are plotted versus the $2pH + pSO_4$ activities (Fig. 21.10) to assess whether any nickel sulfate or nickel hydroxide minerals were acting as a solid-phase control on the solubility of Ni. Lines indicating the solubilities of retrersite ($NiSO_4 \cdot 6H_2O$), morenosite ($NiSO_4 \cdot 7H_2O$), and theophrastite ($Ni(OH)_2$) are included for reference. The data

TABLE 21.4—Thermodynamic data for K, Na, and H jarosite obtained from Alpers et al. (1989).

Reaction	K	DH (kcal/mol)
$KFe_3(SO_4)_2(OH)_6 + 6H^+ \rightleftharpoons K^+ + 3Fe^{3+} + 2SO_4^{2-} + 6H_2O$	$10^{-9.210}$	-36.18
$NaFe_3(SO_4)_2(OH)_6 + 6H^+ \rightleftharpoons Na^+ + 3Fe^{3+} + 2SO_4^{2-} + 6H_2O$	$10^{-5.28}$	-36.18
$HFe_3(SO_4)_2(OH)_6 + 6H^+ \rightleftharpoons H^+ + 3Fe^{3+} + 2SO_4^{2-} + 6H_2O$	$10^{-5.39}$	-55.15

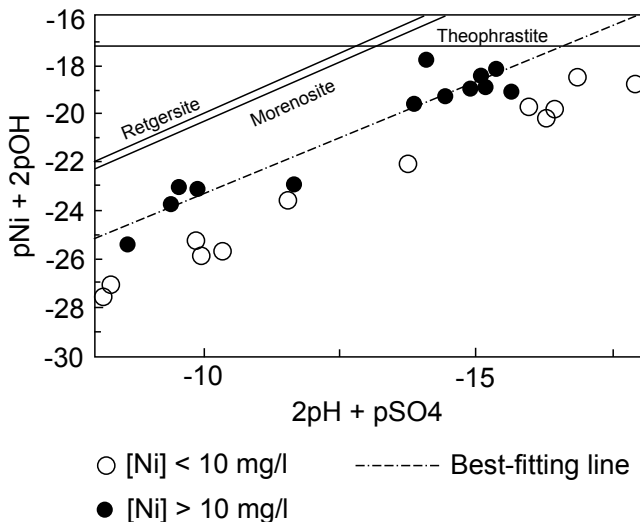


FIGURE 21.10—The plotted relationship of Ni and SO_4 versus pH in the tailings water. The solubility lines for retgersite, morenosite, and theophrastite are included for reference.

points on Figure 21.10 do not fall near the solubility lines of these minerals. The saturation indices for retgersite and morenosite show that the tailings waters are consistently undersaturated with respect to these minerals. No nickel sulfate precipitates of any composition were detected during the mineralogical study. Because some of the measured concentrations of Ni were low (<1 mg/l) in tailings water affected by sulfide oxidation reactions, the tailings water might not always reach equilibrium with a potential solid phase control. Baes and Mesmer (1976) observed theophrastite precipitating slowly at near-neutral pH conditions in laboratory experiments. They concluded that the solubility constant ranges from $10^{-14.7}$ to $10^{-17.2}$ depending on the age of the crystal. As crystal growth occurs, the solid becomes more stable and less soluble. Geochemical calculations using MINTEQA2 indicate that the ion activity product of $\log(\text{Ni}^{2+}) + 2[\log(\text{OH}^-)]$ never exceeds -17.2, suggesting that the tailings water at all piezometers is consistently undersaturated with respect to theophrastite. No $\text{Ni}(\text{OH})_2$ was detected during the mineralogical study.

Small amounts of Ni, accounting for up to 2 mass wt%, were detected within goethite precipitates by energy dispersive X-ray fluorescence (XRF). The coprecipitation or adsorption of Ni with goethite has been inferred as a possible control of dissolved nickel concentrations at other tailings areas (Dubrovsky, 1986; Blowes, 1990). During the polymerization process accompanying the formation of goethite, Ni can be incorporated into the structure of the ferric oxyhydroxide precipitates (Kinniburgh et al., 1976). These geochemical and mineralogical observations suggest that the coprecipitation of Ni with goethite or adsorption of Ni onto goethite surfaces are the only significant solid phase limitations on dissolved Ni concentrations in the shallow tailings. The presence of Ni in altered biotite, detected by electron probe microanalysis and X-ray diffraction studies suggest that biotite alteration may also have some minor influence on Ni mobility.

The maximum concentration of Co (23.3 mg/l) occurs at 1.98 m in IN12. Arnold and Malik (1974) noted that Co was present in weathered ore from the Sudbury Igneous Complex as a solid-solu-

tion component of pentlandite. Thornber (1983) conducted experiments showing that $\text{Fe}(\text{OH})_3$ precipitation can effectively remove Co (and Zn, Pb, and Cu) from solution. Because the Co profile is similar to that of the Fe profile, it is possible that Co might be removed from the tailings water by incorporation into amorphous or crystalline ferric oxyhydroxide precipitates or adsorption onto ferric oxyhydroxide surfaces. Further studies are required to determine the processes controlling Co transport.

Sulfate

Sulfate, the predominant anion in the tailings water, attains concentrations of up to 8700 mg/l (0.7 m, IN13). Sulfate is derived from the oxidation of sulfides and from the mill process water. Geochemical calculations performed using MINTEQA2 indicate that the water throughout the impoundment attains or approaches saturation with respect to gypsum. X-ray diffraction analysis of the tailings indicates that gypsum is present throughout the tailings to a depth of 5 m, the maximum depth analyzed. The relative abundances of gypsum and jarosite within the oxidized zone suggests that the dissolution and precipitation of these minerals and the iron (oxy)hydroxides, limit the pore-water SO_4 , Fe, and Ca concentrations.

Calcium and magnesium

Calcium concentrations range from 350 to 600 mg/l and are relatively constant throughout the cross section (Figs. 21.4 and 21.5). Sources for Ca are the milling reagents and Ca derived from dissolution of carbonate and aluminosilicate minerals. The magnesium concentrations near the tailings surface are low (20 mg/l to 40 mg/l), but sharply increase with increasing depth, reaching 500–1100 mg/l before decreasing to <100 mg/l at greater depths. The distribution of Mg differs greatly from that of Ca at all of the piezometer nests, suggesting different sources for the two elements and/or different controls on their solubility.

Possible sources of Mg, other than dolomite dissolution, include dissolution of aluminosilicates within the tailings and dissolution of limestone used on the surface in the revegetation program. The K and Cl concentrations are similar to the Mg concentrations in the shallow tailings (Figs. 21.4 and 21.5). Weathering of K-bearing aluminosilicates such as biotite will release K to the tailings water; however the largest source of K and Cl in the shallow tailings waters is probably from the fertilizers applied to the surface during the revegetation program, suggesting that the source of most of the Mg in the system was dolomite added with the fertilizer. The revegetation program in the M Impoundment began in 1957. Using the calculated downward ground-water velocity of 0.25 m/a, the front of Mg-rich recharge water should extend to approximately 7.5 m depth, similar to the observed Mg concentrations (Fig. 21.5).

Geochemical calculations indicate that the tailings water reaches saturation with respect to dolomite as the pH approaches 6.7. The pore waters are consistently undersaturated with respect to epsomite $\text{MgSO}_4 \cdot 7\text{H}_2\text{O}$.

Transition metals

Transition metals (Co, Zn, Cu, Pb, Mn, Cr) are present in the tailings as solid-solution components of the major sulfide miner-

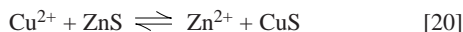
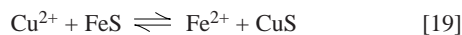
als or as minor sulfides such as cobaltite (CoAsS), sphalerite (ZnS), and galena (PbS) (Hawley and Stanton, 1962; Naldrett and Kullerud, 1967; Naldrett et al., 1982).

The mobility of these metals is dependent on pH and the degree of weathering of the source minerals in the tailings and is controlled by a series of precipitation, dissolution, solid-solution substitution, and adsorption/desorption reactions. The relative mobilities of the more common metals observed in the tailings are: $Fe = Ni = Co > Zn = Pb > Cu$.

Zinc concentrations throughout the Copper Cliff impoundments do not exceed 13.2 mg/l (measured at 1.7 m depth, IN12). Zinc seems to be slightly less mobile than Co. Geochemical equilibrium calculations indicate that the tailings water is undersaturated with respect to all discrete Zn-bearing, secondary minerals in the MINTEQA2 database. No secondary Zn precipitates were detected during the mineralogical study. These observations suggest that adsorption/coprecipitation reactions are probably the dominant solid phase controls on dissolved Zn concentrations.

Lead is similar in mobility to Zn, but is found in concentrations below 1 mg/l throughout the tailings. Saturation indices indicate that where $pH > 3.8$, the tailings water approaches saturation with respect to anglesite ($PbSO_4$), suggesting that anglesite precipitation may act as a solid phase control of Pb concentrations. Anglesite was not detected during the mineralogical study. However, anglesite is associated with acidic tailings waters at other locations (Boorman and Watson, 1976; Dubrovsky, 1986; Blowes and Jambor, 1990). Solubility calculations indicate that the tailings water approaches saturation with respect to cerussite ($PbCO_3$) with increasing pH and attains saturation at IN11 and IN12 where $pH > 6$. However, cerussite was not identified during the mineralogical study and it is unlikely to be present.

Copper is less mobile than Pb or Zn, with maximum concentrations of 12.5 mg/l Cu measured at 1.4 m at IN12. Geochemical calculations indicate that the tailings water is undersaturated to all Cu-bearing hydroxide, sulfate, and carbonate secondary minerals within the MINTEQA2 database. Trace amounts of covellite (CuS) were observed as tiny, anhedral grains near the base of the oxidized zone at piezometer nest IN12 and at shallower depths as incomplete alteration rims on a few pyrrhotite grains. Covellite can form through the replacement of Fe^{2+} or Zn^{2+} cations by Cu^{2+} (Blowes and Jambor, 1990), as shown below:



As with Fe, dissolved-Cu speciation in the water samples was estimated with the Nernst equation and measured Eh values. These calculations suggest that Cu^{2+} is the predominant ion in the zone of oxidized tailings. The formation of CuS through reactions [19] and [20] removes Cu from the tailings water and releases Fe or Zn. At all locations where Cu is removed from the tailings water, Fe and Zn concentrations are sufficient to account for the Cu decrease through reactions [19] and [20].

At and beneath the depths where covellite was observed at IN12, Cu concentrations were consistently below detection (0.05 mg/l). The low dissolved concentrations of Cu suggest that covellite formation is an effective solid phase control on Cu in the M and M1 tailings.

Blowes and Jambor (1990) reported the occurrence of covellite in tailings from the Waite Amulet impoundment, Quebec, and the occurrence of covellite in the Heath Steele tailings impoundment, New Brunswick, was reported both by Boorman and Watson (1976) and Blowes et al. (1991). At both locations the occurrence of covellite coincides with an abrupt decrease in the dissolved Cu concentration.

Manganese was measured at concentrations of up to 0.16 wt% in the Copper Cliff tailings solids, but dissolved Mn concentrations did not exceed 8.35 mg/l (measured at IN13). Manganese speciation was estimated using the Nernst equation and measured Eh, and the calculations suggest that Mn^{2+} is the predominant species in the tailings water. Manganese is as mobile as Fe in the tailings water, with maximum concentrations of dissolved Mn and Fe observed at the same depth at IN13, IN11, and IN12. Geochemical calculations suggest that although the tailings water is undersaturated with respect to all secondary Mn minerals in the MINTEQA2 database, the tailings water does approach saturation with respect to rhodochrosite ($MnCO_3$) (S.I. = -0.317 at 2.5 m, IN10).

Although the tailings solids contain up to 370 ppm Cr, Cr was detected in only two water samples: 0.06 mg/l (IN4) and 0.05 mg/l (IN11), suggesting that Cr is relatively immobile within the Copper Cliff tailings. Geochemical calculations suggest that the tailings water is undersaturated with respect to all secondary Cr minerals in the MINTEQA2 database.

Arsenic

Arsenic was measured at concentrations of 2 to 10 ppm in the Copper Cliff tailings solids. However, dissolved As concentrations do not exceed 0.031 mg/l in any of the water samples. The maximum dissolved As and Fe concentrations are observed at the same depth below ground surface wherever As was detected (IN10, IN11, and IN12), suggesting that As is being displaced through the tailings at approximately the same velocity as Fe.

CONCLUSIONS

Hydrogeological and geochemical investigations at the INCO Ltd. Copper Cliff tailings indicate that the impoundments are a regional ground-water recharge area. Recharge water infiltrates downward and then travels laterally to the southeast, ultimately discharging toward Copper Cliff Creek.

Sulfide oxidation is complete in the surficial 0.10 to 0.25 m of the M1 and M impoundments, but is still occurring in tailings 1 to 2 m below this uppermost zone, thereby producing low-pH waters and high concentrations of dissolved metals. Observed Ni and Co concentrations (641 mg/l and 23 mg/l, respectively) are higher than those observed at other sulfide-bearing, mine-tailings environments and are probably characteristic of tailings in the Sudbury area.

The water table is 0 to 3 m below the zone of oxidation, indicating that sulfide oxidation potential still exists in some areas. Simulations conducted using the analytical solution of Davis and Ritchie (1986) suggest that sulfide oxidation will continue for at least 5–13 years where the vadose zone is <2 m thick and for nearly 400 years where the vadose zone is 5 m thick. The results of the model illustrate the importance of water table elevation in the impoundments.

Jarosite, gypsum, goethite, and other iron oxides cement the tailings at or near their depth of active oxidation. This cemented (hardpan) layer acts as a diffusion barrier to pore gas O_2 and CO_2 , prolonging the time required to completely oxidize the unsaturated tailings. The hardpan also lessens the downward displacement of low-pH waters and the concentration of sulfide oxidation products in the tailings water.

A sequence of carbonate, aluminum hydroxide, aluminosilicate, and iron hydroxide dissolution reactions buffers the low-pH conditions produced by sulfide oxidation. Geochemical calculations with MINTEQA2 suggest that the tailings water attains saturation with respect to siderite and approaches saturation with respect to calcite and dolomite within a pH range of 6.0 to 6.7. Thus, as long as siderite is present in the tailings, its dissolution is an important carbonate dissolution reaction. As a result of these pH-buffering reactions, the transport of H^+ through the tailings system is retarded by a factor of 2.9 to 18.3 relative to Fe, Ni, and SO_4^- .

Dissolved Fe, Ni, and Co exhibit similar mobilities within the tailings water flow system. Although amorphous ferric hydroxide and goethite seem to be acting as solid phase controls on dissolved Fe concentrations, no discrete secondary Ni and Co minerals were observed. However, appreciable amounts of Ni were detected by energy dispersive electron probe microanalysis within goethite precipitates and minor amounts were detected in altered biotite.

The mobilities of dissolved Zn, Cr, Pb, and Cu in the tailings water are strongly dependent upon the pH and are controlled through a series of precipitation, dissolution, adsorption, and desorption reactions with secondary minerals and by solid-solution reactions. Where sulfide oxidation is occurring, the low-pH water is undersaturated with respect to covellite. Covellite was observed at the base of the oxidized zone, just beneath the depth of measurable dissolved Cu. Low concentrations of dissolved Mn and As are present in the tailings water; both elements appear to migrate through the tailings with Fe, Ni, and Co.

In the absence of an effective remedial program, it is anticipated that the observed concentrations of SO_4^- , Fe, and other metals will continue to move downward and laterally through the Copper Cliff tailings impoundments and will ultimately be discharged from the impoundments towards Copper Cliff Creek or into the underlying geologic material.

REFERENCES

- Allison, J.D., Brown, D.S., and Novo-Gradac, K.J., 1990, MINTEQA2/PRODEFA2, a geochemical assessment model for environmental systems—Version 3.0 User's Manual: Environmental Research Laboratory, U.S. Environmental Protection Agency, 106 pp.
- Alpers, C.N., and Nordstrom, D.K., 1991, Geochemical evolution of extremely acid mine waters at Iron Mountain, California—Are there any lower limits to pH?: 2nd Internatl Conference on Abatement of Acidic Drainage, v. 2, pp. 321–342.
- Alpers, C.N., Nordstrom, D.K., and Ball, J.W., 1989, Solubility of jarosite solid solutions precipitated from acid-mine waters, Iron Mountain, California, U.S.A.: *Scientific Geology Bulletin*, v. 42, pp. 281–298.
- Arnold, R.G., and Malik, O.P., 1974, Violarite in some nickel ores from Lynn Lake and Thompson, Manitoba and Sudbury, Ontario, Canada: *Canadian Mineralogist*, v. 12, pp. 320–326.
- Baes, Jr., C.F., and Mesmer, R.E., 1976, *The hydrolysis of cations*: John Wiley and Sons, 489 pp.
- Ball, J.W., and Nordstrom, D.K., 1991, User's manual for WATEQ4F with revised thermodynamic data base and test cases for calculating speciation of major, trace, and redox elements in natural waters: U.S. Geological Survey Open-File Report 91-183, 189 pp.
- Barker, J.F., and Chatten, S., 1982, A technique for determining low concentrations of total carbonate in geologic materials: *Chemical Geology*, v. 36, pp. 317–323.
- Blowes, D.W., 1990, *The geochemistry, hydrogeology and mineralogy of decommissioned sulfide tailings—A comparative study*: Unpub. Ph.D. thesis, University of Waterloo, Waterloo, Canada, 637 pp.
- Blowes, D.W., and Jambor, J.L., 1990, *The pore-water geochemistry and the mineralogy of the vadose zone of sulfide tailings*, Waite Amulet, Quebec, Canada: *Applied Geochemistry*, v. 5, pp. 327–346.
- Blowes, D.W., Reardon, E.J., Cherry, J.A., and Jambor, J.L., 1991, The formation and potential importance of cemented layers in inactive sulfide mine tailings: *Geochimica et Cosmochimica Acta*, v. 55, pp. 965–978.
- Boorman, R.S., and Watson, D.M., 1976, Chemical processes in abandoned sulphide tailings dumps and environmental implications for northeastern New Brunswick: *Can. Inst. Mining Metallurgy Bulletin*, v. 69, pp. 86–96.
- Chapuis, R.P., 1988, Shape factors for permeability tests in boreholes and piezometers: *Ground Water*, v. 27, pp. 647–654.
- Coggans, C.J., 1992, *Hydrogeology and geochemistry of the INCO Ltd. Copper Cliff, Ontario mine tailings impoundments*: Unpub. M.S. thesis, University of Waterloo, Waterloo, Canada, 159 pp.
- Coggans, C.J., Blowes, D.W., and Robertson, W.D., 1991, *The hydrogeology and geochemistry of a nickel-mine tailings impoundment, Copper Cliff, Ontario*: 2nd Internatl Conference on Abatement of Acidic Drainage, Montreal, v. 4, pp. 1–23.
- Davis, G.B., and Ritchie, A.I.M., 1986, A model of oxidation in pyritic mine wastes, I. Equations and approximate solution: *Applied Mathematical Modeling*, v. 10, pp. 314–322.
- Deer, W.A., Howie, R.A., and Zussman, J., 1966, *An introduction to the rock forming minerals*: John Wiley and Sons, 527 pp.
- Dressler, B.O., Gupta, V.K., and Muir, T.L., 1991, *The Sudbury structure; in Geology of Ontario*: Ontario Geological Survey, Spec. Vol. 4, Part 1, pp. 593–625.
- Dubrovsky, N.M., 1986, *Geochemical evolution of inactive pyritic tailings in the Elliot Lake Uranium District*: Unpub. Ph.D. thesis, University of Waterloo, Waterloo, Canada, 373 pp.
- Dubrovsky, N.M., Cherry, J.A., and Reardon, E.J., 1984, Geotechnical evolution of inactive pyritic tailings in the Elliot Lake uranium district: *Canadian Geotechnical Journal*, v. 22, pp. 110–128.
- Felny, A.R., Brown, S.M., Onishi, Y., Yarusaki, S.B., and Argo, R.S., 1983, MEXAMS—The metals exposure analysis modeling system: Final Report for EPA Project 600/3–84–0341, 185 pp.
- Feasby, D.G., Blanchette, M., and Tremblay, G., 1991, *The mine environment neutral drainage (MEND) program*: 2nd Internatl Conference on Abatement of Acid Drainage, v. 1, pp. 1–26.
- Freeze, R.A., and Cherry, J.A., 1979, *Groundwater*: Prentice-Hall, Inc., Englewood Cliffs, N.J., 604 pp.
- Hawley, J.E., and Stanton, R.L., 1962, The facts, the ores, their minerals, metals and distribution in the Sudbury Ores—Their mineralogy and origin: *Canadian Mineralogist*, v. 7, pp. 30–145.
- Hurlbut, Jr., C.S., and Klein, C., 1977, *Manual of mineralogy*: John Wiley and Sons, 532 pp.
- Hvorslev, M.J., 1951, Time lag and soil permeability in groundwater observations: *Experiment Station Bulletin 36*, Vicksburg, Mass., 49 pp.
- Kinniburgh, D.G., Jackson, M.L., and Syers, J.K., 1976, Adsorption of alkaline earth, transition, and heavy metal cations by hydrous oxide gels of iron and aluminum: *Soil Science Society of America Journal*, v. 40, pp. 796–799.
- McLaren, R.G., 1988, CROSSFLO—2-D steady-state flow in cross section: Waterloo Centre for Groundwater Research, University of Waterloo, Waterloo, Canada, 70 pp.
- McReady, R.G.L., 1976, *Microbial assessment of the vegetated test plots on the pyritic uranium tailings in the Elliot Lake area*: CANMET Report MRP/MRL (TR), Department of Natural Resources, Canada, Ottawa, pp. 76–161.

- Miller, S.D., 1980, Sulfur and hydrogen ion buffering in pyritic strip-mine spoil; *in* Trudinger, P.S., and Walter, M.R. (eds.), *Biogeochemistry of Ancient and Modern Environments*, Proceedings, 6th Internatl Symposium on Environmental Biogeochemistry, and Conference on Biogeochemistry in Relation to the Mining Industry and Environmental Pollution, Canberra, Australia, Aug. 26–Sept. 4, 1979: Springer Verlag, Berlin, 723 pp.
- Morin, K.A., Cherry, J.A., Dave, N.K., Lim, T.P., and Vivyurka, A.J., 1988, Migration of acidic groundwater seepage from uranium-tailings impoundment, 1. Field study and conceptual hydrochemical model: *Contaminant Hydrogeology*, v. 2, pp. 271–303.
- Morton, F.I., 1983, Operational estimates of areal evapotranspiration and their significance to the science and practice of hydrology: *Journal of Hydrology*, v. 66, pp. 1–76.
- Munsell Soil Colour Chart, 1975, Macbeth Division of Kollmorgen Corp., Baltimore, Md.
- Naldrett, A.J., 1984, Mineralogy and composition of the Sudbury area: Ontario Geological Survey, Spec. Vol. 1, pp. 309–325.
- Naldrett, A.J., and Kullerud, G., 1967, A study of the Strathcona mine and its bearing on the origin of the nickel-copper ores of the Sudbury district: *Journal of Petrology*, v. 8, pp. 453–531.
- Naldrett, A.J., Innes, D.G., Sowa, J., and Gorton, M.P., 1982, Compositional variation within and between five Sudbury ore deposits: *Economic Geology*, v. 77, pp. 1519–1534.
- Nordstrom, D.K., 1977, Thermodynamic redox equilibria of ZoBell's solution: *Geochimica et Cosmochimica Acta*, v. 41, pp. 1835–1841.
- Nordstrom, D.K., 1982, Aqueous pyrite oxidation and the consequent formation of secondary minerals; *in* *Acid Sulfate Weathering*: Soil Science Society of America, pp. 37–56.
- Norris, P.R., and Parrott, L., 1985, High temperature mineral concentrate dissolution with sulfides; *in* *Fundamental and Applied Biohydrometallurgy*, Proceedings, 6th Internatl Symposium on Biohydrometallurgy, Vancouver, Canada, Aug. 21–24, 1985: Elsevier, Amsterdam, 501 pp.
- Peters, T.H., 1971, The use of vegetation to stabilize mine tailings areas at Copper Cliff: INCO Ltd., Unpub., 23 pp.
- Peters, T.H., 1984, Rehabilitation of mine tailings—A case of complete ecosystem reconstruction and revegetation of industrially stressed lands in the Sudbury area, Ontario, Canada; *in* *Effects of Pollutants at the Ecosystem Level*: John Wiley and Sons, New York, pp. 403–421.
- Reardon, E.J., and Moddle, P.M., 1985, Gas diffusion measurements on uranium mill tailings—Implications to cover layer design: *Uranium*, v. 2, pp. 111–131.
- Shaikh, A.V., and Tallman, D.E., 1979, Species specific analysis of nanogram quantities of arsenic in natural waters by arsine generation followed by graphite furnace atomic absorption spectrometry: Unpub. report from North Dakota State Univ., Fargo, 23 pp.
- Smyth, D.J.A., 1981, Hydrogeologic and Geotechnical studies above the water table in an inactive uranium tailings impoundment near Elliot Lake, Ontario: Unpub. M.S. thesis, Univ. of Waterloo, Waterloo, Canada, 72 pp.
- Starr, R.C., and Ingleton, R.A., 1992, A new method for collecting core samples without a drill rig: *Ground Water Monitoring Review*, v. 41, pp. 91–95.
- Thorner, M.R., 1983, The chemical processes of gossan formation; *in* Smith, R.E. (ed.), *Geochemical Exploration in Deeply Weathered Terrains*: CSIRO Division of Mineralogy, Short Course/Workshop, Floreat Park, Western Australia, pp. 67–73.
- Van Breeman, N., 1973, Dissolved aluminum in acid sulfate soils and in acid mine waters: *Soil Science Society of America Proceedings*, v. 37, pp. 694–697.
- van der Leeden, F., Troise, F.L., and Todd, D.K., 1991, *The water encyclopedia*, 2nd ed.: Lewis Publishers Inc., Chelsea, Mich., 808 pp.

Chapter 22

SEASONAL VARIATION IN METAL CONCENTRATIONS IN A STREAM AFFECTED BY ACID MINE DRAINAGE, ST. KEVIN GULCH, COLORADO

B.A. Kimball

U.S. Geological Survey, 1745 West 1700 South, Salt Lake City, UT 84104-3839

Mining of mineral deposits in the Rocky Mountains has left a legacy of acidic inflows to otherwise pristine upland watersheds. Since 1986, the U.S. Geological Survey has studied physical, chemical, and biological processes that affect the transport and transformation of metals in St. Kevin Gulch, an acidic, metal-rich stream near Leadville, Colorado. Well-known chemical processes have been quantified in the context of on-going physical transport by defining the hydrology with instream tracer-dilution experiments. These processes affect the partitioning of metals between dissolved and colloidal transport phases. In this acidic stream, pH increases during snowmelt runoff. At the most acidic stream site, pH varies from 3.15 to 4.00 during seasonal changes. Conservative effects of dilution are quantified using manganese as a natural, conservative tracer. Aluminum, copper, and zinc also are relatively conservative throughout the seasonal changes. Sulfate and iron, on the other hand, are removed with respect to manganese. The loss of iron through precipitation of hydrous Fe oxide is consistent with thermodynamic calculations. The loss of sulfate, however, cannot be fully explained.

INTRODUCTION

Mining of mineral deposits in the Rocky Mountains has left a legacy of acidic inflows to otherwise pristine upland watersheds (Colorado Water Quality Control Division, 1988). To effectively remediate inflows of acidic, metal-rich water, one must understand the interaction of physical, chemical, and biological processes that affect metal concentrations during downstream transport. Physical processes that affect instream metal concentrations include advection, dispersion, transient storage, and lateral inflow that can cause dilution or add metal load (Bencala et al., 1990; Stream Solute Workshop, 1990). Chemical processes include aqueous speciation, precipitation (including aggregation and settling), dissolution, oxidation, reduction, sorption, and desorption (Chapman et al., 1983; Nordstrom, 1985; Nordstrom and Ball, 1986; Filipek et al., 1987; Helz et al., 1987; McKnight et al., 1988; Hem and Roberson, 1990; McKnight and Bencala, 1990; Smith, 1991; Kieber and Helz, 1992; Ranville, 1992). Biological processes include uptake as micronutrients and oxidation-reduction reactions (Tate et al., 1991).

We have studied these well-known processes in the context of instream transport to compare rates of reaction to rates of transport. Instream reactions affect metal concentrations in a stream reach only if reaction rates are comparable to transport rates. If hydrologic transport moves solutes downstream much faster than

chemical reactions can occur, solute transport will appear conservative rather than reactive. As discharge varies during seasons, the relation between rates of physical transport and chemical reaction will change.

Each of the physical, chemical, and biological processes affecting metal concentrations can vary spatially and temporally (Bencala and McKnight, 1987). Spatial variation of instream solute concentrations can be substantial in upland watersheds because the mass of solutes contributed by inflows and the mass involved in chemical reactions can be as large as the total instream solute mass. This is especially true when inflows to upland watersheds are from acid mine drainage with high metal concentrations. By sampling all visible surface-water inflows and water from pits in many areas of obvious ground-water seepage, Kimball et al. (1994) detailed the spatial variability of instream metal concentrations in St. Kevin Gulch over a 1500 m reach. Areas of ground water seepage to the stream were indicated by dilution of an instream conservative tracer. The detailed sampling allowed simulations of solute transport to account for changes in metal concentration due to inflows and also due to removal by chemical reaction. The simulations indicated that rates of chemical reaction are only comparable to rates of hydrologic transport over short distances in the stream near the acidic inflows. The simulations also indicated net reach-scale rate constants for the removal of iron, aluminum, and sulfate.

Temporal variability of metal concentrations in St. Kevin Gulch has been studied by intensive sampling at fixed sites over 36 hour periods (McKnight et al., 1988). Photoreduction of ferric iron results in an increase in dissolved ferrous iron during the day. An instream injection of a conservative tracer was used to measure discharge at the time that each sample was collected and allowed the calculation of net fluxes of ferrous iron into the stream. Other tracer experiments have shown that the photoreduction can occur in the absence of bacteria and that both dissolved ferric iron and hydrous ferric oxides from the streambed can be affected by photoreduction to ferrous iron (Kimball et al., 1992).

Aspects of both temporal and spatial variability were combined in a study of instream pH modification (Broshears et al., 1994). Injection of sodium carbonate raised instream pH from 3.5 to a maximum of 5.8. Aluminum and iron formed hydroxysulfate solid phases and settled to the streambed. A reactive solute transport model simulated the processes and indicated the importance of chemical interactions between the water column and the streambed and kinetic restraints on the attainment of equilibrium.

Thousands of abandoned and inactive mines discharge acidic water into upland watersheds. To study these sites and evaluate

their environmental effects, it is important to characterize the spatial and temporal variability, and the temporal variability must also include the seasonal variation. The purpose of this paper is to extend techniques for studying instream variability to a seasonal scale. These techniques involve putting well known chemical processes into the context of physical hydrologic transport by using a natural, conservative tracer to evaluate seasonal changes. This may provide a framework for evaluating seasonal variability and for designing studies in the future.

Site description

Since 1986, the Upper Arkansas Surface-Water Toxic Substances Hydrology Project of the U.S. Geological Survey has studied physical, chemical, and biological processes controlling metal concentrations in St. Kevin Gulch near Leadville, Colorado (Fig. 22.1). St. Kevin Gulch is a forested, upland watershed, near Leadville ranging from 2500 to 2800 m in altitude and covering an area of about 10 km². Bedrock is a quartz-biotite-feldspar schist

and granite in some places (Tweto, 1968). This bedrock provides little buffering capacity for acid mine drainage. Silver (about 19 ounces/ton) was mined from a vein deposit between about 1917 and 1924 (Singewald, 1955). Lead (about 3%) from galena and zinc (about 7%) from sphalerite were locally present in the vein. "Chert-like quartz...containing irregularly distributed fine-grained pyrite" is also present.

The seven sampling sites indicated on Figure 22.1 are designated in meters measured downstream from a point above the mine inflows (Broshears et al., 1993). Samples from the site at 449 m are typical of the acidic inflows. Shingle Mill Gulch, at 501 m, is the main non-acidic tributary of St. Kevin Gulch. Sampling sites upstream and downstream from Shingle Mill Gulch are used to quantify processes in the downstream mixing zone. Samples were collected at these seven sites from April to August 1990. Continuous discharge measurements were recorded at a stream-flow gaging station at 1557 m, near the lower end of the study reach. This paper is limited to discussions of seasonal variations in pH, aluminum (Al), copper (Cu), iron (Fe), manganese (Mn), zinc (Zn), and sulfate (SO₄).

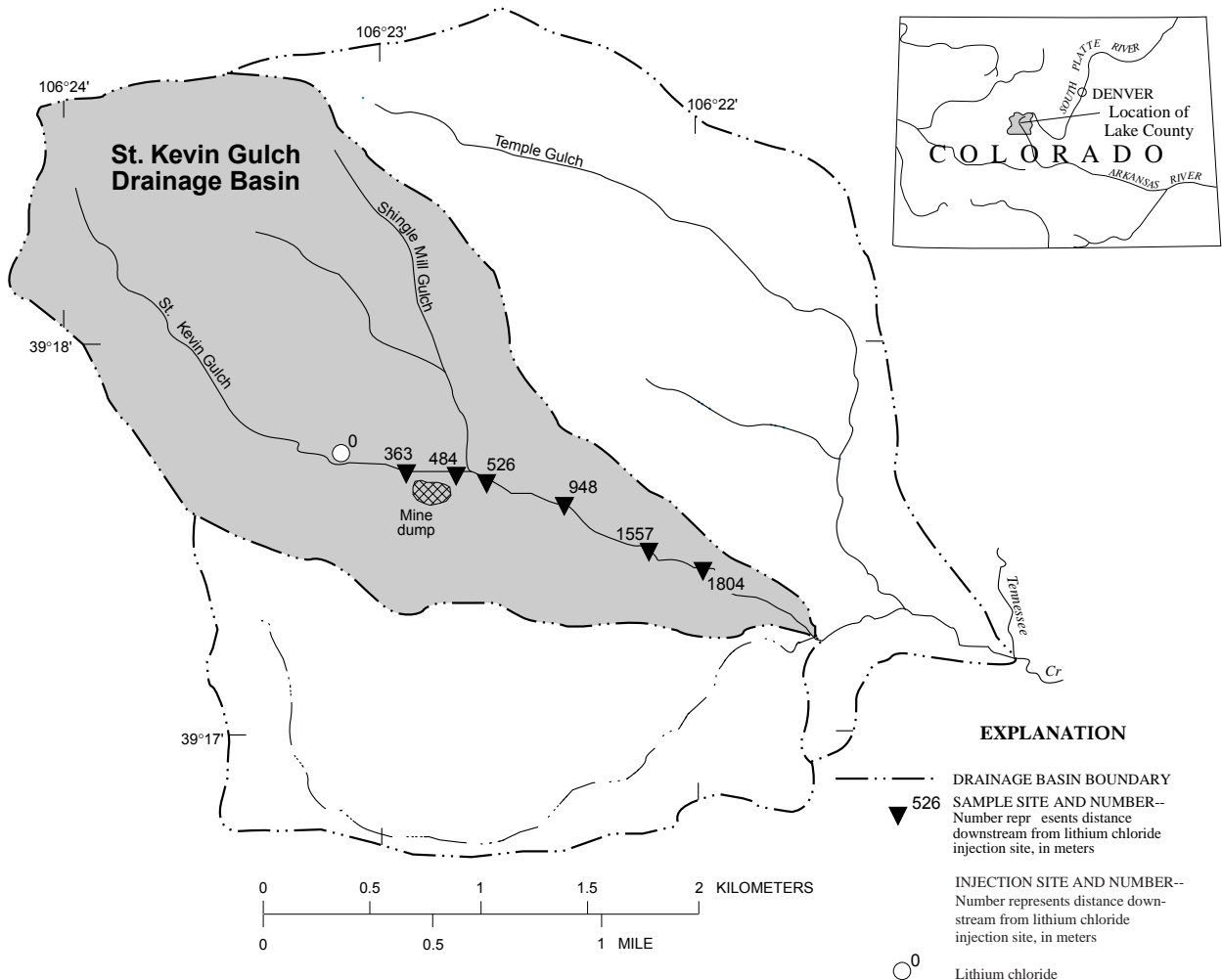


FIGURE 22.1—Location of St. Kevin Gulch indicating sites sampled for seasonal variation.

Methods

The precipitation of hydrous Fe oxides limits the solubility of Fe(III) over a wide range of pH (Pankow, 1991; see fig. 11.3). Even at relatively low values of pH in acid mine drainage, Fe is present in aqueous and colloidal phases (Pankow and McKenzie, 1991). Colloids have a very large surface area (van Olphen, 1977) and their sorption properties can affect the transport of toxic metals (Jenne, 1977; Dzombak and Morel, 1990). In St. Kevin Gulch, individual colloidal monospheres are on the order of 0.0009 μm (micrometer) in diameter, but mostly occur in larger aggregates (Ranville, 1992).

Separation of the aqueous and colloidal phases was accomplished by using ultrafiltration through a nominal pore size of 10,000 Daltons. This is a pore size less than 0.001 μm (Hernandez and Stallard, 1988). The use of ultrafiltration is much more likely to represent the dissolved concentration of metals than the standard 0.45 μm filtration (Kimball et al., 1992), but even ultrafiltration is an operational definition.

Metal concentrations in the colloidal phase were measured indirectly by subtracting the dissolved concentration from a concentration measured in an unfiltered, acidified sample. The colloids are amorphous, Fe-rich precipitates and they dissolve in the bottles when acidified, so the colloidal concentration should represent acid-soluble colloids of hydrous Fe or other metal oxides greater than the 10,000-Dalton filtrate (Smith, 1991; Ranville, 1992). This operational definition of colloids should be applied only to an Fe-rich system. The operational definition includes iron oxides greater than 0.45 μm that normally would be considered as suspended particulates in a standard approach. The same procedure, applied to surface-water environments with organic or aluminosilicate colloids, may not define meaningful colloidal concentrations.

Metal concentrations in St. Kevin Gulch generally fall within the acceptable analytical range for inductively coupled argon plasma atomic emission spectroscopy (Garbarino and Taylor, 1980). Metals were determined in samples that were acidified below pH 2.0 on site with ultrapure nitric acid. Colorimetric determination of Fe(II) was by a bipyridine method (Brown et al., 1970). Anions were determined in a filtered, unacidified sample using ion chromatography. The analytical precision for the range of concentrations of these samples was approximately 10% (relative) for metals, including Fe species, and 3% for SO_4^- .

Hydrologic tracers and analysis equations

Because of the temporal and spatial variability of concentrations, it is useful to normalize instream concentrations with regard to the extremes of the sampled inflows (Bencala and McKnight, 1987). Normalization also allows a more direct comparison among solutes that may have very different concentrations. The normalized concentration is defined as:

$$C_{\text{norm}} = (C - C_{\text{min}}^I) / (C_{\text{max}}^I - C_{\text{min}}^I) \quad [1]$$

where C is the measured instream concentration in mg/l, C_{min}^I is the minimum inflow concentration, and C_{max}^I is the maximum inflow concentration, both in mg/l.

Solutes that do not participate in chemical reactions during transport can serve as tracers to quantify the extent of physical and

chemical processes in mixing zones (Bencala et al., 1987; McKnight et al., 1992). Experimentally injected tracers are well suited for quantifying physical transport under steady flow conditions or short-term perturbations, but are impractical for evaluating seasonal variations during snowmelt runoff (Chapman, 1982; Bencala and Walters, 1983; Bencala et al., 1990; Runkel and Broshears, 1992; Broshears et al., 1993). Conservation of mass in a mixing zone can be written as:

$$Q_B C_B = Q_A C_A + Q_T C_T \quad [2]$$

where Q is discharge, in liters per second, and C is concentration, in milligrams per second. The subscript B is for a site downstream from the tributary, the subscript A is for a site upstream from the tributary, and the subscript T is for the tributary.

If $Q_B = Q_A + Q_T$, then $Q_T = Q_B - Q_A$. Substituting this into [2] and rearranging:

$$Q_B C_B = Q_A C_A + Q_B C_T - Q_A C_T \quad [3]$$

$$Q_B (C_B - C_T) = Q_A (C_A - C_T) \quad [4]$$

$$\frac{Q_A}{Q_B} = \frac{(C_B - C_T)}{(C_A - C_T)} \equiv Q_R \quad [5]$$

For any conservative solute (i.e., non-reactive) the concentration ratio, Q_R , is the ratio of downstream to upstream discharge. Q_R approaches 1 as discharge of the tributary is relatively smaller. The first step in choosing an appropriate conservative solute is to calculate a discharge ratio for each solute. This procedure groups solutes with similar behavior in the mixing zone.

With the discharge ratio, it is possible to evaluate removal of Fe or other solutes by chemical reaction. A predicted downstream concentration for Fe, assuming conservative transport, comes from the equation (Bencala et al., 1987):

$$C_P^{\text{Fe}} = C_A^{\text{Fe}} Q_R + C_T^{\text{Fe}} (1 - Q_R) \quad [6]$$

where C_P^{Fe} is the predicted Fe concentration downstream from the tributary, in mg/l; C_A^{Fe} is the Fe measured concentration upstream from the tributary, in mg/l; Q_R is defined above; and C_T^{Fe} is the Fe concentration of the tributary inflow, in mg/l. This predicted Fe concentration is compared with the measured Fe concentration to calculate a percent loss:

$$\text{Loss} = \frac{C_P^{\text{Fe}} - C_B^{\text{Fe}}}{C_P^{\text{Fe}}} \quad [7]$$

where C_P^{Fe} is defined above, and C_B^{Fe} is the measured Fe concentration downstream from the tributary, in mg/l. The extent of reaction beyond simple dilution can be quantified as discharge changes seasonally by comparing the loss of a solute for the different sampling dates.

RESULTS AND DISCUSSION

Results of chemical determinations are listed in Table 22.1. There was a general pattern of downstream change on each sampling date (Fig. 22.2). At 363 m, the median pH of 4.5 indicates inflow of some acid mine drainage upstream. As the stream flows past a mine dump between 363 and 484 m, several acidic springs discharge into St. Kevin Gulch. These inflows, represented by the acidic inflow at 449 m, cause the pH to be lower at 484 m. At 501 m, Shingle Mill Gulch joins St. Kevin Gulch, causing discharge to double and pH to increase at 526 m. Acidic inflows between 526 and 1557 m are minor and do not affect instream pH like the acidic inflows between 363 and 484 m.

The seasonal variations of discharge and pH are illustrated on Figure 22.3. According to the hydrograph from a recording gage at 1557 m, the weekly samples on 4/11/90 and 8/19/90 represent base flow conditions; samples on 5/10/90, 5/15/90, 6/21/90, and 6/28/90 represent rising and falling flow conditions; and samples on 5/21/90, 5/31/90, 6/4/90, and 6/13/90 represent the highest flow conditions. During snowmelt runoff, pH increases because the pH of snowmelt is high compared to the pH of acid mine drainage. At the most acidic stream site (484 m), pH ranges from 3.15 to 4.00 as discharge increases (Fig. 22.3b). Downstream at 1557 m the variation is similar, but pH is higher mostly attributable to the relatively basic inflow at 501 m.

Normalized concentrations of all these solutes decrease in response to the seasonal increase of discharge (Fig. 22.4). The influence of the acid mine drainage, indicated by a relatively high normalized concentration, is greatest in samples from 4/11/90 and 8/19/90, during periods of base flow. The greatest distinction among sites occurs during base flow. For example, the normalized Mn on 4/11/90 at 484 m is more than double the normalized concentration at 1557 m, and this is true for almost every solute. On the other hand, during the peak of runoff, normalized concentrations are lower and the distinction among sites is smaller. The influence of acid mine drainage is smallest at high flow. The general patterns of normalized Mn, Zn, and SO₄ are similar, and most closely resemble the inverse of discharge. This pattern suggests that these solute variations represent dilution, not reaction.

Beyond these general seasonal patterns there are small details in the variations of normalized concentrations. Some solutes react in response to changing conditions of pH and temperature, or to the variability of the chemical composition of the water, including the amount of dissolved organic carbon. These effects of reaction, however, may be overshadowed by dilution. Although the variations of normalized Al are similar to Mn, Zn, and SO₄, there are differences that indicate reactive behavior. Normalized Fe and Cu are consistently high at 484 m, and follow the general seasonal pattern. At all the other stream sites, however, Fe and Cu show little seasonal pattern; their concentrations are almost constant, indicating reactive behavior. Most of these results are predictable, but these plots indicate the utility of using normalized concentrations to illustrate solute behavior.

Solutes that are conservative in the mixing zone downstream from Shingle Mill Gulch will have similar discharge ratios, calculated from equation [5]. The seasonal patterns of Al, Cu, Mn, and Zn discharge ratios are similar (Figs. 22.5a and b) and most closely resemble the pattern of the hydrograph (see Fig. 22.3a). Simulations of solute transport in St. Kevin Gulch suggest that Mn is the most conservative of these metals (Kimball et al., 1994). The Zn discharge ratio is so similar that Zn must also be conservative.

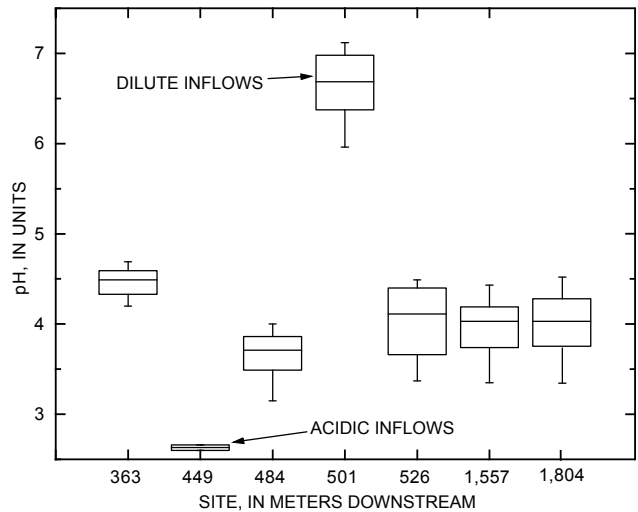


FIGURE 22.2—Box plots showing changes in pH along the stream profile.

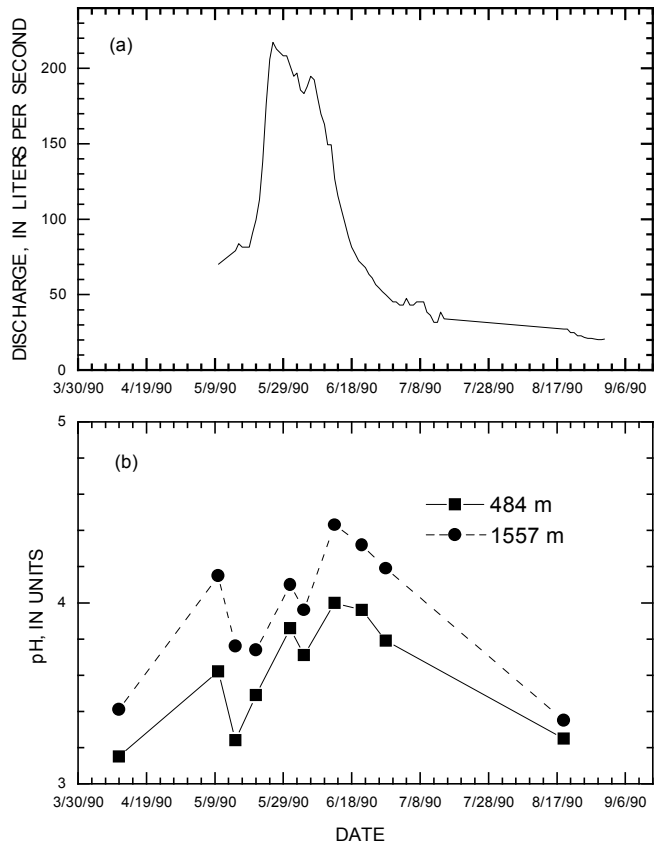


FIGURE 22.3—Variation of (a) discharge, and (b) pH with time.

SEASONAL VARIATION IN METAL CONCENTRATIONS IN A STREAM AFFECTED BY
ACID MINE DRAINAGE, ST. KEVIN GULCH, COLORADO

TABLE 22.1—Results of chemical determinations, in milligrams per liter, for St. Kevin Gulch, 1990.

Date	pH	Aluminum		Copper		Ferrous iron		Iron		Manganese		Zinc		Sulfate
		Filtered	Colloidal	Filtered	Colloidal	Filtered	Colloidal	Filtered	Colloidal	Filtered	Colloidal	Filtered	Colloidal	
900531	4.33	-	-	-	-	363 m	-	-	-	-	-	-	-	41.3
900604	4.20	1.22	0.142	0.164	-	0.560	0.920	1.01	1.41	-	2.13	-	-	38.5
900613	4.59	0.871	0.290	0.150	-	0.580	0.708	0.746	1.23	-	2.02	-	-	36.4
900621	4.49	-	-	-	-	-	-	-	-	-	-	-	-	45.0
900628	4.69	1.63	0.584	0.183	0.011	0.239	0.331	0.454	1.94	0.019	2.94	-	-	46.5
900531	-	-	-	-	-	449 m	-	-	-	-	-	-	-	-
900621	2.66	-	-	-	-	2.61	-	-	-	-	-	-	-	1029
900628	2.60	19.7	1.25	0.764	0.016	6.98	119	6.60	42.6	1.92	112	5.24	-	1157
900411	3.15	3.55	-	0.245	-	484 m	7.95	0.248	9.24	-	13.2	-	-	187
900510	3.62	2.39	0.320	0.219	0.018	2.20	3.35	3.81	4.32	-	7.84	-	-	105
900515	3.24	2.57	0.360	0.208	-	-	1.44	5.50	4.75	-	8.86	-	-	122
900521	3.49	2.20	0.110	0.191	-	2.50	5.47	1.84	4.49	-	8.43	-	-	113
900531	3.86	2.22	-	0.193	0.009	0.390	2.23	2.10	2.24	-	5.04	-	-	65.6
900604	3.71	1.47	-	0.164	-	0.390	2.07	2.02	2.14	-	4.35	-	-	59.1
900613	4.00	1.40	0.200	0.162	-	0.190	1.75	1.56	1.87	0.047	3.93	0.131	-	52.0
900621	3.96	2.23	-	0.226	-	0.127	2.47	1.00	2.80	-	5.36	0.024	-	71.9
900628	3.79	2.29	-	0.193	-	1.15	2.75	1.27	3.52	-	6.77	-	-	83.9
900411	5.96	0.236	-	0.015	-	501 m	0.153	-	0.509	-	0.873	-	-	25.5
900510	6.24	0.007	0.348	0.008	0.008	-	0.031	0.167	0.220	0.076	0.677	-	-	-
900515	6.51	-	-	0.008	-	-	0.014	0.123	0.182	0.035	0.403	0.182	-	14.5
900521	6.63	-	-	-	0.009	0.030	0.057	0.135	0.165	0.033	0.363	0.152	-	13.5
900531	6.74	-	-	-	-	0.390	0.070	0.107	0.184	-	0.368	0.014	-	13.0
900604	-	0.073	0.073	0.005	-	-	0.051	0.080	0.118	0.017	0.219	0.112	-	11.6
900613	6.94	0.018	0.044	-	-	0.190	0.022	0.072	0.085	0.012	0.141	0.087	-	9.58
900621	7.02	0.174	-	0.006	-	-	0.030	0.207	0.119	-	0.189	0.031	-	9.92
900628	7.12	0.141	0.125	0.003	-	0.127	0.026	0.087	0.159	-	0.201	0.124	-	10.8
900819	-	-	-	0.003	-	-	0.040	0.142	0.396	0.009	0.442	0.153	-	-
900411	3.37	-	-	-	-	526 m	-	-	-	-	-	-	-	109
900510	4.14	1.25	0.253	0.115	0.006	0.300	0.555	4.63	2.27	0.022	4.76	-	-	63.5
900515	3.61	1.34	0.262	0.121	0.006	0.130	0.287	3.74	2.69	0.052	5.31	0.572	-	73.6
900521	3.66	1.68	0.025	0.112	-	1.43	1.64	2.58	2.83	0.028	5.50	0.005	-	68.2
900531	4.11	1.79	-	0.161	-	1.64	1.60	1.70	2.12	-	4.79	-	-	39.6
900604	4.02	1.39	-	0.139	-	1.50	1.15	1.62	1.60	-	3.35	-	-	45.5
900613	4.49	0.85	0.025	0.105	-	1.21	0.92	1.10	1.27	-	2.69	-	-	31.4
900621	4.43	1.29	0.114	0.128	-	0.970	1.23	0.968	1.85	-	3.65	-	-	43.4
900628	4.40	1.50	0.080	0.119	-	0.642	0.964	1.62	2.24	0.072	4.53	0.192	-	50.6
900819	-	2.75	-	0.183	-	-	1.83	1.79	4.87	-	8.34	-	-	123

TABLE 22.1—Continued

Date	pH	Aluminum		Copper		Ferroous iron	Iron		Manganese		Zinc		Sulfate
		Filtered	Colloidal	Filtered	Colloidal		Filtered	Colloidal	Filtered	Colloidal	Filtered	Colloidal	
900411	3.41	1.95	-	0.114	-	1557 m 0.864	-	0.864	-	4.33	-	7.78	99.3
900510	4.15	1.22	0.247	0.089	0.003	0.300	1.86	0.454	0.049	2.12	0.173	4.73	60.3
900515	3.76	1.33	0.110	0.120	-	-	2.01	0.359	-	2.47	0.092	5.23	63.1
900521	3.74	1.68	0.075	0.097	-	-	0.831	1.791	0.044	2.50	0.052	5.25	64.0
900531	4.10	1.90	-	0.149	-	1.19	1.53	1.183	-	1.92	-	4.50	53.3
900604	3.96	1.75	0.041	0.140	-	0.990	1.36	1.059	-	1.80	-	4.01	51.1
900613	4.43	1.09	0.317	0.105	-	0.450	1.22	0.641	-	1.37	0.005	3.21	40.3
900621	4.32	1.46	0.251	0.119	-	0.340	1.17	0.567	0.054	1.85	0.125	4.08	52.9
900628	4.19	1.72	0.107	0.122	-	0.395	1.36	0.729	-	2.39	-	5.50	52.3
900819	3.35	3.01	0.026	0.159	-	-	0.618	0.902	-	4.62	-	8.91	120
900515	3.77	1.46	0.007	0.107	-	1804 m 0.470	2.03	0.574	-	2.43	-	5.89	63.5
900521	3.74	1.68	0.011	0.101	-	1.64	0.572	1.90	-	2.60	-	5.79	64.6
900531	4.09	1.95	-	0.142	-	1.19	1.29	1.21	-	1.90	-	4.92	53.8
900604	3.97	1.77	0.15	0.142	0.003	1.07	1.31	1.26	0.028	1.88	0.005	4.47	51.0
900613	4.49	1.11	0.12	0.104	0.004	0.640	1.11	0.783	-	1.38	-	3.22	40.0
900621	4.36	1.42	0.21	0.122	-	0.540	1.88	0.755	0.022	1.89	-	4.19	48.9
900628	4.20	1.40	0.29	0.098	0.015	0.522	1.29	0.772	0.293	1.96	0.806	4.26	53.7
900819	3.35	3.07	-	0.164	-	-	0.827	1.08	-	4.66	-	8.89	120

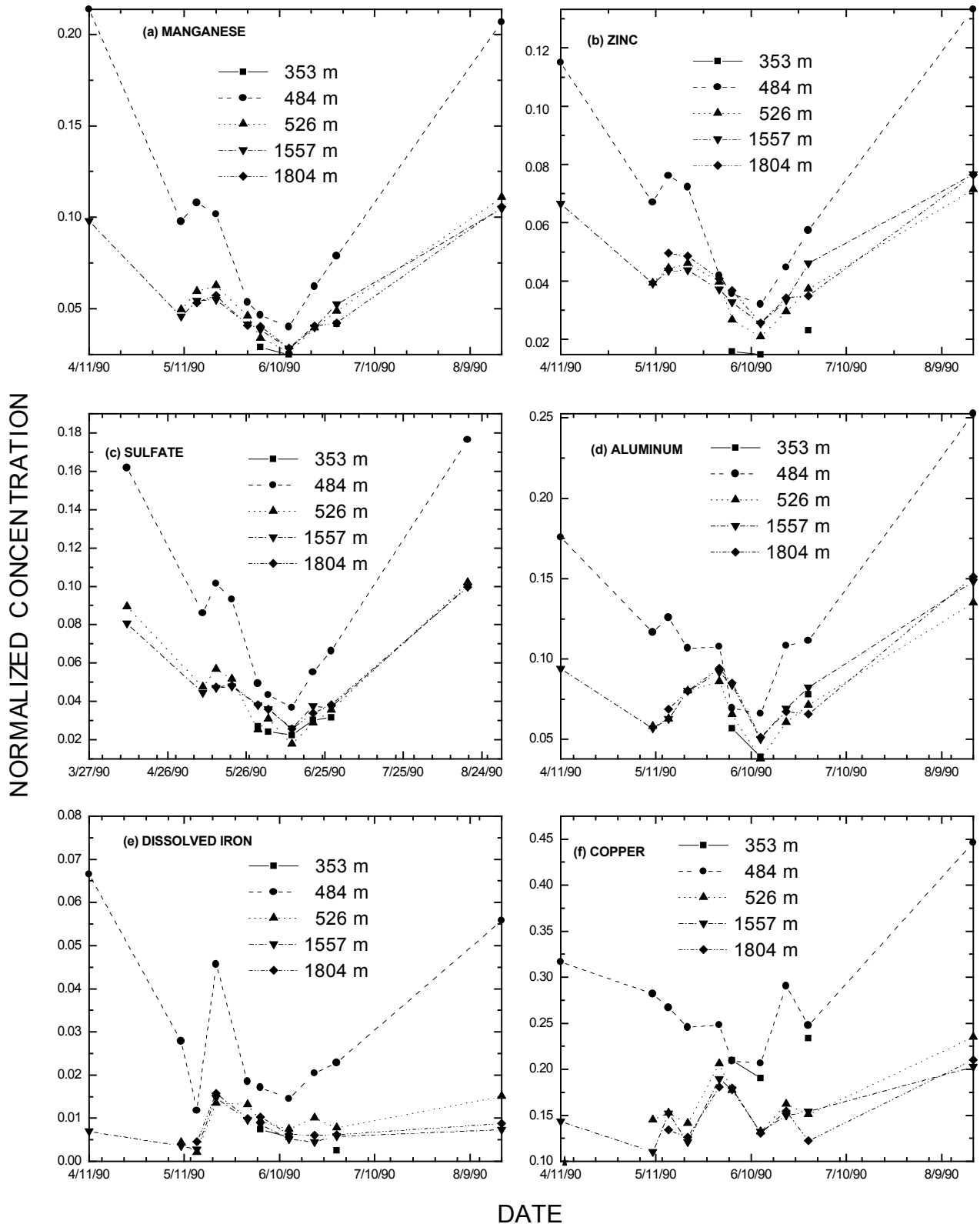


FIGURE 22.4—Variation of normalized concentrations of (a) manganese, (b) zinc, (c) sulfate, (d) aluminum, (e) dissolved iron, and (f) copper with time.

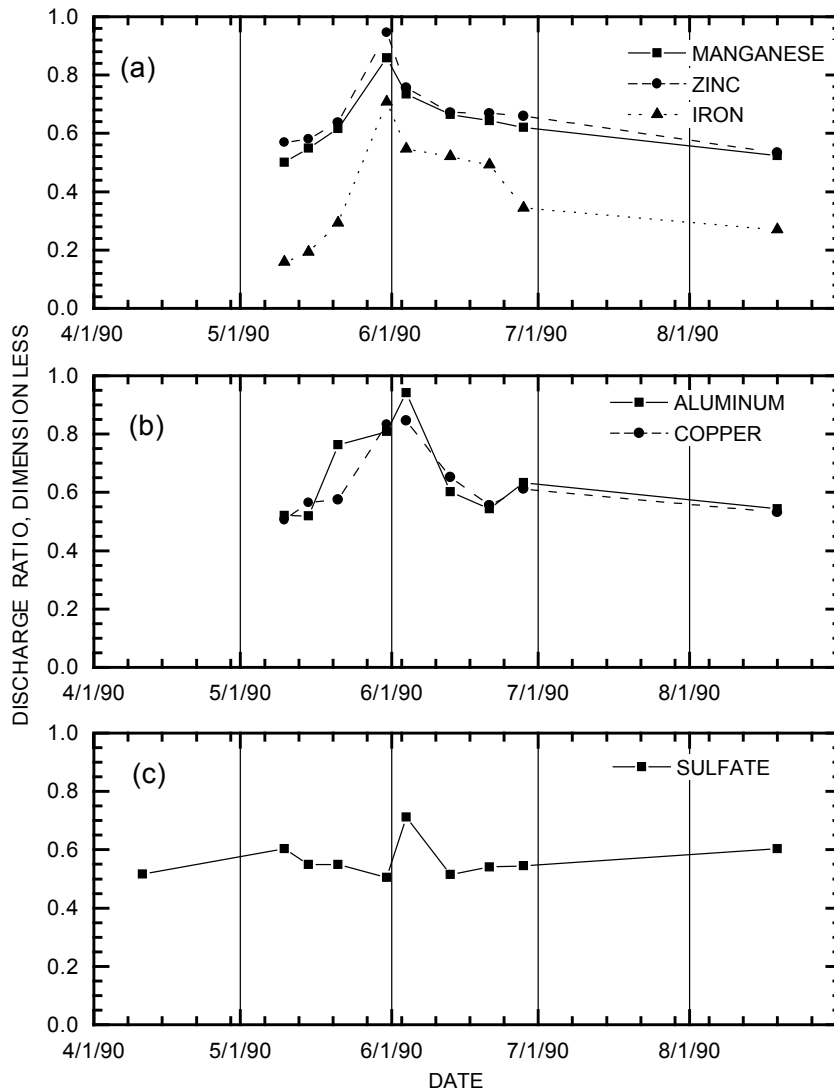


FIGURE 22.5—Variation of discharge ratio calculated for (a) manganese, zinc, and dissolved iron; (b) aluminum and copper; and (c) sulfate with time.

Given the similarity of Mn and Zn discharge ratios and the likelihood that they are not sorbed to Fe coatings when instream pH is less than 5.0 (Smith, 1991), the average of these two discharge ratios will be used in equations [6] and [7].

Patterns of Fe and SO_4 discharge ratios differ substantially from the more conservative solutes (Figs. 22.5a and c). The dissolved Fe discharge ratio has the same seasonal trend as Mn and Zn discharge ratios, but the values are consistently lower than the other solutes. The constant removal of Fe by precipitation is consistent with the trend of Fe^{3+} activity with pH (Fig. 22.6). In general, SO_4 does not vary with the same seasonal pattern; there appears to be a constant process that controls its concentration throughout the runoff period and at base flow.

The loss or gain of Al, Cu, Fe, and SO_4 is quantified by substituting an appropriate discharge ratio into equation [6] to calculate a predicted downstream concentration. The predicted concentration is then put into equation [7] to calculate the percent loss or gain with respect to the predicted concentration. With the excep-

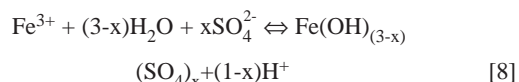
tion of the sample on 6/4/90, Al and Cu are consistently removed from the stream throughout the period of snowmelt runoff (Fig. 22.7a). Possible reactions removing Al and Cu could be the precipitation of hydroxide phases or sorption to the abundant hydrous Fe oxides in the water column and on the streambed. Alternatively, the process could be coprecipitation of Al or Cu. Thermodynamic calculations of the activities of Al^{3+} , Cu^{2+} , Mn^{2+} , and Zn^{2+} , however, do not indicate a trend with pH that is suggestive of either of these controls (Fig. 22.6). On 6/4/90, the gain in Al and Cu corresponds to a change in SO_4 and a relatively lower pH for the high discharge on that day. Given the slightly lower pH for that sampling day, the gains for Al and Cu might be caused by desorption, but the effect would be the opposite for SO_4 . Extra seepage of acid mine drainage, in addition to the sampled inflow of Shingle Mill Gulch also might account for the gain. This would affect Al, Cu, and SO_4 together.

Dissolved Fe is lost by precipitation of hydrous Fe oxides throughout the period of runoff, but the extent of the reaction

varies seasonally (Fig. 22.7b). Colloidal Fe has the opposite trend; reflecting the gain as dissolved Fe is lost (Fig. 22.7c). Changes in discharge and pH should influence the extent of partitioning from the dissolved to the colloidal phase. At higher pH, partitioning should tend toward precipitation of colloids, but as dilution and the velocity of stream flow influence the completion of the chemical reaction, the reaction is less extensive. Percent loss of dissolved Fe varies inversely to the discharge ratio, consistent with this expected variation in the process of Fe removal. Precipitation of Fe colloids should produce 1 mole of precipitate for each mole of dissolved Fe lost from solution. Using the predicted percentages of loss and gain at 526 m, there generally is more dissolved Fe lost than colloidal Fe gained. This does not indicate a lack of mass balance in the system, but indicates that some Fe precipitate settles to the streambed.

Although SO_4 in other acidic mountain streams behaves similarly to Mn (Bencala et al., 1987), there is a seasonal trend with the greatest loss of SO_4 at 526 m during high flow (Fig. 22.7b). The pH variation during the seasonal changes in St. Kevin Gulch is within the range where SO_4 consistently sorbs to hydrous Fe

oxides (Smith, 1991). So the seasonal variation should not substantially decrease the amount of sorption to the sediments. Another explanation could be the inclusion of SO_4 in the precipitation of the hydrous Fe oxide:



Bigham et al. (1990) have identified Schwertmanite, a precipitate of Fe oxyhydroxysulfate in SO_4 -rich, acidic streams with pH values ranging from 2.5 to 4.0. At 526 m pH generally is within this range. The loss of SO_4 , however, generally is much greater than the amount accounted for by the stoichiometry of equation [8], so both precipitation and sorption likely occur.

Formation of colloidal Fe is consistent with thermodynamic calculations that suggest precipitation of Fe minerals (Fig. 22.6). Using the equilibrium constant for ferrihydrite (Ball and

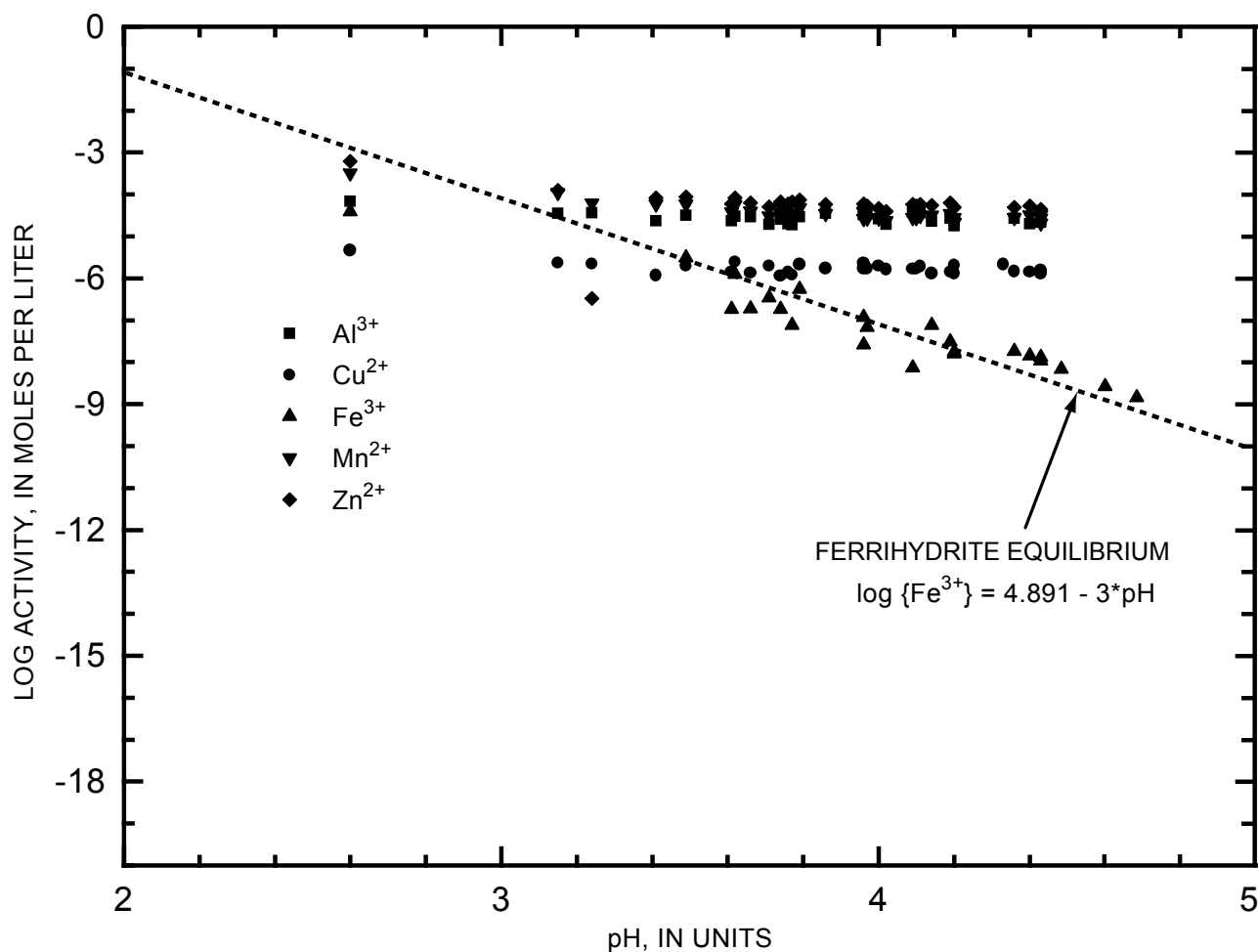


FIGURE 22.6—Activity diagram for the variation of ferric iron and other metals with pH for instream sampling sites in St. Kevin Gulch. Dotted line indicates equilibrium with ferrihydrite at 25°C, using the equilibrium constant from Ball and Nordstrom (1991).

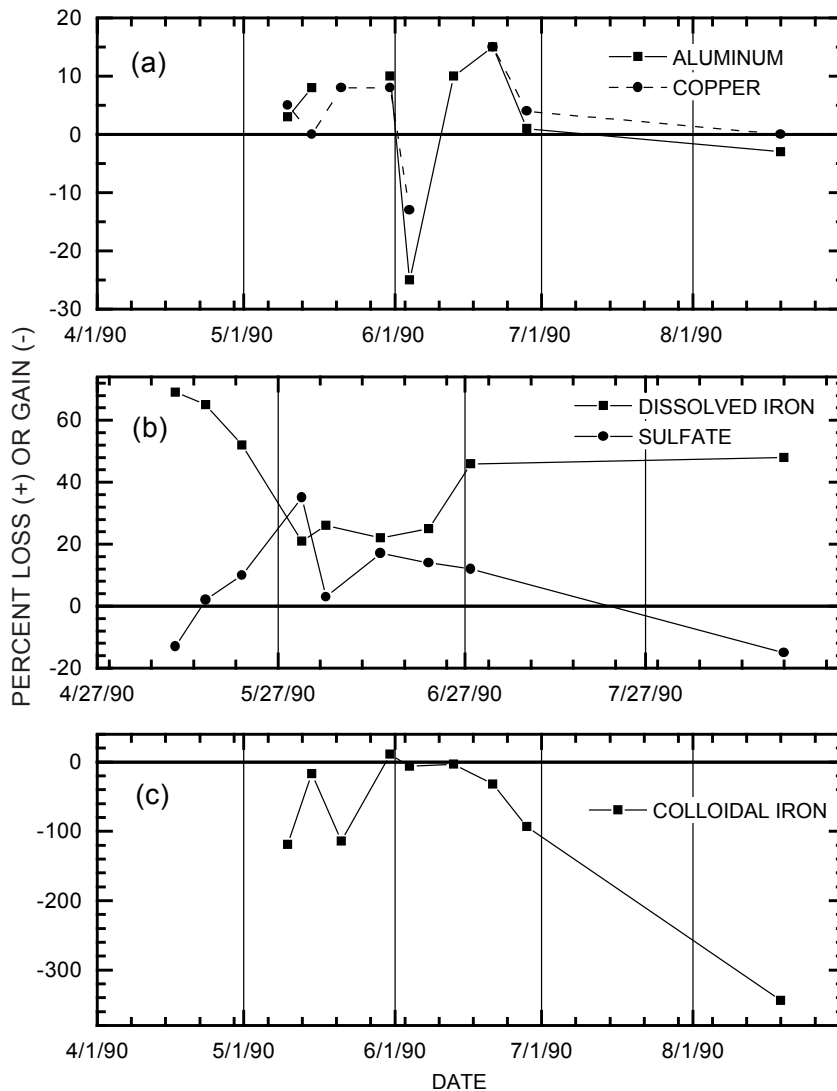


FIGURE 22.7—Variation of percent loss or gain of (a) aluminum and copper; (b) dissolved iron and sulfate; and (c) colloidal iron with time.

Nordstrom, 1991) and the measured values of Fe(II) for estimating redox potential, results showed that samples from each site are consistently near saturation or are supersaturated with respect to ferrihydrite. Variation of the calculated activity of Fe(III) with pH indicates a linear relation with a slope close to -3.0. This could suggest equilibrium with respect to ferrihydrite over the whole range of pH encountered during seasonal changes. A substantial quantity of SO_4 in this precipitate would cause a change of slope to less than -3.0, but any departure from this slope is difficult to discern from these data. Activities of Cu and Al do not follow a trend of negative slope with respect to pH, suggesting that there are no equilibrium controls on these metal concentrations.

Although each of the metals partitions between aqueous and solid phases to some extent, most of the colloidal concentrations in the water column are significantly lower than the dissolved concentrations (Table 22.1). The occurrence of Fe colloids, however, indicates the importance of using ultrafiltration or some other isolation technique to remove colloidal Fe to obtain dissolved Fe concentrations that are appropriate for thermodynamic calculations.

Otherwise, “dissolved” Fe will include colloidal material and result in incorrect predictions of mineral saturation.

CONCLUSIONS

Dilution is the dominant process during runoff, but it is possible to quantify chemical reactions that also occur. Effects of seasonal variation on chemical processes in streams affected by acid mine drainage can be studied in the context of instream transport processes by using patterns of normalized concentrations and by comparison of reactive and conservative solutes. The behaviors of Mn and Zn generally are conservative in the acidic stream, and these solutes can be used to calculate a discharge ratio of upstream to downstream discharge at an inflow. Using the discharge ratio to define conservative transport, the loss or gain of reactive solutes can be calculated. Reactive solutes include Al, Cu, SO_4 , and Fe. Removal of Al and Cu is likely by sorption or coprecipitation with hydrous Fe oxides. Precipitation of Fe occurs throughout the sea-

sonal changes, but the percent of Fe removed decreases at higher flow. The extent of Fe precipitation varies in response to residence time in a given subreach of the stream. Removal of SO_4 is by sorption to hydrous Fe oxides or by precipitation of Schwertmanite, a Fe hydroxysulfate mineral. Increased discharge from snowmelt runoff increased the amount of SO_4 loss, but decreased the extent of Fe loss.

REFERENCES

- Ball, J.W., and Nordstrom, D.K., 1991, User's manual for WATEQ4F, with revised thermodynamic data base and test cases for calculating speciation of major, trace, and redox elements in natural waters: U.S. Geological Survey Open-File Report 91-183, 189 pp.
- Bencala, K.E., and McKnight, D.M., 1987, Identifying in-stream variability—Sampling iron in an acidic stream; *in* Averett, R.C., and McKnight, D.M. (eds.), *Chemical Quality of Water and the Hydrologic Cycle*: Lewis Publishers, Inc., Chelsea, Mich., pp. 255–269.
- Bencala, K.E., and Walters, R.A., 1983, Simulation of solute transport in a mountain pool-and-riffle stream—A transient storage model: *Water Resources Research*, v. 19, pp. 718–724.
- Bencala, K.E., McKnight, D.M., and Zellweger, G.W., 1987, Evaluation of natural tracers in an acidic and metal-rich stream: *Water Resources Research*, v. 23, pp. 827–836.
- Bencala, K.E., McKnight, D.M., and Zellweger, G.W., 1990, Characterization of transport in an acidic and metal-rich mountain stream based on a lithium tracer injection and simulations of transient storage: *Water Resources Research*, v. 26, pp. 989–1000.
- Bigam, J.M., Schwertmann, U., Carlson, L., and Murad, E., 1990, A poorly crystallized oxyhydroxysulfate of iron formed by bacterial oxidation of Fe(II) in acid mine waters: *Geochimica et Cosmochimica Acta*, v. 54, pp. 2743–2758.
- Broshears, R.E., Bencala, K.E., Kimball, B.A., and McKnight, D.M., 1993, Tracer-dilution experiments and solute-transport simulations for a mountain stream, Saint Kevin Gulch, Colorado: U.S. Geological Survey Water-Resources Investigations Report 92-4081, 18 pp.
- Broshears, R.E., Runkel, R.L., and Kimball, B.A., 1994, Development and application of a reactive solute transport model for trace metals in mountain streams; *in* Dutton, A. (ed.), *Toxic Substances and the Hydrologic Sciences*: American Institute of Hydrology, Minneapolis, Minn., pp. 19–34.
- Brown, E., Skougstad, M.W., and Fishman, M.J., 1970, Methods for collection and analysis of water samples for dissolved minerals and gases: *Techniques for Water-Resources Investigations of the U.S. Geological Survey*, Book 5, pp. 101–105.
- Chapman, B.M., 1982, Numerical simulation of the transport and speciation of nonconservative chemical reactants in rivers: *Water Resources Research*, v. 18, pp. 155–167.
- Chapman, B.M., Jones, D.R., and Jung, R.F., 1983, Processes controlling metal ion attenuation in acid mine drainage streams: *Geochimica et Cosmochimica Acta*, v. 47, pp. 1957–1973.
- Colorado Water-Quality Control Division, 1988, Colorado non-point assessment report: Colorado Dept. of Health, Denver, Colo., 160 pp.
- Dzombak, D.A., and Morel, F.M.M., 1990, Surface complexation modeling—Hydrous ferric oxide: John Wiley and Sons, New York, 393 pp.
- Filipek, L.H., Nordstrom, D.K., and Ficklin, W.H., 1987, Interaction of acid mine drainage with waters and sediments of West Squaw Creek in the West Shasta Mining District, California: *Environmental Science and Technology*, v. 21, pp. 388–396.
- Garbarino, J., and Taylor, H.E., 1980, A Babington-type nebulizer for use in the analysis of natural water samples by inductively coupled plasma spectrometry: *Applied Spectroscopy*, v. 34, pp. 584.
- Helz, G.R., Dai, J.H., Kijak, P.J., and Fendinger, N.J., 1987, Processes controlling the composition of acid sulfate solutions evolved from coal: *Applied Geochemistry*, v. 2, pp. 427–436.
- Hem, J.D., and Roberson, C.E., 1990, Aluminum hydrolysis reactions and products in mildly acidic aqueous systems; *in* Melchior, D.C., and Bassett, R.L. (eds.), *Chemical Modeling of Aqueous Systems, II*. ACS Symposium Series 416: American Chemical Society, Washington, D.C., pp. 429–446.
- Hernandez, L.K., and Stallard, R.F., 1988, Sediment sampling through ultrafiltration: *Journal of Sedimentary Petrology*, v. 58, pp. 758–759.
- Jenne, E.A., 1977, Trace element sorption by sediments and soils—Sites and processes; *in* Chappel, W., and Petersen, K. (eds.), *Symposium on Molybdenum in the Environment*, M. Dekker, Inc., New York, 425 pp.
- Kieber, R.J., and Helz, G.R., 1992, Indirect photoreduction of aqueous chromium (VI): *Environmental Science and Technology*, v. 26, pp. 307–312.
- Kimball, B.A., McKnight, D.M., Wetherbee, G.A., and Harnish, R.A., 1992, Mechanisms of iron photoreduction in a metal-rich, acidic stream (St. Kevin Gulch, Colorado, U.S.A.): *Chemical Geology*, v. 96, pp. 227–239.
- Kimball, B.A., Broshears, R.E., Bencala, K.E., and McKnight, D.M., 1994, Coupling of hydrologic transport and chemical reactions in a stream affected by acid mine drainage: *Environmental Science and Technology*, v. 28, pp. 2065–2073.
- McKnight, D.M., and Bencala, K.E., 1990, The chemistry of iron, aluminum, and dissolved organic material in three acidic, metal-enriched, mountain streams, as controlled by watershed and in-stream processes: *Water Resources Research*, v. 26, pp. 3087–3100.
- McKnight, D.M., Kimball, B.A., and Bencala, K.E., 1988, Iron photoreduction and oxidation in an acidic mountain stream: *Science*, v. 240, pp. 637–640.
- McKnight, D.M., Bencala, K.E., Zellweger, G.W., Aiken, G.R., Feder, G.L., and Thorn, K.A., 1992, Sorption of dissolved organic carbon by hydrous aluminum and iron oxides occurring at the confluence of Deer Creek with the Snake River, Summit County, Colorado: *Environmental Science and Technology*, v. 26, pp. 1388–1396.
- Nordstrom, D.K., 1985, The rate of ferrous iron oxidation in a stream receiving acid mine effluent; *in* Subitzky, S. (ed.), *Selected Papers in the Hydrologic Sciences*: U.S. Geological Survey Water-Supply Paper 2270, pp. 113–119.
- Nordstrom, D.K., and Ball, J.W., 1986, The geochemical behavior of aluminum in acidified surface waters: *Science*, v. 232, pp. 54–56.
- Pankow, J.F., 1991, *Aquatic chemistry concepts*: Lewis Publishers, Chelsea, Mich., 683 pp.
- Pankow, J.F., and McKenzie, S.W., 1991, Parameterizing the equilibrium distribution of chemicals between the dissolved, solid particulate matter, and colloidal matter compartments in aqueous systems: *Environmental Science and Technology*, v. 25, pp. 2046–2053.
- Ranville, J.F., 1992, Factors influencing the electrophoretic mobility of suspended sediments in acid mine drainage: Unpub. Ph.D. dissertation T-4213, Colorado School of Mines, Golden, 270 pp.
- Runkel, R.L., and Broshears, R.E., 1992, One-dimensional transport with inflow and storage (OTIS)—A solute transport model for small streams: Center for Advanced Decision Support for Water and Environmental Systems, Boulder, Colo., pp. 1–85.
- Singewald, Q.D., 1955, Sugar Loaf and St. Kevin mining districts, Lake County, Colorado: U.S. Geological Survey Bulletin 1027-E, 299 pp.
- Smith, K.S., 1991, Factors influencing metal sorption onto iron-rich sediment in acid-mine drainage: Unpub. Ph.D. dissertation T-3925, Colorado School of Mines, Golden, 239 pp.
- Stream Solute Workshop, 1990, Concepts and methods for assessing solute dynamics in stream ecosystems: *Journal of the North American Benthological Society*, v. 9, pp. 95–119.
- Tate, C.M., McKnight, D.M., and Spaulding, S.A., 1991, Phosphate uptake by algae in a stream contaminated by acid mine drainage, St. Kevin Gulch, Leadville, Colorado: U.S. Geological Survey Water-Resources Investigations Report 91-4034, pp. 387–391.
- Tweto, O., 1968, Geologic setting and interrelationships of mineral deposits in the Mountain Province of Colorado and south-central Wyoming; *in* Redge, J.D. (ed.), *Ore Deposits of the United States, 1933–1967*: American Institute of Mining and Metallurgical, and Petroleum Engineers, New York, pp. 551–588.
- van Olphen, H., 1977, *An introduction to clay colloid chemistry*, 2nd ed.: John Wiley and Sons, New York, 318 pp.

Chapter 23

NATURAL ATTENUATION OF ACIDIC DRAINAGE FROM SULFIDIC TAILINGS AT A SITE IN WASHINGTON STATE

R.H. Lambeth

Maxim Technologies, Inc., 10220 North Nevada Street, Suite 290, Spokane, WA 99218

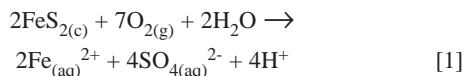
Ground and surface water can be contaminated by the transport of soluble oxidation products from sulfidic mine waste impoundments. A program was designed whereby an impoundment that contained sulfidic waste was studied to characterize pore water in the impoundment and to determine the fate of metals as they were transported downgradient. From this information a method to control dissolved metal transport was identified.

An appropriate field site where a sulfidic tailings impoundment was releasing heavy metals into an unconsolidated aquifer was identified and characterized over a 2.5 year period. Twenty-four piezometers and two lysimeters were installed upgradient from, within, and downgradient from the impoundment. Water samples were analyzed for 12 dissolved constituents, and field measurements for pH, redox potential, dissolved oxygen, temperature, alkalinity, and conductivity were made. Dissolution probably results from oxidation of sulfide minerals in the unsaturated tailings; infiltration transports the oxidation products downward through the saturated tailings into the underlying aquifer. Beneath the impoundment, the acidic water is partially neutralized by calcareous strata; pH-sensitive species precipitate as do some oxidized species. Continuing attenuation downgradient from the impoundment correlates mostly to precipitation of and sorption by oxidized mineral species.

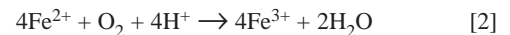
Because oxidation and precipitation and attendant sorption of dissolved metals was identified as the primary downgradient attenuation mechanism, air injection immediately downgradient from the impoundment is postulated as an interim remediation method and an alternative to pump-and-treat procedures. Porosity decrease caused by precipitation may limit the useful life of this method.

INTRODUCTION

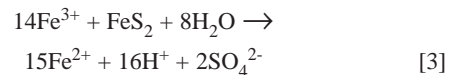
One of the most serious problems and major costs associated with mining is the release of heavy metals into the environment. In most circumstances this release results from oxidation-induced dissolution of sulfide minerals from mill tailings impoundments and waste rock piles. At the field site most dissolution of heavy metals probably takes place in the unsaturated zone of the tailings impoundment, where the most important reaction is the oxidation of pyrite (FeS_2), equation [1] (Nordstrom and Munoz, 1986):



The products of this reaction are sulfuric acid and $\text{Fe}_{(aq)}^{2+}$. Sulfuric acid reacts with the surrounding silicate mineral matrix causing neutralization of the acid and release of numerous ions, including aluminum (Al), calcium (Ca), potassium (K), magnesium (Mg), manganese (Mn), iron (Fe), and silica (SiO_2). Similar reactions may be constructed for other common sulfide minerals, but not all of these produce acid. The sulfide oxidation rates are slow, and most researchers attribute the rapid rates that occur in nature to biomediation by bacteria, especially *Thiobacillus ferrooxidans* (Nordstrom, 1982) after depletion of buffering capacity. Fe^{2+} from reaction [1] then oxidizes pyrite by reactions [2] and [3] (Moses et al., 1987).



and



The oxidation of Fe^{2+} to Fe^{3+} is thought to be the rate-limiting step. Reaction [2] will not occur in the absence of an oxidant such as in oxygen-depleted zones in the lower parts of the unsaturated zone and the saturated zone.

In circumneutral systems most metals have limited solubility and tend to be attenuated as soon as they are transported from an acidic waste impoundment into a more neutral environment. This attenuation is caused by a combination of precipitation, adsorption, ion exchange, and dilution.

At the Spokane Research Center (SRC) of the U. S. Bureau of Mines (USBM), a project was initiated to characterize the hydrogeochemistry downgradient from a sulfidic tailings impoundment to more fully understand the chemical mechanisms of metal attenuation. This information was to be used to develop methods of enhancing natural attenuation mechanisms.

More detailed treatments of the tailings pore waters and downgradient geochemical evolution can be found in Williams (1992) and Lambeth (1992).

SITE DESCRIPTION

The study site is located in north-central Washington State on the east slope of the Cascade Mountains. By agreement with the site owner the location cannot be disclosed. The climate is tem-

perate and semi-arid; average annual precipitation is approximately 30 cm per year. The tailings impoundment, which is approximately 180 m long by 45 m wide by 5 m deep and contains approximately 50,000 mt of tailings, lies within a narrow, north-northwest trending valley at an elevation of 570 m above mean sea level. The valley is a topographic expression of a north-west-striking high-angle fault which consists of a series of discontinuous, slightly rotated segments. These types of faults generally exhibit an open structure compared to compression faults and exhibit locally high ground-water transmissivities. Numerous small ponds and lakes are present along the fault trace, and many of these, including a pond at the northwest end of the impoundment, may receive most of their inflows from springs associated with the fault.

The valley floor, which slopes to the southeast from the tailings impoundment, supports thick brush and phreatophyte growth and is covered with approximately 30 cm of decaying vegetation and root mat. Along the valley axis, this mat is underlain by 20 to 30 cm of oxidized tailings, which were deposited in 1952 when the tailings dam breached. Two small reservoirs, referred to as the Overflow Impoundment and the Spill Impoundment (Fig. 23.1), were constructed to contain the spilled tailings. The spilled tailings are underlain by colluvium and remnant stream gravel (Qal) with a maximum thickness of 10 m. The Qal consists of sub-rounded to rounded clasts up to a few cm in diameter and composed of quartz, quartzite, acidic to midacidic intrusive and metavolcanic rock, schist, and shale. Chlorite and epidote were frequently observed. Calcite cementation was observed in several hand-dug pits located between 50 and 300 m downgradient from the impoundment. The layer is approximately 10 cm thick and appears to coincide with upper portions of the ground-water capillary fringe.

The mine, which is 5 km southwest of the millsite and impoundment, is near a major north-striking fault, and the ore is within a 5- to 20-m-wide silicified shear zone in a felsic horizon of upper Jurassic or lower Cretaceous age andesite breccia. The ore minerals are chalcopyrite, sphalerite, and galena with accessory gold and silver; chalcopyrite and sphalerite were recovered by flotation. Pyrite is the dominant sulfide mineral, but most of the tailings are composed of quartz and feldspar. The deposit was discovered in the late 1800s, but only sporadic production occurred through 1939. At that time the existing mill was commissioned, and production continued through 1955.

METHODS

Monitoring well installation

A monitor well system was installed to sample upgradient ground water in Qal and the underlying fault, tailings pore water, ground water flowing under the impoundment in Qal, and ground water downgradient from the impoundment in both Qal and the underlying fault. The locations of the wells are illustrated on Figure 23.1. Wells BKG and M1 through M5 are nested multiple completion wells which consist of polyvinyl chloride piezometers (PVC) with a 50 cm slotted interval at the bottom. Piezometers less than 8 m deep are sampled through a dedicated PVC tube with a peristaltic pump; positive displacement pumps were installed in wells greater than 8 m depth. The hyphenated number following the borehole number of all wells in text and tables indicates the piezometer completion depth in meters. Base of the Qal

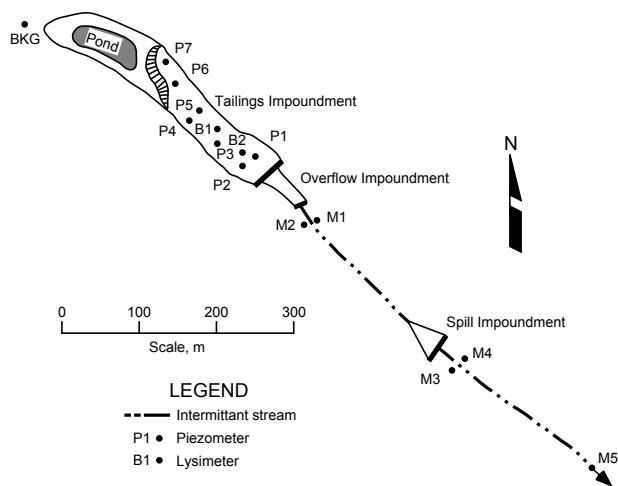


FIGURE 23.1—Plan map of millsite tailings impoundments and monitor wells.

at locations BKG, M1, M2, M3, M4, AND M5 is 8.5, 4.0, 8.0, 8.0, 6.0, and 4.4 m, respectively. Piezometers BKG–06, M1–2 and 3, M2–04 and 06, M3–05, M4–05, and M5–04 are completed in Qal.

In order to define the geometry of the tailings, map the underlying strata, and obtain samples from the saturated zone, seven single completion piezometers and two lysimeters were installed. The lysimeters were completed at 5 m depths at locations B1 and B2; seven PVC piezometers (P1 through P7) were completed at depths of 5, 5.8, 9.3, 4.6, 5.4, 4.9, and 3 m, respectively. Wells P2, P3, P4, P5, and P6 contain water throughout the year; the water table is below well P1 during the dry parts of the year; well P7 never contained water. Wells P1 and P2 were completed slightly below the base of the tailings; P3 was completed in underlying silt; P4, P5, P6, and P7 were completed within the tailings.

From core, it was apparent that the tailings had been deposited on a swampy lake basin. The tailings were underlain by an organic-rich silt and clay layer that ranged in thickness from 15 cm to 2.3 m. This organic-rich layer graded downward into clayey silt and eventually to gravel in some borings. Snail shells were common, particularly in the more organic-rich layer, and the odor of hydrogen sulfide suggested that reducing conditions were present in some zones. The highly oxidized layer at the surface of the tailings ranged from 1 to 2 m in thickness. Only a thin veneer of goethite could be observed with a hand lens on tailings samples taken from below the water table, whereas sulfide particles in the unsaturated zone were intensely oxidized and goethite-coated. This would seem to indicate that most of the oxidation and dissolution was occurring in the unsaturated zone of the tailings. This phenomenon has been observed at other tailings impoundments (Blowes et al., 1988). Ninety-five percent of the tailings particles were composed of silicate minerals, predominantly quartz with lesser amounts of feldspar. The remaining 5% were opaque sulfide minerals, predominantly pyrite with sporadic traces of galena and sphalerite. Although no chalcopyrite was observed, it is probably present in the tailings.

Figure 23.2 is a plan view of the impoundment illustrating the locations of wells P1 through P7. The plan view is projected vertically downward to a fence diagram that provides a limited three-

dimensional view of the organic layer and silt. Included also is a cross section (A-A') of the impoundment through wells P2, P3, P5, and P6 that illustrates the average annual water table as well as impoundment stratigraphy.

Field and laboratory measurements

The final monitoring wells were installed by mid-October 1987, and all wells were developed by the end of that month. After a stabilization period of 1 month, sampling was initiated. Data were collected at approximately 5-week intervals from December 9, 1987 through June 18, 1990. Twenty-two piezometers and two lysimeters were amenable to sampling.

Sampling and sample preservation protocols were those of the EPA (American Water Works Association, 1985), Schuller et al. (1981), and Driscoll (1987). Depths to water table (± 2 mm) was obtained and converted to elevations, and at least two well-casing volumes of water were purged from each piezometer. Samples were pressure-filtered through a stacked filter system that consisted of an acetate fiber prefilter to remove particles, an 0.8-micron borosilicate filter, and a 0.45-micron borosilicate filter. For inductively coupled argon-plasma emission analysis (ICP), samples were collected in acid-washed polyethylene bottles and acidified with concentrated nitric acid to a pH of approximately 1.5. Additional filtered but nonacidified samples were taken for chloride analysis by ion chromatography (IC). Temperature (T), pH, dissolved oxygen (DO), specific conductance (EC), redox potential (Eh), and alkalinity (HCO_3^-) were measured in the field. When an adequate supply of ground water could be obtained from a piezometer, all measurements were taken from a flow-through cell to obtain the greatest accuracy; otherwise a beaker was used, and

the measurements were taken as quickly as possible before equilibrium conditions changed significantly. Alkalinity titrations were obtained only during the last few sampling trips, and they were obtained only at BKG-06, P3-9, M1-2, M2-04, M4-05, and M5-04. A digital titrator and sulfuric acid were used with a pH electrode for determination of alkalinity at the inflection point of the titration plots.

Analyses were performed at the SRC laboratory with a Perkin-Elmer Plasma II inductively-coupled argon plasma emission spectrophotometer (ICP) and a Dionex 400i ion chromatograph (IC). The selected elements, detection limits, analytical method, and potential source minerals are shown in Table 23.1.

Data evaluation methods

All analytical data were initially subjected to the Grubb's Test (Taylor, 1990) to identify and eliminate outlying data. Arithmetic means were calculated for individual constituents and field measurements at each sample point and used to describe their down-gradient variation as well as to locate the contaminant plume. All S was assumed to be in sulfate (SO_4^{2-}) form.

To understand the chemical attenuation mechanisms, it is necessary to determine what minerals may precipitate or dissolve. This was accomplished by using computer simulations that predict the tendency of minerals to precipitate or dissolve by calculating their saturation indices (SI's). The validity of the mineral suite selected from such simulations can be subsequently examined by computer mass balance simulations that identify the combinations of dissolving and precipitating minerals that satisfy changes in concentrations of dissolved constituents in ground water between two points along a flowline.

The models selected for this task were WATEQ4F (Ball and Nordstrom, 1991) and BALANCE (Parkhurst et al., 1982). WATEQ4F is an equilibrium species distribution program that uses pH, Eh or dissolved oxygen, temperature, and concentrations of dissolved constituents to calculate SI's for minerals that might exist in a given solution.

$$SI = \log_{10}(IAP/K_{sp})$$

where

IAP = total ion activity products

and

K_{sp} = solubility product constant.

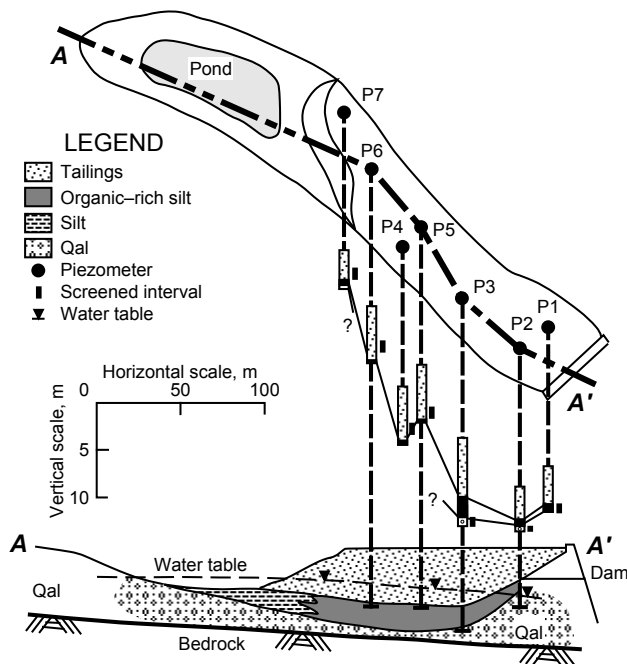


FIGURE 23.2—Plan view of primary impoundment and cross section of the tailings impoundment.

A positive saturation index for a mineral or solid compound indicates that there is more dissolution product from that mineral than would exist at equilibrium, and the mineral is, therefore, oversaturated and will tend to precipitate. A negative saturation index means that there is less dissolution product than would exist at equilibrium, and the mineral will tend to dissolve. A value of zero indicates saturation, but Nordstrom (pers. commun.) recommends that for many minerals values between -1.0 and +1.0 approximate saturation. For many secondary minerals, values between -0.1 and +0.1 approximate saturation. The model is reliable to an ionic strength of approximately 0.72 (Nordstrom, pers. commun.). The user must examine this list of minerals carefully and eliminate those that are unrealistic. For example, the program assumes all reactions are reversible and will often predict that feldspars are oversaturated, but feldspars will not form dominant

TABLE 23.1—Analyzed elements, analytical methods, detection limits, and probable sources.

Element	Symbol	Analytical method	Detection limit (mg/l)	Probable mineral source
aluminum	Al	ICP	0.01	silicate
calcium	Ca	ICP	0.0002	silicate, carbonate
chloride	Cl ⁻	IC	2	inclusion, interstitial
copper	Cu	ICP	0.01	sulfide
iron	Fe	ICP	0.01	sulfide, carbonate, silicate
potassium	K	ICP	0.1	silicate
magnesium	Mg	ICP	0.01	silicate
manganese	Mn	ICP	0.01	silicate, carbonate
sodium	Na	ICP	0.05	silicate
lead	Pb	ICP	0.05	sulfide
sulfur	S	ICP	0.1	sulfide
silica	SiO ₂	ICP	0.01	silicate
zinc	Zn	ICP	0.01	sulfide

silica precipitates under normal ground water conditions. Also the program does not consider the effects of a multiphase system and will produce a saturation index beyond the boundaries of a mineral's normal stability field in complex solutions.

After selection of the potential controlling phases at two different locations along the contaminant plume flowpath the program BALANCE was used to determine which suite of minerals (phases) explain mass balance changes of dissolved constituents between the two points. BALANCE solves a set of simultaneous equations that consist of numerical definitions of the compositions of the selected mineral phases; the amount of a component in a dissolving mineral must be appropriately balanced by that in a precipitating mineral(s). Phases can include ion exchange, and electrons are conserved and treated as a component in redox reactions. The model also performs calculations for situations where waters of two distinct compositions mix to form a third, composite water. The user can constrain the model by forcing it to include certain phases in all models considered, and the program can limit a phase as dissolve-only or precipitate-only. Often phases are never utilized in a simulation, indicating that they may not be an active participant in the system, and the list of potential precipitates and solutes can be reduced.

RESULTS AND DISCUSSION

Ground-water flow

The average hydraulic gradient within Qal (Fig. 23.3) indicates that ground water in Qal potentially flow southeastward from BKG through the impoundment and the confined valley. The mean elevation of the water table within the impoundment was arbitrarily assigned at the location of the tailings dam, because the slope between BKG-06 and the dam is nearly flat.

However, the mean gradient (dh/dl) between M1 and M5 is approximately 0.03 m/m. Given this gradient (dh/dl = -0.03 m/m) and estimates for stream gravel hydraulic conductivity (K = 10⁻⁴ m/s) and effective porosity (n_e = 0.35), the seepage velocity (v_s) of the ground water was estimated to be 9x10⁻⁶ m/s or 0.8 m/day by use of the following formula:

$$v_s = -Kdh/n_e dl \text{ (Fetter, 1980)}$$

Although seasonal variations of the water table and potentiometric levels were observed for all piezometers, concentrations of dissolved solids did not vary temporally. Water levels tend toward a maximum during May and attain a minimum between late September and December. Consistently higher heads from deep within the fractured bedrock system indicate that water flow is potentially upward from bedrock into overlying Qal.

Hydrochemical trends

Means of chemical parameters (pH, EC, Eh, HCO₃⁻, SO₄⁻², Al, Ca, Cl⁻, Cu, Fe, K, Mg, Mn, Na, Pb, Si, and Zn) for the study period are summarized in Table 23.2. Values that were less than detection limit were set to values equal to detection limit for all graphs. The values listed under the column heading TAILS in Table 23.2 are arithmetic means of B1, B2, P4, P5, and P6 values.

Because the contaminant plume was restricted to Qal, only samples from the tailings impoundment and wells in Qal upgradient and downgradient from the tailings dam were examined. Only one piezometer from each well nest was assumed to represent the

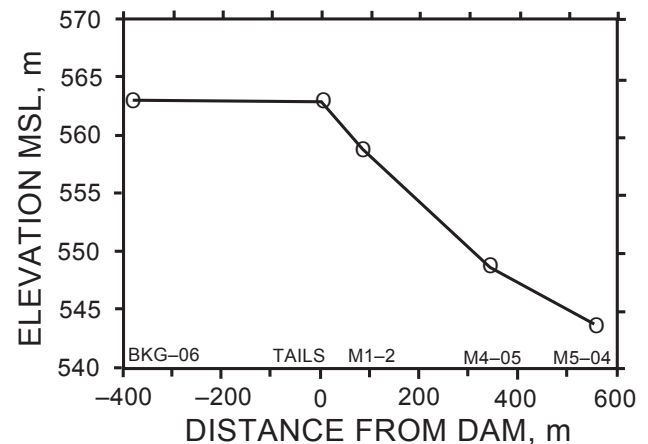


FIGURE 23.3—Mean water table elevation profile in Qal from BKG-06 on left side of graph through the impoundment (P1-P6), M1-2, M4-05, and M5-04.

plume. The selected piezometer at each well had greater amounts of dissolved constituents and other parameters suggestive of contaminants in the plume center. On this basis, hydrogeochemical trends were evaluated considering means for samples from BKG-06, TAILS, M1-2, M4-05, and M5-04, in downgradient sequence. Hydrogeochemical trends are illustrated on Figures 23.4 and 23.5. The value at distance 0 is a mean value from TAILS only; it does not include any values from Qal or lacustrine silt that underlie the impoundment.

As is illustrated in Table 23.2 and on Figures 23.4 and 23.5, all measured ground water parameters tend to return to background levels with increasing distance downgradient from the impoundment. Mean pH is moderately acidic (4.2) within the impoundment, but decreases to background level at 570 m downgradient. Mean Eh values indicate that the entire hydrogeochemical system in the impoundment and Qal is oxidized with an approximate value of 400 mV. Eh in impoundment pore water is only marginally higher than that in Qal. Al, Cl⁻, Cu, Fe, K, Pb, SiO₂, and Zn concentration are elevated within the impoundment, but also attenuate to within twice background concentrations at 570 m downgradient. However, Mg, Mn, and SO₄²⁻, which also attain significant concentrations in the impoundment, only attenuate to 4.1x, 14x, and 4.2x their respective background concentrations. Ca and Na concentrations in general increase downgradient, and at 570 m downgradient are 2.8x and 2.7x their respective background concentrations.

Inverse modeling

In the vicinity of the impoundment the probable path for ground-water flow from the tailings was from the topographic high at the northwest end of the site toward the topographic low at the southeast end through Qal. This pathway would mean that groundwater in Qal would flow from the northwest under, as well as into, the base of the impoundment. That portion of water flowing through the impoundment would mix with pore water infiltrating downward through the tailings. As this water escaped the impoundment at the southeast (downgradient) end it would then mix with groundwater from upgradient that had flowed under and around the impoundment. This contaminated groundwater would then continue to move downgradient to the southeast in Qal. Because the aquifer is confined by impermeable valley walls, transverse dispersion of any dissolved materials derived from tailings will be minimal. Downgradient dilution could occur, however, if deep-seated groundwater flowed upward through the underlying fault and discharged into Qal.

WATEQ4F simulations were conducted for points along the projected contaminant plume flowline only. Included were individual sample analyses rather than mean values for BKG-06, B1-5, B2-5, P4-5, P5-5, P6-5, M1-2, M4-05, and M5-04. Input data consisted of pH, Eh (v), alkalinity (mg/l HCO₃⁻), T (°C), and concentrations (mg/l) of Al, Ca, Cl⁻, Cu, Fe, K, Mg, Mn, Na, SiO₂, SO₄²⁻, and Zn. Measured Eh was used for all species distribution calculations. SI's are tabulated in Table 23.3 for all analyses in which the cation-anion balance was within approximately 10%.

Based on the mineralogy of the tailings and alluvium and the extensive presence of propylitized andesite, the most probable source minerals for dissolved ions are K feldspar, albite, anorthite, chlorite, and quartz. Quartz, the most common mineral in the impoundment, is non-reactive, and would probably not be a dom-

inant source of dissolved SiO₂. The sulfide minerals in the tailings that act as metal and SO₄²⁻ sources are chalcopyrite, galena, pyrite, and sphalerite. Because of the abundance of shells, the lake sediments are a source of aragonite and calcite.

A list of possible precipitate minerals for the entire profile in Qal was compiled from an examination of all acceptable WATEQ4F simulations. Any mineral that was oversaturated or saturated at any piezometer along the profile in the valley fill and that could form a stable precipitate was included in the tabulation. The results of WATEQ4F simulations for these mineral phases for BKG-06, P4-5, P5-5, P6-5, B1-5, B2-5, M1-2, M4-05, and M5-04 are summarized in Table 23.3. Few secondary sulfate, oxide, carbonate, or hydroxide minerals which incorporate Cu, Mg, Mn, Pb, and Zn were saturated or oversaturated; only anglesite, cerussite, magnesite, and rhodochrosite were at or above saturation in any of the WATEQ4F simulations.

Of these minerals, alunite [KAl₃(SO₄)₂(OH)₆] (Mason and Berry, 1968; Nordstrom and Ball, 1986), anglesite (PbSO₄) (Brookins, 1988), basaluminite [Al₂(OH)₁₀SO₄] (Nordstrom and Ball, 1986), jarosite(s) [(H₃O)Fe₃(SO₄)₂(OH)₆] [KFe₃(SO₄)₂(OH)₆] [NaFe₃(SO₄)₂(OH)₆] (Doner and Lynn, 1989), kaolinite [Al₂Si₂O₅(OH)₄] (Dixon, 1989), and melanterite (FeSO₄•7H₂O) (Mason and Berry, 1968) form under acidic conditions. Jurbanite (AlOHSO₄) (Nordstrom and Ball, 1986) forms above pH 4.5 from sulfate-dominated solutions. Allophane ([Al(OH)₃]_{1-x}[SiO₂]_x) (Wada, 1989; Earley and Jones, 1992), cerussite (PbCO₃) (Brookins, 1988), and gibbsite [Al(OH)₃] (Nordstrom and Ball, 1986) precipitate above pH 5. Magnesite (MgCO₃) (Doner and Lynn, 1989), montmorillonite(s) [Ca_{0.17}Al_{2.33}Si_{3.67}O₁₀(OH)₂] [(H,Na,K)_{0.20-0.42}Mg_{0.29-0.46}Fe_{0.23-0.34}Al_{1.68-1.47}Si_{3.93-3.82}O₁₀(OH)₂] (May et al., 1985), and rhodochrosite (MnCO₃) (Brookins, 1988) require neutral to alkaline and often supersaturated conditions to precipitate. Ferrihydrite [Fe(OH)₃] (Schwertmann and Taylor, 1989), gypsum (CaSO₄•2H₂O) (Brookins, 1988), and SiO₂(a) (Brookins, 1988) will form over a broad pH range.

Given this information and the SI's from Table 23.3, and assuming that solubility of minerals close to saturation (-1 to +1) may limit dissolved concentrations most effectively, one could interpret that Al concentration within the impoundment is limited by jurbanite, basaluminite, and kaolinite solubility, whereas downgradient no mineral solubilities clearly limit dissolved Al levels. Gibbsite commonly performs this function. Ca concentration in the impoundment is clearly limited by gypsum solubility; downgradient dissolved Ca concentrations appear to be limited by gypsum and calcite solubility. Dissolved Fe concentration may be limited by jarosite(s), melanterite, and ferrihydrite solubilities within the impoundment; no clear limiting mineral for downgradient Fe concentrations is indicated. Limits of K concentration in the impoundment by jarosite(s) solubility is apparent, but no limiting mineral is indicated downgradient. No Mg- or Mn-bearing precipitates within the impoundment were equilibrated or oversaturated. At the most downgradient sample point, however, magnesite and rhodochrosite appear to influence dissolved Mg and Mn concentrations, respectively. Na concentration does not appear to have any mineral control at any sample point. Pb concentrations in the impoundment are clearly limited by anglesite solubility; no mineral limitation downgradient is evident.

TABLE 23.2—Mean values for constituent characteristics of ground water samples (units are mg/l except as noted; -- indicates no value; * indicates completion in Qal).

	BKG-06*	BKG-20	BKG-43	TAILS	P3-9	M1-2*
pH	7.1	7.5	7.6	4.2	6.9	5.9
EC ($\mu\text{S}/\text{cm}$)	490	960	930	9200	2100	1000
Eh (mV)	400	210	220	440	220	410
HCO_3^{1-}	340	--	--	0	580	0
Al	0.21	0.23	0.30	700	0.43	0.84
Ca	140	47	36	470	380	480
Cl^-	5	4	5	200	--	--
Cu	0.05	0.05	0.05	79	0.08	0.24
Fe	0.77	0.93	0.64	10,000	10	260
K	2.3	2.3	2.6	47	2.0	14
Mg	29	27	19	1,800	130	280
Mn	0.03	0.15	0.03	130	0.85	31
Na	20	180	210	30	38	23
Pb	0.06	0.06	0.07	3.7	0.08	0.11
SO_4^{2-}	280	330	360	33,000	990	2800
SiO_2	31	22	22	68	57	50
Zn	0.11	0.08	0.07	1200	0.41	56
	M1-3*	M1-9	M2-04*	M2-06*	M2-12	M3-10
pH	7.1	7.1	6.4	6.5	6.9	7.2
EC ($\mu\text{S}/\text{cm}$)	1200	1300	1600	1400	1200	830
Eh (mV)	250	190	370	350	280	200
HCO_3^{1-}	--	--	240	--	--	--
Al	0.34	0.38	0.37	0.36	0.26	0.25
Ca	260	290	290	280	270	220
Cl^-	4	5	<2	8	8	7
Cu	0.08	0.05	0.05	0.07	0.07	0.05
Fe	14	13	1.2	4.5	1.4	3.40
K	3.5	3.2	6.5	6.2	2.2	2.2
Mg	79	71	96	91	66	37
Mn	5.6	3.5	22	22	4.7	2.00
Na	72	31	25	25	45	23
Pb	0.07	0.09	0.08	0.07	0.07	0.07
SO_4^{2-}	870	780	870	870	810	420
SiO_2	20	24	31	31	26	24
Zn	0.38	0.14	0.21	0.16	0.08	0.09
	M4-05*	M4-07	M4-10	M5-04*	M5-23	M5-53
pH	6.8	6.9	7.1	7.1	7.6	8.4
EC ($\mu\text{S}/\text{cm}$)	2400	1800	2600	1800	450	450
Eh (mV)	410	360	280	360	340	170
HCO_3^{1-}	480	--	--	440	--	--
Al	0.38	0.38	0.37	0.34	0.36	0.34
Ca	610	625	530	390	74	12
Cl^-	10	20	20	10	<2	<2
Cu	0.10	0.13	0.10	0.08	0.06	0.05
Fe	0.57	1.6	2.7	0.64	1.3	0.52
K	8.7	2.0	5.1	4.3	0.7	0.2
Mg	210	180	140	120	11	0.5
Mn	1.9	1.0	1.1	0.42	0.11	0.03
Na	30	59	210	53	100	120
Pb	0.09	0.09	0.08	0.07	0.06	0.06
SO_4^{2-}	2200	2100	2000	1200	290	170
SiO_2	41	35	46	33	28	14
Zn	0.39	0.12	0.12	0.16	0.14	0.09

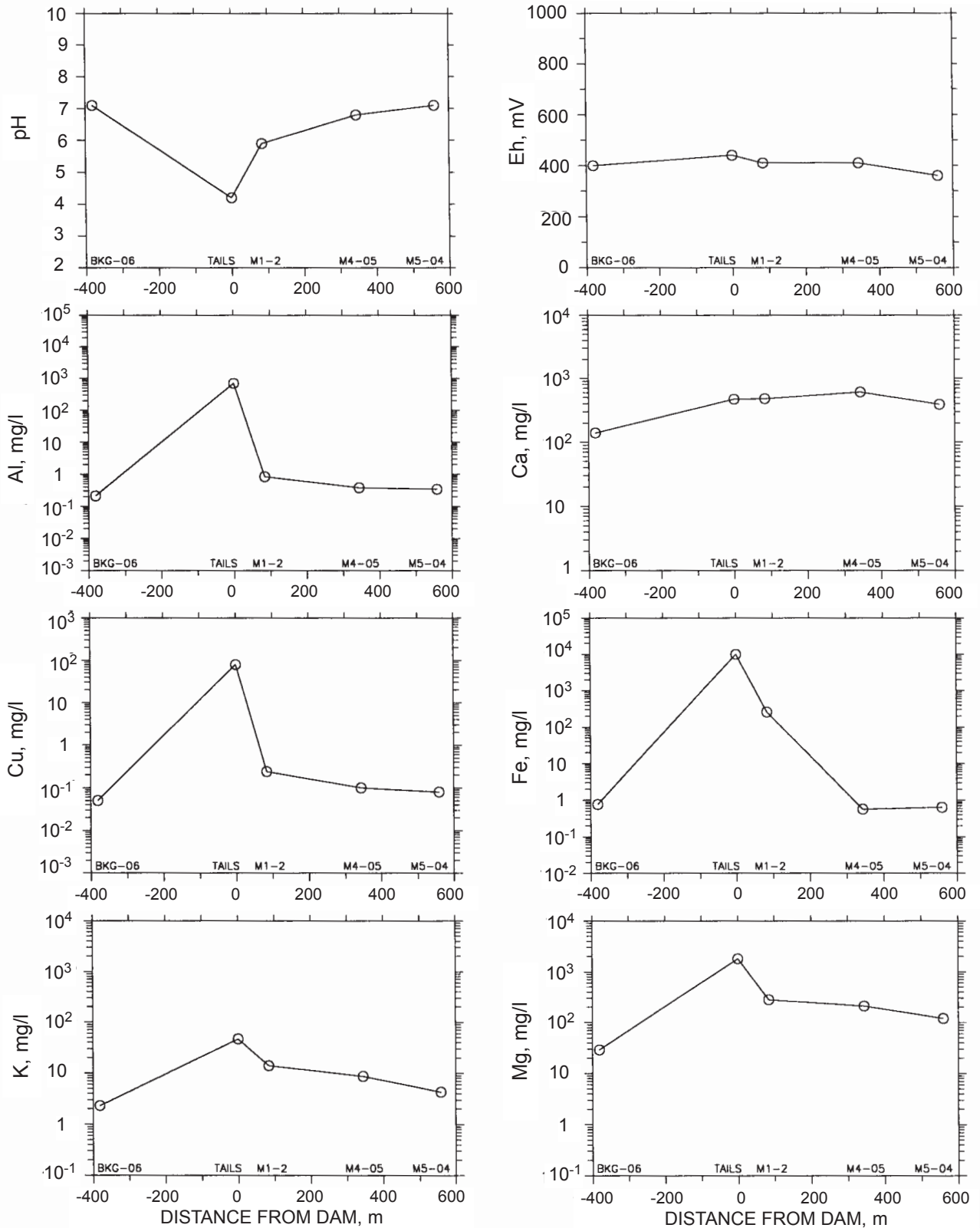


FIGURE 23.4—Variability of pH and Eh and concentrations of Al, Ca, Cu, Fe, K, and Mg along the flowpath.

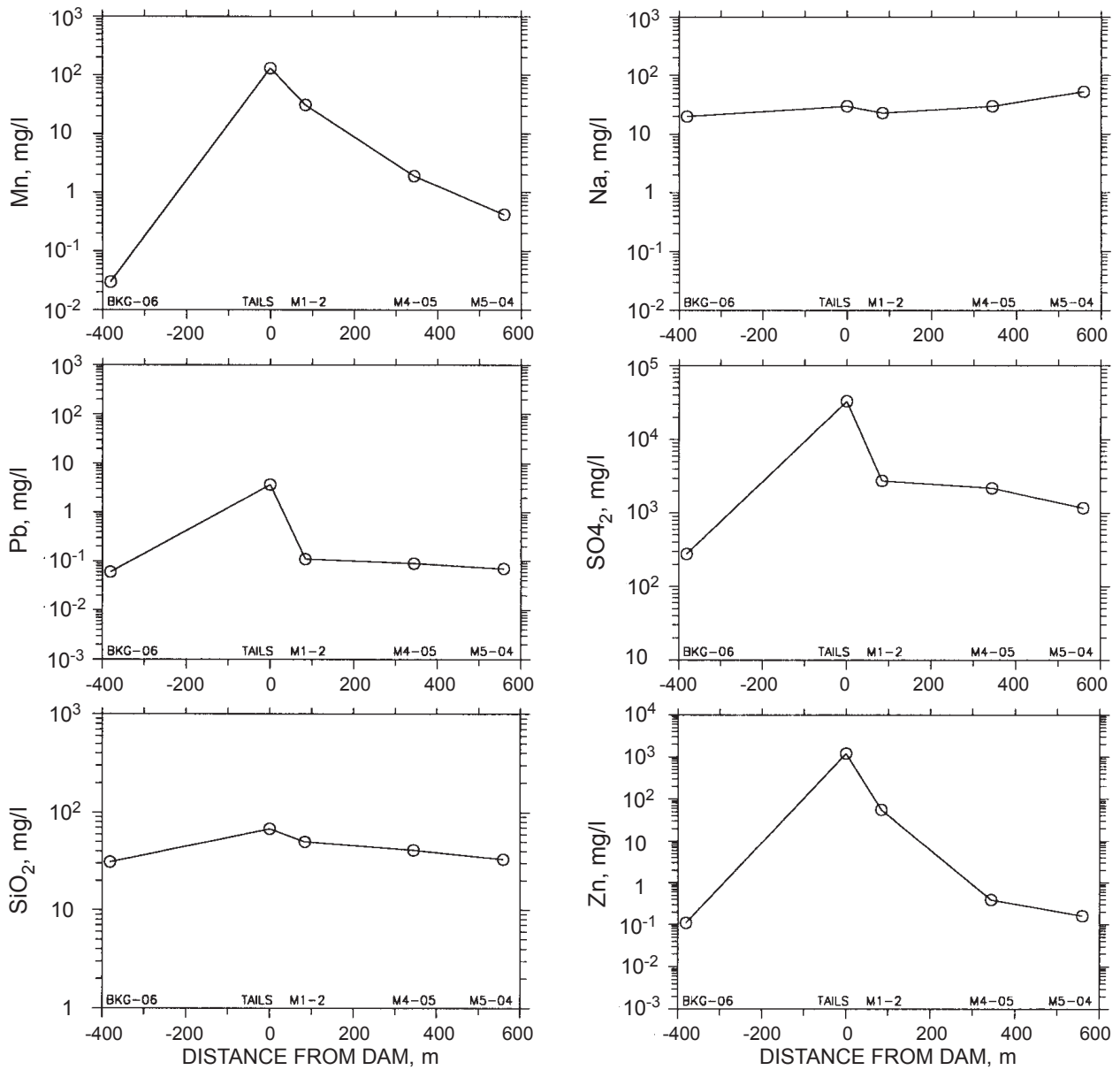


FIGURE 23.5—Variability of Mn, Na, Pb, SO₄²⁻, SiO₂, and Zn concentrations along the flowpath.

TABLE 23.3—Ion balances, ionic strengths, and SI's from WATEQ4F simulations. [Parentheses indicate mineral will probably not form a dominant phase under conditions sampled; values for minerals are saturation indices; NA indicates phase is not applicable]

	BKG-06		P4-5		P5-5		P6-5	
Ion bal. (%)	-3.2	-6.2	7.7	7.2	2.6	-4.2	-1.6	-3.3
Ionic strength	0.015	0.55	0.51	0.50	0.48	0.44	0.51	1.3
allophane	1.7	(0.56)	-0.46	-0.40	-0.50	-0.80	-0.59	-1.1
alunite	(3.5)	11	6.0	5.3	5.4	3.5	4.3	1.5
anglesite	-3.5	0.26	-0.40	-0.19	0.035	0.063	0.30	0.60
basaluminit	(8.4)	9.5	2.3	1.0	1.1	1.7	-1.0	-4.4
cerussite	-0.57		NA			NA		NA
ferrihydrate	3.5	1.2	-0.56	0.72	0.63	1.0	-1.4	0.36
gibbsite	3.1	(2.0)	-0.16	-0.53	-0.75	-0.56	-1.4	-1.9
gypsum	-1.0	0.27	0.070	0.16	0.10	0.18	0.25	0.50
jarosite-H	-7.2	-3.2	-5.6	-1.4	0.32	1.1	-4.9	-2.4
jarosite-K	(0.81)	4.4	0.80	5.0	5.5	4.3	0.21	4.2
jarosite-Na	-2.1	-0.16	-3.1	0.90	1.8	3.0	-3.5	-0.43
jurbanite	-2.3	2.2	1.4	1.8	2.0	2.0	1.8	-0.11
kaolinite	(8.8)	7.4	3.0	2.8	2.1	1.4	0.92	-0.35
magnesite	-0.90		NA			NA		NA
melanterite	-9.4	-0.74	-0.76	-0.79	-0.83	-0.91	-0.81	0.003
Ca-montmoril.	8.6	(7.0)	(1.4)	(1.6)	(0.37)	-1.0	-0.94	-2.3
montmoril.	7.1	(5.3)	(0.088)	(1.0)	-0.89	-2.1	-2.2	(1.9)
rhodochrosite	-2.2		NA			NA		NA
SiO ₂ (a)	-0.47	-0.03	-0.11	0.18	0.029	-0.48	0.090	-0.56
albite	(1.2)	-0.34	-3.6	-3.3	-4.8	-5.7	-5.2	-5.7
anorthite	(1.0)	-4.6	-11	-11	-13	-13	-14	-13
chlorite	-5.8	-20	-32	-33	-39	-40	-42	-32
calcite	-0.26		NA			NA		NA

	B1-5		B2-5		M1-02		M4-05		M5-04	
Ion bal. (%)	6.8	2.3	7.8	-6.1	2.2	11				-2.4
Ionic strength	0.80	0.091	0.093	0.097	0.061	0.060				0.043
allophane	-0.60	-0.82	-1.0	-0.87	0.48	1.7				(2.0)
alunite	4.3	-1.7	-1.5	2.0	(5.8)	(10)				(7.0)
anglesite	0.42	-0.066	-0.069	-0.081	-1.6	-1.7				-2.2
basaluminit	-2.5	-2.7	-7.8	-3.0	(6.6)	(6.6)				(12)
cerussite	NA		NA		NA	NA				0
ferrihydrate	-0.11	-1.6	-1.6	-1.3	5.3	2.0				3.3
gibbsite	-1.9	-1.7	-3.2	-1.8	1.8	3.7				3.7
gypsum	0.32	0.028	0.030	0.045	-0.95	0.009				-0.21
jarosite-H	0.32	-6.3	-4.4	-5.6	(4.8)	-6.5				-6.1
jarosite-K	5.7	-1.8	-0.60	-0.76	(12)	(0.90)				(1.8)
jarosite-Na	1.3	-5.0	-3.7	-4.4	(8.5)	-2.3				-1.1
jurbanite	1.9	0.99	0.45	0.95	-0.20	(0.96)				-0.78
kaolinite	-0.058	-0.080	-3.2	-0.32	(6.4)	(10)				(9.8)
magnesite	NA		NA		NA	-1.2				-0.59
melanterite	-0.51	-2.1	-2.1	-2.1	-5.9	-5.5				-6.2
Ca montmoril.	-2.1	-2.3	-6.2	-2.7	5.6	10				9.7
montmoril.	-2.6	-3.9	-3.3	-4.2	4.9	7.1				7.7
rhodochrosite	NA		NA		NA	-1.7				-0.93
SiO ₂ (a)	0.14	-0.11	-0.14	-0.15	-0.37	-0.42				-0.54
albite	-6.1	-6.3	-8.4	-6.6	-1.2	(1.1)				(1.5)
anorthite	-15	-15	-19	-15	-3.8	(0.75)				(1.9)
chlorite	-44	-47	-55	-47	-17	-10				(3.3)
calcite	NA		NA		NA	-0.24				0.39

However, Pb is strongly sorbed. Dissolved SO_4^{2-} concentrations in the impoundment as well as downgradient are limited by the solubilities of a variety of minerals including gypsum, basaluminite, jarosite(s), and jurbanite in the impoundment; the only evident limiting species downgradient is gypsum. SiO_2 concentrations along the entire flowpath are clearly limited by $\text{SiO}_2(\text{a})$ solubility. pH probably increases downgradient as a result of neutralization by the calcareous lake sediments and calcite in Qal; dilution may also contribute to pH increase. Increasing HCO_3^- downgradient may be caused by reaction with previously precipitated calcite as the acidic contaminant plume advances; concentration is limited by calcite solubility.

The precipitation controls between the TAILS and M5-04 appear to be a combination of pH increase induced by mixing as well as neutralization and oxidation. The tendency for ferrihydrite to be equilibrated to oversaturated suggests that precipitation of ferric Fe minerals is a key factor, and that oxidation and precipitation of redox-active species plays a major role in attenuation. A myriad of secondary, nonferrous base metal minerals are contained in the internal database of WATEQ4F. However, with the exception of anglesite and cerussite, no secondary minerals of Cu, Pb, or Zn were equilibrated or oversaturated. But from Figures 23.4 and 23.5, it is apparent that attenuation does occur. This suggests that coprecipitation with ferric Fe minerals plays a significant role during attenuation.

The flow segments in Qal selected for BALANCE simulations are impoundment (TAILS) to M1-2, M1-2 to M4-05, and M4-05 to M5-04. Mean component concentrations from Table 23.2 were utilized. Phases for each segment were selected as follows:

- 1) The list of stable phases as selected from WATEQ4F for the upgradient and downgradient endpoints of each segment of the flowpath was examined.
- 2) If, at either of the endpoints, a source mineral was equilibrated or undersaturated, that mineral was included in the BALANCE input for that segment and constrained to dissolve only. In a like manner, appropriate precipitates that were equilibrated or oversaturated were also included and constrained to precipitate only. Redox state (RS) was included in all models to maintain electron balance, and Ca/Na and Mg/Na exchanges were only included when required to obtain successful solutions. Very minor phases such as cerussite and anglesite were not utilized.

Ca and Mg often exchange for Na, and Na-bentonite was used for well completion. At BKG, mean Ca concentration in the deep piezometers relative to that in Qal was 2.5 mmol/l less; similarly, mean Mg concentration was 0.25 mmol/l less, while mean Na concentration was 7.8 mmol/l greater. The ideal Ca+Mg:Na exchange ratio is 1:2, a value similar to that from the wells, 1:2.8. Because exchange may have occurred, and because this may have in turn affected concentrations of other components, the analytical mean values of BKG-06 were used for the composition of all mixing simulations during mass balance modeling rather than those of the deep wells.

The BALANCE output file of successful models was then examined, and models that were unrealistic were rejected. The criteria for rejection are the relative amounts of silicate mineral dissolution derived for a model. If a model required more than 1 mmol/l dissolution of K feldspar, anorthite, or albite, a value in excess of their typical solubilities, it was rejected.

TAILS to M1

The segment between TAILS and M1 proceeds from an acidic environment through calcareous sediment to a circumneutral environment and may be characterized by:

- 1) pore water leaving the impoundment and flowing to M1 without mixing with upgradient water, or
- 2) pore water mixing with upgradient water.

The minerals precipitating may be common to an acid condition; they may be characteristic of a neutral condition; or they may be a mixture of both precipitate families. Ca concentrations increase slightly in this segment, and it is highly unlikely that significant quantities of anorthite are being dissolved by the pore water after it leaves the pond. Therefore, it is probable that the pore water is reacting with calcite in the calcareous sediment as it passes into Qal.

Four simulations were conducted:

- 1) without mixing with background water using calcite as a Ca source,
- 2) mixing using calcite as a Ca source,
- 3) no mixing utilizing anorthite as a Ca source, and
- 4) mixing using anorthite as a Ca source.

No solutions were achieved for simulations 1, 3, and 4 even with cation exchange included.

For simulation (2), 817,190 models were tested; 564 solutions were successful, and 374 of the models were acceptable requiring 48 different mixing ratios. Five mixing ratios provided most of the successful solutions: 1 part pore water to 5.74 parts background water (129 solutions); 1 part pore water to 5.73 parts background water (nine solutions); 1 part pore water to 6.76 parts background water (nine solutions); 1 part pore water to 11.9 parts background water (12 solutions); 1 part pore water to 8.45 parts background water (12 solutions). The ratio of 1:5.74 provided the greatest number of successful solutions and incorporated more phases in solutions. Other mixing ratios also used fewer precipitates and did not incorporate several key precipitates such as $\text{SiO}_2(\text{a})$, ferrihydrite, and gypsum into any acceptable solutions. The results of simulation (2) are shown in Table 23.4.

An examination of the preceding data indicates two distinct groups of models that define two different mechanistic pathways for attenuation. One group (50 acceptable solutions) relies on neutralization of acid pore water by calcite coupled with oxidation. These solutions incorporate calcite and O_2 consumption as well as gypsum precipitation and off-gassing of CO_2 . The second group of solutions utilizes a much lower consumption of calcite to neutralize acid pore water and precipitation of melanterite as an iron concentration control. Melanterite normally precipitates as an efflorescent salt during evaporative cycles and is highly soluble. In models which use melanterite, CO_2 off-gasses, but in lesser amounts than in the first pathway, and O_2 is consumed to a much lesser extent. Therefore, the pathway without melanterite is preferable. The dominant control for Ca and SO_4^{2-} in all solutions appears to be gypsum.

M1 to M4

In this segment there is no obvious point of mixing, but ground water could emanate from the fractures to mix with plume water. The average Ca content is greater at M4-05 than at upgradient

well M1–2; therefore, a source of Ca is needed. Again, the most feasible Ca sources are anorthite and calcite. Ca could be derived from anorthite dissolution within the Spill Impoundment. However, concentrations of Fe and SO_4^{2-} are not elevated downgradient from the Spill Impoundment. This indicates that the Spill Impoundment may not be the source of the elevated Ca concentrations. The author has assumed that the plume is equilibrated with any gypsum precipitated during early stages of plume evolution and that gypsum dissolution is not a Ca source. This is also consistent with declining SO_4^{2-} concentrations. The most logical source of Ca is calcite that forms the cement near the top of the capillary fringe in Qal.

Four simulations were conducted:

- 1) no mixing with anorthite as the Ca source;
- 2) mixing with anorthite as the Ca source;
- 3) no mixing with calcite as the Ca source; and
- 4) mixing with calcite as the Ca source.

Magnesite was included even though it is slightly undersaturated. Simulation (1) provided eight solutions from 8,008 possible models; none were acceptable. Simulation (2) provided 28 solutions from 11,440 possible models; none were acceptable. Simulation (3) provided only one acceptable solution from three successful models. Simulation (4) provided 14 successful solutions from 5,005 models, and five of these solutions were within acceptable silicate mineral dissolution limits. In all simulation (4) solutions, the mixing ratio was 3.35 parts M1–2 water to 1 part BKG–06 water. Solutions incorporated all secondary minerals except gypsum (which is consistent with gypsum equilibrium coupled with calcite dissolution) and chlorite. The results of simulation (4), which appear to be the most realistic simulation, are shown in Table 23.5.

All solutions generated during simulation (4) consumed 1.6 mmol/l oxygen. All CO_2 is in-gassing; approximately 2.5 mmol/l of additional CO_2 was required than was available from calcite dissolution. Given the high average partial pressure of CO_2 in typical soils, this is a possibility. However, magnesite, which is slightly undersaturated, was required for all solutions.

M4 to M5

As in the other segments, the hydrologic setting suggests this segment may be characterized by no mixing or mixing with water with the composition of BKG–06 water. However, no Ca source is required, because the Ca concentration decreases from M4–05 to M5–04. Also the SI's in Table 23.3 indicates that albite is slightly oversaturated at both M4–05 and M5–04, and anorthite is equilibrated at M4–05 and oversaturated at M5–04. Only chlorite is consistently undersaturated. Three simulation were conducted. Simulation (1) did not include albite, but did include exchange; no solutions were achieved. Simulation (2) involved no mixing, but included albite. Eight of 8,008 models were successful, but all required silicate mineral consumption in excess of 1 mmol/l; RS and O_2 had to be eliminated to achieve these solutions. Simulation (3) was a mix simulation that also required elimination of RS and O_2 and included albite. Fifty-seven successful solutions from 11,440 model combinations were derived; all required silicate mineral dissolution in excess of 1 mmol/l. None of the solutions for simulations (2) and (3) are realistic, because RS was not considered, excessive silicate dissolution resulted, and albite, an oversaturated phase, was required. Phases included in simulations (2)

and (3) are listed in Table 23.6.

The sequence of geochemical changes at this site as the acidic pore water discharges from the impoundment into the underlying ground water and flows downgradient is very similar to the scenario proposed by Morin et al. (1988) as the attenuation mechanism at the Nordic Main impoundment at Elliot Lake, Ontario. At Nordic Main, acid seepage with a composition similar to that at the project site is entering an underlying aquifer with a ground water velocity of approximately 1 m/day. The aquifer contains a trace amount of calcite particles, and neutralization of the plume begins immediately with postulated precipitation of a siderite-calcite solid solution mineral as well as gypsum, Al hydroxide minerals, and Fe hydroxide minerals. Adsorption and exchange are considered to be minor attenuation factors; substitution for Fe in siderite is thought to be the major attenuation mechanism.

SUMMARY AND CONCLUSIONS

An oxidizing, acid-producing tailings impoundment in north-central Washington State was characterized by installing monitor wells upgradient, within, and downgradient from the impoundment. Over a period of $2\frac{1}{2}$ years, samples were taken approximately every 5 weeks and analyzed for 12 dissolved constituents. pH, Eh, alkalinity, EC, T, DO, and water table elevation measurements were also made. Pore water discharges from the impoundment into the underlying ground water, but with the exception of Ca, Mg, Mn, Na, and SO_4^{2-} , all dissolved constituents attenuate to background concentrations within 570 m from the impoundment.

Through the use of two computer programs, WATEQ4F, an equilibrium species distribution model, and BALANCE, a mass balance computation model, a series of geochemical changes and reactions occurring along a ground water flowpath were characterized. WATEQ4F was used to predict saturation indices of minerals expected to be involved in a series of dissolution and precipitation reactions. BALANCE was then used to determine which mineral suites satisfied mass balance changes along the flowpath.

The geochemical events within and downgradient from the impoundment are as follows:

- 1) Dissolution probably occurs from meteoric water infiltrating into the tailings impoundment. The resulting acid dissolves K feldspar, albite, anorthite, chlorite, and other silicate minerals, adding to the contaminant load.
- 2) This acidic pore water discharges from the tailings impoundment and flows through underlying calcareous lake sediments into a gravel aquifer toward well M1 and is partially neutralized and oxidized. Calcite and possibly trace amounts of albite and K feldspar are dissolved, and the pH-sensitive mineral suite that precipitates is probably a mixture of alunite, gibbsite, montmorillonite(s), kaolinite, $\text{SiO}_2(\text{a})$, gypsum, ferrihydrite, jarosites, allophane, basaluminite, melanterite(?), and jurbanite. The pore water also mixes with approximately 5.7 parts upgradient water flowing under and around the tailings impoundment.
- 3) As the ground water continues flowing downgradient toward well M4 it encounters another source of calcium—possibly calcite in Qal—while mixing with 0.3 parts water from fractures below the Qal. Calcite and possibly trace amounts of albite and K feldspar dissolve, and montmorillonite(s), gibbsite, magnesite(?), $\text{SiO}_2(\text{a})$, and ferrihydrite precipitate.
- 4) The geochemical changes occurring farther downgradient

TABLE 23.4—Results of BALANCE simulation 2), TAILS to M1.

Phases used as ion sources and precipitates (- = phase can only precipitate; + = phase can only dissolve):									
ALUNITE	-	CO ₂ GAS	-	CHLORITE	+	GIBBSITE	-	K FELDSP	+
K-MONT	-	KAOLINIT	-	Mg-MONT	-	O ₂ GAS	+	ALLOPH	-
BASALUNT	-	Ca-MONT	-	FERRIHYD	-	JAROS-H	-	JAROS-K	-
JURBANIT	-	MELANTRT	-	Na-MONT	-	CALCITE	+	ALBITE	+

Preferred solutions (1 part initial water : 5.74 parts BKG water):

Without MELANTRT (50 Models)–	With MELANTRT (79 Models)–
No models utilized:	No models utilized:
CHLORITE	CHLORITE
All models utilized (mmol/l):	All models utilized (mmol/l):
ALBITE (<u>0.0661</u> –0.7133)	ALBITE (<u>0.0662</u> –0.8668)
CALCITE (12.4406–31.2227)	CALCITE (7.2790–13.6961)
CO ₂ GAS (17.2099–35.9906)	CO ₂ GAS (12.0052–17.4654)
GYPSUM (5.4320–23.9856)	K-FELDSP (<u>0.1317</u> –0.9323)
K-FELDSP (0.1315–0.8653)	MELANTRT (<u>0.0662</u> –0.8668)
O ₂ GAS (<u>4.6172</u> –4.6274)	

Note: Underlines indicate most frequent numerical solution.

TABLE 23.5—Results of BALANCE simulation 4), M1 to M4.

Phases used as ion sources and precipitates (- = phase can only precipitate; + = phase can only dissolve):											
ALBITE	+	Ca-MONT	-	CALCITE	+	CHLORITE	+	CO ₂ GAS	-	GIBBSITE	-
GYPSUM	-	K-FELDSP	+	K-MONT	-	MAGNESIT	-	Mg-MONT	-	Na-MONT	-
O ₂ GAS	+	SiO ₂	-	FERRIHYD	-						

Preferred solutions (3.35 parts initial water : 1 part BKG water):

No models utilized:	All models utilized (mmol/l):
CHLORITE	ALBITE (<u>0.3299</u> –0.4113)
GYPSUM	CALCITE (4.9540–4.9894)
	CO ₂ GAS (2.5405–2.5754) (All+)
	FERRIHYD (<u>3.6128</u>)
	K-FELDSP (<u>0.1787</u> –0.2601)
	MAGNESIT (0.8819– <u>0.9172</u>)
	O ₂ GAS (<u>1.6429</u>)
	SiO ₂ (0.8252–1.6022)

TABLE 23.6—Phases incorporated in BALANCE simulations 2) and 3), M4 to M5.

Phases used as ion sources and precipitates (- = phase can only precipitate; + = phase can only dissolve):											
ALBITE	+	ANORTH	+	Ca-MONT	-	CALCITE	-	CHLORITE	+	CO ₂ GAS	-
GIBBSITE	-	GYPSUM	-	K-FELDSP	+	K-MONT	-	MAGNESIT	-	Mg-MONT	-
Na-MONT	-	RHODOCHR	-	SiO ₂	-	FERRIHYD	-				

between M4 and M5 could not be characterized with computer simulations. BALANCE was unable to obtain solutions unless electron accounting was eliminated from consideration, and an oversaturated phase, albite, was used.

The fact that most secondary base metal minerals are undersaturated, but attenuate along the flowpath, indicates that coprecipitation in the form of replacement for Fe and Mn in oxyhydroxide precipitates is a major contributing attenuation factor. The preceding sequence of events needs now to be verified at the site, and additional hydrogeologic information is needed to verify and quantify mixing.

The apparent natural oxidation control at the site can be used to design a remediation procedure at this site. One could accomplish this by injecting air into saturated Qal downgradient from the impoundment to compress the precipitation of secondary Fe and other redox-active minerals into a shorter distance to prevent off-site transportation. This procedure will induce loss of pore volume and transmissivity and is most suitable as an interim rather than long-term remediation procedure. The preceding control method could be effective for redox species, but will have only a limited effect on many other dissolved SO_4^{2-} species.

REFERENCES

- American Water Works Association, 1985, Standard methods for the examination of water and wastewater: American Public Health Association, Washington, D.C., pp. 37–44 and 145.
- Ball, J.W., and Nordstrom, D.K., 1991, User's manual for WATEQ4F, with revised thermodynamic data base and test cases for calculating speciation of major, trace, and redox elements in natural water: U.S. Geological Survey Open-File Report 91–183, 188 pp.
- Blowes, D.W., Cherry, J.A., and Reardon, E.J., 1988, Field observations on the rate of geochemical evolution of tailings pore waters at the Heath Steele Mine, New Brunswick, Proceedings of the International Association of Hydrogeologists Symposium: Halifax, Nova Scotia, Canada, 12 pp.
- Brookins, D.G., 1988, Eh-pH diagrams for geochemistry: Springer-Verlag, New York, 176 pp.
- Dixon, J.B., 1989, Kaolin and serpentine group minerals; *in* Dixon, J.B., and Weed, S.B. (eds.), Minerals in soil environments: Soil Society of America Book Series No. 1, pp. 467–525.
- Doner, H.E., and Lynn, W.C., 1989, Carbonate, halide, sulfate, and sulfide minerals; *in* Dixon, J.B., and Weed, S.B. (eds.), Minerals in soil environments: Soil Society of America Book Series No. 1, pp. 279–330.
- Driscoll, F.G., 1987, Groundwater and wells: Johnson Division, St. Paul, Minn., pp. 719–728.
- Earley, D., III, and Jones, P.M., 1992, Geochemical effects on the hydrology of in-situ leach mining of copper oxide ore at the Cyprus Casa Grande Mine, Arizona, Proceedings of the 1992 Society for Mining Metallurgy, and Exploration Inc. Annual Meeting, Phoenix, Ariz.: Preprint no.92–242, 10 pp.
- Fetter, C.W., 1980, Allied hydrogeology: Charles E. Merrill Publishing Company, Columbus, Ohio, pp. 66–149.
- Lambeth, R.H., 1992, Hydrogeochemical characteristics of an unconsolidated aquifer downgradient from an oxidized, sulfidic mine tailings impoundment: Unpub. M.S. thesis, Eastern Washington University, Cheney, 140 pp.
- Mason, B., and Berry, L.G., 1968, Elements of mineralogy: W. H. Freeman and Company, San Francisco, Calif., pp. 347–374.
- May, H.M., Kinniburgh, D.G., Helmke, P.A., and Jackson, M.L., 1985, Aqueous dissolution, solubilities and thermodynamic stabilities of common aluminosilicate clay minerals—kaolinite and smectites: *Geochimica et Cosmochimica Acta*, v. 50, pp. 1667–1677.
- Morin, K.A., Cherry, J.A., Davé, N.K., Lim, T.P., and Vivuyurka, J., 1988, Migration of acidic groundwater seepage from uranium-tailings impoundments, 1. Field study and conceptual hydrogeochemical model: *Journal of Contaminant Hydrology*, v. 2, pp. 271–303.
- Moses, C.O., Nordstrom, D.K., Herman, J.S., and Mills, A.L., 1987, Aqueous pyrite oxidation by dissolved oxygen and by ferric iron: *Geochimica et Cosmochimica Acta*, v. 51, pp. 1561–1571.
- Nordstrom, D.K., 1982, Aqueous pyrite oxidation and the subsequent formation of secondary iron minerals; *in* Kittrick, J.A., Fanning, D.S., and Hossner, L.R. (eds.), Acid Sulfate Weathering: Soil Society of America Publication 10, pp. 37–56.
- Nordstrom, D.K., and Ball, J.W., 1986, The geochemical behavior of aluminum in acidified surface water: *Science*, v. 232, pp. 54–56.
- Nordstrom, D.K., and Munoz, J.L., 1986, Geochemical thermodynamics: Blackwell Scientific Publications, Palo Alto, Calif., 477 pp.
- Parkhurst, D.L., Plummer, L.N., and Thorstenson, D.C., 1982, BALANCE—A computer program for calculating mass transfer for geochemical reactions in ground water: U.S. Geological Survey Water Resource Investigation 82–14, 29 pp.
- Schuller, R.M., Gibb, J.P., and Griffin, R.A., 1981, Recommended sampling procedures for monitoring wells: *Ground Water Monitoring Review*, v. 1, pp. 42–46.
- Schwertmann, U., and Taylor, R.M., 1989, Iron oxides; *in* Dixon, J.B., and Weed, S.B. (eds.), Minerals in Soil Environments: Soil Society of America Book Series No. 1, pp. 379–438.
- Taylor, J.K., 1990, Statistical techniques for data analysis: Lewis Publishers, Chelsea, Mich., pp. 87–92 and 169.
- Wada, K., 1989, Allophane and imogolite; *in* Dixon, J.B., and Weed, S.B. (eds.), Minerals in Soil Environments: Soil Society of America Book Series No. 1, pp. 1051–1087.
- Williams, B.C., 1992, Comparison of multivariate statistics and the geochemical code WATEQ4F for water quality interpretation in acidic tailings: Unpub. Ph. D. dissertation, University of Idaho, Moscow, 164 pp.

Chapter 24

THE BEHAVIOR OF TRACE METALS IN WATER DURING NATURAL ACID SULFATE WEATHERING IN AN ALPINE WATERSHED

W.R. Miller,¹ R.L. Bassett,² J.B. McHugh,³ and W.H. Ficklin⁴

¹*U.S. Geological Survey, Box 25046, MS 973, Federal Center, Denver, CO 80225-0046*

²*University of Arizona, Department of Hydrology and Water Resources, Tucson, AZ 85721*

³*Retired;* ⁴*Deceased*

Pyrite oxidation in the upper part of Geneva Creek basin has impacted approximately 8 miles of upper Geneva Creek by natural acid drainage (NAD). The maximum concentrations of metals in stream waters for Fe, Mn, and Al are no more than 10 mg/l; Cu, Ni, and Zn are all less than 1 mg/l, and other metals are less than 0.01 mg/l. There are low-volume seeps and flows that exceed these concentrations, but their impact on stream-water chemistry of Geneva Creek is insignificant.

The study area is located in the Colorado Mineral Belt and is underlain by Proterozoic metamorphic and igneous rocks, and intruded by Tertiary felsic stocks with associated pyritic alteration. The naturally acidic waters draining the pyritic altered areas are similar in composition to some of the more familiar acid mine drainage (AMD) waters.

Oxygen-charged waters from snow and rain aggressively oxidize and dissolve pyrite, releasing H^+ , Fe^{2+} , SO_4^{2-} , and trace metals to the waters of the study area. Fe^{2+} is later oxidized forming hydrous iron oxides. The dominant source for trace metals in waters is disseminated pyrite in the pyritic-altered areas, particularly for Cu, Pb, Zn, Bi, Ag, and As.

The geochemical modeling program PHREEQE was used to determine speciation and state of saturation of the waters with respect to mineral phases. The dominant species are Fe^{2+} , Al^{3+} , Mn^{2+} , Zn^{2+} , Cu^{2+} , and Ni^{2+} which are all simple cations, mainly because of the low pH values of the waters. At the majority of sites, jurbanite controls the Al concentrations and ferrihydrite probably controls the Fe concentrations. At a few sites Cu and Zn minerals appear to control the Cu and Zn concentrations, but at most sites the Cu, Ni, and Zn concentrations are probably controlled by sorption onto precipitating hydrous metal oxides. The range of metal contents of waters and the processes controlling the concentrations of metals in water in the study area can probably be considered to be typical for other similarly altered and mineralized areas in the Front Range of Colorado underlain by geochemically similar rocks. The results of this study can contribute to establishing natural geochemical baselines for waters draining areas affected by AMD in many other areas of the Colorado Front Range.

INTRODUCTION

Currently, there is considerable interest in understanding chemical processes that take place in the surficial environment. This has come about mainly because the public has become increasingly concerned about the impact that processes such as acid rain and acid mine drainage (AMD) have on the environment. In a natural

setting, when water comes into contact with rocks and soils, chemical weathering is initiated, elements are released to the waters, and various processes control the mobility of elements soluble in water within the surficial environment. Most studies of chemical weathering are directed toward undisturbed natural settings in which weathering is driven by atmospherically derived water and CO_2 which generate low ionic-strength aqueous solutions as one end member (Garrels and MacKenzie, 1967; Cleaves et al., 1970). Currently another group of studies is investigating anthropogenic processes which generate waters such as acid rain and acid mine drainage as the other end member (Baldwin et al., 1978; Filipek et al., 1987; Nordstrom et al., 1990; Alpers and Nordstrom, 1991). Presently there is very little information on natural geochemical background values of species, particularly trace metals, and the processes which control the concentrations of these species in waters draining areas underlain by sulfide minerals and undisturbed by man.

There is a need, particularly in the western United States, for studies such as this in order to establish baselines for geochemical data of naturally occurring material from areas underlain by sulfide minerals. Recently Runnells et al. (1992) have summarized methods for estimating natural background chemistry. They used geochemical modeling for predictive purposes, but the role of sorption processes in the control of metals was not discussed. Determining natural background values of elements in naturally occurring material is necessary to establish a baseline for restoring the natural environment during remedial cleanup of AMD sites. In addition, these studies contribute to a better understanding of the processes responsible for controlling metal concentrations in water and the natural buffering capacity of a drainage basin impacted by acid drainage; therefore they are useful for designing remedial actions to improve water quality and limit AMD.

Streams draining the Central Mineral Belt (Fig. 24.1) in the Rocky Mountains of Colorado, traverse mineralized and extensively altered areas, some of which contain disseminated pyrite. As a result, pyrite exposed to oxygenated water is oxidized, and many streams draining these areas develop strong acidity. These stream waters have chemical characteristics similar to some surface waters classified as AMD, usually associated with coal strip mining or drainage from mine tailings containing sulfide minerals. These streams and the resultant natural acid stream chemistry are naturally occurring, with no significant influence from mining activities. We label these waters as natural acid drainage (NAD).

We have selected an alpine basin in the Front Range, Colorado, that is underlain by sulfide minerals in a relatively undisturbed

Geology and mineralization

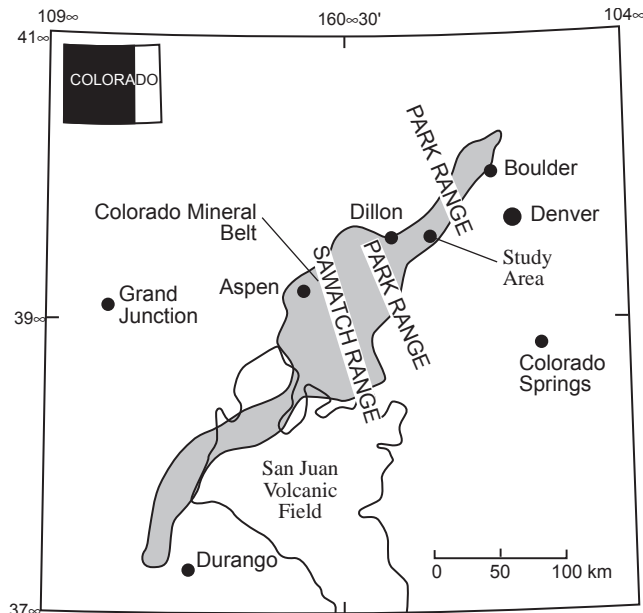


FIGURE 24.1—Map of the Colorado mineral belt showing location of the Geneva Creek study area.

natural setting. Chemical weathering in the upper basin generates acidic waters with $\text{pH} < 3.5$, which have similar characteristics to AMD waters. In the first part of our study (Bassett et al., 1992), we determined the major processes responsible for both the generation of the acid-sulfate waters and the low ionic-strength waters in the study area. This second part of our study is concerned with determining the range of trace-metal concentrations in the natural waters of the study area and with investigating the controls of the trace-metal concentrations in those waters.

SITE DESCRIPTION

The study area consists of the upper quarter of the Geneva Creek drainage basin (Fig. 24.2) which flows into the more extensive drainage system of the North Fork of the South Platte River. It is located approximately 75 km west-southwest of Denver, Colorado and is bounded on the west by the Continental Divide. Total area of the upper watershed is approximately 31 km² with moderate to steep relief. Elevations in the study area range from 3000 to 4000 m at the Continental Divide. About two thirds of the area is above timberline. Vegetation within the basin consists of tundra shrubs and plants above timberline. Engelmann spruce, Douglas fir, lodge pole, yellow and limber pine are the dominant trees in the lower part of the basin. Wetlands are common along Geneva Creek.

Average precipitation is approximately 760 mm/yr (U.S. Dept. Commerce, 1974). Snow is present usually 9 to 10 months in the year. The flow in Geneva Creek is perennial below the 3800 m level, but some small tributaries are intermittent within the study area. The stream flows are at a maximum during spring snowmelt and decrease to a minimum during the winter when many of the tributaries freeze and cease to flow. Flow at the lowest sampling point on the southeastern edge of the study area is about ten-fold greater than flow at the highest sampling point.

The geology of the drainage basin (Fig. 24.2) consists of Proterozoic basement rocks that mainly include a variety of gneisses generally considered to be correlative with the Idaho Springs Formation (Early Proterozoic). These rocks have been intruded and mixed with massive granite and pegmatite that are correlated with the Middle Proterozoic Silver Plume Granite (Lovering, 1935). The metamorphic rocks are fine to medium-grained granulites, gneisses, and schists, locally in migmatitic intergrowth with granitic rock. The dominant mineralogy is biotite, quartz, plagioclase, sillimanite, muscovite, and locally hornblende. The granitic rocks are irregular bodies of small dikes and plutons consisting of biotite-muscovite granite and pegmatite. The pegmatites consist of very coarse-grained biotite, quartz, and alkali feldspar. The petrology of the Proterozoic rocks is described in detail by Robinson et al. (1974).

These basement rocks have been intruded, particularly in the upper reaches of the Geneva Creek drainage, by Tertiary hypabyssal stocks, dikes, and sills with associated alteration and mineralization (Lovering, 1935). Most of the Tertiary intrusive rocks are part of the extensive "porphyry belt" of Eocene or younger rocks present in the Colorado Mineral Belt (Lovering, 1935). The intrusive rocks are aphanitic to very-fine grained calc-alkalic rhyolite and rhyolite porphyry consisting of felsic groundmass with sparse phenocrysts of biotite, feldspar, and quartz.

Sericitic, phyllic and propylitic alteration are associated with the Tertiary intrusive rocks in the upper basin (Fig. 24.2). Approximately 1% pyrite (Neuerburg et al., 1976) is associated with the phyllic alteration in the study area. In addition, a shear zone containing local zones of massive pyrite, is exposed in the cirque wall at the head of Geneva Creek. Gypsum and anhydrite, although not observed in outcrop, were noted in the Roberts water-diversion tunnel (which intercepts the subsurface of the study area) when phyllic-altered rocks were encountered (Warner and Robinson, 1967).

Mines and mine dumps

The Geneva mining district (Henderson, 1926), now considered part of the Montezuma mining district (Lovering and Goddard, 1950), is located in the upper part of the study area. Past mining has been limited. Veins were located in the 1870's and sporadic mining followed. The mineralization consists mainly of small lead-zinc-copper-silver veins which occur mainly in the upper part of Geneva Creek. Recorded production, mostly silver, is around \$100,000 (Jernegan, 1877). The only mine dump in the study area is associated with the Sill mine located in the cirque wall at the head of Geneva Creek. The drainage from the area of the dump is minor compared to other areas of the cirque. In addition, the quality of the waters from the dump area is similar or of better quality than drainage from many other parts of the cirque, particularly below rocks containing disseminated pyrite.

Wisconsin glaciation and formation of iron oxide deposits

The study area has been extensively glaciated and glacial features are abundant. The upper Geneva Creek basin is a Pinedale-age cirque. Medial, terminal, recessional and ground moraines are

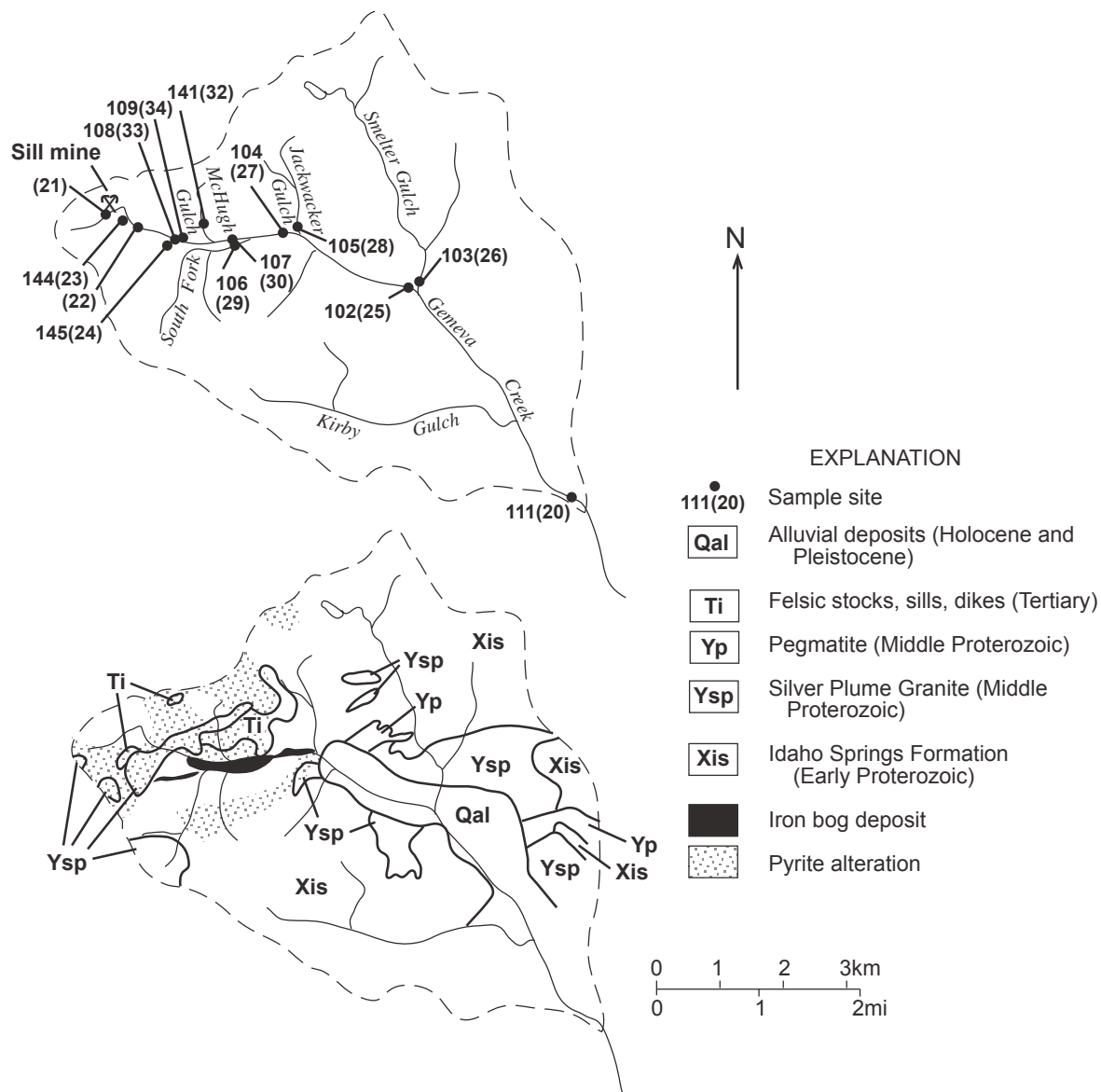


FIGURE 24.2—Map of the Geneva Creek study area showing site locations and geologic map after Lovering and Goddard (1950). Note that the 1990 sites are in parentheses.

present throughout the study area. Pinedale glaciation (late Pleistocene age) was at its maximum approximately 18,000 years ago (Richmond, 1965). The glaciers were in retreat approximately 12,000 years ago, and only minor modification of the topography has taken place since then. Acid drainage and the formation of iron oxide deposits present in Geneva Creek began during the melting of the glaciers and have proceeded since then. Large bedded iron oxide deposits (iron oxides consisting mainly of goethite and limonite) and iron oxide-cemented gravel, conglomerates and talus are present below the pyritic altered rocks. Pyrite, in or near the surface, is rapidly oxidized and removed from the rocks. Because of the steep to moderate relief, mechanical erosion is greater than chemical weathering, thus ensuring that fresh rocks containing pyrite continue to be exposed, continuing the process. Seeps with associated hydrous iron oxide precipitation occur at

the intersection of the lower slopes of the Geneva Creek cirque with the valley floor. In addition, hydrous iron oxide is precipitating along Geneva Creek, particularly below the pyritic altered areas and at the junctions of tributaries such as Smelter and Jackwacker Gulches (Fig. 24.2).

**SUMMARY OF THE FIRST STUDY
(BASSETT ET AL., 1992)**

In the first study, Bassett et al. (1992), mass balance-mass transfer modeling was used to determine potential pathways for reactions controlling the chemistry of the waters of the study area. By constraining the system to identified minerals and thermodynamically valid pathways, and considering the relative rates of dis-

solution, the most probable reaction pathways were determined. The results indicate that biotite, hornblende, plagioclase, pyrite and small quantities of calcite are most readily weathered. The predominant clay minerals are kaolinite, smectite, and vermiculite. Within the zone of pyritic alteration, dissolution of clay minerals provides silica to the waters. About one half of the acidity is buffered by calcite dissolution, even though calcite makes up less than 1% of the rock. Chemical weathering in the study area leads to two end-member type waters. The first type is mainly from tributaries draining areas with no or minor pyritic alteration and is a calcium-bicarbonate type water. The pH values are near neutral with measurable alkalinity. The second type of water is acidic with pH of 4 or less and is derived from areas containing pyrite. Mixing of these two types of water, leads to hydrous iron oxide and hydrous aluminum oxide and possibly sulfate flocculants that precipitate along Geneva Creek, particularly below the confluence of Geneva Creek and tributaries with low ionic-strength waters.

Waters from Smelter and Jackwacker Gulches are examples of calcium-bicarbonate type waters. These low ionic-strength calcium-bicarbonate type waters mix with and dilute the acid-sulfate water from Geneva Creek, and this process represents an important attenuation control on trace-metal contents and pH of waters from Geneva Creek.

METHODS

Samples of water, stream precipitates, iron oxide deposits, rocks, and soils were collected from 1979 to 1990. This study is limited to sets of water samples collected September 18–19, 1979 and July 25–27, 1990. Chemical analyses of samples from selected sites are shown in Tables 24.1 and 24.2. At each site, a 60-ml sample was collected by filtering through a 0.45- μm filter directly into a polyethylene bottle that had been rinsed with 10% HNO_3 . The sample was then acidified with nitric acid to $\text{pH} < 2$. An additional untreated 500-ml sample was also collected in a polyethylene bottle, after rinsing the bottle with the water that was to be sampled. In the 1979 set of water samples, an additional sample was collected by filtering through a 0.1 μm filter to determine if colloidal Fe or Al was passing through the 0.45 μm filter (Kennedy and Zellweger, 1974). A comparison of Fe and Al from the two filtered fractions indicated little or no difference between the two fractions. Subsequent sampling did not include the 0.1 μm filtered fraction. Temperature and pH were measured at each site. Alkalinity, specific conductance, SO_4^{2-} , Cl^- , and F^- were determined on the untreated samples within 30 days of collection. The remaining species were determined using the filtered and acidified sample. Major and minor elements were determined according to methods shown in Table 24.3. Trace metals were determined by graphite furnace atomic absorption spectrometry. Anions were measured with the ion chromatograph except for alkalinity (HCO_3^-), which was determined by titration with sulfuric acid in the laboratory. A complete set of the chemical analyses and analytical methods used for the analysis for water samples collected in 1979 are given in McHugh et al. (1988).

The stream waters are all oxidizing. Measurements of dissolved oxygen in the stream waters ranged from 6 to 8 mg/l, which is near saturated for the specific temperature of the water and elevation of the sample site. Eh measurements were made with a Pt electrode for samples collected during the July 1990 field work. The presence of dissolved oxygen is known to yield unreliable Eh

values so the redox potential was also estimated based on the classical O_2 - H_2O relationship and on the assumption that the water is in equilibrium with ferrihydrite.

Solid phases, which include precipitates, iron oxide deposits, soils, and rocks, were analyzed for chemical composition and mineralogy by X-ray fluorescence, X-ray diffractometry, and inductively coupled plasma atomic emission spectroscopy analysis after acid digestion (Lichte et al., 1987).

RESULTS AND DISCUSSION

Water chemistry

Water samples were collected in the study area September 1979 and July 1990. Therefore, seasonal variation in stream-water chemistry was not determined. Based on stream-flow records of the Snake River directly adjacent to the Geneva Creek basin, on the west side of the Continental Divide, the spring runoff period occurred in mid June in 1979 (USGS, 1980) and the second week in June in 1990 (USGS, 1991). The lowest flows usually occur from October to April. The variation in mean monthly discharge of the Snake River for the water years 1979 and 1990 is shown on Figure 24.3. Studies by past workers, such as Miller and Drever (1977), Baldwin et al. (1978), and a summary by Jeffries (1991), indicate that stream-water chemistry in the Rocky Mountains follows a general pattern with increase in dissolved constituents at the beginning of the spring runoff due to two processes:

- 1) flushing from the soil zone of salts which have built up by capillary action and evaporation during the winter; and

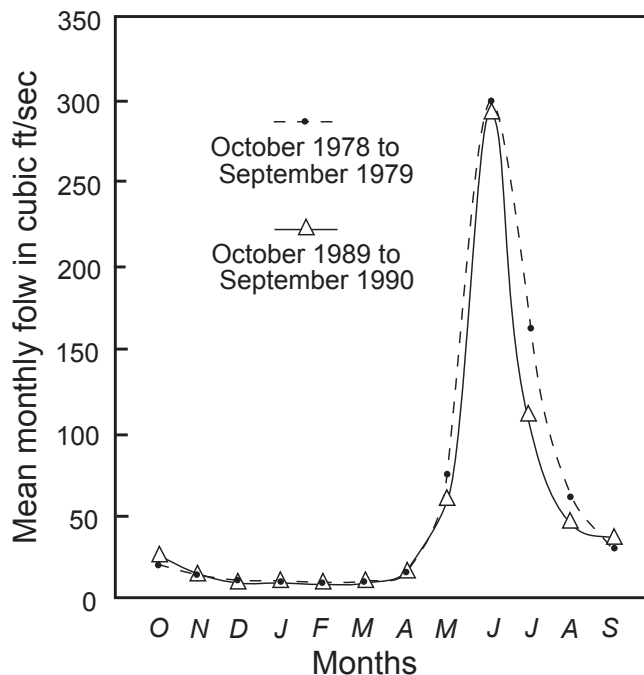


FIGURE 24.3—Variation in mean monthly discharge for the Snake River near Montezuma, Colorado for the water year 1979 (USGS, 1980) and 1990 (USGS, 1991).

TABLE 24.1—Chemical analyses of water samples collected in the Geneva Creek study area in September 1979.

Site no.	Sp. cond.	pH	Eh	Na	K	SiO ₂	SO ₄	F	Fe	Mn	Al	Zn	Cu	Mo	Ag	As	U	V
Stream waters																		
1	160	4.8	.51	1.7	1.1	13	54	0.15	0.6	0.56	2.7	180	10	1.7	0.06	<1	0.9	<5
2	90	7.1	.22	1.2	0.87	5.7	6	0.05	0.01	<.01	0.01	2	<1	1.8	0.07	<1	1.1	<5
3	340	3.6	0.68	1.9	1.2	16	97	0.22	2.7	0.92	6.8	320	44	2.1	0.06	1.7	0.7	<5
4	90	6.9	.21	1.2	0.56	4.2	20	0.15	0.52	<.01	0.01	2	<1	2.0	0.06	<1	1.8	<5
5	460	3.4	.70	2.0	1.3	20	136	0.34	6.3	1.2	9.4	420	62	1.6	0.06	2.1	0.5	<5
6	350	3.6	.66	1.6	1.2	15	90	0.25	5.9	0.70	8.4	360	17	1.7	0.07	1.3	0.2	<5
7	570	3.3	1.00	2.2	1.6	23	184	0.30	7.7	1.7	12.1	520	103	1.7	0.06	2.5	0.9	<5
8	115	4.9	.51	1.4	0.77	14	26	0.11	0.3	1.3	2.2	460	68	1.8	0.05	1.0	<.2	<5
10	230	3.8	.70	1.3	0.76	13	53	0.18	0.7	1.3	3.6	460	16	2.1	0.06	<1	<.2	<5
Ground waters																		
9	800	3.6	.60	2.1	3.2	38	370	0.71	68	2.6	29.2	820	400	1.9	0.06	17	3.5	18
11	2,520	6.1	.25	22	3.1	21	1,370	3.1	5.1	1.1	0.06	90	10	4.0	0.08	72	2.4	15
13	180	4.1	.72	1.1	0.75	14	50	0.10	0.16	1.0	4.1	410	42	1.5	0.06	<1	0.2	<5

Sample locations are indicated on Figure 24.2. Concentrations are in milligrams per liter except for Sp. cond. (specific conductance), which is in microsiemens; calculated Eh, which is in volts; and Zn, Cu, Mo, Ag, As, U, and V, which are in micrograms per liter.

TABLE 24.2—Chemical analyses of water samples collected in the Geneva Creek study area in July 1990.

Site no.	Sp. cond.	pH	Eh	O ₂	Na	K	SiO ₂	SO ₄	F	Fe	Mn	Al	Zn	Cu	Ni	As	Ag	Cd	Co	Cr	Pb
Stream waters																					
1	125	5.13	0.46	7	1.4	0.8	8	44	0.07	0.43	0.40	1.8	190	14	9	<1	<.05	1	5	1	<1
2	70	7.63	.13	7	1.1	0.7	4	5	<.05	0.01	0.01	<.1	4	1	<1	<.05	2	<1	1	1	1
3	225	3.83	.67	7	1.6	0.8	11	80	0.07	1.5	0.68	4.6	350	32	18	2	<.05	1	9	2	1
4	70	7.47	.12	6	1.2	0.5	5	16	<.05	0.03	0.01	<.1	6	<1	<1	<.05	4	<1	1	<1	<1
5	320	3.53	.70	7	1.8	1.0	14	73	0.25	4.2	1.0	7.0	520	55	21	3	<.05	<1	14	6	2
6	290	3.92	.60	7	1.4	0.9	12	53	<.05	5.6	0.54	6.1	400	15	12	2	<.05	<1	11	3	1
7	440	3.56	.66	7	1.7	1.1	17	120	<.05	8.0	1.5	10.0	680	110	31	4	<.05	4	19	5	6
8	140	4.44	.58	6	1.6	0.8	14	52	<.05	0.39	2.2	3.0	840	90	15	1	<.05	5	11	1	<1
10	190	3.98	.66	6	1.4	0.7	10	73	0.08	0.70	1.1	3.2	520	18	15	<1	<.05	4	5	1	7
12	195	3.87	.73	6	1.2	0.6	10	60	0.08	0.71	1.1	2.7	530	16	13	<1	<.05	4	4	1	4
14	95	4.60	.72	6	1.0	0.8	9	70	<.05	<.01	2.7	3.0	810	34	31	1	<.05	6	<1	1	<1
Ground waters																					
9	650	3.74	.57	<1	2.1	3.3	35	520	0.33	93	3.0	41.0	1,400	610	120	20	<.05	10	80	45	<1
11	1,900	6.93	.10	<1	21	2.7	21	490	2.50	6.6		1.1	0.1	<1	6	55	0.12	3	6	2	2
13	210	3.99	.67	6	1.2	0.8	11	70	<.05	0.24	1.7	5.0	660	34	19	1	0.05	4	7	5	<1

Sample locations are indicated on Figure 24.2. Concentrations are in milligrams per liter except for Sp. cond. (specific conductance), which is in microsiemens; calculated Eh, which is in volts; and Zn, Cu, Ni, As, Ag, Cd, Co, Cr, and Pb, which are in micrograms per liter.

TABLE 24.3—Analytical methods used for water analyses, Geneva Creek study area.

Constituents	Method	Reference
Sulfate and fluoride	Ion chromatography	Fishman and Pyen (1979)
Uranium	Laser-excited fluorescence	Scintrex Corp. (1979)
Specific conductance	Conductivity bridge	Skougstad et al. (1979), p. 545
Sodium, potassium, silica, aluminum, iron, manganese, and zinc	Flame atomic-absorption spectrophotometry	Perkin-Elmer Corp. (1976)
Arsenic, silver, vanadium, copper, molybdenum, cadmium, cobalt, chromium, nickel, and lead	Flameless atomic-absorption spectrophotometry	Perkin-Elmer Corp. (1977)

2) the tendency of the first snow melt to be enriched in dissolved solids.

This initial increase in the concentration of dissolved species in stream waters, is followed by dilution in concentration during the remaining spring runoff when the concentration of dissolved species reach a minimum, and a gradual increase in the concentration of dissolved species during the summer to a stable stream water chemistry baseline in late autumn and winter. Precipitation from thunderstorms in the summer and unusually warm weather in the winter cause fluctuations from the normal pattern. During spring runoff, even though the concentrations of species in water reaches a minimum, the total mass, of dissolved species in water reaches a maximum.

The major source for trace metals in the waters of Geneva Creek is disseminated pyrite present in altered rocks in the upper parts of the basin. The pyrite contains significant concentrations of Cu, Pb, Zn, Bi, Ag, and As (Table 24.4). Minor amounts of other sulfide minerals, particularly sphalerite and chalcopyrite, are present in the upper basin and the dissolution of these minerals is an additional source of trace metals.

TABLE 24.4—Chemical analyses of pyrite and altered rock with fine-grained pyrite.

Metal	Coarse crystalline pyrite	Altered rock with fine-grained pyrite
Ag	150	230
As	110	310
Bi	360	370
Co	5	8
Cr	4	5
Cu	850	220
Mo	<2	8
Ni	3	37
Pb	500	990
Sn	40	<10
Zn	410	380

Concentrations are in parts per million.

The trace-metal chemistry of water samples collected from Geneva Creek and tributaries in September, 1979 and July, 1990 is shown in Tables 24.1 and 24.2. There is little variation in concentrations of Ag, As, Pb, Mo, U, and V in the stream waters, but there is significant variation in Cu, Zn, Co, Ni, Fe, Mn, and Al (Tables 24.1 and 24.2). For the 1979 samples, there is a general increase in metal concentrations along the length of the stream, reaching a peak at site 7 for Cu, Zn, Fe, Al, conductivity, and minimum pH (Fig. 24.4). For the 1990 samples, Cu, Co, Ni, Fe, Al, and conductivity reach a peak at site 7. Zinc reaches a peak at site 8 and pH reaches a minimum at site 5 (Fig. 24.5). These sites, except for site 8, are along Geneva Creek where hydrous iron oxides are actively precipitating. Zinc reaches a maximum at the mouth of McHugh Gulch (Fig. 24.2) where the dissolution of a source mineral(s), probably sphalerite, contributes Zn to the water of this tributary. In addition to the stream waters, three ground waters were collected from the same sites in 9/79 and 7/90 (Fig. 24.2 and Tables 24.1 and 24.2). Site 13 is a spring at the base of a snow field in the upper part of the basin. This spring represents water of short residence time from the soil zone. The water is saturated with dissolved oxygen. Site 9 is a flowing bore hole that was

drilled into the iron oxide deposit. The deposit is probably tens of meters thick at this location. The pH was less than 4, which was similar to the surface waters in the vicinity, but the water did not contain detectable dissolved oxygen. The water from the bore hole contains high concentrations of Cu, Zn, Cd, Ni, Co, Cr, U, Fe, and Al (Tables 24.1 and 24.2) compared to the stream waters. Site 11 is flowing water from a drill pipe. The hole is drilled into the iron deposit, but is much deeper than the bore hole, and probably intercepts quartz-monzonite basement rock below the iron oxide deposit. The water does not contain detectable oxygen, and the pH is near neutral. The water from the drill hole generally contains high concentrations of major elements and As, compared to stream waters (Tables 24.1 and 24.2), but low concentrations of other metals, probably because of the near-neutral pH.

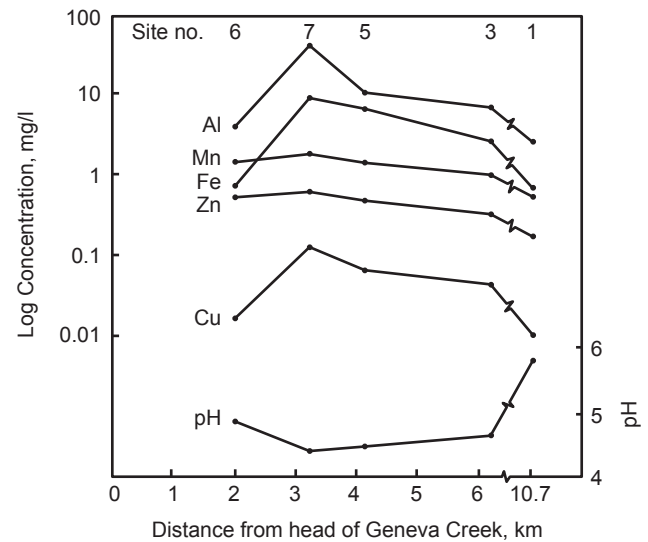


FIGURE 24.4—Profile of the change in pH and concentrations of dominant trace metals along Geneva Creek beginning at the source for samples collected in September 1979.

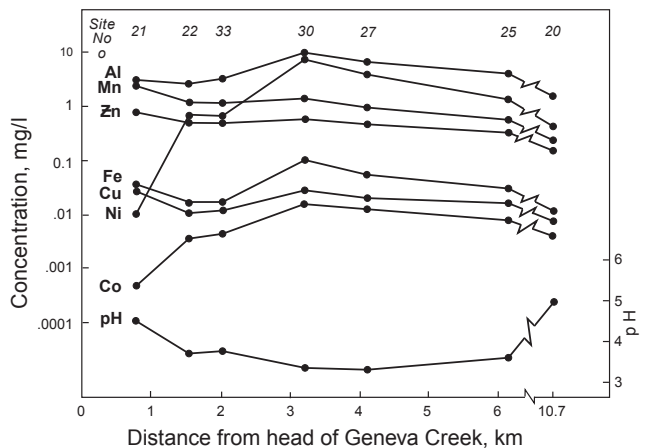


FIGURE 24.5—Profile of the change in pH and concentrations of dominant trace metals along Geneva Creek beginning at the source for samples collected in July 1990.

Changes at A Junctions

Within the study area, major areas of active hydrous iron oxide precipitation occur along the upper part of Geneva Creek where ground waters from springs and seeps emerge along the base of changes in slope. The main area is the base of the Geneva Creek cirque. Precipitation also occurs along Geneva Creek, particularly below the junctions of Geneva Creek with tributaries. Changes in major and trace-element chemistry occur at these junctions as a result of mixing of the streams. These changes were investigated for the junction of Geneva Creek with the South Fork of Geneva Creek (South Fork). Because flow rates were not determined, calculations of relative volumes of Geneva Creek and the South Fork were made using a mass-balance approach. The annual flow of the drainage depends on the annual precipitation which falls within the basin. Type, distribution, and amount of vegetation are similar in both basins. Also both basins are similar in size and physiography. If it is assumed that both drainage basins receive equal proportions of precipitation, and the amount and rate of release of this precipitation is similar, then the relative flow of the stream is dependent on the area of the basin. Therefore, at the junction of the South Fork and Geneva Creek, the relative flows above the junction for the two streams are equal to the relative areas of the two drainage basins above the junction.

Areas were calculated, digitally, using GSMAP (Selner and Taylor, 1993). The areas of Geneva Creek and the South Fork, above the junction, is 3.63 km² and 4.20 km², or 46% and 54% relative area above the junction, respectively. Using these percentages, we calculated the concentration of a species below the junction (see example below). This number can then be compared to what was measured, and the change, if any, determined. Table 24.5 shows the results of these calculations for the September 1979 and July 1990 samples (Tables 24.1 and 24.2). As an example of the calculations for the July 1990 data set, SiO₂ concentrations in stream waters for Geneva Creek and the South Fork above the junction are 17 mg/l and 12 mg/l respectively. We can calculate the amount of SiO₂ below the junction by a mass balance of: .46 (17) + .54 (12) = 14.3 mg/l. This number can be compared to the measured value below the junction (site 5, Table 24.1) of 14 mg/l. The calculated and observed values are equal within analytical limits, therefore no change has taken place in SiO₂ as a result of the mixing of the two streams. Similarly, calculations were made of other species for both the 1979 and 1990 sample sets. We have generally used two or three significant figures in the calculations. Because of analytical error, this may not be justified. The results of gain or loss, particularly <5% or <10% for trace metals, is considered not warranted and is shown as no change in Table 24.5.

This junction represents the mixture of two acid-sulfate type waters. Based on calculations of samples collected in September 1979, there is little or no change in most species. The exceptions are a net loss of Fe (6%) and Al (7%). The amounts are minor, and may be less than analytical precision. The results are not surprising because both streams are acid-sulfate type waters and similar in chemical composition.

For the July 1990 sample set (Table 24.5), there is no change in many of the species, but there is a net loss in SO₄ (13%), Fe (37%), and Al (11%). These results indicate that significant Fe is precipitating below the junction as well as minor Al and SO₄.

We observed that fresh hydrous iron oxide was precipitating below this junction at this time of year. XRD analysis of precipi-

tates collected below this junction identified very poorly crystallized ferrihydrite. The Al loss is best explained by precipitation of aluminum hydroxide or a hydrous aluminum-sulfate complex. Al was identified chemically, but no Al phase was identified by XRD analysis. There is minimal to no loss of Cu and Zn below the junction for either sets of data.

We observed that abundant precipitation of hydrous iron and aluminum oxides was occurring along Geneva Creek in July, 1990, below the junction of Jackwacker Gulch and Smelter Gulch. At these two junctions, acid-sulfate type waters of Geneva Creek are mixing with low-ion strength waters of Jackwacker and Smelter Gulch. The data does not allow the calculation of losses of dissolved species in water occurring below these junctions, but the precipitation of hydrous iron and aluminum oxides is significantly greater than below the junction of the South Fork and Geneva Creek.

TABLE 24.5—Changes in species above and below junction of Geneva Creek with the South Fork. [Concentrations are in milligrams per liter except for Zn, Cu, As, U, Ni, and Co, which are in micrograms per liter]

Species	Calculated amount	Measured amount	Change
Samples collected September 1979			
K	1.36	1.32	no
SiO ₂	19	20	no
SO ₄	133	136	no
Fe	6.7	6.3	6% decrease
Mn	1.2	1.2	no
Al	10.1	9.4	7% decrease
Zn	430	420	no
Cu	57	62	no
As	1.9	2.1	no
U	0.5	0.5	no
Samples collected July 1990			
K	1.0	1.0	no
SiO ₂	14.3	14	no
SO ₄	84	73	13% decrease
Fe	6.7	4.2	37% decrease
Mn	1.0	1.0	no
Al	7.9	7	11% decrease
Zn	529	520	no
Cu	59	55	no
Ni	21	21	no
Co	14.7	14	no

CHEMICAL MODELING OF THE WATERS

To gain further understanding of processes such as speciation of elements, redox conditions, and identification of minerals that may control concentrations of elements in the waters, chemical modeling of the waters using PHREEQE (Parkhurst et al., 1980) was carried out. The chemical modeling program, PHREEQE, assumes mineral-solution equilibrium. One problem associated with chemical modeling is that kinetic effects are not taken into account, and many reactions are inhibited by kinetic effects. These effects may be enhanced by low temperatures such as those encountered in the Geneva Creek basin.

As stated before, all stream-water samples were saturated or near saturated with respect to dissolved oxygen at the temperature

of the water and elevation of the sample site. Of the three ground-water samples, the spring below the snow field, site 13 (Fig. 24.2) is saturated with respect to dissolved oxygen, indicating a short residence time for the water, and that the source for the water is melting snow which infiltrates the soil zone above the site. The dissolved oxygen content of water from the flowing bore hole and the drill pipe was less than 1 mg/l. During the July, 1990 sampling, Eh was measured using a Pt electrode following the procedures of Nordstrom et al. (1979). In addition to the measured values, Eh was calculated using PHREEQE by:

- 1) Using the measured dissolved O₂ and the O₂/H₂O couple and
- 2) Assuming equilibrium of the water with ferrihydrite (Tables 24.1 and 24.2).

Eh values calculated from the O₂/H₂O couple are significantly higher than Eh values measured with a Pt electrode or calculated based on mineral-solution equilibrium with ferrihydrite, similar to the findings of Nordstrom et al. (1979). Although dissolved O₂ in the water is near or in equilibrium with O₂ in the atmosphere, the O₂/H₂O couple is not in equilibrium with the couple controlling the Eh.

As Nordstrom et al. (1979) pointed out, acid waters are well suited to reliable Eh measurements using a Pt electrode because of the high concentrations of Fe species. Therefore, for the acid-sulfate waters in the study area, measured Eh values are probably reasonable estimates for Eh; but for streams with low dissolved solids such as Smelter Gulch, measured Eh is probably not a good estimate. The results of calculated Eh, assuming mineral-solution equilibrium of the waters with ferrihydrite, compare favorably with the measured values of Eh using the Pt electrode (Table 24.6), indicating that ferrous-ferrihydrite couple is probably controlling the Eh, similar to the findings of Nordstrom et al. (1979). In the study area, the acid-sulfate waters show close agreement between calculated and measured Eh except for site 14B, the uppermost site along Geneva Creek. Differences also occur at sites 11, a flowing drill pipe with near-neutral pH, and sites 2 and 4 with low ionic-strength waters. The calculated Eh based on equilibrium with ferrihydrite was used for the chemical modeling.

TABLE 24.6—Measured Eh using a Pt electrode and calculated Eh assuming equilibrium with ferrihydrite for waters collected in July 1990.

Site	Eh measured (mV)	Eh calculated (mV)
1	530	460
2	460	130
3	670	670
4	450	120
5	610	700
6	660	600
7	660	660
8	580	580
9	490	570
10	620	660
11	360	100
12	670	730
13	720	670
14	590	720

The calculated Eh values for the samples collected in July 1990 ranged from 104 to 717 mV (Table 24.2). The lowest calculated Eh value of 104 mV occurs at site 11, the flowing drill pipe. The hole was drilled during evaluation of the area for porphyry

Mo deposit potential in the early 1970's, and the water from the drill pipe probably represents water with the deepest and longest residence time in the study area. The most oxidizing Eh value occurs at site 12, in upper Geneva Creek below the Geneva Creek cirque, where significant inflow from seeps occurs at the base of the slope. Oxidation of disseminated pyrite occurs above this site.

Based on the chemical modeling using PHREEQE, the dominant species in waters in the study area for the most abundant trace metals are Fe²⁺, Al³⁺, Mn²⁺, Zn²⁺, Cu²⁺, and Ni²⁺, all simple cations, mainly because of the low pH. Other species become dominant at a few sites, particularly at higher pH values.

Saturation indexes were calculated for a suite of minerals to determine if concentrations of trace metals in water were controlled by mineral phases. The saturation index is a convenient means of expressing saturation states of minerals (Barnes and Clarke, 1969) where:

$$SI = \log^{10} IAP/K_T$$

In the expression, SI is saturation index, IAP is the ion activity product, and K_T is the equilibrium constant of the dissolution reaction at the temperature in question. We considered mineral phases supersaturated at saturation index (SI) > 1, near saturation at SI = -0.3 to -1 and 0.3 to 1.0, and saturated at SI = -0.3 to 0.3.

The results of the saturation state of waters collected in July 1990, with respect to a suite of minerals, is shown on Figure 24.6. The waters from sites along Geneva Creek are saturated or near saturated with respect to jurbanite (Al(SO₄)OH • 5H₂O), which suggests that concentrations of Al in Geneva Creek are controlled by jurbanite. Nordstrom (1982a), also concluded that under acidic conditions, such as acid mine waters, there is an increasing tendency to form jurbanite. The only waters not in equilibrium with jurbanite are at sites 2 and 4, the two tributaries with low ionic-strength water that have pH values near neutral and Al < 0.1 mg/l, and site 11, the flowing drill hole with pH near neutral and Al = 0.1 mg/l. At these three sites, Al may be controlled by Al(OH)₃ (site 4), boehmite, gibbsite, or halloysite (site 2), and boehmite or gibbsite (site 11). The saturation state of alunite was not considered because of kinetic inhibitions of alunite precipitation at low temperatures (Nordstrom, 1982b).

All the waters of the study area are saturated or nearly saturated with respect to chalcidony, suggesting that chalcidony controls the SiO₂ concentrations of the waters. At site 24, water from the flowing drill pipe, represents the deepest water from the basin, and is saturated or near saturated with respect to calcite. This supports one of the conclusions, in the previous paper (Basset et al., 1992), that calcite present at depth is responsible for buffering much of the acidity in Geneva Creek as it flows from the headwaters downstream. The waters at this site are also saturated with respect to gypsum (present in the altered rocks within the study area), gibbsite, boehmite, anhydrite, fluorite, siderite, cuprite, and ZnSiO₃ (Fig. 24.6). Most of the waters of the study area are highly supersaturated with respect to goethite and jarosite, so these minerals appear to have little control on iron, aluminum, and sulfate concentrations. It was assumed that the waters are in mineral-solution equilibrium with respect to ferrihydrite which would control the Fe²⁺ content of the waters. This assumption appears to be valid for the acid-sulfate type waters.

At a few sites, waters are near saturation with respect to Cu and Zn minerals, suggesting that these minerals control the concentrations of Cu and Zn in the waters at these sites. These include

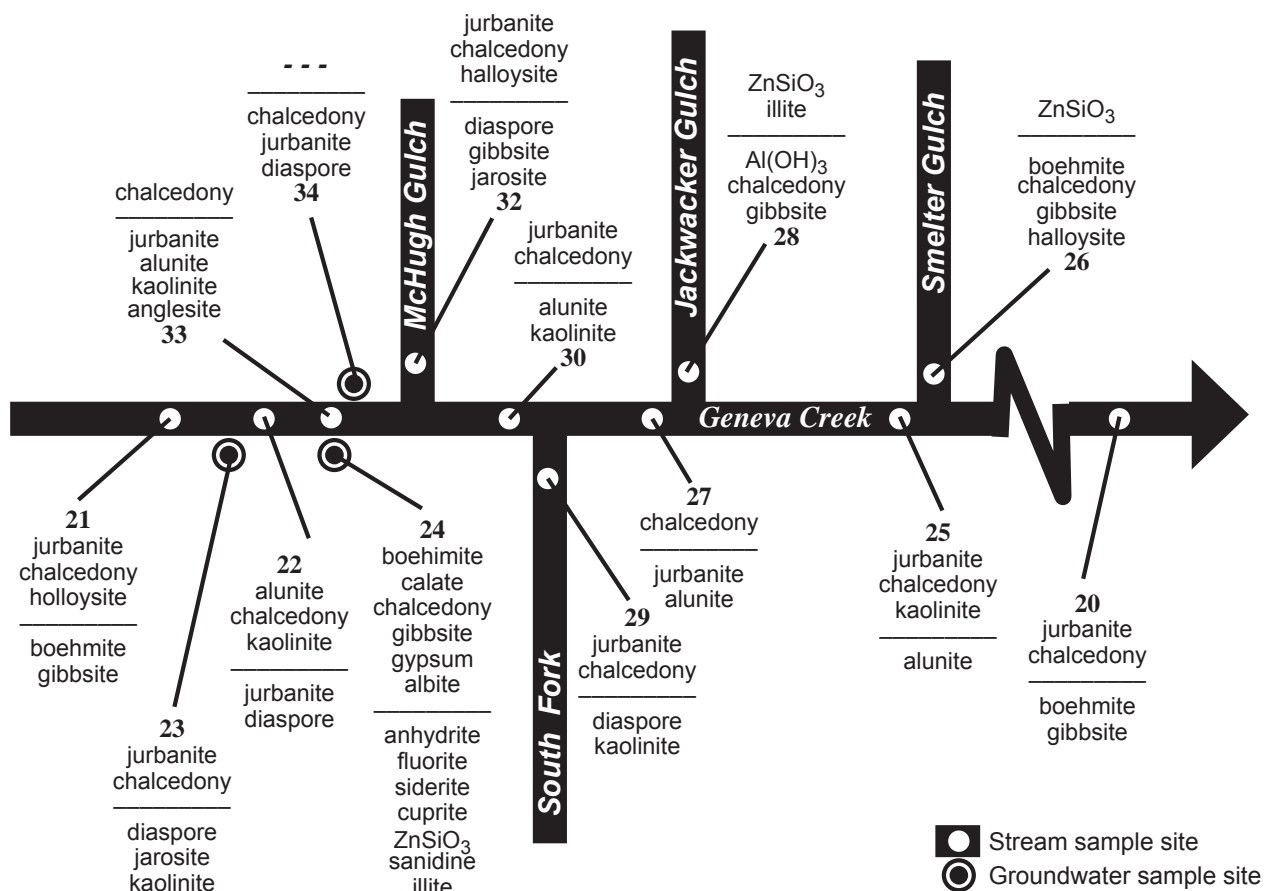


FIGURE 24.6—Saturation state of waters with respect to mineral phases, for samples collected in July 1990. The waters are saturated (SI = -0.3 to 0.3) with respect to minerals above the horizontal line and near saturation (SI = -1.0 to -0.3 and 0.3 to 1.0) for minerals below the horizontal line.

cuprite and ZnSiO₃ at site 11, Cu(OH)₂ and ZnSiO₃ at site 2, and ZnSiO₃ at site 4. At all the other sites, the concentrations of these metals is less than what is predicted by the chemical modeling, suggesting that the concentrations of Zn and Cu in most of the waters of the study area, are probably controlled by sorption onto precipitating hydrous iron oxides. The most ubiquitous precipitate throughout the area is hydrous iron oxide which we identified by XRD as poorly crystalline ferrihydrite. Ferrihydrite probably plays a major role in limiting the concentration of Cu and Zn. The ferrihydrite precipitates are very fine grained, which suggests high surface areas and high adsorption capacities for trace metals. Reddish-colored flocculated material, which appears to be hydrous Fe oxide, also occurs suspended in the stream waters. Cation sorption by ferrihydrite is pH dependent, increasing significantly with increasing pH. Other factors influencing sorption processes are specific metal species and presence of other ligands such as dissolved organic carbon that may interfere with metal sorption. Dzombak and Morel (1987) have comprehensively reviewed adsorption processes in aquatic systems.

Metal contents of precipitates collected in the study area are shown in Table 24.7. Ag, Cd, Mo, Co, Ni, and Pb are generally very low or not detected, suggesting that these metals occur in low concentrations in the stream waters or that ferrihydrite is not con-

trolling concentrations of these elements in the stream waters of the study area. As, Cr, Cu, and Zn are present in the precipitates, suggesting that the precipitation of ferrihydrite has some control on the concentration of these elements in the waters. Not enough information is available to quantify the influence of these precipitates on the concentrations of As, Cr, Cu, and Zn in the waters. The controls on the concentrations of Ni is not known, but sorption onto Mn oxides and(or) organic material may play a role. Mn oxides and organic material are not as ubiquitous as the hydrous iron oxides but are present in the basin.

SUMMARY

Geneva Creek headwaters begin along the east side of the continental divide, as melting snow fields coalesce to form upper Geneva Creek. When Geneva Creek reaches the base of Geneva Creek cirque, its inflow volume is approximately doubled from seeps at the base of the cirque. As Geneva Creek continues eastward from the Continental Divide, tributaries fed by seeps and melting snow fields contribute to the flow of Geneva Creek.

Rain and snow which falls in the study area, infiltrates the soil and rock zones. Retention time is generally short because of the

moderate to steep relief and the shallowness of the soil zone. Only minor amounts of dissolved solids are contributed to the basin from the rain and snow (see Bassett et al., 1992).

Precipitation of hydrous iron and aluminum oxides occurs along Geneva Creek, beginning at the headwaters and continuing along Geneva Creek. Substantial amounts of the precipitates are scoured out and carried out of the study area each season during spring runoff. The precipitates that are preserved, occur in the lower-gradient areas. Considerable wetlands have developed in these areas and series of terraces have formed by hydrous iron oxide precipitates cementing organic debris. These wetlands and terraces trap the hydrous iron oxide precipitates and prevent the spring runoff from carrying away this material, thus establishing iron bogs and eventually iron oxide deposits.

Approximately 8 miles of upper Geneva Creek has been impacted by natural acid drainage (pH<5) because of the oxidation of pyrite in the altered areas in the upper part of the study area. The maximum concentrations of metals in stream waters for Fe, Mn, and Al are no more than 10 mg/l; for Cu, Ni, and Zn, less than 1 mg/l, and less than 0.01 mg/l for other metals. Some low volume seeps and flows from drill holes exceed these concentra-

tions, but their impact on stream water chemistry of Geneva Creek is insignificant.

As shown in the previous study (Bassett et al., 1992), about 50% of the acidity has been buffered naturally by reaction with minerals in the basin, particularly calcite. At low pH values, most of the metals are present in the stream waters as simple cations. For the acid-sulfate waters, mineral-solution equilibrium calculations suggest that the concentrations of Fe, Al, and to a minor extent Zn, are controlled by mineral phases. Dominant controls of Cu and Zn concentrations are probably sorption onto hydrous iron oxides, such as ferrihydrite. Factors that influence the development of natural acid drainage in the study area are summarized in Table 24.8.

Geneva Creek is an example of a relatively undisturbed basin which is underlain by pyritic-altered rocks and impacted by natural acid drainage and elevated metal contents. The range in specie contents of the stream waters establishes a natural baseline of values for this area. The geology, alteration, and mineralization in this area is not unlike many of the mining districts in the Front Range. Therefore the range of metal contents of waters and the processes controlling the concentrations of metals in water in the

TABLE 24.7—Mineralogy and chemistry of precipitates from the Geneva Creek study area, Colorado. [All values are in parts per billion]

Sample no.	XRD pattern	Age	Ag	As	Cd	Co	Cr	Cu	Mo	Ni	Pb	Zn
P 29	ferrihydrite	fresh	<2	<10	<2	6	26	21	<2	<2	4	12
P 34	ferrihydrite, goethite	fresh	<2	260	<2	5	129	36	<2	<2	<4	<2
P 35	ferrihydrite, goethite	<2 yr	<2	230	<2	5	154	91	<2	<2	<4	10
P 36	goethite	<10 yr	<2	40	<2	5	57	311	<2	<2	<4	52
P 37	ferrihydrite, goethite	>10 yr	<2	60	<2	5	51	200	<2	<2	<4	28

TABLE 24.8—Factors controlling the generation of natural acid drainage (NAD) and metal loadings.

Factors (in order of importance)		Comments
1.	Presence, amount, and character of iron sulfides	Influenced by type of mineralization and alteration; fine-grained disseminated iron sulfide has greater capacity for generating NAD than coarse-grained iron sulfides.
2.	Accessibility of iron sulfides to O ₂	Depends on rates of mechanical erosion, chemical reactivity of the host rocks, hydrologic system, fractures, porosity.
3.	Chemistry of gangue and host rocks	Potential acid buffering capacity depends on rock and gangue minerals; acid buffering capacity: carbonates > mafic minerals > felsic minerals; also fine-grained minerals > coarse-grained minerals.
4.	Presence of other sulfide minerals and trace metal contents of the iron sulfides	Contributes to the addition of metal loadings.
5.	Climate	Influences amounts of moisture in contact with iron sulfides, capacity to carry away oxidation products and exposing fresh sulfide minerals; for chemical weathering: humid > arid and warm > cool.
6.	Physical setting	If mechanical erosion > chemical erosion, fresh sulfides will be continuously exposed; otherwise oxidized products will limit accessibility of O ₂ and the generation of NAD; for NAD generation: steep topography > moderate > flat.

study area can probably be considered to be typical for other similar altered and mineralized areas in the Front Range of Colorado underlain by geochemically similar rocks. Since much of the Colorado Front Range falls in this category, the results of this study can contribute to establishing natural baselines for waters draining areas affected by AMD in similar areas of the Colorado Front Range.

REFERENCES

- Alpers, C.N., and Nordstrom, D.K., 1991, Geochemical evolution of extremely acid mine waters at Iron Mountain, California—Are there any lower limits to pH?: Proceedings, 2nd Internat Conference on the Abatement of Acidic Drainage, MEND, v. 2, pp. 321–342.
- Baldwin, J.A., Ralston, D.R., and Trexler, B.D., 1978, Water resource problems related to mining in the Blackbird mining district, Idaho: U.S. Dept. Agriculture, Forest Service Cooperative Agreement 12–11–204–11, Univ. of Idaho, College of Mines, 232 pp.
- Barnes, I., and Clarke, F.E., 1969, Chemical properties of ground water and their corrosion and encrustation effects on wells: U.S. Geological Survey Professional Paper 498–D, 58 pp.
- Bassett, R.L., Miller, W.R., McHugh, J., and Catts, J.G., 1992, Simulation of natural acid sulfate weathering in an alpine watershed: Water Resources Research, v. 28, pp. 2197–2209.
- Cleaves, E.T., Godfrey, A.E., and Bricker, O.P., 1970, Geochemical balance of a small watershed and its geomorphic implications: Geological Society of America Bulletin, v. 81, pp. 3015–3032.
- Dzombak, D.A., and Morel, F.M.M., 1987, Adsorption of inorganic pollutants in aquatic systems: Journal of Hydraulic Engineering, v. 113, pp. 430–475.
- Filipek, L.H., Nordstrom, D.K., and Ficklin, W.H., 1987, Interaction of acid mine drainage with waters and sediments of West Squaw Creek in the West Shasta mining district, California: Environmental Science and Technology, v. 21, pp. 388–396.
- Fishman, J.J., and Pyen, G., 1979, Determination of selected anions in water by ion chromatography: U.S. Geological Survey Water Resource Investigation 79–101, 30 pp.
- Garrels, R.M., and MacKenzie, F.T., 1967, Origin of the chemical composition of some springs and lakes; in Gould, R.F. (ed.), Equilibrium Concepts in Natural Water Systems: Adv. Chem. Ser., v. 67, pp. 222–242.
- Henderson, C.W., 1926, Mining in Colorado: U.S. Geological Survey Professional Paper 138, 263 pp.
- Jeffries, D.S., 1991, Snowpack storage of pollutants, release during melting, and impact on receiving waters; in Norton, S.A., Lindberg, S.E., and Page, A.L. (eds.), Acidic Precipitation—Soils, Aquatic Processes, and Lake Acidification: v. 4, pp. 107–128.
- Jernegan, J.L., Jr., 1877, Notes on a metallurgical campaign at Hall Valley, Colo.: Trans. Am. Inst. Min. Metall. Pet. Eng., v. 5, pp. 560–575.
- Kennedy, V.C., and Zellwiger, G.W., 1974, Filter pore-size effects on the analysis of Al, Fe, Mn, and Ti in water: Water Resources Research, v. 10, pp. 785–790.
- Lichte, F.E., Golightly, D.W., and Lamothe, P.J., 1987, Inductively coupled plasma-atomic emission spectrometry; in Baedecker, P.A. (ed.), Methods for Geochemical Analysis: U.S. Geological Survey Bulletin 1770, pp. B1–B10.
- Lovering, T.S., 1935, Geology and ore deposits of the Montezuma quadrangle, Colorado: U.S. Geological Survey Professional Paper 178, 119 pp.
- Lovering, T.S., and Goddard, E.N., 1950, Geology and ore deposits of the Front Range, Colorado: U.S. Geological Survey Professional Paper 223, 319 pp.
- McHugh, J.B., Ficklin, W.H., and Miller, W.R., 1988, Analytical results for 32 water samples from a hydrogeochemical survey of Geneva Creek area, central Colorado: U.S. Geological Survey Open-File Report 88–365, 8 pp.
- Miller, W.R., and Drever, J.I., 1977, Chemical weathering and related controls on surface water chemistry, Absaroka Mountains, Wyoming: Geochimica et Cosmochimica Acta, v. 41, pp. 1693–1702.
- Neuerburg, G.J., Botinelly, T., and Watterson, J.R., 1976, Ocher as a prospecting medium in the Montezuma District of Central Colorado: U.S. Geological Survey Journal of Research, v. 4, pp. 359–365.
- Nordstrom, D.K., 1982a, The effect of sulfate on aluminum concentrations in natural waters—Some stability relations in the system Al_2O_3 - SO_3 - H_2O at 298 K: Geochimica et Cosmochimica Acta, v. 46, pp. 681–692.
- Nordstrom, D.K., 1982b, Aqueous pyrite oxidation and the consequent formation of secondary iron minerals; in Acid Sulfate Weathering: Soil Science Society of America Spec. Pub. No. 10, pp. 37–56.
- Nordstrom, D.K., Jenne, E.A., and Ball, J.W., 1979, Redox equilibria of iron in acid mine waters; in Jenne, E.A. (ed.), Chemical Modeling in Aqueous Systems—Speciation, Sorption, Solubility and Kinetics: American Chemical Society Symposium Series 93, pp. 51–79.
- Nordstrom, D.K., Bruchard, J.W., and Alpers, C.N., 1990, The production and seasonal variability of acid mine drainage from Iron Mountain, California—A Superfund site undergoing rehabilitation; in Gadsby, J.W., Malick, J.A., and Day, S.J. (eds.), Acid Mine Drainage—Designing for Closure: BioTec Publishers, Vancouver, B.C., pp. 23–33.
- Parkhurst, D.L., Thorstenson, D.C., and Plummer, L.N., 1980, PHREEQE—A computer program for geochemical calculations: U.S. Geological Survey Water Resource Investigations 80–96, 210 pp.
- Perkin-Elmer Corporation, 1976, Analytical methods for atomic-absorption spectrophotometry: Perkin-Elmer Corp., Norwalk, Conn., 586 pp.
- Perkin-Elmer Corporation, 1977, Analytical methods for atomic-absorption spectrophotometry, using the HGA graphite furnace: Perkin-Elmer Corp., Norwalk, Conn., 208 pp.
- Richmond, G.M., 1965, Glaciation of the Rocky Mountains; in Wright, H.E., Jr., and Frey, D.G. (eds.), The Quaternary of the United States, pp. 217–230.
- Robinson, C.S., Warner, L.A., and Wahlstrom, E.E., 1974, General geology of the Harold D. Roberts Tunnel, Colorado: U.S. Geological Survey Professional Paper 831–B, 48 pp.
- Runnells, D.D., Shepherd, T.A., and Angino, E.E., 1992, Metals in water: Environmental Science and Technology, v. 26, pp. 2316–2322.
- Selner, G.I., and Taylor, R.B., 1993, System 9, GSMAP and other programs for the IBM PC and compatible microcomputers, to assist workers in the earth sciences: U.S. Geological Survey Open-File Report 93–511, 363 pp.
- Scintrex Corporation, 1979, UA–3 Uranium Analyzer: Toronto, Canada, 45 pp.
- Skougstad, M.W., Fishman, M.J., Friedman, L.C., Erdmann, D.E., and Duncan, S.S., 1979, Methods for determination of inorganic substances in water and fluvial sediments: Techniques of Water Resources Investigations of the U.S. Geological Survey, Chapter A1, 26 pp.
- U.S. Department of Commerce, 1974, Climatological data: Annual Summary, Colo., 1974.
- U.S. Geological Survey, 1980, Water resources data for Colorado, water year 1979: v. 2, 397 pp.
- U.S. Geological Survey, 1991, Water resources data for Colorado, water year 1990: v. 2, 394 pp.
- Warner, L.A., and Robinson, C.S., 1967, Geology of the Harold D. Roberts Tunnel, Colorado—Station 468 + 49 to the east portal: Geological Society of America Bulletin, v. 78, p. 87–120.

Chapter 25

CALCULATIONS OF GEOCHEMICAL BASELINES OF STREAM WATERS IN THE VICINITY OF SUMMITVILLE, COLORADO, BEFORE HISTORIC UNDERGROUND MINING AND PRIOR TO RECENT OPEN-PIT MINING

W.R. Miller and J.B. McHugh (Retired)

U.S. Geological Survey, Box 25046, MS 973, Federal Center, Denver, CO 80225-0046

INTRODUCTION

The Summitville deposit, located in the San Juan Mountains of southwestern Colorado, was discovered in the 1870s and is an example of an acid-sulfate epithermal Au-Ag-Cu system associated with advanced argillic alteration (Gray and Coolbaugh, 1994; Plumlee et al., 1995). After early mining, the Reynolds adit was constructed in 1887 to dewater existing mines. Limited mining occurred between 1950 and 1984. In 1984, Summitville Consolidated Mining Company, Inc., a subsidiary of Galactic Resources, constructed an open pit heap leach operation to extract gold and ceased operations after declaring bankruptcy in late 1992.

Remediation of environmental problems resulting from the open-pit mining at the Summitville (Fig. 25.1) has raised the question of what the pre-mining geochemical baselines of stream waters may have been in the vicinity of and downstream from the Summitville site. Standards for stream water chemistry set without regard to the watershed may be impossible to meet, depending on the geology of the drainage basins. The mine site lies within the upper Wightman Fork and Cropsy Creek drainage basins (Fig. 25.2). The presence of fossil iron bogs immediately adjacent to and around the Summitville deposit indicates that prior to mining, natural acid drainage generated by the oxidation of sulfides was common at Summitville. Thus, geochemical baselines of Wightman Fork and Cropsy Creek prior to mining were likely

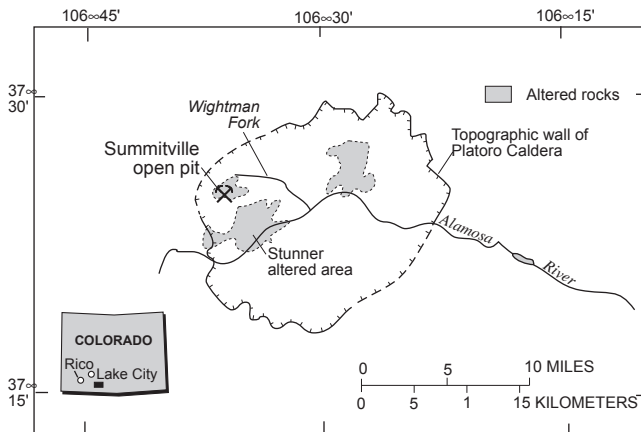


FIGURE 25.1—Map showing Summitville and location of altered rocks in the upper Alamosa River basin.

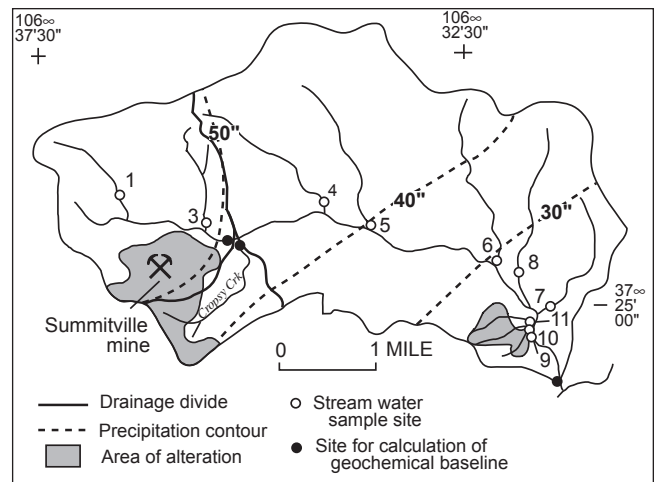


FIGURE 25.2—Map showing drainage basins, altered rocks, precipitation, and stream-water sample sites in the Wightman Fork basin.

lower in pH and probably contained greater concentrations of metals such as iron, aluminum, copper, and zinc than streams draining unaltered areas within the Wightman Fork drainage basin.

This study involves:

- 1) a discussion of the stream water chemistry of the Wightman Fork basin which contains the Summitville mine,
- 2) an examination of possible analogue areas to Summitville and their stream water chemistry,
- 3) a technique is presented and the pre-mining baselines at Summitville are calculated at three sites, and
- 4) geochemical baselines after development of the Reynolds adit, but prior to open-pit mining are calculated for one site.

WIGHTMAN FORK DRAINAGE BASIN

Elevation in the Wightman Fork basin ranges from 12,754 feet for North Mountain to 9400 feet at the junction of Wightman Fork with the Alamosa River. The climate is cool and humid with precipitation ranging from greater than 50 inches per year at the higher elevations to less than 30 inches in the southeastern portion of the drainage basin (Colorado Climate Center, 1984). Thunderstorms are common in summer, particularly during July and August. Spring runoff usually occurs in May and June.

The study area lies within the Platoro complex, which is in the eastern portion of the San Juan volcanic field. The field consists of Oligocene and younger volcanic rocks, beginning with an initial eruption of intermediate composition lavas and breccia, followed by more silicic ash-flow tuffs, and ending with a bimodal association of basalt and rhyolite (Lipman et al., 1970). Two main events of alteration and mineralization occurred in association with the Platoro complex. The first event occurred during late-stage emplacement of monzonitic stocks around 29.1 to 27 m.y. ago (Lipman, 1975). The argillic alteration in the southeastern part of the drainage basin (Fig. 25.2) (referred to as the SE altered area) may have occurred during this event, but it has not been dated. This area was investigated only briefly in this study and appears to contain mostly argillic alteration, although advanced argillic alteration may be present.

The second event was the emplacement of a volcanic dome and underlying monzonitic stock at Summitville at 22.5 m.y. ago (Mehnert et al., 1973). Mineralizing processes associated with this event created intense advanced alteration and later deposited gold, silver, and copper ores in the shallow volcanic dome. Alteration zones grade outward from fractures, and include a core of highly leached rocks in which only vuggy silica and ore minerals remain, to an advanced argillic zone with alunite, to an argillic zone with clay, and finally to propylitized rock containing pyrite, calcite, epidote, and chlorite (Steven and Ratte, 1960; Gray and Coolbaugh, 1994).

Much of the present topography in the study area has been influenced by Pinedale-age glaciation (late Pleistocene), which was at its maximum extent approximately 18,000 years ago (Richmond, 1965). The glaciers were in retreat approximately 12,000 years ago; only minor modification of the topography has taken place since then. Natural acid drainage and the formation of secondary iron oxide deposits began during melting of the glaciers and has continued since then. At the Summitville mine site, both fossil and actively precipitating iron oxide deposits are present below pyritically altered rocks, particularly along the northeast base of South Mountain. These deposits consist mainly of masses of goethite and limonite and iron oxide-cemented gravel, conglomerates, and talus. Many of these deposits are presently or were associated with seeps that occur at the base of the dome and changes in slope, particularly along the valley floor. Plumlee et al. (1995) discusses the geologic controls related to the deposit geology on the location of seeps. In addition, hydrous iron oxide

deposits are precipitating within stream beds of tributaries of Wightman Fork that are draining the SE altered area.

SAMPLING AND ANALYTICAL METHODS

Samples of water were collected from streams and seeps in the Wightman Fork basin, Calico Peak area, and the Redcloud Peak area during summer 1994. Water samples were collected and analyzed according to methods discussed in Miller and McHugh (1994). Temperature and pH were measured at each site. The water samples were determined for major and trace elements by graphite furnace and flame atomic absorption spectrophotometry and inductively coupled plasma mass spectrometry. Sulfate, chloride, fluoride and nitrate were measured by ion chromatography and alkalinity by titration with sulfuric acid.

Areas of precipitation and alteration within drainage basins were determined digitally using GSMAP (Selner and Taylor, 1992) from the annual precipitation map of Colorado (Colorado Climate Center, 1984) and the geologic map by Lipman (1975).

WATER CHEMISTRY OF THE WIGHTMAN FORK BASIN

Stream water samples were collected in August 1994 in the undeveloped areas of the Wightman Fork basin. The chemistry of these waters was used to determine the input of dissolved species from the undeveloped areas for the calculation of the pre-mining geochemical baselines below Summitville. Stream-flow records of a gauging station approximately 10 miles southwest of Summitville indicate a monthly mean flow for August of 53.5 cfs and an average annual mean of 89.3 cfs for water years 1957–1992 (U.S. Geological Survey, 1993). Therefore, the water samples collected in August probably have slightly higher metal concentrations than the mean annual concentrations.

Water samples were collected from 10 streams in the Wightman Fork basin, all draining areas undisturbed by human activities such as mining (Fig. 25.2). The water chemistry ranges from low-ionic strength waters from areas of unmineralized rocks to natural acid drainage waters with high acidity, sulfate, and metals (Table 25.1) from areas of altered mineralized rocks.

TABLE 25.1—Chemical analyses of stream waters from undisturbed areas of the Wightman Fork.

Site no.	pH	Conductivity	SO ₄ ²⁻	Alkalinity	Fe	Al	Mn	Cu	Zn
Unmineralized areas									
WW01	7.47	38	2.8	<1	0.14	<0.1	16	<1	1
WW03	7.25	51	5.4	27	0.15	<0.1	5.6	<1	1
WW04	7.55	72	7.0	37	0.16	<0.1	5.9	<1	1
WW05	8.16	120	10	66	0.10	<0.1	1	1	3
WW06	7.99	90	7.7	48	0.05	<0.1	<0.9	<1	3
WW07	8.23	154	20	62	0.02	<0.1	<0.9	<1	<1
WW08	8.32	172	24	70	<0.01	<0.1	<0.9	<1	<1
Mineralized areas									
WW09	6.94	459	220	4	<0.01	0.1	51	1	13
WW10	7.15	814	440	29	0.04	<0.1	38	<1	10
WW11	3.49	1070	485	<1	27	12	780	3	110

[Conductivity in $\mu\text{S}/\text{cm}$, remaining species in mg/l except for Mn, Cu, and Zn in $\mu\text{g}/\text{l}$]

**UNDEVELOPED GEOLOGIC ANALOGUES
TO SUMMITVILLE**

Undeveloped mineral systems that may be equivalent to Summitville were studied to estimate the background geochemistry of stream waters draining Summitville prior to mining. None of the mineral systems studied is an exact match to Summitville, but permit the likely ranges in composition of stream waters that drained Summitville to be estimated. Geologic analogues were first looked for close to Summitville, in similarly altered areas.

Upper Alamosa River and upper Cropsy Creek drainage

A study of stream waters draining undeveloped altered and mineralized areas within and adjacent to the upper Alamosa River basin, including the upper Cropsy Creek area, was carried out in July 1993 by Miller and McHugh (1994). The upper Cropsy Creek drainage represents an undeveloped area with alteration associated with the Summitville deposit. The ranges in composition of the most anomalous stream waters from this area are shown in Table 25.2. Prior to mining, waters draining the area of acid-sulfate alteration, which includes the Summitville mine site, probably were greater in acidity and trace metal concentrations than waters presently draining upper Cropsy Creek basin above the mine site. The area which includes the mine site and the core of the deposit contained larger amounts of pyrite and sulfides than the area drained by upper Cropsy Creek. In addition, the host rocks at the mine site have less buffering capacity to neutralize the acidity of the waters in contact with the oxidizing pyrite than rocks in upper Cropsy Creek above the mine site. Therefore, the background acidity and metal concentrations generated at Summitville prior to mining were probably greater than what is presently observed in upper Cropsy Creek basin above the mine site.

The upper Alamosa River drainage includes tributaries draining altered areas along the southern flanks of South Mountain, Cropsy Mountain, and Lookout Mountain, of which all occur adjacent to and south of the Summitville mine site. Advanced argillic alteration is present, particularly in the Alum, Bitter, and Iron Creek drainage basins (Bove et al., 1995); referred to here as

the Stunner altered area. Steep slopes form in these areas of soft ground, with sparse to no vegetation. The rate of mechanical erosion for these areas is high. Fresh sulfides, particularly pyrite, are continuously exposed and oxidized, and therefore the streams draining these areas are chemically degraded. The range in concentrations of species for the most anomalous stream waters from these areas are shown in Table 25.2.

The original terrain at the Summitville site was more subdued than Alum or Bitter Creek drainages in the Stunner altered area. In alpine areas with more subdued relief, similar to the area containing the mine site, bogs and wetlands often form, which tend to reduce the exposure of oxygen to sulfides in the underlying rocks, decreasing oxidation and the generation of natural acid drainage. The northeastern slope of South Mountain is partially forested with conifers, which suggests that the slopes are stable and that the soils are not strongly acidic. Therefore, the background acidity and metal concentrations generated at Summitville were probably less than what is presently observed in Alum Creek. The exception to this would be the concentrations of copper and zinc which was assumed to be originally higher in concentration at the mine site, and therefore at higher concentrations in the waters draining the Summitville site prior to mining than Alum Creek.

In summary, at Summitville prior to mining, the larger amounts of pyrite would increase the potential for generation of acid waters, but the more subdued topography and mechanical erosion would lessen the generation of acid waters. Miller and McHugh (1994) concluded that, except for copper and zinc concentrations, the geochemical background of stream waters draining the Summitville mine site prior to mining would probably fall between the geochemistry of stream waters presently draining upper Cropsy Creek above the mine site (a minimum) and Alum Creek at its confluence with the Alamosa River (a maximum).

Calico Peak area

A study was carried out of an undeveloped mineral system analogous to Summitville centered at Calico Peak, northwest of Rico, Colorado. The system occurs in a similar geologic and physical setting with similar climate, rainfall, elevation, relief, and

TABLE 25.2—Chemical analyses of stream waters from undisturbed areas (after Miller and McHugh, 1994).

Site no.	Latitude	Longitude	pH	Conductivity	Sulfate	Alkalinity	Fe	Al	Mn	Cu	Zn
Upper Cropsy Creek											
SW28	37°24'56"	106°35'41"	4.40	150	49	<1	0.07	2.9	1.7	10	1800
SW30	37°24'55"	106°35'39"	4.76	230	70	<1	0.03	1.7	0.82	10	130
SW31	37°24'52"	106°35'39"	6.70	460	220	<1	0.22	17	5.9	46	1200
SW32	37°24'49"	106°35'43"	4.69	140	39	<1	0.01	2.1	0.48	6	86
SW34	37°25'23"	106°37'16"	7.12	80	15	<1	0.09	0.1	0.01	<1	34
SW35	37°25'27"	106°37'13"	7.33	70	7.2	1	0.02	<0.1	0.01	<1	34
Background areas, Alamosa River Drainage Basin											
SW06	37°23'33"	106°23'04"	8.11	130	1.5	38	0.03	0.1	<0.01	<1	4
SW07	37°23'50"	106°25'46"	8.13	150	7.2	50	0.01	<0.1	<0.01	<1	4
SW33	37°26'06"	106°36'31"	7.25	40	0.8	<1	0.04	<0.1	<0.01	1	4
Mineralized area, Upper Alamosa River Drainage Basin											
Alum Ck	37°23'05"	106°33'59"	2.64	1350	800	<1	141	55	2.7	250	710
Bitter Ck	37°23'42"	106°33'07"	3.44	340	95	<1	5.1	3.7	0.58	7	68
Iron Ck	37°22'53"	106°36'09"	3.91	190	56	<1	1.6	3.0	0.22	12	35

[Conductivity in µS/cm; species in mg/l except for Cu and Zn in µg/l]

vegetation. The area around Calico Peak has undergone minimal mining and no significant mines occur in the study area. The study area is underlain by altered porphyritic biotite-hornblende latite of the Calico Peak Porphyry (Pratt et al., 1969), which includes a stock centered at Calico Peak and several dikes. Pervasive alteration includes significant alunite and sericite (Naeser et al., 1979). Pyrite occurs as disseminations and along fractures in the altered area. Fossil iron bogs and ferricrete deposits were observed within and below the altered areas, particularly along the northeastern slope of Calico Peak.

Water samples were collected from 20 streams draining the study area during July 19–20, 1994 (Fig. 25.3, Table 25.3). Waters with pH<5 are from first-order drainages with low-flow volumes at or near their headwaters in the altered area. These waters represent natural acid drainage from the altered and mineralized zone of a mineral system similar to that of Summitville. The Calico Peak area has not been drilled, so the occurrence and amounts of sulfides other than pyrite are unknown. One sample of rock from a prospect pit contained 1.3% copper. The range in pH, iron, manganese, aluminum, and sulfate, may be similar to waters draining Summitville prior to mining at similar times of the year when the samples were collected.

In the headwaters draining the Calico Peak altered area, the waters have low pH and high sulfate and metal concentrations. As the waters mix downstream with tributaries from unmineralized areas, the pH values and sulfate concentrations increase and the copper, zinc, iron, and aluminum concentrations generally decrease. At site 23, which approximates the junction of Wightman Fork above Cropsy Creek in terms of total area and percent of mineralized and unmineralized rocks above the junction, pH = 8.1 and copper, zinc, iron, and aluminum are near background values. Except for sulfate, stream water chemistry for Horse Creek returned to nearly background values in a stream distance of 3.5 km. One difference between the Calico Peak and Summitville mineral systems was that pre-mining copper and zinc concentrations in the rocks were probably greater in the surface

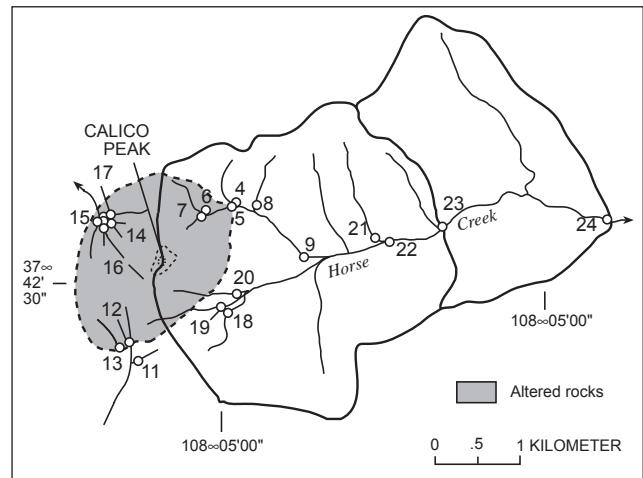


FIGURE 25.3—Map showing location of streams in the Horse Creek drainage basin, altered rocks (gray shaded), and stream-water sample sites in the vicinity of Calico Peak.

and near surface at Summitville prior to mining than at Calico Peak. The Summitville deposit was discovered by early miners and extensively developed because high metal concentrations were found in the surface rocks. This did not occur at Calico Peak.

Redcloud Peak area

The Redcloud Peak area, several miles west and southwest of Lake City, Colorado, was selected for study because no significant mining or acid mine drainage is present in the study area. The area was determined to have high potential for base and precious metals in vein and breccia-pipe epithermal deposits and moderate

TABLE 25.3—Chemical analyses of stream waters from Calico Peak area, Colorado.

Site no.	Latitude	Longitude	pH	Conductivity	Sulfate	Alkalinity	Fe	Al	Mn	Cu	Zn
CW4	37°42'56"	108°04'49"	6.62	66	17	2	0.02	<0.1	<0.01	<0.6	<5
CW5	37°42'55"	108°04'51"	4.63	83	18	<1	0.06	0.5	0.11	65	82
CW6	37°42'53"	108°05'07"	3.33	263	63	<1	0.89	2.0	0.45	350	320
CW7	37°42'51"	108°05'06"	4.15	168	50	<1	1.48	2.4	0.22	12	65
CW8	37°42'54"	108°04'42"	7.11	156	25	60	0.01	<0.1	<0.01	<0.6	<5
CW9	37°42'35"	108°04'22"	7.79	119	25	27	0.15	0.1	0.03	5.8	10
CW11	37°42'02"	108°05'37"	6.19	88	26	7	0.01	0.1	<0.01	<0.6	<5
CW12	37°42'08"	108°05'39"	4.22	88	27	<1	0.05	0.9	0.26	2.0	45
CW13	37°42'07"	108°05'42"	5.77	36	7.1	<1	0.01	<0.1	<0.01	1	6
CW14	37°42'52"	108°05'48"	5.60	82	26	6	0.42	0.4	0.11	0.6	20
CW15	37°42'53"	108°05'52"	3.84	155	48	<1	0.46	2.5	0.11	3.8	47
CW16	37°42'51"	108°05'50"	3.60	122	29	<1	0.65	2.0	0.04	2.9	34
CW17	37°42'53"	108°05'50"	3.98	130	42	<1	0.20	1.1	0.08	140	38
CW18	37°42'19"	108°04'54"	7.10	195	44	40	0.02	<0.1	<0.01	<0.6	5
CW19	37°42'20"	108°04'55"	7.21	82	15	27	0.01	0.1	<0.01	0.9	<5
CW20	37°42'24"	108°04'52"	5.79	75	24	<1	0.05	0.3	0.07	6.0	28
CW21	37°42'42"	108°03'46"	7.45	170	20	59	0.01	<0.1	<0.01	<0.6	<5
CW22	37°42'42"	108°03'43"	7.05	141	42	20	0.38	<0.1	0.62	9.1	66
CW23	37°42'46"	108°03'18"	8.10	316	50	132	0.03	<0.1	<0.01	<0.6	<5
CW24	37°42'47"	108°02'04"	7.94	223	40	78	0.02	<0.1	0.05	0.7	6

[Conductivity in μS/cm; species in mg/l except for Cu and Zn in μg/l]

potential for molybdenum and copper porphyry deposits (Sanford et al., 1987). The area lies mostly within the Lake City caldera and the exposed rocks comprise high silica to quartz trachytic ash-flow tuffs and caldera collapse breccias. Resurgent doming and faulting resulted in the emplacement of quartz syenite and quartz monzonite intrusions into the collapse sequence. Alteration consists of bleached and iron-stained rocks and small silicified and brecciated masses. The physical setting and climate are similar to that of Summitville.

Water samples were collected from 33 streams (McHugh et al., 1995). The acidity and concentrations of metals for most of the waters were near background. Stream water chemistry for only the waters with pH<5 are shown in Table 25.4.

Published literature

The closest undeveloped deposit we have found in the literature that is most nearly equivalent and in a similar physical setting to the Summitville deposit is the Mount McIntosh-Pemberton Hills area in northern Vancouver Island, British Columbia (Koyanagi and Panteleyev, 1993). The deposit is an advanced-argillic, acid-sulfate copper-gold system hosted in volcanic rocks in a temperate-humid climate. Hydrothermally altered and leached silica caps form prominent bluffs along linear alteration zones with base and precious metal deposition. Sulfide mineralization consists of abundant disseminated and massive stratabound iron sulfides, mainly pyrite, with associated enargite and copper sulfides. A study was carried out by Koyanagi and Panteleyev (1993) to investigate natural acid-drainage of streams draining this deposit. Samples were collected from 34 streams and standing swamps. The acidity and metal concentrations of most of the stream waters were at or near background. Geochemical analyses of selected species of four stream waters which contained the highest copper concentrations are shown in

Table 25.5. The maximum copper concentration is 320 µg/l in the small headwater streams. At short distances downstream, these streams return to nearly background levels of copper. The climate in the study area is wetter than at Summitville. Therefore, stream waters draining the Mount McIntosh/Pemberton Hills area are probably slightly more dilute than at Summitville prior to mining.

**CALCULATION OF GEOCHEMICAL BASELINES
PRIOR TO UNDERGROUND MINING**

Using the geochemical data for stream waters draining undeveloped deposits with similar geologic and physiographic characteristics, geochemical baselines prior to mining are calculated for three points downstream of Summitville:

- 1) Wightman Fork above the junction with Cropsy Creek,
- 2) Cropsy Creek above the junction with Wightman Fork, and
- 3) Wightman Fork above the junction with the Alamosa River (Fig. 25.2). Species used for the calculations are pH, sulfate, iron, aluminum, manganese, copper, and zinc.

These were chosen because they have the greatest potential for exceeding water quality standards for streams draining the Summitville mine.

Mass-balance calculations

Wightman Fork and Cropsy Creek drainages receive waters draining both mineralized and unmineralized rocks. The waters from the unmineralized areas dilute concentrations of metals and raise pH values of waters derived from the mineralized areas. The amount of a chemical species contributed by a given drainage above the point for calculation of baselines depends on the percent of mineralized and unmineralized rocks and the amount of water received by and flowing through the drainage basin. The amount

TABLE 25.4—Chemical analyses of stream waters with pH < 5, from Redcloud Peak area, Colorado.

Site no.	Latitude	Longitude	pH	Conductivity	Sulfate	Alkalinity	Fe	Al	Mn	Cu	Zn
RW12	37°56'54"	107°26'19"	4.92	127	49	<1	<0.01	1.6	0.45	4.3	110
RW14	37°56'56"	107°26'25"	3.58	320	106	<1	0.45	2.6	1.6	3.2	280
RW16	37°56'28"	107°27'13"	4.17	148	53	<1	0.07	1.7	1.0	2.5	83
RW30	37°58'22"	107°26'33"	4.42	140	52	<1	0.07	2.1	0.62	2.2	130
RW32	37°57'53"	107°27'04"	3.90	194	74	<1	6	4.4	0.47	5.9	93

[Conductivity in µS/cm; species in mg/l except for Cu and Zn in µg/l]

TABLE 25.5—Chemical analyses of the four most anomalous stream waters in metals from Mount McIntosh-Pemberton Hills area, Vancouver Island, B.C. (from Koyanagi and Panteleyev, 1993).

Site	pH	Conductivity	Sulfate	Fe	Al	Cu	Zn
Hushamu Creek Tributary	3.7	54	228	0.55	16.5	320	40
Hushamu Creek	3.9	163	31	0.01	1.89	120	10
Hepler Creek Tributary	4.1	100	18	0.01	0.82	70	10
Hepler Creek Tributary	3.9	152	51	0.35	3.47	30	10

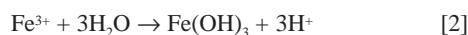
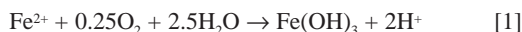
[Conductivity in µS/cm; species in mg/l except for Cu and Zn in µg/l]

of water that flows through a particular basin in a season can be estimated by the drainage area and the amount of annual precipitation received. Some precipitation is lost by evaporation, but it is assumed that evaporation is approximately the same throughout the drainage basins. Some infiltration and underground flow will take place, but because the volcanic bedrock is near the surface in much of the drainage basins, much of the underground flow will return to the surface.

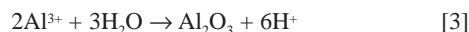
Estimates of the chemical composition of stream waters derived from portions of basins underlain by unmineralized rocks are made directly by chemical analyses of stream waters from tributaries of the Wightman Fork draining unmineralized rocks (Table 25.1). For portions of the drainage basins underlain by mineralized rocks in which water chemistry was not determined, an estimate of the water chemistry using a geologically and physiographic equivalent basin was used for the calculations. Estimates for the composition of pre-mining stream waters of drainage basins that are developed (containing mines with significant acid mine drainage) are made by using data collected from streams draining unmined, mineralized systems discussed earlier that may be comparable to Summitville in geology, climate, and physical setting. The mass of each constituent contributed by the individual basin can be determined by multiplying the amount of mineralized and unmineralized areas of the drainage basin by the average annual precipitation and the concentration of the stream water chemistry determined or estimated for the unmineralized and mineralized portion of the basin. Areas of mineralized rocks, precipitation, and locations of stream water samples collected from undeveloped drainages in the Wightman Fork drainage basin are shown on Figure 25.2. Areas and percent of mineralized and unmineralized rocks and precipitation in the three basins are shown in Table 25.6.

Chemical modeling of in-stream reactions

Although some sulfate may be lost by precipitation of hydrous iron and aluminum oxides, much of the sulfate behaves conservatively. The concentrations of other species are controlled by processes (other than dilution) that take place in the stream channel. As an example, dissolved iron, which is derived from waters draining the altered areas, is composed of species such as Fe²⁺ and Fe³⁺. These species will react with oxygen in the stream bed during mixing, lowering pH according to:



Dissolved aluminum will precipitate as pH trends toward neutral. One possible reaction is:



Most of the aluminum is probably controlled by reaction (3) but some aluminum may be controlled by:



The above reactions may be reversible and consume acid, possibly seasonally, in transitional reaches of streams. Copper, zinc, lead and other metals may precipitate and(or) adsorb or coprecipitate onto freshly precipitated hydrous metal oxides. Therefore these metals are not conservative. Although stream pH values will be lowered by precipitation of hydrous metal oxides, they will tend to rise overall through the neutralizing effect of mixing with tributaries containing carbonate and bicarbonate ions:



Reaction (5) will stop when all the carbonate and bicarbonate ions are used up. The chemical and physical effects of mixing various percentages of water from mineralized and unmineralized portions of a basin can be calculated using PHREEQE (Parkhurst et al., 1980). Sorption of metals, particularly copper and zinc, onto precipitating hydrous oxides is certainly taking place in the stream beds, but this process is not taken into account by the chemical modeling. Therefore the concentration of copper and zinc are probably lower than the estimated concentrations by the chemical modeling. In addition, for the chemical modeling, an assumption is made that 50% of the total dissolved iron and aluminum in stream waters, draining the mineralized areas, react with O₂ and(or) H₂O. This percentage is based on empirical observations of iron and aluminum precipitation in streams draining undeveloped areas underlain by pyritic mineralization. When hydrous metal oxides are precipitated, pH values decrease [reactions (1-4)]. In contrast, pH values increase as the acidic waters mix with the bicarbonate waters [reaction (5)]. PHREEQE was also

TABLE 25.6—Areas and weighted percent (area x precipitation) of mineralized and unmineralized areas of three drainage basins in the vicinity of Summitville, Colorado.

Drainage basin	Area (km ²)			Weighted percent	
	Unmineralized areas	Mineralized areas	Total	Unmineralized areas	Mineralized areas
Cropsy Creek above Wightman Fork	1.67	0.63	2.30	72.2%	27.8%
Wightman Fork above Cropsy Creek	7.46	1.59	9.05	82.5%	17.5%
Wightman Fork above Alamosa River	36.8	3.88	40.71	90.7%	9.3%

used to physically mix the proportions of waters draining the mineralized and unmineralized shown in Table 25.6.

Most likely scenario

The pH, sulfate, iron, manganese, and aluminum concentrations of stream waters draining the altered areas used for the most likely scenario (Table 25.7) is a composite of the chemistry of stream waters derived from both the Stunner altered area and altered areas in upper Cropsy Creek and the geologically analogous Calico Peak area. The copper and zinc concentrations used for the calculations were increased significantly above that in waters draining the Stunner and upper Cropsy Creek altered areas. It is assumed that much more copper and zinc sulfides were present at Summitville prior to mining than the Stunner and upper Cropsy Creek altered areas, and therefore the streams draining Summitville prior to mining contained greater concentrations of copper and zinc than streams draining the Stunner and upper Cropsy Creek altered areas. The calculated pre-mining geochemical baselines for stream waters at the three junctions are shown in Table 25.8.

Conservative scenario

For the conservative scenario, the geochemical baselines are determined by assuming that the compositions of stream waters draining the altered areas in the Wightman Fork basin are equivalent to the chemistry of stream waters draining the Stunner altered area, which is the mineralized area in the Upper Alamosa drainage basin, south of Summitville (Table 25.2). By using this scenario, the natural waters of an area are assumed to be more chemically degraded than the most likely scenario. Concentrations of species used for the conservative scenario (Table 25.7) are estimated by using the composite stream water chemistry of Alum and Bitter Creeks (Table 25.2). Concentrations of species from the unaltered areas in the Wightman Fork basin were determined directly or estimated using equivalent drainages in the Wightman Fork basin (Table 25.1). The amount of mineralized rock which is used in the calculations is based on field mapping. This amount can be in error, so to compensate, the amount of mineralized area was increased by 10% for the conservative scenario (Table 25.9). Using this data, the pre-mining geochemical baselines are calculated at the three junctions (Table 25.8).

TABLE 25.7—Stream water chemistry used for calculation of pre-mining geochemical baselines of three junctions in the vicinity of Summitville, Colorado.

	pH	Sulfate	Alkalinity	Fe	Al	Mn	Cu	Zn
Conservative scenario								
Unmineralized areas	8.0	10	50	0.05	0.1	0.01	1	4
Mineralized areas	3.5	200	0	100	15	0.6	1500	1000
Most likely scenario								
Unmineralized areas	8.0	7	50	0.01	0.1	0.01	1	4
Mineralized areas	3.5	100	0	5	4	0.5	500	500

[Species in mg/l except Cu and Zn in µg/l]

TABLE 25.8—Pre-mining geochemical baselines at three stream junctions in the vicinity of Summitville, Colorado.

Junction	pH	Sulfate	Fe	Al	Mn	Cu	Zn
Conservative scenario							
Cropsy Creek above Wightman Fork	3.67	68	15	2.3	0.19	460	309
Wightman Fork above Cropsy Creek	4.17	47	10	1.5	0.12	290	196
Wightman Fork above Alamosa River	6.20	29	5	0.9	0.07	154	106
Most likely scenario							
Cropsy Creek above Wightman Fork	6.53	33	0.70	0.6	0.15	139	142
Wightman Fork above Cropsy Creek	6.90	23	0.45	0.4	0.09	88	91
Wightman Fork above Alamosa River	7.24	16	0.30	0.3	0.06	47	50

[Species in mg/l except for Cu and Zn in µg/l]

TABLE 25.9—Weighted percent* recalculated assuming 10% greater mineralized area.

Drainage basin	Weighted percent	
	Unmineralized rocks	Mineralized rocks
Cropsy Creek above Wightman Fork	69.4%	30.6%
Wightman Fork above Cropsy Creek	80.7%	19.3%
Wightman Fork above Alamosa River	89.8%	10.2%

*Weighted percent is the area multiplied by annual precipitation for the area and then converted to percent of the total basin.

Comparison of the calculated baselines with stream water chemistry at Calico Peak

The mineral system centered at Calico Peak is an acid-sulfate deposit, similar to Summitville, and occurs in a similar physical and geological setting. Mineralized rocks occur in the headwaters of Horse Creek. The streams draining the mineralized rocks have low pH values and high concentrations of sulfate, iron, aluminum, manganese, copper, and zinc.

The area of the drainage basin above site 23 (Fig. 25.3) is approximately the size of the Wightman Fork basin above Cropsy Creek. In addition, the percent of mineralized and unmineralized rocks is similar. A comparison of the calculated chemical composition of the Wightman Fork above Cropsy Creek with site 23 on Horse Creek is shown in Table 25.10. At site 23 on Horse Creek, the pH is higher and iron, aluminum, manganese, copper, and zinc concentrations are significantly lower compared to the calculated baselines at Summitville. An obvious difference is that the copper and zinc contents of rocks at Summitville were significantly higher than at Calico Peak, which accounted for the higher concentrations of copper and zinc concentrations of the calculated geochemical baselines at Summitville. But the pH and the concentrations of iron, aluminum, and manganese of the surface waters should be similar because both mineral systems contain abundant pyrite and occur in similar physical settings.

The difference is probably attributable to the presence of more reactive rocks in the Horse Creek basin than at Summitville. The stream waters in Horse Creek basin are generally higher in bicarbonate than in the Wightman Fork basin. Calcite occurs as a gangue mineral in lower Horse Creek basin, probably associated with an earlier mineralization event than the system centered at

Calico Peak. Dissolution of calcite would increase the concentration of bicarbonate ions, and thus raise pH values and lower metal contents in the stream waters.

Other considerations

Additional factors can be used to refine the geochemical baselines. The most significant factor, which is not taken into account, particularly during runoff periods, is ratio of mechanical erosion to chemical weathering. When chemical weathering exceeds mechanical erosion, underlying rocks are mantled by a zone of secondary products which insulate much of the sulfides from atmospheric oxygen. When mechanical erosion is greater than chemical weathering, sulfide minerals are continuously being exposed to oxygen, which generates natural acid drainage. This process may result in stream chemistry similar to that produced during mining excavation. As mentioned earlier, the Stunner altered area is an example of soft ground with steep slopes which contributes large amounts of natural acid drainage. One method to estimate this factor would be to determine steepness of slope (using topographic maps) and amount of vegetation and altered ground (using aerial and remote sensing maps). Removing vegetation to make roads and other construction activity will also increase the mechanical erosion within a basin and degrade stream-water chemistry.

Spring runoff and storm events

No attempt was made to calculate geochemical baselines during spring runoff and summer storm events. During these periods, the concentrations of species will be higher during the beginning of the runoff than during annual mean stream flow, mainly because of dissolution of soluble salts that have accumulated during the winter and drier periods by processes such as capillary action/evaporation. After this initial increase, the concentration of species will decrease. However, the total amount of metals or loadings usually will be greater during the runoff period than during mean flow.

To estimate the geochemical baselines during spring runoff and storm events, the calculated concentration of species would be calculated in a manner similar to that done during annual mean flow periods. The estimate of stream water chemistry from the mineralized and unmineralized portions of the basin would be determined by the study of streams draining geologically and physically equivalent areas with similar climates during this runoff period.

TABLE 25.10—Comparison of chemical species of most likely and conservative scenarios for Wightman Fork above Cropsy Creek with site 23, Calico Peak.

	pH	Sulfate	Fe	Al	Mn	Cu	Zn
Most likely scenario	6.9	23	0.45	0.4	0.09	88	91
Conservative scenario	4.2	47	9.7	1.5	0.12	290	196
Site 23, Calico Peak	8.1	50	0.03	<0.1	<0.1	<0.6	<5

[Species in mg/L except for Cu and Zn in µg/l]

**GEOCHEMICAL BASELINES AFTER
DEVELOPMENT OF THE REYNOLDS ADIT,
BUT PRIOR TO OPEN-PIT MINING**

A probable geochemical baseline after development of the Reynolds adit, but prior to open-pit mining can be calculated for stream water below the junction of Cropsy Creek and Wightman Fork, using the same procedure outlined above. The input water chemistry (Table 25.11) for the Reynolds adit is from Brown (1995) and information supplied by Morrison Knudsen (unpub. data). This baseline calculation was made at the request of EPA as part of the initial risk assessment at Summitville.

The geochemistry for stream waters draining the unmineralized and mineralized rocks above the junction of Cropsy Creek and Wightman Fork used in the calculations is similar to that used for the calculation of the pre-mining baseline (Table 25.7), except that pH is reduced from 8.0 to 7.8 and alkalinity has been decreased from 50 to 40 mg/l for the waters from the unmineralized areas. This modification is made because the unmineralized area above the baseline site is near the mineralized zone of the mineral system. These rocks may have been weakly affected by the mineralizing solutions during the emplacement of the Summitville deposit and have lost some of their potential buffering capacity. The pre-mining calculations made earlier were for three sites, two of which received waters derived much further away from the mineral system.

Areas of mineralized rocks, unmineralized rocks, and the area drained by the Reynolds adit (Fig. 25.4) as calculated by GSDRAW (Selner and Taylor, 1992), are shown in Table 25.12. The assumption is made that 50% of the dissolved iron and aluminum precipitates and lowers the pH. The calculations for the estimate of the geochemical baseline at this site were made using the chemical modeling program PHREEQE. The results of the calculated geochemical baselines are shown in Table 25.13.

The amount of dissolved iron and aluminum that precipitates is a factor in the resultant pH value. If no dissolved Al or Fe precipitate, then the resultant pH value is higher, which is shown in Table 25.14. The assumption of 50% precipitation of the dissolved iron and aluminum may be too high. The deposit is near the junction of

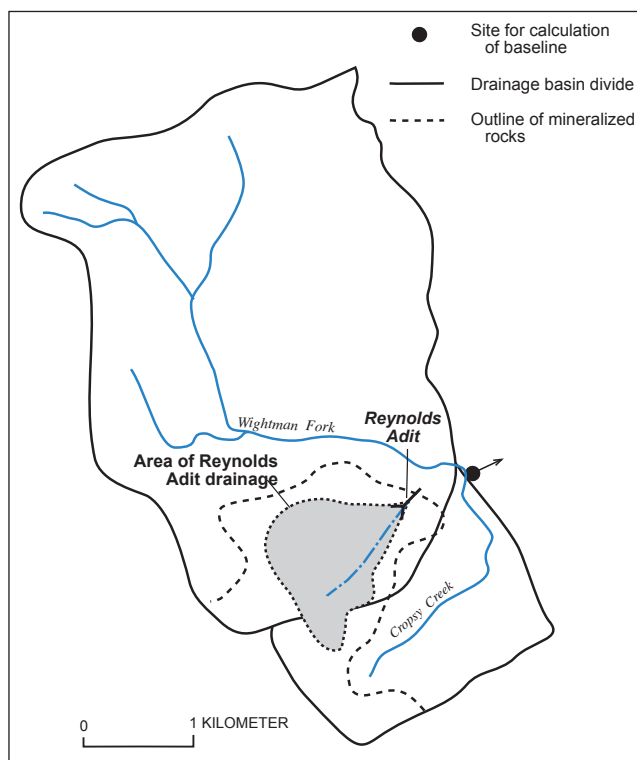


FIGURE 25.4—Map showing location of drainage basins, mineralized rocks, area of drainage of Reynolds adit, and site for baseline calculation.

Cropsy Creek and Wightman Fork and the dissolved iron and aluminum may not have had enough time for the precipitation to take place. If this is the case, the precipitation will still occur, but further downstream, below the junction of Wightman Fork and Cropsy Creek.

Another parameter that influences pH is alkalinity. In the Summitville area, most of the alkalinity is due to the bicarbonate

TABLE 25.11—Estimated water chemistry of streams draining mineralized areas, unmineralized areas, and the Reynolds adit used for the baseline calculations.

pH	Sulfate	Alkalinity	Fe	Al	Mn	Cu	Zn
Unmineralized areas							
7.8	20	40	0.05	0.1	0.01	5	5
Mineralized areas							
3.5	100	0	5	4	0.5	500	500
Reynolds adit							
3.0	450	0	60	25	1	20,000	4000

[Species are in mg/l except for Cu and Zn in µg/l]

TABLE 25.12—Areas and percent of the total for the unmineralized area, mineralized area, and the area drained by the Reynolds adit above the junction of Cropsy Creek and Wightman Fork. The area drained by the Reynolds adit has been subtracted from the mineralized area.

Unmineralized area		Mineralized area		Reynolds adit	
km ²	%	km ²	%	km ²	%
8.88	79.8	1.45	13	0.8	7.2

TABLE 25.13—Calculated post-underground and pre-openpit geochemical compositions for stream waters below the junction of Cropsy Creek and Wightman Fork.

pH	Sulfate	Fe	Al	Mn	Cu	Zn
4.7	60	2.5	1.2	0.15	1500	360

Species in mg/l except for Cu and Zn in µg/l

ion. The effect of varying the amount of alkalinity on the pH is shown in Table 25.14 with alkalinity equal to 50 and 30 mg/l.

TABLE 25.14—The influence of alkalinity and the percent of Fe and Al precipitated on the resultant pH value.

Alkalinity	% Fe and Al Precipitated	Calculated pH
50	50	5.4
40	50	4.7
30	50	3.9
50	0	6.5

Calculated geochemical baselines at the junction of Wightman Fork and Cropsy Creek, prior to the Summitville open pit operations, but after the development of the Reynolds adit, indicate that the early mining and the Reynolds adit contributed substantially (above the pre-mining baseline) to the chemical degradation of the stream waters draining the Summitville mine site.

CONCLUSION

Probable pre-mining geochemical baselines of stream waters in the vicinity of Summitville can be calculated by combining chemical modeling of dominant in-stream reactions with mass balance calculations. This technique consists of the mixing of two types of natural waters above the site for the calculation:

- 1) acid-sulfate waters derived from mineralized portions and
- 2) low-ionic strength-bicarbonate waters derived from unmineralized portions of the drainage basin above the site.

The calculations use as input, water chemistry of streams draining these two types of areas, along with other assumptions. The validity of the calculations depend upon obtaining good geochemical data from an undeveloped analogue area. Exact analogue match is difficult, so extrapolation may be necessary. The assumption on the amount of dissolved iron and aluminum that precipitates is difficult to estimate and contributes to the uncertainty of the calculations. Further studies of these processes is necessary before confidence in this number for a specific area can be established. Meanwhile, the amount of dissolved Fe and Al that is precipitated can be varied and a range determined similar to what is shown in Table 25.14. The technique described is a first approximation on calculating geochemical baselines of stream waters. As more studies of processes that control element mobility in waters are carried out, further refinement in the technique will be possible.

REFERENCES

Bove, D.J., Berry, T., Kurtz, J., Hon, K., Wilson, A.B., Van Luenen, R.E., and Kirkham, R.M., 1995, Geology of hydrothermally altered areas within the upper Alamosa river basin, Colorado, and probable effects on water quality: Colorado Geological Survey Spec. Pub. No. 38, Proceedings, Summitville Forum 95, pp. 35–41.

Brown, A., 1995, Geohydrology and adit plugging: Colorado Geological Survey Spec. Pub. No. 38, Proceedings, Summitville Forum 95, pp. 87–98.

Colorado Climate Center, 1984, Colorado average annual precipitation 1951–1980: Compiled by Dept. of Atmospheric Science, Colo. State Univ., Fort Collins, scale 1:500,000.

Gray, J.E. and Coolbaugh, M.F., 1994, Geology and geochemistry of Summitville, Colorado—An epithermal acid-sulfate deposit in a volcanic dome: Economic Geology, Spec. Issue on Volcanic Centers as Exploration Targets, v. 89, in press.

Koyanagi, V.M. and Panteleyev, A., 1993, Natural acid-drainage in the Mount McIntosh-Pemberton Hills area, Northern Vancouver Island (92L/12); in Grant, B., and Newell, J.M., (eds.), Geological Fieldwork 1992: B.C. Ministry of Energy, Mines and Petroleum Resources, Paper 1994–1, pp. 119–125.

Lipman, P.W., 1975, Evolution of the Platoro caldera complex and related volcanic rocks, southwestern San Juan Mountains, Colorado: U.S. Geological Survey Professional Paper 852, 128 pp.

Lipman, P.W., Steven, T.A., and Mehnert, H.H., 1970, Volcanic history of the San Juan Mountains, Colorado, as indicated by potassium-argon dating: Geological Society America Bulletin, v. 81, pp. 2329–2352.

Mehnert, H.H., Lipman, P.W., and Steven, T.A., 1973, Age of mineralization at Summitville, Colorado, as indicated by K-Ar dating of alunite: Economic Geology, v. 68, pp. 399–401.

McHugh, J.B., Miller, W.R., Meir, A.L., and d'Angelo, W.M., 1995, Chemical analyses of 33 surface water samples from the Redcloud Peak area, Colorado: U.S. Geological Survey Open-File Report 95–79, 5 pp.

Miller, W.R., and McHugh, J.B., 1994, Natural acid drainage from altered areas within and adjacent to the Upper Alamosa River Basin, Colorado: U.S. Geological Survey Open-File Report 94–144, 47 pp.

Naeser, C.W., Cunningham, C.G., Marvin, R.F., and Obradovich, J.D., 1979, Pliocene intrusive rocks and mineralization near Rico, Colorado: U.S. Geological Survey Open-File Report 79–1093, 19 pp.

Parkhurst, D.L., Thorstenson, D.C., and Plummer, L.N., 1980, PHREEQE—A computer program for geochemical calculations: U.S. Geological Survey Water-Resources Investigation 80–96, 210 pp.

Plumlee, G.S., Gray, J.E., Roeber, Jr., M.M., Coolbaugh, M., Flohr, M., and Whitney, G., 1995, The importance of geology in understanding and remediating environmental problems at Summitville: Colorado Geological Survey Spec. Pub. No. 38, Proceedings, Summitville Forum 95, pp. 13–22.

Pratt, W.P., McKnight, I.T., and De Hon, R.A., 1969, Geologic map of the Rico quadrangle, Dolores and Montezuma Counties, Colorado: U.S. Geological Survey Geologic Quadrangle Map GQ–797, scale 1:24,000.

Richmond, G.M., 1965, Glaciation of the Rocky Mountains; in Wright, H.E., Jr., and Frey, D.G. (eds.), The Quaternary of the United States: Princeton Univ. Press, Princeton, N.J., pp. 217–230.

Sanford, R.F., Grauch, R.I., Hon, K., Bove, D.J., and Grauch, V.J.S., 1987, Mineral resources of the Redcloud Peak and Handies Peak wilderness study areas, Hinsdale County, Colorado: U.S. Geological Survey Bulletin 1715, 38 pp.

Selner, G.I., and Taylor, R.B., 1992, System 8. GSMAP, GSMEDIT, GSMUTIL, GSPOST, GSDIG and other programs version 8, for the IBM PC and compatible microcomputers, to assist workers in the earth sciences: U.S. Geological Survey Open-File Report 92–217, 217 pp.

Steven, T.A., and Ratte, J.C., 1960, Geology and ore deposits of the Summitville district, San Juan Mountains, Colorado: U.S. Geological Survey Professional Paper 343, 70 pp.

U.S. Geological Survey, 1993, Water resources data for Colorado, water year 1992: v. 2, 406 pp.

Chapter 26

A CASE STUDY ON THE AEROBIC AND ANAEROBIC REMOVAL OF MANGANESE BY WETLAND PROCESSES

L.A. Clayton,¹ J.L. Bolis,¹ T.R. Wildeman,² and D.M. Updegraff²

¹*McCulley, Frick, and Gilman, 4900 Pearl East Circle, Suite 300W, Boulder, CO 80301*

²*Department of Chemistry and Geochemistry, Colorado School of Mines, Golden, CO 80401*

Constructed wetlands have been utilized to passively remove metals and raise the pH of acid mine drainage. Manganese is typically the most difficult metal to remove from solution due to the high pH (>8) required to form insoluble manganese precipitates. A study of the removal of manganese by wetland processes was conducted using two guidelines. A microbial ecosystem approach was used to select and test reasonable candidates for passive treatment. Also, a staged design approach consisting of laboratory and bench-scale studies was conducted to examine manganese removal by aerobic versus anaerobic constructed wetland processes. Aerobic laboratory experiments found that common green algae (pond scum) removed large concentrations of manganese from solution and raised the pH through photosynthesis. Aerobic bench-scale reservoirs were constructed containing green algae (predominantly *Cladophora*) and mine drainage that had passed through an anaerobic constructed wetland, but still contained 32 mg/l Mn. Static and flow tests were conducted so that manganese was consistently removed to NPDES standards (2 mg/l). Manganese (oxide) coatings on the *Cladophora* appear to be an important removal mechanism. Four anaerobic bench-scale reactors were constructed, however, only the reactors containing a composted manure substrate achieved manganese removal to the NPDES standard for a significant portion of the experiment. In conclusion, manganese removal from severe acid mine drainage through the use of constructed wetlands requires a two-stage process. An aerobic algal pond appears to be a promising treatment method.

INTRODUCTION

Acid mine drainage is produced by the alteration of minerals that have been disturbed by mining activities; it is characterized by a low pH, high sulfate concentration, and high dissolved metals concentration. When acid mine drainage comes into contact with minerals containing manganese such as rhodochrosite (MnCO_3), manganese is released into solution. As a result, manganese concentrations in mine drainage can range from less than 2 to greater than 100 mg/l (Wildeman, 1991).

Iron and manganese are the two most commonly regulated metals in coal mine drainage (Kepler, 1988). Iron is relatively easy to remove from mine drainage chemically, but manganese removal is more difficult and more expensive. This difference arises from two facts: manganese(II) hydroxide solubility is six to seven times greater than iron(II) hydroxide solubility (Crerar et al., 1972) and, over a wide pH range, the kinetics for the oxidation of Mn(II) are

significantly slower than that for the oxidation of Fe(II) (Wehrli and Stumm, 1989). Consequently, chemically raising the pH of mine drainage to near neutral can precipitate many metal contaminants. However, this process may not remove manganese due to the high pH and long time required to form manganese precipitates (Watzlaf, 1985).

Federal National Pollutant Discharge Elimination System (NPDES) regulations require that mine drainage discharge waters meet effluent standards of a daily maximum of 4.0 mg/l total manganese and 2.0 mg/l total manganese on a monthly average (U.S. Code of Federal Regulations, 1997a, b). Also, effluent limitations require the pH of the drainage to be between 6.0 and 9.0 (U.S. Code of Federal Regulations, 1997a, b). The use of microorganisms for the removal of heavy metals from acid mine drainage has become an important alternative to chemical treatment. Constructed wetlands have been proven to substantially increase the pH and remove many of the heavy metals from mine drainage by forming insoluble metal precipitates (Wildeman et al., 1992a; Hedin and Nairn, 1992; Brodie, 1991). However, manganese is often the most difficult metal to remove from solution and microbial manganese removal is rarely achieved. An example of this removal difficulty is seen in the results from the Big Five pilot wetland.

The Big Five wetland was constructed in 1987 in Idaho Springs, Colorado, as a pilot-scale system to passively treat acid mine drainage from the Big Five Tunnel, which has chemical characteristics shown in Table 26.1 (Wildeman et al., 1992a; Machermer et al., 1993). Built by the Colorado School of Mines, the wetland consists of six individual cells, each designed to anaerobically raise the pH and remove the metal contaminants from the Big Five drainage. The adsorption of metals onto the organic substrate contributes initially to the removal of metals from the mine drainage, but the predominant metal removal and acid neutralizing process is the microbially-mediated reduction of sulfate to sulfide and subsequent precipitation of metal sulfides (Reynolds et al., 1991; Machermer and Wildeman, 1992). The sulfate reduction and iron sulfide precipitation reactions, where CH_2O represents organic matter, are as follows:



The sulfate reduction reaction consumes hydrogen ions, thus raising the pH of the mine drainage.

TABLE 26.1—Chemical characteristics of the Big Five mine drainage in Idaho Springs, Colorado (in mg/l except for pH).

pH	2.6	Zn	10.
Al	18	Cd	0.03
Fe	50	Pb	0.01
Mn	32	As	0.02
Cu	1.6	SO ₄ ²⁻	2100

Two year removal results for Big Five Cell E are shown on Figure 26.1. Excellent removals of zinc and copper (≈99%) were obtained at the Big Five wetland and the pH was raised from below 3 to above 6 (Wildeman et al., 1992a). Iron removal was less consistent and varied seasonally, sulfate was reduced by 10 to 15%, but manganese showed essentially no removal. The poor manganese removal is attributed to the high pH (>7) required to precipitate manganese sulfides or carbonates in reducing conditions (Stumm and Morgan, 1981).

The objective of this project was to develop a procedure to maximize the removal of manganese from mine drainage through the use of low-cost, passive, constructed wetlands. It was assumed that the metabolism of microbes and algae would directly remove manganese or provide the reactants for precipitation (Wildeman et al., 1994a). However, based on experience with a bacterial consortium at the Big Five wetland, a microbial ecosystem approach was used to determine the best conditions for treatment. This allows use of conditions more closely approximating the final configuration of the constructed wetland. However, it eliminates the possibility of attributing removal to a specific genus and species of microorganism (Wildeman et al., 1994a). Because aerobic and anaerobic wetlands are different microbial ecosystems and emphasize different metal removal processes, both were used in the study.

Concentrating on microbial ecosystems enables one to take a more systematic approach to wetlands treatment. As opposed to using macrophytes, it is simple to collect and conduct experiments with microbes and algae. In this case, successful development of constructed wetlands starts in the laboratory where the removal

processes are studied and promising ecosystems are chosen for further experiments. Then, bench-scale studies are performed to determine how flow of the contaminated water through the system affects removal efficiency. The goal of these studies is to provide a loading capacity of the wetlands receiving a contaminated water. From the bench-scale results a demonstration system is designed, constructed, and tested. A full-scale system then involves the construction of more demonstration modules. This is the staged design of a wetland system (Reynolds, 1991; Wildeman et al., 1992a). This paper includes the laboratory and bench-scale studies. Based on the bench-scale results, pilot-scale systems have recently been constructed and are currently being evaluated (Wildeman et al., 1993).

LABORATORY INVESTIGATIONS

Introduction

The objectives of the laboratory experiments were as follows:

- 1) Determine an aerobic or anaerobic microbial ecosystem that could remove manganese.
- 2) Examine the conditions (pH, nutrient mix) that will promote maximum activity within this ecosystem.
- 3) Examine the manganese removal efficiency of the ecosystem.
- 4) Based on the results of objectives 1–3, determine the potential of aerobic and anaerobic bench-scale manganese removal treatment systems.

Manganese removal in an aerobic wetland would most likely be by the precipitation of manganese(III) or (IV) oxides. The formation of MnO₂ would be favorable due to the high sorption capacity of MnO₂, which enables it to bind many other trace metals, including manganese(II), to the oxide surface (Lind and Anderson, 1992; Loganathan and Burau, 1973). This autocatalytic process would increase the rate of manganese(II) removal from solution (Nealson et al., 1988), as shown by the following reactions (Stumm and Morgan, 1981):

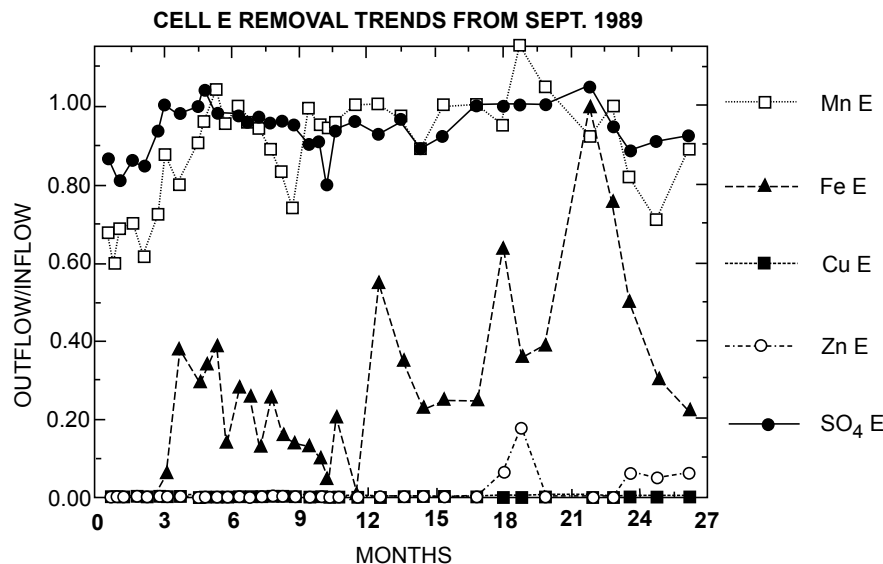
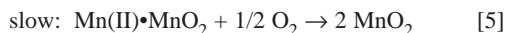
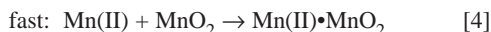
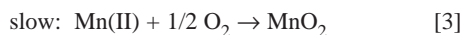


FIGURE 26.1—Big Five Cell E removal trends. Inflow is the mine drainage from Table 26.1; outflow is effluent from the wetland cell.



Manganese oxidation is highly pH-dependent and the kinetics of uncatalyzed manganese oxidation are very slow, often requiring several years to form a manganese oxide precipitate (Diem and Stumm, 1984; Nealson et al., 1988; Wehrli and Stumm, 1989). Measurable rates of uncatalyzed manganese oxidation are only observed at pH >8.5 (Marshall, 1979). Without microbial or surface catalysts, manganese oxide precipitation will not occur without high pH, high Eh, and manganese and oxygen concentrations much greater than saturation (Lind et al., 1987).

Manganese removal in an anaerobic wetland would probably be through formation of a manganese(II) precipitate such as MnCO_3 or adsorption/precipitation of manganese(II) on a solid surface (Bolis et al., 1991; Faulkner and Richardson, 1990). Manganese sulfides are rare and are not likely to be formed by biogeochemical means (Silverman and Ehrlich, 1964).

These constraints on the biogeochemistry of manganese dictated the selection of the microbial ecosystems.

Materials and methods

A complete description of the laboratory study is found in Duggan (1993) and Duggan et al. (1993). This section contains those methods and experiments that best describe the microbial ecosystem approach. Because this was the first time within our group that this approach was used to investigate aerobic wetland processes, these experiments are emphasized. Anaerobic laboratory studies of this type have been described by Wildeman et al. (1994b, c). Therefore, only the conclusions from those experiments abstracted from the complete description (Duggan et al., 1993) will be summarized in the Results and Discussion section.

Based upon the biogeochemistry of manganese that was previously described, algae and muds were collected from several different local streams, eutrophic ponds, and mine drainage areas. Besides biogeochemical criteria, an attempt was made to collect a diversity of ecosystems. The ecosystems collected and their paste pH's are given in Table 26.2. Samples in flasks 30, 31, and 33 were from environments with high levels of manganese. Thus, the organisms living in these samples would be tolerant to high manganese concentrations. The black solid in Flask 33 was collected because it was determined by Sellstone (1990) to be a manganese oxide precipitate. However, in all other cases, collection was purposefully performed so that algae and mucky sediments were taken from several areas at the site and mixed together so that as complete a microbial ecosystem as possible was collected. This type of sampling emphasizes the total ecosystem. However, it makes chemical and mineralogic description of the sediments as well as determination of the genus and species of the microorganisms extremely difficult. For this reason, although local conditions cause the contents of Flask 34 to be blue-green algae dominated by *Cladophora*, the attempt was to collect a "pond scum" type of ecosystem, so that is a more accurate description of the sample. For all ecosystems, excess site water was collected to ensure that

the sample would remain saturated. All experiments were begun within one week to minimize degradation.

TABLE 26.2—Individual inoculum comprising the mixed inoculum.

Ecosystem Sample	Flask number	Paste pH
Algae growing in acid mine drainage	30	≈3
Brown precipitate in effluent pipe at Big Five wetland	31	≈3
Black mud in effluent of a waste water treatment plant	32	≈8
Black manganese oxide solid in acid mine drainage stream	33	≈6.5
Pond scum (green algae, predominantly <i>Cladophora</i>) from freshwater stream	34	≈7.5

The primary aerobic laboratory experiment was conducted in Erlenmeyer flasks that were exposed to the atmosphere to promote aerobic conditions. Each flask contained Big Five mine drainage that had been adjusted to a pH of 7.0 with NaOH in order to form a more hospitable environment for microbes. Microbial manganese oxidation has not been found to occur at very acid pH values (Ehrlich, 1990). Additional manganese, yeast extract, and deionized water were added to some of the flasks. Yeast extract was added as a nutrient source and deionized water was added to bring the volume in each flask to 75 ml. The additional manganese solution was a 30 mmol $\text{MnCl}_2(4\text{H}_2\text{O})$ solution (1650 mg/l Mn), and the yeast extract contained 1 g/l yeast. The final manganese concentration of the flasks containing the Big Five mine drainage and the additional manganese solution was approximately 240 mg/l. Since aerobic wetlands are typically shallow and exposed to the sunlight, half of the flasks were kept in the dark and the other half were kept in the light to examine if light was a necessary factor for manganese removal.

For most of the flasks, a mixed inoculum of equal portions of the five ecosystems described in Table 26.2 was used. In order to determine the percentage of manganese removal attributed to each individual inoculum comprising the mixed inoculum, additional flasks (30–34) were prepared of the individual ecosystems. Each of these five flasks contained 75 ml of an individual inoculum in the water it was collected in, plus an additional 10 ml of the manganese solution used above. No yeast was added to flasks 30–34 and they were kept in the light.

Flasks were tested periodically for pH to monitor whether the processes occurring within the flasks were raising the pH and subsequently encouraging manganese oxidation (Duggan et al., 1993). After 4 weeks, the supernatants from each flask were filtered, acidified, and analyzed for dissolved manganese by flame atomic absorption.

Results and discussion

The initial and final pHs and manganese concentrations of the mixed and individual inoculum flasks for the aerobic experiment are given in Table 26.3. The flask numbers are coded according to the conditions of the flask and the codes are given in the table

footnotes. Values in parentheses are duplicates and <0.3 represents a concentration below the detection limit. Some water evaporated from the flasks, causing the final manganese concentration to be larger than the initial manganese concentration.

TABLE 26.3—Initial and final dissolved manganese concentrations (in mg/l) and pHs for the aerobic experiment. The key to the experiment codes is given at the bottom of the table.

Flask number	Initial Mn	Final Mn	Initial pH	Final pH
Mixed Inoculum in dark:				
1 (D)	17	26	6.7	6.8
2 (MnD)	240	35	6.9	6.7
3 (MnYD)	240	352	6.7	7.7
4 (InD)	17	<0.3	7.3	7.8
5 (MnInD)	240	123	7.4	7.0
6 (MnYInD)	240	336	7.2	7.0
Mixed Inoculum in light:				
13 (L)	17	22 (20)	7.2	6.4
14 (MnL)	240	370	7.1	6.2
15 (MnYL)	240	333	6.5	7.3
16 (InL)	17	<0.3	7.5	7.85
17 (MnInL)	240	75	7.6	7.1
18 (MnYInL)	240	6	7.6	6.7
Individual Inoculum, in light:				
30 (algae, Mn)	220	310 (145)	3	3.0
31 (brown ppt, Mn)	220	392	3	2.3
32 (mud, Mn)	190	147	8	7.9
33 (black ppt, Mn)	200	109	6.5	6.35
34 (pond scum, Mn)	190	<0.3	7.5	7.5

Experiment Key: Mn is additional manganese solution, Y is yeast extract, In is mixed inoculum, D is dark, and L is light.

Of the mixed inoculum flasks, two flasks (#4 InD and 16 InL) removed the manganese to concentrations below the detection limit and one flask (#18 MnYInL) removed the manganese down to 6 mg/l. Flasks #4 (InD) and 16 (InL) were identical except that #4 (InD) was kept in the dark and #16 (InL) was kept in the light. Both flasks contained the manganese found in the Big Five effluent and the mixed inoculum, but no additional manganese solution. Black precipitates and green microbial growth were observed on the walls of flask #16 (InL), whereas black precipitates and small white plants(?) were found in flask #4 (InD). The control flasks containing only Big Five effluent, #1 (D) and 13 (L), did not remove the manganese from solution. Thus, at the lower manganese concentrations (≈ 20 mg/l), the manganese appeared to be removed microbially by the production of black precipitates.

Flask #18 (MnYInL), which contained the Big Five effluent, additional manganese solution, yeast, and inocula, performed the best of the high manganese solution flasks. Black precipitates were observed in this and several of the other high manganese flasks (#5 MnInD and 17 MnInL). It appears that light was an important factor attributing to the manganese removal in flask #18 (MnYInL). Flask #6 (MnYInD), which was identical to #18 (MnYInL) except that it was kept in the dark, contained 336 mg/l Mn at the completion of the experiment, as compared to 6 mg/l for flask #18 (MnYInL). The addition of yeast as a nutrient also appeared to be beneficial to manganese removal as shown by the

comparison of flask #17 (MnInL) to flask #18 (MnYInL).

In summary, for the mixed inoculum, light with yeast, are the most effective conditions for removing high concentrations of manganese under aerobic conditions. At the lower manganese concentrations such as those typically found at the Big Five, the effects of light and yeast were unimportant as long as the inoculum was present. The mixed inoculum obviously contained an important microbe or precipitate that catalyzed the oxidation of manganese. Thus, the objective of finding a source of microbes that could oxidize manganese had been accomplished. To determine which ecosystem sample contained these important microbes, the performance of the individual inoculum flasks was examined.

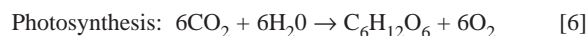
The five individual inoculum flasks provided the most important results of the experiment. The pond scum sample from a freshwater stream (#34) removed the high manganese concentrations down to below detection limit. All four of the other individual inoculum flasks contained greater than 100 mg/l manganese at the completion of the experiment.

Flask #34 formed black precipitates that appeared to be associated with green microbial growth on the walls of the flask. Subsequent studies characterized the pond scum in the Golden, CO area as photosynthetic green and blue-green algae, with the predominant genus being *Cladophora*. If the algae were a catalyst in the manganese removal, this would explain the dependence on light for manganese removal observed in the mixed inoculum experiments (#18 vs. #6). Thus, it appears that the pond scum algae are tolerant of, and have the ability to aerobically remove, high concentrations of manganese from solution.

There was a substantial difference between the manganese concentrations in the sample and duplicate of flask #30. This flask contained a precipitate in the form of very thin slabs floating on the water surface. Viewed under low magnification, these precipitates are composed of orange and black rounded particles. If some of this precipitate was inadvertently collected in the sample to be analyzed, this may have caused a difference in manganese concentrations.

A second aerobic laboratory study was conducted that was similar to the first, except that a different pond scum ecosystem was used and the additional manganese solution was not added (Duggan et al., 1993). All test tubes containing the pond scum decreased the manganese from 19 mg/l to less than 1 mg/l. Also, all experiments containing the inoculum produced brown-black precipitates on the test tube walls. X-ray diffraction study indicated that the black precipitate in one of the test tubes is amorphous and SEM-EDX indicated that it contains calcium and manganese. During this second aerobic experiment, diurnal pH fluctuations were noticed in the test tubes containing pond scum. To examine the extent of these fluctuations, pH measurements were made one day in the mid-afternoon and then the test tubes were placed in the dark to be measured for pH again early the next morning. The changes in the pH values are shown in Table 26.4.

The photosynthetic process increases the pH and redox potential of the solution by the uptake of carbon dioxide, which is an acid, and release of oxygen. Respiration, the reverse of photosynthesis, occurs at night and involves the uptake of oxygen and release of carbon dioxide, resulting in a lower pH. The simplified photosynthesis and respiration reactions are given below:



Materials and methods

Aerobic experiments

Two bench-scale reservoirs were constructed to examine the ability of an algal mixture to tolerate and remove manganese in a larger scale system. The reservoirs were constructed from small plastic swimming pools, each approximately 1.1 m in diameter. Each of the two pools initially contained 97 l of Big Five wetland effluent and 5 l of algae from a local pond. This sample was collected from still another different location than the algal samples collected in the laboratory experiments. It was assumed that aerobic manganese removal would be a second stage process for acid mine drainage. Therefore, the water to be treated was effluent from Big Five Cell E that had a pH of 5.8, but still contained 32 mg/l manganese. The only difference between the two reservoirs was that the bottom of one reservoir was covered with 12 kg of limestone ranging in size from dust to approximately 2 cm in length. This reservoir will be referred to as "reservoir LS" and the reservoir that did not contain limestone will be denoted "reservoir NoLS." The reservoirs were placed on the roof of the Chemistry and Geochemistry building at the Colorado School of Mines to allow for exposure to direct sunlight and other environmental conditions.

The experiment was conducted for approximately four months, from mid-August to mid-December, thus incorporating a wide range of weather conditions. The reservoirs were static for the first two months of the experiment, with approximately 20–40 l/wk of additional effluent added after Day 10 to account for water loss due to evaporation. The weather was typically warm (15–25°C) and sunny during this portion of the experiment.

A flow system was installed during the last two months of the experiment to determine approximate loading and removal rates. This was accomplished using a peristaltic pump to monitor flow from a feed tank into the reservoirs. The outlet tube was located 7 cm above the base of each reservoir. The diameter of the pools was 1 m at the height of the outlet. The outflows were collected in plastic containers that were connected to the reservoirs by Tygon® plastic tubing. The weather during this portion of the experiment was usually cold (0–10°C) and snowy; the reservoirs froze several times.

Because the formation of manganese oxides is highly pH dependent, special attention was paid to its measurement. During the static portion of the experiment, the pH was taken at different areas in each reservoir to account for differences due to the amount of biomass present and because the amount of sunlight received at each location may affect the amount of photosynthesis. The pH values cited below are geometric averages of the several measurements. Each sample collected from the static reservoirs was a composite sample containing water from different areas within the reservoir. During the portion of the experiment when the pump was monitoring the water flow, the pH's (Table 26.5) and samples were taken from the water collected in the outflow containers. The samples were acidified after collection and then filtered and analyzed for manganese by flame atomic absorption spectrophotometry. By acidifying the samples before filtering them, total manganese was measured (NPDES standards are given in terms of total manganese).

Once during the static portion and once during the pump portion of the experiment, a high concentration manganese solution was added to the reservoirs to examine the effectiveness of the

algae in tolerating and removing high manganese concentrations in medium pH waters. This 100 mg/l manganese solution was prepared with manganese sulfate and deionized water had a pH of 4.9.

TABLE 26.5—Flow rate, effluent pH, and effluent Mn concentration in mg/l for reservoirs LS and NoLS.

Day number	Reservoir NoLS			Reservoir LS		
	Flow	pH	Mn	Flow	pH	Mn
71	2.1	9.1	3.2	2.5	9.2	1.0
73	3.9	9.3	nd	3.9	8.7	0.7
84	2.1	8.5	32.1	2.4	8.5	14.0
86	nd	8.5	253	nd	8.8	1.4
91	3.0	8.1	13.0	1.5	8.2	0.6
94	4.5	8.2	10.1	4.5	8.5	1.2
97	4.0	8.6	4.8	4.5	8.6	2.2
99	nd	8.5	3.2	nd	8.4	1.4
100	nd	8.3	2.3	nd	8.4	0.5
103	3.7	8.5	2.3	3.9	nd	1.0
120	3.1	8.1	3.8	1.8	8.1	0.6
125	3.0	8.2	5.0	3.8	8.2	0.3
127	3.0	8.2	7.2	3.7	8.3	0.7

Flow measured in ml/min, Mn in mg/l. nd = data collected. Influent Mn averaged approximately 30 mg/l.

Anaerobic experiments

The anaerobic bench-scale reactors were constructed from four 32 gallon plastic garbage cans in the same manner as described in Bolis et al. (1991) and Wildeman et al. (1992a). Complete details of this experiment were reported by Bolis (1992). Manganese removal was achieved in anaerobic bench-scale studies by Bolis et al. (1991) using a composted manure substrate, therefore, composted manure (75% cow manure and 25% planter soil by volume) was chosen as one of the substrates for this experiment. A second substrate was also tested and was composed of crushed limestone, alfalfa, and inoculum. The inoculum consisted of substrate from currently active cells at the Big Five pilot wetland that have been shown to contain sulfate-reducing bacteria (Batal et al., 1989). Two reactors contained the composted manure substrate and two reactors contained the limestone-alfalfa mix.

Two initial substrate conditions were evaluated: soaked and dry. The two soaked reactors, one with the composted manure substrate and one with the limestone-alfalfa substrate, were filled with mine drainage for one week before the experiment was begun. This allowed the inoculum to incubate and ensure sulfate-reducing activity at the initiation of the experiment. The other two reactors were dry at the beginning of the experiment. Flow rates were maintained as closely as possible to 10 ml/min, based on research that the rate of sulfide production for a wetland treating acid mine drainage is approximately 300 nanomoles/cm³/d (Reynolds et al., 1991; Wildeman et al., 1994a).

This experiment was begun in the summer of 1991 and ran for 132 days, ending in the late fall. The reactors were located on a platform near the Big Five Wetland system in Idaho Springs, Colorado and situated at a level that would allow for gravity flow from the Big Five Tunnel. Unlike the aerobic bench-scale experiment which used effluent that had previously passed through the

wetland treatment, untreated Big Five acid mine drainage flowed through the anaerobic reactors.

Sampling and analytical procedures followed an EPA quality assurance and quality control plan (Wildeman, 1988). The outflow was not continuously collected and stored in containers as in the aerobic flow experiment, therefore, samples and measurements for this experiment are representative of the time of sampling only. During bimonthly sampling of the reactors, 250 ml samples were collected. pH, Eh, conductivity, and temperature measurements were taken and the samples were filtered and acidified in the field. For laboratory analysis, the samples were digested with HNO_3 and HCl. Iron, manganese, copper, and zinc concentrations were determined by flame atomic absorption spectrophotometry. Sulfate was determined gravimetrically by the precipitation of BaSO_4 .

Results

Aerobic experiments

Figure 26.2 shows the changes in pH and manganese concentrations over the course of the static portion of the experiment for the two reservoirs. In addition, to provide indication of photosynthesis, extensive pH measurements were made during the static experiment. The initial pH of the water in each reservoir was 5.8 and contained approximately 32 mg/l manganese. During the first week of the experiment, the pH of each reservoir gradually rose. The pH of reservoir LS was usually slightly higher than the pH of reservoir NoLS. On Day 10, the pH rose 0.3 units in each pool between 7:00 AM and 3:00 PM and reservoir NoLS contained 2.5 mg/l manganese and reservoir LS only 0.5 mg/l.

Much of the water had evaporated from the reservoirs and most of the manganese had been removed from solution. Therefore, on Day 11 at 1:30 PM, 20 l of additional mine drainage effluent from the Big Five Wetland were added (pH = 6.0) to each reservoir. This addition lowered the pH to 7.2 and 7.5 for reservoir NoLS and reservoir LS, respectively, on Day 12 at 6:50 AM. However, on Day 12 at 3:15 PM, the pH increased to 8.2 for reservoir NoLS and 8.5 for reservoir LS. During the remainder of the static portion of the experiment, Big Five Wetland effluent was added about twice a week (20–40 l/wk) and the reservoir pH levels usually recovered within a day or two of the effluent addition.

On Day 20, 40 l of the 100 mg/l manganese solution having a pH of 4.9 were added to each reservoir. Before this addition, the water level in the reservoirs was very low (approximately 40 to 50 l). On Day 25 at 9:30 AM, reservoir NoLS had a pH of 7.6 and contained 51 mg/l of manganese, whereas reservoir LS had a pH of 8.1 and contained 13 mg/l of manganese. For the next two weeks, additional Big Five Wetland effluent was added occasionally, diurnal pH fluctuations continued to be observed, and the outside temperature often fell to near freezing. By Day 42 at 9:30 AM, reservoir NoLS had a pH of 8.8 and contained 10 mg/l of manganese, whereas reservoir LS had a pH of 9.3 and contained less than 0.3 mg/l of manganese. Thus, both reservoirs appeared to be removing the manganese from a medium pH, high manganese solution. During the static portion of the experiment, the algal biomass had grown extensively, appeared healthy, and black precipitates and gas bubbles could be seen in the algal mat.

The pump system was installed in mid-October, on Day 65, with an initial mine drainage effluent flow rate of 3.1 ml/min into

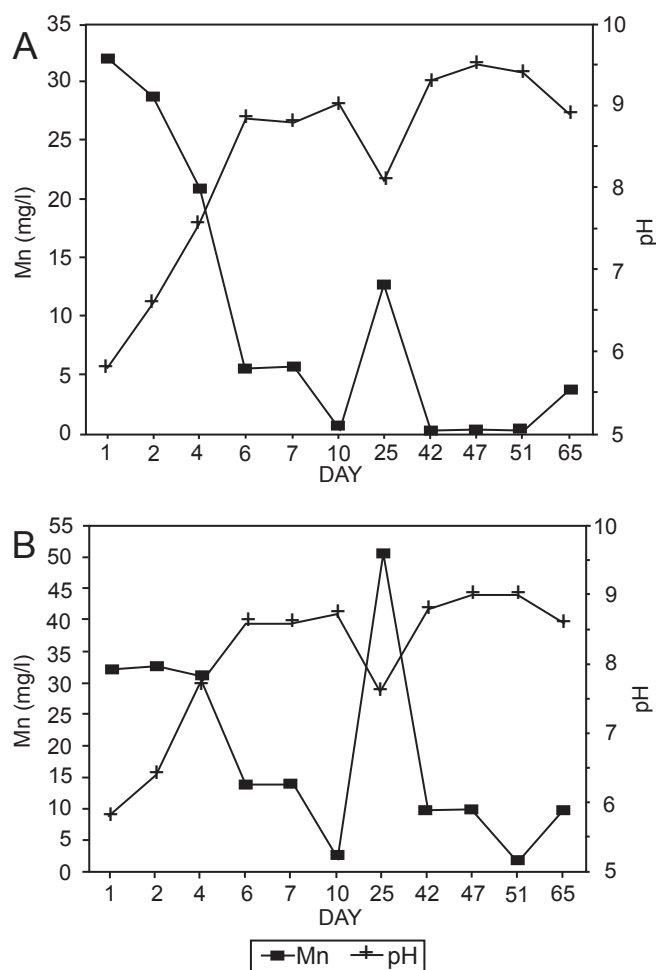


FIGURE 26.2—Results of the aerobic static bench-scale experiment. (A) Reservoir LS, (B) Reservoir NoLS. 100 mg/l Mn solution added on Day 20.

each reservoir. The mine drainage effluent had a pH of 6.3 and contained approximately 23 mg/l of manganese. The effluent was collected weekly from the Big Five Wetland and was stored in plastic feed tanks, so it is unlikely that any change in the water chemistry occurred. It took several days for the water levels in the pools to reach the outlet when the flow system was initiated. The results of the flow experiment are given in Table 26.5. Outflow manganese concentrations and pH values are shown on Figure 26.3.

On Day 79, the mine drainage effluent in the feed tank was replaced with the same 100 mg/l manganese solution that was used in the static experiment. This solution was pumped at 5 ml/min until Day 80, when the flow was adjusted to 3 ml/min because the water and algae in the reservoirs were frozen solid except for a small area around the inlet. On Day 84 samples were collected and the remaining 20 l of manganese solution were mixed with 20 l of Big Five Wetland effluent.

Several processes appeared to be occurring in the reservoirs to remove the manganese from solution. Low magnification microscopy indicated that black precipitates formed as crusts on the filamentous green alga, *Cladophora*. SEM-EDX analyses sug-

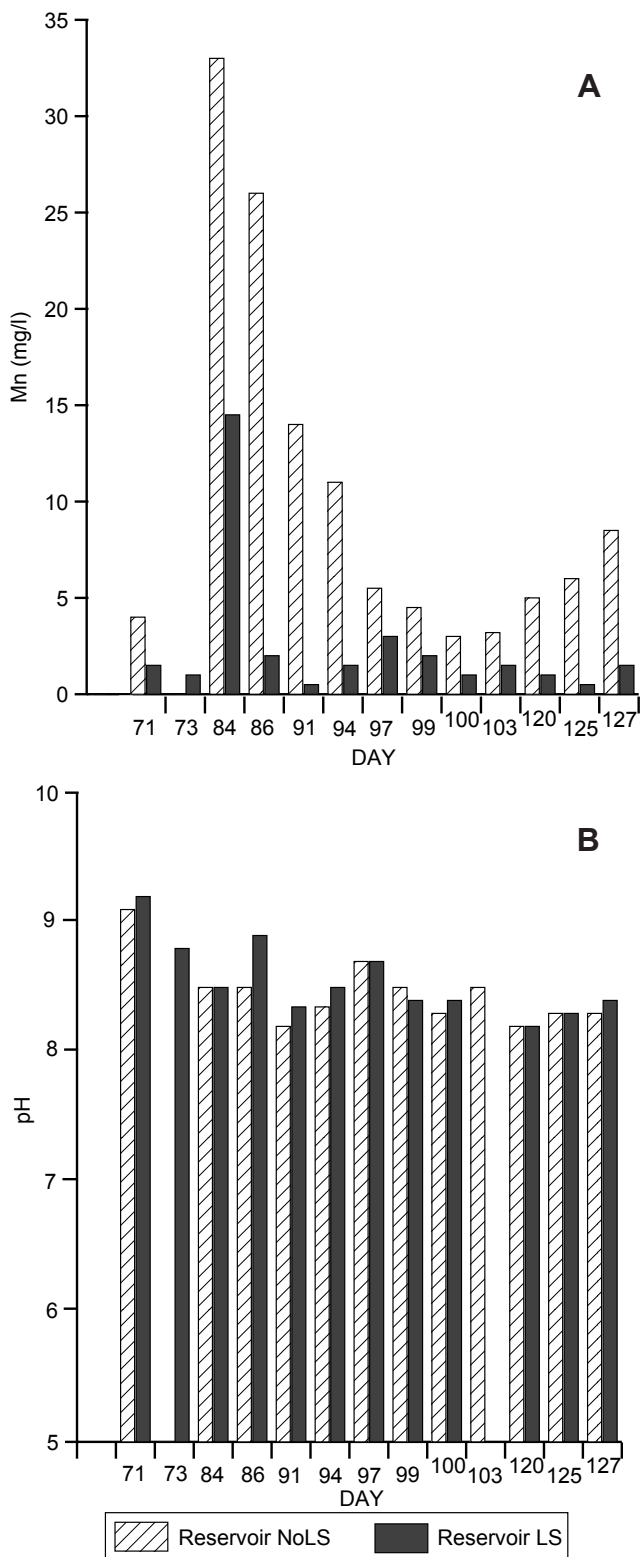


FIGURE 26.3—Results of the aerobic flow bench-scale experiment. (A) Effluent Mn concentration, (B) effluent pH. 100 mg/l Mn solution began on Day 79.

gested that the crusts contained calcium-manganese oxides, which were determined to be amorphous by XRD analysis. Subsequent sequential extraction experiments on these crusts revealed that precipitates are associated with the carbonate, manganese(IV), and ferric oxide phases and not with the easily extracted or organic phases (Duggan, 1993; Duggan and Wildeman, 1994).

Anaerobic experiment

Field data and the manganese and iron concentrations in the mine drainage and composted manure reactor effluents for the anaerobic experiment are given in Table 26.6. The pH measurements for both reactors remained above 7 for the entire study, which should encourage the precipitation of manganese. The Eh measurements were frequently positive, though they did decrease throughout the experiment. A negative Eh is desirable, because it often indicates that sulfate reduction is occurring. The Eh of the soaked reactor was usually lower than the Eh of the dry reactor.

TABLE 26.6—Field data and manganese and iron concentrations for the composted manure reactor effluents.

Reactor		Day number					
		8	23	35	49	84	132
pH	M.D.	3.1	3.1	3.2	3.1	3.0	3.1
	dry	7.3	7.0	7.1	7.3	7.0	7.0
	soaked	7.6	7.4	7.1	7.4	7.3	7.1
Eh	dry	250	140	60	90	90	5
	soaked	220	110	110	-10	40	-80
Flow	dry	13	0	10	7	18	16
	soaked	9	0	9	9	15	34
Mn	M.D.	37	35	35	35	36	37
	dry	1	2	4	6	19	32
	soaked	2	1	1	1	19	29
Fe	M.D.	52	43	40	37	39	40
	dry	2	4	1	1	7	8
	soaked	7	3	1	1	1	3

Eh measured in mV, flow in ml/min, and Mn, Fe in mg/l.
M.D. = Big Five mine drainage

More than 82% manganese removal was achieved by both reactors through Day 49, but declined to approximately 48% on Day 84 and less than 25% on Day 132. There was a slight decrease in pH throughout the experiment and a decrease in temperature which would affect microbial activity. Iron removal began to decrease towards the end of the experiment as the temperature decreased. This can also be caused by decreased microbial sulfate reduction (Wildeman et al., 1994b).

Field data and the manganese concentration of the mine drainage and limestone-alfalfa reactor effluents are given in Table 26.7. The flow rates were more difficult to control for the limestone-alfalfa reactors than the composted manure reactors (Bolis et al., 1992). Both reactors showed gradual pH increases throughout the experiment, from 5.5 to over 6.5, but never reached 7. The limestone-alfalfa reactors were successful in producing anaerobic conditions, with negative Eh measurements for both reactors throughout the last half of the experiment.

TABLE 26.7—Field data and manganese concentration of the mine drainage and the limestone-alfalfa reactor effluents.

Reactor		Day number					
		8	23	35	49	84	132
pH	M.D.	3.1	3.1	3.2	3.1	3.0	3.1
	dry	5.5	5.6	6.0	6.7	6.8	6.6
	soaked	5.5	5.5	5.8	6.4	6.6	6.6
Eh	dry	90	110	30	-60	-100	-90
	soaked	-10	90	10	-60	-90	-80
Flow	dry	0	36	30	0	5	50
	soaked	0	54	40	17	10	20
Mn	M.D.	37	35	35	35	36	37
	dry	63	59	33	29	28	30
	soaked	63	62	44	30	30	27
Fe	M.D.	52	43	40	37	39	40
	dry	94.5	2	11	0.4	0.1	2
	soaked	52	2	66	0.5	0.5	0.7

Eh measured in mV, flow in ml/min, and Mn, Fe in mg/l.
M.D. = Big Five mine drainage

Manganese removal was poor (<30%) for both reactors throughout the entire experiment, which was not surprising because the pH never reached 7. Iron removal was nonexistent initially, with higher concentrations in the effluent than in the influent mine drainage. This may be due to some iron in the limestone initially being leached out. Excellent iron removal was achieved after Day 35 for both reactors.

Discussion

Aerobic experiment

The success of the aerobic laboratory studies and the static portion of this bench-scale study indicated that an algal mixture is effective under warm, sunny conditions. However, a large scale wetland treatment system is more dynamic and subject to more environmental stresses. Thus, the flow portion of this experiment is probably a more accurate indicator of the potential for an algal mixture to be used in a larger scale wetland. Figure 26.3 shows the outflow manganese concentrations for reservoirs NoLS and LS. Considering that the inflow manganese concentration was 100 mg/l from Day 79 through Day 84 and varied between 28 and 65 mg/l during the rest of the experiment, both reservoirs exhibited excellent removal, often reducing the effluent to concentrations below 5 mg/l. Reservoir LS consistently performed better than reservoir NoLS, with 85% of the samples below 2.0 mg/l manganese. However, a pH difference in the two reservoirs could not account for the better performance of reservoir LS, because the pH values of the two reservoirs during this portion of the experiment were very similar. Further laboratory experiments found that 0.16 mg of Mn per g of limestone were bound to the limestone surfaces, which explains the better performance of the limestone reservoir (Duggan and Wildeman, 1994).

Both reservoirs recovered from the addition of the 100 mg/l manganese solution and continued removing manganese during the rest of the experiment. This tolerance of high manganese concentrations is important, because manganese concentrations as

low as 5.5 to 11 mg/l (10–20 units) have been shown to greatly inhibit manganese-oxidizing microbes (Nealson et al., 1988). Reservoir LS once again showed more efficient manganese removal than reservoir NoLS. It is also important to note that the reservoirs were frozen during most of the time that the 100 mg/l manganese solution was added during the flow experiment.

The severe weather conditions present during much of the pump flow experiment had a visible effect on the health of the biomass. During the static experiment, the thick algal mat was bright green and floated on the surface due to the large number of oxygen bubbles produced during photosynthesis. Because flow, sunlight, and temperature were all different than in the static experiment, it is difficult to separate changes in variables. However, throughout the pump flow experiment, the algae lost much of its bright green color and sank below the water surface. Gas bubbles were still observed during the sunlight hours indicating that photosynthesis was occurring, but to a less extent than during the warmer, sunnier months. At the completion of the experiment in mid-December, the reservoirs had frozen several times and the algal biomass did not appear very healthy. However, Figure 26.3 shows that manganese is still being removed from solution during this portion of the experiment. Thus, manganese may have been removed by processes unrelated to photosynthesis. Additional laboratory experiments found that at pH >8, amorphous manganese oxyhydroxides will precipitate (Duggan and Wildeman, 1994). Therefore, as long as enough photosynthesis is occurring to keep the pH above 8, the manganese could be removed from the mine drainage by other processes. However, the oxidation of Mn(III) in the amorphous precipitates and subsequent formation of MnO₂ may require a long time.

Manganese is a required micronutrient involved in the formation of gaseous oxygen from water during photosynthesis (Ehrlich, 1990). Therefore, soluble manganese must be able to pass through the cell wall and has been shown to be accumulated intracellularly to concentrations much higher than usually found in solution (Richardson et al., 1988). However, the presence of manganese precipitates on the filamentous *Cladophora* indicates that much of the manganese is being removed from solution extracellularly in this experiment. Richardson et al. (1988) have shown that different cultures of phytoplankton precipitate manganese oxides by producing a high pH and oxygen microenvironment within the algal aggregates. They found the manganese oxide formation is essentially controlled by pH, as no precipitation occurred when the phytoplankton solution was buffered to pH 7.5. This strong dependence on pH was also observed in the static portion of this experiment as shown on Figure 26.2. It has also been shown that non-living algae have a high affinity for metal adsorption, though additional laboratory experiments with algae and manganese solutions found minimal adsorption (Duggan, 1993).

Anaerobic experiment

Metal removal and a pH increase occurred in all four anaerobic reactors. Essentially complete removal of copper and zinc was achieved by all four reactors, with iron removal being more variable (Duggan et al., 1993). However, there was a large difference in the manganese removal between the composted manure and limestone-alfalfa reactors.

Good manganese removal was achieved by the composted manure reactors during the first half of the experiment, with efflu-

ent pH values ranging from 7.0 to 7.6. However, manganese removal was lost during the last half of the experiment and was accompanied by a slight decrease in pH as the flow was increased. It is difficult to determine whether the decrease in manganese removal was due to the slight decrease in pH or the lack of available adsorption sites on the organic substrate. Other laboratory studies found that initial manganese removal may be attributed to organic complexation (Machemer and Wildeman, 1992) and, therefore, manganese removal was probably lost during the bench-scale study when the adsorption sites were filled. A similar manganese removal pattern was seen in a comparable study by Bolis et al. (1991), when manganese removal significantly decreased after 13 weeks of flowing mine drainage through a bench-scale reactor.

It appears that the limestone-alfalfa reactors required a longer start-up time to reach their optimal pH values than did the organic substrate. However, the pH of these reactors never reached 7, resulting in very poor manganese removal. Thus, a limestone-alfalfa mixture was determined to be an inadequate substrate for the anaerobic removal of manganese.

The initial substrate conditions (soaked vs. dry) had little effect on metal removal. However, the hydraulic conductivity was more consistent in the two soaked reactors, which is important for maintaining a consistent flow through a substrate (Bolis et al., 1992). Though manganese removal was not achieved by the limestone-alfalfa reactors, the rate of sulfate reduction was much higher than in the composted manure reactors (Duggan et al., 1993). A limestone-alfalfa substrate appears promising for iron, copper, and zinc removal from mine drainage, but not manganese.

CONCLUSIONS

Aerobic laboratory tests indicate that common green and blue-green algae (pond scum) can tolerate high concentrations of manganese and remove it from mine drainage under aerobic conditions. Manganese removal is at least partially dependent upon the photosynthesizing ability of the algae. Anaerobic laboratory tests suggest that the removal of manganese may be possible under those conditions, but much less consistent than a sulfate-reducing microbial ecosystem.

The bench-scale investigations extended the examination of possible manganese removal methods. Overall, the aerobic bench-scale experiment appears to have been more successful than the anaerobic experiment with respect to manganese removal. However, the aerobic experiment was conducted as a second-stage treatment system on alkaline waters that focused only on manganese removal. The anaerobic experiment was a single-stage treatment system, attempting to remove all metals and raise the pH in one step. Thus, an important conclusion that can be drawn from this project is that manganese removal from acid mine drainage requires a two-stage wetland treatment process, or a single-stage system that allows for anaerobic and then aerobic treatment cells within one wetland. The use of an algal mixture as a second-stage treatment system for manganese removal appears extremely promising. The exact removal mechanisms require further investigation to determine how important the climate is on the performance and health of the algae. If the algae can continue to remove manganese when they are no longer living, the potential is greater for utilizing an algal pond in harsher climates. Considering the excellent results achieved by the algae in this bench-scale study

for the summer, fall, and early winter, an algal pond pilot-scale study is highly recommended.

One question concerning removal of manganese using algal ponds is whether the pond scum, suggestive of any photosynthesizing algae, can be used or is it necessary to establish a more specific ecosystem. In the pilot study conducted as a result of the laboratory and bench-scale experiments, efforts were made to establish a very specific cyano-bacterial mat (Wildeman et al., 1993). Manganese removal results using this algal mat have been excellent. On the other hand, additional laboratory studies on other circum-neutral drainages using common algae have shown good removal results (Wildeman et al., 1994c). In the same way it has been found that mushroom compost is not necessary for establishing a good sulfate-reducing ecosystem (Wildeman et al., 1994b), it is hoped that future demonstration projects will show that common algal ecosystems will be effective in removal of contaminants from neutral waters.

The anaerobic removal of manganese by a single-stage wetland treatment does not look promising. The composted manure substrate may achieve manganese removal for several months, but after that it is unlikely. This loss of manganese removal may occur in the winter if the bacterial activity decreases and the pH does not increase above 7, the adsorption sites become filled, or the substrate loses its buffering capacity. However, both the composted manure and limestone-alfalfa substrates were effective in removing most of the iron, copper, and zinc, and may therefore be used as a first-stage wetland treatment.

Two results from this study extend beyond the question of Mn removal. Anaerobic laboratory and bench-scale studies have previously been done (Reynolds, 1991; Bolis et al., 1991), however, this is the first time that aerobic laboratory and bench-scale experiments have been done. Previous pilot-scale systems included plants. However, if photosynthesis is important for metal removal and algae can accomplish this function, then aerobic laboratory and bench-scale removal studies can be performed. Such a design will lower the cost and enhance removal efficiencies in the development of aerobic constructed wetlands.

The second result extending beyond the question of Mn removal was the use of a synthetic substrate made of limestone and alfalfa in the bench-scale anaerobic experiment. Most anaerobic systems constructed in the Eastern United States use mushroom compost (Hedin and Nairn, 1992). However, this is not always available. Through extensive laboratory studies testing the effectiveness of substrates (Chang et al., 1991; Plummer et al., 1991), a mixture of alfalfa and limestone proved to be the most effective substrate that did not contain complex soil material. In the bench-scale experiments, this synthetic substrate proved effective at raising the pH and removing Cu, Zn, and Fe even though Mn was not removed.

ACKNOWLEDGMENTS—The authors wish to acknowledge the U.S. Bureau of Mines (Contract No. J021002), which provided support for this research.

REFERENCES

- Batal, W., Laudon, L.S., and Wildeman, T.R., 1989, Bacteriological tests from the constructed wetland of the Big Five Tunnel, Idaho Springs, Colorado; in Hammer, D.A. (ed.), *Constructed Wetlands for Wastewater Treatment*: Lewis Publishers, Chelsea, Mich., pp. 550–557.
- Bolis, J.L., 1992, Bench scale analysis of anaerobic wetlands treatment of

- acid mine drainage: Unpub. M.S. thesis, Colorado School of Mines, Golden, 116 pp.
- Bolis, J.L., Wildeman, T.R., and Cohen, R.R., 1991, The use of bench scale permeameters for preliminary analysis of metal removal from acid mine drainage by wetlands; *in* Oaks, W., and Bowden, J. (eds.), Proceedings of the 1991 National Meeting of the American Society of Surface Mining and Reclamation: Princeton, W.Va., pp. 123–135.
- Bolis, J.L., Wildeman T.R., and Dawson, H.E., 1992, Hydraulic conductivity of substrates used for passive acid mine drainage treatment, Proceedings of the 9th Annual National Meeting of the American Society for Surface Mining and Reclamation: Princeton, W.Va., pp. 79–89.
- Brodie, G.A., 1991, Achieving compliance with staged, aerobic, constructed wetlands to treat acid drainage; *in* Oaks, W., and Bowden, J. (eds.), Proceedings of the 1991 National Meeting of the American Society of Surface Mining and Reclamation: Princeton, W.Va., pp. 151–174.
- Chang, L.K., Updegraff, D.M., and Wildeman, T.R., 1991, Optimizing substrate for sulfate-reducing bacteria [abs.]: 201st National Meeting, American Chemical Society.
- Crerar, D.A., Cormick, R.K., and Barnes, H.L., 1972, Organic controls on the sedimentary geochemistry of manganese: *Mineralogica et Petrographica Acta*, v. 20, pp. 217–226.
- Diem, D., and Stumm, W., 1984, Is dissolved Mn⁺² being oxidized by O₂ in absence of Mn-bacteria or surface catalysts?: *Geochimica et Cosmochimica Acta*, v. 48, pp. 1571–1573.
- Duggan, L.A., 1993, The aerobic removal of manganese from mine drainage through the use of constructed wetlands: Unpub. M.S. thesis, Colorado School of Mines, Golden, 150 pp.
- Duggan, L.A., and Wildeman, T.R., 1994, Processes contributing to the removal of manganese from mine drainage by an algal mixture: Preprints of papers presented at the 207th ACS National Meeting, Div. of Environmental Chemistry, v. 34, no. 2, pp. 488–492.
- Duggan, L.A., Wildeman, T.R., and Updegraff, D.M., 1993, The abatement of manganese in coal mine drainage through the use of constructed wetlands: U.S. Bureau of Mines, Contract Report J021002, 92 pp.
- Ehrlich, H.L., 1990, *Geomicrobiology*: Marcel Dekker, New York, 646 pp.
- Faulkner, S.P., and Richardson, C.J., 1990, Biogeochemistry of iron and manganese in selected TVA constructed wetlands receiving mine drainage: Phase Two Interim Report, Duke Wetland Center Publication 90-03, 69 pp.
- Hedin, R.S., and Nairn, R.W., 1992, Designing and sizing passive mine drainage treatment systems, Proceedings of the 13th Annual West Virginia Surface Mine Drainage Task Force Symposium: Morgantown, W.Va.
- Kepler, D.A., 1988, An overview of the role of algae in the treatment of acid mine drainage: U.S. Bureau of Mines, Circular 9183, pp. 286–290.
- Lind, C.J., and Anderson, L.D., 1992, Trace metal scavenging by precipitating Mn and Fe oxides; *in* Kharaka, Y.F., and Maest, A.S. (eds.), Proceedings of the 7th Water-Rock Interactions Symposium: A.A. Balkema, Brookfield, Vt., pp. 397–402.
- Lind, C.J., Hem, J.D., and Roberson, C.E., 1987, Reaction products of manganese-bearing waters; *in* Averett, R.C., and McKnight, D.M. (eds.), *Chemical Quality of Water and the Hydrologic Cycle*: Lewis Publishers, Chelsea, Mich., pp. 271–301.
- Loganathan, P., and Burau, R.G., 1973, Sorption of heavy metal ions by a hydrous manganese oxide: *Geochimica et Cosmochimica Acta*, v. 37, pp. 1277–1293.
- Machemer, S.D., and Wildeman, T.R., 1992, Adsorption compared with sulfide precipitation as metal removal processes from acid mine drainage in a constructed wetland: *Journal of Contaminant Hydrology*, v. 9, pp. 115–131.
- Machemer, S.D., Reynolds, J.S., Laudon, L.S., and Wildeman, T.R., 1993, Balance of S in a constructed wetland built to treat acid mine drainage, Idaho Springs, Colorado, USA: *Applied Geochemistry*, v. 8, pp. 587–603.
- Marshall, K.C., 1979, Biogeochemistry of manganese minerals; *in* Trudinger, P.A., and Swaine, D.J. (eds.), *Biogeochemical Cycling of Mineral-forming Elements*: Elsevier, New York, pp. 253–292.
- Nealson, K.H., Tebo, B.M., and Rosson, R.A., 1988, Occurrence and mechanisms of microbial oxidation of manganese; *in* *Advances in Applied Microbiology*, v. 33: Academic Press, New York, pp. 279–318.
- Plummer, S.M., Updegraff, D.M., and Wildeman, T.R., 1991, Sulfate reduction versus methanogenesis in substrates designed to treat acid mine drainage [abs.]: 201st National Meeting, American Chemical Society.
- Reynolds, J.S., Machemer, S.D., Wildeman, T.R., Updegraff, D.M., and Cohen, R.R., 1991, Determination of the rate of sulfide production in a constructed wetland receiving acid mine drainage; *in* Oaks, W., and Bowden, J. (eds.), Proceedings of the 1991 National Meeting of the American Society of Surface Mining and Reclamation: Princeton, W.Va., pp. 175–181.
- Richardson, L.L., Aguilar, C., and Nealson, K.H., 1988, Manganese oxidation in pH and O₂ microenvironments produced by phytoplankton: *Limnology and Oceanography*, v. 33, no. 3, pp. 352–363.
- Sellstone, C.J., 1990, Sequential extraction of Fe, Mn, Zn, and Cu from wetland substrate receiving acid mine drainage: Unpub. M.S. thesis, Colorado School of Mines, Golden, 88 pp.
- Silverman, M.P., and Ehrlich, H.L., 1964, Microbial formation and degradation of minerals; *in* Umbreit, W.W. (ed.), *Advances in applied microbiology*: Academic Press, New York, pp. 153–206.
- Stumm, W., and Morgan, J.J., 1981, *Aquatic chemistry*: Wiley and Sons, New York, 780 pp.
- U.S. Code of Federal Regulations, 1997a, Title 30—Mineral Resources: Chapter VII—Office of Surface Mining Reclamation and Enforcement, Department of the Interior; Subchapter B—Initial Program Regulations; Part 715—General Performance Standards; July 1, Section 715.17.
- U.S. Code of Federal Regulations, 1997b, Title 40—Protection of the Environment: Chapter 1, Environmental Protection Agency; Part 434—Coal Mining Point Source Category; Subpart C—Acid or Ferruginous Mine Drainage; July 1.
- Watzlaf, G.R., 1985, Comparative tests to remove manganese from acid mine drainage: U.S. Bureau of Mines Information Circular 9027, pp. 41–47.
- Wehrli, B., and Stumm W., 1989, Vanadyl in natural waters—Adsorption and hydrolysis promote oxygenation: *Geochimica et Cosmochimica Acta*, v. 53, pp. 69–77.
- Wildeman, T.R., 1988, Constructed wetlands-based treatment of degraded waters for toxic metal removal (Quality Assurance Project Plan): Colorado School of Mines Proposal submitted to EPA Office of Research and Development, Hazardous Waste Engineering Laboratory, Cincinnati, Ohio.
- Wildeman, T.R., 1991, Drainage from coal mines—Chemistry and environmental problems; *in* Peters, D.C. (ed.), *Geology in Coal Resource Utilization*: Tech Books, Fairfax, Va., pp. 499–511.
- Wildeman, T.R., Brodie, G.A., and Gusek, J.J., 1992a, Wetland design for mining operations: Bitech Publishing Co., Vancouver, BC, Canada, 300 pp.
- Wildeman, T.R., Duggan, L.A., Bolis, J.L., and Gusek, J.J., 1992b, Constructed wetlands that emphasize sulfate reduction—A staged design process and operation in cold climates; *in* Proceedings of the 24th Annual Conference of the Canadian Mineral Processors: Canadian Institute of Mining, Metallurgy, and Petroleum, Ottawa, Ontario, pp. 32–32-10.
- Wildeman, T.R., Duggan, L.A., Phillips, P., Rodriguez-Eaton, S., Simms, R., Bender, J., Taylor, N., Britt, C., Mehs, D., Forse, J., Krabacher, P., and Herron, J., 1993, Passive treatment methods for manganese—Preliminary results for two pilot sites, Proceedings of the 1993 American Society of Surface Mining and Reclamation Meeting: Princeton, W.Va., pp. 665–677.
- Wildeman, T.R., Updegraff, D.M., Reynolds, J.S., and Bolis, J.L., 1994a, Passive bioremediation of metals from water using reactors or con-

- structed wetlands; *in* Means, J.L., and Hinchey, R.E. (eds.), *Emerging Technology for Bioremediation of Metals*: Lewis Publishers, Boca Raton, Fla., pp. 13–24.
- Wildeman, T.R., Cevaal, J., Whiting, K., Gusek, J.J., and Scheuering, J., 1994b, Laboratory and pilot-scale studies on the treatment of acid rock drainage at a closed gold-mining operation in California, *Proceedings of the Internatl Land Reclamation and Mine Drainage Conference*, v. 2: U.S. Bureau of Mines Spec. Pub. No. SP 06B–94, pp. 379–386.
- Wildeman, T.R., Filipek, L.H., and Gusek, J.J., 1994c, Proof-of-principle studies for passive treatment of acid rock drainage and mill tailing solutions from a gold operation in Nevada, *Proceedings of the Internatl Land Reclamation and Mine Drainage Conference*, v. 2: U.S. Bureau of Mines Spec. Pub. No. SP 06B–94, pp. 387–394.

Chapter 27

GEOCHEMICAL AND BIOGEOCHEMICAL CONTROLS ON ELEMENT MOBILITY IN AND AROUND URANIUM MILL TAILINGS

E.R. Landa

U.S. Geological Survey, 12201 Sunrise Valley Drive, MS 430, Reston, VA 20192

INTRODUCTION

Uranium-bearing ores are mined and milled as the first step in the nuclear fuel cycle. Milling consists of the mechanical and chemical processes that concentrate the uranium fraction from the ore. In conventional uranium milling, the ore is crushed and leached with either alkali or acid. Ores with limestone contents greater than 15% are generally leached under alkaline conditions with sodium carbonate-bicarbonate, whereas most other ores are leached with sulfuric acid. The uranium extracted by the leaching solution is concentrated by solvent extraction or ion exchange and subsequent precipitation (generally with ammonia) of a uranium concentrate (80–85% U_3O_8), referred to as “yellow cake.” For details regarding variants in the milling process, the reader is referred to Merritt (1971), International Atomic Energy Agency (1980), and Organization for Economic Cooperation and Development (1983).

The leached ore residues (“tailings”) are slurried with mill-waste solutions and pumped to an earthen retention pond or a mined-out underground stope for disposal. The waste slurries at acid leach mills are sometimes limed prior to discharge in order to precipitate contaminants and water released from tailings impoundments is typically treated with barium to precipitate $BaSO_4$ and coprecipitate ^{226}Ra . As the ores being exploited are typically low grade, essentially all of the tonnage of ore processed at the mill is disposed of as tailings. The present inventory of uranium mill tailings (UMT) in the United States is about 200 million tons.

Although about 90 to 95% of the uranium in the ore is extracted in the milling process, most of the uranium daughter products remain with the tailings, which thus constitute a low-level radioactive waste material. The leaching of radionuclides from these tailings solids by natural waters creates the potential for human ingestion through water and food. Uranium mill tailings solids can also be sources of gaseous radon in the atmosphere and airborne particulates that can be inhaled (Fig. 27.1) or contaminate vegetation. Nonradioactive substances potentially detrimental to water quality may also be introduced into the surficial environment by activities associated with uranium milling. These substances may be present in the ore or in the process reagents. The ores may contribute elements such as selenium, arsenic, molybdenum, and vanadium, whereas the process reagents may contribute chloride, nitrate, and sulfate. Besides the leached ore residues, milling waste solutions from the leach process with small amounts of entrained or soluble organic solvents also enter the tailings retention pond. These waste streams contain soluble

radionuclides (e.g., small quantities of uranium not recovered by the solvent exchange or ion exchange circuits, ^{230}Th , and other uranium series nuclides) that may (1) persist in solution and migrate in ground water, (2) precipitate by interacting with components from other waste solutions or as a result of liming or other amendment, (3) be sorbed by the tailings or underlying soil in the retention pond (Landa, 1980). Although considerable attention to hydrogeologic and engineering controls is now exercised at uranium mills in the U.S., Canada, Australia and western Europe to avoid the release of contaminants, recent reports (e.g., Keller, 1993) suggest that far less care was taken at some uranium mines/mills in eastern Europe to safeguard against air, water, and soil pollution.

Landa (1980) examined the literature through the late 1970s. A considerable volume of literature on the subject was published during the 1980s, much of the research funded by the U.S. Nuclear Regulatory Commission, the U.S. Department of Energy’s Uranium Mill Tailings Remedial Action (UMTRA), and the National Uranium Tailings Program of Energy, Mines and Resources Canada. This update of the original review covers research on geochemical and biogeochemical aspects of UMT disposal published during the 1980s and early 1990s.

TAILINGS SOLIDS

Because of its high radiotoxicity, ^{226}Ra is typically the uranium daughter product of most concern in hazard assessments of water supplies and food chains associated with uranium mill tailings. The host phase of a radionuclide is a key determinant of its potential mobility in the hydrosphere. The nature of a radionuclide’s retention by UMT will determine its subsequent leaching behavior. Using a sequential selective extraction technique, Landa (1982) compared the leaching of radionuclides from a sandstone uranium ore with the tailings derived therefrom. These samples were from a commercial sulfuric acid leach uranium mill. The tailings had a higher fraction of ^{226}Ra in the water soluble, NaCl-extractable (exchangeable), dilute acetic acid extractable, and alkaline DTPA [(((carboxymethyl)imino) bis-(ethylenenitrilo)) tetraacetic acid] extractable (associated with alkaline earth sulfates and organic matter) phases than did the ore. Although ^{226}Ra content of UMT solids generally accounts for about 98% of the Ra in the parent ore, extensive solubilization and redistribution between particle size fractions occur in both acid (Whitman and Beverly, 1958; Seeley, 1977; Skeaff, 1981) and alkaline (Lakshmanan and Ashbrook, 1978) milling circuits. In general, this redistribution

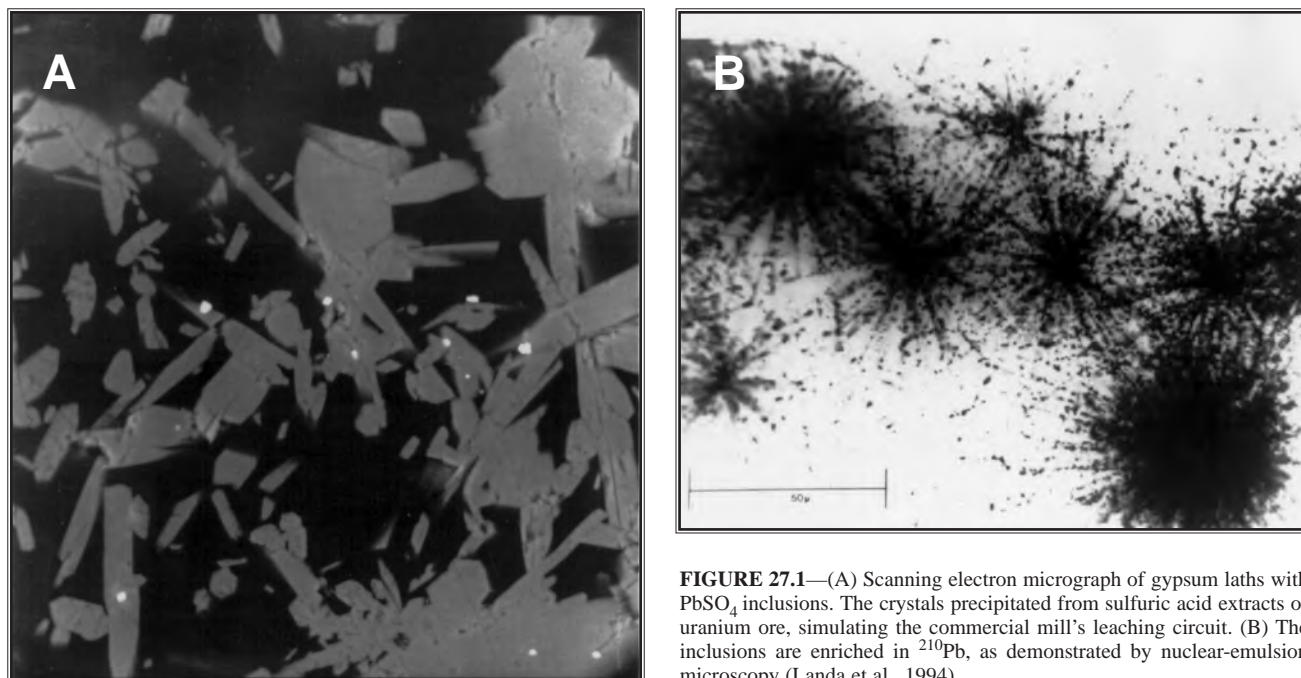


FIGURE 27.1—(A) Scanning electron micrograph of gypsum laths with PbSO_4 inclusions. The crystals precipitated from sulfuric acid extracts of uranium ore, simulating the commercial mill's leaching circuit. (B) The inclusions are enriched in ^{210}Pb , as demonstrated by nuclear-emulsion microscopy (Landa et al., 1994).

involves radium enrichment of the finer particles (-150 mesh (105 μm) or finer). Skeaff (1981) showed that although 58% of the ^{226}Ra in the feed ore sampled at an acid leach mill was in the -200 mesh (74 μm) fraction, about 85% of the ^{226}Ra was in this size fraction in the leaching tank tailings. He noted that the low concentration of ^{226}Ra in the leach liquor and the particle size redistribution of ^{226}Ra that occurs in the acid leaching tank indicate rapid dissolution followed by coprecipitation and/or adsorption of ^{226}Ra preferentially on the fine particles. From studies of leaching kinetics of alkaline UMT (Wiles, 1983) and limed acid UMT (Nathwani and Phillips, 1979a,b), radium is deduced to occur in at least two distinct forms—one that allows for rapid surface exchange or dissolution and a second whose release is slower and diffusion-controlled.

Adherent overgrowths of alkaline earth sulfates and lead sulfate on quartz (Seeley, 1977; Paige et al., 1989a) and on muscovite (Paige et al., 1988, 1989b) have been produced in the laboratory and used to simulate precipitates formed on ore particles during the sulfuric acid leaching process. Work by Snodgrass and Hileman (1985) and Steger and Legeyt (1987) suggest that radium coprecipitates with lead and/or barium sulfate in the mill's ore leaching tanks. Barite crystals, either from the original mineral suite of the uranium ore or as chemical precipitates formed during sulfuric acid leaching or during aging of the tailings effluent, have been observed in UMT (Stieff, 1985; Snodgrass, 1986; Landa and Bush, 1990) and display high specific activities of ^{226}Ra due to coprecipitation or adsorption. Both coprecipitation and adsorption appear to be operative processes in UMT. Morrison and Cahn (1991) examined acid leach tailings from several mills that used Colorado Plateau sandstone ores and found most of the alpha activity to be associated with barium-strontium sulfate grains. Alpha-track maps of polished thin sections showed both grains with uniform track density, as might happen with coprecipitation, and grains with only alpha-tracked rims, indicative of sorption. In

marked contrast to other minerals tested, radium sorbed by preformed barite crystals during simulated acid-mill leach tank conditions was extremely resistant to both 1.0N NH_4Cl and 1.0N HCl extraction (Landa, 1991). ^{230}Th can also coprecipitate with BaSO_4 from sulfuric acid solutions (Sill and Willis, 1964; Ambe and Lieser, 1978), and indeed this mechanism may account for the retention of the radionuclide in UMT solids despite initial solubilization by the hot sulfuric acid leachate of the mill.

Nirdosh et al. (1984) discuss various other radium retention mechanisms in UMT, including sorption on silica and hydrous oxides of iron and manganese and ion exchange on clays. Under conditions simulating acid milling, Landa and Bush (1990) showed that Ra was retained by typical gangue components of uranium ore including clays, feldspars, and oxides. The metabolism of specific microorganisms can essentially act as a selective extraction agent. Using this approach, studies involving the anaerobic incubation of UMT with sulfate-reducing bacteria (Landa et al., 1986) and iron-reducing bacteria (Landa et al., 1991) have shown sulfate minerals and ferric hydrous oxides to be probable hosts for Ra in UMT.

The sorption of radium from aqueous solutions by minerals has been addressed in a series of recent studies under conditions applicable to either ground water and surface water transport, or in-mill and in-pile conditions. Benes et al. (1984, 1985, 1986) used a modified distribution coefficient (K'_D) to compare the sorptive abilities of several minerals at pH's near 7.5–8.0. The K'_D values determined are shown below:

$$\text{muscovite (90,000)} > \text{albite (32,000)} > \text{montmorillonite (8700)} \\ > \text{kaolinite (2900)} > \text{quartz (1700)}.$$

Neither cation exchange capacity nor specific surface area were good predictors of relative radium sorptive ability. The surprising-

ly high K'_D values of muscovite and albite, and the low reversibility of sorption (Benes et al., 1986), reflect a high selectivity of sites for radium binding.

The sorptive capacity of quartz for cations is generally assumed to be low, especially at low pH. Indeed, Benes et al. (1984) showed little Ra sorption by quartz at pH less than 4. However, Nirdosh et al. (1987) have shown that quartz aged in hot sulfuric acid (i.e., conditions typical of an acid leach uranium mill) and washed free of the sulfuric acid could sorb significant quantities of Ra when subsequently exposed to pH 1 (HCl) solutions of RaCl_2 . Sulfuric-acid curing can convert the outer layer of the quartz to a more adsorbent, amorphous form of silica. It appears that either:

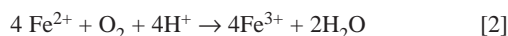
- 1) protonated silanol groups, $\text{Si} \begin{smallmatrix} < \text{OH}_2^+ \\ \text{OH}_2^+ \end{smallmatrix}$ on the surface retain sulfate as counterions and these act to precipitate Ra, or
- 2) weakly hydrated Ra^{2+} ions are specifically sorbed at the surface (Stern layer bonding) despite a net positive charge on the quartz at pH 1.0.

Morrison and Cahn (1991) show petrographic and α -track evidence that silica precipitated in mill ponds, following carbonate leaching of uranium ore, is the major host for α -emitters in alkaline leach UMT. Amorphous silica may also precipitate from simulated acid milling solutions; such precipitates may be very efficient scavengers of ^{226}Ra (Nirdosh and Muthuswami, 1988), ^{230}Th (Johnston, 1990), and U (Zielinski, 1980). Riese (1982) presents extensive experimental and modeling data on the adsorption of radium and thorium onto quartz and kaolinite.

Pyritic tailings present unique environmental problems and have been extensively studied in the Elliot Lake mining district of Ontario, Canada. The Nordic tailings impoundment, which received UMT from 1952–1968, has been the focus of these studies; these tailings were derived from the sulfuric acid treatment of uranium ores containing 3–7% pyrite. The tailings effluent was neutralized to about pH 8 with lime prior to discharge. Surface water was drained from the tailings in 1970. When studied during the mid-1970s through the mid-1980s, the water table was typically several meters below the surface. Because the diffusion of oxygen in air-filled pores is much more rapid than in water-filled pores, the zone above the water table is the zone of extensive pyrite oxidation. The slow abiologic oxidation of pyrite is shown by the reaction:



Aerobic, iron oxidizing bacteria (e.g., *Thiobacillus ferrooxidans*), that are present in the low pH zone of the Elliot Lake tailings (Dubrovsky et al., 1984; Blowes and Gillham, 1988), can obtain energy by oxidizing the ferrous iron to the ferric form (Alexander, 1977):



The Fe^{3+} thus formed may precipitate as ferric hydroxide or jarosite. However, if the Fe^{3+} persists in solution long enough to move below the water table, pyrite dissolution can occur below the water table as represented by the reaction (Alexander, 1977):



The importance of thiobacilli in the oxidation of pyrite in UMT was demonstrated in lysimeter studies (Ritcey and Silver, 1982). The average annual precipitation at Elliot Lake is 996 mm. By applying 9 times this amount of water to the lysimeter each experimental year for 2.5 years, the investigators attempted to simulate the weathering and leaching of the tailings which would occur over a period of about 22.5 years. In one lysimeter, just-discharged, limed Elliot Lake tailings were inoculated with the bacteria; another lysimeter contained the same tailings, but these were uninoculated and were continually treated with a bleach solution to inhibit microbial activity. The effluents collected from the bleach-treated lysimeter contained lower concentrations of iron and sulfate and higher pH than those from the inoculated lysimeter over a simulated 22.5 year period.

The influence of sulfate concentration on radium solubility was also demonstrated. The ^{226}Ra concentration in the effluent from both lysimeters during simulated years 0 to 7.5 was about 100–300 pCi/l. However, during simulated years 7.5 to 17.5, the ^{226}Ra concentration of the bleach-treated lysimeter's effluents increased progressively to about 1000 pCi/l (and up to about 2000 pCi/l at about simulated year 21), while that of the inoculated lysimeter's effluents increased to a steady state around 500 pCi/l. The early similarity probably reflects the mutual suppression of radium solubility by the dissolution of calcium sulfate (gypsum) formed during the liming step.

Moffett and Tellier (1978) studied uranium mill tailings abandoned 17 years earlier at Elliot Lake. Oxygen penetration tends to be less in areas of slimes as compared to sands, because of their fine-grained nature and the comparatively high capillary rise of water within them. This effect is seen in the plot of pyrite content as a function of depth (Fig. 27.2). Water sampled within the tailings at a depth of about 5 m could be classed as either low acid (titratable acidity less than 1000 mg/l as CaCO_3) or high acid. The low acid waters (<50 to 930 mg/l) were all obtained in areas where slimes predominated; the high acid waters were obtained close to dams or the central tailings discharge location where sands predominate. In contrast to the low acid waters, the high acid waters typically had higher levels of total dissolved solids, metals (Fe, Zn), and gross α and β activity. Concentrations of ^{210}Pb , ^{228}Th , ^{230}Th , ^{232}Th , and U were generally much higher in the high acid waters. In contrast, ^{226}Ra concentrations in the high acid waters averaged about half those in the low acid waters, because of the suppressing effect of high concentrations of dissolved sulfate on radium solubility.

The most striking characteristic of the surficial tailings was the depletion of thorium. The ore had an estimated Th content of 170 $\mu\text{g/g}$ and none was commercially recovered. Solubilization of thorium during acid milling can approach 90%, but liming should have precipitated this material. Nevertheless, the tailings contained only about 5 $\mu\text{g Th/g}$ in the top 15–20 cm. Most of the Th has presumably been leached by the sulfuric acid generated by pyrite oxidation during the 17 year period of subaerial weathering.

The Nordic tailings at Elliot Lake have been studied since the late 1970s by Cherry and colleagues at the University of Waterloo. Investigations have been reported on:

- 1) the geochemical evolution of the tailings (Dubrovsky et al., 1984, 1985),

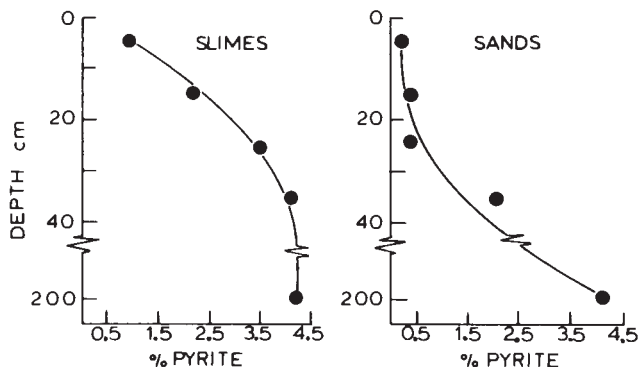


FIGURE 27.2—Distribution of pyrite with depth in sand and slime uranium mill tailings at Elliot Lake, Ontario. Reproduced from Moffett and Tellier, 1978, p. 314; by permission of Journal of Environmental Quality/American Society of Agronomy.

- 2) the migration of the contaminant plume in the underlying aquifer (Morin et al., 1982; 1988a, b; Morin and Cherry, 1986, 1988), and
- 3) possible remediation techniques aimed at limiting pyrite oxidation (Reardon and Moddle, 1985; Nicholson et al., 1989).

A detailed ground-water sampling network using nested piezometers was constructed on the tailings and in a glaciofluvial sand aquifer outside the impoundment. Two distinct water zones were delineated within the tailings: “process water” is neutralized effluent that was discharged to the impoundment in a slurry with the tailings solids, whereas “recharge water” is water that has infiltrated to the ground water after discharge of the tailings solids ceased. Because of pyrite oxidation, the recharge water has a low pH and high concentrations of iron and sulfate. The process water

has a higher pH due to liming of mill effluent and higher chloride content due to milling reagents such as sodium chlorate used as an oxidant during ore leaching and sodium chloride used to elute ion-exchange resins. The Nordic tailings display a two-zone structure: an upper zone in which recharge water has displaced the process water and a deeper zone consisting of the process water. The chemical profile at one site (T6), where the water table is at a depth of about 4 m, shows the stratification clearly (Fig. 27.3). T6 is typical of sites on the Nordic Main tailings with shallow to moderately deep water tables. At sites with deeper water tables and at nearby tailings impoundments that had been inactive for about 10 years longer, the low-pH, high-Fe water extends through the entire tailings thickness. Iron and sulfate appear to be transported conservatively and, along with chloride, can be used to trace the recharge-water/process-water interface. Low pH conditions tended to lag behind the iron and sulfate fronts, suggesting neutralization reactions with the tailings solids.

In the sand aquifer underlying the tailings, the contaminant plume could be classified into three geochemical zones:

- 1) An inner core of unaltered acidic recharge water (pH < 4.8, Fe > 5000 ppm, SO₄²⁻ > 11,000 ppm);
- 2) a neutralization zone in which the inner core water is neutralized by contact with aquifer solids which initially contain about of 0.85 wt% calcite, largely as coatings on sand grains; and
- 3) an outer zone containing neutralized inner core water near the water table, and process water in deeper portions of the aquifer.

The concentrations of most solutes decrease sharply downgradient within the neutralization zone. Among the reactions of importance in the zone are the dissolution of calcite or its solid-solution replacement by siderite (FeCO₃) and the precipitation of gypsum, ferric hydroxide, and aluminum hydroxide. Coprecipitation reactions are thought to be responsible for decreasing concentrations of trace metals and radionuclides. The combination of

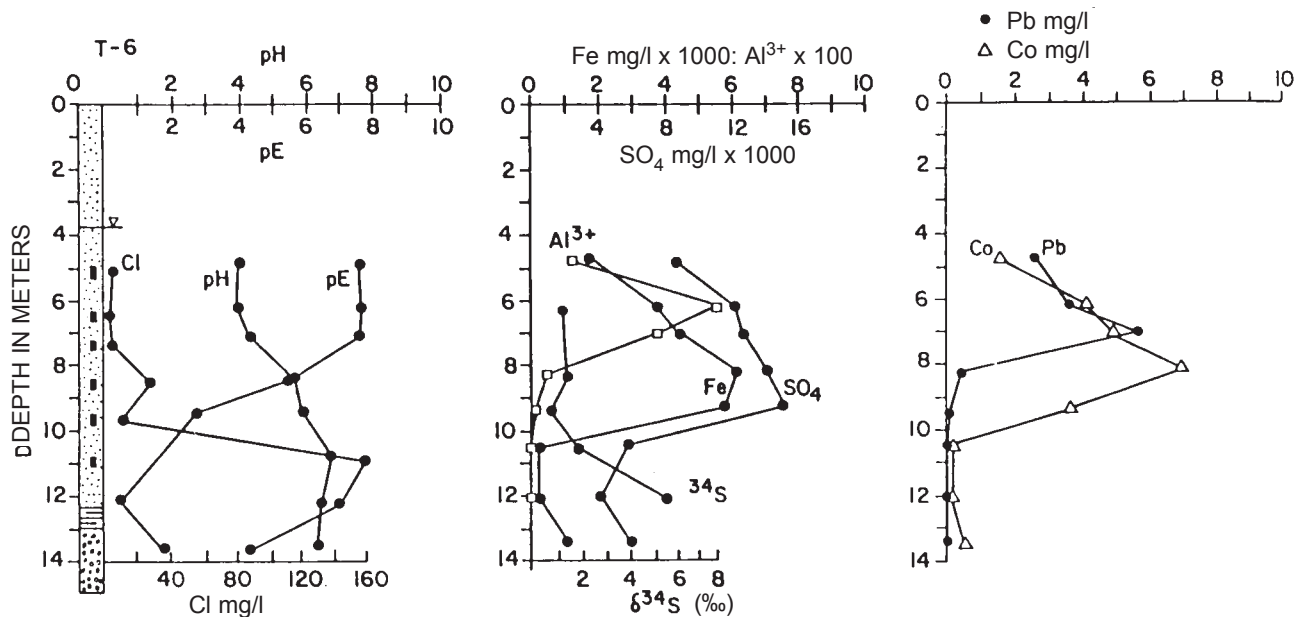


FIGURE 27.3—Profile of groundwater geochemistry at piezometer nest in Elliot Lake, Ontario uranium mill tailings. Reproduced from Dubrovsky et al., 1985, p. 116; by permission of Canadian Geotechnical Journal/National Research Council Canada.

these reactions produces a high degree of contaminant retardation. Although the ground-water velocity is about 440 m/y, the down-gradient migration of the inner core/neutralization zone contact is only about 1–2 m/y (Morin et al., 1982, 1988a, b; Morin and Cherry, 1986, 1988). The reactions occurring in subregions of the neutralization zone can be described by a chemical equilibrium transport model (Morin and Cherry, 1988).

Blowes and Gillham (1988) monitored water quality in a small intermittent stream draining the pyritic Nordic tailings at Elliot Lake during the course of several rain storms and periods of snowmelt. Wells adjacent to and beneath the channel were also sampled. ^{18}O and chloride were used to separate streamflow hydrographs into ground water and surface runoff components. These tracers showed that at this site, where the water table is often within 1.5 m of the tailings surface, and the tailings are predominantly fine sand and silt, the ground-water contribution to streamflow during peak flows was about 30%. Because part of this ground-water contribution is derived from the pore waters of the shallow pyrite oxidation zone of the tailings, the water quality is characterized by low pH and high concentrations of sulfate, iron, zinc, copper, and nickel. The large amounts of Fe^{2+} introduced into the aerated stream precipitate as ferric hydroxides:



The H^+ released to the poorly-buffered stream by the reaction above is a factor in the high acidity (pH 3) measured in the stream. At present, the streamflow here passes through a water treatment plant where the pH is raised and trace metals and radionuclides are removed prior to discharge.

If this study had shown that the ground-water component to streamflow was minor, one might anticipate that contaminant concentrations in the streamflow would decline in a relatively short time as the surficial layer of tailings (i.e., the layer that interacts with the overland flow) was leached of its contaminants. However, as the study showed the ground-water contribution from the tailings to be significant, the water quality problem can be deemed to be more long-term.

Passive waste-management techniques aimed at limiting or mitigating pyrite oxidation in the tailings represent an alternative to water treatment or other active strategies at the site boundary. Such passive strategies that might be employed during close-out of UMT are the use of fine-textured cover layers or organic materials (peat, wood waste, sewage sludge, etc.) to limit oxygen penetration into the tailings and/or to promote sulfate reduction (Reardon and Moddle, 1985; Silver and Ritcey, 1985; Nicholson et al., 1989; D.W. Blowes, written commun., 1990). Deep lake disposal has also been proposed, in which the water cover over the tailings reduces the amount of oxygen available and overlying clay and organic materials limit diffusion of radium and other contaminants into the waters column (Lush et al., 1978). It should be noted that although increasing the growth of sulfate-reducing bacteria may mitigate the effects of acid generation from pyrite, it can promote the leaching of radium from UMT. This effect probably results from the bacterial dissolution of radium-bearing alkaline earth sulfates; the dissolution of radium-bearing hydrous ferric oxides by hydrogen sulfide produced by the sulfate-reducing bacteria may also play a role (Krom and Berner, 1981; Landa et al., 1986).

Although most UMT are disposed of at the surface in dammed ponds or excavated pits, the backfilling of the sand fraction of UMT into underground stopes from which uranium ore has previously been mined has been used at sites in the United States, Canada, and India. Backfilling has been used extensively in the Grants Mineral Belt, New Mexico (Brookins et al., 1982; Thomson et al., 1986). Because native ground water in the mine zone (Ca-bicarbonate type) differs considerably from the initial backfill slurry water (Ca-sulfate type) and redox conditions can be expected to shift from oxidizing conditions to the reducing conditions under which coffinite ore was originally deposited, significant changes in pore fluid chemistry will occur as mine dewatering ends and the backfilled UMT become saturated with native ground water.

Early diagenetic changes in the backfill included precipitation of gypsum and jarosite. The cementing action of the large amounts of gypsum resulted in lithification of the UMT within one year. Jarosite is stable under oxidizing conditions in the presence of high sulfate concentration and low pH. With the flushing of native ground water, jarosite and gypsum can be expected to dissolve. The abiologic process may be enhanced by the action of sulfate-reducing bacteria (Ivarson and Hallberg, 1976). Because jarosite has been shown to be an important host for radium in acidic UMT (Kaiman, 1977), its dissolution can release radium to contacting ground waters. In contrast, other contaminants, such as uranium and selenium, will become less mobile as reducing conditions are established. At the Grants study site, for example, the dissolution of selenium-bearing gypsum may be followed by the reduction of selenate (SeO_4^{2-}) to less soluble selenite (SeO_3^{2-}) or selenide (Se^{2-}), and metallic selenium (Se^0). The precipitation of calcite and aluminosilicates will form late-stage authigenic interstitial cements in the backfill. Mass balance calculations reported by Thomson et al. (1986) suggest that cementation of the tailings will not have a major impact on porosity and permeability.

During the mid-1980s, Waite et al. (1989) measured the concentrations of radionuclides in Langley Bay, a shallow, freshwater bay with a hydraulic turnover (flushing) rate of 14 days, and the flux of radionuclides to the water column coming largely from UMT on the bottom of the bay. Langley Bay is on the northern shore of Lake Athabasca, in northern Saskatchewan. These acidic, unlined UMT came from the mill of the Gunnar mine which operated from 1955 to 1964. The more than 5 million tons of tailings produced were discharged to a small lake draining into Langley Bay. As a result of the demolition of a retaining dam on that lake, UMT were first deposited in Langley Bay. Following this sudden, initial event and continuing to the present, fine tailings escape this upstream lake and flow into Langley Bay, covering its bottom and forming a delta. About 10% of the total ^{226}Ra activity discharged from the mill now resides in the Bay (Waite et al., 1988; Joshi et al., 1989). The concentration of ^{210}Pb in the surficial, lake-bottom sediments/tailings is about 1.5 times that of ^{226}Ra , yet the measured flux rate of ^{226}Ra from the bottom sediments to the overlying water column is about 10 times that for ^{210}Pb (Table 27.1). This may reflect greater ^{210}Pb sorption by bottom sediments compared to ^{226}Ra (Penna Franca et al., 1982). About 80% of the ^{226}Ra in the surface water of the bay could be accounted for by diffusion from the submerged tailings. The UMT represent a long-term contamination source for the waters of Langley Bay (Waite et al., 1989; Joshi et al., 1989). The bones of northern pike and lake whitefish collected from Langley Bay have ^{226}Ra and ^{210}Pb contents about 5 to 100 times those of fish from

uncontaminated control areas on Lake Athabasca. Dose rates to organisms living in the sediment/tailings of Langley Bay are estimated to be on the order of 0.05 to 0.5 gray/y (5–50 rad/y) (Platford and Joshi, 1988). Such doses may be sufficient to cause deformities in benthic invertebrates (Warwick et al., 1987). However no adverse physiological effects (size, hematocrit, cellular anomalies) were observed in the Langley Bay as compared to control area fish (Waite et al., 1990).

TABLE 27.1—Concentration of radionuclides in surface waters and sediments, and flux of radionuclides from sediments, Langley Bay, Saskatchewan (after Waite et al., 1989).

	²¹⁰ Pb	²²⁶ Ra
Average concentration of surface water (pCi/l)	1.6	4.8
Average concentration of surficial (top 1–2 cm) sediment (pCi/g)	700	453
Flux from sediment (pCi/m ² /h)		
1983 data	below detection limit	128
1986 data	15	156

TAILINGS LIQUIDS

The analysis of a typical UMT liquid from an acid leach mill is shown in Table 27.2 (U.S. Nuclear Regulatory Commission, 1980). When a tailings dam at an acid leach uranium mill in New Mexico failed on 16 July 1979, an estimated 94 million gallons of tailings slurry (pH 1.6–1.9) containing about 1100 tons of tailings solids spilled into an adjacent arroyo. Subsequent environmental monitoring of the surficial sediments along a 72 km length of the arroyo downstream of the dam showed that although concentrations of ²¹⁰Pb, ²²⁶Ra and ¹³⁸U were not distinguishable from natural background concentrations, the concentrations of ²³⁰Th ranged from background levels (about 0.8 pCi/g) up to 270 pCi/g (Weimer et al., 1981; Gray and Webb, 1991; Van Metre and Gray, 1992). If this contamination were largely due to tailings solids, one would expect to see elevated levels of ²¹⁰Pb and ²²⁶Ra as well as ²³⁰Th. The findings suggest most of the ²³⁰Th seen in the arroyo sediments was due to soluble ²³⁰Th that became immobilized, probably due to neutralization of the acidic liquid by the riverbed and suspended sediments. ²³⁰Th concentrations in unfiltered tailings water at the time of the accident were about 10,000–12,000 pCi/l (Gray and Webb, 1991).

At this spill site, there is a rough periodicity in ²³⁰Th concentration in channel floor sediments vs. downstream distance; rather than a simple linear or exponential decline, there are alternating highs and lows. Graf (1990) suggest that these fluctuations are related to variations in “unit stream power” (i.e., a measure of the quantity of sediment that the flow is able to transport). He found that high concentrations of ²³⁰Th were found in the channel floor sediments where stream power was low, locations where fluvial geomorphology would predict greater potential for bed storage of sediments (e.g., at wide cross sections and/or shallow gradients). While the occurrence of ²³⁰Th as high specific gravity thorium salt particles as suggested by Graf appears unlikely, the trace quantities of thorium present may be sorbed by high specific gravity minerals such as BaSO₄ and PbSO₄ (Landa et al., 1995). Core

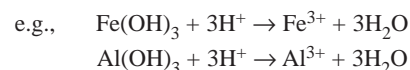
samples showed downward migration of ²³⁰Th up to about 1 m. This may be the result of either: (1) seepage of liquid and retention of the ²³⁰Th by otherwise undisturbed subsurface sediments (Weimer et al., 1981, p. 43–44), or (2) scour of the bed by the flood wave, sediment/contaminant mixing, and redeposition (Graf, 1990).

TABLE 27.2—Chemical properties of tailings liquid at a typical acid-leach uranium mill¹ (U.S. Nuclear Regulatory Commission, 1980, p. 5–6).

pH	2
aluminum, mg/l	2,000
ammonia, mg/l	500
arsenic, mg/l	0.2
calcium, mg/l	500
cadmium, mg/l	0.2
chloride, mg/l	300
copper, mg/l	50
fluoride, mg/l	5
iron, mg/l	1,000
lead, mg/l	7
manganese, mg/l	500
mercury, mg/l	0.07
molybdenum, mg/l	100
selenium, mg/l	0.20
sodium, mg/l	200
sulfate, mg/l	30,000
vanadium, mg/l	0.10
zinc, mg/l	80
total dissolved solids, mg/l	35,000
U-nat, pCi/l	3,300
²²⁶ Ra, pCi/l	250
²³⁰ Th, pCi/l	90,000
²¹⁰ Pb, pCi/l	250
²¹⁰ Po, pCi/l	250
²¹⁰ Bi, pCi/l	250

¹Ore grade about 0.1% U₃O₈

The use of low permeability clay liners in recent years to retard the seepage of milling effluent from UMT impoundments to underlying aquifers has been encouraged by regulatory authorities that license new mills (U.S. Nuclear Regulatory Commission, 1980) and at some UMT remedial action sites (Morrison and Spangler, 1992). Such liners both physically impede fluid flow and act as sorptive barriers to soluble contaminants. Maximum concentrations of inorganic/radioactive constituents for groundwater protection, recently finalized by the U.S. Environmental Protection Agency (1995) for inactive uranium mill tailings sites, are given in Table 27.3. Acidic tailings solutions react with aluminosilicates in the liner to produce secondary clay minerals, jarosite and alunite. Neutralization of the acidic solution occurs in the liner by: (1) reaction with carbonate minerals, (2) ion exchange uptake of H⁺ by clay minerals, and (3) dissolution of amorphous solids



Such amorphous solids may have previously precipitated in the liner under higher pH conditions during initial interaction with the tailings solution. These amorphous solids and secondary minerals will tend to plug pore spaces in the liner and, thus, decrease liner

permeability, as well as acting as sorptive sinks for radionuclides and metals (Gee et al., 1980; Peterson et al., 1983). The precipitation of jarosite will reduce the flux of sulfate and Kaiman (1977) has shown the mineral to be a significant host species for radium in UMT. The high electrolyte concentration and pH-influence of tailings leachates may influence the flocculation behavior of hydrous oxides and clay minerals in liner materials. Such interactions are complex (Sposito, 1984) and may be accompanied by changes in liner permeability with time.

TABLE 27.3—Site boundary ground water concentration limits for inorganic/radioactive constituents established by the U.S. Environmental Protection Agency (1995) for remedial actions at inactive uranium processing sites.

Constituent	Maximum concentration
arsenic	0.05 mg/l
barium	1.0 mg/l
cadmium	0.01 mg/l
chromium	0.05 mg/l
lead	0.05 mg/l
mercury	0.002 mg/l
molybdenum	0.10 mg/l
nitrate (as N)	10 mg/l
selenium	0.01 mg/l
silver	0.05 mg/l
²³⁴ U and ²³⁸ U	30 pCi/l
²²⁶ Ra and ²²⁸ Ra	5 pCi/l
gross alpha particle activity (excluding radon and uranium)	15 pCi/l

With prolonged exposure of a clay liner to acidic tailings solutions, the pH buffering capacity of the clay minerals may eventually be exceeded and the pH of the seepage from the liner can be expected to approach that of the influent. Column studies by Serne et al. (1983) found that arsenic, barium, chromium, lead, silver, thorium, and vanadium were immobilized by the clay liner material during the passage of early pore volumes, when effluent pH was about 8 and were not released after low pH breakthrough when effluent pH fell to a new plateau at about 4. In contrast, aluminum, cadmium, cobalt, copper, manganese, nickel, zinc, and uranium were immobilized in the liner material only as long as the pH remained above 4.5–5, suggesting different sorptive behaviors for the two groups of contaminants.

While the focus of this review is uranium milling, radionuclides and other contaminants are also released to waters by uranium mining activities. For example, Van Metre and Gray (1992) showed that uranium mine dewatering from 1967 to 1986 released about 560 x 10⁶ grams of uranium and 260 Ci of gross alpha activity to the Puerco River in Arizona and New Mexico. This compares with 1.5 x 10⁶ grams of uranium and 46 Ci of gross alpha activity released to the same basin by the tailings spill of 16 July 1979 described earlier; this latter spill was the largest one-time release of uranium mill tailings ever in the U.S. (Gray and Fisk, 1992). Enrichment in natural waters of uranium series nuclides and other elements unique to a specific ore body (e.g., rhenium in the Ranger uranium ore, Northern Territory, Australia) may be used as indications of uranium mining or milling, as opposed to other industrial activities. Where for scientific or regulatory reasons it is necessary to distinguish between contaminants coming

from uranium mining vs. those from uranium milling activities, ions from reagents used in large quantities in the milling process such as sulfate (from the sulfuric acid used in ore leaching) and manganese (from pyrolusite used as an oxidant during ore leaching) may be useful as indicators of milling (Noller, 1991). Wirt (1993) used ²³⁴U/²³⁸U ratios in ground waters of the Colorado Plateau to distinguish those unaffected by mining (ratios of 1.5 to 2.7) from those containing uranium-mine dewatering effluents and uranium milling effluents (ratio about 1.1). The low ratio in the latter case is thought to be due to the rapid dissolution of uranium-bearing minerals by oxygenated ground water in the case of mining or acidic treatment of ore in the case of milling; such a low ratio might also be anticipated in the case of acid mine drainage. The higher ratios in the former case reflect alpha recoil associated with the decay of ²³⁸U in aquifer solids.

Water-soluble forms of arsenic and molybdenum may be present in stockpiled ore and subgrade rock and available for leaching by infiltrating rainfall/snowmelt (Landa, 1984). Pyrite oxidation in overburden and subgrade ore can produce acidic runoff and seepage water high in uranium and other contaminant species (Sumioka, 1991). Table 27.4 shows the concentrations of selected constituents in the water of a retention pond which collects drainage from a pyritic waste rock dump at the inactive uranium mine in eastern Washington. Gypsum and aluminum- and iron/manganese-rich precipitates are visible at springs on the dump. Lime has been added to the retention pond water in an attempt to neutralize the effluent and precipitate contaminants prior to release. At a uranium mine site in Colorado, Yang and Edwards (1984) showed that it may be necessary to treat mine discharge water for uranium removal as well as radium removal (by BaSO₄ precipitation) in order to protect downstream water supplies. In the case of mine dewatering and mine runoff waters, it may be possible to recover uranium in economic quantities by ion exchange resins (Organization for Economic Cooperation and Development, 1983), enzymatic uranium reduction (Lovley and Phillips, 1992), or sorption by immobilized, microbial biomass (Galun et al., 1984; Greene et al., 1986; Macaskie and Dean, 1987; Marques et al., 1990).

TABLE 27.4—Chemical analysis of water samples from retention pond; pyritic, uranium mine site; eastern Washington (data from Sumioka, 1991).

Constituent	Range of values	
specific conductance, μS/cm at 25°C	7130	– 9630
solids, dissolved residue at 105°C	12,300	– 15,700
pH	3.6	– 3.8
calcium, dissolved, mg/l	440	– 590
magnesium, dissolved, mg/l	810	– 1100
sulfate, dissolved, mg/l	8000	– 12,000
aluminum, dissolved, mg/l	490	– 710
manganese, dissolved, mg/l	500	– 640
iron, dissolved, mg/l	3.2	– 4.8
uranium, dissolved, mg/l	160	– 180
²²⁶ Ra, dissolved, pCi/l	48	– 63

BIOGEOCHEMISTRY

Living organisms can mobilize, immobilize, or concentrate radionuclides associated with UMT. Large quantities of uranium ore have been mined and processed in the temperate semiarid western United States, the wet temperate Elliot Lake region of Ontario, Canada, and the wet and dry tropical (monsoon) region of the Australian Northern Territory. Thus, a wide range of fauna, flora, and macro- and micro-organisms have been exposed, or are potentially exposed, to contact with tailings or radionuclides and other contaminants derived therefrom.

Oxygen concentrations of porewaters in uranium mill tailings can vary spatially and temporally, either in the initial disposal environment or following dispersal and redeposition. Aerobic conditions may promote the action of sulfur-oxidizing microorganisms and lead to acidic (i.e., H_2SO_4) conditions promoting the leaching of U, Th, and other contaminants (Moffett and Tellier, 1978). Anaerobic conditions may promote the growth of sulfate-reducing and iron-reducing microorganisms. By their dissolution of alkaline earth sulfate (e.g., BaSO_4) and hydrous ferric oxide coating and particles in UMT, the action of these microorganisms may enhance the leaching of Ra and other contaminants coprecipitated therein (Landa et al., 1986, 1991). Organic acids released by other anaerobes may enhance the dissolution of other radium-host phases such as PbSO_4 (Francis and Dodge, 1986).

Due to process reagents, nitrates are a common constituent in UMT effluents and in ground water beneath UMT impoundments. Denitrification, the process by which microorganisms convert nitrate to nitrogen gas, has been demonstrated to occur in soil beneath tailings (Longmire and Thomson, 1992). The denitrifying bacteria are facultative aerobes; nitrate is used as the electron acceptor for growth in the absence of O_2 (Alexander, 1977). This microbial reduction process may result in attenuation of the nitrate plume downgradient of a UMT disposal area at Maybell, Colorado. Microbial reduction may also enhance the removal from solution of U, Mo, and Se, as soluble species such as uranyl (UO_2^{2+}), selenate (SeO_4^{2-}), and molybdate (MoO_4^{2-}) are reduced to insoluble forms such as uranium oxide (UO_2), elemental selenium, and molybdenum disulfide (MoS_2) (Kauffman et al., 1986; Lovley et al., 1991). Traces of residual organic reagents, such as the kerosene used in the solvent extraction process, may be present in the tailings impoundment and the underlying ground water, and may serve as carbon sources to microorganisms, thus stimulating their activity. The fate and transport of organic contaminants associated with UMT has received little investigative attention. Lysimeter studies by Ritcey and Silver (1982) using neutralized UMT inoculated with thiobacilli suggest that under leaching conditions, which removed about 3% of the radium content of the tailings, more than 95% of added kerosene and Alamine 336 were removed from the tailings. Removal mechanisms for these organic contaminants include elution, volatilization, and microbial degradation.

The ability of microbial biomass (living and dead) to sorb metals from dilute aqueous solutions is well documented. Uptake of U and Ra by biomass from fungi, algae, and bacteria has been studied by various investigators (Galun et al., 1984; Greene et al., 1986; Macaskie and Dean, 1987; Marques et al., 1990; Strandberg et al., 1981; Tsezos, 1985). Tsezos and co-workers (1987) showed that biomass particles prepared from municipal wastewater treatment sludge could be effectively used to remove radium from neutralized UMT effluent from Elliot Lake. Testing by investigators

from Oak Ridge National Laboratory is underway in eastern Germany evaluating the use of immobilized bacterial biomass for removal of uranium, arsenic, and other metals from uranium mill tailings effluent (Anonymous, 1993).

The interaction of plants with UMT is of concern when considering possible radiation doses received through the food chain or other exposure pathways. Native plants may grow on the fringe of UMT disposal areas, and salt- and acid- or alkali-tolerant species may grow on the bare tailings themselves. The roots of vegetation established on cover soils atop reclaimed tailings may penetrate the cover and reach the underlying waste. Riparian vegetation and aquatic macrophytes and phytoplankton in waterways receiving uranium mining and milling effluents may concentrate radionuclides from the water.

For vascular plants rooted in UMT, a novel transport pathway for radon involves the "conduit" transport of ^{222}Rn (daughter product of ^{226}Ra) from soil gas into the root, up the xylem, out the leaves, and into the atmosphere. Allowable ^{222}Rn releases to the atmosphere from reclaimed UMT are set forth in U.S. Nuclear Regulatory Commission standards. Radon moves through the xylem as a dissolved gas in the root-absorbed water, but diffuses out of the entire leaf surface, not just the stomates. This is attributable to the high solubility of radon in fatty acids and triglycerides, a property which allows radon to pass through the leaf cuticle and epicuticular wax layers (Lewis and MacDonell, 1986a, b, 1990). The effect of vegetation on radon fluxes can be significant; experimental field plot studies using UMT have shown up to an order of magnitude greater radon fluxes on vegetated as compared to bare plots (Hinton and Whicker, 1985). Thus, while a vegetative cover can help to stabilize UMT against wind and water erosion (i.e., a benefit), it can also increase the flux of radon to the atmosphere (i.e., a detriment in terms of environmental management). Besides such direct transport of radon to the atmosphere via plants, vegetation can have indirect effects which increase radon flux. For example, a reduction of soil moisture in a cover material due to plant uptake and transpiration of water can increase radon diffusion through the cover. Also, channels created by plant roots can act as conduits for radon transport (Hinton and Whicker, 1985).

The burrows of soil dwelling animals can also increase the "conduit" transport of radon out of buried tailings. Shuman and Whicker (1986) showed that intrusion of reclaimed UMT by prairie dogs can produce local increases in radon flux. The impact on an entire site will depend upon the depth of penetration and extent of colonization of the area by burrowing animals. While data are limited, sandy acidic tailings may be unattractive habitats for such burrowing animals, thereby mitigating the problem. However, even without penetration of the UMT, an extensive network of burrows in the cover soil may increase soil permeability and thereby decrease the effectiveness of the cover soil as a radon barrier. Such burrows may also promote water infiltration to the underlying tailings. Animal intrusion also can bring previously buried UMT to the surface, where they are susceptible to wind and water erosion.

Plant root uptake and translocation of non-gaseous constituents represents another possible pathway for radionuclides from UMT to food chains having humans as the final component. The differing chemical properties of the uranium series nuclides in an acidic sulfate-dominated system, such as an acid leach uranium mill environment, has profound effects on the availability of these nuclides for plant uptake. Ibrahim and Whicker (1992) determined

the concentrations of ^{238}U , ^{230}Th , ^{226}Ra , and ^{210}Pb in native vegetation growing on exposed, weathered tailings near an active acidic (pH 1.8) uranium mill pond in Wyoming. Concentration ratios [CR = concentration in plant tissue/concentration in soil (tailings)] were in the order: $^{238}\text{U} > ^{230}\text{Th} > ^{226}\text{Ra} > ^{210}\text{Pb}$. Uranium and thorium both form water-soluble sulfate salts, whereas radium sulfate and lead sulfate are both quite insoluble (K_{sp} of 4×10^{-11} and 1×10^{-8} , respectively).

The extrapolation of absolute values of concentration ratios from one site to another or from one study to another is very speculative. Some studies have looked predominantly at vegetation on exposed tailings (e.g., Ibrahim and Whicker, 1992), while others have focused on vegetation rooted mainly in an overlying soil cover (e.g., Rumble and Bjugstand, 1986). The CR will vary with plant species, tissue examined, cleansing procedure used on foliage, and soil and (or) tailings properties. The CR can also be expected to vary with the age and degree of weathering of the tailings, as natural diagenetic changes and man-made changes occur. An example of the latter is the application of lime to an inactive, pyritic tailings pile near Elliot Lake, Ontario to produce a gypsum crust that limited wind erosion (Davé et al., 1985).

The UMT environment is one characterized by above normal (i.e., compared to natural background) ionizing radiation levels. The gamma exposure rate at the surface of a tailings pile derived from 0.2% U_3O_8 ore (i.e., typical grade ore in U.S. in 1960s) would be about 1340 $\mu\text{R}/\text{h}$ (Landa, 1980). For comparison, the radiation exposure level in New York City from terrestrial sources (^{40}K ; U and Th series) and cosmic rays is about 10 $\mu\text{R}/\text{h}$ (Shapiro, 1990). While high radiation doses are capable of producing somatic and genetic damage in organisms, the effects of low level radiation typical of uranium mill tailings are more difficult to predict. In field observations and laboratory experiments dealing with UMT, it is also generally not possible to isolate radiation as the only causal agent for biological effects. Nevertheless, at least two studies have suggested the occurrence of mutations in response to some agent associated with UMT. Campbell and Rechel (1979) studied *Tradescantia*, a radiation-sensitive perennial herbaceous plant grown under greenhouse conditions on UMT from the Vitro pile in Salt Lake City, Utah. Radiation exposure levels (mR/h; an indirect measure of radionuclide content) associated with tailings samples showed a statistically significant correlation with the number of somatic mutations (e.g., color changes in flower petals; changes in cell size from normal to giant or dwarf; occurrence of branched stamen hairs) and with the number of stunted hairs per stamen on plants grown on tailings for 30 days. Warwick and co-workers (1987) showed a greater incidence of mouth-part deformities in the larvae of *Chironomus*, a freshwater benthic invertebrate collected from sediments in the heavily polluted inner harbor area at Port Hope on Lake Ontario, as compared to the less polluted outer harbor. Port Hope harbor received wastes from radium and uranium extraction and refining operations and other non-radioactive wastes. The dose rate to the chironomids in the inner harbor sediment was estimated to be about 1 mGray/day. This level is below the 10 mGy/d threshold value for deleterious effects to aquatic organisms suggested recently by the National Council on Radiation Protection and Measurements (Nelson, 1993). The biological effects of environmental variables other than radiation (e.g., in the Port Hope case, heavy metals and elevated water temperatures) cannot be ruled out.

BIBLIOGRAPHIC NOTES

When reviewing a field, selective vision is the rule and comprehensiveness is a seldom-realized goal. With this in mind, reference is made briefly below to other post-1979 UMT information sources in which geochemical and geotechnical issues are addressed:

- 1) For a discussion of siting criteria, monitoring needs, and engineering design aspects of modern UMT management, the reader is referred to the 3-volume "Final Generic Environmental Impact Statement on Uranium Milling," published by the U.S. Nuclear Regulatory Commission (1980).
- 2) During the years 1978–1986, the Geotechnical Engineering Program (Civil Engineering Department) at Colorado State University published annual volumes from its symposia on UMT management.
- 3) The Office of Scientific and Technical Information of the U.S. Department of Energy issued bibliographies (with abstracts) on "Uranium Mill Tailings" in November 1982 and March 1985 (DOE/TIC-3393 and -3393(Suppl. 1)). A more recent bibliographic series, "Nuclear Facility Decommissioning and Site Remedial Action" (e.g., ORNL/EIS-154/V10; Sept. 1989) also covers the UMT literature. More recent references are available using DOE's on-line Energy Data Base, accessible by the Dialog¹ system.
- 4) The International Atomic Energy Agency (1980, 1982, 1990, 1992) issued technical reports and a symposium volume on "Significance of Mineralogy in the Development of Flowsheets for Processing Uranium Ores," "Management of Wastes from Uranium Mining and Milling," "The Environmental Behavior of Radium," and "Current Practices for the Management and Confinement of Uranium Mill Tailings."
- 5) The National Research Council (1986) published a report on risk assessment and waste management practices associated with UMT.
- 6) The Organization for Economic Cooperation and Development/Nuclear Energy Agency (1982, 1984) issued reports addressing long-term aspects of UMT disposal (including geomorphologic stability).
- 7) In 1980, the Society of Mining Engineers sponsored a conference on Uranium Mine Waste Disposal (Brawner, 1980).
- 8) Thermodynamic modeling of UMT systems is discussed by Riese (1982, focusing on Ra and Th), Johnston (1990, focusing on Th), and Opitz et al. (1985). The latter two references also have intensive discussions of tailings liquid neutralization experiments. White et al. (1984) and Narasimhan et al. (1986) present static and dynamic geochemical mixing models, respectively, to look at the interaction of UMT process water with native ground water at the Riverton, Wyoming UMTRA site. Erikson et al. (1990) describes a chemical transport model which considers the effects of various geochemical processes (aqueous speciation, precipitation/dissolution, adsorption) on the ground-water transport of uranium at UMT disposal sites.
- 9) The Canadian government's National Uranium Tailings Program (1985) published a "Uranium Tailings Sampling Manual," covering tailings solids, surface water and seepage, tailings pore water, and wind-blown dust and radon. Also included are two case studies from tailings impoundments in the Elliot Lake, Ontario area dealing with sampling programs

¹Any use of trade, product, or firm names in this publication is for descriptive purposes only and does not imply endorsement by the U.S. Government.

carried out for routine monitoring for regulatory compliance, environmental impact assessment, and decommissioning design.

REFERENCES

- Alexander, M., 1977, Introduction to soil microbiology, 2nd ed.: John Wiley and Sons, New York, 467 pp.
- Ambe, S., and Lieser, K.H., 1978, Coprecipitation of thorium with barium sulfate: *Radiochimica Acta*, v. 25, pp. 93–98.
- Anonymous, 1993, Ogden to test Oak Ridge process on contaminated water in Germany: Inside Energy/with Federal Lands, McGraw Hill Newsletter, February 22, 1993, p. 7–8.
- Benes, P., Strejc, P., and Lukavec, Z., 1984, Interaction of radium with freshwater sediments and their mineral components, I. Ferric hydroxide and quartz: *Journal of Radioanalytical Nuclear Chemistry, Articles*, v. 82, pp. 275–285.
- Benes, P., Borovec, Z., and Strejc, P., 1985, Interaction of radium with freshwater sediments and their mineral components, II. Kaolinite and montmorillonite: *Journal of Radioanalytical Nuclear Chemistry, Articles*, v. 89, pp. 339–351.
- Benes, P., Borovec, Z., and Strejc, P., 1986, Interaction of radium with freshwater sediments and their mineral components, III. Muscovite and feldspar: *Journal of Radioanalytical Nuclear Chemistry, Articles*, v. 98, pp. 91–103.
- Blowes, D.W., and Gillham, R.W., 1988, The generation and quality of streamflow on inactive uranium tailings near Elliot Lake, Ontario: *Journal of Hydrology*, v. 97, pp. 1–22.
- Brawner, C.O., 1980, First international conference on uranium mine waste disposal: Society of Mining Engineers, American Institute of Mining, Metallurgical and Petroleum Engineers, New York, 626 pp.
- Brookins, D., Thomson, B., and Longmire, P., 1982, Early diagenesis of uranium mine stops backfill; in Symposium on uranium mill tailings management: Colorado State Univ., Ft. Collins, pp. 27–37.
- Campbell, W.F. and Rechel, E.A., 1979, *Tradescantia*, a “super-snooper” of radioactivity from uranium mill wastes: Utah Science, Utah Agricultural Experiment Station, Utah State Univ., Logan, v. 40, pp. 100–103.
- Davé, N.K., Lim, T.P., and Cloutier, N.R., 1985, Ra-226 concentrations in blueberries *Vaccinium angustifolium Ait.* near an inactive uranium tailings site in Elliot Lake, Ontario, Canada: *Environmental Pollution (Series B)*, v. 10, pp. 301–314.
- Dubrovsky, N.M., Morin, K.A., Cherry, J.A., and Smyth, D.J.A., 1984, Uranium tailings acidification and subsurface contaminant migration in a sand aquifer: *Water Pollution Research Journal of Canada*, v. 19, pp. 55–89.
- Dubrovsky, N.M., Cherry, J.A., Reardon, E.J., and Vivyurka, A.J., 1985, Geochemical evolution of inactive pyritic tailings in the Elliot Lake uranium district: *Canadian Geotechnical Journal*, v. 22, pp. 110–128.
- Erikson, R.L., Hostetler, C.J., and Kemner, M.L., 1990, Mobilization and transport of uranium at uranium mill tailings sites—Applications of a chemical transport model: U.S. Nuclear Regulatory Commission report NUREG/CR-5169 (PNL-7154).
- Francis, A.J., and Dodge, C.J., 1986, Anaerobic bacterial dissolution of lead oxide: *Archives of Environmental Contamination Toxicology*, v. 15, pp. 611–616.
- Galun, M., Keller, P., Malki, D., Feldstein, H., Galun, E., Siegel, S., and Siegel, B., 1984, Removal of uranium(VI) from solution by fungal biomass—Inhibition by iron: *Water, Air, and Soil Pollution*, v. 21, pp. 411–414.
- Gee, G.W., Campbell, A.C., Sherwood, D.R., Strickert, R.G. and Phillips, S.J., 1980, Interaction of uranium mill tailings leachate with soils and clay liners—Laboratory analysis/progress report: U.S. Nuclear Regulatory Commission report NUREG/CR-1494 (PNL-3381), 49 pp. and appendix.
- Graf, W.L., 1990, Fluvial dynamics of thorium-230 in the Church Rock event, Puerco River, New Mexico: *Annals of the Association of American Geographers*, v. 80, pp. 327–342.
- Gray, J.R., and Fisk, G.G., 1992, Monitoring radionuclide and suspended-sediment transport in the Little Colorado River basin, Arizona and New Mexico, USA, International Symposium on Erosion and Sediment Transport Monitoring Programmes in River-Basins: International Association of Hydrological Sciences No. 210, IAHS Press, Wallingford, Oxfordshire, U.K., pp. 505–516.
- Gray, J.R., and Webb, R.H., 1991, Radionuclides in the Puerco and Lower Little Colorado River Basins, New Mexico and Arizona, before 1987: U.S. Geological Survey Bulletin 1971, pp. 297–311.
- Greene, B., Henzl, M.T., Hosea, J.M., and Darnall, D.W., 1986, Elimination of bicarbonate interference in the binding of U(VI) in mill-waters to freeze-dried *Chlorella vulgaris*: *Biotechnology and Bioengineering*, v. 28, pp. 764–767.
- Hinton, T.G., and Whicker, F.W., 1985, A field experiment on radon flux from reclaimed uranium mill tailings: *Health Physics*, v. 48, pp. 421–427.
- Ibrahim, S.A., and Whicker, F.W., 1992, Comparative plant uptake and environmental behavior of U-series radionuclides at a uranium mine-mill: *Journal of Radioanalytical Nuclear Chemistry*, v. 156, pp. 253–267.
- International Atomic Energy Agency, 1980, Significance of mineralogy in the development of flowsheets for processing uranium ores: IAEA, Vienna, Technical Reports Series No. 196, 267 pp.
- International Atomic Energy Agency, 1982, Management of wastes from uranium mining and milling: IAEA, Vienna, Proceeding Series, Report STI/PUB/622, 735 pp.
- International Atomic Energy Agency, 1990, The environmental behavior of radium: Technical Report Series No. 310, IAEA, Vienna, v. 1, 599 pp. and v. 2, 446 pp.
- International Atomic Energy Agency, 1992, Current practices for the management and confinement of uranium mill tailings: Technical Report Series No. 335, IAEA, Vienna, 140 pp.
- Ivarson, K.C., and Hallberg, R.O., 1976, Formation of mackinawite by the microbial reduction of jarosite and its application to tidal sediments: *Geoderma*, v. 16, pp. 509–518.
- Johnston, R.M., 1990, Mineralogical controls on the mobility of thorium-230 from uranium mine and mill tailings: Unpub. Ph.D. thesis, Univ. of New England, Armidale, New South Wales, Australia, 299 pp.
- Joshi, S.R., Waite, D.T., and Platford, R.F., 1989, Vertical distribution of uranium mill tailings contaminants in Langley Bay, Lake Athabasca sediments: *Science of the Total Environment*, v. 87/88, pp. 85–104.
- Kaiman, S., 1977, Mineralogical examination of old tailings from the Nordic Lake Mine, Elliot Lake, Ontario: Canada Centre for Mineral and Energy Technology Report, ERP/MSL 77-190 (IR).
- Kauffman, J.W., Laughlin, W.C., and Baldwin, R.A., 1986, Microbiological treatment of uranium mine waters: *Environmental Science and Technology*, v. 20, pp. 243–248.
- Keller, G., 1993, Radioecological aspects of former mining activities in Saxon Erzgebirge: *Environment International*, v. 19, pp. 449–454.
- Krom, M.D., and Berner, R.A., 1981, The diagenesis of phosphorus in a nearshore marine sediment: *Geochimica et Cosmochimica Acta*, v. 45, pp. 207–216.
- Lakshmanan V.I. and Ashbrook, A.W., 1978, Radium balance studies at the Beaverlodge mill of Eldorado Nuclear Limited; in Seminar on management, stabilization and environmental impact of uranium mill tailings: Organization for Economic Cooperation and Development/ Nuclear Energy Agency, Paris, pp. 51–64.
- Landa, E.R., 1980, Isolation of uranium mill tailings and their component radionuclides from the biosphere—Some earth science perspectives: U.S. Geological Survey Circular 814, 32 pp.
- Landa, E.R., 1982, Leaching of radionuclides from uranium ore and mill tailings: *Uranium*, v. 1, pp. 53–64.
- Landa, E.R., 1984, Leaching of molybdenum and arsenic from uranium ore and mill tailings: *Hydrometallurgy*, v. 13, pp. 203–211.
- Landa, E.R., 1991, Leaching of ²²⁶Ra from components of uranium mill tailings: *Hydrometallurgy*, v. 26, pp. 361–368.

- Landa, E.R., and Bush, C.A., 1990, Geochemical hosts of solubilized radionuclides in uranium mill tailings: *Hydrometallurgy*, v. 24, pp. 361–372.
- Landa, E.R., Miller, C.L., and Updegraff, D.M., 1986, Leaching of ^{226}Ra from uranium mill tailings by sulfate-reducing bacteria: *Health Physics*, v. 51, pp. 509–518.
- Landa, E.R., Phillips, E.J.P., and Lovley, D.R., 1991, Release of ^{226}Ra from uranium mill tailings by microbial Fe(III) reduction: *Applied Geochemistry*, v. 6, pp. 647–652.
- Landa, E.R., Stieff, L.R., Germani, M.S., Tanner, A.B., and Evans, J.R., 1994, Intense alpha-particle emitting crystallites in uranium mill wastes: *Nuclear Geophysics*, v. 8, pp. 443–454.
- Landa, E.R., Le, A.H., Luck, R.L., and Yeich, P.J., 1995, Sorption and coprecipitation of trace concentrations of thorium with various minerals under conditions simulating an acid uranium mill effluent environment: *Inorganica Chimica Acta*, v. 229, pp. 247–252.
- Lewis, B.G., and MacDonell, M.M., 1986a, Predicting radon transport by vegetation; in Cawley, W.A., and Morand, J.M. (eds.), *Proceedings of Special Conference of Environmental Engineering Division: American Society of Civil Engineering*, pp. 37–42.
- Lewis, B.G., and MacDonell, M.M., 1986b, Radon transport through a cool-season grass: *Journal of Environmental Radioactivity*, v. 4, pp. 123–132.
- Lewis, B.G., and MacDonell, M.M., 1990, Release of radon-222 by vascular plants—Effect of transpiration and leaf area: *Journal of Environmental Quality*, v. 19, pp. 93–97.
- Longmire, P., and Thomson, B.M., 1992, Evidence for denitrification at a uranium-mill tailings site, Maybell, Colorado, USA; in Kharaka, Y.K., and Maest, A.S. (eds.), *Proceedings of 7th Internatl Symposium on Water-Rock Interaction: A.A. Balkema, Rotterdam*, pp. 295–300.
- Lovley, D.R., and Phillips, E.J.P., 1992, Bioremediation of uranium contamination with enzymatic uranium reduction: *Environmental Science and Technology*, v. 26, pp. 2228–2234.
- Lovley, D.R., Phillips, E.J.P., Gorby, Y.A., and Landa, E.R., 1991, Microbial reduction of uranium: *Nature*, v. 350, pp. 413–416.
- Lush, D., Brown, J., Fletcher, R., Goode, J., and Jurgens, T., 1978, An assessment of the long term interaction of uranium tailings with the natural environment; in *Management, Stabilization and Environmental Impact of Uranium Mill Tailings: Organization for Economic Cooperation and Development/Nuclear Energy Agency, Paris*, pp. 373–398.
- Macaskie, L.E., and Dean, A.C.R., 1987, Use of immobilized biofilm of *Citrobacter* sp. for the removal of uranium and lead from aqueous flows: *Enzyme and Microbial Technology*, v. 9, pp. 2–4.
- Marques, A.M., Bonet, R., Simon-Pujol, M.D., Fuste, M.C., and Congregado, F., 1990, Removal of uranium by an exopolysaccharide from *Pseudomonas* sp: *Applied Microbiology and Biotechnology*, v. 34, pp. 429–431.
- Merritt, R.C., 1971, *The extractive metallurgy of uranium: Colorado School of Mines Research Institute, Golden*, 576 pp.
- Moffett, D., and Tellier, M., 1978, Radiological investigations of an abandoned uranium tailings area: *Journal of Environmental Quality*, v. 7, pp. 310–314.
- Morin, K.A., and Cherry, J.A., 1986, Trace amounts of siderite near a uranium-tailings impoundment, Elliot Lake, Ontario, Canada and its implication in controlling contaminant migration in a sand aquifer: *Chemical Geology*, v. 56, pp. 117–134.
- Morin, K.A., and Cherry, J.A., 1988, Migration of acidic groundwater seepage from uranium-tailings impoundments, 3. Simulation of conceptual model with application to seepage area A: *Journal of Contaminant Hydrology*, v. 2, pp. 323–342.
- Morin, K.A., Cherry, J.A., Lim, T.P., and Vivuyurka, A.J., 1982, Contaminant migration in a sand aquifer near an inactive uranium tailings impoundment, Elliot Lake, Ontario: *Canadian Geotechnical Journal*, v. 19, no. 1, pp. 49–62.
- Morin, K.A., Cherry, J.A., Dave, N.K., Lim, T.P., and Vivuyurka, A.J., 1988a, Migration of acidic groundwater seepage from uranium-tailings impoundments, 1. Field study and conceptual hydrogeochemical model: *Journal of Contaminant Hydrology*, v. 2, pp. 271–303.
- Morin, K.A., Cherry, J.A., Dave, N.K., Lim, T.P., and Vivuyurka, A.J., 1988b, Migration of acidic groundwater seepage from uranium-tailings impoundments, 2. Geochemical behavior of radionuclides in groundwater: *Journal of Contaminant Hydrology*, v. 2, pp. 305–322.
- Morrison, S.J., and Cahn, L.S., 1991, Mineralogical residence of alpha-emitting contamination and implications for mobilization from uranium mill tailings: *Journal of Contaminant Hydrology*, v. 8, pp. 1–21.
- Morrison, S.J., and Spangler, R.R., 1992, Extraction of uranium and molybdenum from aqueous solutions—A survey of industrial materials for use in chemical barriers for uranium mill tailings remediation: *Environmental Science and Technology*, v. 26, pp. 1922–1931.
- Narasimhan, T.N., White, A.F., and Tokunaga, T., 1986, Groundwater contamination from an inactive uranium mill tailings pile, 2. Application of a dynamic mixing model: *Water Resources Research*, v. 22, pp. 1820–1834.
- Nathwani, J.S., and Phillips, C.R., 1979a, Rate-controlling processes in the release of radium-226 from uranium mill tailings, I. Leaching study: *Water, Air, and Soil Pollution*, v. 11, pp. 301–308.
- Nathwani, J.S., and Phillips, C.R., 1979b, Rate-controlling processes in the release of radium-226 from uranium mill tailings, II. Kinetic study: *Water, Air, and Soil Pollution*, v. 11, pp. 309–317.
- National Research Council, 1986, *Scientific basis for risk assessment and management of uranium mill tailings: National Academy Press, Washington, D.C.*, 245 pp.
- National Uranium Tailings Program, 1985, *Uranium tailings sampling manual: Canada Centre for Minerals and Energy Technology, Ottawa*, Report NUTP-1E, 87 pp.
- Nelson, C.B., 1993, Book review—Effects of ionizing radiation on aquatic organisms: *NCRP Report No. 109, Health Physics*, v. 64, pp. 329–330.
- Nicholson, R.V., Gillham, R.W., Cherry, J.A., and Reardon, E.J., 1989, Reduction of acid generation in mine tailings through the use of moisture-retaining cover layers as oxygen barriers: *Canadian Geotechnical Journal*, v. 26, pp. 1–8.
- Nirdosh, I., and Muthuswami, S.V., 1988, Distribution of ^{230}Th and other radionuclides in Canadian uranium mill streams: *Hydrometallurgy*, v. 20, pp. 31–47.
- Nirdosh, I., Muthuswami, S.V., and Baird, M.H.I., 1984, Radium in uranium mill tailings—Some observations on retention and removal: *Hydrometallurgy*, v. 12, pp. 151–176.
- Nirdosh, I., Trembley, W.B., Muthuswami, S.V., and Johnson, C.R., 1987, Adsorption-desorption studies on the radium-silica system: *Canadian Journal of Chemical Engineering*, v. 65, pp. 928–934.
- Noller, B.N., 1991, Non-radiological contaminants from uranium mining and milling at Ranger, Jabiru, Northern Territory, Australia: *Environmental Monitoring and Assessment*, v. 19, pp. 383–400.
- Opitz, B.E., Dodson, M.E., and Serne, R.J., 1985, Uranium mill tailings neutralization—Contaminant complexation and tailings leaching studies: *U.S. Nuclear Regulatory Commission report NUREG/CR-3906, PNL-5179*, 45 pp. and appendix.
- Organization for Economic Cooperation and Development/Nuclear Energy Agency, 1982, *Uranium mill tailings management: OECD/NEA, Paris*, 237 pp.
- Organization for Economic Cooperation and Development/Nuclear Energy Agency, 1983, *Uranium extraction technology: OECD/NEA, Paris*, 270 pp.
- Organization for Economic Cooperation and Development/Nuclear Energy Agency, 1984, *Long-term radiological aspects of management of wastes from uranium mining and milling: OECD/NEA, Paris*, 112 pp.
- Paige, C.R., Hileman, Jr., O.E., and Snodgrass, W.J., 1988, The formation of heteroepitaxial deposits of lead, barium and (barium/lead) sulfates on mica surfaces: *Journal of Radioanalytical Nuclear Chemistry, Letters*, v. 127, pp. 341–348.
- Paige, C.R., Hileman, Jr., O.E., Kornicker, W.A., and Snodgrass, W.J., 1989a, The formation of hetero-epitaxial deposits of lead, barium and (barium/lead) sulfates on quartz surfaces: *Journal of Radioanalytical*

- Nuclear Chemistry, Letters, v. 135, pp. 299–305.
- Paige, C.R., Hileman, Jr., O.E., Kornicker, W.A., and Snodgrass, W.J., 1989b, The formation of hetero-epitaxial deposits of strontium sulfate on mica surfaces: *Journal of Radioanalytical Nuclear Chemistry, Letters*, v. 137, pp. 319–325.
- Penna Franca, E., Amaval, E.C.S., and Stoffel, M.G., 1982, Behavior of Ra-226 and Pb-210 in the aquatical environment of the first Brazilian uranium mine and mill; *in* Vohra, K.G., Pillai, K.C., Mishra, U.C., and Sadasivan, S. (eds.), 2nd Spec. Symposium on Natural Radiation Environment, Bhabha Atomic Research Centre, Bombay, India: John Wiley and Sons, New York, pp. 93–101.
- Peterson, S.R., Felmy, A.R., Serne, R.J., and Gee, G.W., 1983, Predictive geochemical modeling of interactions between uranium mill tailings solutions and sediments in a flow-through system: U.S. Nuclear Regulatory Commission Report NUREG/CR-3404 (PNL-4782).
- Platford, R.F. and Joshi, S.R., 1988, Dose rates to aquatic life near a U waste site: *Health Physics*, v. 54, pp. 63–68.
- Reardon, E.J., and Moddle, P.M., 1985, Suitability of peat as an oxygen interceptor material for the close-out of pyritic uranium tailings: *Uranium*, v. 2, pp. 83–110.
- Riese, A.C., 1982, Adsorption of radium and thorium onto quartz and kaolinite—A comparison of solution/surface equilibria models: Unpub. Ph.D. thesis, Colorado School of Mines, Golden, 292 pp.
- Ritcey, G.M., and Silver, M., 1982, Lysimeter investigations on uranium tailings at CANMET: *Canadian Institute of Mining and Metallurgy Bulletin*, v. 75, pp. 134–143.
- Rumble, M.A., and Bjugstad, A.J., 1986, Uranium and radium concentrations in plants growing on uranium mill tailings in South Dakota: *Reclamation and Revegetation Research*, v. 4, pp. 271–277.
- Seeley, F.G., 1977, Problems in the separation of radium from uranium ore tailings: *Hydrometallurgy*, v. 2, pp. 249–263.
- Serne, R.J., Peterson, S.R., and Gee, G.U., 1983, Laboratory measurements of contaminant attention of uranium mill tailings leachates by sediments and clay liners: U.S. Nuclear Regulatory Commission Report NUREG/CR-3124 (PNL-4605), 78 pp. and appendix.
- Shapiro, J., 1990, Radiation protection—A guide for scientists and physicians: 3rd ed., Harvard Univ. Press, Cambridge, 494 pp.
- Shuman, R., and Whicker, F.W., 1986, Intrusion of reclaimed uranium mill tailings by prairie dogs and ground squirrels: *Journal of Environmental Quality*, v. 15, pp. 21–24.
- Sill, C.W., and Willis, C.P., 1964, Precipitation of submicrogram quantities of thorium by barium sulfate and application to fluorometric determination of thorium in mineralogical and biological samples: *Analytical Chemistry*, v. 36, pp. 622–630.
- Silver, M., and Ritcey, G.M., 1985, Effects of iron-oxidizing bacteria and vegetation on acid-generation in laboratory lysimeter tests on pyrite-containing uranium tailings: *Hydrometallurgy*, v. 15, pp. 255–264.
- Skeaff, J.M., 1981, Survey of the occurrence of Ra-226 in the Rio Algom Quirke I uranium mill, Elliot Lake: *Canadian Institute of Mining and Metallurgy Bulletin*, v. 74, pp. 115–121.
- Snodgrass W.J., 1986, Study of radiobarites in uranium mill tailings research report (contract no. 23317–5–1721) by Beak Consultants Ltd. for National Uranium Tailings Program: Energy, Mines and Resources, Ottawa, Canada.
- Snodgrass, W.J., and Hileman, O.E., 1985, On the geochemical mechanism controlling Ra-226 dissolution in uranium mill wastes (tailings) research report (contract no. 23241–4–1678) by Beak Consultants Ltd. for National Uranium Tailings Program: Energy, Mines and Resources, Ottawa, Canada.
- Sposito, G., 1984, The surface chemistry of soils: Oxford University Press, New York, 234 pp.
- Steger, H.F., and Legeyt, M., 1987, Radium-226 in uranium mill tailings, I. Fate and consequent dissolution: *Journal of Radioanalytical Nuclear Chemistry, Articles*, v. 111, pp. 95–104.
- Stieff, L.R., 1985, The characterization of uranium mill tailings using alpha-sensitive nuclear emulsions; *in* Symposium on Uranium Mill Tailings Management: Colorado State Univ., Ft. Collins, pp. 559–568.
- Strandberg, G.W., Shumate II, S.E., Parrott Jr., J.R., and North, S.E., 1981, Microbial accumulation of uranium, radium and cesium; *in* Brinckman, F.E., and Fish, R.H. (eds.), DOE/NBS workshops on Environmental Speciation and Monitoring Needs for Trace Metal Containing Substances from Energy-Related Processes: NBS Spec. Pub. No. 618, p. 274–283.
- Sumioka, S.S., 1991, Quality of water in an inactive uranium mine and its effects on the quality of water in Blue Creek, Stevens County, Washington, 1984–85: U.S. Geological Survey Water-Resources Investigations Report 89–4110, 62 pp.
- Thomson, B.M., Longmire, P.A., and Brookins, D.G., 1986, Geochemical constraints on underground disposal of uranium mill tailings: *Applied Geochemistry*, v. 1, pp. 335–343.
- Tsezos, M., 1985, The selective extraction of metals from solution by micro-organisms—A brief overview: *Canadian Metallurgical Quarterly*, v. 24, pp. 141–144.
- Tsezos, M., Baird, M.H.I., and Shemilt, L.W., 1987, The use of immobilized biomass to remove and recover radium from Elliot Lake uranium tailing streams: *Hydrometallurgy*, v. 17, pp. 357–368.
- U.S. Environmental Protection Agency, 1995, Groundwater standards for remedial actions at inactive uranium processing sites—Final rule: *Federal Register* 40 CFR Part 192, v. 60 (Jan. 11, 1995), pp. 2854–2871.
- U.S. Nuclear Regulatory Commission, 1980, Final generic environmental impact statement on uranium milling: Washington, D.C., Report NUREG-0706.
- Van Metre, P.C., and Gray, J.R., 1992, Effects of uranium mining discharges on water quality in the Puerco River basin, Arizona and New Mexico: *Hydrological Sciences Journal*, v. 37, pp. 463–480.
- Waite, D.T., Joshi, S.R., and Sommerstad, H., 1988, The effect of uranium mine tailings on radionuclide concentrations in Langley Bay, Saskatchewan, Canada: *Archives of Environmental Contamination and Toxicology*, v. 17, pp. 373–380.
- Waite, D.T., Joshi, S.R., and Sommerstad, H., 1989, Movement of dissolved radionuclides from submerged uranium mine tailings into the surface water of Langley Bay, Saskatchewan, Canada: *Archives of Environmental Contamination and Toxicology*, v. 18, pp. 881–887.
- Waite, D.T., Joshi, S.R., Sommerstad, H., Wobeser, G., and Gajadhar, G.G., 1990, A toxicological examination of whitefish (*Coregonus clupeaformis*) and northern pike (*Esox lucius*) exposed to uranium mine tailings: *Archives of Environmental Contamination and Toxicology*, v. 19, pp. 578–582.
- Warwick, W.F., Fitchko, J., McKee, P.M., Hart, D.R., and Burt, A.J., 1987, The incidence of deformities in *Chironomus* spp. from Port Hope Harbour, Lake Ontario: *Journal of Great Lakes Research*, v. 13, pp. 88–92.
- Weimer, W.C., Kinnison, R.R., and Reeves, J.H., 1981, Survey of radionuclide distributions from the Church Rock, New Mexico, uranium mill tailings pond dam failure: U.S. Nuclear Regulatory Commission Report NUREG/CR-2449 (PNL-4122), 59 pp. and appendix.
- Whitman, A., and Beverly, R.G., 1958, Radium balance in the Monticello acid R.I.P. uranium mill: U.S. Atomic Energy Commission WIN-113, 23 pp.
- White, A.F., Delany, J.M., Narasimhan, T.N., and Smith, A., 1984, Groundwater contamination from an inactive uranium mill tailings pile, 1. Application of a chemical mixing model: *Water Resources Research*, v. 20, pp. 1743–1752.
- Wiles, D.R., 1983, The radiochemistry of radium and thorium in uranium mine tailings: *Water, Air, and Soil Pollution*, v. 20, pp. 99–108.
- Wirt, L., 1993, Use of $^{234}\text{U}/^{238}\text{U}$ as an environmental tracer of uranium-mining contamination in ground water [abs.]: *Eos*, v. 74, p. 298.
- Yang, I.C., and Edwards, K.W., 1984, Releases of radium and uranium into Ralston Creek and Reservoir, Colorado, from uranium mining; *in* Barney, G.S., Navratil, J.D., and Schulz, W.W. (eds.), *Geochemical behavior of disposed radioactive waste*: American Chemical Society, Washington, D.C., ASC Symposium Series 246, pp. 271–285.
- Zielinski, R.A., 1980, Uranium in secondary silica—A possible exploration guide: *Economic Geology*, v. 75, pp. 592–602.

Chapter 28

BIOOXIDATION PRETREATMENT OF REFRACTORY SULFIDIC AND SULFIDIC-CARBONACEOUS GOLD ORES AND CONCENTRATES

J.A. Brierley

Newmont Technical Facility, 10101 East Dry Creek Road, Englewood, CO 80112

Bacterial oxidation of refractory sulfidic gold ores and concentrates can be used as a pretreatment process to enhance the recovery of gold. Sulfide minerals that occlude gold, such as pyrite, arsenopyrite, pyrrhotite, and marcasite, are biooxidized by acidophilic, chemolithotrophic bacteria. The biooxidation process results in the solubilization of the sulfide minerals with increased exposure of gold for subsequent recovery using standard metallurgical processes such as cyanide leaching. The mineralogy of the refractory gold ore determines the effectiveness of the biooxidation process. The ore must possess sufficient iron sulfide to support the bacterial growth and carbonate minerals, which can consume the acid, must be absent or present in such low concentrations that the biooxidation will result in a net production of acid. Several mining operations currently utilize biooxidation as a pretreatment process for refractory gold ore concentrates. Research and development are in progress to extend the use of biooxidation for pretreatment of lower grade sulfidic, refractory ores.

INTRODUCTION

Many gold ores and mineral concentrates produced from these ores are considered refractory because the gold cannot be economically recovered using conventional metallurgical procedures, for example extraction using cyanide. The refractory nature of the ore can be attributed to one or more factors: encapsulation of the gold within sulfide minerals and silicates, occurrence of gold with tellurium in non-leachable compounds, and (or) coexistence of gold with an organic component that complicates extraction and recovery of the metal. Locking of gold within iron sulfide minerals accounts for a large proportion of refractory gold ores. These minerals are principally pyrite or arsenopyrite, but marcasite and pyrrhotite are also commonly involved. In order to liberate the gold from the sulfide mineral matrix, the sulfide must be oxidized.

Oxidation of the sulfide is considered a pretreatment process for recovery by cyanide extraction. Several pretreatment processes are available for oxidizing iron sulfide minerals, thus rendering the refractory ore amenable to conventional recovery techniques. These methods include roasting, pressure oxidation, and chemical oxidation. Each process has been successfully used for refractory, precious metal ore pretreatment, but their use can be precluded by capital and operating costs relative to the value of the ore.

An alternative to the physical-chemical methods is bacterial oxidative pretreatment (biooxidation), a biological process whereby iron sulfide minerals are degraded and the liberated precious metal values are subsequently recovered by conventional technologies.

Bacterial oxidation of sulfide minerals has been applied for extraction of copper (see reviews by Bruynesteyn, 1970; C.L. Brierley, 1978; Torma, 1989; Flett and Bonney, 1991) and uranium (McCready and Gould, 1990). Bacterial oxidation of minerals with concurrent release of metals into the acid solution is termed bioleaching. Bioleaching may have been practiced as early as the 15th or 16th century, when soluble copper was precipitated from mine waters (see Brierley, 1990a). Presumably, microbial activity was involved in the solubilization of copper, but neither the role of bacteria nor the bacteria themselves were known at that time.

The bioleaching process can be applied to the bacterial pretreatment of refractory, sulfidic, gold ores and mineral concentrates. However, in the case of gold, the process should be referred to as biooxidation rather than bioleaching, as the precious metal value is not concurrently extracted by the bacterial oxidation of the sulfide minerals.

Recent reviews of biooxidation pretreatment of refractory sulfidic gold ores have been published by Lawrence (1990) and Lindström et al. (1992).

BIOOXIDATION PROCESS

Microbiology

Some members of the bacterial physiological group described as chemolithotrophic, autotrophic, iron- and sulfur-oxidizing bacteria are well suited for use in biooxidation of refractory sulfidic gold ores. These bacteria have simple requirements for growth: an oxidizable inorganic energy source, such as ferrous iron, elemental sulfur, or a sulfide mineral; carbon dioxide as a source of carbon for synthesis of cell material; some inorganic nutrients such as ammonia, nitrogen, and phosphate; and several trace metals (e.g., magnesium, potassium, zinc, copper, manganese, molybdenum). Furthermore, these bacteria can live in conditions of high acidity, pH 3.5 to pH <1.0, and high metal and sulfate concentrations. Additionally, some bacteria can tolerate temperatures up to 90°C (thermophiles). The few nutritional requirements of these bacteria and their ability to exist in "severe" environmental conditions make them well suited to live and function in the bioleaching/biooxidation environment.

The bacteria most commonly associated with biooxidation of sulfide minerals include *Thiobacillus ferrooxidans* and *Leptospirillum ferrooxidans*. *T. ferrooxidans* are small (0.5 x 1.0 µm), rod-shaped bacteria; *L. ferrooxidans* are vibroid-shaped cells that may form short chains with an apparent spirillum, or "corkscrew," morphology. Both bacteria can function in a temper-

ature range of about 10° to 40°C and in acid environments from around pH 2.5 down to about pH 1.0.

T. ferrooxidans were first found by Colmer and Hinkle (1947) during study of acid mine drainage. The role of this bacterium in bioleaching was defined during the mid 1950s (see Bryner et al., 1954; Bryner and Anderson, 1957; Bryner and Jameson, 1958). In 1958 a patent was issued to the Kennecott Copper Corporation for the use of the iron-oxidizing bacteria in bioleaching (Zimmerley et al., 1958).

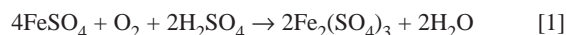
Other bacteria conducting the same biooxidation activities as *T. ferrooxidans* function at higher temperatures. Categorized by temperature range of growth, there are two groups of thermophilic bacteria:

- 1) The moderately thermophilic bacteria grow at about 30°C up to about 55°C and include the *Sulfobacillus thermosulfidooxidans* and other similar but unnamed bacteria (Norris, 1990);
- 2) The extremely thermophilic bacteria, for example *Sulfotobus* sp., *Acidianus brierleyi*, and *Metallosphaera sedula*, grow at maximum temperatures from 70° to 90°C.

These moderately and extremely thermophilic bacteria have also been considered for use in bioleaching and biooxidation processes (Brierley and Brierley, 1986; Brierley, 1990b).

The bioleaching/biooxidation environment is very complex with regard to the indigenous microflora. The environmental system is not composed of a single type of bacterium, for example *T. ferrooxidans*, but rather a mixed, heterogenous microflora composed of *T. ferrooxidans*, *L. ferrooxidans*, and perhaps even moderately thermophilic bacteria, all of which coexist with other bacteria that have no known role in bioleaching or biooxidation (Tuovinen et al., 1991). The interactions among the known and the yet-to-be discovered bacteria in bioleaching and mineral biooxidation systems are not well defined.

The function of the bacteria in bioleaching and biooxidation is associated with their use of inorganic elements and compounds as substrates for energy. The principal biooxidation reaction from which these microorganisms obtain energy is the oxidation of ferrous iron (equation [1]):



This biooxidation process takes place in acidic conditions and requires molecular oxygen (O₂), because the bacteria are aerobic. Pyrite oxidation by the bacteria is illustrated in equation [2]:

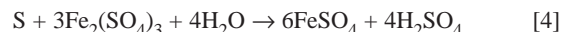


This equation also indicates that the bacterial oxygen requirement is of considerable importance in the practical applications of mineral sulfide biooxidation. Pyrite oxidation can also occur inorganically with ferric iron species (equation [3]):



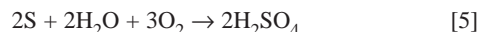
subsequently resulting from the oxidation of ferrous ions and iron compounds by the bacteria. Elemental sulfur may accumulate from ferric iron oxidation of the pyrite or the sulfur may be further

oxidized to sulfate by ferric iron (equation [4]):

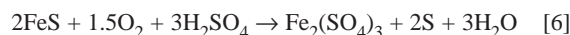


The ferrous iron produced would then be re-oxidized by the bacteria [equation 1] to perpetuate the cycle.

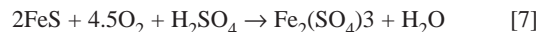
The bacterium *Thiobacillus thiooxidans*, also found in bioleaching and biooxidation habitats, oxidizes sulfur to sulfuric acid (equation [5]):



The iron sulfide pyrrhotite can also be oxidized by the bacteria according to equations [6] and [7]:



and



to provide energy for growth functions. Elemental sulfur may also result from biooxidation of pyrrhotite (equation [6]) or the sulfur may be completely oxidized to sulfate (equation [7]). Sulfur accumulation is probably related to the availability of oxygen in that oxygen limitation could inhibit sulfate formation but facilitate the formation of elemental sulfur. There is no apparent accumulation of elemental sulfur in biooxidation pretreatment processes.

Arsenopyrite, often associated with refractory, sulfidic, gold ores, can also be oxidized by bacteria (equation [8]):



Solubilization of different forms of iron, arsenic, and sulfide occurs during biooxidation of arsenopyrite. The *T. ferrooxidans* have a relatively high tolerance to the normally toxic effects of arsenic. Collinet and Morin (1990) report toxic levels of 5 g arsenite/l and 40 g arsenate/l for *T. ferrooxidans*.

Mineralogy

The mineralogy of refractory gold ores is of paramount importance in the biooxidation pretreatment process. Mineralogy will determine the possibility of biooxidation, the rate of biooxidation, and the extent of biooxidation required for economic gold recovery.

Suitable ore for biooxidation pretreatment must be net acid producing. In this regard, the presence of carbonate minerals can have a deleterious influence on the biooxidation process, because of the acidophilic nature of the bacteria. A low concentration of carbonate in the ore, less than 0.5% by weight, can be neutralized with sulfuric acid to facilitate the initial growth of the bacteria. This, however, assumes that the ore contains a sufficient amount

of sulfide, which, when oxidized to sulfuric acid, yields a pH of 2 or less.

Baldi et al. (1992) report wide variations in the rate of microbial oxidation of pyritic materials from differing sources, mineral pyrite and pyrites associated with coal. The described differences could not be attributed to metal toxicity or oxygen starvation, although there was uncertainty regarding the availability of oxygen at the mineral surface during biooxidation. The susceptibility of the various pyrites to biooxidation attributed to chemical reactivities may be a function of subtle differences in the composition and crystal structure of the pyrite.

Odekirk reports (see reference of Brierley and Wan, 1990) that, initially *T. ferrooxidans* preferentially oxidizes the late-stage, fine-grained anhedral pyrite (which may contain arsenic) that commonly replaces, cements, and rims earlier-stage pyrite. The pyrite that is most susceptible to bacterial oxidation also contains the greater proportion of gold compared to the more refractory, coarse-grained, euhedral pyrite. The early-stage euhedral pyrite can subsequently be biooxidized at a much slower rate.

Arsenopyrite is more rapidly biooxidized than pyrite. Apparently, the more "contaminated" the pyrite crystal is with either arsenic and (or) gold, the less stable the crystal structure and the greater its susceptibility to biooxidation.

During the biooxidation of sulfide minerals, cylindrical pores develop along weaknesses in the sulfide lattice (Lazer et al., 1986). The structural weaknesses are dislocations in the crystal and are the "preferred" sites for biooxidation of the sulfide. The greater association of gold with the structural dislocations leads to accelerated gold release during biooxidation and decreased amounts of total sulfide requiring oxidation for economic gold recovery.

Mustin et al. (1992) determined the average pore size resulting from biooxidation of pyrite to be 2 μm in diameter. The reactive area was located at the base of the pit, resulting in increased intragranular porosity. This corrosion process increased the surface area of the pyrite grains, up to 42% for the test specimen. This phenomenon would result in exposure of the occluded gold if present.

Some refractory sulfidic ores may also contain carbon that interferes with gold recovery. The carbon, referred to as acid-insoluble carbon (i.e., not carbonate) or "organic" carbon, is preg-robbing. Preg-robbing is the sorption of aurocyanide complex, formed during cyanide leaching, by the organic matter of the ore. Preg-robbing results in reduced gold recoveries because the gold is unavailable for adsorption onto activated carbon or precipitation by zinc, the two major processes used for gold recovery from solution. The biooxidation process can effectively mitigate the influence of the sulfide component of sulfidic-carbonaceous ores; however, it is not effective for pretreatment or inactivation of the carbon component. The carbon is not likely to be metabolized by bacteria (autotrophic or heterotrophic), however, there is some indication that bacterial activity can partially inactivate the preg-robbing function by blinding the carbon surface (Brierley and Kulpa, 1992, 1993; Kulpa and Brierley, 1993). Alternatives to cyanide, such as thiourea or ammonium thiosulfate, can be used for gold recovery following biooxidation of refractory, sulfidic-carbonaceous ores (Brierley and Wan, 1990; Wan et al., 1994). Neither the thiourea-gold complex nor the ammonium thiosulfate-gold complex are sorbed by the preg-robbing carbon.

A unique approach to pretreatment of refractory, sulfidic ores involves the mixing of a manganese-containing, precious metal

ore with a refractory, sulfidic precious metal ore in the presence of bacteria to facilitate oxidation of the sulfidic ore (Wu et al., 1988). Reportedly, the sulfide reduces and solubilizes some of the manganese causing release of precious metals locked in both the manganese ore and the sulfidic ore. The bacteria were required for more extensive oxidation of the sulfidic ore.

Pretreatment concept

The biooxidation of the sulfide minerals of a precious metal ore exposes the locked gold for recovery by conventional leaching with cyanide or other lixiviants. The refractory sulfidic gold is, in effect, converted to an "oxide" gold ore as a result of the bacterial solubilization of the sulfide minerals. The biooxidation-pretreatment concept is shown on Figure 28.1, which illustrates the relationship of sulfide oxidation to gold extraction. For gold evenly distributed throughout all sulfide minerals in an ore, the gold extraction is dependent upon sulfide oxidation with a curve of slope 1 (example curve "A"). Complete gold extraction can only be achieved with complete oxidation of the sulfide.

More commonly, however, the gold in refractory, sulfidic ores is enriched in a specific sulfide mineral or grain-size fraction, and effective gold extraction can be achieved with only partial oxidation of the total available sulfide. The gold ore may be deemed very refractory because leaching of the ore with cyanide, prior to any pretreatment, results in little or no gold extraction. However, high gold extraction can be achieved with oxidation of that sulfide phase containing the gold (curve "B"). This "selective" oxidation of the gold-enriched sulfide is primarily a function of the mineralogical character of the ore, as discussed above, in which the gold predominantly occurs in the later-stage anhedral pyrite or arsenopyrite.

Curve "C" illustrates gold extraction from an ore containing free gold (about 45 wt% of the total gold in the ore) as well as gold enriched in a particular portion of the sulfide mineral(s). Only partial oxidation is required for effective extraction of the gold value.

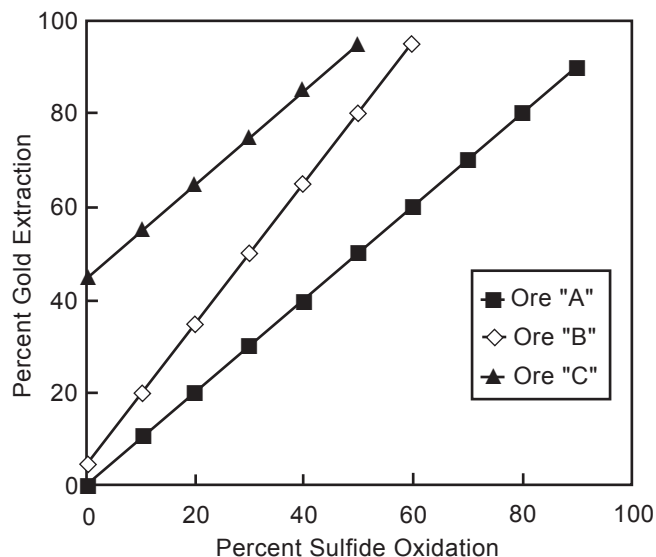


FIGURE 28.1—Effect of biooxidation of sulfide on gold extraction.

PROCESS APPLICATION

Biooxidation pretreatment development

During the decade of the 1980s, experimentation specifically for development of the biooxidation pretreatment process was initiated. In 1975, Pinches published a report dealing with bacterial leaching of an arsenic-bearing sulfide concentrate. This report could be considered a foundation for biooxidation of refractory gold-bearing sulfide concentrates. Most early research focused on the biooxidation pretreatment of sulfidic concentrates (Lawrence and Bruynesteyn, 1983; Lawrence and Gunn, 1985). Bruynesteyn (1988) summarized the early progress.

Bacterial oxidation was tested for pretreatment of a refractory gold-bearing sulfide concentrate from Olympias, Greece (Komnitsas and Pooley, 1990, 1991). Initial testing was conducted using air-stirred pachuca reactors. The arsenopyrite in this concentrate contained 80.4 wt% of the gold, whereas the pyrite contained only 4.7 wt% of the total gold; the remaining gold was either free or present in non-sulfides. High gold recoveries, >70 wt%, were achieved when arsenopyrite oxidation exceeded 70 wt%. However, the biooxidation process was sensitive to the concentrate pulp density over a range from 5 to 30%; as the pulp density increased, the gold recovery decreased from 87 to 62%. Reduction of the concentrate-particle size from -63 to -32 μm decreased the biooxidation time from 8 to 6 days for a 5% pulp density slurry.

Moderately thermophilic bacteria, grown at 50°C, and the thermophilic *Acidianus brierleyi*, grown at 60°C, were evaluated for their ability to biooxidize sulfidic and sulfidic-carbonaceous ores to increase gold recovery (Hutchins et al., 1988a, b). Relative to *T. ferrooxidans* (at 30°C), the moderately thermophilic bacteria were similar in pretreatment effect (56% gold recovery) of a sulfidic, flotation concentrate (gold recovery was only 5% without biooxidation pretreatment). By comparison, the thermophile *A. brierleyi* was more effective for pretreatment of this particular gold concentrate, producing a 91% gold recovery. Although the *A. brierleyi* was effective for oxidation of the sulfide minerals of a sulfidic-carbonaceous ore, neither this thermophile nor the *T. ferrooxidans* deactivated the preg-robbing ability of the carbon component of the ore.

A mixed culture of moderately thermophilic (grown at 45°C) bacteria, isolated from a mine in Western Australia, were evaluated by Barrett et al. (1988) for their oxidation of pyrite and arsenopyrite. Spencer and Budden (1990) also used this culture for biooxidation pretreatment of an arsenopyrite concentrate containing 16.7% arsenic, 28% iron, 34% sulfur and 50g Au/t (1.46 oz Au/ton). The biooxidation rate, determined at 40° to 45°C in an aerated, stirred-tank, batch reactor, increased with pulp density up to 15% w/v. However, further increases in pulp density did not increase the biooxidation rate. The culture was resistant to arsenic, with reported soluble arsenic concentrations between 20 and 28 g/l. Biooxidation of the concentrate by the mixed culture improved gold extraction using cyanide leaching from about 30% without biooxidation to about 90% following biooxidation.

Field testing of biooxidation pretreatment using the moderately thermophilic, mixed culture was conducted using a small pilot plant (Budden and Spencer, 1991; Spencer et al., 1991a, b). The pilot unit consisted of four biooxidation reactors with a total capacity of 32 m³ (8,454 gallons). Because biooxidation by the mixed culture was conducted at 55°C, cooling of the reactors,

which can be required using *T. ferrooxidans* and *L. ferrooxidans*, was eliminated. The results of the pilot plant closely matched the laboratory results; gold recovery increased from about 50% to over 80% using a feed rate of 500 kg concentrate/day (at 15% w/v solids).

Other studies have indicated potential problems with use of the thermophilic *Sulfolobus* bacteria, growing at 70°C, for biooxidation pretreatment of sulfide concentrates. Lindström and Gunneriusson (1990) reported growth limitation of the microbes at 1.5% w/v pulp density of an arsenopyrite concentrate. One possible explanation for this low limit is that the *Sulfolobus* do not have a rigid cell wall that provides protection against the abrasive action of a mineral slurry. Lawrence and Marchant (1988) reported no advantage in using *S. acidocaldarius*, growing at 64°C, compared with *T. ferrooxidans*, growing at 33°C, for biooxidation of sulfide concentrates. There was no apparent increase in rate of biooxidation at the higher temperature. Additional comparative work is required to determine the relative capabilities of thermophilic and mesophilic bacteria.

Laboratory research led to the development of the "BIOTANKLEACH" process by Giant Bay Biotech¹ in 1984 (Bruynesteyn et al., 1986). This process used *T. ferrooxidans* to oxidize refractory pyrite and arsenopyrite gold concentrates. Their testing established that biooxidation of refractory gold ores could be done on a large, commercial scale.

Implementation of biooxidation technology has been advanced by development of kinetic models of the process (Lazer et al., 1986; Pinches et al., 1988; Hansford and Bailey, 1992). The experimental data agree well with the logistic equation for biooxidation of sulfide minerals. The logistic equation and its integrated forms for various reactor configurations provide a quantitative association between reaction kinetics and the physical processes in reactors. Important factors are oxygen mass transfer, heat transfer, and solids mixing.

Tank-reactor systems

Application technology for biooxidation pretreatment has been developed primarily for use with refractory, sulfidic, gold ore concentrates of high economic value. Production-scale biooxidation pretreatment plants are now operating in several localities: Fairview Mine in South Africa, processing 35 tons/day; Sao Bento, Brazil, 150 tons/day; and Harbour Lights, Australia, 40 tons/day (Hansford and Bailey, 1992). Biooxidation pretreatment plants are also in operation at the Wiluna Gold Mine, treating up to 115 tons/day (Brown et al., 1994), and at the Youanmi Mine (Budden and Bunyard, 1994; Brierley and Brans, 1994), both in Western Australia. The largest biooxidation pretreatment facility has been commissioned at the Gold Fields Ashanti Mine, Obuasi, Ghana. This plant treats 800 tons/day concentrate of refractory, sulfidic ore (Nicholson et al., 1994).

The biooxidation pretreatment plant with the longest history of operation is Genmin's BIOX[®] process at the Fairview Mine. This plant, operating since October 1986 (van Aswegen et al., 1991; Marais, 1990), treats a refractory arsenopyrite/pyrite concentrate. The bacterial culture, which has been adapting as the system operates, functions optimally at 45°C and tolerates temperature excursions

¹Any use of trade, product, or firm names in this publication is for descriptive purposes only and does not imply endorsement by the U.S. Government.

sions up to 53°C. Sulfide oxidation in the system is about 75 to 90% with gold extraction of over 90%.

Genmin also developed their BIOX® process for use as a pretreatment stage prior to further oxidation in a pressure autoclave at the Sao Bento, Brazil facility (Slabbert et al., 1992). The purpose of the biooxidation stage was to oxidize pyrrhotite and decompose siderite with acid to increase oxidation rates and optimize oxygen usage within the autoclave. Operation of the Sao Bento facility identified three conditions leading to loss of bacterial activity in a production plant:

- 1) failure of the air supply to the reactor,
- 2) cooling coil mechanical failure resulting in escape of biocides and toxic descalant reagents from the cooling water into the reactor, and
- 3) thiocyanate toxicity.

The thiocyanate resulted from increased recycling of tailings dam water in which cyanide reacted with residual forms of sulfur. Use of fresh water prevents thiocyanate toxicity.

There have been several pilot plant applications of biooxidation pretreatment. One of the largest, Vaal Reefs in South Africa, treated 20 tons per day of a pyritic flotation concentrate (Dempsey et al., 1990). These authors report that a large bacterial population, which can be greater than 10⁹ bacteria/ml, is required for acceptable pyrite oxidation rates. The reactor was started using an inoculum of 20% by volume of an active slurry containing the bacteria. Bacterial growth and pyrite oxidation became evident after a 14-day lag period following inoculation. An additional 14 days were required for production of the bacterial population in the reactor system. Thereafter, the bacterial population remained active and stable.

A pilot plant test, using a 225 m³ (59,445 gallon capacity) reactor, was successfully operated at the Congress Gold property near Goldbridge, British Columbia (Hackl, 1990a, b). The apparent rate of biooxidation was independent of oxygen concentration in the reactor until the dissolved oxygen decreased below 1.2 mg/l (the critical oxygen concentration necessary to sustain the process).

The design of bioreactors for the biooxidation pretreatment of concentrates and possibly high grade ores must take into account several factors that facilitate the growth of the bacteria on the mineral particles: oxygen supply, slurry mixing, and heat transfer. Heat transfer may not be problematic if the reactor uses thermophilic bacteria for the biooxidation process.

EIMCO Process Equipment Company developed a reactor, based on the principles of waste-water treatment technology, for biooxidation of refractory sulfidic ores (Sitarski et al., 1989). The reactor system was tested at pilot scale in Zimbabwe. Oxygen was supplied via fine bubble diffusers mounted on rotating rake arms. The rake arms moved settled solids to a central airlift mixer for resuspension. A separately driven impeller, mounted on the center column, was used to supplement slurry mixing.

Impellers used for agitation and gas dispersion in reactors have been studied to improve the biooxidation process. Traditionally, vertical, flat-blade turbine impellers have been used. Recently, Riley et al. (1990) described a hydrofoil impeller which can be used effectively with the biooxidation process. This type of impeller provides the mixing and gas dispersion necessary for aerobic biooxidation.

Biooxidation heap system

Another potential application of biooxidative pretreatment is oxidation of the sulfide of lower grade, lower economic value ores. This approach requires a simple "reactor" system, such as a heap, for economic pretreatment and subsequent recovery of the precious metal value. The basis for this approach is the successful use of bioleaching of copper from low grade ores and mine wastes in dumps.

The first consideration for the biooxidation pretreatment of refractory gold ores in heaps can be attributed to Livesey-Goldblatt (1986), who discussed biooxidation for enhancing gold recovery from mill tailings. Testing demonstrated that slimes, loosened into a granular mass and inoculated with iron- and sulfide-oxidizing bacteria, could be effectively biooxidized to facilitate subsequent gold leaching. Livesey-Goldblatt's pioneering work has been extended by Lawson et al. (1990), who confirmed that *T. ferrooxidans* offer an alternative to flotation-roasting for gold recovery from slimes dams.

Column test studies, simulating biooxidation of refractory sulfidic gold ore in heaps, have been reported by Burbank et al. (1990) and Greene (1990). Both studies showed that after several months of biooxidation, gold recovery from refractory ores was substantially increased. The importance of this approach is process development for economic recovery of gold from lower grade ores which cannot be treated economically by other means. Success of this process would result in expanded mineable reserves.

Newmont Gold Company and Newmont Mining Corporation are evaluating the potential use of the biooxidation heap process for pretreatment of refractory gold ore. Testing of the process was begun in the laboratory using columns containing up to 45 kg ore (Brierley and Luinstra, 1993) and continued in field trials using ore heaps of 500 to 600 metric tons and one heap of about 27,000 metric tons (Brierley, 1994).

A process for inoculation/agglomeration of the refractory ore for biooxidation heap pretreatment was developed (Brierley and Hill, 1993, 1994) and tested by Newmont Gold Company. The process adds *T. ferrooxidans* grown on ferrous iron to the crushed ore concurrent with formation of the heap. This process ensures distribution of an active population of bacteria throughout the entire mass of the heap for rapid initiation of the biooxidation process and to achieve homogenous biooxidation of the sulfides. Addition of the acidic bacterial culture to the ore also benefits the process through a degree of agglomeration of the ore fine particles. Ores used for six field site tests of the biooxidation heap process are characterized in Table 28.1.

TABLE 28.1—Characteristics of respective ore samples used for the biooxidation heap test program.

Test heap	Amount tonnes	Particle size % <1.9 cm	Au g/tonne	Sulfide S %	AIC %	Carbonate %
1	432	49	1.76	0.2–0.4	0.24	0.1–0.2
2	449	42	2.24	1.15	1.21	0.3
3	635	100	8.62	1.5	0.08	0.3–0.5
4	771	85	2.55	0.82	1.03	0.3
5	25,900	70	3.52	1.35	2.42	1.75–2.20
6	4082	98	1.62	0.78	0.67	1.25

AIC = acid-insoluble carbon content of the ore

The gold grades in the test samples varied from 1.62 g Au/tonne to 8.62 g Au/tonne. With one exception, 8.62 g Au/tonne, the respective ore grades for testing were consistent with the range of low grade ore, 1.0 to 2.4 g Au/tonne, for which the biooxidation heap pretreatment process is considered to offer a practical option to either pressure oxidation or roasting pretreatment. Only one of the test ores had an unusually low sulfide S content, 0.2 to 0.4%, in order to evaluate a possible limiting concentration of oxidizable sulfide.

The carbonate content of ore is also an important consideration for use of the biooxidation heap pretreatment process. High acid consumption, due to occurrence of high concentration of carbonate in the ore, can preclude the biooxidation heap process because of the cost of acid added to establish proper pH conditions for the growth of the bacteria (Bruynesteyn, 1993). The ore samples used for field testing of the process had low carbonate content.

A solution containing iron, ammonium sulfate, and potassium phosphate was applied to each heap with a system of drip-emitter tubing. The solution was applied at a rate of about 10 to 12 l m⁻² h⁻¹. The effluent from each heap was collected in either tanks or a pond for recirculation to the top of the heap. Routine monitoring of the progress of the biooxidation pretreatment process was accomplished by determination of the pH, redox potential, ferrous, ferric and total iron concentrations in samples of the solution effluent from each heap.

The biooxidation process, as shown by the increase in total dissolved iron for the respective test heaps, is presented on Figure 28.2. The total iron was almost entirely in the ferric form and the solution Eh range of +495 to +770 mV Standard Calomel Electrode (SCE) indicated effective bacterial activity. Initiation of iron solubilization was rapid, occurring in less than 10 to 20 days for all the test heaps with the exception of heap 6. The ore sample used for the biooxidation heap 6 contained some acid-consuming carbonate, in the form of calcite, which precipitated iron and limited the use of iron solubilization as an indicator of biooxidation activity. Acid was added to heap 6 in an amount of 5.4 kg H₂SO₄/tonne. The short lag for the biooxidation process found with the other test heaps demonstrates the utility of the inoculation/agglomeration process for distributing an active culture of the bacteria throughout the heap. The population of the acidophilic iron-oxidizing bacteria increased to 3.5–8.7 × 10⁷/g in the minus 10 mesh fraction of ore samples by 30 days biooxidation, indicating suitable conditions within the test heaps for growth of the bacteria.

The solubilization of iron reached a plateau for test heaps 1, 2, and 4 in less than 60 days, and less than 80 days for test heap 5. A plateau in the increase of the total soluble iron was considered an indicator of achieving effective oxidation of the iron-sulfide minerals exposed to biooxidation.

The ore in test heaps 2 and 4 responded very well to biooxidation (Fig. 28.2). Total iron in solution reached levels of about 29 and 18 g/l respectively. The active bacterial oxidation of the sulfide minerals was a function of good solution percolation and associated effective aeration. No solution ponding on the surface of these heaps occurred.

The apparent slowest response of the ore to the biooxidation heap pretreatment process was in heap test 3. Iron solubilization was a linear process throughout the biooxidation period, rather than the apparent exponential curves occurring with four of the test heaps (Fig. 28.2). This ore had favorable characteristics of grade (8.62 g Au/tonne), high sulfide S content (1.5%), very low

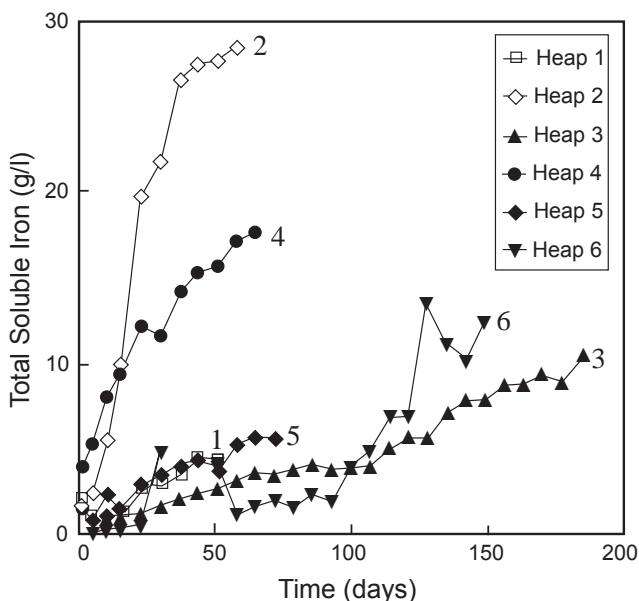


FIGURE 28.2—Iron solubilization from six field site pilot plant tests of the biooxidation heap pretreatment process.

acid-insoluble carbon (0.08%) and apparent low carbonate content (0.3–0.5%). However, there was also some acid-consumption (7 kg H₂SO₄/tonne) by this ore even at the low carbonate concentration. Acid consumption was attributed to presence of more calcite than analyzed in a composite head sample. The slower apparent sulfide oxidation in this heap test was attributed to ore particle size; following crushing, 100% of the ore was <1.9 cm with 65% <0.64 cm. The small size and occurrence of clayey fines caused poor solution percolation through the heap resulting in poor aeration and limited oxygen supply for the biooxidation process. Ponding of solution on the surface of the heap was observed.

Low sulfide content of ore, 0.2–0.4% (test heap 1), did not prevent occurrence of biooxidation as indicated by solubilization of iron (Fig. 28.2). Even with the low pyrite content, biooxidation resulted in rapid solubilization of iron up to about 4 g/l. At this low sulfide mineral concentration the refractory nature of the ore could be attributed to factors other than sulfide locking of gold, such as the presence of preg-robbing carbon in this case. Nevertheless, the biooxidation heap process has a low (<0.2–0.4%) sulfide S concentration requirement for support of bacterial activity.

Gold extraction results for the biooxidized ores from the respective test heaps are presented in Table 28.2 (Brierley et al., 1995a).

Although test heap 1 had a high degree of sulfide oxidation, 50–75%, gold extraction with cyanide was low, 30% (Table 28.2). This heap contained some preg-robbing carbonaceous sulfidic ore in addition to the cyanide amenable sulfidic ore. However, there was some apparent benefit of the biooxidation heap process for enhancing gold extraction.

Test heap 3 was leached using cyanide because the ore was sulfidic and not preg-robbing. The resulting extraction of 50%, an increase in gold extraction of 41% above an unoxidized ore sample (Table 28.2), would have been greater with further oxidation of the sulfide. Figure 28.2 shows that iron solubilization was continuing at the termination of the biooxidation period, indicating

potential for further sulfide oxidation. The preponderance of small particle size ore and clays in this heap affected solution flow by decreasing porosity. Biooxidation was deleteriously affected by poor solution flow and ventilation of the heap. Leaching was also likely affected by the hydrological characteristics of this heap attributed to small particle size of the ore. This heap demonstrated the importance of proper heap design and operation in order to enhance aeration to support biooxidation.

TABLE 28.2—Gold extraction from ore biooxidized using a heap pretreatment process.

Test heap	Untreated CN extraction %	Sulfide oxidation %	Leach process	Extraction %
1	14	50–75	cyanide	30
2	nil	35–40	thiourea	18
3	4	45	cyanide	50
4	nil	42	thiosulfate	51
5	41	48	thiosulfate	61
6	nil	47	thiosulfate	65

Test heap 2 was composed entirely of preg-robbing carbonaceous sulfidic ore which cannot be leached with cyanide following biooxidation. Details of the biooxidation pretreatment process have been reported (Brierley et al., 1995b). Thiourea leaching was tested as a lixiviant for leaching the gold from this heap. Thiourea leaching was attractive for use with biooxidation pretreatment since thiourea functions in acidic conditions eliminating the need to neutralize acidic ore. However, very low extraction (18%, Table 28.2) was achieved, even though laboratory column tests provided more encouraging extraction results, and thiourea was not used for extraction in subsequent biooxidation heap tests. The thiourea leaching yielded poor gold extraction kinetics because of large particle size ore (29.3% >2.54 cm) in the heap and cold temperatures during the leach process. In addition, thiourea consumption was relatively high and found to undergo oxidation reactions with unfavorable end-products, such as elemental sulfur, making the process uneconomical for use with biooxidation heap pretreatment (Wan et al., 1995).

Given the preg-robbing nature of much of Newmont Gold Company's refractory ore, an alternative to cyanide and thiourea is required for leaching the biooxidized ore. Ammonium thiosulfate was found to provide a process for leaching gold from biooxidized ore with preg-robbing carbon and a process patent was granted (Wan et al., 1994). Five tonne composite samples from test heaps 5 and 6 were leached using thiosulfate (Table 28.2). Test heaps 4 and 6 contained actively preg-robbing ores, and test heap 5 contained sulfidic carbonaceous ore which had little preg-robbing activity. Leach results from ore samples of test heaps 5 and 6 indicated gold extraction of 61 and 65% respectively for an economically favorable commercial process. The gold extraction of 51% (test heap 4) is also considered adequate for economic recovery.

SUMMARY

The acidophilic chemolithotrophic iron- and sulfur-oxidizing bacteria can be used for oxidative pretreatment of refractory sul-

fidic gold ores and concentrates to economically increase recoverable gold values. These bacteria include: *Thiobacillus ferrooxidans* and *Leptospirillum ferrooxidans*, which grow at temperatures up to 40°C; moderately thermophilic bacteria, capable of growth up to 55°C; and extremely thermophilic bacteria such as *Sulfolobus acidocaldarius*, *Acidianus brierleyi*, and *Metallosphaera sedula*, capable of growth at temperatures from 70° to 90°C. These bacteria oxidize sulfide minerals to obtain energy for growth processes. This oxidation results in the liberation of gold locked within the mineral matrix; the gold can subsequently be solubilized with cyanide or other reagents.

Sulfide minerals vary in their susceptibility to biooxidation. Fine-grained anhedral pyrites, particularly those with gold present, are more easily biooxidized than coarse-grained pyrite minerals. Arsenopyrite will be preferentially biooxidized over pyrite. The presence of gold and arsenic in association with iron sulfide minerals facilitates the biooxidation process, because these constituents create crystal discontinuities. Biooxidation of the sulfides results in formation of cylindrical pores along dislocations in the crystal lattice increasing the mineral surface area.

Biooxidation of refractory sulfidic gold bearing ores has been demonstrated by extensive laboratory investigations to improve gold extraction when followed by conventional metallurgical processes. These studies have led to the employment of commercial-sized bioreactors for pretreatment of refractory sulfidic gold ore concentrates. Currently, research and development are in progress for use of biooxidation pretreatment for lower grade ores in heaps.

REFERENCES

- Baldi, F., Clark, T., Pollack, S.S., and Olson, G.J., 1992, Leaching of pyrites of various reactivities by *Thiobacillus ferrooxidans*: Applied and Environmental Microbiology, v. 58, no. 6, pp. 1853–1856.
- Barrett, J., Hughes, M.N., Ewart, K., and Poole, R., 1988, The isolation and characterization of a moderately thermophilic mixed culture of autotrophic bacteria—Application to the oxidation of refractory gold concentrates; in Perth Gold 88: Randol International Ltd., Golden, Colorado, pp. 148–150.
- Brierley, C.L., 1978, Bacterial leaching: CRC Critical Reviews in Microbiology, v. 3, pp. 207–262.
- Brierley, C.L., and Brans, R., 1994, Selection of BacTech's thermophilic biooxidation process for Youanmi Mine; in Biomine '94: Australian Mineral Foundation, Glenside, South Australia, pp. 5.1–5.7.
- Brierley, J.A., 1990a, Biotechnology for the extractive metals industries: Journal of Metals, v. 42, no. 1, pp. 28–30.
- Brierley, J.A., 1990b, Acidophilic thermophilic archae-bacteria: potential application for metals recovery: FEMS Microbiology Reviews, v. 75, pp. 287–292.
- Brierley, J.A., 1994, Biooxidation-heap technology for pretreatment of refractory sulfidic gold ore; in Biomine '94: Australian Mineral Foundation, Glenside, South Australia, pp. 10.1–10.8.
- Brierley, J.A., and Brierley, C.L., 1986, Microbial mining using thermophilic microorganisms; in Brock, T.D. (ed.), Thermophiles—General, Molecular, and Applied Microbiology: John Wiley and Sons, Inc., New York, pp. 279–305.
- Brierley, J.A., and Hill, D.L., 1993, Biooxidation process for recovery of gold from heaps of low-grade sulfidic and carbonaceous sulfidic ore materials: U.S. Patent 5,246,486.
- Brierley, J.A., and Hill, D.L., 1994, Biooxidation process for recovery of metal values from sulphur-containing ore materials: U.S. Patent 5,332,559.
- Brierley, J.A., and Kulpa, C.F., 1992, Microbial consortium treatment of

- refractory precious metal ores: U.S. Patent 5,127,942.
- Brierley, J.A., and Kulpa, C.F., 1993, Biometallurgical treatment of precious metal ores having refractory carbon content: U.S. Patent 5,244,493.
- Brierley, J.A., and Luinstra, L., 1993, Biooxidation-heap concept for pretreatment of refractory gold ore; *in* Torma, A.E., Wey, J.E., and Lakshmanan, V.I. (eds.), *Biohydrometallurgical Technologies*, v. 1, Bioleaching Processes: The Minerals, Metals and Materials Society, Warrendale, Pa., pp. 437–448.
- Brierley, J.A., and Wan, R.Y., 1990, Enhanced recovery of gold from a refractory sulfidic-carbonaceous ore using bacterial pretreatment and thiourea extraction; *in* Hausen, D.M., Halbe, D.N., Petersen, E.U., and Tafuri, W.J. (eds.), *Gold '90: Society for Mining, Metallurgy, and Exploration, Inc.*, Littleton, Colo., pp. 463–466.
- Brierley, J.A., Wan, R.Y., Hill, D.L., and Logan, T.C., 1995a, Biooxidation-heap pretreatment technology for processing lower grade refractory gold ores; *in* Vargas, T., Jerez, C.A., Wiertz, J.V., and Toledo, H. (eds.), *Biohydrometallurgical Processing: v. 1*, Univ. of Chile, Santiago, pp. 253–262.
- Brierley, J.A., Wan, R.Y., and Luinstra, L., 1995b, Gold recovery from refractory sulfidic-carbonaceous ore, Part I: Biooxidation-heap pretreatment; *in* Warren, G.W. (ed.), *Extraction and Processing Division (EPD) Congress 1995: The Minerals, Metals and Materials Society*, Warrendale, Pa., pp. 155–163.
- Bruynesteyn, A., 1970, Microbiological leaching research to date and future applications: Society of Mining Engineers AIME, Pre-print no. 70-B-104.
- Bruynesteyn, A., 1986, The BIOTANKLEACH process; *in* Fivaz, C.E., and King, R.P. (eds.), *Gold 100, Extractive Metallurgy of Gold*, v. 2: South African Institute of Mining and Metallurgy, Johannesburg, pp. 353–365.
- Bruynesteyn, A., 1988, Biotechnology for gold ores—The state of the art; *in* Perth Gold 88: Randol International Ltd., Golden, Colo., pp. 141–143.
- Bruynesteyn, A., 1993, Biological treatment of refractory gold ores, advantages and disadvantages; *in* *Biomine '93: Australian Mineral Foundation*, Glenside, South Australia, pp. 3.1–3.7.
- Bruynesteyn, A., Hackl, R.P., and Wright, F., 1986, The BIOTANKLEACH process; *in* Fivaz, C.E., and King, R.P. (eds.), *Gold 100, Extractive Metallurgy of Gold*, v. 2: South African Institute of Mining and Metallurgy, Johannesburg, pp. 353–365.
- Bryner, L.C., and Anderson, R., 1957, Microorganisms in leaching sulfide minerals: *Industrial and Engineering Chemistry*, v. 49, pp. 1721–1724.
- Bryner, L.C., and Jameson, A.K., 1958, Microorganisms in leaching sulfide minerals: *Applied and Environmental Microbiology*, v. 6, pp. 281–287.
- Bryner, L.C., Beck, J.V., Davis, D.B., and Wilson, D.G., 1954, Microorganisms in leaching sulfide minerals: *Industrial and Engineering Chemistry*, v. 46, pp. 2587–2592.
- Budden, J.R., and Bunyard, M.J., 1994, Pilot plant testwork and engineering design for the BacTech bacterial oxidation plant at the Youanmi Mine; *in* *Biomine '94: Australian Mineral Foundation*, Glenside, South Australia, pp. 4.1–4.8.
- Budden, J.R., and Spencer, P.A., 1991, The effect of temperature and water quality on bacterial oxidation—The advantages of a moderately thermophilic culture over conventional *Thiobacillus* cultures; *in* Cairns '91: Randol International Ltd., Golden, Colo., pp. 271–274.
- Burbank, A., Choi, N., and Prisbrey, K., 1990, Biooxidation of refractory gold ores in heaps; *in* Fuerstenau, M.C., and Hendrix, J.L. (eds.), *Advances in Gold and Silver Processing: Society for Mining, Metallurgy, and Exploration, Inc.*, Littleton, Colo., pp. 151–159.
- Collinet, M.N., and Morin, D., 1990, Characterization of arsenopyrite oxidizing *Thiobacillus*—Tolerance to arsenite, arsenate, ferrous and ferric iron: *Antonie van Leeuwenhoek Journal of Microbiology and Serology*, v. 57, pp. 237.
- Colmer, A.R., and Hinkle, M.E., 1947, The role of microorganisms in acid mine drainage—A preliminary report: *Science*, v. 106, pp. 253–256.
- Dempsey, P., Human, P., Pinches, A., and Neale, J.W., 1990, Bacterial oxidation at Vaal Reefs; *in* *Innovations in Metallurgical Plant: South African Institute of Mining and Metallurgy*, Johannesburg, pp. 111–123.
- Flett, D.S., and Bonney, C.F., 1991, The use of micro-organisms in the minerals and metals industries—A technical review: Minerals Industry Research Organization, Lichfield, England, 91 pp.
- Greene, J.W., 1990, Microbial column leaching of a refractory, carbonaceous gold ore; *in* *Randol Gold Forum '90: Randol International Ltd.*, Golden, Colo., pp. 89–92.
- Hackl, R.P., 1990a, Operation of a commercial scale bio-leach reactor at the Congress gold property; *in* Fuerstenau, M.C., and Hendrix, J.L. (eds.), *Advances in Gold and Silver Processing: Society for Mining, Metallurgy, and Exploration, Inc.*, Littleton, Colo., pp. 131–141.
- Hackl, R.P., 1990b, Operating a commercial-scale bioleach reactor at the Congress gold property: *Mining Engineering*, December, pp. 1325–1326.
- Hansford, G.S., and Bailey, A.D., 1992, The logistic equation for modeling bacterial oxidation kinetics: *Minerals Engineering*, v. 5, no. 10–12, pp. 1355–1364.
- Hutchins, S.R., Brierley, J.A., and Brierley, C.L., 1988a, Microbial pretreatment of refractory sulfide and carbonaceous ores improves the economics of gold recovery: *Mining Engineering*, v. 40, no. 4, pp. 249–254.
- Hutchins, S.R., Davidson, M.S., and Brierley, J.A., 1988b, Thermophilic microbial treatment of precious metal ores: U.S. Patent 4,729,788.
- Komnitsas, C., and Pooley, F.D., 1990, Bacterial oxidation of an arsenical gold sulphide concentrate from Olympias, Greece: *Minerals Engineering*, v. 3, no. 3/4, pp. 295–306.
- Komnitsas, C., and Pooley, F.D., 1991, Optimization of the bacterial oxidation of an arsenical gold sulphide concentrate from Olympias, Greece: *Minerals Engineering*, v. 4, no. 12, pp. 1297–1303.
- Kulpa, C.F., and Brierley, J.A., 1993, Microbial deactivation of preg-robbing carbon in gold ore; *in* Torma, A.E., Wey, J.E., and Lakshmanan, V.I. (eds.), *Biohydrometallurgical Technologies*, v. 1, Bioleaching Processes: The Minerals, Metals and Materials Society, Warrendale, Pa., pp. 427–435.
- Lawrence, R.W., 1990, Biotreatment of gold ores; *in* Ehrlich, H.L., and Brierley, C.L. (eds.), *Microbial Mineral Recovery: McGraw-Hill Publishing Co.*, New York, pp. 127–148.
- Lawrence, R.W., and Bruynesteyn, A., 1983, Biological pre-oxidation to enhance gold and silver recovery from refractory pyritic ores and concentrates: *Canadian Institute of Metallurgy Bulletin*, v. 76, no. 857, pp. 107–110.
- Lawrence, R.W., and Gunn, J.D., 1985, Biological pre-oxidation of a pyrite gold concentrate; *in* Spisak, J.F., and Jergensen, G.V. (eds.), *Frontier Technology in Mineral Processing: Society of Mining Engineers of the American Institute of Mining, Metallurgical, and Petroleum Engineers, Inc.*, New York, pp. 13–17.
- Lawrence, R.W., and Marchant, P.B., 1988, Comparison of mesophilic and thermophilic oxidation systems for the treatment of refractory gold ores and concentrates; *in* Norris, P.R., and Kelly, D.P. (eds.), *Biohydrometallurgy: Science and Technology Letters*, Kew, Surrey, pp. 359–374.
- Lawson, E.N., Taylor, J.L., and Hulse, G.A., 1990, Biological pretreatment for the recovery of gold from slimes dams: *Journal of South African Institute of Mining and Metallurgy*, v. 90, pp. 45–49.
- Lazer, M.J., Southwood, M.J., and Southwood, A.J., 1986, The release of refractory gold from sulphide minerals during bacterial leaching; *in* Fivaz, C.E., and King, R.P. (eds.), *Gold 100, Extractive Metallurgy of Gold*, v. 2: South African Institute of Mining and Metallurgy, Johannesburg, pp. 287–297.
- Lindström, E.B., and Gunneriusson, L., 1990, Thermophilic bioleaching of arsenopyrite using *Sulfolobus* and a semicontinuous laboratory procedure: *Journal of Industrial Microbiology*, v. 5, pp. 375–382.
- Lindström, E.B., Gunneriusson, L., and Tuovinen, O.H., 1992, Bacterial oxidation of refractory sulfide ores for gold recovery: *Critical Reviews in Biotechnology*, v. 12, no. 1/2, pp. 133–155.
- Livesey-Goldblatt, E., 1986, Bacterial leaching of gold, uranium, pyrite

- bearing compacted mine tailing slimes; *in* Lawrence, R.W., Branion, R.M.R., and Ebner, H.G. (eds.), *Fundamental and Applied Biohydrometallurgy*: Elsevier, New York, pp. 89–96.
- Marais, H.J., 1990, Bacterial oxidation of arsenopyritic refractory gold ore—Barberton Mine's answer to pollution control; *in* *Innovations in Metallurgical Plant*: South African Institute of Mining and Metallurgy, Johannesburg, pp. 125–129.
- McCready, R.G.L., and Gould, W.D., 1990, Bioleaching of uranium; *in* Ehrlich, H.L., and Brierley, C.L. (eds.), *Microbial Mineral Recovery*: McGraw-Hill Publishing Co., New York, pp. 107–125.
- Mustin, C., de Donato, P., and Berthelin, J., 1992, Quantification of the intragranular porosity formed in bioleaching of pyrite by *Thiobacillus ferrooxidans*: *Biotechnology and Bioengineering*, v. 39, pp. 1121–1127.
- Nicholson, H.M., Smith, G.R., Stewart, R.J., Kock, F.W., and Marais, H.J., 1994, Design and commissioning of Ashanti's Sansu BIOX[®] plant; *in* *Biomine '94*: Australian Mineral Foundation, Glenside, South Australia, pp. 2.1–2.8.
- Norris, P.R., 1990, Acidophilic bacteria and their activity in mineral sulfide oxidation; *in* Ehrlich, H.L., and Brierley, C.L. (eds.), *Microbial Mineral Recovery*: McGraw-Hill Publishing Co., New York, pp. 3–27.
- Pinches, A., 1975, Bacterial leaching of an arsenic-bearing sulphide concentrate; *in* Burkin, A.R. (ed.), *Leaching and Reduction in Hydrometallurgy*: The Institute of Mining and Metallurgy, London, pp. 28–35.
- Pinches, A., Chapman, J.T., De Riele, W.A.M., and Van Staden, M., 1988, The performance of bacterial leach reactors for the preoxidation of refractory gold-bearing sulphide concentrates; *in* Norris, P.R., and Kelly, D.P. (eds.), *Biohydrometallurgy: Science and Technology Letters*, Kew, Surrey, pp. 329–344.
- Riley, R.P., Baguley, W., and Greenhalgh, L.P.H., 1990, Development of the VELMIX biooxidation reactor; *in* *Innovations in Metallurgical Plant*: South African Institute of Mining and Metallurgy, Johannesburg, pp. 131–140.
- Sitariski, J., Griffin, E.A., and Emmett, B., 1989, Bioleaching—Bioreactor design issues; *in* *Gold and Silver Recovery Innovations*: Randol International Ltd., Golden, Colo., pp. 145–147.
- Slabbert, W., Dew, D., Godfrey, M., Miller, D., and Van Aswegen, P., 1992, Commissioning of a BIOX[®] module at Sao Bento Mineracao; *in* *Randol Gold Forum Vancouver '92*: Randol International Ltd., Golden, Colo., pp. 447–452.
- Spencer, P.A., and Budden, J.R., 1990, Metallurgical considerations in the design of a biooxidation plant—A case study for a refractory arsenopyrite concentrate; *in* Gaskell, D.R. (ed.), *Extraction and Processing Division (EPD) Congress '90: The Minerals, Metals and Materials Society*, Warrendale, Pa., pp. 295–303.
- Spencer, P.A., Budden, J.R., and Barrett, J., 1991a, Pilot-plant biooxidation of gold-bearing arsenopyrite concentrates—*Transactions of the Institute of Mining and Metallurgy, Section C: Mineral Processes Extractive Metallurgy*, v. 100, pp. C21–C24.
- Spencer, P.A., Budden, J.R., and Rhodes, M.K., 1991b, Bacterial oxidation—An economic alternative for the treatment of refractory gold concentrates; *in* *World Gold '91: The Australasian Institute of Mining and Metallurgy*, Victoria, Australia, pp. 59–64.
- Torma, A.E., 1989, Present standing and future challenges in biohydrometallurgy; *in* Sastry, K.V.S., and Fuerstenau, M.C. (eds.), *Challenges in Mineral Processing*: Society of Mining Engineers, Inc., Littleton, Colo., pp. 550–563.
- Tuovinen, O.H., Kelley, B.C., and Groudev, S.N., 1991, Mixed cultures in biological leaching processes and mineral biotechnology; *in* Zeikus, J.G., and Johnson, E.A. (eds.), *Mixed Cultures in Biotechnology*: McGraw-Hill, New York, pp. 373–427.
- van Aswegen, P.C., Godfrey, M.W., Miller, D.M., and Haines, A.K., 1991, Developments and innovations in bacterial oxidation of refractory ores: *Society for Mining, Metallurgy, and Exploration*, Preprint no., 91–75.
- Wan, R.Y., LeVier, K.M., and Clayton, R.B., 1994, Hydrometallurgical process for the recovery of precious metal values from precious metal ores with thiosulfate lixiviant: U.S. Patent 5,345,359.
- Wan, R.Y., Luinstra, L., and Brierley, J.A., 1995, Gold recovery from refractory sulfidic-carbonaceous ore, Part II. Thiourea leaching following biooxidation-heap pretreatment; *in* Warren, G.W. (ed.), *Extraction and Processing Division (EPD) Congress 1995: The Minerals, Metals and Materials Society*, Warrendale, Pa., pp. 165–173.
- Wu, R., Tsui, L.B., Krebs-Yuill, B.A., Milligan, D.A., Troncoso, N.J., McBride, J.S., and Knecht, A.T., 1988, Treating manganese-containing ores with a metal sulfide: U.S. Patent 4,752,332.
- Zimmerley, S.R., Wilson, D.G., and Prater, J.D., 1958, Cyclic leaching process employing iron oxidizing bacteria: U.S. Patent 2,829,964.

Chapter 29

DETERMINATION OF THE SOURCE AND PATHWAY OF CYANIDE-BEARING MINE WATER SEEPAGE

L.H. Filipek

5061 Indiana Street, Golden, CO 80403-1743

INTRODUCTION

All human activities, including mining, carry risks. The role of the environmental consultant in mining is to help design environmentally sound mining approaches and facilities, and also to solve problems quickly and effectively when something doesn't work exactly as planned. This chapter shows an example of the type of geochemical problem that can be addressed within a very short time frame using simple, inexpensive geochemical tools. The name of the mine site is not given at the request of the mine owner.

THE SITE AND THE PROBLEM

The site is a gold mining operation in Nevada at an elevation of about 5500 feet above mean sea level. The area has an arid to semi-arid temperate climate, in which most of the precipitation occurs as snowfall. At the site, gold is extracted with cyanide in a mill. The mill waste, or tailing, is deposited in a drained tailing storage facility, shown on Figure 29.1.

In 1990, two areas of seepage containing measurable cyanide concentrations were discovered bordering the tailing facility (Fig. 29.1). One seep, referred to as the lower seep, was east of the underdrainage collection pond; the other, referred to as the upper seep, was southwest of the toe of the tailing impoundment embankment (tailing dam). Based on initial test-pit observations, the seepage appeared to be traveling through the embankment fill and along the fill/subsoil contact.

The source(s) of the seepage needed to be determined in order to stop them. Three hypotheses were developed regarding the source(s). One possible source was an excess of water in the supernatant pond ("tailing pond") of the tailing facility; another was a failure of the underdrainage system from the facility. A third, less likely source was water traveling from a neighboring tailing facility through a highly permeable tuffaceous ash layer. Geophysical, geochemical, trenching, and boring investigations were conducted to determine the source of the seepage and the capacity of the intercepted soils to chemically attenuate the seepage. This chapter presents the results of the geochemical investigation.

In this investigation, the potential source waters and the four soil types in the vicinity of the seeps were characterized geochemically. The waters and soils were then subjected to a series of sequential-batch soil-attenuation tests to investigate the attenuation capacities of each soil type for cyanide and metals and to develop a "fingerprint" of the effect of each soil type on water chemistry. Piper trilinear plots and Stiff diagrams were used to

interpret water types; HC-GRAM, a computerized geochemical mixing model (McIntosh, 1990), was used to investigate potential interaction of different water types. The batch tests and analyses were conducted at Core Laboratories, Aurora, Colorado.

BACKGROUND

Cyanide geochemistry

Cyanide complexation with gold and silver is presently the most common method of extracting low concentrations of these elements from rock. The cyanide anion, CN^- , can form a large number of inorganic and organic complexes. The complexes most likely to occur in mill tailing solutions include free cyanide, simple cyanide compounds, and complex alkali-metal cyanides. (These complexes are discussed in detail in Huiatt, 1984, and are only summarized here.) The simplest of these is hydrogen cyanide (HCN), commonly called "free cyanide." The stability of this complex in solution is pH-dependent. At a pH of less than about 9.4, free cyanide exists mainly as HCN, a dissolved gas that can easily volatilize. Above this pH, it exists as the anion CN^- (e.g., Fuller, 1984). To reduce cyanide losses due to volatilization, cyanide milling or leach solutions are always basic, typically with a pH greater than 10.

The next simplest set of cyanide compounds are simple cyanides, with a formula $\text{A}(\text{CN})_x$, where A is an alkali or metal and x is the number of cyanide groups. Alkali cyanides ionize easily to release CN^- . The simple metal cyanides are less soluble than free cyanide.

Complex alkali-metal cyanides have the formula $\text{A}_y\text{M}(\text{CN})_x$, where A is an alkali, M is a heavy metal, y is the number of alkali ions, and x is the number of cyanide groups. The typical metals are ferric and ferrous iron, cadmium, copper, zinc, nickel, cobalt, silver, and gold. Soluble complex cyanides dissociate into the complex ion $\text{M}(\text{CN})_x$, rather than the CN group. Each of these metal complex ions has a different relative stability, ranging from weak, through moderately strong, to strong. Iron, cobalt, and gold produce some of the strongest complexes, which are extremely stable. The weak complexes are easily dissociated in mild acid solutions. Some states have set standards based on these weak cyanide complexes and analytical schemes have been developed specifically to measure weak acid dissociable (WAD) cyanide.

Polythionates and polysulfides produced by oxidation of sulfide minerals in ore can react with free cyanide to form thiocyanate, SCN^- , which is not considered toxic. Cyanides can also

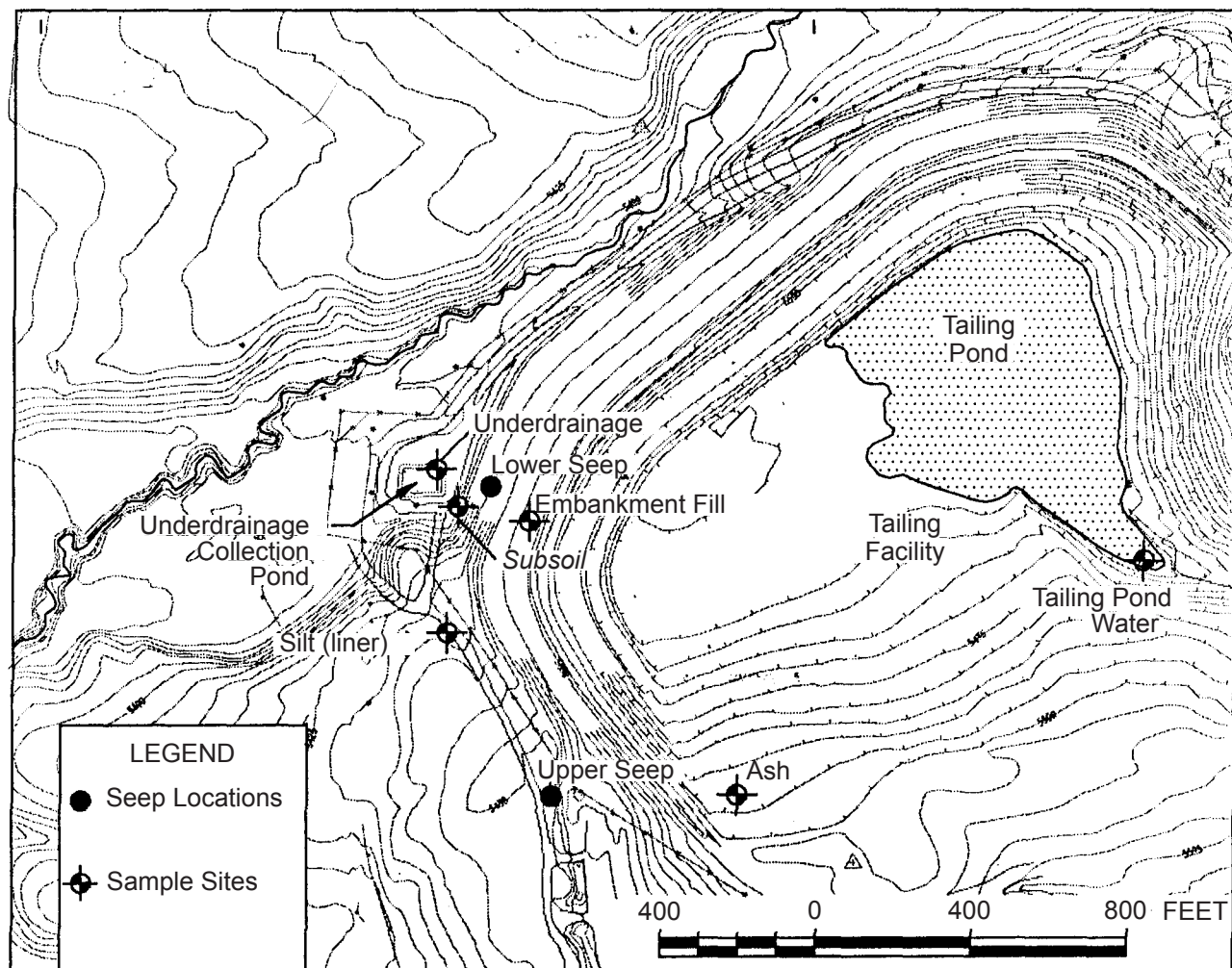


FIGURE 29.1—Layout of tailing facility, including seeps and sample sites for water and soils. Contour interval is 5 feet (1.5 m).

degrade naturally by bacterial mediation to carbon dioxide and ammonia. The ammonia can react, through denitrification processes, to nitrate, nitrite, and nitrogen gas (e.g., Fuller, 1984).

Attenuation capacities of soils

Most soils have the ability to react with the fluids that move through them. They do so by a number of mechanisms, including ion exchange, adsorption, precipitation, hydrolysis, volatilization, and biological reactions. Many of these mechanisms tend to “attenuate” (remove from solution) trace substances such as heavy metals or cyanide. The effectiveness of any of these mechanisms depends on the geochemical characteristics of both the soil and the water moving through it, as well as on physical factors such as climate and degree of soil saturation.

The attenuation capacity of a soil or other solid material for a particular constituent is defined as the maximum weight of that constituent removed from solution per unit weight of the material. In the most common situation, attenuation of a dissolved constituent by a soil is due to adsorption and ion exchange.

Attenuation tends to follow certain rules (e.g., Fuller et al., 1980). For example, at a given solution pH and constant concentration of all other ions, the mass-action law requires that the attenuation capacity of a soil for a given ionic constituent will increase as the concentration of that constituent in solution increases. At a given concentration of a constituent in solution and a constant pH, the total attenuation capacity of a soil for that constituent will increase with decreasing concentrations of competing ions. (Competing ions are those ions whose charge is of the same sign as the constituent of interest, i.e., cations compete with cations and anions compete with anions.) As the pH of the solution changes, the attenuation capacity of a particular soil for a given constituent changes. Typically, as the pH increases, the attenuation capacity increases for ions and decreases for anions.

Methods to determine attenuation capacities

Changes due to attenuation can be simulated in the laboratory through column leach tests or sequential batch tests (SBT's). The column leach test typically entails adding a solution to the top (or

bottom) of a tube or column filled with soil or rock pieces and collecting the solution that exits at the other end of the column. The column test is typically run until several "pore volumes" of solution have been flushed through the column (Fuller, 1982).

A pore volume is defined as the amount of solution necessary to fill all of the interstitial void spaces of a given volume of soil or rock, for example, an entire column. It is a function of the porosity of the soil or rock. Porosity is the ratio of the void volume to the total volume of a soil or rock in situ. Thus, the amount of solution in a pore volume for a high porosity soil or rock will be greater than the amount of solution in a pore volume for a low porosity rock. The permeability of the soil or rock affects the time it takes to run a column test. If the permeability is low, one pore volume of solution may require several weeks to traverse the column.

Many pore volumes of fresh solution may be run through the same column of soil or rock to test the changes in its ability to leach or attenuate elements over continued exposure. At the other extreme, the same solution may be recirculated through the same column many times until the solution reaches a constant concentration of the constituent of interest. In either case, the test can take several months to more than a year to be completed.

In a batch test, solution and soil or rock pieces are put into a container at a predetermined ratio by weight. The container is shaken or rolled to increase contact between the solution and the solid. In a bottle-roll test, the container is typically a 5 gallon bot-

tle that is laid on its side and rolled mechanically. In a typical batch test, the stirring, shaking, or rolling is continued until the solution reaches a constant concentration of the constituent of interest. The water:rock volume ratio used in the batch test can be converted to an equivalent pore volume if the in situ porosity of soil (or rock) is known. The effects of permeability are removed, so the duration of the test is a function only of reaction rate. The test can take as little as a few hours if sorption processes control the constituent's concentration.

A sequential batch test (SBT) is a series of batch tests. The series may use the same soil (or rock) sample with a succession of fresh solutions to simulate successively more pore volumes, or it may use the same solution on a succession of fresh soil samples to simulate successively fewer pore volumes. The results of a sequential batch test can mimic the results of a column leach test in a fraction of the time if sorption and rapid dissolution processes control the behavior of a constituent (Houle and Long, 1980; Rouse and Pyrih, 1988).

A schematic of a typical SBT procedure is presented on Figure 29.2. An aliquot of solution is advanced through successive batches of soil from left to right on the diagram. Solution A1 represents the initial contact of soil and solution. In A2, fresh soil is exposed to solution that has previously been in contact with soil. Similarly, a given batch of soil is subjected to successive doses of solution from top to bottom on Figure 29.2.

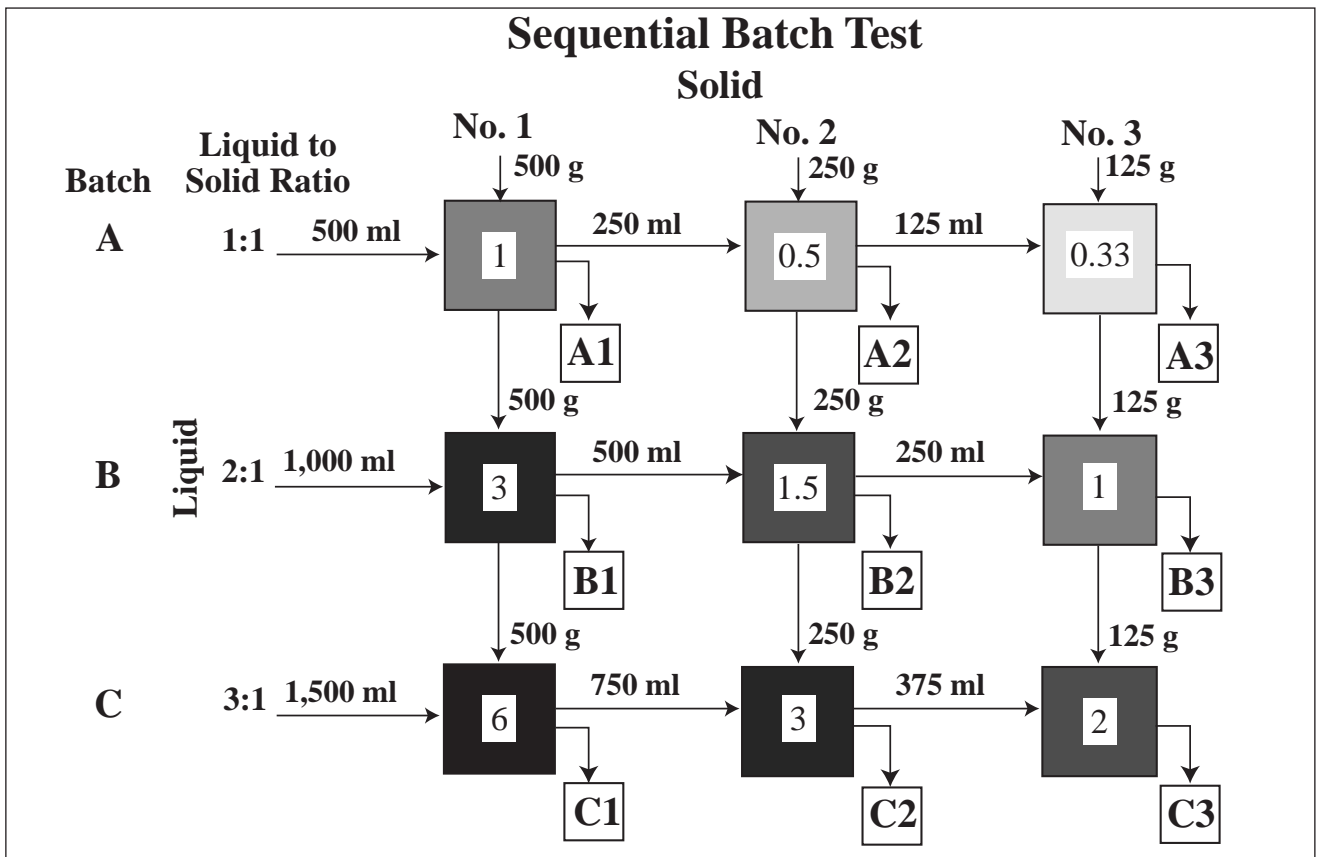


FIGURE 29.2—Schematic of Sequential Batch Test showing equivalent liquid:solid ratios for solutions from each step. Shading is explained in text.

The effective liquid:solid ratios for each batch are given in the shaded boxes on Figure 29.2. The intensity of shading in the boxes corresponds to the liquid:solid ratio. The lighter the shading, the lower the effective liquid:solid ratio, the less the exposure of soil to solution, and thus the greater the attenuation of constituents from solution. The darker the shading, the greater effective liquid:solid ratio, the greater the exposure of soil to solution, and thus the lower the capacity of the soil to attenuate additional solution.

Thus, batch A3, with an effective liquid:solid ratio of 0.33, would be expected to show the greatest attenuation compared to the original solution because the solution in A3 has already been exposed to a large volume of solid. Batch A3 therefore represents what might be expected in fresh soil or rock far from the source of a seepage. Batch C1, with an effective liquid:solid ratio of 6, would be expected to produce the least attenuation of the test batches, because it has already been exposed to a large volume of solution. It represents what might be expected for soil or rock close to a seepage source after significant exposure to the solution.

A three-by-three matrix including nine sets of tests is shown on Figure 29.2. This set of tests allows a reasonable range of pore volumes to be tested and also supplies a measure of redundancy for quality control purposes. Two sets of batches represent the same nominal number of liquid:solid ratios (or pore volumes): batches A1 and B3 both represent a liquid:solid ratio of 1, whereas batches B1 and C2 both represent a liquid:solid ratio of 3. Differences in the results for these two pairs help set boundaries for the accuracy of the results. For cost savings, sometimes six sets of tests are conducted that include only A1, A2, A3, B1, B2, and C1.

METHODS

Sample selection

The location of the seeps adjacent to the tailing facility implicated either the tailing pond or the underdrainage from the facility as the source of the seepage. Based on initial test pit observations, the seepage appeared to be traveling through the embankment fill of the tailing facility and along the fill/subsoil contact.

Water samples were collected from the upper and lower seeps, the tailing pond, and the underdrainage pond (Fig. 29.1). In order to investigate temporal variability, water samples from the seeps and the tailing pond were collected first in August and again in October.

Field observations of the seeps and test pits suggested that four major soil/rock types might have come in contact with the seepage:

- 1) Embankment fill, which is a silty sand and gravelly mine waste;
- 2) subsoil underlying the facility, which is a low-organic, low-carbonate silty sand;
- 3) ash, which is a high-permeability fine tuffaceous sandstone; and
- 4) silt liner, which is a local low-permeability silty material.

Each of these soil/rock types was collected for characterization and subsequent sequential batch testing.

Geochemical characterization

Water samples were collected and analyzed for pH, conductivity, major ions, metals, total and WAD cyanide, thiocyanate, and nitrate nitrogen. The waters were filtered through a 0.45 micron

filter before analysis, so the analyses represent dissolved constituents.

All water samples were preserved according to EPA guidelines: samples collected for metals were preserved with nitric acid, those collected for nitrate nitrogen were preserved with sulfuric acid, and those collected for cyanide were preserved with sodium hydroxide. All samples were analyzed within the appropriate holding times.

Soil/rock samples were collected and analyzed for metals, paste pH, WAD cyanide, acid (HCl) soluble iron and manganese, carbonate content and base neutralization potential, cation exchange capacity and exchangeable cations, and organic carbon. Acid soluble iron and manganese gives an approximation of the amount of hydrous iron and manganese oxides. In addition, texture (percent sand, silt, and clay) and moisture were determined. Porosities of the soils/rocks were previously determined by Knight Piésold and Co. to range from about 20% for the embankment fill to 45% for the ash.

Sequential batch test procedures

The tailing pond water and the underdrainage water collected on 23 August 1990 (Table 29.1) were used for the SBT's, along with the four soil/rock types listed in Table 29.2, for a total of eight sets of tests. The waters were kept refrigerated prior to use. The soils/rocks were sieved to minus 10 mesh because the smaller particles were expected to be more reactive in that they have greater surface area per unit mass.

The SBT procedure used for this study involved placing weighed amounts of soil/rock into polyethylene bottles and adding measured volumes of liquid in the ratios and amounts shown on Figure 29.3. The volume of the bottles was large compared with the combined volume of liquid and solid, so abundant air space existed in the bottles during the tests. The resultant mixtures were rolled for 24 hours, then filtered. Half of the resultant solution was added to the next batch of soil/rock from left to right in the diagram. The remaining solution was set aside for analysis. The filtered soil/rock was then returned to the bottle. The next aliquot (moving from top to bottom on the diagram) of liquid was added and the procedure was repeated.

Each large box on Figure 29.3 shows the equivalent pore volume for each soil/rock type assuming the porosities and specific gravities for the soils/rocks given in Table 29.2. In the boxes, "A" is the number of pore volumes for ash, "S" the number of pore volumes for silt liner and subsoil material, both of which have the same porosity, and "E" the number for embankment fill. The lower the porosity of the soil/rock used in these tests, the higher the number of pore volumes represented. For example, leachate solution A3, which has a liquid:solid ratio of 0.33 (Fig. 29.2), is equivalent to 0.9 pore volumes of seepage throughput for the high-porosity ash and 3.5 pore volumes for the low-porosity embankment fill. Solution C1, which has a liquid:solid ratio of 6 (Fig. 29.2), is equivalent to about 16 pore volumes of seepage throughput for the ash to 62 pore volumes for the embankment fill.

Each of the leachate solutions was analyzed for pH, conductivity, WAD cyanide, arsenic, cadmium, zinc, and copper. All tests were conducted by Core Laboratories and all constituents were analyzed by Core Laboratories in accordance with their quality assurance program.

TABLE 29.1—Water chemistry of seeps, tailing pond and underdrain¹.

	Lower Seep		Upper Seep		Tailing Pond		Reclaim	Slurry	Underdrain	
	8/14/90	10/15/90	8/14/90	10/15/90	8/14/90	8/23/90	10/15/90	10/15/90	8/14/90	8/23/90
Alkalinity (Total)	350	340	216	220	113		113	189	92	
Bicarbonate	440	410	264	268	<5	<5	<5	<5	99	101
Carbonate	<1	<1	<1	<1	58	49	56	76	6	6
Chloride	131	110	123	105	136	126	30	23	48	42
Conductivity	1740	1780	1430	1510	1060	1310	1370	1470	811	836
Cyanide (Total)	0.82		5.11		26.2	31.1			16.8	14.6
Cyanide (WAD)	0.06	0.25	2.14	0.88	23.7	25.7	42.2	61.9	8.5	7.11
Thiocyanate	<0.1	<0.1	0.1	0.1	19.6	35.6	27.8	29.4	11.0	9.6
Hydroxide	<1		<1		6				<1	
Nitrogen (Nitrate)	37.3	35.8	24.5	20.1	2.8		9.2	3.2	3.6	
pH	7.7	7.71	8.17	8.11	10.16	10.03	10.11	10.46	8.48	8.77
Sulfate	336	318	263	341	263	470	344	342	180	187
Aluminum	<0.05	<0.05	<0.05	<0.05	<0.05	<0.05	<0.05	<0.05	<0.05	<0.05
Antimony	<0.1	<0.1	<0.1	<0.1	0.3	0.3	0.1	0.2	<0.1	0.1
Arsenic	<0.05	0.06	0.06	0.06	2.61	2.22	1.07	1.21	2.18	2.40
Barium	0.10	0.09	0.14	0.12	0.02	0.03	0.04	0.03	0.09	0.09
Beryllium	<0.005	<0.005	<0.005	<0.005	<0.005	<0.005	<0.005	<0.005	<0.005	<0.005
Boron	0.37	0.37	0.22	0.35	0.06	0.12	0.11	0.12	0.07	0.11
Cadmium	<0.005	<0.005	<0.005	<0.005	0.018	0.026	0.047	0.046	0.017	0.011
Calcium	232	235	170	192	95	126	146	160	46	50.0
Chromium	<0.01	<0.01	0.01	<0.01	<0.01	<0.01	<0.01	<0.01	<0.01	<0.01
Cobalt	0.07	0.09	0.20	0.28	0.19	0.32	0.09	0.39	0.22	0.24
Copper	0.01	<0.01	<0.01	<0.01	2.95	2.32	6.15	11.5	0.13	0.09
Iron	0.31	0.23	1.16	1.70	0.03	0.20	0.14	3.58	0.43	0.51
Lead	<0.05	<0.05	<0.05	<0.05	<0.05	<0.05	<0.05	<0.05	<0.05	<0.05
Magnesium	55	55.3	32	37.3	0.40	0.43	0.74	0.14	7.98	8.01
Manganese	0.07	<0.01	0.05	0.02	<0.01	<0.01	<0.01	<0.01	0.06	0.06
Molybdenum	<0.05	<0.05	<0.05	<0.05	0.31	0.40	0.52	0.50	0.30	0.34
Nickel	<0.04	<0.04	<0.04	<0.04	0.72	0.73	0.33	0.35	0.22	0.22
Potassium	5	<5	10	9	16	22	22	22	9	9
Selenium	<0.1	<0.1	<0.1	0.1	0.5	1.0	0.4	0.4	0.4	0.4
Silver	<0.01	<0.01	<0.01	<0.01	<0.01	<0.01	<0.01	0.02	<0.01	<0.01
Sodium	116	109	88	115	126	176	168	165	103	99
Strontium	1.19	1.19	0.75	0.88	0.22	0.29	0.36	0.36	0.34	0.34
Vanadium	<0.05	<0.05	<0.05	<0.05	0.13	0.16	0.12	0.14	0.10	0.10
Zinc	<0.01	<0.01	<0.01	<0.01	0.55	1.40	2.30	2.28	<0.01	0.01

¹Concentrations in mg/l, except for pH (in pH units) and conductivity (in mmhos/cm)

TABLE 29.2—Physical and geochemical properties of soil types potentially intercepting seepage.

	Embankment fill	Subsoil	Silt	Ash
pH (on 1:1 Paste)	8.13	7.64	8.1	8.19
Texture (%)				
Sand	55.9	66.1	50.2	38.0
Silt	24.1	27.3	45.8	60.0
Clay	20.0	6.6	4.0	2.0
Porosity ¹	0.2	0.41	0.41	0.48
Specific Gravity* (g/cm ³)	2.7	2.6	2.6	2.47
HCl Soluble Cation (%)				
Iron	0.3	1.07	0.33	0.11
Manganese	0.02	0.04	0.01	<.01
Carbonate Content (%) (as CaCO ₃)	1.6	0.2	0.1	<.1
Base Neutralization Potential (meq/kg)	<5.0	<5.0	<5.0	<5.00

TABLE 29.2—Continued

	Embankment fill	Subsoil	Silt	Ash
Cation Exchange Capacity (meq/100 g)	30.6	15.2	59.8	2.72
Exchangeable Cation (meq/100 g)				
Calcium	37.4	10.0	27.7	1.31
Magnesium	6.15	4.0	9.86	0.4
Sodium	1.61	0.13	3.05	0.21
Potassium	0.52	1.08	0.88	0.12
Moisture (Air Dried) (%)	2.0	2.3	7.9	1.3
Organic Carbon (Walkley Black) (%)	1.23	0.7	1.17	1.15

*Ash measured; others estimated

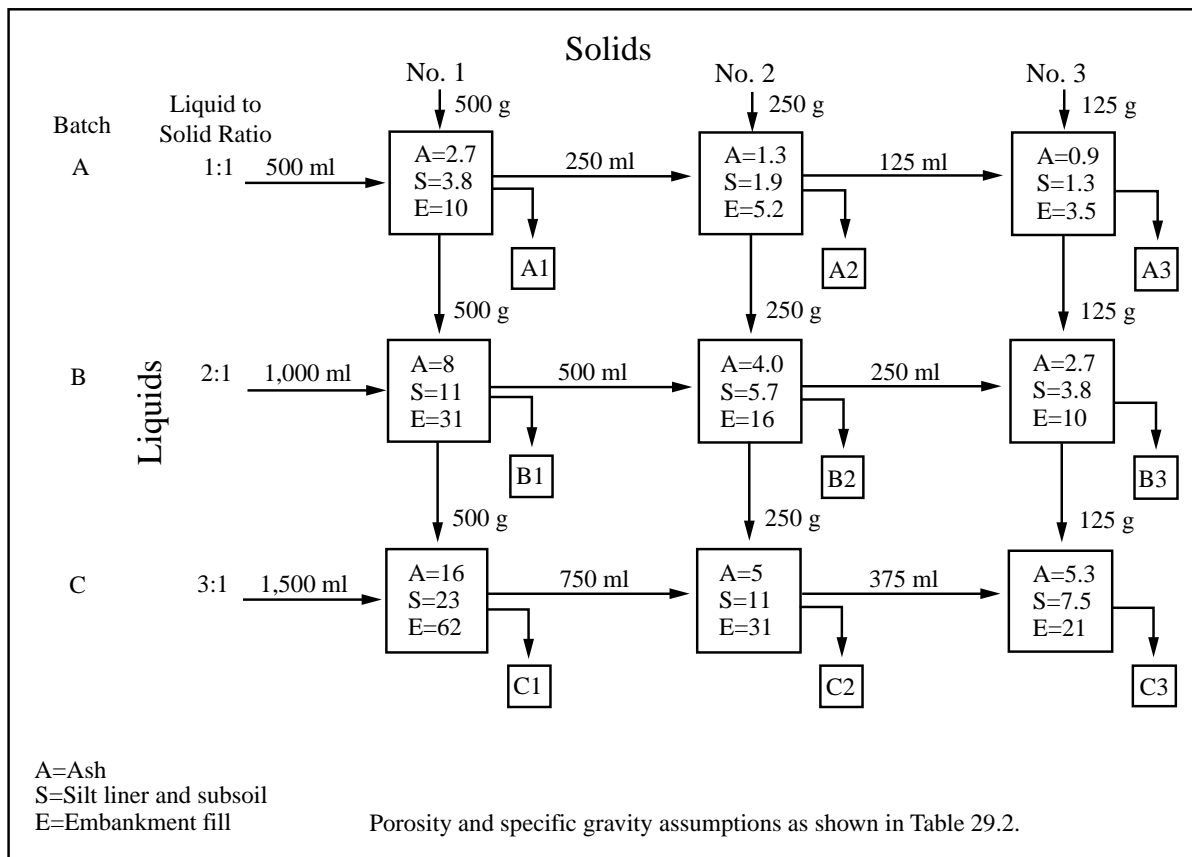


FIGURE 29.3—Schematic of Sequential Batch Test showing pore volume equivalents for solutions for each step for each of the soil/rock types investigated.

RESULTS

Geochemical characterization

The chemical compositions of the upper and lower seeps, the tailing pond water, and the underdrainage water are listed in Table 29.1. The underdrainage water has lower pH and lower concentrations of almost all other constituents than the present tailing pond water, probably because the underdrainage is supernatant that has been substantially diluted by precipitation that falls on the part of the tailing facility contributing to the underdrainage system.

The upper seep has higher pH, higher concentrations of cyanide, and lower concentrations of nitrate, alkalinity, bicarbonate, calcium, and magnesium than the lower seep. Both seeps have higher nitrate, alkalinity, bicarbonate, magnesium, and calcium and lower pH, cyanide, and thiocyanate concentrations than either the tailing pond or the underdrainage water.

The major geochemical characteristics of the soil types through which the seepage may have flowed are listed in Table 29.2. All the soils are slightly alkaline. All have low carbonate content, low base neutralization potential, and relatively low organic carbon content. The silt liner material and the embankment fill have the highest cation exchange capacity. The subsoil has the highest hydrous iron oxide content.

Sequential batch tests

Table 29.3 gives the results of the SBT's for the four soils using tailing pond water and Table 29.4 gives the results using underdrainage. Figures 29.4a through 29.4g show the results as a function of pore volume for the four soils using tailing pond water. The underdrainage results are similar to the tailing pond results, but with generally lower initial concentrations.

Tables 29.5 and 29.6 summarize the capacities of the soils to attenuate constituents of concern from the tailing pond water (Table 29.5) and underdrainage (Table 29.6), respectively. In the tables, the initial concentration is the value from Table 29.1 for fresh unreacted tailing pond water or underdrainage. The minimum concentration given on each table is the lowest concentration for that constituent reported within a test sequence. The lowest concentration is most commonly in the A3 solution, because this batch had the lowest liquid:solid ratio and thus the most adsorption sites per unit volume of solution.

The total amount of a constituent attenuated by a given weight of sample during the course of a test was calculated. The calculation consisted of summing the amount of the constituent that was removed from the solution during contact A1, B1, and C1. The results are reported as milligrams (mg) of constituent attenuated per kilogram (kg) of soil (mg/kg) after the method of Houle and Long (1980).

TABLE 29.3—Leachate analyses from sequential batch test using tailing pond water.

Batch number	A1	A2	A3	B1	B2	B3	C1	C2	C3
Embankment fill									
Pore Volumes (approx.)	10	5.2	3.5	31	16	10	62	31	21
Conductivity (mmhos/cm)	1230	1160	1200	1230	1290	1350	1290	1310	1280
Cyanide, WAD (Filt.)	17.2	11.2	7.67	21.1	16.1	13.3	27.1	17.6	14.7
pH (Units)	8.28	8.24	8.07	8.52	8.42	7.86	9.27	8.77	7.92
Arsenic, Diss. (mg/l)	0.70	0.32	0.25	1.51	0.77	0.37	2.14	1.36	0.74
Cadmium, Diss. (mg/l)	0.009	<0.005	<0.005	0.036	0.008	<0.005	0.035	0.025	0.006
Copper, Diss. (mg/l)	4.04	3.35	5.45	2.75	3.22	3.31	2.73	4.93	2.85
Zinc, Diss. (mg/l)	0.13	0.02	0.01	0.91	0.09	0.02	1.49	0.48	0.04
Subsoil									
Pore Volumes (approx.)	3.8	1.9	1.3	11	5.7	3.8	23	11	7.5
Conductivity (mmhos/cm)	1300	1410	1350	1420	1480	1430	1410	1370	1340
Cyanide, WAD (Filt.)	18.4	11.0	8.44	20.2	16.9	13.8	21.8	17.9	14.9
pH (Units)	8.07	7.97	8.16	8.40	8.11	8.01	8.81	8.17	7.88
Arsenic, Diss. (mg/l)	0.44	0.07	0.05	1.23	0.45	0.17	1.64	0.96	0.50
Cadmium, Diss. (mg/l)	0.009	0.005	0.005	0.031	0.009	0.006	0.051	0.018	0.010
Copper, Dis. (mg/l)	6.15	4.81	1.80	3.94	6.25	7.35	2.79	4.06	3.81
Zinc, Diss. (mg/l)	0.04	0.02	0.01	0.53	0.03	0.02	1.25	0.19	0.02
Silt Linear Material									
Pore Volumes (approx.)	3.8	1.9	1.3	11	5.7	3.8	23	11	7.5
Conductivity (mmhos/cm)	1330	1210	1180	1280	1230	1260	1250	1260	1310
Cyanide, WAD (Filt.)	13.6	6.16	3.33	19.7	14.5	10.1	20.2	18.6	12.8
pH (Units)	7.55	7.49	8.06	8.32	7.80	7.95	8.44	7.99	7.82
Arsenic, Diss. (mg/l)	0.71	0.16	0.09	1.48	0.66	0.27	2.05	1.40	0.77
Cadmium, Diss. (mg/l)	<0.005	<0.005	<0.005	0.015	<0.005	<0.005	0.025	0.014	<0.005
Copper, Dis. (mg/l)	3.71	2.07	0.41	2.36	2.38	2.34	4.06	2.45	2.64
Zinc, Diss. (mg/l)	0.02	<0.01	<0.01	0.18	<0.01	<0.01	0.62	0.05	0.01
Ash									
Pore Volumes (approx.)	2.7	1.3	0.9	8	4	2.7	16	8	5.3
Conductivity (mmhos/cm)	1280	1450	1410	1290	1340	1400	1310	1320	1350
Cyanide, WAD (Filt.)	16.3	10.7	8.5	22.6	17.2	12.5	25.7	18.9	16.3
pH (Units)	8.07	8.50	8.08	8.63	8.19	7.63	8.93	8.43	7.99
Arsenic, Diss. (mg/l)	1.48	1.07	0.99	1.94	1.78	1.60	2.00	1.89	1.72
Cadmium, Diss. (mg/l)	0.020	0.005	<0.005	0.029	0.027	0.012	0.025	0.039	0.029
Copper, Dis. (mg/l)	4.52	6.66	3.66	2.42	4.02	3.46	2.61	3.50	2.64
Zinc, Diss. (mg/l)	0.56	0.07	0.03	1.26	0.54	0.08	1.42	1.38	0.57

pH

The initial pH of the tailing pond water was 10.0. In all cases the final pH was less than the original pH (Table 29.3 and Fig. 29.4a), indicating that the soils were able to neutralize a portion of the tailing solution. The silt liner material tended to be the most effective in lowering the solution pH.

The initial pH of the underdrainage was 8.8. The final pH values from the SBT's using underdrainage tended to remain within the range of 7.9 to 8.8 (Table 29.4). The silt liner material again tended to be most effective in lowering the initial pH of the underdrainage. However, the final pH values in this test are actually somewhat higher than for the tailing solution (Fig. 29.4a).

For comparison, the pH values of the upper and lower seep are 8.1 and 7.7, respectively (Table 29.1). From the SBT results on pH, therefore, either the tailing pond or the underdrain could be the source of the seepage.

Tables 29.5 and 29.6 summarize the capacities of the soils to attenuate WAD cyanide. The results indicate that all the soils were able to attenuate the cyanide. For the tailing pond water, the silt liner material proved to have the highest attenuation capacity (40.6

mg/kg); the ash had the lowest (13.6 mg/kg). With the lower initial pH and cyanide content of the underdrainage, the attenuation capacities of most of the soils decreased slightly. That of the silt decreased to about one-fourth of its capacity with the tailing pond water.

Comparison of the SBT WAD cyanide results (Fig. 29.4b) with the seepage chemistry (Table 29.1) shows lower WAD cyanide in either seep than in any of the SBT's.

Conductivity

Conductivity is an effective way to estimate the total amount of dissolved solids in a solution. The SBT conductivity results for both the tailing pond solution (Table 29.3 and Fig. 29.4c) and for the underdrainage (Table 29.4) showed little variation, especially for the underdrainage. It appears that the embankment fill and the silt liner decreased the conductivity of the tailing pond solution slightly, whereas the subsoil and the ash increased it slightly.

Comparison of the conductivity values of the seeps, tailing pond water, and underdrainage (Table 29.1) shows that conductiv-

TABLE 29.4—Leachate analyses from sequential batch test using underdrainage.

Batch number	A1	A2	A3	B1	B2	B3	C1	C2	C3
Embankment fill									
Pore Volumes (approx.)	10	5.2	3.5	31	16	10	62	31	21
Conductivity (mmhos/cm)	800	780	800	810	870	820	840	860	850
Cyanide, WAD (Filt.)	4.86	4.07	3.34	4.57	4.92	4.39	3.67	4.59	4.63
pH (Units)	8.33	8.39	8.37	8.56	8.36	8.69	8.79	8.75	8.31
Arsenic, Diss. (mg/l)	0.91	0.48	0.35	1.90	1.31	0.79	2.30	1.90	1.37
Cadmium, Diss. (mg/l)	<0.005	<0.005	<0.005	<0.005	<0.005	<0.005	0.006	<0.005	<0.005
Copper, Diss. (mg/l)	1.25	1.04	0.69	0.52	1.84	1.10	1.08	0.50	1.14
Zinc, Diss. (mg/l)	0.01	<0.01	<0.01	<0.01	<0.01	<0.01	<0.01	<0.01	<0.01
Subsoil									
Pore Volumes (approx.)	3.8	1.9	1.3	11	5.7	3.8	23	11	7.5
Conductivity (mmhos/cm)	830	900	890	890	880	900	890	900	830
Cyanide, WAD (Filt.)	3.20	2.40	2.00	3.16	2.52	2.32	2.83	2.67	2.52
pH (Units)	8.22	8.14	7.92	8.28	8.26	8.21	8.50	8.23	8.30
Arsenic, Diss. (mg/l)	0.56	0.09	<0.05	1.36	0.52	0.16	1.87	1.22	0.64
Cadmium, Diss. (mg/l)	0.007	<0.005	<0.005	0.008	0.006	<0.005	0.006	<0.005	0.005
Copper, Diss. (mg/l)	0.46	0.04	0.02	1.08	0.59	0.09	0.82	0.99	0.49
Zinc, Diss. (mg/l)	0.01	0.01	0.01	<0.01	<0.01	<0.01	<0.01	<0.01	<0.01
Silt Linear Material									
Pore Volumes (approx.)	3.8	1.9	1.3	11	5.7	3.8	23	11	7.5
Conductivity (mmhos/cm)	870	790	840	810	790	830	800	770	850
Cyanide, WAD (Filt.)	4.59	2.34	1.37	6.14	4.85	2.84	5.28	5.43	4.01
pH (Units)	7.98	7.95	8.02	8.23	8.19	8.07	8.30	8.02	8.19
Arsenic, Diss. (mg/l)	0.87	0.24	0.07	1.64	0.91	0.47	2.04	1.76	1.16
Cadmium, Diss. (mg/l)	<0.005	<0.005	<0.005	<0.005	<0.005	<0.005	<0.005	<0.005	<0.005
Copper, Diss. (mg/l)	0.25	0.05	0.01	0.58	0.90	0.33	0.48	0.93	0.87
Zinc, Diss. (mg/l)	<0.01	<0.01	<0.01	<0.01	<0.01	<0.01	<0.01	<0.01	<0.01
Ash									
Pore Volumes (approx.)	2.7	1.3	0.9	8	4	2.7	16	8	5.3
Conductivity (mmhos/cm)	856	868	885	848	876	843	860	867	849
Cyanide, WAD (Filt.)	5.48	3.97	3.36	4.87	4.38	4.21	4.61	4.40	4.10
pH (Units)	8.23	8.36	8.13	8.39	8.30	8.37	8.64	8.42	8.33
Arsenic, Diss. (mg/l)	1.82	1.43	1.16	2.15	1.99	1.77	2.11	2.20	2.00
Cadmium, Diss. (mg/l)	<0.005	<0.005	<0.005	<0.005	<0.005	<0.005	<0.005	<0.005	0.007
Copper, Diss. (mg/l)	2.87	2.31	1.65	1.24	2.61	2.07	0.70	1.43	2.33
Zinc, Diss. (mg/l)	<0.01	<0.01	<0.01	<0.01	<0.01	<0.01	<0.01	<0.01	0.01

ity in the tailing pond water varies over time, but is similar to the conductivity of the seeps. The underdrainage conductivity is lower than that in the tailing pond or the seeps.

Arsenic

All of the tested soils attenuated arsenic (Tables 29.3 and 29.4, Fig. 29.4d). In no case was attenuation ability exhausted, even after the many pore volumes represented by batch C (Tables 29.5 and 29.6). The subsoil showed the highest attenuation capacity for arsenic, whereas the ash showed the least. The arsenic concentrations in the seeps are near or below the lower detection limit of 0.05 mg/l.

Cadmium and zinc

Cadmium and zinc usually display similar geochemical behavior. Therefore, they are discussed together. All of the tested soils

attenuated cadmium and zinc (Tables 29.3 and 29.4, Figs. 29.4e and 29.4f). The silt liner had the highest attenuation capacity for both metals. In tests using tailing pond water, the attenuation ability was actually exhausted for cadmium by batch B (3:1 liquid:solid ratio) for all soil types except the silt liner material. The seeps had low (less than the lower limit of detection) for both metals.

Copper

Unlike the results for the other metals, copper was not attenuated, but actually leached in the first and most batches of all tests using tailing pond water (Fig. 29.4g). This leaching is probably due to formation of soluble copper cyanide complexes. The silt liner material showed some attenuation capacity as the chemistry of the solution changed at the lowest pore volume or liquid:solid ratios (Fig. 29.4g).

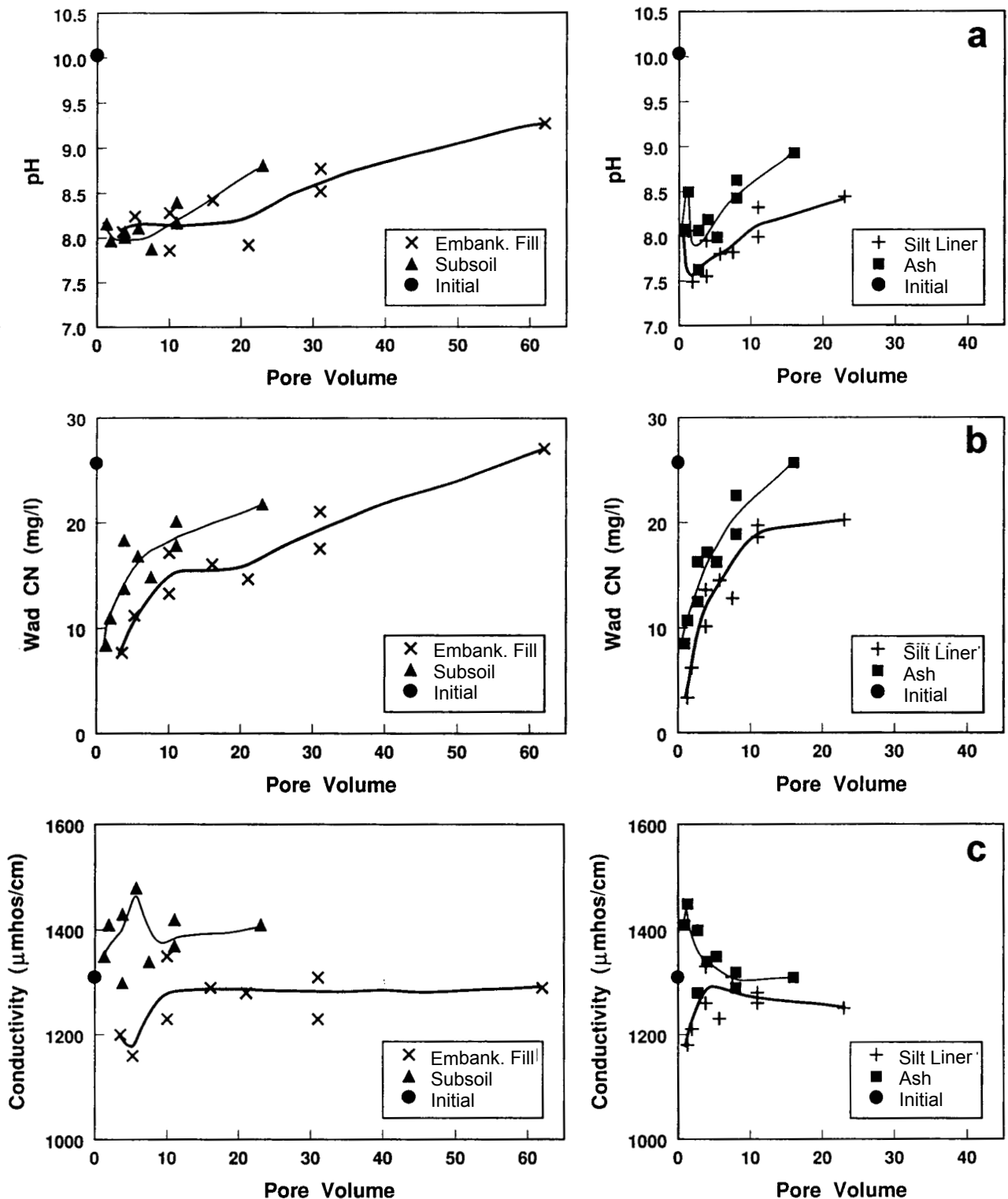


FIGURE 29.4—Concentrations of pH and selected elements in solution as a function of pore volume from Sequential Batch Tests using tailing pond water. The initial concentration in the tailing pond water is shown on the y-axis. a) pH; b) Weak acid dissociable (WAD) cyanide; c) Electrical conductivity; d) Arsenic; e) Cadmium; f) Zinc; g) Copper.

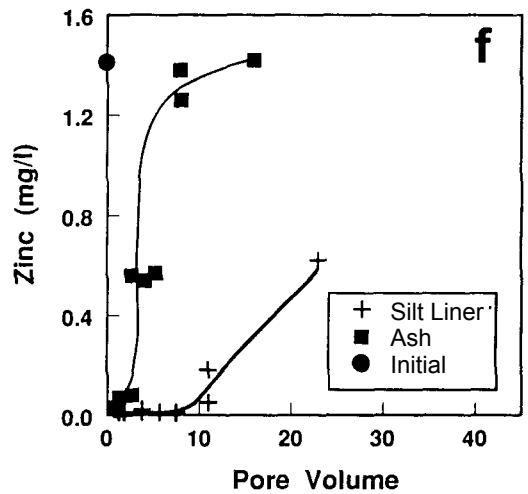
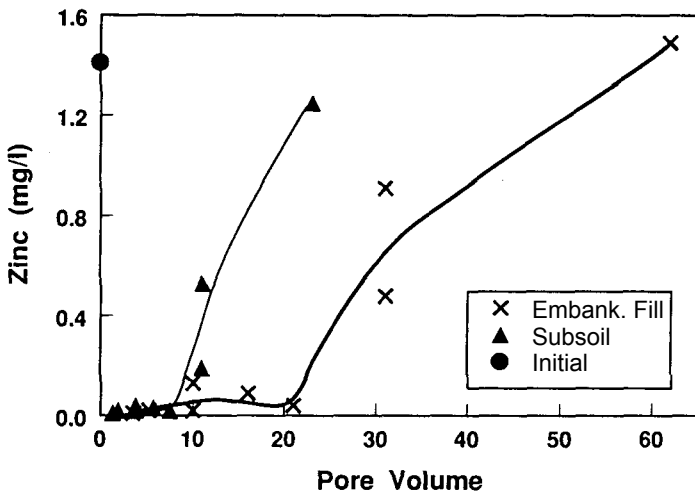
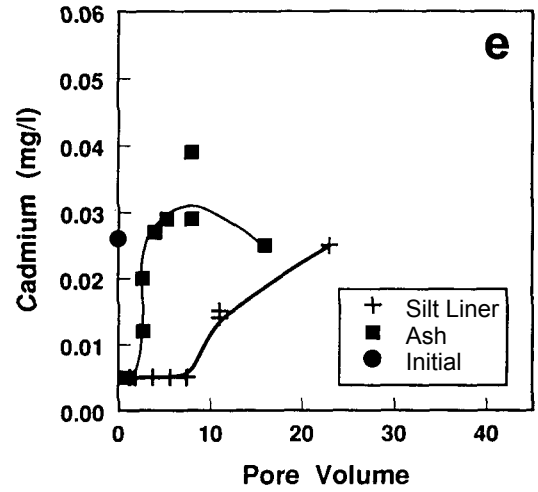
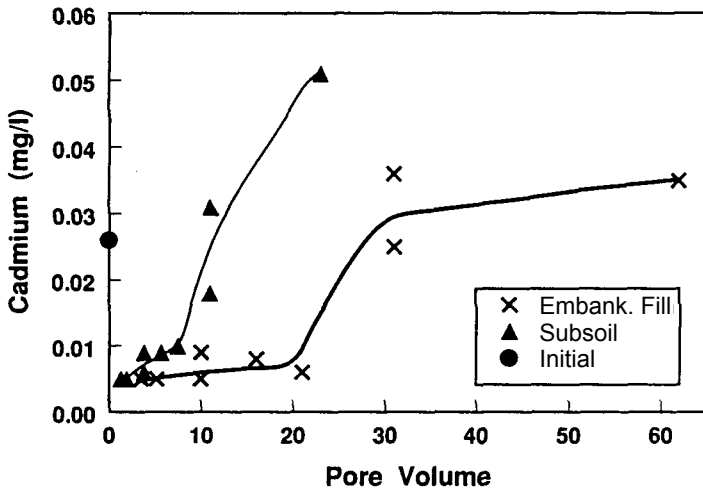
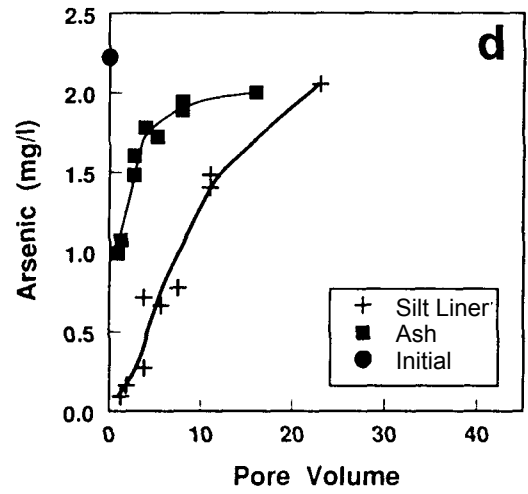
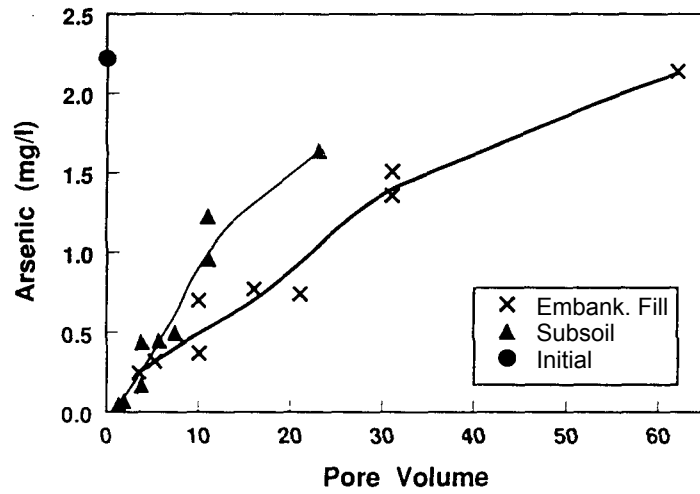


FIGURE 29.4—Continued

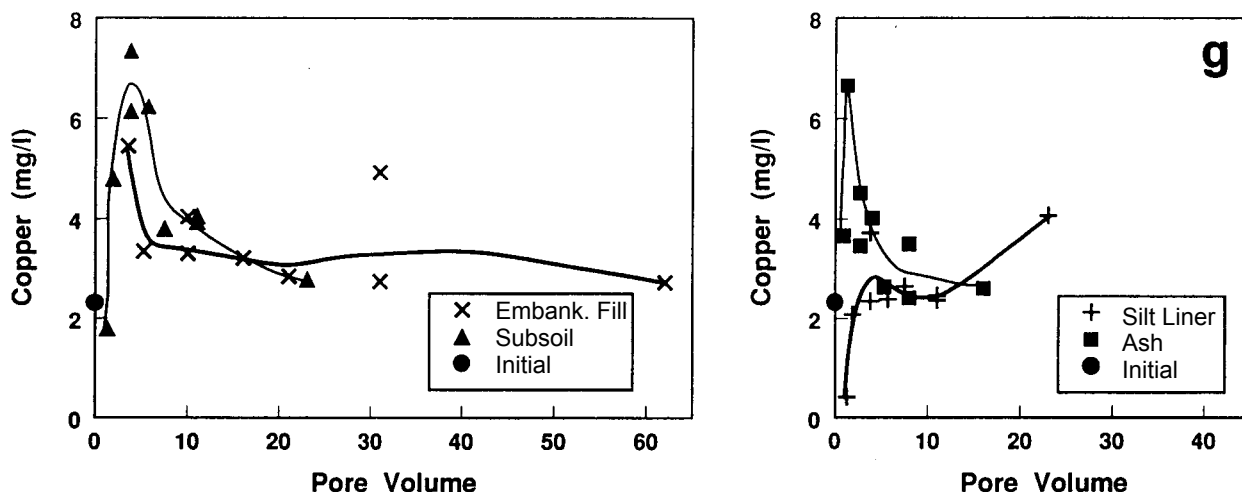


FIGURE 29.4—Continued

TABLE 29.5—Tailing pond water sequential batch tests. Solution concentrations (mg/l) and attenuation capacity (mg/kg).

Constituent		Embankment fill	Subsoil	Silt	Ash
WAD Cyanide	Initial Concentration	25.7	25.7	25.7	25.7
	Minimum Concentration	7.67	8.44	3.33	8.57
	Final (C3) Concentration	14.7	14.9	12.8	16.3
	Attenuation Capacity	17.7	30.0	40.6	15.6
Arsenic	Initial Concentration	2.22	2.22	2.22	2.22
	Minimum Concentration	0.25	<0.05	0.09	0.79
	Final (C3) Concentration	0.74	0.50	0.77	1.72
	Attenuation Capacity	3.18	5.50	3.50	1.96
Cadmium	Initial Concentration	0.026	0.026	0.026	0.026
	Minimum Concentration	<0.005	0.005	<0.005	<0.005
	Final (C3) Concentration	0.006	0.01	<0.005	0.029
	Attenuation Capacity	0.017	0.017	0.046	0.006
Zinc	Initial Concentration	1.40	1.40	1.40	1.40
	Minimum Concentration	0.01	0.01	<0.010	0.03
	Final (C3) Concentration	0.04	0.02	0.01	0.57
	Attenuation Capacity	2.29	3.55	6.16	1.12
Copper	Initial Concentration	2.32	2.32	2.32	2.32
	Minimum Concentration	2.73	1.80	0.41	2.42
	Final (C3) Concentration	2.85	3.81	2.64	2.64
	Attenuation Capacity ¹	--	--	--	--

¹No attenuation capacity was calculated because copper was leached from the

TABLE 29.6—Underdrainage sequential batch tests. Solution concentrations (mg/l) and attenuation capacity (mg/kg).

Constituent		Embankment fill	Subsoil	Silt	Ash
WAD Cyanide	Initial Concentration	7.11	7.11	7.11	7.11
	Minimum Concentration	3.34	2.00	1.37	3.36
	Final (C3) Concentration	4.63	2.52	4.01	4.10
	Attenuation Capacity	17.6	24.6	10.0	13.6
Arsenic	Initial Concentration	2.40	2.40	2.40	2.40
	Minimum Concentration	0.35	<0.05	0.07	1.16
	Final (C3) Concentration	1.37	0.64	1.16	2.00
	Attenuation Capacity	2.79	5.51	4.13	1.95
Cadmium	Initial Concentration	0.011	0.011	0.011	0.011
	Minimum Concentration	<0.005	<0.005	<0.005	<0.005
	Final (C3) Concentration	<0.005	0.005	<0.005	0.007
	Attenuation Capacity	>0.033	0.025	>0.036	>0.036
Zinc	Initial Concentration	0.01	0.01	0.01	0.01
	Minimum Concentration	<0.01	<0.01	<0.01	<0.01
	Final (C3) Concentration	<0.01	<0.01	<0.01	0.01
	Attenuation Capacity	>0.01	>0.01	>0.01	>0.01
Copper	Initial Concentration	0.09	0.09	0.09	0.09
	Minimum Concentration	0.50	0.02	0.01	0.70
	Final (C3) Concentration	1.14	0.49	0.87	2.33
	Attenuation Capacity ¹	--	--	--	--

¹No attenuation capacity was calculated because copper was leached from the soils.

DISCUSSION

As discussed previously, cyanide can exist in several forms and react through several processes. During transport through soils, cyanide can be removed from solution by volatilization of free cyanide, reaction with metals to form less soluble cyanide complexes, reaction with polysulfides and(or) polythionates to form thiocyanate, and bacterial oxidation to carbon dioxide and ammonia.

The SBT procedure, by its nature, tends to exaggerate the role of volatilization as the main mechanism for removing cyanide from solution, because the procedure is of short duration (24 hours per batch) and requires exposure of solids and solution to the atmosphere during transfer and filtering. The SBT test results suggest that if volatilization is the main mechanism reducing cyanide in the seeps, less than one to two pore volumes of fluid could have been in contact with the soils (results that would have been equivalent to an A4 or A5 batch, if such a batch had been done). In other words, relatively small amounts of water would have traveled through a relatively large areal extent of soil.

Formation of strong alkali-metal cyanide complexes could also account for some of the loss of WAD cyanide in the SBT's. The leaching of copper into the SBT solutions is evidence of reaction of copper with cyanide to form soluble copper-cyanide complexes. In contrast to the SBT solutions, the seep waters have low to nondetectable levels of copper. Thiocyanate could also have been a reaction product to lower WAD cyanide in the SBT solutions. If this is the case, however, the reaction in the SBT's would be counter to results for seep waters, in which thiocyanate is at or below its lower limit of detection (Table 29.1).

The final mechanism for decreasing cyanide in water is microbial degradation of cyanide, ultimately, to nitrate and bicarbonate. Significant microbial degradation of cyanide to nitrate would not be expected to occur during the short duration of the SBT's (Chatwin, 1990; Fuller, 1984; Simovic et al., 1984). Nitrate nitrogen was measured in the A3 fractions of the SBT's using ash and tailing pond water and ash and underdrainage. The concentrations were 9.9 and 6.1 mg/l, respectively. These values were similar to the values in the original tailing water and underdrainage, shown in Table 29.1, suggesting that little or no microbial degradation took place in the experiments. Therefore, the WAD cyanide results from the SBT's are conservative from the standpoint of microbial degradation and can give an underestimate of cyanide attenuation by this mechanism.

Comparison of nitrate nitrogen concentrations in the seeps with those in the tailing pond water and underdrainage (Table 29.1) shows that concentrations in the seeps (20 to 37 mg/l) are substantially higher than either the tailing pond (3 to 9 mg/l) or the underdrainage (about 3.5 mg/l). They are also higher than the average baseline ground water (not shown), at <1 mg/l. If the seeps traveled through embankment fill, they could have picked up some nitrate as a residue from blasting operations. On the other hand, the nitrate data suggest that much of the cyanide may have been converted to nitrate in the seeps, rather than volatilized.

In Table 29.7, the nitrogen in cyanide, thiocyanate, and nitrate was calculated for the lower and upper seeps, tailing pond water, and underdrainage from the samples collected on 14 August 1990. The tailing pond water collected near the reclaim pump on 15 October 1990, is also included. Comparison of the two samples of tailing pond water shows that the sum of the nitrogen species is variable over time, probably dependent on the amount of cyanide

used in the mill process. Another possibility is that substantial but variable amounts of nitrogen exist in ammonia and nitrite, which were not measured. In the August sampling, in which data exist for all water types, the underdrainage water has less nitrogen than the tailing pond or either seep. The conductivity results further suggest that the source of the seeps is excess water in the tailing pond, rather than underdrainage.

TABLE 29.7—Nitrogen species¹ in seeps, tailing pond water, and drainage.

Constituents	Lower seep	Upper seep	Tailing water	Tailing (reclaim) water	Under-drainage water
	8/14/90	8/14/90	8/14/90	10/15/90	8/14/90
Total CN	0.82	5.11	26.2	42.2 ²	16.8
SCN	<0.1	<0.1	19.6	27.8	11.0
NO ₃ -N	37.3	24.5	2.8	9.2	3.6
Converted to Equivalent N:					
CN-N	0.44	2.76	14.1	22.8	9.1
SCN-N	0.02	0.02	4.7	6.7	2.6
NO ₃ -N	37.3	24.5	2.8	9.2	3.6
Total N	37.8	27.3	21.6	38.7	15.3

¹Concentrations from Table 29.1 (mg/l); ammonia and nitrite nitrogen were not measured

²Only WAD cyanide was measured. Total cyanide concentration is probably higher

As discussed previously, the seeps (Table 29.1) have low to nondetectable copper concentrations. These low copper concentrations can be consistent with excess water in the tailing pond as the source of the seeps if very large amounts of soil, including silt liner material, have been in contact with small amounts of overflow. In such a case, the chemistry of the water after it has reacted with large amounts of fresh soil could be sufficiently changed to allow attenuation of copper, as was discussed above for the silt liner material. More likely, the microbial degradation of cyanide within the embankment fill reduced the amount of cyanide available to complex with copper so that the copper in the seepage was sorbed by the fill similar to the behavior of cadmium and zinc.

DETERMINATION OF SOURCE

The results of the SBT's and the original water concentrations, especially for nitrogen and conductivity, indicate that excess water in the tailing pond is a more likely source for the seeps than seepage of underdrainage. However, the differences in calcium and magnesium between the seeps and the tailing pond water (Table 29.1) could not be addressed with the initial analyses of the SBT's. The possibility that the seeps came from a third, more distant source could also not be addressed. Consequently, additional tests and geochemical modeling were conducted. The purpose of this additional work was to "type" the water chemistry after interaction with the various soil types and compare the water types to the seeps. This comparison would allow determination of probable flow paths of the seeps.

The A3 leachate solutions were analyzed for major ions. These results were plotted on Piper trilinear plots and Stiff diagrams for visual inspection. Groundwater data collected by Geraghty and

Miller in 1989 from existing monitoring wells were also plotted for comparison. The tailing pond and underdrainage solutions were then compared with A3 solutions and seep waters using HCGRAM.

The Piper trilinear plot allows the cation and anion compositions of many samples to be represented on a single plot so that groupings in the types of samples can be discerned visually. The plot represents the concentrations as percentages. The Stiff diagram is a graphical representation of chemical analyses that allows rapid comparison as a result of distinctive shapes.

Time variation of waters

Before discussing the results of the A3 analyses, it is instructive to investigate the temporal variability of the geochemistry of the seeps, tailing pond water, and underdrainage and the spatial variability of the tailing pond water. Figure 29.5 is a Piper trilinear plot of seep, tailing pond, and underdrainage water. On the plot, waters with different total dissolved solids concentrations may be represented by a single point as long as the relative proportions of the major ions are the same for both. The mixture of

two different water types will plot on the straight line connecting the points representing the two waters.

The seep samples shown on the plot were collected on 14 August and 15 October 1990; tailing pond samples were collected on 14 and 23 August and 15 October 1990; and underdrainage samples were collected on 14 and 23 August 1990. The tailing pond water in all three samplings was collected in the general vicinity of the reclaim pump. On 15 October, slurry entering the tailing pond was also collected as it exited the discharge pipe. All data were taken from Table 29.1.

Based on Figure 29.5, the lower seep shows the least temporal variability, followed by the upper seep and the underdrainage. Most of the temporal variability is in the ratio of anions, especially chloride and sulfate, as can be seen from the lower left field of the Piper plot. As can be seen from Table 29.8, the ratio of chloride to sulfate decreased over time in all of the water samples. The tailing pond water showed the highest initial ratio and the greatest decrease. The upper seep had a higher initial ratio and a greater decrease with time than the lower seep. The slurry had the lowest concentration of all waters sampled in October.

These results suggest that the ore being milled has been variable in sulfur content over time and(or) that the mill process has

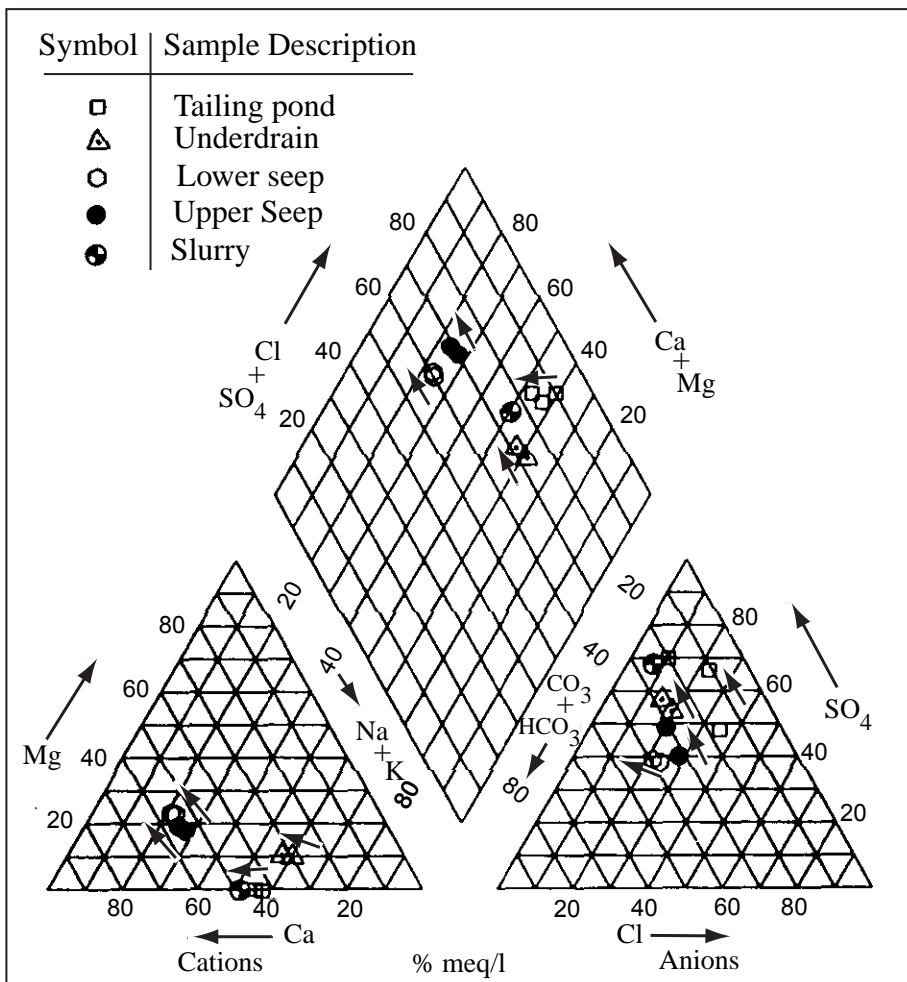


FIGURE 29.5—Trilinear Piper Plot showing the variation of major ion chemistry in the seeps, tailing pond and slurry water, and underdrainage as a function of time. Arrows on diagram point from earlier to later sample dates.

changed somewhat, and the tailing facility as a whole is reflecting the variability. (Chloride is typically a byproduct of treating tailings with a hypochlorite solution to reduce cyanide to levels that are not toxic to water fowl.)

TABLE 29.8—Variability with time of chloride-to-sulfate ratios in seeps and tailing facility waters.

	Cl/SO ₄		
	8/14/90	8/23/90	10/15/90
Lower seep	0.39		0.35
Upper seep	0.47		0.31
Underdrainage	0.27	0.22	
Tailing pond water	0.52	0.27	0.09
Slurry			0.07

The seeps appear to be tracking the variability in the tailing facility and are consistent with the hypothesis that the tailing pond, rather than a more distant location, is likely to be the source. The chemistry of the upper seep is more similar to the tailing pond water than the lower seep. Thus, if the tailing pond is the source of the seepage, the upper seep has probably had a shorter reaction path (i.e., is closer to the source) than the lower seep.

A3 analyses

The A3 fraction of the SBT's is that fraction most likely to show the greatest changes in water chemistry due to reaction with soils. Therefore, analysis for major ions, including calcium, magnesium, sodium, potassium, bicarbonate, chloride, and sulfate permits the determination of the major geochemical changes that would take place after passage of potential seep source water through the various soils. Comparison of these results with the major ion geochemistry of the actual seep waters gives evidence as to the probable soil types through which the seep waters passed.

Piper trilinear plots of the A3 SBT solutions for the tailing pond water and underdrainage water are shown on Figures 29.6a and 29.6b, respectively. The first point of note is that the A3 solutions from the tuffaceous ash are least like the seeps in water type, especially in terms of cations. The seep waters have higher relative calcium and magnesium contents than the tailing pond water and global underdrainage water, whereas the ash A3's have lower relative calcium and magnesium. This result tends to rule out ash layers as the likely flow channels.

Based on the trilinear plots, all of the other soil types tended to react with the tailing pond water or underdrainage to produce a water more similar to the seeps. None is an exact mix, however, since none lies on a straight line in all three fields of the plot. The mixing model was also unable to obtain any of the A3 results by mixing either seep with tailing pond water or underdrainage.

Stiff diagrams of the A3 SBT solutions for the tailing pond water and underdrainage are shown on Figures 29.7a and 29.7b, respectively. The center vertical line is the zero concentration level. Cations are plotted to the left of the center line and anions to the right. The order of the ions vertically is always the same: sodium plus potassium, calcium, magnesium, and (sometimes) iron for cations, and chloride, bicarbonate, sulfate, and (sometimes) carbonate for anions. Lines are drawn connecting the val-

ues to form distinctive shapes. The closer two waters are to each other in shape, the more similar they are in terms of water type. The closer two waters are in size of their shapes, the more similar they are in terms of total dissolved solids.

In terms of size on the Stiff diagrams, the tailing pond waters are more similar to the seeps than the underdrainage waters. This result was already noted in the discussion of SBT conductivity results. In terms of shapes, none of the SBT results is identical to the seeps. However, the A3 results do indicate that the embankment fill tends to alter the tailing pond water and underdrainage waters to a shape closer to that of the seep waters on the basis of the ratios of calcium and magnesium to sodium plus potassium (Fig. 29.7a).

Mixing model

The principle behind the SBT tests is that seepage flowing through a soil or porous rock will react with the material through which it flows. The reactions can sometimes be modeled by reaction path models if a detailed mineralogy of the material is known. As mentioned previously, mixtures of two water types will lie on a straight line connecting the two waters on each of the three fields of a trilinear plot. Thus, a simplified alternative to reaction path modeling would be to use the trilinear plots to evaluate whether the two seepage water chemistries can be extrapolated back to a single source water. If so, then they have likely come from the same source water and traveled through the same type of material.

The equations for the straight lines on the trilinear plots can be calculated and compared with data from any water type. The calculation and comparison are done automatically by the computer HC-GRAM. In the present study, all waters that deviated by less than 20% from a straight line in all three fields of the trilinear plot were considered possible mixtures.

Mixing model calculations showed that the upper seep waters fell on a mixing line between the tailing pond water and the lower seep waters in terms of major ion chemistry (Table 29.9). This results suggests that either:

- 1) the flow path is from the tailing pond to the upper seep to the lower seep, more or less parallel to the embankment or
- 2) both the upper and lower seep waters travel on a path more or less perpendicular to the embankment through the same type of material between the tailing pond and the seep outlet, and the lower seep water has a longer flow path.

TABLE 29.9—HC-GRAM mixing model using upper seep as a mixture of tailing pond water and lower seep water. Samples collected on 14 August 1990.

Ion	Lower Seep	Tailing Pond	Calculated Mix	Upper Seep	Percent Error
Total Concentration	36.1	21.9	31.8	26.6	20
Mg	4.52	0.03	3.68	2.63	40
Ca	11.6	4.74	10.30	8.48	21
Na+K	5.17	5.89	5.31	4.08	30
HCO ₃ +CO ₃	7.21	1.95	4.79	4.33	11
SO ₄	7.00	5.48	6.30	5.48	15
Cl	4.30	3.88	4.11	3.87	6.2
Mixing Factors	70%	30%			

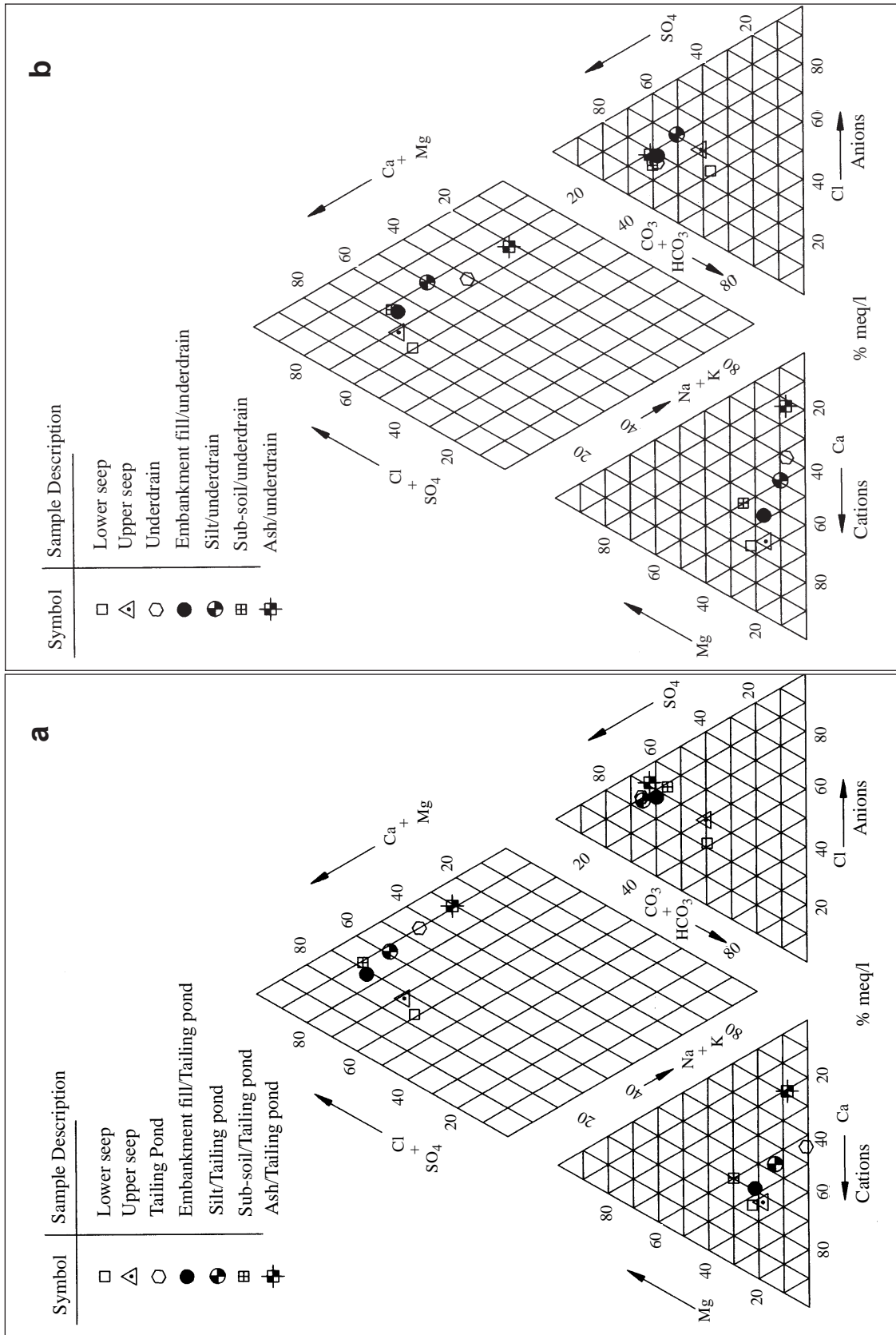


FIGURE 29.6—Trilinear Piper Plot showing the chemistry of the seeps, (a) tailing pond water or (b) underdrainage, and the solution from the A3 step of the corresponding Sequential Batch Tests. The A3 step corresponds to the smallest pore volume tested.

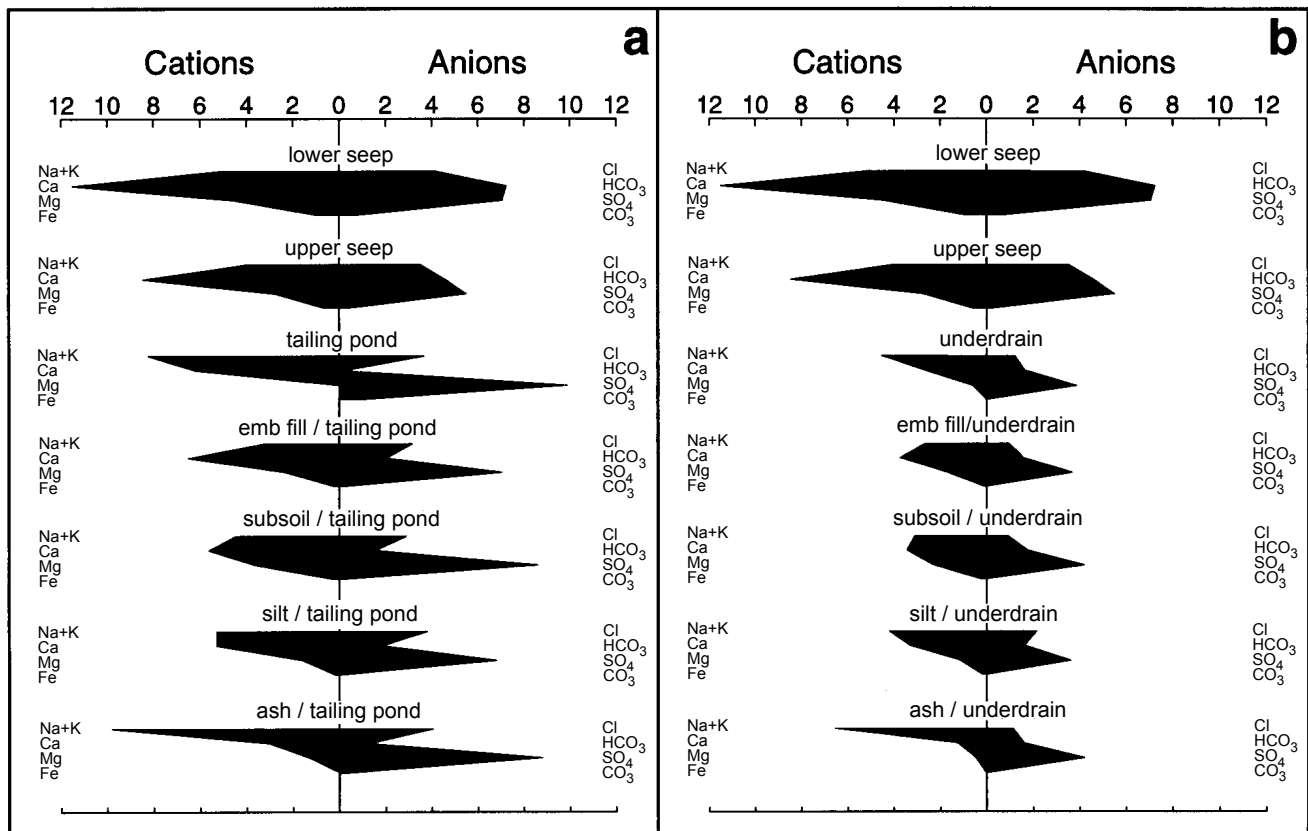


FIGURE 29.7—Stiff Diagram showing the chemistry of the seeps, (a) tailing pond water or (b) underdrainage, and the solution from the A3 step of the corresponding Sequential Batch Tests. The A3 step corresponds to the smallest pore volume tested.

SUMMARY AND CONCLUSIONS

An investigation using simple, inexpensive geochemical tools was conducted within a short time-frame to determine the source of two seeps bordering a gold mill tailing facility. The methods were simple, but were complementary and attacked the problem from several angles, so that important conclusions could be drawn. Additional geochemical tools such as nitrogen isotopes, mineralogical analyses, and more complicated computerized reaction path models would have provided additional corroborating evidence, but would likely not have changed the relevant conclusions.

The upper seep water had higher pH, higher concentrations of nitrate, alkalinity, bicarbonate, calcium, and magnesium than the lower seep. Both seep waters had higher total dissolved solids, as evidenced by conductivity, and a different mix of major ions than either the tailing pond water or the underdrainage water. The underdrainage water was more dilute than the tailing pond water, probably because the underdrainage water was diluted by precipitation that falls on the part of the tailing facility contributing to the underdrainage system. Cyanide, thiocyanate, arsenic, cadmium, zinc, and copper were significantly depleted in the seep waters compared with either the tailing pond or underdrainage waters.

Soils likely to come in contact with the seepage water (embankment fill, underlying subsoil, silt liner material, and tuffa-

ceous ash) were characterized geochemically. Characterization included properties that affect attenuation in natural earth materials. On the whole, soils showed geochemical properties favorable to cyanide and metal attenuation. The silt liner material and the embankment fill had the highest cation exchange capacity.

The attenuation properties of the soils toward concentrations of constituents in the tailing pond and underdrainage were determined from sequential batch tests (SBT's). In the SBT's, the soils neutralized a portion of the alkalinity of the high-pH tailing pond water (pH 10) and the underdrainage (pH 8.5). The final pH's tended to be in the range of 7.5 to 9, similar to the seep pH's. The silt liner material was most effective in lowering the solution pH.

Conductivity values in the SBT solutions changed little throughout the tests. The results indicated that the source of the seeps was more likely to be the tailing pond water than the underdrainage.

Contact with the soils reduced the WAD cyanide in all soils tested in the SBT's. Volatilization of cyanide due to the drop in pH is probably the primary mechanism for the decrease in cyanide in the SBT's due to their short duration. However, comparison of amounts and forms of nitrogen in the tailing pond water and the seeps suggests that if the source of the seeps is the tailing pond water, most of the decrease in cyanide in the seeps is likely due to degradation to nitrate, with relatively little volatilization. This degradation to nitrate has resulted in nitrate levels in the seeps on the order of 20 to 40 mg/l of nitrate nitrogen. Volatilization may

have been inhibited in the tailing embankment due to saturated conditions and(or) minimal ventilation.

All the soils tested in the SBT's attenuated arsenic, cadmium and zinc, in agreement with the observed low concentrations of these elements in the seeps. However, the ability to attenuate cadmium was exhausted in the course of the testing in all soils except the silt liner material in the tailing pond water test.

Copper was leached from most soil types in the SBT's, rather than attenuated, as suggested by the concentrations of copper in the seeps. The high copper in the SBT solutions was probably due to complexing with cyanide during the short exposure time in the tests. During the longer exposure time available in the seepage, microbial degradation of cyanide probably reduced the amount of cyanide available to complex with the copper.

These results indicate that the SBT's were effective in predicting the behavior of constituents such as pH, conductivity, arsenic, cadmium, and zinc, which appear to be controlled by rapid sorption and dissolution processes in the seeps. The SBT's were less effective in predicting the behavior of cyanide and copper, which appear to be controlled by slower microbial processes.

Comparison of the temporal variability of the seeps, tailing pond water, and the underdrainage resulted in several observations. The ratios of chloride to sulfate appeared to be changing over time, presumably reflecting changes in ore chemistry and(or) the mill process. Because the seeps appeared to reflect the changes in the tailing pond, the tailing pond water, rather than some more distant water, was likely to be the source. Also, the upper seep water was more similar than the lower seep water to the tailing pond water and, thus, probably had a shorter reaction path than the lower seep water; i.e., the upper seep was closer to the source.

Geochemical characterization of the seep and tailing pond waters showed that the seep waters had a different mix of major ions than the tailing pond water. In order to determine if passage of the tailing pond water through any of the soil types could produce the mix of major ions observed in the seeps, simple tools including Piper trilinear plots, Stiff diagrams, and simple computerized mixing models were used to compare the major ion chemistries of the seeps and results of the most attenuated solution batch of each of the SBT's.

The results showed that ash changed the chemistry of the tailing pond water to make it look less like the seeps. Therefore, it is unlikely that the seep water has come in contact with ash layers.

The other soil types, especially the embankment fill, changed the tailing pond water to make it look more like the seep waters. These results implicate an overfilled tailing pond as the most likely source of the seeps.

EPILOGUE

The geochemical results presented in this report complemented the geophysical work and led to a model of lateral seepage flow paths through areas of geophysical self-potential anomalies. The combination of conditions that appear to have caused the seepage have been corrected by improvements in operating plans as well as design modifications implemented during a tailing facility expansion program initiated in 1990.

REFERENCES

- Chatwin, T.D., 1990, Cyanide attenuation/degradation in soil (Appendix): Resource Recovery and Conservation Company, Salt Lake City, Utah.
- Fuller, W.H., 1982, Methods for conducting soil column tests to predict pollutant migration: Proceedings, Land Disposal of Hazardous Wastes Symposium, EPA-600/9-82-002, pp. 87-105.
- Fuller, W.H., 1984, Cyanides in the environment with particular attention to the soil: Proceedings, Conference on Cyanide and the Environment, Tucson, Ariz., pp. 19-46.
- Fuller, W.H., Amoozergar-Fard, A., Niebla, E.E., and Boyle, M., 1980, Influence of leachate quality on soil attenuation of metals: Proceedings, Disposal of Hazardous Waste Symposium, EPA-600/9-80-010, pp. 108-117.
- Huiatt, J.L., 1984, Cyanide from mineral processing—Problems and research needs: Proceedings, Conference on Cyanide and the Environment, Tucson, Ariz., pp. 65-81.
- Houle, M.J., and Long, D.E., 1980, Interpreting results from serial batch extraction tests of wastes and soils: Proceedings, Disposal of Hazardous Waste Symposium, EPA-600/9-80-010, pp. 60-81.
- McIntosh, G.E., 1990, HC-GRAM: U.S. Department of the Interior, Office of Surface Mining.
- Rouse, J.V., and Pyrih, R.Z., 1988, Natural geochemical attenuation of trace elements in migrating precious-metal process solutions: Proceedings, Randol International Gold Conference, Perth, pp. 77-81.
- Simovic, L., Snodgrass, W.J., Murphy, K.L., and Schmidt, J.W., 1984, Development of a model to describe the natural degradation of cyanide in gold mill effluents: Proceedings, Conference on Cyanide and the Environment, Tucson, Ariz., pp. 413-432.

Chapter 30

USE OF LEAD ISOTOPES AS NATURAL TRACERS OF METAL CONTAMINATION—A CASE STUDY OF THE PENN MINE AND CAMANCHE RESERVOIR, CALIFORNIA

S.E. Church,¹ C.N. Alpers,² R.B. Vaughn,¹ P.H. Briggs,¹ and D.G. Slotton³

¹*U.S. Geological Survey, Box 25046, MS 973, Federal Center, Denver, CO 80225-0046*

²*U.S. Geological Survey, Placer Hall, 6000 J Street, Sacramento, CA 95819-6129*

³*Division of Environmental Science and Policy, University of California, Davis, CA 95616*

Lead isotopes have been used as tracers of geologic processes in both ore-genesis and petrogenesis studies. Recently, they have found increased application in contamination studies. There are two requirements for their application in contamination studies: (1) that the isotopic signature of the contaminant is different from the rock lead in the area, and (2) that the signature of the source is known or can be determined. In this study, we examined lead isotope data for sediments from Camanche Reservoir near Stockton, California. We identified two sources of contamination in the sediments and soils of the area: one from acid-mine drainage from the Penn Mine within the drainage basin, and a second exotic lead, probably from airborne deposition from combustion of leaded gasoline in the early 1970s, found in soils.

Lead isotope data for sediments from the drowned channel of the Mokelumne River in Camanche Reservoir plot on a mixing line between the lead isotope signature of massive sulfide Cu-Zn-Pb ores from the Penn Mine and unaffected sediments derived from tributaries draining into Camanche Reservoir. The contribution of lead from the source of these metals, the Penn Mine, is diluted by sediments supplied by these tributaries. Distribution profiles for copper and zinc mimic the behavior of lead. Geochemical and lead isotope data for a sediment sample recovered from the fish hatchery at Camanche Dam following the 1989 fish kill indicate that the sediment was from the deep portion of Camanche Reservoir. The water intake from the hatchery was subsequently moved to reduce the probability of intake of sulfidic, anoxic waters and associated metal-rich sediments from deep in the reservoir. Since 1994, the water level of the reservoir has been maintained at 180 feet or more as recommended by Slotton et al. (1994) on the basis of their sediment resuspension studies. Installation of a hypolimnetic aeration system has resulted in no subsequent fish kills in the fish hatchery at Camanche Dam.

Four of the five shallow soil samples collected from within the watershed in 1976 for the National Uranium Resources Evaluation (NURE) contain relatively high concentrations of lead with an isotopic signature similar to that reported in the Sierra Nevada by Shirahata et al. (1980). These lead isotope data are interpreted to indicate the presence of airborne lead contamination derived from the combustion of leaded gasoline. The NURE soils in the USGS National Geochemical Sample Archive represent a valuable suite of samples of historical significance that can be used to evaluate the effect of legislation designed to reduce industrial impact of metals on the environment.

INTRODUCTION

The oxidation of sulfide minerals in mine wastes and weathering of *in situ* mineralization has resulted in the generation of acid rock drainage (ARD) in many mineralized areas. Metals such as copper, lead, and zinc are of economic value but also are potentially toxic to aquatic organisms and humans, depending on concentrations, speciation, and exposure pathways. These metals occur commonly in ore deposits as discrete sulfide minerals in association with the iron-sulfide minerals pyrite, marcasite, or pyrrhotite. The iron-sulfide minerals, when exposed to oxidizing conditions, release sulfuric acid during weathering. The acid attacks other metal-bearing sulfides that release the potentially toxic metals (e.g., Nordstrom, 1982; Alpers et al., 1994a; Plumlee et al., 1994; Nordstrom and Alpers, 1999). As metal-rich ARD solutions oxidize and mix with more dilute waters, dissolved trace metals tend to precipitate with or sorb to secondary minerals such as hydrous iron, aluminum, and manganese oxides that occur as discrete mineral grains or coatings on sediment particles. In addition, sediments containing primary sulfide minerals can be mobilized by natural erosion processes, commonly accelerated greatly by past mining and mineral processing practices.

The amount of metal released from a mined deposit either as acidic drainage or contaminated sediment is controlled largely by the geology and mineralogy of the ore deposit, the amount of water available to the mine wastes and the mine workings (e.g., Plumlee and Nash, 1995), the milling procedures used at the time the ore was processed, the waste handling procedures in place during mining and milling operations, and the strategies for containment and isolation of mine wastes adopted at the time of mine closure (e.g., Jambor and Blowes, 1994). Uncontrolled erosion of mine-waste piles and past practices of discharging mill tailings slurries directly to surface waters have led to large-scale problems with metal-contaminated sediments in many watersheds (e.g., Clark Fork River, Montana: Moore and Luoma, 1990; Arkansas River, Colorado: Church et al., 1993, 1994; Walton-Day et al., 1996; Animas River, Colorado: Church et al., 1997). Contaminated water and sediment from some historical abandoned mine sites have impacted drinking water supplies and affected aquatic and riparian habitats downstream within these watersheds.

Volcanogenic massive sulfide deposits, of which the Penn Mine is one of several in the Sierra Nevada Foothills copper belt (Fig. 30.1) of northern California (Heyl, 1948; Fig. 1), are gener-

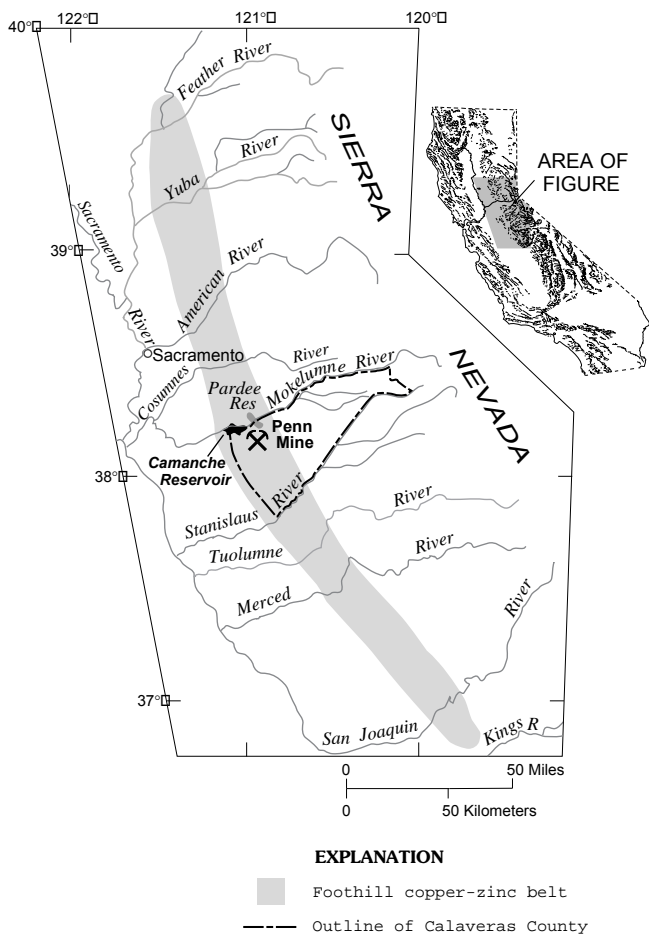


FIGURE 30.1—Map showing the location of the Foothill copper-zinc belt, the Penn Mine, Camanche Reservoir, and other localities mentioned in the text (after Peterson, 1988).

ally among the most prolific generators of ARD and associated potentially toxic metals. Studies of the Iron Mountain Mine in Shasta County, California have documented ARD with pH values less than 1.0 and total metal contents in excess of 100,000 mg/l (Alpers and Nordstrom, 1991; Nordstrom et al., 1991; Alpers et al., 1992, 1994a, c; Nordstrom and Alpers, 1999). Plumlee et al. (1994) demonstrated that the environmental effect of weathering volcanic-hosted massive sulfide deposits can produce some of the most acidic, metal-laden waters known. This is because volcanogenic massive sulfide deposits contain large amounts of acid-producing iron-sulfide minerals and occur in rocks that have little potential to neutralize the acid produced upon weathering (Taylor et al., 1995). The acidic drainage from abandoned mine sites not only contributes acidic waters, but also transports a substantial metal load that impacts downstream aquatic and riparian habitats.

Lead isotope data have been used in numerous studies to evaluate geologic processes. For example, Doe (1970) used lead isotope data as a tracer of ore-forming processes and Gulson (1986) has used them as indicators of the presence of ore in mineral exploration programs. Gulson et al. (1992) studied the distribution of lead isotopes on pebble coatings in streams that drained a well-

characterized porphyry-molybdenum deposit and showed that lead isotope compositions changed quickly as a function of distance in the stream, reflecting local sources of lead added to the stream by ground water. Thus, if metal-rich effluents contain a sufficient concentration of lead, they can readily be traced to their source, be it industrial, mining-related, or natural, by using the lead isotope signature associated with specific ore deposits or industrial processes. Applications of this lead isotope tracer approach to measure the metal dispersion caused by historical mining in watersheds have been used in the western U.S.A. by Church et al. (1993, 1994, 1995, 1997) and in Sweden by Östlund et al. (1995).

Environmental studies by Patterson (1971, 1972) used lead isotope and lead-concentration data to demonstrate that human activities have contaminated the Earth's surface with lead from smelting of sulfide ores beginning about 4500 B.P. Shirahata et al. (1980) showed that lead in gasoline in the U.S.A. had raised the concentration of leachable lead in sediments in a remote alpine pond in the Sierra Nevada from 5.7 ppm in 1894 to 27.6 ppm by 1972. Lead isotope data confirmed that the source of lead was airborne contamination from the combustion of gasoline. Heyvaert (1998) confirmed lead enrichment in sediment cores from pristine Lake Tahoe, dated using ²¹⁰Pb. Other lead isotope studies have indicated that this same process of airborne transport of lead from the combustion of gasoline was responsible for the changes in the concentration of lead in both the near-shore marine environment (Patterson et al., 1976; Ng and Patterson, 1979; Sañudo-Wilhelmy and Flegal, 1994) and the urban and industrial corridor in the northeastern U.S.A. (e.g., Riston et al., 1994; Graney et al., 1995).

The Mokelumne River drainage, east of Stockton, California (Fig. 30.1), has been adversely affected by acidic drainage and metal-laden sediments from the Penn Mine (Finlayson and Rectenwald, 1978). The U.S. Geological Survey (USGS), in conjunction with the University of California at Davis, participated in the present study of bottom sediments in Camanche Reservoir to help define the potential role of sediments and ARD from the Penn Mine site on periodic mortalities of fish in the Mokelumne River Fish Facility located just below Camanche Dam. In this report, we investigate the distribution of labile trace metals in the sediments of Camanche Reservoir and source materials at Penn Mine, and demonstrate the utility of lead isotopes as natural tracers in the study of metal contamination. We identified two sources of metal contamination in the study area. One source is tied directly with the ARD from past production at the Penn Mine. A second source found in the soils collected during the NURE program (1976) from near the Camanche Reservoir contains an exotic lead component, probably derived from the historical combustion of leaded gasoline.

STUDY AREA

Camanche Reservoir was built in the Sierra Nevada foothills, about 60 km southeast of Sacramento, California (Fig. 30.1), on the Mokelumne River in 1964 by the East Bay Municipal Utility District (EBMUD) 5 years after mining and exploration activities ceased at the Penn Mine. The reservoir is used primarily as a flood control basin as well as a source of agricultural irrigation water, and is also the source of water for the Mokelumne River Fish Facility located just below Camanche Dam. Metavolcanic and metasedimentary rocks of Jurassic and Triassic age crop out at the head of the reservoir (Strand and Koenig, 1965; Peterson, 1985).

Located in these rocks is a series of volcanogenic massive sulfide deposits forming the California Foothill copper-zinc belt (CFB; Fig. 30.1), of which the now abandoned Penn Mine was the largest producer. The Penn Mine site is adjacent to the former Mokelumne River channel, which is now inundated by Camanche Reservoir.

The effects of metal contamination from past mining at the Penn Mine on sediment chemistry and water quality in Camanche Reservoir were summarized by Slotton et al. (1994). Historically, numerous fish kills have been associated with the low flows in the Mokelumne River following the construction of Pardee Reservoir 5 km upstream from Penn Mine in 1928. The first of such documented fish kills was recorded in 1937 (Shaw and Towers, 1937). At that time, ARD from the Penn Mine flowed directly into the Mokelumne River through a tributary known as Mine Run (Fig. 30.2). Periodic fish kills were documented in the river between 1937 and 1960, when construction of the Camanche Dam began (Dunham, 1961; Finlayson and Rectenwald, 1978). Fish kills in the salmon and steelhead hatchery built just below Camanche Dam were reported in 1967, 1973, 1977, 1987, and 1989 (Bond, 1988; S.R. Bond, California Regional Water Quality Control Board—Central Valley Region, written commun., 1989) even though no surface waters were released from the Penn Mine into the reservoir from June, 1986 through January, 1993 (T. Pinkos, California Regional Water Quality Control Board—Central Valley Region, written commun., 1995). Although EBMUD had no role in the mining activity, it undertook remediation efforts during low-water conditions in 1977–78, removing several tons of sulfidic metal-laden sediment from Camanche Reservoir and from an area known as Oregon Bar. EBMUD, in conjunction with the California Regional Water Quality Control Board (RWQCB), also constructed Mine Run Dam (Fig. 30.2), a clay-core dam designed to prevent acidic drainage and metals from sulfidic sediment in waste rock and tailings piles on the abandoned Penn Mine site from running off directly into Camanche Reservoir. Elevated metal concentrations remain in the sediments of Camanche Reservoir and were a suspected source of metal contaminants for the fish kills between 1983 and 1989 (Bond, 1988).

The USGS participated in ground-water monitoring in the vicinity of Mine Run Dam from 1991–94 and documented an acidic metal-rich zone of contaminated ground water apparently leaking from Mine Run Reservoir through bedrock fractures in the north abutment of Mine Run Dam (Alpers and Hamlin, 1993; Hamlin and Alpers, 1995, 1996; Alpers et al., 1999). A plume of acidic ground water with pH <4 and elevated concentrations of dissolved metals occurs beneath the slag pile down gradient from Mine Run Dam (Fig. 30.2) at the former smelter site on the shoreline of Camanche Reservoir. Fluxes of metals to Camanche Reservoir in contaminated ground water are difficult to estimate because of the transient nature of hydraulic head gradients in the slag area, which are affected by seasonal fluctuations of up to 50 feet in the elevation of Camanche Reservoir (Hamlin and Alpers, 1995; Alpers et al., 1999).

GEOLOGIC AND HYDROLOGIC SETTING

The rocks of the Sierra Nevada foothills are accreted terranes of the western Cordillera. The geologic map (Fig. 30.3) shows the outcrop pattern of the upper Paleozoic and Mesozoic marine metasedimentary and metavolcanic rocks that form the western

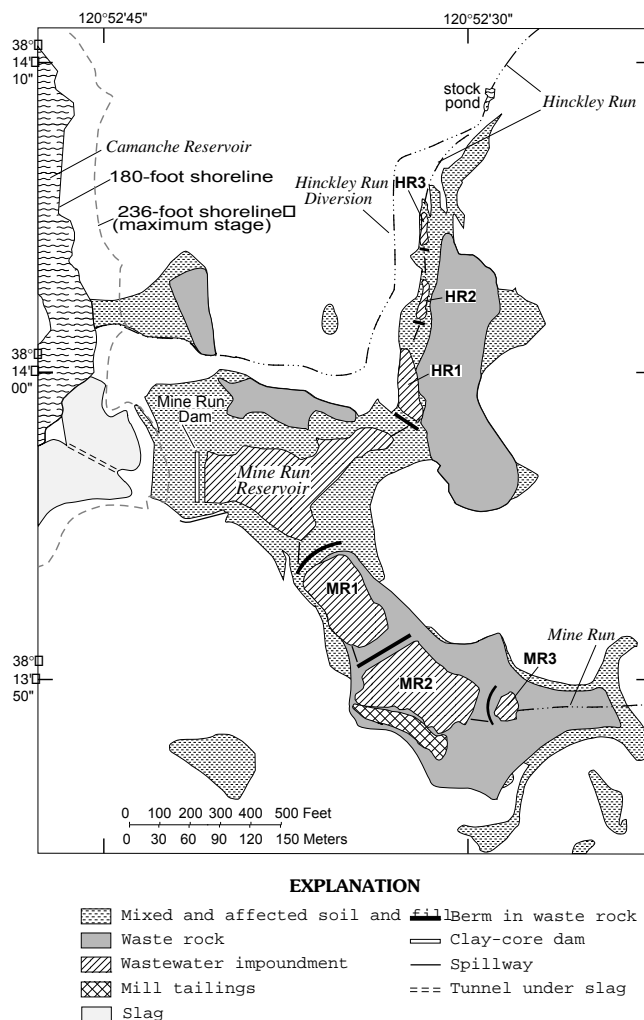


FIGURE 30.2—Map showing location of waste impoundments and monitoring wells at the Penn Mine, Camanche Reservoir, California (from Hamlin and Alpers, 1996; after Davy Environmental, 1993).

margin of the Sierra Nevada batholith and underlie the watershed in which Camanche Reservoir is located. Intrusive rocks of the Sierra Nevada batholith have been studied extensively and range in age from Triassic to Cretaceous (e.g., Chen and Moore, 1982). Syngenetic mineral deposits, such as the massive sulfide deposits of Jurassic age represented by the Penn Mine in this study area, are pre-accretionary and reflect the hydrothermal and geochemical processes that occurred at the time the rocks were formed (e.g., Albers, 1981). These processes formed economic deposits of copper and zinc in a setting similar to the back-arc spreading regime currently active in the Japan Sea, host to Kuroko-type massive sulfide deposits (e.g., Tono, 1974; Ohmoto and Skinner, 1983; Singer, 1986, 1992).

Mother Lode gold deposits, which were formed during the accretionary metamorphic process (Böhlke and Kistler, 1986), and the associated gold placer deposits have been exploited extensively beginning with the 1849 California gold rush. Production of gold occurred both from Mother Lode vein deposits such as those

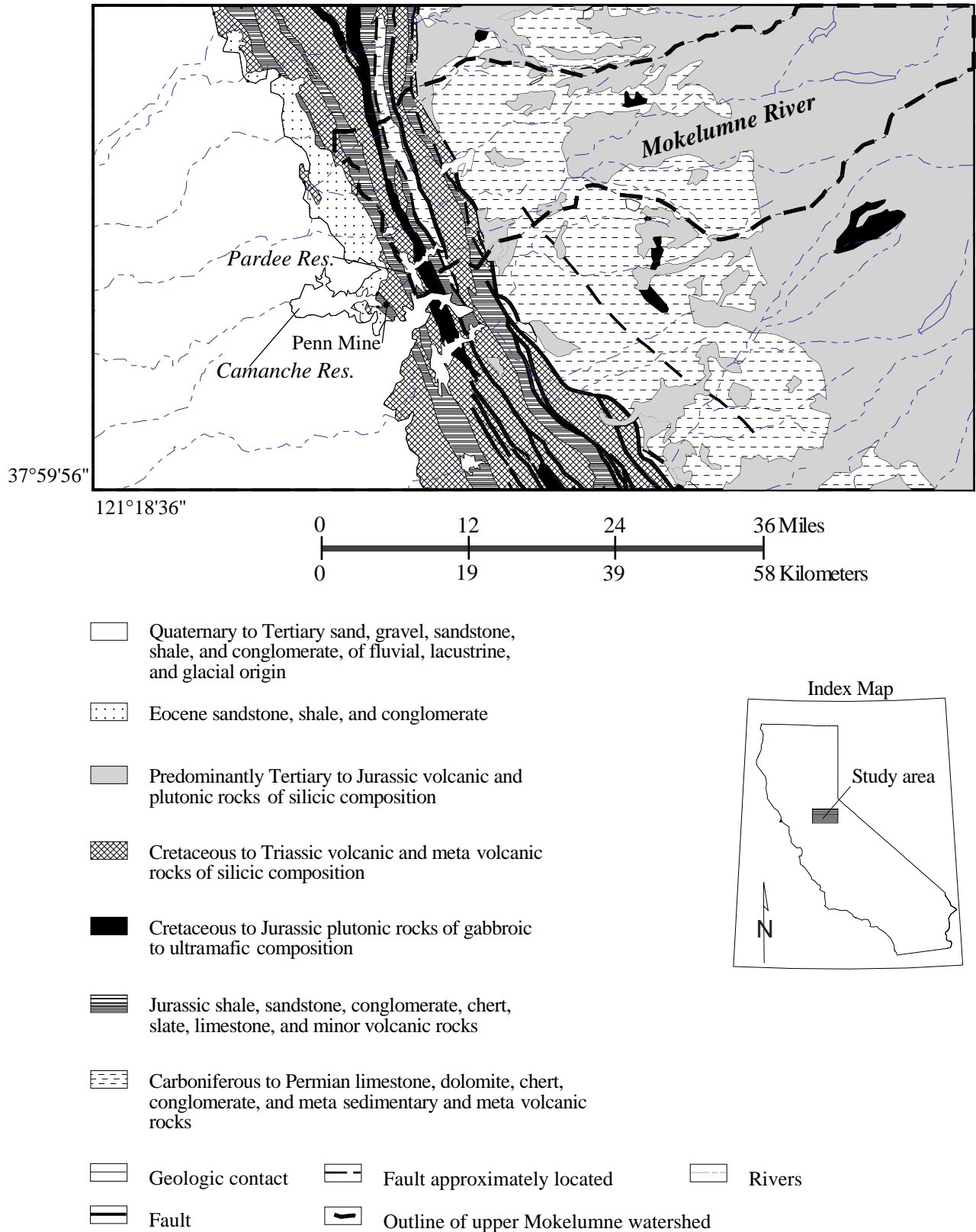


FIGURE 30.3—Geologic map of Mokelumne River drainage basin (after Strand and Koenig, 1965).

near Jackson and Angel's Camp in Calaveras County (Fig. 30.1) as well as from the extensive Tertiary gravel deposits on the western flank of the Sierra Nevada foothills (Lindgren, 1911; Knopf, 1929). Placer gold production from the Tertiary gravels in the drowned channel of the Mokelumne River was documented on the Jackson folio (Turner, 1894). Hydraulic mining of these gravels resulted in the dredge tailings shown on the Wallace 7.5' quadrangle map (USGS, 1962) in Camanche Reservoir (Lindgren, 1911) and some historical waste piles from hydraulic placer mining also exist on upland areas immediately adjacent to the Penn Mine. The bulk of the placer mining activity in the Mokelumne River channel occurred prior to the peak copper production at the Penn Mine (Turner, 1894; Lindgren, 1911; Clark and Lyndon, 1962). Base-metal skarn and polymetallic vein deposits formed during the emplacement of plutons into the roof pendants within the Sierra Nevada batholith and also have been exploited (e.g., Knopf, 1929; Albers, 1981). The Sierra Nevada batholith and associated rocks have had a long history of mineral production from a variety of mineral deposit types.

REGIONAL GEOCHEMISTRY

A regional geochemical soil survey of the Sacramento 1° x 2° quadrangle was carried out during the National Uranium Resources Evaluation (NURE) hydrogeochemical and stream-sediment reconnaissance program in the mid-1970s (NURE, 1982). Because the Sacramento quadrangle is in a semiarid climate, 1,374 of the 1,925 samples collected by the NURE program in this quadrangle were soils (NURE, 1982). These soil samples were collected at a depth of 10 to 50 cm below the surface, sieved, and analyzed using the same procedures as were the stream sediment samples (Price and Jones, 1979). Geochemical maps of these data clearly show that variations of elemental concentrations are controlled by the local geology; that is, the geochemistry of the soils and stream sediments reflect the underlying bedrock. Maps of copper, lead, and zinc concentrations in soils and stream sediments indicate localized sources of high concentrations of metals within the Sacramento 1° x 2° quadrangle. Sporadic high values of lead occur near some highways. Pardee Reservoir (Fig. 30.1), constructed in 1928 by EBMUD, acts as a trap for sediments derived from the upper reaches of the Mokelumne River watershed. A drainage overlay on the geochemical maps shows no sources for these metals other than the Penn Mine in the Mokelumne drainage below Pardee Reservoir that could contribute directly to the metal load in Camanche Reservoir. The major sources of sediments for Camanche Reservoir are therefore the small tributary streams draining into Camanche Reservoir from the north and south, and the short stretch of the Mokelumne River below Pardee Dam.

PENN MINE AREA

Copper was discovered in the California Foothill copper-zinc belt (CFB) in 1860 at the Quail Hill Mine about 30 km southeast of the Penn Mine (Fig. 30.1). By 1863, sixteen mines were operating in the CFB and smelters were operating at the Penn, Buchanan, and La Victoria Mines (Heyl, 1948). The mines of the CFB had a varied history of production and quiescence over the period from 1860 to 1957. The bulk of the production at the Penn Mine occurred between 1899–1919 (Clark and Lyndon, 1962).

Six thousand tons of zinc were recovered between 1943 and 1946 from the early mill tailings which averaged 7.5% zinc. More than 100,000 tons of massive sulfide ore was produced between 1947 and 1952 (Goodwin, 1957). The last production was in the 1955–1957 time period; exploration for additional ore reserves at the Penn Mine was discontinued in 1959. The Penn Mine was the largest producer in the CFB with a combined production of nearly 1 million tons of massive sulfide ore through 1957. According to Clark and Lyndon (1962), cumulative production from the Penn Mine was 41,250 tons of copper, 11,100 tons of zinc, 600 tons of lead, 2.2 million ounces of silver and 68 thousand ounces of gold. Following accepted industry practice during this period, waste rock and mill tailings were placed in Mine Run and Hinckley Run (Fig. 30.2), tributaries to the Mokelumne River (Finlayson and Rectenwald, 1978; Peterson, 1985, 1988; Bond, 1988); smelter slag was placed along the shoreline of the Mokelumne River (Wiebelt and Ricker, 1948), in an area that is now inundated seasonally by Camanche Reservoir (Parsons et al., 1998).

Peterson (1985) mapped chloritic, hematitic, sericitic, and silicified alteration zones surrounding the shafts of the Penn Mine. The various phases of the Gopher Ridge Volcanics (Clark, 1964) dip near vertically in the vicinity of the mine, and the hydrothermal alteration is assumed to be associated with the ore horizons. Near the mine, the rocks are mostly pyroclastic with less abundant flows and an intrusive felsic quartz porphyry. The massive sulfide ore bodies are within and adjacent to these felsic quartz porphyry intrusions (Heyl et al., 1948). Parts of the tuffs and the felsic quartz porphyry have been altered and subsequently metamorphosed to a sericitic schist (Schmidt, 1978; Peterson, 1985). Heyl et al. (1948) described lenses of banded and schistose massive sulfide ore that plunge downdip along two north-northwest-trending zones of alteration. Contacts of the ore and wall rock are gradational and the intensity of the alteration decreases away from ore. The massive ore is a mixture of fine-grained pyrite, chalcopyrite, and sphalerite with lesser amounts of galena, bornite, and tetrahedrite-tennantite. Gangue minerals include calcite, barite, and quartz. Gypsum is noted in some museum specimens from Penn Mine (M. Parsons, Stanford Univ., written commun., 1996) however the origin of the gypsum is unknown.

Geochemical studies of the alteration zones surrounding the Penn Mine (Peterson, 1988) showed that copper, zinc, lead, cadmium, silver, barium, and boron are concentrated in the ore bodies. Concentrations of copper, zinc, and lead in the surrounding rocks away from the ore zones (Peterson, 1988) are generally near crustal abundance (CA) values (Fortescue, 1992). In the surrounding rocks, copper ranges from <10 to 150 ppm, [CA_{Cu} = 68 ppm], zinc ranges from 50 to 150 ppm [CA_{Zn} = 76 ppm], and lead ranges from <10 to 20 ppm [CA_{Pb} = 13 ppm]. Iron and manganese are slightly enriched in chloritic alteration zones surrounding ore, and potassium is enriched in the sericitic schist. Peterson (1988) stated that the metal zonation patterns are very similar to those surrounding the Kuroko-type massive sulfide deposits in the Hokuroko District in Japan (Tono, 1974).

Prior to the construction of Mine Run Dam in 1978, erosion of these historical mine waste piles from production at the Penn Mine resulted in discharge of metal-rich sediments from Mine Run into the upper part of Camanche Reservoir (Fig. 30.2). The construction of Mine Run Dam and associated upstream impoundments has been largely successful at blocking the transport of metal-rich sediment eroded from the waste piles at Penn Mine, but has been less successful in preventing the discharge of acidic metal-rich

drainage waters to Camanche Reservoir. Uncontrolled releases of ARD occurred at Mine Run Dam during six of the wet seasons (November-April) between 1978–86, and then again in March 1993 after a prolonged drought during 1987–92. In March 1993, EBMUD installed a lime neutralization plant designed to treat the acidic discharge during high-flow conditions to pH values between 7 and 9 and to remove more than 99% of the dissolved Cu, Zn, and Cd (J. Landy, U.S. Environmental Protection Agency, written commun., 1995). Litigation in state and federal courts has resulted in classification of Mine Run Dam as a point source. The issuance of an NPDES (National Pollutant Discharge Elimination System) permit for the site has been suspended pending settlement between the litigants, during which time a draft Environmental Impact Report for long-term remediation of the site was prepared (Golder and Associates Inc., 1996).

SEDIMENTS IN CAMANCHE RESERVOIR

Camanche Reservoir contains sediments with elevated concentrations of copper, zinc, and cadmium that have been suspected of contributing to fish mortality during specific events since its construction in 1964 (Slotton et al., 1994). The historical waste piles at the Penn Mine were assumed to be the source of these metals (E.V.S. Consultants, 1989). These studies also showed that elevated ore-metal concentrations had accumulated in the deepest part of the reservoir near the dam where the particle size of the sediment was smallest. The present study was conducted to evaluate the distribution and lead isotope signature of trace and ore metals in sediments as a function of distance along the drowned stream channel within Camanche Reservoir.

SAMPLE COLLECTION AND PRESERVATION

Detailed sampling of the water and bottom sediments of Camanche Reservoir was conducted in June 1992 by a team of researchers from the University of California, Davis. The overall sampling plan (Slotton et al., 1994) included about 65 sites; localities of the most intensively studied sites are shown on Figure 30.4. Eleven intact core samples were carefully collected by divers from eight sites in the drowned Mokelumne River channel. Refrigerated samples of surficial sediment were shipped to the USGS laboratories in Denver shortly thereafter for chemical and lead isotope analysis. Steven Bond (California Regional Water Quality Control Board—Central Valley Region) provided a sample of sediment retrieved from the state fish hatchery below Camanche Dam following the 1989 fish kill. We report chemical and lead isotope data here for samples from these sites, plus the sample from the fish hatchery. The sample from site W4-4, although not from a drowned channel locality, is from the deepest part of the reservoir where fine-grained suspended sediment has accumulated and will be treated as a channel sample from the W4 transect. In addition, five NURE soil samples (NURE, 1982) collected in 1976 were retrieved from the National Geochemical Sample Archive for analysis to evaluate the isotopic composition of lead in the surrounding soils.

ANALYTICAL METHODS

To determine the labile metal concentrations, we have adapted the partial digestion procedures developed by Chao (1984). We used a 2M HCl-1% H_2O_2 partial digestion procedure for the study

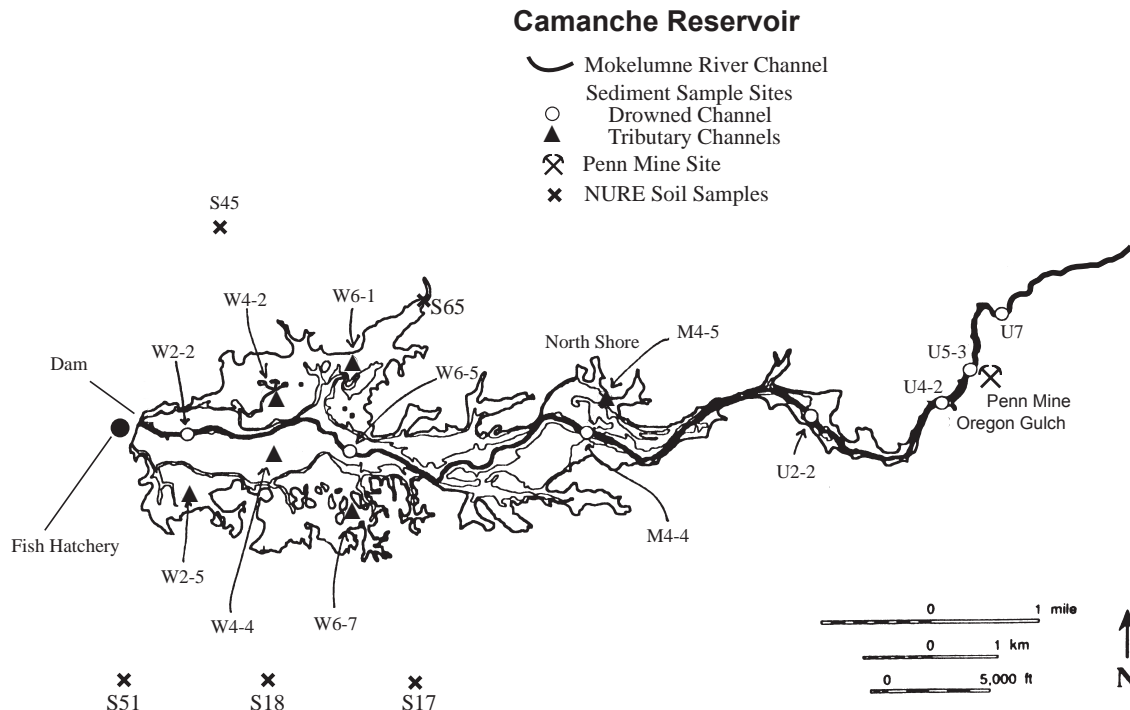


FIGURE 30.4—Map of Camanche Reservoir showing localities of sediment samples and NURE soil samples.

of metals derived from ARD (Gulson et al., 1992). Metals carried in ARD tend to precipitate with the iron- and manganese-oxhydroxide phases. Two grams of dried sediment were placed in a sealed 50 ml centrifuge tube and agitated in a warm (55°C) water bath for two hours. After digestion, the samples were centrifuged and the solution pipetted off for determination of the labile metal concentrations and the lead isotope compositions. Total digestion chemistry (HCl, HNO₃, HF, and HClO₄; 0.2 g dried and ground sediment) and ICP-AES analyses were performed using the methods described by Briggs (1990). The 2M HCl-H₂O₂ partial digestion procedure is described by Church et al. (1993). Lead was separated from the 2M HCl-H₂O₂ solution by ion chromatography in the HBr medium and was analyzed on a 68° sector, 12" NBS-type solid-source mass spectrometer (Church et al., 1993). Analytical precision of the ICP data is 1–2% and the precision of the lead isotope ratios is ± 0.1% per mass unit. The Buffalo River sediment

certified standard reference material (SRM–2704) was run as an external check on analytical precision and accuracy.

RESULTS

Lead isotope data for the NURE soil samples, the sediment sample from the fish hatchery collected in 1989, the Camanche Reservoir sediments and Penn Mine ores are in Table 30.1. Geochemical data for the Camanche Reservoir sediment samples are in Table 30.2 (total digestion) and labile metal concentrations are in Table 30.3 (2M HCl-H₂O₂ digestion). Minor discrepancies between the 2M HCl-H₂O₂ digestion data and the total digestion data at low concentrations are the result of differences in analytical precision and dilution factors in the two methods. Comparisons of our total digestion lead data with graphite furnace

TABLE 30.1—Lead isotope and chemical data for sediment samples from Camanche Reservoir, California study area.

Sample no.	Distance km	Latitude Deg Min Sec	Longitude Deg Min Sec	Pb ppm ^{1,2}	Pb ppm ³	²⁰⁶ Pb	²⁰⁷ Pb	²⁰⁸ Pb
						²⁰⁴ Pb	²⁰⁴ Pb	²⁰⁴ Pb
Drowned Channel Samples, Camanche Reservoir								
U7	1.0	38° 14' 33"	120° 52' 18"	28	11	18.868	15.622	38.588
U5-3	3.2	38° 14' 2"	120° 52' 47"	54	30	18.530	15.600	38.287
U4-2	4.0	38° 13' 42"	120° 53' 8"	--	27	18.504	15.576	38.215
U2-2	6.8	38° 13' 30"	120° 54' 30"	63	29	18.632	15.585	38.325
M4-4	10.7	38° 13' 45"	120° 56' 50"	--	28	18.743	15.612	38.455
W6-5	14.7	38° 13' 17"	120° 59' 8"	49	29	18.844	15.614	38.534
W4-4B	16.5	38° 13' 10"	120° 59' 58"	--	21	18.905	15.652	38.668
W4-4BD	16.5	38° 13' 10"	120° 59' 58"	--	21	18.896	15.640	38.630
W4-4C	16.5	38° 13' 10"	120° 59' 58"	--	17	18.900	15.641	38.647
W4-4 (n=3)	16.5	38° 13' 10"	120° 59' 58"	39	20	18.900	15.644	38.648
W2-2	18.0	38° 13' 23"	121° 0' 48"	46	27	18.984	15.648	38.642
Drowned Tributary Samples, Camanche Reservoir								
M4-5	10.5	38° 13' 18"	120° 56' 10"	--	18	18.980	15.638	38.723
W6-1	14.6	38° 14' 4"	120° 59' 8"	19	16	18.944	15.654	38.726
W6-7	14.8	38° 12' 47"	120° 59' 9"	25	22	18.901	15.634	38.636
W4-2B	16.6	38° 13' 47"	120° 59' 58"	10	14	19.425	15.672	39.300
W2-5	17.9	38° 12' 53"	121° 0' 45"	12	18	19.047	15.654	38.787
Average (n=5)						18.968	15.645	38.718
Sediment from Camanche Dam Fish Hatchery (1989)								
Hatchsd-89	20	38° 13' 30"	121° 1' 30"	--	23	18.86	15.623	38.537
NURE Soil Samples								
SXDE017 ⁴	13.0	38° 12' 22"	120° 58' 11"	15	20	19.187	15.643	38.855
SXDE065	13.4	38° 14' 23"	120° 58' 32"	25	18	18.753	15.681	38.630
SXDE018	16.3	38° 12' 14"	120° 59' 54"	44	48	18.768	15.616	38.288
SXDE045	16.8	38° 14' 25"	121° 0' 19"	23	24	18.885	15.621	38.499
SXDD051	19.8	38° 12' 13"	121° 2' 6"	17	18	18.800	15.651	38.504
Average (n=4)						18.877	15.648	38.569
Ores from the Penn Mine								
Penn Mine	3.2	38° 13' 52"	120° 52' 25"			18.284	15.577	38.079
Penn Mine						18.302	15.569	38.075
Penn Mine						18.296	15.565	38.057
Penn Mine						18.278	15.562	38.045
Average (n=4)						18.290	15.568	38.064
Buffalo River Sediment Standard								
SRM-2704 ⁵					130	18.757	15.623	38.394

¹Lead concentration data for the Camanche Reservoir sediments are from Slotton et al. (1994)

²Lead concentration data for the NURE soil samples are from NURE (1982).

³Lead concentration data are from this study, total digestion data.

⁴Sample treated as an outlier for calculation of average lead isotope composition.

⁵Lead isotope data from this study; no certified value available from NIST.

TABLE 30.2—Geochemical data from total digestions¹ of sediment samples from Camanche Reservoir, California study area.

Sample no.	Na wt. %	K wt. %	Mg wt. %	Ca wt. %	Al wt. %	Fe wt. %	Ti wt. %	P wt. %	Mn ppm	V ppm	Cr ppm	Co ppm	Ni ppm
Drowned Channel Samples, Camanche Reservoir													
U7	1.50	2.20	2.30	1.20	9.10	5.60	0.48	0.10	1000	210	210	29	87
U5-3	1.30	1.70	1.90	1.30	9.20	6.40	0.54	0.13	760	200	170	40	76
U4-2	1.10	1.40	1.50	1.20	7.70	4.90	0.47	0.10	830	170	140	31	61
U2-2	1.10	1.50	1.20	1.20	9.60	5.80	0.53	0.11	1000	180	120	32	55
M4-4	1.10	1.70	1.00	1.20	9.70	5.10	0.54	0.10	1400	150	94	28	44
W6-5	1.20	1.70	1.00	1.30	9.80	5.50	0.55	0.12	2900	140	73	31	39
W4-4B	1.50	1.70	1.30	2.00	9.70	5.40	0.61	0.12	1600	150	83	26	40
W4-4BD	1.50	1.70	1.20	1.90	9.40	5.30	0.60	0.11	1500	140	80	26	39
W4-4C	1.60	1.70	1.40	2.30	9.00	5.20	0.61	0.11	1400	150	91	24	37
W4-4 (n= 3)	1.50	1.70	1.30	2.10	9.40	5.30	0.61	0.11	1500	150	85	25	39
W2-2	1.10	1.60	1.00	1.10	10.00	5.90	0.56	0.15	2700	150	73	33	41
Drowned Tributary Samples, Camanche Reservoir													
M4-5	2.50	2.70	0.28	1.90	7.70	2.20	0.25	0.03	280	55	14	6	5
W6-1	2.60	2.20	0.59	2.50	8.90	2.20	0.34	0.03	490	61	22	9	11
W6-7	2.40	1.80	0.77	2.70	8.90	2.80	0.46	0.05	630	86	42	14	17
W4-2A	2.50	2.10	0.76	2.80	8.30	2.40	0.25	0.03	510	61	12	9	6
W4-2B	2.60	2.00	0.84	3.00	8.40	2.80	0.30	0.04	590	78	16	10	6
W4-2C	2.70	2.10	0.97	3.10	8.80	3.70	0.36	0.04	620	99	21	13	7
W4-2(mean)	2.60	2.10	0.86	3.00	8.50	2.90	0.30	0.04	570	79	16	11	6
W2-5	2.60	2.10	0.76	2.50	9.40	3.20	0.45	0.06	610	86	34	13	16
Sediment from Camanche Dam Fish Hatchery (1989)													
Hatchsd-89	0.54	0.85	0.65	0.75	5.80	4.80	0.31	0.33	3500	100	51	21	32
NURE Soil Samples													
SXDE017	2.10	1.20	1.20	3.50	8.50	4.70	0.63	0.08	720	170	97	17	29
SXDE065	2.00	1.20	0.77	2.80	9.30	4.20	0.63	0.07	1400	150	65	20	27
SXDE018	2.20	1.40	1.10	3.20	9.40	3.90	0.57	0.07	550	130	58	16	21
SXDE045	1.20	1.10	0.88	1.40	9.30	3.90	0.46	0.03	450	72	27	14	17
SXDD051	2.00	1.60	0.90	2.60	9.00	4.30	0.56	0.10	820	150	54	17	25
Buffalo River Sediment Standard (SRM-2704)													
This Study	0.68	2.10	1.30	2.90	6.70	4.50	0.36	0.11	620	98	160	18	47
Certified value ²	0.55	2.00	1.20	2.60	6.11	4.11	0.46	0.10	555	95	135	14	44
USGS value ³	0.61	1.93	1.24	2.70	6.10	4.15	0.41	0.10	577	94	142	15	43

atomic absorption spectroscopy (GFAAS) data in split samples reported by Slotton et al. (1994) are not as good as we would have hoped (Table 30.4); lead concentrations reported by Slotton et al. (1994) are generally higher than our total digestion results, copper data are generally comparable, and our zinc results are generally somewhat higher than those of Slotton et al. (1994). These discrepancies are judged to have no impact on the conclusions drawn from this study. Published lead concentrations for the NURE samples and the Buffalo River sediment (SRM-2704) compare well with our total digestion data and are within acceptable analytical limits of error (Table 30.1).

Slotton et al. (1994) and Slotton and Reuter (1995) also reported chemical analysis of the sediment samples from Camanche Reservoir for a limited number of metals by two methods, a total digestion followed by AAS/GFAAS and a cold, 6N HCl digestion in combination with extraction of acid volatile sulfide (AVS) followed by ICP-MS. Simultaneously extracted metal (SEM) data from Slotton et al. (1994) for copper and zinc from these samples are in Table 30.4. Our warm, 2M HCl-H₂O₂ digestion is considerably more aggressive than the AVS digestion. Where there is a significant concentration of iron oxides bonding metals in the sediments, the 2M HCl-H₂O₂ digestion recovers a larger portion of the

metals in the sediments than does the AVS digestion (compare the Cu and Zn concentrations by these two methods in Table 30.4).

DISCUSSION

Camanche Reservoir is an excellent site at which to demonstrate the utility of the lead isotope tracer method to fingerprint specific point sources of anthropogenic contamination. The reservoir is isolated from particulate metal sources upstream by the presence of Pardee Reservoir, built in 1928 (Fig. 30.3). The Penn Mine operated for many years following the completion of the Pardee Reservoir with major ore production taking place during World War II (Heyl, 1948). The surrounding tributaries to the reservoir contribute no additional anomalous sources of metals. Metals in the rocks can be separated from metals released by weathering and contamination using the chemical leach procedures outlined above. The fundamental reason that the lead isotope tracer technique works so well as a tracer of ARD is that the lead isotope signature of an ore deposit is often both uniform and distinct from that in the surrounding rocks, and the deposit has a large concentration enrichment of labile lead. In sharp contrast, the lead

TABLE 30.2—Continued

Sample no.	Cu ppm	Zn ppm	Pb ppm	As ppm	Cd ppm	Li ppm	Be ppm	Sr ppm	Ba ppm	Y ppm	La ppm	Ce ppm	Yb ppm
Drowned Channel Samples, Camanche Reservoir													
U7	74	200	11	11	<2.0	43	2	140	940	16	20	39	2
U5-3	690	2700	30	19	6.0	43	1	140	790	24	24	49	3
U4-2	260	1100	27	11	2.0	37	1	140	680	18	22	43	2
U2-2	230	840	29	12	<2.0	47	1	170	720	22	32	60	2
M4-4	170	640	28	12	<2.0	43	2	200	780	21	36	65	2
W6-5	99	480	29	<10	<2.0	40	2	250	870	23	42	76	2
W4-4B	81	390	21	<10	<2.0	36	2	330	870	22	38	71	3
W4-4BD	79	380	21	<10	<2.0	35	2	320	860	21	37	70	2
W4-4C	64	320	17	<10	<2.0	30	2	340	830	21	36	67	3
W4-4 (n=3)	75	360	20	<10	<2.0	34	2	330	850	21	37	69	3
W2-2	98	460	27	<10	<2.0	44	2	240	910	22	44	80	2
Drowned Tributary Samples, Camanche Reservoir													
M4-5	8	51	18	<10	<2.0	10	1	380	1100	13	23	42	1
W6-1	14	81	16	<10	<2.0	13	2	450	1000	16	24	46	2
W6-7	26	120	22	<10	<2.0	15	2	510	890	17	27	54	2
W4-2A	8	55	15	<10	<2.0	12	1	450	890	11	18	29	1
W4-2B	7	65	14	<10	<2.0	12	1	450	840	14	18	33	2
W4-2C	9	83	15	<10	<2.0	15	1	460	860	14	21	39	1
W4-2 (n=3)	8	68	15	<10	<2.0	13	1	450	860	13	19	34	1
W2-5	26	150	18	<10	<2.0	20	2	430	920	17	29	55	2
Sediment from Camanche Dam Fish Hatchery (1989)													
Hatchsd-89	100	650	23	16	<2.0	26	2	130	600	16	25	47	2
NURE Soil Samples													
SXDE017	20	81	20	<10	<2.0	19	3	570	710	21	30	57	2
SXDE065	26	89	18	13	<2.0	24	3	700	1000	18	34	56	2
SXDE018	24	87	48	<10	<2.0	23	2	610	910	19	29	55	2
SXDE045	24	92	24	<10	<2.0	40	3	350	790	29	45	89	3
SXDD051	19	98	18	<10	<2.0	18	3	490	860	17	29	50	2
Buffalo River Sediment Standard (SRM-2704)													
This Study	110	480	130	17	3.0	54	2	150	450	20	35	68	3
Certified value ²	99	438	161	23	3.5	--	--	130	414	--	--	--	--
USGS value ³	99	464	160	25	3.3	50	2	135	410	23	33	60	2

¹Analytical results from total digestion of 0.2 g of dried sediment, analyses by ICP-AES using method of Briggs (1990).

²Certified values from NIST (1988).

³USGS values from Wilson et al. (1994).

leached from uncontaminated sediments is characterized by variable and radiogenic lead isotope signatures and low concentrations. The large amounts of lead in the ore deposit overwhelm the contribution of labile lead released by weathering of unmineralized rocks. The effect of this mixing process is shown clearly by the data from this study (Fig. 30.5).

The lead isotope data from sediments from Camanche Reservoir (Fig. 30.6) show that the labile lead in sediment samples from the drowned Mokelumne River channel are the result of mixing between two well-defined end members: massive sulfide ores from the Penn Mine and sediments added to Camanche Reservoir by side tributaries. The lead isotope data from the Penn Mine are from five ore samples collected by Schmidt (1978) who studied the genesis of the deposit. The lead isotope data from four of the five sediment samples collected in this study from the drowned tributaries to Camanche Reservoir have very similar lead-isotope values and lie along a mixing line within analytical error and geologic variability (sampling variance) of the source rocks making up the sediments of the reservoir. The fifth tributary sample (W4-2B) is more radiogenic than the others; therefore, for the purpose of calculating a mean lead isotope composition of unmineralized rocks in the drainage basin, the lead isotope results

from this sample (W4-2B) were treated as an outlier.

The lead isotope data from sediment samples collected within the drowned Mokelumne River channel contrast sharply with those from the drowned tributary channels within Camanche Reservoir. The isotopic composition of labile lead in the stream-sediment sample (U7) collected from the Mokelumne River channel upstream of Camanche Reservoir is very similar to that of the tributaries (Fig. 30.6, Table 30.1). However, the results from sites adjacent to the Penn Mine (U5-3 and U4-2) show a marked difference in lead isotope composition indicating that the Penn Mine site is the source of significant lead contamination. Samples collected from successively greater distances down-channel from the Penn Mine show progressive dilution of the lead-isotope signature found in the sediments near the Penn Mine indicating that the effect of this contamination source is diluted by mixing with sediments derived from the surrounding unmineralized rock. On Figures 30.7A and 30.7B, the lead-isotope data have been used to calculate the percentage of the lead in each sample that can be attributed to sulfide mine wastes or acidic drainage from the Penn Mine. Average values calculated from the tributary drainages (see Table 30.1) were used as the starting lead isotope compositions (data are shown as dashed lines on Figs. 30.7A and B). Note that

TABLE 30.3—Geochemical data from 2M HCl-H₂O₂ leaches of sediment samples from Camanche Reservoir, California study area.

Sample no.	Na ppm	K ppm	Mg ppm	Ca ppm	Al ppm	Fe ppm	Ti ppm	P ppm	Mn ppm	V ppm	Cr ppm
Drowned Channel Samples, Camanche Reservoir											
U7	23	220	4400	2700	7100	16000	64	810	580	17	29
U5-3	66	740	6500	3200	14000	36000	260	1300	560	53	40
U4-2	67	910	6800	4000	13000	30000	310	1200	810	54	40
U2-2	68	1100	4700	3300	10000	24000	350	800	790	54	27
M4-4	74	1200	3600	3000	8300	19000	360	680	1100	50	12
W6-5	160	2800	4800	3800	13000	28000	760	1100	3700	88	15
W4-4B	150	2700	4400	3300	11000	23000	800	1000	1400	69	27
W4-4BD	160	3100	5000	3700	13000	26000	900	1100	1500	74	29
W4-4C	130	2800	4400	3100	11000	22000	890	1100	1400	59	30
W4-4 (n=3)	150	2900	4600	3400	12000	24000	860	1100	1400	67	29
W2-2	150	2600	4500	3700	13000	28000	660	1200	2900	82	27
Drowned Tributary Samples, Camanche Reservoir											
M4-5	26	450	600	509	1400	3100	160	190	120	6	2
W6-1	98	1400	2000	2000	4200	7300	580	280	300	28	6
W6-7	130	1500	2300	2800	5400	8700	600	480	430	29	9
W4-2A	49	1700	2400	1100	3600	7800	670	320	290	21	3
W4-2B	58	1800	2600	1400	3800	8200	720	430	300	22	4
W4-2C	71	2100	3000	1400	4500	9700	860	460	240	21	4
W4-2 (n=3)	60	1900	2700	1300	4000	8600	750	400	280	21	4
W2-5	82	1800	3100	2600	6000	11000	760	510	380	27	10
Sediment from Camanche Dam Fish Hatchery (1989)											
Hatchsd-89	90	900	1400	2300	5300	27000	170	3000	3200	44	8
NURE Soil Samples											
SXDE017	67	190	1700	2600	2300	3800	130	510	120	13	5
SXDE065	200	660	1700	5900	3600	9000	630	590	1700	35	9
SXDE018	260	1100	3100	5100	4700	5800	410	660	200	23	5
SXDE045	57	660	2500	5100	3100	2200	71	130	110	7	2
SXDD051	130	1100	1400	4500	3800	6200	200	780	550	27	7
Buffalo River Sediment Standard											
SRM-2704	71	340	7700	26000	7300	21000	57	900	440	13	86

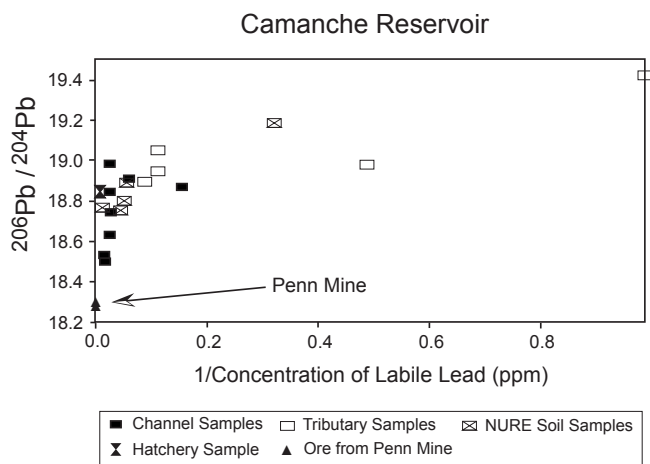


FIGURE 30.5—Plot of ²⁰⁶Pb/²⁰⁴Pb data versus 1/concentration of labile lead (in ppm-1) in shallow NURE soils, Camanche Reservoir sediments, sediment from the Camanche Dam fish hatchery, and Penn Mine ores. The isotopic composition of lead in sediments unaffected by the ore-lead from the Penn Mine becomes systematically more radiogenic as the concentration of labile lead decreases.

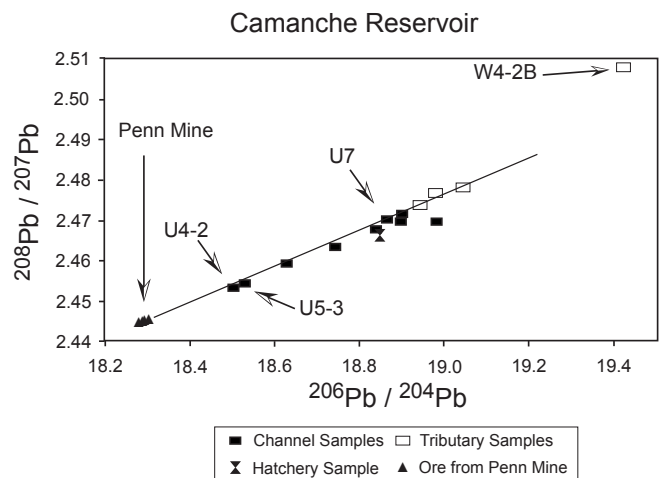


FIGURE 30.6—Plot of ²⁰⁶Pb/²⁰⁴Pb versus ²⁰⁸Pb/²⁰⁷Pb of lead isotope data from Table 30.1; lead isotope data for sediment samples from the Mokelumne River, Camanche Reservoir, and the fish hatchery lie along a mixing line between Penn Mine ore and sediment samples from the tributary streams that drain into Camanche Reservoir.

TABLE 30.3—Continued

Sample no.	Co ppm	Ni ppm	Cu ppm	Zn ppm	Pb ppm	As ppm	Cd ppm	Li ppm	Be ppm	Sr ppm	Ba ppm
Drowned Channel Samples, Camanche Reservoir											
U7	17	29	46	98	6	5	< 0.3	12	0.2	29	69
U5-3	40	40	780	2800	40	12	7.9	13	0.5	26	150
U4-2	27	40	350	1300	40	11	4.0	13	0.5	40	180
U2-2	27	27	200	700	27	4	1.4	11	0.5	41	160
M4-4	12	12	140	500	25	4	2.5	9	0.5	37	170
W6-5	29	15	120	500	29	6	1.5	10	1.2	59	380
W4-4B	14	14	82	370	14	4	1.0	10	1.0	41	300
W4-4BD	15	15	88	400	15	3	1.0	10	1.0	44	340
W4-4C	15	15	74	330	15	4	0.7	9	0.7	44	280
W4-4 (n=3)	14	14	82	370	15	4	1.0	10	1.0	43	310
W2-2	27	14	82	410	27	5	0.8	10	1.1	55	380
Drowned Tributary Samples, Camanche Reservoir											
M4-5	2	1	6	32	2	< 2	< 0.3	1	< 0.3	6	32
W6-1	7	4	14	70	8	< 3	< 0.5	3	0.4	28	170
W6-7	9	6	29	100	10	< 3	< 0.5	3	0.4	29	180
W4-2A	5	2	7	35	1	< 2	< 0.3	4	< 0.2	14	91
W4-2B	5	2	7	44	1	< 2	< 0.3	4	0.1	15	88
W4-2C	6	3	7	57	2	< 2	< 0.3	5	0.1	14	110
W4-2 (n=3)	5	2	7	45	2	< 2	< 0.3	5	0.1	14	96
W2-5	8	5	27	120	8	< 3	< 0.5	4	0.4	27	140
Sediment from Camanche Dam Fish Hatchery (1989)											
Hatchsd-89	17	11	68	670	16	7	2.4	3	0.5	23	170
NURE Soil Samples											
SXDE017	6	4	5	13	3	< 2	< 0.3	1	0.2	26	120
SXDE065	11	6	17	36	18	< 3	< 0.5	1	0.7	87	330
SXDE018	7	5	11	34	43	< 2	< 0.3	3	0.4	66	270
SXDE045	3	3	5	13	15	< 2	< 0.3	1	1.0	77	160
SXDD051	9	7	7	41	16	3	< 0.3	2	0.4	43	150
Buffalo River Sediment Standard											
SRM-2704	10	29	100	390	140	13	2.9	14	0.4	43	86

Analytical results by ICP-AES using method of Church et al. (1993).

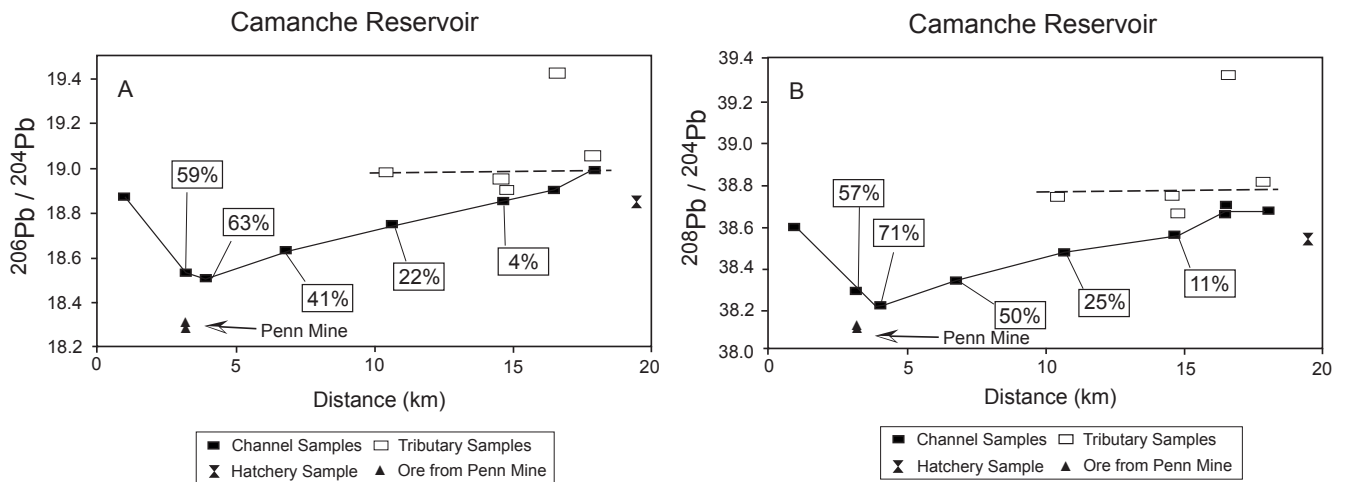


FIGURE 30.7—Plot of lead-isotope data for sediments from Camanche Reservoir and ore samples from Penn Mine versus distance along the drowned Mokelumne River channel: A. $^{206}\text{Pb}/^{204}\text{Pb}$ and B. $^{208}\text{Pb}/^{204}\text{Pb}$. For each of the samples from the drowned Mokelumne River channel, the isotope data have been used to calculate the percentage of the lead in each sample that can be attributed to the Penn Mine. Average values calculated from the tributary drainages (see Table 30.1) were used as the starting lead isotope compositions (data are shown as a dashed line).

TABLE 30.4—Lead, copper and zinc concentrations in sediment samples from Camanche Reservoir, California determined by different analytical procedures.

Sample no.	Pb	Pb	Pb	Cu	Cu	Cu	Cu	Zn	Zn	Zn	Zn
	ppm (TD) ¹	ppm (TD) ²	ppm (LH) ²	ppm (TD) ¹	ppm (TD) ²	ppm (LH) ²	ppm (AVS) ¹	ppm (TD) ¹	ppm (TD) ²	ppm (LH) ²	ppm (AVS) ¹
	GFAAS	ICPAES	ICPAES	GFAAS	ICPAES	ICPAES	ICPMS	GFAAS	ICPAES	ICPAES	ICPMS
Drowned Channel Samples, Camanche Reservoir											
U7	28	11	6	56	74	46	<0.1	125	200	98	1
U5-3	54	30	40	654	690	780	450	2345	2700	2800	1887
U4-2	--	27	40	258	260	350	--	903	1100	1300	--
U2-2	63	29	27	217	230	200	170	759	840	700	639
M4-4	--	28	25	20	170	140	--	122	640	500	--
W6-5	49	29	29	86	99	120	160	457	480	500	339
W4-4 (n=3)	39	20	15	82	75	82	32	397	360	370	230
W2-2	46	27	27	89	98	82	57	438	460	410	355
Drowned Tributary Samples, Camanche Reservoir											
M4-5	--	18	2	5	8	6	5	34	51	32	24
W6-1	19	16	8	25	14	14	10	133	81	70	32
W6-7	25	22	10	38	26	29	20	195	120	100	64
W4-2 (n=3)	10	15	2	16	8	7	2	77	68	45	16
W2-5	12	18	8	17	26	27	22	95	150	120	88

¹GFAAS and ICPMS, data from Slotton et al. (1994); (TD), total digestion; (AVS), acid volatile sulfide, simultaneously extracted metals.

²ICPAES, data from this study; (TD), total digestion; (LH), 2M HCl-1%H₂O₂ leach

the source of contamination can be readily traced even though the massive sulfide deposits at Penn Mine are relatively low in lead compared with other massive sulfide deposits, and the maximum concentration of labile lead in reservoir sediment samples reaches only 40 ppm.

Comparison of the distribution patterns of labile copper and zinc in Camanche Reservoir sediments show that the concentrations of these metals mimic the trace-metal distribution pattern of lead. We interpret these data to indicate that the Penn Mine is also the source of these metals (Figs. 30.8 A-C). This behavior contrasts with that of titanium, strontium, and cobalt which are not

enriched in the Penn Mine deposit but rather reflect the litho-geochemistry (Figs. 30.8 D-F), and with manganese and vanadium (Figs. 30.8 G-H) which are enriched in the fine-grained sediments in the deepest part of the reservoir near the dam site (Slotton et al., 1994). Other lithophile element concentrations are given in Tables 30.2 and 30.3; the behavior of these groups of trace metals is indicated by the elements plotted on Figures 30.8 D-F. Note that the concentrations of metals in sediment samples from the tributaries and the NURE soil samples are markedly lower for the ore metals copper and zinc, nearly identical for titanium and strontium, and somewhat lower for cobalt, manganese, and vanadium. These

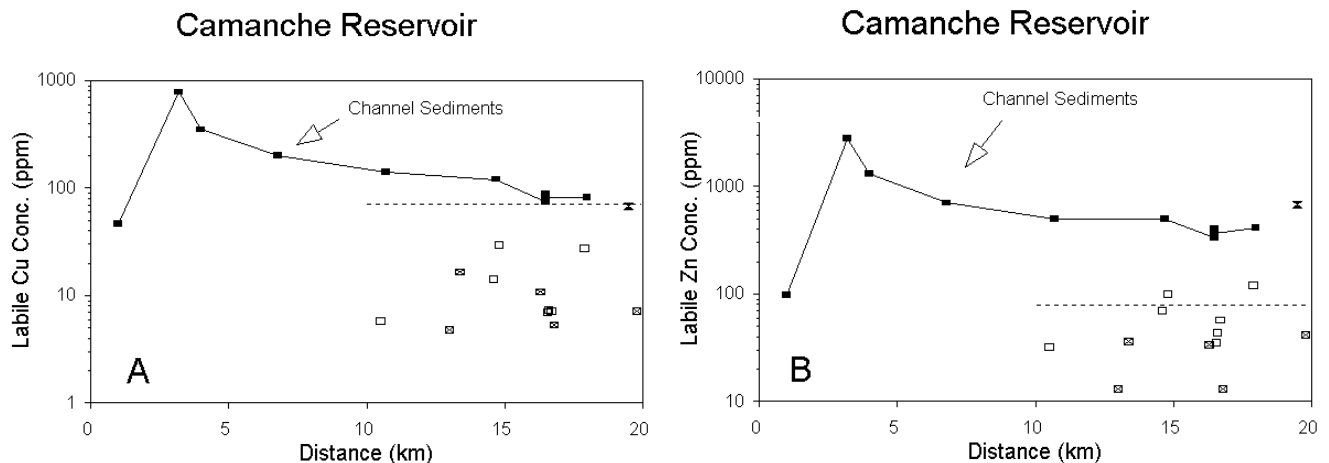


FIGURE 30.8—Log plots showing the profile of selected metal concentrations leached from various sediment and soil samples (Table 30.3; sample key is the same as on Figs. 30.5–30.7) plotted against distance along the drowned Mokelumne River channel: A, copper (Cu); B, zinc (Zn); C, lead (Pb); D, titanium (Ti); E, strontium (Sr); F, cobalt (Co); G, manganese (Mn), and H, vanadium (V). Dashed lines represent average crustal abundances (Fortescue, 1992).

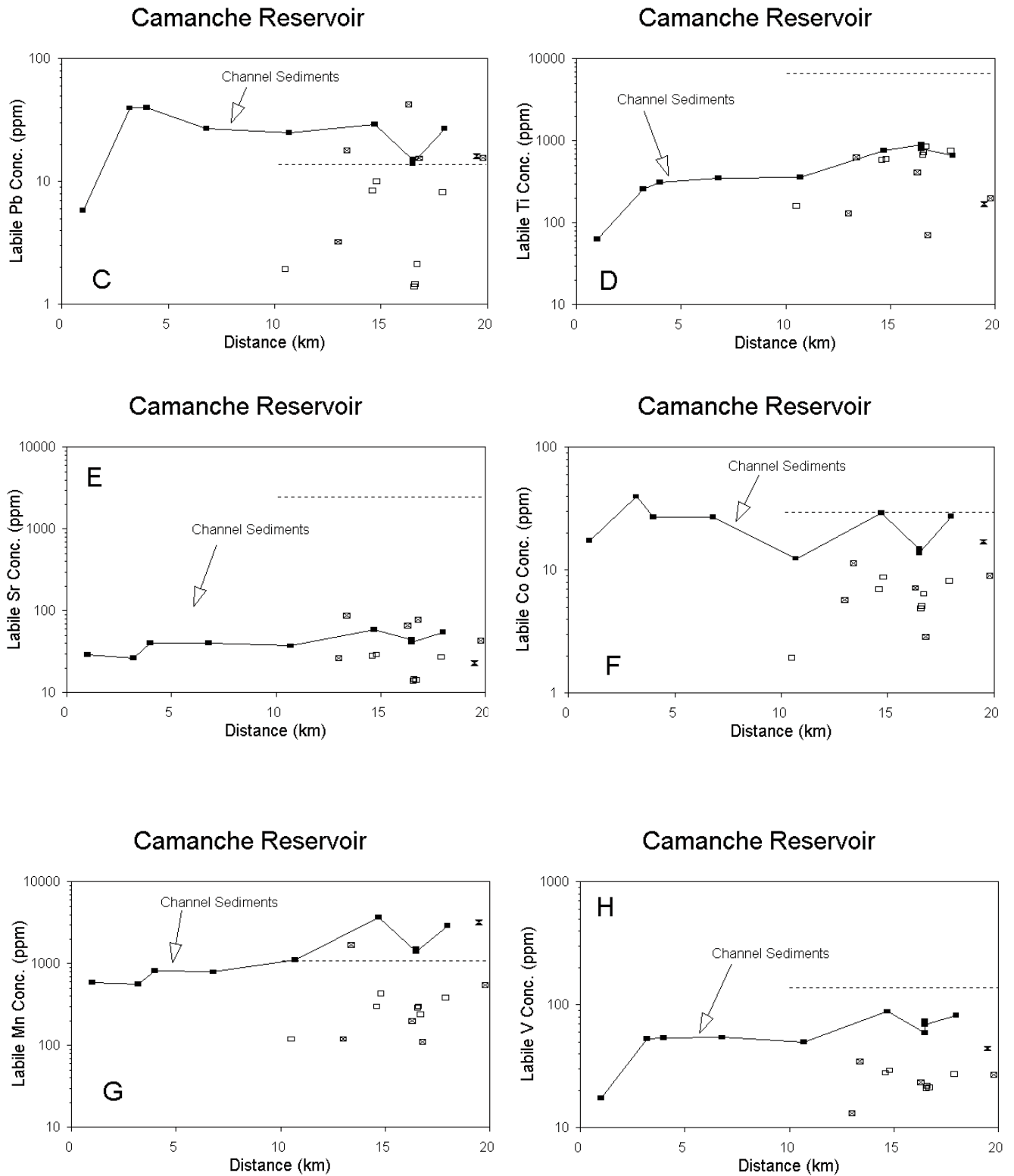


FIGURE 30.8—Continued

trace element data indicate that metals derived from the erosion and transport of materials to the reservoir by surface streams from the surrounding area do not contain elevated concentrations of copper, lead, and zinc. Thus, this is a second line of evidence that indicates that the source of the contaminant metals is from the Penn Mine alone.

The contrast in behavior between titanium and strontium with that of manganese and vanadium is of fundamental importance in understanding the distribution of labile metals (Church et al., 1987). Because titanium is a high-field-strength metal, it is tightly bound in silicate phases in rocks and is not readily mobilized during weathering processes. Strontium is likewise tightly bound in silicate mineral lattices substituting for calcium. Notice that the concentration of labile titanium and strontium are substantially less than the crustal abundances (Fortescue, 1992) shown by the dashed line on each of the figures. The concentration of labile titanium in the drowned channel samples increases in the sediments of Camanche Reservoir as a function of distance reflecting the increased concentration of titanium in sediments from the side tributaries, whereas the concentration of strontium is nearly constant. Thus, the distributions of these two metals in the sediments of the reservoir reflect the geology of the source rocks present in the drainage basin.

The behavior of manganese and vanadium, however, is quite different; both metals are readily mobilized during weathering. The concentrations of these two transition metals are markedly lower in the sediments from the tributaries than in those from the drowned Mokelumne River channel. Enrichment of these metals is a very common phenomenon in the hydromorphic mineral phases, that is, these labile metals are readily sorbed by iron-oxide coatings on sediment grains in streams. Likewise, the other transition metals copper, cobalt, nickel, and zinc behave similarly to manganese, as does lead. Microscopic examination of the sediment grains in these samples following the acid leach procedure shows that the iron-oxide coatings on the sediment grain surfaces had been completely removed. Thus, we interpret the site of residence of these potentially toxic metals to be the hydromorphic, cryptocrystalline (amorphous-to-poorly-crystalline) hydrous iron-oxide minerals that coat the sediment grains.

Comparison of the lead isotope (Fig. 30.7) and geochemical data (Fig. 30.8) from the 1989 fish hatchery sediment sample with data from the drowned channel sediment samples indicates that the sediment in the fish hatchery at the time of the 1989 fish kill has both a chemical and lead isotope composition like that of the sediment from the deep part of Camanche Reservoir. At the time, the water intake for the fish hatchery was low in the dam. Following this fish kill incident, the water intake for the hatchery was replaced with a hypolimnetic aeration system to provide water for the fish hatchery (J. Miyamoto, EBMUD, oral commun., 1999). There have been no subsequent fish kills in the fish hatchery at Camanche Dam following these recommended changes in operation. Slotton et al. (1994) showed that the metal-laden sediments in the reservoir occurred primarily below the 140-foot level and that resuspension of these sediments by wind action is the most likely scenario for mobilization of metal-laden sediments to the water column. Because the metal-laden sediments occurred primarily below the 140-foot level within the reservoir, Slotton et al. (1994) recommended maintaining the water level at 180 feet or higher to minimize contamination of the fish hatchery with metal-laden sediments.

Comparison of the lead data in the tributary samples with the NURE soil samples indicates a separate, exotic source of lead is present in at least three of the five NURE soil samples. Total lead concentrations in the tributary samples are below the crustal abundance value (Fig. 30.8C). However, the concentration of lead in the NURE soil samples is markedly enriched in four of the five samples as shown on Figures 30.5 and 30.8C. Three of these samples plot to the right of the mixing line between the Penn Mine ore lead and the tributary samples as shown on Figure 30.9, indicating the presence of an exotic component of lead derived from a different geologic provenance. Also shown on this figure are the total and labile lead isotopic compositions determined by Shirahata et al. (1980) from dated sediment intervals from an isolated alpine lake in the Sierra Nevada range. The higher the labile lead concentration in these alpine lake sediment samples, the farther away from the mixing line the labile lead components plot. In their study of the labile lead component in dated sediments from the Great Lakes, Graney et al. (1995) also defined an exotic lead component that plots to the right of the mixing line shown on Figure 30.9, but at higher $^{206}\text{Pb}/^{204}\text{Pb}$ values. Estimates of the historical production of atmospheric lead from combustion of leaded gasoline exceeds the total production of atmospheric lead contributed from smelting of ores and from the combustion of coal worldwide by almost two orders of magnitude by 1970 (Graney et al., 1995, Fig. 5). We interpret the data from the NURE soil samples to represent this exotic atmospheric gasoline-lead component. NURE soil samples collected from semiarid climatic zones and archived by the USGS thus represent a major historical resource for the measurement of changes in lead contamination from the combustion of gasoline in these soil samples. Recollection of materials from the same sites

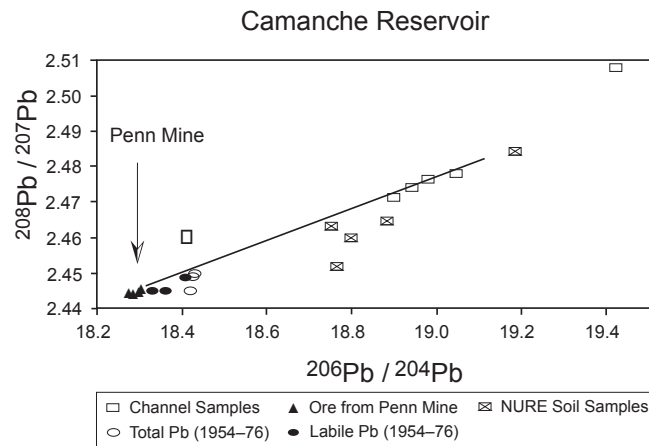


FIGURE 30.9—Plot of $^{206}\text{Pb}/^{204}\text{Pb}$ versus $^{208}\text{Pb}/^{207}\text{Pb}$ data from Table 30.1; lead isotope data for sediment samples from tributaries of the Mokelumne River and ore samples from the Penn Mine are shown along the mixing line from Figure 30.6 (channel samples not shown). At least three of the five NURE soil samples plot to the right of this mixing line indicating an exotic component of lead has been added and preserved. Labile and total lead compositions from Shirahata et al. (1980) are shown to indicate a similar source of an exotic component of lead in dated sediments from an isolated alpine lake in the Sierra Nevada range. This exotic component of lead is interpreted to be atmospheric lead introduced by the combustion of leaded gasoline.

would allow the measurement of the change in atmospheric lead flux as a direct result of the environmental regulations enacted in the 1970s on atmospheric emissions resulting from the combustion of leaded gasoline.

SUMMARY

This case study clearly demonstrates the utility of lead isotope fingerprinting to identify the source of metals in contaminated stream sediments and soils. It further demonstrates the value of archived samples to monitor the effects of environmental regulation on the geochemistry of the landscape. The Penn Mine is clearly the source of elevated copper and zinc concentrations in sediments in the drowned channel of the Mokelumne River in Camanche Reservoir. The lead isotope and chemical data indicate that the source of sediments to the fish hatchery in 1989 was deep within the reservoir. These data confirm the model proposed by Slotton et al. (1994) which suggested that wind action coupled with low reservoir levels could cause resuspension of bottom sediments into the water column. Because the metal-laden sediments occurred primarily below the 140-foot level within Camanche Reservoir, Slotton et al. (1994) recommended maintaining the water level at a minimum elevation of 180 feet to minimize contamination of the fish hatchery with metal-laden sediments. They further concluded that ore-metal contamination from these deep sediments was not the primary cause of the 1989 fish mortality events. Our lead isotope and geochemical data from the sediment recovered from the fish hatchery in 1989 confirm their general conclusions about the source of sediments to the intake for the fish hatchery.

ACKNOWLEDGMENTS—The authors thank coworkers in the Limnology Group, University of California, Davis, for assistance with sample collection. We also thank Steven Bond, California Regional Water Quality Control Board, for providing the sample of sediment collected from the fish hatchery in 1989, and the Stanford University Department of Geology for access to rock samples collected at the Penn Mine. The authors thank the East Bay Municipal Utility District for access to Camanche Reservoir and the Penn Mine site. Funding for collection of the Camanche Reservoir sediment samples was provided by the California State Water Resource Control Board under Interagency Agreement 1-198-150-0 with the University of California.

REFERENCES

- Albers, J.P., 1981, A lithologic-tectonic framework for the metallogenic provinces of California: *Economic Geology*, v. 76, pp. 765-790.
- Alpers, C.N., and Hamlin, S.N., 1993, Geochemistry and hydrogeology of an acidic ground-water plume in fractured metamorphic rocks at Penn Mine, Calaveras County, California [abs.]: *EOS*, v. 74, no. 16, p. 326.
- Alpers, C.N., and Nordstrom, D.K., 1991, Are there any lower limits to pH?—The geochemistry of extremely acid mine water from Iron Mountain, California; in *Proceedings, 2nd Internatl Conference on the Abatement of Acidic Drainage*, Montreal, Quebec, Sept. 16-18, 1991: *MEND (Mine Environment Neutral Drainage)* v. 2, pp. 321-342.
- Alpers, C.N., Nordstrom, D.K., and Burchard, J.M., 1992, Compilation and interpretation of water-quality and discharge data for acidic mine waters at Iron Mountain, Shasta County, California, 1940-1991: U.S. Geological Survey Water-Resources Investigations Report 91-4160, 173 pp.
- Alpers, C.N., Blowes, D.W., Nordstrom, D.K., and Jambor, J.L., 1994a, Secondary minerals and mine-water geochemistry; in Jambor, J.L., and Blowes, D.W. (eds.), *Environmental Geochemistry of Sulfide Mine- Wastes: Mineralogical Association of Canada, Nepean, Ontario, Short Course Handbook*, v. 22, pp. 247-270.
- Alpers, C.N., Hamlin, S.N., and Rye, R.O., 1994b, Stable isotopes (O, H, S) distinguish sources of acid drainage at Penn Mine, California [abs.]: *Abstracts of the 8th Internatl Conference on Geochronology, Cosmology, and Isotope Geology: U.S. Geological Survey Circular 1107*, p. 4.
- Alpers, C.N., Nordstrom, D.K., and Thompson, J.M., 1994c, Seasonal variations of Zn/Cu ratios in acid mine water from Iron Mountain, California; in Alpers, C.N., and Blowes, D.W. (eds.), *Environmental Geochemistry of Sulfide Oxidation: American Chemical Society Symposium Series 550*, pp. 324-344.
- Alpers, C.N., Hamlin, S.N., and Hunerlach, M.P., 1999, Hydrology and geochemistry of acid mine drainage in ground water in the vicinity of Penn Mine and Camanche Reservoir: *Summary Report, 1993-1995. U.S. Geological Survey Water-Resources Investigations Report 96-4287 (in press)*.
- Böhlke, J.K., and Kistler, R.W., 1986, Rb-Sr, K-Ar, and stable isotope evidence for the ages and sources of fluid components of gold-bearing quartz veins in the northern Sierra Nevada foothills metamorphic belt: *Economic Geology*, v. 81, pp. 296-322.
- Bond, S.R., 1988, Penn Mine Toxic Pits Cleanup Act Technical Investigation Report, California Regional Water Quality Control Board: Central Valley Region, Groundwater Protection and Investigation Section, 36 pp., 3 appendices.
- Briggs, P.H., 1990, Elemental analysis of geological material by inductively coupled plasma-atomic emission spectrometry; in Arbogast, B.F. (ed.), *Quality Assurance Manual for the Branch of Geochemistry: U.S. Geological Survey Open-File Report 90-688*, pp. 83-91.
- Chao, T.T., 1984, Use of partial dissolution techniques in geochemical exploration: *Journal of Geochemical Exploration*, v. 20, pp. 101-135.
- Chen, J.H., and Moore, J.G., 1982, Uranium-lead isotopic ages from the Sierra Nevada Batholith: *Journal of Geophysical Research*, v. 87, pp. 4761-4784.
- Church, S.E., Mosier, E.L., and Motooka, J.M., 1987, Mineralogical basis for the interpretation of multi-element (ICP-AES), oxalic acid and aqua regia partial digestions of stream sediments for reconnaissance exploration geochemistry: *Journal of Geochemical Exploration*, v. 29, pp. 207-233.
- Church, S.E., Holmes, C.W., Briggs, P.H., Vaughn, R.B., Cathcart, J., and Marot, M., 1993, Geochemical and Pb-isotope data from stream and lake sediments, and cores from the upper Arkansas River drainage—Effects of mining at Leadville, Colorado on heavy-metal concentrations in the Arkansas River: U.S. Geological Survey Open-File Report 93-534, 61 pp.
- Church, S.E., Wilson, S.A., Vaughn, R.B., and Fey, D.L., 1994, Geochemical and Pb-isotopic studies of river and lake sediments, upper Arkansas River basin, Twin Lakes to Pueblo, Colorado: U.S. Geological Survey Open-File Report 94-412, 44 pp.
- Church, S.E., Wilson, S.A., and Briggs, P.H., 1995, Geochemical and Pb-isotopic studies of stream and river sediments, Alamosa River basin, Colorado: U.S. Geological Survey Open-File Report 95-250, 71 pp.
- Church, S.E., Kimball, B.A., Fey, D.L., Ferderer, D.A., Yager, T.J., and Vaughn, R.B., 1997, Source, transport, and partitioning of metals between water, colloids, and bed sediments of the Animas River, Colorado: U.S. Geological Survey Open-File Report 97-151, 136 pp.
- Clark, L.D., 1964, Stratigraphy and structure of part of the western Sierra Nevada metamorphic belt, California: U.S. Geological Survey Professional Paper 410, 70 pp.
- Clark, W.B., and Lydon, P.A., 1962, Mines and mineral resources of Calaveras County, California: California Division of Mines and Geology County Report 2, pp. 28-31.
- Davy Environmental, 1993, Site Characterization Report, Penn Mine,

- Calaveras County, California: Prepared for California Regional Water Quality Control Board, Central Valley Region, 174 pp., 8 maps, 2 appendices.
- Doe, B.R., 1970, Lead isotopes: Springer-Verlag, New York, 137 pp.
- Dunham, R., 1961, Report on pollution at the Mokelumne River by the Penn Mine, Calaveras County, California: California Dept. of Fish and Game, Report to Central Valley Regional Water Pollution Control Board, 28 pp.
- E.V.S. Consultants, Inc., 1989, Camanche Reservoir water quality studies, Project No. 4/233-07.
- Finlayson, B.J., and Rectenwald, H.J., 1978, Toxicity of copper and zinc from the Penn Mine area on king salmon (*Oncorhynchus tshawytscha*) and steelhead trout (*Salmo gairdneri*) in the Mokelumne River Basin California: Fish and Wildlife Water Pollution Control Laboratory, California Department of Fish and Game, Environmental Services Branch Administrative Report No. 78-1, 42 pp.
- Fortescue, J.A.C., 1992, Landscape geochemistry—retrospect and prospect—1990: Applied Geochemistry, v. 7, pp. 1–54.
- Golder and Associates, Inc., 1996, Environmental Impact Report, Penn Mine, unpub. manuscript.
- Goodwin, J.G., 1957, Lead and zinc in California: California Journal of Mines and Geology, v. 53, No. 3–4, 728 pp.
- Graney, J.R., Halliday, A.N., Keeler, G.J., Nriagu, J.O., Robbins, J.A., and Norton, S.A., 1995, Isotopic record of lead pollution in lake sediments from the northeastern United States: Geochimica et Cosmochimica Acta, v. 59, pp. 1715–1728.
- Gulson, B.L., 1986, Lead isotopes in mineral exploration: Elsevier, New York, 245 pp.
- Gulson, B.L., Church, S.E., Mizon, K.J., and Meier, A.L., 1992, Lead isotopes in iron and manganese oxide coatings and their use as an exploration guide for concealed mineralization: Applied Geochemistry, v. 7, pp. 495–511.
- Hamlin, S.N., and Alpers, C.N., 1995, Hydrogeology and geochemistry of acid mine drainage in ground water in the vicinity of Penn Mine and Camanche Reservoir, Calaveras County, California, First year summary: U.S. Geological Survey Water-Resources Investigations Report 94-4040, 45 pp.
- Hamlin, S.N., and Alpers, C.N., 1996, Hydrogeology and geochemistry of acid mine drainage in ground water in the vicinity of Penn Mine and Camanche Reservoir, Calaveras County, California, Second year summary, 1992–1993: U.S. Geological Survey Water-Resources Investigations Report 96-4257, 44 pp.
- Heyl, G.R., 1948, Foothill copper-zinc belt of the Sierra Nevada, California: Calif. Div. of Mines and Geology Bulletin 144, pp. 11–29.
- Heyl, G.R., Cox, M.W., and Eric, J.H., 1948, Penn zinc-copper mine, Calaveras County, California: Calif. Div. of Mines and Geology Bulletin 144, pp. 61–84.
- Heyvaert, A.C., 1998, The biogeochemistry and paleolimnology of sediments from Lake Tahoe, California–Nevada: Unpub. PhD. thesis, Univ. of California, Davis.
- Jambor, J.L., and Blowes, D.W. (eds.), 1994, Environmental Geochemistry of Sulfide Mine-Wastes: Mineralogical Association of Canada, Nepean, Canada, Short Course Notes, v. 22, 438 pp.
- Knopf, A., 1929, The Mother Lode System of California, U.S. Geological Survey Professional Paper 157, 88 pp.
- Lindgren, W., 1911, The Tertiary gravels of the Sierra Nevada of California: U.S. Geological Survey Professional Paper 73, 226 pp.
- Moore, J.W., and Luoma, S.N., 1990, Hazardous wastes from large-scale metal extraction: Environmental Science and Technology, v. 24, pp. 1278–1285.
- National Institute for Standards and Technology (NIST), 1988, Certificate: Standard Reference Material 2704, Buffalo River Sediment.
- National Uranium Resource Evaluation (NURE), 1982, Hydrogeochemical and stream sediment reconnaissance basic data for Sacramento quadrangle, California: Open-File Report 82-GJBX-22, 165 pp.
- Ng, A.C., and Patterson, C.C., 1979, Chronological variations in barium concentrations and lead isotopic compositions in sediments of four Southern California offshore basins—Southern California Baseline Study: Benthic Year 2, Vol II, Report 14, Bureau of Land Management, Department of the Interior Contract AA550-CT6-40.
- Nordstrom, D.K., 1982, Aqueous pyrite oxidation and consequent formation of secondary minerals; in Karl, D.M. (ed.), Acid-Sulfate Soils: Soil Science Society of America, Spec. Pub. No. 10, pp. 37–56.
- Nordstrom, D.K., and Alpers, C.N., 1999, Geochemistry of acid mine waters; in Plumlee, G.S., and Logsdon, M.J. (eds.), The Environmental Geochemistry of Mineral Deposits, Part A. Processes, Methods and Health Issues: Society of Economic Geologists, Reviews in Economic Geology, v. 6A, pp. 133–160.
- Nordstrom, D.K., Alpers, C.N., and Ball, J.W., 1991, Measurement of negative pH and extremely high metal concentrations in acid mine water from Iron Mountain, California: Geological Society of America, Abstracts with Programs, v. 23, no. 5, p. A383.
- Ohmoto, H., and Skinner, B.J., (eds.) 1983, The Kuroko and related volcanogenic massive sulfide deposits: Economic Geology Monograph, v. 5, The Economic Geology Publishing Co., 604 pp.
- Östlund, P., Torssander, P., Morth, C.-M., and Claesson, S., 1995, Lead and sulphur isotope dilution during dispersion from the Falun mining area: Journal of Geochemical Exploration, v. 52, pp. 91–95.
- Parsons, M.B., Einaudi, M.T., Bird, D.K., and Alpers, C.N., 1998, Geochemical and mineralogical controls on trace-element release from base-metal slag deposits at the Penn Mine, Calaveras County, California [abs.]: Eos, Transactions, American Geophysical Union, v. 79, no. 45, 1998 Fall Meeting Supplement, p. F354.
- Patterson, C.C., 1971, Native copper, silver, and gold accessible to early metallurgists: American Antiquity, v. 36, pp. 286–321.
- Patterson, C.C., 1972, Silver stocks and losses in ancient and medieval times: Economic History Review, 2nd series, v. 25, pp. 205–235.
- Patterson, C.C., Settle, D.M., and Glover, B., 1976, Analysis of lead in polluted coastal seawater: Marine Chemistry, v. 4, pp. 305–319.
- Peterson, J.A., 1985, Geologic map of the Penn mine, Calaveras County, California: U.S. Geological Survey Miscellaneous Field Studies Map MF-1797, scale 1:1,200.
- Peterson, J.A., 1988, Distribution of selected trace and major elements around the massive sulfide deposit at the Penn Mine, California: Economic Geology, v. 83, pp. 419–427.
- Plumlee, G.S., and Nash, J.T., 1995, Geoenvironmental models of mineral deposits—fundamentals and applications; in du Bray, E.A. (ed.), Preliminary Compilation of Descriptive Geoenvironmental Mineral Deposit Models: U.S. Geological Survey Open-File Report 95-831, pp. 1–9.
- Plumlee, G.S., Smith, K.S., and Ficklin, W.H., 1994, Geoenvironmental models of mineral deposits, and geology-based mineral-environmental assessments of public lands: U.S. Geological Survey Open-File Report 94-203, 7 pp.
- Price, V., and Jones, P.L., 1979, Training manual for water and sediment geochemical reconnaissance: Department of Energy Open-File Report 91-GJBX-420, 104 pp.
- Riston, P.I., Esser, B.K., Niemeyer, S., and Flegal, A.R., 1994, Lead isotopic determination of historical sources of lead to Lake Erie, North America: Geochimica et Cosmochimica Acta, v. 58, pp. 3297–3305.
- Sañudo-Wilhelmy, S.A., and Flegal, A.R., 1994, Temporal variations in lead concentrations and isotopic composition in the Southern California Bight: Geochimica et Cosmochimica Acta, v. 58, pp. 3315–3320.
- Schmidt, J.M., 1978, Volcanogenic massive sulfides at Campo Seco, (Calaveras County) California: Unpub. M.S. thesis, Stanford Univ., 104 pp.
- Shaw, P., and Towers, C.L., 1937, Water pollution problems in California: Fish and Game, Calif., v. 23, no. 4, pp. 262–285.
- Shirahata, H., Elias, R.W., Patterson, C.C., and Koide, M., 1980, Chronological variations in concentrations and isotopic compositions of anthropogenic atmospheric lead in sediments of a remote subalpine pond: Geochimica et Cosmochimica Acta, v. 44, pp. 149–162.
- Singer, D.A., 1986, Descriptive model of Kuroko massive sulfide; in Cox, D.P., and Singer, D.A. (eds.), Mineral Deposit Models: U.S. Geological Survey Bulletin 1693, pp. 189–190.

- Singer, D.A., 1992, Grade and tonnage model of Sierra Kuroko deposits; *in* Bliss, J.D. (ed.), *Developments in Mineral Deposit Modeling*: U.S. Geological Survey Bulletin 2004, pp. 29–30.
- Slotton, D.G., and Reuter, J.E., 1995, Heavy metals in intact and resuspended sediments of a California Reservoir, with emphasis on potential bioavailability of copper and zinc: *Marine and Freshwater Research*, v. 46, pp. 257–265.
- Slotton, D.G., Reuter, J.E., Goldman, C.R., Jepson, Richard, and Lick, Wilbert, 1994, Camanche Reservoir bottom sediment study—heavy metal distribution and resuspension characteristics: Final Report for California State Water Resources Control Board, Interagency Agreement 1–198–150–0, 205 pp., 6 appendices.
- Strand, R.G., and Koenig, J.B., 1965, Geologic map of California, Sacramento sheet; *in* Jenkins, O.P. (ed.), *California Division of Mines and Geology, Sacramento*, scale 1:250,000.
- Taylor, C.D., Zierenberg, R.A., Goldfarb, R.J., Kilburn, J.E., Seal, R.R., II, and Kleinkopf, M.D., 1995, Volcanic-associated massive sulfide deposits; *in* du Bray, E.A. (ed.), *Preliminary Compilation of Descriptive Geoenvironmental Mineral Deposit Models*: U.S. Geological Survey Open-File Report 95–831, pp. 137–144.
- Tono, N., 1974, Minor element distribution around Kuroko deposits of northern Akita, Japan: *Society Mining Geologists Japan, Special Issue 6*, pp. 399–420.
- Turner, H.W., 1894, Jackson Folio, California: U.S. Geological Survey, *Geologic Atlas of the United States (No. 11)*, scale 1:125,000.
- U.S. Geological Survey, 1962, Topographic map of the Wallace 7.5' quadrangle, California: U.S. Geological Survey, scale 1:24,000.
- Walton-Day, K., Jerz, J.K., Ranville, J.F., Evans, J.F., and Smith, K.S., 1996, Effects of fluvial tailings deposits on the quality of surface and ground water at a site in the upper Arkansas River basin, Colorado [abs.]: *Geological Society of America*, v. 28, no. 7, pp. 466.
- Wiebelt, F.J., and Ricker, S., 1948, Penn Mine slag dump and mine water, Calaveras County, California: U.S. Bureau of Mines, *Report of Investigations 4224*, 6 p.
- Wilson, S.A., Briggs, P.H., Mee, J.S., and Siems, D.F., 1994, Determination of thirty-two major and trace elements in three NIST soil SRMs using ICP-AES and WDXRF: *Geostandards Newsletter*, v. 18, pp. 85–89.